Amino Acids

Chemistry, Biology and Medicine

I am highly indebted to Ajinomoto Co., Inc. for generous support of the First Amino Acid Congress.

Gert Lubec

Amino Acids

Chemistry, Biology and Medicine

Edited by

Gert Lubec
Department of Pediatrics
University of Vienna
A-1090 Vienna, Austria

with an introduction by

Gerald A. Rosenthal
T.H. Morgan School of Biological Sciences and
The Graduate Center for Toxicology
University of Kentucky
Lexington, Kentucky 40506-0225, USA

ESCOM • Leiden • 1990

CIP-Data Koninklijke Bibliotheek, Den Haag

Amino

Amino Acids: Chemistry, Biology and Medicine / ed. by G. Lubec and G.A. Rosenthal.
Leiden: ESCOM. – Ill.
With index, ref.
SISO 546 UDC 547.96
Subject heading: Amino acids.

ISBN 90-72199-04-9 (hardbound)

Published by:

ESCOM Science Publishers B.V.
P.O. Box 214
2300 AE Leiden
The Netherlands

Preface

There is little wonder in the fact that the investigation of amino acids is of fundamental interest to scientists from so many diversified fields. If amino acids were only basic constituents of enzymes as well as structural and other proteins, this property alone would elevate them to real scientific importance. Added to this role, however, is their ability to serve as building blocks for the production of many classes of secondary metabolites. They can support the biosynthesis of a myriad of natural products including nonprotein amino acids, cyanogenic glycosides, pharmacologically active alkaloids, certain phenols, purines and pyrimidines, nucleic acids, condensed tannins, lignins and other metabolites.

The approximately twenty or so amino (and imino) acids that comprise proteins are well known; less familiar are what is now approaching 600 nonprotein amino acids that have been isolated and characterized from plant, fungal or animal sources. Investigations of the protein amino acids have proven of outstanding value in enhancing our understanding of a variety of physiological and neurological topics that affect human health and well being. Amino acids are used to probe inhibitory and excitatory transmission receptors in the brain. They contribute to our understanding of epilepsy, development of anti-epileptic drugs, production of novel γ-aminobutyric acid uptake inhibitors, and acute and chronic neurodegenerative disorders. Amino acids can be helpful in understanding metabolite turnover and function in the brain of animals with epileptic syndromes or Parkinson's disease, and the effects of excitatory amino acid antagonists on seizure phenomena. Amino acids have been employed to investigate cirrhosis and other liver diseases, to study encephalomyelopathy, amyotrophic lateral sclerosis, insomnia and to gain a basic understanding of human nutrition and many aspects of animal physiology.

Certain nonprotein amino acids have proven of considerable experimental value in probing amino acid chemistry and function, as a tool for enhanced understanding of the roles and functions of protein amino acids, in understanding the chemistry and biochemistry of ecological interactions between living systems, and as analogs and/or competitive inhibitors of protein amino acids in biochemical studies.

This text had its inception in an International Congress on Amino Acid Research held in Vienna, Austria from August 7–12, 1989. The collection of papers presented at or created in response to this meeting will appeal to researchers in the fields of biochemistry, vascular and cell biology, physiology, pharmacology, endocrinology, and clinical medicine. The offerings of this treatise reflect the broad interest in amino acids among researchers in chemistry, biochemistry, neurology, pharmacology, physiology and medicine.

Chirospecific synthesis and the separation and analysis of optically active mixtures of amino acids is of considerable current interest. Much of this interest emanates from expanding research on and the synthesis of new drugs. This treatise reflects the increasing interest in the study of nonprotein amino acids as well. These compounds have proven of value in understanding the life processes of higher plants, probing structural and functional aspects of specific proteins, protein synthesis, and post-translational modification of proteins.

This text details the use of amino acids to probe important nutritional and physiological questions. Amino acids have been employed for their therapeutic potential as excitatory amino acid antagonists, for analyzing excitatory amino acid receptors, and for understanding aspects of central nervous system function. They have allowed us to better understand transport phenomena and its regulation.

While this treatise is not intended to be exhaustive in its coverage, it will provide a basic introduction to many areas of study that are being enthusiastically explored today using amino acids as highly effective experimental tools. Hopefully, it will serve to stimulate and motivate further investigations of this important group of metabolites.

Gerald A. Rosenthal

Contents

Section II: Neurochemistry/Neurobiology

Section I
Basic chemistry, Analysis and Synthesis

Novel amino acids from plants

Sir Leslie Fowden

Lawes Trust Fellow, Rothamsted Experimental Station, Harpenden, Herts AL5 2JQ, U.K.

The availability of new chromatographic techniques in the late 1940s facilitated the study of complex mixtures of compounds present in extracts of plants, and paper chromatography was particularly useful for the separation, and subsequent characterization, of amino acid constituents. During the last 40 years, several hundred novel amino acids have been identified within the plant kingdom, and new characterizations continue as analytical techniques become more refined and sensitive. These 'newer' amino acids are not present normally in protein molecules of the 'producer' species, and for that reason often are called non-protein amino acids. Since they are now so numerous, it is not surprising that they display a very wide range of structural features. Some molecules contain groupings not encountered among the 20 protein amino acids, e.g. ethylenic and acetylenic linkages as part of aliphatic C chains, cyclopropane rings, novel heterocycles containing N, S or O atoms, etc. As a distinct group of plant secondary products, these metabolites pose many interesting problems in regard to biosynthesis and function. Some of the compounds are toxic, which sometimes can be explained by direct antagonism of intermediary metabolic processes concerned with amino acid biosynthesis, degradation, or incorporation into protein molecules. The poisonous nature of some of these substances suggests possible roles as protective agents produced by particular plants to confer a degree of resistance to attack by pests or pathogens. The remainder of this paper will elaborate the concepts expressed above through suitable examples.

Structures and analogue features

The structures of many of the non-protein amino acids closely resemble those of normal protein constituents, and therefore can be grouped into alkyl (neutral, basic and acidic), S-containing, aromatic (phenyl and heterocyclic), and imino acid classes in the manner applied to the protein amino acids.

My own early work [1] led to the isolation and characterization of 4-methyleneglutamic acid (I) and 4-methyleneglutamine (II) from *Arachis hypogaea* (peanut). Subsequently, many other C-4 substituted glutamic acids have been characterized; also a range of N^5(amide)-substituted glutamines and N^4(amide)-asparagines. Later, the cyclopropane ring containing compounds, *cis*- and *trans*- α-(carboxycyclopropyl)glycine (III and IV, R=H) were isolated from *Aesculus* spp. [2] and

recognized as potential analogues of glutamic acid: the *cis*-isomer inhibits the growth of mung bean seedlings, and has been tested as a metabolic antagonist in animal systems. A range of 4-substituted glutamic acids have been assayed for possible antagonism of glutamic acid/γ-amino butyric acid functions in mammalian and insect nervous systems.

Two other cyclopropylamino acids, hypoglycin A (V,R=H) [3] and α-(methylenecyclopropyl)glycine (VI,R=H) [4], both isolated from plants from the family Sapindaceae (where they coexist with the related γ-glutamyl peptides, V and VI, R= γ-glutamyl), behave as hypoglycaemic compounds by dramatically reducing blood glucose levels. The mode of action apparently involves an initial oxidative deamination and decarboxylation of the amino acids to give cyclopropylcarboxylic acids that inhibit normal ß-oxidation of fatty acids, so placing an extra demand on glucose as a respiratory energy substrate.

Proline (VII) is the only imino acid invariably present in plant proteins, although certain structural proteins may contain *trans*-4-hydroxy-L-proline. However, additional imino acids exist as free constituents. A variety of substituted L-prolines exist, e.g. *cis*-4-hydroxy, *trans*-3-hydroxy, *trans*-4-methyl, *cis*-4-hydroxymethyl, and 4-methylene. The homologous azetidine-2-carboxylic acid (VIII) is present in many liliaceous species (5), in selected legumes, and in occasional unrelated species. Pipecolic acid (IX), the higher homologue, occurs more widely in plants being formed by cyclization of lysine. *Trans*-4- and *trans*-5-hydroxy derivatives have been characterized, as have isomeric 4,5-dihydroxypipecolic acids. *Cis*-3,4-methanoproline (X) is a fascinating analogue displaying features of both proline and pipecolic acid [2]. Azetidine-2-carboxylic acid and 3,4-methanoproline strongly antagonize proline metabolism: they compete with proline uptake into cells (i.e. are permease inhibitors), limit the rate of proline biosynthesis, and azetidine-2-carboxylic acid is introduced into protein molecules in place of proline residues. *Trans*-4-hydroxyproline also reduces proline synthesis in plant cells, acting as a mimic end-product inhibitor of proline biosynthetic enzymes.

Nice examples of naturally-occurring structural analogues have been found among the group of basic amino acids. S-aminoethylcysteine (XI, thialysine) is a bacterial product that has a similar molecular conformation to lysine (XII), and so the compound mimics lysine in regard to end-product inhibition phenomena and can compete with lysine during the processes of amino acid activation and incorporation into protein molecules. Canavanine (XIII), produced by many species within the Papilionoideae, is an isostere of arginine (XIV), in which an -O- replaces a normal $-CH_2-$ group. In a similar fashion, indospicine (XV) from the legume *Indigofera spicata* [6] also behaves as an arginine analogue: in this instance, a guanidino-NH of the parent amino acid is replaced by CH_2. Both canavanine and indospicine are toxic, and interference seems likely at three levels of arginine metabolism (permease, amino acid biosynthesis, and aminoacyl-tRNA synethase action).

Avoidance of analogue autotoxicity

Azetidine-2-carboxylic acid, canavanine and indospicine are examples of analogue molecules that are believed to confer protection upon the producer plant species against damaging organisms, particularly insect pests; they also may confer a degree of competitive advantage by acting as growth inhibitors of other plants seeking to colonize the same niche. If such allochemical action is to be successful, *a priori* the compounds must not affect the growth and development of the producer plants in any way, i.e. such species must have developed appropriate mechanisms to avoid the toxic action of their own products. A common mechanism for effecting detoxification is transport and accumulation of a compound in the cell vacuole, which isolates the material from the functional cytoplasm and sub-cellular organelles. Another mechanism entails conjugation of the toxic compound to produce a larger molecule that no longer has lethal properties. However, detailed comparisons of plants with and without the ability to synthesize azetidine-2-carboxylic acid or canavanine has indicated that a more exact and discriminating mode of avoiding autotoxicity has been evolved, in which the substrate specificity of aminoacyl-tRNA synthetase enzymes differs between plants and leads to the selective exclusion of the toxic analogues from the proteins of producer species.

Studies with prolyl-tRNA synthetases have demonstrated the existence of such differences in enzyme specificity most clearly. Purified enzymes prepared from three types of plant producing large quantities of azetidine-2-carboxylic acid were compared with similar enzymes from plants unable to synthesize the imino acid [7]. Data in Table 1 show that the analogue is used as a substrate by the enzymes from non-producer species, but is essentially inactive with the enzymes from producer plants. Therefore it appears that during evolution the prolyl-tRNA synthetase has undergone subtle mutations in producer species that render the enzymes' active site no longer capable of binding the analogue molecule. The available evidence suggests that the configuration at the active site of the enzyme from producer plants has altered in a way that makes the fit of the analogue too loose for effective binding to occur.

Table 1. Kinetic parameters of prolyl-tRNA synthetases from azetidine-2-carboxylic acid (A2C) producer and nonproducer plants

Species	A2C Producer	Proline K_m ($\times 10^{-4}$M)	A2C	
			K_m ($\times 10^{-3}$M)	Vmax*
Convallaria majalis	Yes	4.5	∞	≈0
Delonix regia	Yes	1.82	∞	≈0
Parkinsonia aculeata	Yes	4.35	∞	≈0
Phaseolus aureus	No	1.37	1.43	55
Hemerocallis fulva	No	6.25	5.3	75
Ranunculus bulbosa	No	2.9	2.0	66

* These V_{max} values are expressed as percentages of those obtained for proline.

Less detailed work with the arginyl-tRNA synthetase from *Canavalia ensiformis*, a major canavanine-producing species, has led to a similar conclusion; namely, the *Canavalia* enzyme is unable to activate canavanine although enzymes from plants not producing canavanine accept the compound as a substrate prior to its incorporation into protein molecules in place of arginine [8].

Canavanine is accumulated especially in the seeds of producer plants, where concentrations may reach 12% on a D.W. basis, and the amino acid plays a strong defensive role against seed-boring insects. Test insects fed on a diet containing canavanine may show significant developmental malformations, and canavanine becomes incorporated into the insects' proteins. However, larvae of the bruchid beetle, *Caryedes brasiliensis* are able to live solely on seed of *Dioclea megacarpa*, which contains 8–12% canavanine. This insect's ability to overcome the toxic action of canavanine again rests on the evolution of a modified arginyl-tRNA synthetase that fails to activate canavanine in contrast to enzymes isolated from sensitive insect species [9].

Amino acids in crop improvement

The majority of the N assimilated via plant roots is incorporated ultimately into amino acids and proteins. The overall amino acid composition varies significantly between different major crop species; for example, the cereal seed proteins contain relatively low concentrations of lysine and threonine in comparison with the seed proteins of legumes or brassicas. For this reason, the cereal seed proteins are of low quality in human nutrition, especially by comparison with animal protein, and interest surrounds any opportunity to boost seed lysine and threonine concentrations.

Amino acid synthesis in plants is regulated by end-product inhibition of key biosynthetic enzymes, and in this way cellular concentrations of particular amino acids normally are maintained within closely defined ranges. The aspartate family of amino acids which includes the protein constituents, lysine, threonine and methionine, has been studied to illustrate this concept. Each of the end-products (lysine, threonine and methionine) inhibits certain key enzymes involved in the aspartic pathways. Isosteric analogues can mimic the normal end-product, e.g. S-aminoethylcysteine shows similar inhibitory action to lysine itself. If plant cells or tissues are subjected to high concentrations of a combination of two of the normal end-products (lysine and threonine), then synthesis of the third (methionine) is interrupted, and normal growth is quickly restricted. Since advantage could result from the deregulation of synthesis of those 'essential' amino acids present in low amount in major food plants (e.g. lysine and threonine in cereals), Dr. S.W.G. Bright and colleagues at Rothamsted sought mutant lines of plants in which synthesis within the aspartate family of amino acids was no longer seriously subject to end-product inhibition. For this purpose, immature embryos of barley (var. Bomi) were isolated from seeds previously treated with a chemical mutagen,

Table 2. Free amino acid levels in barley grain (n mol g^{-1} D.W.)

Cultivar/mutant	Threonine	Lysine	Methionine
Bomi	118	84	24
R2501	6129	1266	149
R2506	9032	1620	72

and rare individuals able to grow in the presence of lysine plus threonine were analysed in detail for their amino acid composition and the kinetic parameters of the initial biosynthetic enzyme, aspartic kinase. A few mutants possessing greatly elevated concentrations of free lysine, threonine and methionine were characterized, and some comparative information is given in Table 2. Although the composition of the barley proteins remained unaffected, the magnitude of the increase in concentration of the free amino acids represents significant percentage increases in total amounts present in the mutant barleys. Thus, some of the mutant lines were made available to plant breeders in the expectation that the new traits may be combined with other desirable agronomic features in new barley cultivars.

Bright's group have used analogues of proline in a similar manner to screen for mutant lines of barley in which proline biosynthesis is partially deregulated. The selected plants accumulated 5–7 times the normal amounts of proline. This approach is of interest in elucidating the possible role of proline in relation to drought resistance in plants – certainly, plants subject to water stress accumulate proline in much higher concentrations (up to 50-fold) than normal plants. The mutant barleys having higher proline contents exhibited marginally greater salt tolerance and were slightly less sensitive to water stress than the parent cultivar.

In a very different way proline analogues have been employed as potential chemical gametocides for the production of hybrid wheats. This development was initiated with the knowledge that free proline is accumulated in very high concentration in pollen grains of many plant species, and that it may play a role as an energy source during processes leading to the rapid growth of pollen tubes. Proline analogues were then evaluated as potential, specific inhibitors of pollen grain germination and pollen tube growth by scientists at the Shell group of companies.

Normally, wheat is self pollinating, and a successful chemical gametocide should inhibit intra-specific pollination after application to plants at anthesis. 3,4-Methanoproline was shown to act in this way if sprayed onto the potential female parent of a hybrid – and thus it facilitated cross-pollination and hybridization dependent upon pollen transfer from an adjacent but different wheat cultivar behaving as the male parent. The technique was reasonably successful in producing hybrid seed, but the compound proved slightly too phytotoxic to the wheat plants. An alternative synthetic analogue, azetidine-3-carboxylic acid (XVI), was

Annex of chemical structures

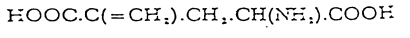

I

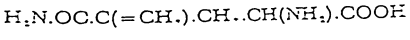

II

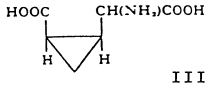

III

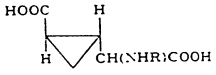

IV

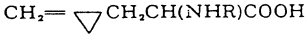

V

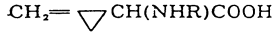

VI

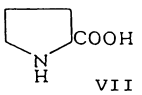

VII

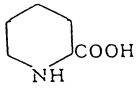

IX

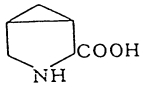

X

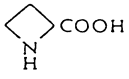

VIII

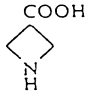

XVI

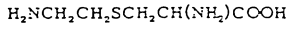

XI

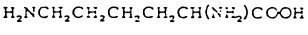

XII

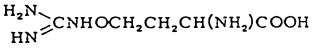

XIII

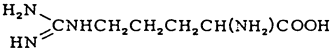

XIV

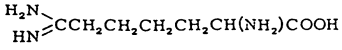

XV

Key to structures:

I. 4-Methyleneglutamic acid
II. 4-Methyleneglutamine
III. *Cis*-α-(carboxycyclopropyl)glycine
IV. *Trans*-α-(carboxycyclopropyl)glycine
V. Hypoglycin A (R=H)
VI. α-(Methylenecyclopropyl)glycine (R=H)
VII. Proline
VIII. Azetidine-2-carboxylic acid
IX. Pipecolic acid
X. 3,4-Methanoproline
XI. S-aminoethylcysteine
XII. Lysine
XIII. Canavanine
XIV. Arginine
XV. Indospicine
XVI. Azetidine-3-carboxylic acid

produced and fulfilled most requirements for a successful chemical hybridizing agent. This latter compound has been tested widely in field trials, and has given hybrids showing useful yield increases (up to about 12%) over the parent varieties. However, XVI like many other potential agrochemicals is experiencing difficulty in satisfying all of the increasingly stringent environmental and toxicological regulatory criteria.

References

1. Done J and Fowden L (1952) Biochem. J. 51: 451–458.
2. Fowden L, Smith A, Millington DS and Sheppard RC (1969) Phytochemistry 8: 437–443.
3. Ellington EV, Hassall CH, Plimmer JR and Seaforth CE (1959) J. Chem. Soc. 80–85.
4. Gray DO and Fowden L (1962) Biochem. J. 82: 385–389.
5. Fowden L (1956) Biochem. J. 64: 323–332.
6. Hegarty MP and Pound AW (1968) Nature, London. 217: 354.
7. Norris RD and Fowden L (1972) Phytochemistry 11: 2921–2935.
8. Fowden L and Frankton JB (1968) Phytochemistry 7: 1077–1086.
9. Rosenthal GA, Dahlman DL and Janzen DH (1976) Science 192: 256–258.

Chirospecific synthesis of amino acids and analogues

Tomihisa Ohta[a], Akio Hosoi[a], Toshihiko Kimura[a], Nobuaki Sato[a], Kunisuke Izawa[b] and Shigeo Nozoe[a]

[a]Faculty of Pharmacy, Tohoku University, Aobayama, Sendai 980, Japan
[b]Basic Research Department, Central Research Laboratories, Ajinomoto Co., Inc., Kawasaki 210, Japan

Use of *N*-carbamoylpyroglutamate as an effective precursor

Proline and its analogues demonstrate a wide range of biological activity, inview of that we have synthesized amino acid analogues having pyrrolidine ring starting from *N*-carbamoylpyroglutamate (**1**). In this process we have established regioselective mono-addition reaction, stereospecific substitution at C-4 and pyrrolidine ring formation.

The combination of physical, chemical and stereochemical nature of amino acids and its analogues constructs the three dimensional geometry of peptides, proteins and other physiologically active compounds, which dominates the intermolecular interactions of the molecules. Proline and its derivatives demonstrate a variety of activities such as inhibition of enkephalinase B [1], antileukemic [2], antihypertensive [3–6] and prolyl endopeptidase inhibition [7]. Proper modification of the pyrrolidine ring in those compounds and the introduced substituent effects on an activity may afford a three dimensional information about an active site of interacted proteins such as enzymes and receptors [1,5]. In view of that, we have planned the chirospecific synthesis of variously substituted prolines and related amino acid analogues from simple and naturally abundant starting materials, glutamic acid. Mimicking the biosynthesis of proline from glutamic acid, we designed the modification of C-5 carbonyl group so that we could synthesize 4- and 5-substituted prolines which have been suggested to be an important constituent of antihypertensive agent such as angiotensin converting enzyme (ACE) inhibitor [4,5].

Results and Discussion

As a starting material for this study, we chose *N*-carbamoylpyroglutamate (**1**) in which 5-carbonyl group was found to be more reactive than ester carbonyl group at C-1. Namely, regioselective mono-addition of carbon nucleophiles, such as Grignard reagents and ester enolates gave exclusively 5-oxoamino acid derivatives which was subsequently cyclized to afford 5-substituted prolinates [8,9].

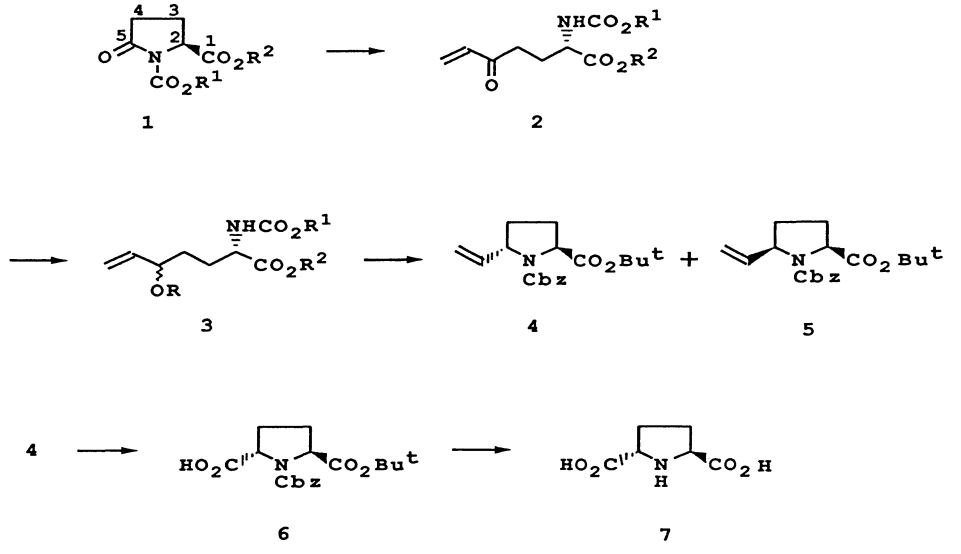

Scheme 1.

For the synthesis of 5-vinylprolinate and pyrrolidine-2,5-dicarboxylate, the pyroglutamate (**1**) was treated first with vinylmagnesium bromide at –40°C to give the vinylketone (**2**). The vinylketone (**2**) was reduced with $NaBH_4$-$CeCl_3$ at –15°C and the resulting alcohol (**3**: R=H) was transformed to the mesylate (**3**: R=Ms) which was rather unstable and rearranged gradually into prolinates **4** and **5** on stirring with Et_3N in CH_2Cl_2, at room temperature. Two diastereomers **4** and **5** were separated by silica gel in 46 and 9% yield, respectively. 2,5-*Trans* 5-vinylprolinate (**4**) was successively oxidized to the carboxylic acid (**6**) which on deprotection gave the acid (**7**). Overall yield from the pyroglutamate (**1**) was 13%. The amino acid (**7**) was found identical in all respects with (2*S*,5*S*)-pyrrolidine-2,5-dicarboxylic acid, the acidic amino acid constituent of the marine red alga *Schizymenia dubyi* [8, 10]. (Scheme 1)

Because of the higher nucleophilicity of lithium enolate than that of Grignard reagents, the addition reaction of **1** with lithium enolate of esters proceeded faster even at –78°C and gave 5-oxoamino acid derivatives (**8**) in excellent yields as shown in Table 1. In spite of the strong basicity of the lithium enolate, *S*-configuration at C-2 was retained throughout the reaction pathway which was confirmed by ^{13}C NMR (125.65 MHz) [9]. Catalytic hydrogenolysis of the adduct (**8**) under medium pressure of hydrogen, was accompanied with reductive pyrrolidine ring formation to give 2,5-*cis* substituted pyrrolidine (**10**). It was assumed that the stereospecific hydrogenation of the intermediate pyrroline (**9**) gave 5-substituted proline (**10**), which indicated the 2,5-*cis* stereochemistry. This was con-

Table 1. Reaction of pyroglutamates (**1**) with Ester Enolates

1	R^1	R^2	R^3	R^4	yields of **8**
1a	Bzl	Bzl	H	tBu	95 (%)
1b	Bzl	Bzl	Me	tBu	93
1c	Bzl	Bzl	Et	tBu	81
1d	Bzl	Bzl	iPr	tBu	83
1e	Bzl	Bzl	Bzl	tBu	81
1f	Bzl	Me	H	tBu	84
1g	Bzl	Me	Et	Bzl	71
1h	tBu	Bzl	H	tBu	97

firmed by the direct comparison with 2,5-*trans* pyrrolidine (**12**) which was synthesized from 5-vinylprolinate (**11**). HPLC analysis of amino acid (**10**: R^3=H, R^4=*t*-Bu and **12**) showed that **10** contains 4% of the *trans* isomer (**12**). The amino acid (**10**) was transformed into (+)-carbapenam (**14**) and 6-ethyl analogue (**10**: R^3=Et, R^4=t-Bu) which was useful for the synthesis of antibiotic (+)-PS-5 (**15**) [11]. (Scheme 2) (+)-Carbapenam (**14**) was isolated from *Serratia* and *Erwinia* species and suggested its putative role in the biosynthesis of the more complex carbapenem antibiotics [12].

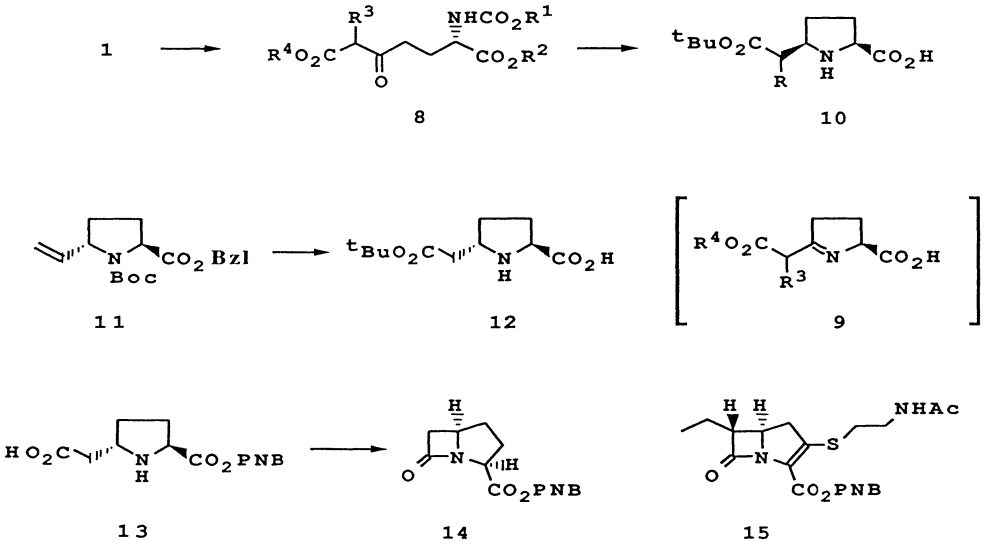

Scheme 2.

The fact that C-5 carbonyl group of the pyroglutamate (**1**) is more reactive than that of ester carbonyl indicated that a regioselective enolization at C-5 may be possible, which results in a diastereoselective substitution at C-4 such as 4-alkylation and 4-hydroxylation. For that purpose the lithium enolate (**16**) was derived from **1** (R^1=Bu^t, R^2=Bzl) with lithium hexamethyldisilazide (LiHMDS) and then treated with methyl iodide to give 4-methylpyroglutamates **17** and **18** in 48 and 27%, respectively. A high diastereoselectivity, however, was observed when **16** was hydroxylated with 2-toluenesulfonyl-3-phenyloxazilidine [13]. 4(*R*)-Hydroxypyroglutamate (**19a**) was obtained as a sole product. HPLC analysis of **19a** and its 4-epimer (**20a**) which is derived from **19a** *via* 4-formate (**20b**) showed >98% of diastereomeric excess for **19a**. (+)-α-Methoxy-α-trifluoromethylphenyl-acetoxy [(+)-MTPA] derivatives (**19b**, and mixture of **19b** and **20c**) indicated that the hydroxylation proceeded with no racemization at C-2. (4*R*)-Configuration of the alcohol (**19a**) was determined by the NMR analysis of alcohols **19a** and **20a**. Namely, desielded signals of 2- and 4-hydrogen (δ 4.61 and 4.41, respectively) of the alcohol (**19a**) compared to those ($\delta_{H\text{-}2}$ 4.44 and $\delta_{H\text{-}4}$ 4.24) of the epimer (**20a**) clearly indicates the 2,4-*trans* relationship of the alcohol (**19a**).

As an extension of our methodology, we synthesized 4,5-disubstituted proline analogue, (−)-bulgecinine (**24**) which is the main component of bulgecines, the unique glycopeptides isolated from *Pseudomonas acidophila* and *P. mesoacido-*

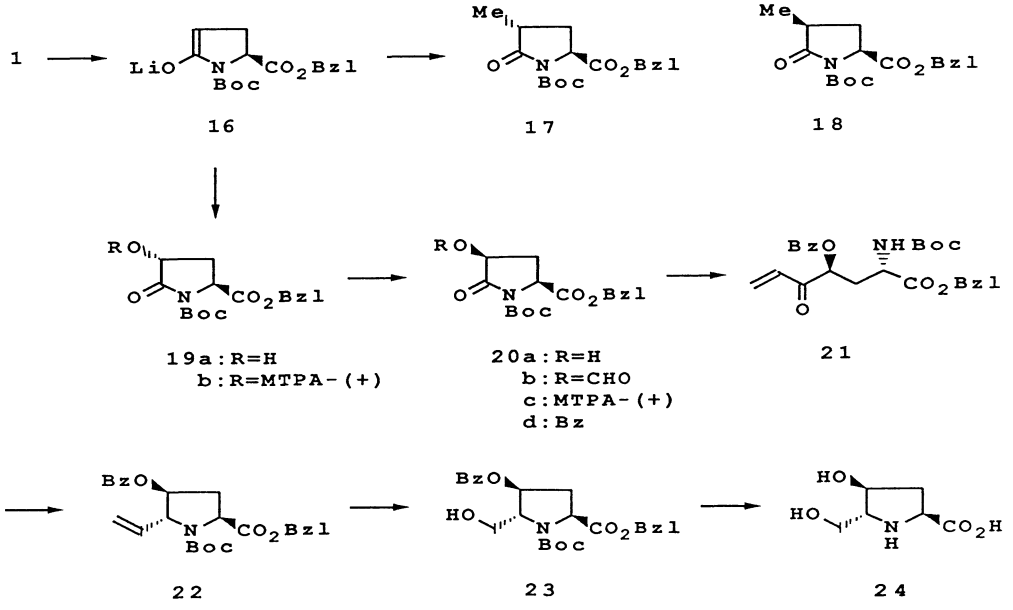

Scheme 3.

phila [14, 15]. According to the procedure we developed [8], (4*S*-)benzoxypyroglutamate (**20d**) was treated with vinylmagnesium bromide at –40°C in THF to afford the enone (**21**). Reduction of the enone (**21**) was followed by mesylation at 0°C and cyclization over silica gel to give the vinylprolinate (**22**). Observation of two sets of NMR signals for 2- and 5-hydrogens of **22** is characteristic for the 2,5-*trans* substituted *N*-carbamoylpyrrolidine derivatives. Moreover, the observed small coupling constant between 4- and 5-hydrogens, 0.7 or 1.1 Hz, clearly indicates the *trans* relationship of those hydrogens [14]. The vinylprolinate (**22**) may regard as an interesting substitute for bulgecinine (**24**) or proline itself in physiologically active compounds. (Scheme 3)

Finally we synthesized proline (**28a**) and 4-hydroxyproline (**28b**) from the pyroglutamate (**1**), as models of isotopically labeled prolinates which may be useful in a metabolism study or protein analysis. The high reactivity of C-5 carbonyl of the lactam (**1**) allowed us to reduce it with sodium borohydride ($NaBH_4$) to yield the aminal (**25**) in addition to **26** as a by-product. Excellent yield of **25** was given by suppressing over reduction at low temperature. Quenching procedure also influenced yields of aminal (**25**) as shown in Table 2. As an aldehyde equivalent, the aminal (**25**) reacted slowly with a stable Wittig reagent giving C_1 amino acid derivative (**27**). And moreover, the aminals (**25** and **29**) were found to be easily transformed under deprotective condition to proline (**28a**) or hydroxyproline (**28b**). (Scheme 4)

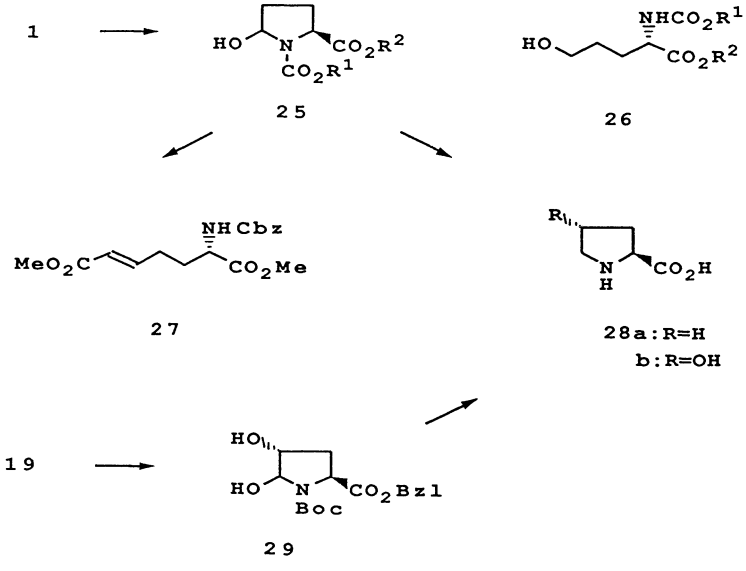

Scheme 4.

Table 2. Reduction of pyroglutamates (**1**)

			Reduction conditions			Yield (%)	
1	R^1	R^2	Temp. (°C)	Time (h)	Work up	**25**	**26**
1a	Bzl	Bzl	0≈ 20	4.5	AcOH	4.7	48[a]
			−15≈−10	0.5	$NaHCO_3$ aq.	94	3.4
1b	Bzl	Me	−15≈−10	1	AcOH	69	27
			−15≈−10	1	$NaHCO_3$ aq.	78	7.2
1c	t_{Bu}	Bzl	−15≈−10	1	$NaHCO_3$ aq.	95	–
1d	t_{Bu}	Me	−15≈−10	1.5	$NaHCO_3$ aq.	94	5.1

[a] R^2=Me, Benzyl ester was exchanged with MeOH.

Thus we have established facile and chirospecific synthesis of amino acids and analogues having pyrrolidine ring. Our synthetic procedures and compounds we synthesized may be useful for biosynthetic study, drug design or stereochemical study of proteins. Further application of this study for the synthesis of physiologically active amino acid analogues are under investigation.

Experimental section

General methods

Tetrahydrofuran was distilled from sodium and Benzophenone. Methylene chloride was distilled from P_2O_5. Amines were distilled from CaH_2. NMR spectra were recorded on a JEOL FX100 or GX500 system. Chemical shifts were referred to internal Me_4Si. Other spectral data were obtained on the following spectrometers: IR on a JASCO A-100S, MS on a JEOL JMS-01SG-2, and optical rotation on a JASCO Dip-4 Digital Polarimeter.

t-Butyl (S)-2-benzyloxycarbamido-5-oxo-6-heptenoate (**2**)

To the pyroglutamate (**1**, 4.83 g, 15 mmol) in dry THF (50 ml) was added 2M vinylmagnesium bromide THF solution (10 ml, 20 mmol) dropwise at −40°C and the mixture was stirred at −40°C for 1 h. After quenching with MeOH-AcOH (1:1, 1 ml), the mixture was diluted with Et_2O, washed with 10% citric acid, water and evaporated. The residue was chromatographed on silica gel and elution with 20% Et_2O in hexane gave the enone (**2**): 2.84g (55%); IR 3300, 1740, 1720, 1680, 1620 cm^{-1}; ^1H NMR ($CDCl_3$) δ 1.45 (9H, s), 2.4–2.8 (2H, m), 4.0–4.4 (1H, m), 5.0 (2H, s), 5.1–5.4 (1H, m), 5.7 (1H, dd, J=4, 8 Hz), 6.13 (1H, d, J=4 Hz), 6.14 (1H, d, J=8 Hz), 7.2 (5H, s). MS *m/z* (FD) 347 (M^+).

t-Butyl (S)-2-benzyloxycarbamido-6-hydroxy-7-heptenoate (**3**)

The mixture of enone (**2**, 300 mg, 0.386 mmol) and $CeCl_3.7H_2O$ (370 mg, 1 mmol) was cooled to −15°C (ice+MeOH) and $NaBH_4$ (37 mg, 1 mmol) was added portionwise to the mixture. After 5 min of stirring, the mixture was diluted with Et_2O, washed with 10% citric acid, water and sat. brine, dried and evaporated. Silica gel chromatography (30% Et_2O in hexane elution) of the residue gave the alcohol (**3**): 275 mg (91%); IR 3400,1740, 1720, 1640 cm^{-1}; ^1H NMR ($CDCl_3$) δ 1.45 (9H, s), 3.8–4.4 (2H, m), 5.0 (2H, s), 4.9–6.0 (4H, m), 7.2 (5H, s). MS *m/z* (FD) 349 (M^+).

t-Butyl N-carbobenzoxy-5-vinylprolinate (**4**) *and* (**5**)

To the mixture of alcohol (**3**, 970 mg, 2.8 mmol) and Et_3N (0.8 ml, 6 mmol) in dry CH_2Cl_2 (15 ml) was added MsCl (0.27 ml, 3.5 mmol) dropwise at 0°C. The mixture was stirred at 0°C for 2 h, diluted with Et_2O, washed with water and sat. NaCl aq., dried and evaporated. The residue in CH_2Cl_2 (2 ml) was stirred with Et_3N (0.8 ml, 6 mmol) at rt for 3 days. Evaporation at reduced pressure was followed by silica gel chromatography (10% Et_2O in hexane elution) of the residue gave isomeric mixture of vinylprolinates, 560 mg, which were separated by HPLC (20% Et_2O in hexane elution). *2,5-Trans 5-vinylprolinate* (**4**) : 422 mg (46%); t_R 5 min; $[\alpha]_D^{20}$ −41.6° (c 0.52, $CHCl_3$) ; IR 1740, 1710, 1640 cm^{-1}; ^1H NMR ($CDCl_3$) δ 1.32 (9/2H, s), 1.44 (9/2H, s), 4.25 (1H, m), 4.55 (1H, m), 4.8–5.2 (5H, m), 5.7 (1H, m), 7.29 (5H, s). MS *m/z* (FD) 331 (M^+). *2.5-Cis 5-vinylprolinate* (**5**): 83 mg (9%); t_R 7.5 min. $[\alpha]_D^{20}$ − 66.1° (c 0.19, $CHCl_3$); IR 1740, 1710, 1640 cm^{-1}; ^1H NMR ($CDCl_3$) δ 1.35 (27/5H, s), 1.43 (18/5H, s), 4.1–4.5 (2H, m), 4.9–5.3 (3H, m), 5.10 (2H, m), 5.9 (1H, m), 7.29 (5H, s). MS *m/z* (FD) 331 (M^+).

t-Butyl (2S, 5S)-N-benzyloxycarbonyl-5-carboxyprolinate (**6**)

Vinylprolinate (**4**, 2.2 g, 6.6 mmol) in MeOH (15 ml) was ozonized at −78°C. After treating with Me_2S (1 ml, 15 mmol), the mixture was evaporated and subjected to silica gel chromatography. Elution with 20% Et_2O in hexane gave *t-butyl (2S, 5S)-N-carbobenzoxy-5-formylprolinate*, 2.10 g (95%). To the mixture of 1.8 g of the 5-formylprolinate in dry DMF (20 ml) was added pyridinium dichromate (7 g, 20 mmol) stirred at rt overnight. Dilution with EtOAc was followed by washing with 10% citric acid, water and brine. The residue obtained by evaporation of solvent was subjected to silica gel chromatography and elution with 50% EtOAc in hexane gave the carboxylic acid (**6**); 1.36 g (70%); mp 120–122°C; IR 3300-2500, 1740, 1720 cm^{-1}; ^1H NMR ($CDCl_3$) δ 1.30 (9/2H, s), 1.40 (9/2H, s), 4.2–4.6 (2H, m), 5.00 (2H, br s), 7.15 (5H, s), 8.00 (1H, br s). MS *m/z* 349 (M^+).

(2S, 5S)-Pyrrolidine-2,5-dicarboxylic acid (**7**)

To the acid (**6**, 1.0 g, 3 mmol) in anisole (0.5 ml) was added TFA (2 ml) at 0°C. After 2 h of stirring the mixture was diluted with water and extracted with EtOAc. EtOAc layer was washed with ice-water, and brine. Evaporation of EtOAc left the residue which was chromatographed on silica gel. Elution with 50% EtOAc in CH_2Cl_2 gave *(2S,5S)-N-benzyloxycarbonylpyrrolidine-2,5-dicarboxylic acid* which was crystallized from EtOAc: 780 mg (96%); mp 167–168°C; IR 3300-2500, 1720, 1420 cm^{-1}; ^1H NMR ($CDCl_3$) δ 2.0–2.5 (4H, m), 4.3–4.6 (2H, m), 5.00 (2H, s), 7.15 (5H, s), 7.75 (2H, br s). MS *m/z* 277 (M^+). 360 mg of the dicarboxylic acid (1.3 mmol) in MeOH (10 ml) was hydrogenated with 5% Pd-C as a catalyst. The mixture was filtered through Celite pad and evaporated. The residue was crystallized from EtOH to give the amino acid (**1**): 177 mg (86%); mp >300°C; $[\alpha]_D^{20}$ −107°C (c 1.0, H_2O); IR 1680, 1560 cm^{-1}. Anal. Calcd for $C_6H_9NO_4$: C, 45.28; H, 5.70, N, 8.80. Found: C, 44.99, H, 5.30: N, 8.57.

Benzyl (−)-(S)-2-benzyloxycarbamido-6-t-butoxycarbonyl-5-oxohexanoate (**8**)

t-Butyl acetate (0.54 ml, 4.00 mmol) in THF (4 ml) was added to lithium diisopropylamide in THF (48 ml) prepared from diisopropylamine (0.68 ml, 4.80 mmol) and 15% n-butyl lithium in hexane (3.07 ml, 4.80 mmol) at −78°C. After stirring the mixture for 30 min, benzyl N-Cbz-pyroglutamate (**1**, 1.41 g, 4.00 mmol) in THF (15 ml) was added to it... The reaction mixture was stirred for 30 min at −78°C, and then quenched with AcOH-MeOH (1:1, 2 ml). Silica gel chromatography (20% EtOAc in hexane) of the crude product afforded the ketoester (**8**): 1.65 g, 95%; $[\alpha]_D^{20}$ −4.58° (c 1.27, $CHCl_3$); IR 3400, 1735, 1715, 1700 cm^{-1}; ^1H NMR ($CDCl_3$) δ 1.42 (9H,s), 3.25 (2H, s), 4.08–4.54 (1H, m) 5.03 (2H, s), 5.08 (2H, S), 5.40 (1H, d, J=8.0 Hz), 7.31 (10H, m). Anal. Calcd for $C_{26}H_{31}NO_7$: C, 66.51; H, 6.66, N, 2.98 Found: C,66.66; H, 6.81; N, 3.05.

(2S, 5R)-5-t-Butoxycarbonylmethyl-2-pyrrolidinecarboxylate (**10**)

The ketoester (**8**, 4.17 g, 8.88 mmol) in MeOH (206 ml) was shaken with 5% Pd-C (416 mg) for 12 h under H_2 at 4.0 kg/cm^2. The reaction mixture was filtered through Celite pad and the filtrate was evaporated in vacuo. The residue was chromatographed on silica gel and elution with CH_3CN-MeOH (7:3) gave the amino acid (**10**): 1.97 g (97%); mp 188–189 °C (decomp); $[\alpha]_D^{20}$ −66.93° (c 0.89, MeOH); IR 3400, 1720, 1615 cm^{-1}; ^1H NMR (D_2O) δ 1.28 (9H, s), 2.64 (2H, d, J=8.0 Hz), 3.6–3.8 (1H, m), 3.96 (1H, dd, J=6.0, 8.0 Hz). MS *m/z* 230 [$(M+1)^+$]. Anal. Calcd for $C_{11}H_{19}NO_4$: C, 57.62; H, 8.35; N, 6.11. Found: C, 57.74; H, 8.34; N, 5.89.

Benzyl (2S, 4R)-N-t-butoxycarbonyl-4-hydroxypyroglutamate (**19a**)

Butyl lithium (6.5 ml, 10 mmol) was added dropwise to HMDS (2.1 ml, 10 mmol)

in dry THF (20 ml) at 0°C and the mixture was stirred for 30 min. The $LiN(TMS)_2$ solution was transferred to the THF (30 ml) solution containing the pyroglutamate (**1**, 3.2 g, 10 mmol), at −78°C using 'kanule' (1 mm od × 300 mm). After 15 min of stirring, the oxaziridine (2.7 g, 10 mmol) in THF (20 ml) was added dropwise and the reaction mixture was stirred at −78°C for 30 min. Addition of (+)-camphorsulfonic acid (10 g) in THF (20 ml) to the mixture was followed by dilution with Et_2O. The mixture was washed with 5% $NaHCO_3$ aq., water and sat. brine, dried and evaporated. Silica gel chromatography (30% EtOAc in hexane elution) of the residue gave the alcohol (**19a**) : 2.0 g (60%); mp 108–109°C; IR 3450, 1790, 1740, 1720, 1620, cm^{-1}; ^1H NMR ($CDCl_3$) δ 1.40 (9H, s), 4.41 (1H, dd, J=8, 10 Hz), 4.61 (1H, dd, J=2, 9 Hz), 5.19 (2H, s), 7.30 (5H, 5). MS *m/z* 335 (M^+).

Benzyl (2S, 4S)-N-t-butoxycarbonyl-4-benzoxypyroglutamate (**20d**)

The alcohol (**19a**, 670 mg, 2 mmol) in THF (5 ml) was treated with triphenylphophine (730 mg, 3 mmol) in THF (10 ml), diethyl azodicarboxylate (0.37 ml, 2.2 mmol) and benzoic acid (305 mg, 2.5 mmol) in THF 5 ml, at −20°C for 1 h and then the reaction mixture was stirred at room temperature for 15 h. Evaporation of the solvent was followed by dilution with Et_2O and filtration of precipitates. The filtrate, after evaporation of Et_2O, was chromatographed on silica gel. Et_2O-hexane (1:4) elution gave the benzoate (**20d**): 670 mg (76%); mp 104–105°C; IR 1785, 1740, 1715 cm^{-1}; ^1H NMR ($CDCl_3$) δ 1.40 (9H, s), 4.55 (1H, dd, J=10, 13 Hz), 5.10 (2H, s), 5.45 (1H, dd, J=10, 13 Hz), 7.15 (5H, s), 7.1–8.0 (5H, s). MS *m/z* 439 (M^+)

Benzyl (2S, 4S)-N-t-butoxycarbonyl-4-benzoxy-5-oxo-6-heptenoate (**21**)

Following the procedure for **2**, the pyroglutamate (**20d**, 400 mg, 0.9 mmol) in THF (10 ml) was treated with 1M vinylmagnesium bromide in THF (1.2 ml) to give the enone (**21**): 340 mg (80%); IR 3350, 1795, 1720, 1690 cm^{-1}; ^1H NMR ($CDCl_3$) δ 1.37 (9H, s), 4.20(1H, dd, J=7, 13 Hz), 5.10 (2H, s), 5.1 (1H, m), 5.80 (1H, dd, J=4, 8 Hz), 6.4–6.5 (2H, m), 7.30 (5H, s), 7.2–8.1 (5H, m). MS *m/z* 467 (M^+).

Benzyl (2S, 4S, 5R)-N-t-butoxycarbonyl-4-benzoxy-5-vinylprolinate (**22**)

The enone (**21**, 625 mg, 1.25 mmol) was reduced with $NaBH_4$ (62 mg, 1.75 mmol) and $CeCl_3$ (650 mg, 1.75 mmol). To the allylalcohol (550 mg, 1.2 mmol) obtained and Et_3N (0.36 ml, 3 mmol) in CH_2Cl_2 (10 ml) was added MsCl (0.12 ml, 1.5 mmol) and the mixture was stirred for 1 h at 0°C. It was quenched with water, diluted with Et_2O, washed with water and brine, dried and evaporated. The residue was chromatographed on silica gel and eluted with 20% Et_2O in hexane to give the vinylprolinate (**22**): 338 mg (64%); mp 74–75°C; IR 1750, 1710 cm^{-1}; ^1H NMR ($CDCl_3$) δ 1.37 (9/2H, s), 1.43 (9/2H. s), 4.5–4.8 (2H, m), 4.9–5.4 (5H, m), 5.6–6.1 (1H, m), 7.22 (5H, m), 7.1–8.0 (5H, m). MS *m/z* 467 (M^+).

Benzyl (2S, 4S, 5R)-N-t-butoxycarbonyl-4-benzoxy-5-hydroxymethylprolinate (**23**)

The vinylprolinate (**22**, 500 mg, 1.1 mmol) in MeOH (20 ml) was ozonized at −78°C. The mixture was treated with $NaBH_4$ (160 mg, 4 mmol) at −78°C – room temperature. It was diluted with Et_2O, washed with 10% citric acid and brine, dried and evaporated. Silica gel chromatography of the residue and 30% EtOAc in hexane elution gave the alcohol (**23**): 470 mg (93%); IR 3700-310, 1750, 1700 cm^{-1}; ^1H NMR ($CDCl_3$) δ 1.35 (9H, s), 4.5 (1H, m), 5.10 (2H,s), 5.3 (1H, m), 7.23 (5H, s), 7.2–8.0 (5H, m). MS *m/z* 451 (M^+).

(−)-Bulgecinine (**24**)

The alcohol (**23**, 220 mg, 0.5 mmol) in MeOH (10 ml) was hydrolyzed with 1N NaOH (1.1 ml, 1.1 mmol). The hydrolyzate was chromatographed on silica gel (EtOAc elution) to obtain the acid (110 mg, 87%): IR 3500-3400, 1725, 1675, 1170 cm^{-1}. MS *m/z* 261 (M^+). 120 mg of the acid (0.64 mmol) in anisole (0.1 ml) was treated with trifluoroacetic acid (0.2 ml) at 0°C for 1 h. The mixture was diluted with water and adsorbed in Dowex 50 W resin. Elution with 1N pyridine gave (−)-bulgecinine (**24**) which was crystallized from MeOH to yield colorless prisms: 40 mg (54%); mp 195–196°C; $[\alpha]_D^{29}$ −14.1° (c 0.80, H_2O); IR 3400, 1630, 1410, 1080, 1040 cm^{-1}; ^1H NMR (D_2O) δ 2.15 (1H, ddd, J=6, 7, 15 Hz), 2.67 (1H, ddd, J=7, 9, 15 Hz), 3.78 (2H, d, J=5 Hz), 3.81 (1H, m), 4.21 (1H, dd, J=7, 9 Hz), 4.38 (1H, m). Anal. Calcd for $C_6H_{11}NO_4$: C, 44.72; H, 6.88; N, 8.69. Found: C, 39.89, H, 6.31; N, 7.48.

(2R, 5RS)-1,2-Dibenzyloxycarbonyl-5-hydroxypyroglutamate (**25**)

To benzyl N-benzyloxycarbonylpyroglutamate (**1**, 3.58 g, 10.1 mmol) in CH_2Cl_2-MeOH (1:1, 50 ml) was added $NaBH_4$ (1.92 g, 50.8 mmol) at 0°C and the mixture was stirred for 30 min. The reaction mixture was poured into the stirred mixture of CH_2Cl_2-sat. $NaHCO_3$ aq. (1:1, 200 ml) and the whole was stirred for 10 min. Water layer was extracted with CH_2Cl_2 and the combined organic phase was washed with sat.brine, dried and evaporated. The residue was cromatographed on silica gel and elution with hexane-EtOAc (3:1) gave the aminal (**25**) as an oil: 3.40 g (94%): IR 3450, 1755, 1712 cm^{-1}; ^1H NMR ($CDCl_3$) δ 4.56 (1H, m), 5.04 (2H, brs), 5.20 (2H, brs), 5.63 (1H, brs), 7.30 (5H, s), 7.37 (5H, s). MS calcd for $C_{20}H_{21}NO_5$: *m/z* 355.1420. Found: 355.1402. Elution with hexane-EtOAc (1:1) gave benzyl (*S*)-2-benzyloxycarbamido-5-hydroxypentanoate (**26**): 124 mg (3.4%); mp 51–53°C; $[\alpha]_D^{26}$–2.97° (c 1.41, $CHCl_3$) ; IR 3720, 3420, 1740, 1720 cm^{-1}; ^1H NMR ($CDCl_3$) δ 3.53 (2H, t, J=6 Hz), 4.17–4.57 (1H, m), 5.03 (2H, s), 5.10 (2H, s), 5.23–5.50 (1H, m), 7.23 (10H, s). Anal. Calcd for $C_{20}H_{23}NO_5$: C, 67.21; H, 6.49; N, 3.92. Found: C, 67.16; H, 6.56; N, 3.88.

Dimethyl (2S, 5E)-2-benzyloxycarbamido-5-heptene-1,7-dicarboxylate (**27**)

The mixture of the aminal (**25**, R^1=Bzl, R^2=Me, 291 mg, 1.04 mmol) and methyl (triphenylphosphoranylidene) acetate (522 mg, 1.56 mmol) in benzene (10 ml) was stirred under reflux for 5 h. The reaction mixture was evaporated and the residue was chromatographed on silica gel. Elution with hexane-EtOAc (3:1) gave the ester (**27**): 320 mg (91.6%); $[\alpha]_D^{27}$ +18.46° (c 2.35, $CHCl_3$); IR 3350, 1745, 1725, 1660 cm^{-1}; ^1H NMR ($CDCl_3$) δ 3.60 (6H, s), 4.35 (1H, m), 5.10 (2H, s), 5.43 (1H, brd, J=8 Hz), 5.80 (1H, dd, J=1, 16 Hz), 6.90 (1H, dt, J=6, 16 Hz), 7.30 (5H, s). MS calcd for $C_{17}N_{21}HO_6$: *m/z* 335.1368. Found: 335.1370.

(−)-Proline (**28a**)

The aminal (**25**, R^1=R^2=Bzl, 342 mg, 0.96 mmol) and 10% Pd-C (35 mg) in MeOH (10 ml) was shaken under H_2 for 90 min. The mixture was filtered through Celite pad and evaporated to give crude proline (109 mg). Crystallization from abs. EtOH-Et_2O gave needles (**28a**): 70.5 mg (64%); mp 220–222°C; $[\alpha]_D^{24}$ −83° (c 1.0, H_2O). IR and ^1H NMR were identical to those of authentic (−)-proline.

References

1. Inaoka Y, Naruto S (1988) J. Biochem. 104: 706–711.
2. Laduree D, Lancelot JC, Robba M, Chenu E and Mathe G (1989) J. Med. Chem. 32: 456–461.
3. Hardy GW, Bull D, Jones HT, Mills G and Allan G (1988) Tetrahedron Lett. 29: 799–802.
4. Hunt AH, Mynderse JS, Samlaska SK, Fukuda DS, Maciak GM, Kirst HA, Occolowitz JL, Swartzendruber JK and Jones ND (1988) J. Antibiot. 41: 771–779.
5. Smith EM, Swiss GF, Neustadt BR, Gold EH, Sommer JA, Brown AD, Chiu PJS, Moran R, Sybertz EJ and Baum T (1988) J. Med. Chem. 31: 875–885.
6. Krapcho J, Turk C, Cushman DW, Powell JR, DeForrest JM, Spitzmiller ER, Karanewsky DS, Duggan M, Rovnyak G, Schwartz J, Natarajan S, Godfrey JD, Ryono DE, Neubeck R, Atwal KS and Petrillo Jr. EW (1988) J. Med. Chem. 31: 1148–1160.
7. Tsuru D, Yoshimoto T, Koriyama N and Furukawa S (1988) J. Biochem. 104: 580–586.
8. Ohta T, Hosoi A, Kimura T and Nozoe S (1987) Chemistry Lett. 2091–2094.
9. Ohta T, Kimura T, Sato N and Nozoe S (1988) Tetrahedron Lett. 29: 4303–4304.
10. Impellizzeri G, Mangiafico S, Oriente G, Piattelli M, Sciuto S, Fattorusso E, Magno S, Santacroce C and Sica D (1975) Phytochemistry 14: 1549–1557.
11. Ohta T, Sato N, Kimura T, Nozoe S and Izawa K (1988) Tetrahedron Lett. 29: 4305–4308.
12. Bycroft BW, Maslen C, Box SJ, Brown AG and Tyler JW (1987) J. Chem. Soc. Chem. Commun. 1623–1625.
13. Evans DA, Morrisseey MM and Dorow RL (1985) J. Am. Chem. Soc. 107: 4346–4388.
14. Ohta T, Hosoi A and Nozoe S (1988) Tetrahedron Lett. 29: 329–332.
15. Shinagawa S, Kasahara F, Wada Y, Harada S and Asai M (1984) Tetrahedron 40: 3465–3470.

Toxic and non-toxic nonprotein amino acids in the Vicieae

Fernand Lambein,[a] Yu-Haey Kuo,[a] Fumio Ikegami[b] and Isamu Murakoshi[b]

[a]*Lab. of Physiological Chemistry, State University of Gent, K.L. Ledeganckstraat 35, B-9000 Gent, Belgium*

[b]*Faculty of Pharmaceutical Sciences, Chiba University, Yayoi-cho 1-33, Chiba 260, Japan*

Abstract

Over 665 nonprotein amino acids have been recognized as secondary metabolites. Forty-two of these natural products were found in members of the *Vicieae*. The highest concentrations of such compounds, and often the greatest variety, may be found in young seedlings of the genera: *Lathyrus, Vicia, Lens* and *Pisum*.

Relatively high concentrations of isoxazolinone amino acids are found characteristically in all species and varieties of *Pisum* and *Lens*, and in most species of *Lathyrus* and in part of the *Vicia* species. Outside the tribe *Vicieae*, isoxazolinone derivatives are not found in the plant kingdom.

Of the fifty species of *Lathyrus* seedlings examined, forty contain isoxazolinone amino acids. The analysis of these seedlings mostly reveal unique compositions of nonprotein amino acids and derivatives, including up to nine isoxazolinone derivatives, homoarginine, lathyrine, homoserine, *O*-acetyl-homoserine, *O*-oxalyl-homoserine, the osteolathyrogen: 3-aminopropionitrile and its 4-glutamyl derivative as well as the neurotoxins 2,4-diaminobutyric acid and 3-*N*-oxalyl-2,3-diaminopropionic acid.

Introduction

A recent comprehensive list of naturally occurring amino acids contains over seven hundred compounds. [1] Some 665 of these are secondary metabolites. The tribe *Vicieae* consists of the genera: *Vicia, Pisum, Lathyrus, Lens* and *Vavilovia*. The monotypic genus *Vavilovia* has not yet been examined for its amino acids and was also not available to us. Some 42 nonprotein amino acids have been isolated from plant species belonging to the *Vicieae*. Some of these metabolites have been found in only one species; e.g., 2-hydroxymethylserine in *Vicia pseudo-orobus* [2] the chlorinated tryptophanes in pea seeds [3] and 4-hydroxynorvaline [4] and 2-(4-glutamylaminoethyl)-isoxazolin-5-one [5] in *Lathyrus odoratus*. The distribution of other nonprotein amino acids in the seeds of *Lathyrus* species or *Vicia* species was used by Bell to make a chemotaxonomic classification of these genera. [6,7]

Some members of the genera *Vicia* and *Lathyrus* are toxic to mammals and fowls since they cause skeletal deformations or neurological symptoms. The compounds responsible for this toxicity are known to be nonprotein amino acids that are present in high concentrations in the seeds. [8] The seeds of the genera *Pisum, Lens* and *Lathyrus* [9,10] have been used for human consumption since

earliest history without adverse effects. The seeds of *Lathyrus sativus* are used presently for food in large areas in Asia and Africa and are responsible for human lathyrism. While most work on those toxic species is limited to the study of the seeds, it was recognized by Ressler that the young seedlings are the most toxic stage of certain *Lathyrus* species [8]. Seedlings of *Vicieae*, in particular toxic species, not only accumulate higher concentrations of nonprotein amino acids – some of which are toxic – they also often produce compounds that are absent from the dry seeds. The occurrence and biosynthesis of the toxic amino acids and some nonprotein amino acids occurring mainly in seedlings are discussed below.

Toxic amino acids

3-Cyanoalanine (BCA) and its 4-glutamyl peptide accumulate in seeds and seedlings of *Vicia sativa*. In experimental animals, these compounds can cause strychnine-like convulsions lasting up to 24 hr [8]. BCA is found in 16 of 48 species of *Vicia* [7] and also in some *chromobacteria*. Recently it was found that many if not all plants can detoxify HCN with the formation of BCA; the HCN arising from ethylene biosynthesis can be linked to cysteine by a BCA-synthase or to *O*-acetylserine by an isoenzyme of cysteine synthase. Both enzymes produce BCA [11].

3-Aminopropionitrile (BAPN) and its 4-glutamyl peptide are the osteolathyrogens of *L. odoratus*. BAPN inhibits the formation of crosslinks in collagen and elastin, resulting in a number of skeletal deformations and even aortic rupture [8]. 4-Glu-BAPN is present in the seeds of 3 out of 49 species of *Lathyrus* [6]. We found BAPN or 4-glu-BAPN in the seedlings of 22 out of 56 species of *Lathyrus* [12].

2,4-Diaminobutyric acid (DABA) is the neurotoxic amino acid occurring in *Lathyrus sylvestris*. It is present in the seeds of 13 out of 49 species of *Lathyrus* [6] and in the seedlings of 14 out of 56 species. Although the toxicity of DABA is not high (LD_{50} 69 mg/100 g body weight) the concentration in seeds of *L. sylvestris* is such that a single meal of the seeds can be lethal to rats [8]. DABA is metabolically derived from homoserine [13].

3-*N*-oxalyl-2,3-diaminopropionic acid (ODAP) is the major toxin of *L. sativus* and the cause of human lathyrism [14]. It is present in all *Lathyrus* species linked to lathyrism [15]. *L. sativus* is the agronomically most important species of the genus. Partly because of its drought tolerance, it is cultivated on several million hectare in Asia and Africa. Selection of low toxin varieties is being pursued on a large scale in several institutes in different parts of the world [16]. Together with other nonprotein amino acids, ODAP was found to be present in the chloroplasts, the potential site of biosynthesis [17].

Isoxazolin-5-one derivatives

Two natural compounds present in seedlings of *Lathyrus* species and containing the heterocyclic isoxazolinone ring are toxic to animals: 2-(3-amino-3-carboxy-

propyl)-isoxazolin-5-one (compound **VI**, Scheme 1) can be hydrolysed or photolysed with the formation of DABA [12]. When given to day-old chicks *per os* or *i.p.* neurolathyrism symptoms develop, similar to the effect of DABA. Free DABA [19] was found in the blood and in the excrement of the experimental animals. Compound **VI** can thus be metabolised into a neurotoxic amino acid. Compound **VI** is not present in dry seeds in a detectable amount, but it can influence the toxicity of the seedlings and foliage of a number of *Lathyrus* species, including *L. sativus*.

2-Cyanoethyl-isoxazolin-5-one (**VIII**) can be hydrolysed or photolysed with the formation of BAPN, the osteotoxin from *L. odoratus* [18]. Compound **VIII** is present in all species containing BAPN or 4-glu-BAPN (*L. venosus* is the only exception known). A possible involvement of **VIII** in the biosynthesis of BAPN was postulated [12].

The higher toxicity of *Lathyrus* seedlings in comparison to the seeds is illustrated by the presence of these two isoxazolinone compounds in the seedlings of 17 of 56 species examined, while they are virtually absent from the dry seeds. In addition, 4-glu-BAPN is present in the seedlings of 28 species of 56. *L. odoratus* has been described as only osteolathyritic. However, when feeding freeze-dried seedlings to day-old chicks they develop the symptoms of both neurolathyrism and osteolathyrism, obviously due to the presence of **VI** in a concentration of 3% of the dry weight of the seedlings. Also *L. sativus* that is described as only neurotoxic, contains **VIII** in the seedling stage. The presence of small concentrations of **VIII** in the dry seeds of *L. sativus* may be responsible for the minor skeletal lesions observed in older lathyrism patients [20].

Nontoxic amino acids

No toxic properties towards higher animals have been found for the compounds described below, however some less stable compounds may not have been examined adequately.

The presence of homoserine as a free amino acid in the seedlings and foliage seems to be a common property among the *Vicieae*. This compound has been studied by Virtanen in pea seedlings, where it can reach 10% of the dry matter [21]. The *O*-acetyl derivative of homoserine is very abundant in the pericarp of *Pisum sativum*. In the pericarp of *L. sativus*, *O*-oxalylhomoserine is the dominant amino acid, while *O*-acetylhomoserine is a major amino acid in the young seedlings and stems of the mature plants.

The heterocyclic amino acid lathyrine as well as homoarginine occur together in the seedlings of only 10% of the species of the genus *Lathyrus* that have been examined, although they are metabolically linked [22]. Some 60% of the *Lathyrus* species contain detectable concentrations of either lathyrine or homoarginine [12]. While these two amino acids seem to be specific for the genus *Lathyrus*, we also found homoarginine in seedlings of *Pisum abyssinicum* and lathyrine in seedlings of *Lens nigricans*.

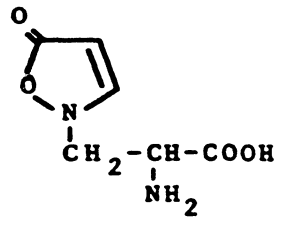

I

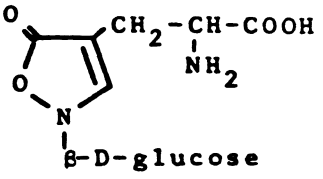

III

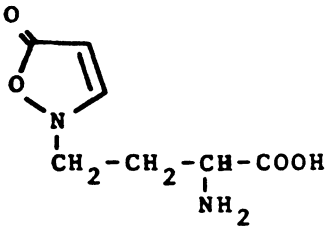

VI

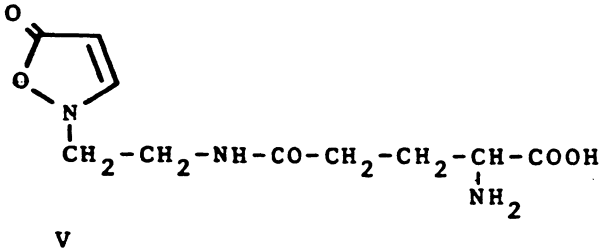

V

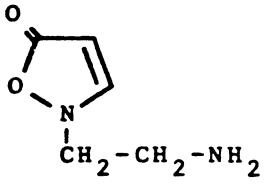

VII

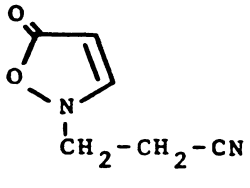

VIII

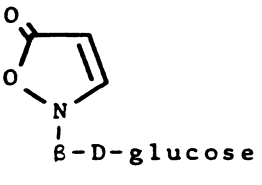

IX

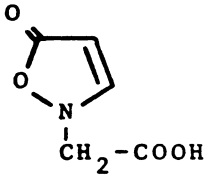

X

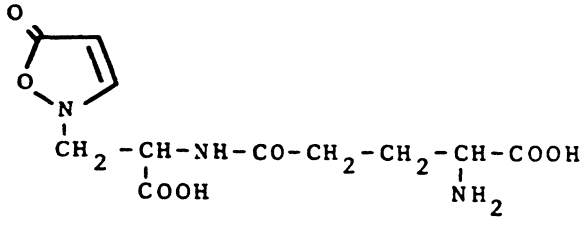

XI

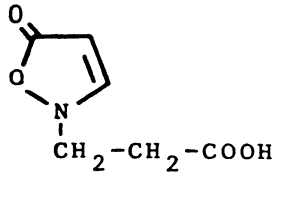

XII

Scheme 1. Structures of isoxazolin-5-one derivatives naturally occurring in species of the *Vicieae*.

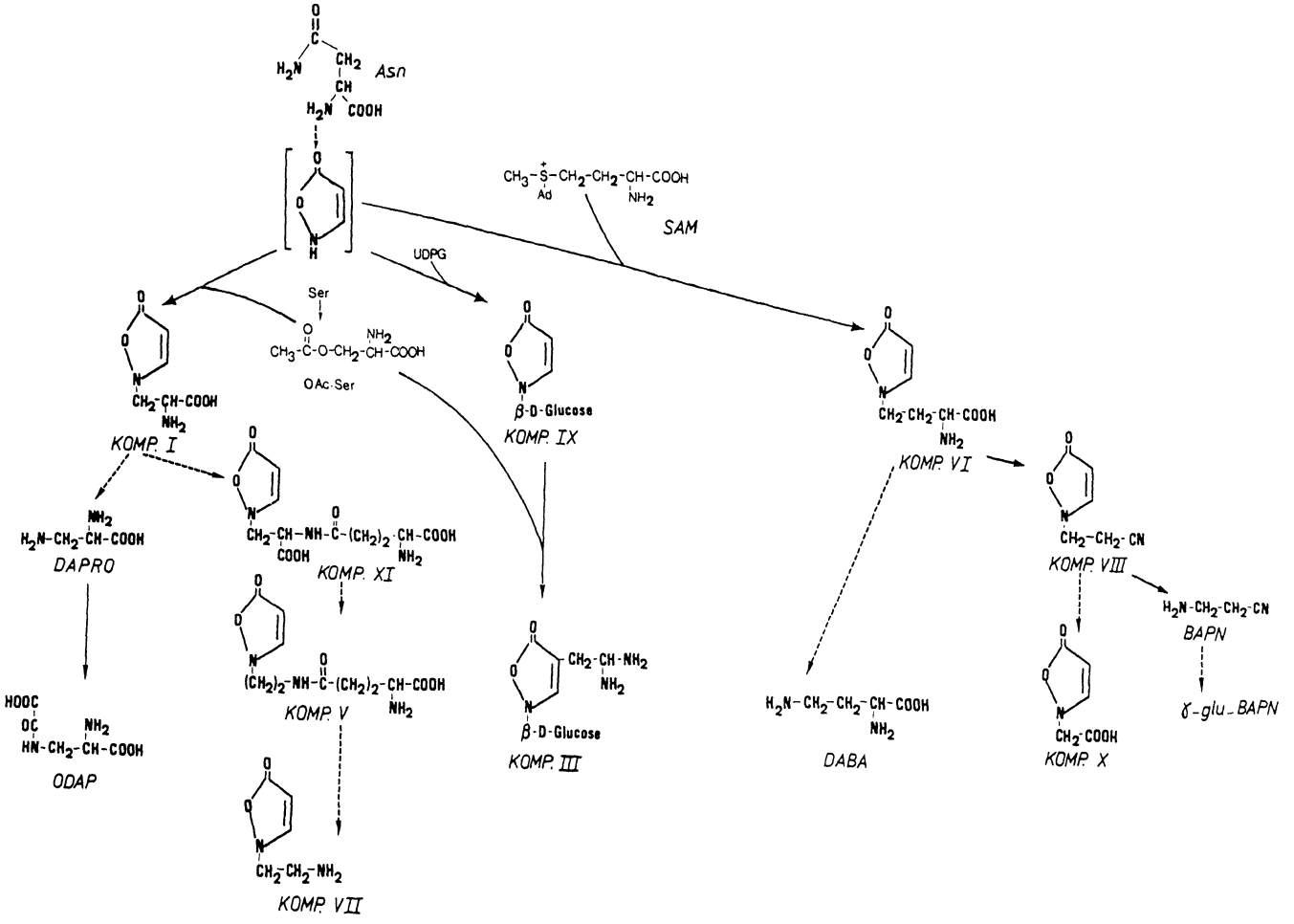

Scheme 2. Pathways for the biosynthesis of isoxazolin-5-one derivatives and the *Lathyrus* toxins. Dashed lines represent steps that remain to be confirmed.

The uracyl-alanines: willardiine and isowillardiine occur together in seedlings of all accessions of the genus *Pisum* examined. The biosynthesis of these compounds from free uracil and *O*-acetylserine has been examined independently by Brown [23] and Murakoshi [24]. The argument of whether two different enzymes are involved in the biosynthesis of the two isomers is not yet resolved. While willardiine occurs in some *Acacia* species and isowillardiine in some *Crotalaria* species [25], the occurrence of both isomers seems to be consistent within seedlings of the genus *Pisum*. Only one species of *Lathyrus*, i.e. *L. luteus* contains isowillardiine in the seedling stage.

Isoxazolin-5-one derivatives

In Scheme 1 the structures of a number of natural compounds containing the five membered isoxazolin-5-one ring are shown. This ring is very sensitive to alkali and UV-irradiation. *L. odoratus* is the species that is the richest in this class of natural products. In young seedlings up to 10% of the dry weight consists of nine different known isoxazolin-5-one derivatives, and several unknown compounds, whose UV-spectrum and UV-sensitivity point to the isoxazolinone-ring. Only the dipeptide **XI** is absent from *L. odoratus*. 3-(Isoxazolin-5-on-2-yl)-alanine (**I**) makes up 2% of the dry weight of pea seedlings and it is present in all seedlings of the genera *Pisum* and *Lens*, as well as in 80% of the *Lathyrus* species examined, and in about 50% of the *Vicia* species. Its biosynthesis involves the alanylation of the free ring with *O*-acetylserine as donor of the side chain [26].

The neurotoxin **VI** is the higher homologue of **I**. **VI** only occurs in the genus *Lathyrus*, in the seedlings of 20% of the species examined. The biosynthesis has not yet succeeded *in vitro*. *In vivo* experiments with [^{14}C]labelled precursors demonstrate that the amino acid moiety of S-adenosylmethionine (SAM) is incorporated at an acceptable rate (4% of the label). With [^{14}C]methionine as precursor, the rate of incorporation in **VI** was much less [27]. When SAM, labelled at the C-2 of the methionine moiety instead of the carboxyl group, is given to *L. odoratus*, the isoxazolinone **VIII** and 4-glu-BAPN are also labelled. This indicates that the osteolathyrotoxin BAPN is metabolically linked to the isoxazolinones **VI** and **VIII**.

In *L. sylvestris*, neither **VI** nor **VIII** are present, but when [^{14}C]-SAM is fed to the seedlings, labelled DABA is found [28]. We cannot yet prove whether **VI** may be a short lived precursor in the biosynthesis of this neurotoxin. This is in agreement with Nigam and Ressler [13], who found that homoserine is incorporated in DABA, because homoserine is also a precursor for methionine and for SAM.

The glucosylated amino acid 3-(2-glucosyl-isoxazolin-5-on-4-yl)-alanine (**III**) is present in the seedlings of all members of the genera *Pisum* and *Lens*, and in over 40% of the species of the genus *Lathyrus*, mostly together with its precursor 2-glucosyl-isoxazolin-5-one (**IX**). When **III** is hydrolysed or photolysed, glutamic acid is formed. Compound **III** can thus represent a metabolic link between serine and glutamic acid.

Influence of osmotic stress on the amino acids of L. sativus

A major reason for the persistence of *L. sativus* as a popular crop in large areas of Asia and Africa is its tolerance to drought. Since many plants react to osmotic stress by increasing the concentration of proline or other amino acids and the toxin responsible for human lathyrism is an amino acid, it is important to assess the eventual role of ODAP in this drought tolerance. While in the dry seeds the toxin ODAP is by far the most important compound in the amino acid profile, during the germination homoserine and its *O*-acetyl and *O*-oxalyl derivatives become more prominent.

When seedlings of *L. sativus* were grown in a medium with increasing osmotic potential (NaCl, mannitol or PEG 20 000) the concentration of many amino acids increases about two-fold [29].

When NaCl or mannitol is used as the osmoticum, homoserine and its derivatives seem to act as the major osmotic compounds: these compounds making up 70% or more of the free amino acid pool [30]. When PEG is used as the osmoticum, there is also a marked increase in proline and ODAP concentration. This increase in ODAP concentration under osmotic stress may also indicate an increased toxicity of *L. sativus* in periods of drought.

Conclusions

Besides the interesting chemical and biochemical aspects of the nonprotein amino acids present in this agronomically very important group of plants, these natural products are also of very high importance from ecological viewpoints and even for the food supply of a sizable section of the world population.

In the genus *Lathyrus* the variation in the nonprotein amino acids may form the barrier for crosspollination between species by inhibiting the growth of pollen tubes [31]. The exudation of nonprotein amino acids through the roots can influence the microbial life in the rhizosphere and the germination of seeds [32–34]. The presence of nonprotein amino acids in the sieve-tubes of the foliage may have a selective effect on sucking insects [35]. In these areas the information available is very limited. The major obstacle for this kind of research may be that most of these natural compounds are not commercially available.

The fact that many thousands of people have been paralysed for life, after consumption of the seeds of *L. sativus* containing a toxic nonprotein amino acid, should induce biologists to develop ways to make this plant non-toxic without losing its attractive agronomic traits. Perhaps genetic engineering can bring the answer to this problem when sufficient biochemical information is available.

Acknowledgements

This work is supported by the Belgian 'Fonds voor Kollektief Fundamenteel Onderzoek' under contract 2.0025.87. We also thank Prof. W. Fiers for the use of a scintillation counter and the Botanical Garden of the State University of Gent for facilities and for seeds.

References

1. Hunt S (1985) In: Barett GC (ed.) Chemistry and Biochemistry of the Amino Acids. Chapman and Hall, London, pp. 55–138.
2. Saito K, Furukawa J, Okuda S and Hatanaka SJ (1985) Phytochemistry 24: 853–854.
3. Bell EA (1973) In: Hey DH and John DI (eds.) MTP International Review of Science, Organic Chemistry, Series I. Butterworths, London, Vol. 6, p. 1.
4. Fowden L (1966) Nature 209: 807.
5. Lambein F and Van Parijs R (1974) Biochem. Biophys. Res. Comm. 61: 155–162.
6. Bell EA (1962) Biochem. J. 83: 225–229.
7. Bell EA and Tirimanna ASL (1965) Biochem. J. 97: 104–111.
8. Ressler C (1975) In: Runeckles VC (ed.) Recent advances in phytochemistry. Plenum Press, New York, Vol. 9, pp. 155–166.
9. Marinval P (1986) In: Kaul AK and Combes D (eds.) Lathyrus and Lathyrism. Third World Medical Research Foundation, New York, pp. 39–45.
10. Kislev ME (1986) In: Kaul AK and Combes D (eds.) Lathyrus and Lathyrism. Third World Medical Research Foundation, New York, pp. 46–51.
11. Ikegami F, Takayama K and Murakoshi I (1988) Phytochemistry 27: 3385–3389.
12. Lambein F, De Bruyn A, Ikegami F and Kuo YH (1986) In: Kaul AK and Combes D (eds.) Lathyrus and Lathyrism. Third World Medical Research Foundation, New York, pp. 246–256.
13. Nigam SN and Ressler C (1966) Biochemistry 5: 3426–3431.
14. Spencer PS, Roy DN, Ludolph A, Hugon J, Dwivedi MP and Schaumburg HH (1986) The Lancet 8515: 1066.
15. Bell EA (1971) In: Harborne JB, Boulter JB and Turner BL (eds.) Chemotaxonomy of the leguminosae. Academic Press, London, pp. 179–206.
16. Spencer PS, Roy DN, Palmer VS and Dwivedi MP (1986) In: Kaul AK and Combes D (eds.) Lathyrus and Lathyrism. Third World Medical Research Foundation, New York, pp. 297–305.
17. Kuo YH, Kobori M, Ongena G and Lambein F (1989) Arch. Int. Physiol. Biochim. 97: 12
18. Lambein F, Kuo YH and Van Parijs R (1976) Heterocycles 4: 567–593.
19. Lambein F and De Vos B (1981) Arch. Int. Physiol. Biochim. 89(2): 66–67.
20. Cohn DF (1986) In: Kaul AK and Combes D (eds.) Lathyrus and Lathyrism. Third World Medical Research Foundation, New York, pp. 315–317.
21. Virtanen AI, Berg AM and Kari S (1953) Acta. Chem. Scand. 7: 1423–1424.
22. Brown EG and Al-Baldawi F (1977) Biochem. J. 164: 589-594.
23. Ahmad MAS, Maskall CS and Brown EG (1984) Phytochemistry 23: 265.
24. Ikegami F, Kaneko M, Lambein F, Kuo YH and Murakoshi I (1987) Phytochemistry 26: 2699–2704.
25. Pilbeam DJ and Bell EA (1979) Pytochemistry 18: 973–985.
26. Murakoshi I, Kato F, Haginiwa J and Fowden L (1973) Chem. Pharm. Bull. 21(4): 918–920.
27. Callebaut A, Lambein F and Van Parijs R (1977) Arch. Int. Physiol. Biochim. 85: 157–158.
28. Lambein F, Kuo YH and Ikegami F (1982) Abstr. 12th Internat. Congr. of Biochem. Perth. W. Australia Abstr. Pos. 005–215, p. 400.
29. Ongena G, Kuo YH and Lambein F (1989) Arch. Int. Physiol. Biochim. 97: 39.
30. Ongena G (1989) Thesis. State University of Ghent, Belgium.
31. Simola LK (1986) In: Kaul AK and Combes D (eds.) Lathyrus and Lathyrism. Third World Medical Research Foundation, New York, pp. 225–239.
32. Kuo YH, Lambein F, Ikegami F and Van Parijs R (1982) Plant Physiol. 70: 1283–1289.
33. Schenk S (Personal communication).
34. Wilson MF and Bell EA (1979) Phytochemistry 18: 1883–1884.
35. Srivastava PN, Lambein F and Auclair JL (1988) Entomol. Exp. Appl. 48: 109–115.

3-Amino-2*H*-azirines, equivalents of α,α-disubstituted α-amino acids in the synthesis of heterocycles and peptides

Heinz Heimgartner

Organisch-chemisches Institut der Universität Zürich, Winterthurerstrasse 190, CH-8057 Zürich, Switzerland

Abstract

The easily available 2,2-disubstituted 3-amino-2*H*-azirines **1** react with a variety of acidic compounds, e.g. NH-acidic heterocycles, to give novel heterocycles containing α,α-disubstituted α-amino acids. These reactions proceed *via* formation of an intermediate aziridine, which is rearranged to a bicyclic zwitterion. This zwitterion is the key intermediate in all reactions proceeding *via* cleavage of the C=N bond of **1**. The reaction of **1** with carboxylic acids leads to the formation of diamides, e.g. acyl-amino isobutyramides. The general character of this reaction has been demonstrated in particular with amino acids and oligopeptides. Together with the selective hydrolysis of the C-terminal amide group, this reaction sequence ('*Azirine/Oxazolone-Method*') represents a new and efficient strategy for the synthesis of peptides with α,α-disubstituted α-amino acids.

The scope of the '*Azirine/Oxazolone-Method*' for the synthesis of linear and cyclic peptides and depsipeptides is demonstrated by the synthesis of segments of the peptaibols *Alamethicin F-30* and *Trichotoxin A-50* as well as of model peptides, used for studies of the influence of α,α-disubstitution on the conformation of the peptide. *Via* an analogous approach, the synthesis of *cyclo*[Gly-Phe(2Me)-Aib-Aib-Gly] is achieved by the pentafluorophenol/DCC cyclization of H-Gly-Phe(2Me)-Aib-Aib-Gly-OH. In the case of cyclic depsipeptides, the linear precursors can be cyclized directly by treatment with HCl-gas in a non-nucleophilic solvent ('*Direct Amide Cyclization*').

Introduction

The first synthesis of 3-amino-2*H*-azirines **1**, which are cyclic three-membered amidines with an endocyclic C=N bond, has been described 19 years ago [1]. Because of the ring strain of these heterocyclic bases, a considerable reactivity to ring opening reactions was expected. Whereas photolysis and thermolysis lead to the formation of nitrile ylides [2] and 2-aza-butadienes [3], respectively, *via* cleavage of the C-C bond, treatment with electrophiles, e.g. acyl chlorides [4,5] yields 1-aza-allyl cations as reactive intermediates *via* cleavage of the N-C bond. The hydrolysis of 3-(dimethylamino)-2,2-dimethyl-2*H*-azirine (**1a**) with aqueous potassium hydrogen phosphate leads to aminoisobutyric-acid dimethylamide (Aib-NMe_2) *via* cleavage of the C=N bond [6]. In this reaction, the 3-amino-2*H*-azirine **1** can be considered as amino-acid building block.

In the last few years, we did show [cf. 7,8] that the easily available 2,2-disubstituted 3-amino-2*H*-azirines **1** react with a variety of acidic compounds (pK_a

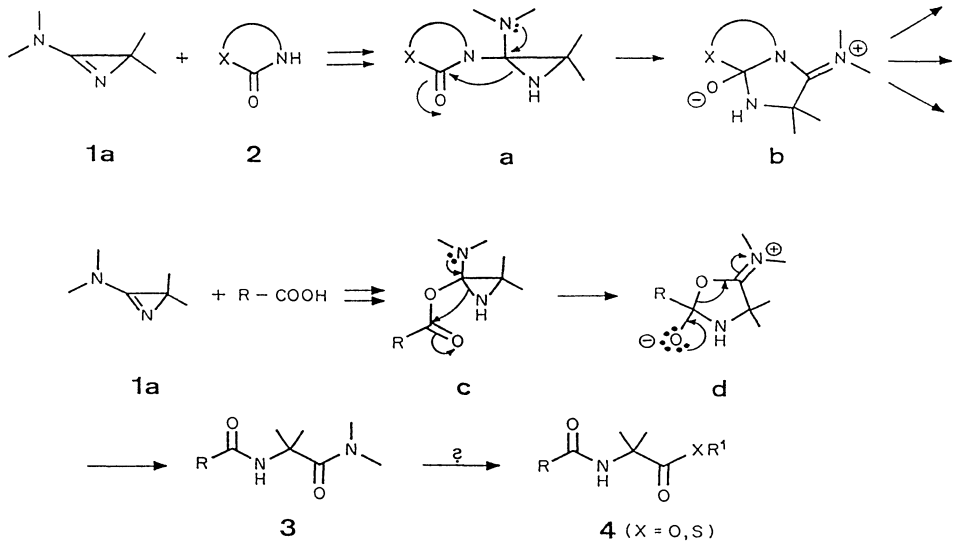

Fig. 1. Reactions of 3-(dimethylamino)-2,2-dimethyl-2*H*-azirine (**1a**) with NH-acidic heterocycles **2** and with carboxylic acids. The bicyclic zwitterions of type **b**, key intermediates in the reactions with **2**, are stabilized through different routes, e.g. ring expansion *via* cleavage of the central C-N bond or ring opening *via* cleavage of the C-X bond. With carboxylic acids, the zwitterion **d** is formed *via* ring expansion of the aziridine **c**. Subsequent ring opening leads to diamide **3**.

of 4–8) to give novel heterocycles containing α,α-disubstituted α-amino acids. The specificity of the ring cleavage has been confirmed using (1-^{15}N)-labelled 3-(dimethylamino)-2,2-dimethyl-2*H*-azirine (**1a***) and ^{15}N-NMR spectroscopy [9]. Analogous reaction mechanisms are proposed for all these transformations (Fig. 1): protonation of the ring-N-atom of **1a** followed by nucleophilic attack of the lactam anion yields the aziridine **a**, which is rearranged to the zwitterion **b**. Cleavage of the central C-N bond in **b** gives enlarged heterocycles [10–13], whereas cleavage of the C-X bond leads to dipolar products [14,15]. Direct evidences for the intermediate **b** are gained from its hydrolysis, methylation followed by hydrolysis, and reduction [15,16].

With activated phenols, **1a** reacts also *via* cleavage of the C=N bond [17] yielding N-aryl-substituted Aib-dimethylamides. Enolized 1,3-dicarbonyl compounds with $pK_a<8$ react in an analogous manner to give N-(3-oxo-1-alkenyl)-substituted Aib-dimethylamides [18,19]. The reactions with sulfinic acids and thiocarboxylic acids lead to N-sulfinyl- [19] and N-thioacyl-substituted Aib-dimethylamides [20], respectively.

Of special interest is the reaction of carboxylic acids with the 3-amino-2*H*-azirine **1a** [18], leading to N-acyl-substituted amino-acid amides **3**. This smooth

reaction already takes place at 0°C to give the diamides in excellent yields. The first reaction step is most probably a protonation of the azirine ring-N-atom, followed by nucleophilic attack of the carboxylate to yield an aziridine intermediate **c**, which, *via* ring expansion to a five-membered zwitterion **d** and subsequent ring opening, leads to the product **3** (Fig. 1). So, this reaction allows the direct coupling of a carboxylic acid with an α,α-disubstituted α-amino acid under mild conditions. Since no additional coupling reagents are needed, bifunctional carboxylic acids, e.g. hydroxy-, mercapto-, and amino-acids can be used in their unprotected form [21,22].

The reaction of 3-amino-2*H*-azirines **1** with carboxylic acids is a potential method for the extension of peptide chains with amino-acid units. The crucial step involving **1** in peptide synthesis is the conversion of the terminal amide group into a carboxylic-acid or carboxylate group (Fig. 1). A selective hydrolysis is accomplished under remarkably mild conditions [21–24]: treating a suspension or solution of diamides of type **3** with aqueous HCl yields the corresponding acid **4** (XR^1 = OH) *via* intermediate formation of a 1,3-oxazol-5(4*H*)-one. In the case of terminal N-methylanilides, the hydrolysis is achieved with 3N HCl in THF/H_2O at 25–35°C. In an analogous manner, compounds **3** are transformed into esters (XR^1 = OR, OAr, SPh) using HCl in alcohols or in toluene in the presence of phenols or thiophenol.

Via repetitive reaction of an acid with 3-amino-2*H*-azirine **1a** and hydrolysis of the resulting amide, a series of Aib-peptides or peptide-like compounds have been synthesized, e.g. PhCH(OH)-CO-$(Aib)_5$-NMe_2, H-$(Aib)_4$-OCH_3, Z-$(Aib)_6$-N(Ph)Me, etc. [22,25].

Results and Discussion

Synthesis of heterocyclic compounds

As mentioned in the introduction, 3-amino-2*H*-azirines **1** react with NH-acidic heterocycles *via* a common zwitterionic intermediate of type **b**. The reaction with 1,3-thiazolidine-2-thione (**5**) in acetonitrile at room temperature leads to a mixture of two 1:1 adducts, the imidazo-[4,3-*b*]thiazole-5-thione **6** (Fig. 2) and N,N-dimethyl-N'-[1-methyl-1-(4,5-dihydro-1,3-thiazol-2-yl)ethyl]thiourea [26]. It has been shown that **6** is the primarily formed product, which is slowly rearranged into the thiourea. This rearrangement is faster in polar solvents; in 2-propanol at room temperature **1** and **5** react to give only the thiourea-derivative. A reaction mechanism for the formation of **6** is depicted in Fig. 2. Cleavage of the C-S bond in the intermediate zwitterion **b'** leads to the dipolar intermediate **e**, which undergoes a ring closure *via* nucleophilic attack of the thiolate to give the bicyclic product **6**. Confirmation of the position of the azirine-*N*(1)-atom in **6** was possible by ^{15}N-NMR spectroscopy using ^{15}N-labelled **1a*** [9].

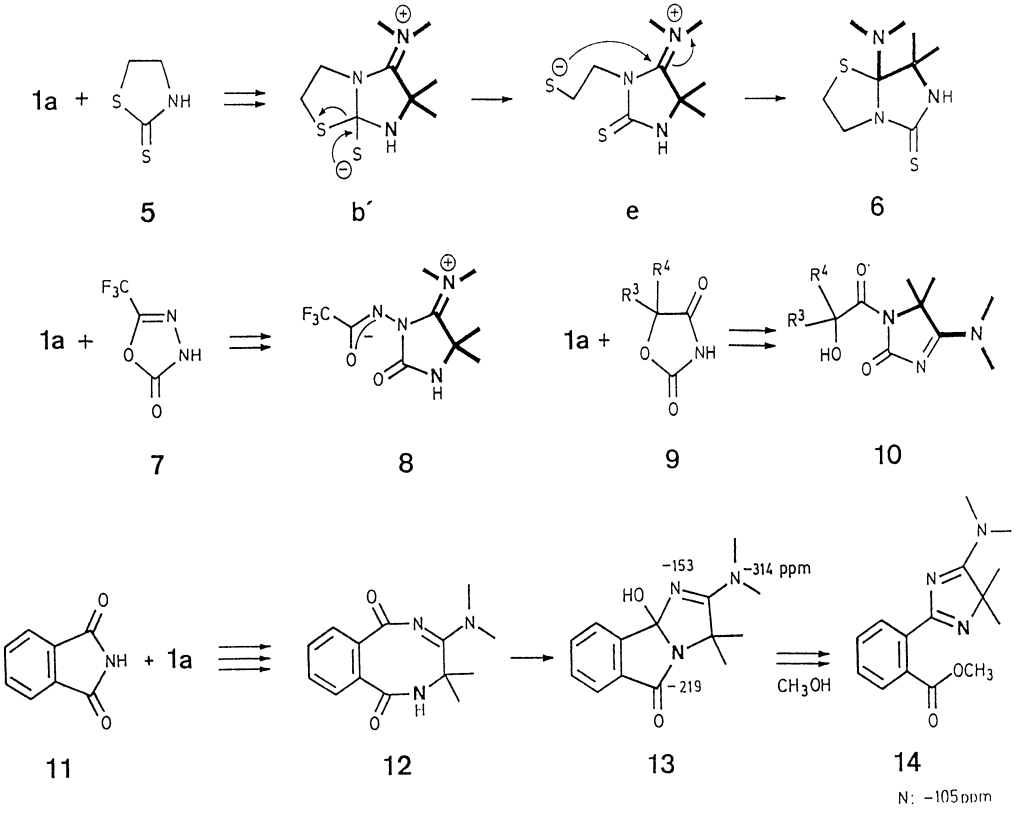

Fig. 2. Reaction of 3-(dimethylamino)-2,2-dimethyl(1-^{15}N)-2*H*-azirine (**1a***) with 1,3-thiazolidine-2-thione (**5**), 5-trifluoromethyl-1,3,4-oxadiazol-2(3*H*)-one (**7**), 1,3-oxazolidine-2,4-dione (**9**), and phthalimide (**11**). The structure of the 1:1 adducts **6**, **8**, and **13** has been established by X-ray crystallography, the position of the azirine-N(1)-atom in **6**, **8**, **10**, and **13** has been confirmed by ^{15}N-NMR spectroscopy.

The reaction of **1** with 1,3,4-oxadiazol- and 1,3,4-thiadiazol-2(3*H*)-ones, performed in 2-propanol at room temperature, yields stable dipolar 1:1 adducts of type **e**, e.g. **8** [14,15]. In contrast to **e**, the negative charge is perfectly stabilized as amidate or thioamidate, respectively. These transformations formally can be described as an annellation of **1** onto the -CO-NH- group of the heterocycle **7** and concomitant ring opening.

Again *via* the same mechanism, the reaction of **1** with 1,3-oxazolidine-2-thione leads to 5,5-disubstituted 3-(2-hydroxyethyl)-2-thiohydantoins. In this case, the dipolar intermediate of type **e** is hydrolyzed during workup.

An unexpected product is formed in the reaction of **1** with 1,3-oxazolidine-2,4-diones **9**. In acetonitrile at room temperature, 3,4-dihydro-2*H*-imidazol-2-ones **10** are formed in very good yield. It has been shown by ^{15}N-NMR spectroscopy that **1a*** yields **10**, in which N(3) is exclusively labelled. From this result we conclude that the reaction proceeds *via* a sequence of ring expansion, ring contraction, and ring opening.

As a last example, the reaction of **1a*** with phthalimide (**11**) shall be discussed (Fig. 2). *Via* ring-expansion of the bicyclic zwitterion, the eight-membered heterocycle **12** is formed. During workup, **12** undergoes a transannular ring contraction to give the azacyclol **13** [27]. The ^{15}N-NMR spectrum of **13** clearly shows that only N(4) is labelled. In methanolic solution at room temperature, **13** is rearranged to yield the methyl 2-(4*H*-imidazol-2-yl)benzoate **14**. The structure of the latter is closely related to 2-(4,5-dihydro-5-oxo-imidazol-2-yl)pyridine-3-carboxylates, which are very potent herbicides [28,29].

In all examples presented, the new heterocycles contain the azirine fragment N-CR^1R^2-C(NR_2), i.e. the cleavage of the azirine-ring occurs at the C=N bond, implying that the azirine atoms are incorporated as α,α-disubstituted α-amino acid moiety.

Synthesis of peptides

The smooth reaction of 3-amino-2*H*-azirines **1** with carboxylic acids (cf. Fig. 1) and the astonishingly mild and selective cleavage of the terminal amide group (Fig. 3; **16** → **17**) proceed without any epimerization at the second-to-last amino acid of the oligopeptide [24]. Together with an efficient DCC coupling with another amino component *via in situ* generated 1,3-oxazol-5(4*H*)-ones **18** in the presence of additives like $ZnCl_2$ or camphor-10-sulfonic acid [30], the reaction of a peptide **15** with **1**, followed by hydrolysis, represents an attractive strategy for the synthesis of peptides containing α,α-disubstituted α-amino acids (Fig. 3). This new procedure is called the '*Azirine/Oxazolone-Method*'.

The general character of the method has been demonstrated in several synthesis of model peptides [31,32]. These peptides, containing α,α-disubstituted α-amino acids, are of current interest because of their extraordinary conformational properties [33].

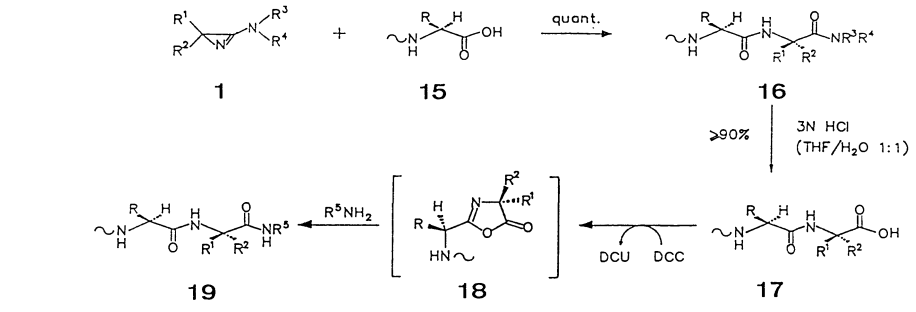

Ac–Aib–Pro–Aib–Ala–Aib–Ala–Gln–Aib–Val–Aib–Gly–Leu–Aib–Pro–Val–Aib–Aib–Glu–Gln–Pheol

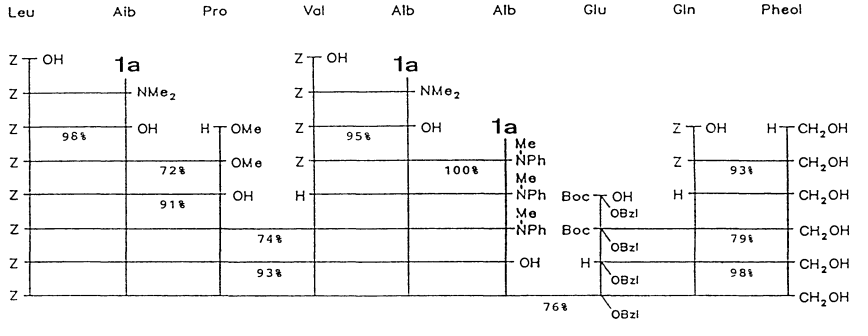

Fig. 3. Synthesis of peptides containing α,α-disubstituted α-amino acids using the '*Azirine/Oxazolone-Method*'. Following this procedure, segments of the peptaibols *Alamethicin F-30* and *Trichotoxin A-50 (G)* have been synthesized.

For testing the scope of the '*Azirine/Oxazolone-Method*' in the synthesis of longer peptide sequences, we have chosen peptaibols as target molecules. Peptaibols are amphiphilic polypeptide ionophores and antibiotics [34] with membrane modifying properties [35]. The characteristic feature of this class of peptides is their high content of α,α-disubstituted α-amino acids, a *C*-terminal amino-alcohol, and a *N*-terminal acetyl group. As the first model, we synthesized the protected *C*-terminal nonapeptide of *Alamethicin*, which was also used in a recently described total synthesis [36]. The accomplished synthesis of the segment Z-Leu-Aib-Pro-Val-Aib-Aib-Glu(O^5-Bzl)-Gln-Pheol, based on our new strategy, is depicted in Fig. 3 [37].

Alamethicin F-30 Ac-Aib-Pro-Aib-Ala-Aib-Ala-Gln-Aib-Val-Aib-Gly-Leu-Aib-Pro-Val-Aib-Aib-Glu-Gln-Pheol

As a second target molecule, we have selected *Trichotoxin A-50* (G) [38,39]. Using the '*Azirine/Oxazolone-Method*', the fragments Ac-Aib-Gly-Aib-Leu-Aib-N(Ph)-Me (1–5), Z-Ala-Ala-Aib-Pro-OBzl (10–13), and Z-Leu-Aib-Iva-Gln-Valol (14–18), have already been synthesized in good yields [40]. A special problem arises by the introduction of an isovaline (Iva, 2-ethyl-2-methylglycine) in position 16. Our synthetic equivalent for Iva is the racemic 2-ethyl-2-methyl-3-[*N*-methyl-*N*-(phenylamino)]-2*H*-azirine (**1**, R^1 = Et, R^2,R^3 = Me, R^4 = Ph). Coupling reaction with Z-Leu-Aib leads to a 1:1 mixture of the epimers Z-(*S*)-Leu-Aib-(*R*,*S*)-Iva-N(Ph)Me in excellent yield. Separation of the two diastereoisomers is achieved by HPLC.

Trichotoxin A-50 (G) Ac-Aib-Gly-Aib-Leu-Aib-Gln-Aib-Aib-Aib-Ala-Ala-Aib-Pro-Leu-Aib-Iva-Gln-Valol

Synthesis of cyclic depsipeptides and peptides

As already discussed in the previous section, diamides or peptides of type **16** are selectively transformed into acids or esters under acidic conditions. The intermediate 1,3-oxazol-5(4*H*)-one is attacked by a nucleophile in an intermolecular reaction. In the absence of external nucleophiles, cyclization reactions, proceeding *via* intramolecular nucleophilic attack, take place [41,42]. This '*Direct Amide-Cyclization*' has been applied for the formation of cyclic depsipeptides with 6-, 9-, 12-, and 15-membered rings. As an example, the synthesis of *cyclo*[(*R*)-Mns-Aib-(*R*)-Mns-Aib] (**24**) is shown in Fig. 4.

Cyclopeptides with an alternating sequence of (*R*)-α-hydroxy carboxylic acids and (*S*)-α-amino acids are called *Enniatines* [43,44]. Usually, in the synthesis of

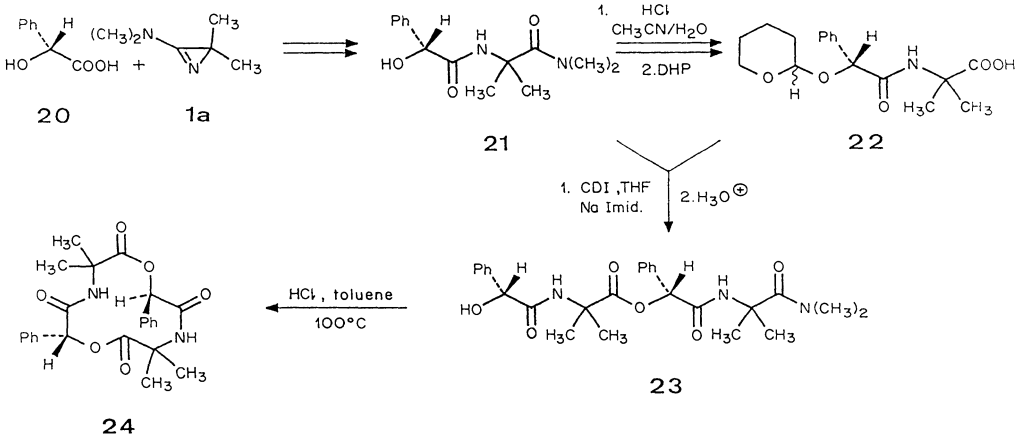

Fig. 4. Synthesis of cyclo[(*R*)-Mns-Aib-(*R*)-Mns-Aib] (**24**) by '*Direct Amide Cyclization*'.

these ionophores, the ring closure is achieved by a lactamic linkage. In our synthesis of the 12-membered analog **24**, cyclization occurs *via* lactone formation. The linear precursor H-(*R*)-Mns-Aib-(*R*)-Mns-Aib-NMe_2 (**23**) is prepared *via* **21**. One half of this sample is then selectively hydrolyzed and the free hydroxy group is protected with THP to give **22**. Coupling of this fragment with **21** through a modified CDI procedure, using sodium imidazolide in THF, affords **23** in 66% yield based on mandelic acid (**20**). Cyclization with HCl in toluene at 100°C leads to **24** in 88% yield [45]. Cleavage of the ester group in **23** could not be observed under these conditions.

As expected, the '*Direct Amide-Cyclization*' of peptide derivatives to give cyclopeptides, using HCl in toluene, cannot be accomplished. Therefore, we used a combination of our new strategy and conventional procedures to synthesize these compounds. As the last example, the synthesis of a cyclic pentapeptide containing three α,α-disubstituted α-amino acids shall be discussed (Fig. 5). The linear pentapeptide **25** is synthesized using the '*Azirine/Oxazolone-Method*' with 2-benzyl-2-methyl-3-[*N*-methyl-*N*-(phenylamino)]- and 2,2-dimethyl-3-[*N*-methyl-*N*-(phenylamino)]-2*H*-azirine as Phe(2Me) and Aib synthons, respectively, with the yields shown in Fig. 5 [25]. Cyclization of the pentapeptide is achieved by the pentafluorophenol (PFP)/DCC method: a *ca.* 10^{-4}M CH_2Cl_2 solution of **25**, 2 equivalent of PFP, and 1 equivalent of DCC is stirred for 30 hours at room temperature. After HPLC purification, cyclopeptide **26** is obtained in 40% yield. The conformation of the linear pentapeptide **25** as well as of the cyclic **26** is established by single-crystal X-ray analysis, which reveals that **25** forms in the

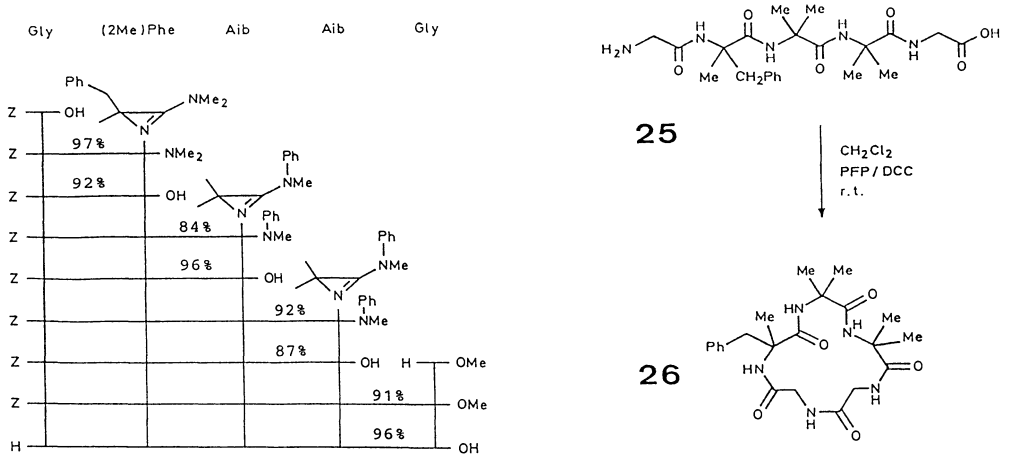

Fig. 5. Synthesis of the cyclic pentapeptide cyclo[Gly-Phe(2Me)-Aib-Aib-Gly] (**26**). The linear precursor (**25**) has been synthesized using the '*Azirine/Oxazolone-Method*', the cyclization has been achieved by the pentafluorophenol/DCC method.

crystal a left-handed 3_{10}-helix with two intramolecular H-bonds, and the rigid conformation of **26** is also stabilized by two intramolecular H-bonds.

Conclusions

It has been shown that 3-amino-2*H*-azirines **1** react with proton acids *via* cleavage of the C=N bond. These reactions lead to synthons which can be considered as α,α-disubstituted α-amino-acid building blocks. Since several heterocyclic systems containing α-amino acid moieties show remarkable biological activities, e.g. as herbicides etc., new synthetic methods for the incorporation of these building blocks are of current interest. The strained 3-membered heterocycles **1** can be used to insert the amino-acid fragment *via* ring expansion. All reactions of **1** and NH-acidic heterocycles proceed *via* a zwitterionic intermediate. Depending on the charge-distribution influenced by a variety of hetero-atoms and substituents, this intermediate is stabilized through different routes. This fact makes it rather difficult to plan a synthesis of a heterocyclic system, using amino-azirines **1**.

This is not the case, when amino-azirines **1** are used as synthons for α,α-disubstituted α-amino acids for the build-up of peptides and peptide-like compounds. Coupling of a peptide with **1** generally proceeds under very mild conditions, without any further activation, and in excellent yield. Together with the selective hydrolysis of the terminal amide group, a new, versatile methodology for the insertion of α,α-disubstituted α-amino acids into peptides, the '*Azirine/Oxazolone-Method*', has been developed. The scope of this new strategy has been demonstrated by syntheses of peptaibol fragments.

A special feature of the selective transformation of a terminal amide function is the smooth cyclization with a hydroxy group of the linear peptide. This reaction facilitates formation of cyclic depsipeptides, which, in turn, are potential ionophores.

Acknowledgements

The support of our work by the Swiss National Science Foundation and F. Hoffmann-La Roche AG, Basel, is gratefully acknowledged. I also thank my able and diligent coworkers, whose names are cited in the references, for their skill and enthusiasm during the laboratory work.

References

1. Rens M and Ghosez L (1970) Tetrahedron Lett. 3765.
2. Dietliker K and Heimgartner H (1983) Helv. Chim. Acta 66: 262.
3. Demoulin A, Gorissen H, Hesbain-Frisque AM and Ghosez L (1975) J. Am. Chem. Soc. 97: 440.
4. Schaumann E, Kausch E and Walter W (1975) Chem. Ber. 108: 2500.

5. Widmer U, Heimgartner H and Schmid H (1978) Helv. Chim. Acta 61: 815.
6. Hoet P (1975) Dissertation Université Catholique de Louvain.
7. Heimgartner H (1981) Israel J. Chem. 21: 151.
8. Heimgartner H (1986) Israel J. Chem. 27: 3.
9. Ametamey SM, Hollenstein R and Heimgartner H (1988) Helv. Chim. Acta 71: 521.
10. Chaloupka S, Vittorelli P, Heimgartner H, Schmid H, Link H, Bernauer K and Oberhänsli WE (1977) Helv. Chim. Acta 60: 2476.
11. Scholl B, Bieri JH and Heimgartner H (1978) Helv. Chim. Acta 61: 3050.
12. Schläpfer-Dähler M, Prewo R, Bieri JH and Heimgartner H (1984) Heterocycles 22: 1667.
13. Hostettler B, Obrecht JP, Prewo R, Bieri JH and Heimgartner H (1986) Helv. Chim. Acta 69: 298.
14. Prewo R, Bieri JH and Heimgartner H (1985) Chimia 39: 354.
15. Ametamey SM (1989) Dissertation Universität Zürich.
16. Chaloupka S, Bieri JH and Heimgartner H (1980) Helv. Chim. Acta 63: 1797.
17. Chandrasekhar BP, Heimgartner H and Schmid H (1977) Helv. Chim. Acta 60: 2270; Chandrasekhar BP and Heimgartner, unpublished results.
18. Vittorelli P, Heimgartner H, Schmid H, Hoet P and Ghosez L (1974) Tetrahedron 30: 3737.
19. Chandrasekhar BP, Schmid U, Schmid R, Heimgartner H and Schmid H (1975) Helv. Chim. Acta 58: 1191.
20. Jenny Ch and Heimgartner H (1986) Helv. Chim. Acta 69: 374.
21. Obrecht D and Heimgartner H (1981) Helv. Chim. Acta 64: 482.
22. Obrecht D and Heimgartner H (1987) Helv. Chim. Acta 70: 102.
23. Obrecht D, Scholl B and Heimgartner H (1985) Helv. Chim. Acta 68: 465.
24. Wipf P and Heimgartner H (1987) Helv. Chim. Acta 70: 354.
25. Dannecker-Doerig I (1989) unpublished results.
26. Ametamey SM, Prewo R, Bieri JH, Heimgartner H and Obrecht JP (1986) Helv. Chim. Acta 69: 2013.
27. Schläpfer-Dähler M, Prewo R, Bieri JH, Germain G and Heimgartner H (1988) Chimia 42: 25.
28. Los M (1984) ACS Symp. Ser. 255: 29; Amer. Cyanamid Co., US Patent 4188487, 1980; US Patent 4221586, 1980.
29. Obrecht JP, Schönholzer P, Jenny Ch, Prewo R and Heimgartner H (1988) Helv. Chim. Acta 71: 1319.
30. Wipf P and Heimgartner H (1986) Helv. Chim. Acta 69: 1153.
31. Wipf P and Heimgartner H (1988) Helv. Chim. Acta 71: 140.
32. Sahebi M, Wipf P and Heimgartner H (1989) Tetrahedron 45: 2999.
33. Wipf P and Heimgartner H (1988) Helv. Chim. Acta 71: 258; Wipf P, Kunz RW, Prewo R and Heimgartner H (1988) ibid. 71: 268.
34. Toniolo C, Bonora GM, Bavoso A, Benedetti E, di Blasio B, Pavone V and Pedone C (1983) Biopolymers 22: 205.
35. Müller P and Rudin DO (1968) Nature 217: 713.
36. Schmitt H and Jung G (1985) Liebigs Ann. Chem. 321 and 345.
37. Wipf P (1987) Dissertation Universität Zürich.
38. Jung G, Brückner H and Schmitt H (1981) In: Voelter W and Weitzel G (eds.) Structure and Activity of Natural Peptides. de Gruyter, Berlin, p. 75.
39. Brückner H, Przybylsky M, Dietrich I and Manz I (1984) Biomed. Mass. Spectrom. 11: 569; Brückner H and Przybylsky M (1984) J. Chromatogr. 296: 263 and ref. cited therein.
40. Altherr W (1988) Diplomarbeit Universität Zürich.
41. Obrecht D and Heimgartner H (1983) Tetrahedron Lett. 24: 1921; (1987) Helv. Chim. Acta 70: 329.
42. Obrecht D and Heimgartner H (1984) Helv. Chim. Acta 67: 526.
43. Schröder E and Lübke K (1963) Experientia 19: 57.
44. Ovchinnikov, Yu A (1976) In: Rydon HN (ed.) MTP Int. Rev. of Science, Organic Chemistry, Series Two. Butterworths, London, Vol. 6, p. 219.
45. Obrecht D (1983) Dissertation Universität Zürich.

Chemistry of glutamate analogues

Haruhisa Shirahama, Kimiko Hashimoto, Miwa Yanagida and Manabu Horikawa

Department of Chemistry, Faculty of Science, Hokkaido University, Sapporo 060, Japan

Abstract

Stereoselective syntheses of four diastereoisomers of ß-benzylglutamic acid were performed through Michael addition of benzylphenylsulfide to the lactone and the lactam which were prepared from serine and glutamic acid respectively. (2S,3R)-ß-Benzylglutamic acid whose configuration was the same as that of kainic acid exhibited threefold neuroexcitatory activity in the isolated rat spinal cord than glutamate and other isomers showed very little activity. A new synthetic method of acromelic acid families was also developed. The enolate of an aromatic aldehyde and a vinyl group, both of which were linked with amino nitrogen, underwent intramolecular Diels-Alder addition reaction with excellent stereoselectivity to give the proline derivative with desired configuration. From this product, a methoxyphenyl kainoid (3-carboxymethylproline with methoxyphenyl group at C4) with the same configuration in pyrrolidine ring as kainic acid was derived. The methoxyphenyl kainoid showed potent activity comparable to that of acromelic acid B or domoic acid.

Introduction

The amino acid glutamate functions are recognized as a fast excitatory transmitter in the mammalian brain. Recent studies demonstrate that glutamate is a powerful neurotoxin, capable of killing neurons in the central nervous systems when its extracellular concentration is sufficiently high. The glutamate and its analogues cause a marked depolarization of a mammalian central neuron which lead to specific neuronal death in the brain. The compounds related to the glutamate probably play a key roll in ischemic brain damage [1–5]. Among many excitatory glutamate analogues, N-methyl-D-aspartic acid (NMDA), quisqualic acid (QA) and kainic acid (KA) exhibit extraordinarily potent activity and they have served to classify the glutamate receptors into three subtypes [6–9]. Studies on the function of the NMDA type receptor have been fortunately achieved by the aid of selective antagonists. For instance, selective impairment of learning and blockage of long-term potentiation by a NMDA receptor antagonist were recently reported [10]. However, the function of QA and KA type receptors still remained to be studied. Recently from the Japanese toadstool, *Clitocybe acromelalga*, we isolated a minute amount of poisonous principles named as acromelic acids A and B which were revealed to be the most potent neuroexcitatory kainoids in the world [11–13]. Because of this strongest activity, these acids are very much expected as useful tools in the field of neurophysiology. The appearance of the acromelic acids

remind of the introduction of kainic acid into this field in previous time. The toadstool was not popular and contains so little acromelic acids and besides it could not be cultured. We synthesized them from kainic acid but it was not for supplying the new kainoids but for the determination of their absolute configuration [11]. Now we need a new synthesis. Furthermore clarification of the reason why the acromelic acids have so potent activity must serve to design a new and very potent kainoid which is easily accessible by chemical synthesis. In order to examine a roll of an aromatic group at C4 of the proline nucleus and the conformation of the glutamate moiety of kainoids in neuroexcitatory activity, we achieved two syntheses and estimated the activity of the synthetic products. We would like to report the results of these studies.

Syntheses of acyclic analogues of kainoids

The potent neuroexcitatory activity of kainoids probably depends on both the restricted conformation of the glutamate moiety involved as a constitutional structure and a π-electron system attached to C4 of the proline skeleton. Therefore we are interested in the structure **7** where the pyrrolidine ring is cleaved to release the limited movement of the glutamate moiety and the configuration of the benzyl group placed at ß-position to the carboxyl group is the same as that of biologically active kainoids (Fig. 1). We synthesized possible four stereoisomers of ß-benzylglutamic acid. Synthetic route was outlined in Fig. 2. Michael addition of a benzyl group to lactone **10** or lactam **14** would provide (2S,3R)-(or(2R,3S)-) and (2S,3S)-(or(2R,3R)-) 3-benzylglutamic acids respectively. The lactone **10** and also the lactam **14** should be easily accessible through ordinary syntheses from ordinary amino acids. The syntheses were performed through this line [14].

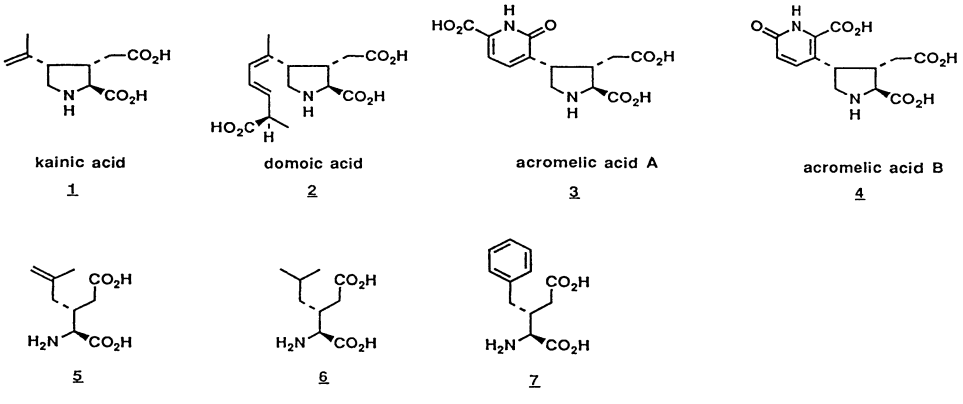

Fig. 1. Neuroexcitatory kainoids and its acyclic analogues.

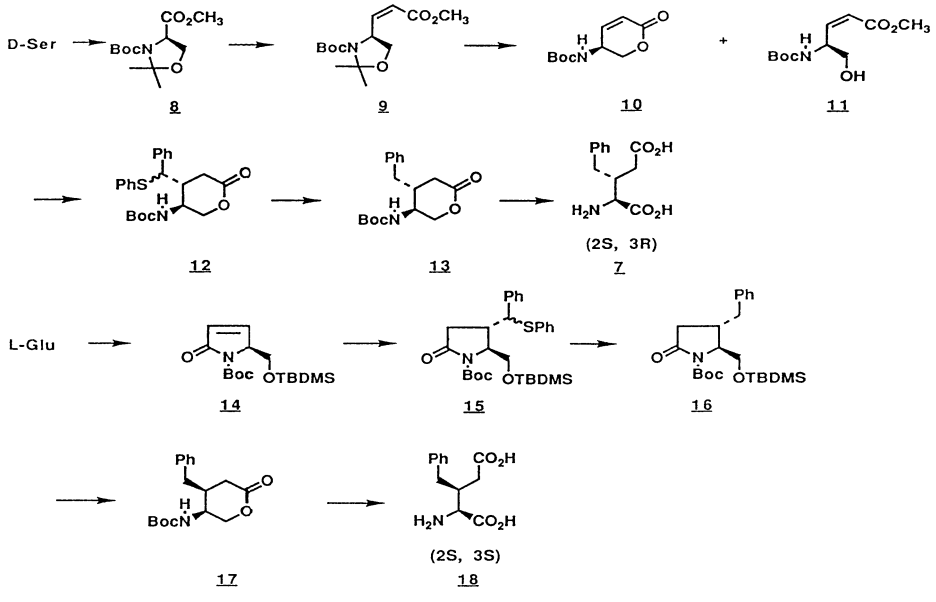

Fig. 2. Synthetic scheme of acyclic analogues of kainoids.

New synthetic method of acromelic acid families

Acromelic acids were most likely biosynthesized through condensation of a DOPA derivative with a glutamic acid followed by cyclization to form pyrrolidine ring. The biogenesis hinted us a new synthetic scheme of acromelic acid derivatives. The target molecule could be derived from a compound consisting of two parts, an aromatic group and a glutamic acid precursor, which were linked together with nitrogen. The key step of the synthesis was the stereoselective formation of pyrrolidine ring which was performed probably by the intramolecular Diels-Alder reaction of an enolate of an aromatic aldehyde and vinyl group which would be leading to γ-carboxylic acid of glutamic acid (see **22** to **25**). The part of glutamic acid precursor could be derived from L-methionine, therefore an asymmetric synthesis of acromelic acid families should be available.

Experimental procedures

Syntheses of acyclic analogues of kainoids

(2S,3R)-3-Benzylglutamic acid was obtained as follows. The amino, carboxyl and hydroxyl groups of D-serine were protected as a *t*-butyl carbamate, methyl ester

and N,O-acetonide respectively to afford **8** in 39% yield (3 steps). The ester was reduced to alcohol with lithium aluminum hydride followed by oxidation of resulting alcohol with Swern's method (oxalyl chloride with dimethyl sulfoxide and then triethyl amine) at low temperature (−78°C) to give aldehyde, which was converted to *cis*-α,ß-unsaturated ester **9** under Still's condition [15]. Treatment of **9** with dl-10-camphorsulfonic acid (CSA) in methanol yielded a mixture of unsaturated lactone **10** and deprotected alcohol **11**. The latter could be converted to the former with CSA in dichloromethane. The stereoselective introduction of benzyl group to lactone **10** was successfully carried out using a Michael addition reaction of benzylphenylsulfide in N,N,N',N'-tetramethylethylenediamine (TMEDA) at −78°C. The mixture of Michael adducts **12** was desulfurized with tributyltin hydride to give a desired product **13** as a single product which was converted to (2S,3R)-3-benzylglutamic acid **7** by the following sequence of reactions: (1) hydrolysis of lactone ring followed by oxidation of resulting alcohol with $KMnO_4$ (2) deprotection of amino protecting group with trifluoroacetic acid (TFA) (59% 2 steps). Using the same method, **5** and **6** were prepared from the lactone **10** by conjugate addition of corresponding Grignard reagents in the presence of copper (I) bromide dimethyl sulfide complex. Enantiomer of **7** was also prepared starting from L-serine by the use of the same procedure.

On the other hand, (2S,3S)-isomer was synthesized from the known γ-lactam **14** [16], which was prepared from L-glutamic acid through 8 steps. The lactam **14** was allowed to react with benzylphenylsulfide to afford Michael adducts **15**, which was then desulfurized with Raney nickel (W-2) to give desired *trans*-substituted lactam **16**. Successive reaction involving hydrolysis of lactam, esterification, desilylation gave *cis*-substituted lactone **17**. Oxidation followed by deprotection yielded (2S,3S)-isomer **18**. Enantiomer of **18**, (2R,3R)-isomer was also synthesized from (2R)-**14**.

New synthetic method of acromelic acid families

2-Indanone was converted to lactol **19** by the sequence of following reactions: (1) Baeyer-Villiger oxidation with *m*-chloroperbenzoic acid (mCPBA) (2) reduction of resulting lactone with diisobutylaluminum hydride. On the other hand, known vinyl glycinol derivative **20** was prepared from L-methionine through 5 steps [17]. Condensation of lactol **19** with amine part **20** was achieved as follows. The masked amine **20** was deprotected with trifluoroacetic acid (TFA) in dichloromethane and the resulting TFA salt was dissolved in methanol. The pH of this solution was adjusted to 6 with dropwise addition of triethylamine. To this solution **19** and sodium cyanoborohydride in methanol were added to afford N-alkylated product **21** in 62% yield. The amino and C1-hydroxyl groups were protected as a cyclic carbamate ((1) benzyl chloroformate (ZCl), (2) KOH) followed by oxidation of benzyl alcohol with MnO_2 to give a key intermediate **22**. Intramolecular Diels-Alder reaction was achieved under irradiation of **22** by the use of medium-pressure mercury arc lamps in toluene at 15°C to afford cyclized products in 75% yield.

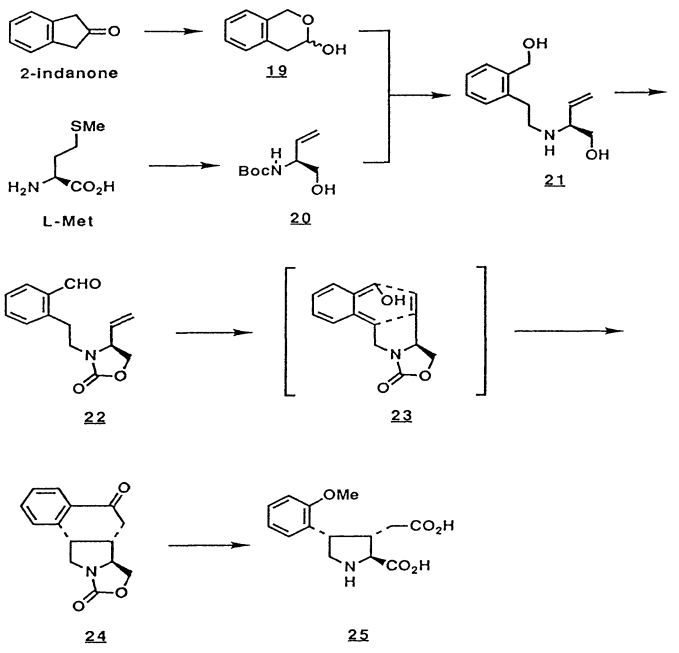

Fig. 3. Synthetic scheme of new kainoids.

Oxidation of resulting alcohols with MnO_2 gave desired ketone **24** along with its C4 epimer in the ratio of 99 to 1. Ketone **24** was converted into amino acid **25** by the following reactions. (1) Deprotection with KOH followed by reprotection of amino group with ZCl. (2) Oxidation of resulting alcohol to carboxylic acid using pyridinium dichromate (PDC) in dimethylformamide followed by esterification with diazomethane. (3) Baeyer-Villiger oxidation with mCPBA followed by esterification. (4) Methylation of hydroxyl group with methyl iodide and sodium hydride as a base. (5) Hydrolysis of esters followed by N-deprotection with hydrogenolysis.

Neuroexcitatory activity

Synthetic compounds were applied to electrophysiological experiment in the isolated newborn rat spinal cord following the method described in reference 12.

Results and Discussion

In the syntheses of acyclic analogues of kainoids, the key step was the Michael addition of an aromatic component to the lactone **10** and lactam **14**. Both the reactions were successfully achieved employing benzylphenysulfide which added to give completely stereoselectively *trans*-addition products. They were smoothly converted to diastereomerical benzylglutamates.

Neuroexcitatory activity of ß-benzylglutamates was shown by the relative potency ratio in the rat spinal cord (Fig. 4). The (2S,3R)-isomer **7** whose configuration was the same as that of kainic acid exhibited threefold activity than the glutamate and other isomers showed very little activity. Since kainic acid showed much more stronger activity than glutamic acid, fission of the pyrrolidine ring of kainoid much reduced activity. A little stronger activity of **7** implied that configuration of C2 and C3 played a key roll in the potentiation of the glutamate. (2S,3R)-Isomer **7** seemed to have allokainic acid like conformation judging from the coupling constants between vicinal protons in the ^{1}HNMR spectrum. These facts should explain that conformation was also very important and the pyrrolidine ring of kainoids made their conformations arrange properly to exhibit potent activity. The activity of (2S,3R)-ß-substituted glutamates with different substituents suggested that π-electron system at C3 enhanced activity and the stronger activity was due to the larger π-system. According to Shinozaki and Ishida, NMDA antagonist did not block the effect of benzylglutamates (private communication). The benzylglutamate bound probably with a KA or QA type receptor which should have another binding site with π-electron system.

In the development of a new synthetic method of acromelic acid families, we focused how stereoselectively the pyrrolidine ring was assembled. This reaction was performed by two groups so far [18–19], but both of them were not satisfactory. The intramolecular Diels-Alder reaction of the enolate of aromatic aldehyde and vinyl group was successfully achieved and gave the desired product, 2,3-*trans*-3,4-*cis* isomer, with excellent stereoselectivity (**22** to **24**). The key point of this reaction was the selection of protective groups of amino and C1 hydroxymethyl group. We first carried out the reaction of the compound with separately protected

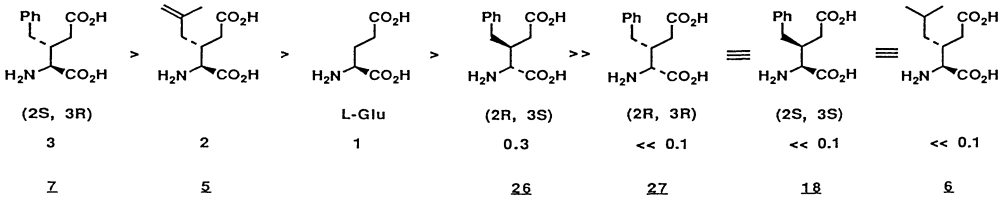

Fig. 4. Relative potency ratio of synthetic glutamate analogues in the rat spinal cord.

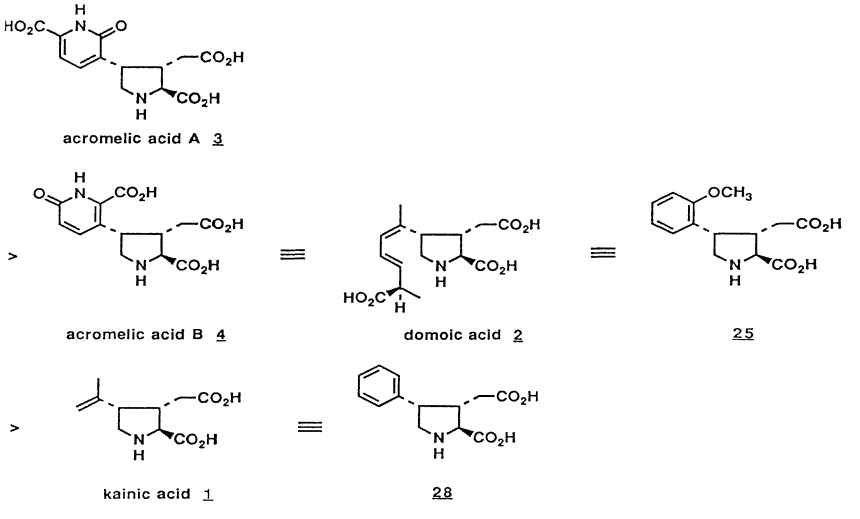

Fig. 5. Neuroexcitatory activity of new kainoids in the rat spinal cord.

amine and alcohol, and poor selectivity was obtained. Molecular model studies on the stereochemistry of the transition state suggested that the assemblage of five membered ring with formation of a carbamate bridge between the amino and hydroxyl groups yielded an adequate arrangement of the enolate and the vinyl group so as to give the product with desired configuration. The surmise was beautifully realized.

A new kainoid with methoxyphenyl moiety **25** which had the same configuration to kainic acid exhibited potent activity comparable to acromelic acid B or domoic acid. A methoxyphenyl, pyridone, and 1,3-diene fragments might be effective to arrange the conformation of glutamate skeleton adequately to exhibit neuroexcitatory activity and they themselves might carry some function to potentiate the activity. Acromelic acid families or phenyl kainoids might be classified to two groups by the time courses of the responses. Acromelic acids A and B, methoxyphenyl kainoid **25** showed significantly short half decay time and domoic acid, kainic acid and phenyl kainoid **28** showed rather long half decay time of the response.

Addendum

Methoxyphenyl kainoid **25** was later found to have much more potent neuroexcitatory activity than acromelic acid A. Details of this compound will be published shortly.

Acknowledgement

We are very grateful to Drs. H. Shinozaki and M. Ishida (Tokyo Metropolitan Institute for Medical Science) for the estimation of neuroexcitatory activity and valuable discussion.

References

1. Olney JW (1985) Int. Rev. Neurobiol. 27: 337–362.
2. Meldrum BS (1985) Clin. Sci. 68: 113–122.
3. Meldrum BS (1986) Adv. Neurol. 43: 687–706.
4. Greenamyre JT (1986) Arch. Neurol. 43: 1058–1063.
5. Rothman SM and Olney JW (1986) Ann. Neurol. 19: 105–111.
6. Fagg GE, Foster AC and Ganong AH (1986) Trends Pharmacol. Sci. 7: 357–363.
7. Mayer ML and Westbrook GL (1987) Prog. Neurobiol. 28: 197–276.
8. McLennan H (1983) Prog. Neurobiol. 20: 251–271.
9. Watkins JC and Evans RH (1981) Ann. Rev. Pharmacol. Toxicol. 21: 165–204.
10. Morris RGM, Anderson E, Lynch GS and Baudry M (1986) Nature 319: 774–776.
11. Konno K, Hashimoto K, Ohfune Y, Shirahama H and Matsumoto T (1988) J. Am. Chem. Soc. 110: 4807–4815.
12. Ishida M and Shinozaki H (1988) Brain Res. 474: 386–389.
13. Shinozaki H, Ishida M and Okamoto T (1986) ibid. 399: 395–398.
14. Yanagida M, Hashimoto K, Ishida M, Shinozaki H and Shirahama H (1989) Tetrahedron Lett. 30: 3799–3802.
15. Still WC and Gennari C (1983) ibid. 24: 4405–4408.
16. Ohfune Y and Tomita M (1982) J. Am. Chem. Soc. 104: 3511–3513.
17. Ohfune Y and Kurokawa N (1984) Tetrahedron Lett. 25: 1071–1074.
18. Baldwin JE and Li C-S (1988) J. Chem. Soc. Chem. Commun. pp. 261–263.
19. Takano S, Iwabuchi Y and Ogasawara K (1987) J. Am. Chem. Soc. 109: 5523–5524.

A simple conversion of tryptophan to a yohimbane derivative

Eugène Neuzil, Eliane de Tinguy-Moreaud, Gilles Précigoux, Nguyen Ba Chanh and Christian Courseille

Department of Medical Biochemistry, University of Bordeaux II and the Laboratory of Crystallography and Crystal Physics, University of Bordeaux I, France

Abstract

DL-Tryptophan in 0,1 N HCl reacts with ninhydrin (triketoindane hydrate) at room temperature to give a brown precipitate; washing the precipitate with cold methanol leaves a yellow compound which is crystallized from boiling methanol ($C_{20}H_{14}O_4N_2$, 1 CH_3OH). X-ray diffractometry showed that the crystals belong to the monoclinic system, with $P2_{1/n}$ as a spatial symmetry group; the unit cell (a = 12.016 Å; b = 13.336 Å; c = 12.128 Å; ß = 113.45°) contains four molecules, each one formed by the association of a molecule of methanol with 5-carboxy-14-hydroxy-(3,14,15,16,17,18,19,20) octadehydro-yohimban-21-one, a hitherto not described compound possessing the same ring skeleton as yohimbine and reserpine, two major indole alkaloids. The structure of a spiro derivative of 2,3,4,5-tetrahydro-ß-carboline, previously proposed [16], can thus be eliminated.

The synthesis of the new yohimbane compound may be explained by the opening of the cyclopentane ring of ninhydrin, followed by the condensation of the resulting *o*-carboxyphenyl glyoxal with the indole amino acid or by a mechanism involving the transient formation of a spirane.

Tryptophan and tryptamine are the fundamental building blocks required for the biosynthesis of indole alkaloids, which include more than a thousand representatives of widely differing molecular structure and pharmacological activity [1–3]. Various tryptophan derivatives condense with secologanin to give strictosidine, a precursor which, after an eventual opening or rearrangement of its secologanin moiety, leads to the group of monoterpenoid-derived indole alkaloids [4]. In this group, the pentacyclic skeleton of yohimbane (I) and of 3-epi-allo-yohimbane (III) appears respectively in two alkaloids of major interest, yohimbine (II) and reserpine (IV).

Since the first isolation of yohimbine [5,6] and the elucidation of its chemical structure [7–11], a great number of syntheses of compounds possessing the yohimbane nucleus have been described [12–15]. These syntheses are generally multi-step strenuous techniques.

In this paper, we show that tryptophan reacts with ninhydrin (triketoindane hydrate) in a hydrochloric medium at room temperature, to give a crystalline yellow product which was identified by X-ray diffractometry to 5-carboxy-14-hydroxy-(3,14,15,16,17,18,19,20)octadehydro-yohimban-21 one (V) and not to the spiro indolo-indanic zwitterion (VI) previously postulated [16].

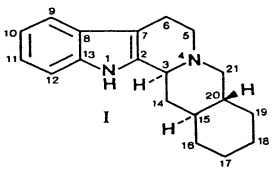

I

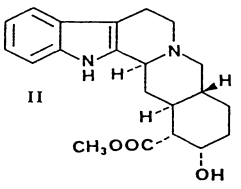

II

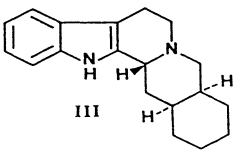

III

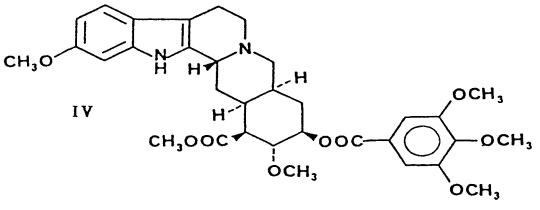

IV

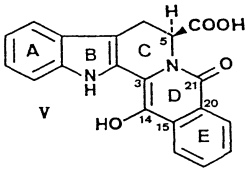

V

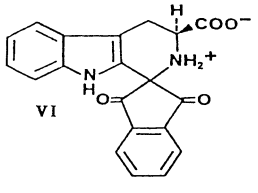

VI

Materials and Techniques

Chemicals

DL- and L-tryptophan as well as L-tryptophanamide were from Cyclo Chemical Inc., Los Angeles, Ca, USA. α-Methyl- and 1-methyl-DL-tryptophan were purchased from Sigma, St Louis, Mo, USA. DL-Tryptophan monomethyl derivatives in positions 4, 5, 6 or 7-; 5-hydroxy- and 5-methoxy-DL-tryptophan; 4-methyl-DL-tryptophol were provided by Bachem, Bubendorf, Switzerland. Analytical grades of ninhydrin, methanol and hydrochloric acid were used (Merck, Darmstadt, West Germany).

Syntheses

DL-Tryptophan (2.04 g, 10 mmoles) was dissolved in warm hydrochloric acid (0.1 N, 75 ml); ninhydrin (1.78 g, 10 mmoles) was equally dissolved in the same volume of 0.1 N HCl. The two solutions, brought to room temperature, were mixed. A precipitate appeared rapidly and was collected on sintered glass after 48 h. The brown precipitate was washed with ice-cold methanol; the first washings were dark-brown; the washed yellow precipitate was crystallized from hot methanol to

give small yellow crystals [17]. The yield of 20 percent could be improved by collecting the filtrate of the initial preparation and the methanol used for washing.

Similar yellow crystals could be obtained when DL-tryptophan was replaced by one of its five methyl derivatives [18], by L-tryptophanamide or by 4-methyl-DL-tryptophol. Reacting L-tryptophan with ninhydrin in the same experimental conditions also led to yellow crystals, but the yield was much smaller.

Apparatus

An automatic X-ray diffractometer CAD-4-Eonius was used with λ (CuKα) 1.5418 Å; the structure was resolved by direct Mithril methods [19]. The other apparatus were a Varian DMS 90 UV-visible spectrophotometer and a Beckman Aculab-1 IR-spectrophotometer.

Results

The crystals obtained by reacting DL-tryptophan with ninhydrin contained one molecule of methanol

$C_{20}H_{14}O_4N_2$, 1 CH_3OH (PM = 378.34)	% C	% H	% N
Theor	66.6	4.79	7.4
Found	65.85	4.84	7.09
	65.92	4.75	7.24

The crystals gave excellent X-Ray diffraction patterns; 3508 reflections could be noted, among which 2170, with $I>2\sigma(I)$, could be selected to achieve the resolution of the structure; a reliability factor of R = 0.056 was obtained. The crystals correspond to the five ring structure of a yohimbane derivative. The molecule is almost flat (Fig. 1); cycles A and B are coplanar with one another as well as cycles D and E; a slight twist appears at cycle C level. Crystals belong to the monoclinic system, with a spatial symmetry group $P2_{1/n}$; the unit cell (A = 12.016 Å; b = 13.336 Å; c = 12.128 Å; ß = 113°45) contains four molecules, each one resulting from the association of a molecule of methanol with V (Fig. 2). The complete crystallographic data [20] are limited in this paper to interatomic distances and angles (Table 1).

Compound V differs from yohimbane a) by the aromatic character of ring E, which eliminates stereochemical ambiguities at C15 and C20, b) by the enol group O(24)H at C14, another elimination of a stereochemical difficulty at C3, c) by the lactam character of cycle D, a consequence of the presence of an oxygen atom at C21, d) by an unionized carboxylic group at C5.

Within the unit cell, the carboxylic group of V is linked by a hydrogen bond to the carboxylic group of another molecule of V; a second hydrogen bond occurs between O(26)H of the carboxylic group and the oxygen atom of the hydroxylic group at C24.

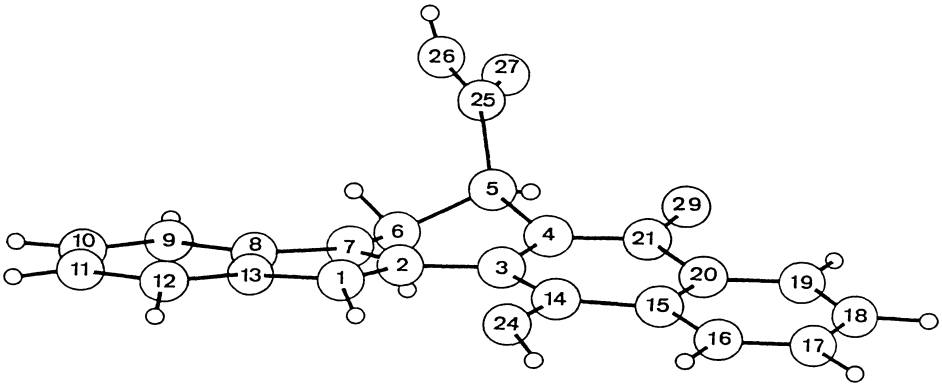

Fig. 1. Three dimensional structure of compound V: 5-carboxy-14-hydroxy-(3,14,15,16,17,18,19,20)octadehydro-yohimban-21-one.

Some physico-chemical characteristics (chromatographic behaviour; UV and IR spectroscopic data) of compound V have been published elsewhere [17]. Compound V is insoluble in water and sparingly soluble in methanol or ethanol; dilute methanolic or ethanolic solutions are instable and very sensitive to light.

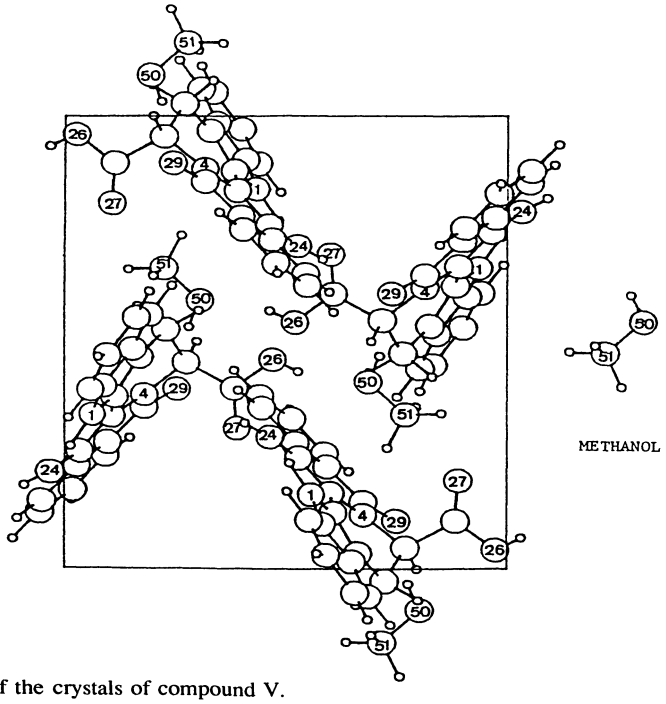

Fig. 2. Unit cell of the crystals of compound V.

Table 1. Molecular characteristics of the yohimbane compound V. Interatomic distances and angles

Distances				Angles				
N1	– C2	1.391(5)		C2	– N1	– C13	107.9(3)
N1	– C13	1.375(6)					
C2	– C3	1.438(6)		N1	– C2	– C3	125.5(4)
C2	– C7	1.365(5)		N1	– C2	– C7	110.5(3)
				C3	– C2	– C7	124.0(4)
C3	– N4	1.436(5)		C2	– C3	– N4	114.6(3)
C3	– C14	1.358(6)		C2	– C3	– C14	125.7(4)
				N4	– C3	– C14	119.6(4)
N4	– C5	1.478(5)		C3	– N4	– C5	120.0(3)
N4	– C21	1.362(6)		C3	– N4	– C21	122.6(3)
				C5	– N4	– C21	116.8(3)
C5	– C6	1.539(6)		N4	– C5	– C6	112.1(3)
C5	– C25	1.525(6)		N4	– C5	– C25	108.8(3)
				C6	– C5	– C25	111.9(3)
C6	– C7	1.500(6)		C5	– C6	– C7	108.1(3)
C7	– C8	1.426(6)		C2	– C7	– C6	121.4(4)
				C2	– CT	– C8	106.9(4)
				C6	– C7	– C8	131.7(4)
C8	– C9	1.389(6)		C7	– C8	– C9	133.8(4)
C8	– C13	1.427(6)		C7	– C8	– C13	106.8(4)
				C9	– C8	– C13	119.4(4)
C9	– C10	1.383(7)		C8	– C9	– C10	118.6(4)
C10	– C11	1.414(7)		C9	– C10	– C11	121.1(5)
C11	– C12	1.379(7)		C10	– C11	– C12	121.8(5)
C12	– C13	1.396(7)		C11	– C12	– C13	116.6(4)
				N1	– C13	– C8	107.9(4)
				N1	– C13	– C12	129.7(4)
				C8	– C13	– C12	122.4(4)
C14	– C15	1.424(6)		C3	– C14	– C15	121.1(4)
C14	– O24	1.380(6)		C3	– C14	– O24	117.0(4)
				C15	– C14	– O24	121.9(4)
C15	– C16	1.410(6)		C14	– C15	– C16	122.9(4)
C15	– C20	1.423(6)		C14	– C15	– C20	118.1(4)
				C16	– C15	– C20	119.0(4)
C16	– C17	1.363(7)		C15	– C16	– C17	120.0(4)
C17	– C18	1.412(7)		C16	– C17	– C18	121.0(4)
				C17	– C18	– C19	120.3(4)
C19	– C20	1.402(6)		C18	– C19	– C20	119.7(4)
C20	– C21	1.442(5)		C15	– C20	– C19	120.0(4)
				C15	– C20	– C21	121.3(4)
				C19	– C20	– C21	118.6(4)
C21	– O29	1.275(5)		N4	– C21	– C20	117.1(4)
				N4	– C21	– O29	120.2(4)
				C20	– C21	– O29	122.7(4)
C25	– O26	1.317(6)		C5	– C25	– O26	109.1(4)
C25	– O27	1.190(6)		C5	– C25	– O27	125.5(4)
				O26	– C25	– O27	125.3(4)
O50	– C51	1.413(7)					

Discussion

The new yohimbane derivative V described in this paper is related to several products of biological interest which all possess a pentacyclic structure associated with an aromatic E ring.

Demethoxycarbonyl-3,14-dihydrogambirtannine (VII) isolated from *Ochrosia lifuana*, is devoid of any functional group on its hexadehydroyohimbane skeleton [21,22]. The lactam structure of V, a consequence of the presence of a carbonyl group at C21 is also found in compound VIII [8,23,22], as well as in two synthetic products: compound IX, only differing by the contraction of ring D [24,25], and the oxa analogue X [26]. The hydroxy group of the enolic function at C14 of compound V, is replaced by a phenolic hydroxy group in the completely aromatic structure of the zwitterionic anhydroalstonatine (XI) from *Alstonia venenata* [27].

Some natural alkaloids, despite the occurrence of an additional heteroatom, are nevertheless linked to V by their lactam structure; this is the case when a nitrogen

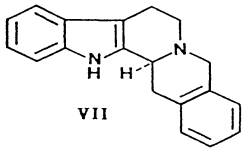

VII

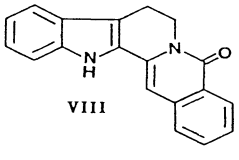

VIII

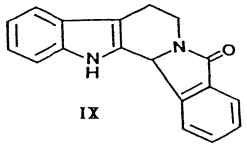

IX

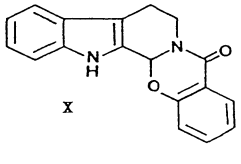

X

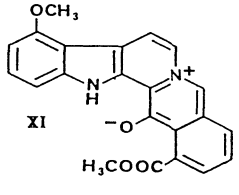

XI

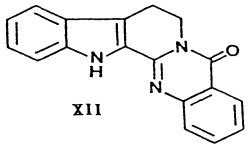

XII

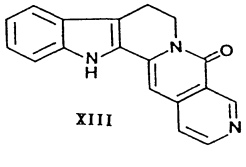

XIII

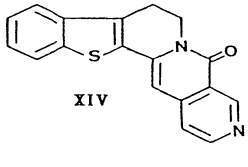

XIV

heteroatom replaces the carbon atom at position 14, as in rutaecarpine from *Evodia rutaecarpa* (XII) [28–30], or at position 18 as in nauclefine from *Nauclea latifolia* (XIII) [31,32] and in its synthetic thia analogue XIV [33] or in angustidine, a 17-methyl derivative of XIII extracted from *Strychnos angustiflora* [34,21].

The formation of a yohimbane derivative implies the replacement of the indanic pentagonal ring by the hexagonal heterocyclic lactam in cycle D, a new type of ring-enlargement reaction of ninhydrin [35]. A first pathway can be advanced (Scheme 1). Ninhydrin (XV) reacts through a more active form, *o*-carboxyphenylglyoxal (XVI) [36] which condenses in acidic medium with tryptophan (XVII) to give the ketonic lactam XVIII, finally isolated under its crystalline enolic form V (Scheme 2). The preferential formation of *o*-carboxyphenylglyoxal in alkaline medium [37] does not favour this hypothesis.

The transient formation of the spiro β-carboline VI should not however be eliminated, as oxogambirtannine (XXII), an alkaloid from *Uncara gambier* [38], is formed by UV irradiation of the spirane XXI [39] with the corresponding indanedione XX (Scheme 3). A similar reaction occurs with a methoxy derivative of a spiro ß-carboline [40].

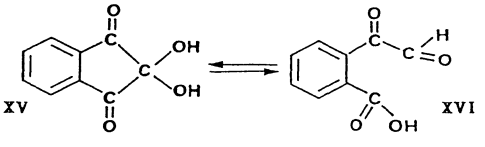

Scheme 1.

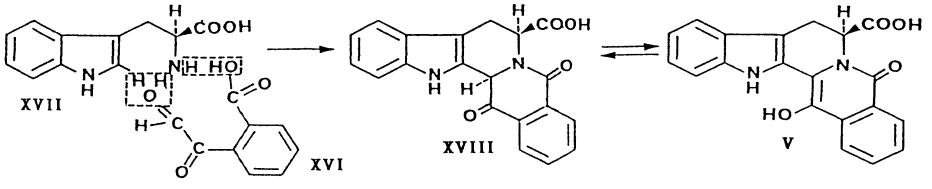

Scheme 2.

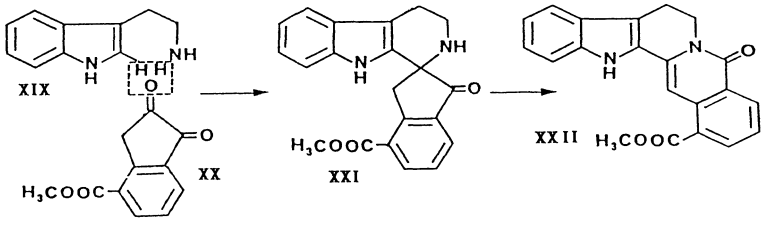

Scheme 3.

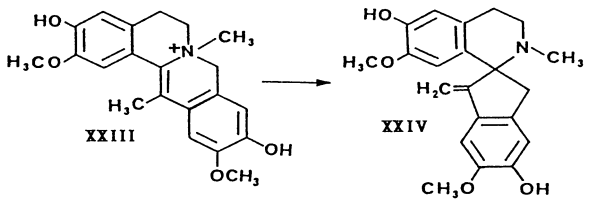

Scheme 4.

This type of rearrangement is not limited to the yohimbane series. The reverse reaction (Scheme 4) has been described in the group of protoberberine alkaloids: the diphenolic N-methosalt XXIII gives the spirane XXIV when refluxed in aqueous ethanolic sodium hydroxide [41]. The reaction illustrated in scheme 4 may be involved in the biogenesis of spirobenzylisoquinoline alkaloids [42].

These examples of a reversible rearrangement between a spirane and a compound with condensed-cycles call for an urgent confirmation (or revision) of the spiro structures described when ninhydrin reacts with cysteine [43] or with other amino compounds.

References

1. Marion L (1952) In: Manske RHF (ed.) The Alkaloids 2. Academic Press. New York, pp. 369–498.
2. Saxton JE (1960) In: Manske RHF (ed.) The Alkaloids 7. Academic Press, New York, pp. 1–199.
3. Cordell GA (1981) Introduction to Alkaloids, a Biogenetic Approach. Wiley-Interscience, New York, pp. 655–697.
4. Szantay C, Blasko G, Honty K and Dörnyei G (1986) In: Brossi A (ed.) The Alkaloids 27. Academic Press, New York, pp. 131–268.
5. Spiegel L (1896) Chem. Zeit 20: 970–971.
6. Thoms H (1897) Ber. Pharm. Ges. 7: 279–283.
7. Witkop B (1943) Ann. Chem. 554: 83–126.
8. Clemo GR and Swan GA (1946) J. Chem. Soc. 617–621.
9. Clemo GR and Swan GA (1949) J. Chem. Soc. 487–492.
10. Swan GA (1949) J. Chem. Soc. 1720–1724.
11. Swan GA (1950) J. Chem. Soc. 1534–1539.
12. Ninomiya I and Naito T (1983) In: Brossi A (ed.) The Alkaloids 22. Academic Press, New York, pp. 189–27.
13. Blasko G, Kerekes P and Makleit S (1987) In: Brossi A (ed.) The Alkaloids 31. Academic Press, New York, pp. 1–28.
14. Martin SF, Rüeger H, Williamson SA and Grzejszczak S (1987) J. Am. Chem. Soc. 109: 6124–6134.
15. Hiemstra H and Speckamp WN (1988) In: Brossi A (ed.) The Alkaloids. Academic Press, New York, pp. 271–339.
16. Heesing JA, Muller-Mathesius R and Rose H (1970) Ann. Chem. 735: 72–76.
17. Tinguy-Moreaud E de, Cicirello S, Chanh NgB and Neuzil E (1989) Bull. Soc. Pharm. Bordeaux 128: 19–31.

18. Cicirello S, Tinguy-Moreaud E de and Neuzil E (1989) Bull. Soc. Pharm. Bordeaux 128: 32–39.
19. Gilmore CJ (1984) J. Appl. Cryst. 17: 42–46.
20. Précigoux G, Courseille C, Chanh NgB, Leroy F, Tinguy-Moreaud E de and Neuzil E (1990) Acta Cryst., submitted for publication.
21. Ninomiya I, Naito T and Takasugi H (1976) J.C.S., Perkin I. 1865–1868.
22. Pandey GD and Tiwari KP (1980) Synth. Comm. 10: 523–527.
23. Ninomiya I, Takasugi H and Naito T (1973) J.C.S., Chem. Comm. 732.
24. Atta-ur-Rahman and Waheed N (1979) Tetrahedron Letters 19: 1715–1710.
25. Laguerre M, Boyer C and Atfani M (1988) Tetrahedron 44: 7109–7118.
26. Kametani T, Higa T, Van Loc C, Ihara M and Fukumoto K (1977a) Chem. Pharm. Bull. (Japan) 25: 2735–2738.
27. Chattergee A and Mukhopadhyay S (1977) Indian J. Chem. 15B: 183–184.
28. Ashamina Y and Kashiwaki K (1915) J. Pharm. Soc. Japan (Yakugakuzasshi) 35: 1273–1292.
29. Kametani T, Van Loc C, Higa T, Koizumi M, Ihara M and Fukumoto K (1977b) J. Am. Chem. Soc. 99: 2306–2309.
30. Kametani T, Ohsawa T, Ihara M and Fukumoto K (1978) Chem. Pharm. Bull. (Japan) 26: 1922–1926.
31. Hotellier F, Delareau P and Pousset JL (1975) Phytochemistry 14: 1407–1409.
32. Atta-ur-Rahman and Ghazala M (1982) Z. Naturforsch. 37B: 762–771.
33. Shafiee A and Rashidbalgi A (1977) J. Heterocycl. Chem. 14: 1317–1320.
34. Au TY, Cheung HT and Sternhell S (1973) J.C.S., Perkin I. 13–16.
35. Lukats B and Clauder O (1972) Acta Chim. Acad. Sc. Hungar. 71: 93–100.
36. Bernatek E (1958) Tetrahedron 4: 213–222.
37. Ruhemann S (1910) J. Chem. Soc. 2025–2031.
38. Merlini L, Mondelli R, Nasini G and Hesse M (1967) Tetrahedron 23: 3129–3145.
39. Irie H, Fukudome J, Ohmori T and Tanaka J (1975) J.C.S. Chem. Comm. 63.
40. Kametani T, Hirai Y, Kajiwara M, Takabashi T and Fukumoto K (1975) Chem. Pharm. Bull. (Japan) 23: 2634–2642.
41. Shamma M and Nugent JF (1970) Tetrahedron Letters 30: 2625–2628.
42. Shamma M (1971) In: Manske RHF (ed.) The Alkaloids 13. Academic Press, New York, pp. 165–188.
43. Prota G and Ponsiglione E (1973) Tetrahedron 29: 4271–4274.

Peptide and protein hydrolysis by microwave irradiation: Kinetics and refinement of hydrolysis conditions for peptide-bond cleavage

Kung-Tsung Wang and Shyh-Horng Chiou

Institute of Biochemical Sciences, National Taiwan University and Institute of Biological Chemistry, Academia Sinica, P.O. Box 23-106, Taipei, Taiwan, R.O.C.

Abstract

A rapid peptide-bond hydrolysis by means of microwave irradiation is introduced for the facile preparation of protein and peptide hydrolysates used for amino acid analysis. The optimal hydrolysis conditions have been determined using several enzymes and toxins with known amino acid compositions. The effects of hydrolysis time on the recoveries of various labile and hydrophobic amino acids are also exemplified in the microwave heating of standard amino acids. It provides a radical expedition of protein and peptide hydrolysis via commercial microwave ovens and specially-designed Teflon vials/tubes, showing greater ease than the conventional method of heating at 110°C for more than 24 h. The kinetics for the release of amino acids from various hydrophobic dipeptides is also studied in order to provide some insights into the mechanism underlying this novel type of microwave chemistry associated with specific peptide-bond cleavage.

Introduction

The advances in instrumentation of amino acid analysis have shortened the net analysis times from several hours to less than an hour for each individual sample [1]. Therefore the rate-determining and most essential step of a successful amino acid analysis now lies in the skillful preparation of protein hydrolysates. The commonly used conventional protocol of Hirs *et al.* [2] utilizes 6M hydrochloric acid and 110–120°C for more than 24 h has been the method of choice for the past thirty years. Although the recent development of gas-phase hydrolysis of protein samples [3] has been widely promoted, the reproducible and complete amino acid analysis data for most proteins are not easily obtained, except in some cases of short peptides.

We have introduced a rapid method of microwave heating for the facile preparation of protein and peptide hydrolysates [4,5]. The hydrolysis time was shortened from thirty minutes (gas phase hydrolysis) [3] to only a few minutes by microwave irradiation. This paper reports refinements of the method in order to establish microwave irradiation as a rapid and novel means of protein hydrolysis with special regard to its general application to amino acid analysis. The optimal hydrolysis conditions have been determined using several dipeptides including

Val-Val, Ile-Val and various proteins and peptides. The complete amino acid analysis of peptides and proteins with a single nonvolatile solvent of methanesulfonic acid is accomplished with good recoveries of tryptophan and half-cystine. It provides a radical method of protein and peptide hydrolysis via commercial microwave ovens and specially designed Teflon vials with the potential of on-line automation of protein hydrolysis and analysis.

Experimental

Custom-made Teflon vials (70 mm × 30 mm × 5 mm I.D.) and Teflon-Pyrex reusable hydrolysis tubes (150 mm × 4 mm I.D.) were purchased locally (The Continuity Enterprise, Taipei, Taiwan). Each vial can contain up to 0.5 ml of hydrolysis solvent. In practice, ca 0.3 ml of solvent was added for the preparation of each protein hydrolysate. The basic designs of the vials are based on inert gas flushing for removal of oxygen inside the vials [6]. The Reacti-Therm dry block heating system (Pierce, Rockford, IL, U.S.A.) was used for the conventional hydrolysis procedure of 24 h heating at 110°C. Two models of the commercial microwave ovens were used. Model MW 3500 XM (Whirlpool, Benton Harbor, MI, U.S.A.) can be controlled at several different powers for different time periods and Samsung RE 330 D is the inexpensive microwave oven with time control for one pre-set power (500 W).

4 M methanesulfonic acid containing 0.2% 3-(2-aminoethyl)-indole and standard amino acid mixture in 1 ml ampoules were obtained from Pierce. Individual amino acids in crystal form were from Merck (Darmstadt, F.R.G.) and various dipeptides, oxidized ribonuclease and oxidized insulin chain were from Sigma (St. Louis, MO, U.S.A.). Constant-boiling 12 M hydrochloric acid is redistilled in our laboratory and somatostatin derivatives synthesized by solid-phase method.

The samples (0.1–0.5 mg) were analyzed for amino acid compositions by microwave irradiation or the conventional procedure [2]. The proteins or peptides were dissolved in 0.1 ml–0.3 ml of hydrolysis solvent in the Teflon vials or the Teflon-Pyrex tubes, which were then directly flushed with nitrogen or argon gases for 1 min and sealed by screwing down the Teflon cap or Teflon plunger [6]. The vials or tubes were then put in the microwave oven at the pre-set power for different time periods or on a dry heating block set at 110°C for 24 h. At the end of heating, the hydrolysed protein solutions were pipetted into acid-cleaned vials and evaporated to dryness in a Speed Vac concentrator (Savant Instruments, Farmingdale, NY, U.S.A.) with refrigerated condensation trap.

In the HPLC analysis of *o*-phthaldehyde derivatized hydrolysates, the pH of hydrolysates was adjusted to 6.0, and then added 500 µl of *o*-phthaldehyde solution prepared according to Hurst [7] and analysed by HPLC with fluorescence detector.

Amino acid compositions were determined with the Beckman high-performance amino acid analyser (Model 6300) with dual-channel data system using a single

ion-exchange column. Reversed-phase HPLC was carried out either on a Hitachi liquid chromatograph with a Model L-6200 pump and a variable-wavelength UV monitor or Waters liquid chromatography system, consisting of Soma Model S-3350 fluorescence spectrophotometer, two Model 6000 pumps, Model 450 variable-wavelength UV detector, Model 660 solvent programmer, and Shimadzu C-R2AX chromapack. The column (300 mm × 4.0 mm I.D., Synchropak RP-C18 6.5 μm or Nucleosil C-18 7 μm beads) was used to analyse the hydrolysis products from microwave irradiation for completeness of hydrolysis.

Results and Discussion

Previous experience with Pyrex tubes commonly used for 6 M hydrochloric acid hydrolysis of proteins has indicated that the high pressure and temperature induced in the sealed hydrolysis tubes by microwave irradiation easily caused tubes to explode. The design of Teflon vials and Teflon-Pyrex tubes that can resist high temperature and pressure under microwave oven condition was described in the previous reports [4,5], and rapid protein hydrolysis can be achieved by microwave irradiation without expensive instrumentation.

Table 1. Effect of microwave irradiation on stability of amino acids

	Irradiation duration			
Amino acids	0	2 min	4 min	8 min
1/2 Cys	1.18	1.17	1.16	1.14
Asx	1.04	1.05	1.04	1.04
Thr	1.07	1.06	1.04	0.95*
Ser	1.04	1.02	0.95	0.89*
Glx	1.06	1.05	1.06	1.07
Pro	1.12	1.13	1.15	1.15
Gly	1.04	1.05	1.04	1.05
Ala	1	1	1	1
Val	1.08	1.07	1.05	1.06
Met	1.00	0.98	0.96	0.93*
Ile	0.94	0.96	0.97	1.01
Leu	1.00	1.02	1.01	1.02
Tyr	1.03	1.04	0.97	0.92*
Phe	1.01	1.03	1.02	0.99
His	1.03	1.04	1.01	0.91*
Lys	1.01	0.99	1.05	0.98
Arg	0.97	0.98	0.97	0.99

Data are expressed as relative molar ratios of 17 amino acids in standard amino-acid mixture (Pierce) detected in the chromatograms of amino acid analyzer before and after different times of microwave irradiation in 6 M HCl using alanine as the reference. Values marked with * indicated some destruction with 8 min irradiation.

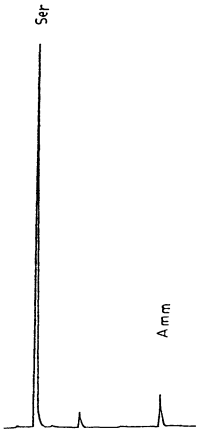

Fig. 1. Heating of serine in microwave oven: 5 min; power 80%; 12 N HCl/TFA 4:1; OPA derivative on HPLC.

Table 1 shows the effect of hydrolysis time by microwave irradiation on the recoveries of standard amino acids. It is clearly evident that microwave irradiation of amino acids in 6 M hydrochloric acid for 2–8 min did not cause destruction of most amino acids, except for some minor degradation of labile amino acids such as serine, threonine, methionine, tyrosine and histidine, which is also commonly observed during conventional analysis. These findings formed the basis for the potential application of microwave irradiation in the routine hydrolysis of peptides and proteins before amino acid analysis. Figure 1 showed the HPLC chromatogram of serine after 5 min microwave irradiation in 12 N HCl-TFA (4:1) solvent. This also showed no significant degradation during microwave irradiation.

We first applied microwave hydrolysis to oxidized insulin B chain and oxidized ribonuclease A [4]. The data correspond quite well to the theoretical values of sequence and those obtained by the conventional protocol (6 N HCl at 110°C, 24 h). The only amino acids which deviated more from the predicted values are serine and threonine, methionine, tyrosine and histidine which are also commonly observed during conventional analysis.

It is known that the nature of microwave heating precludes the conventional means of temperature determination. We have conducted a calibration of the temperature inside the Teflon vials on microwave irradiation by use of several organic compounds with known melting points. The setting of 80% full power (ca. 0.96 kW input/power) and 4 min on the control pad of the microwave oven corresponded to the temperature range between the melting points of semicarbazid hydrochloride (178°C) and p-anisic acid (186°C). Therefore the temperature of our microwave hydrolysis is tentatively shown to be ca. 180 ± 5°C by the indirect

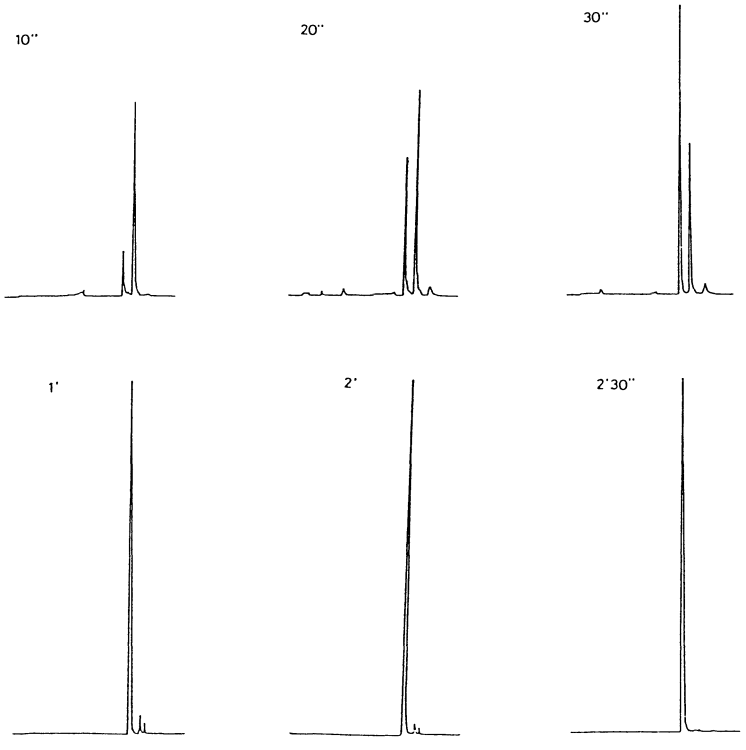

Fig. 2. The time course of hydrolysis of Val-Val; 10 sec to 2.5 min; power 80%; 12 N HCl/TFA 4:1; OPA derivative on HPLC.

method; however, the pressure inside the hydrolysis tube remains to be determined. It is to be emphasized that any commercially available microwave oven can be adapted for the purpose of rapid protein hydrolysis. For the purpose of calibrating microwave oven, we used several dipeptides to evaluate the relationship between power and time required for peptide cleavage. Previous experience has indicated that Val-Val is the most difficult to hydrolyse [8]. Therefore the hydrolysis of Val-Val dipeptide by microwave irradiation coupled with *o*-phthaldehyde derivatization and HPLC was used to follow peptide-bond cleavage and search for optimal 'power' and 'time' of different microwave ovens. Figure 2 shows the time course of hydrolysis. The same dipeptide, Val-Val, was used to determine the best acid-solvent composition. Table 2 shows the best conditions of hydrolysis with various acid solvents.

We also tried to analyze the amino acid content on Merrifield resin by microwave irradiation. Table 3 gives the results for 18 amino acid resin esters obtained by the microwave technique using the propionic acid – 12 M hydrochloric acid (1:1, v/v) with preset power of 70% of full power and a heating time of 7 min. It is

Table 2. Acidic solvents for hydrolysis of Val-Val: optimal conditions

Solvent	Time (min)	%
6 N HCl	8	78
12 N HCl	6	94
12 N HCl/TFA[a] 4/1 v/v	2	100
4 M Methanesulfonic acid	6	100

[a]TFA: Trifluoroacetic acid.

evident that this fast microwave heating yielded reproducible recoveries with standard deviations of less than 5% for most samples.

4 M Methanesulfonic acid is used to hydrolyse somatostatin derivatives which contain tryptophan and cysteine. Figure 3 shows its chromatogram of amino acid analysis. It is clear from these results, the complete amino acid analysis with a single nonvolatile methanesulfonic acid in aqueous solution could be accomplished with good recoveries of tryptophan and cysteine.

Table 3. Recovery of amino acids after microwave hydrolysis

Boc-amino acid resin[a]	Stated concentration (mmol/g resin)[b]	Found concentration (mmol/g resin)[c]	Recovery (%)
Nt-Boc-Ala	0.61	0.64 ± 0.03	103.0 ± 2.2
Nt-Boc-NO_2-Arg	0.17	0.10 ± 0.01	100.3 ± 3.1
Nt-Boc-Asn	0.40	0.33 ± 0.02	104.9 ± 0.9
Nt-Boc-Bzl-Asp	0.38	0.44 ± 0.02	99.4 ± 1.4
Nt-Boc-(S-Bzl)-Cys	0.29	0.33 ± 0.08	105.2 ± 1.7
Nt-Boc-Gln	0.35	0.41 ± 0.04	102.2 ± 3.2
Nt-Boc-Bzl-Glu	0.13	0.32 ± 0.06	102.1 ± 4.7
Nt-Boc-Gly	0.44	0.36 ± 0.03	102.4 ± 3.7
Nt-Boc-Ile	0.29	0.34 ± 0.05	117.2 ± 1.6
Nt-Boc-Leu	0.24	0.36 ± 0.03	97.6 ± 4.4
Nt-Boc-Met	0.27	0.50 ± 0.06	102.2 ± 5.1
Nt-Boc-Phe	0.70	0.78 ± 0.05	101.0 ± 4.6
Nt-Boc-Pro	0.38	0.44 ± 0.07	103.1 ± 2.5
Nt-Boc-(O-Bzl)-Ser	0.20	0.13 ± 0.04	343.7 ± 3.6
Nt-Boc-(O-Bzl)-Thr	0.37	0.30 ± 0.03	113.8 ± 2.7
Nt-Boc-Cbz-Lys	0.46	0.23 ± 0.02	103.8 ± 3.7
Nt-Boc-(O-Bzl)-Tyr	0.05	0.31 ± 0.04	107.0 ± 2.8
Nt-Boc-Val	0.13	0.40 ± 0.03	102.0 ± 3.6

[a] All N-t-Boc amino acid resin esters were obtained from Sigma, except that of alanine, which was synthesized in our laboratory. NO_2=nitro; Bzl=benzyl; Cbz=chlorobenzyloxycarbonyl.

[b] Analytical data on the labels supplied by Sigma.

[c] Data (mean ± S.D., n=3) obtained by hydrolyses of the amino acid resin esters using propionic acid-12 M hydrochloric acid at 140°C for 3 h.

Recovery (mean ± S.D., n=3) by the method of microwave heating with the mixed acid assuming the corresponding data in the previous column to represent 100%.

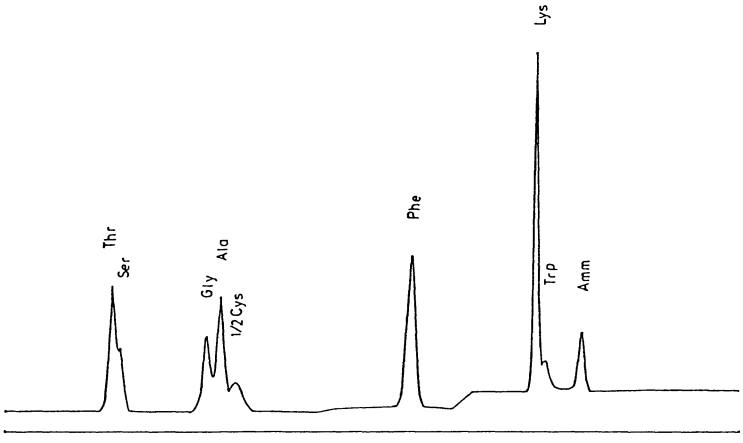

Fig. 3. Hydrolysis of bis-s-t-butyl dihydrosomatostatin; 6 min; power 80%; 4 M methanesulfonic acid; Beckman 6300 amino acid analyzer.

The selective cleavage at aspartic acid residue of protein was discussed by Inglis [9] who described the use of dilute hydrochloric acid and dilute formic acid heating under vacuum for 2 h at 108°C. We tried the same acid solvents in the hydrolysis of peptides by microwave irradiation. As shown in Fig. 4 Asp-Phe-OMe bond was hydrolysed much faster than other peptide bonds. It is possible to cleave selectively at the aspartyl bond (by microwave irradiation) and obtain specific fragments for protein sequence studies. (in preparation).

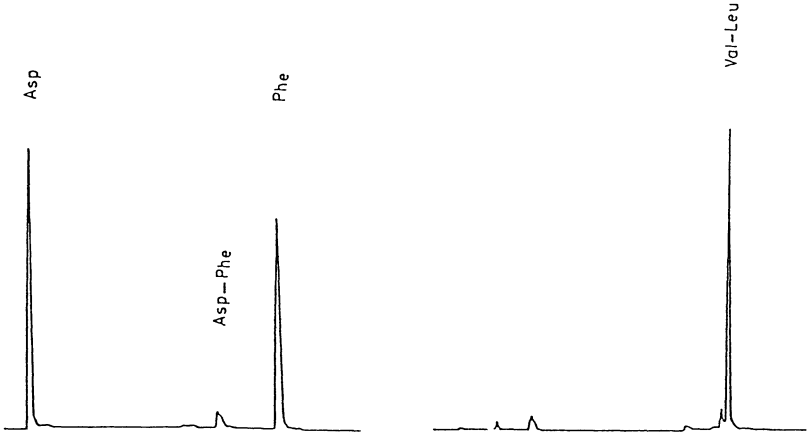

Fig. 4. Hydrolysis of Asp-Phe-OMe and Val-Leu by dilute hydrochloric acid; 2 min; power 100%; dilute HCl [9]; OPA derivatives on HPLC.

References

1. Beckman Instruments, Inc. High performance amino acid analyzers, the system 6300 series, Instruction manual.
2. Hirs CHW, Stein WH and Moore S (1954) J. Biol. Chem. 211: 941–950.
3. Instruction Manual for Waters' PICO-TAG System.
4. Chen ST, Chiou SH, Chu YH and Wang KT (1987) Int. J. Peptide Protein Res. 30: 572–576.
5. Yu HM, Chen ST, Chiou SH and Wang KT (1988) J. Chromatogr. 456: 357–362.
6. Chiou SH and Wang KT (1988) J. Chromatogr. 448: 404–410.
7. Hurst WJ, CRC Handbook of HPLC for the separation of amino acids, peptides and proteins. CRC Press, Vol. 1, p. 325.
8. Tsugita A, Uchida T, Mewes HW and Ataka T (1987) J. Biochem. 102: 1593–1597.
9. Inglis AS (1983) Methods in Enzymology 91: 324–332.

^{13}C-Leucine-Tracer-Technique in clinical research on postoperative protein metabolism

H.-J. Günther[a], W. Park[b], H. Paust[b], P. Scigalla[b], V. Schenkelberger[a], I. Reichardt[a], J.-P. Striebel[c] and H.-D. Saeger[a]

[a]Surgical Clinic, University Heidelberg, Mannheim, F.R.G.
[b]Pediatric University Hospital, Free University of Berlin, F.R.G.
[c]Department of Anaesthesia, University Clinic, Mannheim, F.R.G.

Abstract

The non-invasive ^{13}C-Leucine Infusion-Technique allows quantitative information about protein decarboxylation as well as the dynamics of the protein metabolism like protein synthesis, protein oxidation, protein degradation and protein retention. In clinical research it is possible to compare the quality of different nutrition regimen with regard to protein-sparing effects by this method without irritation of the patient and without interrupting his nutrition. Two clinical investigations had been performed at the Surgical University Clinic Mannheim to study postoperative protein metabolism:

1. on the influence of different carbohydrates (Xylitol/Glucose) concerning postoperative protein metabolism during a hypocaloric nutrition regimen and
2. on the course of the individual postoperative protein metabolism during different phases after the operation and in comparison of two requirement-adapted nutrition regimen.

Results

1. Our first study showed no influence of the applied carbohydrate (Xylitol or Glucose) to the postoperative protein metabolism.
2. The comparison of a peripheral-venous nutrition regimen composed of maltose (12%), amino acid solution (7%) and fat (20%) (2,000 kcal, 650 mosm/l) with a central-venous nutrition regimen composed of glucose/laevulose/xylitol (40%) and amino acid solution (7%) (2,000 kcal, >2,000 mosm/l) showed no changes in postoperative protein metabolism. Contrary to the accumulated nitrogen balance the ^{13}C-Leucine-Tracer-Technique showed still a light catabolism even on the fifth day after operation.

Introduction

Investigations of the last years showed that the determination of the 'classic' parameters of the protein metabolism like amino acid analysis, nitrogen balances, analysis of the short lived proteins, often cannot give exact and quantitative results. Because ethical reasons do not allow the use of radioactive tracers for *in vivo* investigations anymore, stable isotopes have been established in clinical research more and more. The non-invasive ^{13}C-Leucine-Tracer-Technique yields quantitative information about protein decarboxylation and dynamics of the protein metabolism such as protein synthesis, protein oxidation, protein degradation and protein

retention [1–3]. For example with this method it is possible to compare the quality of different nutrition regimen with regard to their protein-sparing effect without bothering the patient and without interrupting his (e.g., parenteral) nutrition.

During the last two years two clinical randomised studies had been performed with the ^{13}C-Leucine Tracer-technique in order to study the postoperative protein metabolism rising two questions:

1. Do different carbohydrates (Glucose or Xylitol) take influence on the post-operative protein metabolism in a hypocaloric nutrition regimen?
2. Does a requirement-adapted parenteral nutrition (2,000 kcal) applied by peripheral-venous catheter and composed of maltose (12%), amino acids (7%) and fat (20%) have the same effects on postoperative protein metabolism as an isocaloric parenteral nutrition applied by a central venous catheter?
3. Is it possible to compare accumulated nitrogen balances with the results of the ^{13}C-Leucine-Tracer-Technique with regard to protein retention and catabolism.

Materials and Methods

Essential reasons for the use of ^{13}C-labelled Leucine are:

1. Leucine as an essential amino acid is not synthesised by the organism itself, that means plasma levels of leucine only can be maintained by exogenous intake or proteolysis; an additional effect is the regulatory influence of leucine on the other branched chain amino acids [3,4].

2. The very special biochemical breakdown of leucine (Fig. 1). The first step in breakdown is the deamination to α-cetoisocaproate; this is a reversible step which takes place in the muscle. As supplier of amino acids, muscle tissue plays the most important part in maintenance of their homeostasis.

The next (irreversible) step is the decarboxylation, done in the liver into iso-valeryl-coenzyme A (which leads into the citric-acid circle after decomposition to acetyl-coenzyme A) and CO_2, which will be expired through the lungs.

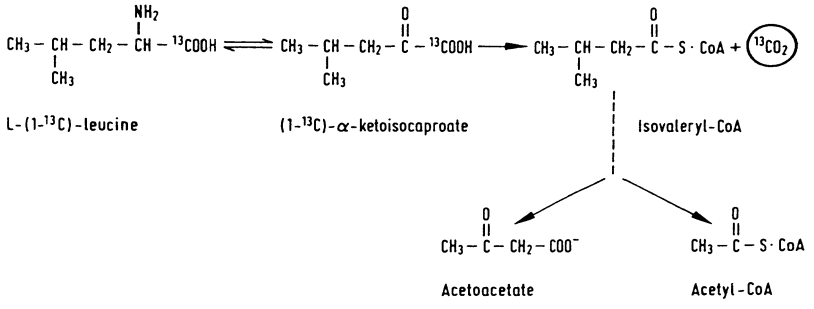

Fig. 1. L-(1-^{13}C)-leucine metabolism.

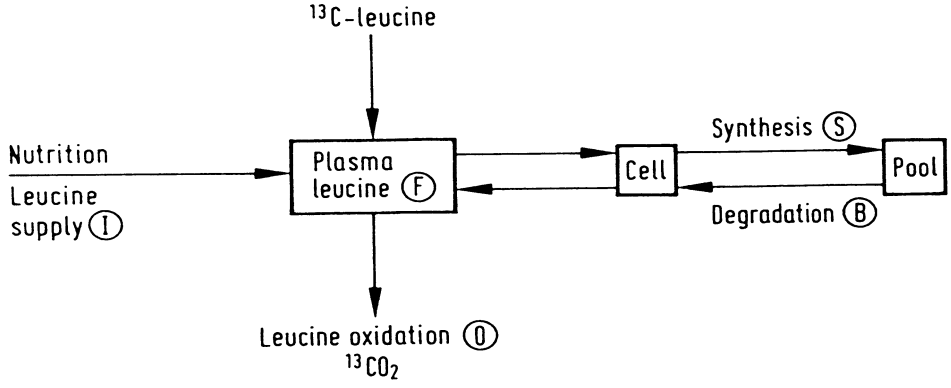

Fig. 2. 'Pool model' (Sprinson and Rittenberg).

If Leucine is labelled on its carboxyl-group with ^{13}C and then infused, it is possible to determine during the steady state the decarboxylation rate (and so the oxidation rate) by analysing the expired CO_2.

For analysing the dynamic aspects of the protein metabolism Sprinson and Rittenberg developed their pool model [5], which was modified by Matthews and Bier (Fig. 2). Their idea was the appearance of a steady state between the single

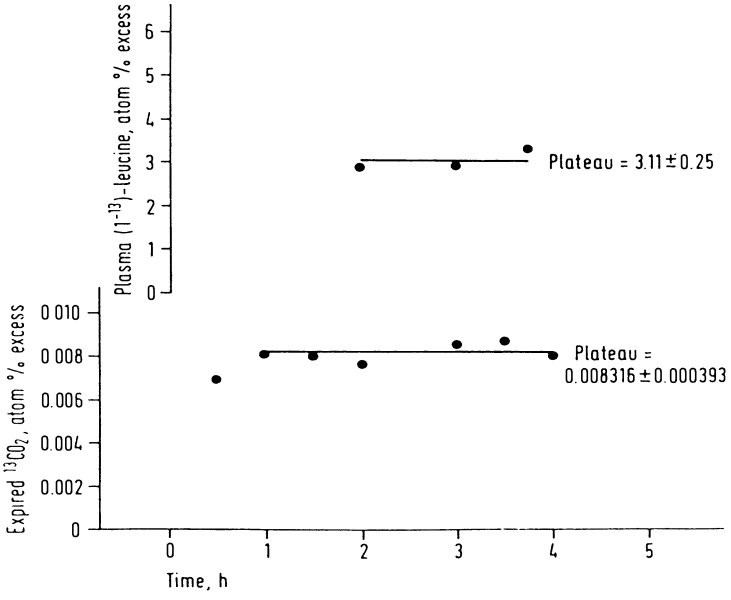

Fig. 3. ^{13}C-enrichment (atom%-excess) in plasma and breath during L-(1-^{13}C)-leucine infusion (exemplary).

compartments under a continuous ^{13}C-Leucine infusion [1,2]. By doing that, these parameters, which describe the leucine metabolism, could be determined (Fig. 3):

$$\text{Flux} = \text{Oxidation} + \text{Synthesis} = \text{Intake} + \text{Breakdown}$$

The quantity of the infused leucine is known. The oxidation rate is measured by analysing the expired CO_2. Flux is determined by gaschromatography/mass-spectrometry of the ^{13}C-Leucine-concentration in plasma. With the above mentioned equation both synthesis rate and breakdown can be calculated [1,3].

Project 1

Under a hypocaloric nutrition regimen the protein sparing effect of the infused carbohydrates is well known. Today glucose as well as fructose, sorbitol (precursor of fructose) and xylitol are in common use. Because of a possible intolerance the use of fructose (and therefore sorbitol) is being questioned again. It has not been decided yet, wether glucose or xylitol have better effects on the postoperative protein metabolism. In the current literature the discussion is still controverse [6,7].

Test conditions

Our first study was performed at the Surgical University Clinic Mannheim including 20 patients (mean age: 52.4 years). After the operation (e.g., intestinal resection or gastric resection) the patients had been divided in two groups by randomisation:

Group I was fed by a hypocaloric nutrition regimen containing Glucose (120 g/day) and amino acids (1 g/kg/day).

Group II was fed by a hypocaloric nutrition regimen containing xylitol (120 g/day) and amino acids (1 g/kg/day).

On day 3 postoperative day we performed the ^{13}C-Leucine-breath-test. Over the whole period of our study we analysed also the 'classic' parameters of the protein metabolism like urea-production-rate, nitrogen balances, short-lived-proteins and the usual laboratory parameters.

Results

In group I (glucose) the protein retention was –0.43 g/kg/day, in group II (xylitol) –0.56 g/kg/day; the difference is not significant (Table 1). Also all the other laboratory parameters showed no difference. The rapid increase of total protein, albumin and pre-albumin point at the positive effect of the hypocaloric nutrition regimen. On the basis of our investigations, especially the results of the ^{13}C-Leucine-Tracer-technique, we can conclude that the positive effect of the hypocaloric parenteral nutrition is independent of the applied carbohydrate.

Table 1. Results of the ^{13}C-leucine-infusion-technique (project 1: xylitol vs. glucose)

	Xylitol	Glucose
Leucine-Oxidation-Rate (%)	x = 18.17 ± 4.60	x = 18.14 ± 5.31
Protein-Turnover (g/kg/day)	x = 7.91 ± 2.75	x = 7.05 ± 2.13
Protein-Synthesis (g/kg/day)	x = 6.55 ± 2.36	x = 5.82 ± 1.75
Protein-Breakdown (g/kg/day)	x = 7.11 ± 2.75	x = 6.25 ± 2.13
Protein-Rentention (g/kg/day)	x = –0.56 ± 0.65	x = –0.43 ± 0.49

Project 2

In case a patient needs a total parenteral nutrition for a time longer than 5 days, he will need a requirement-adapted nutrition regimen (= 2,000 kcal/day). Usually the osmolarity of those kind of infusions is over 800 mosm/l (mostly >2.000 mosm/l) and can only be applied by a central venous catheter including the possible high risks of this kind of application [8]. Therefore we tried to find out whether it would be possible to apply a requirement-adapted nutrition regimen by a peripheral-venous catheter (see above).

Test conditions

Our second study with stable isotopes was also performed as a randomised study including 20 patients. This study was done similar to the first project.

The composition of both parenteral nutritions is mentioned above. The ^{13}C-Leucine-breath-test was performed on day 3 and day 5 postoperative. All the usually taken laboratory parameters had been analysed, also short-lived proteins and amino acids-levels in plasma.

Results

The results of the ^{13}C-Leucine-Tracer-Technique (protein oxidation, protein synthesis, protein breakdown, protein retention) are shown in Table 2 and 3.

Comparing the metabolic utilisation of both nutrition regimen, we found no difference. Both plasma amino acid and short-lived protein levels also showed no difference. While the protein retention (measured by the ^{13}C-Leucine-Tracer-Technique) is still negative on the 5th postoperative day, the accumulated nitrogen balance shows a strong increase after the operation and is already positive on the 3rd postoperative day (Fig. 4).

Conclusions of project 1 and 2

1. Postoperative protein metabolism is completely independent of the type of carbohydrate during hypocaloric parenteral nutrition.

Table 2. Results of the ^{13}C-leucine-infusion-technique, postoperative day 3 (project 2: maltose/amino acids/fat vs. glucose/laevulose/sorbitol/amino acids)

	Maltose	Glucose
Leucine-Oxidation-Rate	x = 1.01 ± 0.21	x = 1.35 ± 0.75
Protein-Turnover	x = 5.24 ± 0.91	x = 8.31 ± 2.85
Protein-Synthesis	x = 4.22 ± 0.75	x = 6.96 ± 2.25
Protein-Breakdown	x = 4.42 ± 0.91	x = 7.56 ± 2.86
Protein-Rentention	x = –0.20 ± 0.21	x = –0.60 ± 0.71

Table 3. Results of the ^{13}C-leucine-infusion-technique postoperative day 5 (project 2: maltose/amino acids/fat vs. glucose/laevulose/sorbitol/amino acids)

	Maltose	Glucose
Leucine-Oxidation-Rate	x = 1.33 ± 0.68	x = 1.20 ± 0.24
Protein-Turnover	x = 6.39 ± 1.72	x = 6.73 ± 2.08
Protein-Synthesis	x = 5.06 ± 1.15	x = 5.53 ± 1.84
Protein-Breakdown	x = 5.58 ± 1.73	x = 5.99 ± 2.09
Protein-Rentention	x = –0.52 ± 0.69	x = –0.46 ± 0.25

2. It is possible to apply a requirement-adapted parenteral nutrition regimen by a peripheral venous catheter using maltose (12%), amino acids (7%) and fat (20%), which has the same metabolic quality as a common parenteral nutrition applied by a central-venous catheter.
3. Calculated accumulated nitrogen balances are not suitable to judge correctly the postoperative protein metabolism. Obviously the catabolism in the postoperative period is not as strong as suspected yet, but it lasts longer.

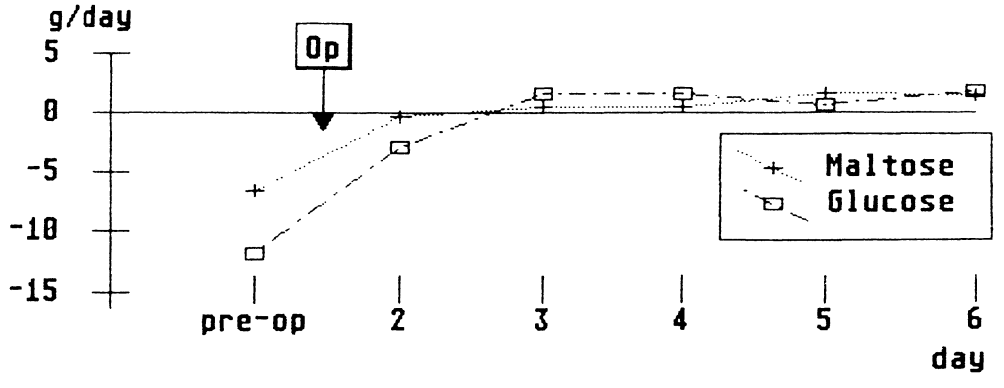

Fig. 4. Accumulated nitrogen balance (project 2).

References

1. Matthews DE, Motil KJ, Rohrbaugh DH, Burke IF, Young VR, Bier DM (1980) Measurement of leucine metabolism in man from a primed continuous infusion of L-(1-^{13}C)-leucine. Am. J. Phys. 238: E473–E479.
2. Matthews DE, Schwarz HP, Yang RD, Motil KJ, Young VR, Bier DM (1982) Relationship of plasma leucine and α-ketoisocaproate during a L-(1-^{13}C)-leucine infusion in man: a method for measuring human intracellular leucine tracer enrichment. Metabolism 31: 1105–1112.
3. Park W, Paust H, Knoblach G, Frauendienst-Egger G, Scigalla P (1988) Untersuchungen zur Dynamik des Proteinmetabolismus mit ^{13}C-markierten Aminosäuren. In: Eckart J, Wolfram G (eds.) Klinische Ernahrung. Zuckschwerdt, München, Vol. 31, pp. 121–134.
4. Bier DM, Matthews DE (1982) Stable Isotope Tracer Methods for *In Vivo* Investigations. Fed. Proc. 41: 2679–2685.
5. Sprinson DB, Rittenberg D (1949) The Rate of Interaction of the Amino Acids of the Diet with the Tissue Proteins. J. Biol. Chem. 180: 715-716.
6. Georgieff M, Moldawen LL, Bistrian BR, Blackburn GL (1985) Xylitol an Energy Source for Intravenous Nutrition. JPEN 9: 199–209.
7. Löhlein D, Zick R (1981) Zuckeraustauschstoffe oder Glucose bei der peripherven̈sen hypokalorlschen Ernährung. Infusionstherapie 3: 133–140.
8. Förster H, Hoos I, Boecker S (1976) Versuche mit Probanden zur parenteralen Verwertung von Maltose Z. Ernährungswiss. 15: 284–293.

Adress for correspondence: Dr. Hans-Joachim Günther, Surgical Clinic, Theodor-Kutzer-Ufer, Klinikum Mannheim der Universität Heidelberg, D-6800 Mannheim 1, F.R.G.

Effect of Na^+ electrochemical potential energy on system A Amino acid transport in rat skeletal muscle during endotoxic shock

Michael D. Karlstad[a,b] and John T. Chesney[b]

[a]Departments of Medical Biology and [b]Department of Anesthesiology, The University of Tennessee Medical Center at Knoxville, Knoxville, TN 37920, USA

Abstract

We previously reported a decrease in Na^+ dependent amino acid (AA) transport by endotoxic rat soleus muscle, *in vitro*. This study evaluated the kinetics of AA transport *in vitro*, active AA transport *in vivo* and intra- and extracellular Na^+ concentration (mmol/L) and the calculated chloride equilibrium potential (mv) in endotoxic soleus muscle. Fasted male rats (90 g) received an i.v. injection of the system A AA analog alpha-aminoisobutyric acid (AIB) (1 mg/kg) and *Salmonella enteritidis* endotoxin (ETX) (20 mg/kg) or saline (SAL) and were killed 4–5 h later. Kinetic parameters V_{max} (nmol/g dry wt/min) and K_m (mM) were estimated from initial rates of AIB uptake during incubations in O_2-Krebs with various [AIB] (0.1–20 mM). AIB uptake by muscle *in vivo* was expressed as a distribution ratio (DR; [AIB]intracell/[AIB]extracell) to assess active AA transport.

	AIB DR	V_{max}	Km	[Na^+]intra	[Na^+]extra	Cl^- Eq. Pot.
SAL	4.7 ± .3	56 ± 3.3	1.7 ± 1	9.3 ± 1.1	134 ± 0.9	−89.4 ± 3.5
ETX	2.8 ± .2[a]	18 ± 1.9[a]	1.6 ± .2	15.9 ± 0.9[a]	119 ± 1.3[a]	−52.7 ± 1.6[a]

Values = mean ± SE, [a]P<0.01 ETX vs SAL.

The 40% decrease in active AA transport *in vivo* in endotoxic rats is comparable to that measured previously *in vitro*. The altered transport is likely due to a decrease in the number of system A transport carriers and/or a decrease in the activity of existing transporters in the membrane (V_{max}) and not due to a change in membrane carrier affinity (K_m) for AIB. The change in active AA transport is consistent with a decrease in the energy of the Na^+ electrochemical potential gradient in endotoxic muscle. Alterations in AA transport may limit the availability of AA for skeletal muscle protein synthesis in endotoxic shock.

Introduction

Endotoxemia is associated with marked alterations in amino acid and protein metabolism [1–4]. The effects of injury on plasma and tissue amino acid concentrations may be linked to changes in amino acid incorporation and release rates from tissue proteins combined with alterations of specific cell membrane amino acid transport systems. Protein synthesis and neutral amino acid transport by system A are depressed in skeletal muscle during sepsis [5] and following an

intravenous injection of endotoxin in rats [1–4]. This inhibition of system A amino acid transport in skeletal muscle may be due to a decrease in the free energy of the transmembrane Na^+-electrochemical potential gradient [3]. The free energy of this gradient and the presence of extracellular Na^+ are required for active transport of neutral amino acids by system A [1,6–8].

One of the metabolic responses to injury is an increase in skeletal muscle protein breakdown and the release of amino acids for increased hepatic gluconeogenesis necessary to meet the needs of glucose dependent tissues [9,10]. The accelerated release of amino acids from skeletal muscle in injury is due to an increase in the rate of protein breakdown and possibly to a loss of energy used to maintain amino acid concentration gradients across the cell membrane. Amino acids transported into the intracellular compartment of skeletal muscle can be oxidized for energy or incorporated into newly synthesized protein. An inhibition of amino acid transport could limit the availability of amino acids for cellular metabolism and contribute to the loss of protein by limiting protein synthesis in skeletal muscle.

In this study we investigated active amino acid transport *in vivo* and the kinetics of system A amino acid transport *in vitro* in skeletal muscle during endotoxic shock and show that the mechanism of decreased alpha-aminoisobutyric acid (a non-metabolizable amino acid analog of system A) transport is due to a decrease in the number of carriers and/or a decrease in the activity of existing transporters in the membrane and not due to a change in membrane carrier affinity for amino acid. In addition, we examined the effects of endotoxic shock on electrolyte concentration gradients and calculated chloride equilibrium potential in soleus muscle and show that the decrease in active amino acid transport *in vivo* may be due, at least in part, to a decrease in the energy of the Na^+-electrochemical potential gradient.

Methods

Measurement of alpha-aminoisobutyric acid uptake, in vitro

Male Sprague-Dawley rats (Holtzman Co., Madison, WI) weighing 80–100 g were fasted overnight and allowed water *ad libitum* prior to experiments. Rats were briefly anesthetized with diethyl ether for a sublingual vein injection of saline or 20 mg/kg *Salmonella enteritidis* endotoxin (LD_{32} at 5 h) (Boivin, Difco Laboratories, Detroit, MI). Two additional groups of rats were given an intravenous injection of a non-lethal dose of 1 or 10 mg/kg endotoxin. Rats were killed five hours later by decapitation and the soleus muscles removed and placed in chilled oxygenated Krebs-Ringer bicarbonate buffer (KRB). The tendons were attached to a stainless steel holder to maintain normal muscle resting length. Isolated soleus muscles (40 mg) were incubated at 37°C in a Dubnoff metabolic shaker incubator for up to 3 h in KRB (3–5 ml), pH 7.4, which was equilibrated with 95% O_2:5% CO_2 and contained 5.6 mM glucose. The incubation medium also contained alpha-amino-(1-^{14}C) isobutyric acid (AIB) (0.23–1.4 μCi/ml) with sufficient unlabeled AIB to

yield AIB concentrations up to 20 mM. Soleus muscles were removed from the medium at the end of incubation and lightly blotted on filter paper to remove adherent surface radioactivity. Muscles were weighed and solubilized in 2 ml TS-1 tissue solubilizer (Research Products International, Mount Prospect, IL). Scintillation fluor was added to vials containing dissolved muscles and media samples (0.1 ml) and radioactivity counted in a Packard Tri-Carb 460C liquid scintillation counter. Quenching of radioactive counts was corrected by an external standard technique.

Measurement of alpha-aminoisobutyric acid uptake, in vivo

Soleus muscle amino acid transport *in vivo* was determined in control and endotoxic rats by sublingual vein injection of 1 mg/kg or 10 mg/kg AIB (2 μCi/ml) dissolved in 0.9% saline. Shock was induced by the intravenous injetion of 20 mg/kg *S. enteritidis* endotoxin subsequent to the injection of AIB. AIB uptake was determined in control and endotoxic soleus muscles at 1, 2, 3, 4, 5 hours later and at 8 and 24 hours for the controls. Radioactivity in muscle and plasma was determined as above.

Determination of soleus muscle extracellular space

Extracellular space was determined in separate experiments by measuring soleus muscle uptake of inulin-(^{14}C)carboxylic acid (0.2 μCi) (Amersham, specific activity 17.1 mCi/mmol) *in vitro*. Extracellular space of soleus muscle *in vivo* was determined by intravenous injection of inulin(^{14}C)carboxylic acid (0.1 μCi/kg) in control and endotoxic rats. Rats were bilaterally nephrectomized 30 minutes prior to inulin injection to prevent the clearance of inulin from the plasma compartment by the kidneys [11]. Extracellular space was calculated as the ratio of muscle radioactivity (dpm/g) to media or plasma radioactivity (dpm/ml). The concentration of inulin in plasma or media was assumed to be equal to the concentration in muscle interstitial water. Total tissue water (ml/g) was calculated for each muscle from its wet weight/dry weight ratio.

Calculations and electrolyte measurements

AIB transport into the intracellular compartment of skeletal muscle was calculated after determining the content of AIB in the extracellular (inulin) compartment. The distribution ratio of AIB was calculated by dividing the intracellular concentration of AIB by the extracellular AIB concentration. Muscles were dried in a vacuum oven for 24 hours at 100°C. Cellular AIB uptake was calculated as the amount present in the intracellular fluid divided by the dry weight of the muscle and was expressed in nmol/g dry tissue. Electrolytes were determined in tissues of control and endotoxic rats. Na^+ and K^+ were analyzed in plasma (0.1 ml) and nitric acid digestations of soleus muscles by means of atomic absorption spectroscopy (Perkin-Elmer, Model 603). Cl^- was analyzed in plasma and muscle by means of

electrometric titration in a Buchler-Cotlove chloridometer [12]. Concentrations of Na^+, K^+, and Cl^- in muscle were determined using the calculations described above.

Statistical analysis

Data were expressed as means ± SE. Results were analyzed using a one- or two-way analysis of variance, least significant difference test, or Student's t-test modified for unpaired replicates. For the double reciprocal plots, the error values of the slope and the intercept were determined and used to calculated the SE for V_{max} and K_m. Slopes were analysis with analysis of covariance. A 'P' value less than or equal to 0.05 was considered significant.

Results

Table 1 shows soleus muscle AIB uptake and AIB distribution ratios ([AIB]intracell/[AIB]extracell) in rats following an intravenous injection of saline or 1, 10, or 20 mg/kg endotoxin. AIB uptake by endotoxic muscle was similarly depressed over the twenty fold range of endotoxin doses as compared with the saline group. The distribution ratio was similarly depressed in endotoxic muscle as compared to the controls. These data show that soleus muscle AIB transport is similarly affected over a wide range of endotoxin doses and indicate that amino acid transport is sensitive to relatively low levels of endotoxin.

To determine if decreased AIB uptake by endotoxic muscle was due to an alteration of the Na^+ dependent portion of AIB uptake, Na^+ was removed from the incubation medium and replaced with another monovalent cation, choline (see Fig. 1). Previous investigators have shown that choline does not, by itself, affect total tissue water, extracellular space or membrane permeability to nonpermeant solutes [8,13]. Figure 1 shows that AIB uptake in the presence of Na^+ (Na^+=142 mM) by endotoxic soleus muscles was 34% lower than controls. AIB uptake in the presence of choline chloride ([Na+]=0 mM) was not significantly different between control and endotoxic soleus muscles ($P>0.05$). AIB uptake in the absence of Na^+ was approximately one half its value in the presence of Na^+ for control muscles. The AIB distribution ratio for control and endotoxic muscles in the absence of Na^+ was less than one, indicating a loss of active AIB transport.

Table 1. AIB transport in control and endotoxic soleus muscles, *in vitro*

Endotoxin (mg/kg)	N	AIB uptake (nmol/g dry wt/2 h)	AIB distribution ratio ($[AIB]_{IC}/[AIB]_{EC}$)
Control	16	15.10 ± 0.49	1.48 ± 0.05
1	15	9.5 ± 0.37[a]	0.97 ± 0.04[a]
10	22	10.15 ± 1.03[a]	1.03 ± 0.03[a]
20	12	10.03 ± 0.40[a]	1.06 ± 0.06[a]

N = no. of muscles; [a]$P \leq 0.001$ compared to control muscles.

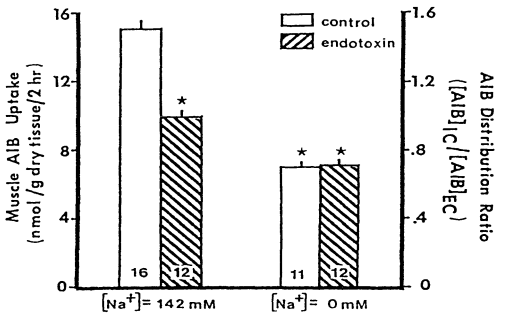

Fig. 1. Effect of Na^+ on cellular AIB uptake and AIB distribution ratio by control and endotoxic soleus muscles. Values are means ± SE for no. of muscles given within bars. *Stars*, values significantly different ($P<0.001$) from control muscle AIB uptake in the presence of Na^+.

The kinetic behavior of system A amino acid transport was investigated in order to better understand the mechanism of amino acid transport disturbances in soleus muscle during endotoxic shock. The maximum rate of entry (V_{max}) and apparent K_m for saturable AIB uptake by control and endotoxic soleus muscles were determined from reciprocal plots of initial rates of entry and extracellular AIB

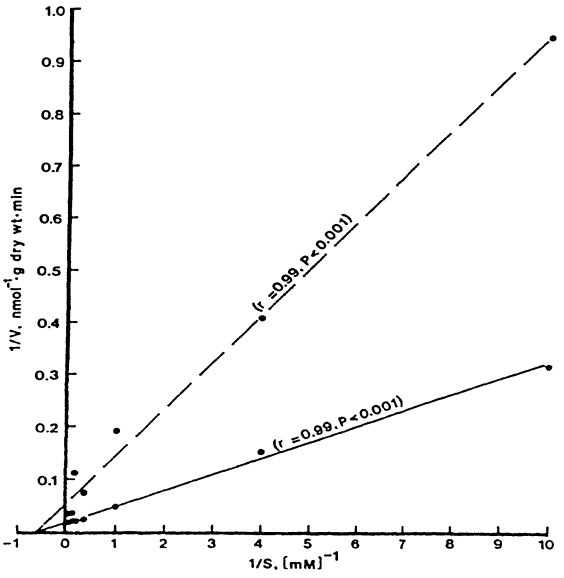

Fig. 2. Double reciprocal plot of initial rates of saturable alpha-aminoisobutyric acid (AIB) transport vs. AIB concentration for control and endotoxic soleus muscles. (———), control; (– – –), endotoxin. Correlation coefficients (r) and significance of individual regression lines are shown (least-square analysis). Slopes are significantly different between control and endotoxic muscles ($P<0.001$). See Table 2 for values of maximal rate of AIB transport and apparent K_m.

Table 2. V_{max} and K_m of control and endotoxic soleus muscles

Group	n	V_{max} (nmol × g dry wt^{-1} × min^{-1})	K_m (mM)
Control	62	55.6 ± 3.3	1.68 ± 0.12
Endotoxin	67	18.3 ± 1.9[a]	1.64 ± 0.19

Values are means ± SE, *n*, no. of muscles, [a]P≤0.01 compared to control.

concentration according to the graphical method of Lineweaver-Burk [14] (see Fig. 2). The method of least squares was used to fit regression lines of these plots to determine the kinetic parameters, V_{max} and K_m. The large decrease in the rate of entry of saturable AIB transport into endotoxin muscles was due to a 69% decrease in V_{max} (P≤0.01). The values of apparent K_m for saturable AIB transport were not different between control and endotoxic soleus muscles (P>0.05) (see Table 2).

The following experiments were performed to determine if the *in vitro* transport disturbances in soleus muscles were present *in vivo* during endotoxic shock. Fig. 3 shows for control and endotoxic rats the AIB distribution ratio in soleus muscle at various times after an intravenous injection of AIB (1 mg/kg). The distribution ratio was calculated using muscles from separate experiments at each time point. A distribution ratio greater than one indicates active AIB transport by soleus muscle. The distribution ratio was greater than 1 by 1 hour and increased to a steady-state level by 4 hours and was not different at the 5, 8 or 24 hour measurement in control muscles (P≥0.05). The AIB distribution ratio was greater than 1 by 1 hour in endotoxic soleus muscle and increased further until 3 hours and then did not change from this level for the next 2 hours (P≥0.05). The capacity for active accumulation of AIB in endotoxic soleus muscle at 4 and 5 hours was significantly lower than controls (P≤0.0001). The steady state AIB distribution ratio is an

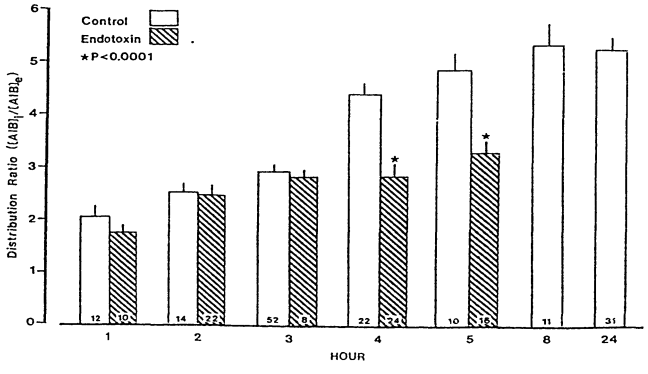

Fig. 3. AIB distribution ratios in control and endotoxic soleus muscles at various times after intravenous injection of AIB. Values are means ± SE for number of muscles given at each time point. (*), significant differences (P<0.0001) between control and endotoxic muscles at each time point.

accurate index of AIB transport by skeletal muscle because it is independent of plasma AIB concentration or changes in AIB delivery to muscle [15,16]. Increasing the concentration of AIB in plasma 10-fold (by altering the dose) increased the content of AIB in muscle but did not produce significant changes in the distribution ratio. The distribution ratio of AIB in control muscle 4 hours after intravenous injection of 1 mg/kg or 10 mg/kg AIB was 4.4 ± 0.2 (n=22) and 4.2 ± 0.2 (n=14), respectively ($P \geq 0.05$).

Electrolyte concentrations were determined in soleus muscles removed from control and endotoxic rats without *in vitro* incubation and are shown in Table 3. The decrease in plasma Na^+ and increase in plasma K^+ in endotoxin rats was small but significantly different as compared to controls ($P \leq 0.05$). Plasma Cl^- concentration was not different between the groups ($P > 0.05$). Changes in the intracellular concentrations of electrolytes in the endotoxic muscles included a 70% increase in Na^+, an 11% decrease in K^+, and a 257% increase in Cl^- as compared to control muscles ($P \leq 0.005$). The calculated chloride equilibrium potential was significantly lower in endotoxic muscles as compared to the control muscles. For the *in vivo* experiments, the intracellular concentrations of Na^+, Cl^-, K^+ and AIB were calculated using values of 0.216 ± 0.005 ml/g (n=18) for the extracellular space and 0.774 ± 0.005 ml/g (n=18) for the water content of control soleus muscles. The intracellular concentrations in endotoxic soleus muscles were calculated using values of 0.168 ± 0.004 ml/g (n=36) for the extracellullar space and 0.771 ± 0.001 ml/g (n=36) for total water. The intracellular space in endotoxic muscle (0.603 ± 0.004 ml/g; n=36) was significantly greater as compared to control muscles (0.558 ± 0.008 ml/g; n=18) ($p \leq 0.001$). The increase in intracellular water in endotoxic soleus muscle could be due to a shift of fluid from the extracellular space as there was no change in total tissue water.

Discussion

System A amino acid transport has been shown to transport neutral amino acids such as alanine, proline, serine, glycine, and the non-metabolizable analog, alpha-aminoisobutyric acid [7,17,18]. It has been shown that most if not all the energy used to transport type A amino acids is supplied by the free energy of the Na^+-electrochemical gradient [6,19,20]. Thus, the driving force for the active accumulation of amino acids is dependent on both the activity of the Na^+/K^+-pump and membrane ion permeabilities to Na^+ and K^+. It follows that a reduction of Na^+-electrochemical energy would adversely influence the transport characteristics of system A and decrease active amino acid transport. The results of this study show that the *in vivo* steady state distribution ratio of AIB in endotoxic muscle was substantially lower than controls, and that this was associated with a lower capacity for active amino acid transport. This study and others have shown that the plasma AIB concentration over a wide range (100-fold) does not affect the steady state AIB distribution ratio in soleus muscle [15,16]. The decrease in AIB distribution

Table 3. Electrolyte concentrations and Cl^- equilibrium potential in control and endotoxic muscles

Group	Extracellular Electrolytes[a] (mmol/L)			Intracellular Electrolytes (mmol/L cell water)			Cl^- Equilibrium potential (mV)
	[Na]	[K]	[Cl]	[Na]	[K]	[Cl]	
Control	134 ± 0.9	4.5 ± 0.3	101 ± 1.0	9.3 ± 1.1	164 ± 1.5	4.1 ± 0.6	−89.4 ± 3.5
(n)	(6)	(6)	(16)	(12)	(12)	(16)	(16)
Endotoxin	119 ± 1.3[b]	5.4 ± 0.3[c]	102 ± 1.0	15.9 ± 0.9[b]	145 ± 1.7[b]	14.6 ± 0.9[b]	−52.7 ± 1.6[d]
(n)	(11)	(11)	(9)	(21)	(21)	(10)	(18)

[a]Concentrations in plasma; values are means ± SE; n, no. of muscles; [b]$P \leq 0.0005$, [c]$P \leq 0.05$ and [d]$P \leq 0.0001$ compared with control.

ratio in endotoxic muscle was not a function of plasma AIB concentration or AIB delivery to muscle but rather due to an intrinsic alteration of system A amino acid transport.

This study has also shown a decrease in system A amino acid uptake by skeletal muscle of rats in endotoxic shock, *in vitro*. The depression of cellular AIB uptake by endotoxic muscle was similar over a twenty-fold range of endotoxin doses. The fact that AIB uptake in Na^+-free media was the same in control and endotoxic muscle implies that the membrane carrier responsible for the facilitated transport of AIB into skeletal muscle was functional during endotoxic shock. The decrease in basal AIB uptake by endotoxic muscles was therefore due to an alteration in the Na^+-dependent portion of the uptake process. Na^+-dependent AIB uptake, calculated as the difference between AIB uptake in the presence and absence of Na^+, was decreased in shock to 36% of the control value.

The chloride equilibrium potential was calculated for control and endotoxic soleus muscles as an approximation of the membrane potential. The decrease in intracellular $[K^+]$ and chloride equilibrium potential and intracellular accumulation of $[Na^+]$ and $[Cl^-]$ in endotoxic muscle indicate an alteration of the transmembrane movement of ions and are consistent with an increase in the ratio of membrane permeability to Na^+ relative to K^+ and/or a decrease in the activity of the Na^+/K^+ pump. The lower values of membrane potential and Na^+ and K^+ concentration gradients for endotoxic muscle, as compared with controls, would indicate a loss of Na^+-electrochemical potential energy for active amino acid transport. Previous studies have shown that the transport of Na^+ and K^+ is altered in skeletal muscle and liver during shock and other forms of trauma [21–25]. Others have shown a large reduction of transmembrane potential in skeletal muscle during endotoxic shock [22,23,25]. Since the magnitude of the electrochemical potential gradient for Na^+ across the cell membrane determines the extent of AIB accumulation in skeletal muscle, the decrease in active AIB transport measured *in vitro* and *in vivo* are consistent with a decrease in the availability of energy of the Na^+-electrochemical gradient in muscle.

The lowering of Na^+-electrochemical potential energy in skeletal muscle would offer an explanation for the decrease in V_{max} for amino acid transport by endotoxic muscle since the activity of AIB transport carriers in the membrane would be affected by the availability of energy. Since the apparent affinity (K_m) of amino acid carrier for AIB is not affected in endotoxic muscle, the mechanism of altered amino acid transport is likely due to a decrease in the number and/or activity of existing AIB transport carriers in the membrane. Altered amino acid transport in endotoxic shock may limit intracellular availability of amino acids for cellular energy and protein synthesis. Futhermore, the efflux of neutral amino acids from muscle's intracellular amino acid pools may play a role in the redistribution of amino acids from skeletal muscle to viscera in stress states.

References

1. Karlstad MD and Sayeed MM (1985) Am. J. Physiol. (Regulatory, Integrative Comp. Physiol. 17) 248: R142–R146.
2. Karlstad MD and Sayeed MM (1986) Am. J. Physiol. (Regulatory, Integrative Comp. Physiol. 20) 251: R150–R156.
3. Karlstad MD and Sayeed MM (1987) Am. J. Physiol. (Regulatory, Integrative Comp. Physiol. 21) 252: R674–R680.
4. Jepson MM, Pall JM, Bates PC and Millward DJ (1986) Biochem. J. 235: 329–336.
5. Hasselgren PO, James JH and Fischer JE (1986) Ann. Surg. 203: 360–365.
6. Moore RD (1983) Biochim. Biophys. Acta 737: 1–49.
7. Narahara HT and Holloszy JO (1974) J. Biol. Chem. 249, 5435–5443.
8. Parrish JE and Kipnis DM (1964) J. Clin. Invest. 43: 1994–2002.
9. Clowes GHA Jr., O'Donnell TF, Blackburn GL and Maki TN (1976) 56: 1169–1184.
10. Rosenblatt S, Clowes GHA Jr., George BC, Hirsch E and Lindberg B (1983) Arch. Surg. 118: 167–175.
11. Williams JA, Withrow CD and Woodbury DM (1971) J. Physiol. (London) 212: 117–128.
12. Cotlove E (1961) Stand. Meth. Clin. Chem. 3: 81–98.
13. Kipnis DM and Parrish JE (1965) Fed. Proc. 24: 1051–1059.
14. Lineweaver H and Burk D (1934) J. Am. Chem. Soc. 56: 658–666.
15. Goldberg AL and Goodman HM (1969) Am. J. Physiol. 216: 1111–1115.
16. Riggs TR and Walker LM (1963) Endocrinology 73: 781–788.
17. Akedo H and Christensen HN (1962) J. Biol. Chem. 237: 118–122.
18. Riggs TR and McKirahan KJ (1973) J. Biol. Chem. 248: 6450–6455.
19. Crane RK (1977) Rev. Physiol. Biochem. Pharmacol. 78: 99–159.
20. Geck P and Heinz E (1976) Biochim. Biophys. Acta 443: 49–53.
21. Sayeed MM (1984) Am. J. Physiol. (Regulatory, Integrative Comp. Physiol. 16) 247: R465–R474.
22. Flear CTG (1970) J. Clin. Path. 23: 16–31.
23. Flear CTG, Bhattacharya S and Singh CM (1980) JPEN 4: 98–120.
24. Illner HP and Shires GT (1981) Arch. Surg. 116: 1302–1305.
25. Gibson WH, Cook JJ, Gatipon G and Moses ME (1977) Surgery 81: 571–577.

Address for correspondence: Michael D. Karlstad, Department of Anesthesiology, University of Tennessee Medical Center, 1924 Alcoa Highway, Knoxville, TN 37920, USA.

The effect of arginine on glycolysis by oral bacteria

R. Duguid

Department of Periodontology and Community Dentistry, University of Dundee, Dundee DD1 4HR, Scotland, U.K.

Abstract

Arginine and arginine peptides reduce the sugar-associated drop in pH of dental plaque and suspensions of oral bacteria. This slowing of the fall in pH reduces the amount of acid in the local microenvironment of the teeth and is, on balance, likely to benefit dental health. There are two possible explanations as to how arginine affects the pH of dental plaque. It could be that arginine acts simply as a buffer. It could be that arginine acts directly or indirectly on the glycolysis pathway reducing the amount of acid produced. Some combination of these two explanations may also be possible. The experiments reported here show that lactic acid production by bacteria from salivary sediment is reduced by arginine. This supports the hypothesis that arginine acts directly or indirectly on glycolytic processes in oral bacteria and has more than a simple buffering effect on the pH of dental plaque.

Dental caries is caused by the glycolytic breakdown of fermentable sugars in the diet to organic acids by bacteria next to the tooth surface [1]. These bacteria, known as dental plaque, break down sugars to produce a range of organic acids of which the most important is lactic acid. Any factor which reduces the rate of glycolysis, the production of acid or elevates the pH next to the tooth surface will tend to reduce susceptibility to dental caries. Arginine and arginine peptides, such as the salivary tetrapeptide sialin, elevate the pH of dental plaque and thus have the potential to slow the rate of appearance of dental caries. At least part of the elevation in pH is thought to arise from the breakdown of arginine by dental plaque bacteria to citrulline and NH_3. There is evidence that arginine can elevate the pH in suspensions of a number of different oral bacteria – including *Streptococcus mutans* the bacterium most frequently implicated in dental caries [2].

There are two possible explanations for the rise in dental plaque pH seen following the addition of arginine and arginine peptides. One possibility is that the rise is a simple pH buffering effect resulting from ammonia production. The other possibility is that arginine, or its breakdown products, interferes with glycolysis by oral bacteria reducing glucose uptake and/or lactate production by these bacteria. Previous experiments performed by the author have shown evidence that arginine is able to slow the rate of glycolysis in *S. mutans* [2].

The experiments reported here were designed to answer the question – does arginine elevate the pH of suspensions of oral bacteria by means of a simple buffering effect or is there evidence that arginine directly or indirectly alters the rate of glycolysis by these bacteria?

Materials and Methods

Oral bacteria suspension: Whole saliva from healthy volunteers was collected and centrifuged at low speed (400 g) for 15 mins, washed and resuspended in PBS.

Incubation

The oral bacteria suspension was preincubated for 30 min before the addition of any sugar containing solutions in order to remove any traces of fermentable carbohydrate. To 15 ml of oral bacteria suspension 15 ml of glucose or glucose-arginine solution prewarmed to 37°C was added. Glucose concentrations of 5, 50 and 500 mM and an arginine concentration of 10 mM were investigated. The diluted suspensions were well mixed, left for 1 min to stabilize, pH readings were taken and aliquots removed for analysis at intervals over 4 h.

Isotachophoresis

Measurements of levels of lactic acid produced were made using an LKB 2127 Tachophor (LKB Instruments, Bromma, Sweden) with a 5 mM solution of NCl containing 0.2% hydroxy methyl cellulose buffered to pH 3.9 with B-alanine as the leading electrolyte. The terminating electrolyte was 5 mM hexanoic acid adjusted to pH 5.5 by the addition of solid tris (hydroxymethyl) methylamine. Separations were performed at a constant current of 40 μA with the Tachophor set at 12°C.

pH measurements

These were made using a combination gel-filled pH electrode (Orion Research, Cambridge, MA, U.S.A.) and an Orion Microprocessor ionalyser/901 calibrated for use at 37°C (Slope: +61.5 mV/pH unit).

Results

Tables 1 and 2 show the effect of 10 mM arginine on acid production by salivary sediment at different concentrations of glucose. Ten mM arginine had little obvious effect at 5 mM glucose, but at 50 mM and 500 mM glucose, arginine reduced the observed pH drop and significantly ($p<0.05$) reduced the concentration of lactate in the medium.

Discussion

Suspensions of salivary sediment have been widely used for studying the metabolism of dental plaque bacteria [3,4]. Basic amino acids and peptides such as

Table 1. The effect of 10 mM arginine on the pH of salivary sediment in the presence of 5, 50 and 500 mM glucose (pH values are mean of three measurements)

	5 mM glucose		50 mM glucose		500 mM glucose	
Time (hours)	−arg	+arg	−arg	+arg	−arg	+arg
0	7.3	7.1	7.3	7.2	7.2	7.2
0.5	5.6	6.3	5.5	6.0	5.1	5.5
1	5.1	5.6	5.0	5.6	4.4	4.7
2	5.2	5.5	4.6	4.9	4.0	4.4
4	5.4	5.5	4.7	4.8	4.1	4.5

arginine and arginine peptides are now recognized as important factors which moderate the fall in pH observed when salivary sediment is incubated with glucose [5]. Distler and Kronker [6] incubated a number of strains of *S. mutans* in a Warburg apparatus with and without arginine. They found that arginine reduced the amount of CO_2 produced during incubation but had no effect on lactate production. Duguid [2] also investigated the effect of arginine on lactate, acetate and formate production by *S. mutans NCTC 10449* but found that, in this organism, arginine reduced the production of organic acids, suggesting that the effect of arginine was more than that accounted for by simple buffering.

The results reported here extend the previous studies with *S. mutans* to a mixed suspension of oral bacteria in salivary sediment. The effect of arginine and arginine peptides on the pH of these suspensions is well known and has been previously investigated in detail [7]. These results demonstrate a similar effect with oral bacteria in salivary sediment. It could be that arginine acts on the entry of glucose into the cells or it could be that it acts on the subsequent metabolism of glucose. The experiments reported here do not distinguish between these possibilities. Keevil, Marsh and Ellwood [8] have suggested that arginine may divert glucose metabolism from acid production to glycogen synthesis. Kleinberg *et al.*, [4] found that in the salivary sediment system, salivary supernatant, containing the arginine peptide sialin, increased glucose consumption by the mixed bacteria sediment.

Table 2. The effect of 10 mM arginine on lactate production by salivary sediment in the presence of 5, 50 and 500 mM glucose (lactate concentrations -mM- mean ± std. deviations)

	5 mM glucose		50 mM glucose		500 mM glucose	
Time (hours)	−arg	+arg	−arg	+arg	−arg	+arg
0	4.8 ± 0.1	4.7 ± 0.1	4.7 ± 0.1	4.7 ± 0.2	4.8 ± 0.2	4.7 ± 0.2
0.5	8.7 ± 0.2	8.3 ± 0.1	9.3 ± 0.3	8.6 ± 0.2	10.1 ± 0.3	9.2 ± 0.2
1	9.1 ± 0.2	8.8 ± 0.1	11.0 ± 0.3	10.2 ± 0.3	12.1 ± 0.3	10.6 ± 0.3
2	9.2 ± 0.2	8.9 ± 0.1	17.1 ± 0.3	15.6 ± 0.3	18.6 ± 0.3	16.1 ± 0.4
4	9.2 ± 0.3	8.9 ± 0.1	20.8 ± 0.4	16.8 ± 0.3	22.9 ± 0.3	19.5 ± 0.4

Whatever mechanisms are involved, these results show that the effect of arginine on the pH of the oral bacteria in salivary sediment is more than a simple buffering effect. Not only is acid neutralized but the production of organic acids by these bacteria is reduced.

References

1. Marsh PD and Martin M (1984) Oral Microbiology, van Nostrand Reinhold (U.K.) Co. Ltd., England.
2. Duguid R (1987) Archs. Oral Biol. 32: 175–179.
3. Kleinberg I (1967) Archs. Oral Biol. 12: 1457–1473.
4. Kleinberg I, Craw D and Komiyama K (1973) Archs. Oral Biol. 18: 787–798.
5. Tavss EA and Eigen E (1986) Caries Res. 20: 244–250.
6. Distler W and Kronke A (1985) Caries Res. 19: 175.
7. Kleinberg I, Jenkins GN, Chatterjee R and Wiyeyeweava L (1982) J. Dent. Res. 61: 1139–1147.
8. Keevil CW, Marsh PD and Ellwood DC (1984) J. Bact. 157: 560–567.

Methionine sulfoxide in the hinge-ligament protein of molluscan bivalve species*

Yasuo Kikuchi and Nobuo Tamiya

Department of Chemistry, Faculty of Science, Tohoku University, Aobayama, Sendai, Miyagi 980, Japan

Abstract

Methionine sulfoxide, an oxidized form of methionine, was detected at extremely high levels (15–30 mol% of total amino acids) in the protein from the elastic hinge-ligaments of molluscan bivalve species. The presence of methionine sulfoxide in the intact protein was confirmed by amino acid analysis of the NaOH-hydrolysate of the protein, non-destructive analyses of the ligament with solid-state ^{13}C-NMR and IR-spectrometries and by the observation that the protein was resistant to the BrCN treatment. The conversion of methionine into its sulfoxide is almost complete. The oxidation process may be non enzymatic because two diastereomers, (5*R*)-L- and (5*S*)-L-methionine sulfoxide, were detected in the protein. The methionine sulfoxide residues might contribute to keep the protein highly hydrophilic and to promote the swelling of the ligaments.

The protein with a high content of methionine sulfoxide (MetO), an oxidized form of methionine (Met)[1], seems unusual because Met is one of the least abundant amino acid constituents of proteins [1], and because there has been no obvious instance for the presence of MetO in the intact proteins from normally functioning tissues of bio-organisms [2,3]. In the present communication we describe a high content of MetO in the hinge-ligament proteins of molluscan bivalve species. The hinge-ligaments are elastic only when they are wet and swollen, and function to open the shells: When the shells are closed by the contraction of adductor muscles, the hinge-ligaments are compressed and strained, and when the adductor muscles relax, the shells are opened by the elastic properties of the ligaments. The hinge-ligaments are composed of proteins and aragonite crystals of calcium carbonate [4,5], of which the protein is primarily important for the elastic properties and the uni-axial arrangement of calcium carbonate crystals is essential for the elastic anisotropy of the ligaments [6].

* This work was supported in part by the fund for Scientific Research from the Ministry of Education, Science and Culture of Japanese Government. One of the authors (Yasuo Kikuchi) was financially supported for the participation in the congress by The Japan Association of Chemistry (Sendai, Japan).

[1]All amino acids except for glycine are of L-configuration. The sulphur in methionine sulfoxide was treated as a carbon in the numbering.

Table 1. Bivalve species and their hinge-ligament layers subjected to the present work

Sample No.	Bivalve species	Ligament layer
A Mactracea species		
1.	*Pseudocardium sachalinensis* (Sakhalin surf clam)[a]	Resilium
2.	*Spisula (Hemimactra) solidissima* (Atlantic surf clam)[b]	Resilium
3.	*Spisula solidia* (Solid mactra)[c]	Resilium
4.	*Mactra chinensis* (Chinese mactra)[d]	Resilium
5.	*Tresus keenae* (Keen's graper)[a]	Resilium
6.	*Coecella chinensis* (Chinese anapella clam)[c]	Resilium
B Veneracea species		
	Saxidomus purpuratus (Purplish Washington clam)[e]	Inner layer
C Pteriacea species		
	Malleus (Malleus) albus (White hammer oyster)[c]	Fibrous layer
D Limacea species		
	Acesta (Acesta) goliath (Giant lima)[d]	Resilium
E Ostreacea species		
	Crassostrea gigas (Giant pacific oyster)[d]	Fibrous layer

The common names are given in the parentheses. [a] from Fukushima, Japan.; [b] from Woods Hole, MA. U.S.A.; [c] provided by Dr. T. Habe (National Scientific Museum, Tokyo, Japan); [d] from Miyagi, Japan.; [e] from Mie, Japan.

Experimental procedures

Bivalve species and their hinge-ligaments

Table 1 shows the bivalve species and their hinge-ligament layers subjected to the present study. The classification and the common names of the species are given according to Habe [7] and Abbott and Dance [8]. The hinge-ligaments of the species in superfamilies Mactracea and Limacea are a big rubber-like mass called 'resilium' (internal hinge-ligament). The ligaments of Veneracea species are composed of two histologically distinct layers, outer and inner layers. The liga-

ments of species in superfamilies Pteriacea and Ostreacea are also composed of two layers; fibrous layer and lamellar layer. The resiliums, inner layers and fibrous layers were employed in the present study. They are ontogenetically homologous to one another [9].

Reduction of MetO residues in the hinge-ligament proteins

The powdered resilium of Sakhalin surf clam (*Pseudocardium sachalinensis*; A-1 in Table 1) (8.9 g) was stirred in 50% (w/v) aqueous *N*-methylmercaptoacetamide [10] (100 ml) at room temperature for 11 days. The protein powder was washed with H_2O, 50% (v/v) methanol, methanol and acetone (50 ml × 5 times, each) and dried *in vacuo* (7.1 g).

Methionine sulfoxide

An authentic DL-MetO was purchased from Wako Pure Chem. Ind. Co. Ltd. (Osaka, Japan), and L-MetO was prepared from L-Met and hydrogen peroxide as described by Toennies and Kolb [11]. Two diastereomers were resolved by fractional crystallization of the picrates as described by Lavine [12]. Their absolute configurations were determined by Christensen and Kjær [13].

Amino acid analyses

The amino acid compositions of the hinge-ligament proteins were determined on the HCl-hydrolysates prepared from ligament pieces (2–3 mg) in 6 M HCl (0.3 ml) at 105°C for 24 h *in vacuo*. The amino acid analyses were carried out with JLC 8AH, 10-D or 200A amino acid analyzer (JEOL Co. Ltd., Tokyo, Japan). The MetO contents were determined on NaOH-hydrolysates prepared from ligament pieces (2–3 mg) in 2.5 M NaOH (0.3 ml) at 105°C for 15 h *in vacuo*. No correction was made for hydrolytic losses.

Infrared spectra

Infrared spectra were measured on a Hitachi 260–10 IR spectrophotometer (Hitachi Co., Ltd., Tokyo, Japan) by KBr disk method.

Solid-state ^{13}C-NMR spectra

The ^{13}C cross-polarization/magic angle spinning spectra were obtained at room temperature on a Bruker CXP-300 NMR spectrometer, operated at 75.46 MHz. A matched single-contact Hartmann-Hahn spin-locked cross-polarization was established by applying radio frequency fields of 1.5 mT (15 G) for ^1H and 6 mT (60 G) for ^{13}C. A contact time was set at 2 ms with a recycle time of 2.0 s. About 300 mg of solid samples were packed into rotors made of poly (perdeuterated methylme-

thacrylate) and rotated at 3.9 kHz at the magic angle [14]. Chemical shifts were expressed as parts per million with reference to external tetramethylsilane. The initial calibration was made on adamantane.

Proteolytic solubilization of the hinge-ligament protein

A suspension of decalcified ligament powder (4 mg) in 0.1 M sodium borate buffer solution (pH 8.8) (1 ml) and one drop of chloroform as preservative was added with 0.1 ml aliquots of crystalline bacterial alkaline protease (Katayama Chem. Ind. Co. Ltd., Osaka, Japan) (4 mg/ml in the same buffer solution) at the time intervals of 24 h and the mixture stirred at 25°C for 120 h. The extent of the solubilization was monitored by the combined contents of Met, MetO and homocysteic acid in the HCl-hydrolysates of the supernatant aliquots (30 µl) taken out from the mixture at every 24 h.

Proteolytic liberation of MetO

The above mixture was stirred at 25°C and added with 0.1 ml aliquots of leucine amino peptidase (cytosole) (Sigma) (2 mg/ml) at the incubation times of 0, 27, 50 and 90 h. The contents of free MetO in the supernatant aliquots (30 µl) were determined with amino acid analyzer at the incubation times of 27, 50, 90 and 120 h.

Analyses of MetO diastereomers

Two columns (0.8 cm × 70 cm each) of sulphonated polystyrene resine (JLC-R-2, JEOL Co. Ltd. Tokyo, Japan) were tandemly connected and equipped on an amino acid analyzer, JLC 8AH (JEOL Co. Ltd.). The analysis was carried out at 54°C with 0.067 M sodium citrate-NaCl buffer solution (pH 2.85, ionic strength = 0.2) at a flow rate of 0.5 ml/min. Under these conditions the diastereomers, (5*S*)- and (5*R*)-MetO, were equally sensitive to ninhydrin and eluted at 4.4 and 4.6 h, respectively. The peak areas were proportional to the amounts of materials up to 230 nmol and the routine analyses were carried out with 50–80 nmol each of the diastereomers.

Results

Amino acid composition of the hinge-ligament proteins

The amino acid compositions of the hinge-ligament proteins determined on their HCl-hydrolysates are shown in Fig. 1. The contents of MetO, Met and homocysteic acid, the latter two of which were derived from MetO during the HCl-hydrolysis [15,16], were combined and taken as Met content. The MetO-contents were determined on the NaOH-hydrolysates (Table 2, column 2).

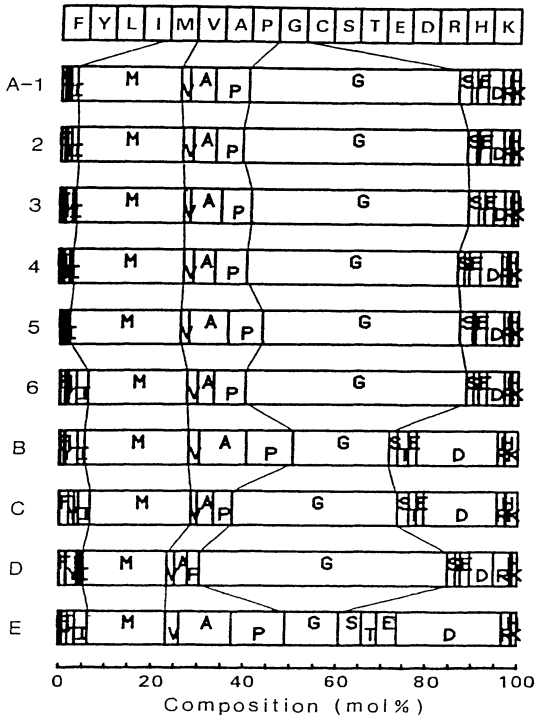

Fig. 1. Amino acid compositions of the hinge-ligament proteins of bivalve species. The numbers for the species and ligament laysers are the same as those in Table 1.

Table 2. Methionine sulfoxide in the hinge-ligament protein of various bivalve species

Species and ligament layer[a]	Contents: MetO/(Met + MetO) ratio in the NaOH-hydrolysate	Diastereomer ratios: (5*S*)-MetO/(5*R*)-MetO
A Mactracea species		
1	1.0	1.1
2	1.0	1.2
3	1.0	1.2
4	1.0	1.2
5	1.0	1.2
6	0.9	1.2
B Veneracea species	1.0	1.1
C Pteriacea species	1.0	1.1
D Limacea species	1.0	1.5
E Ostreacea species	1.0	1.1

[a] Numbers for the bivalve species and the ligament layers are the same as those in Table 1.

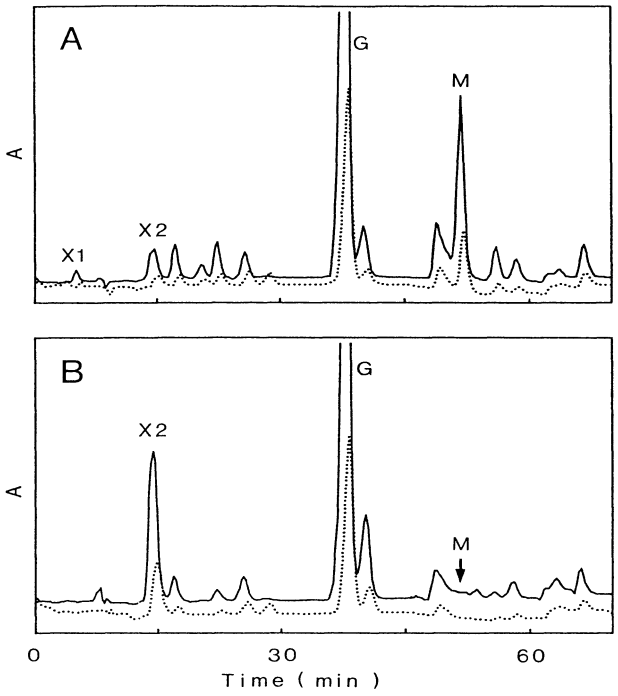

Fig. 2. Analyses of acidic and neutral amino acids in (A) HCl-hydrolysate and (B) NaOH-hydrolysate of the resilium (internal hinge-ligament) of Sakhalin surf clam (*P. sachalinensis*) on a JLC 8AH amino acid analyzer. A_{570} (——); A_{440} (. . . .).

MetO in the intact hinge-ligament proteins

On the amino acid analysis of the HCl-hydrolysate of the resilium (internal hinge ligament) of Sakhalin surf clam (*P. sachalinensis*) (Fig. 2A), one of the unidentified components, X2, coincided with MetO in its retention time. In a NaOH-hydrolysate, an increased amount of X2 but no Met was detected (Fig. 2B). The X2 containing part of the eluate from the amino acid analyzer was collected from the NaOH-hydrolysate of the resilium (30 mg) seven times, and X2 was isolated from the eluate by ionic exchange chromatography on a column (2.4 cm × 15 cm) of Amberlite IR-120 (H^+-form in H_2O) (9 mg). The IR spectrum of X2 agreed with that of an authentic DL-MetO (not shown).

The powdered resilium (168 mg) was treated with BrCN (1.2 g) in 70% (v/v) formic acid for 4 days at room temperature. Only 4% (w/w) of the material was solubilized and could pass through a column of Sephadex G-25. The content of homoserine in the solubilized material was less than 1 mol% of amino acids.

IR-spectrum of the resilium showed the absorption band at 1020 cm^{-1}, which was assigned to S-O stretching vibration of sulphinyl group (Fig. 3-a). The

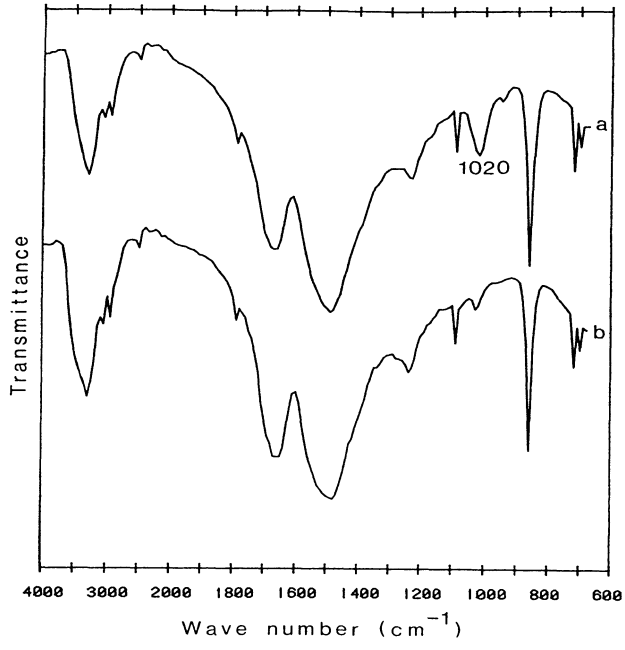

Fig. 3. IR spectra of (a) resilium and (b) reduced resilium of Sakhalin surf clam (*P. sachalinensis*).

corresponding band was not observed in the spectrum of the reduced resilium in which MetO had been converted into Met with reducing reagent (Fig. 3-b). The S-O stretching vibration band of an authentic MetO preparation appeared as split peaks at 1020 and 1030 cm^{-1} (not shown).

In the solid-state ^{13}C-NMR spectrum of the powdered resilium (Fig. 4A), the signal at 38.2 ppm is assigned to C_ε of MetO in the resilium protein because its chemical shift is close to that of C_ε-signal (40.0 ppm) of authentic MetO. The signal of C_β is included in the peak at 24–26 ppm and the signals of C_α and C_γ are in the peak at 51.8 ppm. The signal at 43.9 ppm is that of C_α of Gly, the most abundant amino acid in the resilium protein. In the spectrum of reduced resilium (Fig. 3B), the C_ε-signal of MetO (38.2 ppm) was not detected. On the other hand, the C_ε-signal of Met appeared at 15.4 ppm. The C_α-signal of Met is at 51.6 ppm, and the C_β- and C_γ-signals are in the peak at 30.5 ppm. The C_α of Gly appeared at 43.7 ppm.

MetO diastereomers

The hinge-ligament proteins were solubilized by the proteolysis with crystalline bacterial alkaline protease. The extent of solubilization was 80% or more in most of the cases examined. Amino acids were released from the solubilized peptides by

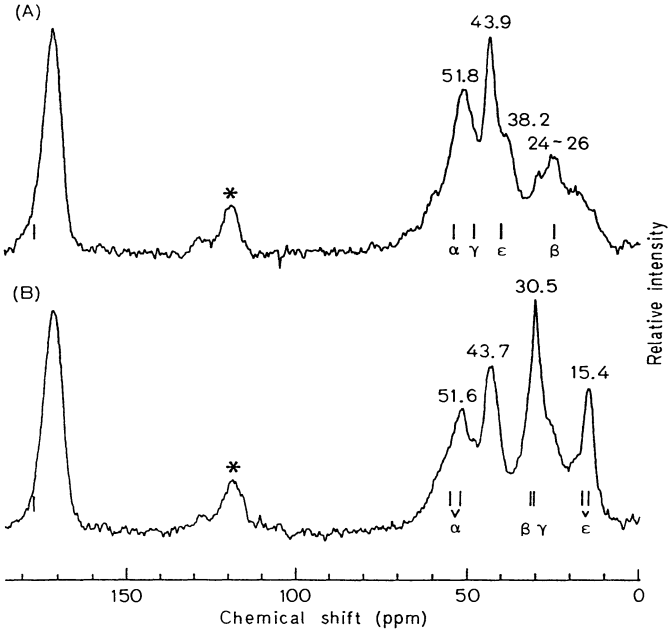

Fig. 4. Solid-state ^{13}C-NMR spectra of (A) resilium and (B) reduced resilium obtained by 3000 (2000 for B) times of integration. The bars in (A) and (B) show the position of the signals of L-methionine sulphoxide and L-methionine, respectively. The signals with asterisks are the scanning sidebands.

the action of an exopeptidase, leucine amino peptidase. About 80% of MetO was detected as a free amino acid in the digests of the ligament proteins from Mactracea species (A1–A6 in Tables 1 and 2) and Giant pacific oyster (*C. gigas*) (E in Tables 1 and 2), but only 30–40% of MetO was liberated from the peptides in the other cases. The ratio of MetO diastereomers was determined with an amino acid analyzer. Figure 5 shows the results on the MetO from the resilium protein of

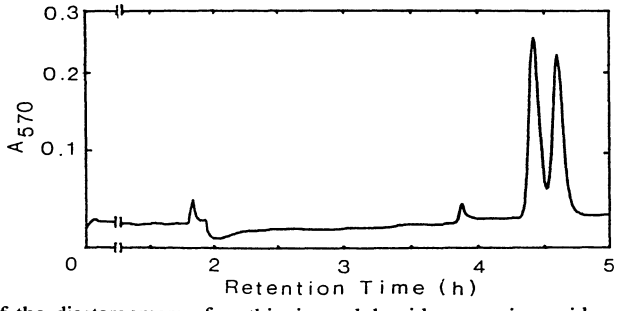

Fig. 5. Separation of the diastereomers of methionine sulphoxide on amino acid analyzer. For detailed chromatographic conditions see experimental section.

Sakhalin surf clam (*P. sachalinensis*). The peaks at 4.4 and 4.6 h were assigned to (5*S*)- and (5*R*)-MetO, respectively. From their peak areas, the (5*S*)-MetO/(5*R*)-MetO ratio was determined as 1.1. Table 2 (column 3) shows the ratios of MetO diastereomers in the ligament proteins from various bivalve species. The values are 1.1 – 1.2 in most cases and 1.5 for the MetO from the resilium protein of Giant lima, *A. (A.) goliath.*

Discussion

While only 20 amino acids are involved as monomer building blocks in the protein synthesis, more than 140 amino acids have been identified in natural proteins because some amino acids are modified after they are incorporated into the peptide chain of proteins [2,3]. Methionine sulphoxide (MetO) had been detected in some proteins [3,17–19], but its contents were low. As methionine (Met) can be oxidized *in vitro* into MetO during the isolation procedures of proteins, the presence of MetO in an intact protein should be demonstrated excluding the possibility of formation as an artefact or, preferably, without any chemical treatment. The amino acid compositions of resilium proteins of the Mactracea species are similar to one another in containing Gly and Met to the extent of 50 and 20 mol%, respectively (Fig. 1, A1–A6). The ligament proteins from other species (B–E) also contain Met as predominant constituent. The presence of Met in its sulphoxide form was suggested by the amino acid analyses on the hydrolysates of the resilium (internal hingeligament) of Sakhalin surf clam (*P. sachalinensis,* superfamily Mactracea). Although MetO was low in the HCl-hydrolysate, it was an unique Met analogue detected in the NaOH-hydrolysate (Fig. 2A and B). As MetO is reduced slowly into Met during the HCl-hydrolysis procedures [15,16], Met might be present exclusively in its sulphoxide form in the intact protein [4]. The observation that the resilium protein was resistant to the BrCN treatment also supported the presence of Met in its oxidized form. The presence of MetO in the intact resilium protein was confirmed by the non-destructive analyses. The IR-spectrometry detected the sulphinyl group in the resilium (Fig. 3) to confirm the presence of MetO in the resilium protein [5]. As shown in Fig. 4, the solid-state ^{13}C-NMR was successfully applied to detect MetO and Gly in the resilium, and Met and Gly in the reduced resilium [20]. These results demonstrated the presence of Met exclusively in its sulphoxide form in the intact resilium protein of Sakhalin surf clam. The MetO-content was extremely high as compared with the Met-contents of usual proteins. This was the first solid evidence for the presence of MetO in an intact protein. And the Met residues in the hinge-ligament protein of other bivalve species were mostly in sulphoxide form (Table 2, column 2) [21]. Since free MetO cannot be utilized as such in protein synthesis [22] the MetO residues must have been formed *in vivo* by post-translational oxidation of Met in the proteins. The conversion of Met into MetO introduces another asymmetric center into the amino acid molecule, namely sulphoxide group of *S*- and *R*-configurations; they are designated as (5*S*)-MetO and

(5*R*)-MetO, respectively. The optically active sulphoxide groups are formed in many natural products by enzymatic oxidations of sulphide groups [23]. On the other hand, the Met-oxidation was suggested to be unfavorable for most proteins because the *in vitro* oxidation of Met residues caused the loss of the biological activities of various proteins, and the biologically produced molecules such as superoxide, hydroxyl radicals, H_2O_2 and hypochlorite ion were proposed as the detrimental oxidizing agents [24]. The non-enzymatic mechanism was also suggested [3,24] for the *in vivo* oxidation of Met residues in the proteins from pathologically defective tissues such as brown cataract lens [25] or rheumatoid arthritis synovial fluid [26]. In contrast to the above proteins, however, the ligament proteins are from nondefective and normally functioning hinge-ligaments of the bivalve species. Their Met-contents are high and the extent of Met-oxidation in them is almost complete. Only one of the diastereomers can be expected when the Met-oxidation is catalyzed by enzymes, and even when the oxidation is non-enzymatic, the molecular size of the oxidant and the three-dimensional environments of the target Met residues may affect the stereochemical specificities in the Met-oxidation. Since the hinge-ligament proteins were insoluble because of the presence of cross-linking components [27], they were solubilized with proteolytic enzyme under the conditions mild enough to prevent the interconversion of the MetO diastereomers. And MetO was released as free amino acid from the solubilized fragments by the action of exopeptidase. The extent of the MetO liberation, however, was different from one sample to another (see Experimental section). It might be due to the difference in amino acid sequence of the protein. The diastereomer analysis (Fig. 5) showed that the two diastereomers are present in approximately equal amounts in the hinge-ligament proteins from bivalve species of a wide variety of the taxonomic classes (Table 2, column 3) [21]. From these results, the *in vivo* Met oxidation may be a non-enzymatic reaction as suggested previously, although the active oxidizing species is not identified yet. And, the conformation of the hinge-ligament proteins may be random and the two MetO diastereomers can be formed with equal probabilities. Alternatively, the protein conformation may determine the stereospecificities at every Met-oxidation sites in the protein to form the two MetO diastereomers in equal amounts. As the MetO is a predominant constituent of the hinge-ligament proteins of some bivalve species, and as the conversion of Met into MetO is almost complete in these proteins, the MetO residues are supposed to play some essential roles in the properties of the hinge-ligaments. The MetO side chains make the protein highly hydrophilic and promote the swelling of the hinge-ligaments (Y. Kikuchi *et al.*, unpublished data). The relationship between the MetO residues and the elastic properties of the ligaments will be discussed elsewhere.

Acknowledgements

The authors are grateful to Professor Tadashige Habe (National Scientific Museum,

Tokyo, Japan) for providing the hinge-ligaments of some bivalve species, and to Mr. Hisaku Abe of this laboratory for amino acid analysis.

References

1. Dayhoff MD (1972) Atlas of Protein Sequence and Structure. Natl. Biom. Foundation, Washington DC.
2. Uy R and Wold F (1977) Science 198: 890–896.
3. Harding JJ (1985) Advances in Protein Chemistry 37: 247–334.
4. Kikuchi Y and Tamiya N (1981) J. Biochem. (Tokyo) 89: 1975–1976.
5. Kikuchi Y and Tamiya N (1984) Bull. Chem. Soc. Jpn. 57: 122–124.
6. Ono K, Kikuchi Y, Higashi K, Tamiya N and Yasuoka N (1990) J. Biomechanics (in press).
7. Habe T (1977) Systematics of Mollusca in Japan: Bivalvia and Scaphopoda (in Japanese), Hokuryu-kan, Tokyo.
8. Abbott RT and Dance SP (1982) Compendium of Seashells. EP Dutton, New York; Japanese edition by Habe T and Okutani T (1985) Heibonsha Publishers, Tokyo.
9. Trueman ER (1969) Ligament. In: Moore RC (ed.) Treatise on Invertebrate Paleontology. Geological Society of America, Boulder, and University of Kansas, Lawrence. Part N, Vol. 1, pp. N58–N64.
10. Houghten RA and Li CH (1979) Anal. Biochem. 98: 34–46.
11. Toennies G and Kolb JJ (1939) J. Biol. Chem. 128: 399–405.
12. Lavine TF (1947) J. Biol. Chem. 169: 477–491.
13. Christensen BW and Kjær A (1965) Chem. Commun. 1965: 225–226.
14. Floyd NF and Cammaroti MS and Lavine TF (1963) Arch. Biochem. Biophys. 102: 343–345.
15. Morihara K (1964) Bull. Chem. Soc. Jpn. 37: 1781–1784.
16. Andrew ER (1971) In: Emsley JW, Feeney J and Sutcliffe LH (eds.) Progress in Nuclear Magnetic Resonance Spectrometry. Pergamon Press, Oxford, Vol. 8, pp. 1–101.
17. Hudson BG and Spiro RG (1972) J. Biol. Chem. 247: 4229–4238.
18. Brewer Jr. BH, Keutmann HT, Potts Jr. JT, Reisfeld RA, Schleuter R and Munson PL (1968) J. Biol. Chem. 243: 5739–5747.
19. Adelstein RS and Huehl WM (1970) Biochemistry 9: 1355–1364.
20. Kikuchi Y, Tamiya N, Nozawa T and Hatano M (1982) Eur. J. Biochem. 125: 575–577.
21. Kikuchi Y, Higashi K and Tamiya N (1988) Bull. Chem. Soc. Jpn. 61: 2083–2087.
22. Lemoine E (1958) Eur. J. Biochem. 4: 213–221.
23. Kjær A (1974) Tetrahedron 30: 1551–1554.
24. Brot N and Weissbach H (1983) Arch. Biochem. Biophys. 223: 271–281.
25. Truscott RJW and Augusteyn RC (1977) Biochim. Biophys. Acta 492: 43–52.
26. Wong PS and Travis J (1980) Biochem. Biophys. Res. Commun. 96: 1449–1454.
27. Kikuchi Y, Tsuchikura O, Hirama M and Tamiya N (1987) Eur. J. Biochem. 164: 397–402.

Address for correspondence: Yasuo Kikuchi, Department of Chemistry, Faculty of Science, Tohoku University, Aobayama, Sendai, Miyagi 980, Japan.

Separation of D- and L-amino acids by ion exchange column chromatography in the form of 2-sulfonic acid alanyl dipeptides

J. Csapó, I. Tóth-Pósfai and ZS. Csapó-Kiss

Pannon Agricultural University, Faculty of Animal Science Kaposvár, H-7401 Kaposvár, Dénesmajor 2. Hungary

Abstract

A method of ion exchange column chromatography was developed for the determination of D- and L-amino acids in the form of diastereomer dipeptide. First the protein containing samples were hydrolized with 6 mole hydrochloric acid then the single amino acids were separated in an LKB automated amino acid analyzer with the LKB fraction collector. Following lyophilization the single amino acids were transformed with (t-BOC)$_2$-L-CySS-(ONSu)$_2$ active ester into 2 sulfonic acid-alanyl dipeptide after inserted oxidation by performic acid. The 2-sulfonic acid-alanyl dipeptides appear on the chromatogram directly after cysteic acid. They separate easily from one another and from the cysteic acid formed from the excess of active ester. Accuracy of the determination is satisfactory. The coefficient of variation amounts to 4–10%.

The use of the method is suggested to laboratories having an amino acid analyzer and wish to determine D- and L-amino acids in synthetic amino acids complements, peptides or natural materials.

Introduction

The alanyl dipeptides – as has been found in the experiments aimed at separating them – even in the case of aspartic acid, appear in the chromatogram after Ala, thus, separation takes at least 1–1.5 h. We tried to find a way to make the synthesized diastereomer dipeptides appear in a shorter time on the chromatogram. Therefore, we selected as the second acylating amino acid cystine (CySS) hoping that after the active ester condensation a tripeptide is formed which will break down after oxidation with performic acid into two dipeptides. One of the two peptides, cysteic acid accelerates the elution of the dipeptide thereby significantly shortening the time needed to separate the diastereomer dipeptides.

Experimental procedure

Materials used

We synthesized the bis-tercier-butyl-oxy-carbonyl-L-cystine-bis-N-hydroxy-succinimide ester (t-BOC)$_2$-L-CySS-(ONSu)$_2$ with the intention of using the neutral or basic amino acids. The protected active ester of the amino acid was synthesized as described by Bajusz [1].

Subsequent to the synthesis of the active ester diastereomer dipeptides were prepared from crystallized amino acids (standards) or from the single amino acids separated in the amino acid analyzer.

Separation of the protein building amino acids

The determination and separation of amino acids have been carried out with LKB 4101 type amino acid analyzer and the connected LKB fraction collector. The test-tubes corresponding to individual amino acids were identified and lyophilised to the dry. Then the diastereomer dipeptides were produced from the individual amino acids or from the mixture of several amino acids.

Synthesis of diastereomer dipeptides

The synthesized amino acid or the residue separated with the amino acid analyzer and dried by lyophilisation was dissolved in water to obtain a solution of 1–10% concentration for everyone of the amino acids. The pH of the solution was set at pH=8 by adding 1–2 sodium hydrogen carbonate crystal, then the protected active ester of CySS, dissolved in dioxane-water 1:1 was added in 2 to 2.5 times excess. In the case of CySS, the reaction mixture was shaken in a shaking apparatus for 8 h at room temperature, then lyophilised to dry. After drying, the protective BOC group was cleaved off with 1 mol HCl in glacial acetic acid solution (reaction time 1 h), finally lyophilization was repeated. The cystinyl dipeptide was oxidized with performic acid according to Hirs [2]. After breaking down the disulfide bridge two dipeptides containing cysteic acid were obtained. The performic acid was removed, the residue was dissolved in citric acid buffer of pH2,2 and the solution was applied to the ion exchange column of the analyzer. Concentrations were set by dilution so that the dipeptides formed should fall between 50 and 100 nmol.

The reaction equations are as follows:

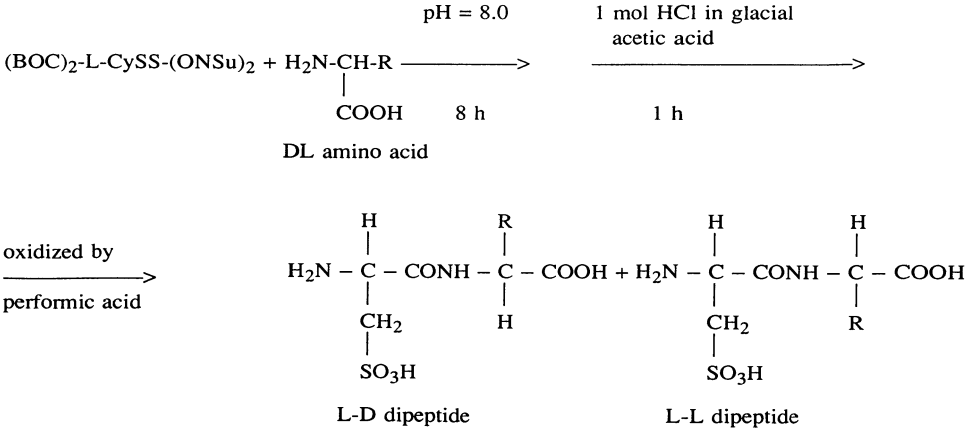

Separation of the diastereomer dipeptides

The sulfonic acid-alanyl-dipeptides were separated and determined in the LKB 4101 type automated amino acid analyzer.

In the chromatogram, cysteic acid appears in the eleventh min directly after the front and is followed by two peaks, one of them in the nineteenth min forming about 25% of the cysteic acid peak and the second in the twenty-second min forming about 5% of the cysteic acid peak. The higher peak is probably that of cysteine-sulfinic acid, while the smaller peak could not be identified so far.

These two peaks do not cause any difficulty in relation to Asp, Thr, Ser, Glu, Pro or Ala because the two diastereomer 2-sulfonic acid-alanyl dipeptides formed from the above amino acids appear in the chromatogram in the free space between cysteic acid and the second peak. The separation of the diastereomer dipeptides from cysteic acid is satisfactory, it can be compared to the separation of Thr-Ser in normal amino acid analysis. The first methodological difficulty arises in relation to valine where the separation of L-L dipeptide peak and the peak ascribable to $CySO_2H$ is imperfect; they partly overlap. This problem gets modified in the case of Ile so that the separation from D-L-dipeptide is perfect, while the peak of $CySO_2H$ merges, without causing trouble, into that of D-L-dipeptide. The situation is similar with isoleucine, too. In the case of tyrosine the problem modifies so that the D-L-dipeptide, appearing in the chromatogram first is directly after the two peaks and in the case of Phe nothing interferes with separation. Since performic acid oxidizes not only cysteine but also methionine producing methionine sulfone, the 2-sulfonic acid-alanyl-methioninesulfone dipeptide, similarly to aspartic acid, appears in the chromatogram directly after cysteic acid. In this case special care has to be taken to finish oxidation by performic acid completely, otherwise a mixture of the dipeptide of methionine sulfone and methionine sulfoxide is obtained in which case determination is almost impossible.

Since during the retention period of 2-sulfonic acid-alanyl-dipeptides differences are only slight for the consecutive amino acids. The advantage of this method in comparison to the former one is that the determination of the D- or L-isomer of any one amino acid takes much less time than that of the alanyl dipeptides. On the other hand, it is disadvantageous that the D- or L-isomer of only a single amino acid can be determined at any one time.

Results and Discussion

Accuracy of the determination of optical amino acid isomers in the form of diastereomer 2-sulfonic acid-alanyl-dipeptides

In Table 1 the results of experiments with 2-sulfonic acid-alanyl dipeptides are presented. As can be seen, the mean values of the theoretical results and those determined are practically identical. The standard deviations, however, are much

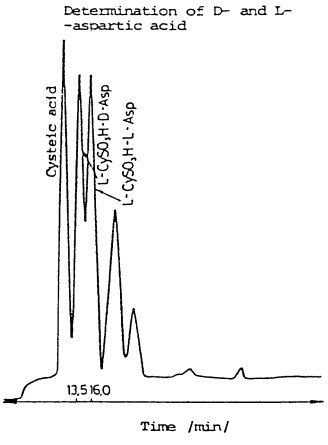

Fig. 1. Chromatogram of the DL-Asp.

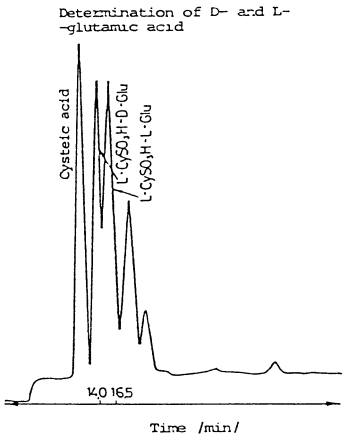

Fig. 2. Chromatogram of the DL-Glu.

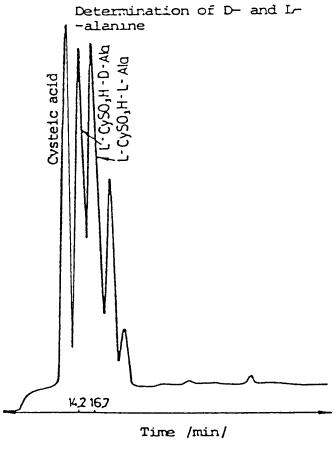

Fig. 3. Chromatogram of the DL-Ala.

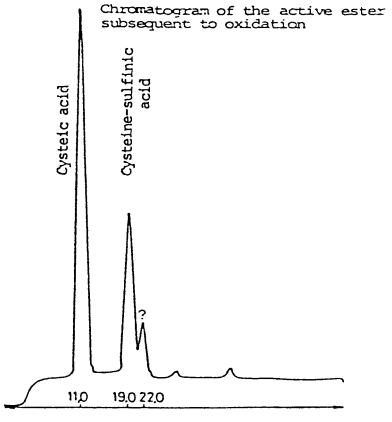

Fig. 4. $(BOC)_2$ L-CySS-$(ONSu)_2$ active ester after preparation as described above. Conditions of separation are as follows: Temperature of column: 40°C during the whole process of separation. Buffer A: pH = 2.9; Na molarity = 0.2; to the end of analysis Na-hydroxide = 0.4 mol; 15 min. Equilibration: Buffer A (pH = 2.9); 45 min.

Table 1. Determination of the D- and L-amino acids in various mixtures in the form of 2-sulfonic acid-alanyl-diastereomer dipeptides

Material tested	Theoretical value (%)		Value measured (%)		Number of measure-ments	Standard deviation		Coefficient of variation	
	D	L	D	L		D	L	D	L
Glutamic acid	50	50	51.7	48.2	5	3.02	2.54	5.84	5.27
	25	75	25.3	75.1	5	1.94	3.22	7.67	4.29
	5	95	4.8	94.9	5	0.51	4.85	10.63	5.11
	1	99	0.99	99.2	5	0.092	4.99	9.29	5.03
Alanine	50	50	49.9	51.0	5	2.98	2.63	5.97	5.16
	25	75	24.6	24.9	5	2.00	3.11	8.13	4.15
	5	95	5.1	95.2	5	0.54	4.62	10.59	4.85
	1	99	1.02	98.4	5	0.085	5.03	8.33	5.11
Valine	50	50	50.3	48.9	5	2.79	2.71	5.55	5.54
	25	75	24.7	75.3	5	2.11	3.33	8.54	4.42
	5	95	4.89	95.2	5	0.48	4.71	9.82	4.95
	1	99	1.11	98.7	5	0.091	5.11	8.20	5.18
Isoleucine	50	50	48.7	49.9	5	2.94	2.48	6.04	4.97
	25	75	25.3	74.8	5	1.85	3.01	7.31	4.02
	5	95	5.11	95.2	5	0.47	4.90	9.20	5.15
	1	99	0.97	98.8	5	0.101	4.97	10.41	5.03

higher than those given at alanyl dipeptides. Probably one of the reasons for this lies in the fact that the production of 2-sulfonic acid-alanyl dipeptides requires one more step (performic acid oxidation) than that of alanyl dipeptides. Another reason maybe that the isolation of the diastereomer dipeptides of very short retention time is not as perfect as with alanyl dipeptides. Finally, the third reason may be that cysteic acid, cystein sulfinic acid and the hitherto unidentified small peak may occasionally disturb the determination of sulfonic acid containing dipeptides.

The value of the coefficients of variation exceeds 10 in 3 cases only and even then only very slightly. In every other case it is below 10. Thus, this method is also reliable and its reproducibility is satisfactory.

Conclusion

In order to accelerate the method (to be able to elute the diastereomer dipeptides in less time) it seemed more expedient to synthesize a dipeptide containing an acidic amino acid. Knowing the difficulties involved in protecting and later freeing the amino, carboxyl and hydroxy groups our choice has fallen on cysteic acid appearing directly after the front. The *N*-hydroxy-succinimide ester of cystine, protected by the *t*-BOC group was connected to the amino acid to be determined. Then the *t*-BOC group was removed and the cystine was oxydized by performic acid into cysteic acid and the 2-sulfonic acidalanyl-diastereomer dipeptides were thus obtained. These dipeptides appeared – as expected – directly behind cysteic acid in the chromatogram and in most cases they were easy to isolate from cysteic acid as well as from one another. The advantage of this method over the former one lies in its rapidity. An analysis takes hardly 20–25 min, however, it is more labour intensive and standard deviations, particularly at lower concentrations, are nearly twice as high (Table 1). The methods are suitable for the detection of at least 1% D-(or L-) amino acid in the presence of 99% L-(or D-) amino acid. This method is recommended to all the laboratories which are equipped with an amino acid analyzer and want to determine the D- and L-amino acids in synthetic amino acids, peptides or natural substances.

The financial help provided by the Protein Program Bureau of the National Technical Development Committee, Budapest, is also highly appreciated.

References

1. Bajusz S (1980) Synthesis of Peptides. Budapest, Akadémiai Kiadó.
2. Hirs CHW (1956) J. Biol. Chem. 219: 611.

Chiroptical properties of fluorescamine and MDPF condensation compounds with amino acids, amino acid esters and dipeptides

Voldemar Toome and Bogda B. Wegrzynski

Roche Research Center, Hoffmann-La Roche Inc., Nutley, NJ 07110, U.S.A.

Abstract

2-Methoxy-2,4-diphenyl-3(2H)furanone (MDPF) and 4-phenylspiro[furan 2(3H),1'-phthalan]-3,3'-dione (fluorescamine, Fluram®) react efficiently with primary amino groups to form pyrrolinone type (*N*-substituted 3,5-diphenyl-5-hydroxy-2-pyrrolin-4-ones) chromophores with UV absorption maxima at 270–280 nm and 380–390 nm regions. In Circular Dichroism (CD) measurements, in ethanol, the synthesized MDPF derivatives of twenty-four L-, and D-amino acids showed three characteristic Cotton effects: *first* at 400–370 nm, *second* at 335–315 nm, and *third* at 290–270 nm displaying in L-series (+)-, (−)-, (+)-, signs. Chromophoric reactions of MDPF and fluorescamine with α-amino acids, their esters and dipeptides can be performed in test tubes. CD spectra are obtained from the resulting reaction mixtures *in situ*. Investigations showed that in configurational studies of fluorescamine derivatives only the second and third Cotton effects should be used following the empirical rule: in L-series the second CD band at 340–315 nm is negative, whereas the third one at 290–270 nm is positive. For the MDPF condensation compounds with dipeptides, only the sign of the third Cotton effect is reliable. A pyrrolinone chirality rule is proposed. The experimental parameters, solvent, and pH effects on the sign of the Cotton effects are discussed. The main advantage of these chromophoric reactions is their simplicity, reliability and the fact that they can he carried out under mild conditions within minutes.

Introduction

There are several hundred amino acids (in addition to the twenty common building elements of proteins) known to occur in nature [1,2]. Most of them possess L-configuration[1] at the asymmetric α-carbon atom, but the number of D-amino acids, isolated mainly from microbial products are encountered with increasing frequency. Therefore, the determination of their absolute configuration is an important recurring task. Chiroptical methods, such as Optical Rotatory Dispersion (ORD) and Circular Dichroism (CD) have been utilized (among other techniques, such as chromatographic methods, single crystal x-ray analysis, etc.) in various ways for conformational assignments of amino acids [4–6]. All aliphatic L-α-amino acids show, in their CD spectrum at pH 1, a positive Cotton effect near 209 nm, which is generally assigned to the $n \rightarrow \pi^*$ transition of the carbonyl chromophore [7–10]. The CD spectra of D-α-amino acids exhibit a negative Cotton effect in the same area. Their spectra are relatively simple and can be measured directly with the state-of-the-art ORD/CD spectropolarimeters which are extending to the vacuum UV region.

In the presence of additional chromophoric substituents such as in the case of the aromatic amino acids etc., a more complex chiroptical pattern occurs. In addition, the substitution pattern at the aromatic moiety, as described in the case of o-, m-, and p-tyrosine, influences the sign of the long wavelength CD band (^1L_b transition) in the 275 nm region [11]. Therefore, in practice, it is advantageous to form new chromophoric derivatives whose chiroptical properties reflect the absolute configuration at the α-carbon atom, and whose absorption is shifted to the longer wavelength region (above 300 nm) where the aromatic compounds and other chromophoric substituents (and possible impurities) are transparent. The new chromophoric derivatives should preferably have a rather high Kuhn's dissymmetry factor g, which is defined as $\Delta\varepsilon/\varepsilon$, to effect CD spectra with favorable signal-to-noise ratios.

A number of reagents and methods for the preparation of the chromophoric derivatives of α-amino acids, have been described in the literature and their properties have been previously reviewed [5,6]. Some of their adherent disadvantages have also been noted: for example, derivatization is often accompanied by partial racemization, reaction mixtures have to be heated over a period of time, or stand at ambient temperature for at least 24 h. In other instances, the sign of the Cotton effect of the derivative is not a function of the configuration alone, but it is also dependent upon the nature of the substituents at the α-carbon as well. In addition, some of the reagents may also react with hydroxy or sulfhydryl groups.

This report describes the application of 2-methoxy-2,4-diphenyl-3(2H)-furanone (MDPF,I) and 4-phenylspiro[furan-2(3H),1'-phthalan]-3,3'-dione (fluorescamine, Fluram®,III) as suitable chromophoric reagents for the determination of the absolute configuration of α-amino acids, α-amino acid esters, and the NH_2-terminal amino acids of dipeptides (or any peptide or protein). Both react readily with the free amino group of these compounds [12] to form *N*-substituted 3,5-diphenyl-5-hydroxy-2-pyrrolin-4-ones (Scheme 1), compounds of general structure of IIa,b,c, and IVa,b,c.

The UV spectra of these chromophores are similar [12] and show maxima in ethanol at 270–285 nm (ε = 16,000–18,000), and at 380–390 nm (ε = 6,000–7,500); an inflection is observed at 215–220 nm (ε = 10,000–12,000). Derivatives containing an aromatic moiety such as a phenol (Tyr) or an indole (Trp) in the side chains show additional UV absorption stemming from these substituents. As expected, these electronic transitions of the pyrrolinone chromophore recognize the chirality of the α-carbon atom of an amino acid and the sign of their Cotton effects can be used for configurational assignments.

Based on the empirical data, a pyrrolinone chirality rule is proposed. Simple test tube procedures which allow measurements (also on microscale) of ORD and CD spectra of the reaction mixtures *in situ* are described. Experimental parameters set forth previously have been updated and refined; these differences as well as the influence of the solvent polarity and the pH on the sign of the Cotton effects are discussed.

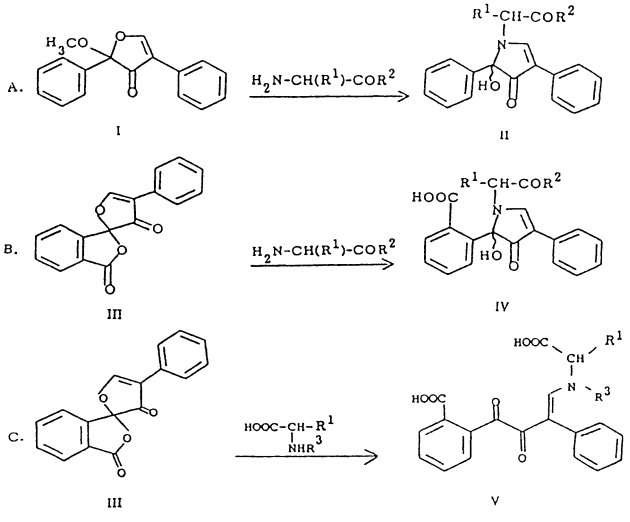

Scheme 1. Summary of the MDPF (I) and fluorescamine (III) reactions (A and B) with α-amino acids (R^2 = OH), α-amino acid esters (R^2 = O-methyl, O-t-butyl, O-benzyl, O- benzyl-p-tosyl) and dipeptides (R^2 = COOH-terminal amino acid of a dipeptide) affording the corresponding pyrrolinone-type chromophores: IIa, IIb, IIc, IVa, IVb, and IVc. Reaction C depicts the reaction of fluorescamine (III) with secondary amino acids (R^2 = methyl, Pro, or azetidine residue) forming aminoenone-type chromophores V.R^1 represents the substituent at the α-carbon of an amino acid.

Materials and Methods

The derivatization and isolation of chromophoric derivatives with MDPF have previously been described [12,13]. Some compounds were recently obtained from Dr. S. De Bernardo, Hoffmann-La Roche Inc. Amino acids, amino acid esters and dipeptides were purchased from Aldrich Chemical Co., Cyclo Chemical CO., ICN Life Science, Mann Research Laboratories, Pfaltz and Bauer Inc., Pierce Chemical Co. and Vega-Fox Biochemicals and were used without further purification.

Some less common amino acids were donated by Dr. J. P. Scannell, Hoffmann-La Roche Inc. Fluorescamine (Fluram®) and MDPF were obtained from Hoffmann-La Roche Inc. Histological grade dioxane and spectral grade dimethylformamide, ethanol, and methanol were purchased from Fisher Scientific Co. The borate and phosphate buffers (0.05 M) were prepared according to Clark and Lubs [14] using analytical grade chemicals from Mallinckrodt Chemical Works. Triethylamine was obtained from Eastman Kodak Co.

Preparation of reference compound solutions

0.002–0.01 M solutions of the isolated MDPF condensation compounds with α-amino acids were prepared in ethanol and dioxane.

Preparation of the in situ *solutions*

Since the introduction of MDPF and fluorescamine as chromophoric reagents for the determination of the absolute configuration of α-amino acids, our preliminary experimental conditions have been updated and optimized and are described below.

Chromophoric reactions of MDPF

In general, 18 equivalents of triethylamine are added to a test tube containing a 0.02 M (concentration may range between 0.1 and 0.002 M) solution of an α-amino acid, α-amino acid ester, or a dipeptide in 0.05 M phosphate buffer pH 8. Reagents are stirred on a Vortex-type mixer, and 2.5 equivalents of MDPF in methanol[2] are added to the test tube. The reaction mixture is stirred for 20 seconds and CD spectra recorded after one minute. When necessary, the initial solution is diluted with methanol/phosphate buffer pH 8 (50:50).

In a nonaqueous procedure, two ml of dimethylformamide (DMF) is added to 0.04 millimoles of an α-amino acid, α-amino acid ester or a dipeptide. Since most of the compounds used in studies were found to be insoluble in DMF, suspensions were used. The suspension is neutralized with 0.1 ml of triethylamine and 1.9 ml of 0.0527 M solution of MDPF in methanol is added. The reaction mixture is stirred for 20 seconds on Vortex-type mixer and allowed to stand for up to 20 h at ambient temperature before recording CD spectra.

On a microscale, (0.1–10 μg range) in order to avoid working with dilute solutions where the reaction is slow or incomplete, about 10 μg of an α-amino acid (or ester) is dissolved in 0.01 ml of methanol/water (50:50) and reacted under stirring, in a test tube, with 2.5 eq of MDPF in 0.01 ml methanol containing 18 eq of triethylamine. The reaction mixture is stirred, and after standing at ambient temperature for about one h, it is diluted with 5 ml of methanol/buffer solution (50:50).

Chromophoric reactions of fluorescamine

An equal aliquot containing two equivalents of fluorescamine in dioxane is added to a 0.002 M (concentration may range between 10^{-2}M and 0.5×10^{-6}M) solution of an α-amino acid, a-amino acid ester, dipeptide, or a peptide in 0.05 M phosphate or borate buffer pH 8.0–9.0, or in a different solvent system in a test tube. Reagents are stirred on Vortex-type mixer for 20 seconds and CD spectra are recorded. On the average, in qualitative analyses, CD spectra can be recorded after one minute,

but in some cases, it might be advisable to allow the reaction mixture to stand for 20–45 minutes for optimum chemical yield. When necessary, dilutions are made with an appropriate solvent system.

Modifications to the general procedure were made as indicated by preliminary studies for each group of the compounds under investigation. In the case of α-amino acids esters the excess of fluorescamine is increased from two to four fold. Secondary α-amino acids are routinely dissolved in 0.05 M borate buffer pH 9. For some peptides the reaction of fluorescamine was carried out in methanol/0.05 M phosphate buffer pH 8 (50:50) and (20:80) solvent systems. In two cases, L-Lys-L-Trp and L-Phe-L-Ile, the dipeptides were dissolved in methanol. In this solvent system, the maximum dichroic intensity was reached after 4 h.

Further, in a nonaqueous procedure, two ml of 0.004 M solution of fluorescamine in dioxane is added to two ml of 0.002 M suspension of an α-amino acid, α-amino acid ester, and dipeptide in DMF. The reagents are stirred on Vortex-type mixer and allowed to stand at ambient temperature in a dark place. CD spectra are recorded after 16–24 h.

Preparation of solutions for pH studies

Synthesized chromophores

The synthesized MDPF condensation compounds with α-amino acids are dissolved in ethanol (0.02 M) and are diluted 1:10 with 0.1 N HCl, 0.1 N KOH, and with a buffer of a desired pH.

In situ *chromophores*

0.01 M stock solutions of the chromophoric derivatives are prepared as described above. For pH studies above 7, the initial solutions are diluted 1:10 with 0.1 N NaOH or a buffer of a desired pH. Below pH 7, the initial solution is first diluted 1:9 with the original solvent system, and then an appropriate aliquot of 1.0 N HCl is added to give the final dilution factor of 10. CD spectra are recorded after one minute.

Measurements of UV, ORD, and CD

Absorption measurements were taken on a Cary Recording Spectrophotometer, Model 14. Earlier ORD and CD spectra were recorded on Durrum-Jasco Spectropolarimeter, Model ORD/CD/UV-5 and Jasco Spectropolarimeter, Model J-20. Latest studies were carried out using Jasco J-500A Spectropolarimeter. All spectropolarimeters are calibrated with d-10-camphorsulfonic acid in water. CD spectra are recorded at ambient temperature, between 450 and 220 nm. The increased sensitivity of Model J-500A allows for CD measurements below 260 nm. The CD

intensity calculations are based on the concentrations of substrates containing the NH_2 group and are expressed in molecular ellipticities [θ], (deg·cm^2·dmole^{-1}).

Results and Discussion

Reaction conditions

Since our preliminary reports [15,16], the reaction conditions have been reworked and improved, and series of experiments have been repeated[4]. Initially, the reaction yields of MDPF with amino acids *in situ* were ca. 30–70% of those of the isolated standards [13], but they have been improved and are now ca. 50–90%. Since the Cotton effects are strong, these yields are sufficient for *in situ* determination of the absolute configuration of α-amino acids. Further, it has been demonstrated that there is no need to heat the MDPF reaction mixture. Under standard conditions, it is carried out in methanol/water or methanol/buffer solution. And, it has been documented that an increase from 1 to 18 eq of triethylamine greatly improves the chemical yield of the reaction. A two to three fold excess of the reagent is sufficient when the amino acid concentration is ca. 0.02 M. Lower amino acid concentrations require higher excess of the reagent.

For reasons previously described [17], the fluorescamine reaction is carried out in a phosphate or borate buffer pH 8–9/dioxane system (50:50). When the amino acid, ester, or dipeptide concentrations are in the range of 0.01–0.001 M, a two fold excess of fluorescamine is sufficient for the maximum chemical yield *in situ,* but lower concentrations require a 20–40 fold excess of the reagent [18].

Although the chromophoric reactions *in situ* are complete within 1 minute, it is sometimes advisable to let the reaction solutions stand for one h at room temperature for optimum development of the Cotton effects. The chromophores are stable for at least 1–2 h.

Under standard conditions, the fluorescamine reaction is more sensitive and reproducible than the MDPF technique. The Beer's law is obeyed in the 0.1 to 0.001 M range [19], and therefore, the fluorescamine method is more suitable for quantitative analyses [18,19]. The CD bands of the fluorescamine reaction mixture are on the average higher (70–90% of the MDFF standards) than those obtained with MDPF.

However, for the determination of the absolute configuration of more complex amino acids or their derivatives it may be essential to isolate and characterize the chromophoric derivative. In such cases MDPF will be the reagent of choice [13].

CD spectra of synthesized MDPF derivatives of α-amino acids (IIa)

Since the fluorescamine derivatives with α-amino acids tend to undergo secondary reactions and isomerize upon isolation, for reference purposes, twenty-four amino acids representing a wide variety of standard types were derivatized with MDPF

(to form pyrrolinones IIa), isolated, and characterized [13]. Their ORD[3] and CD spectra were measured in ethanol. And, as anticipated, the electronic transitions of the pyrrolinone-type chromophores recognize the chirality of the α-C atom. The CD spectra exhibit characteristic strong Cotton effects at 390–370 nm (1st CD band), at 330–310 nm (2nd CD band) and at 290–260 nm (3rd CD band). Additional two to three Cotton effects are observed below 260 nm depending on the character of the amino acid (Figs. 1,2 and Table 1). The second Cotton effect appears in the area where the UV spectrum has a minimum and it might be explained by a dipole coupling mechanism [20] between the transition moments of the pyrrolinone and carboxyl chromophores, the latter having a weak maximum at 270–280 nm [21].

In the L-series, without an exception, the sign of the first Cotton effect was found to be positive , that of the second one negative and the third Cotton effect is again positive. The CD spectra of the chromophoric derivatives of D-amino acids are mirror images to those of L-series (within the experimental error). A number of the CD spectra of these chromophoric derivatives have now been remeasured and the original data have been confirmed. The chromophoric derivatives consist of two diastereoisomeric components, but this does not interfere with this empirical method.

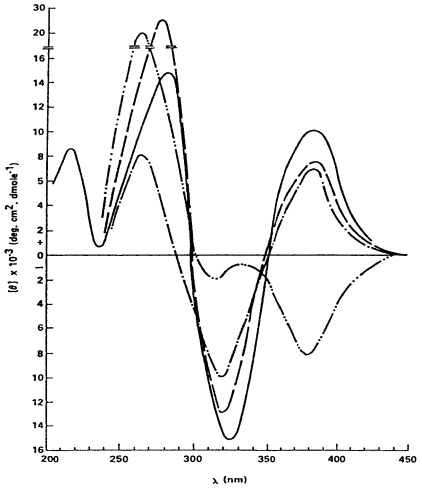

Fig. 1. CD spectra of synthesized (isolated) MDPF derivative of L-Leu in ethanol (–) and of the *in situ* reaction mixtures of MDPF with L-Leu (– –), with L-Leu methyl ester (– · –) and with L-Leu-L-Ala (– ·· –) in methanol/phosphate buffer pH 8 (50:50) in presence of 18 eq of triethylamine. Note the unexpected sign of the first Cotton effect of the MDPF reaction product with L-Leu methyl ester *in situ*.

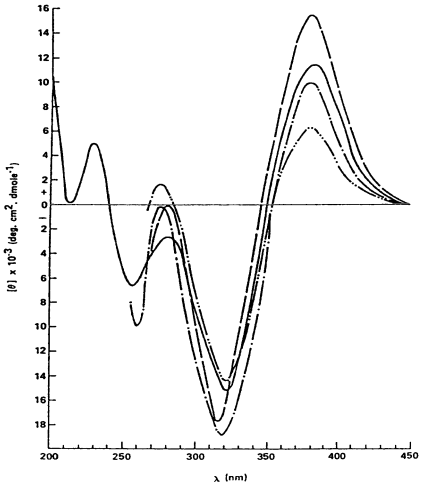

Fig. 2. CD spectra of synthesized (isolated) MDPF derivative of L-Phe in ethanol (–) and of the *in situ* reaction mixtures of MDPF with L-Phe (– –), with L-Phe methyl ester (– · –) and L-Phe-L-Val (– ·· –) in methanol/phosphate buffer pH 8 (50:50) in presence of 18 eq of triethylamine.

Table 1. Summary of CD spectral data[a] of MDPF and Fluorescamine (Fluram®) chromophoric derivatives of α-amino acids, α-amino acid esters and dipeptides: [θ] deg·cm^2·mole^{-1}.

Derivative	First		Second		Third Cotton Effect[b]	
	λ nm	[θ] × 10^{-3}	λ nm	[θ] × 10^{-3}	λ nm	[θ] × 10^{-3}
1. MDPF and L-α-amino acids	391–375	(+)1.6 – (+)16.7	327–317	(–)4.4 – (–)19.4	280–260	(+)6.0 – (+)18.0
2. MDPF and L-α-amino acids	389–375	(+)1.3 – (+)14.0[c]	325–315	(–)4.0 – (–)18.5	285–260	(+)5.5 – (+)17.5
3. MDPF and L-α-amino acid esters	395–380	( )1.7 – ( )13.5[d]	327–315	(–)3.95 – (–)19.5	290–260	(+)6.7 – (+)20.5
4. MDPF and dipeptides (L-NH_2-)	397–377	( )1.8 – ( )21.0[d]	333–295	( )1.8 – ( )29.5[d]	285–255	(+)6.8 – (+)33.5
5. Fluram® and L-α-amino acids	389–377	(+)1.8 – (+)18.5[c]	325–310	(–)1.1 – (–)15.5	280–260	(+)6.0 – (+)16.7
6. Fluram® and less common L-α-amino acids	414–388	(+)2.8 – (+)23.0[e]	324–301	(–)2.7 – (–)30.1	290–280	(+)7.5 – (+)17.8
7. Fluram® and secondary L-α-amino acids	369–345	( )1.2 – ( )8.5[d,f]	325–319	(+)2.5 – (+)21.5[f]	310–290	(–)2.0 – (–)24.5
8. Fluram® and L-α-amino acid esters	400–370	( )2.7 – ( )14.5[d]	330–320	(–)6.0 – (–)34.0	294–268	(+)1.5 – (+)29.7
9. Fluram® and dipeptides (L-NH_2-)	403–376	( )2.2 – ( )29.5[d]	333–308	(–)4.1 – (–)30.5	286–263	(+)5.5 – (+)66.7

[a] Entry 1 data for synthesized standards, entries 2–9 data for chromophoric derivatives *in situ*. The intensities of the Cotton effects vary, they depend on the size and the nature of the alkyl substituents: Ala derivatives showed the lowest intensities, whereas the CD bands of the chromophoric derivatives of the aromatic amino acids are relatively high. Therefore, only the ranges of the molecular ellipticities [θ] are given, calculated for the molar concentrations of amino acids and their analogues used in experiments.

[b] In the presence of aromatic amino acids, the spectra are difficult to obtain below 260 nm, because of their own Cotton effects in this area and due to the high UV absorption of the reagent.

[c] The only exception is L-Ala, whose derivative *in situ* has a first negative Cotton effect.

[d] No sign for the first Cotton effect is given since it relates to the absolute configuration of the compound under investigations and it varies: it is negative for aliphatic amino acid esters and dipeptides and positive when the α-substituent contains a chromophore. It is also sensitive to solvent polarity.

[e] The only exception is L-*threo*-ß-hydroxyaspartic acid, where the sign of the first Cotton effect is negative.

[f] The first, second and third Cotton effects are always present in the case of the cyclic amino acid derivatives, but the chromophoric derivatives of the acyclic amino acids showed first and second CD bands only in few instances.

CD spectra of fluorescamine and MDPF condensation compounds *in situ*

α-*Amino acids*

Subsequently, it was demonstrated that under standard conditions the chromophoric reactions between fluorescamine and MDPF with α-amino acids can be carried out in a test tube [15,16]. These reactions are simple, fast and the CD spectra can be obtained from the resulting reaction mixtures without isolating the chromophores IIa and IVa. An excess of the reagents can be tolerated because they are not optically active.

A number of α-amino acids were reacted with MDPF (Figs. 1,2 and Table 1) and fluorescamine (Figs. 3,4 and Table 1) and the CD spectra of the reaction mixtures were recorded. The spectra show (as in the case of the standards) three characteristic Cotton effects between 400–260 nm. Additional Cotton effects are observed below 260 nm, but in this wavelength region the spectra are difficult to obtain due to the high UV absorption of the reagents, especially if their concentration is higher than 0.004 M.

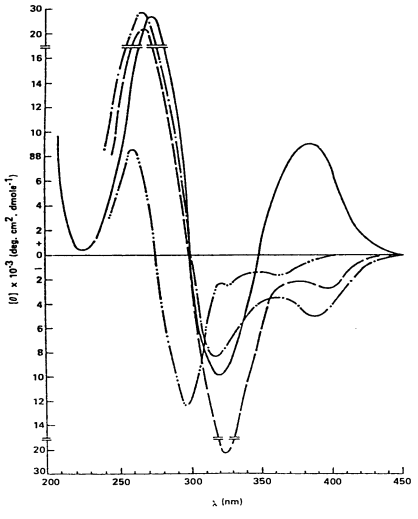

Fig. 3. CD spectra of the *in situ* reaction mixtures of fluorescamine with L-Leu(–), with L-Leu methyl ester (– –), with L-Leu-L-Ala (– · –) and with *N*-methyl-L-Leu (– ·· –) in dioxane/phosphate buffer pH 8 (50:50).

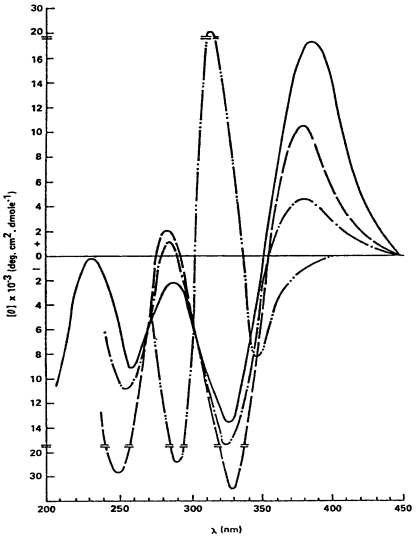

Fig. 4. CD spectra of the *in situ* reaction mixtures of fluorescamine with L-Phe (–), with L-Phe methyl ester (– –), with L-Phe-L-Ile (– · –) and with *N*-methyl-L-Phe (– ·· –) in dioxane/phosphate buffer pH 8 (50:50).

The signs of the *in situ* measured and predicted Cotton effects (based on those of the synthesized ones) are in agreement with each other. In the L-series, the first Cotton effects (at 390–375 nm) are positive, the second ones (at 330–315 nm) are negative and third Cotton effects (at 290–260 nm) are again positive. Within the experimental error, the CD curves of the D-amino acid derived chromophores are mirror images of those of the L-amino acids. The only exceptions to this empirical rule are the L-, (or D-,) Ala reaction products where the sign of the first Cotton effect is reversed, but the sign of the second Cotton effect remains unchanged and can safely be used for configurational assignments[4]. Therefore, it is advisable to measure all Cotton effects. However, as seen from Table 1, the intensities of the Cotton effects vary with the nature of the α-substituent, and they are sensitive to the solvent polarity. Generally, the intensities increase with the size of the aliphatic side chain (e.g. Ala has the lowest CD extrema) and the CD bands of the chromophoric derivatives of the aromatic amino acids are relatively strong. To further demonstrate the usefulness of chromophoric reagents, fluorescamine was reacted, *in situ*, with secondary [22] and less common L-α-amino acids [23], (no D-enantiomers were available). In addition, both fluorescamine and MDPF were reacted with α-amino acid esters [24] and dipeptides [25,26]. With some exceptions, which will be discussed for each group, the signs of the recorded Cotton effects were in agreement with those of the common α-amino acids in all the groups.

Less common α-amino acids

In the case of the less common L-α-amino acids (Table 1) the only exception (confirmed by additional recent experiments) is the L-*threo*-ß-hydroxyaspartic acid reaction product, where the sign of the first Cotton effect is reversed. The only difference in the CD spectral pattern of the less common L-α-amino acid derivatives, when compared with those of the common α-amino acids, is the appearance of a weak CD band (sometimes shown only as an inflection or shoulder) in the 365–343 nm region. At present, we have no explanation for this extra band. No experiments have been carried out with MDPF as a chromophoric reagent.

Secondary α-amino acids

The *N*-methyl α-amino acids, Pro, its derivatives and azetidine carboxylic acid when reacted with fluorescamine form the aminoenone-type chromophore V with absorption maxima in the 250–255 (ε = 13,500–15,500) and 300–320 nm (ε = 16,000–18,000) regions, and an inflection is observed at 340–360 nm (ε = 8000–10,000). The chromophore V (Scheme 1) is chiroptically active and the characteristic CD spectra can be obtained from the reaction mixtures *in situ*. The strongest Cotton effects are observed in the 310–290 nm region (Figs. 3,4 and Table 1) corresponding to the main UV maxima and without exception, they are negative for the chromophores derived from L-amino acids and positive in the case

of D-amino acid derivatives. As described before [22] and confirmed by recent measurements, the UV spectra of the chromophores are quite similar, but there are characteristic differences in the pattern of the CD curves between 380 and 320 nm which might be helpful for an early classification of an unknown secondary amino acid [22]. The most significant difference is observed between the CD spectra of chromophores formed with cyclic and alicyclic amino acids, presumably due to differences in the conformational mobility. Under standard conditions, MDPF does not react with secondary amino acids.

α-Amino acid esters

As in the case with the α-amino acid derivatives with MDPF and fluorescamine, the corresponding α-amino acid ester chromophoric derivatives also exhibit three characteristic Cotton effects between 400–260 nm (Figs. 1–4 and Table 1). Additional two to three Cotton effects can be detected below 260 nm, but they are difficult to record due to the unfavorable anisotropy factor $\Delta\varepsilon/\varepsilon$. The sign of the first Cotton effect varies. It is not a function of the configuration alone, but remains dependent upon the nature of the substituent at the α-carbon as well. In the case of the fluorescamine and MDPF derivatives of aliphatic amino acid esters of L-configuration (except L-Leu methyl ester derivative with MDPF), it is negative, i.e. reversed, when compared with standards [13] (in the free α-amino acid series only L-Ala behaved similarly), but when the α-substituent contains a chromophore such as an aromatic moiety or a carboxyl group, the sign of the first Cotton effects is preserved. Similar behavior of the sign of the Cotton effects of several other chromophoric derivatives of α-amino acids and esters had been reported in the literature [27–30]. The change of the sign has been linked with the change of the conformational equilibrium in solution; however, the size of the ester group (methyl vs. t-butyl) does not seem to influence the sign of the Cotton effects.

In any case, the sign of the second (330–320 nm) and third Cotton effects (285–265 nm) can be safely used for the determination of the absolute configuration of the α-amino acid esters using the following general rule:[4,5]

Configuration	Sign of the 2nd	and 3rd Cotton effect
L	−	+
D	+	−

Dipeptides

Because of the pattern of irregularities observed during the CD investigations of the fluorescamine and MDPF derivatives of α-amino acid esters, it was important to examine the chiroptical properties of fluorescamine and MDPF condensation compounds with dipeptides [25,26].

As in the case of amino acid esters, the signs of the first Cotton effects at (400–370 nm) of fluorescamine and MDPF condensation compounds with dipeptides *in situ* vary (Figs. 1–4 and Table 1). It is not a function of the configuration alone, but it also depends upon the nature of the amino acid side chain. When the NH_2-terminal L-α-amino acid of a dipeptide is an aliphatic one, the sign of the first Cotton effect is negative i.e. opposite to the originally proposed empirical rule [13]. The few exceptions are Val-Val-dipeptides, and in some cases, when the COOH-terminal amino acid of a dipeptide is an aromatic one. It will be shown later that the sign of the first Cotton effect is sensitive to the polarity of the solvent. But in any case, the sign of the second and third Cotton effect of the fluorescamine condensation compounds with dipeptides can be safely used for the determination of the absolute configuration of a NH_2-terminal amino acid of a dipeptide: in the L-series they are negative and positive respectively[5]. Furthermore, it is interesting that the configurational characteristics are transmitted through the Gly moiety, as has been demonstrated in the case of Gly-Leu and GLy-Phe, although the intensities of the Cotton effects are reduced.

Some additional irregularities were observed in the CD spectra of the MDPF condensation compounds with dipeptides [27]. Several experiments have now been repeated and the earlier results have been confirmed. The signs of the first and also the second Cotton effects may vary, but without an exception, the sign of the third Cotton effect at 280–260 nm reflects the absolute configuration of the NH_2-terminal amino acid: it is positive for the NH_2-terminal L-amino acid of a dipeptide and negative for the D-amino acid. Here the empirical rule [13] holds only when the NH_2-terminal amino acid is an aromatic one. Interestingly, in the case of the aliphatic dipeptides of L,L-, or L,D-, type, the second Cotton effect also obeys the empirical rule. If the third Cotton effect of a MDPF chromophoric derivative of an aliphatic or an aromatic dipeptide cannot be measured properly, it is advisable to react a proper model dipeptide with known absolute configuration with MDPF and to compare the CD spectra. For the determination of the absolute configuration of an α-amino acid in a more complex dipeptide, it may be essential to isolate and characterize the chromophoric derivative.

It should be emphasized that the experimental results have clearly shown, that the sign of the third Cotton effect of the pyrrolinone-type chromophores IIc and the signs of the second and third CD bands of chromophores IVc depend only on the configuration of the NH_2-terminal amino acid of the corresponding dipeptide. Evidently, the configuration of the COOH-terminal amino acid has only a minor influence on the amplitude of the Cotton effect.

As discussed under α-amino acid esters, the change of the sign of the first, and sometimes the second Cotton effect may be caused by the changed conformational equilibria with the character of the α-substituent and the solvent[6]. Solvent effects will be discussed below. The additional COOH group at the phenyl ring of the pyrrolinone-type chromophore IV might be responsible for the difference in the chiroptical properties of the reaction products of dipeptides with fluorescamine and MDPF.

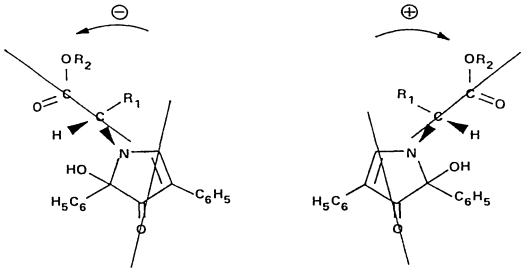

VI VII

Fig. 5. Pyrrolinone chirality rule: negative or positive 2nd Cotton effect arising from the interaction of the pyrrolinone-type chromophores with the carboxyl moiety of L-α-amino acid VI, (L-α-amino acid ester, or dipeptide) or D-α-amino acid VII,(D-α-amino acid ester, or dipeptide).

Pyrrolinone chirality rule

Based on the empirical data, a pyrrolinone chirality rule has been introduced. The second Cotton effect of the fluorescamine and MDPF condensation compounds with α-amino acids, α-amino acid esters and dipeptides is observed in the area (330–320 nm) where their UV spectra show minima. It presumably represents the long wavelength portion of the couplet (short wavelength band at 285–265 nm) resulting from the exciton splitting [20,31], electric dipole-dipole or magnetic dipole-electric dipole coupling (depending on the nature of the carboxylate or ester moiety transitions) between the 280–285 nm transition moment of electron transfer band of the pyrrolinone chromophore and the recently described transition ($\varepsilon = \approx 10^{-2}$, supposedly a singlet → triplet transition of the carbonyl group) of the carboxylic acids, esters and amides in the vicinity of 275 nm [21]. As demonstrated in Fig. 5, the pyrrolinone chirality rule predicts, in agreement with the experimental data, a negative Cotton effect at 330–320 nm for the pyrrolinone derivatives of L-amino acids, their esters and dipeptides, and a positive one for the D-derivatives [24]. The sign of the second Cotton effect is the same for the fluorescamine and MDPF derivatives of α-amino acids, α-amino acid esters and for fluorescamine derivatives of dipeptides. Furthermore, it is unaffected by the nature of the amino acid side chain (alkyl or aromatic), the size of the esters moiety (methyl, benzyl, or t-butyl, or the solvent polarity. Therefore, the proposed chirality rule can be safely used for the determination of the absolute configuration of α-amino acids, esters, and NH_2-terminal amino acids of dipeptides (few exceptions are observed in the case of MDPF derivatives of certain aliphatic dipeptides).

Solvent and pH effects on the CD spectra of MDPF and fluorescamine chromophoric derivatives

Solvent effects

The CD spectra of the isolated MDPF chromophoric derivatives of amino acids (as standards) were measured in ethanol and dioxane, and the spectral pattern was found to be similar in both solvents [13].

However, when amino acids were reacted with MDPF or fluorescamine in a test tube, in the presence of water or buffer and their CD spectra were measured *in situ*, it was found that in the case of the Ala chromophoric derivative, the sign of the first Cotton effect was inverted in L-series from negative to positive. The signs of the other Cotton effects were preserved. Subsequently, additional deviations from this rule were detected in the CD spectra of the MDPF and fluorescamine derivatives of amino acid esters and dipeptides.

For comparison, the CD spectra of synthesized MDPF derivatives of L-Leu-L-Ala were also recorded in phosphate buffer pH 8/methanol (50:50) and in methanol/DMF (50:50), and compared with those of the reaction products obtained *in situ*. It was found that the influence of solvent polarity on the sign of the CD bands of the isolated compounds parallels those of the reaction mixtures *in situ*. Again, the signs of the second and third Cotton effects are independent of the solvent, but those of the first ones are not. Similar observations were made in the case of L-Ala-D-Ala, D-Val-L-Val derivatives. Furthermore, in the CD spectra of the MDPF chromophoric derivatives of L-Val-L-Trp, and L-Ile-L-Phe in methanol DMF (50:50), the signs of the first and second Cotton effects were reversed, but so far, the sign of the third Cotton effect has been found to be independent of solvent polarity[7] and can be safely used for the determination of the absolute configuration of the NH_2-terminal amino acid of a dipeptide.

Several dipeptides, such as L-Lys-L-Trp, and L-Phe-Ile were also reacted with fluorescamine in dioxane/methanol (50:50) and the CD spectra of the reaction mixtures were recorded *in situ*. It was found that the sign at the first Cotton effect in the 400–375 nm is sensitive to the polarity of the solvent, but here the sign of the second and third Cotton effect can be safely used in configurational assignments of the NH_2-terminal amino acid of a dipeptide.

In cases where the empirical rule was not obeyed under standard reaction conditions, the CD spectra of the MDPF chromophoric derivatives *in situ* in organic solvents exhibit spectral pattern in agreement with our empirical rule which applies to the MDPF derivatives of α-amino acids. Lately, repeated experiments have confirmed these observations.

The reaction of MDPF and fluorescamine with α-amino acids, their esters and dipeptides in organic solvents, such as methanol/DMF (50:50), is much slower (the CD spectra of the reaction mixtures are usually recorded after 20 hours) than in the presence of phosphate buffer. Also, there are marked differences in their chiroptical characteristics in solvent systems of a different polarity. Therefore, when the

fluorescamine or MDPF reaction with an amino acid ester or a dipeptide has to be carried out in an organic solvent system (because of solubility problems, etc.), it is advisable to carry out a parallel reaction under the same conditions with a similar compound of a known absolute configuration.

pH effects

Since the introduction of the empirical rule, which correlates the sign of the first, second, and also third Cotton effect with the absolute configuration at the α-carbon atom of an α-amino acid, several exceptions concerning the sign of the first Cotton effect have been observed in the CD spectra of the *in situ* reaction mixtures (especially in the case of α-amino acid esters and dipeptides). Therefore, the CD spectra of several standards such as isolated MDPF condensation compounds with L-Ala, L-Phe, and L-alle were recorded in 0.1 N HCl, in 0.05 M phosphate buffer pH 7, and in 0.1 N KOH containing 5–40% ethanol for solubility purpose. In the case of the Ala chromophore, the sign of the first Cotton effect at around 385 nm is reversed from positive to negative (it is also reversed just by adding 5% H_2O to the ethanolic solution), but the signs of the second and third Cotton effects are preserved in buffer pH 7 and in 0.1 N HCl. The chromophore seems to be unstable in 0.1 N KOH and new bands appear below 350 nm.

The CD spectra of the *in situ* reaction mixtures of L-Leu and L-Phe with MDPF were also recorded at pH 1.8, 8.4, and 12.1. At pH 1.9 and 8.4, the signs of the three Cotton effects are preserved, but at pH 12.1, the signs of the first and second Cotton effect are reversed.

The pH effects on the CD spectra of fluorescamine reaction mixtures with L-Leu and L-Phe have also been investigated *in situ*. As in the case of the MDPF derivatives, there is no change in the spectral pattern at pH 1.9 and pH 8.0. But in 0.1 N KOH, the chromophores are not stable and several spectral shifts occur.

In conclusion, the MDPF or fluorescamine derivatives are not stable above pH 10. On the other hand, acidification of the reaction mixture intensifies the second (at around 330–310 nm) and third (at 290–260 nm) Cotton effects on the average of 30–50% and this pH influence might be useful when a limited amount of material is available.

No pH studies have been carried out with the dipeptide chromophoric derivatives.

Conclusions

The main advantage of the fluorescamine and MDPF methods is their simplicity. These chromophoric reactions are fast and carried out under mild conditions (no isomerization of amino acids has been observed). Under standard conditions, as little as 0.1–1.0 μg of amino acids or esters have been routinely reacted with fluorescamine and useful CD spectra of the reaction mixtures *in situ* are obtained.

It should be noted that on the average rotational values of the fluorescamine and MDPF condensation compounds with α-amino acids and its derivatives are also increased 50-to-200 fold in the 700–400 nm range. Therefore, accordingly less material is needed for the determination of optical purity or the sign of rotation at sodium D-line.

Acknowledgements

We thank Dr. M. Weigele for helpful discussions and Dr. S. De Bernardo for donating several MDPF derivatives of amino acids and dipeptides.

References

1. Fowden L (1973) In: Miller LP (ed.) Phytochemistry Vol. II. Van Nostrand Reinhold, New York, pp. 1–29.
2. Scannell JP and Preuss L (1974) In: Weinstein B (ed.) Chemistry and Biochemistry of Amino Acids, Peptides and Proteins, Vol. III. Marcel Dekker, New York, pp. 189–244.
3. Cahn RS, Ingold CK and Prelog V (1966) Angew. Chem. Internat. Edit. 5: 385–415.
4. Toniolo C and Signor A (1972) Experientia 28: 753–759.
5. Toome V and Weigele M (1981) In: Gross E and Meienhofer J (eds.), The Peptides, Analysis, Synthesis, Biology Vol. IV. Academic Press, New York, pp. 85–184.
6. Toniolo C (1985) In: Barrett GC (ed.) Chemistry and Biochemistry of the Amino Acids, Chapman and Hall, New York, pp. 545–572.
7. Listowsky I, Avigad G and Englard S (1979) J. Org. Chem. 35: 1080–1085.
8. Fowden L, Scopes PM and Thomas RN (1971) J. Chem. Soc. (C) 833–840.
9. Polonski T (1975) Tetrahedron 31: 347–352.
10. Korver D and Liefkens TF (1980) Tetrahedron 36: 2019–2020.
11. Hooker TM Jr. and Schellman JA (1970) Biopolymers 9: 1319–1348.
12. Weigele M, De Bernardo SL, Tengi JP and Leimgruber W (1972) J. Am. Chem. Soc. 94: 5927–5928.
13. Toome V, De Bernardo SL and Weigele M (1975) Tetrahedron 31: 2625–2627.
14. Clark WM and Lubs HA (1916) J. Biol. Chem. 25: 470–484.
15. Toome V and Reymond G (1975) Biochem. Biophys. Res. Commun. 66: 75–80.
16. Toome V, Wegrzynski B and Reymond G (1976) Biochem. Biophys. Res. Comm. 69: 206–211.
17. De Bernardo S, Weigele M, Toome V, Manhart K, Leimgruber W, Bohlen P, Stein S and Udenfriend S (1974) Arch. Biochem. Biophys. 163: 390–399.
18. Toome V, De Bernardo S, Manhart K and Weigele M (1974) Anal. Letters 7: 437–443.
19. Toome V and Wegrzynski B (1981) Anal. Letters 14(B20): 1725–1733.
20. Shellman JA (1968) Acc. Chem. Res. 1: 144–151.
21. Caswell LR, Howard MF and Onisto TM (1976) J. Org. Chem. 41: 3312–3316.
22. Toome V, Wegrzynski B and Dell J (1976) Biochem. Biophys. Res. Comm. 71: 598–602.
23. Toome V, Wegrzynski B (1980) Biochem. Biophys. Res. Comm. 90: 447–451.
24. Toome V and Wegrzynski B (1978) Biochem. Biophys. Res. Comm. 85: 1496–1502.
25. Toome V, Wegrzynski B and Dell J (1977) Biochem. Biophys. Res. Comm. 74: 825–830.
26. Toome V and Wegrzynski B (1983) Biochem. Biophys. Res. Comm. 114: 433–439.
27. Crabbe P, Halpern B and Santos E (1968) Tetrahedron 24: 4315–4326.
28. Toniolo C, Nisato D, Biondi L and Signor A (1972) J. Chem. Soc. Perkin Trans. 1: 1179–1189.
29. Tortorella V, Bettoni G, Halpern B, and Crabbe P (1972) Tetrahedron 28: 2991–2997.
30. Smith HE, Burrows EP, Marks MJ, Lynch RD and Chen FM (1977) J. Am. Chem. Soc. 29: 2908–2916.
31. Harada N and Nakanishi K (1972) Accounts Chem. Res. and references therein 5: 257–263.

Footnotes

1. The L-, or L_S-configuration at C-2 in α-amino acids is usually, but not always (S) in the Cahn-Ingold-Prelog convention [3].
2. When MDPF is dissolved in dioxane, a decrease in the intensity of the CD bands has been observed.
3. We have routinely measured ORD and CD spectra of the synthesized chromophores and those of the reaction mixtures *in situ*. They correlate well with each other. However, the CD spectra are simpler, and therefore, in this paper, only the CD spectral characteristics are discussed.
4. Recently, Kovacs KL (1979) Biochem. Biophys. Res. Commun. 86: 995–1001, came to the same conclusion. However, he apparently was not aware of our recent publications [16 and 25] where we stressed the importance of the second Cotton effect in the 325–300 nm region. Even in our first publication [15] to which Kovacs refers, mentioning a need for revision of our proposed rule, we clearly advised measuring the first and the second Cotton effect. Furthermore, we have been unable to reproduce Kovac's results in cases of Ile, Val, Thr, and Glu, whereas we can consistently reproduce our results.
5. In our preliminary report, Toome V and Wegrzynski B (1983) Biochem. and Biophys. Res. Commun. 114: 433–439, there is a typing error on page 436: under *'Configuration'* (8th line from the bottom) the letters D and L on the 7th and 6th line should read L and D respectively.
6. In a recent communication Toome V and Wegrzynski B (1983) Biochem. and Biophys. Res. Commun. 114: 433–439, on page 434, in the 11th line from the bottom it should state : L-Leu-L-Ala instead of L-Ile-LPhe. In the 8th line it should read: entries 9 and 10 instead of entries 16 and 17.
7. Additional experiments about the influence of the temperature on the sign of the Cotton effects are planned.

Chemo-enzymatic synthesis of enantiomerically pure α-H and α-alkyl α-amino acids and derivatives

J. Kamphuis, H.F.M. Hermes, J.A.M. van Balken, H.E. Schoemaker, W.H.J. Boesten and E.M. Meijer

DSM Research BV, Bio-organic Chemistry Section, P.O. Box 18, 6160 MD Geleen, The Netherlands

Abstract

At DSM a chemo-enzymatic process based on the enantioselective hydrolysis of efficiently prepared amino acid amides by an L-specific amidase from *Pseudomonas putida* has been developed. This chemo-enzymatic method can be used to synthesize natural and synthetic L- as well as D-α-H-amino acids. The use of *in vivo* protein engineering has made it possible to generate a mutant strain of *P. putida*, possessing next to the L-amidase- also D-amidase- and amino acid amide racemase activity. Direct and quantitative conversion of the D,L-amino acid amide, into the D- or L-amino acid is in principle possible.

Enantioselective hydrolysis of α-alkyl α-amino acid amides can be achieved using an amidase from *Mycobacterium neoaurum*. This chemo-enzymatic method provides access to enantiomeric pure L- as well as D-α-alkyl α-amino acids. Both biocatalysts illustrate the exceptional feature that they accept a broad structural range of substrates.

HPLC and NMR analytical techniques have been developed in order to establish the enantiomeric purity of the α-H- and α-alkyl α-amino acids and amides.

Introduction

In the last two decades there has been a growing public awareness and concern with regard to the exposure of man and his environment to an ever increasing number of chemicals. The benefits, however, arising from the use of therapeutic agents, pesticides, food and feed additives, etc. are enormous. Hence there is still an ever increasing demand for more selective drugs and pesticides which are targeted in their mode of action, exhibit less toxic side-effects and are more environmentally acceptable. To this end a central role will be played by chiral (optically pure) compounds as nature at the molecular level is intrinsically chiral. Consequently, this provides an important stimulus to companies to market chiral products as pure optical isomers. This in turn results in an increasing need for efficient methods for the industrial synthesis of optically active compounds.

The advantages of applying biocatalysis to the synthesis of optically pure compounds include: high selectivity (regio- and stereo-), high efficiency, activity under mild reaction conditions and so on. It is therefore expected that biocatalytic methods will play a dominant role in the synthesis of these compounds.

In the present paper we describe the chemo-enzymatic syntheses of α-H-and α-alkyl α-amino acids using amidases from *Pseudomonas putida* and *Mycobacterium neoaurum* respectively. New HPLC and NMR techniques have been developed in order to determine the enantiomeric purity of the α-H and α-alkyl α-amino acids and amides.

Results

Chemo-enzymatic synthesis of enantiomerically pure α-H amino acids

Enantiomerically pure α-H amino acids and their derivatives are important intermediates for the production of pharmaceuticals (see Fig. 1). The well-known fermentation processes used can, however, only be applied to the synthesis of natural L-α-H amino acids. Enzymatic methods, however, can be used for the synthesis of D- as well as L-α-H amino acids.

Starting from readily available aldehydes, aminonitriles are obtained via the Strecker reaction (HCN, NH_3). For the conversion of these aminonitriles to amino acid amides, we have already perfected an efficient one step procedure under alkaline condition in the presence of a catalytic amount of ketone or aldehyde to the desired amide (yield >90%) [1].

The general principle of the enzymatic resolution process [2,3] is based on the use of an L-specific amidase from *P. putida* ATCC 12633 [4]. The crude biocatalyst is used in the soluble form, since in this manner poorly soluble amino acids can also be resolved without difficulties. We observed a nearly 100% stereoselectivity in the hydrolysis of selectively the L-amino acid amides of a broad range of amino acid amides (Table 1). Moreover, no enzymic side effects are observed and substrate concentrations up to 20% by weight can be used without affecting the enzyme activity. The biocatalyst is also active at a broad pH-range of 8–10.

After enzymatic hydrolysis, the L-amino acid has to be separated from the D-amino acid amide (see Fig. 2). Ingeniously we found at DSM that the addition of one equivalent of benzaldehyde to the enzymic hydrolysate solution, afforded the

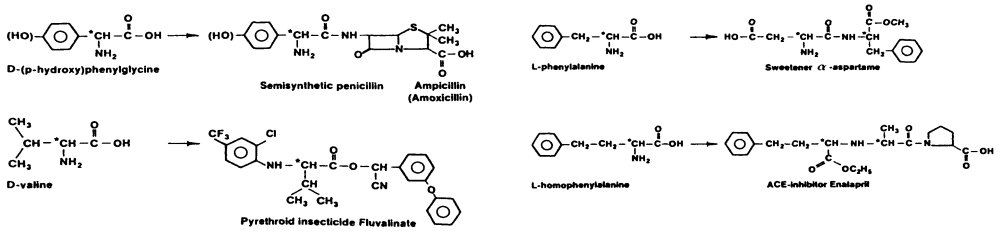

Fig. 1. Some potential applications of α-H amino acids as chiral building blocks for pharmaceuticals, agrochemicals and sweeteners.

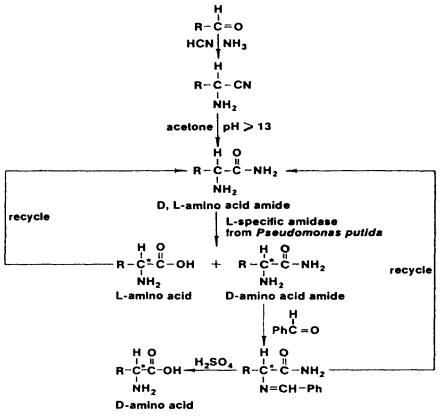

Fig. 2. DSM process for the synthesis of optically pure L-as well D-α-H amino acids.

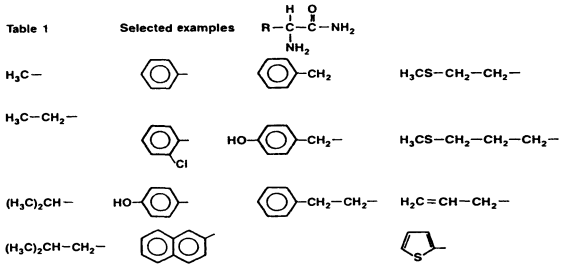

Table 1. Some selected examples of substrates that are stereospecifically converted using an L-amidase from *Pseudomonas putida.*

insoluble Schiff base of benzaldehyde and the D-amino acid amide, thus allowing it to be easily isolated by filtration. It was also discovered that these N-benzylidene amino acid amides are prone to racemisation and in organic solvent, using a small amount of base (depending on the substituent R), racemisation can take place within minutes [5]. In this way the D-enantiomer can be efficiently recycled making quantitative yields (100%) of L-α-H-amino acids possible (conversely, 100% conversions to the D-amino acid will also be possible provided that the L-amino acid amide is first prepared from the amino acid) [6,7].

However, if a biocatalyst could be found with D-amidase – respectively L-amidase – in combination with amino acid amide racemase activity, no chemical recycling procedures would be necessary. Direct conversion of the D,L-amino acid amide into the D-amino acid resp. L-amino acid would then be possible (see Fig. 3).

Using *in vivo* protein engineering not only mutant strains of *P. putida* exhibiting L-amidase-but also D-amidase and amino acid amide racemase activity were obtained [8].

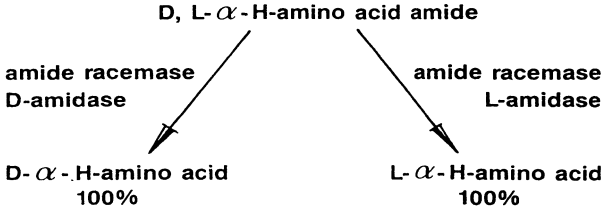

Fig. 3. DSM process using mutant strains of *Pseudomonas putida* having L-amidase or D-amidase activity in combination with amino acid amide racemase activity.

It is noteworthy that the α-hydrogen is an essential structural feature for the biocatalytic activity.

These enantiomerically pure compounds (amino acids) are members of the chiral pool and therefore very well suited to be chemically derivatized into intermediators for ACE inhibitors like Enalapril, Lysinopril, etc. (see Fig. 1).

Chemo-enzymatic synthesis of α-alkyl α-amino acids

In recent years medicinal chemists have been increasingly interested in bioactive peptides (like neuropeptides, chemotactic peptides and for example enkephalins) containing α-alkyl α-amino acids, since they tend to freeze specific conformations and slow enzymatic degradation processes down dramatically.

Through screening, a new biocatalyst was found enabling access to this interesting class of α-alkyl α-amino acids. The amidase biocatalyst from *M. neoaurum* is capable of stereoselectively hydrolyzing a whole range of α-alkyl α-amino acid amides [7,9] (see Table 2 and Fig. 4).

Several of these amino acids are now incorporated into bioactive peptides [10,11]. Many more of these are found in nature, for example L-isovaline is found in peptaibol antibiotics [12,13]. Their influence on the conformational behaviour of peptides is presently under intensive investigation [14].

Determination of the enantiomeric purity of α-H- and α-alkyl α-amino acids and their corresponding acid amides by means of HPLC [15]

Derivatization with *o*-phthalaldehyde in combination with N-acetyl-L-cysteine has proven to be a useful method for the optical resolution of enantiomeric α-H amino acids, α-alkyl α-amino acids and the corresponding acid amides. By using reversed-

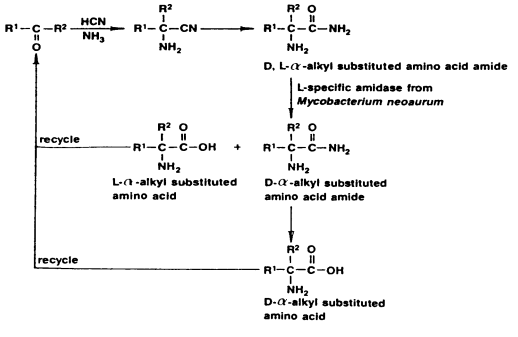

Fig. 4. Process for the syntheses of optically pure α-alkyl α-amino acids.

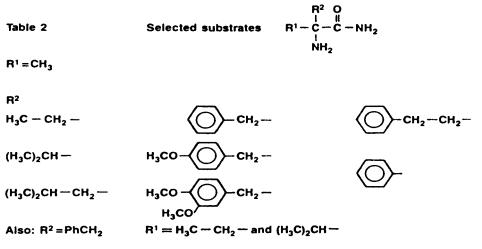

Table 2. Types of substrates which can be stereospecifically converted using the amidase from *Mycobacterium neoaurum.*

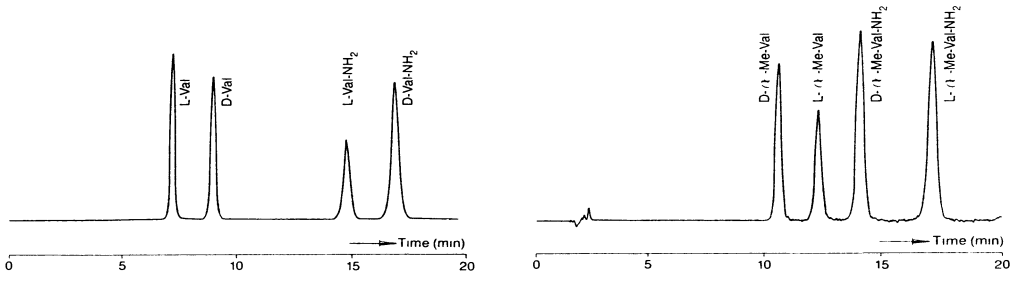

Fig. 5. Chromatogram of OPA – NAC derivatives of L-, D-Val, D-, L-Val-NH_2, D-, L-α-CH_3-Val and D-, L-α-CH_3-Val-NH_2.

phase high-performance liquid chromatography with a mobile phase containing copper (II) acetate and L-proline, the diastereomeric derivatives of the α-amino compounds can be separated under isocratic conditions. The rate of reaction of α-alkyl α-amino compounds with *o*-phthalaldehyde-*N*-acetyl-L-cysteine can be increased by selectively increasing the amount of *o*-phthaladehyde in the reaction mixture. When the derivatization parameters were controlled automatically, the derivatization process showed good reproducibility and the method was found to be suitable for quantitative measurements. The method was successfully applied to the monitoring of the enantiomeric purity of α-H α-amino acids and α-alkyl α-amino acids obtained by enantioselective hydrolysis of the corresponding acid amides using an aminopeptidase [7,9]. (See Fig. 5).

A novel single-step method for enantiomeric excess determination of α-H and α-alkyl α-amino acids by NMR [9]

A procedure for ee determination has been recently described in which esters of amino acids are coupled with the achiral reagent CH_3PSCl_2 [16]. The extra steric hindrance present in α-alkyl α-amino acids unfortunately inhibits both the esterification and the coupling with CH_3PSCl_2. We found, however, that Schotten-Baumann coupling of S-2-chloropropionyl chloride, with the free amino acids followed by analysis of the ratio of diastereomers by 'H NMR provides a fast and accurate analysis of the ee's of normal as well as α-alkyl α-amino acids [9]. (See Fig. 6).

By proper choice of solvent and signal, sufficient signal separation can be obtained to allow accurate integration of the diastereomer ratio (see Table 3).

Conclusions

We believe that the methods here described provide a simple access to large-scale synthesis of enantiomerically pure natural and synthetic L- and D-α-H- and

Table 3. 'H NMR data for (S)-2-chloropropionyl derivatives of racemic amines and amino acid

Entry	Amino acids	Chemical shift, δ		Solvent
		CH_3CHCl	$NHCCH_3$	
1	$(CH_3)_2CHCHNH_2CO_2H$	1.79, 1.77 (J = 7.0 Hz)		CD_3OD
		1.75, 1.74 (J = 7.0 Hz)		$CDCl_3$
		1.51, 1.49 (J = 6.8 Hz)		C_6D_6
2	$C_6H_5CH_2CHNH_2CO_2H$	1.73, 1.67 (J = 6.7 Hz)		CD_3OD
		1.68, 1.63 (J = 7.0 Hz)		$CDCl_3$
3	$CH_3SCH_2CH_2CHNH_2CO_2H$	no separation		$CDCl_3$
		1.60, 1.57 (J = 7.0 Hz)		C_6D_6
		1.79, 1.78 (J = 7.0 Hz)		CD_3OD
4	$C_6H_5C(CH_3)NH_2CO_2H$	1.76, 1.72 (J = 7.4 Hz)		$CDCl_3$
5	$C_6H_5C(CH_3)NH_2CO_2H$	1.73, 1.69 (J = 7.3 Hz)		$CDCl_3$
6	$(CH_3)_2CHC(CH_3)NH_2CO_2H$	1.76, 1.74 (J = 7.0 Hz)	1.64, 1.62	CD_3OD
7	$C_6H_5CH_2C(CH_3)NH_2CO_2H$	no separation	1.69, 1.60	CD_3OD
		no separation	1.62, 1.59	D_2O
8	$C_6H_5CH_2CH_2C(CH_3)NH_2CO_2H$	no separation	1.74, 1.71	CD_3OD
		no separation	1.58, 1.54	C_6D_6
9	p-$CH_3OC_6H_4CH_2C(CH_3)NH_2CO_2H$	no separation	1.68, 1.60	CD_3OD
10	$(CH_3)_2CHCH_2C(CH_3)NH_2CO_2H$	no separation	1.67, 1.66	CD_3OD
			1.78, 1.76	C_6D_6

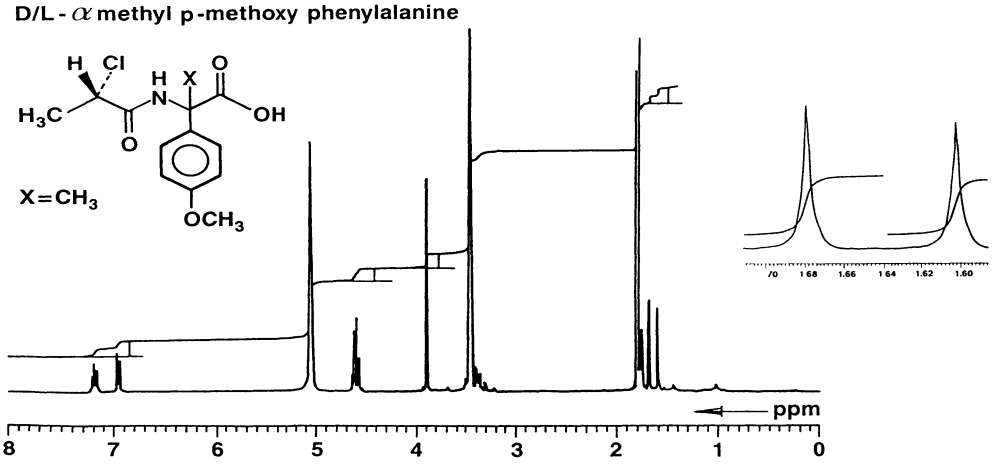

Fig. 6. 'H NMR of the Schotten-Baumann coupling adduct of S-2-chloropropionyl chloride and α-CH_3-paramethoxyphenylglycine.

α-alkyl amino acids and amides. We also are convinced that the easy and accurate analytical techniques described here (HPLC and NMR) are general methods for the determination of the enantiomeric excess.

References

1. Boesten WHJ (1986) Eur. patent 0.232.562.
2. Meijer EM, Boesten WHJ, Schoemaker HE and van Balken JAM (1985) In: Tramper J, van der Plas HC and Linko P (eds.) Biocatalysis in Organic Synthesis. Elsevier, pp. 135–156.
3. Boesten WHJ, Dassen BHN, Kerkhoffs PL, Roberts MJA, Cals MJH, Peters PJH, van Balken JAM, Meijer EM and Schoemaker HE (1986) In: Schneider MP (ed.) Enzymes as Catalysts in Organic Synthesis, pp. 335–360.
4. Boesten WHJ and Meijer-Hoffman LRM (1978) U.S.A. patent 4.080.259.
5. Boesten WHJ, Schoemaker HE and Dassen BHN (1986) Eur. patent 1.994.07.
6. Sheldon RA, Schoemaker HE, Kamphuis J, Boesten WHJ and Meijer EH (1988) In: Ariens EJ, van Rensen JJS and Welling W (eds.) Stereoselectivity of Pesticides 14: 409–451.
7. Kamphuis J, Kloosterman M, Schoemaker HE, Boesten WHJ and Meijer EH (1987) Chiral intermediates and applications, Proc. 4th European Congress on Biotechnology 4: 331–348.
8. Hermes HFM *et al.* (priority date Febr. '87) (publ. 1989) Eur. patent appl. 0.307.023, WO 89/01525.
9. a) Kruizinga WH, Bolster J, Kellogg RM, Kamphuis J, Boesten WHJ, Meijer EM and Schoemaker HE (1988) J. Org. Chem. 53: 1826.
   b) Boesten WHJ and Peters PJH (1984) Eur. patent 0.150.854.
   c) Boesten WHJ and Kamphuis J (1986) Eur. patents 0.231.548, 0.236.591, 0.232.562.
10. Pandey RC, Meng H, Cook JC and Rinehart KL (1977) J. Am. Chem. Soc. 99: 5203.
11. Fox RO and Richard FM (1982) Nature 300: 325–327.
12. Goodman M (1985) Biopolymers 24: 137–155.
13. Marshall GR (1982) In: Lubitt AG and Creighton AM (eds.) Chemical Regulation of Biological Mechanisms. London.
14. a) Barone V, Fraternali F, Cristinziano PL, Lelj F and Rosey A (1988) Biopolymers 27: 1673–1685 and references cited therein.
   b) Toniolo C and Benedetti E (1988) ISI Atlas of Science Biochemistry pp. 225–230.
15. Duchateau A, Crombach M, Kamphuis J, Boesten WHJ, Schoemaker HE and Meijer EM (1989) J. Chromatography 471: 263–270.
16. Feringa BL, Strijtveen B and Kellogg RM (1986) J. Org. Chem. 51: 5484.

Synthesis of ^{11}C-labelled amino acids

G. Antoni, P. Bjurling, K.J. Fasth, A. Gee and B. Långström

Department of Organic Chemistry, University of Uppsala, Box 531, S-751 121 Uppsala, Sweden

Abstract

In this paper the synthesis of amino acids labelled in different positions with the short-lived positron emitting radionuclide carbon-11 are described. Both aliphatic and aromatic amino acids have been synthesized. To obtain the labelled amino acids enantiomerically pure or enriched in the L-form different approaches such as resolution of racemic mixtures or asymmetric syntheses by chemical or enzymatic methods have been used. The importance of the labelling position in the molecule and some special problems encountered when working with short-lived radionuclides of high specific radioactivity are discussed.

Introduction

Isotopically labelled compounds have been used to elucidate biochemical pathways for a long time. Compounds specifically labelled with tritium or carbon-14 in combination with the autoradiography technique have for example been used to study the distribution of biologically interesting compounds in different organs. These investigations are, however, restricted to experimental animals or *in vitro* studies on post-mortem human tissue. The positron emission tomography (PET) technique on the other hand has the potential to study the biodistribution of exogenic and endogenic compounds *in vivo* both in humans and animals. Another important feature of the PET technique is the possibility to study non-invasively biochemical and physiological processes *in vivo* [1,2].

The decay characteristics of the radionuclides used (^{11}C, $t_{1/2}$ = 20.4 min, ^{18}F, $t_{1/2}$ = 110 min ^{13}N, $t_{1/2}$ = 10 min, and ^{15}O, $t_{1/2}$ = 2 min) are the basis for the possibility to apply the PET technique to *in vivo* studies. These radionuclides decay by emitting a positron which in an annihilation reaction with an electron creates two photons traversing in opposite directions from each other. The high energy photons formed in the annihilation (511 keV) easily penetrate tissue and can be detected by external detectors enabling reconstruction of an image showing the spatial distribution of the labelled compound in the studied organ.

Biomedically interesting compounds labelled with the short-lived positron emitting radionuclides mentioned, is a requirement for the successful employment of the PET technique. The possibility to produce ^{11}C, ^{18}F, ^{13}N and ^{15}O with high specific radioactivity means that compounds labelled with these radionuclides can be used in tracers studies i.e., without disturbing the studied system.

The development of the PET technique depends to a great extent on improved labelling syntheses. During the last decade especially, the access to ^{11}C-labelled compounds has increased considerably due to the development of reactive ^{11}C-labelled synthons and fast labelling procedures. Amino acids labelled with carbon-11 have proved to be versatile research tools in studies of important biological processes and also in some clinical applications. Examples of PET investigations using ^{11}C-labelled amino acids are in studies of cerebral protein synthesis [3] delineation of brain tumours [4] and neurotransmitter synthesis [5].

This paper deals mainly with the synthesis of amino acids specifically labelled with carbon-11. Several synthetic approaches leading to amino acids and α-methylamino acids labelled in different positions are presented. The stereochemistry of the ^{11}C-amino acids is important. Fast methods for the resolution of racemic amino acids as well as chemical and enzymatic syntheses resulting in products enantiomerically pure or enriched in the desired enantiomeric form are shown.

Experimental

General

[^{11}C]Carbon dioxide was produced by the ^{14}N(p,α)^{11}C nuclear reaction in a gas target. The 10 MeV protons used were produced by the tandem van de Graaff accelerator at the The Svedberg laboratory, University of Uppsala. The [^{11}C]-carbon dioxide obtained was trapped in a lead shielded oven containing 4-Å molecular sieves and transported to the chemistry laboratory.

The ^{11}C-labelled alkyl iodides used in the alkylation reactions were obtained according to previously described procedures [6–9]. Hydrogen [^{11}C]cyanide was produced according to a well known procedure [10].

Synthesis of [3–^{11}C]amino acids

Racemic [3–^{11}C]amino acids have been obtained by a phase transfer alkylation reaction with ^{11}C-labelled alkyl iodides on an achiral protected glycine derivative

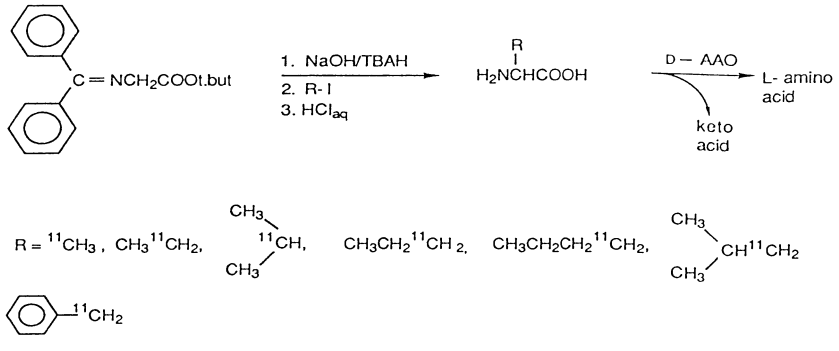

Scheme 1.

as shown in Scheme 1 [11]. The alkylation product was subjected to acid hydrolysis to remove the protecting groups. ^{11}C-Labelled L-alanine, L-valine and L-phenylalanine were then obtained by treatment of the racemic mixture with D-amino acid oxidase (EC 1.4.3.3).

In Scheme 2 another approach is shown. An alkylation reaction employing anhydrous reaction conditions with ^{11}C-labelled alkyl iodides on a chiral protected glycine derivative followed by a two-step hydrolysis of the protecting groups resulted in 3-^{11}C-amino acids enriched in the L-form [12,13].

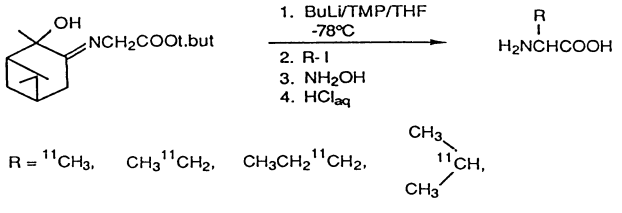

Scheme 2.

Another example of asymmetric synthesis is shown in Scheme 3. The diastereomeric alkylation products were obtained in unequal amounts and were separated by HPLC which after hydrolysis of the protecting groups resulted in enantiomerically pure L-3-^{11}C-amino acids [14].

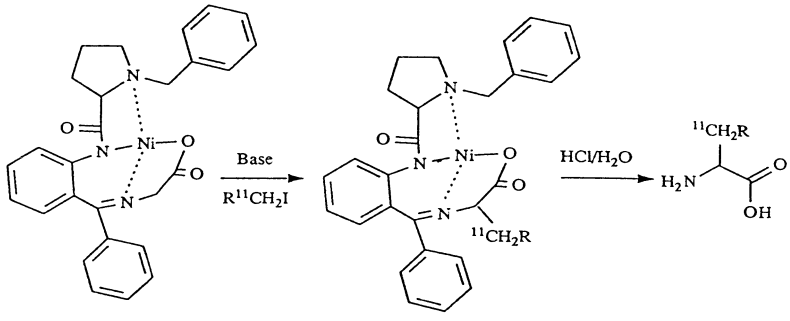

Scheme 3.

Enzymatic synthesis of aromatic ^{11}C-amino acids

In Scheme 4 the synthesis of the carboxylic or ß-^{11}C-labelled enantiomerically pure 3,4-dihydroxy-L-phenylalanine (L-DOPA), L-tyrosine, L-tryptophan and 5-hydroxy-L-tryptophan are shown [15–17].

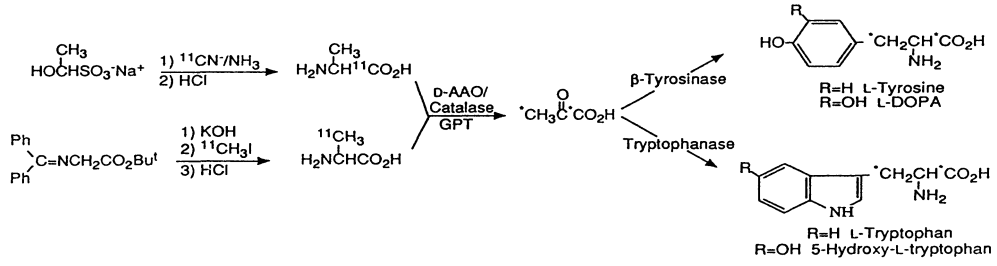

Scheme 4.

For these syntheses 1-^{11}C-, and 3-^{11}C-labelled alanine were needed as precursors for the subsequent multi-enzymatic syntheses. Racemic [1-^{11}C]Alanine was synthesized by reacting hydrogen [^{11}C]cyanide with the bisulfite adduct of acetaldehyde and ammonia followed by acid hydrolysis [18]. DL-[3-^{11}C]Alanine was obtained in a similar way as shown in Scheme 1. The ^{11}C-labelled alanine was enzymatically converted to the aromatic L-amino acids by the use of D-amino acid oxidase (EC 1.4.3.3), catalase (EC 1.11.1.6), glutamic-pyruvic transaminase (EC 2.6.1.2), and ß-tyrosinase (EC 4.1.99.2) or tryptophanase (EC 4.1.99.1) together with the appropriate precursor. The enzymatic reactions were performed in a one-pot reaction.

Synthesis of ^{11}C-labelled α-methylamino-acids

L-α-methyl[methyl-^{11}C]amino acids were synthesized according to Scheme 5 [19]. Alkylation of the appropriate alkylmalonic diester with [^{11}C]methyl iodide gave the α-methylalkyl derivative. By the use of an enzymatic de-esterification reaction using pig liver esterase (EC 3.1.1.1.) the enantiomerically pure L-monoesters were obtained [20]. A modified Curtius rearrangement followed by acid hydrolysis gave the labelled L-α-methylamino acids.

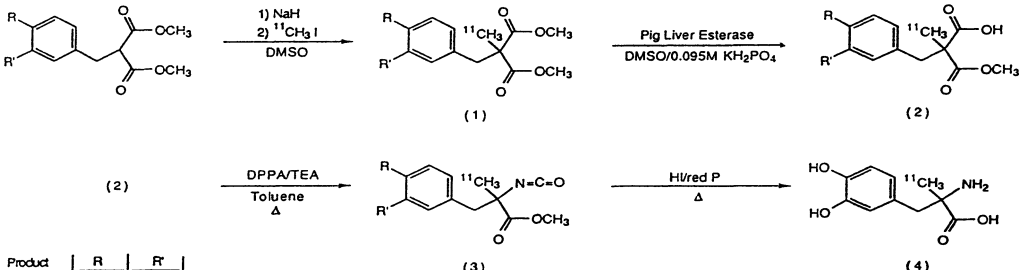

Product	R	R'
αMePhe	H	H
αMeTyr	OMe	H
αMeDopa	OMe	OMe

Scheme 5.

Synthesis of ^{11}C-amino acids using [^{11}C]cyanide

The synthesis of γ-amino[4-^{11}C]butyric acid (GABA) is shown in Scheme 6. A Michael addition reaction on ethyl acrylate with [^{11}C]cyanide followed by a selective reduction of the nitrile obtained gave the labelled GABA after alkaline hydrolysis [21].

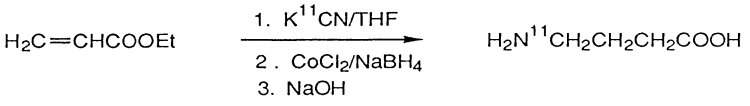

Scheme 6.

Another example of a Michael addition reaction using [^{11}C]cyanide is shown in Scheme 7. The addition product obtained was reduced to the corresponding amine followed by acid hydrolysis forming DL-2,4-diamino[4-^{11}C]butyric acid (DABA) [22].

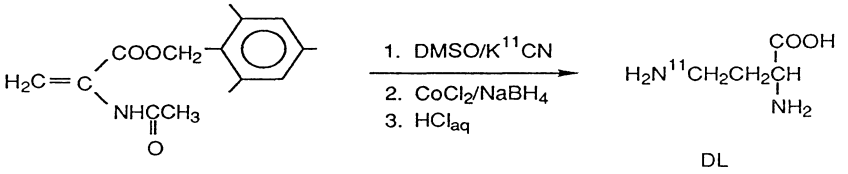

Scheme 7.

Synthesis of L- or D-[methyl-^{11}C]methionine

The synthesis of the labelled methionine was performed according to Scheme 8 [6].

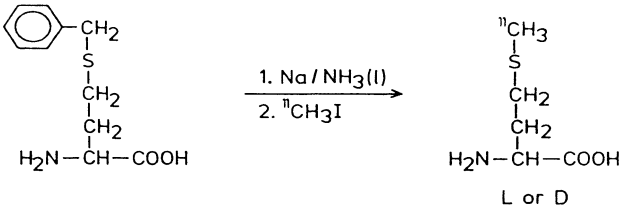

Scheme 8.

The alkylation reaction was performed in liquid ammonia/sodium on the corresponding sulfide anion of D- or L-*S*-benzylhomocysteine with [^{11}C]methyl iodide.

The solvent was removed and the residue purified by semi-preparative HPLC yielding the enantiomerically pure product.

All the ^{11}C-labelled amino acids obtained were purified either by a cation-exchange resin or by preparative HPLC.

Results and Discussion

The short half-life of carbon-11 and the limited access to labelled precursors restricts the possible synthetic pathways that can be used. Another complicating factor in designing a synthetic strategy is that the label should be introduced as late as possible in the synthesis. A rule of thumb is that a synthesis, including purification should not take more than three half-lives (60 min in the case of ^{11}C). It is however, as we show in this paper, possible to perform a 7-step synthesis within this rather short time span (c.f. Scheme 5).

In work with radionuclides of high specific radioactivity small volumes, typically 0.1–1 ml are used. In order to minimize losses of product on the surface of the reaction vessels it is important to reduce the number of transfers from one vessel to another during the reaction sequence. One-pot procedures are therefore to be preferred and have been used when possible in the syntheses presented. The technical handling is further complicated by the need for radioprotection.

In synthesis with short-lived radionuclides the synthesis time is, as mentioned, important. Apart from the usual criteria used to describe the results of a synthesis i.e. yield and purity, synthesis times must be included. The syntheses that are described in this paper were typically performed in 40–60 min starting from [^{11}C]carbon dioxide. In the synthesis of the aromatic ^{11}C-labelled amino acids (c.f Scheme 4) the synthesis times were reduced considerably by performing the enzymatic reactions in a one-pot reaction and adding the enzymes instantaneously instead of consecutively.

The results of the described syntheses are summarised as follows. The radiochemical purities were in all cases higher than 98% with radiochemical yields ranging from 20–70%, decay corrected and based on the amount of [^{11}C]carbon dioxide or hydrogen [^{11}C]cyanide used. The enantiomeric purities of the amino acids obtained by enzymatic synthesis (Scheme 1, 4 and 5) were higher than 99%. The enantiomeric purity of the L-3-^{11}C-amino acids obtained by asymmetric synthesis were 80–87%. D- or L-[methyl-^{11}C]methionine were obtained enantiomerically pure i.e. with an enantiomeric excess higher than 99%. In the methionine synthesis the stereochemistry was already established prior to the labelling. The specific radioactivities of the amino acids were in the order of 10–100 mCi/μmol. The radiochemical purities as well as the identity of the obtained products were determined by the use of at least two different HPLC systems. Also the enantiomeric purities were determined by chromatographic methods either directly using chiral stationary phases or after derivatisation to diastereomers.

Before use in biomedical application in animals or humans, the solutions of the labelled amino acids were made isotonic and adjusted to physiological pH with phosphate buffer and saline. Filtration through a 0.22 μm filter ensured that the solutions were sterile. No pyrogens could be detected by the limulus test. Details of the experimental conditions and the results of the syntheses are found in the respective papers.

The importance of the position of the label in the amino acid is exemplified in the PET study of the *in vivo* synthesis of dopamine from DOPA. After enzymatic decarboxylation carboxylic ^{11}C-labelled DOPA results in [^{11}C]carbon dioxide and unlabelled dopamine whereas ß-^{11}C-labelled DOPA gives unlabelled carbon dioxide and labelled dopamine. The corresponding PET images show very different distributions of the radioactivity in the brain.

The application of ^{11}C-labelled amino acids as *in vivo* tracers for different purposes has been only briefly discussed here whereas several methods used to obtain them have been presented. It must, however, be emphasized that the demands of new labelled tracers to be used in PET is one incentive for the further developments in the field of labelling synthesis.

Acknowledgements

We are indebted to Fil. Lic Petter Malmborg for radionuclide production and to the Swedish Natural Science Research Council for financial support grant K-KU 3463

References

1. Greitz T, Ingvar DH and Widen L (eds.) (1985) The Metabolism of the Human Brain Studied with Positron Emission Tomography. Raven Press, New York.
2. Hayashi O and Torizaku K (eds.) (1986) Biomedical Imaging. Academic Press, New York.
3. Phelps ME, Barrio JR, Huang SC, Keen RE, Chugani H and Mazziotta JC (1984) Ann. Neurol. 192.
4. Lilja A, Bergström K, Hartvig P, Spännare B, Halldin C, Lundqvist H and Långström B (1985) A.J.N.R. 6: 505.
5. Långström B, Bjurling P and Hartvig P (1989) to be submitted.
6. Långström B, Antoni G, Gullberg P, Halldin C, Någren K, Rimland A and Svärd H (1986) Int. J. Appl. Radiat. Isot. 37: 1141–1145.
7. Långström B, Antoni G, Gullberg P, Halldin C, Malmborg P, Någren K, Rimland A and Svärd H (1987) J. Nuc. Med. 28: 1037–1040.
8. Antoni G and Långström B (1987a) Appl. Radiat. Isot. 38: 655–659.
9. Fasth KJ, Antoni G and Långström B (1989a) Appl. Radiat. Isot. submitted.
10. Christman DR, Finn RD, Karlstrom K and Wolf AP (1975) Int. J. Appl. Radiat. Isot. 26: 435.
11. Antoni G and Långström B (1987b) J. Labelled. Compd. Radiopharm. 24: 125–143.
12. Antoni G and Långström B (1986) Acta. Chem. Scand. B 40: 152–156.
13. Antoni G and Långström B (1987c) Acta. Chem. Scand. B 41: 511–517.
14. Fasth KJ, Antoni G and Långström B (1989b) Acta. Chem. Scand. to be submitted.
15. Bjurling P, Watanabe Y, Tokushige M, Oda T and Långström B (1989) J. Chem. Soc. Perkin Trans. 1: 1331–1334.
16. Bjurling P, Watanabe Y, Oka S, Nagasawa T, Yamada H and Långström B (1989) J. Org. Chem. submitted.

17. Bjurling P, Antoni G, Watanabe Y and Långström B (1989) Appl. Radiat. Isot. submitted.
18. Iwata R, Ido T, Takahashi T, Nakanishi H and Iida S (1987) Appl. Radiat. Isot. 38: 97.
19. Gee AD and Långström B (1989) J. Labelled Compd. Radiopharm. 26: 327.
20. Björkling F, Boutelje J, Gatenbeck S, Hult, Norin T and Szmulik P (1985) Tetrahedron 41: 1347.
21. Antoni G and Långström B (1989a) J. Labelled Compd. Radiopharm. 27: 571–576.
22. Antoni G and Långström B (1989b) to be submitted.

Chemoenzymatic syntheses of enantiomerically pure hydroxy amino acids

H. Hönig, P. Seufer-Wasserthal and H. Weber

Graz University of Technology, Institute of Organic Chemistry, Stremayrgasse 16, A-8010, Austria

Abstract

Hydroxy amino acids constitute essential partial structures of many biologically important compounds. While there are several ways of controlling the stereochemistry of condensation- or ring opening reactions leading to *erythro*- or *threo*- products of high diastereomeric purity there is no generally applicable method of separation of these racemates into their respective optical antipodes. Here we describe the enantiomeric resolution of easily obtainable precursors, namely azido hydroxy derivatives. The resolutions are accomplished by hydrolysis of the respective O-acyl derivatives of the hydroxy azido carboxylic acid esters with the aid of commercially available lipases, mainly from *Candida cylindracea* and *Pseudomonas fluorescens*. The rates of conversion and the enantiomeric purities attainable are demonstrated with all four diastereomers of azido hydroxy 3-phenylpropionic acid (precursors of phenylserine and phenyl-*iso*-serine). Details on the dependence of the stereospecifity of the hydrolysis on the kind of the ester used as well as on the regiosisomer employed are given. The simplicity of the method easily allows for scale up of the preparative procedure and thus shows promise for the extension to other systems of biological interest.

Introduction

Besides the well known essential amino acid threonine, there are several rare natural hydroxy amino acids, most of them occurring as part of bigger molecules with distinct biological effects. Thus bestatin, *N*-[(2*S*,3*R*)-3-amino-2-hydroxy-4-phenylbutanoyl]-L-leucine (**1**) and analogues thereof are known to exhibit strong aminopeptidase B inhibitory effects and act as immunomodulators useful in cancer treatment [1,2]. Statine, (3*S*,4*S*)-4-amino-3-hydroxy-6-methylheptanoic acid (**2**) is part of the natural peptide pepstatin (Iva-Val-Val-Sta-Ala-Sta). Incorporation of statine and analogs thereof into appropriate peptide sequences has led to the discovery of potent human renin inhibitors [3]. Moreover, the (3*S*,4*R*)-diastereomer has received considerable attention as a key component of the didemnins, with significant antitumor and antiviral activity [4–6]. Pepstatin and statine itself can act as inhibitors of the human immune deficiency virus-1 protease [7,8] ß-Hydroxyhistidine (**3**) as part of the bleomycins is essential for the complexation of iron and copper ions, important for the activation of oxygen which in turn leads to their useful activity against squamous cell carcinomas and malignant lymphomas, including Hodgkin's disease [9].

While there are some excellent syntheses of single representatives of these rare amino acids [10–14], there is no simple and general method for the preparation of

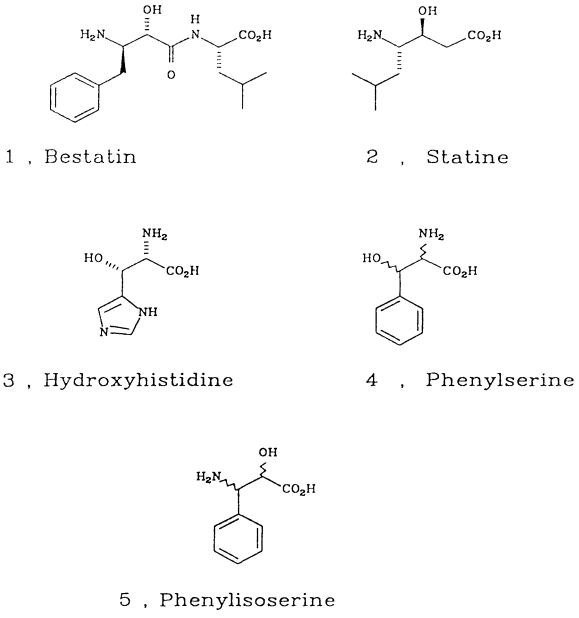

Fig. 1. Structures of some naturally occurring hydroxy amino acids.

optically pure hydroxy amino acids, which allows to produce all isomers in equal quantities. This is very important for practical reasons, because substantial amounts of either pure enantiomer are needed for well founded pharmacokinetic data without the 'enantiomeric ballast' [15] of the other isomer.

We have shown in the cyclic [16,17] and acyclic series [18] of simple azido alcohols – which are suitable precursors for amino alcohols – that enzymatic hydrolyses of the respective butyrates proceed with acceptable conversion rates and in excellent optical yields. Since it is known that introduction of a carboxylic acid functionality in molecules which otherwise give moderate optical yields often improves the resolution [19], the application of our methodology to hydroxy azido carboxylic acids looked very promising.

We have chosen 3-phenylserine (**4**) and 3-phenylisoserine (**5**) as model compounds for this class of substances. They exhibit some distinct biological effects like inhibition of growth of influenza-viruses [20,21] as well as reducing the death rate of rats infected by rabies [22]. Moreover, the necessary precursors are prepared very easily (Fig. 2). The diastereomers of (**6**) and (**7**) are also well suited from a theoretical point of view, since they bear sterically demanding substituents in the vicinity of the function to be resolved. Enzymatic resolution on these model compounds provided, from the experience gained by own experiments and the

results of many other groups, the extension to the systems mentioned above should be straightforward. There is an early report on protease catalyzed resolution of the *N*-trifluoracetyl derivative of DL-**4** with the aid of a carboxypeptidase [23].

Experimental procedures

Optical rotations were measured on a JASCO DIP-360 polarimeter in CH_2Cl_2 solution. The optical yields were determined by ^1H- and ^{19}F-NMR of the respective (*S*)-MTPA esters [24]. NMR spectra were recorded in $CDCl_3$ on a Bruker MSL 300 at 300 MHz (^1H), 75.47 MHz (^{13}C), and 282.27 MHz (^{19}F). All esters were purified by bulb-to-bulb distillation before enzymatic hydrolysis.

Reactions were monitored by t.l.c. using silica gel Merck $60F_{254}$ plates; purifications of products and separations of esters and alcohols after the enzymatic conversions were performed on silica gel Merck 60 with mixtures of ethyl acetate and petrolether as mobile phase. All commercially obtained compounds were used as received. The esterifications with different acyl residues were done according to standard procedures [25]. All new compounds showed the correct elemental analysis together with the spectral characteristics expected (^1H-NMR and ^{13}C-NMR). *Erythro-* and *threo-* isomers could be distinguished unambiguously by their respective pattern of the chemical shifts and coupling constants (^1H-NMR) of the protons attached to the chiral centers [26]. The basic operational steps and details of the enzymatic resolutions are described elsewhere [16–18]. Crude enzyme preparations were employed without further purification. Lipase P (30 μ/mg) is a product from Amano Pharmaceutical Co., *C. cylindracea* lipase (12 μ/mg) was purchased from Sigma (1 μ is able to liberate 1 μmol fatty acid/min at pH 7.0 and 25°C). All enzymatic hydrolyses were performed with a Schott TR 156 pH-stat.

Results

For the preparation of the starting materials there are several alternative strategies (see Fig. 2). Although there are ways of controlling the stereochemistry of condensation reactions like **b** or **g** at least to a certain extent [22], tedious separation procedures for the *threo-* and *erythreo*-diastereomers are not very appealing when aiming at a simple and efficient method for the synthesis of larger quantities. In addition path **g** uses ethyl azido acetate, the preparation of which might contain some safety risks.[1] Thus we referred to the stereochemically well defined pathways **a** – **c** – $\mathbf{e}_2$ for **7a** and **7b** respectively, whereas steps **d** – $\mathbf{e}_1$ – $\mathbf{f}_1$ lead to **6a** and **6b**.

These sequences start from readily available α,ß-unsaturated carboxylic ester derivatives. The availability of the starting materials is an essential prerequisite in

[1] Although prepared for several times without problems, the residue of one of the distillations detonated without any obvious reason.

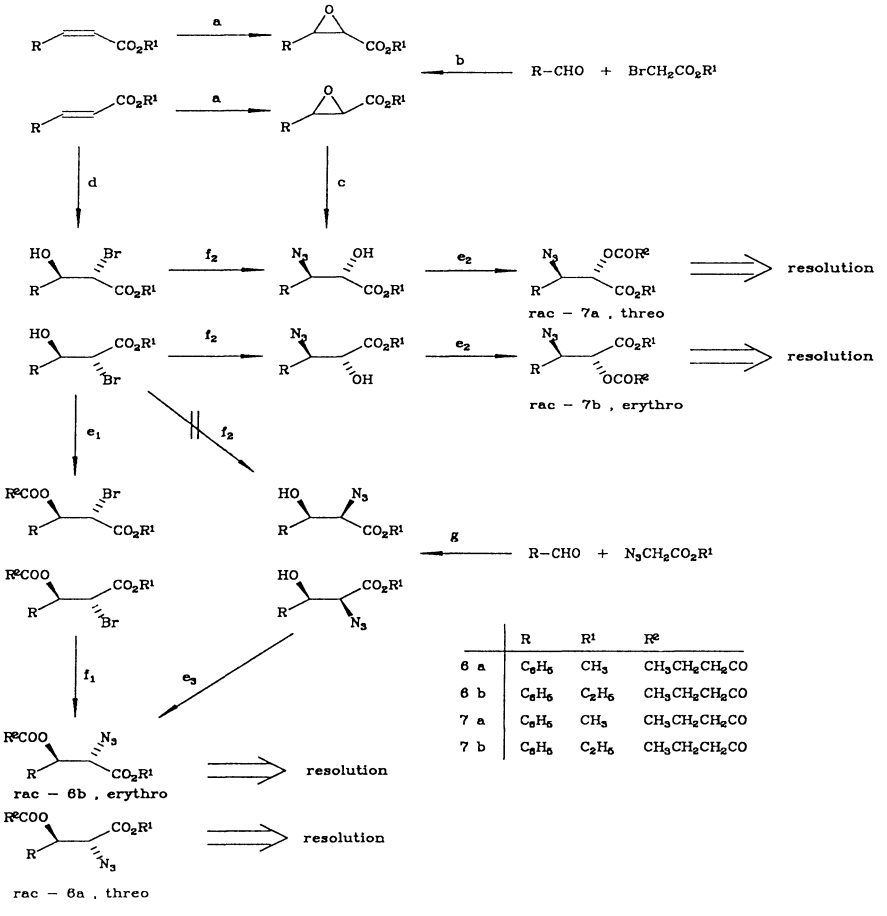

Fig. 2. Pathways to O-acyl derivatives of hydroxy azido carboxylic acid esters.
a: *m*-chloroperbenzoic acid / CH_2Cl_2
b: base
c: NaN_3 / EtOH / H_2O / NH_4Cl
d: *N*-bromosuccinimide / tetrahydrofurane / H_2O
e: $(R^2CO)_2O$ / pyridine / 4-dimethylaminopyridine / CH_2Cl_2
f: NaN_3 / dimethylformamide
g: base

designing a simple and general synthetic pathway. Contrary to the literature [27], direct exchange of bromohydrines to azido alcohols (path $\mathbf{f_2}$) did not yield the expected 2-azido series (**6a** and **6b**) but the 3-azido compounds (**7a** and **7b**)

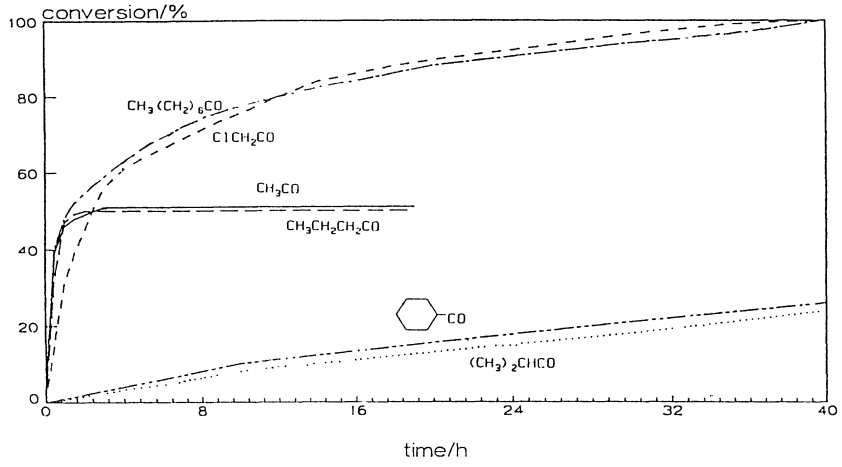

Fig. 3. Rates of conversion of different O-acyl analogs of **7b** with lipase P.

instead. This seems to be effected by the formation of an intermediate epoxide (with the aid of the weakly basic azide anion), which is cleaved in turn by azide ions in the usual way to give the kinetically favored 3-azides. Therefore the esterifications (path **e**) were done prior to azide exchange, thus preventing the intermediate formation of epoxides. In preliminary experiments it was found that blocking of the acid functionality with simple and small alcohols like methanol or ethanol did not affect the enzymatic hydrolysis of the O-acyl part (derived from the

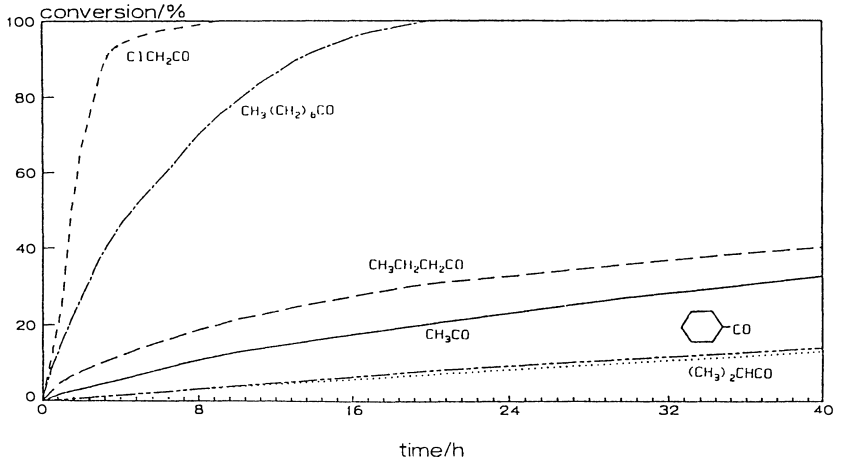

Fig. 4. Rates of conversion of different O-acyl analogs of **7b** with lipase CC.

Table 1. Enantiomeric excesses obtained by enzymatic hydrolyses of different O-acyl analogs of **7b**

Analog of **7b** $R^1 = CH_3$	Lipase CC activity µmol/h mg	c[a] %	ee %	E[b]	Lipase P activity µmol/h mg	c[a] %	ee %	E[b]
$R^2 = CH_3CO$	0.26	25	85	16	17.30	40	97	128
$ClCH_2CO$	3.09	50	2	1	10.20	40	86	13
$CH_3CH_2CH_2CO$	0.62	40	67	8	22.95	40	>98	200
$(CH_3)_2CHCO$	0.07	24	84	15	0.20	40	>98	200
$CH_3(CH_2)_6CO$	5.76	40	36	3	21.60	40	85	12
$C_6H_{11}CO$	0.06	27	72	8	0.23	27	93	39

[a] conversion; [b] Enatiomeric ratio (28): $E = \ln[1-c(1+ee)]/\ln[1-c(1-ee)]$

azido *alcohol* moiety). In fact, the methyl or ethyl esters were not hydrolyzed at all. The results of the hydrolysis of different acyl analogs of **7b** with lipases from *P. fluorescens* (lipase P) and *C. cylindracea* (lipase CC) are given in Fig. 3, Fig. 4 and Table 1 respectively. Other commercially available lipases (porcine pancreas lipase, pig liver esterase and lipase from *Aspergillus sp.*) were far less active and/or less enantioselective. As can be seen, in accordance with results obtained earlier [16–18], butanoates were found to be most suitable for this type of enzymatic resolution. Thus, the butanoates **6a**, **6b**, **7a** and **7b** were subjected to the enzymatic hydrolyses with the aid of the two lipases CC and P. In the course of these investigations it was found that only **7a** and **7b** exhibited activity with lipase P, whereas **6a** and **6b** showed virtually no turnover. Thus, although the curve for **7b** with lipase P showed more promising behaviour than with lipase CC (see Fig. 3

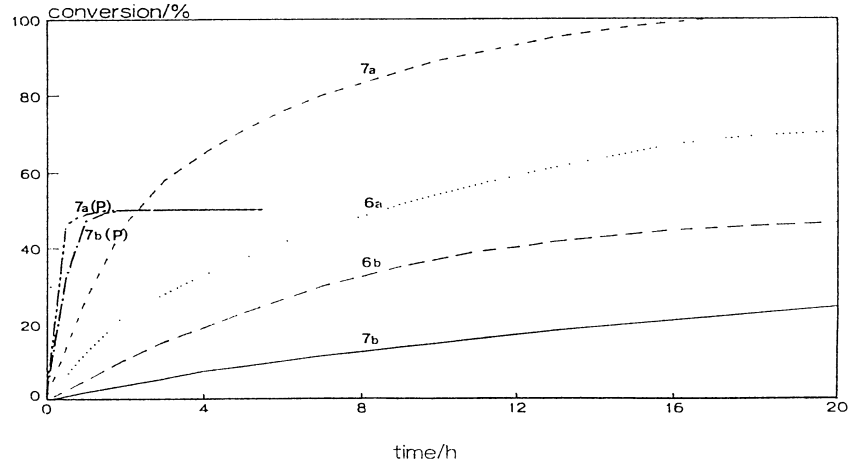

Fig. 5. Rates of conversion of **6a**, **6b**, **7a** and **7b** with lipase CC.

Table 2. Enantiomeric excesses obtained by enzymatic hydrolyses of butanoates **6a**, **6b**, **7a** and **7b** with lipases CC and P resp.

Substrate	Lipase	activity µmol/h mg	C[a] %	ee %	E[b]
6a	CC	0.52	40	>98	200
6b	CC	0.41	36	>98	170
7a	CC	2.28	40	75	11
7a	P	20.11	40	>98	200
7b	CC	0.97	40	67	8
7b	P	18.03	40	>98	200

[a] conversion; [b] Enatiomeric ratio (28): E = ln[1−c(1+ee)]/ln[1−c(1−ee)]

and 4), all remaining hydrolyses were done with lipase CC. The pertinent results are shown in Fig. 5 and Table 2.

Discussion

As can be seen in Fig. 2 general access to compounds **6** and **7** is straightforward and simple. Most (*E*) – configurated unsaturated acids as the basic starting materials can be obtained commercially or prepared by simple standard procedures. (*Z*)-Unsaturated acids are somewhat more difficult to get, but either dibromination of the (*E*)-acid, elimination and hydrogenation with the aid of a Lindlar catalyst or stereospecific Wittig-reactions starting from abundant aldehydes pose virtually no problems for the quick access to these starting materials too.

The surprising fact that in the bifunctional molecules used only the ester with the simple acyl and more complicated alcoholic residue is cleaved, could be rationalized as follows: Apparently both lipases exhibit an active site with enough space for bigger substituents at the alcoholic residue to be cleaved. Once the molecule is attached and the hydrolysis can proceed, the other ester functionality with the small alcoholic residue is excluded from this process simply by being not in the correct position for hydrolysis. That the size of this cavity must be somewhat smaller in lipase P than within lipase CC is demonstrated by the fact that only **7a** and **7b** could be hydrolyzed by lipase P. The other substrates apparently need the less restrictive (but therefore also less ideal) bigger cavity of lipase CC.

By looking at Fig. 3 one can easily depict the esters with good conversion rates. Regardless of the type of lipase, esters with more bulky acyl residues (2-methylpropanoate and cyclohexanecarboxylate) were hydrolyzed much slower than the others. Although they might show quite good enantiodifferentiation, for practical purposes, because of the long reaction times needed, they were not explored further. Of the faster reacting esters, at least with lipase P (Fig. 3), the chloroacetate and octanoate were hydrolysed very quickly, but the conversion did not stop at

around 50%. Thus these curves demonstrated that the respective esters were also not very suitable for the resolution of racemates, since there was no good enantiodifferentiation to be expected. Acetate and butanoate however showed ideal behaviour. Because butanoates have proved their general applicability in a number of different substrates, we used this acyl residue throughout the further investigations. As mentioned above, for substrates **6a** and **6b** we had to go back to the somewhat less ideal results with lipase CC. With this lipase, all four diastereomers could be resolved. The enantiomeric excesses reached in either case are summarized in Table 2.

From a comparison of the physical data of the compounds obtained by our method with the literature data and the known behaviour of lipase CC it can be concluded, that the (*S*)- configurated O-acyl compounds are hydrolyzed preferentially.

In summary we have shown that our methodology is well suited for the resolution of racemic precursors of hydroxy amino acids. The hydrogenation of the homochiral azides thus obtained to the respective amino compounds by hydrogen with the aid of a palladium catalyst is state of the art and known to proceed in almost quantitative yields.

Acknowledgements

Financial support by the *Fonds zur Förderung der Wissenschaftlichen Forschung*, Vienna (projects 6257 and 6893) is gratefully acknowledged. We are indebted to G. Kothleitner for synthetic assistance.

References

1. Nishizawa R, Saino T, Suzuki M, Fujii T, Shirai T, Aoyagi T and Umezawa H (1983) J. Antibiotics 36: 695–699.
2. Harbeson SL and Rich DH (1988) Biochemistry 17: 7301–7310.
3. Boger J, Lohr NS, Ulm EH, Poe M, Blaine EH, Fanelli GM, Lin TY, Payne LS, Schorn TW, Lamont BI, Vassil TC, Stabilito II, Veber DF, Rich DH and Boparai, AS (1983) Nature (London) 303: 81–84.
4. Rinehart KL Jr, Gloer JB, Cook JC Jr., Mizsak SA and Scahill TA (1981) J. Am. Chem. Soc. 103: 1857–1859.
5. Rinehart KL Jr, Gloer JB, Hughes RG Fr., Renis HE, McGovern JP, Swynenberg EB, Stringfellow DA, Kuentzel SL and Li LH (1981) Science (Washington, D.C.) 212: 933–935.
6. Jiang TL, Liu RH and Salmon SE (1983) Cancer Chemother. Pharmacol. 11: 1–4.
7. Billich S, Knoop MT, Hansen J, Strop P, Sedlacek J, Mertz R and Moelling K (1988) J. Biol. Chem. 263: 17905–17908.
8. Navia MA, Fitzgerald PMD, McKeever BM, Leu CT, Heimbach JC, Herber WK, Sigal IS, Darke PL and Springer JP (1989) Nature (London) 337: 615–620.
9. Umezawa H (1976) Prog. Biochem. Pharmacol. 11: 18–32.
10. Woo PWK (1985) Tetrahedron Lett. 26: 2973–2976.
11. Mulzer J, Büttelmann B and Münsch H (1988) Liebigs Ann. Chem. 445–448.

12. Maibaum J and Rich DH (1988) J. Org. Chem. 53: 869–873.
13. Schuda PF, Greenlee WJ, Chakravarty PK and Eskola P (1988) Ibid. 873–875.
14. Kuneda T, Ishizuka T, Higuchi T and Hirobe M (1988) Ibid. 3383–3384.
15. Ariens JE (1988) Eur. J. Drug. Metab. Pharmacokin. 13: 307–308.
16. Faber K, Hönig H and Seufer-Wasserthal P (1988) Tetrahedron Lett. 29: 1903–1904.
17. Hönig H, Seufer-Wasserthal P and Fülöp F (1989) J. Chem. Soc., Perkins Trans. 1: 2341–2345.
18. Foelsche E, Hickel A, Hönig H and Seufer-Wasserthal P (1990) J. Org. Chem. 55, in press.
19. Scilimati A, Ngooi TK and Sih CJ (1988) Tetrahedron Lett. 29: 4927–4930.
20. Dickinson L and Thompson MJ (1957) Brit. J. Pharmacol. Chemotherapy 12: 66–72.
21. Kundin WD and Robbins ML (1961) Virology 15: 164–168.
22. Pons MW and Preston WS, Ibid. 192–198.
23. Fones WS (1953) J. Biol. Chem. 204: 323–328.
24. Sullivan GR, Dale JA and Mosher HS (1973) J. Org. Chem. 38: 2143–2147.
25. Höfle G, Steglich W and Vorbrüggen H (1978) Angew. Chem. 90: 602–615; Angew. Chem. Int. Ed. Engl. 17: 569–582.
26. Kamandi E, Frahm AW and Zymalkowski F (1984) Arch. Pharm. 307: 871–878.
27. Shin C, Yonezawa Y, Unoki K and Yoshimura J (1979) Bull. Chem. Soc. Jap. 52: 1657–1660.
28. Chen CS, Fujimoto Y, Girdaukas G and Sih CJ (1982) J. Am. Chem. Soc. 104: 7294–7299.

Amino acid analysis by derivatization with *o*-phthaldialdehyde and chiral thiols

Hans Brückner[a], Robert Wittner[a] and Herbert Godel[b]

[a]*Institute of Food Technology, University of Hohenheim, D-7000 Stuttgart 70, F.R.G.*
[b]*Hewlett-Packard, Research and Development Division, D-7517 Waldbronn 2, F.R.G.*

Abstract

The chiral resolution of standard mixtures composed of a large number of DL-amino acids was investigated by reversed-phase high-performance liquid chromatography (HPLC) of the corresponding isoindolyl derivatives, formed by automated precolumn derivatization with *o*-phthaldialdehyde (OPA) and a series of chiral *N*-acyl-L-cysteines (acyl = *n*-octanoyl, *n*-butyryl, isobutyryl) which had been synthesized in our laboratory. The resolutions were compared with those obtained when *N*-acetyl-D-penicillamine and the thiol drug 'Captopril' (1-[(2S)-3-mercapto-2-methylpropanoyl]-L-proline) were used as chiral reagents. All reagents made the more or less complete enantioseparation of amino acid mixtures possible; however, *n*-butyryl-L-cysteine and isobutyryl-L-cysteine (*i*-But-Cys) in particular gave high resolution coefficients for most of the DL-amino acids. For HPLC the liquid chromatograph was equipped with a device for automated precolumn derivatization, a fluorescence detector and a workstation for data processing. Chromatography was performed by employing octadecylsilyl silica (3 µm) as the stationary phase and gradients of sodium acetate buffers with acetonitrile as the eluents. The utility of the method for the determination of minor amounts of enantiomers is demonstrated by the detection of 0.2% D-Trp and 0.5% D-Ser in the presence of an excess of the respective L-enantiomer by use of the OPA/*i*-But-Cys reagent.

Among the various methods for quantitative amino acid analysis by precolumn derivatization, three routine procedures, in particular, rival for acceptance, i.e. derivatization with phenyl isothiocyanate, with 9-fluorenylmethoxycarbonyl chloride, or with OPA together with thiols such as mercaptoethanol or 3-mercaptopropionic acid. Chiral variations have been described for all of these approaches [1–3]. The use of the OPA/chiral thiol method has the advantage that several chiral thiols such as *N*-acetyl-L-cysteine (Ac-Cys), *N-tert.*-butyloxycarbonyl-L-Cys (Boc-Cys), or *N*-acetyl-D-penicillamine (NAP) are commercially available. We have very recently shown [4] that L-cysteine (L-Cys) in particular serves as an economic building block for the synthesis of a number of systematically modified *N*-acyl-L-cysteines [acyl = *n*-butyryl (*n*-But), isobutyryl (*i*-But), pivaloyl, benzoyl]. The OPA/chiral thiol approach also made possible the enantioseparation of nonprotein amino acids [5,6] as well as the determination of D-amino acids in complex matrices such as foodstuffs [4,7,8]. In this paper, we compare the resolution behaviour of a new *N*-acyl-L-cysteine (acyl = *n*-octanoyl) with that of *n*-But-Cys, *i*-But-Cys and *N*-acetyl-D-penicillamine (NAP) and show that OPA together with

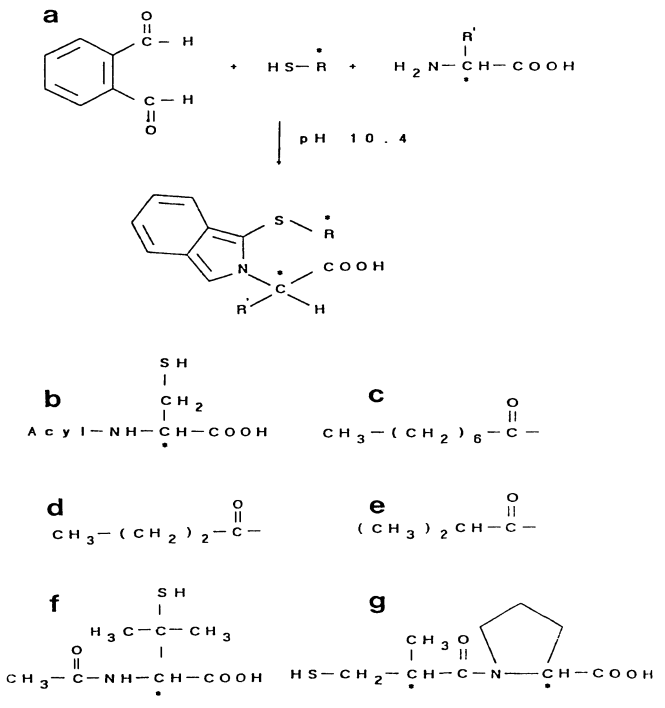

Fig. 1. Structures of derivatives and reagents. (a) Proposed reaction scheme and general structure of diastereomeric isoindolyl derivatives formed by reaction of OPA with thiols (HS-R*) and amino acids (H_2N-CHR'-COOH), general formula of (b) Acyl-Cys with acyl (c) *n*-octanoyl, (d) *n*-butyryl, (e) isobutyryl; (f) *N*-acetyl-penicillamine (NAP), and (g) Captopril. R* and R' refer to residues of chiral thiols and amino acid side chain residues, respectively; asterisks mark chiral centers.

the chiral thiol drug 'Captopril' (for formulae of these reagents, see Fig. 1) also makes possible the enantioseparation of complex amino acid mixtures (cf. Fig. 2).

Materials and Methods

Instruments

Analyses were carried out with a 1090 LC system, equipped with a device for automated precolumn derivatization of amino acids and a Model 1046 A fluorescence detector equipped with a xenon-arc flash lamp and operated at an excitation wavelength of 230 nm and an emission wavelength of 450 nm. The workstation was composed of a Series 9000 computer, Model 300, with fixed disc and floppy

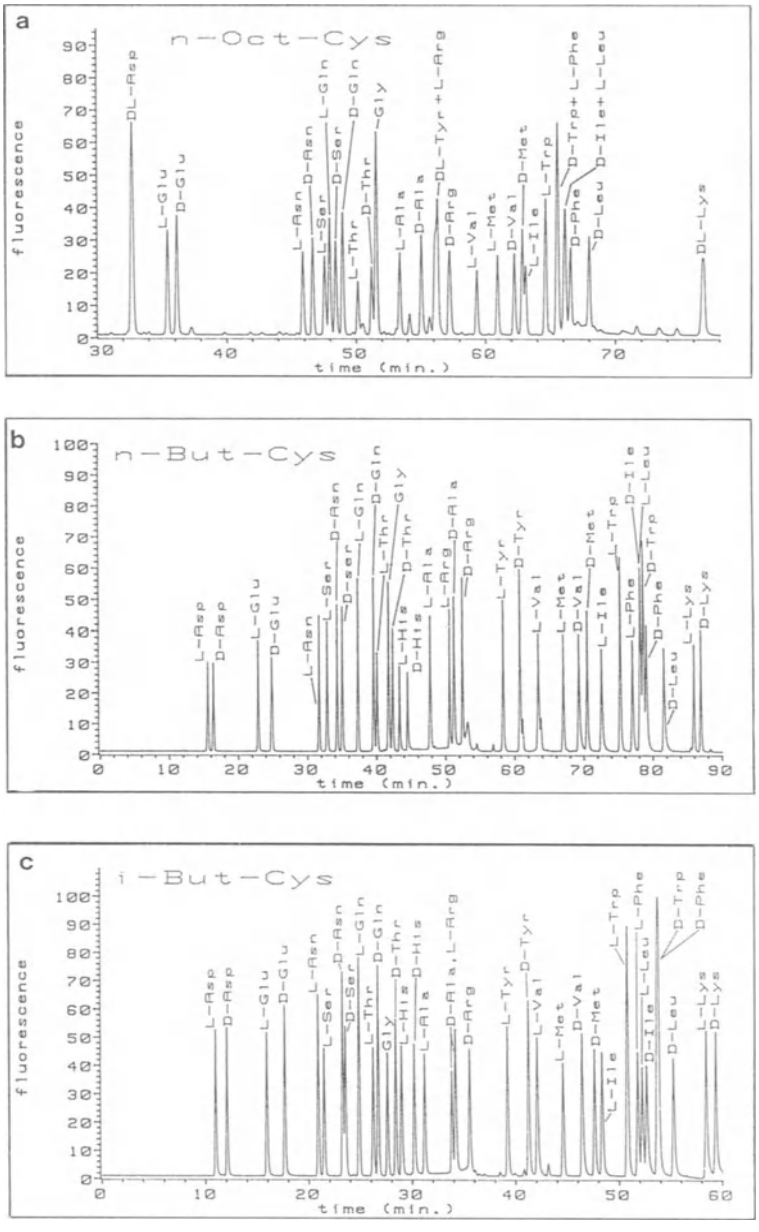

Fig. 2. HPLC of the enantioseparation of diastereomeric derivatives of (a–e) standard mixtures of DL-amino acids and Gly and of (f) L-Ser with 0.5% D-Ser and (g) L-Trp with 0.2% D-Trp after precolumn derivatization with *o*-phthaldialdehyde and various chiral thiols and fluorescence detection at 230 nm *(continued)*

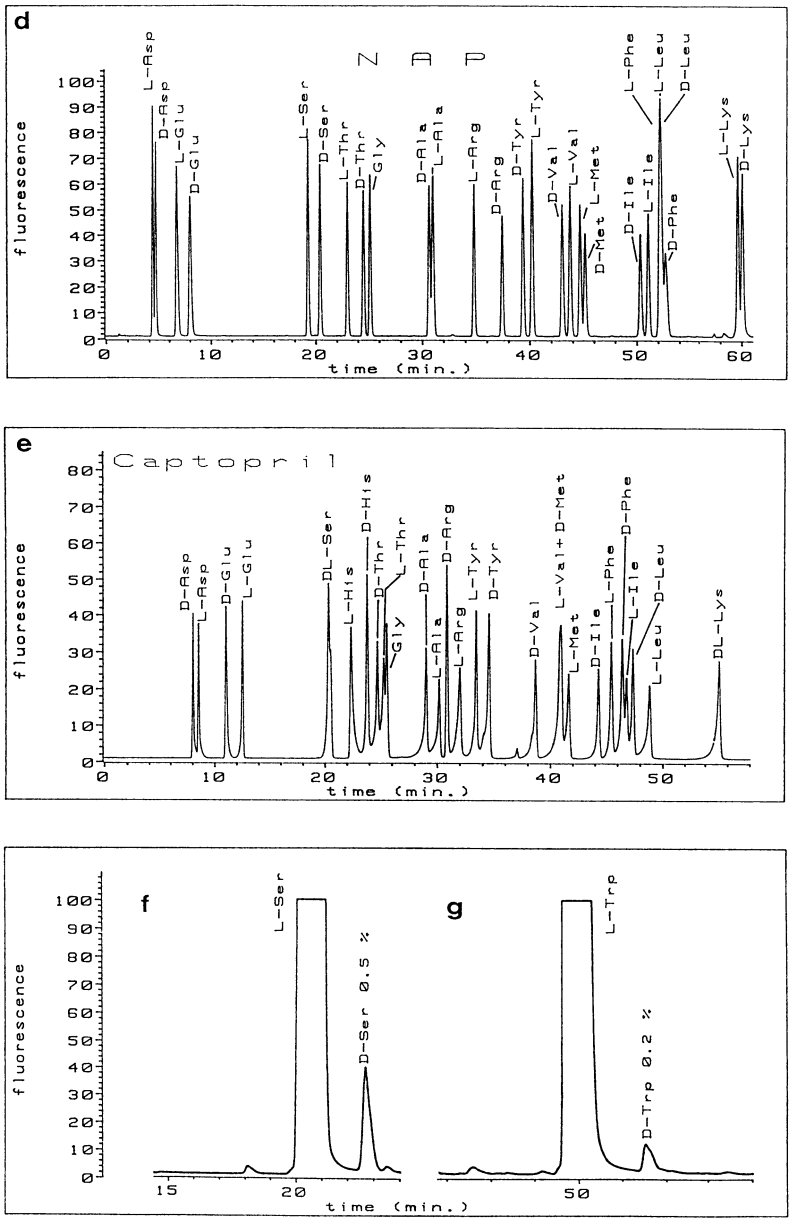

Fig. 2 (cont'd)

(excitation) and 450 nm (emission). (For abbreviations see Material and Methods; NaAc, sodium acetate; AA, amino acid). (a) *n*-Oct-Cys, (b) *n*-But-Cys, (c), (f), (g) *i*-But-Cys, (d) NAP, (e) Captopril. Chromato-

(continued)

graphic conditions: Spherisorb ODS II, 3 μm, column (a), (c)–(g) 125 mm × 4.6 mm I.D., precolumn 20 mm × 4 mm I.D.; (b) 250 mm × 4 mm I.D. Buffer gradients: Eluent B in all instances 100% acetonitrile; (a) eluent A 30 m*M* NaAc (pH 7.2) with 2% acetonitrile, linear gradient, in 80 min to 33% B; flow rate, 0.9 ml/min, temperature 25°C; amplifier stage of fluorescence detector (PMT) 8, (b), eluent A 25 m*M* NaAc (pH 6.4), linear gradient, in 90 min to 24% B; flow rate, 0.75 ml/min; temperature, 26°C; PMT 8, changed at 84 min to 9; (c), (f), (g) eluent A 30 m*M* NaAc (pH 6.3), linear gradient, in 60 min to 23% B; flow rate, 0.9 ml/min; temperature, 25°C; (c) PMT 8, changed at 56.5 min to PMT 9, (f), (g) PMT 11; (d) eluent A 25 m*M* NaAc (pH 7.2), gradient, isocratically for 5 min, then in 55 min linear to 18.5% B; flow rate, 0.9 ml/min; temperature, 23°C; PMT 12, changed after 57 min to PMT 13; (e), 50 m*M* NaAc (pH 7.2), linear gradient, in 60 min to 25% B; flow rate, 0.9 ml/min; temperature 25°C; PMT 8. Conditions for precolumn derivatization: Reagents were mixed automatically (for composition of reagents and procedure cf. Materials and Methods): (a)–(c), (f), (g) 5 μl borate buffer, 2 μl OPA-reagent, (a) 2 μl *n*-Oct-Cys reagent, (b) 2 μl *n*-But-Cys reagent or (c), (f), (g) 2 μl *i*-But-Cys reagent, and (a)–(c) 0.5 nmol of each AA enantiomer (b,c His 1 nmol) and (f), (g) 10 nmol of each AA in totally 1 μl [(a) 1.5 μl] standard solution; (d), 4 μl borate buffer, 2 μl OPA-reagent, 2 μl NAP-reagent, 1 nmol of each AA enantiomer in totally 2 μl standard solution; (e) 5 μl borate buffer, 2 μl OPA-reagent, 2 μl captopril reagent, 0.5 nmol of each AA (His 1 nmol) enantiomer in totally 0.5 μl solution.

disc, Model 9153, and a plotter, ColorPro Model 7440 (all instruments from Hewlett-Packard, Waldbronn, F.R.G.).

Chromatography

HPLC was performed using Spherisorb ODS II (3 μm) (Phase Separations, Queensferry, U.K.) as stationary phase packed in columns of the size 125 mm × 4.6 mm I.D. (250 × 4 mm I.D., cf. legend of Fig. 2) of which the former were equipped with precolumns (Manufit System, Bischoff Analysentechnik, Leonberg, F.R.G.). Buffer compositions and gradient programs are given in the legend of Fig. 2.

Chiral thiol reagents

N-acyl-L-cysteines (acyl = *n*-octanoyl, *n*-butyryl, isobutyryl) were synthesized by Schotten-Baumann acylation of L-cystine with the respective acyl chlorides (octanoyl chloride, *n*-butyryl chloride, isobutyryl chloride, all from Fluka, Buchs, Switzerland) and reduction of the respective bisacyl-L-cystines with zinc powder in 2 *M* HCl or, in the case of the *n*-octanoyl derivative, with conc. HCl/acetone.

N-acetyl-D-penicillamine was purchased from Fluka, and Captopril was a generous gift from Dr. Grote, Schwarz GmbH, Monheim, F.R.G.

Chemicals and composition of amino acid standards

Methanol and acetonitrile were obtained from Baker, Deventer, The Netherlands and of 'Baker analyzed quality' for HPLC, sodium acetate was of *pro analysi* grade from Merck, Darmstadt, F.R.G. Buffer solutions prepared from these reagents were filtered (0.45 μm filter) and degassed by sonification prior to use. DL-amino acids were purchased from Sigma (St. Louis, MO, U.S.A.) and were of analytical

grade. Standard mixtures of DL-amino acids (and Gly) were prepared as (a) 0.5 m*M* solution of each enantiomer (His 2 m*M*) in 0.01 *M* HCl, (b) 1 m*M* solutions of each enantiomer in 0.01 *M* HCl and (c) 1 m*M* solution of each enantiomer of DL-Asn, DL-Gln and DL-Trp in water/methanol (80:20), and 10 m*M* L-Trp with 0.2% D-Trp and 10 m*M* L-Ser with 0.5% D-Ser dissolved in water. For precolumn derivatization suitable amounts of the amino acid standard mixtures (cf. Figure legends) were mixed automatically (10 mixing cycles for approx. 5 min) at 25°C with 5 µl or 4 µl (cf. legend to Fig. 2) of 0.4 *N* borate buffer of pH 10.4 (Pierce, Rockford, Ill., U.S.A.) and 2 µl of *o*-phthaldialdehyde (OPA) reagent [5 mg OPA (Fluka) in 1 ml borate buffer]. Chiral reagents were prepared by dissolving the respective thiols in 0.4 *N* borate buffer [*n*-But-Cys, *i*-But-Cys (20 mg/ml), NAP (10 mg/ml), Captopril (11 mg/ml), and *n*-Oct-Cys (35 mg/ml) in acetone/borate buffer 6:4].

Results and Discussion

The enantioseparations of standard mixtures composed of DL-amino acids and the achiral Gly by use of OPA and the chiral thiols *n*-Oct-Cys (*n*- octanoyl-L-cysteine), *n*-But-Cys, *i*-But-Cys, (NAP) [2], and captopril are shown in Figs. 1a–e. The resolution times and calculated resolutions of the corresponding pairs of enantiomers are compiled in Table 1. The chromatograms show that in principle all thiol reagents are able to separate even complex mixtures of DL-AA. Which of the reagents finally will be chosen depends on the aim of the work. In cases where minor amounts of one enantiomer have to be determined quantitatively in an excess of the other the latter should elute second from the column and the resolution should be as high as possible in order to achieve highest accuracy (cf. Figs. 1f–i). In instances where complex mixtures of components have to be separated the overall resolution of DL-AA (inclusive separation of Gly) has to be considered. Owing to the different chromatographic behaviour of the respective AA derivatives optimization of the chromatographic conditions for an individual pair of AA enantiomers may result in a less satisfactory separation of others, or give rise to peak overlap of other DL-AA in the chromatogram. Optimization of the enantioseparation is therefore a laborious work since the chromatographic conditions may be altered successively or simultaneously and these alterations may act contrarily on the resolution of certain pairs of DL-AA. One has to consider the kind of stationary phase, size of particles, dimensions of the column, composition and pH of buffers, selection of organic modifier, gradient program and temperature. Moreover the nature of the chiral derivatization reagent plays a major role for the overall enantioseparation since it drastically influences the hydrophobicities and conformational behaviour of the derivatives formed. This can be recognized from Figs. 2a–c, where the derivatives formed by derivatization with *n*-Oct-Cys, *n*-But-Cys, and *i*-But-Cys are compared. As a result of the highest hydrophobicity of *n*-Oct-Cys as compared to the other reagents (cf. Figs. 1a–e) the steepest linear

Table 1. Retention times (min) of the first (r_{t1}) and second eluted (r_{t2}) DL-amino acid enentiomers after derivatization with OPA/chiral thiols and resolution R given

Reagent	*n*-Oct-Cys			*n*-But-Cys			*i*-But-Cys			NAP			Captopril		
DL-amino acid[a]	r_{t1}	r_{t2}	R[b]	r_{t1}	r_{t2}	R	r_{t1}	r_{t2}	R	r_{t1}	r_{t2}	R	r_{t1}	r_{t2}	R
Asp	32.7	32.7	0	15.6	16.4	2.2	11.0	12.1	3.8	4.3	4.6	1.2	8.0	8.5	1.9
Glu	35.4	36.1	2.1	22.9	24.8	5.3	15.9	17.7	5.2	6.7	8.0	3.5	11.0	12.5	4.7
Asn	45.9	46.6	2.1	31.7	34.3	7.9	20.9	23.2	7.4	n.d.	n.d.	–	n.d.	n.d.	–
Ser	47.6	48.4	2.1	32.9	35.1	6.0	21.5	23.5	6.0	19.2	20.4	3.9	20.3	20.5	0.5
Gln	47.9	49.0	3.0	37.3	39.6	6.7	24.8	26.7	5.8	n.d.	n.d.	–	n.d.	n.d.	–
Thr	50.1	51.2	3.0	40.1	42.4	6.1	6.2	28.4	6.5	23.0	24.5	4.2	24.7	25.3	1.2
Gly	51.5	achiral	–	41.8	achiral	–	27.6	achiral	–	25.1	achiral	–	25.6	achiral	–
His	n.d.	n.d.	–	43.4	44.5	3.2	29.0	30.2	3.4	n.d.	n.d.	–	22.4	23.8	3.0
Ala	53.4	55.0	4.3	47.8	51.2	8.6	31.2	33.8[c]	7.6	30.6	31.0	0.9	29.0	30.2	2.3
Arg	56.3	57.2	1.7	50.6	52.4	5.3	34.2[c]	35.5	3.7	34.8	37.4	6.7	30.9	32.0	2.3
Tyr	56.3	56.3	0	58.3	60.7	6.2	39.2	41.2	5.6	39.3	40.2	2.1	33.4	34.6	2.4
Val	59.3	62.2	7.8	63.4	69.3	12.3	42.1	46.4	10.8	43.0	43.7	1.6	38.7	41.0	3.6
Met	60.9	62.8	7.8	67.0	70.5	8.6	44.6	47.6	8.0	44.6	45.1	1.0	41.0	41.7	1.1
Ile	63.1	66.1	7.8	72.6	78.1	11.3	48.3	52.6	10.1	50.3	51.0	1.6	44.3	46.8	5.4
Trp	64.6	65.5	2.3	75.3	78.5	7.4	50.8	53.7	5.8	n.d.	n.d.	–	n.d.	n.d.	–
Phe	65.5	66.5	2.5	77.0	79.0	4.3	51.8	53.7	3.9	52.1	52.6	0.9	45.5	46.4	1.8
Leu	66.1	68.0	4.7	78.1	81.6	7.1	52.2	55.2	7.5	52.1	52.1	0	47.4	48.9	2.7
Lys	76.7	76.7	0	85.9	86.9	2.6	58.4	59.3	2.2	59.6	60.0	0.9	55.3	55.3	0

[a] For elution order of DL-amino acid enentiomers see Figs. a)–e).

[b] Resolution R is calculated according to the formula $R = (r_{t2} - r_{t1})/(pw_1 + pw_2)$, pw_1 and pw_2 refer to the half-height peak width of the first and second eluted peak of amino acid derivatives.

[c] Tentative assignment of the elution order of D-Ala and L-Arg.

n.d. not determined.

gradient, resulting in the relatively highest amount of organic modifier at the end of the analysis, has to be used in order to achieve reasonable elution times. Use of the chromatographic conditions described in this paper made possible the enantioseparation of 13 pairs of DL-AA and Gly by use of *n*-Oct-Cys (Fig. 2a, DL-Tyr and L-Arg, D-Trp and L-Phe, D-Ile and L-Leu are eluted together under these conditions and DL-Lys and DL-Asp are not resolved). Each of 17 pairs of DL-AA and Gly are resolved by *n*-But-Cys (Fig. 2b, D-Ile and L-Leu are eluted together), and by *i*-But-Cys (Fig. 2c, D-Trp and D-Phe are not separated).

It had been shown already [2] with the resolution of 7 pairs of DL-AA that OPA/*N*-Acetyl-D-penicillamine (NAP) also enables the enantioseparation of amino acids. The application of this reagent to a mixture of 12 DL-AA pairs and Gly is shown in Fig. 1d. Under the conditions used a satisfactory resolution was achieved with the exception of L-Phe, L-Leu and D-Leu, which elute together. Among the relatively few commercially available chiral thiol reagents, the L-proline derivative 'Captopril' 1-[(2S)-3-mercapto-2-methylpropanoyl]-L-proline is noteworthy since it has found wide application in the therapy for hypertension [9]. Although this reagent has the disadvantage of having two chiral centers, a feature that usually does not favour the chiral resolution when using the diastereomeric approach, it also made possible the enantioseparation of 12 pairs of DL-AA and Gly (Fig. 1e). L-Val and D-Met elute together and DL-Ser and DL-Lys are not resolved. However, in contrast to the other reagents described in this paper, the peak shapes in the chromatogram show an asymmetry ('heading') in most instances and are therefore unsatisfactory. It might be possible, however, that the reversed approach, i.e. derivatization of Captopril with OPA and an optically pure amino acid such as D- or L-Glu will provide a routine procedure for the determination of the optical purity of the drug. Finally, the determination of minor amounts of one enantiomer in the presence of an excess of the other by derivatization with OPA and *i*-But-Cys and fluorescence detection is shown for Ser and Trp in Fig. 1f and 1g, respectively. These amino acids are of particular interest since nephrotoxicity of D-Ser in experimental animals has been reported [10] and L-Trp is used as an antidepressant. As can be seen from the chromatograms 0.5% and 0.2% of the respective D-enantiomers are easily detectable.

References

1. Nimura N, Toyama A and Kinoshita T (1984) J. Chromatogr. 316: 547–552.
2. Buck RH and Krummen K (1987) J. Chromatogr. 387: 255–265.
3. Einarsson S, Josefsson B, Möller P and Sanchez D (1987) Anal. Chem. 59: 1191–1195.
4. Brückner H, Wittner R and Godel K (1989) J. Chromatogr. 476: 73–82.
5. Brückner H, Kühne S, Zivy S, Langer M, Kamiński ZJ and Leplawy MT (1988) In: Aubry A, Marraud M and Vitoux B (eds.) Second Forum on Peptides. John Libbey Eurotext, London, pp. 291–295.
6. Kamiński ZJ, Leplawy MT, Esna-Ashari A, Kühne S, Zivny S, Langer M and Brückner H (1989) In: Bayer E and Jung G (eds.) Peptides 1988. Walter de Gruyter, Berlin, pp. 298–300.
7. Brückner H, Wittner R, Hausch M and Godel H (1989) Fresenius Z. Anal. Chem. 333: 775–776.

8. Brückner H and Hausch M (1989) In: Frank H, Holmstedt B and Testa B (eds.) Chirality and Biological Activity. Liss, New York, pp. 129–136.
9. Romankiewicz JA, Brogden RN, Heel RC, Speight TM, Avery GS (1983) Drugs 25: 6–40.
10. Kaltenbach JP, Ganote CE and Carone FA (1979) Exp. Mol. Pathology 30: 215–229.

Address for correspondence: Hans Brückner, Institute of Food Technology, University of Hohenheim, D-7000 Stuttgart 70, F.R.G.

Chiral ligand-exchange chromatography of amino acid derivatives

Hans Brückner[a], Barbara Sorsche[a], Ali Esna-Ashari[a] and Rolf Jöster[b]

[a]Institute of Food Technology, University of Hohenheim, D-7000 Stuttgart 70, F.R.G.
[b]Perkin Elmer Analytic, Gewerbestraße 42, D-7000 Stuttgart 80, F.R.G.

Abstract

The chiral resolution of various *N*-acyl-DL-amino acids [acyl = formyl, acetyl, monochloroacetyl, trifluoroacetyl, benzyloxycarbonyl (Z), *tert.*butyloxycarbonyl (Boc)] as well as dansyl-DL-amino acids and side chain protected DL-serines was investigated by ligand-exchange high-performance liquid chromatography (LE-HPLC) using a commercially available stationary phase of silica bonded L-proline ('Chiral ProCu') and aqueous eluents containing Cu^{2+} as complex forming ion. In the instances investigated the D-enantiomers eluted before the L-enantiomers. Since in most cases baseline resolution, or almost baseline resolution, of the diastereomeric amino acid/Cu^{2+} complexes was achieved LE-HPLC is considered as a suitable method for the determination of the optical purity of the respective amino acid derivatives. The investigation of Boc- and Z-protected amino acids is of particular interest because these derivatives are among the most frequently used in peptide synthesis. However, 9-fluorenylmethyloxycarbonyl(Fmoc)-DL-amino acids were not, or unsatisfactorily, resolved by LE-HPLC under the conditions used.

For the synthesis of peptide drugs by either classical methods such as stepwise elongation of peptide chains, by segment condensations or by solid phase procedures using an insoluble solid support [1–3] the most frequently used amino protected amino acids (AA) are currently the respective Boc-, Fmoc-, and Z-derivatives (Boc, *tert.*butyloxycarbonyl; Fmoc, 9-fluorenylmethyloxycarbonyl; Z, benzyloxycarbonyl). In pharmacology a number of *N*-acylated L-α-amino acids such as the mucolytic agent *N*-acetyl-L-cysteine, the antihypertensive drug 1-[(2S)-3-mercapto-2-methyl-propanoyl]-L-proline ('Captopril') or certain N-acetylated α-amino acids for parenteral nutrition are of particular interest. Owing to the highly stereospecific interaction of AA (and the peptides derived therefrom) under physiological conditions, the optical purity (ideally the presence of exclusively one enantiomer, usually the L-enantiomer in instances of protein amino acids) has to be proved prior to use in synthesis or pharmacology. The respective L-AA might have racemized (epimerized) to a certain degree in the course of the derivatization procedures, or during storage and treatment of derivatives under unfavorable conditions. It has been shown that chiral ligand-exchange high-performance liquid chromatography (LE-HPLC) using silica bonded amino acids such as L-Pro and aqueous eluents containing Cu^{2+} is a highly suitable technique for the direct enantioseparation of the diastereomeric complexes formed with DL-AA [4]. In particular the commercially available chiral stationary phase named

Chiral ProCu (see Materials and Methods) shows an excellent chiral recognition for protein amino acids [5] as well as for *N*-methyl-α-amino acids and nonprotein α-alkyl-α-amino acids [6] or α-hydroxymethyl-α-amino acids [7]. In this paper we show that LE-HPLC using Chiral ProCu and eluents containing Cu^{2+} makes also possible the enantioseparation of a large number of the diastereomeric Cu^{2+}-complexes formed by the stationary phase and mono- or disubstituted AA as used in peptide synthesis and which have free carboxy groups.

Materials and Methods

High-performance liquid chromatography

For HPLC a Perkin Elmer Liquid Chromatograph Series 10 equipped with a Rheodyne injector Model 7125, a variable wavelength detector Model LC 85 B and an integrator LCI 100, or a recorder Model 561, were used.

The column had the size 250 mm × 4 mm i.d. (pre-column 20 mm × 4 mm i.d.; Manufit System, Bischoff Analysentechnik, Leonberg, F.R.G.) and was kept at suitable temperatures by a water jacket (Knauer, Bad Homburg, F.R.G.) and two thermostates connected in series (Desaga Frigostat, Desaga, Heidelberg, F.R.G.) in order to control the temperature precisely.

The column was packed with the chiral stationary phase Chiral ProCu (5 μm, Serva, Heidelberg, F.R.G.; cf. Fig. 1k).

The eluents used were **A**, 1 m*M* aqueous copper(II)sulfate, pH 6.0; **B**, 1 m*M* copper(II)acetate in water/acetonitrile 9:1 (v/v), pH 5.0; **C**, 1 m*M* copper(II)acetate in 0.1 m*M* ammonium acetate/acetonitrile 7:3 (v/v), pH 6.9; **D**, 0.25 m*M* copper(II) acetate in water/acetonitrile 1:1 (v/v). Eluents were degassed by sonification prior to use.

Copper(II)acetate and copper(II)sulfate × 5 H_2O were of *pro analysi* grade (Merck, Darmstadt, F.R.G.) and acetonitrile for HPLC was from Baker (Baker Chemicals, Deventer, The Netherlands). Amino acid derivatives were purchased as DL-, L-, or D-compounds from either Bachem Feinchemikalien, Bubendorf, Switzerland or from Sigma Chemicals, St. Louis, MO, U.S.A. Amino acids and derivatives are abbreviated according to the literature [1-3]. The following amino acid derivatives have been used (for formulae of the protecting groups see Fig. 1a–j):

(a), For-DL-Phe-OH (*N*-formyl-DL-phenylalanine); (b), Ac-DL-Trp-OH (*N*-acetyl-DL-tryptophane); (c), Ac-DL-Leu-OH (*N*-acetyl-DL-leucine); (d), Mca-DL-Phe-OH (*N*-monochloroacetyl-DL-phenylalanine); (e), Tfa-DL-Phe-OH (*N*-trifluoroacetyl-DL-phenylalanine); (f), Tfa-DL-Val-OH (*N*-trifluoroacetyl-DL-valine); (g), Bz-DL-Ala-OH (*N*-benzoyl-DL-alanine); (h), Bz-DL-Met-OH (*N*-benzoyl-DL-methionine); (i), Z-DL-Ala-OH (*N*-benzyloxycarbonyl-DL-alanine); (j), Z-DL-Val-OH (*N*-benzyloxycarbonyl-DL-valine); (k), Z-DL-Leu-OH (*N*-benzyloxycarbonyl-DL-leucine); (1), Z-DL-Ser(tBu)-OH (*N*-benzyloxycarbonyl-*O-tert.*-

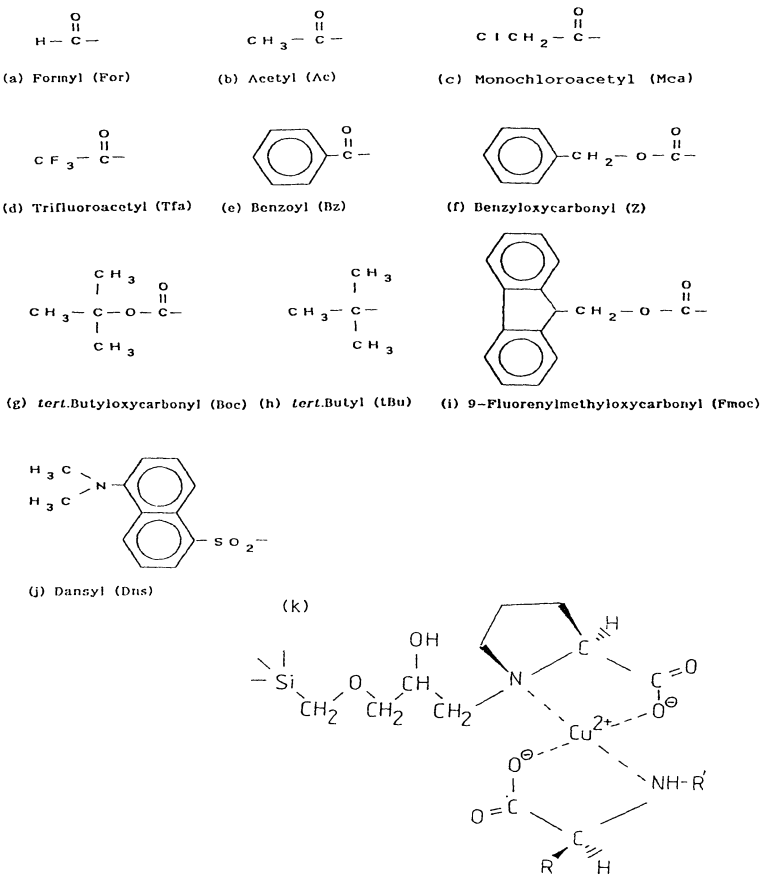

Figs. 1a-k. (a)–(j) Structures and abbreviations of amino acid protecting groups and (k) tentative structure of the diastereomeric copper complex formed by the chiral stationary phase 'Chiral ProCu' and *N*-acyl-L-amino acids. R, amino acid side chain; R', acyl- or dansyl residue.

butyl-DL-serine); (m) Fmoc-DL-Phe-OH (*N*-9-fluorenylmethyloxycarbonyl-DL-phenylalanine); (n), Fmoc-DL-Val-OH (*N*-9-fluorenylmethyloxycarbonyl-DL-valine); (o), Boc-DL-Ala-OH (*N-tert.*butyloxycarbonyl-DL-alanine); (p), Boc-DL-Val-OH (*N-tert.*butyloxycarbonyl-DL-valine); (q), Boc-DL-Leu-OH (*N-tert.*butyloxycarbonl-DL-leucine); (r), Boc-DL-Orn(Z)-OH (N^{α}-*tert.*butyloxycarbonyl-N^{δ}-benzyloxycarbonyl-DL-ornithine); (s), H-DL-Ser(Ac)-OH (*O*-acetyl-DL-serine); (t), H-Ser(tBu)-OH (*O-tert.*butyl-DL-Serine); (u), Dns-DL-Thr-OH (*N*-dansyl-DL-threonine); (v), Dns-DL-Leu-OH (*N*-dansyl-DL-leucine); (w), Dns-DL-Glu-OH (*N*-dansyl-DL-glutamic acid).

Results and Discussion

The enantioseparation of a number of DL-amino acid derivatives by LE-HPLC using the chiral stationary phase Chiral ProCu and eluents containing Cu^{2+} as complex forming ions is shown in Figs. 2a–w. It can be seen from the chromatograms that formyl-, acetyl-, haloacetyl-, and benzoyl DL-AA are resolved (Figs. 2a–h) as well as AA derivatized with the urethane-type protecting groups Z (Figs. 2i–l) and Boc (Figs. 2o–r), and side chain protected AA having free α-amino groups such as H-DL-Ser(Ac)-OH (Fig. 2s) or H-DL-Ser(tBu)-OH (Fig. 2t). Even bis-substituted AA such as Z-DL-Ser(tBu)-OH (Fig. 21) or Boc-DL-Orn(Z)-OH (Fig. 2r) are separated into enantiomers. However, when a number of Fmoc-DL-amino acids was investigated by LE-HPLC only Fmoc-DL-Phe-OH (Fig. 2m) and

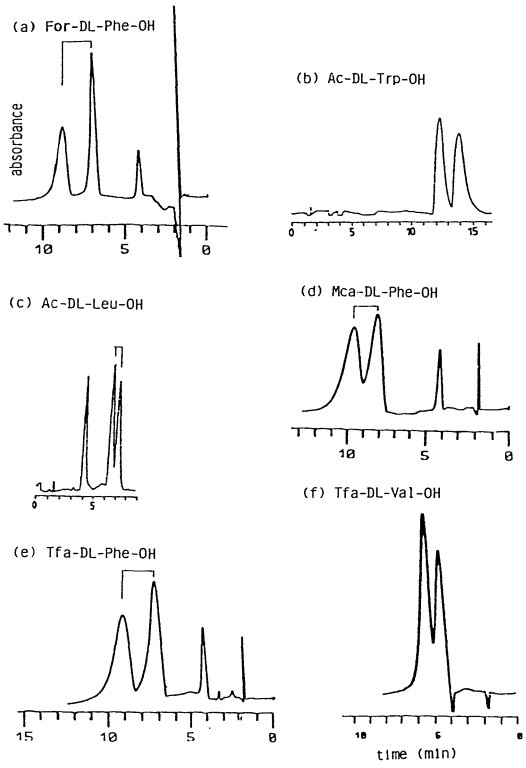

Figs. 2a–w. Chiral ligand-exchange chromatography of DL-amino acid derivatives by use of Chiral ProCu as stationary phase and aqueous eluents containing Cu^{2+}. For chromatographic conditions and for compositions of eluents A–D see Materials and Methods: a, d, e, f, **A**; b, c, g–l, o–t, **B**; u–w, **C**; m, n, **D**; flow rate: a–t, 1.5 ml/min; u–w, 1.1 ml/min; photometer absorbance: a–e, g, h, o–t, 245 nm; f, 236 nm; i–l, 254 nm; m, n 260 nm; u–w, 310 nm; column temperature: a, d–f, ambient temperature; b, c, g–t, 40°C; u–w, 60°C. D-enantiomers elute before L-enantiomers.

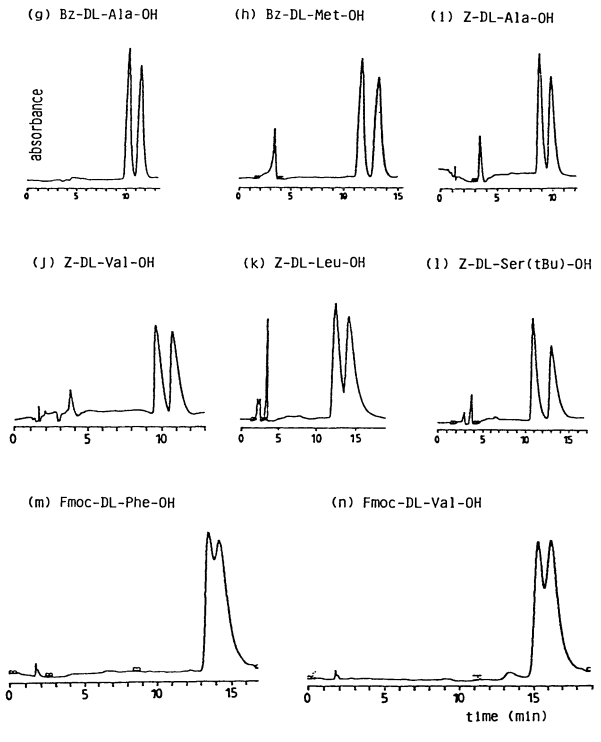

Fig. 2g–n.

Fmoc-DL-Val-OH (Fig. 2n) showed just the beginning of enantioseparation. This behaviour is attributed to the low solubility of hydrophobic Fmoc-DL-amino acids in aqueous eluents. In the instances shown 50% acetonitrile had to be added to the mobile phase in order to achieve sufficient solubilities and the beginning of a resolution of the analytes. Other Fmoc-DL-AA such as Fmoc-DL-Ala-OH, Fmoc-DL-Lys-OH and Fmoc-DL-Ser(tBu)-OH were not resolved under these conditions. That not alone the bulkiness of the Fmoc-group is responsible for the deviating behaviour is shown with Dns-DL-Thr, Dns-DL-Leu-Phe and Dns-DL-Glu-OH (Figs. 2u–w). The Fmoc- and Dansyl-group are of comparable size; the latter, however, is more hydrophilic and the eluent requires addition of less organic modifier (cf. Materials and Methods). It is remarkable that independent from the structures of the *N*-acyl groups baseline resolution, or almost baseline resolution, of the derivatives is achieved, with the exception of Fmoc-DL-Phe-OH and Fmoc-DL-Val-OH as mentioned above. This result is of interest since it is generally accepted that the DL-AA derivatives of the analyte form bidentate, tetracoordinated copper complexes with the chiral selector (L-Pro in the present instances, cf. Fig. 1k) of the stationary phase giving rise to diastereoisomers. Since

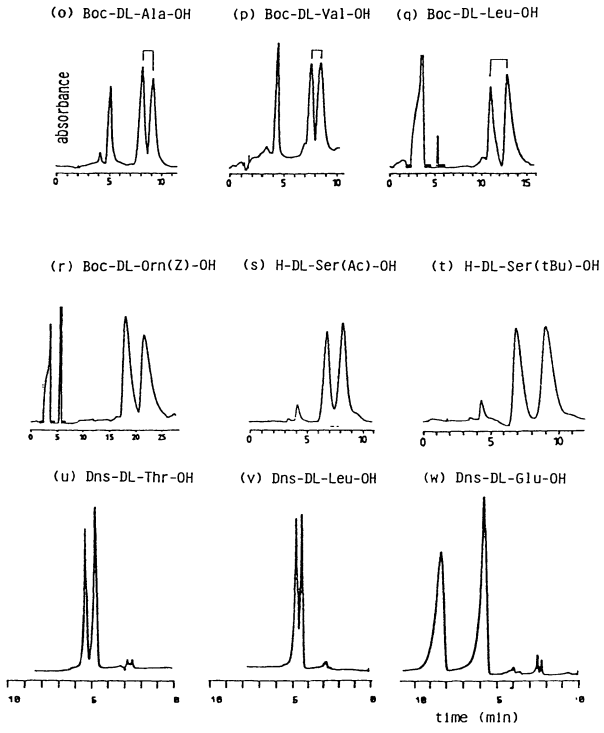

Fig. 2o–w.

the basic electron pair of the α-amino group in *N*-substituted amino acids acts as electron donator for Cu^{2+} one would expect that strong electron withdrawing acyl groups, such as the trifluoroacetyl group (Tfa), should decrease the resolution factor when compared to less electron withdrawing substituents. However, in contrast to *N*-methyl-α-amino acids, where the enhanced basicities of the alkyl substituted α-amino groups leads to high resolutions in LE-HPLC [6] no pronounced effect is observed with the various *N*-acyl derivatives (cf. Figs. 1a, d and e). The enantioseparation of Boc- and Z-amino acids is of particular interest, since the respective mono- or bifunctional protected AA derivatives (together with Fmoc-AA) are the most frequently used in peptide synthesis by either classical stepwise chain-lengthening and segment condensations or by solid phase procedures using various types of insoluble polymeric supports [2,3]. Since the acylation of the amino acids is usually carried out under alkaline conditions, which may contribute to the racemization of AA, the optical purity of the protected AA has to be checked carefully by the manufacturer in quality control, and by the peptide chemist prior to their use in peptide synthesis. It is assumed that chiral LE-HPLC of protected amino acid acids as described above is a suitable method

for the determination of the optical purity of amino acid derivatives. Furthermore, since *N*-acetyl and *N*-trifluoroacetyl DL-AA are well resolved by LE-HPLC, this method makes possible the monitoring of the stereospecific enzymic cleavage of acetyl amino acids. This has recently been shown with the preparative cleavage of non-proteinogenic α-alkyl-α-amino acid derivatives such as Tfa-DL-α-propionyl alanine and Tfa-DL-α-methyl leucine by carboxypeptidase A and acylase I [8]. It should be mentioned in this context that chiral columns for LE-HPLC which are comparable to Chiral ProCu are Nucleosil Chiral-1 (Macherey-Nagel, Düren, F.R.G.) and Chiralpak WH and WM (Daicel Chemical Industries, Tokyo; distributed in Europe by Baker Chemicals).

Conclusions

1. It is shown that LE-HPLC using silica bonded L-Pro ('Chiral ProCu') and eluents containing Cu^{2+} as complex forming ions enable the chiral resolution of *N*- and *O*-protected DL-amino acid derivatives having free carboxy groups.
2. Since no further derivatization steps are necessary this method is considered as being very suitable for the determination of the optical purity of amino acid derivatives, in particular also for Boc- and Z-amino acids which are important in synthetic peptide chemistry. Under the conditions used Fmoc-amino acids are not separated or show just the beginning of a separation.
3. Although in many instances baseline resolution, or almost baseline resolution, of *N*-acyl-DL-amino acids is achieved the resolutions obtained are in principle lower as compared to the respective *N*-methyl-DL-AA [6]. The nature of the *N*-acyl group, therefore, is of minor importance for the resolution of the various derivatives of a certain amino acid.
4. From the results it is assumed that the method will make possible the enantioseparation and prove of the optical purity of many more *N*-acylated or otherwise derivatized DL-amino acids.

References

1. Wünsch E (1974) Synthese von Peptiden, Teil 1. In: Müller E (ed.) Methoden der Organischen Chemie, Teil XV. Thieme Verlag, Stuttgart.
2. Bodansky M and Bodansky A (1984) The Practice of Peptide Synthesis. Springer, Berlin.
3. Bodansky M (1984) Principles of Peptide Synthesis. Springer, Berlin.
4. Davankov VA (1984) In: Hancock WS (ed.) Handbook of HPLC for the Separation of Amino Acids, Peptides and Proteins. CRC Press, Boca Raton, U.S.A., Vol. 1, pp. 393ff.
5. Gübitz G, Jellenz W and Santi W (1981) J. Chromatogr. 203: 377–384.
6. Brückner H (1987) Chromatographia 24: 725–738.
7. Brückner H, Kühne S, Zivny S, Langer M, Kamiński ZJ and Leplawy MT (1989) In: Aubry A, Marraud M and Vitoux B (eds.) Second Forum on Peptides. John Libbey Eurotext, London, pp. 291–295.
8. Brückner H, Kühne S, Zivny S and Currle M (1987) In: Shiba T and Sakakibara S (eds.) Peptide Chemistry 1987. Protein Research Foundation, Osaka, Japan, pp. 175–178.

Address for correspondence: Hans Brückner, Institute of Food Technology, University of Hohenheim, D-7000 Stuttgart 70, F.R.G.

Enantioseparation of C^{α}-disubstituted glycines*

Hans Brückner[a], Mathias Langer[a], Ali Esna-Ashari[a], Anik Labudda[a], Zbigniew J. Kamiński[b], Miroslaw T. Leplawy[b] and Rolf Jöster[c]

[a]Institute of Food Technology, University of Hohenheim, D-7000 Stuttgart 70, F.R.G.
[b]Institute of Organic Chemistry, Technical University, 90-924 Lodz, Poland
[c]Perkin Elmer Analytic, Gewerbestraße 42, D-7000 Stuttgart 80, F.R.G.

Abstract

The enantioseparation of α-alkyl-α-amino acids (AAA) was achieved as their *N(O)*-pentafluoropropionyl S(+)-3-methyl-2-butyl esters by capillary gas chromatography on dimethylpolysiloxane (CP-Sil 5) as the stationary phase. Chiral resolution of AAA and α-hydroxymethyl-α-amino acids was also possible by ligand-exchange chromatography using either a chiral stationary phase in which L-Pro had been bonded covalently to silica ('Chiral ProCu'), or by use of octadecylsilica as stationary phase and a chiral eluent composed of an aqueous solution of *N,N*-dimethyl-L-phenylalanine and copper(II)sulfate.

The formal substitution of the C^{α}-hydrogen atoms in glycine by alkyl or aryl groups, which may be further substituted, results in the formation of non-proteinogenic α-amino acids with the general structure H_2N-C(RR')-COOH and referred to as C^{α}-disubstituted glycines. The compouds are chiral when $R \neq R'$; and in instances where R is a protein amino acid side chain residue and R' is an alkyl group, the resulting amino acid may also be designated as α-alkyl-α-amino acid (AAA). An example is α-ethylalanine, α-Et-Ala, H_2N-C(C_2H_5)(CH_3)-COOH, that also may be designated as α-methyl-α-amino-*n*-butyric acid, α-Me-Abu. The common name for this compound is isovaline (Iva). In analogy, substitution of the C^{α}-hydrogen atom in a protein amino acid by a hydroxymethyl (CH_2OH) group leads to α-hydroxymethyl-α-amino acids (α-HmA). An example is α-hydroxymethylalanine, α-Hm-Ala, H_2N-C(CH_2OH)(CH_3)-COOH that, in turn, may be also designated as α-methylserine, α-Me-Ser. Based on the simple rule that the title compounds are regarded as derivatives of protein amino acids (or well-known analogs such as α-amino-*n*-butyric acid, Abu, norvaline, Nva, or phenylglycine, Phg) the abbreviations used in Figs. 1 and 2 are easily understandable.

In particular, AAA are attracting continuing attention since they may act as antagonists for protein amino acids; α-methyldopa (α-Me-Dopa) for example, is used for the treatment of Parkinson's disease. Furthermore, the substitution of protein amino acids by C^{α}-disubstituted glycines offers high potential for peptide

* This presentation was awarded the Ajinomoto Prize for the best poster of the Congress.

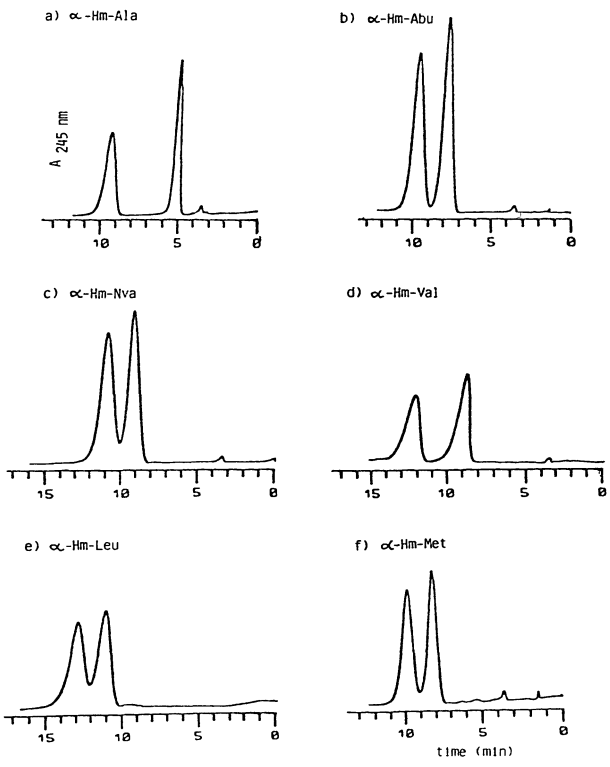

Fig. 1. Enantioseparation of DL-α-hydroxymethyl-α-amino acids and DL-α-alkyl-α-amino acids by ligand-exchange HPLC. (a)–(f), stationary phase **A** and eluent **I**; (g), (j), (k), stationary phase **B** and eluent **II**; (h), (i), stationary phase **B** and eluent **III** (for abbreviations and chromatographic conditions see Materials and Methods).

drug design since, as a result of considerable restrictions in the ϕ/ψ torsion angles of the peptide backbone, the resulting amino acids may give rise to particular or significantly stabilized peptide conformations [1]. Moreover, the peptide bonds formed by C^{α}-disubstituted glycines are almost completely resistant towards cleavage by proteases, a feature which is expected to make possible the synthesis of analogs of peptide hormones with dramatic durations of activity when used as pharmacons. Use of chiral C^{α}-disubstituted glycines in either the free or derivatized form necessitates methods for the preparative and analytical resolution of the respective enantiomers. In the following we show that C^{α}-disubstituted glycines can be separated as their diastereomeric esters or, in the underivatized form, by chiral ligand-exchange chromatography.

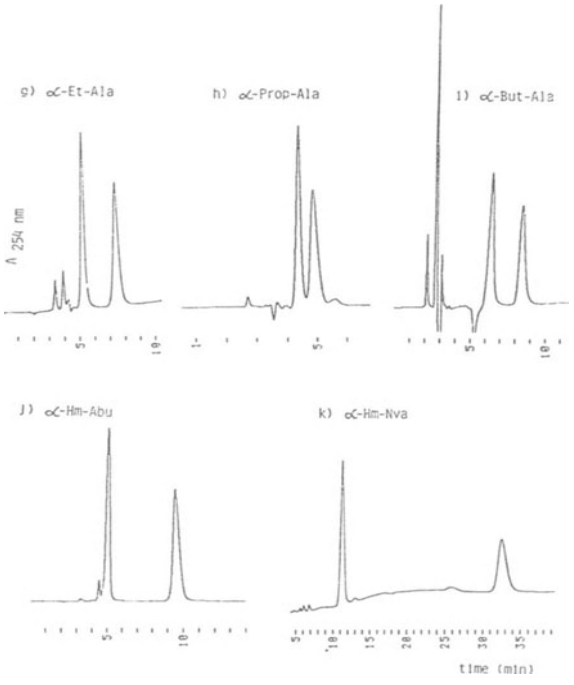

Fig. 1g–k.

Materials and Methods

Instruments

Gas Chromatography

For GC a Hewlett Packard Model 5880A gas chromatograph equipped with a flame ionization detector (FID) and a fused silica capillary column coated with CP-Sil 5 (26 m × 0.22 mm i.d., 0.21 µm dimethylpolysiloxane; Chrompack, Middelburg, The Netherlands) was used. Conditions: carrier gas, helium; pressure, 100 kPa; split injection of ca. 0.8 µl samples, split ratio ca. 1:30; injector and detector temperature, 250°C.

High-performance liquid chromatography

For HPLC a Perkin-Elmer Liquid Chromatograph Series 10 equipped with a variable wavelength detector LC 85B and a recorder of the Series 561 were used. Columns were 250 mm × 4 mm i.d. (Novogrom system, Grom, Herrenberg, F.R.G.) and equipped with precolumns (20 mm × 4.6 mm i.d.). Stationary phases

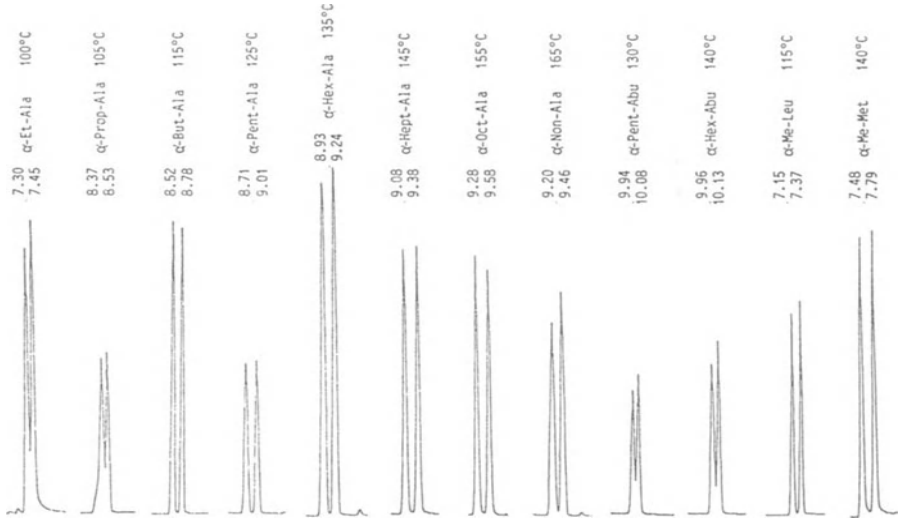

Fig. 2. Enantioseparation of DL-α-alkyl-α-amino acids by gas chromatography of PFP-amino acid S(+)-3-methyl-2-butyl esters. Netto retention times (min) and isothermal temperature programs are given; *S*-enantiomers elute before *R*-enantiomers. For chromatographic conditions and abbreviations of amino acids see Materials and Methods.

used were **A**, Chiral ProCu, 5 µm (Serva, Heidelberg, F.R.G.) and **B**, Nucleosil 5 C 18, 5 µm (Macherey-Nagel, Düren, F.R.G.). Mobile phases used were **eluent I**, 1 m*M* aqu. copper(II)sulfate, pH 6.0; flow rate, 2 ml/min; 50°C; **eluent II**, 2 m*M* *N,N*-dimethyl-L-phenylalanine in 1 m*M* aqu. copper(II)acetate, pH 4.5; flow rate, 1 ml/min, ambient temperature; eluent III, 2 m*M* *N,N*-dimethyl-L-phenylalanine and 1 m*M* copper(II)acetate in water/acetonitrile (9:1), pH 4.5; flow rate, 1 ml/min, ambient temperature.

Origin and abbreviations of materials

DL-α-methylaspartic acid (α-Me-Asp), DL-α-methylglutamic acid (α-Me-Glu), DL-α-methylserine (α-Me-Ser), DL-α-methylornithine (α-Me-Orn), DL-α-methyl-*meta*-methoxyphenylalanine (α-Me-*m*-PheOMe), DL-α-methyl-*para*-tyrosine (α-Me-Tyr), DL-α-methyl-*meta*-tyrosine (DL-α-*m*-Tyr). DL- and L-α-methyl-(3,4-dihydroxyphenyl)-alanine (α-Me-Dopa) were purchased from Sigma (St. Louis, MO, U.S.A.); DL-α-methylleucine (α-Me-Leu) was from Bachem (Bubendorf, Switzerland), and DL-α-ethylphenylglycine (α-Et-Phg) was from EMKA Chemie (Markgröningen-Talhausen, F.R.G.).

DL-α-methyl-*homo*-phenylalanine (α-Me-*homo*-Phe) was a gift from Dr. J. Kamphuis (DSM Research, Geleen, The Netherlands).

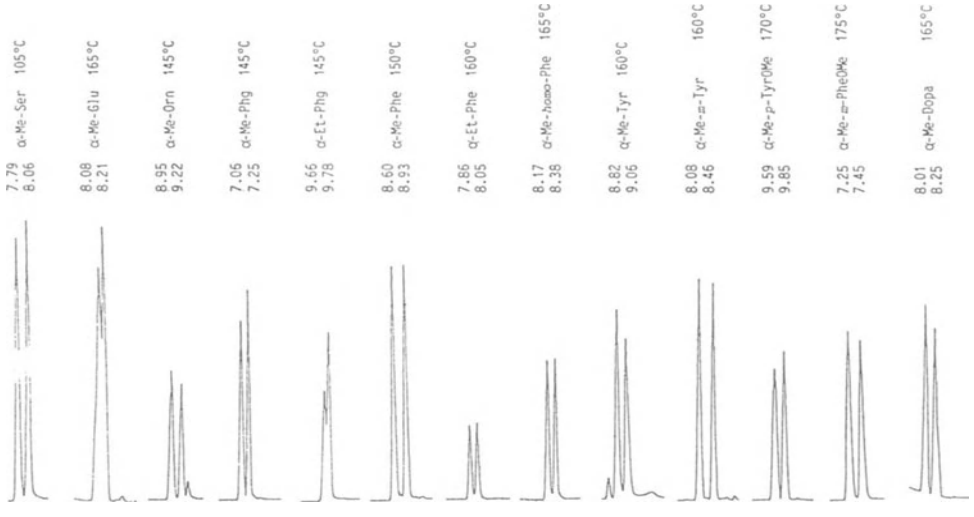

Fig. 2. (cont'd)

The following, commercially unavailable amino acids were synthesized in our laboratory according to the Schotten-Baumann procedure or in analogy to methods described previously [2]: DL-α-ethylalanine (α-Et-Ala), DL-α-propylalanine (α-Prop-Ala), DL-α-butylalanine (α-But-Ala), DL-α-pentylalanine (α-Pent-Ala), DL-α-hexylalanine (α-Hex-Ala), DL-α-heptylalanine (α-Hept-Ala), DL-α-octylalanine (α-Oct-Ala), DL-α-nonylalanine (α-Non-Ala), DL-α-pentyl-α-amino-*n*-butyric acid (α-Pent-Abu), DL-α-hexyl-α-amino-*n*-butyric acid (α-Hex-Abu), DL-α-hydroxymethylalanine (α-Hm-Ala), DL-α-hydroxymethyl-α-amino-*n*-butyric acid (α-Hm-Abu), DL-α-hydroxymethylnorvaline (α-Hm-Nva), DL-α-hydroxymethylvaline (α-Hm-Val), DL-α-hydroxmethylleucine (α-Hm-Leu), DL-α-hydroxymethylmethionine (α-Hm-Met).

Reagents, derivatization procedures and eluents

S(+)-3-methyl-2-butanol was from Sigma, pentafluoropropionic anhydride (PFPA) was from Pierce, Rockford, Ill., U.S.A., acetyl chloride, copper(II)sulfate × 5 H_2O, and N,N-dimethyl-L-phenylalanine were from Merck, Darmstadt, F.R.G.

For the derivatization of aliphatic and aromatic amino acids for GC ca. 0.6 mg of the respective amino acid in 100 µl of a solution of acetyl chloride in S(+)-3-methyl-2-butanol (2:8, v/v) was heated in a 1 ml 'reacti-vial' (Wheaton, Milleville, U.S.A.) at 100°C for 1 h. Solvents were removed in a stream of nitrogen, 100 µl dichloromethane (DCM) and 25 µl PFPA were added, and the mixture was heated at 100°C for 20 min. Reagents were removed in a stream of nitrogen, the residue was dissolved in 50 µl of DCM and aliquots were subjected to GC. For the derivatization of acidic and basic amino acids transesterification was carried out:

300 µl 2 *M* HCl in methanol were added to 0.6 mg of the respective amino acid and the mixture heated at 100°C for 1 h. Reagents were removed in a stream of nitrogen, acetyl chloride in S(+)-3-methyl-2-butanol was added, and the derivatization procedures and analyses were carried out as described above.

Results and Discussion

We have recently shown [3–5], that the enantioseparation of a number of AAA is possible by HPLC and precolumn derivatization with *o*-phthaldialdehyde and chiral thiols such as *N*-acetyl-L-cysteine and *N-tert.*-butyloxycarbonyl-L-cysteine, or with Marfey's reagent. Another approach was ligand-exchange chromatography [6] using a chiral stationary phase in which L-Pro was covalently bonded to silica and an eluent containing Cu^{2+}-ions were used [7,8]. In Fig. 1a–f we show that ligand-exchange chromatography using Chiral ProCu as stationary phase and copper sulfate as eluent also makes possible the enantioseparation of α-HmA such as α-Hm-Ala, α-Hm-Abu, α-Hm-Val, α-Hm-Nva, α-Hm-Leu, and α-Hm-Met. As shown in Fig. 1g–k with α-Et-Ala ('isovaline'), α-Prop-Ala, α-But-Ala, α-Hm-Abu, and α-Hm-Nva chiral resolution of C^{α}-disubstituted glycines by ligand-exchange chromatography is also possible with a nonchiral stationary phase, when a chiral additive to the eluent is used which is capable of forming diastereomeric copper complexes with amino acids. In particular, the chiral selector *N,N*-dimethyl-L-phenylalanine gives very high resolution coefficients, as has already been shown for a number of protein amino acids [9]. In a previous communication we have shown that capillary gas chromatography of *N(O)*-pentafluoropropionyl (=PFP) S(+)-3-hexyl esters on a dimethylpolysiloxane stationary phase gave excellent resolutions for a homologous series of α-alkyl-alanines [4]. Since very good chiral resolutions of protein amino acids by use of S(+)-3-methyl-2-butyl esters have also been reported [10], we have compared the resolution behaviour of the homologous series S(+)-2-butyl to S(+)-2-octyl esters of a large number of AAA with that of the respective S(+)-3-methyl-2-butyl esters. As can be seen in Fig. 2, enantioseparation of all PFP derivatives of S(+)-3-methyl-2-butyl esters of AAA is possible and, in most cases, a baseline resolution is achieved. In particular, α-Me-Tyr, α-Me-*m*-Tyr, α-Me-*p*-TyrOMe, α-Me-*m*-PheOMe and α-Me-Dopa show higher resolution coefficients for this ester when compared to the series of PFP derivatives of 2-butyl esters to 2-octyl esters. From the results it is concluded that appropriate selection of the above GC or HPLC method, or the other methods described previously [3–5,8] will make possible the enantioseparation of almost any C^{α}-disubstituted glycine or, if necessary, furnish proof of its enantiomeric purity.

Acknowledgements

This work has been supported in part by the Deutsche Forschungsgemeinschaft and the Polish Academy of Sciences.

References

1. Marshall GR, Clark JD, Dunbar JB, Smith GD, Zabrocki J, Redlinski AS and Leplawy MT (1988) Int. J. Peptide Protein Res. 32: 544–555.
2. Kamiński ZJ, Leplawy MT and Slomczynska U (1983) In: Bláha K and Malõn P (eds.) Peptides 1982. Walter de Gruyter, Berlin, pp. 323–326.
3. Brückner H, Kühne S, Zivny S and Currle M (1988) In: Shiba T and Sakikabara S (eds.) Peptide Chemistry 1987. Protein Research Foundation, Osaka, Japan, pp. 175–178.
4. Brückner H, Kühne S, Zivny S, Langer M, Kamiński ZJ and Leplawy MT (1989) In: Aubry A, Marraud M and Vitoux B (eds.) Second Forum on Peptides. Colloque, Inserm John Libbey Eurotext, London, pp. 291–294.
5. Kamiński ZJ, Leplawy MT, Langer M, Sorsche S and Brückner H (1989) In: Bayer E and Jung G (eds.) Peptides 1988. Walter de Gruyter, Berlin, pp. 298–300.
6. Davankov VA and Semechkin AV (1977) J. Chromatogr. 141: 313–353.
7. Gübitz G, Juffmann F and Jellenz W (1983) Chromatographia 16: 103–106.
8. Brückner H (1987) Chromatographia 24: 725–738.
9. Wernicke R (1985) J. Chromatogr. Sci. 23: 39–47.
10. König WA, Rahn W and Eyem J (1977) J. Chromatogr. 133: 141–146.

Address for correspondence: Hans Brückner, Institute of Food Technology, University of Hohenheim, D-7000 Stuttgart 70, F.R.G.

Enzymatic synthesis and biochemical reactions of fluorinated analogues of L-tyrosine and L-dopa*

Robert S. Phillips, Robert L. Von Tersch, Joel G. Fletcher and Ah H. Lai

Departments of Chemistry and Biochemistry, School of Chemical Sciences, University of Georgia, Athens, GA 30602, U.S.A.

Abstract

2-Fluoro-L-tyrosine and 3-fluoro-L-tyrosine have been prepared from 3-fluorophenol and 2-fluorophenol, respectively, pyruvate and ammonia using tyrosine phenol-lyase from *Citrobacter freundii*. Evidence was obtained that 6-fluoro-L-dopa can be made from 4-fluorocatechol by this method. Both fluorotyrosines are substrates for mushroom tyrosinase. Oxygenation of 2-fluoro-L-tyrosine results in 6-fluoro-L-dopa, while 3-fluoro-L-tyrosine gives 5-fluoro-L-dopa. Both fluorotyrosines produce fluoride ion in reactions with tyrosinase, as measured by a fluoride-specific electrode. However, ascorbic acid can suppress fluoride release from 3-fluoro-L-tyrosine, but not from 2-fluoro-L-tyrosine.

Introduction

The properties of fluorinated analogues of biologically active molecules are interesting and frequently therapeutically useful. 5-Fluorouracil is in widespread clinical use as an antineoplastic drug [1], while dexamethasone is a fluorinated steroid with potent antiinflammatory properties [2]. Due to the small atomic radius of fluorine, it is able to substitute for either hydrogen or hydroxy groups in molecules with retention or even enhancement of biological activity. Thus, there is great interest in methods of preparation of fluorinated biomolecules.

We have been studying the preparation and biochemical properties of fluorinated analogues of L-tyrosine and L-dopa. 6-Fluorodopa, labeled with [^{18}F], has been successfully used in diagnostic screening for Parkinson's disease by PETT scanning [3]. We have investigated the use of a microbial enzyme, tyrosine phenol-lyase, for the preparation of 2- and 3-fluoro-L-tyrosines and 6-fluoro-L-dopa from simple precursors, 2- or 3-fluorophenols or 4-fluorocatechol, pyruvic acid and ammonia. We have also studied the reaction of mushroom tyrosinase[1] with the resultant fluorotyrosines, and we have found that the aromatic fluorine is released as fluoride ion during enzymatic oxygenation [4].

* This work was supported by grants (CHM-382 and CHM-382A) from the American Cancer Society to R.S.P.

[1] Abbreviations are: TLC, thin layer chromatography; HPLC, high performance liquid chromatography; tyrosinase, monophenol, dihydroxy-phenylalanine; oxygen oxidoreductase [EC 1.14.18.1].

Experimental procedures

Chemicals

2-Fluorophenol and 3-fluorophenol were obtained from Aldrich Chemical Co. 4-Fluorocatechol was synthesized from 4-aminoveratrole (Aldrich) by a thermal Schiemann reaction of the diazonium fluoborate, followed by BBr_3 cleavage of the 4-fluoroveratrole. Authentic samples of fluorodopas were a generous gift of Dr. Kenneth L. Kirk of the National Institutes of Health [5].

Enzymes and assays

Tyrosine phenol-lyase [EC 4.1.99.2] was obtained from cells of *Citrobacter freundii* (ATCC 29063) grown on a medium containing 0.1% (w/v) L-tyrosine, as described [6]. Mushroom tyrosinase and bovine liver catalase were obtained from Sigma Chemical Co. as lyophilized powders. Tyrosine phenol-lyase activity was measured spectrophotometrically at 370 nm ($\Delta\varepsilon = -1860\ M^{-1}\ cm^{-1}$) with 0.6 mM S-(*o*-nitrophenyl)-L-cysteine [7]. Tyrosinase activity was determined using a YSI Model 53 Oxygen Monitor with a polarographic electrode. The Oxygen Monitor response was calibrated with the L-amino acid oxidase/L-phenylalanine reaction.

Preparation of fluorinated analogues

Typical reaction mixtures contained, in a total volume of 1 L, 50 mM pyruvic acid, 100 mM ammonium acetate, 50 μM pyridoxal 5'-phosphate, 5 mM 2-mercaptoethanol, and 20–60 units of tyrosine phenol-lyase. The pH of the reaction mixtures was adjusted to about 8 with aqueous NH_3. The phenols were added in portions so that the concentration of the phenol does not exceed 10 mM. When the reaction equilibrium was established, in 3 to 5 days, the solutions were acidified with glacial acetic acid, filtered through Celite to remove precipitated protein, and concentrated *in vacuo* to about 100 mL. The crude products which precipitated upon storage at 4°C were collected and recrystallized from hot water. Isolated yields were 63% for 3-fluoro-L-tyrosine and 30% for 2-fluoro-L-tyrosine. The 300 MHz ^1H and 282.4 MHz ^{19}F NMR spectra were consistent with the assigned structures. Reactions with 4-fluorocatechol were performed in the presence of 0.1% sodium sulfite and under N_2 to prevent oxidation.

High performance liquid chromatography of tyrosinase reactions

The reaction mixtures contained 1 mM 2-fluoro- or 3-fluoro-L-tyrosine, 10 mM ascorbic acid, 50 μg/mL catalase and 50 μg/mL tyrosinase in air-saturated 0.1 M potassium phosphate, pH 7.0. The reaction mixtures were incubated for 30 minutes to 1.5 h. The products were separated from the proteins by centrifugation through an Amicon MPS-1 centrifugal ultrafiltration filter using a YMP membrane.

Products of tyrosinase oxygenation reactions were determined using a Rainin high performance liquid chromatography (HPLC) system in 0.1% trifluoroacetic acid, 5% acetonitrile on an Applied Biosystems 2.1 × 220 mm C_{18} column at 0.2 ml/minute, with detection by absorbance at 270 nm. This wavelength was selected as the optimum for detection of the fluorotyrosine and fluorodopa isomers in a single run, although it is less sensitive for 6-fluorodopa (λ_{max} = 283 nm). Before injection, samples were diluted twenty-fold with 0.1% trifluoroacetic acid, 5% acetonitrile. The predilution step was essential for efficient separation of the fluorinated isomers of L-dopa.

Fluoride electrode measurements

Fluoride release upon oxygenation of fluorotyrosines was measured with a Corning Fluoride Electrode using an Ag/AgCl reference electrode. Reactions were performed as described for HPLC experiments, except that 100 μg/mL tyrosinase was added, and reaction mixtures were incubated for one h. Samples were diluted with equal volumes of total ionic strength adjustment buffer (TISAB) [8]. Standard curves were prepared by addition of known amounts of NaF (10^{-6} to 10^{-3}M) to a blank reaction mixture, followed by dilution with TISAB. Fluoride ion concentrations in the reaction mixtures were then determined by comparison with the standard curve. Control experiments containing L-tyrosine were also performed, and gave no evidence for fluoride production.

Results and Discussion

Preparation of fluorinated analogues

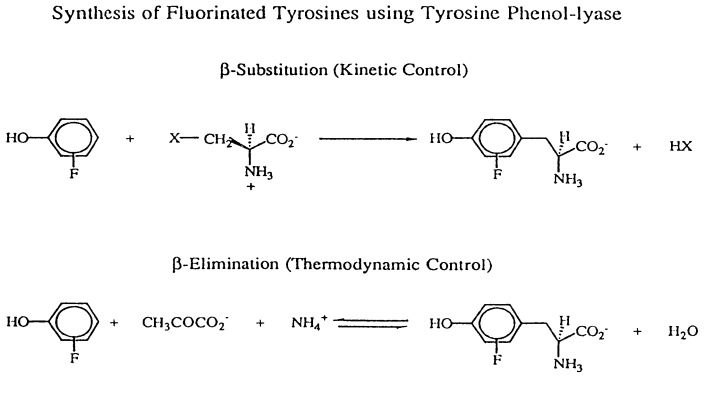

Scheme 1.

Table 1. Kinetic Constants for Tyrosinase Reactions

Substrate	K_m[a]	V_{max} (relative)[a]	V_{max}/K_m (relative)[a]
L-Tyrosine	0.13 mM	1	1
3-F-L Tyrosine	0.016 mM	0.15	1.27
2-F-L Tyrosine	0.32 mM	0.71	0.30

[a] Kinetic parameters were measured using a polarographic O_2 electrode as described in the Experimental Procedures section. The specific activity for the enzyme preparation was found to be 2.7 μmol/min-mg with 1 mM L-tyrosine as the substrate.

2-Fluoro-L-tyrosine and 3-fluoro-L-tyrosine are readily prepared in moderate to good yields from 3-fluorophenol and 2-fluorophenol, respectively, using bacterial tyrosine phenol-lyase (Scheme 1), as previously reported by Nagasawa *et al.* [9]. 6-Fluoro-L-dopa also could be prepared from 4-fluorocatechol under these conditions, as seen from thin layer chromatography (TLC) and HPLC of reaction mixtures (data not shown). However, isolation of 6-fluoro-L-dopa is complicated by the extreme lability of this compound. This reaction can be performed under kinetic control, using the ß-substitution activity of tyrosine phenol-lyase [6], or it can be performed under thermodynamic control, by reversal of the ß-elimination activity (Scheme 1). Although the reactions are much slower, we have obtained higher yields of the fluorinated tyrosines under the thermodynamically controlled conditions.

Reactions with tyrosinase

Kinetic parameters for oxygenation of fluorinated tyrosines were determined using a polarographic oxygen electrode assay, with the results summarized in Table 1 [4]. Both monofluorinated tyrosines are good substrates; however, 3-fluoro-L-tyrosine is a better substrate based on comparison of values of V_{max}/K_m, while 2-fluoro-L-tyrosine exhibits a greater V_{max}. These results suggest that the 2-fluoro substituent has a greater effect on binding, while the proximity of the 3-fluoro substituent to the site of reaction retards the oxygenation reaction. The K_m value for L-tyrosine obtained in these experiments is in good agreement with literature values [10].

The reaction products were readily identified by HPLC analysis of reaction mixtures containing ascorbic acid, as shown in Fig. 1 [4]. 2-Fluorotyrosine and the likely reaction products, 2-fluorodopa and 6-fluorodopa, are readily separated under the described HPLC conditions (Fig. 1A). The reaction of 2-fluoro-L-tyrosine gave a single product, tentatively identified by its retention time as 6-fluoro-L-dopa (Fig. 1B). Furthermore, upon extended incubation, there was no further increase in the 6-fluoro-L-dopa, but another product with retention time of 3.7 minutes was observed (data not shown). Control HPLC experiments with tyrosinase and 6-fluorodopa demonstrated that synthetic 6-fluorodopa is not stable under the reaction conditions, but is rapidly converted to a product with a retention time of 3.7 min. In contrast, similar experiments with 2-fluorodopa demonstrated that it

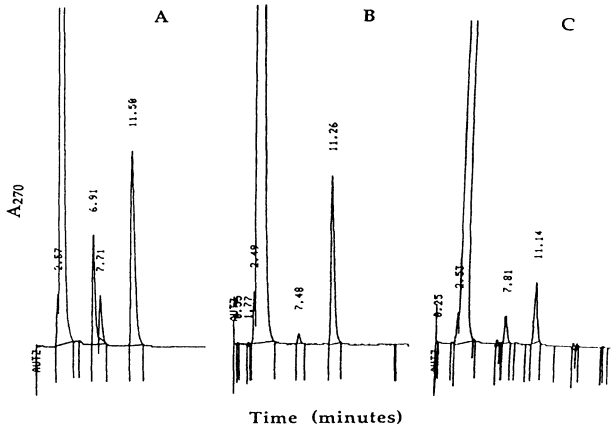

Fig. 1. A. Separation of 2-fluorotyrosine (t_R = 11.5 minutes), 2-fluorodopa (t_R = 6.91 minutes), and 6-fluorodopa (t_R = 7.71 minutes) by HPLC as described in Materials and Methods. B. Reaction mixture of 2-fluorotyrosine with mushroom tyrosinase after 30 minutes of incubation. A new peak, with t_R = 7.48 minutes, is seen, which is assigned to 6-fluorodopa. C. Reaction mixture of 3-fluorotyrosine with mushroom tyrosinase after 1 h of incubation. 3-Fluorotyrosine (t_R = 11.14 minutes) and 5-fluorodopa (t_R = 7.81 minutes) are seen in the reaction.

is stable under the reaction conditions, so it should have been detected if it were formed. Thus, hydroxylation of 2-fluoro-L-tyrosine is highly regioselective, producing only 6-fluoro-L-dopa (Fig. 1B). This is the expected effect of fluorine on electrophilic aromatic substitution reactions. For example, the partial rate factor for nitration of fluorobenzene at the *p*-position is 14-fold that for an *o*-position [11].

The relatively low stoichiometry for 6-fluoro-L-dopa observed in the reaction mixtures containing 2-fluoro-L-tyrosine (see Fig. 1B) was initially puzzling. Quantitative analysis of HPLC data indicated that the 2-fluorotyrosine was 47% consumed after 1.5 h, but the amount of L-fluorodopa formed accounted for only 14%. However, 6-fluorodopa was not stable under the reaction conditions (*vide supra*). The presence of ascorbic acid also does not prevent formation of fluoride ion from 2-fluoro-L-tyrosine in the reactions (Table 2). Thus, it is clear that tyrosinase is catalyzing the rapid decomposition of nascent 6-fluorodopa. In previous studies, Rice *et al.* found that 6-fluorodopa was oxidized by tyrosinase even more rapidly than dopa, while electrochemical oxidation of 6-fluorodopa was found to release fluoride ion in a 2-electron process, and electrochemical oxidation of dopa and 2- and 5-fluorodopas proceeds through a 4-electron process [12]. Thus, it was proposed that 6-fluorodopaquinone must rapidly cyclize to release fluoride [12]. Our results agree with these previous conclusions. The proposed reaction pathway is summarized in Scheme 2. Loss of fluoride from the 6-fluorodopaquinone would be expected to lead directly to 5,6-dihydroxyindole-2-carboxylic

Table 2. Release of fluoride from fluorinated tyrosines

Substrates[a]	Ascorbate[b]	[fluoride],μM
2-F-L-Tyr	+	194.5
2-F-L-Tyr	–	424.4
3-F-L-Tyr	+	13.2
3-F-L-Tyr	–	173.0

[a] Initial concentrations of fluorinated tyrosines were 0.5 m*M*.
[b] Ascorbate concentration was 10 m*M* "+" indicates the reaction mixtures containing ascorbate; "–" indicates reation mixtures from which ascorbate was omitted.

acid, which is generated in the normal melanin biosynthetic pathway by another 2-electron oxidation [13].

Reaction mixtures with 3-fluoro-L-tyrosine gave one product, identified as the expected 5-fluoro-L-dopa by its retention time (Fig. 1C) [4]. No evidence for L-dopa formation from 3-fluoro-L-tyrosine was detected in these reactions, although oxygenative defluorination has been observed in other oxygenase reactions [14,15]. Since rapid cyclization of the quinone derived from 5-fluorodopa does not occur [12], one observes stoichiometric conversion of 3-fluorotyrosine to 5-fluorodopa under our reaction conditions. The presence of ascorbic acid strongly suppresses the formation of fluoride ion (Table 2). The release of fluoride from 3-fluorotyrosine which we observed in the absence of ascorbic acid may be occurring during subsequent melanogenesis.

The production of fluoride ion during biological oxygenation of aryl fluorides has been observed in several other systems. Hydroxylation of 4-fluorophenylalanine by phenylalanine hydroxylase results in L-tyrosine and fluoride ion [14]. Also, hydroxylation of 3,5-difluoro-4-hydroxybenzoic acid catalyzed by *para*-hydroxybenzoate hydroxylase results in 3-fluorobenzoquinone-5-carboxylic acid

Proposed Reaction of Fluorotyrosines with Tyrosinase

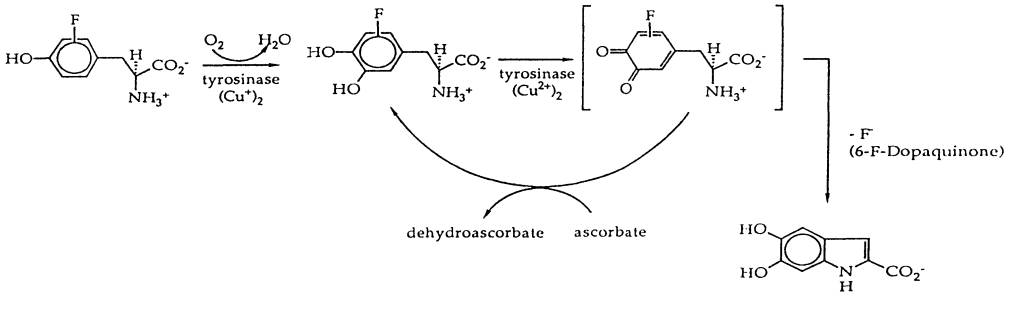

Scheme 2.

and fluoride ion [15]. However, these examples involved direct oxygenative defluorination of a C-F bond. The results in this paper demonstrate a novel mode for fluoride release, by oxygenation to an electrophilic product which undergoes subsequent nucleophilic substitution. Fluoride release from 2-fluorotyrosine is more efficient than that from 3-fluorotyrosine (Table 2). Furthermore, 3-fluorotyrosine is highly toxic, due to its conversion to fluoroacetate in liver metabolism [16], while 2-fluorotyrosine is relatively nontoxic. The release of fluoride ion through the action of tyrosinase on 2-fluorotyrosine in tissues containing high levels of tyrosinase (e.g., melanoma tumors) might lead to selective cytotoxicity. 2-Fluorotyrosine has been submitted for testing for inhibitory activity against melanoma cell lines.

References

1. Heideberger C (1970) Cancer Res. 30: 1549–1569.
2. Weltstein A (1972) In: Ciba Symp., p. 298.
3. Calne DB, Langston JW, Martin WRW, Stoessl AF, Ruth TJ, Adam MJ, Pate BD and Schulzer M (1985) Nature (London) 317: 246–248.
4. Phillips RS, Fletcher JG, Von Tersch RL and Kirk KL (1990) Arch. Biochem. Biophys. 276: 65–69.
5. Creveling CR and Kirk KL (1985) Biochem. Biophys. Res. Comm. 130: 1123–1131.
6. Phillips RS, Ravichandran K and Von Tersch RL (1989) Enz. Microb. Technol.
7. Phillips RS (1987) Arch. Biochem. Biophys. 256: 302–310.
8. Frant MS and Ross JW Jr. (1968) Anal. Chem. 40: 1169–1170.
9. Nagasawa T, Utagawa T, Goto J, Kim C-J, Tani Y, Kumagai H and Yamada H (1981) Eur. J. Biochem. 117: 33–40.
10. Toussaint O and Lerch K (1987) Biochem. 26: 8567–8571.
11. Sykes P (1986) In: A Guidebook to Mechanism in Organic Chemistry, 6th Edition. John Wiley and Sons, Inc., New York, p. 160.
12. Rice ME, Maghaddam B, Creveling CR and Kirk KL (1987) Anal. Chem. 59: 1534–1538.
13. Robb DA (1984) Copper Proteins and Copper Enzymes, II. CRC Press, Inc, pp. 208–240.
14. Kaufman S (1961) Biochim. Biophys. Acta 51: 619–621.
15. Husain M, Entsch B, Ballou DP, Massey V and Chapman PJ (1980) J. Biol. Chem. 255: 4189–4197.
16. Koe BK and Weissman A (1967) J. Pharmacol. Exp. Therm. 157: 565–573.

Address for correspondence: Robert S. Phillips, Departments of Chemistry and Biochemistry, School of Chemical Sciences, University of Georgia, Athens, GA 30602, U.S.A.

The presence of 4-methylproline in the mammalian system

I. Graef, B. Bartosch, Chr. Prusa, J. Häusler and G. Lubec

University of Vienna, Department of Paediatrics, Währinger Gürtel 18, A-1090 Vienna, Austria

Introduction

During tests to determine whether 4-methylproline (4-mp) is incorporated into collagen after feeding rats orally for a period of one month we found the presence of 4-mp in the non-treated group as well. Thus the first evidence of the presence of this imino acid in the mammalian system was obtained. Up to this point 4-mp had only been described in antibiotics [1] and fruit [2–4]. This observation made us examine whether 4-mp was present regularly in the mammalian system, and in which tissues and structures it could be found. Questions about whether species- or organ-specific distributions existed were raised.

Materials and Methods

Animals

Twenty white, female rats weighing 120–140 g were used in the experiments. Ten animals were given 4-methyl proline orally 30 mg/kg body weight/day for a period of 1 month. Ten animals served as controls on tap water. The animals had free access to rat cake. The animals were kept under a day/night rhythm and were sacrificed at the end of the month by decapitation.

Autopsy was performed, kidney and liver fixed and embedded for light microscopy. Kidney, liver and heart were kept frozen at –70°C until homogenization and isolation of collagens occurred.

Collagen type IV was extracted from rat kidney by the method of Dixit [5] and interstitial collagens from liver and heart by a standard method.

Human samples

Kidney and liver were obtained at autopsy within 12 h after death. In addition, human serum, red blood cells and urine were subject to analysis.

We tested human serum and urine from two women who were on an exclusive apple diet for three days.

Collagen Type IV from human placenta (Sigma No. C-7521) and collagen type I from bovine achilles tendon (Sigma No. C-8886) were also analyzed for the presence of 4-mp.

Other samples

A commercially available histone (calf thymus histone, Type II S, Sigma H 6005) was examined.

Rat cake was also analysed.

Apple specimens were homogenized and tested by the method outlined below. Organs were homogenized and used for the extraction of collagen. Proteins were hydrolyzed under the same conditions.

Standard

Racemic *cis/trans* 4-methylproline, identified by NMR and infrared spectroscopy, was the generous gift of Dr. J. Häusler, Institute of Organic Chemistry, Vienna.

Analytical procedures

SDS-PAGE of collagens extracted from treated and non-treated rats were performed in order to show molecular changes due to eventual incorporation [6].

Hydrolyzed samples were ion exchanged using a method described in a previous publication [7]. The evaporated samples were used for thin layer chromatography and/or high pressure liquid chromatography.

Thin layer chromatography was carried out by a method given elsewhere [8].

High pressure liquid chromatography was performed according to the principle of Lindblad and Diegelmann [9] with the following modifications.

Sample and standard derivatization

The evaporated protein hydrolyzate was redissolved in a minimal volume (150 µl) of 1 M potassium borate buffer pH 10.4 (Pierce). The 4-mp standard (1 mg/ml HPLC water (Rathburn)) was mixed with an aliquot of borate buffer.

Forty µl *o*-Phthaldehyde Reagent Solution (Pierce) was added to 50 µl of sample and standard and incubated for 10 min in the dark at 23°C.

Then 40 µl of NBD-Cl (7 chloro 4-nitrobenz 2 oxa 1,3,diazole) (8 mg/ml ethanol) was added. NBD-Cl was purchased from Sigma No. C-5261.

The mixture was incubated again for 10 min in the dark. After the addition of 20 µl of $HClO_4$ the samples were centrifuged on a TDX TM centrifuge (Abbott) for 3 min and the supernatant was taken for HPLC analysis.

Instrumentation

The samples were analyzed using a Shimadzu LC-6A Liquid chromatograph, equipped with a Shimadzu RF-535 fluorescence HPLC monitor.

The column used was an RP 18 Partisil 35 U column.

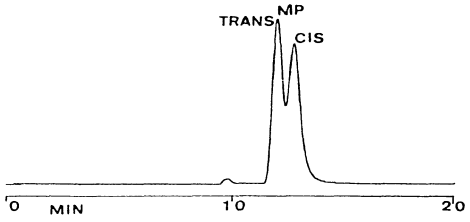

Fig. 1a. The 4-mp standard at a flow rate of 0.6 ml/min.

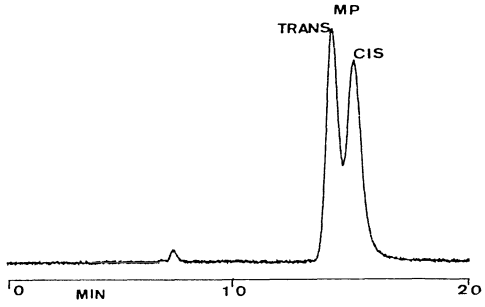

Fig. 1b. The 4-mp standard at a flow rate of 0.5 ml/min.

Chromatographic conditions

The analysis was performed with a flow rate of 0.6 ml/min and/or 0.5 ml/min. The elution buffer used consisted of: 650 ml HPLC water, 10 ml triethylamine (Pierce) – pH was adjusted to 6.0 with acetic acid – and 350 ml methanol.

To confirm whether the peak found in the samples was 4-methylproline the samples were spiked with 4-methylproline standard.

In order to control the methods applied bands obtained on thin layer chromatography were scratched from the plates, suspended in methanol, incubated for half an hour at room temperature, spun down, evaporated and the pellet redissolved in borate buffer and applied onto HPLC under the conditions described above.

The peak assigned to methylproline was collected (depending on the flow; 0.6 ml/min: 11–13 and/or 0.5 ml/min: 14–16) (Fig. 1a, 1b) applied on HPTLC plates and two dimensional thin layer chromatography employed. The solvent mixture for the first dimension consisted of: 40 ml of acetone, 25 ml of methanol, 120 ml of chloroform adjusted to a volume of 200 ml with TEA and for the second dimension of: 80 ml acetone, 80 ml toluol, 30 ml methanol and 10 ml TEA (Fig. 2).

Results

Rat samples

Autopsy and light microscopy

No pathological macroscopical or microscopical findings were obtained on autopsy.

Thin layer chromatography

The TLC was done on kidney collagen, liver collagen and heart collagen hydrolyzates from rats who had been fed with 4-mp and from the control group. The presence of 4 mp in kidney collagen (Fig. 3a) and heart collagen in both groups was demonstrated. In liver collagen hydrolyzates 4-mp could not be detected paralleling our findings in the human samples.

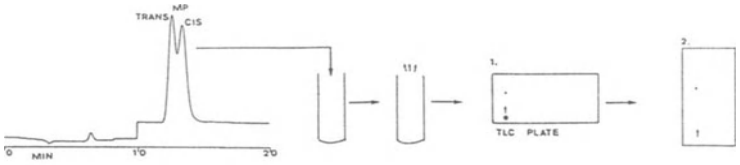

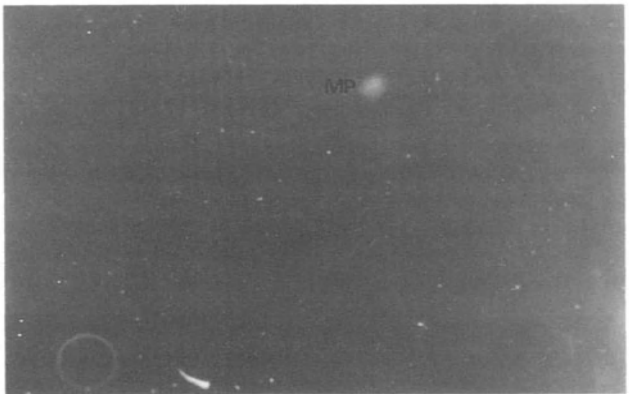

Fig. 2. The mp peak obtained on HPLC was collected, evaporated and redissolved for application on two dimensional thin layer chromatography and photo of the two dimensional TLC plate of the 4-mp standard.

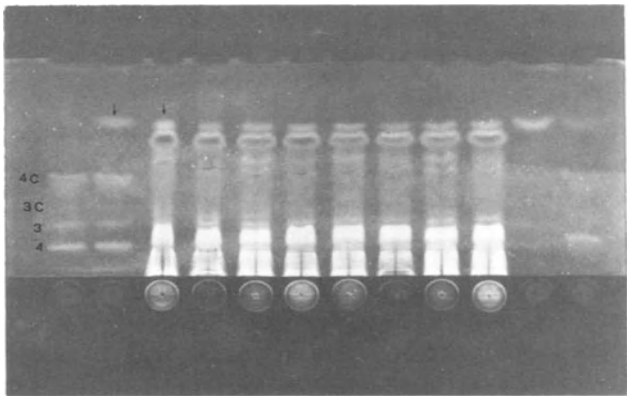

Fig. 3a. Thin layer chromatographical demonstration of 4-mp in kidney collagen hydrolyzates (arrow indicates the position of 4-mp) 4 = 4 *trans*-, 3 = 3 *trans*-, 3c = 3 *cis*, 4c = 4 *cis*-hydroxyproline; c= control, mpf = methylproline fed rats.

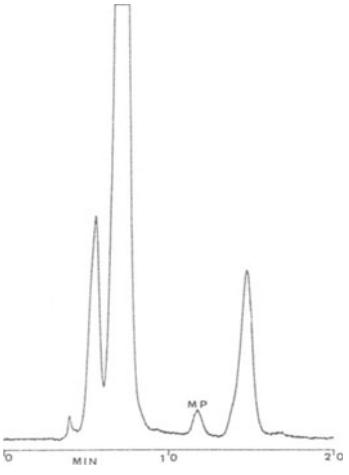

Fig. 3b. The HPLC pattern of hydrolyzed kidney collagen taken from the band on TLC.

HPLC

Kidney collagen hydrolyzates and the bands from the TLC, which were suspected to contain 4-mp, were analyzed on HPLC. 4-mp was detected in kidney collagen hydrolyzates (Fig. 3b, c, d) and in heart collagen hydrolyzates (Fig. 4a–c) which were scratched from the TLC plates and in the samples of kidney collagen hydrolyzates applied directly onto HPLC (Fig. 5 a, b).

No 4-mp was detectable in liver collagen hydrolyzates from TLC. In order to verify that the peaks found were evoked by 4-mp, all samples were spiked with 4-mp standard confirming cochromatography of the standard with mp in the specimen.

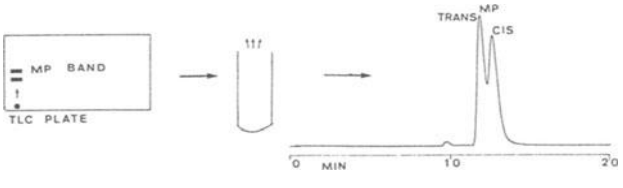

Fig. 3c. The mp standard taken from the TLC plate and applied onto HPLC.

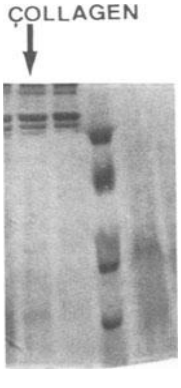

Fig. 3d. SDS-PAGE showing the purity of collagen type IV isolation from kidney

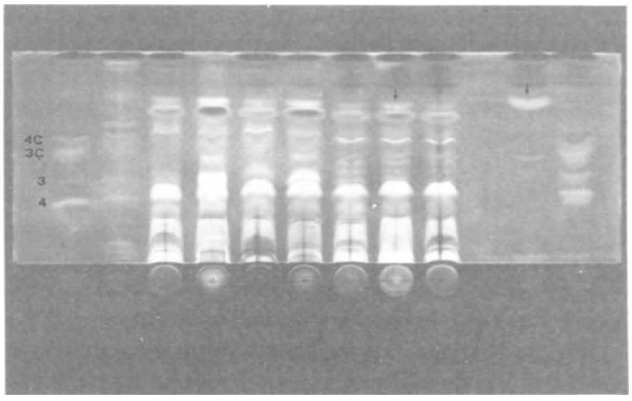

Fig. 4a. TLC pattern of heart collagen hydrolyzates. 4 = 4 *trans-*, 3 = 3 *trans-*, 4c = 4 *cis-*, 3c = 3 *cis*-hydroxyproline, c = control, mpf = mp fed rats, arrow indicates 4-mp.

Fractions from HPLC suggested to contain mp were collected and applied on two dimensional TLC showing the identity with pure standard of mp (Fig. 5c).

Human samples

TLC

There was no detectable urinary excretion of 4-mp before or after exclusive apple diet, whereas 4-mp was demonstrated in serum after the apple diet.

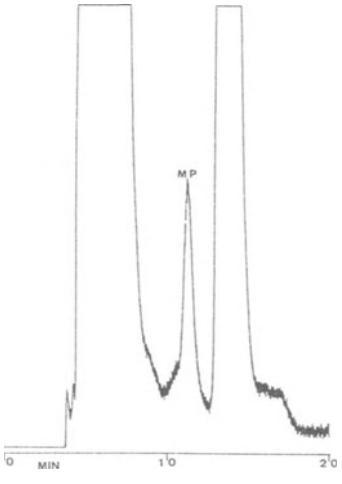

Fig. 4b. HPLC pattern of the band obtained from TLC – original chromatogram.

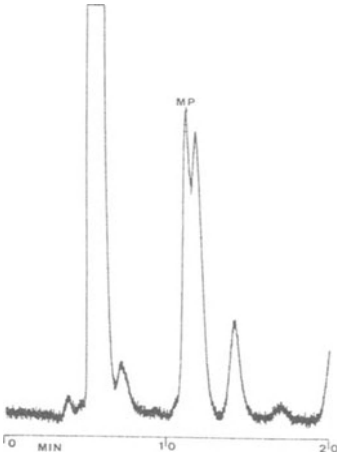

Fig. 4c. The sample of Fig. 4b spiked with 4-mp.

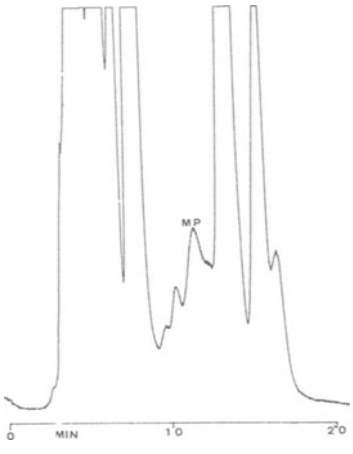

Fig. 5a. HPLC pattern of kidney collagen hydrolyzate, unspiked sample.

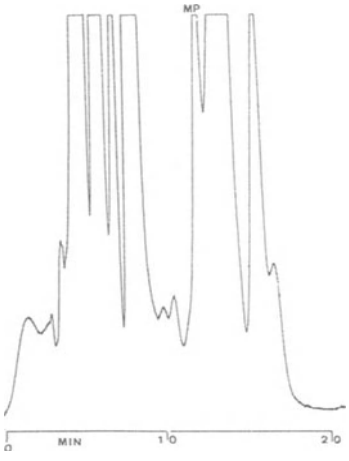

Fig. 5b. HPLC pattern of kidney collagen hydrolyzate, spiked with 4-mp.

HPLC

Kidney collagen hydrolyzates (Fig. 6a,b) and collagen type IV hydrolyzates from human placenta (Fig. 6c,d) contained 4-mp. In liver collagen hydrolyzates and in red blood cells (Fig. 6e,f) no 4-mp was detectable.

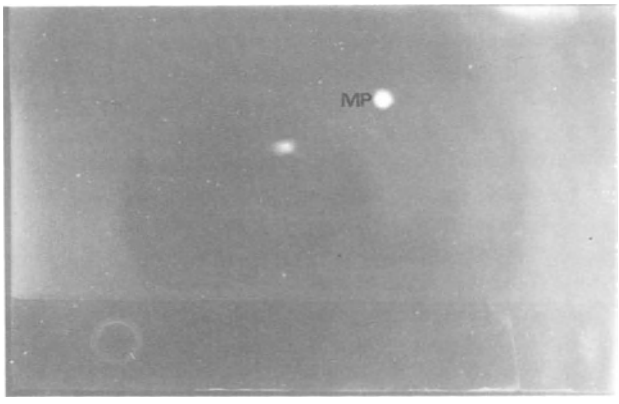

Fig. 5c. The postcolumn collected fraction on two dimensional TLC.

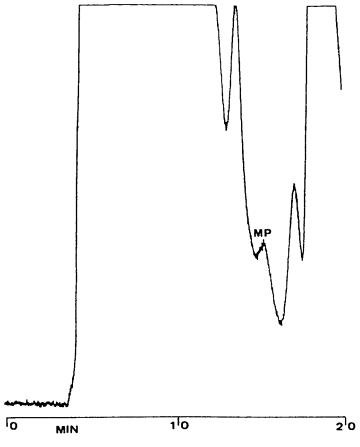

Fig. 6a. Kidney collagen hydrolyzate: HPLC pattern of the unspiked human sample.

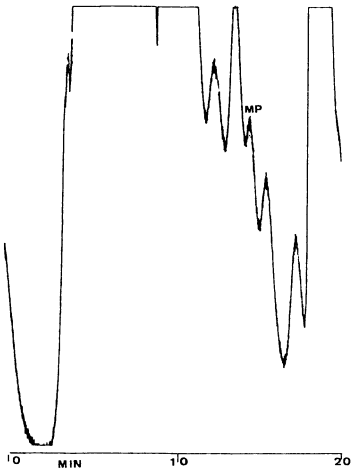

Fig. 6b. Kidney collagen hydrolyzate: HPLC pattern of the spiked human sample.

Other samples

In the hydrolyzates of rat cake 4-mp was detected on HPLC. Apples, which were examined on TLC, contained as already known 4-mp.

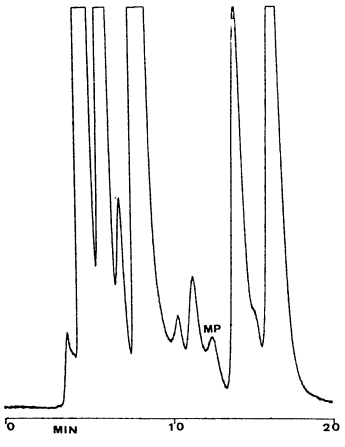

Fig. 6c. Collagen type IV from placenta, unspiked human sample.

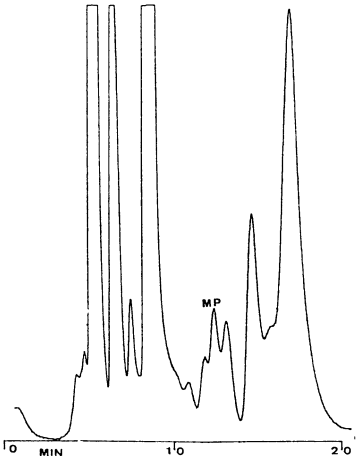

Fig. 6d. Collagen type IV from placenta, spiked human sample.

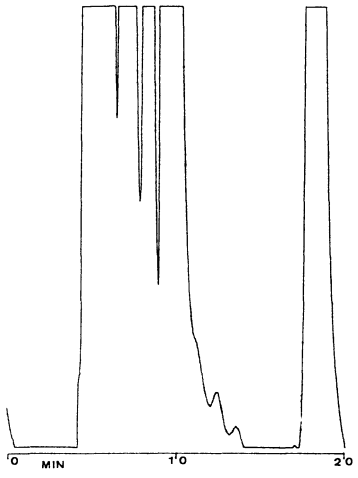

Fig. 6e. Red blood cells hydrolyzed, unspiked human sample.

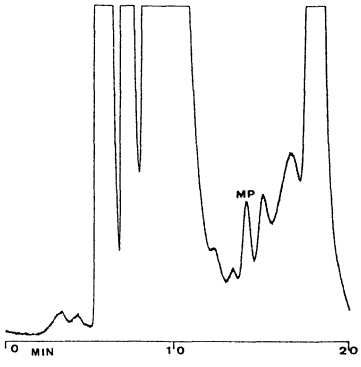

Fig. 6f. Red blood cells hydrolyzed, spiked human sample.

In collagen type I hydrolyzates, analysed by HPLC, no 4 mp was detectable (Fig. 7a,b). Histone-hydrolyzates examined by HPLC did not demonstrate 4-mp. 4-mp standard scratched from TLC plates showed on HPLC 2 peaks corresponding to 4 *cis* and *trans* mp at the same position as the standard which was applied directly onto HPLC.

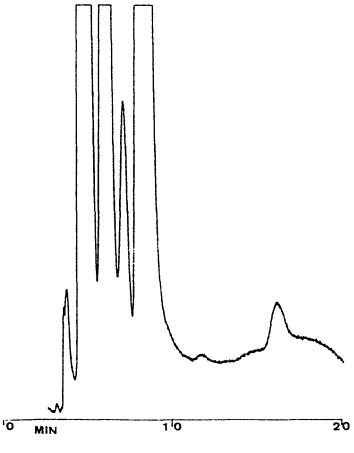

Fig. 7a. HPLC pattern of collagen type I, the unspiked sample does not show the presence of 4-mp.

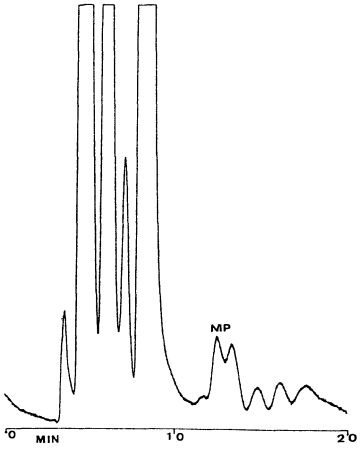

Fig. 7b. HPLC pattern of collagen type I, spiked sample.

Discussion

As shown in the results, the presence of 4-methylproline could be documented in the mammalian system. This observation was never reported before. The question, however, whether this proline analogue in mammals is derived from alimentation or is synthesized by the mammalian organism itself cannot be answered fully: though 4-mp was described for some fruits only it was present e.g. in food of our experimental animals (rat cake). This theoretically could have led to the ingestion and subsequent incorporation into mammalian proteins. This explanation for the presence of 4-mp in proteins such as collagen is highly improbable from a practical point of view as high proline analogue amounts are necessary to compete with the naturally occurring substrate of the prollyl t-RNA, proline and there is no doubt that proline is more abundant than its methylated analogue in food sources. On the other hand volunteers failed to show the presence of 4-mp in urine and serum before the apple diet rich in 4-mp but showed detectable concentrations in serum afterwards.

Human kidney collagen as well as placental type IV collagen contained 4-mp in contrast to human liver collagen and human red blood cells. If the theory is valid that 4-mp is derived from alimentation one would suggest that all forms of collagen contain this proline analogue. It seems more likely that a tissue specific methylation process was involved. This tissue specific enzymatic reaction is well known in mammalian biology: 3-methylhistidine is present in the skeletal muscle of adult animals but not in cardiac muscles indicating a tissue specific methyltransferase activity [10].

In the rat system kidney and heart collagen were shown to contain 4-mp, whereas 4-mp could not be detected in liver collagen which is in congruence with human data.

There was no significant difference between the 4-mp content of collagen of controls versus animals fed with 4-mp for a period of 1 month. This seems to contradict the suggestion that 4-mp in collagen is nutrition derived.

Organ hydrolyzates and free 4-mp in tissues and biological fluids were not determined as this would have given no additional information: as outlined above, we found 4-mp in serum after the apple mono diet.

Provided the hypothesis of enzymatic methylation of proline by the mammalian organism is correct we do not find C-methylation for amino acids as acceptors in literature. C-methyltransferases have been reported for nucleic acids exclusively [11]. N-methyltransferases, however, are abundant in the organism and described for N-methylation of amino acids [12–14]. Also proline is subject to N-methylation in histones under certain circumstances [15].

Another possibility for the origin of methylproline in the mammalian system is the nonenzymatic way of cyclization of an aliphatic amino acid. A pathway regularly occurring during proline synthesis.

The suggestion that nonenzymatic methylation of proline was caused during isolation or separation of amino acids can be ruled out as the specimens under examination were treated by the same procedure and collagen type I, histones etc. failed to show methylation of proline. Nonenzymatic methylation can be seen after treatment with methylating organic solvents under certain conditions.

The biological significance of methylation lies in the described effects as protection against proteolytic enzymes [15]. Proline methylation could be influencing secretion [16–18], hydroxylation [16,19–21], helical conformation [17,20] regulation of proline [22] and collagen [20,21] biosynthesis.

Summing up we have obtained evidence, using appropriate methodologies combining thin layer chromatography (two and one dimensional form) and high pressure chromatography that 4-mp is present in mammalian connective tissue protein. We suggest that an enzymatic reaction converts proline to 4-mp either methylating free proline or intrachain proline in analogy to other posttranslational modifications such as hydroxylation and glycosylation.

In our laboratory we are presently looking for prolyl methyl transferase activity in human placental and kidney samples in order to test our first hypothesis on the origin of methylproline.

References

1. Arroyo J, Hall MJ, Hassall C and Yamasaki K (1976) J. Chem. Soc. Comm. 21: 845.
2. Hulme AC and Arthington W (1952) Nature 170: 659.
3. Hulme AC and Arthington W (1954) Nature 173: 588.
4. Dalby J, Kenner GW and Sheppard RC (1962) In: Peptides. Academic press, p. 4387.
5. Dixit SN (1979) FEBS Letters 106: 379.
6. Lämmli UK (1970) Nature 227: 680.
7. Lubec G, Weiis M, Häusler J, Vycudelik W and Herkner K (1987) Labor aktuell 4: 16.
8. Bellon G, Berg R, Chastang F, Malgras L and Borel JP (1984) Anal. Biochem. 137: 151.
9. Lindblad WJ and Diegelmann RF (1984) Anal. Biochem. 138: 390.
10. Huszar G (1984) Meth. Enzym. 106: 287.
11. Dixon M and Webb EC (1979) Enzymes. Longman, London, 762.
12. Heady JE and Kerr SJ (1973) J. Biol. Chem. 248: 69.
13. Paik WK and Di Maria P (1984) Meth. Enzym. 106: 274.
14. Paik WK (1984) Meth. Enzym. 106: 265.
15. Desrosiers R and Tanguay RM (1988) J. Biol. Chem. 263: 4686.
16. Rosenbloom J and Prockop DJ (1970) J. Biol. Chem. 245: 3361.
17. Uitto J, Dehm P and Prockop DJ (1970) BBA 278: 661.
18. Rosenbloom J and Prockop DJ (1971) J. Biol. Chem. 246: 1549.
19. Hutton JJ, Marylin JR, Witkop B, Kurtz J, Berger A and Udenfried S (1968) Arch. Biochem. Biophys. 125: 779.
20. Uitto J and Prockop DJ (1974) BBA 336: 734.
21. Takhuchi T and Prockop DJ (1969) BBA 175: 142.
22. Tristram H and Thurston CF (1966) Nature 212: 74.

Infrared spectroscopical studies on the non-enzymatic glycosylation of arginine and collagen

K. Kranewitter and G. Lubec

University of Vienna, Department of Paediatrics, Währinger Gürtel 18, A-1090 Vienna, Austria

Abstract

Non-enzymatic glycosylation is a post-translational process that is increased in the diabetic state. In order to determine whether the non-enzymatic reaction can be followed by multiple reflection infrared spectroscopy, we performed studies on the non-enzymatic glycosylation of arginine and collagen. Spectra clearly showed that a reaction between the amino acid and glucose and the collagen and glucose occurred. The major finding was the disappearance of the 1722 cm^{-1} peak derived from the carbonyl function of glucose after reaction with arginine, indicating that the carbonyl grouping had been blocked by the reaction, a finding in the reduction of carbonyl functions agreement with Schiff base formation. This interpretation is confirmed by changes of the 1219 cm^{-1} band. When glucose binds to collagen, the presence of the glucose derived 1026 cm^{-1} band is evident in the spectrum of the glycosylated molecule. This simple non-destructive method provides a useful tool with which to follow non-enzymatic glycosylation.

Introduction

Non-enzymatic glucosylation of proteins may occur as a post-translational modification process. Either the *N*-terminal amino acid residue or the Σ-amino groups of lysine residues are initially involved in Schiff's base formation; the resulting ketoamine eventually undergoes cyclization.

This group of reactions is called the early stage non-enzymatic glycosylation and is shown in Fig. 1. This reaction underlies the so-called 'browning', well known to the food technologist, when protein or amino acids and sugars react together. In human pathophysiology, i.e. in the diabetic state, non-enzymatic glycosylation seems to be the cause of the diabetic long-term complications. Collagens, if non-enzymatically glycosylated become more rigid and less soluble, which in turn results in a net positive synthesis and accumulation. Infrared spectra of collagens have been published [1] but no studies on non-enzymatic glycosylation of collagen are reported. This paper then provides process using the technique of multiple internal reflection infrared spectroscopy data on the non-enzymatic glycosylation of arginine and collagen.

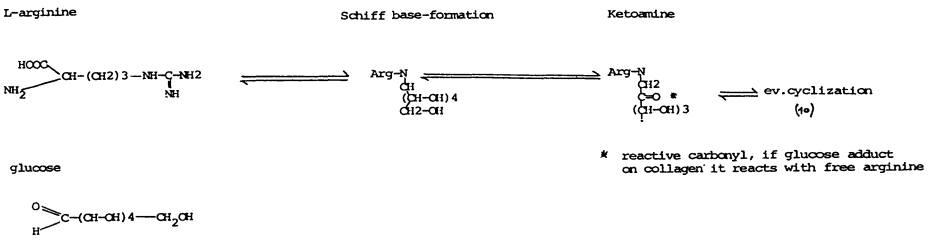

Fig. 1. Reaction mechanism of non-enzymatic glycosylation, early stage [8].

Materials and Methods

L-arginine (Merck, FRG, 1542) and collagen (lyophilized, achilles tendon, Merck, FRG, 24014) type I were used in the experiments.

The experiments were performed in the presence of NaN_3 in order to prevent bacterial or fungal growth.

As a model for non-enzymatic glycosylation, L-arginine and glucose were incubated at 23°C for different times; 'zero', i.e. immediately after mixing the solution was frozen in liquid nitrogen and 1,2,4,8,30 days. The buffer used in all the experiments was a 0.01 M phosphate buffer pH 7.8.

Collagen was incubated with glucose alone and together with glucose and arginine for times given above.

At the end of each incubation the mixtures were centrifuged at 3000 ×g for 10 min in order to remove non-bound compounds: Collagen itself is highly insoluble at this pH and molarity. Washing procedures were repeated 3 times with distilled water. Immediately at the end of the washing procedure samples were lyophilized.

Infrared spectroscopy

The technique described in a previous publication [2,3] was applied: The reflection principle of the multiple internal reflection technique is given in Fig. 2.

The dried samples (lyophilized) were applied onto a 45° KRS (T1J-T1Br) crystal on a Nicolet 60 SX spectrophotometer and spectra were taken scanning from 400–4000 cm^{-1} at 24°C in an H_2O and CO_2 free atmosphere.

Results

Spectra of the native compounds are given in the Fig. 3a,b,c.

Spectra of the glucose-arginine reaction mixture at times 'zero' and after one month are given in Fig. 4 a,b.

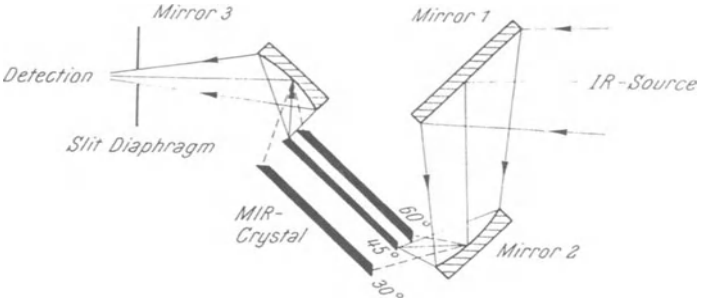

Fig. 2. Reflexion principle of the ATR-technique M.I.R. = Multiple internal reflexion.

The spectrum of collagen and glucose reaction at times 'zero' and one month is given in Fig. 5 a,b.

The spectrum of the collagen-glucose-arginine reaction at times 'zero' and after one month is listed in Fig. 6 a,b.

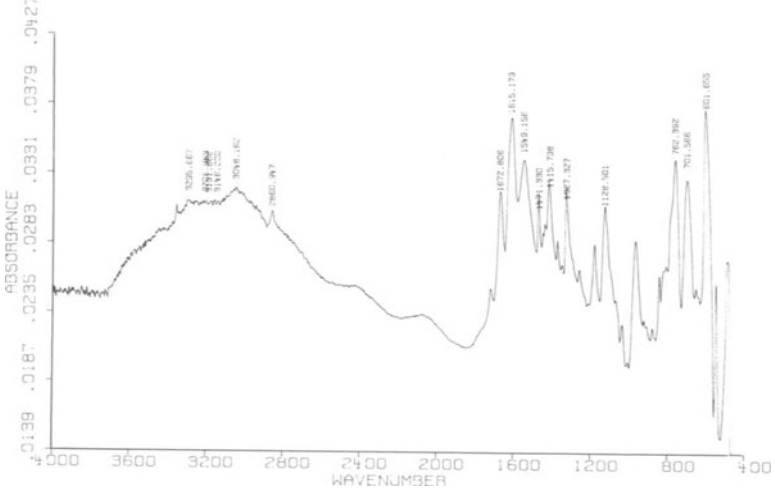

Fig. 3a. The spectrum of arginine (solid phase).

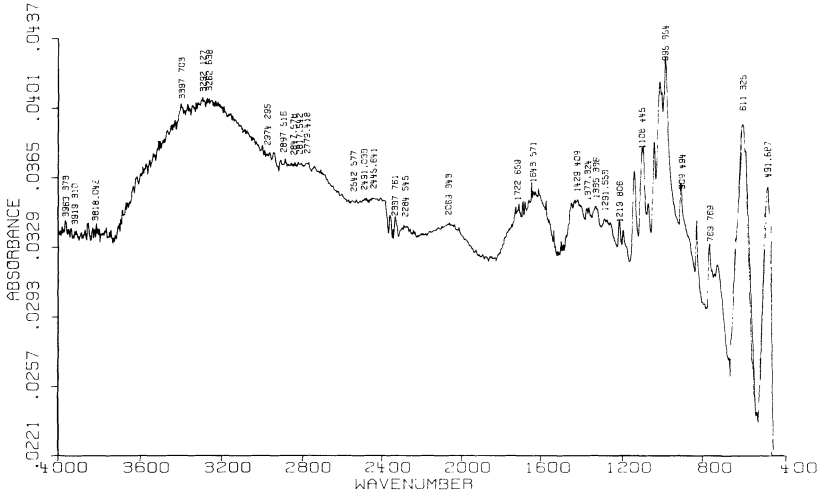

Fig. 3b. The spectrum of solid phase glucose.

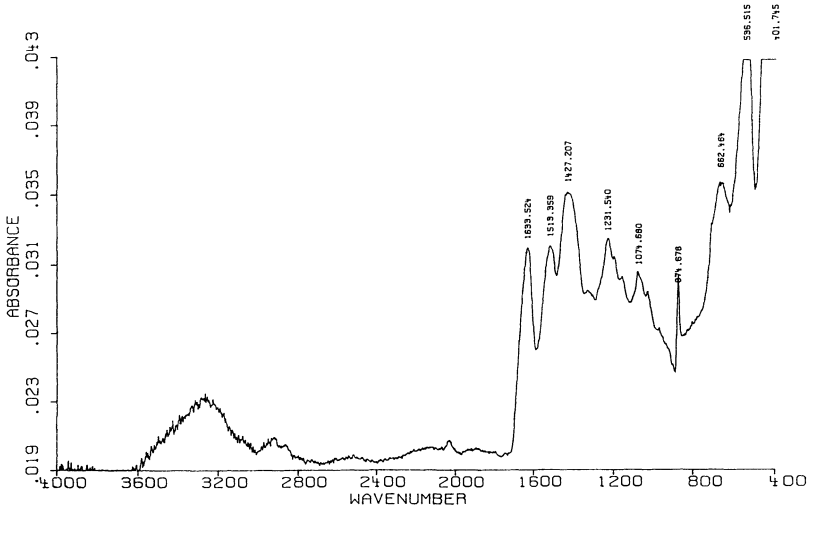

Fig. 3c. The spectrum of collagen type I in the solid state.

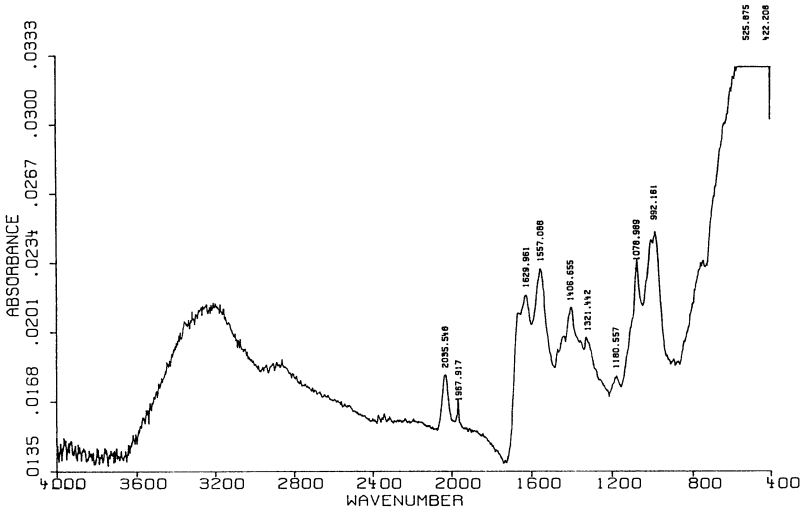

Fig. 4a. Spectrum of the arginine-glucose mixture at time 'zero'.

Discussion

One could expect that non-enzymatic glycosylation could lead to IR-spectroscopical changes of the glycosylated molecules. These postulated changes could affect structural and radical changes.

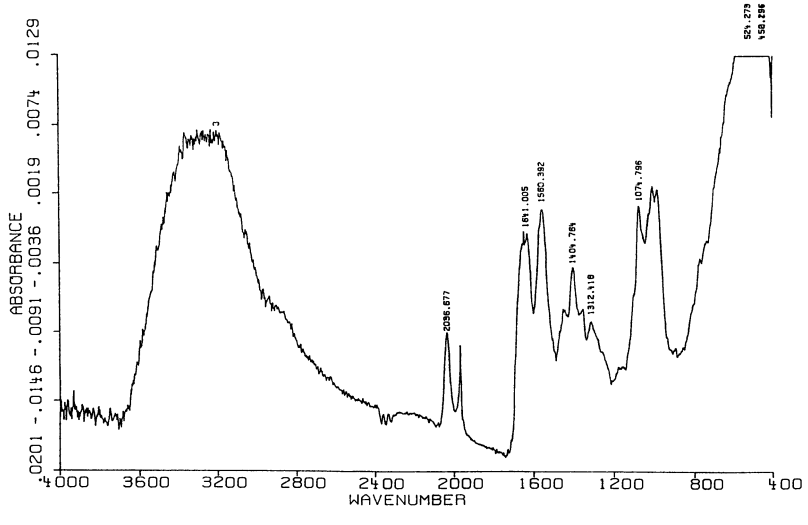

Fig. 4b. The spectrum of the arginine-glucose mixture after 1 month of incubation.

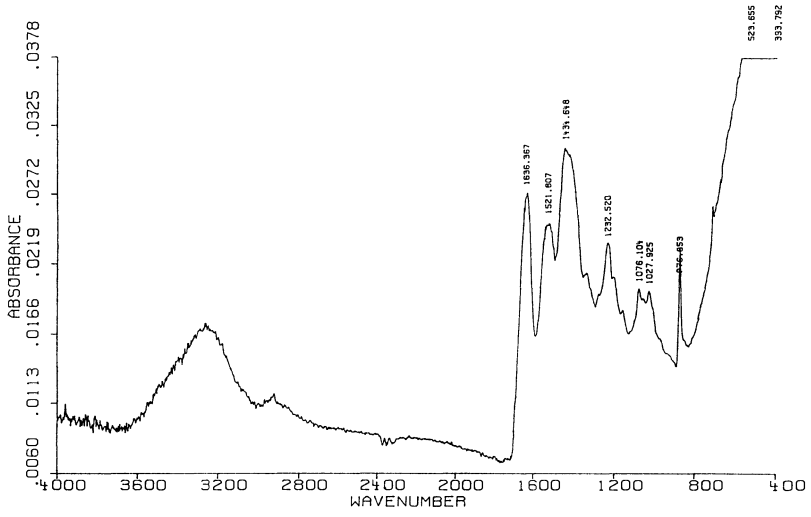

Fig. 5a. The spectrum of collagen and glucose incubation at the time 'zero'.

In the case of the reaction of L-arginine with glucose carbonyl residues and amino groups could be involved primarily. The same could be postulated for glycated collagen but in addition the collageneous structures i.e. conformation might have been altered.

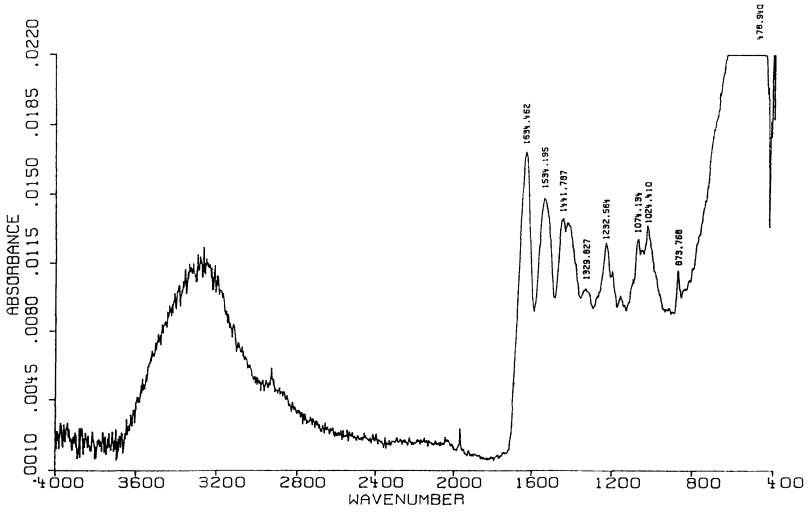

Fig. 5b. The spectrum of the collagen-glucose mixture after 1 month.

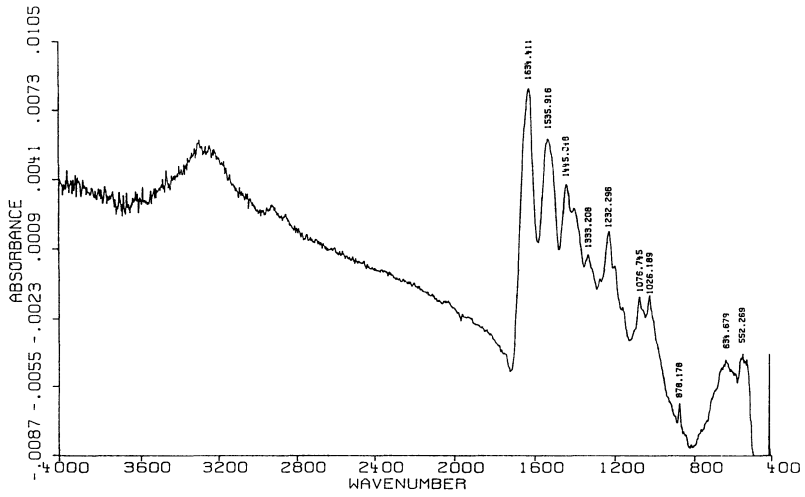

Fig. 6a. The spectrum of the collagen, glucose, arginine incubation at time 'zero'.

Based upon the primary reaction partners, Arg and Glu (spectra in Fig. 3a,b), the reaction immediately after the mixture (mixing Arg and Glu, liquid nitrogen freezing, lyophilization) was measured in the solid state on IR. As shown in the results spectra presented that a reaction had taken place: No additional peaks could be detected but the amide I band showed a different pattern and the amide II band became the dominant peak. This could be due to the amino group-carbonyl reaction.

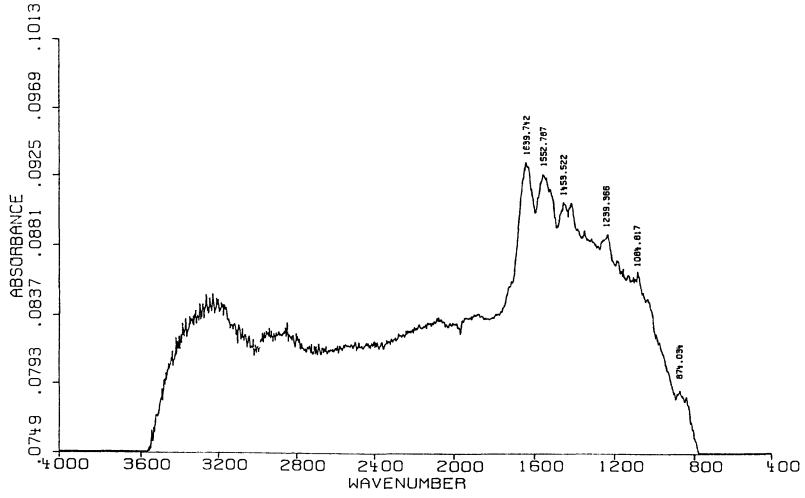

Fig. 6b. The spectrum of glucose, collagen, arginine after 1 month incubation.

A major finding was the disappearance of the 1722 cm peak derived from the carbonyl functions of glucose after the reaction with Arg. As the 1722 band can clearly be assigned to the carbonyl function of glucose, the disappearance shows the blockade of this residue [4,5]. This wave number can be found in other aldehyde/carbonyl compounds as well confirming the assignment [6]. The reduction of carbonyl functions which is in congruence with formal reactions of Schiff base formation is shown by the disappearance of the 1219 band after the Glu-Arg reaction. This band can be assigned to carbonyl functions in the solid state (pp. 1050–1300, [7]). According to the thermodynamics and kinetics of the Schiff base formation the early changes detected on IR are realistic [8–10], as the Schiff base formation is a rapid process. The intermediates (day 2 and following) did not show other useful new information. The spectrum obtained after one month of Glu-Arg incubation (Fig. 4b) in comparison to the spectrum at time 'zero' only showed the reduction of the 1180 band (not a carbonyl function per se) and the inverse switch of the 995–1027) vibration. This however, cannot be interpreted as reflection of the later stage non-enzymatic glycosylation reactions as ketoamine formation or even cyclization [10].

Collagen and glucose reacted in the sense of the model Arg-Glu: the glucose derived 1027 cm^{-1} band was found to be almost as high as the 1074 band (Fig. 5a after short time incubation (time 'zero').

No conformational changes were observed after the reaction with glucose which would have been seen in the amide I band [1].

After one month of collagen-Glu incubation the 1024 band becomes even more prominent and the CH2-CH-vibrations reduced (wave number 1441 [11]) as documented in Fig. 5b.

Incubation of collagen-Glu-Arg at time 'zero' in comparison to time 'zero' incubation of glucose-coll did not show differences on IR. The glucose must have attached to both types of molecules. The following intermediates of incubation however showed clearly that arginine must have had reacted with glucose free or bound to collagen as the 1027 glucose derived wave number was no more prominent in the one month coll-Glu-Arg spectrum (Fig. 6b, and for the probable reaction mechanism Fig. 1).

Summing up we can state that we can follow the glucose IR-multiple internal reflection technique, a non-invasive, non-destructive and non-sophisticated method which can easily be performed.

References

1. Lazarev YA, Grishkovsky BA and Khromova TBi (1985) Biopolymers 24: 1449–1478.
2. Lubec G and Nauer G (1984) Lancet I: 804.
3. Krimm S (1962) J. Mol. Biol. 4: 528–539.
4. Potts WJ (1963) Chemical and Infrared Spectroscopy Vol. I. N.Y.
5. An Index of Published Infrared Spectra Vol. I, II. (1960) HMSO, London.
6. Lubec G, Nauer G, Pollak A, Coradello H and Ratzenhofer E (1982) Z. Hautkr. 58: 637–645.

7. Williams DH and Fleming I (1966) Spectroscopic Methods in Organic Chemistry. McGraw-Hill Publ., Maidenhead.
8. Bunn HF, Haney DN, Kamin S, Gabbay KH and Gallpo PM (1976) J. Clin. INV. 57: 1652–1659.
9. Flückiger R (1978) Inaugural dissertation, Basel.
10. Flückiger R and Winterhalter KH (1976) FEBS Lett. 71: 356–360.
11. Lubec G and Nauer G (1988) Päd. Pädol. 23: 101–108.

Biosynthesis of epidermal growth factor having nonprotein amino acid residues by *Escherichia coli**

Hiroshi Koide[a], Mitsuko Oishi[a], Takanori Oka[b], Tetsuo Miyake[b], Toru Fuwa[b], Shigeyuki Yokoyama[a] and Tatsuo Miyazawa[c]

[a]*Department of Biophysics and Biochemistry, Faculty of Science, the University of Tokyo, Bunkyo-ku, Tokyo 113, Japan*

[b]*Central Research Laboratories, Wakunaga Pharmaceutical Co., Ltd., Koda-cho, Takata-Gun, Hiroshima 729-64, Japan*

[c]*Faculty of Engineering, Yokohama National University, Hodogaya-ku, Yokohama 240, Japan*

Abstract

For development of a novel method in protein engineering, we studied the use of nonprotein amino acids, namely, amino acids other than the 20 protein-constituting amino acids. We succeeded in *in vivo* production of human epidermal growth factor (hEGF) substituted with norleucine, an analog of methionine. In the present study we attempted production of hEGF substituted with *p*-fluorophenylalanine residue (*p*FPhe), although hEGF does not have Phe residues. We prepared two genes of mutant hEGF; Tyr^{22} or Tyr^{29} was replaced by Phe by oligonucleotide-directed mutagenesis. To enhance incorporation of *p*-fluorophenylalanine, these mutant hEGF genes were introduced into an *Escherichia coli* strain auxotrophic for phenylalanine. The optimum concentration of *p*-fluorophenylalanine for production of *p*FPhe-substituted hEGFs was 50 μg/ml. By gel filtration chromatography, and reverse-phase and ion-exchange high performance liquid chromatography, we succeeded in purification of *p*FPhe-substituted hEGFs. Fluorine substitution of the aromatic ring of each Phe residue probably induces a conformational change of hEGF.

A variety of analogs of protein-constituting amino acids have been used for studies on protein synthesis, post-translational protein modification, and conformation – function correlations of peptides. We attempted production of proteins substituted with nonprotein amino acids (alloproteins) [1] and further development of novel protein engineering taking advantage of unnatural side chains of nonprotein amino acids. We succeeded in the preparation of human epidermal growth factor (hEGF[1]) substituted with norleucine (Nle) [1]. Preparation of Nle-substituted proteins has also been reported by other groups [2–4].

* This work was supported in part by a Bioscience Grant for International Joint Research Project from the NEDO, Japan and a Grant-in-Aid 60060004 for Distinguished Research from the Ministry of Education, Science and Culture of Japan.

[1] The abbreviations used are: EGF, epidermal growth factor; hEGF, human EGF; HPLC, high performance liquid chromatography; Nle, norleucine; [Nle^{21}]hEGF, hEGF having Nle residue at position 21; *p*FPhe, *p*-fluorophenylalanine; [*p*FPhe^{22}]hEGF, hEGF having *p*FPhe residue at position 22; [*p*FPhe^{29}]hEGF, hEGF having *p*FPhe residue at position 29; [Phe^{22}]hEGF, hEGF having Phe residue at position 22; [Phe^{29}]hEGF, hEGF having Phe residue at position 29.

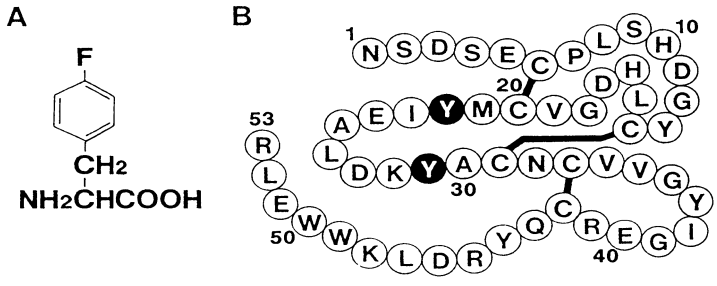

Fig. 1. (A) Structure of *p*-fluorophenylalanine and (B) amino acid sequence of hEGF.

p-Fluorophenylalanine (Fig. 1A) is known to be highly cytotoxic [5]. In the present study, however, we attempted incorporation of *p*FPhe residue in place of Tyr residues in hEGF (Fig. 1B). By the basic strategy worked out previously [1], we succeeded in preparation of *p*FPhe-substituted hEGF.

Experimental procedures

Materials

Escherichia coli strain KA197 (λ^-, *pheA97, relA1, spoT1, thi-1*) was given by Dr. B.J. Bachmann of Yale University. *p*-Fluoro-DL-phenylalanine was purchased from Sigma.

Synthesis and purification of oligonucleotides

Oligonucleotides for site-specific mutagenesis were synthesized using an automatic DNA synthesizer NS-1 (Shimadzu, Kyoto, Japan) and purified according to the method described [6]. Reagents for DNA synthesis were purchased from Shimadzu.

Construction of mutant hEGF genes

The gene of hEGF was isolated by treatment of plasmid pTA1522 [1] with *Eco*RI and *Sal*I, and subcloned into the multicloning site of M13mp19 DNA. By mutagenesis using a Muta-Gene™ kit (Bio Rad) with the synthetic oligonucleotides, two mutant hEGF genes were obtained; the second position of each of two Tyr codons (TAT for Tyr^{22} and TAC for Tyr^{29}) was converted to T. The mutations were confirmed by sequencing the genes on M13mp19 DNA. The *Eco*RI-*Sal*I fragment of each mutant clone was substituted for the corresponding region of pTA1522. Thus we obtained plasmids pTA152-22F and pTA152-29F carrying the genes

coding for two mutant hEGFs ([Phe^{22}]hEGF and [Phe^{29}]hEGF) that have Phe in positions 22 and 29, respectively.

Preparation of [Phe^{22}]hEGF and [Phe^{29}]hEGF

E. coli strain KA197 harboring plasmid pTA152-22F or pTA152-29F was cultured overnight in TG+20 medium [7] containing phenylalanine (50 μg/ml) at 37°C. The cells were transferred to low-phosphate medium TG+1 [7] containing phenylalanine (50 μg/ml), and harvested after incubation at 37°C for 6 h. The protein product [Phe^{22}]hEGF or [Phe^{29}]hEGF was recovered by osmotic shock procedure [1], and purified by gel filtration chromatography on a column of Sephadex G-50 (Pharmacia) and high performance liquid chromatography (HPLC) using an LC-4A system (Shimadzu) equipped with a reverse-phase ODS-120T column (0.46 × 15 cm) (Tosoh, Tokyo) and an LC-6A system (Shimadzu) equipped with a DEAE-5PW column (0.75 × 7.5 cm) (Tosoh) as described [1].

Preparation of pFPhe-substituted hEGFs

*p*FPhe-substituted hEGFs ([*p*FPhe^{22}]hEGF and [*p*FPhe^{29}]hEGF) having *p*FPhe residue in positions 22 and 29, respectively, were prepared by the same procedures as in the cases of [Phe^{22}]hEGF and [Phe^{29}]hEGF except that TG+1 medium contained *p*-fluorophenylalanine instead of phenylalanine. Final purification with ion-exchange HPLC was repeated twice.

Results and Discussion

Site-directed mutagenesis of hEGF gene

The amino acid sequence of hEGF [8] does not include Phe residues (Fig. 1B). Thus, for incorporating *p*FPhe residue at specific position in hEGF, it was necessary to introduce a Phe codon to the hEGF gene. Among the protein-constituting amino acid residues, Tyr residues were chosen as the sites for conversion to Phe residues because the side chain structure of Tyr is similar to that of Phe. hEGF has five Tyr residues and two of them, Tyr^{22} and Tyr^{29}, lie in the loop Cys^{20}-Cys^{31} (Fig. 1B) that has been found to be important for binding with the receptor [9]. Accordingly, each of these two Tyr residues was converted to Phe residue by oligonucleotide-directed mutagenesis.

Problems in preparation of alloprotein

When we attempt preparation of proteins substituted with nonprotein amino acids (alloproteins), we have to overcome difficulties, firstly the cytotoxicity of nonprotein amino acids and secondly the instability of proteins having nonprotein

amino acid residues in the cell. When cells are cultured in the medium containing nonprotein amino acids, those amino acids are incorporated in the target protein hEGF and also in proteins of the host cell. This disturbs functions of the proteins of host cell and/or induces heat-shock like responses, which stop cell growth. However, such cytotoxicity of nonprotein amino acids may be suppressed by reducing synthesis of the proteins of host cell while allowing biosynthesis of alloproteins [1]. Secondly, proteins having nonprotein amino acid residues are degraded much faster than normal cell proteins [10]. However, proteins are more stable in the periplasm than in the cytoplasm [11]. Therefore secretion to periplasm may be useful for avoiding degradation of alloproteins. From these two points of view, in the present study, we again chose the system of *E. coli phoA* promoter and signal peptide [1].

Yield of p*FPhe-substituted hEGF*

Incorporation of *p*-fluorophenylalanine into proteins is known to be in competition with phenylalanine. Thus in order to raise the efficiency of incorporation of *p*-fluorophenylalanine, it is necessary to reduce the concentration of phenylalanine in the host cell. In the present study, we used a phenylalanine auxotroph *E. coli* strain KA197 as the host cell and added *p*-fluorophenylalanine in place of phenylalanine to TG+1 medium. On one hand, a higher concentration of *p*-fluorophenylalanine in the medium will be favorable to efficient incorporation of this nonprotein amino acid. On the other hand, excessive incorporation of this cytotoxic amino acid in proteins of the host cell should depress biosynthesis of *p*FPhe-substituted hEGF. Thus, yield of this alloprotein will reach a maximum at an optimum concentration of *p*-fluorophenylalanine.

*Preparation of [*p*FPhe^{22}]hEGF*

E. coli strain KA197 harboring plasmid pTA152-22F was cultured in TG+1 medium containing *p*-fluorophenylalanine at a concentration range of 10–200 μg/ml and the protein product was recovered from the periplasm. In the steps of gel filtration chromatography and reverse-phase HPLC, [*p*FPhe^{22}]hEGF and [Phe^{22}]hEGF were eluted at nearly the same retention time. However, in the step of ion-exchange HPLC, three peaks were observed (Fig. 2). The second peak (peak b) was found to be due to [Phe^{22}]hEGF from the comparison with the elution profile of the preparation of [Phe^{22}]hEGF (data not shown). The height ratio of peak a to peak b was increased as the concentration of *p*-fluorophenylalanine in the medium was raised (Fig. 2A-D). This indicates that peak a is due to [*p*FPhe^{22}]hEGF, which was confirmed by the analysis of amino acid compositions of the two peak fractions[2].

[2] H. Koide, S. Yokoyama and T. Miyazawa, unpublished.

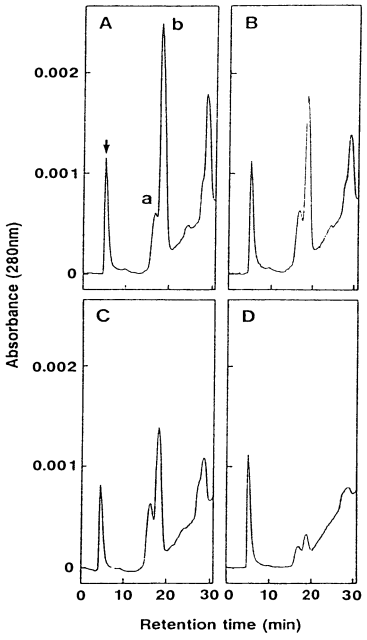

Fig. 2. HPLC profile of [*p*FPhe^{22}]hEGF and [Phe^{22}]hEGF. *Escherichia coli* strain KA197 harboring pTA152-22F was cultured in 200 ml of TG+1 medium containing *p*-fluorophenylalanine at the concentration of 10 μg/ml (A), 50 μg/ml (B), 100 μg/ml (C) and 200 μg/ml (D). The protein product was partially purified with gel filtration chromatography and reverse-phase HPLC, and then dissolved in 100 mM ammonium acetate buffer (pH 6.0). The protein solution was loaded on ion-exchange HPLC and elution was performed with a linear gradient of 100–400 mM ammonium acetate buffer. The peak due to an injection shock is shown with an arrow.

Table 1. Incorporation of *p*-fluorophenylalanine into hEGF

Concentration of *p*FPhe (μg/ml)	10	50	100	200
Sum of [*p*FPhe^{22}]hEGF and [Phe^{22}]hEGF[a]	1.0	0.7	0.6	0.1
Ratio of [*p*FPhe^{22}]hEGF to [Phe^{22}]hEGF	0.2	0.3	0.4	0.7
Yield of [*p*FPhe^{22}]hEGF[a]	1.0	1.0	1.0	0.3

[a] Relative to the case of *p*FPhe concentration of 10 μg/ml.

Optimum concentration of p-fluorophenylalanine

From the peak heights in the elution profile of ion-exchange HPLC (Fig. 2), the yields of [*p*FPhe^{22}]hEGF and [Phe^{22}]hEGF were obtained as shown in Table 1. As the concentration of *p*-fluorophenylalanine in the medium was raised from 10 to 200 μg/ml, the yield ratio of [*p*FPhe^{22}]hEGF to [Phe^{22}]hEGF was increased, but the sum of the yields of two products was decreased. The yield of [*p*FPhe^{22}]hEGF was nearly constant over the *p*-fluorophenylalanine concentration range of 10–100 μg/ml, but was reduced as the concentration was raised from 100 to 200 μg/ml. Thus, the optimum concentration of *p*-fluorophenylalanine was found to be 50 μg/ml.

Preparation of [pFPhe^{29}]hEGF

E. coli strain KA197 harboring plasmid pTA152-29F was cultured in TG+1 medium containing *p*-fluorophenylalanine at the optimum concentration of 50 μg/ml. In the steps of gel filtration chromatography and reverse-phase HPLC, [*p*FPhe^{29}]hEGF and [Phe^{29}]hEGF were eluted at nearly the same retention time.

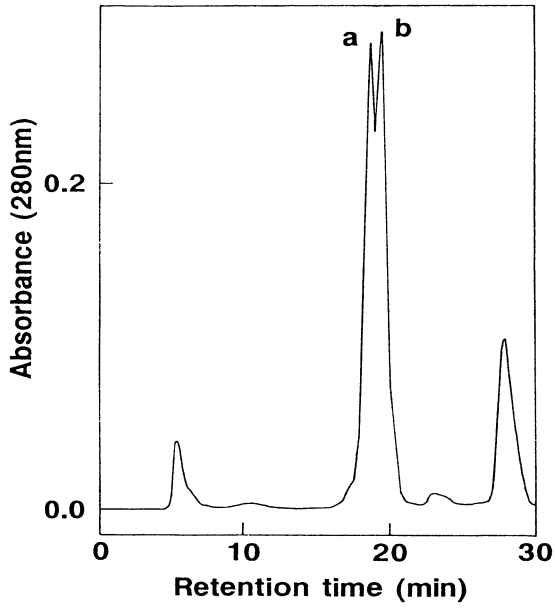

Fig. 3. HPLC profile of [*p*FPhe^{29}JhEGF and [Phe^{29}]hEGF. *Escherichia coli* strain KA197 harboring pTA152-29F was cultured in 2l of TG+1 medium containing *p*-fluorophenylalanine (50 μg/ml). After gel filtration chromatography and reverse-phase HPLC, the whole fraction containing [*p*FPhe^{29}]hEGF was loaded on ion-exchange HPLC.

However, in the step of ion-exchange HPLC, three peaks were observed (Fig. 3). The first peak (peak a) and the second peak (peak b) were found to be due to [Phe^{29}]hEGF and [*p*FPhe^{29}]hEGF, respectively, from the comparison with the elution profile of [Phe^{29}]hEGF (data not shown). This was again confirmed by the analysis of amino acid compositions of the two peak fractions[2]. Thus, in the present study, we succeeded in the preparation of two species of *p*FPhe-substituted hEGF.

Effect of incorporation of *p*FPhe in hEGF

The incorporation of *p*FPhe in place of Phe in hEGF will not directly affect the ionization state of the protein. However, [*p*FPhe^{22}]hEGF and [*p*FPhe^{29}]hEGF were separated from [Phe^{22}]hEGF and [Phe^{29}]hEGF, respectively, by ion-exchange HPLC (Figs. 2 and 3). This suggests that the incorporation of *p*FPhe in place of Phe caused some change in the native conformation of hEGF. We note that the fluorine atom in the para position of the aromatic ring of *p*-fluorophenylalanine is more bulky than the hydrogen atom. This substitution could cause some distortion of the protein conformation, if the *p*FPhe residue is buried in the interior of the protein. In fact, residues Tyr^{22} and Tyr^{29} in the antiparallel ß-sheet may be buried in the core of EGF [12,13]. The strong cytotoxicity of *p*-fluorophenylalanine is possibly due to perturbations of conformations and functions upon incorporation of this non-protein amino acid in proteins in the host cell.

Concluding remarks

We have succeeded in the *in vivo* preparation of three alloproteins, [Nle^{21}]hEGF [1], [*p*FPhe^{22}]hEGF and [*p*FPhe^{29}]hEGF. Recently, site-specific *in vitro* incorporation of some nonprotein amino acids was reported [14]. Novel design of nonprotein amino acids for incorporation in proteins and efficient syntheses of alloproteins will have much potential application in protein engineering.

Acknowledgements

We are grateful to Dr. B.J. Bachmann of Yale University for the generous gift of *E. coli* strain KA197.

References

1. Koide H, Yokoyama S, Kawai G, Ha J-M, Oka T, Kawai S, Miyake T, Fuwa T and Miyazawa T (1988) Proc. Natl. Acad. Sci. USA 85: 6237–6241.
2. Gilles A-M, Marliere P, Rose T, Sarfati R, Longin R, Meier A, Fermandjian S, Monnot M, Cohen GN and Barzu O (1988) J. Biol. Chem. 263: 8204–8209.

3. Tsai LB, Lu HS, Kenney WC, Curless CC, Klein ML, Lai P-H, Fenton DM, Altrock BW and Mann MB (1988) Biochim. Biophys. Res. Commun. 156: 733–739.
4. Bogosian G, Violand BN, Dorward-King EJ, Workman WE, Jung PE and Kane JF (1989) J. Biol. Chem. 264: 531–539.
5. Richmond MH (1962) Bact. Rev. 26: 398–420.
6. Sproat BS and Gait MJ (1984) In: Gait MJ (ed.) Oligonucleotide Synthesis: A Practical Approach. IRL Press, Oxford, pp. 83–116.
7. Garen A and Levinthal C (1960) Biochim. Biophys. Acta 38: 470–483.
8. Gregory H (1975) Nature (London) 257: 325–327.
9. Komoriya A, Hortsch M, Meyers C, Smith M, Kanety H and Schlessinger J (1984) Proc. Natl. Acad. Sci. USA 81: 1351–1355.
10. Goldberg AL (1972) Proc. Natl. Acad. Sci. USA 69: 422–426.
11. Talmadge K and Gilbert W (1982) Proc. Natl. Acad. Sci. USA 79: 1830–1833.
12. Marco AD, Menegatti E and Guarneri M (1983) FEBS Lett. 159: 201–206.
13. Kohda D and Inagaki F (1988) J. Biochem. 103: 554–571.
14. Noren CJ, Anthony–Cahill SJ, Griffith MC and Schultz PG (1989) Science 244: 182–188.

Address for correspondence: Hiroshi Koide, Department of Biophysics and Biochemistry, Faculty of Science, University of Tokyo, Hongo, Bunkyo-ku, Tokyo 113, Japan.

Determination of methylated basic amino acids, 5-hydroxylysine, and elastin crosslinks in proteins and tissues*,**

Constantinos G. Zarkadas[a], Edward A. Meighen[b], James A. Rochemont[c], George C. Zarkadas[d], Ali D. Khalili[e] and Quang Nguyen[e]

[a]*Agriculture Canada's Food Research Centre, Saint-Hyacinthe, Canada*
[b]*Department of Biochemistry, McGill University, Canada*
[c]*The Molecular and Biochemical Neuroendocrinology Laboratories, Clinical Research Institute of Montreal, Canada*
[d]*McGill Nutrition and Food Science Centre and the Department of Animal Science, Canada*
[e]*Macdonald College of McGill University, Ste. Anne de Bellevue, Quebec H9X 1CO, Canada*

Abstract

Myosin, actin, collagen, and elastin of adult bovine diaphragm and porcine and avian skeletal muscle tissues and their separated intracellular and extracellular muscle protein fractions have been determined by chromatographic methods developed to quantitate their unique basic amino acids. In this direct chemical approach the determination of the myofibrillar myosin and actin content of skeletal muscle is based on the amounts of Nτ-methylhistidine present, and collagen from the amount of 5-hydroxylysine present. Elastin was also determined from the amounts of desmosine found. Skeletal muscles were found to contain between 10.2–11.5% actin and 21.3 to 24.0% myosin, corresponding to 21.1% and 44.0% of the myofibrillar proteins (52.3% of the total muscle proteins), between 37.6–46.3% other SDS-soluble intracellular proteins, and 4.7 to 10.2% SDS-insoluble extracellular matrix muscle proteins. Total skeletal muscle collagan ranged from 2.8 to 5.9%, while elastin accounted for an estimated 0.063–0.143%, and the transcellular matrix SDS-insoluble proteins accounted for the remaining 1.8%.

Introduction

The enzymatic methylation of the side chains of specific lysines, histidines and arginines in proteins is a very common phenomenon in nature. It involves numerous classes of proteins in both prokaryotic and eukaryotic cells (reviewed in [1–2]), and has been studied extensively using a number of chromatographic procedures [3–5]. These studies have led to the discovery of eight methylated derivatives of lysine, histidine, and arginine [6] present in proteins such as histones, ribosomal proteins, cytochrome c, flagellar proteins [1], and proteins with even more complex biochemical functions and properties including myosin [2], actin [7], and the encephalitogenic basic A1 protein in myelin.

* This investigation was supported by Grant FY-82/84 from the Muscular Dystrophy Association of Canada and by Agriculture Canada in the form of a DSS Contract (No. 05081-00523) with McGill University.
** Contribution No. 115, Saint-Hyacinthe Food Research Centre.

Quantitation of $N\tau$-methylhistidine [His(τ-Me)], a unique basic amino acid found in both myosin and actin [2,7–8], has been used for determining the myofibrillar proteins in tissues [9–11], and the turnover rates of muscle protein breakdown [12]. High urinary excretion of His(τ-Me) and ω-*N*-methylarginines has been found, for example, in patients with Duchene muscular dystrophy [13–14], suggesting possible changes in the structure of myofibrillar, myelin sheath, and heterogeneous nuclear RNA proteins [1]. In addition, measurements of the levels of 5-hydroxylysine [Lys(5-OH)] in tissues or urine [15–16], and desmosine [17], the main lysine-derived stable crosslink of elastin (reviewed in [7]), are of great clinical importance [15,10]. Low levels of Lys[5-OH) and type III collagen, and crosslinking defects in elastin, have been implicated in certain heritable disorders of connective tissue including Marfan's syndrome [19–21], Ehlers-Danlos syndrome IV [20–21], and possibly atherosclerosis [22]. Similarly, low levels of Lys(5-OH) and structural collagen defects have been reported recently as prime factors in avian muscular dystrophy [23]. However, to quantitate the extent of the above post-translational side chain modifications occurring in trace amounts in proteins, cellular extracts, and tissues, analytical methods of high sensitivity and resolving power are required.

This paper describes the application of the new analytical chromatographic methods developed [24–25] to quantitate the unique methylated basic amino acids, including Lys(5-OH), desmosine, isodesmosine and related compounds in the adult bovine diaphragm and typical porcine skeletal muscle tissues, in purified actin, and the two major intracellular muscle protein and extracellular matrix protein fractions, prepared and quantitated by the methods of McCollester [26] and Laurent *et al.* [27]. The aim was to determine whether the levels of these unique basic amino acids in the selected skeletal muscle tissues could be used for the determination of their myofibrillar and connective tissue proteins from the amounts of protein-bound His(τ-Me) and Lys(5-OH) found in their acid hydrolysates, respectively. The elastin content in muscles can also be calculated from the amounts of desmosine found [24]. These calculations are based on the total protein content of the skeletal muscle and the isolated intracellular muscle protein and extracellular matrix fractions determined by their detailed amino acid compositions [9–11].

Experimental procedures

Preparation of intracellular SDS-soluble (F1) and extracellular SDS-insoluble (F2) skeletal muscle proteins fractions

The procedure employed for the extraction and preparation of the intracellular muscle protein (F1) and extracellular matrix connective tissue protein fractions (F2) combines the original method of McCollester [26] and the procedure described by Laurent *et al.* [27]. Intracellular and extracellular skeletal muscle

protein fractions were isolated from the costal region of the adult bovine diaphragm, three typical porcine skeletal muscles from Yorkshire sows, (*External sternomandibularis, Semimembranousus, Semitendinosus*), and from the legs and breasts of young and adult White Leghorn chickens and were quantified by detailed amino acid analysis. This involved repeated homogenization of the muscle tissue in the presence of 50 mM $CaCl_2$, neutral phosphate-buffered saline (pH 7.4), followed by solubilization with 2% sodium dodecyl sulfate (SDS), and centrifugation to separate all intracellular muscle proteins (fraction F1) from the extracellular matrix SDS-insoluble (F2) fraction, as described previously [9–11].

Actin purification

Skeletal muscle G-actin was purified from acetone-extracted avian muscle tissue (leg and breast), and from the porcine *Semimembranosus* muscle by the low salt buffer extraction method of Spudich and Watt [29], followed by the polymerization and depolymerization steps as recommended by Pardee and Spudich [30]. Both porcine and avian skeletal muscle actins were further purified by gel permeation chromatography on a 2.6 × 95 cm Sephacryl S-200 column eluted with the depolymerization buffer of Pardee and Spudich [30]. Homogeneity of the protein was checked by SDS-polyacrylamide gel electrophoresis by the method of Weber and Osborn [32]. The technique described by Laemmli [33] using 10% acrylamide gel with a 3% stacking gel, followed by two-dimensional SDS-PAGE according to O'Farrell [34], were applied to further test the purity of skeletal muscle actins, as described previously [10].

Procedures for amino acid analyses

Amino acid analyses were carried out on either a conventional (Beckman Model 120C) or an updated and fully automated amino acid analyzer (equivalent to Beckman Model 121MB).

Complete amino acid analyses were carried out on each of the two major muscle protein fractions, F1 and F2, and on both avian and porcine actins as described previously [10–11, 24–25]. Duplicate samples of 10.0 μg of the actins were used both for regular amino acid analysis and for the methionine and cysteine determinations. Separate samples of 80 μg were used for determination of tryptophan [24]. Determinations of the methylated basic amino acids, the diastereoisomers of Lys(5-OH), and related compounds were carried out with concentrated 96 h hydrolysates (equivalent to 100 to 250 μg protein/analysis) by the single-microcolumn (50 × 0.28 cm) system packed with Dionex DC-4A resin so that peaks adequate for these components (100 to 250 pmol) could be obtained [10–11,24–25].

Theory of the method

Calculation of the protein mass in skeletal muscle

The protein mass of each acid hydrolysate was determined by the procedure described by Horstmann [31]. According to this method, a mean residue weight

(WE in μg/nmol) is calculated for the amino acids constituting the proteins in skeletal muscle as:

$$WE = \sum_{i=1}^{20} (a_i \cdot b_i) \tag{1}$$

where a_i is the mole fraction of an amino acid *i* found in the analyzed aliquot and b*i* is the molecular weight of amino acid residue *i*.

Determination of a specific protein in skeletal muscle

The amount of a specific protein *j* present in skeletal muscle and the separated intracellular and extracellular protein fractions (F1 and F2) can be calculated from the quantitative determination of a given amino acid *i* known to occur exclusively in that specific protein (*j*), according to

$$P_j = C_i \cdot \frac{[1000]}{n'_i} \cdot \frac{WE_{Pj}}{M_{ri}} \tag{2}$$

where P_j is the concentration of a specific protein *j* expressed in grams per kilograms of total protein, WE_{p_j} is the weight equivalent of a specific muscle protein *j* determined from equation 1 as described by Horstmann [31] C_i is the mean concentration in grams per kilogram of total protein of a unique protein-bound amino acid *i* found in the analyzed acid hydrolysate of skeletal muscle or its protein fractions, n_i is the number of amino acid residues, *i*, per 1000 amino acid residues and M_{r_i} is the anhydrous molecular weight of the unique amino acid *i* [9].

The following analytical conventions, derived from equation 2, can therefore be used for calculating the:

(i) amt of collagen (P_c) = amt of 5-hydroxylysine × 63.3 (2a)

(ii) amt of elastin (P_E) = amt of desmosine × 62.4 (2b)

(iii) amt of connective tissue (P_{CT}) = amt of 4-hydroxyproline × 8.03 (2c)

Determination of the myofibrillar proteins myosin and actin

Sequence studies [7–8] have shown that 1 mol of actin (A) contains 1 mol of His(τ-Me) and that 1 mol of myosin (M) contains 2 mol of His(τ-Me). Thus, the total amount (C_T) of His(τ-Me) in skeletal muscle determined by the present method [25] represents the sum of the distribution of His(τ-Me) the myosin (P_M) and actin (P_A) present in skeletal muscle (g/kg total protein) by the following equation.

$$\sum_{j=1}^{2} [P_A + P_M] = \left[\frac{A}{A + 2M} \cdot \frac{41{,}782}{151.2} + \frac{M}{A + 2M} \cdot \frac{521{,}000}{151.2} \right] \cdot C_T \quad (3)$$

Substituting the molar ratio of actin to myosin reported by Murakami and Uchida [35] [A/B = 6] in equation (3) the sum of actin and myosin in skeletal muscles can be made as follows:

$$\sum_{j=1}^{2} [P_A + P_M] = [207 + 431] \cdot C_T \quad (3a)$$

or

$$\sum_{j=1}^{2} [P_A + P_M] = 638 \cdot C_T \quad (3b)$$

Yates and Greaser [47] have shown that the sum of actin and moysin in the myofibril accounts for 65% of the total myofibrillar protein by weight. Thus, the total myofibrillar protein in g/kg total protein in skeletal muscles can also be calculated as shown below:

amt of myofibrillar protein

$$\frac{\sum_{j=1}^{2} [P_A + P_M]}{0.65} \cdot C_T = 981 \cdot C_T \quad (3c)$$

Results and Discussion

The separation of all methylated basic amino acids, the diastereoisomers of Lys(5-OH), desmosine, isodesmosine, the amino sugars and related compounds was carried out on an updated amino acid analyzer (equivalent to Beckman Model 121 MB) under a variety of chromatographic conditions to obtain complete resolution in a minimum of time [25]. The chromatographic separations shown in Fig. 1 are typical of those obtained when a synthetic mixture of all methylated basic amino acids and related compounds was analyzed on a 50 × 0.28 cm microcolumn of Dionex type DC-4A resin (sized to 9.0 ± 0.5 μm). In this chromatographic system (Fig. 1) ionic interactions between these unique basic amino acids and the DC-4A (Dionex) resin are primarily responsible for their separation. Thus, as may be seen in Fig. 1, by selecting the optimum conditions of

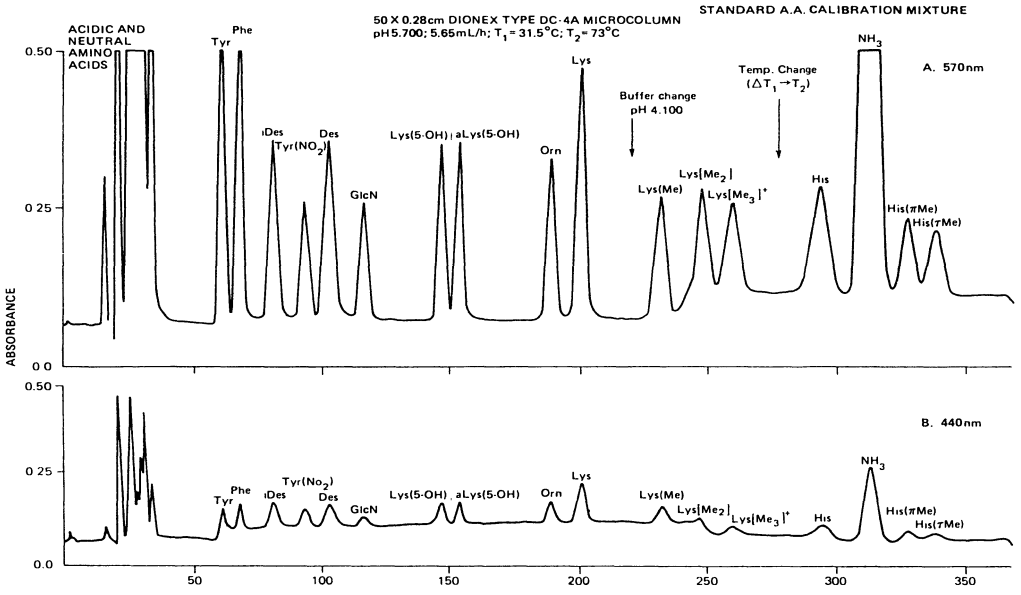

Fig. 1. Chromatographic separation of methylated lysines and histidines, the diastereoisomers of 5-hydroxylysine, desmosine, isodesmosine and related compounds (2 nmol each) on an analytical 50 × 0.28 cm microcolumn of Dionex DC-4A resin. Two sodium citrate buffers (0.35 M) were pumped through the column at 5.65 mL/h to achieve the indicated separation. The second buffer, pH 4.500, was introduced at 215.7 min as indicated by the arrow. Column temperature: 31.5°C changed to 73°C at 294.7 min. Ninhydrin flow rate was 5.60 mL/h. The upper curve shows absorbance at 570 nm and the lower curve the absorbance at 440 nm. Peak identification: Tyr(NO_2), 3-nitrotyrosine; iDes, isodesmosine (0.9609 nmol); Des, desmosine (1.0378 nmol); GlcN, glucosamine, GalN, galactosamine; Lys (5-OH), 5-hydroxylysine; aLys(5-OH), *allo*-5-hydroxylysine; Orn, ornithine; Lys(Me), N^6-methyllysine; Lys(Me_2), dimethyllysine; Lys(Me_3)$^+$, N^6-trimethyllysine; His(πMe), N^{π}-methylhistidine; His(τ-Me), N^{τ}-methylhistidine.

column temperature (initial 31.5°C; reset at 295 min to reach 73°C in 50 min), composition, and pH of the sodium citrate buffer systems (0.35M; pH 5.700 changed to 4.501 at 215 min) and by adjusting the eluant linear flow velocity to 1.56 cm/min (5200 kN/m^2, 1000 psi) all of the 17 basic components of the mixture (2.0 nmol each) applied to the microcolumn emerged as discrete, well-separated peaks. Since the separation of these unique basic compounds is affected by temperature, pH, flow rate, composition, and nature of the eluant, other interactive forces in the resin must also be involved in their resolution. According to Hancock and Harding [5], ion-exchange resins contain several interactive groups (i.e., sulfonic acid, nonpolar alkyl chains, and aromatic rings), each of which contribute to the separation, and that both hydrophobic and van der Waals, and possibly aromatic π–*π interactions, are also responsible for 12 amino acid separations. On

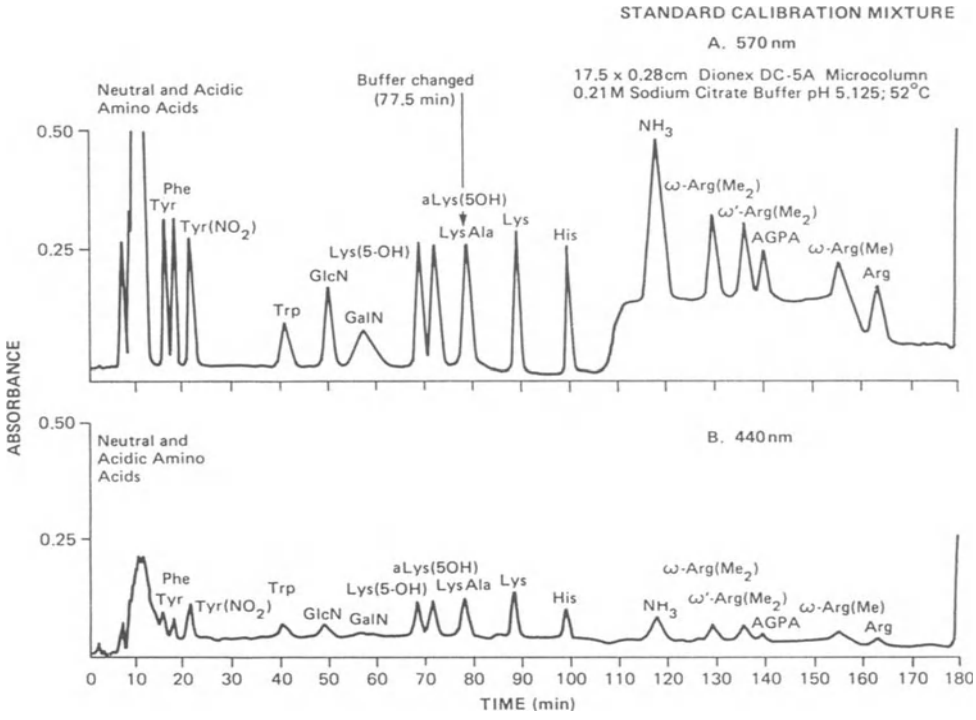

Fig. 2. Typical separation of a synthetic mixture containing 0.500 nmol of each of the 19 basic amino acids including ω-*N*-methylarginines on an analytical 17.5 × 0.28 cm microcolumn of Dionex type DC-5A resin. The microcolumn was operated at 52°C with 0.21 M sodium citrate buffer (pH 5.125) containing 2% isopropanol. The second 0.35 M sodium citrate buffer, pH 5.700, was introduced at 77.5 min, after lysinoalanine. Buffer and ninhydrin flow rates 25 were 5.75 and 5.60 mL/h, respectively. The upper curve shows absorbance at 570 nm and the lower curve at 440 nm. Peak identification: Tyr(NO_2), 3-nitrotyrosine: GlcN, glucosamine; GalN, galactosamine; Lys (5-OH), 5-hydroxylysine; aLys(5-OH), *allo*-5-hydroxylysine; LysAla, N^6-lysinoalanine; ω-Arg(5Me_2), ω-*N*,ω-*N*-dimethylarginine; ω^1-Arg(Me_2), ω-*N*,ω^1-*N*-dimethylarginine; ω-Arg(Me), ω-*N*-methylarginine.

the basis of these findings, therefore, the separation achieved by this system (Fig. 1) would be the method of choice for analyzing complex protein or tissue hydrolysates, which on hydrolysis yield picomole levels of all these amino acids. The possibility of overlap or coincidence of peaks and interference from artifacts has thus been eliminated.

The determination of all ω-*N*-methylarginines and related compounds was carried out at picomole levels in the minimum time using small diameter microporous resins, sized to 6.0 ± 0.5 μm [25]. Thus, by developing the 17.5 × 0.28 cm microcolumn of Dionex DC-5A resin at 52°C with 0.21 M sodium citrate buffer, pH 5.125, followed (min 77.5) by a 0.35 M buffer, pH 5.700, and eluant linear flow velocity of 1.56 cm min at 3100 kN/m^2 (600 psi), excellent resolution of the 19

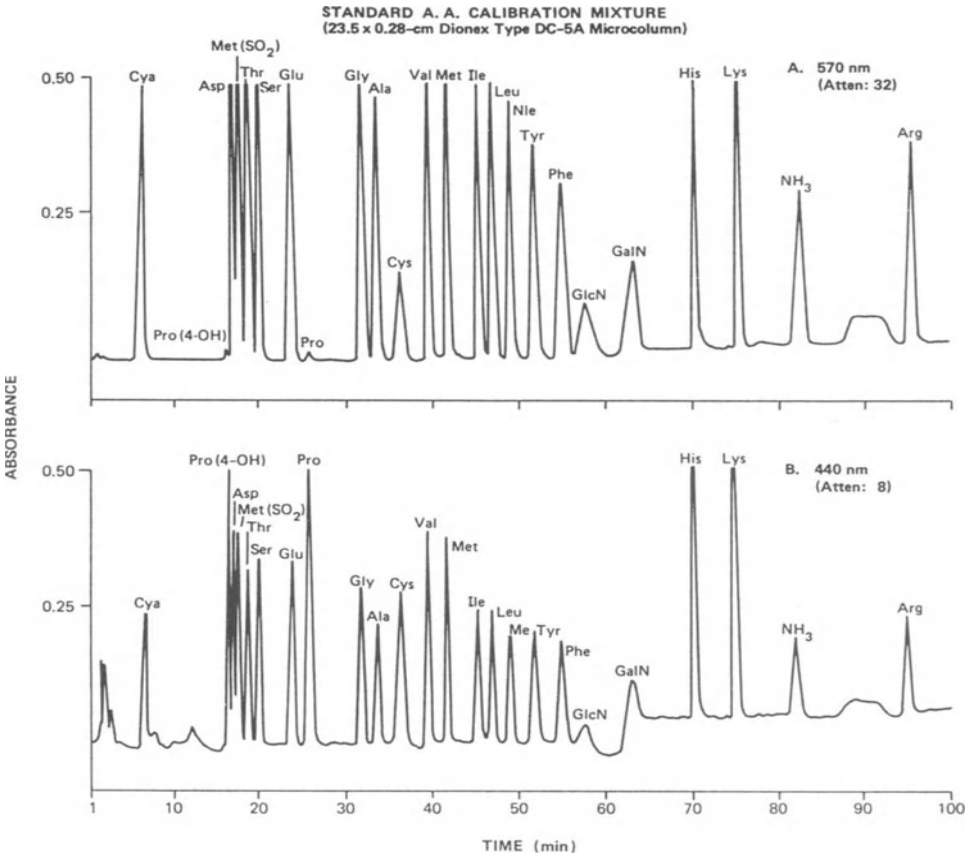

Fig. 3. Resolution of a standard amino acid mixture (500 pmol each) on a 23.5 × 0.28 cm microcolumn of Dionex DC-5A cation-exchange resin operated at 5.75 mL/h with the Beckman microcolumn buffer system: Buffers A, 0.20 M Na^+ at pH 3.28; B, 0.20 M Na^+ at pH 4.25; C, 1.0 M Na^+ pH 6.40. Buffers changed at 27.1 min (ΔA → B) and 5.26 min. (ΔB → C) after injection. Initial colum Temperature: 42.5°C changed to 73°C at 12.7 min. The ninhydrin reaction was carried out at 129°C with a flow rate of 5.60 mL/h. The upper curve denotes absorbance at 570 nm and the lower curve absorbance at 440 nm.

basic amino acids components of a synthetic calibration mixture (Fig. 2) was achieved. The internal standards selected to test the accuracy of the procedure were 3-nitrotyrosine and L-2-amino-3-guanidinopropionic acid. Since the limit for detection by this system was about 20 pmol, it has been possible to achieve accurate quantitative determinations of the unusual basic amino acids at the 50 to 200 pmol levels, with a reproducibility of 100 ± 2.5%.

The present study also extends the work and refines the standard single-column methodology described previously [36] to include the complete separation of

S-carboxymethylcysteine, 4-hydroxyproline, methionine S,S-dioxide, and the amino sugars likely to be encountered in collagen, elastin, and various proteins or tissue hydrolysates. Figure 3 shows the elution pattern obtained when a synthetic calibration mixture of 25 standard amino acids was analyzed on a 23.5 × 0.28 cm microcolumn of Dionex DC-5A resin using the Beckman microcolumn sodium citrate buffer system (A:0.20 M Na^+ at pH 3.28; B:0.20 M Na^+ at pH 4.25; C: 1.0 M Na^+ pH 6.40) recommended for ninhydrin analysis [36]. As may be seen in Fig. 3, complete separation of S-carboxymethylcysteine, 4-hydroxyproline, aspartic acid, methionineS,S-dioxide, and the hydroxyamino acids threonine and serine was achieved in 7 min by adjusting the pH of buffer A to 3.28 ± 0.002 and the initial column temperature to 42.5°C (changed to 73°C at 12.7 min). S-carboxymethylcysteine (data not shown in Fig. 3) was completely resolved from the microcolumn at 15.1 min. Although a large number of specific chromatographic procedures for separating the diastereoisomers of 4-hydroxyproline have appeared in the literature using pH 2.9 buffer, its separation from aspartic acid by this single column system is important in the analysis of connective tissue proteins or complex tissue hydrolysates [25]. The complete separation and quantitation of the amino sugars glucosamine and galactosamine has also been carried out by this single-microcolumn system.

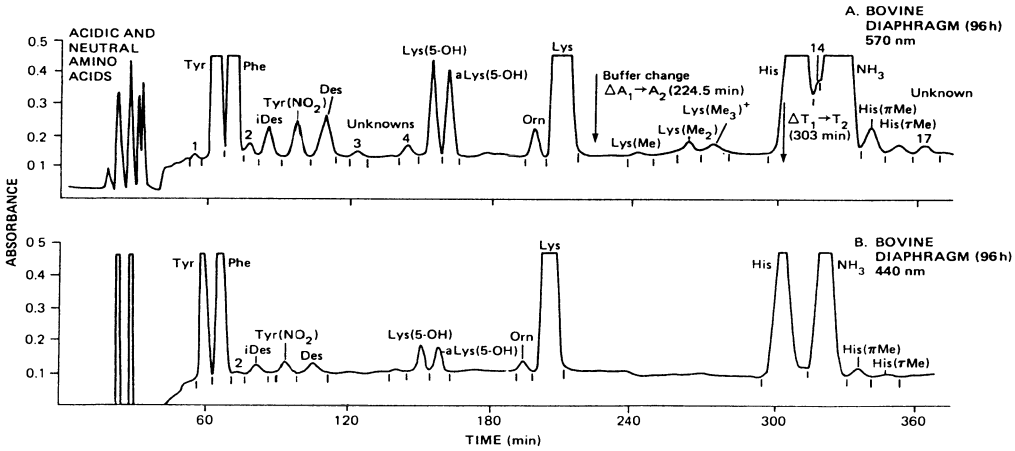

Fig. 4. Chromatographic separation of all methylated lysines and histidines, the diastereoisomers of 5-hydroxylysine, stable crosslinking amino acids and related compounds in normal bovine diaphragm tissue hydrolysates (96 h) by method 1. The second 0.35 M sodium citrate buffer, pH 4.501, was introduced at 224.5 min and column temperature: 31.5°C changed to 73°C at 303 min, as indicated by arrows. The upper curve indicates absorbance at 570 nm and the lower curve the absorbance at 440 nm. Peak identification: iDes, isodesmosine: Tyr(NO_2), 3-nitrotyrosine; Des, desmosine; Lys(5-OH), 5-hydroxylysine; aLys(5-OH, *allo*-5-hydroxylysine; Lys(Me), N^6-methyllysine; Lys(Me_2), N^6-dimethyllysine; Lys(Me_3)$^+$, N^6-trimethyllysine; His($^\pi$Me), $N\pi$-methylhistidine; His(τ-Me), $N\tau$-methylhistidine.

Application of this methodology to complex tissues was also tested with acid hydrolysates of various muscle tissues including the bovine diaphragm, avian red and white muscles and select porcine skeletal muscles, and the separated intracellular and extracellular protein fractions [9–11]. As shown in Fig. 4A, the analysis of a diaphragm hydrolysate sample (100 μL equivalent to 400 μg protein) by the present analytical chromatographic methods revealed the complete separation, at pH 5.700, of isodesmosine, desmosine the diastereoisomers of Lys(5-OH), and all methylated lysines along with six as yet unidentified ninhydrin-positive peaks, designated 1, 2, 3, 4, 14 and 17. One complication, however, often encountered in the analysis of His(τ-Me) in muscle tissue hydrolysates is the presence of variable amounts of soluble histidine dipeptides, including carnosine, homocarnosine, anserine, and balenine, which on acid hydrolysis yield ß-alanine, histidine, N^{π}-methylhistidine and His(τ-Me) [37–38]. Although the physiological function of anserine and balenine in skeletal muscle tissues has not been established, and only carnosine and its analogues are now considered as endogenous antioxidants in brain and muscle [38], these dipeptides must be extracted from muscle tissues prior to acid hydrolysis.

Unique basic amino acid content of skeletal muscles

The combined procedures of McCollester [26] and Laurent *et al.*, [27] effectively separated the intracellular SDS-soluble muscle protein fraction (F1) from the

Table 1. Recoveries of the intracellular (F1) and extracellular (F2) muscle protein fractions from selected skeletal muscles by the combined methods of McCollester [26] and Laurent *et al.* [27]

Skeletal muscle		Yields, % of total muscle protein[a]	
		F1 Myofibrillar SDS-soluble proteins[b]	F2 Myofibrillar SDS-soluble proteins[b]
Bovine	Costal diaphragm	95.27 ± 2.50	4.73 ± 0.07
Porcine	*External Sternomandibularis*	89.78 ± 0.80	10.22 ± 1.21
	Semitendinosus	94.55 ± 0.37	5.45 ± 0.07
	Semimembranosus	94.80 ± 0.01	5.20 ± 0.21
Avian Leg	6-month-old	94.54 ± 3.59	5.46 ± 1.04
	1.2-year-old	93.21 ± 2.35	5.20 ± 0.57
Breast	6-month-old	94.12 ± 0.74	5.87 ± 0.05
	1.2-year-old	93.49 ± 2.66	6.51 ± 1.29

[a] Protein content was determined by amino acid analysis according to Horstmann [31].
[b] Mean ± standard error of measurements (S.E.M.) for 3 raplicates and 48 determinations.

Table 2. Comparison of the unique basic amino acid (AA) content of the intracellular (F1) and extracellular (F2) muscle protein fractions from selected skeletal muscles

	Bovine	Porcine			Avian	
	Costal diaphragm	*External sternomandibularis*	*Semifendino*	*Semi-membranosus*	Red (leg)	White (breast)
			SDS-solubilized intracellular F1			
N^6-methyllysine		0.10	0.095	0.109	0.095	0.112
N^6,N^6,N^6-trimethyllysin	0.121	0.41	0.350	0.453	0.405	3.346
N^τ-methylhistidine	0.548	0.592	0.589	0.521	0.556	0.449
Total AA N[b]	170.17	172.53	168.63	180.82	164.24	165.07
WE, µg/nmol[b]	112.84	112.62	112.95	112.78	112.15	112.22
			SDS-insoluble extracellular fraction F2			
4-hydroxyproline	70.23	111.50	118.12	107.10	111.99	105.07
5-hydroxylysine	8.85	9.11	9.81	8.64	9.89	7.84
Isodesmosine	0.43	0.224	0.291	0.185	–	–
Desmosine	0.44	0.225	0.291	0.194	0.178	–
Ornithine	0.320	0.362	0.458	0.588	–	–
Total AA N[b]	190.46	199.28	203.55	219.07	186.89	196.02
WE, µg/nmol[b]	93.94	93.10	93.73	95.32	96.57	95.49

[a] Determined by the procedures of Zarkadas *et al.* (9–11,24,25).

[b] Calculated according to Horstmann [31].

extracellular SDS-insoluble protein fraction (F2) of bovine, porcine and avian skeletal muscles [9–11], and the results obtained are summarized in Table 1. The intracellular skeletal muscle protein fraction F1 accounts for an estimated 89.3 to 95.3% of the total skeletal muscle mass, while the extracellular protein fraction (F2) ranged from 4.7 to 10.22%, of the total muscle protein.

A summary of the unique basic amino acid content of SDS-solubilized intracellular (F1) and SDS-insoluble extracellular (F2) muscle protein fraction isolated from three porcine skeletal muscles and from the bovine diaphragm is given in Table 2. These results show that while the protein-bound His(τ-Me) content of both the bovine costal diaphragm (0.548 g/kg protein) and the porcine *External sternomandibularis* (0.592 g/kg of protein) and *Semitendinosus* (0.589 g/kg protein) muscles appeared to be very similar, there was a small but statistically significant variation ($P<0.01$) in the (His(τ-Me) content (0.521 g/kg of protein) of the *Semimembranousus* muscle [11]. The mean His(τ-Me) values in avian muscles ranged from 0.542 to 0.578 g/kg protein in adult and young leg (slow) muscles, respectively, and from 0.416 g/kg in young breast muscle to 0.467 g/kg protein in adult breast muscles [10]. While most of this variation may be attributed to the presence of variable amounts of fast (Type IIA), slow (Type I) and mixed fast/slow (Types IIA and IIB) or slow tonic fibers (Types I, or IIIA and IIIB), the factors responsible for the small differences in His(τ-Me) contents among porcine or avian skeletal muscles are less clear. The distribution of heavy myosin chain isoforms among different muscle fiber types with fast, mixed fast/slow, and slow properties has been shown to vary in a muscle specific manner [41–43].

N^{τ}-methylhistidine content of G-actin

To establish whether the small variation in protein-bound His(τ-Me) among skeletal muscles could be attributed to myosin heavy chain isoforms or to actin isotypes, the His(τ-Me) content of purified G-actin from both the legs and breasts of chickens as well as from sows *Semimembranosus* muscle was determined by the present method [10–11,25]. A single band was observed on both the one- and two-dimensional SDS-polyacrylamide gels which had been stained for protein, demonstrating that actins purified from porcine *Semimembranosus* muscle as well as from chicken breasts or leg muscles [10,11] were essentially homogeneous. Porcine G-actin contained 0.97 moles of His(τ-Me) compared to avian G-actin which contained between 0.96 and 1.09 moles of His(τ-Me) per mole of protein. The results obtained confirmed and extended those reported by Elzinza *et al.*, [17] for the amino acid sequence of rabbit skeletal actin, demonstrating that the structure of muscle actins in the vicinity of His(τ-Me) appears to be highly conserved in different species.

Myofibrillar and connective tissue protein components of skeletal muscles

From the levels of these unique basic amino acids found in the selected skeletal muscle tissues investigated (Table 2), it has been possible to calculate the myo-

fibrillar myosin and actin, and collagen contents of both skeletal muscles and the separated intracellular and extracellular matrix protein fractions from the amounts of protein-bound His(τ-Me) and Lys (5-OH), respectively. The elastin content of muscles were also calculated from the amounts of Des found [9]. These calculations are based on the total protein content of the skeletal muscle and the isolated intracellular muscle protein and extracellular matrix fractions, as determined by their detailed amino acid compositions [9,25].

The results of Table 3 show that the bovine costal diaphragm contained 11.0% actin and 23.0% myosin corresponding to 21.1% and 44.0% of the myofibrillar proteins (52.3% of the total protein). Similar results were obtained with selected avian and porcine skeletal muscles [10]. Actin accounted for an estimated 10.2–11.5% of the total porcine muscle mass or about 21.1% of the total myofibrillar protein, while myosin ranged from 21.3 to 24.0% of the total muscle protein corresponding to 43.9% of the myofibrillar proteins (52.14% of total protein). These results are in accord with those reported by Yates and Greaser [47] and Hanson and Huxley [45] who have used different methods and different muscle tissue for these determinations. These authors have shown that the myofibrillar protein of the rabbit *Psoas* muscle represent 57.71% of the total muscle mass, and that the myofibrils contain 22% actin and 43% myosin by weight.

Table 3 shows that the bovine costal diaphragm contained 4.73% SDS-insoluble extracellular matrix muscle proteins, which corresponds to 2.62% collagen, 0.13% elastin, and 1.8% other transcellular matrix proteins. The *External sternomandibularis* porcine muscle contained the highest levels (10.2%) of extracellular matrix proteins, compared to the other two porcine muscles, which ranged from 5.20 to 5.45 g protein per 100 g total muscle protein. Total collagen in porcine muscle ranged from 2.84% in *Semimembranosus*, 3.38% in *Semitendinosus*, to 5.89% in the *External sternomandibularis* muscle, while elastin accounted for an estimated 0.063–0.143% of the total muscle mass. The highest level of elastin (0.143%) was found in the *External sternomandibularis* muscle. These results are in reasonably good agreement with those reported by Bendall [39], Dransfield [40] and Light *et al.*, [44] for the distribution of collagen (average 4.35%, range 1.22–15.1%) in 34 bovine skeletal muscles investigated. These results also demonstrate that the content of collagen is higher in slow twitch postural muscles than in locomotory muscles which contain primarily fast twitch fibertypes.

Other muscle soluble proteins

From the foregoing results, it became apparent that, in addition to myofibrillar and connective tissue proteins of the extracellular matrix (Table 3), a large quantity of SDS-soluble proteins is found in the intracellular muscle protein fraction of bovine diaphragm and porcine muscles, which ranged from 37.64 to 46.4% of the total muscle proteins. These results are considerably higher than those found (28–34%) by Hanson and Huxley [45] as soluble proteins (sarcoplasmic) washed out of the glycerol-extracted muscle after it has been broken up into fibrils, but they are in

Table 3. Myofibrillar and connective tissue protein contents of selected skeletal nuscles (% of total muscle protein)

	Bovine	Porcine			Avian		*Psoas* major (rabbit)		
Skeletal muscle proteins[a]	Costal diaphragm	*External Sterno-mandibularis*	*Semi-tendinosus*	*Semi-membranosus*	legs (red)	Breast (white) *Pectoralis thoracica*	Yates and Greaser [47]	Hanson and Huxley [45]	Szent-Gyorgi *et al.* [46]
				F1, intracellular; SDS-solubilized proteins[b]					
1. Myofibrillar	52.26	52.14	54.63	48.45	53.2	57.98	57.71	62.00	40–48
Actin	11.04	11.00	11.53	10.22	11.22	12.23	12.69	12.00	
Myosin	22.94	22.91	24.00	21.29	23.36	25.47	24.82	34.00	
Actomyosin	83.98	33.91	35.53	31.51	34.58	37.70	37.52	46.00	
2. Other soluble proteins	43.00	37.64	39.92	46.35	39.86	38.95	–	34.00	41.6
				F2, Extracellular matrix: SDS-insoluble proteins[b]					
3. Connective tissue	2.59	9.15	5.17	4.47	5.38	1.94			
4. Collagen	2.62	5.89	3.38	2.84	6.87	3.08			
5. Elastin	0.128	0.143	0.099	0.063					
6. Total 4 + 5	2.752	6.033	3.480	2.903					

[a] Calculated from unique basic amino acid data (Table 2) as described by Zarkadas *et al.* [8].

[b] Fraction F1 and F2 were separated by the combined procedures of McCollester [26] and Laurent *et al.* [27].

accord with the 41.6% figure quoted by Szent-Gyorgi *et al.*, [46] using two different extraction procedures. These results suggest that the intracellular muscle protein fraction includes sarcoplasmic proteins, organelles, Z-band and other membrane proteins, etc., which are soluble in 2% sodium dodecyl sulfate.

From the data presented in this paper, it may be concluded that these sensitive methods for determining all methylated basic amino acids, Lys(5-OH), the stable elastin cross-links and related compounds in proteins and muscle tissues can be applied for the determination of the myofibrillar and connective tissue protein contents of the bovine diaphragm and other skeletal muscles [9–11]. These methods of analysis should be especially valuable for studying the molecular and cellular mechanisms involved during morphogenetic and developmental processes in muscle cells. They can also be applied to the study of protein methylation, hydroxylation, and elastin cross-linking formation of contractile and extracellular matrix proteins in biological systems, under both normal and pathological conditions.

References

1. Paik WK and Kim S (1980) In: Meister A (ed.) Biochemistry. Wiley, New York, Vol. 1, pp. 1–250.
2. Huszar G (1984) In: Wold F and Moldave K (eds.) Methods in Enzymol. Academic press, Orlando, FL. Vol. 106, pp. 287–295.
3. Zarkadas CG (1975) Canad. J. Biochem. 53: 96–101.
4. Zarkadas CG (1978) Canad. J. Biochem. 56: 952–957.
5. Hancock WS and Harding DRK (1984) In: Hancock NS (ed.) CRC Handbook of HPLC for the Separation of Amino Acids, Peptides and Proteins. CRC Press Inc., Boca Raton, FL. Vol. 1, pp. 235–262.
6. Cohn WE (1984) In: Methods in Enzymol. 106: 3–17.
7. Elzinza M, Collins JH, Kuehl WM and Adelstein RS (1973) Proc. Natl. Acad. Sci. USA 70: 2687–2691.
8. Maita T, Hayashida M, Tanioka Y, Komine Y, Matsuda G (1987) Proc. Natl. Acad. Sci. USA 84: 416–420.
9. Zarkadas CG, Meighen EA, Zarkadas GC, Karatzas CH, Khalili AD, Rochemont JA and Berthelet M (1988) J. Agric. Food Chem. 36: 1095–1109.
10. Khalili AD and Zarkadas CG (1988) Poultry Sci. 67 1593–1614.
11. Zarkadas CG, Karatzas CH, Khalili AD, Khanizadeh S and Morin Q (1988) J. Agric. Food Chem. 36: 1131–1146.
12. Munro HN and Young VR (1979) Amer. J. Clin. Nutr. 31: 1608–1616.
13. McKeran RO, Halliday D and Purkiss P (1977) J. Neurol. Neurosurg. Psych. 40: 979–981.
14. Lou MF (1979) Science 203: 668–670.
15. Weis JB (1984) Top. Mol. Struct. Biol. 5: 17–53.
16. Farris B, Ferrera R, Glembourt M, Mongayzel PJ Jr., Crombie G and Franzblau C (1981) Anal. Biochem. 116: 71–74.
17. Paz MA, Keith DA and Gallop PM (1982) Methods in Enzymol. 82: 571–587.
18. Starcher BC (1982) Methods in Enzymol. 82: 759–762.
19. Gunja-Smith Z and Banek RJ (1981) Biochem. J. 193: 915–918.
20. Krane SM, Pinnel SR and Erbe RW (1972) Proc. Natl. Acad. Sci. USA 69: 2899–2903.
21. Eyre PR and Glimcher MJ (1972) Proc. Natl. Acad. Sci. USA 69: 2594–2598.

22. Franzblau C and Farris B (1982) Method in Enzymol. 82: 615–637.
23. DeMichele SJ, Brown RG, Krasin BW and Sweeny PR (1985) Comp. Biochem. Physiol. B81: 149–157.
24. Zarkadas CG, Zarkadas GC, Karatzas CN, Khalili AD and Nguyen Q (1986) J. Chromatogr. 378: 67–76.
25. Zarkadas CG, Rochemont JA, Zarkadas GC, Karatzas CN and Khalili AD (1987) Anal. Biochem. 160: 251–266.
26. McCollester DL (1962) Biochim. Biophys. Acta 57: 427–437.
27. Laurent GJ, Cockerill P, McAnulty RJ and Hastings JRB (1981) Anal. Biochem. 113: 301–312.
28. Light N and Champion AE (1984). Biochem. J. 219: 1017–1026.
29. Spudich JA and Watt S (1971) J. Biol. Chem. 246: 4866–4871.
30. Pardee JD and Spudich JA (1982) Methods Enzymol. 85: 164–181.
31. Horstmann JH (1979) Anal. Biochem. 96: 130–138.
32. Weber K and Osborn M (1975) In: Neurath HG, Hill RL and Boeder CL (eds.) The Proteins Vol. 1, pp. 179–223.
33. Laemmli UK (1970) Nature 227: 680–685.
34. O'Farrell PH (1975) J. Biol. Chem. 250: 4007–4021.
35. Murakami U and Uchida M (1985) J. Biochem. 98: 187–197.
36. Fauconnet M and Rochemont J (1978) Anal. Biochem. 91: 403–409.
37. Harris CI and Milne G (1987) Comp. Biochem. Physiol. 86B: 273–279.
38. Kohen R, Yamamoto Y, Cundy KC and Ames BN (1988) Proc. Natl. Acad Sci. USA 85: 3175–3179.
39. Bendall JR (1967) J. Sci. Food Agric. 18: 53–558.
40. Dransfield EJ (1977) J. Sci. Food Agric. 28: 833–842.
41. Lowey S (1986) Med. Sci. Sports Exercise 18: 284–291.
42. Mahdavi V, Strehler EE, Periasamy M, Wreczarek DF, Izumo S and Nadal-Ginard B (1986) Med. Sci. Sports Exercise 18: 299–308.
43. Staron RS and Pette D (1987) Biochem. J. 243: 695–699.
44. Light N, Champion AE, Voyle C and Bailey AJ (1985) Meat Sci. 13: 137–149.
45. Hanson J and Huxley HE (1957) Biochim. Biophys. Acta 23: 250–260.
46. Szent-Gyorgi AG, Mazia D and Szent-Gyorgi A (1955) Biochim. Biophys. Acta 16: 339–342.
47. Yates LD and Greaser ML (1983) J. Mol. Biol. 168: 123–141.

Address for correspondence: Dr. C.G. Zarkadas, P.O. Box 205, Macdonald College, Ste. Anne de Bellevue, Quebec H9X 1C0, Canada.

Section II
Neurochemistry/Neurobiology

Cerebroprotective and anticonvulsant action of competitive and non-competitive NMDA antagonists

Astrid G. Chapman, Jeanette H. Swan, Smita Patel, Joanne L. Graham and Brian S. Meldrum

Department of Neurology, Institute of Psychiatry, De Crespigny Park, Denmark Hill, London SE5 8AF, U.K.

Abstract

Both competitive (e.g. AP5, AP7, CPP, CGS 19755, CGP 37849, CGP 39551) and non-competitive (e.g. MK 801, PCP, ketamine, tiletamine, dextrorphan, dextromethorphan and ketamine) NMDA antagonists have cerebroprotective activity in a number of ischemia, hypoxia and trauma models, as well as anticonvulsant activity in a wide range of animal seizure models. Their pharmacological efficacies, on the whole, correlate well with their affinities for the NMDA receptor.

Administration of pharmacologically active doses of non-competitive NMDA antagonists cause significant metabolic activation of multiple brain regions, especially the limbic structures, in contrast to pharmacologically comparable doses of competitive antagonists which cause little or no metabolic activation. Following the systemic administration of non-competitive NMDA antagonists more severe motor abnormalities (increased locomotion, ataxia, stereotypy) are observed in rodents or primates than following the administration of pharmacologically comparable doses of competitive antagonists.

Competitive NMDA antagonists are therefore more promising candidates for anticonvulsant therapy, considering the chronic drug administration required under these conditions. For the acute therapeutic conditions encountered in ischemia management, competitive and non-competitive NMDA antagonists appear equally suitable as potential clinical cerebroprotective agents.

Introduction

The therapeutic potential of excitatory amino acid antagonists, especially those acting at the *N*-methyl-D-aspartate-(NMDA)-receptor, was recognized in the early 1980s, first as anticonvulsant agents [1] and subsequently as cerebroprotective agents. The ensuing explosive development of research relating to the function of the NMDA-receptor has confirmed and extended the original pharmacological observations and has firmly established the NMDA antagonists as the most potent wide-spectrum experimental anticonvulsants available, and has demonstrated a potent cerebroprotective activity of both competitive and non-competitive NMDA antagonists in a wide range of experimental ischemia and trauma models [2–5].

The aim of the present chapter is to evaluate, based on their action in appropriate rodent and primate models, the therapeutic potential of existing competitive and non-competitive NMDA antagonists in two clinical areas; as antiepileptic drugs, and as potential cerebroprotective agents administered following stroke or cardiac arrest.

Experimental procedures

Anticonvulsant studies

DBA/2 mice, in the age range of 16 to 30 days, are susceptible to sound-induced seizure [6]. Exposure to a sound-stimulus (109 dB) triggers a characteristic sequence of responses; a wild running phase (onset 1–5 second), followed by clonic seizures (onset 5–15 second), tonic extension (onset 8–20 second) and occasional respiratory arrest (20–30 second). Drugs or vehicle were administered to the mice by one of three routes; intraperitoneally (i.p., 0.1 ml per 10 g body weight), intracerebroventricularly (i.c.v.; 10 μl, or orally (p.o.; 0.2 ml per 10 g body weight). Optimal pretreatment times were determined by preliminary experiments and ranged typically around 30–60 min. Groups of around 10 mice were used per dose of drug, and ED_{50} values for the suppression of the different seizure phases were determined from dose response curves according to Litchfield and Wilcoxon method [7].

Photically-induced seizures in baboons. Intermittent light stimulation (ILS, 15–35/second) evokes a myoclonic response in 60% of baboons (Papio papio) from the Casamance region of Senegal [8]. Adolescent baboons, seated in a primate chair, were tested for seizure susceptibility at hourly intervals by exposure to stroboscopic stimulation for up to 5 min before and after drug administration [9]. Susceptible individuals responded to ILS with a graded response of 1) myoclonus of eyelids, 2) myoclonus of face and neck, 3) myoclonus of all limbs, and 4) myoclonus continuing beyond ILS. Drugs were administered intravenously (i.v.) or orally.

Global ischemia in rats

Blood pressure (BP), body temperature and blood gases were monitored and maintained within a narrow physiological range in paralyzed and ventilated rats. Transient incomplete forebrain ischemia was induced for 10 min by bilateral carotid occlusion and decrease in SP to 50 mmHg. Following the ischemic period, drugs or vehicle were administered twice i.p. (at 15 min and 5 h post-ischemically). The rats were allowed to recover for a 7 day period before their brains were assessed for hippocampal damage following perfusion fixation, Nissl staining of brain sections, and light microscopy examination of surviving neurons in the CA1 region of the hippocampus [10].

Regional cerebral glucose utilization

Glucose utilization was determined by the Sokoloff method following the i.v. administration of ^{3}H-2-deoxy-glucose to fasted, conscious male Wistar rats. Rats were pretreated with i.p. administration of either saline or an NMDA antagonist. Following decapitation 45 min after the ^{3}H-2-deoxy-glucose administration the

frozen brains were cut into 20 μm sections, which were placed in contact with ^{3}-H-sensitive film and developed along with ^{3}-H-standards. The resulting autoradiographs were analyzed for regional densities using an IBAS 2000 computerized densitometry system [11,12].

Results and Discussion

Competitive NMDA antagonists as anticonvulsant agents

Some of the most potent and selective competitive NMDA antagonists available are shown in the upper half of Fig. 1. The competitive antagonists are all structural analogues of the endogenous NMDA agonists, the dicarboxylic excitatory amino acids glutamate and aspartate, where one of the carboxylic acids have been replaced by a phosphonic acid group. A potent anticonvulsant activity was the first therapeutic property described for this group of compounds, when 2-amino-7-phosphonoheptanoic acid (AP7) and 2-amino-5-phosphono-pentanoic acid (AP5) were shown to protect against sound-induced seizures in DBA/2 mice [13]. More recently synthesized antagonists, 3-((±)-2-carboxypiperazin-4-yl)-propyl-1-phosphonate (CPP), CGS 19755, and CGP 37849 and its ethyl ester, CGP 39551, have subsequently been shown to be 10–20 fold more active than AP7 as NMDA antagonists in *in vitro* and *in vivo* studies [14].

The top half of Fig. 2 shows dose-dependent suppression of sound-induced clonic seizures in DBA/2 mice by the same competitive NMDA antagonists following their i.c.v. administration. CPP, CGS 19755, and CGP 37849 are approximately equipotent with ED_{50}, values 40, 20 and 40 pmol, respectively;

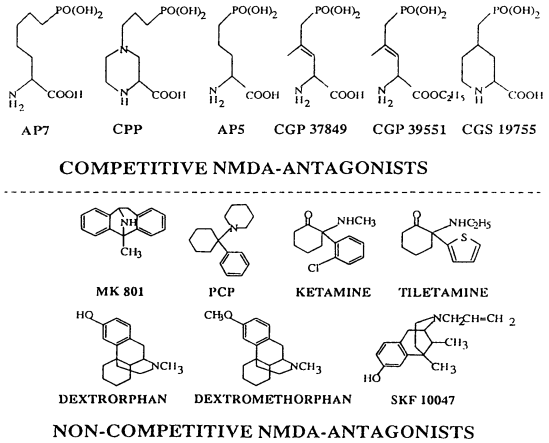

Fig. 1. Chemical structures of selected competitive and non-competitive NMDA antagonists.

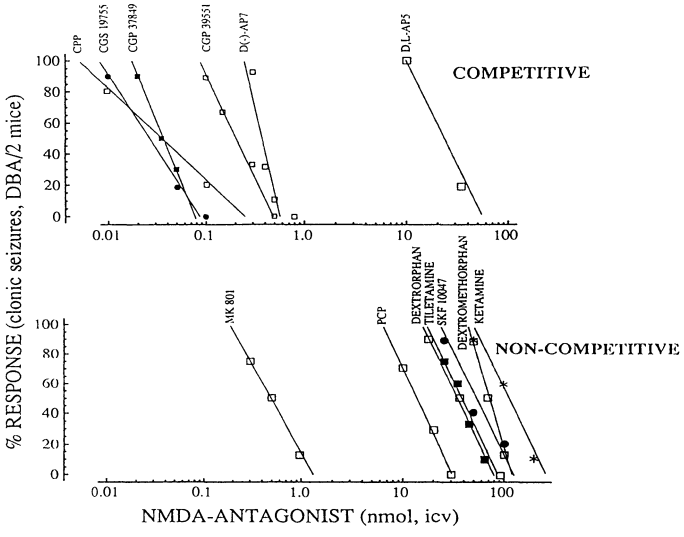

Fig. 2. Dose-dependent inhibition of sound-induced clonic seizures in DBA/2 mice following the i.c.v. administration of competitive (top) and non-competitive (bottom) NMDA antagonist. [1,7,11,14–17].

CGP 39551 is 5–10 fold less potent, with an icv ED_{50} value of 210; the corresponding icv ED_{50} values for AP7 and AP5 are 1.8 and 15 nmol, respectively. The same

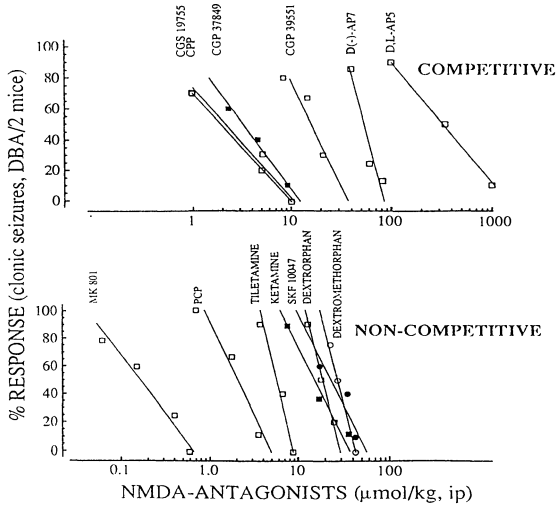

Fig. 3. Dose-dependent inhibition of sound-induced clonic seizures in DBA/2 mice following the i.p. administration of competitive (top) and non-competitive (bottom) NMDA antagonist. [1,7,11,14–17].

Table 1. Inhibition of seizures in rodent models by competitive NMDA-antagonists

	ED_{50} (μmol/kg, i.p.)					
	CPP	CGS 19755	CGP 37849	CGP 39551	AP7	AP5
DBA/2 mice, clonic	2.6	1.8	3.3	19.4	40	320
SS Gerbils					530	
ES, threshold	7.1				100	
MES	24.2	16.3	11.1	38.0	370	
NMDA	7.5	9.9			150	>800
PTZ	3.6				80	
3-MPA	6.0				60	
Receptor affinity (^{3}H-CPP displacement) K_i, μM	0.1–0.5	0.05–0.1	0.04	0.31	1.7	0.2–0.6

Binding data from [16,18]. Anticonvulsant data from: DBA/2 mice [1,14,16,17]; seizure susceptible gerbils [15,19]; electroshock threshold (ES) 3-mercaptopropionic acid (3-MPA) and pentylenetetrazol (PTZ) [20]; maximal electroshock (MES) [16,20–22]; NMDA [23,24].

ranking order and relative anticonvulsant potencies are encountered following the ip administration of the competitive NMDA antagonists to DBA/2 mice (top half, Fig. 3). The corresponding ED_{50} values are listed in the first line of Table 1, which also tabulates the anticonvulsant activities of the same antagonists in a number of rodent seizure models. With the exception of maximal electroshock seizures that require higher doses of competitive NMDA antagonists for their suppression, the anticonvulsant activities of the antagonists are quite consistent in the different seizure models. Table 1 also shows that the anticonvulsant activities of CPP, CGS 19755, CGP 37849, CGP 39551 and AP7 correlate directly with their affinities for the NMDA-receptor (measured as ^{3}H-CPP-displacement). AP5 represents an anomaly in this context, as its affinity for the NMDA-receptor and activity in *in vitro* electrophysiological studies [25] is 3–8 fold greater than that of AP7, while its *in vivo* pharmacological activity is consistently 3–10 fold less than that of AP7.

When some of the same competitive NMDA antagonists are used to protect against photically-induced seizures in baboons, the same ranking order and relative anticonvulsant activities are observed (Table 2). The Table also shows that the non-competitive NMDA antagonist, MK 801, is a remarkably potent anticonvulsant in this model, both compared to the competitive NMDA antagonists and to conventional antiepileptic drugs. However, as will be discussed in a later section, its administation at pharmacologically active doses is associated with acute motor abnormalities both in primates and in rodents.

Compared to antiepileptic drugs in current clinical use, the competitive NMDA antagonists have very potent anticonvulsant activity in rodent models, especially following central (i.c.v.) administration where they have been shown to be more

Table 2. Inhibition of photically induced seizures in baboons by NMDA-antagonists

	Fully protective dose mmol/kg i.v.
Competitive	
CGP 37849	0.18
CGP 39551	0.68
AP7	0.1
APS	3.3
Noncompetitive	
MK 801	0.0003
Anti epileptic drugs	
Diazepam	0.0018
Phenobarbital	0.065
Valproate	1.39

See references [5,9,26]

than 3 orders of magnitude more potent than benzodiazepines, the most potent of existing antiepileptic drugs [5]. Despite a relatively poor uptake of the competitive NMDA antagonists into the brain [27], the anticonvulsant efficacies of the competitive NMDA antagonists compare favorably with those of the existing antiepileptic drugs even following systemic (i.p.) administration [5]. The recent introduction of two competitive NMDA antagonists, CGP 37849 and CGP 39551, with potent anticonvulsant activity in rodents and primates following oral administration [5,17,22] heralds an encouraging development towards possible clinical use of these NMDA antagonists. Furthermore, the anticonvulsant protection provided by one of these compounds, CGP 39551, is exceptionally long-lasting (in excess of 2 days) following i.p. or oral administration both in rodents and baboons.

Chronic (9 days) administration twice daily to DBA/2 mice did not affect the anticonvulsant potency of AP7 [3], however, more prolonged administration in additional seizure models are required to establish if the development of tolerance will diminish the anticonvulsant potencies of NMDA antagonists.

Non-competitive NMDA antagonists as anticonvulsant agents

A heterogenous group of compounds, including MK 801, phencyclidine (PCP), sigma receptor ligands (SKF 10047), the 'dissociative anasthetic', ketamine, and morphinan derivatives, dextrorphan and dextromethorphan, act as non-competitive antagonists at the NMDA receptor, at a 'use-dependent' site proposed to be located within the ion channel of the NMDA receptor complex [28]. The structures of a selection of these non-competitive NMDA antagonists are shown in the bottom part of Fig. 1. Anticonvulsant activity was attributed to MK 801 [29–31] and PCP [32] before it was known that these compounds act as NMDA antagonists.

Table 3. Inhibition of seizures in rodent models by noncompetitive NMDA-antagonists

	ED_{50} (μmol/kg, i.p.)					
	Mk 801	PCP	Dextrorphan	SKF 10047	Dextromethorp.	Ketamine
DBA/2 mice, clonic	0.14	1.9	18.5	23.5	28.0	15.5
Spont. absence, rats	0.3					
Kindled, motor	0.6–0.8	17.9			99	
MES	0.44	5.4–21.4	23.7	24.1	33.5	55.1
Quinolinate	0.6					102
PTZ, tonic		10.7–13.5		34.1		73
Receptor affinity (^{3}H-TCP displacement) K_I, nM	3.8	52.9	470.0	311.4		812.8

Binding data from [ref. 15,33]. Anticonvulsant data from: DBA/2 mice [27]; spontaneous absence seizures [34]; kindled seizures [32,35–37]; maximal electroshock (MES) [20,29,38–41]; quinolinate [42,43]; pentylenetetrazol (PTZ) [20,44].

Subsequent studies have shown that all the non-competitive NMDA antagonists have anticonvulsant activity in a number of rodent seizures models (Table 3), as well as in baboons (Table 2). MK 801 is the most potent of the non-competitive NMDA antagonists available, and the ED_{50} values for seizure protection is similar (0.15–0.8 μmol/kg i.p.) in all the rodent seizure models listed in Table 3. PCP is around 10 fold less potent than MK 801, while dextrorphan, SKF 10047, dextromethorphan and ketamine are grouped together as being around 100 fold less potent than MK 801 as anticonvulsant agents. The ranking order and the relative anticonvulsant potencies of the non-competitive NMDA antagonists correlate perfectly with their affinities for the NMDA receptor (measured as ^{3}H-TCP displacement) as shown at the bottom of Table 3.

A direct comparison of the anticonvulsant potencies of the competitive and the non-competitive NMDA antagonists against sound-induced seizures in DBA/2 mice are shown in Fig. 2 (i.c.v. administration) and Fig. 3 (i.p. administration). Following i.c.v. administration, only MK 801 approaches the most active of the competitive antagonists (Fig. 2). However, this situation is altered when the same compounds are assessed as anticonvulsants following their systemic administration. The blood-brain barrier penetration is more favorable for the non-competitive than for the competitive NMDA antagonists, making MK 801 10–20 fold more potent than the best of the competitive antagonists following i.p. administration, while the remaining non-competitive NMDA antagonists match the anticonvulsant potencies of leading competitive antagonists. However, as will be discussed in the following section, the therapeutic ratio (dose required for anticonvulsant action versus dose producing behavioral side-effects) appears to be less favorable for the non-competitive than for the competitive NMDA antagonists.

Effect of NMDA atagonists on behavior and regional cerebral metabolism

Following the demonstration of an interaction between PCP and the NMDA receptor, the remaining NMDA antagonists, competitive and non-competitive, have been scrutinzed for possible signs of inducing PCP-like behavior in animals [45]. Three approaches to assessing the behavioral correlates of NMDA antagonism will be considered; 1) observation of acute motor function and overt behavioral excitation following antagonist administration to unconditioned animals, 2) test for the ability of antagonists to substitute for PCP (or NMDA or ketamine) in animals trained to discriminate between PCP and saline, and 3) determine the effect of NMDA antagonists on regional metabolic rates (glucose utilization) in the brain.

Systemic administration of competitive NMDA antagonists (AP7, AP5, and CGS 19755) causes ataxia in rodents (assessed by direct observation, or by impaired performance in rotarod or horizontal screen tests) at doses that range from 3–35 fold their anticonvulsant ED_{50} values [38,46–48]. Leander *et al.* [41] have reported a similar 'protective index' (ED_{50} for motor impairments divided by anticonvulsant ED_{50} value), range from 1.2–5, for the non-competitive NMDA antagonists, in general agreement with similar ratios (0.2–7 fold) reported by other authors [31,47,49]. Hence, both competitive and non-competitive NMDA antagonists induce ataxia in rodents, but the therapeutic ratio is slightly more favorable for the competitive antagonists.

Stereotypy (increased locomotion, rearing, sniffing, gnawing, head-bobbing, grooming) is commonly observed following non-competitive antagonists (at approximately 2–5 fold anticonvulsant dose), but is only observed at very much higher doses of competitive NMDA antagaonists (25–70 fold anticonvulsant dose) [30,38,47,48,50]. Competitive NMDA antagonists have been reported to cause stereotypy following focal injection into specific brain structures, or following i.c.v. administration at high concentrations [45].

Drug discrimination studies have shown that both non-competitive (MK 801, PCP, ketamine) and competitive (AP7, CPP, CGS 19755) antagonists will antagonize a NMDA-discriminative cue in a dose-dependent fashion in rats [48]. In rhesus monkeys trained with a ketamine discriminative stimulus, MK 801 will potently substitute for ketamine, but CGS 19755 will not [52]. In rats trained with a PCP discriminative stimulus, both MK 801 and ketamine will readily substitute for PCP, whereas systemically administered AP7 (330 μmol/kg, or 8 fold the anticonvulsant ED_{50} value) will not. However, following i.c.v. administration (13–26 nmol i.c.v., or 7–15 fold anticonvulsant ED_{50} value) even AP7 will substitute for PCP [53]. Therefore, both competitive and non-competitive antagonists will recognize an agonist (NMDA) cue, but it is less certain whether competitive antagonists will recognize a non-competitive antagonist cue when the compounds are administered at reasonable doses (compared to anticonvulsant potencies) in rodents or monkeys.

Large increases in regional cerebral metabolic rates (and blood flow) are frequently encountered during seizures [54], while the administration of anti-

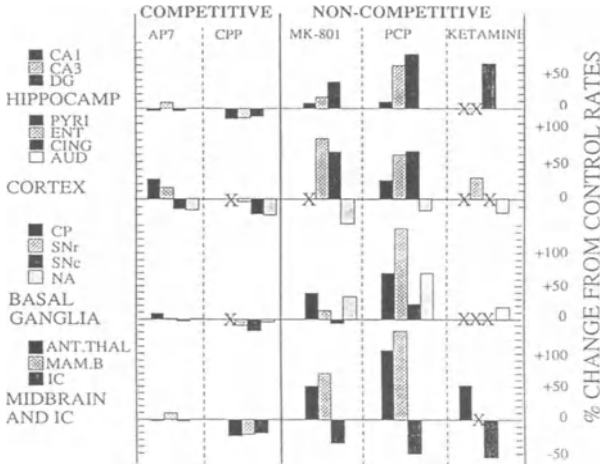

Fig. 4. The effect of competitive and non-competitive NMDA antagonists on the regional cerebral metabolic rates in selected brain structures of rat. The regional rates of glucose utilization in antagonist-treated rats are expressed as percent of matched regional control rates in hippocampal areas (CA1, CA3 and dentate gyrus), cortical areas (pyriform-, entorhinal-, cingulate- and auditory-cortex), basal ganglia areas (caudate putamen, substantia nigra reticulata, substantia nigra compacta, nucleus accumbens), and midbrain structures (anterior thalamus, mamillary bodies and inferior colliculus) Antagonist doses administered (μmol/kg, i.p.) were; AP7, 500; CPP, 40; MK 801, 1.5-3; PCP, 14-18; ketamine 365. [11,12,17,59–64].

epileptic drugs generally has a modest generalized inhibitory effect on metabolism [55–58].

Figure 4 summarizes the effects of pharmacologically comparable doses (10–20 fold their anticonvulsant ED_{50} values) of competitive and non-competitive NMDA antagonists on regional metabolic rates in rat brain. PCP administration [60,61,63] produces a characteristic pattern of regional activation where the limbic areas, substantia nigra, cingulate cortex, anterior thalamus and mamillary bodies exhibit activation (up to 2–3 fold) of glucose utilization, while the rates of glucose utilization in the auditory cortex and inferior colliculus are selectively inhibited. This pattern of regional PCP-induced metabolic activation is closely mirrored by MK 801 [12,62,64,65] and ketamine [59]. However, the administration of pharmacologically comparable doses of the competitive NMDA antagonists, CPP and AP7, has only a very minor effect on regional metabolic rates [11,12,17,63], suggesting that the competitive NMDA antagonists have a less severe effect on cerebral metabolism than do the non-competitive antagonists.

NMDA antagonists as cerebroprotective agents

The cerebroprotective actions of excitatory amino antagonists have recently been extensively reviewed [66] and only a brief summary will be provided here.

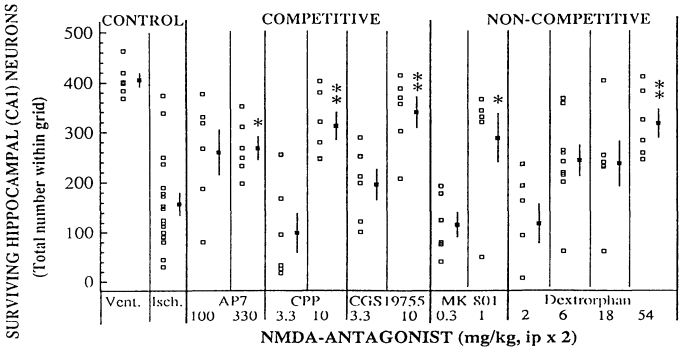

Fig. 5. Protection against delayed hippocampal neuronal loss following transient (10 min) forebrain ischemia in rats by the systemic administration of competitive and non-competitive NMDA antagonists. The numbers below the names of the antagonists indicate doses administered twice (15 min and 5 h postischemically) expressed in mg/kg. [10].

Selective neuronal loss occurs in the CA1 region of the hippocampus following 10 min of ischemia and 7 day survival [10]. Fig. 5 shows that only around 160 (or 40%) of the neurons in the hippocampal CA1 region survive the ischemic insult in a rat. Competitive (AP7, CPP and CGS 19755) and non-competitive (MK 801, dextrorphan) NMDA antagonists administered systemically after the ischemic episode (i.p. twice, at 15 min and 5 h from the onset of ischemia) provide a dose-dependent protection against this selective delayed neuronal death. The relative cerebroprotective potencies (lowest dose that gives significant protection against neuronal loss during ischemia) of the NMDA antagonists correlate with their anticonvulsant activities and with their affinities for the NMDA receptor. The NMDA antagonists are believed to protect against ischemic cell damage by blocking excessive excitatory action of glutamate or aspartate at the postsynaptic receptor during the early reperfusion phase. It has been demonstrated that there is an increased release of glutamate and aspartate, an increased burst firing, and an increased calcium influx during this phase [66]. The 'permitted' delay between the ischemic episode and the administration of a protective dose of NMDA antagonist, varies between species. In gerbils it was observed that MK 801 could be administered as late as 24 h following a 2 vessel occlusion and still provide significant protection against ischemic cell damage [67]. However, in rats the time window is smaller. When competitive (CGS 19755) and non-competitive (MK 801) antagonists were administered 5 h and 10 h after the ischemic episode, no significant cerebro-protection was observed [10].

Table 4 summarizes a series of different ischemia/hypoxia/trauma studies where excitatory amino acid antagonists have been reported to provide significant protection against neuronal loss or to reduce the infarct size of the affected brain area. In the majority of the studies the antagonists were administered following the ischemic episode (15 min to 24 h). The pattern of protection provided by competi-

Table 4. Protection by NMDA antagonists against ischemic cell damage in different ischemia and trauma models in rodents

Model	Drug	Dose mg/kg i.p. unless indicated	Time drug adm (h) (Time 0=onset isch)	Reference
Global ischaemia				
2 VO Gerbils	MK 801	0.3– 1.0	1	68
		3 – 10	2,24	67
	APH	100 × 4	0,2,4,6	69
	CGS 19755	10 × 4	–0.25,2,4,6	70
	CPP	30 × 4	0.25,2,4,6	70
2 VO Rats	APH	675 × 3	0,4,10	71
		300 × 2	0.25,5	10
	CPP	10 × 2	0.25,5	10
	CGS 19755	10 × 2	0.25,5	10
	MK 801	1 × 2	0.25,5	10
	Dextrorphan	54 × 2	0.25,5	10
Middle cerebral artery occlusion				
Rats	MK 801	0.5	–0.5 or 0.5	72
	Kynurenate	300 × 3	0,4,8	73
Fischer 344	SL 82.0715	1 p.o.	0.5	74
	TCP	1 i.p.	0	74
Mice	MK 801	0.3	0.1,6,18	75
	SL 820715	1 i.p.	0.1,6,18	75
Cats	MK 801	5.0		76
	Ifenprodil	3		74
Neonatal hypoxia/ischaemia				
Rats	Dextrorphan	10–35		77
	Kynurenate	300		78
	MK 801	1	–1 or +1.25	79
CNS trauma				
Rat spinal cord	MK 801	1 i.v.	0.25	80
Rat brain	Dextrorphan	10 i.v.	0.5	81
	CPP	100 μg i.c.v.	0	81

tive and non-competitive antagonists is similar, and there is no rational basis at this point for preferring one antagonist above the others as the principle cerebroprotective candidate.

References

1. Croucher MJ, Collins JF and Meldrum BS (1982) Science 216: 899–901.
2. Schwarcz R and Meldrum BS (1985) The Lancet ii: 140–143.

3. Chapman AG (1988) Frontiers in Excitatory Amino Acid Research. In: Cavalheiro EA, Lehmann J and Turski L (eds.) Neurology and Neurobiology. Alan R. Liss, New York. Vol. 46, pp. 203–210.
4. Patel S, Chapman AG, Millan MH and Meldrum BS (1989) In: Lodge D (ed.) Excitatory Amino Acids in Health and Disease. John Wiley & Sons, Chichester. pp. 353–378.
5. Meldrum BS, Chapman AG, Patel S and Swan JH (1989) In: Watkins JC and Collingridge G (eds.) The NMDA Receptor. IRL Press, Oxford, pp. 207–216.
6. Chapman AG and Meldrum BS (1987) In: Jobe PC and Laird II, HE (eds.) Neurotransmitters and Epilepsy. The Humana Press, Clifton, New Jersey. pp. 9–40.
7. Chapman AG and Meldrum BS (1990) Eur. J. Pharmacol. 178: in press.
8. Naquet R and Meldrum BS (1972) In: Purpura D, Penry JK, Tower DB, Woodbury DM and Walter RD (eds.) Experimental Models of Epilepsy. Raven Press, New York. pp. 373–406.
9. Meldrum BS, Croucher MJ, Badman G and Collins JF (1983) Neurosci. Lett. 39: 101–104.
10. Swan JH and Meldrum BS (1990) J. Cereb. Blood Flow Metab., in press.
11. Chapman AG, Swan JK and Meldrum BS (1989b) J. Cereb. Blood Flow Metab. 9 Suppl. 1, s310.
12. Kurumaji A, Nehls DG, Park CK and McCulloch J (1989) Brain Research, in press.
13. Deleted in proof.
14. Chapman AG, Meldrum BS, Nanji N and Watkins JC (1987) Eur. J. Pharmacol. 139: 91–96.
15. Lehmann J, Hutchison AJ, McPherson SE, Mondadori C, Schmutz M, Sinton CM, Tsai C, Murphy DE, Steel DJ, Williams DL, Cheney DL and Wood PL (1988a) J. Pharm. Exp. Ther. 246: 65–75.
16. Lehmann J, Chapman AG, Meldrum BS, Hutchison A, Tsai C and Wood PL (1988b) Eur. J. Pharmacol. 154: 89–93.
17. Chapman AG, Graham JL and Meldrum BS (1989a) J. Cereb. Blood Flow Metab. 9 Suppl. 1, s309.
18. Fagg GE, Olpe HR, Bittiger H, Schmutz M, Angst C, Brundish D, Allgeier H, Heckendorn R and Dingwall JG (1988) 18th Annual Meeting of Society for Neuroscience Toronto Nov. Abstract 381.1 pp. 13–18.
19. Löscher W (1985) J. Pharm. Exp. Ther. 233: 204–213.
20. Nevins ME and Arnold SM (1987) 17th Annual Meeting of Society for Neuroscience, New Orleans, Nov. Abstract 432.6 pp. 16–21.
21. Czuczwar SJ, Cavalheiro EA, Turski L, Turski WA and Kleinrok Z (1985a) Neurosci. Res. 3: 86–90.
22. Schmutz M, Kleps K, Olpe HR, Fagg GE, Allgeier H, Heckendorn R, Angst C, Brundish D, Dingwall JG (1988) 18th Annual Meeting of Society for Neuroscience, Toronto, Nov. Abstract 345.3 pp. 13–18.
23. Czuczwar SJ, Frey HH and Löscher W (1985b) Eur. J. Pharmacol. 108: 273–280.
24. Lehmann J, Schneider J, McPherson S, Murphy DE, Bernard P, Tsai C, Bennett DA, Pastor G, Steel DJ, Boehm DL, Cheney JM, Liebman JM, Williams M and Wood PL (1987) J. Pharm. Exp. Ther. 240: 737–746.
25. Watkins JC and Olverman HJ (1987) Trend Neurosci. 10: 265–272.
26. Naquet R and Meldrum BS (1986) In: Fahn S, Marsden, CD, and Woert MV (eds.) Advances in Neurology. Raven Press, New York. Vol 43, pp. 611–627.
27. Chapman AG, Collins JF, Meldrum BS and Westerberg E (1983) Neurosci. Lett. 37: 75–80.
28. Kemp JA, Foster AC and Wong EHF (1987) Trend Neurosci. 10: 294–298.
29. Clineschmidt BV, Martin GE and Bunting PR (1982a) Drug Dev. Res. 2: 123–134.
30. Clineschmidt BV, Martin GE, Bunting PR and Papp NL (1982b) Drug Dev. Res. 2: 135–145.
31. Clineschmidt BV, Williams M, Witoslawski JJ, Bunting PR, Risley EA and Totaro JA (1982c) Drug Dev. Res. 2: 147–163.
32. Freeman FM, Jarvis MF and Duncan P (1982) Pharmacol. Biochem. Behav. 16: 1009–1011.
33. Sircar RM, Rappaport M, Nictenhauser R and Zukin SR (1987) Brain Research 435: 235–240.
34. Peeters BWMM, Van Rijn CM, Van Luijtelaar ELJM and Coenen AML (1989) Epilepsy Res. 3: 178–181.
35. McNamara JO, Russell RD, Rigsbee L and Bonhaus DW (1988) Neuropathol. 27: 563–568.
36. Williamson JM and Lothman EW (1989) Ann. Neurol. 26: 85–90.

37. Feeser HR, Kadis JL, Wong BY and Prince DA (1987) 17th Annual Meeting of Society for Neuroscience New Orleans, Nov. Abstract 317.12 16–21.
38. Ornstein P, Zimmerman DM, Hynes MD and Leander JD (1987) In: Nick TP, Lodge D and McLennan H (eds.) Excitatory Amino Acid Transmission. Alan R. Liss, New York. pp. 123–126.
39. Tortella F and Musacchio JM (1986) Brain Research 383: 314–318.
40. Tortella F, Ferkany JW and Potecorvo MJ (1988) Life Science 42: 2509–2514.
41. Leander JD, Rathburn RC and Zimmerman DM (1988a) Brain Research 454: 368–372.
42. Marranes R and Wauquier A (1987) Neuroscience (Suppl.) s663.
43. Vezzani A, Stasi MA, Serafini R, Wu HQ and Samanin R (1988) Frontiers in Excitatory Amino Acid Research. In: Cavalheiro EA, Lehmann J and Turski L (eds.) Alan R. Liss, New York. Neurology and Neurobiology, Vol. 46, pp. 279–286.
44. Hayes BA and Balster RL (1985) Eur. J. Pharmacol. 117: 121–125.
45. Snell LD and Johnson KM (1988) In: Lodge D (ed.) Excitatory Amino Acids in Health and Disease. John Wiley & Sons, Chichester. pp. 261–273
46. Bennett DA and Amrick CL (1986) Life Science. 39: 2455–2461.
47. Compton RP, Contreras PC, O'Donohue TL and Monahan JB (1987) Eur. J. Pharmacol. 136: 133–134.
48. Bennett DA, Bernard PS, Amrick CL Wilson DE and Hutchison AJ (1987) 17th Annual Meeting of Society for Neuroscience, New Orleans, Nov. Abstract 433.17 pp. 16–21.
49. Koek W and Woods JK (1988) Frontiers in Excitatory Amino Acid Research, In: Cavalheiro EA, Lehmann J and Turski L (eds.) Neurology and Neurobiology. Alan R Liss, New York, Vol 46, pp. 535–542.
50. Koek W and Woods JH and Ornstein P (1987) Psychopharmacol. 91: 297–304.
51. Amrick CL and Bennett DA (1987) 17th Annual Meeting of Society for Neuroscience, New Orleans, Nov. Abstract 433.16 pp. 16–21.
52. France CP Woods JH and Ornstein P (1989) Eur. J. Pharmacol. 159: 133–139.
53. Tricklebank MD, Singh L, Oles RJ, Wong EHF and Iversen SD (1987) Eur. J. Pharmacol. 141: 497–501.
54. Chapman AG (1985) In: Pedley TA and Meldrum BS (eds.) Recent Advances in Epilepsy. Churchill Livingstone, Edinburgh. Vol. 2, pp. 19–63.
55. Theodore WH, Bairamian D, Newmark ME, DiChiro G, Porter RJ, Larson S and Fishbein D (1986) J. Cereb. Blood Flow Metab. 6: 315–320.
56. Kelly PAT and McCulloch J (1986) Neuroscience 19: 257–265.
57. Cudennec A, Duverger D, Lloyd KG, MacKenzie ET, McCulloch J, Motohasbi N, Nishiknwa T and Scatton B (1987) Brain Research 423: 162–172.
58. Theodore WH, Bromfield E and Onorati L (1989) Ann. Neurol. 25: 516–520.
59. Cavazzuti M, Porro CA, Biral GP, Benassi C and Barbieri GC (1987) J. Cereb. Blood Flow Metab. 7: 806–811.
60. Tamminga CA, Taqnimoto K, Kuo S, Chase TN, Contreras PC, Rice KC, Jackson AE, O'Donohue TL (1987) Synapse 1: 497–504.
61. Weissman AD, Dam M, London ED (1987) Brain Research 435: 29–40.
62. Nehls DG, Kurumaji A, Park CK and McCulloch J (1988) Neurosci. Lett. 91: 204–210.
63. Piercey MF and Ray CA (1988) Life Science 43: 379–385.
64. Piercey MF, Hoffmann WE and Kaczkofsky P (1988) Psychopharmacol. 96: 561–562.
65. Cavazzuti M, Porro CA, Bonatesta P and Barbieri GC (1989) J. Cereb. Blood Flow Metab. 9 Suppl. 1, s287.
66. Meldrum BS (1990) Cereb. Brain Metab. Rev. 2: 27–57.
67. Gill R, Foster AC and Woodruff GN (1988) Neurosci. 25: 847–855.
68. Gill R, Foster AC and Woodruff GN (1987) J. Neurosci. 7: 3343–3349.
69. Boast CA, Gerhardt SC and Janak P (1987) In: Hick TP, Lodge D and McLennan H (eds.). Excitatory Amino Acid Transmission. Alan R. Liss, New York. pp. 249–252.
70. Boast CA, Gerhardt SC, Pastor G, Lehmann J, Etienne PE, Liebmann JM (1988) Brain Research 442: 345–348.

71. Swan JH, Evans MC, Meldrum BS (1988) J. Cereb. Blood Flow Metab. 8: 64–78.
72. Park CK, Nehls DG, Graham DI, Teasdale GM and McCulloch J (1988) Ann. Neurol. 24: 543–551.
73. Germano IM, Pitts LH, Meldrum BS, Bartkowski KM, and Simon RP (1987) Ann. Neurol. 22: 730–734.
74. Gotti B, Duverger D, Bertin J, Carter C, Dupont R, Frost J, Gaudilliere B, MacKenzie ET, Rousseau J, Scatton B, and Wick A (1988) J. Pharm. Exp. Ther. 247: 1211–1220.
75. Benavides J, Cornu P, Dubois A, Gotti B, Mackenzie ET and Scatton B (1989) In: Krieglstein J (ed.) Pharmacology of Cerebral Ischemia 1988. CRC Press, Boca Raton, Florida. pp. 187–196.
76. Ozyurt E, Graham DI, Woodruff GM and McCulloch J (1988) J. Cereb. Blood Flow Metab. 8: 138–143.
77. Prince DA and Feeser HR (1988) Neurosci. Lett. 85: 291–296.
78. Andine P, Lehmann A, Ellren K, Wennberg E, Kjellmer I, Nielsen T and Hagberg H (1988) Neurosci. Lett. 90: 208–212.
79. McDonald JW, Silverstein FS and Johnston MV (1987) Eur. J. Pharmacol. 140: 359–361.
80. Faden Al and Simon RP (1988) Ann. Neurol. 23: 623–626.
81. Faden Al, Demediuk P, Panter SS and Vink R (1989) Science 244: 798–800.

Address for correspondence: A.G. Chapman, Department of Neurology, Institute of Psychiatry, De Crespigny Park, Denmark Hill, London SE5 8AF, U.K.

Differential effects of competitive and noncompetitive NMDA receptor antagonists on GABA turnover in the mouse brain

Raymond Bernasconi, Therese Leonhardt, Pierre Martin, Anne F. Steulet, Chantal Portet, Kurt Stöcklin, Graham Fagg and Markus Schmutz

Research and Development Department, Pharmaceuticals Division, CIBA-GEIGY Ltd, CH-4002 Basle, Switzerland

Abstract

The modulation of GABA-mediated neurotransmission by excitatory amino acid inputs was examined by testing the effects of competitive NMDA receptor antagonists (CPP, CGS 19755, CGP 37849 and CGP 39551) and noncompetitive antagonists (dizocilpine, PCP, ketamine, dextromethorphan and SKF 10047) on the rate of GABA synthesis and depletion, two indices of GABAergic neuronal activity. The rate of GABA synthesis in the mouse was assessed in four brain regions by the elevation in GABA levels after inhibition of GABA-T with gabaculine. The rate of GABA depletion was estimated from the decrease in GABA concentrations observed after inhibition of GAD with isoniazid. The administration of anti-convulsant doses of all competitive NMDA antagonists dose-dependently decreased the rate of GABA synthesis. With the exception of CGP 39551, the time course of effects of competitive antagonists on the rate of GABA synthesis corresponded with the time course of their anticonvulsant potencies. Unlike the competitive antagonists, the noncompetitive blockers, dizocilpine, PCP, dextromethorphan and SKF 10047 had no effect on the rate of GABA synthesis.

The competitive NMDA receptor antagonists did not alter the rate of GABA depletion, but dose-dependently prolonged the latency to isoniazid-induced seizures. The time course for this anti-isoniazid effect correlated with that observed in other epilepsy models; i.e. it lasted more than 24 h in the case of CGP 39551 (60 mg/kg) and less than 24 h with CGS 19755 (10 mg/kg) and CGP 37849 (30 mg/kg). Dizocilpine (0.3 mg/kg) showed moderate and dextromethorphan (30 mg/kg) no anticonvulsant properties in this model.

These results indicate that GABAergic pathways are subject to regulation by GLU-mediated excitatory transmission and suggest that NMDA receptors are involved in this interaction.

In the mammalian CNS, GABA and L-glutamate (GLU) are the major transmitters mediating inhibitory and excitatory synaptic events, respectively. Alterations in transmission mediated by these two amino acids have been proposed to play a critical role in several animal models of epilepsy [1]. GLU exerts its effects via distinct receptor subtypes which are named according to the preferred agonists, i.e. *N*-methyl-D-aspartate (NMDA), kainate (KA), and quisqualate (QA) [2]. Studies utilizing selective antagonists have shown that NMDA receptors are critically involved in epileptogenesis and that these compounds possess anticonvulsant properties [3]. Perhaps surprisingly, NMDA receptor antagonists block seizures induced not only by hyper-activation of GLUergic neurons, but also those elicited by impairment of GABA-mediated inhibition. Thus, seizures induced by 3-

mercaptopropionic acid (which blocks GABA release; [4]), or by the convulsant ß-carboline, DMCM, (an inverse agonist at the GABA/benzodiazepine receptor complex; [5]) are potently blocked by the competitive receptor antagonist 2-amino-7-phosphonoheptanoate (2-APH) [3,6]. Noncompetitive NMDA receptor antagonists also protect against convulsions induced by impairment of GABA-mediated inhibition, and dizocilpine is one of the most potent anticonvulsants in antagonizing bicuculline-elicited seizures [7]. These and other results indicate that, whatever their primary mechanism of induction, epileptic seizures represent the summed effects of abnormal firing in both excitatory and inhibitory neurotransmitter systems. As a means of characterizing the interactions between GLU and GABA neuronal systems, we have examined the effects of four competitive antagonists of NMDA receptors (CPP, CGS 19755, CGP 37849 and CGP 39551; Fig. 1) [8–12] on the rates of GABA synthesis and depletion in four brain regions and compared them with those of the noncompetitive antagonists, dizocilpine, phencyclidine (PCP), ketamine, dextromethorphan and SKF 10047 [see 13]. We report that competitive and noncompetitive antagonists differ in their effects on GABA-mediated inhibitory transmission (Fig. 1).

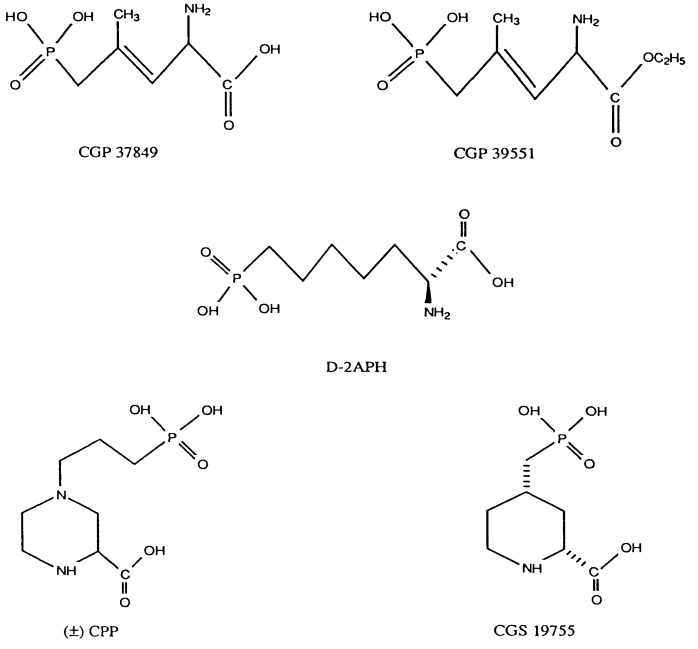

Fig. 1. Structures of various competitive antagonists of NMDA. CGP 37849 and CGP 39551 are, at the moment, the only orally active NMDA antagonists.

Experimental procedures

Animals

Male Tif:MAGf (SPF) mice, 21–22 g body-weight, 4–6 weeks of age (Tierfarm Sisseln, Switzerland) were used. Mice were housed (8 mice per cage) for 2 to 5 days before the experiments, with a light-dark cycle of 12–12 h. All experiments were performed between 8:30 and 11:00 a.m.

Drug treatment

The following drugs were used: isoniazid (Fluka), CPP (Tocris Neuramin), PCP, ketamine and SKF 10047 (Research Biochemicals Incorporated), and dextromethorphan (Sigma). Gabaculine, CGP 37849, CGP 39551 and CGS 19755 were synthesized in the laboratories of CIBA-GEIGY at Basel and Summit. Dizocilpine was a gift from Merck Sharp and Dohme Research Laboratories, Harlow, U.K. All compounds were dissolved in 0.9% saline, the pH adjusted to 5–7, and administered i.p. or s.c. The volumes for i.p. and s.c. injection were 10 and 4 ml/kg body-weight, respectively.

Measurement of steady-state GABA levels

Mice were sacrificed by microwave irradiation, decapitated, the brains removed, cooled on dry ice, dissected immediately into four regions and extracted as described previously [14]. This procedure prevents post-mortem increases in GABA content. The brain extracts were analyzed by gas-chromatographic analysis according to procedure already described [14,15].

Measurement of the rate of GABA synthesis

The rate of GABA synthesis in the mouse brain was assessed by the elevation in GABA levels after inhibition of 4-aminobutyrate: 2-oxoglutarate aminotransferase (EC 2.6.1.19; GABA-T) with gabaculine. The method has been reported previously [14], the dose of gabaculine used was 150 mg/kg i.p. and mice were sacrificed 60 min after injection of the GABA-T inhibitor.

Measurement of the rate of GABA depletion

The rate of GABA depletion was estimated from the decrease in GABA concentrations observed after inhibition of L-glutamate-1-decarboxylase (EC 4.1.1.15: GAD), a marker of the neuronal GABA pool, with isoniazid. The content of cortical GABA was measured according to Bernasconi *et al.* [16]. The measurement of GABA was performed in pairs consisting of a protected and a non-protected animal: Mice were sacrificed at the onset of seizures (t_{iso}, $t_{CGP37849}$, $t_{CGP39551}$ etc),

and just after a 'non-protected' mouse had been sacrificed, another mouse which did not show preconvulsive behaviour was also sacrificed. The latter mice formed the 'protected group'. The rate of GABA synthesis and of GABA depletion are dependent on nerve impulse flow [17,18], and reflect changes in GABAergic neuronal activity.

Isoniazid-induced seizures

Concomitantly to the measurement of the rate of GABA depletion, the anti-convulsant effects (prolongation of the latency to the onset of seizures and percentage of mice with and without convulsions) were also measured. In male mice, clonic seizures, followed in most animals by tonic convulsions, were induced by injection of 250 mg/kg isoniazid i.p.. Fifteen mice were used for each group. After the injection of isoniazid the animals were observed for 2 h, and the time to onset of seizures and the pattern of the convulsion types were recorded.

Statistics

Results were expressed as means ± S.E.M. Drug-treated mice were compared to saline-treated animals by the multiple comparison of Dunnet.

Results

Effects of NMDA-antagonists on the rate of GABA synthesis

CGP 37849 (injected 2 h before sacrifice) did not alter steady-state levels of GABA in the mouse brain, but it potently and dose dependently decreased its rate of synthesis (Fig. 2). The effects were observed in the cortex and hippocampus (Fig. 2) as well as in the striatum and cerebellum (results not shown). The threshold dose was less than 3 mg/kg i.p. in the four brain structures. At 30 mg/kg the reduction was more than 60%, the extent being similar in all brain structures. Severe side effects (ataxia, sedation) observed at 30 mg/kg prevented the injection of higher doses.

CGP 39551 produced a weaker effect on the rate of GABA synthesis than CGP 37849: the threshold dose was between 3 and 6 mg/kg i.p. and at 30 mg/kg the decrease was less than 30–35%. The threshold dose for CGS 19755 was between 1 and 3 mg/kg i.p., peak effects were observed after the administration of 10 mg/kg (50–60% reduction of the rate of GABA synthesis) which then levelled off. The decrease of the rate of GABA synthesis elicited by CPP was weaker than with CGS 19755.

Dizocilpine (0.1, 0.3, 0.6 mg/kg i.p.), PCP (3, 10, 30 mg/kg i.p.), dextro-methorphan (3, 10, 30 mg/kg i.p.) and SKF 10047 (6, 20 and 60 mg/kg s.c.) changed neither GABA levels nor its rate of synthesis. The effects of these

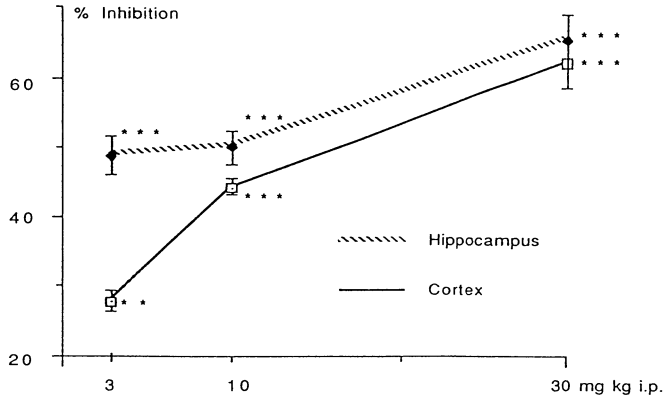

Fig. 2. Dose-dependent increase in the inhibition of cortical and hippocampal rate of GABA synthesis by CGP 37849. CGP 37849 was injected 60 min before gabaculine (150 mg/kg i.p.) and mice were sacrificed 60 min later. The data are expressed as percent inhibition of the rate of GABA synthesis in controls and are given as means ± S.E.M. for groups of six mice. Cortical GABA levels were: saline group 1.57 ± 0.05 μmol/g, gabaculine group 6.04 ± μ0.15 μmol/g, CGP 37849 (30 mg/kg) 1.47 ± 0.07 μmol/g, CGP 37849 (30 mg/kg) + gabaculine 3.12 ± 0.18 ***μmol/g, CGP 37849 (10 mg/kg) + gabaculine 3.91 ± 0.10 ***μmol/g, CGP 37849 (3 mg/kg) + gabaculine 4.64 ± 0.24 **μmol/g. Statistical calculations were made by means of Dunnett's test, ** $p<0.01$, *** $p<0.001$ when compared to the gabaculine treated group.

compounds were evaluated at a time corresponding to their peak anticonvulsant effects [12]. In addition, dizocilpine was also tested 1, 2, 4, 8 and 16 h after administration and found to be either inactive or marginally active (10% inhibition in the striatum at 4 h). Ketamine, which is a moderate to weak inhibitor of GABA uptake [19], had no effect on steady-state GABA levels, but reduced the rate of synthesis: the inhibition was 20–40% at 30 mg/kg i.p.

Time course for the decrease in the rate of GABA synthesis elicited by NMDA receptor antagonists

The peak inhibition of GABA synthesis by CGP 37849 (10 mg/kg i.p.; Fig. 3) was observed between 1 and 2 h post-administration and coincided with the maximal protection against electrically- and sound-induced seizures [12,20]. The decrease in the rate of GABA synthesis lasted for 4–8 h. This interval corresponds to the duration of the anticonvulsant protection by CGP 37849 [12,20]. The time course for the reduction in the rate of synthesis of GABA by CGP 39551 (10 and 60 mg/kg) and CGS 19755 (10 mg/kg) showed the same profile: the peak inhibitory activity was seen after 2 h and disappeared after 8 h. This corresponds to the duration of the anticonvulsant protection by CGS 19755 while the protective effect of CGP 39551 lasted for more than 24 h [12,20]. An increase in the dose of CGP 39551 from 10 to 60 mg/kg increased only the efficacy of the degree of inhibition of GABA synthesis but not its duration.

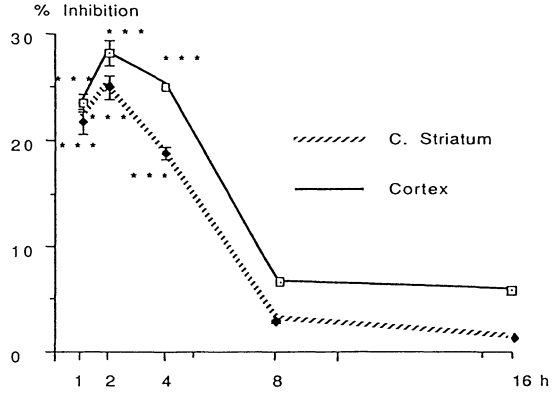

Fig. 3. Time course of the inhibition of the rate of GABA synthesis elicited by CGP 37849 in cortex and striatum. CGP 37849 (10 mg/kg) was injected 1 h before gabaculine and mice were sacrificed at the intervals indicated. The results are expressed as percent inhibition of the increase in GABA levels of mice treated with gabaculine alone (150 mg/kg i.p.) and are the means ± S.E.M. for groups of 6 mice. Cortical GABA levels in mice receiving gabaculine were 9.94 ± 0.13 μmol/g, striatal GABA concentrations in the same group were 9.11 ± 0.24 μmol/g. Statistical calculations were made by means of Dunnett's test. *** $p<0.001$ versus the group treated with gabaculine only.

Effects of CGP 37849, CGS 19755, dizocilpine and dextromethorphan on GABA depletion and on seizures elicited by isoniazid treatment

One of the critical factors in convulsions induced by inhibition of GAD is a decrease of brain GABA levels below a critical value [21]. Competitive NMDA antagonists such as CGP 37849 (3, 10 and 30 mg/kg) dose-dependently delayed the onset of seizures induced by isoniazid, the effect being already highly significant at the dose of 3 mg/kg. At 10 mg/kg the latency was extended from 32 ± 3 min (mice treated with isoniazid alone; t_{iso}) to 60 ± 4 min in the group treated first with CGP 37849 and 90 min later with isoniazid ($t_{CGP37849}$). As seen in Fig. 4, CGP 37849 significantly decreased cortical GABA levels and marginally modified the rate of GABA depletion measured after inhibition of GAD by isoniazid; however, these effects were extremely small. Mice treated with CGP 37849 were free of convulsions at t_{iso}, although their GABA levels at that time were even lower than in those animals treated with isoniazid alone, all of which had convulsions. At $t_{CGP37849}$, GABA levels were still lower than at t_{iso}, in protected as well as in nonprotected mice. Results with CGS 19755 (10 mg/kg) were similar to those with CGP 37849.

Dizocilpine weakly but reproducibly prolonged the latency of seizures elicited by isoniazid from 31 ± 1 min for mice receiving isoniazid only, to 39 ± 1 min ($p<0.05$) for animals treated first with dizocilpine (0.3 mg/kg) and 30 min later with isoniazid. The dose response curve showed a bell-shaped form: the threshold

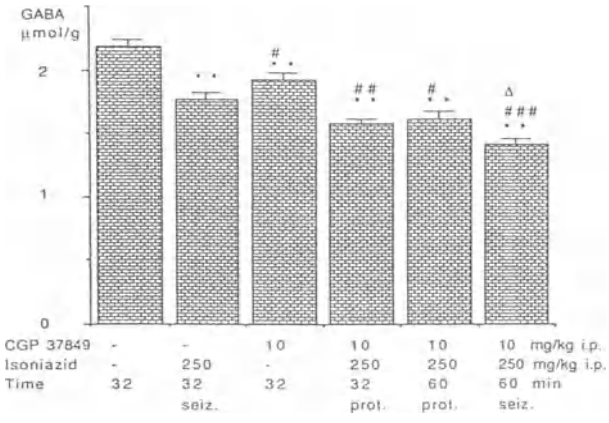

Fig. 4. Time course of the action of CGP 37849 on isoniazid-induced seizures and the related depletion of cortical GABA levels in mouse. Saline or CGP 37849 (10 mg/kg i.p.) were injected 90 min before isoniazid (250 mg/kg i.p.) and mice were sacrificed at t_{iso} or $t_{CGP37849}$. Fifteen mice for each group were used for the pharmacological results and 10 for the determination of GABA levels. The times indicated are calculated from the injection time of isoniazid. Results are given as means ± S.E.M. Statistical calculations were made by means of Dunnett's test. t_{iso} and $t_{CGP37849}$ were 32 ± 3 min and 60 ± 4 min, respectively ($p<0.01$). ** $p<0.01$ versus saline group, # $p<0.05$, ## $p<0.01$, ### $p<0.001$ compared to the group treated with isoniazid alone, Δ $p<0.05$ mice with seizures versus protected mice at $t_{CGP37849}$.

dose was about 0.1 mg/kg and peak activity was reached at 0.3 mg/kg. However, at 0.5 mg/kg the protective effect disappeared. As with CGP 37849 and CGS 19755, this anti-isoniazid activity was not caused by any normalization in levels of GABA, demonstrating that these compounds do not interfere with the metabolism of GABA. Dextromethorphan modified neither the latency to convulsions induced by isoniazid nor the concomitantly decreased GABA levels.

Time course of the effects of CGP 39551 on GABA depletion and on protection against seizures induced by isoniazid

The time course for the protection by CGP 39551 against seizures induced by isoniazid differed from that of other competitive NMDA antagonists. In contrast to CGP 37849 and CGS 19755 the duration of the protective action of CGP 39551 lasted for more than 24 h when doses above 30 mg/kg were administered. As shown in Fig. 5, 24 h after the administration of 60 mg/kg CGP 39551 all mice were free of seizures at t_{iso} (29 ± 2 min) although their cortical GABA levels were lower than in those receiving isoniazid alone and which all had convulsions. $t_{CGP39551}$ was 42 ± 2 min ($p<0.01$). GABA levels measured concomitantly were no different in mice with or without convulsions. A subgroup (21%) of mice treated with CGP 39551 was still free of seizures 2 h after administration of isoniazid; cortical GABA levels in this group were similar to those observed at $t_{CGP39551}$.

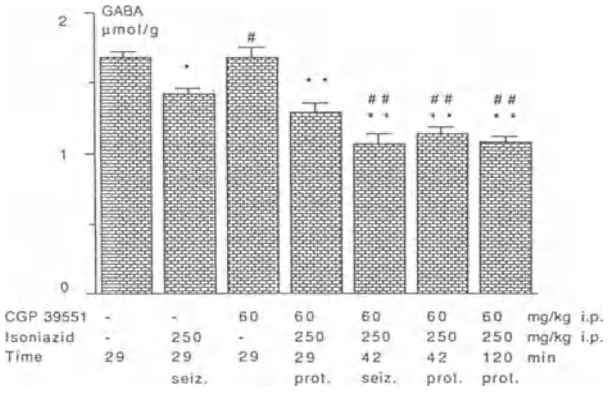

Fig. 5. Time course of the long term anticonvulsant action of CGP 39551 on isoniazid-induced seizures and related changes in cortical GABA levels. Saline or CGP 39551 (60 mg/kg i.p.) were injected 24 h before isoniazid (250 mg/kg i.p.) and mice sacrificed at the intervals indicated. Fifteen mice per group were used for the pharmacological results and 10 for the determination of GABA levels. Time values given in the figure are based on the injection time of isoniazid = 0. Results are given as means ± S.E.M. Statistical calculations were made by means of the Dunnett's test. t_{iso} 29 ± 2 min, $t_{CGP39551}$ 42 ± 2 min ($p<0.01$), t_{120} group of mice protected 120 min after the administration of isoniazid. * $p<0.05$, ** $p<0.01$ compared to the control group, # $p<0.05$, ## $p<0.01$ compared to the group treated with isoniazid only.

Discussion

The electrophysiological consequences of competitive and noncompetitive antagonism at the NMDA receptor-ionophore complex are essentially similar, except that noncompetitive blockade is use-dependent (i.e. it requires the presence of an agonist) [22]. Following the demonstration of an interaction between PCP and the NMDA receptor complex, competitive NMDA receptor antagonists have been scrutinized for possible signs of inducing PCP-like behaviour in animals [23]. Surprisingly, marked biochemical differences have been reported recently between competitive and noncompetitive antagonists. Nehls *et al.* [24] and Chapman *et al.* [25] found that, following systemic administration of pharmacologically-active doses of the noncompetitive NMDA antagonists, dizocilpine, PCP or ketamine to rats, there is a marked metabolic activation in some brain regions. In contrast, competitive NMDA receptor antagonists (CPP, 2-APH) had no, or minimal effects on glucose utilization in the same brain structures, suggesting that competitive NMDA receptor antagonists have a less severe effect on cerebral metabolism than do the noncompetitive antagonists. One explanation of these results is that the functional consequences of NMDA receptor blockade *in vivo* depend on the precise molecular mechanism whereby such blockade is induced [26]. In line with this concept, France *et al.* [27] reported that, in contrast to the noncompetitive antagonist dizocilpine, the competitive antagonist CGS 19755 did not produce ketamine-like discriminative stimulus effects in rhesus monkeys. These results

have now been confirmed with CGP 37849 and CGP 39551 (France and Woods, personal communication). Quantitative differences in the behavioral consequences of competitive and noncompetitive NMDA receptor blockade have been reported by a number of investigators: e.g. following the systemic administration of noncompetitive NMDA receptor antagonists more severe motor abnormalities (increased locomotion, ataxia, stereotypy) are observed in rodents and primates than following the administration of pharmacologically comparable doses of competitive antagonists [28].

The results of this report describe another difference between competitive and noncompetitive NMDA-antagonists: competitive NMDA blockers appear to modify the rate of GABA synthesis more strongly than the noncompetitive antagonists. The competitive antagonists used in this study have no direct action on $GABA_A$, $GABA_B$, chloride channel or central benzodiazepine binding sites (at 100 μM), or on GABA uptake (Bernasconi *et al.*, to be published) and GABA levels (or only marginally), and these results could therefore suggest that the rate of GABA synthesis in inhibitory neurons is modified by the excitatory input to those cells [29]. However, this interpretation is complicated by the lack of effect of the noncompetitive NMDA receptor antagonists utilized.

While it is tempting to speculate that the different functional consequences, with regard to GABAergic transmission, following administration of competitive and noncompetitive NMDA antagonists might be due to hitherto unknown subtypes of NMDA receptors (which are not coupled to PCP receptors) other explanations are possible. One is that some effects of competitive NMDA receptor antagonists are mediated via 'non-NMDA' receptors. However, this seems unlikely. Based on currently published results, the evidence is that both classes of antagonists act highly selectively at NMDA receptor sites [9–11,30].

Another possibility is that competitive antagonists, by virtue of their structural similarity to GLU, interact directly with GAD. However, the lack of effect of competitive NMDA receptor antagonists on steady-state GABA levels and their potent anticonvulsant action against seizures elicited by inhibition of GAD tend to invalidate this hypothesis.

The data also suggest that the level of GABA-mediated inhibitory transmission in the brain may play a role in determining whether NMDA receptors are or are not activated in various types of seizure discharges. Electrophysiological studies *in vitro* previously have demonstrated that the contribution of the NMDA receptor to synaptic responses depends on factors such as the Mg^{2+} content of the extracellular medium (Mg^{2+} blocks the NMDA-receptor channel) and the level of $GABA_A$ receptor-mediated synaptic inhibition [31–34]. Thus, convulsant drugs such as bicuculline or picrotoxin unmask an NMDA receptor-mediated component of the synaptic response, presumably by allowing the neuronal membrane potential to more readily rise in response to excitatory inputs to a level at which the NMDA receptor-ionophore complex is not blocked by Mg^{2+}. The present data suggest that GABA-mediated inhibition may play a similar regulatory role *in vivo*. Thus, under conditions when GABA levels are increased (gabaculine), the frequency of NMDA

receptor channel opening would be predicted to be reduced and noncompetitive blockers (dizocilpine) would be expected to be less effective than competitive antagonists. This was in fact observed to be the case. Conversely, when GABA-mediated inhibition is reduced (isoniazid), NMDA receptor mechanisms are more readily activated and both noncompetitive and competitive antagonists are effective anticonvulsants.

Conclusion

The present study indicates that the level of inhibitory amino acid transmission plays an important role in regulating the contribution of NMDA receptor mechanisms to neuronal physiology and pharmacology.

Acknowledgements

The authors would like to thank Dr. L. Iversen for generously providing dizocilpine.

References

1. Meldrum BS (1986) In: Meldrum, BS and Porter, RI (eds.) New Anticonvulsant Drugs. John Libbey Ltd., London, pp. 17–30.
2. Foster AC and Fagg GE (1984) Brain Res. Rev. 7: 103–164.
3. Meldrum BS and Chapman AG (1986) In: Nistico G, Morselli PL, Lloyd KG, Fariello RG and Engel J. Jr. (eds.) Neurotransmitters, Seizures, and Epilepsy III. Raven Press, New York, pp. 223–232.
4. Fan SG, Wusteman M and Iversen LL (1981) Brain Res. 228: 379–387.
5. Braestrup C, Schmiechen R, Neef G, Nielsen M, and Petersen EN (1982) Science 216: 1241–1243.
6. Czuczwar SJ and Meldrum BS (1982) Eur. J. Pharmacol. 83: 335–338.
7. Clineschmidt BV, Martin GE and Bunting PR (1982) Drug Dev. Res. 2: 123–134.
8. Fagg GE, Olpe HR, Bittiger H, Schmutz M, Angst C, Brundish D, Allgeier H, Heckendorn R and Dingwall JG (1988) Soc. Neurosci. Abs. 14: 381.1.
9. Fagg GE, Olpe HR, Schmutz M, Pozza MF, van Riezen H, Bittiger H, Angst C, Brundish D, Allgeier H, Heckendorn R and Dingwall JG (1989) In: Williams M (ed.) Current and Future Trends in Anticonvulsant, Anxiety and Stroke Therapy. Alan R. Liss, New York, in press.
10. Lehmann J, Schneider J, McPherson S, Murphy DE, Bernard P, Tsai C, Bennett DA, Pastor G, Steel DJ, Boehm DL, Cheney JM, Liebman JM, Williams M and Wood PL (1987) J. Pharm. Exp. Ther. 240: 737–746.
11. Lehmann J, Hutchison AJ, McPherson SE, Mondadori C, Schmutz M, Sinton CM, Tsai C, Murphy DE, Steel DJ, Williams M, Cheney DL and Wood PL (1988) J. Pharm. Exp. Ther. 246: 65–75.
12. Schmutz M, Kleps K, Olpe HR, Fagg GE, Allgeier H, Heckendorn R, Angst C, Brundish D and Dingwall JG (1988) Soc. Neurosci. Abs. 14: 345.3.
13. Kemp JA, Foster AC and Wong EHF (1987) Trend Neurosci. 10: 294–298.
14. Bernasconi R, Klein M, Martin P, Portet Ch, Maitre L, Jones RSG, Baltzer V and Schmutz M (1985) J. Neural. Transm. 63: 169–189.

15. Bernasconi R, Klein M, Martin P, Christen P, Hafner T, Portet C and Schmutz M (1988) J. Neural. Transm. 72: 213–233.
16. Bernasconi R, Marescaux C, Vergnes M, Klebs K, Klein M, Martin P, Portet C, Maitre L and Schmutz M (1988) J. Neural. Transm. 71: 11–27.
17. Carmona E, Gomes C and Trolin G (1980) Naunyn-Schmiedeberg's Arch. Pharmacol. 313: 221–224.
18. Lindgren S and Anden NE (1984) Acta. Pharmacol. Toxicol. 55: 41–49.
19. Wood ID and Hertz L (1980) Neuropharmacology 19: 805–808.
20. Chapman AG, Graham JL and Meldrum BS (1989) J. Cereb. Blood Flow Metab. 9 (Suppl. 1): S309.
21. Bernasconi R, Martin P, Steulet AF, Portet C, Leonhardt T and Schmutz M (1990) In: Engel J, Avanzini G, Fariello R and Heinemann U (eds.) Advances in Neurobiology of Epilepsy, Vol. 1: Neurotransmitters, Seizures and Epilepsy. Demos Press, New York, in press.
22. Lodge D, Aram JA, Church J, Davies SN, Martin D, Millar J and Zeman S (1988) In: Lodge D (ed.) Excitatory Amino Acids in Health and Disease. John Wiley & Sons, Chichester, pp. 237–259.
23. Snell LD and Johnson KM (1988) In: Lodge D (ed.) Excitatory Amino Acids in Health and Disease. John Wiley & Sons, Chichester pp. 261–273.
24. Nehls DG, Kurujami A, Park CK and McCulloch J (1988) Neurosci. Lett. 91: 204–210.
25. Chapman AG, Swan JH and Meldrum BS (1989) J. Cereb. Blood Flow Metab. 9 (Suppl. 1): S310.
26. Costa E, Fada E, Kozikowski AP, Nicoletti F, Wroblewski JT (1988) In: Ferrendelli JA, Collins RC and Johnson EM, (eds.) Neurobiology of Amino Acids, Peptides and Trophic Factors. Kluwer Academic Publishers, Boston, pp. 35–50.
27. France CP, Woods JH, Ornstein P (1989) Eur. J. Pharmacol. 159: 133–139.
28. Chapman AG, Swan JH, Patel S, Graham JL and Meldrum BS (1990) In: Lubec G and Rosenthal GA (eds.) Amino Acids: Chemistry, Biology and Medicine. ESCOM Science Publishers B.V., Leiden, this volume.
29. Wood PL, Moroni F, Cheney DL and Costa E (1979) Neurosci. Lett. 12: 349–354.
30. Wong EHF, Kemp JA, Priestley T, Knight AR, Woodruff GN and Iversen LL (1986) Proc. Natl. Acad. Sci. 83: 7104–7108.
31. Herron CE, Williamson R, Collingridge GL (1985) Neurosci. Lett. 61: 255–260.
32. Baldino F, Wolfson B, Heinemann U, Gutnick MJ (1986) Neurosci. Lett. 70: 101–105.
33. Horne AL, Harrison NL, Turner JP and Simmonds MA (1986) Eur. J. Pharmacol. 122: 231–238.
34. Dingledine R, Hynes MA and King GL (1986) J. Physiol. 380: 175–189.

Address for correspondence: Dr. R. Bernasconi, Research Laboratories, Pharmaceuticals Division, CIBA-GEIGY Ltd., CH-4002 Basel, Switzerland.

Excitatory amino acid receptors coupled to phosphoinositide metabolism: Characterization and possible role in physiology and physiopathology

M. Récasens and J. Guiramand

INSERM U. 254, Laboratoire de Neurobiologie de l'Audition, Hôpital St-Charles, 300, rue A. Broussonnet, F-34059 Montpellier Cedex 01, France

Introduction

It is now widely established that a large variety of neurotransmitters activate receptors linked to phospholipase C. This enzyme catalyses the hydrolysis of membrane phosphoinositides to yield two second messengers; inositol triphosphate and diacylglycerol. The former acts by mobilizing intracellular Ca^{2+}, the latter by stimulating protein kinase C [1,2]. Since the first publications [3–5] indicating that excitatory amino acids (EAAs) stimulate the phosphoinositide cascade in rat striatal neurons, granule cells and hippocampal slices, a large number of reports have confirmed and extended these previous findings using various models [6–8]. However, until recently, the characterization of the EAAs receptor involved in the increase in inositol phosphates (IPs) production remained rather obscure. For instance, ibotenate, a rigid structural analogue of glutamate, was reported as the most active of the EAAs in stimulating IPs formation in adult rat hippocampal slices [5] while EAAs were found inactive in this same area [9]. In primary cultures of striatal neurons [3], in Xenopus oocytes injected with rat brain mRNA [10], in granule cells [4] and in rat brain synaptoneurosomes [7] quisqualate, another glutamate agonist, proved to be the most efficient EAAs agonist for inositol phospholipid hydrolysis. These apparent discrepancies may originate from various key factors which may be identified as: 1) the experimental model (slices, cells in culture or membrane vesicles), 2) the anatomical origin of the model (hippocampus, cerebellum, striatum...), 3) the age of the animal used and to a lesser extent 4) the species. In fact, in slices or cells in culture, the IPs formation induced by neuroactive substances results from several events which are: the direct effect of the substance tested on its receptor coupled to the phosphoinositide metabolism, but also indirect effects due for example to the release of other substances able to stimulate or to inhibit themselves the IPs synthesis. The choice of a given brain structure may lead to the study of a specific receptor particularly enriched in that region and linked to IPs formation. Finally, the density and the pharmacological characteristics of receptors may change during development. These considerations may explain the rather confusing situation concerning the EAAs receptors involved in IPs production.

To overcome most of the difficulties described above, we have chosen to study the IPs metabolism elicited by EAAs on a membrane preparation from rat forebrains called synaptoneurosomes [11]. Synaptoneurosomes contain many synaptosomes with attached resealed postsynaptic entities (neurosomes). This preparation is useful for studying transduction systems [12–14] because cell-cell interactions as well as most of the intracellular regulations are eliminated. Moreover, since the synaptoneurosomes were prepared from rat forebrain and not from a specific brain region, one may expect that most, if not all, of the EEAs receptors are present in this preparation.

In this paper, we investigate the characterization of the EAAs receptors coupled to phosphoinositide metabolism and compare them to the electrophysiologically defined EAAs receptors subtypes, termed *N*-methyl-D-aspartate (NMDA) or AA1, quisqualate or AA2 and kainate or AA3 [15–16]. We also investigate the sequential steps which lead from the EAAs receptor activation to the increase in the IPs metabolism and finally, we examine the developmental changes of the EAAs receptors linked to the IPs synthesis in order to understand the physiological role of this EAAs induced production of second messenger molecules.

Materials and Methods

Myo[2–^{3}H] inositol (17 Ci/mmol; 0.63 TBq/mmol) was purchased from the Commissariat à l'Energie Atomique (France). The amino acid structural analogs and antagonists were purchased from Cambridge Research Biomedicals or Tocris Chemicals (U.K.). All other reagents were from Sigma.

Synaptoneurosomes were prepared according to [11]. Briefly, 10 forebrains of 8-day-old Long-Evans rats (for developmental studies, the number of forebrains was chosen in order to obtain the same protein concentration in the synaptoneurosome preparation, whatever the age of the rats) were dissected and homogenized in 9 volumes of Krebs-Ringer buffer previously gassed with O_2/CO_2 (95%/5%) with a glass-glass dounce homogenizer. The Krebs-Ringer buffer contained 125 mM sodium chloride, 3.5 mM potassium chloride, 1.25 mM potassium dihydrogen phosphate, 1.25 mM magnesium sulfate, 1.5 mM calcium chloride, 25 mM sodium hydrogen carbonate and 10 mM D-glucose. The homogenate was filtered first through two layers of nylon blutex (153 µm, Tripette and Renaud, France) then through 8 µm pore Millipore filters SCWP 04700 under a pressure of carbogen. The filtrate was centrifuged at 1000 g for 15 min and the supernatant was discarded.

The phosphoinositides were labelled by incubating the synaptoneurosomes for 60 min in 30 ml of buffer containing 150 µCi myo[2–^{3}H] inositol and 1 mM cytidine. The excess of myo[2–^{3}H] inositol was removed by centrifugation as previously described [7]. After 12 min of incubation with 10 mM lithium chloride, synaptoneurosomes were then incubated with stimulating agents (20 min at 37°C) or buffer for control samples. When used, antagonists were added at the same time

as lithium chloride. [^{3}H]]IPs extraction and separation on Dowex 1 X 8 formate columns were performed according to [17]. No attempt was made to separate the various inositol phosphates metabolites, since preliminary experiments have shown that inositol monophosphate (IP_1) represents more than 95% of the IPs produced following 20 min of stimulation in presence of lithium chloride. The IPs fraction was eluted with 24 ml of 2 M ammonium formate, 0.1 M formic acid. The [^{3}H]IPs measurements were systematically corrected for possible contaminations due to [^{3}H]inositol or other tritiated compounds as previously indicated [18].

Results

Pharmacological characterization of the EAAs receptors coupled to IPs formation

All the EAAs agonists tested stimulate the IPs formation. These include glutamate, aspartate, NMDA, quisqualate, kainate, ibotenate and DL-alpha-amino-3-hydrox-5-methyl-4-isoxazole propionate (AMPA). The following order of potency was observed: quisqualate (EC_{50} = 0.4 μM) >> glutamate (EC_{50} = 8 μM) ibotenate (EC_{50} 13 μM) >> AMPA, NMDA, kainate. The latter three compounds are partial agonists (Fig. 1).

Several antagonists of EAAs-induced depolarization were tested for their effect on the inositol phosphate formation elicited by glutamate, NMDA, quisqualate and kainate (Table 1). Glutamate diethylester (GDEE), glutamate aminomethyl sulfonate (GAMS) and particularly 6-nitro-7-cyanoquinoxaline-2,3-dion (CNQX), antagonists acting preferentially on the ionotropic quisqualate receptor subtype did not inhibit IPs formation evoked by quisqualate (10^{-5} M) when assayed at a concentration of 10^{-3} M (Table 1). The antagonists of the other ionotropic EAAs receptor subtypes also did not affect the IPs production induced by quisqualate (Table 1). On the contrary, the classical NMDA antagonist, DL-2-alpha-amino-5-phosphonovalerate (APV) blocks at a concentration of 10^{-3} M about 50% of the IPs accumulation elicited by NMDA (10^{-3} M). None of the antagonists tested inhibit the kainate induced IPs formation. It must be noted that DL-2-amino-phosphonobutyrate (APB) did not block any of the EAAs induced IPs formation (Table 1).

Ionic mechanisms involved in the activation of IPs synthesis by EAAs

NMDA, quisqualate and kainate were tested for their ability to stimulate IPs accumulation in the presence of variable concentrations of K^+ and compared to that produced by carbachol, a cholinergic muscarinic agonist. K^+ *per se* stimulates IPs production (150% of the control value). K^+ has a biphasic effect on the IPs production induced by quisqualate (10^{-5} M) and high concentrations of glutamate (Fig. 2). Between 10 and 25 mM of K^+, the glutamate and quisqualate elicited IPs formation is inhibited, while at concentrations above 50 mM, these excitatory

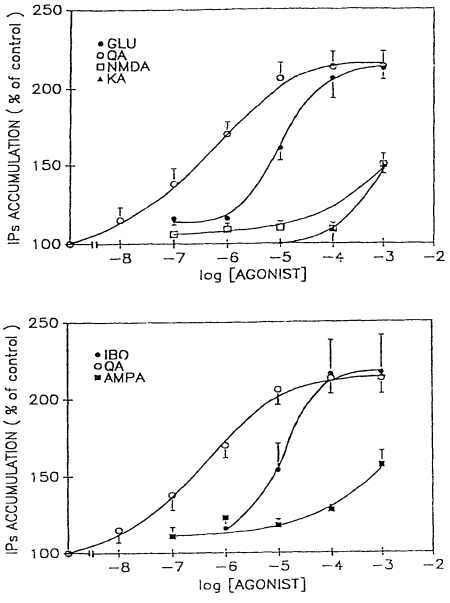

Fig. 1. Dose-dependent accumulation of [^{3}H]-IPs accumulation elicited by various EAAs agonists in rat brain synaptoneurosomes.

Synaptoneurosomes prepared from 8-day-old rat forebrain were labelled for 60 min with [^{3}H] inositol. After preincubation with 10 mM lithium at 37°C for 12 min, increasing concentrations of agonists were added and the synaptoneurosomes were further incubated for 20 min. [^{3}H]-IPs accumulation was measured as previously indicated. Results, expressed as percentages of the basal IPs accumulation, are means ± S.E.M. of at least 4 experiments performed in triplicate. a) Glutmate-(●), quisqualate-(○), NMDA-(□) and kainate-(▲) induced IPs formation. The apparent EC_{50} value estimated graphically from these dose-response curves is about 8 µM for glutamate and 0.4 µM for quisqualate. b) Quisqualate-(○), AMPA-(■) and ibotenate-(●) induced IPs formation. EC_{50} value is 13 µM for ibotenate and more than 100 µM for AMPA.

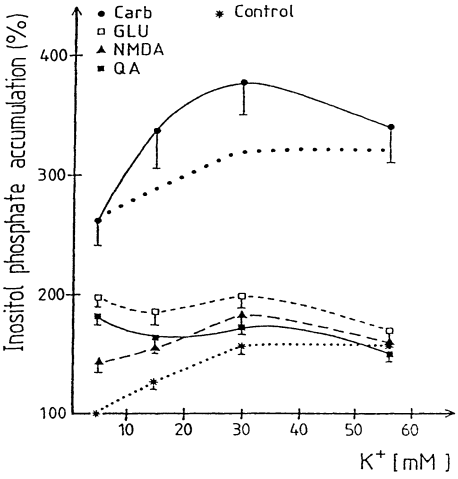

Fig. 2. Effect of increasing concentrations of potassium ions on EAAs- and carbachol-elicited IPs formation. EAAs- and carbachol-induced IPs formation have been measured in modified Krebs-Ringer buffer containing various K^+ concentrations. This buffer was obtained by equimolar substitution of KCl by NaCl. The results are expressed as percentages of the basal IPs accumulation obtained in normal Krebs-Ringer buffer (4.75 mM K^+). They are means ± S.E.M. of 3–5 experiments. Glutamate, NMDA and carbachol were used at 10^{-3}M, whereas quisqualate was tested at 10^{-5}M. For each agonist, these concentrations give the maximal IPs stimulation. The upper dotted line in this figure represents the theoretical IPs accumulation if carbachol (10^{-3}M) and K^+ ions responses were additive (whatever the K^+ concentration). At 15 mM and 30 mM K^+, the experimental values obtained for carb are significantly different from the corresponding theoretical value ($p<0.02$, using Student's t-test).

amino acids did not further enhance IPs synthesis. The NMDA evoked IPs accumulation is additive with that of K^+ up to a concentration of 30 mM and inhibited at higher concentrations of this ion (Fig. 2). On the contrary, the carbachol elicited IPs formation is potentiated by concentrations of K^+ ranging from 15 to 30 mM and strictly additive for higher concentrations (Fig. 2).

Table 1. Effect of high concentrations of EAA antagonists on the IPs accumulation induced by QA, NMDA, KA and GLU on rat forebrain synaptoneurosomes

Agonists	GDEE (10^{-2} M)	GAMS (10^{-3}M) – (10^{-2}M)		CNQX (10^{-4}M)	DL-APV (10^{-3}M) – (5×10^{-3}M)		γ-DGG (10^{-3}M) – (10^{-2}M)		DL-APB (5×10^{-3}M)	None
QA (10^{-5}M)	258±18	236±14	218±15[a]	245±20	239±8	224±23	236±12	244±20	229±13	250±20
NMDA (10^{-3}M)	—	169±11	—	—	143±10[a]	114±4[b]	164±15	152±10[a]	169±17	183±4
KA (10^{-3}M)	—	150±18	—	—	132±10	136±12	158±7	148±8	161±14	150±8
GLU (10^{-4}M)	—	239±14	—	250±9	243±22	245±23	243±22	—	246±28	254±24

Results are expressed as a percentage of the control value (^{3}H-IPs accumulation in the absence of any agonist or antagonist and represent the means ± S.E.M. of 3 to 5 separate experiments, each performed in triplicate. All the antagonists (glutamate-diethylester (GDEE), glutamate amino-methyl-sulfonate (GAMS) 6-nitro-7-cyanoquinoxaline-2-3 dion (*CNQX*) DL-2-amino-5-phosphonovalerate (DL-APV), γ-D-glutamylglycine (-DGG) and DL-2-amino-phosphonobutyrate DL-APB)) tested alone did not significantly differ from the control value. The absolute value for the control was 1780 dpm ± 169 per mg of protein.

[a]$p<0.05$, [b]$p<0.01$: Significance of the inhibitory effect of the antagonist on the agonist-induced IPs formation as estimated by a Student's t test.

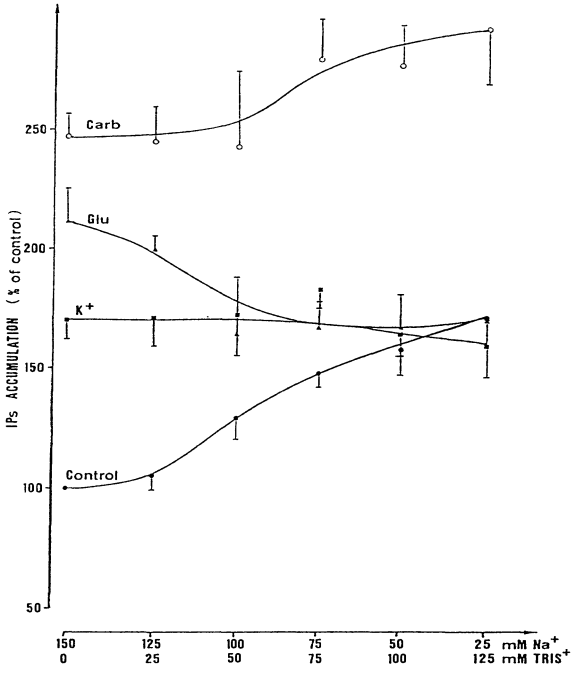

Fig. 3. Influence of replacing Na^+ ions by $TRIS^+$ on Glutamate-, Carbachol-, and K^+-induced IPs accumulation in rat brain synaptoneurosomes.

Glutamate (10^{-3}M)-, carbachol (10^{-3}M)- and K^+ (30 mM)-stimulated IPs formation were measured in modified Krebs-Ringer buffer obtained by equimolar substitution of NaCl by TRIS-HCl. The results, expressed as percentages of basal IPs accumulation obtained in normal Krebs-Ringer buffer (150 mM Na^+), are means ± S.E.M. of 3 experiments, each performed in triplicate.

The replacement of external Na^+ by $Tris^+$ ions (unable to cross the membrane by Na^+ channels) resulted in an increase of the basal IPs formation and a concomitant inhibition of the glutamate stimulated IPs accumulation (Fig. 3). Conversely, the carbachol response parallels that of the basal IPs production (Fig. 3). Similar patterns were obtained by substituting Na^+ ions by Li^+ or *N*-methyl-D-glucamine$^+$ (data not shown).

Developmental changes in the basal and agonist stimulated IPs production

The basal IPs accumulation decreases dramatically between synaptoneurosomes prepared from 4-day-old rat forebrains (2900 dpm/mg protein) and synaptoneurosomes prepared from 15-day-old rat forebrains (1000 dpm/mg protein) (Fig. 4a). Subsequently, the basal IPs formation remains more or less constant up to the age of 2 years (Fig. 4a). The IPs accumulation elicited by glutamate and quisqualate is

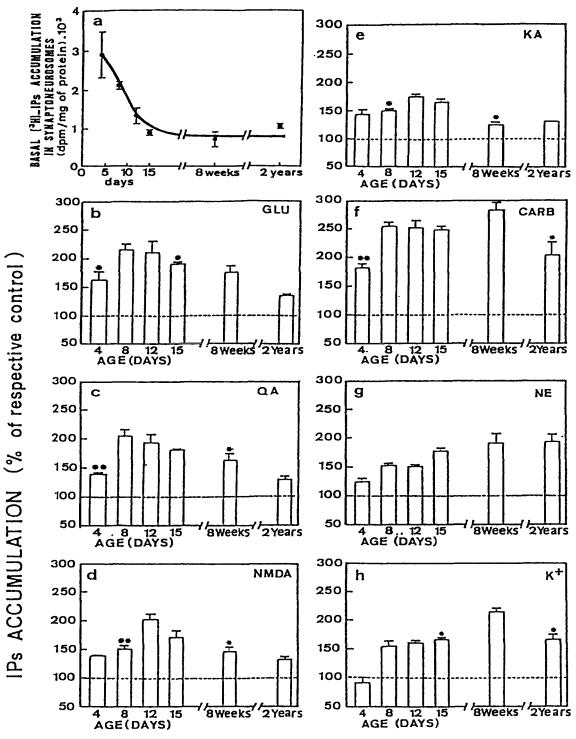

Fig. 4. Evolution of basal- and agonist-stimulated IPs formation in rat forebrain synatoneurosomes during post-natal development. Basal and agonist-stimulated IPs accumulation have been measured in synaptoneurosomes prepared from rats of different ages (4-day- to 2-year-old rats). a) Basal IPs accumulation is expressed as dpm per mg of proteins. b–e) EAAs-stimulated IPs synthesis during post-natal development: The main EAAs agonists, glutamate 1 mM (4b), quisqualate 0.01 mM (4c), NMDA 1 mM (4d) and kainate 1 mM (4e) were tested. The results, expressed as percentages of the corresponding basal value, are means ± S.E.M. of at least 3 experiments, each performed in triplicate. The significance of the difference observed in IPs accumulation during development was tested using Student's t-test (*$p<0.01$, **$p<0.001$) with the maximal value being taken as the reference. f–h) Other agonist-stimulated IPs formation during post-natal development: Different stimulating agents have been tested: carbachol 1 mM (4f), noradrenaline (NE) 1.5 mM (4g) and K^+ 30 mM (4h).

similar and peaks in synaptoneurosomes prepared from 8-day-old rat forebrains (220% of the control value for glutamate and 210% for quisqualate). Thereafter, a continuous decrease is observed so that the IPs formation observed in synaptoneurosomes of 2-year-old rats is only 30% of the maximal one. The NMDA-induced IPs synthesis increases slightly between 4- and 8-day-old rat forebrains synaptoneurosomes and sharply between 8- and 12-day-old The kainate elicited IPs formation presents a similar pattern to that found for NMDA (Fig. 4e). The carbachol induced IPs accumulation in rat forebrain synaptoneurosomes increases with age until 8 weeks and decreases significantly in very old animals (Fig. 4f).

The developmental profile of noradrenaline stimulated IPs formation shows a regular age-related augmentation up to adult animals and then levels off (Fig. 4g). K^+ ions (30 mM) induced IPs synthesis increases with the age of the animals and reaches its maximal value with 8-week-old rats (220% of the basal value) (Fig. 4h). Then, a substantial decrease was observed in older animals.

Discussion

Our results indicate that EAAs enhanced IPs formation in rat forebrain synaptoneurosomes in a saturable and dose-dependent manner (Fig. 1). The three main agonists, NMDA, quisqualate and kainate, which defined the three subtypes of ionotropic EEAs receptors [15,16] activate the IPs formation although to different extents. Among them, quisqualate was the most potent ($EC_{50} = 0.4$ μm). However, the pharmacological characterization of the quisqualate receptor involved in the IPs synthesis did not correspond to that previously described for the ionotropic quisqualate receptor as evidenced by the facts that: 1) Usual antagonists of the quisqualate-induced depolarization (GAMS, GDEE and CNQX) are ineffective in inhibiting quisqualate evoked IPs formation (Table 1) [18]. 2) AMPA, a quisqualate agonist on the ionotropic receptor subtype is about 300 times less potent than quisqualate (Fig. 1). 3) The quisqualate induced IPs response decreases from the age of 8 days in synaptoneurosomes prepared from rat forebrain (Fig. 4) [7] without any change in the apparent affinity [19]. The depolarizing potency of quisqualate remains at whatever age. Our data are in agreement with the fact that the Joro Spider Toxin, known to block quisqualate associated ion channels [20] did not block the quisqualate evoked membrane current expressed in Xenopus oocytes injected with rat brain mRNA [21]. It has also been reported that GDEE and *cis*-2,3-piperidine dicarboxylate did not affect the quisqualate induced IPs formation in hippocampal slices [5]. These data strongly suggest that a new EAAs receptor is coupled to the phosphoinositide metabolism, which could be defined as a quisqualate metabotropic receptor, tentatively named sAA_2 (slow acting) according to the previously proposed nomenclature [16]. Conversely, NMDA may activate IPs accumulation via the same receptor subtype as that defined in electrophysiological experiments. In fact, specific or broad antagonists (APV, gamma-D-glutamylglycine) inhibit both NMDA-induced depolarization and NMDA-elicited IPs formation. Similar blocking effects of APV and of Mg^{2+} on the IPs synthesis was reported in cerebellar granule cells [22]. Very high concentrations of kainate are required to slightly stimulate IPs formation. Moreover, APV inhibits although not significantly the kainate-induced response (Table 1). The developmental pattern of kainate induced IPs formation parallels that obtained with NMDA. This may suggest that the kainate response is not due to the activation of the ionotropic kainate receptor subtype, which only requires micromolar concentrations, but is likely due to an effect of a high concentration of kainate on the NMDA receptor. Such overlapping of kainate on NMDA receptor was reported in binding experi-

ments [23]. It was reported that ibotenate was the most potent agonist (in magnitude) in stimulating IPs synthesis in adult rat hippocampal slices [5,24]. This ibotenate induced IPs response was blocked by APB [5,24]. In our model, the IPs response related to ibotenate was as potent in magnitude as quisqualate, but ibotenate has a much lower apparent affinity (EC_{50} = 13 μM) than quisqualate (EC_{50} = 0.4 μm). As opposed to the effect observed in brain slices, in synaptoneurosomes APB does not block the ibotenate-induced IPs accumulation. Consequently, it may be suggested that ibotenate and quisqualate act at the same receptor subtype. These apparent discrepancies may be explained by the fact that we used 8-day-old rats to prepare synaptoneurosomes while other authors used adult rats for obtaining hippocampal slices. However, the main explanation of that difference may lie in the existence of indirect effects in slices as compared to synaptoneurosomes. Following this idea, it was recently published that IPs stimulation via quisqualate receptors is inhibited by NMDA receptor activation [25]. Ibotenate is known to interfere preferentially with the NMDA receptor [26] and is likely to undergo enzyme-catalysed decomposition to give muscimol, a GABA agonist, in brain tissue [27].

The pharmacological characterization studies of the EAAs receptors involved in the phosphoinositide breakdown may thus lead to the following conclusions: 1) Existence of a new quisqualate receptor subtype called sAA_2 2) Probable involvement of the classical NMDA receptor 3) Complex effect of ibotenate, not necessarily implicating the presence of a specific ibotenate receptor 4) Improbable participation of a kainate receptor.

The second question that we have asked is: What are the sequential steps which lead from EAAs receptor activation to the IPs formation? Our experiments were conducted in order to mainly study the multistep mechanism associated with the activation of the metabotropic quisqualate receptor. Indirect evidence has suggested that quisqualate activates IPs metabolism through GTP binding regulatory proteins (Gi or Go) in Xenopus oocytes injected with rat brain mRNA [10]. It was reported that agents enhancing sodium influx such as batrachotoxin, veratridine, aconitine, scorpion toxins, pumiliotoxin B, and agents augmenting intracellular sodium concentration, such as ouabain, monensin, increase IPs formation [13,28,29]. We found that K^+- and glutamate-induced IPs metabolism are not additive (Fig. 2). Moreover, the replacement of external Na^+ by $Tris^+$ ions inhibit both K^+- and glutamate-induced IPs production. These results indicate that these two compounds interact at least at one of the sequential steps which occur between receptor activation and IPs synthesis. Among numerous possibilities, two appear most likely: 1) depolarization induced Na^+ influx 2) K^+ induces glutamate release. In fact, depolarizing substances release glutamate in brain slices [30,31]. However, the glutamate concentration (about 1 μM) resulting from K^+ ions is insufficient to explain the magnitude of K^+ induced IPs formation. Similar conclusions were drawn in granule cells [22]. Thus one of the sequential steps where K^+ and glutamate interfere may be the depolarization induced Na^+ influx. It must be emphasized that this step appears to be specific for glutamate stimulation, since

carbachol elicited IPs synthesis is potentiated by K^+ ions (Fig. 2) and not affected by the replacement of Na^+ ions by other monovalent cations (Fig. 3).

The third point that we have begun to investigate is the physiological significance of the EAAs elicited IPs production in the brain. Our results indicate that the postnatal developmental pattern of EAAs evoked IPs response is characteristic as compared to those observed with other neuroactive substances (carbachol, noradrenaline and K^+) (Fig. 4).

Indeed, EAAs actively stimulate IPs synthesis in rat brain synaptoneurosomes during the two first postnatal weeks where synaptogenesis occurs. These data may imply that quisqualate and NMDA have a crucial role in events linked to neuronal development and synaptic plasticity. This possibility is further supported by the facts that glutamate induces sprouting in isolated snail ganglia [32]; NMDA receptor activation stimulates neurite outgrowth and differentiation in cerebellar granule cells [33,34]; simultaneous applications of quisqualate and NMDA induce long-term potentiation in hippocampal slices [35] and protein kinase C inhibitors eliminate this potentiation [36]; lesions of some glutamatergic pathways result, 2 days later, in an increase in IPs formation elicited by glutamate or quisqualate [37]; post hypoxic brain injury enhances quisqualate stimulated IPs turnover [38]; and finally, kindling increases IPs formation induced by ibotenate [39,40].

The stimulating EAAs ability is impaired in adult rat brain and continues to decrease with aging (Fig. 4). Since aging does not modify the apparent affinity of EAAs for their respective receptors coupled to the phosphoinositide metabolism [19], the IPs decrease observed likely results from a decrease of the number in receptors, suggesting a degeneration of specific neurons. This was found to be the case in some neurodegenerative pathologies such as Alzheimer's disease, where NMDA and quisqualate receptors binding are reduced [41,42].

Acknowledgements

We are grateful to Dr. Honoré (Ferrosan Research Division, Denmark) for providing us with CNQX and Prof. Krogsgaard-Larsen (Royal Danish School of Pharmacy) for the gift of AMPA. We thank I. Sassetti for technical assistance, A. Bara for typing the manuscript and E. Mayat for reading it. This work was supported by grants from the Centre National de la Recherche Scientifique (ATP Medicament, AIP 953134), M.R.E.S., C.N.A.M.T.S.-INSERM, IPSEN, Air Liquide and the Institut H. Beaufour (Paris).

References

1. Berridge MJ (1987) A. Rev. Biochem. 56: 159–193.
2. Downes CP and Michell RH (1985) In: Cohen P and Housley MD (eds.) Molecular Mechanism of Transmembrane Signalling. Elsevier, Amsterdam, pp. 3–56.

3. Sladeczek F, Pin J-P, Récasens M, Bockaert J and Weiss S (1985) Nature 317: 717–719.
4. Nicoletti F, Wroblewski JT, Novelli A, Alho H, Guidotti A and Costa E (1986) J. Neurosci. 6: 1905–1911.
5. Nicoletti F, Meek JL, Iadarola MJ, Chuang DM, Roth BL and Costa E (1986) J. Neurochem. 46: 40–46.
6. Pearce B, Albrecht J, Morrow C and Murphy S (1986) Neurosci. Lett. 72: 335–340.
7. Récasens M, Sassetti I, Nourigat A, Sladeczek F and Bockaert J (1987) Eur. J. Pharmacol. 141: 87–93.
8. Schoepp DD and Johnson BG (1988) J. Neurochem. 50: 1605–1613.
9. Baudry M, Evans J and Lynch G (1986) Nature 319: 329–331.
10. Sugiyama H, Ito I and Hirono C (1987) Nature 325: 531–533.
11. Hollingsworth EB, McNeal ET, Burton JL, Williams RJ, Daly JW and Creveling CR (1985) J. Neurosci. 5: 2240–2253.
12. Hollingsworth EB, Sears EB, De La Cruz RA, Gusovsky F and Daly JW (1986) Biochim. Biophys. Acta 883: 15–25.
13. Gusovsky F, Hollingsworth EB and Daly JW (1986) Proc. Natl. Acad. Sci. USA 83: 3003–3007.
14. Schwartz RD, Jackson JA, Weigert D, Skolnick P and Paul SM (1985) J. Neurosci. 5: 2963–2970.
15. Watkins JC and Evans RH (1981) A. Rev. Pharmac. Toxic. 21: 165–204.
16. Fagg GE, Foster AC and Ganong AH (1986) Trends Pharmacol. Sci. 7: 357–363.
17. Bone EA, Fretten P, Palmer S, Kirk CJ and Michell RH (1984) Biochem. J. 221: 803–809.
18. Récasens M, Guiramand J, Nourigat A, Sassetti I and Devilliers G (1988) Neurochem. Int. 13: 463–467.
19. Guiramand J, Sassetti I and Récasens M (1989) Int. J. Dev. Neurosci. 7: 257–266.
20. Akaike N, Kawai N, Kiskin NI, Kljuchko EM, Krishtal OA and Tsyndrenko A (1987) Neurosci. Lett. 79: 326–330.
21. Sugiyama H, Ito I and Hirono C (1987) Nature 325: 531–533.
22. Nicoletti F, Wroblewski JT and Costa E (1987) J. Neurochem. 48: 967–973.
23. Monahan JB and Michel J (1987) J. Neurochem. 48: 1699–1708.
24. Schoepp DD and Johnson BG (1988) J. Neurochem. 50: 1605–1613.
25. Palmer E, Monaghan DT and Cotman CW (1988) Mol. Brain Res. 4: 161–165.
26. Krogsgaard-Larsen P, Nielsen E and Curtis DR (1984) J. Med. Chem. 27: 585–591.
27. Nielsen E, Schousboe A, Hansen SH and Krogsgaard-Larsen P (1985) J. Neurochem. 45: 725–731.
28. Gusovsky F, McNeal ET and Daly JW (1987) Mol. Pharmacol. 32: 479–487.
29. Gusovsky F and Daly JW (1988) Neuropharmacology 27: 95–105.
30. Toggenburgen G, Wiklund L, Henke H and Cuenod M (1983) J. Neurochem. 41: 1606–1613.
31. Recasens M, Fagni L, Baudry M and Lynch G (1984) Neurochem. Int. 6: 325–332.
32. Barnes DM (1986) Science 234: 1325–1326.
33. Balazs R, Hack N and Jorgensen OS (1988) Neurosci. Lett. 87: 80–86.
34. Pearce IA, Cambray-Deakin MA and Burgoyne RD (1987) FEBS Lett. 223: 143–147.
35. Izumi Y, Miyakawa H, Ito K and Kato H (1987) Neurosci. Lett. 83: 201–206.
36. Lovinger DM, Wong K, Murakami K and Routtenberg A (1987) Brain Res. 436: 177–183.
37. Nicoletti F, Wroblewski JT, Alho H, Eva C, Fadda E and Costa E (1987) Brain Res. 436: 103–112.
38. Chen C-K, Silverstein FS, Fisher SK, Statman D and Johnston MV (1988) J. Neurochem. 51: 353–359.
39. Iadarola MJ, Nicoletti F, Naranjo JR, Putnam F and Costa E (1986) Brain Res. 374: 174–178.
40. Akiyama K, Yamada N and Sato M (1987) Exp. Neurol. 98: 499–508.
41. Greenamyre JT, Penney JB, D'Amato CJ and Young AB (1987) J. Neurochem. 48: 543–551.
42. Monaghan DT, Geddes JW, Yao D, Chung C and Cotman CW (1987) Neurosci. Lett. 73: 197–200.

Address for correspondence: Dr. M. Récasens, INSERM U. 254, Laboratoire de Neurobiologie de l'Audition, Hôpital St-Charles, 300, rue A. Broussonnet, F-34059 Montpellier Cedex 01, France.

Excitatory amino acid actions on membrane potential and conductance of brainstem motoneurones

J. Durand and J.P. Gueritaud
INSERM U6 and CNRS URA 634, 280 Bd Ste Marguerite, 13009 Marseille, France

Introduction

N-methyl-D-aspartate (NMDA), quisqualate and kainate receptors are widely studied in the central nervous system and their participation in synaptic transmission of different pathways has been well established [for reviews: 1–5,16,19]. Relatively little is known about the excitatory transmitters in the oculomotor system. Our earlier observations on intracellularly recorded activity indicated that L-glutamate and NMDA excited cat abducens motoneurones in different ways [8]. We report here a comparison of NMDA effects on membrane potential and conductance of these brainstem motoneurones of the rat *in vivo* and in a brainstem slice preparation. *In vivo* the excitatory amino acids (EAA) were applied by iontophoretic injections while perfusion or droplets were used in the slice preparation. The first mode of application had a local effect on the somatic region of the motoneurone. The second mode had a diffuse effect in reaching all parts of the neurone together with its microenvironment. We used two receptor antagonists (DL-aminophosphonovalerate and kynurenate) to study the involvement of EAA receptors in the synaptic responses evoked in these motoneurones.

Experimental procedures

Full details of surgical and experimental procedures were described previously [6,7,14]. Briefly, *in vivo* experiments were carried out on male wistar rats anaesthetized with pentobarbital. The animal was placed in a stereotaxic device and a craniotomy was performed over the cerebellum which was partially removed. Microelectrodes were guided into the region of the oculomotor (nerve III) or the abducens (nerve VI) nuclei which were identified by the antidromic field potentials evoked by the stimulation of the muscular nerves in the orbit. Trigeminal afferent fibers were also stimulated in the orbit inducing excitatory post-synaptic potentials in ocular motoneurones. *In vitro* experiments were made on 400 μm rat brainstem parasagittal slices kept in a chamber (1 ml) containing a buffered solution at pH 7.35 at 36°C, continuously perfused and bubbled with 0_2 95% and CO_2 5%. The modified Krebs-Ringer solution consisted of (mM): NaCl, 124: KCl, 5; $CaCl_2$, 2.5:

KH_2PO_4, 1.20: $MgSO_4$, 1.30: Glucose, 10: $NaHCO_3$, 24. Oculomotor neurones were antidromically identified following electrical stimulation of the motor axons. Excitatory post-synaptic potentials (probably vestibular and partly monosynaptic) could be evoked by stimulation of the medial longitudinal fasciculus (MLF). Recording microelectrodes were filled with 3 M KCl or 2 M *K*-citrate. In the slice preparation, the EAA and their antagonists were applied extracellularly by droplet either directly on the slice or through the bubble trap in the perfusion line. In a few experiments, the substances were applied by iontophoresis using a micropipette close to the intracellular recording electrode. *In vivo* the compounds were iontophoresed onto the motoneurone with a seven-barrelled assembly [9] surrounding an intracellular recording electrode (intertip distance: 50 μm–100 μm). The iontophoresed substances were: *N*-methyl-D-aspartate (NMDA: 0.1 M); kynurenate (KY; 0.2 M); (±) 2-aminophosphonovalerate (APV: 0.2 M in 150 mM NaCl) and NaCl 3 M. Intracellular potentials were recorded on fast and slow chart recorders, stored on magnetic tape and digitized for further analysis. Conductance measurements were made from hyperpolarizing current pulses of 40 ms to 120 ms duration, delivered at 0.5 to 2 Hz.

Results

Stable intracellular recordings for periods of up to 1 h *in vivo* and 3 h in slices were obtained from antidromically identified ocular motoneurones. Resting membrane potentials were between –50 mV and –80 mV with action potentials of 70 mV to 110 mV. Mean membrane resting potentials were similar for both *in vivo* and *in vitro* motoneurones.

NMDA responses were different in these motoneurones according to the application mode of NMDA: either close to the soma by local iontophoretic application *in vivo* or diffuse application by perfusion of the slice preparation.

In vivo, iontophoretic local applications of NMDA on oculomotor neurones evoked a slow depolarization and an apparent membrane resistance increase followed by a stable repetitive firing of action potentials. Figure 1 illustrates the NMDA responses of an oculomotor neurone during extracellular iontophoresis (50 nA) through the NMDA barrel located at 65 μm from the somatic recording site. The repetitive firing outlasted the NMDA application. Similar responses were obtained in abducens motoneurones. Similar responses were also obtained *in vitro* following droplet or iontophoretic applications on oculomotor neurones and they can be compared to those obtained in spinal motoneurones [11].

When NMDA was applied by droplets (5 μl or 10 μl; 40 mM) in the perfusion line of the slice chamber, dose-dependent NMDA responses occurred in oculomotor neurones as shown in Fig. 2. Slow depolarizations developed together with an increase of synaptic noise, an apparent membrane conductance decrease and repetitive firing. The repetitive firing of action potentials was usually 'quenched' (Fig. 2B) or blocked during a 'plateau' potential at an apparent Em level of about

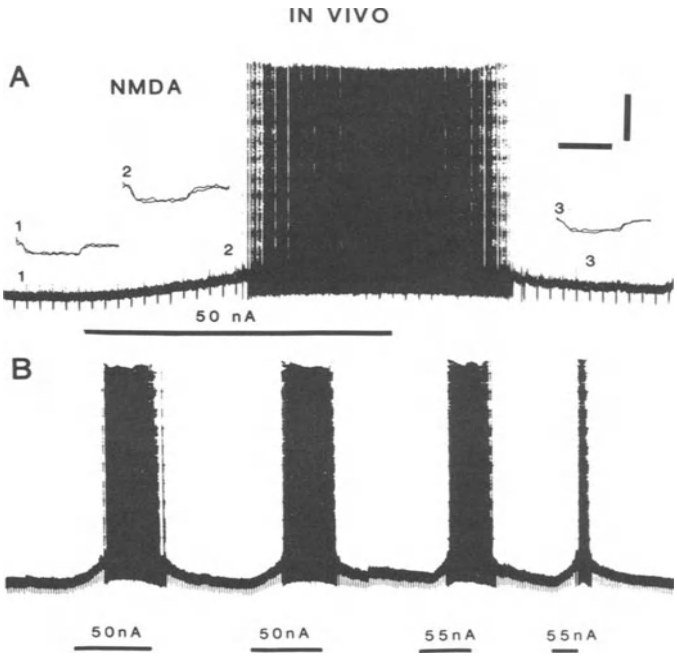

Fig. 1. Oculomotor neurone *in vivo*, –75 mV. A) Membrane potential and conductance changes during iontophoretic NMDA application (50 nA). Three conductance pulses taken at different times (1, 2 and 3) are shown with delayed time scale (70 msec) before, during and after the NMDA application. B) Repeated NMDA applications and dose-dependent responses with different duration pulses.
Calibrations: time in A, 4 sec and B, 20 sec; voltage, 20 mV.

–50 mV (Figs. 3B and 3D). The plateau potential lasted a few seconds, then after a slow decay of the membrane potential to the level of discharges, the repetitive firing started again, lasting 1–2 min. The membrane potential returned slowly to its resting level. During the plateaus, only rebound action potentials were observed following hyperpolarizing conductance pulses (Fig. 3B or 3D, see legends). Such rebound action potentials could also be evoked during NMDA repetitive firing (Fig. 2B). In Fig. 2C, membrane potential and conductance changes during two NMDA responses are plotted in function of time. The input membrane conductance (Gm), measured by intracellular current pulses, decreased by 10% to 25% during the slow depolarization (Fig. 2C, left). During the plateau potential, Gm increased by more than 100% (Fig. 2C, right) and then decreased before the action potentials started to fire again.

The NMDA-induced responses were blocked by the antagonists APV and KY in slice and *in vivo*. The droplet application in the perfusion line of APV (20 µl; 0,2 M) or KY (15 µl; 0,2 M) preceding those of NMDA strongly reduced the NMDA responses (Fig. 3). Simultaneous local applications of APV or KY from the

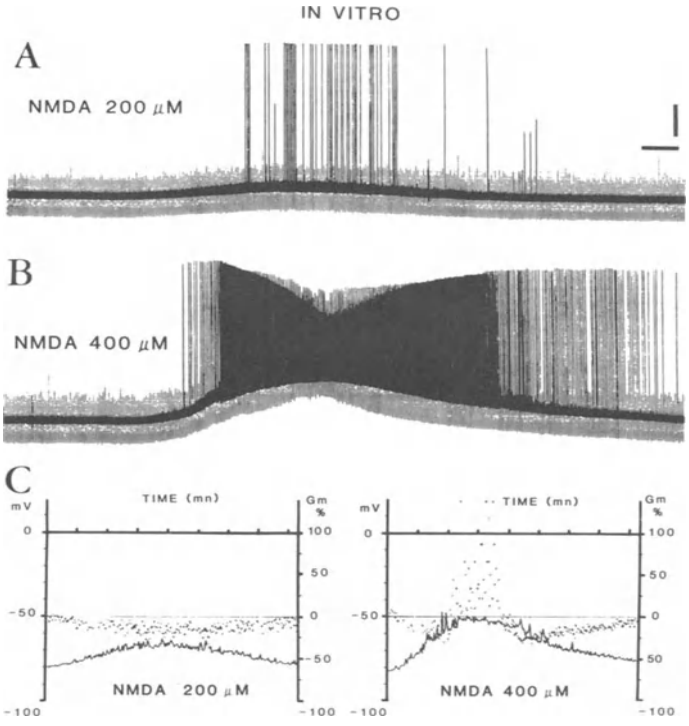

Fig. 2. Oculomotor neurone *in vitro* –82 mV. A) and B) NMDA-induced responses following NMDA droplet application through the perfusion line (5–10 μl; 40 mM). C) Graphs showing membrane potential and conductance changes (dots) during two NMDA applications in the same motoneurone. Graph on the left corresponds to Fig. 2A and graph on the right to Fig. 3D.
Calibrations: time, 20 sec; voltage, 20 mV.

7-barrelled electrodes, during NMDA pulses, gave a partial blockade of the NMDA responses *in vivo* (Fig. 4). NMDA induced responses following iontophoretic applications (100 nA) were reduced during continuous application of APV (45 nA for 5 min, Fig. 4B). Simultaneous application of KY (30 nA) and APV (45 nA) blocked the NMDA responses (Fig. 4C). The two antagonist effects could be additive. A partial recovery was obtained under APV without KY (Fig. 4D).

Trigeminal EPSPs, evoked *in vivo* by orbital electrical stimulation, were not affected by APV and KY iontophoretic applications at doses which blocked the NMDA-induced responses (Fig. 5A). *In vitro,* EPSPs evoked by the MLF stimulation were not modified during antagonist perfusion which strongly reduced NMDA responses (Fig. 5B). The absence of antagonist effect on EPSPs was tested on 21 motoneurones *in vivo* and 8 motoneurones *in vitro*. For each motoneurone, 25 to 100 EPSPs were digitized and the calculated area of the EPSPs showed no

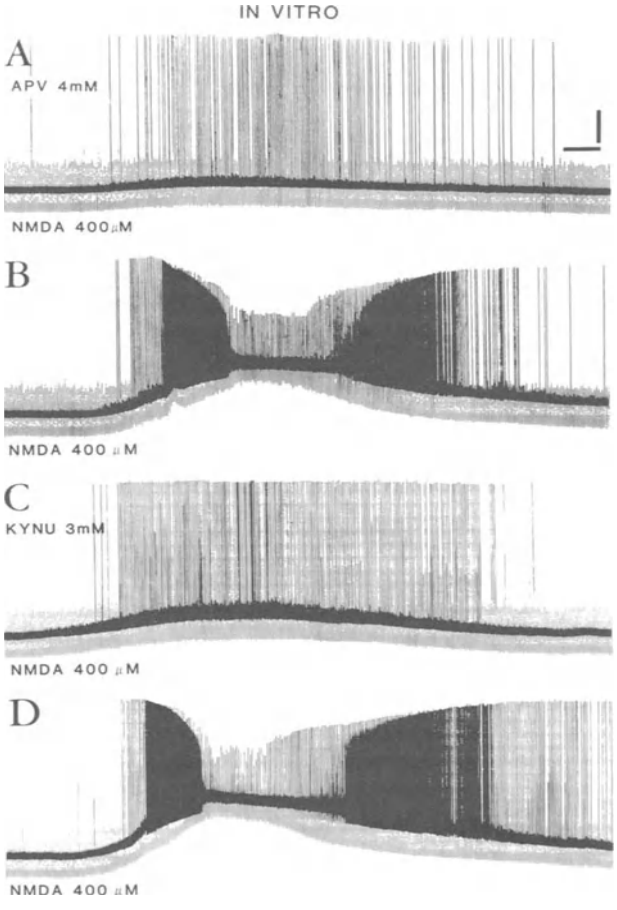

Fig. 3. Same motoneurone as in Fig. 2, control NMDA response was shown in Fig. 2A. A) Effect of APV (20 μl; 0.2 M) applied 40 sec before the NMDA application. B) Recovery of the NMDA-induced response (400 μM). C) Effect of KY (15 μl; 0,2 M) applied 40 sec before the NMDA application. D) Recovery of the NMDA-induced response. Only rebound action potentials with different amplitudes could be observed following hyperpolarizing conductance pulses, during the plateaus.
Calibrations: time, 20 sec; voltage, 20 mV.

modification before, during and after the antagonist application. During NMDA depolarizations, the trigeminal EPSPs were amplified, as shown in Fig. 5D, giving rise to bursts of action potentials followed by a large hyperpolarization. Trigeminal EPSPs were not affected by intracellular injection of hyperpolarizing or depolarizing currents (Fig. 5C).

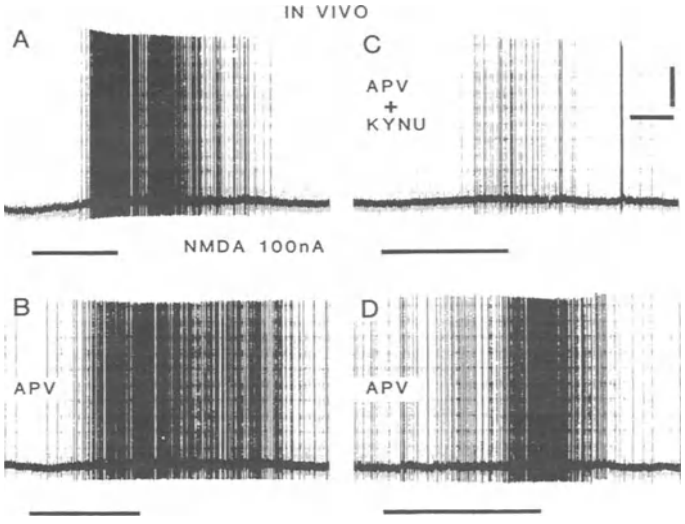

Fig. 4. Abducens motoneurone –70 mV recorded *in vivo*. Antidromic action potential was evoked at a rate of 1 Hz during all the recordings. A–D) NMDA induced responses following iontophoretic applications of (100 nA) NMDA. A) Control; B) during APV application (45 nA for 5 min). C) APV (45 nA) for 6 min and KY applications (30 nA) for 1 min. D) APV application (45 nA) for 7 min and KY application off since 2 min.
Calibrations: time, 20 sec; voltage, 20 mV.

Discussion

Our results show that different NMDA-induced responses were obtained in the same type of motoneurones, following extracellular local iontophoretic applications and applications by perfusion of the brainstem slice. When NMDA was applied locally close to the soma of the motoneurone (50 μm–100 μm), a stable repetitive firing appeared after a slow depolarization and no plateau potential was induced. On the contrary, plateau potentials were obtained during NMDA application by perfusion in the slice. This difference in the NMDA effect might be explained by the different modes of application. *In vitro,* the whole somatodendritic membrane of the motoneurone can be affected by NMDA and/or local circuits can be activated simultaneously. We suggest that some NMDA receptors are located at dendritic sites and their activation may account for the observed different responses. Plateau potentials have been induced by NMDA in different neurones [10,13,15]. NMDA or DL-homocysteate responses were observed as far as 400 μm from the soma of spinal motoneurones [12]. It has been suggested that NMDA receptors are concentrated on cortical neurones proximally [18] or at dendritic sites predominantly [17]. We speculate that both dendritic and somatic

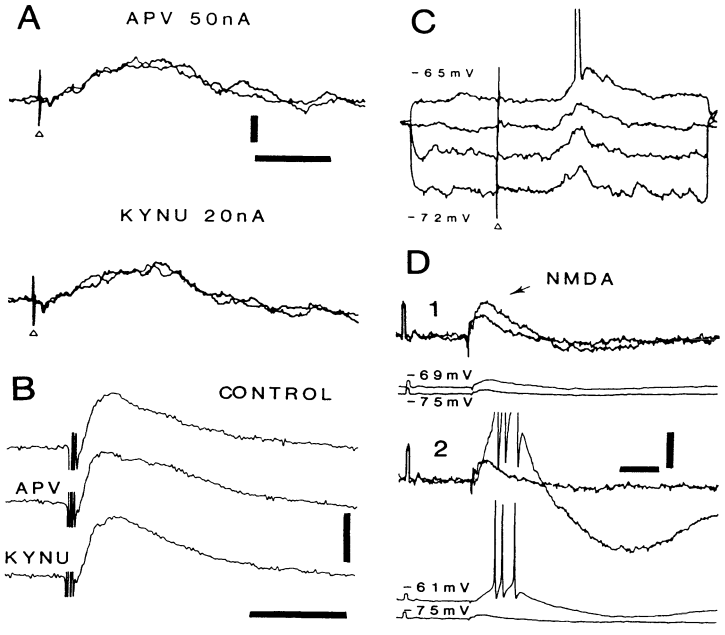

Fig. 5. EPSPs in ocular motoneurones during APV, KY or NMDA applications. A) *In vivo* trigeminal EPSPs during APV or KY with control EPSP in superimposed traces. Calibrations: time, 10 msec; voltage, 2 mV. B) *In vitro,* EPSPs evoked by MLF stimulation before (control) and during APV or KY applications. C) Trigeminal EPSPs during hyperpolarizing or depolarizing current pulses. (100 msec). D) Trigeminal EPSPs during NMDA depolarization. D1) EPSP control superimposed with amplified EPSP at −69 mV. D2) EPSP control with amplified EPSP at −61 mV. NMDA applications: 100 nA. Calibrations: time, 10 msec in A, 5 msec in B, 10 msec in D, pulses duration in C, 70 msec; voltage, 2 mV in A, 10 mV in B, 5 mV (high gain) and 20 mV (low gain) in D.

NMDA sites are present on ocular motoneurones. These results also suggest that NMDA receptors are not involved in vestibular and trigeminal EPSPs. Vestibular EPSPs produced by MLF stimulation *in vitro* and trigeminal EPSPs *in vivo,* were not modified by APV or KY applications. A possible explanation for the lack of antagonists effects on trigeminal EPSP would be that local iontophoretic application of antagonists did not reach the excitatory synapses. The trigeminal EPSPs were amplified during NMDA receptors activation, probably due to a region of negative slope conductance in the I/V characteristic of the neuron [13]. We suggest the presence of NMDA receptors on the motoneuronal membrane between the trigeminal synapses and the somatic application site. The increase in synaptic noise, under NMDA perfusion *in vitro,* may be relevant to the same amplification mechanism of synaptic events during NMDA receptors activation.

Acknowledgements

We thank N. Cannavo and N. Seyfritz for technical assistance.

References

1. Ascher P and Nowak L (1987) Trends in Neurosci. 10: 284–288.
2. Cotman CW and Iversen LL (1987) Trends in Neurosci. 10: 263–265.
3. Cotman CW, Monaghan DT and Ganong AH (1988) Ann. Rev. Neurosci. 11: 61–80.
4. Cotman CW, Monaghan DT, Ottersen OP and Storm-Mathisen J (1987) Trends in Neurosci. 10: 273–280.
5. Collingridge GL and Bliss TVP (1987) Trends in Neurosci. 10: 288–293.
6. Durand J (1989) Exp. Brain Res. 76: 141–152.
7. Durand J (1989) Neuroscience 30: 639–649.
8. Durand J, Engberg I and Tyc-Dumont S (1987) Neurosci. Lett. 79: 295–300.
9. Engberg I, Flatman JA and Lambert JDC (1979) J. Physiol. (Lond) 288: 227–261.
10. Engberg I, Flatman JA and Lambert JDC (1984) Acta Physiol. Sci. 121: 6A.
11. Engberg I, Flatman JA, Lambert JDC and Lindsay A (1983) In: Fuxe K, Roberts P and Schwarcz R (eds.) Excitotoxins. Macmillan, London, pp. 170–183.
12. Flatman JA, Lambert JDC and Engberg I (1985) Acta Physiol. Scand. 124: 421–427.
13. Flatman JA, Schwindt PC and Crill WE (1986) Brain Res. 363: 62–77.
14. Gueritaud JP (1988) Neuroscience 24: 837–852.
15. Herrling PL, Morris R and Salt T (1983) J. Physiol. (Lond) 339: 207–222.
16. Macdermott AB and Dale N (1987) Trends in Neurosci. 10: 280–284.
17. Sutor B and Hablitz JJ (1989) J. Neurophysiol. 61: 621–634.
18. Thomson AM (1986) Neuroscience 17: 37–47.
19. Watkins JC and Olverman HJ (1987) Trends in Neurosci. 10: 265–272.

Blockade of audiogenic seizures by a GABA-uptake inhibitor, NO-328, in the genetically epilepsy-prone rat

Carl L. Faingold, Marcus E. Randall and Catherine A. Copley

Department of Pharmacology, Southern Illinois University, School of Medicine, Springfield, IL 62794, U.S.A.

Abstract

Previous studies indicate that a critical audiogenic seizure (AGS) initiation mechanism in genetically epilepsy-prone rats (GEPRs) is the reduced effectiveness of exogenously applied or endogenously evoked release of GABA in inhibiting inferior colliculus (IC) neurons. NO-328 [R-(-)-1-(4,4-(3-Methyl-2-thienyl)-3-butenyl)-3-piperidine carboxylic acid], is a new anticonvulsant that selectively blocks GABA uptake. In this study, systemically administered NO-328 was effective in blocking AGS in GEPRs [ED_{50} of 11 (tonus), 29.5 mg/kg (wild running and clonus), 30 min post-injection. Bilateral microinjection of 40–80 nMol/side of NO-328 reduced AGS severity in GEPRs. Animals were quiescent with higher systemic or microinjected doses. These data further support the importance of the reduced effectiveness of GABA in AGS initiation in GEPRs and indicate that NO-328 is a potentially important new anticonvulsant drug.

Introduction

The inhibitory amino acid, GABA, is implicated as an important neurotransmitter in the inferior colliculus (IC) [1]. The IC is an obligate nucleus of the ascending auditory pathway, and recent studies have suggested that several forms of acoustically-evoked inhibition in IC neurons may be mediated by GABA [1,2]. Recent studies indicate that the function of GABA in the IC of the genetically epilepsy-prone rat substrain exhibiting maximal AGS (GEPR-9) is abnormal. The IC is strongly implicated in audiogenic seizures (AGS) initiation in the GEPR [3–5]. GABA levels and the number of GABAergic neurons in the IC of the GEPR-9 are elevated [6,7]. The effectiveness of GABA exogenously applied and the efficacy of GABA-mediated forms of acoustically-evoked inhibition are reduced in IC neurons of the GEPR-9 as compared to normal IC neurons [8,9]. Previous studies in the submaximal seizures of the original AGS-susceptible rat strain from which the GEPR-9 was derived indicated that GABA agonists microinjected into the IC blocked AGS susceptibility [10,11], and this was confirmed in recent studies in the maximal severity seizures of the GEPR-9 [12]. However, the effectiveness of GABA agonists in blocking AGS only indicates that GABA receptors may be activated exogenously to attenuate seizures, but it is not clear from these studies if GABA released from IC, implied by studies on its role in IC physiology, is capable

of affecting seizure susceptibility in the GEPR-9. NO-328 [R-(-)-1-(4,4-(3-Methyl-2-thienyl)-3-butenyl)-3-piperidine carboxylic acid], is a new drug (Novo Industries) that selectively blocks GABA uptake without GABA agonist properties [13]. NO-328 is anticonvulsant against AGS in DBA/2 mice and against convulsant drugs in mice and rats. The purpose of the present study was to examine if administration of NO-328, which increases the effect of endogenous GABA, is capable of affecting AGS susceptibility in the GEPR utilizing systemic administration or bilateral microinjection directly into the IC.

Methods

GEPR-9s obtained from Dr. Phillip Jobe at the University of Illinois in Peoria or offspring of these animals were used in these experiments. The animals were anesthetized with ketamine/xylazine (85/3 mg/kg i.m.) and bilateral guide cannulae (21 gauge) were cemented into place with dental acrylic on the surface of the brain over the inferior colliculus (IC). The following coordinates (in mm) from Paxinos and Watson [14] were utilized for the implantations in inferior colliculus: AP –9.3 (posterior to bregma), L 1.5 (from the midline), V –3.5 (ventral to the surface of the brain). At least one week later the animals were tested for AGS susceptibility, and only those exhibiting characteristic maximal AGS, score of 9 on the scale of Jobe [15], were utilized in these experiments.

Microinjection experiments involved bilateral infusion of NO-328 into the IC of GEPR-9s. The drug was dissolved in 0.5–1.0 µl of phosphate buffer (pH 7.0) and administered over a 2–4 min period. This study also examined effects of systemic administration of NO-328 by the intraperitoneal route. Following drug administration the animals were tested for AGS susceptibility by being individually placed in a cylindrical chamber in which an electrical bell (122 dB SPL) was mounted. The animals were exposed to the bell until the onset of convulsions, or for a maximum of 60 seconds. AGS severity scores were evaluated until recovery at 30 min, 1, 2, 3 and 4 h and subsequently at 24 h intervals after the end of the infusion. At the end of the experiment the animals were sacrificed with an overdose of pentobarbital (100 mg/kg i.p.) and the brains were removed for histological verification of the position of the cannula tips. Only those animals in which the cannula tips were positioned in the IC were included in the results. The one sample Student's t test was used to evaluate the changes in seizure scores. ED_{50} calculations were done using probit analysis.

Results

As shown by the dose-response curves in Fig. 1, systemically administered NO-328 was effective in blocking AGS in GEPR-9s. The i.p. doses of NO-328 ranged from 4–60 mg/kg, and the highest dose showed nearly complete anti-

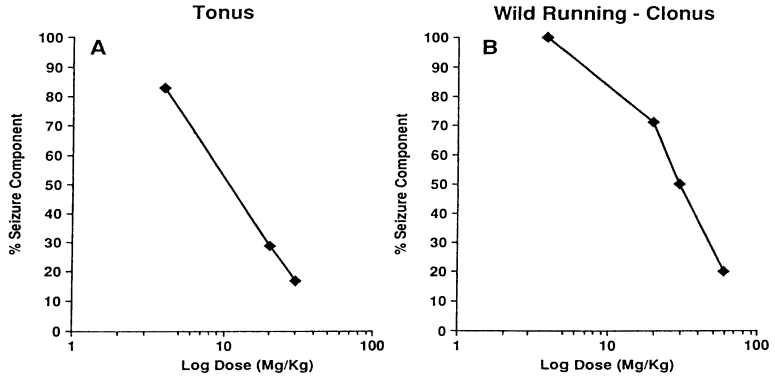

Fig. 1. Dose response curves for NO-328 against audiogenic seizure components A) tonus and B) clonus and wild running in the GEPR-9. The ED_{50} for tonus was 11 mg/kg, and for clonus and wild running it was 29.5 mg/kg (probit analysis).

convulsant efficacy, reducing the AGS score to zero in most animals. The ED_{50} for blockade of tonic hindlimb extension was 11 mg/kg as seen in Fig. 1A, and a higher dose (ED_{50}, 29.5 mg/kg) was required to block wild running and clonus, as shown in Fig. 1B. The drug reached complete efficacy at 30 min post-injection. Only modest behavioral changes were noted, which include a quieting effect on the animal's normal exploratory behavior at the highest systemic doses, but no overt signs of sedation were observed. Complete reversal of anticonvulsant effects was observed by 24 h.

The effects of bilateral microinjection of 10–80 nmol/side of NO-328 into the IC on AGS severity were examined in GEPR-9s. Typical placement sites within the IC are shown in Fig. 2. Animals were also quiescent with higher microinjected doses. Higher doses produced a statistically significant lowering of the AGS scores (Table 1). The seizure blockade was usually observed by 2–3 h after infusion, and recovery was often protracted, lasting up to two days, as seen in the time course of the curves in Fig. 3. Lower doses were ineffective at reducing seizure severity and vehicle infusions were without effect. Recovery occurred by 24 to 48 h. The time course of effects is prolonged as compared with those of GABA agonists, which is consistent with inhibition of GABA uptake rather than receptor blockade.

Discussion

The results of this study support the previous findings of the importance of GABA in the AGS susceptibility of the GEPR. The ability of NO-328, which blocks the uptake of GABA [13], to block AGS suggests that endogenous release of this inhibitory amino acid acts to reduce the firing of neurons important for seizure

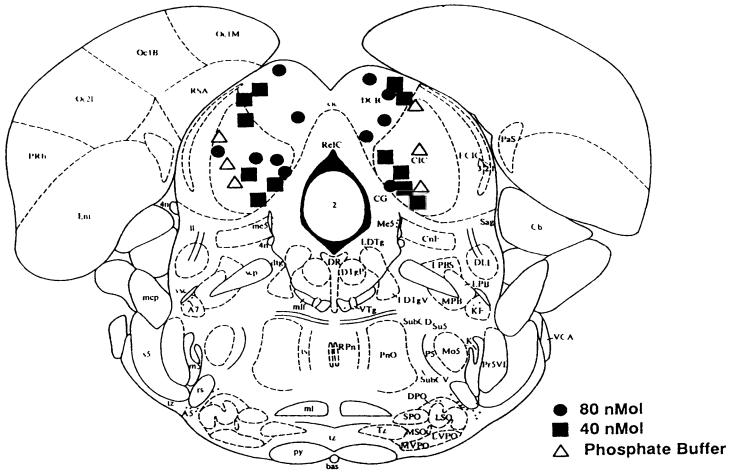

Fig. 2. Distribution of placement sites for cannula tips in the inferior colliculus in the GEPR-9. The circle = 80 nmol, square = 40 nmol/side and triangle = sites of vehicle injection. Filled symbols indicate sites that were effective in reducing AGS severity, and unfilled symbols are sites without effect. Stereotaxic coordinates in mm from Paxinos and Watson [14]: inferior colliculus: –9.3 (posterior to bregma), 1.8 (ventral to brain surface), –3.5 (vertical).

initiation. Previous studies have suggested that the IC is the most critical brain region for initiation of AGS [3,5]. Alterations in the action of GABA have been strongly implicated in the initiation mechanisms for AGS. Thus, recent studies have shown blockade of AGS in GEPR-9s with microinjection of GABA agonists,

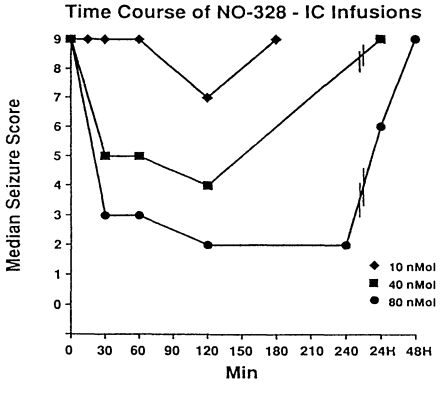

Fig. 3. Time course of effects of NO-328 in three doses microinjected bilaterally into inferior colliculus. Significant reductions in AGS severity were observed with the higher doses and prolonged durations were also observed with these doses.

Table 1. Effects of focal bilateral microinfusion into IC of NO-328 on AGS in the GEPR-9

Drug	Structure	N	Dose (nmol/side)	median seizure score before	after
NO-328	IC	5	10	9	9 ns
		7	40	9	4[a]
		6	80	9	2[b]

[a] Significantly different from pre-injection score at $p<0.05$.
[b] Significantly different from pre-injection score at $p<0.001$.
ns not significantly different from pre-injection score.
(One sample Student's t test).

muscimol or baclofen into the IC [12,16]. The GABA-transaminase inhibitor, gabaculine, reduces GABA levels when injected into the IC [17,18], and AGS are also blocked by this procedure. Microinjection of bicuculline into the IC of normal rats causes the animals to become susceptible to AGS [19]. Abnormalities in the GABAergic neurons in the GEPR-9 IC have been observed. Thus, an increase in the number of GABAergic neurons and GABA content is observed particularly in the central nucleus of IC of the GEPR-9 [6,7]. The effectiveness of iontophoretically applied GABA and a benzodiazepine are reduced in the GEPR-9 IC, and two forms of endogenous GABA-mediated inhibition, binaural inhibition and non-monotonic rate intensity functions, are also less effective [8,9]. Several possibilities have been suggested to reconcile the seemingly conflicting anatomical and physiological findings. These include the possibility that there is an increased GABA release onto IC neurons, which leads to down-regulation of GABA receptors. Another possibility is that the increase in GABAergic neurons results in increased uptake of normally released GABA back into these neurons. Preliminary evidence has been observed which supports the latter possibility [20]. The finding that the GABA-uptake inhibitor, NO-328, is an effective anticonvulsant upon administration directly into the IC would be consistent with this hypothesis. These results indicate that NO-328 is a potentially important new anticonvulsant drug, and this new mechanism of action, blockade of GABA uptake, may hold promise for improved therapy of epilepsy.

Acknowledgements

The authors gratefully acknowledge the technical assistance of Vipul Trivedi and Novo Industries for providing the NO-328. This study was supported in part by NIH NS 13849, and NS 21281. The Division of Biomedical Illustration and Photography prepared the figures.

References

1. Faingold CL, Gehlbach G and Caspary DM (1989) On the Role of GABA as an Inhibitory Neurotransmitter in Inferior Colliculus Neurons: Iontophoretic Studies. Brain Res. 500: 302–312.
2. Faingold CL, Gehlbach G and Caspary DM (1990) Functional Pharmacology of Inferior Colliculus Neurons. In: Altschuler RA, Hoffman DW, Bobbin RP and Clopton B (eds.) Neurobiology of Hearing. Raven Press, New York. Vol. 2, (in press).
3. Browning R (1986) Neurobiology of seizure disposition – the genetically epilepsy-prone rat VII. Neuroanatomical localization of structures responsible for seizures in the GEPR: Lesion Studies. Life Sci. 39: 857–868.
4. Faingold CL (1987) The Role of the Brain Stem in Generalized Epileptic Seizures. Metab. Brain Dis. 2: 81–112.
5. Faingold CL (1988) The Genetically Epilepsy-Prone Rat. Gen. Pharmacol. 19: 331–338.
6. Roberts RC, Ribak CE and Oertel WH (1985) Increased numbers of GABAergic neurons occur in the inferior colliculus of an audiogenic model of genetic epilepsy. Brain Res. 361: 324-338.
7. Ribak CE, Byun MY, Ruiz GT and Reiffenstein RJ (1988) Increased levels of amino acid neurotransmitters in the inferior colliculus of the genetically epilepsy-prone rat. Epilepsy Res. 2: 9–13.
8. Faingold CL, Gehlbach G and Caspary DM (1986) Decreased effectiveness of GABA-mediated inhibition in the inferior colliculus of the genetically epilepsy-prone rat. Exp. Neurol. 93: 145–159.
9. Faingold CL and Boersma-Anderson CA (1988) Inferior Colliculus (IC) Unit Activity and Audiogenic Seizures (AGS) in Behaving Genetically Epilepsy-Prone Rats (GEPRs) Soc. Neurosci. Abs. 14: 253.
10. Duplisse BR, Picchioni AL, Chin L and Consroe PF (1974) Relationship of the inferior colliculus and gamma-aminobutyric acid (GABA) to audiogenic seizure in the rat. Fed. Proc. 33: 468.
11. Frye GD, McCown TJ, Breese GR and Peterson SL (1985) GABAergic modulation of inferior colliculus excitability: Role in the ethanol withdrawal audiogenic seizures. J Pharmacol. Exp. Ther. 237: 478–485.
12. Browning RA, Lanker ML and Faingold CL (1989) Effect of Inferior Colliculus Injections of Noradrenergic and GABAergic Agonists on Audiogenic Seizures in Genetically Epilepsy Prone Rats. Epilepsy Res. 4: 119–125.
13. Nielsen EB, Wolffbrandt KH, Andersen KE, Knutsen LJS, Sonnewald U and Braestrup C (1987) NO-328: A new potent GABA-uptake inhibitor. Soc. Neurosci. Abs. 13: 968.
14. Paxinos G and Watson C (1986) The Rat Brain in Stereotaxic Coordinates. Academic Press: Orlando, FL.
15. Dailey JW and Jobe PC (1985) Anticonvulsant drugs and the genetically epilepsy-prone rat. Fed. Proc. 44: 2640–2644.
16. Faingold CL, Copley CA and Boersma-Anderson CA (1988) Effects on Audiogenic Seizures (AGS) of Microinfusion of Baclofen (BAC) or 5-Hydroxytryptamine (5HT) into the Inferior Colliculus (IC) of Genetically Epilepsy-Prone Rats (GEPRs). Generalized Epilepsy Symposium Montreal, Quebec, Canada, p. 2.
17. Faingold CL, Millan MH, Boersma CA and Meldrum BS (1989) Induction of Audiogenic Seizures in Normal and Genetically Epilepsy-Prone Rats by Focal Microinjection of an Excitant Amino Acid into Auditory and Reticular Formation Nuclei. Epilepsy Res. 3: 199–205.
18. Faingold CL, Arneric SP, Randall ME and Copley CA (1989) Increased GABA levels or decreased glutamate (GLU) levels in inferior colliculus (IC) block audiogenic seizure (AGS) susceptibility in genetically epilepsy-prone rats (GEPRs). Soc. Neurosci. Abs. 15: 46.
19. Millan MH, Meldrum BS and Faingold CL (1986) Induction of audiogenic seizure susceptibility by focal infusion of excitant amino acid or bicuculline into the inferior colliculus of normal rats. Exp. Neurol. 91. 634–639.
20. Browning RA, Marcinczyk M and Jobe PC (1989) Assessment of GABA uptake and glutamic acid decarboxylase (GAD) in the genetically epilepsy-prone rat (GEPR) brain. Soc. Neurosci. Abs. 15: 1074.

Address for correspondence: Carl L. Faingold, Ph.D., Dept. Pharmacology, Southern Illinois University, School of Medicine, PO. Box 19230, Springfield, IL 62794-9230, U.S.A.

N-Methyl-D-aspartate antagonists stimulate locomotor activity in monoamine depleted rats: Implications for the therapy of Parkinson's disease

Thomas Klockgether[a], Lechoslaw Turski[b], Peter-Andreas Löschmann[b] and Helmut Wachtel[b]

[a]*Department of Neurology, University of Tübingen, Hoppe-Seyler-Str. 3, D-7400 Tübingen, F.R.G.*

[b]*Research Laboratories of Schering AG, Müllerstr. 170–178, D-1000 Berlin 65, F.R.G.*

Abstract

Recent experimental evidence suggests that the subthalamic and pallidal projections in 1-methyl-4-phenyl-1,2,3,6-tetrahydropyridine (MPTP) treated monkeys are abnormally active. In addition, immunocytochemical and electrophysiological studies have shown that the subthalamic nucleus receives a glutamatergic cortical input and subthalamic neurons projecting to the internal pallidal segment (GPi) themselves are glutamatergic. On the basis of these findings we have hypothesized that glutamate antagonists may be beneficial in the therapy of Parkinson's disease. To test the validity of this hypothesis in a rodent model of Parkinson's disease we subjected rats to reserpine (5 mg/kg, i.p.; 24 h) and α-methyl-p-tyrosine (250 mg/kg, i.p.; 3.5 h) treatment and tested whether glutamate antagonists, MK-801 (5-methyl-10,11-dihydro-5H-dibenzo(a,d)cycloheptan-5,10-imine maleate) (0.39–6.25 mg/kg, i.p.), a non-competitive antagonist at the *N*-methyl-D-aspartate (NMDA) receptor subtype and CPP (3-((±)-2-carboxypiperazin-4-yl)-propyl-1-phosphonate) (0.39–6.25 mg/kg, i.p.), a competitive NMDA antagonist, stimulate locomotor activity. The results show that MK-801 dose-dependently stimulates locomotor activity in monoamine depleted rats and markedly potentiates the action of L-DOPA. CPP also showed stimulatory effects, however its effect was less than MK-801. These observations support the notion that antagonism at NMDA receptors restores locomotion in monoamine depleted animals and raises hopes that adjuvant therapy with NMDA antagonists might improve therapy of patients suffering from Parkinson's disease.

Introduction

It is now firmly established that L-glutamate plays an important role as neurotransmitter in the basal ganglia. Cortical ablation reduces high-affinity glutamate uptake in the neostriatum (NEO) and substantia nigra suggesting a neurotransmitter role of L-glutamate in the corticostriatal and corticonigral pathway [1,2]. The glutamatergic nature of the corticostriatal pathway is further substantiated by electrophysiological investigations demonstrating excitatory effects of cortical stimulation on striatal neurons which are mediated by the non-*N*-methyl-D-

aspartate (non-NMDA) subclass of L-glutamate receptors [3]. Recently, it has been shown by immunocytochemical methods that in contrast to earlier belief neurons of the subthalamic nucleus (STH) are not GABAergic, but glutamatergic [4,5]. In addition, electrical stimulation of the STH has excitatory effects on neurons in its projection fields, the substantia nigra pars reticulata (SNR) and the internal pallidal segment (GPi) [4]. Electrophysiological experiments using microiontophoretic technique further suggest that the STH receives a glutamatergic cortical input [6].

In contrast to L-glutamate's well-established role in physiological processes of the basal ganglia there is only limited knowledge to which degree glutamate transmitter metabolism is affected in pathophysiological states, such as Parkinson's disease. Parkinsonian symptomatology is caused by a deficiency of dopamine within the NEO due to degeneration of the dopaminergic nigrostriatal tract. Electrophysiological recordings and measurements of local deoxyglucose uptake in monkeys made parkinsonian by treatment with 1-methyl-4-phenyl-1,2,3,6-tetrahydropyridine (MPTP) revealed an increased neuronal activity in the STH and the output stations of the basal ganglia, the GPi and SNR [7,8], suggesting overactivity of the glutamatergic system projecting from the cortex via the STH to the basal ganglia output stage [9]. An increased neuronal output from the basal ganglia suppresses thalamocortical activity via GABAergic projections and is thought to lead to akinetic-rigid symptomatology in Parkinson's disease [10–13].

Given the hypothetical role of L-glutamate to mediate the consequences of dopamine deficiency in the NEO, we decided to investigate if antagonists of L-glutamate induced excitation are capable of reversing the depression of locomotor activity in a rodent model of Parkinson's disease. As a test model we chose reserpine- and α-methyl-p-tyrosine-treated rats which – due to depletion of their monoamine pools and blockade of dopamine synthesis – exhibit a marked reduction of locomotor activity. As antagonists we used MK-801 (5-methyl-10,11-dihydro-5H-dibenzo(a,d)cycloheptan-5,10-imine maleate), a non-competitive antagonist at the NMDA receptor subtype [14] and CPP (3-((±)-2-carboxypiperazine-4-yl)-propyl-l-phosphonate), a competitive antagonist at the same site [15]. Unfortunately, compounds which block specifically non-NMDA receptors are short-acting and do not pass the blood-brain-barrier [16].

Materials and Methods

Drugs

The following drugs were used: reserpine (Ciba-Geigy, Basle, Switzerland), D,L-α-methyl-p-tyrosine methylester hydrochloride (Labkemi AB, Göteborg, Sweden), benserazid (Hoffmann-La Roche, Basle, Switzerland), L-DOPA (Sigma, St. Louis, MO, U.S.A.), MK-801 (5-methyl-10,11-dihydro-5H-dibenzo(a,d)cycloheptan-5,10-imine maleate) (Merck Sharp and Dohme, Harlow, Essex, UK), and

CPP (3-(±)-2-carboxypiperazin-4-yl)-propyl-l-phosphonic acid) (Tocris, Buckhurst Hill, U.K.). Reserpine was dissolved in a drop of glacial acetic acid and diluted to the final concentration with demineralised water. Benserazid was dissolved in isotonic saline solution. All other drugs were dissolved in isotonic saline solution containing 10% (w/v) Cremophor EL® (polyethoxylated castor oil) (BASF, Ludwigshafen, F.R.G.).

Animals and treatment

Male Wistar rats (Schering AG, Berlin, F.R.G.) weighing 100–130 g were used. The animals were kept in a temperature-controlled room (22°C ± 1°C) with a 12 h light/dark cycle. The room was illuminated between 06.00 and 18.00 h. The rats received a standard diet (Altromin®, Altromin Spezialfutterwerke GmbH, Lage, F.R.G.) with free access to water. The drugs were administered intraperitoneally (i.p.) in a volume of 0.5 ml/100 g body weight. Control animals received a corresponding volume of vehicle. All drug doses refer to the base.

Locomotor activity

Locomotor activity was measured using circular photocell activity cages as described in detail elsewhere [17]. Every interruption of the photocell beam was recorded as one count. Immediately following the injection of the NMDA antagonists or vehicle, individual rats were placed in a motility cage and the counts accumulated over 10 min intervals were recorded for up to 120 min.

Statistics

Means ± S.E.M. were calculated and the statistical significances of the differences between the means for the various drug treatments and the corresponding control were determined by one-way analysis of variance in conjunction with the Dunnett test.

Results

Depletion of endogenous brain catecholamines by pretreatment with reserpine and α-methyl-p-tyrosine produces a pronounced depression of locomotor activity in rats. Administration of the non-competitive NMDA antagonist MK-801, 0.39–6.25 mg/kg i.p., reduced the hypokinesia; this effect was statistically significant at 6.25 mg/kg of MK-801 (Fig. 1). The competitive NMDA antagonist CPP, 0.39–6.25 mg/kg i.p., also showed a dose-related stimulatory effect, however its activity was less pronounced compared to MK-801 (Fig. 2).

Administration of MK-801 in the dose of 0.39 mg/kg highly potentiated the stimulatory (sub-threshold) effect of L-DOPA and benserazide in reserpinised rats (Table 1).

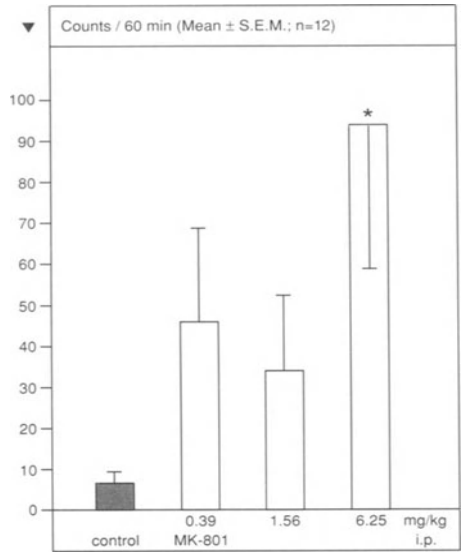

Fig. 1. Effect of various doses of MK-801 on the locomotor activity of rats depleted of brain monoamines by pretreatment with reserpine (5 mg/kg i.p., 24 h) and α-methyl-p-tyrosine (250 mg/kg i.p., 3.5 h). Immediately after MK-801 or vehicle administration, rats were individually placed in a circular photocell motility cages, and the number of light beam crossings was recorded for 1 h. The statistical significance of the differences between the means of the various MK-801-treated groups and the control was determined by one-way analysis of variance in conjunction with the Dunnett test (* $p<0.05$).

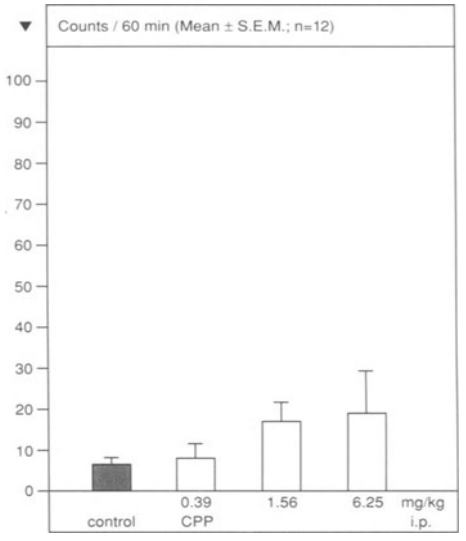

Fig. 2. Effect of various doses of CPP on the locomotor activity of rats depleted of brain monoamines by pretreatment with reserpine and α-methyl-p-tyrosine. See legend to Fig. 1. for further details.

Table 1. Effect of MK-801 (0.39 mg/kg i.p.) on locomotor activity of rats pretreated with reserpine (RES; 5 mg/kg i.p., 24 h), benserazid (B; 100 mg/kg i.p., 30 min) and L-DOPA (125 mg/kg i.p., 15 min) or the corresponding vehicle (C). The counts/60 min (mean ± S.E.M.; n = 9) are shown. See legend to Fig. 1 for further details.

RES+C+C+C	RES+C+C+MK-801	RES+B+L-DOPA+C	RES+B+L-DOPA+MK-801
	Counts/60 min (mean ± S.E.M.)		
332.4 ± 93.6	387 ± 131.1	351.8 ± 81.6	1743.0 ± 411.7[a]

[a]$P<0.01$ ANOVA/Dunnett test.

Discussion

We have shown that MK-801 and CPP dose-dependently reverse the depression of locomotor activity in monoamine depleted rats and that MK-801 markedly potentiates the stimulatory effect of L-Dopa in these animals. Both, MK-801 and CPP block NMDA-induced excitation although being of different chemical structure and working by a different mode of action. Extensive biochemical investigations have given no evidence of an interaction of these compounds with any transmitter receptor system other than NMDA receptors [14,15]. With these considerations in mind, it seems justified to conclude that the observed locomotor stimulatory effects of MK-801 and CPP in monoamine depleted rats are due to antagonism at the NMDA receptor subtype of L-glutamate receptors.

The significance of the present results is underlined by the recent finding of Schmidt and Bubser [18] using a different rodent model of Parkinson's disease that MK-801 dose-dependently reverses haloperidol-induced catalepsy in rats. In addition Carlsson and Carlsson [19] reported that MK-801 stimulates locomotor activity in monoamine depleted mice.

In an earlier paper [9] we have hypothetically predicted anti-parkinsonian activity of NMDA antagonists. This prediction was based on observations made in MPTP treated monkeys. Whereas no systematic changes of striatal cell activity were detectable as a consequence of dopamine loss in these animals, electrophysiological and metabolic studies revealed dramatic changes of neuronal activity in nuclei of the basal ganglia lying downstream of the NEO [7,8]. The most conspicuous findings were an increase of activity within the STH and within the output stations of the basal ganglia, the GPi and SNR. Since the STH receives a glutamatergic input from the cortex and subthalamic neurons projecting to the GPi and SNR themselves are glutamatergic, it is a viable hypothesis that the observed locomotor effects of MK-801 and CPP are due to blockade of excitation in the STH, GPi and SNR. This hypothesis is corroborated by an earlier electrophysiological finding in parkinsonian monkeys bearing experimental lesions of the dopaminergic part of substantia nigra that administration of dopamine agonists led to a diminution of cell activity in the GPi that parallelled clinical improvements [20]. In addition, local injections of glutamate agonists into the SNR of rats induce a Parkinsonian-like state of immobility and rigidity [21].

There are, however, alternative ways to explain the locomotor stimulatory effects of NMDA antagonists. Schmidt [22] found that local injection of the competitive NMDA antagonist 2-amino-5-phosphonovalerate into a restricted region of the anterodorsal NEO increased locomotion in drug-naive rats. On the other hand, Turski *et al.* [23] identified a region in the ventral part of the NEO adjacent to the pallidum, where the NMDA antagonist 2-amino-7-phosphonoheptanoate elicited immobility and muscular rigidity. Donzanti and Uretsky [24] performed local injections into the nucleus accumbens and observed both, locomotor inhibition and stimulation after injections of various glutamate antagonists. There is an obvious need for further, carefully conducted studies using the

microinjection technique to identify the precise site of the locomotor action of NMDA antagonists.

The present experimental results, in conjunction with those of Schmidt and Bubser [18] and Carlsson and Carlsson [19], raise hopes that antagonism at NMDA receptors might represent a new therapeutic principle in the treatment of Parkinsonian patients. Adjuvant treatment with NMDA antagonists might help to save dopaminergic medication and so retard the appearance of long-term side effects of dopaminergic medication [25]. Clinical trials testing the safety and efficacy of MK-801 in the treatment of epilepsy and stroke are currently under way, although there are still concerns with respect to undesired side effects of the compound. On the other hand, knowledge about structure and function of the NMDA receptor with its various modulatory sites is rapidly growing [26] so that there are hopes for advent of novel classes of NMDA antagonists which may be more appropriate for clinical use.

References

1. Fonnum F (1984) J. Neurochem. 42: 1–11.
2. Young AB, Penney JB, Dauth GW, Bromberg MB and Gilman S (1983) Neurology 33: 1513–1516.
3. Herrling PL (1985) Neuroscience 14: 417–426.
4. Kitai ST and Kita H (1986) In: Carpenter MB and Jayaraman A (eds.) The Basal Ganglia. Plenum Press, New York, Vol. 2, pp. 357–373.
5. Smith Y and Parent A (1988) Brain Res. 453: 353–356.
6. Rouzaire-Dubois B and Scarnati E (1987) Neuroscience 21: 429–440.
7. Miller WC and DeLong M (1986) In: Carpenter MB and Jayaraman A (eds.) The Basal Ganglia. Plenum Press, New York, Vol. 2, pp. 415–427.
8. Mitchell IJ, Cross AJ, Sambrook MA and Crossman AR (1986) Neurosci. Lett. 63: 61–66.
9. Klockgether T and Turski L (1989) Trends in Neurosci. 12: 285–286.
10. Penney JB and Young AB (1986) Movement Disorders 1: 3–15.
11. Scheel-Krüger J (1986) Acta Neurol. Scand. 107: S1–S54.
12. Reavill C, Jenner P and Marsden CD (1984) In: Evered D and O'Connor M (eds.) Functions of the Basal Ganglia. Pitman, London, pp. 164–171.
13. Klockgether T, Schwarz M, Turski L, Wolfarth S and Sontag K-H (1985) Exp. Brain Res. 58: 559–569.
14. Wong EHF, Kemp JA, Priestley T, Knight AR, Woodruff GN and Iversen LL (1986) Proc. Natl. Acad. Sci. USA 83: 7104–7108.
15. Davies J, Evans RH, Herrling PL, Jones AW, Olverman HJ, Pook P and Watkins JC (1986) Brain Res. 382: 169–173.
16. Honore T, Davies SN, Drejer J, Fletcher EJ, Jacobsen P, Lodge D and Nielsen FE (1988) Science 241: 701–703.
17. Wachtel H (1982) Psychopharmacology 77: 309–316.
18. Schmidt WJ and Bubser M (1989) Pharmacol. Biochem. Behav. 32: 621–623.
19. Carlsson M and Carlsson A (1989) J. Neural Transm. 75: 221–226.
20. Filion M (1979) Brain Res. 178: 425–441.
21. Turski L, Klockgether T, Turski WA, Schwarz M and Sontag K-H (1987) Brain Res. 424: 37–48.
22. Schmidt WJ (1986) Psychopharmacology 90: 123–130.
23. Turski WA, Klockgether T, Ikonomidou C, Turski L, Schwarz M and Sontag K-H (1988) In: Cavlheiro EA, Lehmann J, and Turski L (eds.) Frontiers in Excitatory Amino Acid Research. Alan Liss, New York, pp. 497–500.

24. Donzanti BA and Uretsky NJ (1984) Naunyn-Schmiedeberg's Arch. Pharmacol. 325: 1–7.
25. Marsden CD and Parkes JD (1976) Lancet 1: 292–296.
26. Johnson JW and Ascher P (1987) Nature 325: 529–531.

Motor neuron degeneration linked to excitatory amino acids: Histological and immunocytochemical approaches

J. Hugon[a,b], J.M. Vallat[a], P.S. Spencer[c] and D. Barthe[b]

[a]Departments of Neurology and [b]Histology, University Hospital, 87 042 Limoges, France
[c]Center for Occupational Disease Research, Oregon Health Sciences University, Portland, Oregon, U.S.A.

Introduction

Excitatory amino acids are now associated with the pathophysiology of various neurological diseases such as brain ischemia and hypoglycemia, epilepsia [1–3] and some neurodegenerative disorders including Huntington's disease [4,5] and olivo-ponto-cerebellar atrophy [6]. We have shown recently that two human motoneuron diseases might be reproduced in primates after chronic intoxication with certain uncommon amino acids.

Lathyrism is characterized by the occurrence of a spastic paraparesia of rapid or delayed onset in subjects consuming large amounts of *Lathyrus sativus* in various regions of India, Bangladesh and Ethiopia [7]. *L. sativus* contains an uncommon amino acid B-oxalyl-amino-L-alanine (BOAA) which induces seizures in experimental animals. We have intoxicated primates with *L. sativus* or with the pure BOAA. Two (BOAA) to fourteen months *(L. sativus)* after the beginning of intake, clinical signs occurred consisting of tremor, myoclonic jerks, increased muscle tone of lower extremities. Physiological evaluations revealed a corticospinal tract deficit and pathological changes were observed in upper motoneurons of the cortex area [8].

Another motoneuron disease, Guam amyotrophic lateral sclerosis, is clinically marked by the progressive occurrence of upper and lower motoneuron involvements with amyotrophy, brisk tendon reflexes and pyramidal syndrome. The prevalence of this particular type of amyotrophic lateral sclerosis was greater among Chamoros people living in Guam as compared with the other regions of the world. One of the possible aetiology was a chronic intoxication with a plant *Cycas circinalis* containing another uncommon excitatory amino acid; B-*N*-methyl-amino-L-alanine (BMAA). We have demonstrated [9] that chronic primate intoxication with BMAA produces after two months a disease characterized by diffuse amyotrophy, increased muscle tone and behavioural changes. Pathological alterations of motoneurons were found in the cerebral cortex and anterior horns of the spinal cord. They consisted of neurons with eccentric nuclei, swollen cytoplasm and accumulation of neurofilaments. Guam amyotrophic lateral sclerosis is often associated with another disease: Parkinson-dementia complex. Behavioural signs

(akinesia) in the BMAA intoxicated primates were partially reduced by an oral administration of levodopa.

These results showed that chronic primate intoxication with two plant excitotoxins BOAA and BMAA can reproduce clinically, physiologically and histologically the particular features of the corresponding human disorders.

Histopathological changes of motoneurons in human sporadic amyotrophic lateral sclerosis have been clearly described [10,11]. They include degenerative changes with chromatolytic aspect, eccentric nucleus, proximal axonal enlargements and accumulation of neurofilaments [12]. Phosphorylated forms of neurofilaments were shown to be abnormally present in motoneuron cell bodies of the spinal cord in amyotrophic lateral sclerosis patients [13].

The goal of the present study was to experimentally reproduce the histological and immunocytochemical features of the human amyotrophic lateral sclerosis with kainic acid intoxication in rats.

Methods

Male Wistar rats, of 200–250 g body weight, received intrathecally a sterile aqueous solution of sodium chloride alone (vehicle control) or containing kainic acid (SIGMA). For this purpose, animals were anesthetized with sodium barbitone (30 mg/kg i.p.), the back shaven, and a percutaneous lumbar puncture performed with a 26/0 stainless steel needle. The tip of the needle was located intrathecally between the L4 and L5 vertebrae. Group 1 animals (n = 18) received a single injection of 0.02 μmol of kainic acid (pH 7.0) in 20 μl of sodium chloride solution (9 g/l), while Group II (n = 18) similarly received 20 μl of vehicle alone. Solutions were delivered intrathecally over a 5-min period using a hand-held microsyringe. Body temperature was kept constant by placing the animal on a warm pad. Two h, 1, 3, 6 and 14 days after intrathecal injections, rats were re-anesthetized and systemically perfused via the aortic arch with 4% paraformaldehyde (30 sec) followed by 5% glutaraldehyde (10 min), each fixative in a 0.1 M phosphate buffer. After excision of the spinal cord, sections from cervical (C6), thoracic (T6) and lumbar (L5) cords were postfixed in 2% Dalton's chrome osmium solution, dehydrated stepwise and infiltrated with epoxy resin. One-micrometer epoxy sections were prepared from hardened blocks of tissue, mounted on slides, stained with toluidine blue, and examined by light microscopy. Ultrathin sections were prepared from selected blocks, stained with uranyl acetate followed by lead citrate, and examined by transmission electron microscopy.

Immuno histochemical procedure

Vibratome sections were immersed in 0.3% hydrogene peroxyde in PBS then rinsed in pure PBS and normal swine serum was applied for 10 min for background blocking. Two hundred Kd neurofilament monoclonal antibodies (Mouse) (Amersham)

was applied on sections for 1 h at room temperature. Sections were rinsed 3 times in PBS. Rabbit anti-mouse IgG was used for the second layer then peroxydase conjugated swine anti-rabbit IgG was applied for 30 min at room temperature. Diaminobenzidine was utilized for peroxydase development.

Results and Discussion

After intrathecal injection, kainic acid produced acute muscle spasms in the tail and hind limbs whereas myoclonus occurred in forelimbs when animals recovered from anesthesia. One third of the kainic acid injected rats displayed a persistent spastic paraplegia in the following days. In sodium chloride injected rats, no comparable signs were noted.

Histological changes could be differentiated in acute and delayed morphological abnormalities. Acute signs (2 h – 1 day) comprised shrunken and hyperchromatic neurons (Fig. 1) with many cytoplasmic vacuoles. Diffuse oedema was noted corresponding to dendrite and glial swellings. Pathological signs were mainly located in the ventral horn and, to a lesser extent, in the dorsal horn, whereas dorsal root ganglia were unaffected. Except in two animals, axons of the anterior and posterior roots entry zones were not affected. Delayed changes (3, 6, 14 days after injection) were obviously different (Figs. 2, 3, 4). They essentially consisted in chromatolytic-like aspect of motoneurons. Three days after injection, many neurons displayed condensed and vacuolated cytoplasms with eccentric nuclei and dispersion of Nissl bodies. Six days after injection, the cytoplasm appeared swollen and rounded with proximal neurite enlargements. Characteristic lesions of axons in the grey matter were dilatation and splitting of the myelin sheath with condensed filament accumulations. A glial reaction was observed 6 and 14 days after injection of kainate. Proximal part of the ventral roots of lumbar and dorsal spinal cord were free of abnormalities. Neurons of the dorsal root ganglia and peripheral nerves were unaffected.

Ultrastructural analysis confirms these findings revealing neurons with indented nuclear membranes, dispersion of rough endoplasmic reticulum and accumulation of lipid-like materials, mitochondria, dense bodies and neurofilaments (Figs. 3, 4).

Fig. 1. Acute motoneuronal lesions 24 h after kainic acid administration: condensed and vacuolated cytoplasm with diffuse oedema of the neuropil. (E.M. × 896).

Fig. 2. Delayed motoneuronal lesions 6 days after kainic acid administration: eccentric nucleus with accumulations of lipid-like material in the cytoplasm. (× 160).

Fig. 3. Accumulation of neurofilaments in the cytoplasm of a motoneuron 14 days after injection of kainic acid. (E.M. × 7200).

Fig. 4. Delayed motoneural lesions 14 days after kainic acid administration dispersion of the Nissl substance with subplasmalemnal vacuoles and indented nuclear membrane. (E.M. × 1200).

Fig. 5. Diffuse immunohistochemical staining of a motoneuron using a 200 Kd monoclonal antibody (Peroxydase anti-peroxydase technique) 14 days after kainic acid intrathecal injection. (× 152).

1

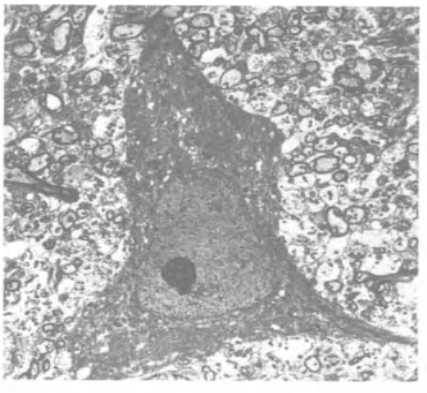

2

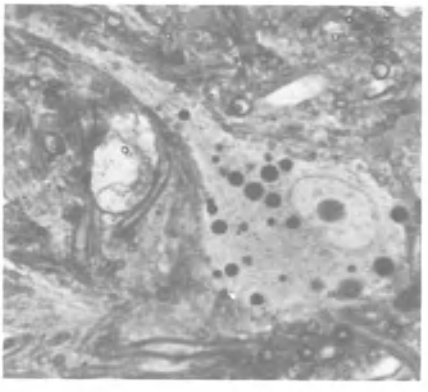

3

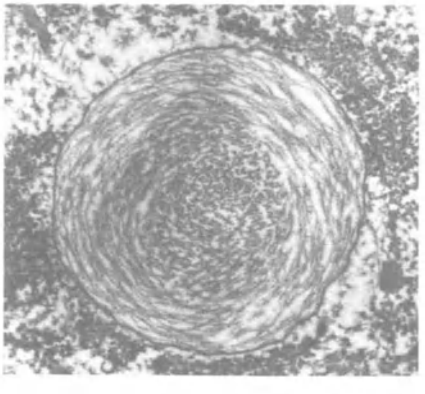

4

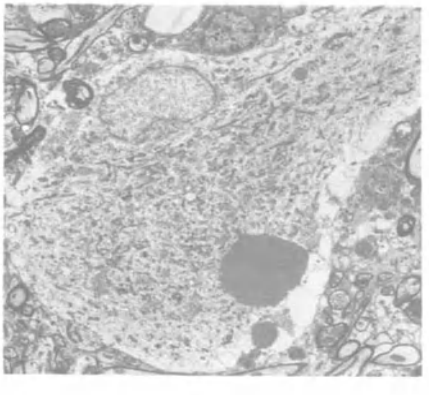

5

An immuno-histochemical study using a 200 Kd neurofilament antibody showed at 3 days a progressive staining under the plasma membrane of motoneurons, then at 6 and 14 days after injection, a diffuse cytoplasmic and proximal staining (Fig. 5). As it has been shown for phosphorylated neurofilaments, immuno-histochemical study of control animals did not reveal stainings of the cell bodies as compared with those observed in kainic acid injected rats.

Delayed neuropathological findings detected in motoneurons after kainic acid administration are reminiscent of the morphological abnormalities seen in patients with sporadic Amyotrophic lateral sclerosis i.e. chromatolytic-like aspect of motoneurons with eccentric nucleus, proximal axonal or dendrite swellings, accumulation of phosphorilated neurofilaments.

This study demonstrates that excitatory amino acids (kainic acid) can reproduce certain morphological signs of the human amyotrophic lateral sclerosis. Recently, various anomalies have been described concerning the excitatory amino acid metabolism in such patients: increased aspartate level in the C.S.F. related to the severity of the disease [14], abnormal glutamate metabolism [15] and decreased glutamate dehydrogenase activity [16]. These findings and the two experimental models of lathyrism and Guam amyotrophic lateral sclerosis argue in favor of a possible relation between excitatory amino acid toxicity and chronic degenerative disorders of the human motor system. Further studies are needed on this promising line of research.

References

1. Greenamyre JT (1986) Arch. Neurol. 43: 1058–1063.
2. Rothman SM and Olney JW (1986) Ann. Neurol. 19: 105–111.
3. Auer RN and Siesjö BK (1988) Ann. Neurol. 24: 699–707.
4. Coyle JT and Schwazrcz R (1976) Nature 263: 244–246.
5. McGeer EG and McGeer PL (1976) Nature 263: 517–519.
6. Plaitakis A, Berl S and Melvin DY (1984) Ann. Neurol. 15: 144–153.
7. Ludolph A, Hugon J, Dwivedi MP, Schaumburg HH and Spencer PS (1987) Brain 110: 149–165.
8. Spencer PS, Roy DN, Ludolph A, Hugon J, Dwivedi MP and Schaumburg HH (1986) Lancet 2: 1066–1067.
9. Spencer PS, Nunn PB, Hugon J, Ludolph A, Robertson RC, Ross SM and Roy DN (1987) Science 237: 517–522.
10. Hirano A, Donnenfeld H, Sasaki S and Nakano I (1984) J. Neuropathol. Exp. Neurol. 43: 461–470.
11. Nakano I, Donnenfeld H and Hirano A (1983) Neurol. Med. (Tokyo) 18: 136–144.
12. Carpenter S (1968) Neurology 18: 841–851.
13. Munoz DG, Greene C, Perl DP and Selkoe DJ (1988) J. Neuropathol. Exp. Neurol. 47: 9–18.
14. Patten BM, Harati Y, Acosta L, Jung SS and Felmus MT (1978) Ann. Neurol. 3: 305–309.
15. Plaitakis A and Coroscio JT (1987) Ann. Neurol. 22: 575–579.
16. Hugon J, Tabaraud F, Rigaud M, Vallat JM and Dumas M (1989) Neurology 39: 956–958.

Address for correspondence: Dr. J. Hugon, Department of Neurology, University Hospital, 2 rue Alexis Carrel, 87 042 Limoges Cedex, France.

Acromelic acid as a tool for the study of specific neurone damages

H. Shinozaki[a], M. Ishida[a], Y. Gotoh[a] and S. Kwak[b]

[a]*The Tokyo Metropolitan Institute of Medical Science, 3-18-22, Honkomagome, Bunkyo-ku, Tokyo 113, Japan*

[b]*National Institute of Neuroscience, 4-1-1, Ogawahigashi, Kodaira, Tokyo 187, Japan*

Abstract

Acromelic acid, one of kainoids which possess a constitutional moiety of kainic acid, has been isolated from a poisonous mushroom. Acromelic acid proved to be one of the most potent excitatory amino acids in both vertebrates and invertebrates; superior to other kainoids in depolarizing activity on newborn rat spinal motoneurones. A single systemic injection of acromelic acid caused a marked tonic extension of the rat hind limb, which was ultimately replaced by persistent spastic paraplegia, through causing a transient flaccid paralysis of the lower part of the rat. In the course of these experiments, most rats receiving acromelic acid died from generalized tonic-clonic convulsions. These abnormal symptoms were quite distinct from those induced by kainic acid, and lasted until the rat was sacrificed without a further administration of acromelic acid. Histopathological studies suggested selective neuronal damages of small neurones in the spinal cord. The most striking changes occur in the dorsal horn of lumbar and sacral segments, suggesting an animal model for the stiff-man syndrome.

Introduction

Kainic acid has been the object of many experimental investigations for elucidating physiological functions of glutamate. At present, some kainic acid analogues (kainoids) are available for neuroscience research [1]. Biologically active kainoids, such as kainic acid and domoic acid, possess some characteristic neuropharmacological properties [1,2]: (I) depolarizing actions on the mammalian central neurones and invertebrate muscles; (II) selective neuronal death in mammalian central neurones; (III) potentiation of responses to bath-applied glutamate in invertebrates; and (IV) inhibitory action on the response to quisqualic acid in invertebrates. In general, kainoids are not particularly active to depolarize the invertebrate muscle fibre [3–6], in spite of the fact that they have marked neuroexcitatory and neurotoxic properties in the mammalian central nervous system (CNS) [7,8]. Among the kainoids, domoic acid has so far been the most potent excitant at the crayfish neuromuscular junction (NMJ). However, in our previous examinations [1,9,10], acromelic acid (Fig. 1), a new kainoid, demonstrated an extremely potent excitatory action at the crayfish NMJ with quite similar pharmacological properties to kainic acid. At this junction, acromelic acid was about 10 times as potent as domoic acid in its depolarizing activity, and was about 100 times more powerful

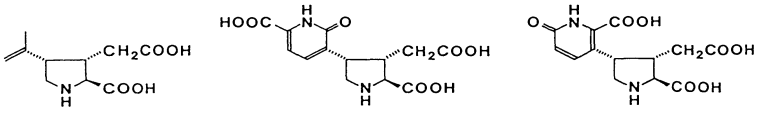

Fig. 1. Chemical structure of kainic acid, acromelic acid A and B. Note that they possess a common moiety in their molecules.

than kainic acid on a molar basis, when the threshold concentration for depolarization was compared [9]. Therefore, we expected that acromelic acid would possess a novel action on the mammalian CNS, in particular, an extremely potent depolarizing action. In fact, in our preliminary examinations, acromelic acid demonstrated extremely potent depolarizing actions in the newborn rat spinal cord. Thus, acromelic acid was expected to prove valuable for elucidating the functions of kainate receptors [1,10,11].

Two isomers of acromelic acid (acromelic acid A and B) have so far been isolated from a poisonous mushroom, *Clitocybe acromelalga* [12–15]. About a week after a man ingests the poisonous mushroom erroneously, a sharp pain and a marked reddish edema (erythromelalgia) are induced in his hand and foot, which persist for about a month. Shirahama *et al.*, who succeeded in the isolation of both isomers of acromelic acid [12–15], designed a method for their chemical synthesis to confirm their proposed chemical structure [13–16]. Recently, small samples of acromelic acid finally became available for biological experiments. In the present study, we describe characteristic excitotoxic actions of systemic acromelic acid on the rat CNS, such as abnormal behavioural signs and specific neuronal damage, which are quite distinct from those induced by systemic kainic acid. In addition to established excitatory amino acids, such as kainic acid and domoic acid, acromelic acid will be a very useful tool for neuroscience research. In most cases of systemic administration of a centrally active substance, a site of action for the substance is obscure. However, in cases where the mode of actions of a compound relatively is well documented and it acts on a specific site, the characteristic behavioural change after the systemic administration of the compound would provide a useful piece of information about future experiments in the CNS.

Materials and Methods

Newborn rat spinal cord

On account of limited availability of acromelic acid B, acromelic acid A was almost exclusively used in the present study. The excitatory activity of acromelic acid (unless otherwise specified, acromelic acid A) was examined on the newborn

rat spinal cord. The spinal cords of 1–5-day-old Wistar rats were used for the experiments, and the experimental methods were similar to those previously described [17–19]. Under ether anesthesia, the lumbar-sacral spinal cord was isolated, hemisected sagittally and placed in a 0.15 ml bath perfused with artificial cerebrospinal fluid (mM: NaCl 138.6, KCl 3.4, $CaCl_2$ 1.3, $MgCl_2$ 1.0, $NaHCO_3$ 20.9, NaH_2PO_4 0.6, glucose 10.0) which was oxygenated with a gas mixture of 95% O_2 and 5% CO_2. Tetrodotoxin (TTX) was always added to the perfusing solution throughout the experiment in a concentration of 0.5 μM to block spontaneous depolarization and indirect drug effects. In some cases, $MgCl_2$ was replaced with NaCl to examine whether the action was dependent on Mg^{2+} concentrations. Perfusion rate was 6 ml/min, and the bath temperature was kept at 27°C. The potential changes generated in the motoneurones were recorded extracellularly from the L3-L5 ventral root with a glass capillary, whose inner diameter fitted tightly with the recorded ventral roots. Test compounds were applied to preparation either by perfusion or by brief-pulse injection into the perfusion system as described previously by Otsuka and Yanagisawa [20].

Before the examination of actions of excitatory amino acids, the spinal reflex was evoked by the electrical stimulation (duration 100 μs, 10 V, at an interval of about 1 min) of dorsal root (L4 or L5), in order to test the viability of the spinal cord preparation. After selecting only those spinal cord preparations which demonstrated polysynaptic reflexes of above 2 mV in amplitude in the Mg^{2+}(1.0 mM)-containing and TTX-free saline, TTX (0.5 μM) was added to the perfusing fluid throughout the experiments.

Histopathological observations

Acromelic acid was systemically administered to the rat in various doses (male Wistar rats, body weight 121–251 g, 2–5.5 mg/kg s.c., i.p. and i.v., N = 24). For histological assessment, rat brains and spinal cords were fixed *in situ* by transcardiac perfusion with a 3% paraformaldehyde and 0.25% glutaraldehyde in 0.1 M phosphate buffer (pH 7.4) under deep pentobarbital-Na anesthesia (50 mg/kg i.p.) 7 and 86 days after the injection of acromelic acid. Transverse sections of the CNS were processed for histopathological examination by routine paraffin technique and stained with hematoxylin and eosin, and by Kluver and Barrera's method.

Results

Potent depolarizing actions in the newborn rat spinal cord

Acromelic acid caused a depolarization of motoneurones in a dose-dependent manner as well as other kainoids. When peak amplitudes of the depolarization induced by kainic acid, domoic acid, and acromelic acid were compared following a 10 s duration of application and a concentration of 1 μM, there was no significant

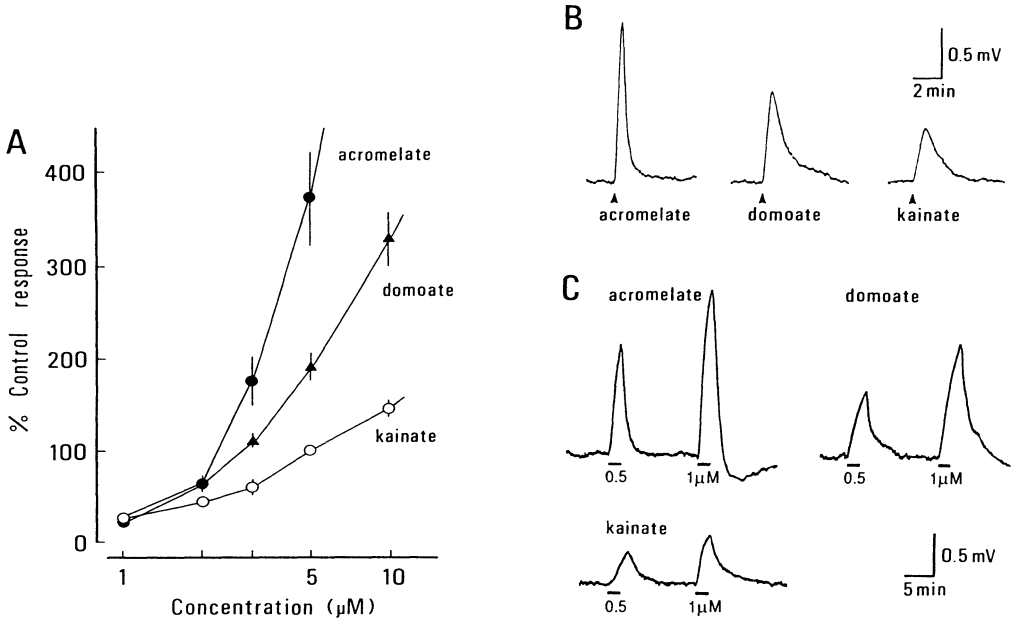

Fig. 2. A: Dose response relationships for acromelic acid, domoic acid and kainic acid in the isolated newborn rat spinal cord. These kainoids were added to the perfusing fluid for a period of 10 s. The responses to these kainoids were recorded from the ventral root extracellularly in Mg^{2+}-free, TTX(0.5 μM)-containing solution. Peak amplitudes of responses from individual preparations have been normalized, so that results are expressed as a percentage of the control depolarization induced by 5 μM kainic acid. Vertical bars represent S.E.M. (N = at least 5). B: Sample records of responses (10 s application) to kainic acid, domoic acid and acromelic acid in a concentration of 3 μM. Each compound was added to the perfusing fluid at a mark point for a period of 10 s. Note the significant difference in the time course of the responses. C: Sample records of responses (2 min application) to kainoids in concentrations of 0.5 and 1 μM. Each compound was added for a period (2 min) indicated by horizontal bars.

difference among them. However, acromelic acid caused a larger depolarization than other kainoids as the concentrations were increased. For the experiment shown in Fig. 2A, kainic acid, domoic acid and acromelic acid were repeatedly added to the perfusing solution in various concentrations at a fixed interval and a 10 s duration. Acromelic acid was the most potent among them.

Acromelic acid possesses a chemical moiety of kainic acid as shown in Fig. 1. However, some differences are detected in depolarizing responses between acromelic acid and other kainoids. An interesting difference was the short time course of depolarizing responses to acromelic acid. As shown in Fig. 2B, the tail of responses to acromelic acid more quickly decreased in amplitude than that to

kainic or domoic acid. The half-decay time of responses to kainic acid (64 ± 3 s, N = 5) and domoic acid (54 ± 2 s, N = 5) were approximately similar at a concentration of 3 μM, but that of acromelic acid (26 ± 1 s, N = 5) was considerably shorter than that of kainic acid or domoic acid. The half-decay time was slightly increased as the concentration increased, but responses to acromelic acid always decayed more quickly than those to other kainoids.

When the depolarizing activity of agonists was compared in terms of the peak amplitudes of depolarizing responses, responses measured after 10 s application (Fig. 2A) might lead to an underestimate of the more slowly developing responses (e.g. kainic acid) relative to the fast responses. So, the depolarizing activity of excitatory amino acids administered for a longer period was compared, but the relative potency of acromelic acid to kainic acid was quite similar even when these kainoids were administered for a period of 2 min (Fig. 2C). For the experiment shown in Fig. 3, quisqualic acid, kainic acid, acromelic acid and *N*-methyl-D-

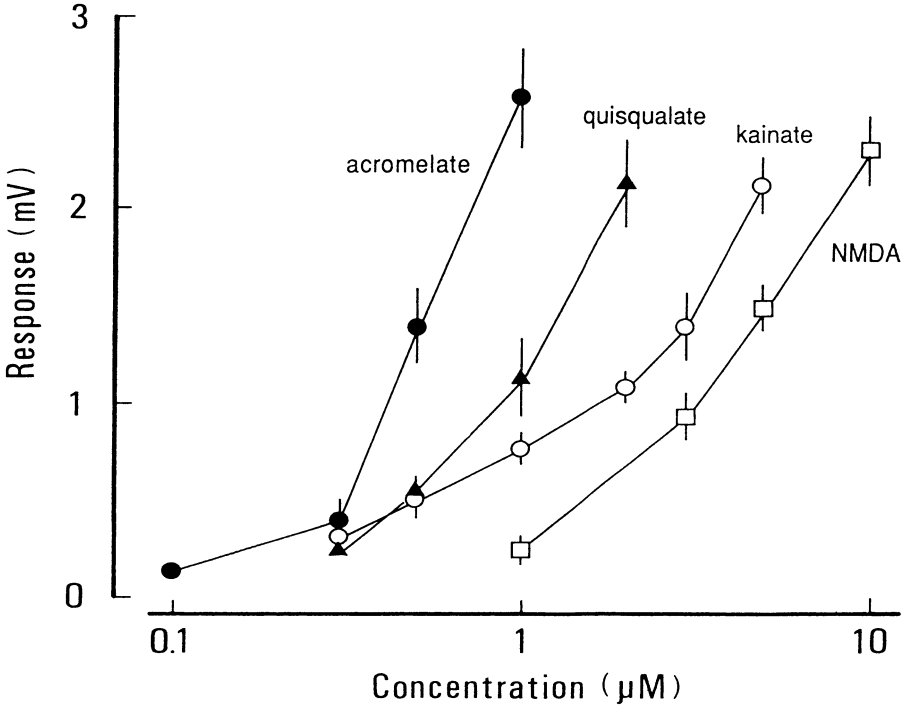

Fig. 3. Comparison of the excitatory activity of glutamate agonists in the newborn rat spinal cord. Agonists were added to the perfusing fluid for a period of 2 min. Experimental conditions were similar to those described in Fig. 2. Peak amplitudes of depolarizing responses (mV) were plotted against concentrations (μM). Vertical bars represent S.E.M. (N = at least 5). Note that acromelic acid is the most potent among the excitatory amino acids.

aspartic acid (NMDA) were repeatedly added to the perfusing fluid in various concentrations for a 2 min duration, and the potency was compared in terms of the peak amplitude of responses to these excitatory amino acids. Acromelic acid was the most potent among them.

In order to examine the possibility that the depolarization induced by acromelic acid was a result of the release of neurotransmitters, actions of some antagonists for neurotransmitters were examined. γ-Aminobutyric acid (GABA) (1 mM) causes a slight depolarization in this preparation, which was usually blocked by 20 μM picrotoxin. The acromelate-induced depolarization was not affected by picrotoxin (50 μM), suggesting that the depolarization induced by acromelic acid was not mediated by GABAergic systems. In a similar way, strychnine (10 μM) did not reduce amplitudes of responses to kainic acid (5 μM) and acromelic acid (3 μM). In the case of the perfusing solution containing TTX (0.5 μM), high Mg^{2+} (4.7 mM) and low Ca^{2+} (0.1 mM), axonal transmission of action potentials should be blocked and transmitter release from presynaptic terminals of adjacent neurones to motoneurones should be considerably suppressed. Under these conditions, amplitudes of responses to kainic acid (5 μM) and acromelic acid (3 μM) were hardly affected, suggesting that acromelic acid acted directly on the motoneurone.

It is necessary to test whether acromelic acid activates other subtypes of glutamate receptors as well, such as quisqualate- or NMDA-type receptors. At present, there is no specific pharmacological method to differentiate between actions on kainate- and quisqualate-type receptors, but it is possible to block the actions of NMDA-type agonists effectively without appreciable actions on responses evoked by non-NMDA agonists. Magnesium ions primarily act by blocking the NMDA ion channel in a voltage-dependent manner [21–23]. When the Mg^{2+}-free solution was changed to the Mg^{2+}(1 mM)-containing one, responses to acromelic acid were not affected at all (Fig. 4A), in spite of the fact that the depolarizing response to NMDA was almost completely reduced by Mg^{2+}. In addition, the amplitude and the time course of the response to acromelic acid and kainic acid was hardly affected by D(-)-2-amino-5-phosphonovaleric acid (APV) (20 μM–0.1 mM) or 3-((±)-2-carboxypiperazin-4-yl)-propyl-1-phosphonic acid (CPP) (20 μM), suggesting that there is little chance that acromelic acid activates NMDA-type receptors. 6,7-dinitroquinoxaline-2,3-dione (DNQX) (10 μM) markedly reduced the depolarizing response of acromelic acid in a similar way to that of kainic acid. At a high concentration of 0.1 mM, 6-cyano-7-nitroquinoxaline-2,3-dione (CNQX) completely abolished the responses to acromelic acid and kainic acid. In the newborn rat spinal cord, acromelic acid did not reduce depolarizing responses to quisqualic and glutamic acids at all, but augmented them in an additive manner.

The excitatory activity of acromelic acid A seemed superior to that of acromelic acid B in the newborn rat spinal cord, and the time course of their responses seemed quite similar. The potency of acromelic acid B was similar to that of domoic acid.

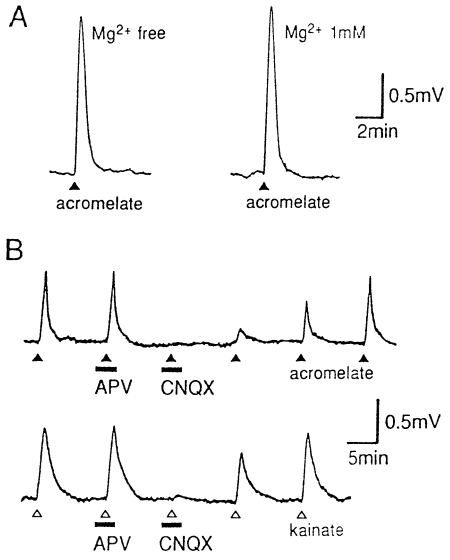

Fig. 4. A: Sample records of responses to acromelic acid in the absence and presence of Mg^{2+} (1 mM). Acromelic acid (5 μM) was added to the perfusing fluid at a mark point for a period of 10 s. There was no significant difference in amplitude between both responses. B: Responses to acromelic acid and kainic acid in the absence and presence of APV and CNQX. Upper trace: responses to acromelic acid (▲). Lower trace: responses to kainic acid (Δ). Agonists (acromelic acid: 1 μM, kainic acid: 2 μM) were added to the perfusing fluid for a period of 30 s. Antagonists (APV: 0.1 mM, CNQX: 0.1 mM) were applied 90 s prior to administration of agonists, as indicated by horizontal bars. Note that both responses were markedly reduced by CNQX but not by APV.

Behavioural symptoms

The intravenous minimum lethal dose of acromelic acid was estimated to be about 4 mg/kg in Wistar rats and about 3 mg/kg in ICR mice, while that of kainic acid was about 10 mg/kg in rats and 40–60 mg/kg in mice. From the structural similarity of acromelic acid to kainic acid (Fig. 1), it is reasonable to predict kainate-type excitotoxic actions of acromelic acid in the mammalian CNS. However, to our surprise, acromelic acid induced quite distinct behavioural symptoms from kainic acid, of which neurotoxic actions have been well documented [8,24–32]. The most pronounced behavioural change was severe spastic paraplegia, which persisted semi-permanently after one-shot application of acromelic acid. When acromelic acid was subcutaneously administered to 6 rats at a dose of 5 mg/kg, there was no incidence of 'wet-dog-shakes (WDS)' throughout the experiment. About 1 h after the injection, rats began to develop a marked tonic extension of the hind limb and the tail, without causing severe salivation nor apparent disturbance in respiratory

functions. The extension of the hind limb closely resembled strychnine-induced convulsions, but the upper part of the rat body was associated with no convulsions. The rats demonstrated righting reflexes and struggled to be in a normal position using the forepaw. This tonic extension of the hind limb lasted for more than 30 min. Before this stage, the tails of the rats sometimes moved like snakes, and the rats walked on tiptoe of the hind limb when they altered their position. When they stopped walking, both heels of the hind limbs were gradually raised like a slow motion picture and the rats fell forward as they stood, being seized with a cramp in both hind limbs on repeated occasions. Later, (about 80 min after the injection), most rats developed marked generalized tonic-clonic convulsions, and 4 of 6 rats died at this stage, but 1 of 6 rats did not develop generalized tonic-clonic convulsions. The surviving rats were also prone to severe seizures, the duration of which was markedly shorter than that evoked by systemic kainic acid [24–26]. In passing, the kainate-induced limbic seizures persisted for more than 3 h or until death (kainic acid 10 mg/kg i.p.). From around the time when the severe acromelate-induced seizures disappeared (about 2 h later), the tonic extension of the hind limb was followed by a transient flaccid paralysis of the lower part of the body, which persisted for more than 2 h. At this stage, no response was evoked by sensory stimuli to the hind limb, but the rat sometimes walked using the forepaw only. However, the rat did not always develop transient flaccid paralysis, even after developing the tonic extension of the hind limb. On the day following the injection of acromelic acid, the surviving rats which had shown transient flaccid paralysis developed severe spastic paraplegia and this was significantly reinforced by sensory stimuli such as touching and poking. The incidence of transient flaccid paralysis seemed to play a key role for the development of spastic paraplegia. The rats shuffled their hind limb along, and could not sit in a normal posture. The spastic paraplegia persisted until the rat was sacrificed for histological analysis (at least more than 3 months after the one-shot application) without a further administration of acromelic acid.

At doses less than 3 mg/kg of acromelic acid, even intravenously dose, the tonic extension of the hind limb was never induced and the mortality rate at this dose was zero, but at a dose of 4 mg/kg about half the rats died from generalized tonic-clonic convulsions. At a dose of 5.5 mg/kg, all rats died from severe seizures. Of 24 rats receiving acromelic acid, only two rats developed spastic paraplegia, and most rats were compelled to die from severe seizures while some rats demonstrated slight behavioural changes only. It was, therefore, very difficult to select the dose to extend to spastic paraplegia. However, the incidence will certainly be increased by improved techniques for the administration of acromelic acid, such as using sustained-release pharmaceuticals. Similar abnormal behavioural signs were also observed in mice receiving acromelic acid.

Histopathological observations

Seven and 86 days after acromelate administration, the surviving rats (2 rats) were sacrificed for histological analysis of the central and peripheral nervous systems

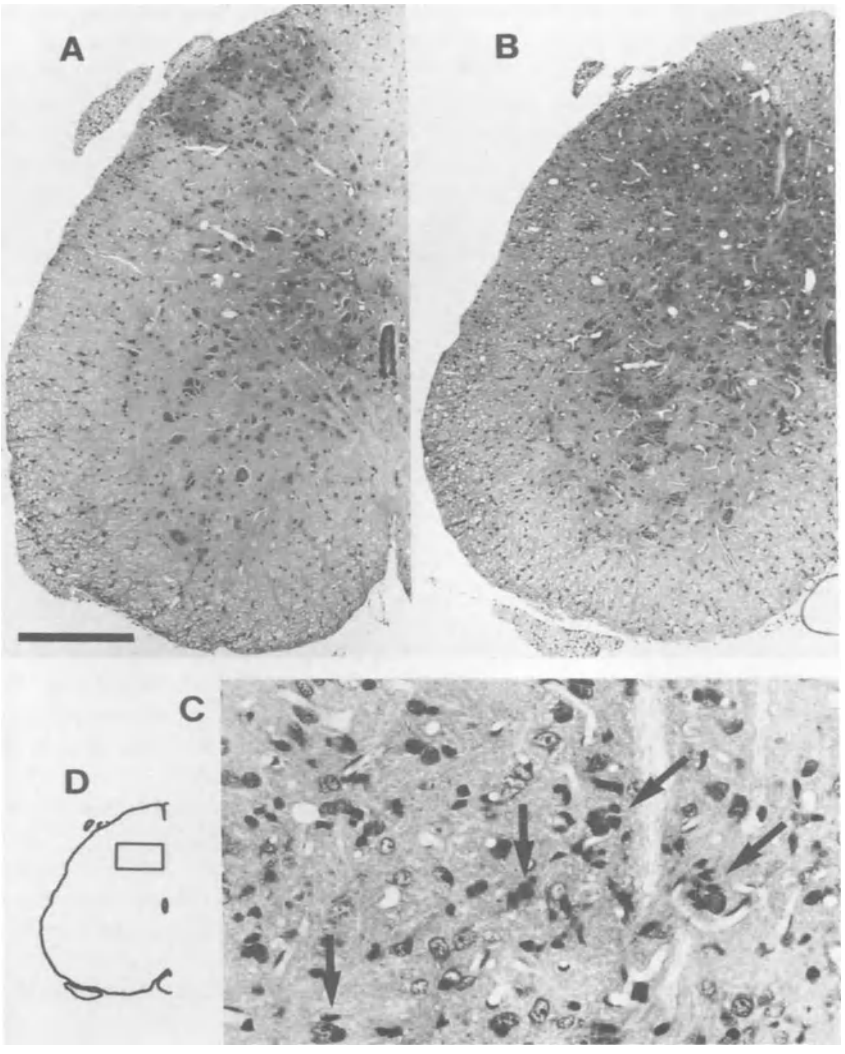

Fig. 5. Transverse sections of the rat sacral (S_1) spinal cord. A) Normal control. B) Seven days after the subcutaneous injection of acromelic acid (5 mg/kg). Scale bar, 200 μm (common in A and B). C) A higher magnification of the boxed region in D, which is a schematic reduced drawing of B. Scale bar, 50 μm. Small glial cell nuclei are considerably increased in number in the middle and dorsal portion of the spinal cord. Some neurones appear pyknotically shrunken and surrounded by glial cells (indicated by arrows). Note that the large anterior horn cells are preserved both in number and in configuration.

and the muscles. The animal that had developed spastic paraplegia as a result of systemic acromelic acid showed marked neuronal damage in the lower spinal cord

rather than other areas 7 days after injection. In particular, the neuronal damage became marked from the lower level of thoracic part. Marked gliosis was distributed diffusely in the lower spinal cord. The most striking changes occurred in the middle and dorsal gray matter (sparing I and II layers of Rexed) of the lumbar and the sacral, where there were several pyknotic cells and a decrease in number of small neurones (Fig. 5). Preservation of large anterior horn cells and the myelinated spinal tracts predicted that both primary and secondary pyramidal tracts and ascending sensory tracts were not affected. Mild glial proliferation was observed in the hippocampal CA4 by immunohistochemistry against glial fibrillary acidic protein (GFAP) without apparent loss of pyramidal cells. The rest of the structures were not affected including large anterior horn cells and the white matter of the spinal cord. Acromelic acid did not affect muscle fibres and peripheral nerves, and demyelination as a result of systemic injection of acromelic acid was not observed, insofar as the routine histological analysis. Histological investigation of the rat sacrificed 86 days after injection of acromelic acid showed recovery from the acute phase 7 day histological reactions (details will be described elsewhere in these proceedings).

Discussion

In the present study acromelic acid proved to be one of the most potent excitants in the mammalian CNS. Responses to acromelic acid are not at all affected by NMDA antagonists, but they are effectively blocked by DNQX or CNQX, suggesting that acromelic acid is a non-NMDA-type excitatory agonist. Acromelic acid is one of the kainoids, therefore, as a matter of course, acromelic acid is expected to bind exclusively to kainate receptors. The examination of the receptor binding assay suggests that acromelic acid has the most potent binding activity to kainate receptors among kainoids in the frog spinal cord (Maruyama, personal communications). Thus, acromelic acid is expected to be a useful tool for elucidating the function of kainate receptors in the mammalian CNS as well as kainic acid.

Systemic or local administration of kainic acid induces selective neuronal damages in the mammalian CNS. In adult rats, a single subcutaneous injection of kainic acid induces a seizure syndrome which begins with staring, mouth movements, head nodding and WDS and progresses to a 'rearing, praying, salivating' limbic seizure. These recur with increasing frequency until the animal is in *status epilepticus*. When the brains of these animals are examined following sustained kainic acid induced seizures, there is a characteristic pattern of limbic brain damage involving some or all of the following: amygdala, pyriform and entorhinal cortices, hippocampus, several thalamic nuclei and lateral septum [33]. The chain of above mentioned abnormal behavioural signs induced by systemic acromelic acid, including the tonic extension of the hind limb, were quite distinct from those induced by systemic kainic acid. Kainic acid caused neither spastic paraplegia nor tonic extension of the hind limb of the rat even in lethal doses, but caused severe

limbic motor seizures [8,24–26]. Contrary to our speculations, there were no limbic motor seizures and only a few incidents of WDS in rats receiving acromelic acid even in lethal doses. The central action of acromelic acid was evidently ascending from the lower spinal cord toward the brain with the lapse of time after the injection, but the spinal cord seemed to be exquisitely sensitive, so far as we observed their behavioural signs.

It is of great interest that there are some striking differences in behavioural signs and areas of neuronal damage between systemic injections of kainic and acromelic acid. In the case of intracerebral and systemic administration of kainic acid, there are interesting differences in the pathological manifestations. Intracerebral or intraventricular injection of kainic acid produces neuronal loss selectively in the CA3-4 cell fields of hippocampus [28] which correlates well with the high density of kainate receptors in this area. In contrast, systemic kainic acid causes seizures and extensive brain edema and the most consistent neuronal cell loss in the hippocampus is in the CA1 region [26,27,31] where there is a low density of kainate receptors [24,34]. The CA1 damage caused by systemic kainic acid closely resembles that produced by cerebral ischemia [35]. Thus, the distribution of the lesions induced by kainic acid does not always correlate with the brain regions of high density of kainate receptors. As mentioned above, acromelic acid is considered to activate kainate receptors and is superior to kainic acid in terms of its depolarizing activities in the newborn rat spinal motoneurones [19]. At present, there is no clear-cut explanation for the above discrepancy, but the idea that there are more than two subtypes of kainate receptors is very attractive, although we cannot immediately jump to such a conclusion. Kainoids are thought to exert their excitotoxic activity through activation of glutamate receptors. Almost all neurones with kainate receptors in the mammalian CNS should be equally activated by systemic kainoids. In fact, iontophoretically applied acromelic acid induces markedly spike discharges in the rat cortical neurones (unpublished observations). Therefore, differences in functional organization of inhibitory and excitatory pathways as a result of activation of concerned neurones may also play a key role for the development of specific neuronal damages induced by kainoids. Further studies will be required to elucidate the function of kainate receptors.

The convulsant action of the drug has often been attributed to interference with central inhibitory processes. The pathological observation above indicates that the selective loss of spinal internuncial cells, which might exert inhibitory actions on spinal reflexes, is responsible for the development of persistent spastic paraplegia. The generalized tonic clonic convulsion observed about 1.5 h after injection of acromelic acid seemed to be attributed to other than the spinal pathology. As the convulsion was a transient episode, it may be reasonable that no definitive histological changes are detected in the brain. These histopathological changes account for the abnormal behavioural signs evoked by systemic acromelic acid. Acromelic acid is expected to be a useful tool for the study on underlying mechanisms of human spastic paraplegia, and rats receiving acromelic acid may be useful as an animal model of the stiffman syndrome [36,37].

The new material, acromelic acid, will play a key role as a very useful pharmacological tool for neuroscience research in addition to established excitatory amino acids, and moreover will provide useful information about elucidating the pharmacology of the glutamatergic system in both vertebrates and invertebrates. One of the purposes of this paper is to encourage the utilization of this new and potentially valuable compound.

Acknowledgement

The authors wish to thank Professor H. Shirahama, Drs. K. Konno and K. Hashimoto for a generous gift of acromelic acid, and Dr. Y. Ohfune for domoic acid. This work was supported in part by a Grant-in-Aid for Scientific Research from the Ministry of Education, Science and Culture of Japan.

References

1. Shinozaki H (1988) Prog. Neurobiol. 30: 399–435.
2. Shinozaki H (1980) Prog. Neurobiol. 14: 121–155.
3. Shinozaki H and Shibuya I (1974) Neuropharmacol. 13: 1057–1065.
4. Shinozaki H and Shibuya I (1976) Neuropharmacol. 15: 145–147.
5. Takeuchi A and Onodera K (1975) Neuropharmacol. 14: 619–625.
6. Onodera K and Takeuchi A (1980) J. Physiol. (Lond.) 306: 233–250.
7. Shinozaki H and Konishi S (1970) Brain Research 24: 368–371.
8. McGeer EG, Olney JW and McGeer PL (eds.) (1978) Kainic Acid as a Tool in Neurobiology. Raven Press, New York.
9. Shinozaki H, Ishida M and Okamoto T (1986) Brain Research, 399: 395–398.
10. Shinozaki H and Ishida M (1988) In: Lunt GG (ed.) Neurotox '88: Molecular Basis of Drugs and Pesticide Action. Elsevier Science Publishers B.V., Amsterdam, pp. 91–104.
11. Shinozaki H and Ishida M (1988) In: Kanazawa I (ed.) Neurotransmitters: Focus on Excitatory Amino Acids. Excerpta Medica, Tokyo, pp. 17–30.
12. Konno K, Shirahama H and Matsumoto T (1983) Tetrahedron Lett. 24: 939–942.
13. Shirahama K, Konno K, Hashimoto K and Matsumoto T (1988) In: Lunt GG (ed.) Neurotox '88: Molecular Basis of Drugs & Pesticide Action Elsevier Science Publishers B.V., Amsterdam, pp. 105–122.
14. Konno K, Hashimoto K, Ohfune Y, Shirahama H and Matsumoto T (1986) Tetrahedron Lett. 27: 607–610.
15. Konno K, Hashimoto K, Ohfune Y, Shirahama H and Matsumoto T (1988) J. Amer. Chem. Soc. 110: 4807–4815.
16. Hashimoto K, Konno K, Shirahama H and Matsumoto T (1986) Chem. Lett. 1399–1400.
17. Otsuka M and Konishi S (1974) Nature 252: 733–734.
18. Ishida M and Shinozaki H (1988) Brain Research 473: 193–197.
19. Ishida M and Shinozaki H (1988) Brain Research 474: 386–389.
20. Otsuka M and Yanagisawa M (1980) J. Exp. Biol. 89: 201–214.
21. Ault B, Evans RH, Francis AA, Oakes DJ and Watkins JC (1980) J. Physiol. (Lond.) 307: 413–428.
22. Mayer ML, Westbrook GL and Guthrie PB (1984) Nature 309: 261–263.
23. Nowak L, Bregestovski P, Ascher P, Herbert A and Prochiantz A (1984) Nature 307: 462–465.
24. Ben-Ari Y (1985) Neurosci. 14: 375–403.

25. Collins RC, McLean M and Olney J (1980) Life Sci. 27: 855–862.
26. Lassman H, Petsche V, Kitz K, Baran G and Sperk G (1984) Neurosci. 13: 691–704.
27. Lothman EW and Collins RC (1981) Brain Research 218: 299–318.
28. Nadler JV, Perry BW and Cotman CW (1978) Nature 271: 676–677.
29. Nadler JV (1981) Life Sci. 29: 2031–2042.
30. Olney JW, Rhee V and Ho OL (1974) Brain Research 77: 507–512.
31. Schwob JE, Fuller T, Price JL and Olney JW (1980) Neurosci. 5: 991–1014
32. Olney JW, Fuller T and de Gubareff T (1979) Brain Research 176: 91–100.
33. Olney JW and de Gubareff T (1978) In: McGeer E, Olney JW and McGeer PL (eds.) Kainic Acid as a Tool in Neurobiology. Raven Press, New York, pp. 201–217.
34. Foster AC, Mena EE, Monaghan DT and Cotman CW (1981) Nature 289: 73–75.
35. Brown AW and Brierly IB (1972) J. Neurol. Sci. 16: 59–84.
36. Howell DA, Lees AJ and Toghill PJ (1979) J. Neurol. Neurosurg. Psychiat. 42: 773–785.
37. Kasperek S and Zebrowski S (1971) Arch Neurol. 24: 22–30.

Address for correspondence: H. Shinozaki, The Tokyo Metropolitan Institute of Medical Science, 3-18-22, Honkomagome, Bunkyo-ku, Tokyo 113, Japan.

Studies on the role of NMDA, GABA and adenosine receptors within discrete brain nuclei in the high pressure neurological syndrome in rats

Maria H. Millan[a], Bridget Wardley-Smith[b], Michael J. Halsey[b] and Brian S. Meldrum[a]

[a]Institute of Psychiatry, Department of Neurology, De Crespigny Park, Denmark Hill, SE5 8AF, U.K.
[b]Northwick Park Hospital, Division of Anaesthesia, Clinical Research Centre, Harrow, Middlesex HA1 3UJ, U.K.

Abstract

We investigated the influence of brain focal injections of 2-amino-7-phosphonoheptanoate (APH), *N*-methyl-D-aspartate (NMDA), muscimol and 2-chloroadenosine (CAD) on behavioural symptoms of the high pressure neurological syndrome (HPNS) in rats. Each compound was bilaterally injected (in nmole range doses) into the *substantia nigra pars reticulata* (SNR), entopeduncular nucleus (EP) or ventromedial thalamic nucleus (VLTh) prior to exposure to hyperbaric conditions. Threshold pressure for the occurrence of tremor, myoclonic jerks and convulsions were recorded for drug and vehicle-injected animals. A decrease in threshold pressure for a particular symptom indicates that the reaction to hyperbaric conditions is more pronounced, while an increase in threshold pressure is indicative of protection against HPNS.

Injection of NMDA (an agonist of excitatory NMDA receptor subtype) into the SNR, EP or VLTh produced a decrease in threshold pressure for the occurrence of tremor and its intensity. Injection of APH (a selective antagonist at the NMDA receptor) resulted in protection against tremor in all three structures (the most potent effect was produced by entopeduncular injection). An increase in threshold pressure for convulsions also followed APH injection into each structure (with the most pronounced effect after nigral injection). Injection of muscimol did not change the animals' response to compression, while injection of CAD produced increased reaction to hyperbaric conditions significantly affecting tremor (nigral and thalamic injections) and convulsions (entopeduncular injection).

Introduction

Animals exposed to hyperbaric conditions develop high pressure neurological syndrome (HPNS). Behavioural symptoms appearing consecutively with increase of atmospheric pressure are tremor, myoclonus, clonic seizure and clonic-tonic seizure.

Rats can be protected (i.e. threshold pressure for each behavioural symptom rises) by systemic injection of some anaesthetics, flurazepam or sodium valproate [1]. However, the best protection so far is produced by the i.p. injection of 2-amino-7-phosphonoheptanoic acid (APH) a selective antagonist at the *N*-methyl-D-aspartate (NMDA) excitatory receptor [2]. Antagonists at other receptor subtypes (kainate and quisqualate) or mixed antagonists without preference for any particular subtype of excitatory receptor are also effective when injected either systemically or i.c.v. [3,4]. Systemic injection of muscimol, DABA and nipecotic acid (GABA agonists) is not protective against HPNS [5].

In this study APH, NMDA, muscimol and 2-chloroadenosine (CAD – an agonist of adenosine A_1 receptor) were injected into the *substantia nigra pars reticulata* (SNR), entopeduncular nucleus (EP), or ventro-lateral thalamic nucleus (VLTh). The SNR and EP belong to the basal ganglia system, thus they are involved in the transmission of motor events from brain centers to the spinal cord. Injection of excitatory amino acid antagonists or muscimol into either of these nuclei results in protection against seizures in various models of epilepsy [6–12].

Thalamo-cortical connections originating in the VLTh are essential for the development of postural tremor. Electrical activity in the VLTh increases during episodes of Parkinsonian tremor in human beings and destruction of its link with the cortex abolishes tremor [13].

The role of excitatory (NMDA) inhibitory (GABA) and purinergic (adenosine) transmission within these nuclei in HPNS was investigated.

Experimental procedures

Male Sprague-Dawley rats (240–250 g) were chronically implanted with bilateral guide cannulae attached to the skull and placed 2.5–3 mm above the target structures. Five to seven days after surgery, animals were injected through injection cannulae with drugs or vehicle (buffered saline or phosphate buffer) into the nuclei. Drugs were delivered in 0.5 µl volume to each side by slow infusion (2.5 min). The stereotaxic coordinates based on Paxinos & Watson atlas [14] were SNR: A + 2.3, V + 1.5 (from intra-aural line) L ± 2.5; EP: A + 5.0, V + 2.9, L ± 2.5, VLTh: A + 4.6, V + 7.1, L ± 2.2.

Drugs were applied in the following doses: APH – 1, 5 and 10 nmole/side in the SNR; 5 and 10 nmoles in the VLTh and 1 and 5 nmoles in the EP. NMDA – 1, 5 and 10 nmole in the SNR and EP and 5 nmoles in the VLTh. Muscimol – 20 nmoles in the EP and the SNR. CAD: 25 nmoles in the EP and 12.5 nmoles in the SNR.

After the injection, a rectal probe was inserted for monitoring body temperature and the rats were placed in the small cage mounted on a gauge connected to an oscilloscope. The cage was placed in the hyperbaric chamber with the TV camera installed in the front window.

The chamber was filled with O_2 (0.5–0.6 ATA – maintained through the compression). Compression with helium at 3 ATA/min was started 10–30 min after injection.

Behaviour of animals was observed on the TV screen and the onset of tremor monitored on the oscilloscope. Threshold pressure for the occurrence of each behavioural sign was recorded. The following motor signs were observed: T_1 – fine tremor of ears and head, T_2 – mild tremor of head, tremor occasionally visible in the body, T_3 – mild tremor of the body, T_4 – severe periodic tremor of the body, T_5 – severe continuous tremor of the body, myoclonus – single jerks, clonic seizure, clonic-tonic seizure.

After the final stage of HPNS appeared the animal was anaesthetised with nitrous oxide and decompressed over 20–30 min. The brain was taken and histologically examined for the placement of the injection cannulae tips. The statistical significance of changes in threshold pressure for each behavioural syndrome was performed using the Mann-Whitney U-test.

Results

Histological examination of the brains showed that most of the injection placements aimed at the SNR were situated within the SNR, and on the dorsal border of SNR and SNC (*substantia nigra pars compacta*).

Entopeduncular injections were mostly placed within and just dorsal to this nucleus.

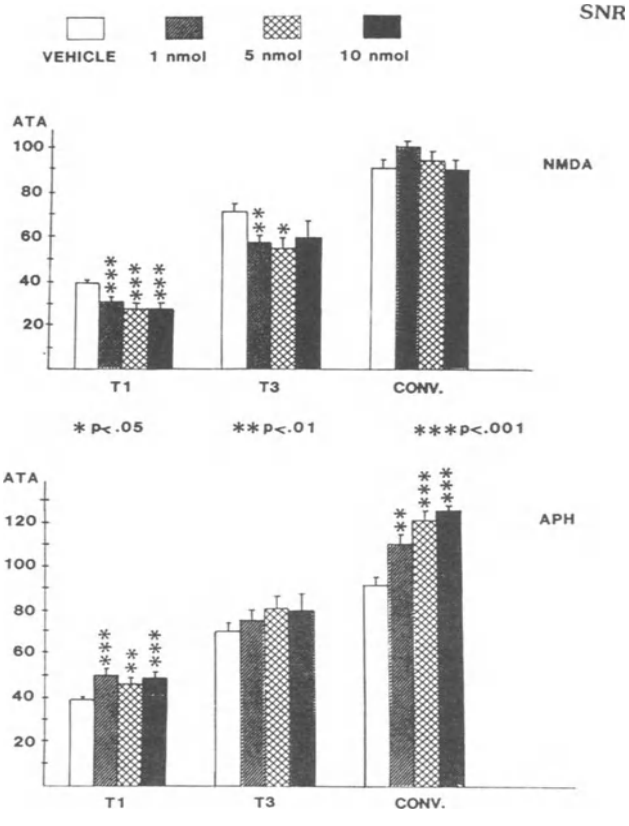

Fig. 1. Effect of focal injections of NMDA and APH into the SNR on behavioural symptoms of HPNS in rats (conv. – convulsions, ATA – atmospheres).

Fig. 2. Effect of focal injections of NMDA and APH into the EP on behavioural symptoms of HPNS in rats (conv. – convulsions, ATA – atmospheres).

Thalamic injections were mostly placed in the anterior part of VLTh and on the border of this nucleus with adjacent anteroventral and ventromedial nuclei.

In all groups a small percentage of animals had their injection sites slightly misplaced due to imperfection of the stereotaxic technique. The results obtained from these rats were not included into the groups analysed statistically.

During injections of NMDA into the SNR became increasingly ataxic and cataleptic. The onset of tremor in these rats occurred significantly, dose dependently, at lower pressure than in the control group.

The higher intensity tremor (tremor of whole body) also developed at significantly lower pressure after injection of NMDA 1 and 5 nmoles than in vehicle-injected group. Threshold pressure (TP) for myoclonus and convulsions was not affected by these injections (Fig. 1).

NMDA injected into the EP caused motor activation. NMDA 5 and 10 nmol also produced forelimb clonus. TP for T_1 was decreased in these animals as compared

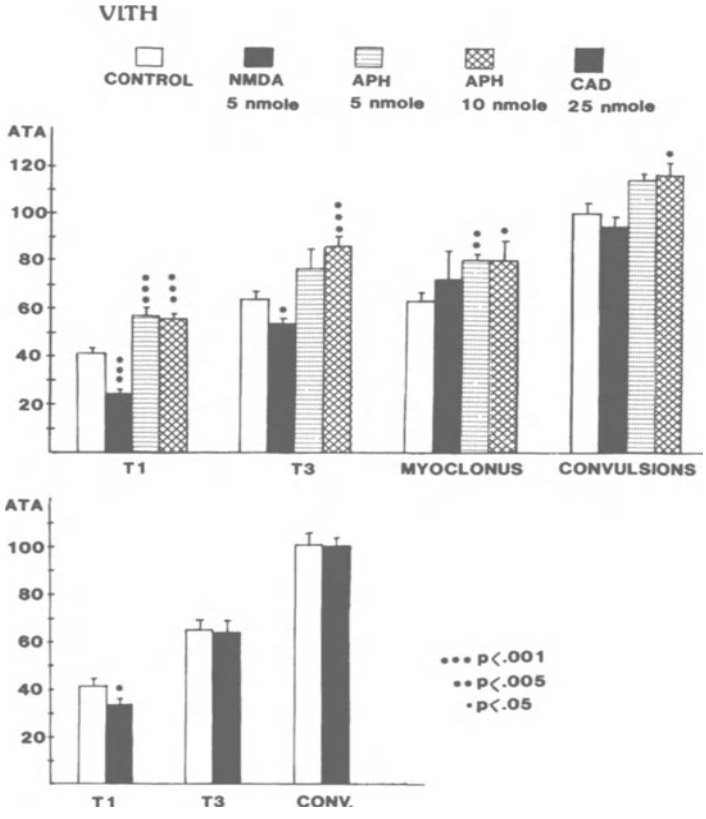

Fig. 3. Effect of focal injections of NMDA, APH and CAD into the VLTh on behavioural symptoms of HPNS in rats (conv. – convulsions, ATA – atmospheres).

to the control group. In animals injected with NMDA 5 nmol convulsions also occurred at significantly lower pressure (Fig. 2).

Injection of NMDA into the VLTh had similar effect on the onset and development of tremor (Fig. 3).

Immediately after the end of NMDA injection a pronounced transient, spontaneous tremor was visible in some rats.

APH injection into each of the areas had an opposite effect to NMDA. SNR-injected animals developed motor activation and stereotypic sniffing. Their TPs for T_1, T_3 and convulsions were significantly higher than those of the control group (Fig. 1).

Entopeduncular injections of APH resulted in similar increases for each of these behavioural symptoms (Fig. 2). However the onset of tremor was more affected while the occurrence of convulsions was less effected than in SNR-injected rats (Fig. 5).

Thalamic injections of APH did not cause any remarkable change in the motor behaviour of the animals. Their TPs for T_1, T_3 and myoclonus were significantly increased and APH 10 nmol was also significantly protective against convulsions (Fig. 3).

Injection of muscimol 20 nmol into the SNR produced pronounced stereotypic sniffing while entopeduncular injection resulted in severe ataxia and catalepsy. Either injection failed to change behavioural response to hyperbaric conditions (not shown).

CAD had a similar effect to APH on motor behaviour i.e. it produced stereotypic sniffing in the SNR-injected and ataxia in the EP-injected rats. Thalamic injections did not change motor behaviour. Surprisingly CAD failed to protect rats against HPNS, but resulted in decrease of TP for T_1 in the SNR and VLTh-injected and a decrease in TP for convulsions in the EP-injected animals (Fig. 3 and 4).

Discussion

It was previously reported that the i.p. injection of APH provides a uniquely potent protective effect against HPNS. In particular the threshold pressure (TP) for tremor is increased by 120% [2].

Focal injections of APH into the SNR, EP and VLTh are also protective against HPNS. The anticonvulsant effect of these injections is similar to that produced by their systemic injection. However the antitremorgenic effect of focal injections is much less pronounced than reported by Meldrum *et al.* [2] for systemic injections (32.8, 48.2 and 39% v/s 120%).

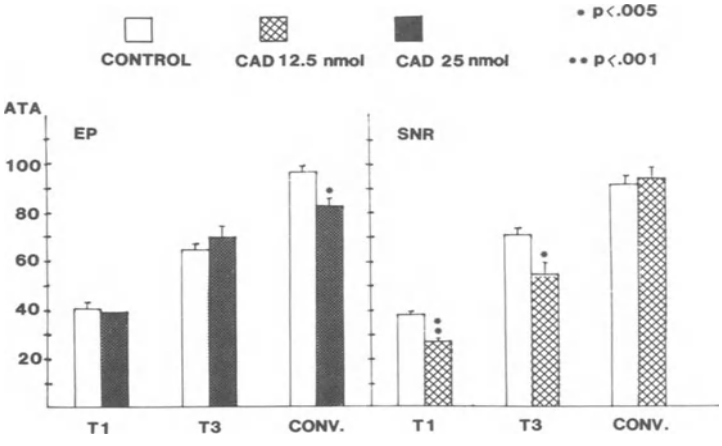

Fig. 4. Effect of focal injection of CAD into the SNR and EP on behavioural symptoms of HPNS in rats (conv. – convulsions, ATA – atmospheres).

Injection of NMDA into each nucleus produces the opposite effect i.e. a significantly lowered TP for tremor. The TP for convulsions is non-significantly lowered by NMDA injection into any of the structures investigated.

The TP for myoclonus is not affected by any of the nigral or entopeduncular injections but significantly increased by APH injection into the VLTh.

Drugs increasing GABA-mediated inhibition have been widely reported to have potent anticonvulsant effects in several animal models of epilepsy [for review see ref. 15]. Systemic injection of muscimol, (a GABA agonist) or nipecotic acid and DABA (GABA uptake inhibitors) does not however protect against HPNS behavioural symptoms. Sodium valproate which is protective, shows in addition to GABAergic facilitation, anti-excitatory amino acid action [5]. Focal injections of muscimol into the nigra or the EP have anticonvulsant effect in various models of epilepsy [9,16].

In this study muscimol injected into the SNR or EP produces no protection against HPNS although it has been applied in much higher doses than those used in the studies on epilepsy. The report by Chapman *et al.* [17] indicates however that there is some involvement of GABAergic brain system in the development of HPNS. At a pressure of 85 ATA, GABA levels in the hippocampus are increased by 72.2%.

Purinergic transmission seems to be also involved in controlling convulsions. Activation of adenosine (A_1 in particular) receptors has been shown to protect against various experimental seizures [18–20]. In fact some investigators describe adenosine as an endogenous anticonvulsant [21]. Also one clinically used anticonvulsant – carbamazepine is supposedly acting at A_1 receptor [22,23]. Blockade of A_1 receptors by methylxanthines in high doses is convulsant [24] and has a proconvulsant effect in experimental limbic epilepsy [25].

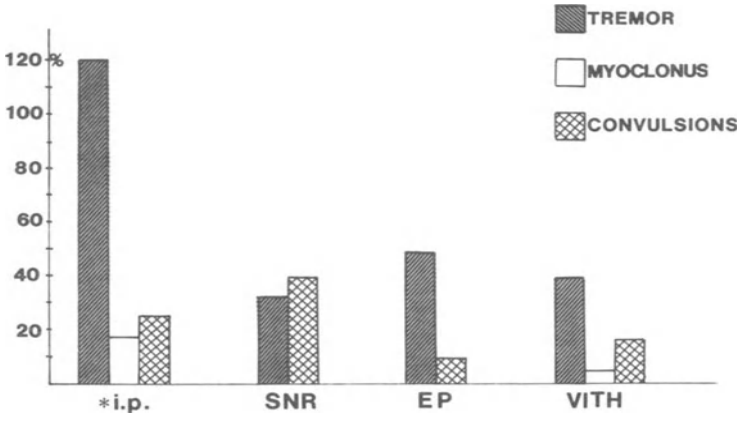

Fig. 5. Comparison of the protective effect of APH, injected focally into the SNR, EP, VLTh or given i.p., on HPNS in rats, presented as percent of TP increase* [2].

On the basis of the known anticonvulsant properties of adenosine receptor agonists we expected that focal injections of CAD would show a protective effect against HPNS. This however was not the case. In fact injection into each of investigated nuclei produced the opposite effect, decreasing TP for tremor or convulsions (Fig. 3 and 4).

These results indicate that increased excitatory transmission may be involved in the HPNS. Blockade of excitatory amino acid receptors protects against behavioural symptoms of HPNS (by increasing threshold pressure.)

As shown in Fig. 5 the best protection against tremor has been produced by the i.p. injection of APH, while the anticonvulsant effect of both systemic and focal SNR and VLTh injections were within similar range. It indicates that there are probably other tremorgenic sites located either in some other part of the brain or in the spinal cord – where APH acts to inhibit motoneurons [26]. Increase in GABAergic inhibition remains without effect. Application of an adenosine receptor agonist (CAD) paradoxically potentiates HPNS.

High pressure alters synaptic function [27] and may alter receptor properties Helium pressure increases the sensitivity of NMDA receptor in the hippocampus [28]. It is likely that GABA and purinergic receptors function is also altered in hyperbaric conditions and the effects of their agonists are modified.

References

1. Angel A, Halsey MJ, Little J, Meldrum BS, Ross JAS, Rostain JC and Wardley-Smith B (1984) Phil. Trans. R. Soc. Lond. B304: 85–94.
2. Meldrum BS, Wardley-Smith B, Halsey MJ and Rostain J-C (1983) Eur. J. Pharmacol. 87: 501–502.
3. Wardley-Smith B, Meldrum BS and Halsey MJ (1987) Eur. J. Pharmacol. 138: 417–420.
4. Wardley-Smith B and Meldrum BS (1984) Eur. J. Pharmacol. 105: 351–354.
5. Rostain J-C, Wardley-Smith B, Farni C and Halsey MJ (1986) Neuropharmacol. 25: 545–554.
6. De Sarro G, Meldrum BS and Reavill C (1984) Eur. J. Pharmacol. 106: 175–179.
7. Turski L, Cavalheiro EA, Turski A and Meldrum BS (1986) Neurosci. 18: 61–77.
8. Gale K (1985) Fed. Proc. Fed. Am. Soc. Exp. Biol. 44: 2414.
9. Patel S, Millan MN, Mello LM and Meldrum BS (1986) Neurosci. Lett. 64: 226–230.
10. Millan KH, Meldrum BS, Boersma CA and Faingold CL (1988) Exp. Neurol. 99: 687–798.
11. De Sarro G, Patel S and Meldrum BS (1986) Eur. J. Pharmacol. 132: 225–236.
12. McNamara JO, Galloway MT, Rigsbee LC and Shin C (1984) J. Neurosci. 4: 2410–2417.
13. Poirier LJ, Pechadre JC, Larochelle L, Dankova J and Boucher R (1975) In: Meldrum BS and Marsden CD (eds.) Advances in Neurology. Vol. 10, Raven Press, New York.
14. Paxinos C and Watson C (1982) The Rat Brain in Stereotaxic Coordinates. Academic Press, Sydney.
15. Meldrum BS (1989) Br. J. Clin. Pharmacol. 27: 35–115.
16. Garant D and Gale K (1986) Eur. J. Pharmac. 124: 365–369.
    Iadarola MJ and Gale K (1982) Science 218: 1237–1240.
17. Chapman AG, Halsey MJ, Hart GP, Luff NP, Meldrum BS and Wardley-Smith B (1986) J. Neurochem. 47: 314–317.
18. Lee US, Schubert P and Heineman U (1984) Brain. Res. 321: 160–164.
19. Barraco RA, Swanson TH, Phillis JW and Berman RF (1984) Neurosci. Lett. 46: 317–322.
20. Dunwiddie TV and Worth T (1982) J. Pharmacol. Exp. Ther. 220: 70–76.
21. Dragunov M, Goddard GV and Laverty R (1985) Epilepsia 26: 480–487.

22. Marangos PJ, Post RM, Patel J, Lander K, Parma A and Weiss S (1983) Eur. J. Pharmacol. 93: 175.
23. Skerritt JH, Davies LP and Johnston GAR (1982) Eur. J. Pharmacol. 82: 195–197.
24. Chu NS (1982) Epilepsia 22: 88–94.
25. Albertson TE, Stark LG, Joy RM and Bowyer JF (1983) Exp. Neurol. 81: 703–713.
26. Polc P (1985) Eur. J. Pharmacol. 117: 381–389.
27. Wann KT and MacDonald AG (1988) Progr. Neurobiol. 30: 271–307.
28. Fagni L, Zinebi F and Hugon M (1987) Neurosci. Lett. 81: 285–290.

Cerebral amino acids in neonate from caffeine-drinking dam

H. Tanaka and M. Arima

National Center of Neurology and Psychiatry, 4-1-1 Ogawahigashi, Kodaira, Tokyo 187, Japan

Abstract

The cerebral free amino acids in neonatal rats, from dams given 0.04% caffeine in the drinking fluid *ad libitum* before and/or during pregnancy throughout the lactational period, were examined on days 1, 5 and 10. Significantly reduced cerebral weight was observed on day 1. The tyrosine concentration in the cerebrum, but not that in the liver, was increased on days 1 and 5. The tyrosine level showed a positive correlation with the caffeine level in neonatal cerebrum only on day 1. These results suggest that maternal caffeine disturbs the neonatal cerebrum through tyrosine and tyrosine hydroxylase, and then produces behavioral abnormalities in developing rats.

Introduction

Caffeine has long been a principal component of many commonly consumed beverages. The possible harmful effect of caffeine in human pregnancy cannot be neglected because of the pharmacological and embryofetopathic action of caffeine or its dimethylxanthines under experimental conditions [1–4]. Low caffeine levels of 1.5–3.0 μg caffeine per ml or g wet weight, in mothers and fetuses, lowered the fetal cerebral weight [4]. In the present study the effect of maternal caffeine on the levels of free amino acids in the neonatal cerebrum was examined to elucidate the factors related to cerebral function. We present here for the first time an increase in free tyrosine level in the neonatal cerebrum induced by maternal caffeine ingestion.

Materials and Methods

The experimental procedures used for the preparation of fetal models were essentially as described previously [1,2,4]. Virgin female albino rats of the Wistar strain were given 0.04% caffeine (C) or tap water (W) as the drinking fluid. According to the drinking fluid, the rats were divided into three groups; W-W, W-C and C-C. The W-W and C-C groups were given tap water and 0.04% caffeine diluted with tap water, respectively, throughout the experimental periods. The W-C group was given 0.04% caffeine during pregnancy and lactation.

The isolation of amino acids in the cerebrum and liver was performed basically by the method of Kalyanasundaram and Ramanamurthy [5]. Determination of

amino acids was performed by high-performance liquid chromatography with the post-labelling method with o-phthalaldehyde as described previously [6–8].

Data were statistically analyzed by analysis of variance and Scheffe's multiple comparison.

Results

The mean neonatal cerebral weight was significantly reduced in the C-C group and tended to reduce in the W-C group as compared to in the W-W group only on day 1. In the neonatal cerebrum on days 1, 5 and 10, there were no significant differences in the levels of aspartic acid, glutamic acid, glutamine and taurine, among the three groups; W-W, W-C and C-C. Compared to in the W-W group, the concentration of tyrosine in the C-C group was significantly higher on days 1 and 5, and that in the W-C group was only higher on day 5. On the other hand, there were no significant differences among the three groups on all three experimental days in the concentration of phenylalanine.

The correlation between the caffeine and tyrosine concentrations in neonatal cerebrum was calculated on the three experimental days. A significant positive correlation was found in the W-C group on day 1 ($r = 0.75$, $p<0.02$).

The concentrations of tyrosine and phenylalanine in neonatal liver were not significantly different among the three groups on any of the three experimental days (data not shown).

Discussion

In addition to the fetal period examined in our previous studies [1–4], this investigation was an attempt to clarify the effect of maternal caffeine on the neonatal cerebrum during the period of days 1–10 postpartum, which are taken to correspond to the third trimester in human pregnancy. Reduced fetal cerebral weight [1,2,4] also continued on day 1, i.e., the 24 h after birth, in the C-C group.

There have been no studies on the amino acid levels in offspring exposed to caffeine *in utero*. Unexpectedly, our present study showed a significantly high tyrosine but not a high phenylalanine level in the cerebrum with low caffeine levels of 1.5–2.0 μg/g wet weight on day 1–5. The discrepancy between the levels of tyrosine in the cerebrum and liver may depend on the enzyme which catalyzes the hydroxylation of phenylalanine, that is, tyrosine hydroxylase in the cerebrum and phenylalanine hydroxylase in the liver [9]. Therefore, an increased tyrosine level in the cerebrum may suggest that caffeine activates tyrosine hydroxylase, which also catalyzes the rate-limiting step in catecholamine biosynthesis; e.g., dopamine, norepinephrine and epinephrine [10,11]. On the other hand, caffeine stimulates cyclic AMP levels [12] through inhibition of phosphodiesterase [13]. When the

Table 1. Cerebral weights (number of newborns) and concentrations of aspartic acid, glutamic acid, glutamine, taurine, tyrosine, and phenylalanine (10 newborns) at 1, 5, and 10 days after birth

	Cerebral wt	Asp	Glu	Gln	Taurine	Tyr	Phe
	mg			μmol/g wet wt			
1 day							
W–W	175(31)	2.04	5.20	3.74	9.25	0.15	0.13
W–C	92(34)	102	95	84	100	113	100
C–C	86(47)[a]	98	94	84	109	147[a]	100
5 days							
W–W	337(23)	1.88	5.81	1.93	7.33	0.20	0.13
W–C	103(26)	99	102	121	100	130[a]	85
C–C	94(37)	103	97	102	96	135[a]	92
10 days							
W–W	656(23)	2.00	7.22	1.66	5.84	0.29	0.12
W–C	105(32)	110	99	105	106	103	117
C–C	100(37)	110	101	111	96	97	100

Values in W–W are expressed as means and those in W–C and C–C are expressed as percent of W–W values.
[a] Significantly different from the W–W, $p<0.01$.

level of cyclic AMP is elevated, tyrosine hydroxylase is activated in association with cyclic AMP-dependent protein kinase [10,11]. Following this step, tyrosine hydroxylase catalyzes the synthesis of catecholamines through a flux-generating step with several regulators [14]. Based on these findings our result suggests the possibility that maternal caffeine induces a disturbance of catecholamine metabolism in the fetal and neonatal cerebrum.

Recently correlation between non-therapeutic doses of caffeine and human neonatal behavior have been reported [15]. Therefore, we can suppose that prenatal caffeine consumption affects the developing cerebrum and results in a postnatal abnormality with no more biochemical changes. As the cause and treatment of abnormal behavior in human being, the change in cerebral tyrosine levels should be studied.

References

1. Tanaka H, Nakazawa K and Arima M (1983) Brain Dev. (Tokyo) 5: 397–406.
2. Tanaka H, Nakazawa K, Arima M and Iwasaki S (1984) Brain Dev. (Tokyo) 6: 355–361.
3. Nakazawa K, Tanaka H and Arima M (1985) J. Pharmacobio.-Dyn. 8: 151–160.
4. Tanaka H, Nakazawa K and Arima M (1987) Biol. Neonate 51: 332–339.
5. Kalyanasundaram S and Ramanamurthy PSV (1982) Neurochem. Res. 7: 469–476.
6. Nakazawa K, Tanaka H and Arima M (1982) J. Chromatogr. 233: 313–316.
7. Tanaka H, Nakazawa K, Arima M, Morooka K, Suzuki F, Aoki, T and Kohno Y (1983) Brain Dev. (Tokyo) 5: 450–456.
8. Tanaka H, Nakazawa K, Arima M and Hayashi A (1987) Brain Dev. (Tokyo) 9: 37–42.
9. Ikeda M, Levitt M and Udenfriend S (1965) Biochem. Biophys. Res. Commun. 18: 482–488.
10. Ames MM, Lerner P and Lovenberg W (1978) J. Biol. Chem. 253: 27–31.
11. Vulliet PR, Langan TA and Weiner N (1980) Proc. Natl. Acad. Sci. USA 77: 92–96.
12. Schreiner CM, Zimmerman EF, Wee EL and Scott WJ (1986) Teratology 34: 21–27.
13. Smellie FW, Davis CW, Daly JW and Wells JN (1979) Life Sci. 24: 2475–2482.
14. Newsholme EA and Leech AR (1983) In: Biochemistry for the Medical Sciences. John Wiley & Sons Ltd., Chichester, pp. 777–797.
15. Emory EK, Konopka S, Hronsky S, Tuggey R and Davé R (1988) Psychopharmacology 94: 64–68.

Address for correspondence: Dr. Harumi Tanaka, Division of Mental Retardation and Birth Defect Research, National Institute of Neuroscience, NCNP (National Center of Neurology and Psychiatry), 4-1-1 Ogawahigashi, Kodaira, Tokyo 187, Japan.

Inhibitory effects of L-*threo*-3,4-dihydroxyphenylserine against maximal electroconvulsion and brain norepinephrine in mice

Motoaki Yoshida, Kazuo Yoshizawa and Takao Nakanishi

Department of Neurology, Institute of Clinical Medicine, University of Tsukuba, Ibaraki 305, Japan

Abstract

L-*threo*-3,4-dihydroxyphenylserine (L-DOPS) is a synthetic amino acid, which is decarboxylated to form L-norepinephrine *in vivo*. The effects of L-DOPS on maximal electroshock seizure (MES) were investigated in mice here. All substances were injected intraperitoneally. L-DOPS (100–400 mg/kg) significantly decreased extension/flexion (E/F) ratios, though it could not abolish MES (tonic hind leg extension). However L-DOPS (400 mg/kg) significantly abolished MES, when combined with desipramine (5–20 mg/kg), maprotiline (20–40 mg/kg) or nialamide (30 mg/kg). Similar doses of desipramine, maprotiline, nialamide or L-DOPS could not inhibit MES when used alone.

In the combined treatment with desipramine (20 mg/kg), maprotiline (40 mg/kg) or nialamide (30 mg/kg), the ED_{50} (95% CL) of L-DOPS for abolition of MES was 160 (100–256), 95 (50–181) or 210 (145–305) mg/kg respectively. The determination of brain NE was made by HPLC. The significant increase of NE was observed in the treatment with L-DOPS, nialamide, or L-DOPS combined with either nialamide, desipramine or maprotiline. Desipramine mildly increased NE, but maprotiline did not alter NE. It was presumed that an anticonvulsant action of L-DOPS and L-DOPS with the combined drugs was due to the modification of brain nonadrenergic transmission.

Introduction

L-*threo*-3,4-dihydroxyphenylserine (L-DOPS) is a synthetic norepinephrine (NE) precursor, which has been demonstrated to form natural NE by enzymatic decarboxylation *in vitro* [1]. Recently L-DOPS has been tried for different neurological disorders including Parkinson's disease and beneficial effects have been reported [2,3]. On the other hand, NE has been shown to play an important role in the pathophysiology of some experimental epilepsies [4–6]. Though an anticonvulsant action of DL-DOPS has been described [7], the effect of L-DOPS on experimental epilepsies has not been reported. We investigated whether L-DOPS suppressed electroconvulsions in mice.

Materials and Methods

Animals

Male, ddY mice weighing from 23 to 30 g were used. Mice fed on standard food (Toyojozo Co., Tokyo) were maintained on a 12 h light/dark cycle and allowed

free access to water and food during experiments. Experiments were performed between 12:00 and 17:00 h. Animals were used only once.

Maximal electroshock seizure (MES) test

Electroshock was applied with an electroshock apparatus (USA-201, Unique Medical Co. Ltd., Tokyo), using corneal electrodes. Maximal electroshock consisted of 50 Hz a.c., 50 mA and 0.2 second duration [8]. The tonic extensor component of hind legs was used as a criterion for electroconvulsions. When the angle of hind legs was less than 90°, it was defined as the abolishment of/or the protection from electroconvulsions. The protection rate meant a ratio of the number of animals protected from electroconvulsions to the number of all tested ones.

Extension/flexion (E/F) ratio was calculated. The durations of the two seizure components were measured [9] as follows: hind leg tonic flexion was measured from the time of application of stimulus to the time of onset of hind leg tonic extension; hind leg tonic extension was measured from the time of the extensor thrust of hind legs to the time of onset of generalized clonus.

Measurements of brain NE

A whole brain was used in the determination of NE. A brain was homogenized with 0.4 N perchloric acid and centrifuged. After absorbing with alumina, NE was eluted with 0.5 N HCl. HPLC was performed using Coulochem Model 5100A. The content of protein was assayed by the method of Lowry. NE content was presented as ng/mg protein.

Treatments

L-DOPS (Sumitomo Pharm. Co., Osaka, Japan) was suspended in 0.5% carboxymethylcellulose sodium salt. Desipramine and maprotiline both in the hydrochloride form (Ciba Geigy Co.) were dissolved in distilled water. Nialamide was dissolved in distilled water with the aid of dilute hydrochloric acid. All substances were injected intraperitoneally (i.p.) in a volume of 0.1 ml/10 g body weight. L-DOPS or its vehicle was injected 2 h or 3 h before MES test or decapitation. When other drugs were combined, they were injected 1 h before the administration of L-DOPS.

Statistics

Protection rates were analysed using Fisher's exact probability test. ED_{50} and 95% confidence limit of drugs for anticonvulsant effects were calculated by the method of Litchfield and Wilcoxon [10]. NE contents were analysed using Student's t test.

Results

E/F ratios were significantly reduced to 76% or 63% of vehicle control respectively at 2 or 3 h after the injection with L-DOPS (400 mg/kg) (Table 1). Therefore

Table 1. Effects of L-DOPS on E/F ratio in relationship to intervals between injection of L-DOPS and maximal electroshock seizure (MES) test

Treatment	Dose (mg/kg i.p.)	Time of injection before MES test	E/F ratio (mean ± S.D.)	N	P
Vehicle[a]	–	3 h	12.27 ± 1.62	7	–
L-DOPS	400	1 h	11.08 ± 2.82	7	N.S.
L-DOPS	400	2 h	9.30 ± 1.60	7	<0.005
L-DOPS	400	3 h	7.75 ± 1.85	7	<0.001

[a] Vehicle: 0.5% carboxymethylcellulose sodium salt.

Table 2. Effects of different doses of L-DOPS on maximal electroshock seizure (MES)

Treatment	Dose (mg/kg i.p.)	Number protected[a] N	E/F ratio (mean ± S.D.)	(n)	% alteration of E/F ratio
Vehicle[b]	–	1/12	11.81 ± 2.17	(11)	100
L-DOPS	100	0/12	9.26 ± 2.20[c]	(12)	78
L-DOPS	200	0/12	8.22 ± 3.36[d]	(12)	69
L-DOPS	400	0/12	8.70 ± 2.23[e]	(12)	73

Mice received vehicle or L-DOPS 3 h before MES test.
[a] The term 'protect' means the abolishment of tonic hind limb extensions.
Number protected/N was not significantly different between vehicle group and L-DOPS group.
[b] Vehicle: 0.5% carboxymethylcellulose sodium salt.
[c] $p<0.02$.
[d] $p<0.01$.
[e] $p<0.005$.

Table 3. Effects of L-DOPS in combination with nialamide on maximal electroshock seizure (MES)

Group	Treatment	Dose (mg/kg i.p.)	Number protected N	P
I	Vehicle 1[a] + Vehicle 2[b]	–	1/15	—
II	Nialamide + Vehicle 2	30 + –	1/15	N.S. (I/II)
III	Vehicle 1 + L-DOPS	— + 400	1/15	N.S. (I/III; II/III)
IV	Nialamide + L-DOPS	30 + 100	4/15	N.S. (I/IV; II/IV; III/IV)
V	Nialamide + L-DOPS	30 + 200	6/15	<0.1 (I/V; II/V; III/V)
VI	Nialamide + L-DOPS	30 + 400	12/15	<0.01 (I/VI; II/VI; III/VI)

Mice received vehicle 1 or nialamide, 4 h before and vehicle 2 or L-DOPS, 3 h before MES test.
[a] Vehicle 1; dilute acid water.
[b] Vehicle 2; 0.5% carboxymethylcellulose sodium salt.

Table 4. Effects of desipramine, L-DOPS, or their combination treatment on maximal electroshock seizure (MES)

Group	Treatment	Dose (mg/kg i.p.)	Number protected N	P
I	Vehicle 1[a] + Vehicle 2[b]	—	0/15	—
II	Vehicle 1 + L-DOPS	— + 400	1/15	N.S. (I/II)
III	Desipramine + Vehicle 2	10 + –	2/15	N.S. (I/III; II/III)
IV	Desipramine + Vehicle 2	20 + –	2/15	N.S. (I/IV; II/IV)
V	Desipramine + L-DOPS	5 + 400	3/15	N.S. (I/V; II/V; III/V)
VI	Desipramine + L-DOPS	10 + 400	4/15	N.S. (I/VI; II/VI; III/VI)
VII	Desipramine + L-DOPS	20 + 50	4/15	N.S. (I/VII; II/VII; IV/VII)
VIII	Desipramine + L-DOPS	20 + 100	4/15	N.S. (I/VIII; II/VIII; IV/VIII)
IX	Desipramine + L-DOPS	20 + 200	9/15	<0.01 (I/IX; II/IX), <0.05(IV/IX)
X	Desipramine + L-DOPS	20 + 400	11/15	<0.01 (I/X; II/X; IV/X)

Mice received desipramine or vehicle 1, 4 h before and L-DOPS or vehicle 2, 3 h before MES test.

[a]Vehicle 1; distilled water.

[b]Vehicle 2; 0.5% carboxymethylcellulose sodium salt.

L-DOPS was injected 3 h before MES test in the following studies. L-DOPS in doses ranging from 100 to 400 mg/kg was unable to abolish tonic hind leg extensions. However it significantly reduced E/F ratios almost in a dose-dependent manner (Table 2). When animals were pretreated with nialamide (30 mg/kg) 4 h before MES test, L-DOPS at a dose of 400 mg/kg protected 80% of animals from electroconvulsions ($P<0.01$), while it was not effective at a dose of either 100 or 200 mg/kg (Table 3).

When combined with nialamide (30 mg/kg), ED_{50} (95% confidence limit) of L-DOPS for an anticonvulsant action was 210 (145–305) mg/kg (Table 6).

When desipramine at a dose of 20 mg/kg was pretreated 4 h before MES test, L-DOPS at a dose of 200 or 400 mg/kg significantly protected 60% and 73% of animals from electroconvulsions respectively (Table 4).

However L-DOPS at doses of 100 mg/kg or less was not effective even under this condition. Therefore ED_{50} (95% CL) of L-DOPS for an anticonvulsant action was 160 (100–256) mg/kg, when combined with desipramine (20 mg/kg).

When maprotiline at a dose of 40 mg/kg was injected 4 h before MES test, L-DOPS significantly protected animals from electroconvulsions (Table 5). Protection rates and corresponding doses of L-DOPS were as follows: 53%, 100 mg/kg; 67%, 200 mg/kg; 73%, 300 mg/kg; 73%, 400 mg/kg. L-DOPS at a dose of 50 mg/kg was ineffective. Therefore ED_{50} (95% CL) of L-DOPS for an anticonvulsant action was 95 (50–181) mg/kg, when combined with maprotiline (40 mg/kg).

Even in those combination treatments, not only desipramine but also maprotiline were ineffective when used at doses smaller than the above mentioned ones.

However an anticonvulsant effect was obtained, when interval periods between injection times of those drugs and MES test were shortened. When desipramine and L-DOPS (400 mg/kg) were injected 3 h and 2 h respectively before MES test, electroconvulsions were significantly abolished at a dose of 5 mg/kg or 10 mg/kg of desipramine (Table 7).

Under the same injection times, maprotiline at a dose of 20 mg/kg significantly reduced electroconvulsions in combination with L-DOPS (-400 mg/kg) (Table 8).

Brain NE contents were significantly increased by either L-DOPS or nialamide alone (Table 9). The combination treatment with nialamide and L-DOPS increased NE still more, compared to the treatment with either one of these drugs. Brain NE contents were not increased by desipramine (10 mg/kg) and not altered by maprotiline (20 mg/kg) (Table 10). The combination treatment with those antidepressants and L-DOPS significantly increased brain NE contents.

Discussion

When administered alone, L-DOPS could not abolish MES. However, it significantly decreased E/F ratios. This suggests that L-DOPS has a property to reduce the intensity of seizure.

Table 5. Effects of maprotiline, L-DOPS, or their combination treatment on maximal electroshock seizure (MES)

Group	Treatment	Dose (mg/kg i.p.)	Number protected N	P
I	Vehicle 1[a] + Vehicle 2[b]	—	0/15	—
II	Vehicle 1 + L-DOPS	— + 400	1/15	N.S. (I/II)
III	Maprotiline + Vehicle 2	20 + –	1/15	N.S. (I/III; II/III)
IV	Maprotiline + Vehicle 2	40 + –	3/15	N.S. (I/IV; II/IV)
V	Maprotiline + L-DOPS	20 + 400	0/15	N.S. (I/V; II/V; III/V)
VI	Maprotiline + L-DOPS	40 + 50	5/15	<0.05 (I/VI), N.S. (II/VI; IV/VI)
VII	Maprotiline + L-DOPS	40 + 100	8/15	<0.01 (I/VII), <0.025 (II/VII), N.S. (IV/VII)
VIII	Maprotiline + L-DOPS	40 + 200	10/15	<0.01 (I/VIII; II/VIII), <0.05 (IV/VIII)
IX	Maprotiline + L-DOPS	40 + 300	11/15	<0.01 (I/IX; II/IX; IV/IX)
X	Maprotiline + L-DOPS	40 + 400	11/15	<0.01 (I/X; II/X; IV/X)

Mice received maprotiline or vehicle 1, 4 h before and L-DOPS or vehicle 2, 3 h before MES test.

[a]Vehicle 1; distilled water.

[b]Vehicle 2; 0.5% carboxymethylcellulose sodium salt.

Table 6. ED_{50} of L-DOPS for an anticonvulsant effect shown in combined use with other drugs

Combined drug	Dose (mg/kg i.p.)	ED_{50}[a] of L-DOPS (mg/kg i.p.)
Nialamide	30	210 (145–305)[b] [2.55][c]
Desipramine	20	160 (100–256) [3.74]
Maprotiline	40	95 (50–181) [7.48]

Mice received nialamide, desipramine or maprotiline 4 h before and L-DOPS 3 h before MES test.
[a] Dose necessary to abolish tonic hind limb extension in 50% animals.
[b] 95% confidence interval in parentheses.
[c] Slope of regression line in brackets.

When pretreated with nialamide, desipramine or maprotiline, L-DOPS abolished MES dose-dependently. At doses used for the combination these drugs were not effective, when used alone. Both L-DOPS and nialamide (MAO-inhibitor) significantly increased brain NE content. Combination treatment increased brain NE content still more. These results are reasonable, since there is an interaction between the MAO-inhibitor and NE produced by L-DOPS.

On the other hand, desipramine did not increase brain NE, and maprotiline did not do so at doses used here. Both drugs produced a significant increase in brain NE in a combination treatment with L-DOPS.

Those anti-depressants are known to block preferentially the re-uptake of NE into synaptic terminals, resulting in the increase of NE in synaptic clefts [11–17]. Therefore, it is reasonable to infer that the combination treatment activated central noradrenergic transmission more than with L-DOPS alone.

In view of those biochemical results, it is reasonable to infer that the anticonvulsant action of L-DOPS combined with the antidepressants or the MAO-inhibitor was caused by the modification of central noradrenergic transmission.

An anticonvulsant action of NE has been suggested in various experimental epilepsy models [4–6,18–24]. However, most of those studies were performed in animals whose cerebral NE was lowered artificially or genetically.

Ko *et al.*, (1981) reported that the selective increase of brain NE reduced seizure intensity in genetically epilepsy-prone rats [25]. They suggested that there was an inverse relationship between the seizure intensity and the level of noradrenergic transmission in brains of the rats. This suggestion seems to conform to the present findings, since E/F ratios were reduced by L-DOPS.

Cox and Lomax (1976) reported that DL-DOPS attenuated seizure severity in genetically-seizure-prone Mongolian gerbils [7]. There are two differences between their study and our study. We used L-DOPS and the electroshock seizure model in mice, while they used DL-DOPS and genetically seizure-prone gerbils. However, an anticonvulsant action of DOPS is common in the two studies.

Table 7. Effects of L-DOPS in combination with smaller doses of desipramine on maximal electroshock seizure (MES)

Group	Treatment	Dose (mg/kg i.p.)	Time of injection before MES test		Number protected N	P
I	Vehicle 1[a] + L-DOPS	— + 400	2 h 15 min	1 h 45 min	0/15	—
II	Desipramine + Vehicle 2[b]	10 + –	2 h 15 min	1 h 45 min	0/15	—
III	Desipramine + L-DOPS	5 + 400	2 h 15 min	1 h 45 min	8/15	<0.01 (I/III; II/III)
IV	Desipramine + L-DOPS	5 + 400	3 h	2 h	5/15	<0.05 (I/IV; II/IV)
V	Desipramine + L-DOPS	10 + 400	3 h	2 h	11/15	<0.005 (I/V; II/V)

Though doses of combined desipramine were smaller than 20 mg/kg, protective effects were obtained, when intervals between drug injections and MES test were shorter than that presented in Table 4.

[a] Vehicle 1; distilled water.

[b] Vehicle 2; 0.5% carboxymethylcellulose sodium salt.

Table 8. Effects of L-DOPS in combination with smaller doses of maprotiline on maximal electroshock seizure (MES)

Group	Treatment	Dose (mg/kg i.p.)	Time of injection before MES test		Number protected / N	P
I	Vehicle 1[a] + L-DOPS	— + 400	3 h	2 h	0/15	—
II	Maprotiline + Vehicle 2[b]	20 + –	3 h	2 h	1/15	—
III	Maprotiline + L-DOPS	10 + 400	3 h	2 h	1/15	N.S. (I/III; II/III)
IV	Maprotiline + L-DOPS	20 + 400	3 h	2 h	10/15	<0.005 (I/IV; II/IV; III/IV)

Though doses of combined maprotiline were smaller than 40 mg/kg, protective effects were obtained, when intervals between drug injections and MES test were shorter than that presented in Table 5.

[a,b] as presented in Table 7.

Table 9. Brain norepinephrine (NE) in mice treated with L-DOPS, nialamide or a combination of both drugs

Group	Treatment	Dose (mg/kg i.p.)	Time of injection before decapitation		Norepinephrine mean ± S.E. (ng/mg protein)	N
I	Vehicle 1 + Vehicle 2	—	4 h	3 h	2.99 ± 0.07	6
II	Vehicle 1 + L-DOPS	— + 400	4 h	3 h	3.76 ± 0.22[a]	6
III	Nialamide + Vehicle 2	30 + –	4 h	3 h	4.98 ± 0.34[b]	6
IV	Nialamide + L-DOPS	30 + 400	4 h	3 h	6.26 ± 0.24[b]	6

Vehicle 1: distilled water, Vehicle 2: 0.5% CMC-Na, [a]$p<0.01$, [b]$p<0.001$, from Group 1.
Either L-DOPS or nialamide increased brain NE significantly.
The combination of both drugs increased NE more than when used alone.

Table 10. Brain norepinephrine (NE) in mice treated with L-DOPS, antidepressants or a combination of both drugs

Group	Treatment	Dose (mg/kg i.p.)	Time of injection before decapitation		Norepinephrine mean ± S.E. (ng/mg protein)	N
I	Vehicle 1 + Vehicle 2	—	3 h	2 h	3.25 ± 0.07	6
II	Vehicle 1 + L-DOPS	— + 400	3 h	2 h	4.25 ± 0.14[a]	5
III	Desipramine + Vehicle 2	10 + –	3 h	2 h	3.48 ± 0.14	6
IV	Maprotiline + Vehicle 2	20 + –	3 h	2 h	3.17 ± 0.06	6
V	Desipramine + L-DOPS	10 + 400	3 h	2 h	4.06 ± 0.07[a]	6
VI	Maprotiline + L-DOPS	20 + 400	3 h	2 h	4.09 ± 0.13[a]	6

Vehicle 1: distilled water, Vehicle 2: 0.5% CMC-Na, [a]$p<0.001$, from Group 1.
Neither maprotiline nor desipramine increased brain NE significantly when used alone though L-DOPS did so.
The combination of L-DOPS with either desipramine or maprotiline increased NE significantly.

There have been clinical case reports of seizures with desipramine, imipramine or maprotiline [26–30]. On the other hand, Fromm *et al.*, (1972; 1978) reported a beneficial effect against petit mal epilepsy with imipramine [31,32]. Pineda and Russell (1974) reported an anti-epileptic effect of desipramine [33].

In experimental models of epilepsy, tricyclic anti-depressants have been reported to exert a biphasic effect with an anticonvulsant action shown at a low dose and a proconvulsant action at a high dose [34,35]. In kindled hippocampal seizures in rats, desipramine, imipramine and maprotiline significantly reduced afterdischarge duration and seizure severity [36]. Trimble (1978) noted that maprotiline was less seizurogenic than other antidepressants in animal studies [28], yet it is not so in humans.

The present study suggests that L-DOPS could limit the proconvulsant side-effects of desipramine and/or maprotiline in the clinical use of these antidepressants.

References

1. Inagaki C and Tanaka C (1978) Biochem. Pharmacol. 27: 1081–1086.
2. Narabayashi H, Kondo T, Hayashi A, Suzuki T and Nagatsu T (1981) Proc. Japan Acad. 57: 351–354.
3. Senda Y, Muto T, Matsuoka Y, Takahashi A and Sobue I (1987) Clin. Neurol. (Tokyo) 27: 300–304.
4. Kilian M and Frey HH (1973) Neuropharmacology 12: 681–729.
5. Mason ST and Corcoran ME (1978) Life Sci. 23: 167–172.
6. Mason ST and Corcoran ME (1979) Brain Res. 170: 497–507.
7. Cox B and Lomax P (1976) Pharmacol. Biochem. Behav. 4: 263–267.
8. Swinyard EA, Brown WC and Goodman LS (1952) J. Pharmacol. Exp. Ther. 106: 319–330.
9. Tedeshi DH, Swinyard EA and Goodman LS (1956) J. Pharmacol. Exp. Ther. 116: 107–113.
10. Litchfield JT and Wilcoxon F (1949) J. Pharmacol. Exp. Ther. 96: 99–113.
11. Carlsson A, Corrodi H, Fuxe K and Hökfelt T (1969) Eur. J. Pharmacol. 5: 357–366.
12. Carlsson A, Corrodi H, Fuxe K and Hökfelt T (1969) Eur. J. Pharmacol. 5: 367–373.
13. Fuxe K and Ungerstedt U (1968) Eur. J. Pharmacol. 4: 135–144.
14. Göthert M, Schlicker E and Köstermann F (1983) Naunyn-Schmiedeberg's Arch. Pharmacol. 322: 121–128.
15. Lidbrink P, Jonsson G and Fuxe K (1971) Neuropharmacology 10: 521–536.
16. Maitre L, Waldmeier PC, Baumann PA and Staehelin M (1974) Adv. Biochem. Psychopharmacol. 10: 297–304.
17. Waldmeier PC, Baumann P, Greengrass PM and Maitre L (1976) Postgrad. Med. J. 52 (Suppl. 3): 33–39.
18. Jobe PC, Picchioni AL and Chin L (1973) J. Pharmacol. Exp. Ther. 184: 1–10.
19. Jobe PC, Stull RE and Geiger PF (1974) Neuropharmacology 13: 961–968.
20. Gross RA and Ferrendelli JA (1982) Neuropharmacology 21: 655–661.
21. Corcoran ME and Mason ST (1980) Brain Res. 190: 473–484.
22. Trottier S, Berger B, Chauvel P, Dedek J and Gay M (1981) Neuroscience 6: 1069–1080.
23. Mohr E and Corcoran ME (1981) Exp. Neurol. 72: 507–511.
24. Laird II, HE (1983) Epilepsia 24: 107.
25. Ko KH, Dailey JW and Jobe PC (1982) J. Pharmacol. Exp. Ther. 222: 662–669.
26. Lamont ES (1965) Br. Med. J. 2: 483.
27. Kiloh LG, Davison K and Osselton JW (1961) Electroencephalogr. Clin. Neurophysiol. 13: 216–223.
28. Trimble M (1978) Epilepsia 19: 241–250.
29. Schwartz L and Swaminathan S (1982) Am. J. Psychiatry 139: 244–245.
30. Holliday W, Brasfield Jr. KH and Powers B (1982) Am. J. Psychiatry 139: 673–674.
31. Fromm GK, Amores CY and Thies W (1972) Arch. Neurol. 27: 198–204.
32. Fromm GH, Wessel HB, Glass JD, Alvin JD and Van Horn G (1978) Neurology 28: 953–957.
33. Pineda MR and Russell SC (1974) Dis. Nero. Syst. 35: 322–323.
34. Lange SC, Julieu RM and Fowler GW (1976) Epilepsia 17: 183–196.
35. Wood TW, Jobe PC, Laird HE and Dailey JW (1983) Fedn. Proc. 42: 363.
36. Clifford DB, Rutherford JL, Hicks FG and Zorumski CF (1985) Ann. Neurol. 18: 692–697.

Address for correspondence: M. Yoshida, Dpt. Neurology, Inst. Clin. Med., Univ. Tsukuba, City of Tsukuba, Ibaraki 305, Japan.

Small neurons in the lower spinal cord are selectively damaged in the spastic rat by acromelic acid

S. Kwak[a], H. Aizawa[a], M. Ishida[b], Y. Gotoh[b] and H. Shinozaki[b]

[a]National Institute of Neuroscience, 4-1-1 Ogawahigashi, Kodaira, Tokyo 187, Japan
[b]The Tokyo Metropolitan Institute of Medical Science, 3-18-22, Honkomagome, Bunkyo-ku, Tokyo 113, Japan

Abstract

A single systemic injection of acromelic acid, one of kainoids, caused semipermanent severe spastic paraparesis in the rat. One week after the injection, routine histological examination disclosed chromatolysis of small neurons with marked reactive gliosis in the spinal cord, particularly the lumbar and sacral segments. These changes were observed throughout the gray matter except the most dorsal margin of the posterior horn (I and II layers of Rexed). Glial processes were intensely stained by immunohistochemistry against glial fibrillary acidic protein (GFAP) which was maximal at the ventral part of the dorsal horn at the sacral and lumbar segment. Mild glial proliferation was visualized only by the immunohistochemistry of GFAP in the hippocampal CA4, but pyramidal cells appeared intact by ordinary staining. The remaining structures were not affected including large anterior horn cells and the white matter of the spinal cord. The following points are deduced from these results; 1) The selective loss of small neurons in the lower spinal cord is responsible for the marked spastic paraparesis produced by the injection of acromelic acid. Destroyed neurons may belong to a group of inhibitory interneurons of spinal reflex arcs. 2) By analogy to the excitotoxic action of kainic acid, acromelic acid may have caused neural degeneration through excessive depolarization. This suggests that degenerated neurons might bear receptors with great affinity to acromelic acid. 3) Acromelic acid conceivably acts through a different glutamate receptor subtype from the kainate receptor in the rat central nervous system because of the different pattern of cell vulnerability from that following systemic kainic acid injection. 4) Selective destruction of small neurons of the spinal cord, possibly by extrinsic neurotoxin, might give a clue to the pathophysiology of human spastic paraparesis such as the 'stiff-man syndrome'.

Introduction

Acromelic acid which has been recently extracted from a Japanese poisonous mushroom *Clitocybe acromelalga* [1–3], possesses a common moiety with and similar pharmacological properties to kainic acid [4]. Recent pharmacological studies have revealed that its depolarizing effect on the crayfish muscle [4] and newborn rat spinal cord [5] was the most potent among kainoids. Because of this potent depolarizing action, investigating the neuronal response to acromelic acid would provide useful information on roles of kainate receptors and on the effects of the excitatory amino acid. With this aim, we investigated the behavioral responses and the neuropathological changes induced by systemic acromelic acid in the rat.

Materials and Methods

Twenty four male Wistar rats, weighing 121–251 g, were injected systemically with acromelic acid in various doses (2–5.5 mg/kg s.c., i.p., and i.v.). Seven and 86 days after the injection of acromelic acid, spastic rats were transcardially perfused with 200 ml of 3% paraformaldehyde, 0.25% glutaraldehyde in 0.1 M phosphate buffer (pH 7.4) under pentobarbital anaesthesia. Whole brains, spinal cords, sciatic nerves and quadriceps muscles were dissected and immersed in the cold fixative for 2 h, then transferred to 0.1 M phosphate buffer pH 7.4 containing 5% sucrose and incubated overnight. After several changes of the phosphate buffer containing increasing amounts of sucrose, tissues were trimmed and mounted in paraffin and cut at 8 μm. In addition to the routine hematoxylin and eosin (H.E.), Kluver-Barrera (K.B.) and Bodian's silver staining, some sections were immunohistochemically stained with monoclonal antibody against glial fibrillary acidic protein (GFAP) (Labsystems, Helsinki) in dilution of 1:500 using avidin biotin method (Vector lob Inc.). 3,3-diaminobenzidine was used as a chromogen and sections were counterstained with hematoxylin. For cytometry, 5 randomized paraffin sections of lumber segment (L5) from the normal and the injected rat were used and only the neurons having nucleolei were counted. Neurons were arbitrarily divided into two groups; whose diameter over 15 μm are designated as large neurons and those less than 15 μm as small neurons. Numbers are expressed as the mean ± S.D. of five slices.

Results

The most pronounced ultimate change of the rat behavior induced by systemic acromelate was the persistent spastic paraparesis. About 30 min after the injection of acromelic acid (5 mg/kg), all 6 rats began to move their tail like a snake and to bite their tail occasionally as if it were itching. Then the back became flexed (severely kyphotic) with the gradual raising of the hips and the extension of hind limbs. They could walk only on their toes because of the forced extension of hind limbs. The hind limbs sometimes became cramped and hind paws took a plantar flexed posture when they were standing, and rats occasionally lost their balance and fell forward. They demonstrated righting reflexes and struggled to be in a normal position using their forelimbs. The hind limbs extended intermittently which lasted more than half an hour. Subsequently, rats developed a marked tonic cramp of the hind limb and the tail, but they hardly salivated or panted. Rats were fully conscious and used their forelimbs skillfully when they crawled or stood up from the recumbent position. As the hind limb cramps repeated, most of the rats developed marked generalized tonic-clonic convulsions. Four out of 6 rats died at this stage, although one did not develop convulsion. Rats which survived the phase of convulsion lasting about 30 min, developed flaccid but not spastic paralysis of the lower part of the body. The flaccid hind limbs did not respond to external

noxious stimuli and rats walked using forelimbs only, dragging the hind limbs and the tail. Some rats did not become flaccid, even though the tonic extension of hind limbs were severe in the previous phase. On the next day, only the rats that passed

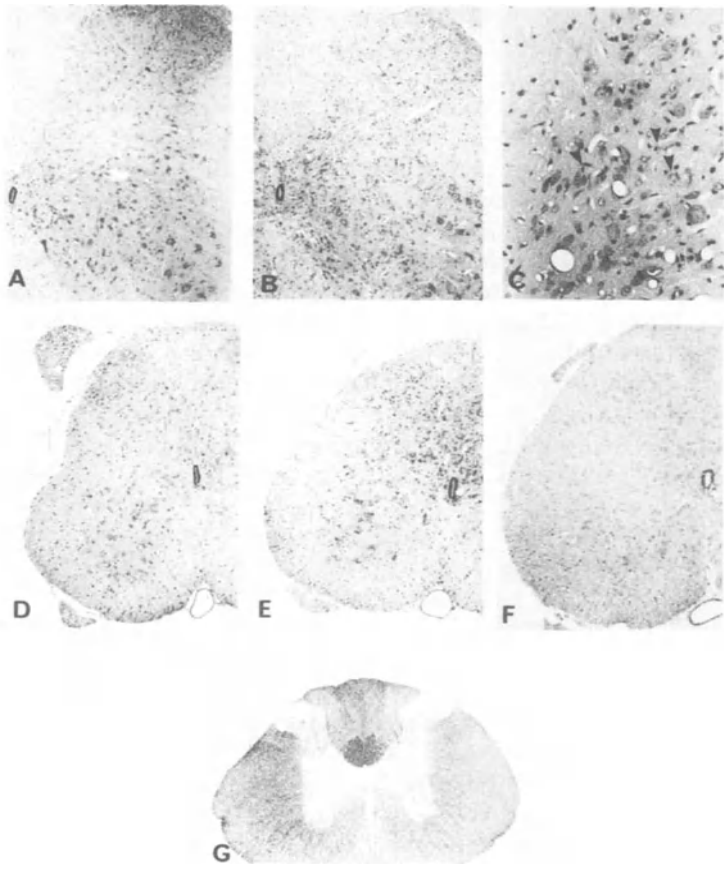

Fig. 1. Spinal cord sacrificed 7 and 86 days after the acromelic acid injection with control. A) L5 segment of the normal rat spinal cord. H.E. × 38. B) Corresponding segment of the rat 7 days after the injection. Note the marked increase of small microglial nuclei at the entire gray matter except the outermost area of the dorsal horn and the lateral ventral horn. Large anterior horn cells were preserved. C) Magnified view from the same section to Fig. B) at the border of the gray and the white matter most ventral dorsal horn. Several neurons appear pyknotic and surrounded by dark glial nuclei (arrowheads). H.E. × 150. D) Sacral segment of the normal rat. H.E. × 38. E) Sacral segment of the rat 7 days after the injection. Small glial proliferation is marked at the dorsal area. H.E. × 38. F) Sacral segment of the rat 86 days after the injection. A slight increase in the glial nuclei is notable. Small neurons are decreased in number. H.E. × 38 G). Thoracic segment of the rat 86 days after the injection. Entire white matter is well myelinated. K.B. × 17.

through the transient phase of flaccidity developed severe spastic paraparesis which was significantly reinforced by sensory stimuli such as touching and poking. The paretic rats dragged their hind limbs and the hind pads usually faced the ceiling. However, they could use hind limbs, although only rarely indicating that the hind limbs were not completely paralysed. This spastic paralytic phase persisted until they were sacrificed for the histopathological analysis. Contrary to this, rats that did not exhibit the flaccid phase appeared normal on the next day. The death rate of rats that received 3 mg/kg acromelic acid and did not change their behaviors was zero, of those received 4 mg/kg 50%, and of those receiving 5.5 mg/kg 100%. Among 24 rats receiving acromelic acid, only two developed persistent paraplegia.

Two spastic rats were transcardially perfused on 7 and 86 days after the injection, respectively. The histological change was almost confined to the gray matter of the lower spinal cord (Fig. 1). On 7 days post-injection, several pyknotic neurons were found to be surrounded by small glia whose number was markedly increased throughout the gray matter except the 1 and 2 layers of Rexed (Fig. 1). Cytometry showed clearly that only the population of small neurons was decreased; the mean ± S.D. of large and small neurons in the lumbar segment of the injected rat as compared to that of the control were 21.8 ± 2.13 vs 22.0 ± 1.41 and 298 ± 11.9 vs 531 ± 21.5, respectively. The result of cytometry indicated that the pyknotic, degenerated neurons were small sized. The total number of pyknotic neurons was 70.0 ± 7.01 in the injected rat and the ratio of degenerated neurons against the sum of small neurons and degenerated neurons was 17.4:85.5 (20%) in the ventral, 21.3:82.6 (25%) in the middle and 32.1:222 3 (12%) in the dorsal area when the gray matter was divided into three areas. The degenerated neurons were frequent at the areas near the central canal. Preservation of large anterior horn cells (Figs. 1B, 1C) and the myelination in the white matter (Fig. 1G) support the selectivity of the small neuronal damage. Astroglial immunoreactivity against glial fibrillary acidic protein (GFAP) was intensely increased and glial processes became prominent in the ventral part of dorsal horn in the lumbar segment 2A, 2B) but the reaction was more diffuse throughout the gray matter in the sacral segment 2D). These changes were most striking at the sacral segment and became less pronounced more rostrally. In the lower thoracic segment, only trace signs of cell degeneration and a slight increase of immunoreactivity of GFAP were observed and the cervical cord was apparently intact (Fig. 2C). Outside the spinal cord, a mild increase of the immunoreactivity to GFAP was observed at hippocampal CA4 area (Fig. 2G) although no pyramidal cell change was detected there by routine histological observation (Fig. 3A). The other structures were histologically intact including the areas where liable to systemic kainic acid such as pyriform and entorhinal cortices, amygdaloid nucleus, and lateral septum (Fig. 3). Normal appearance of muscles suggests that both motor neurons and muscles are free from the pathological change (Fig. 3G).

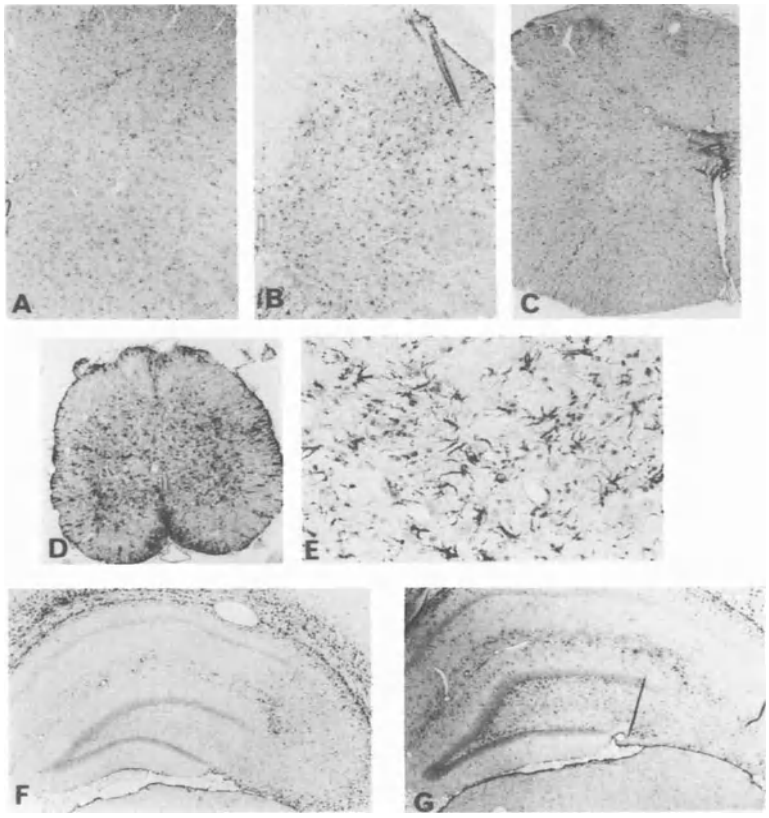

Fig. 2. Immunohistochemistry against GFAP of the spinal cord from rat sacrificed 7 days after the acromelic acid injection. All the sections were counter stained with hematoxylin. A) Control lumbar segment (L5). × 38. B) L5, injected rat. Glial reaction is marked at the central and dorsal gray matter. Again, the reaction is not increased at the dorsal edge of the posterior horn. At the ventral horn, glial reaction in the lateral part is rather less pronounced than in the medial part. × 38. C) Cervical cord (C4) of injected rat. No glial reaction is detectable. The same as the view of the control. × 25. D) Sacral segment from the injected rat. Note that the astroglias become prominent and their processes become markedly thickened. Glial reaction appears not increased at the most dorsal sector of the posterior horn. × 38. E) Magnified view. Thickened, arborized astroglial processes are seen. × 150. F) Control hippocampus. × 15. G) Hippocampus, injected rat. Immunoreaction is slightly increased at CA4 sector. × 15.

Discussion

Semipermanent spastic paraplegia after a single shot of acromelic acid was quite noteworthy. Initial changes in the tail and the hind limbs suggest a strong preponderance of the affinity of acromelate for the caudal spinal cord. Hind limbs

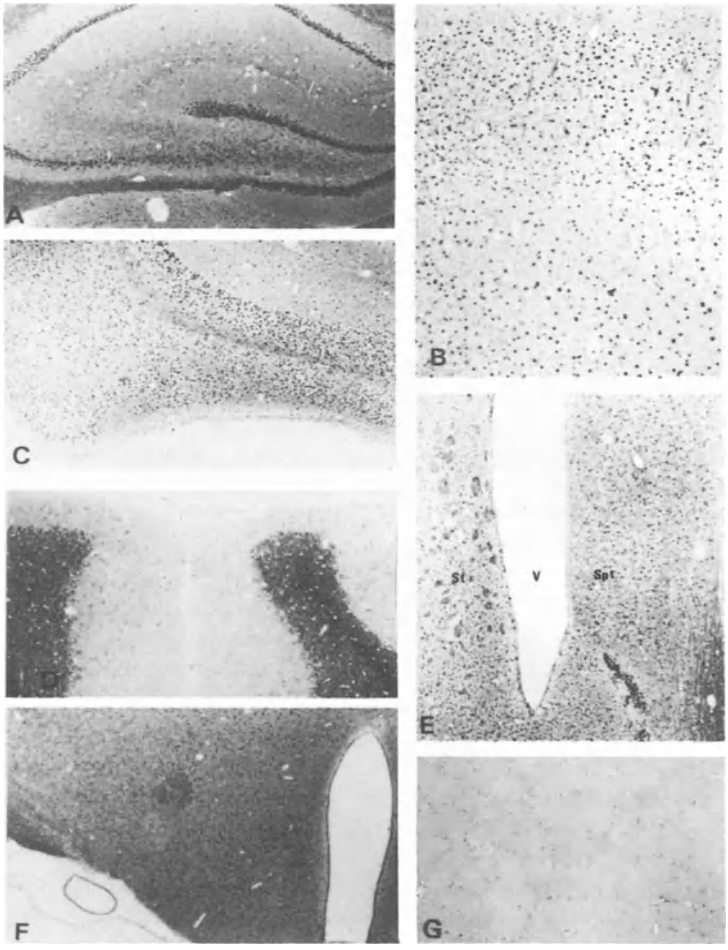

Fig. 3. Histology from the rat 86 days after the injection. No histopathological alteration is detectable. Bodian stain except G). A) Hippocampus. × 15. B) Frontal cortex. × 50. C) Entorhinal cortex. × 50. D) Cerebellar cortex. × 50. E) Striatum and Septum. Spt: septum, V: lateral ventricle, St: striatum. × 15. F) Hypothalamus. × 15. G) Quadriceps muscle. H.E. × 50.

extended gradually although rats could still use them when they moved, and the back was flexed but not extended like the posture characteristic of decerebrate rigidity. These postural changes suggested that the spasticity could hardly be attributed to the cessation of the corticospinal tract above the level of the thoracic segment. Generalized seizures that occurred after an intensification of the hind limb extension may be based on the nonselective, excessive neuronal depolarization in all the neurons in the central nervous system. Subsequent phase of flaccid

paraplegia is based on a functional neuronal damage after the exaggerated neural firing. It could be an analogous state to the 'spinal shock' which is frequently observed after an acute spinal injury or post-icteric paralysis because the flaccid paraplegia recovered within 24 h and replaced by permanent spasticity. Even after the development of permanent spastic paraparesis, rats could use their hind limbs on some occasions indicating that the muscles and the motor neurons were functioning and escaped severe histological change. However, permanency of the symptoms suggests that the behavioral change observed here must be accompanied by at least some histopathological alteration. Since the permanent behavioral change is the spastic paraparesis, the primary site of the lesion is predicted to be located in the lower spinal cord, sparing alpha motoneurons. Namely, internuncial neurons that act to inhibit spinal reflexes are most likely to have been destroyed by the action of acromelic acid.

As predicted from the observation of behavioral change, neuropathological alteration was confined to the spinal cord, particularly the sacral and lumbar cord. White matter myelination was well preserved as far as the myelin staining disclosed. Finding that the most external layer of dorsal horns were spared from the glial reaction and from cell degeneration on 7 days after the injection indicates that the primary afferent fibers were not involved. Neither alpha nor gamma motoneurons were selectively affected because the degenerated neurons were infrequent in the ventral horn and also because the nerve fibers in the ventral root were intact (data not shown). The selective loss of small sized neurons was also supported by the cytometrical results. A large proportion of the small neurons in the spinal cord are the internuncial neurons. In contrast to the diffuseness of the distribution of degenerated neurons in our study, Renshaw's recurrent inhibitory neurons localize in the restricted ventromedial area of the anterior horn [6]. Thus, vulnerability is not confined to Renshaw cells, interruption of the spinal arc by the degeneration of inhibitory interneurons must be the pathophysiological basis as we predicted from the behavioral observation. Since this semi-permanent behavioral change was produced by a single injection, the excitotoxic action of acromelic acid must be so potent as to cause excessive depolarization of the affected neurons.

After the systemic injection of kainic acid, on the other hand, rats have been known to display seizure syndrome (rearing, praying, salivating) and a characteristic 'wet dog shake' behavior [7–11]. The recurrence of these 'limbic seizures' is said to continue for more than 3 h which ultimately ends in the long-standing status epileptics [8]. Symptoms confined to the hind limbs and the tail as we observed in our experiment have never appeared in the animals with kainate injection. Histopathological changes were reported not in the spinal cord but mainly in the limbic systems; hippocampus, amygdala, pyriform and entorhinal cortices, thalamic nuclei and septum [7,8,12]. Therefore, the distribution of neuropathological changes was comparable to the occurrence of 'limbic seizure'. A lack of behavioral similarity between the cases of systemic injection of kainic acid and those of acromelic acid could explain the difference of the extent and the distribution of neuropathological changes between them.

Mechanisms by which kainic acid produces tissue damage in the central nervous system have not been fully clarified. Kainic acid receptors are localized most abundantly in the hippocampal CA3 area [13] whereas the neuronal degeneration is more pronounced at the CA1 than CA4 and CA3 sector when administered systemically [7,8,12]. Although a direct effect of kainic acid on the affected neurons was proposed [14], a part of the histological change was attributable to the extensive brain edema [10].

Selective loss of lumbar spinal cord interneurons has been reported in the ischemic lesion produced by the ligation of thoracic aorta in the dog and cats [15–17]. The behavioral change was quite similar to our spastic rats. Histologically, the small neurons were most vulnerable to ischemia and large neurons were destroyed only if the ischemia prolonged further [15]. The exact nature of the selective death of small neurons has not been elucidated. Whether acromelic acid produces local lumbosacral ischemia in the rat through acting directly on the small arteries is not known, but it is unlikely that acromelic acid acts directly on the small vessels and causes strong ischemia comparable to the effect of more than 30 min aortic ligation [15,16]. However, because of the exact concordance of the neuropathological change, it is worthy to investigate a basis of the selective neuronal death by acromelic acid in relation to the mechanism underlying the cell death in ischemia.

Clinically, we can easily recall a similar clinicopathological state called 'stiff-man syndrome', a progressive neurological disease characterized by ascending rigidospasticity without muscle wasting [18,19]. Although this disease is considered to be a heterogeneous entity, gliosis of the gray matter sparing the anterior horn cell is the histopathological characteristic in common to the reported autopsy cases, although some associated findings such as the white matter lesion are always present [20–22]. Signs of Renshaw cells dysfunction have been reported by electrophysiological studies [22]. Because of the clinical and neuropathological similarities, the discovery of a compound reported here causing an animal model of 'stiff-man syndrome' is invaluable to understand the pathophysiology of this miserable progressive neurological disease of unknown etiology. This compound is also a useful tool to investigate selective neuronal death, which is a key question of degenerative neurological diseases.

Further study is necessary to elucidate which class of neurons are vulnerable to acromelic acid in terms of their neurotransmitters. In addition, effect of low dose administration of acromelic acid is important if the accumulation of an excitotoxin is a real cause of a certain degenerative neurological disease.

Acknowledgement

The authors thank Prof. H. Shirahama for the generous gift of acromelic acid.

References

1. Hashimoto K, Konno K, Shirahama H and Matsumoto T (1986) Chem. Lett. 1399–1400.
2. Konno K, Hashimoto K, Ohfune Y, Shirahama H and Matsumoto T (1986) Tetrahedron Lett. 27: 607–610.
3. Konno K, Shirahama H and Matsumoto T (1983) Tetrahedron Lett. 24: 939–942.
4. Shinozaki H, Ishida M and Okamoto T (1986) Brain Res. 399: 395–398.
5. Ishida M and Shinozaki H (1988) Brain Res. 474: 386–389.
6. Thomas RC and Wilson VJ (1965) Nature 206: 211–213.
7. McGeer EG, Olney JW and McGeer PL (eds.) (1978) Kainic Acid as a Tool in Neurobiology, Raven Press, New York.
8. Ben-Ari Y (1985) Neurosci. 14: 375–403.
9. Collins RC, McLean M and Olney J (1980) Life Sci. 27: 855–862.
10. Lassman H, Tetsche V, Kitz K, Baran G and Sperk G (1984) Neurosci. 13: 691–704.
11. Olney JW and de Gubareff T (1978) In: McGeer EG, Olney JW and McGeer PL (eds.) Kainic Acid as a Tool in Neurobiology. Raven Press, New York, pp. 201–217.
12. Schwob JE, Fuller T, Price JL and Olney JW (1980) Neuroscience 5: 991–1014.
13. Foster AC, Mena EE, Monaghan DT and Cotman CW (1981) Nature 289: 73–75.
14. Garthwaite J and Garthwaite G (1983) Nature 305: 138–140.
15. Gelfan S and Tarlov IM (1959) J. Physiol. 146: 594–617.
16. Gelfan S and Tarlov IM (1963) Am. J. Physiol. 205: 606–616.
17. Davidoff RA, Graham LT Jr., Shank RP, Werman R and Aprison MH (1967) J. Neurochem. 14: 1025–1031.
18. Moersch FP and Woltman HW (1956) Mayo Clin. Proc. 31: 421–427.
19. Gordon AS, Rewcascle NB, Humphrey JG and Stewart BM (1967) Am. J. Med. 42: 582–599.
20. Howell DA, Lees AJ and Toghill PJ (1979) J. Neurol. Neurosurg. Psychiat. 42: 773–785.
21. Whitely AM, Swash M and Urich H (1976) Brain 99: 27–42.
22. Watanabe K, Kawai M, Shimpo T, Shimada Y and Toyokura Y (1981) Clinical Neurol. 14: 574–581. (Eng. abstr.)

Address for correspondence: S. Kwak, National Institute of Neuroscience, 4-1-1, Ogawahigashi, Kodaira, Tokyo 187, Japan.

Alteration of the NMDA associated ion channel binding sites in the epileptic mutant mouse quaking

Yves Maurin[a], Marie Jo Besson[a] and Nadia Mitrovic[a,b]

[a]CNRS-UPMC, Institut des Neurosciences, Dept. Neurochimie-Anatomie, 9 Quai St. Bernard, 75005 Paris, France

[b]Laboratoire de Neurochimie, INSERM U134, Hop. Salpétrière, 75 Bld. de l'Hopital, 75651 Paris Cedex 13, France

Abstract

Two competitive (CPP and CGS 19755) and two non-competitive (TCP and MK-801) antagonists of the NMDA receptor/ion channel complex inhibited in a dose dependent manner the convulsions of the quaking mice, a model of inherited epilepsy. However, the effects of the competitive antagonists (which bind to the NMDA recognition site) were not complete, and were accompanied by a marked ataxia, while the non-competitive antagonists (which interact with the NMDA-receptor associated ion channel) fully protected the quaking mice and did not induce any noticeable side effect. The binding of ^{3}H-glutamate to thoroughly washed brain membranes did not show any difference between the mutants and their controls. Moreover, CPP and CGS 19755 appeared equally potent at displacing the binding of ^{3}H-glutamate in the two strains. The binding of ^{3}H-TCP appeared to be markedly higher in the quaking mice than in the controls (B_{max} qk: 3.11 ± 0.47 pmol/mg prot, n=5; controls: 1.80 ± 0.18 pmol/mg prot, n=6), without any change of the affinity constant (Kd qk: 70.8 ± 14.4 nM, n=5; controls: 54.3 ± 3.6 nM, n=6). In both quaking and control mice, ^{3}H-TCP binding could be modulated by glutamate and glycine. In addition, the ability of glutamate and glutamate + glycine to enhance the binding of ^{3}H-TCP was higher in the mutants than in the controls.

The quaking (qk) mutation [1] is a recessive mutation which maps on chromosome 17. The affected mice exhibit several alterations of the central nervous system structure and function. The differentiation of oligodendrocytes, the glial cells which produce the brain myelin, is profoundly affected [2], thus giving rise to an immature myelin sheath [3]. Brain levels of myelin proteins are markedly reduced [for review, see ref. 4], probably via an indirect mechanism, since none of their structural genes maps on chromosome 17. Behaviorally, the trait of the qk mutation is a tremor of the voluntary movements and tonic clonic convulsions which appear by post-natal day 40 [5]. Such convulsions are either spontaneous or may be readily elicited by tactile or auditory stimulation [6]. Several studies have demonstrated that the convulsions of the qk mice are associated with profound alterations of the brain noradrenergic system [5,7–11]. Among the amino acid neurotransmitters, it has been shown that GABA is probably not associated with the qk mice convulsions [12]. In the present study, we have been interested in the possible involvement of the glutamatergic neurotransmission in the convulsions of the qk mutants.

Materials and Methods

Animals

Male adult qk mice (C57B1/6J strain), 10 to 12 weeks old, weighing 19–21 g, raised in our colony under standard laboratory conditions (free access to food and water; 12 h (7:00–19:00) dark-light cycle), were used.

Behavioral experiments

The anticonvulsant effects of CPP (3-((±)-2-carboxypiperazin-4-yl)-propyl-1-phosphonate) (Sandoz), CGS 19755 (cis-4-phosphonomethyl-2-piperidine carboxylic acid) (Ciba-Geigy), TCP (1-(1-(2-thienyl)cyclohexyl)piperidine) (kindly provided by Dr. Kamenka) and MK-8O1 (5-methyl-10,11-dihydro-5H-dibenzo(a,d)cyclohepten-5,10-imine maleate) (a generous gift from Dr. Pin), all administered i.c.v., in solution in 0.1 M phosphate buffer (pH 7.4), were measured according to the following protocol: for each mouse, the number of seizures (N_1) elicited by a first set of twenty tactile stimulations (one stimulation every 60 s, consisting of an attempt to place rapidly the mouse in the dorsal decubitus position) was determined prior to the treatment; at the end of the set, the drugs (or the vehicle) were injected in a final volume of 1 µl. After 15 min (i.c.v.), the response (N_2) induced by another set of 20 convulsive stimuli was determined. The percent change of seizure response (100(N2-N1/N1)) was taken as an index of the anticonvulsant properties of the drug tested. ED_{50} values (corresponding to the dose of compound inducing 50% inhibition of the convulsive response) were calculated from log dose-probit transformation.

Mice were prepared for the experiment in the following manner: the day preceding the experiment, they were prepared by fixation of a plastic guide (0.3 mm internal diameter) over a hole in the skull drilled under anesthesia (either halothane for TCP and MK-801 experiments or 0.25 mg acepromazine base followed 15 min later by 1 mg ketamine, for CPP and CGS 19755) at the following stereotaxic coordinates 3.7 mm anterior to the lambda, 1.4 mm lateral to the interhemispheric suture. The mice were left overnight to recover from surgery. On the day of the experiment, drugs were injected through the plastic guide with a Hamilton syringe fitted with a needle of 0.3 mm external diameter at a depth of 2.1 mm from the surface of the cortex. The site of i.c.v. injection was checked histologically.

Binding assays

^{3}H-glutamate binding

The binding of ^{3}H-glutamate was performed on whole brain synaptic membranes (one brain/binding assay). Mice were killed by cervical dislocation. The brains were rapidly removed and homogenized in 0.32 M sucrose with a Potter. The

homogenate was centrifuged at 1000 g for 10 min. The pellet was discarded and the supernatant recentrifuged at 20,000 g for 10 min. The pellet (P_2) was homogenized with a Polytron (setting 6, 15 sec.) in 20 ml of cold bidistilled water and centrifuged for 15 min at 48,000 g. The pellet was frozen during 15 min at −20°C. The washing procedure (Polytron, centrifugation, freezing) was repeated three more times. On the day of the experiment, the final pellet was thawed at room temperature, resuspended in 25 ml of bidistilled water, homogenized, incubated for 10 min at 37°C, and centrifuged at 48,000 g for 15 min. After a second resuspension in 25 ml of bidistilled water, homogenization and centrifugation in the same conditions, the final pellet was suspended in 25 ml of 50 mM Tris-acetate buffer (pH 7.4) to reach a protein concentration of approximately 1 mg/ml [determined according to Lowry *et al.*, ref. 13]. For the binding assays, 200 µl of the membrane preparation were incubated during 1 h with varying concentrations of ^{3}H-glutamate (S.A. 1961 Gbq/mmol, Amersham) ranging from 10 to 300 nM (final concentrations), in the absence (total binding) or the presence (non-specific binding) of 1 mM (final concentration) unlabelled glutamic acid. The incubation was stopped by filtration under vacuum over Whatman GF/B glass fiber filters. The filters were washed twice with 3.5 ml of the incubation buffer, and the radioactivity retained on the filters was determined by liquid scintillation counting at an efficiency of approximately 33%. Equilibrium constants (Kd and B_{max}) were calculated from non-linear regression curves [14], derived from specific binding values (defined as the difference between total and non-specific binding).

For the displacement studies, membranes prepared as described above were incubated at 4°C in Tris-acetate buffer during 1 h with a single concentration of ^{3}H-glutamate (270 nM), in the presence of CPP or CGS 19755 at concentrations ranging from 1×10^{-9} M to 3×10^{-5} M.

^{3}H-TCP binding

The P2 fractions were prepared in the same way as for ^{3}H-glutamate binding. They were resuspended in 30 ml Tris-HCl buffer (5mM, pH 7.7) with a Polytron (setting 6, 15 sec) and washed by 5 centrifugations (48,000 g, 15 min) with intermediate resuspension in Tris-HCl buffer and Polytron homogenization. The final pellet was resuspended and homogenized in 10 ml of Tris-HCl buffer and frozen at −20°C until utilization.

The frozen pellet was then thawed at room temperature, suspended in 30 ml of 5 mM Tris-HCl buffer, homogenized in the same conditions as above, and centrifuged 3 times (48,000 g, 15 min) with intermediate homogenization in Tris-HCl buffer containing 0.1 mM EDTA. The final pellet was resuspended in 10 ml of Tris-HCl buffer containing 0.1 mM EDTA and used for the binding assay.

Saturation studies

Aliquots (200 µl) of the membrane preparation were incubated during 4 h with 20 µl ^{3}H-TCP (S.A.: 1702 GBq/mmol, CEA) at various concentrations in the presence

(non-specific binding) or absence (total binding) of 20 µl phencyclidine (PCP, final concentration 10^{-4} M). The incubation was stopped by filtration under vacuum over GF/B glass fiber filters (presoaked during 1 h in 0.05% polyethylene imine). The incubation tubes and the filters were washed three times by 3.5 ml of incubation buffer, and the radioactivity retained on the filters was determined by liquid scintillation counting at an efficiency of approximately 33%.

Modulation studies

The experiments were done as described above except that single concentrations (5 nM) of ^{3}H-TCP were used and that the assays were carried out in the presence of glutamate, or glycine, or glutamate + glycine in concentrations ranging from 1×10^{-8} M to 1×10^{-4} M.

When the effects of glutamate or glycine on the equilibrium constants of ^{3}H-TCP binding were determined, the assays were carried out as described in the 'saturation studies' section, except that all tubes contained varying concentrations of ^{3}H-TCP plus a single concentration (10^{-5} M) of either glutamate or glutamate + glycine.

Results

Behavioral experiments

As shown in Fig. 1a, the two competitive antagonists CPP and CGS 19755 inhibited the convulsions of the quaking mice in a dose dependent fashion, with ED50 values of 0.18 and 0.105 nmol/mouse, respectively. Both compounds also induced a marked ataxic side effect. In addition, at concentrations above 0.5 nmol/mouse, their protective action disappeared, and a convulsant effect could be observed (not shown).

The two non-competitive antagonists TCP and MK-801 (Fig. 1b) fully inhibited the convulsions of the quaking mice with ED50 values of 4.5 and 2.7 nmol/mouse, respectively. Both compounds were devoid of any noticeable side effect, and no reversal of the protection could be observed.

^{3}H-glutamate binding

The binding of ^{3}H-glutamate to P2 fractions was saturable, and specific binding represented 50–60% of total binding at concentrations close to the Kd (not shown). The equilibrium constants are presented on Table 1. As can be seen, no difference in the Kd and B_{max} values could be detected between the mutants and their controls.

In the two strains, the binding of ^{3}H-glutamate was displaced in a concentration dependent manner by CPP and CGS 19755 (data not shown). The potency and the

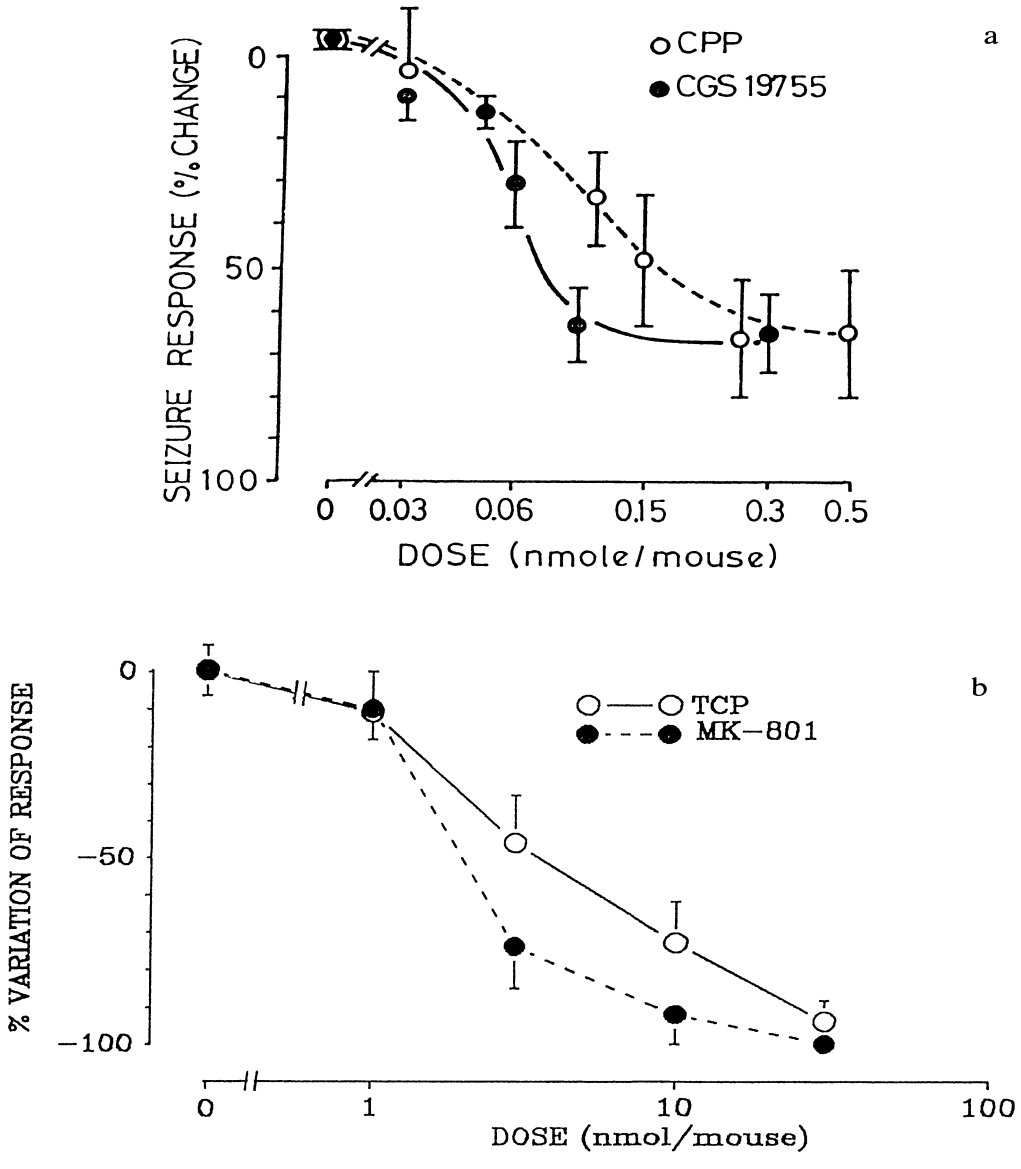

Fig. 1. Anticonvulsant effect of CPP and CGS 19755 (1a) and of TCP and MK-801 (1b) injected i.c.v in the quaking mutants. Twenty tactile stimulations were applied prior to the injection and 15 min after. Drugs were solubilized in a 0.1 M phosphate buffer and injected in a volume of 1 µl. Their effect was expressed as the percentage of variation of seizure response. Each values is the mean ± S.E.M. of the results of 3 to 6 independent experiments. The ED50's (expressed in nmol/mouse, and calculated from log probit transformations) were: CPP : 0.18; CGS 19755 : 0.105; TCP : 4.5 and MK-801 : 2.7.

Table 1. Binding of ^{3}H-glutamate and ^{3}H-TCP to cerebral membranes of control and quaking mice. Aliquots of thoroughly washed membranes of quaking (qk) or control (N) mice were incubated in duplicates in 50 mM Tris-Acetate buffer during 60 min (^{3}H-glutamate) or during 240 min in 5 mM Tris-HCl buffer containing 0.1 mM EDTA (^{3}H-TCP) in the presence of concentrations of labeled ligand ranging from 10 to 300 nM (^{3}H-glutamate) or from 5 nM to 100 nM (^{3}H-TCP). Non specific binding was determined in the presence of 1 mM unlabelled glutamate or 0.1 mM phencyclidine (^{3}H-TCP). Values are expressed as mean ± S.E.M. of (n) separate determinations

Ligand	Mice	n	Kd (nM)	B_{max} (pmol/mg prot.)
^{3}H-glutamate	N	6	151.5 ± 25.5	1.25 ± 0.15
	qk	6	150.3 ± 32.3	1.41 ± 0.32
^{3}H-TCP	N	6	54.3 ± 3.60	1.80 ± 0.18
	qk	5	70.8 ± 14.4	3.12 ± 0.47[a]

[a] $p<0.05$ (Student's t-test).

maximal efficacy of the two compounds were very similar in the quaking mice and their controls, reaching approximately 60% inhibition at 30 μM (data not shown).

^{3}H-TCP binding

The binding of ^{3}H-TCP was saturable and the specific binding represented approximately 70–80% of the total binding at concentrations close to the Kd (data not shown). No significant difference was observed between the quaking mice and their controls with regard to the Kd value (Table 1). However, the B_{max} value was markedly increased in the brain of the mutants.

Modulation of ^{3}H-TCP binding by glutamate and glycine

In both the quaking mice and their controls, the binding of ^{3}H-TCP was modulated by glutamate and glycine in a concentration dependent manner (Figs. 2 and 3). Glycine was only slightly effective. Glutamate increased the binding of 5 nM ^{3}H-TCP with a maximal effect reached at 10^{-5} M. At a higher concentration of glutamate (10^{-4} M), this facilitatory effect disappeared. When glutamate and glycine were added in combination, the facilitatory effect of glutamate was potentiated. At low concentrations (10^{-8} M), glycine or glutamate added alone did not modify the binding of ^{3}H-TCP, whereas they significantly increased it when they were added together.

When saturation studies were performed in the presence of glutamate (10^{-5} M) or glutamate + glycine (10^{-5} M), the binding of ^{3}H-TCP was differently affected in the mutant mice and their controls (Table 2). In the control mice, glutamate alone induced a significant increase of the B_{max}, which was not further modified by the addition of glycine. On the other hand, the affinity constant was not changed by glutamate alone, but was diminished significantly by glutamate and glycine in

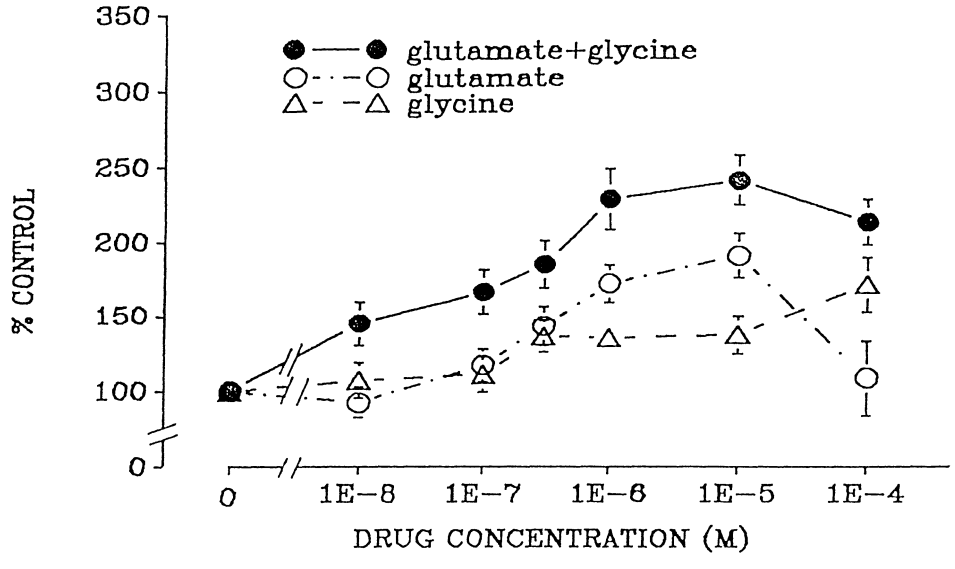

Fig. 2. Modulation of ^{3}H-TCP binding by either glutamate or glycine alone or glutamate + glycine in combination, on membrane preparations of control mice. Experiments were performed with one concentration of ^{3}H-TCP (5 nM) and various concentrations of drugs ranging from 10^{-8} M to 10^{-4} M. Values are the mean ± S.E.M. of 5 to 6 independent determinations.

combination. In the mutant mice, the facilitatory effect of glutamate and glycine on ^{3}H-TCP binding appeared to result solely from a Kd change. It should also be

Table 2. Equilibrium constants of ^{3}H-TCP binding on P2 membranes of control or quaking mice in the absence or presence of either 10^{-5} M glutamate alone or glutamate + glycine in combination. Assays are performed in duplicate as described in the text. Values are the mean ± SEM of (n) separate determinations

Mice	Drug added	n	Kd (nM)	B_{max} (pmol/mg prot.)
Controls				
	none	6	54.3 ± 3.6	1.80 ± 0.18
	Glutamate 10^{-5} M	5	44.7 ± 6.2	2.70 ± 0.23[a]
	glutamate 10^{-5} M + Glycine 10^{-5} M	5	30.2 ± 2.8[c]	2.76 ± 0.12[b]
Quaking				
	none	5	70.8 ± 14.4	3.12 ± 0.47
	Glutamate 10^{-5} M	5	31.5 ± 5.4[a]	3.75 ± 0.26
	Glutamate 10^{-5} M + Glycine 10^{-5} M	5	24.3 ± 2.7[a]	3.36 ± 0.20

[a] $p<0.05$; [b] $p<0.01$; [c] $p<0.001$ (Student's t-test).

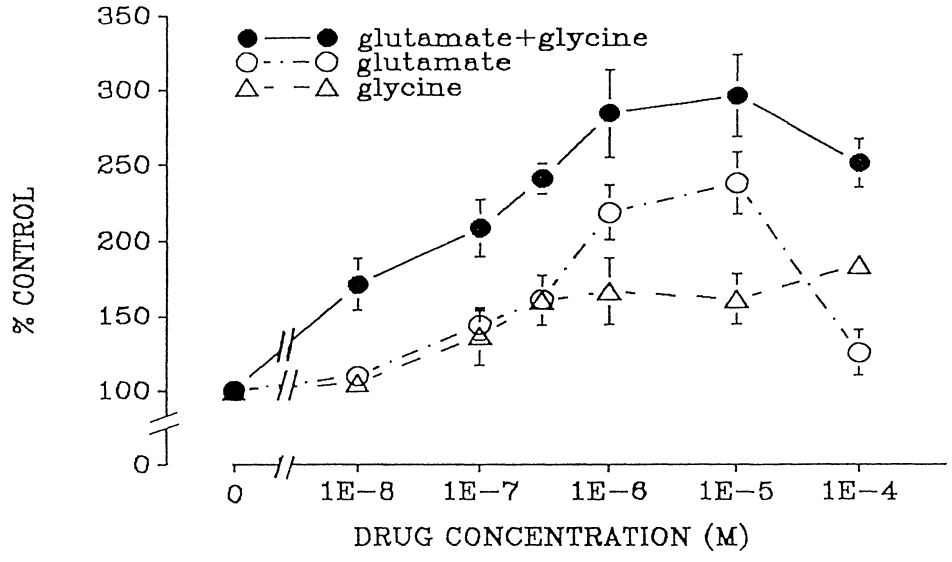

Fig. 3. Modulation of ^{3}H-TCP binding by either glutamate or glycine alone or glutamate + glycine in combination, on membrane preparations of quaking mice. Experiments were performed with one concentration of ^{3}H-TCP (5 nM) and various concentrations of drugs ranging from 10^{-8} M to 10^{-4} M. Values are the mean ± S.E.M. of 5 to 6 independent determinations.

mentioned that for any given experimental conditions, no difference could be detected between the mutants and their respective controls with regard to the affinity constant, while the density of binding sites remained always higher in the mutants.

Discussion

Our results of the anticonvulsant properties of NMDA receptor antagonists and of the increased binding of ^{3}H-TCP in the brain of the quaking mice strongly suggest that the inherited epilepsy of the quaking mice is associated with endogenous modifications of the NMDA receptor/ion channel complex.

The observation that the non-competitive antagonists TCP and MK-801 (which block the NMDA associated ionic channel [15,16] completely inhibit the seizures of the qk mice, whereas the competitive antagonists CPP and CGS 19755 (which act on the NMDA site [17–20] exert a partial anticonvulsant effect suggest that in this latter situation, a certain proportion of ionic channels remain active, even when NMDA sites are fully blocked. However, if such were the case, one would expect to observe two categories of ^{3}H-TCP binding sites in the presence of glutamate. As

a matter of fact, it has been shown [21–24] that the binding of PCP-like drugs to NMDA-associated ion channel sites is enhanced by glutamate, and that only one population of sites is found. We also obtained a single category of glutamate enhanced ^{3}H-TCP binding sites. Therefore, it is unlikely that a certain proportion of ion channels remain active when the NMDA sites are blocked. Other mechanisms than the blockade of NMDA receptors might be triggered by the competitive antagonists, and could account for their partial anticonvulsant effects.

The density of NMDA sites did not appear to be modified in the brain of the qk mice, as suggested by the results of ^{3}H-glutamate binding. This conclusion is supported by the similar potencies of 30 μM CPP or 30 μM CGS 19755 at displacing 60% of ^{3}H-glutamate binding in the mutants and their controls. It is noteworthy that the binding of ^{3}H-glutamate in human temporal cortex preparations is also inhibited at approximately 60% by 300 μM DL-APH, a competitive NMDA antagonist [25]. In contrast, the density of ionic channel sites was markedly increased in the mutants. As mentioned above, the existence of a single population of glutamate-sensitive ^{3}H-TCP binding sites suggests that all the ion channels are part of NMDA receptor complexes. This would imply that in the brain of the quaking mice, the activation of a given proportion of NMDA sites might trigger the activation of an abnormally high number of ionic channels. This conclusion is supported by the observation that glutamate (alone or in combination with glycine) exerts a slightly greater facilitation of ^{3}H-TCP binding in the mutants than in their controls. Another difference between the two strains lies in the enhancement of ^{3}H-TCP binding by glutamate. In the mutants, this facilitation results solely from a Kd change, in agreement with previously reported results [23]. On the contrary, in the controls, the facilitation results from both a Kd and a B_{max} change, suggesting that glutamate might unmask ion channel sites in the controls but not in the mutants.

Thus, the ratio of ion channel sites to NMDA sites appears to be higher in the brain of the qk mice than in the brain of their controls. The question remains as whether this abnormality concerns the whole population of NMDA receptor complexes. In this respect, it is noteworthy that in the rat hippocampus, the ratio ^{3}H-TCP/^{3}H-glutamate binding varies during ontogeny [26]. It would also be interesting to know whether this abnormality in the qk mice is evenly distributed throughout the brain or only in discrete regions. Recent studies revealing similar patterns of binding for ^{3}H-TCP and for ^{3}H-CPP in the rat brain [27] would favorise the former possibility.

In summary, our results show an increased density of NMDA associated ionic channel binding sites in the brain of the quaking mice. This abnormality is not accompanied by a concomitant change of NMDA binding sites. This alteration probably mediates the convulsions of the mutants, since the blockade of NMDA associated ionic channels fully inhibited the seizures, without any side effect. To our knowledge, this is the first report of a simultaneous investigation of the anticonvulsant properties of competitive and non-competitive NMDA antagonists in a model of inherited epilepsy. Furthermore, our results, which demonstrate the

correlation between anticonvulsant properties and endogenous perturbations of the NMDA/ion channel receptor complex, provides new information on the involvement of glutamatergic systems in epileptic dysfunctions.

Acknowledgements

This project was supported by dret grant no. 86/1502/DS/SR.

References

1. Sidman RL, Dickie MM and Appel SH (1964) Science 144: 309–311.
2. Billings-Gagliardi S, Adcock LH and Wolf MK (1980) Brain Res. 194: 325–338.
3. Bourre JM, Pollet S, Daudu O, Le Saux F and Baumann N (1977) Biochimie 59: 819–824.
4. Campagnoni AT (1988) J. Neurochem. 51: 1–14.
5. Maurin Y, Berger B, Le Saux F, Gay M and Baumann N (1985) Neurosci. Lett. 57: 313–318.
6. Chauvel P, Louvel J, Kurcewicz I and Debono M (1980) In: Baumann N (ed.) Neurological Mutations Affecting Myelination. Elsevier, Amsterdam, pp. 513–516.
7. Chermat R, Doaré L, Lachapelle F and Simon P (1981) Naunyn-Schmiedeberg's Arch. Pharmacol. 318: 94–99.
8. Chermat R, Lachapelle F, Baumann N and Simon P (1979) Life Sci. 25: 1471–1476.
9. Maurin Y, Arbilla S, Dedek J, Lee CR, Baumann N and Langer SZ (1982) Naunyn-Schmiedeberg's Arch. Pharmacol. 320: 26–33.
10. Maurin Y, Le Saux F, Graillot C and Baumann N (1985) Dev. Brain Res. 22: 229–235.
11. Maurin Y, Enz A, Le Saux F and Besson MJ (1986) Brain Res. 366: 379–384.
12. Caboche J, Mitrovic N, Le Saux F, Besson MJ, Sauter A and Maurin Y (1989) J. Neurochem. 52: 419–427.
13. Lowry OH, Rosebrough MJ, Farr AL and Randall RJ (1951) J. Biol. Chem. 193: 265–275.
14. Vindimian E, Robaut C and Fillion G (1983) J. Appl. Biochem. 5: 261–268.
15. Stirling JM, Cross AJ and Green AR (1989) Neuropharmacol. 28: 1–7.
16. Wong EH, Kemp JA, Priestley T, Knight A, Woodruff GN and Iversen LL (1986) Proc. Natl. Acad. Sci. 83: 7104–7108.
17. Olverman HJ, Monaghan DT, Cotman C and Watkins JC (1986) Eur. J. Pharmacol. 131: 161–162.
18. Lehmann J, Schneider J, McPherson S, Murphy DE, Bernard P, Tsai C, Bennett DA, Pastor G, Steel DJ, Boehm C, Cheney DL, Liebman JM, Williams M and Wood PL (1987) J. Pharmacol. Exp. Ther. 240: 737–746.
19. Lehmann J, Chapmann AG, Meldrum BS, Hutchison A, Tsai C and Wood PL (1988) Eur. J. Pharmacol. 154: 89–93.
20. Lehmann J, Hutchison AJ, McPherson SE, Mondatori C, Schmutz M, Sinton CM, Tsai C, Murphy DE, Steel DJ, Williams M, Cheney DL and Wood PL (1988) J. Pharmacol. Exp. Ther. 246: 65–75.
21. Bonhaus DW, Burge BC and McNamara JO (1987) Eur. J. Pharmacol. 142: 489–490.
22. Johnson KM, Sacaan AI and Snell LD (1988) Eur. J. Pharmacol. 152: 141–146.
23. Ransom RW and Stec NL (1988) J. Neurochem. 51: 830–836.
24. Reynolds IJ, Murphy SN and Miller RJ (1987) Proc. Natl. Acad. Sci. 84: 7744–7748.
25. Cowburn RF, Hardy JA and Roberts PJ (1988) J. Neurochem. 50: 1872–1878.
26. Tremblay E, Roisin MP, Represa A, Charriaut-Marlangue C, Flexor MA and Ben-Ari Y (1989) Difference entre L'Ontogenese des Sites NMDA et des Sites TCP dans L'Hippocampe de Rat. 3eme Colloque National des Neurosciences, p. 293.
27. Jarvis MF, Murphy DE and Williams M (1987) Eur. J. Pharmacol. 141: 149–152.

$GABA_A$-similar-receptor-subtypes mediate excitatory neurotransmission in the mammalian labyrinth: An experimental and clinical study

Klaus Ehrenberger[a] and Dominik Felix[b]

[a]First E.N.T.-Department, University of Vienna, Austria
[b]Division of Neurobiology, University of Berne, Switzerland

Abstract

The inhibitory action of GABA, mediated by the bicuculline-sensitive $GABA_A$- and the bicuculline-insensitive $GABA_B$-receptors in the central and peripheral nervous system is generally accepted. In contrast, the existence of an additional excitatory GABA-receptor in the labyrinth of warm blooded animals and in the corresponding structures in cold blooded animals is still controversial. Both the evident excitatory effects of GABA and the inhibitory effects of the GABA-antagonists bicuculline and picrotoxin on the vestibular postsynaptic afferent activity are discussed as having either a direct influence on the afferents, mediated by a postsynaptic GABA-receptor, or an indirect presynaptic effect mediated by the efferents. With the aid of microiontophoretic techniques, we have demonstrated that, in cats, GABA acts quantitatively as an amplifier whereas the presynaptic activity, mediated by the efferent vestibular system, acts qualitatively as a modulator of the vestibular postsynaptic afferent activity. The GABA action is antagonized by bicuculline and it is assumed that a postsynaptic bicuculline-sensitive GABA-receptor is involved. Picrotoxin, a GABA-antagonist correspondent to bicuculline, suppresses induced labyrinthine nystagmus in healthy subjects and pathological labyrinthine (peripheral) spontaneous nystagmus in patients. Similarities in the direction and time courses of the action of the GABA-antagonists in humans and in cats suggest that in humans an excitatory bicuculline- and picrotoxin-sensitive GABA-receptor mediates the afferent vestibular information. The possibility of influencing this $GABA_A$ similar-receptor-subtype by picrotoxin in humans is the basis of a successful therapy programme for labyrinthine nystagmus and vertigo, including motion sickness.

Introduction

As well as the known inhibitory bicuculline- and picrotoxin-sensitive $GABA_A$- and bicuculline- and picrotoxin-insensitive $GABA_B$-receptors in the peripheral and central nervous system (for a review, see Ref. [1]), we have been able to demonstrate the presence of a further, namely excitatory bicuculline- and picrotoxin-sensitive GABA-receptor in the cat labyrinth [2,3]. Subsequently, on the basis of the hypothesis that GABA acts as the excitatory neurotransmitter between the vestibular hair cells and their afferents, we commenced a series of clinical experiments aimed at finding out whether certain vestibular dysfunctions in humans could be influenced by modulating the peripheral excitatory GABA system by means of the GABA-antagonist picrotoxin [4]. In fact, protracted i.v. application of low doses of picrotoxin results in a suppression of spontaneous

labyrinthine (peripheral) nystagmus without CNS side effects. This objective suppression of the peripheral nystagmus coincides with a suppression of the patient's subjective feeling of vertigo. In contrary thereto, picrotoxin does not significantly influence a manifest spontaneous nystagmus of central origin.

We have discussed the possibility that the excitatory action of GABA in the labyrinth could be an indirect one [2,3]. In the last few years, the discussion about a postsynaptic excitatory GABA action in the labyrinth of warm blooded animals [5–8] and the corresponding structures of cold blooded animals [9–12] has become controversial. Influenced by these controversies there is increasing criticism as to the existence of an excitatory postsynaptic GABA-receptor [13].

Akoev and Andrianov [14] assumed that the apparent excitatory GABA actions are indirect presynaptic effects. This means that GABA and its antagonists must have an influence on the presynaptic efferent innervation which is only present in the large population of vestibular type II sensory cells [15].

The epithelial layer of the mammalian labyrinth consists of two different types of hair cells [15]. The spontaneous activity of the afferents of the type I hair cells is always irregular in pattern, whereas the population of the afferents of the type II cells integrates the postsynaptic spontaneous activity to a regular one [16–18]. The labyrinth receives an efferent innervation originating bilaterally in the brain stem [19,20]. Numerous efferent terminals contact each afferent chalice supplying a type I cell and contact each type II cell [15]. The former axo-dendritic innervation has been designated postsynaptic, the latter axo-somatic innervation, presynaptic [20]. There is evidence that acetylcholine acts as the efferent vestibular neurotransmitter [21]. Studies on the functional role of the efferent system demonstrated both a weak inhibitory effect [22] and an excitatory effect combined with a modulation [19,23] on the spontaneous afferent discharge.

If the GABA, bicuculline and picrotoxin effects which we have found are, in fact, indirect presynaptic ones, they would have to be comparable to the direct efferent effects on the afferent activity. The first part of this paper deals with a study on the regular spontaneous activity of the type II hair cells and the effects that GABA, bicuculline and the efferents have on this spontaneous activity.

In the second part, a comparison of the results of the animal experiments and the clinical picrotoxin experiments is made. The aim is to describe, in more detail, the location of the effect in humans, despite the experimental black box conditions.

Experimental procedures and Results

Comparison between the effects of GABA, bicuculline and the efferents on the regular afferent spontaneous activity by means of interspike-interval histograms (IIH)

The study was carried out on 11 adult cats. The regular spontaneous discharges of 39 identified afferent units of the type II hair-cells were biochemically tested using microiontophoretic techniques. Full details of anesthesia, preparation of the animals,

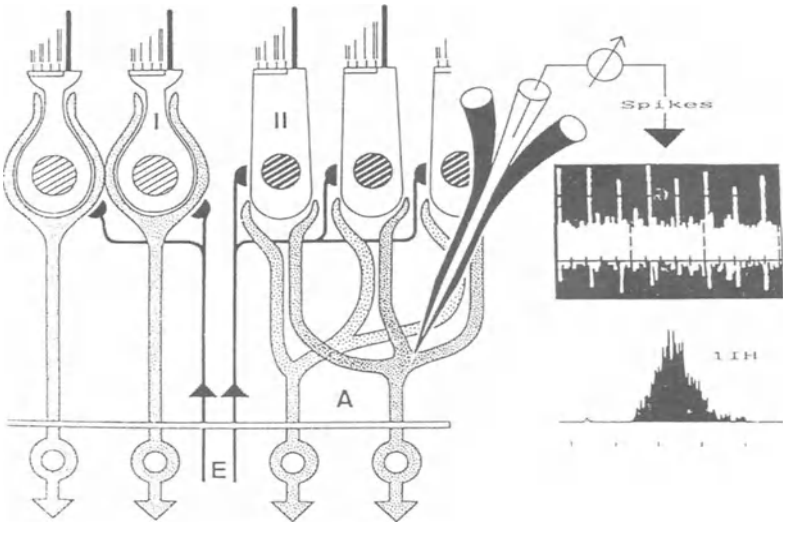

Fig. 1. Schematic diagram showing the recording site. A: afferent integrating neuron of the type II hair cells (II). Original oscilloscope tracing demonstrates the regular pattern of the spike train. Consequently, interspike interval-histogram (IIH: Computer PDP 11) forms a 'quasi-Gaussian' distribution. E: efferent postsynaptic axo-dendritic innervation of type I hair cells (I), and efferent presynaptic axo-somatic innervation of type II hair cells (II).

preparation of the electrodes and testing solutions, recording and analysis of the spike trains by interspike interval-histograms and rate-histograms have been described elsewhere [2,18]. After preparation of the middle ear, opening of the oval window to reach the sacculus or opening of the wall of the lateral semicircular canal, a multibarrel microelectrode with a tip diameter of about 5 μm is inserted into the subsynaptic region of the type II cells. The regular spontaneous discharges of the type II integrating neurons recorded with the 4M NaCl filled centre barrel are characterized by a 'quasi-Gaussian' distribution of the interspike intervals in the histogram (Fig. 1).

The action of GABA and bicuculline

The outer channels of the multibarrel micropipette contain the test compounds GABA and the GABA-antagonist bicuculline to be ejected microiontophoretically with the appropriate currents. Both substances diffuse in the synaptic cleft and the perisynaptic space.

The application of GABA (Fluka, 0.5 M, current 50 nA for 30 sec.) causes the firing rate to rise. In contrast, a similar ejection of bicuculline (bicuculline hydrochloride, Labatec, 5 mM in 165 mM NaCl, current 50 nA for 50 sec.) results in a decrease in the firing rate. In both test situations the regularity of the discharge patterns remains unchanged. As shown in Fig. 2A, GABA shifts the Gaussian distribution to the left, indicating the increase in the firing rate, bicuculline shifts the data of the histogram to the right, corresponding to the decrease of the discharge.

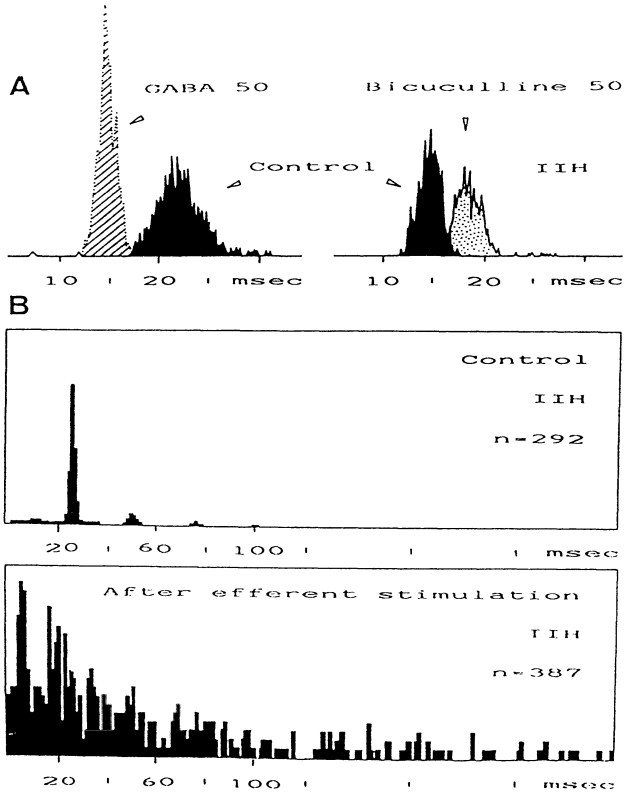

Fig. 2. Qualitative effects of GABA, bicuculline and efferents on afferent spontaneous activity in cats.

A) IIHs, showing the effect of 50 nA GABA and 50 nA bicuculline on regular discharge patterns of two different units. GABA shifts the data to the left (= increase of activity), bicuculline to the right (= decrease of activity). The Gaussian distribution (regularity) remains unchanged.

B) Efferent modulatory effect: transition of the Gaussian distribution in IIH of the regular discharge pattern (control) into an asymmetric distribution indicating a stochastic process (after efferent stimulation). Note different time scales in A and B.

Influence of efferent activity

The efferents of the lateral labyrinth ampulla may be stimulated physiologically by caloric utriculopedal stimulation of the corresponding contralateral structure [24,25]. Under these test conditions (water irrigation of the contralateral ear) the stimulation of the efferents not only causes a moderate change in the spontaneous spike rate, but the regular spontaneous activity becomes irregular as well. The Gaussian distribution gives way to a unimodal, asymmetric distribution indicating the transition into a stochastic discharge pattern (Fig. 2B).

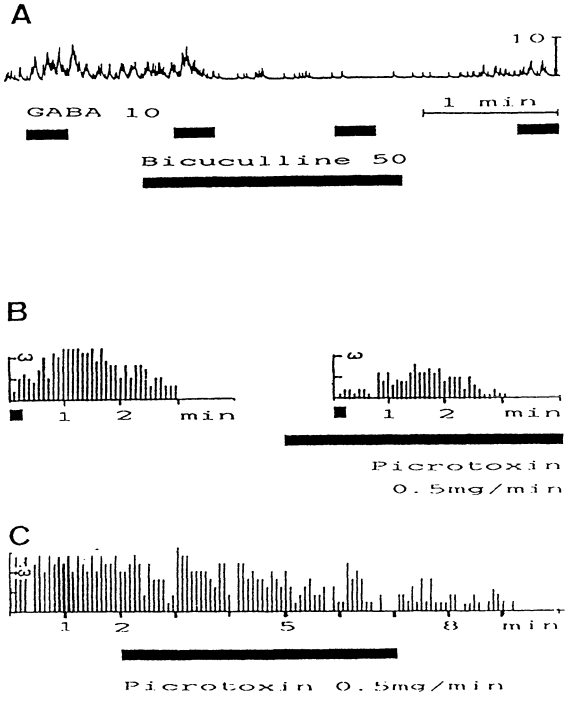

Fig. 3. Quantitative effects of GABA-antagonists on induced labyrinthine activity in cats and in humans: Effects of GABA-antagonists in experimental and pathological induced activity, demonstrated by rate-histograms (integrated firing frequency: for example A: Nuclear Enterprises 4667, Bell & Howel 5-137. For examples B and C: Computer Hewlett-Packard 2100 A).

A) Perisynaptic applied 50 nA bicuculline for 2 min blocks the GABA induced postsynaptic spontaneous activity of a unit in the cat labyrinth.

B) Rate-histograms of the angle-velocity of the slow component of the nystagmus during the period of caloric induced nystagmus in a healthy subject. Stimulation (black square): warm water irrigation of the outer ear: 44°C, 20 ccm for 20 sec. Picrotoxin (2.5 mg i.v., infusion rate 0.5 mg/min.) suppresses the excitability of the labyrinth (right) in contrary to the test control 30 min. before (left).

C) Rate-histogram in case of a pathological labyrinthine nystagmus (unilateral acute loss of labyrinthine function). Picrotoxin (2.5 mg i.v., infusion rate 0.5 mg/min.), within several minutes, suppresses the pathological nystagmus. Note the corresponding time courses of the GABA-antagonistic effect on the single fiber activity in cats and on the nystagmus in humans.

Comparison of cat and human rate-histograms of the time course of the GABA antagonistic effect on the induced afferent vestibular activity

Cats

As shown in Fig. 3A, repeated simultaneous iontophoretic application of GABA (10 nA for 30 sec.) and bicuculline (50 nA for a period of 2 min) lead to a blockage

of the GABA induced afferent activity with a continuous exponential decrease of the spike rate to zero for a duration of several minutes.

Humans

The experiments were carried out in 5 healthy subjects and 45 patients. An imbalance in the activity of the left and right labyrinth leads to a spontaneous labyrinthine peripheral nystagmus. In the healthy subjects, the nystagmus was set off by a unilateral caloric labyrinthine stimulation by warm water irrigation via the outer ear (44°C, 20 ccm for 20 sec.).

In the patients, unilateral pathophysiological conditions of the labyrinths were the cause of the nystagmus. Figure 3B shows examples of the time course of the angle-velocity of the slow nystagmus component in rate-histograms of healthy subjects during the period of caloric stimulated nystagmus with and without simultaneous application of picrotoxin (Serva, 1 mg% in 0.9 NaCl; infusion rate: 0.5 mg/min for 5 min). The caloric excitability of the labyrinth is clearly suppressed under the influence of the GABA-antagonist picrotoxin.

In patients, a picrotoxin dosage between 1–5 mg at an infusion rate of 0.5–0.75 mg/min results, within minutes, in a distinct reduction or total suppression of the spontaneous peripheral nystagmus (Fig. 3C). The blocking effect depends both on the degree of the nystagmus and the total amount of the infused picrotoxin.

Note the similarity of the exponential decrease of the firing rate in the three rate histograms of the Figs. 3B and 3C.

Discussion

Perisynaptically applied GABA and bicuculline only have a quantitative and not a qualitative influence on the regular spontaneous postsynaptic activity of the vestibular type II cell afferents in cats. GABA increases and bicuculline decreases and even completely blocks the spike rate, but both substances do not change the regularity of the discharge pattern. In contrast, a presynaptic efferent stimulation has a dramatic qualitative effect on the spontaneous postsynaptic activity, transforming the regular discharge pattern into an irregular stochastic process. The synaptic GABA action amplifies, but the presynaptic efferent activity modifies the tested parameter, corresponding to the previously assumed functions of the efferent vestibular system [19]. This modulating efferent effect is mediated by acetylcholine [21].

Although it is known that there is an acetylcholine-$GABA_A$-receptor interaction at the adrenomedullary chromaffin cells in the periphery [26], it is not possible to transfer this model to the labyrinth because acetylcholine and GABA have independent, qualitatively different effects on the vestibular sensory system. Therefore, it is not possible for the excitatory GABA effect in the labyrinth to be indirect and presynaptic in nature [14].

Bicuculline completely antagonizes the amplifying effect of GABA. In a dose dependent way, the time course of the bicuculline action is characterized by a continuous exponential decrease of the spike rate to zero. On the other hand, efferent stimulation never leads to a total blockage of the afferent labyrinthine activity [19,22,23,27].

Picrotoxin, like bicuculline, acts as a $GABA_A$-receptor blocker [1]. Applied systemically, picrotoxin is able to suppress caloric induced nystagmus in healthy subjects. The time course of picrotoxin's effect corresponds to the time course of the effect of bicuculline on the GABA induced postsynaptic afferent activity in cats. The caloric nystagmus is due to a unilateral vestibular hair cell excitation which leads to the release of the transmitter at the afferent synapses [20]. A comparison of the described bicuculline effects in cats with those of picrotoxin in humans supports the hypothesis that GABA also functions as the excitatory neurotransmitter of the human labyrinth.

Pathological spontaneous peripheral nystagmus originates in the imbalance of excitation between the right and the left labyrinths. A reduction in the unilateral, predominant afferent excitation through picrotoxin results in the disappearance of the nystagmus and its related subjective vertigo. The time course of the suppression of the pathological, labyrinthine nystagmus corresponds to the time course of the suppression of the caloric induced nystagmus. This picrotoxin effect also supports the view that there is a picrotoxin-sensitive excitatory GABA-receptor in the human labyrinth.

In summary, the above findings confirm the hypothesis of a postsynaptic excitatory GABA-receptor in the labyrinth of mammals. This excitatory receptor is sensitive to bicuculline and picrotoxin and therefore has certain similarities to the inhibitory $GABA_A$-receptor. Whether the sometimes inhibitory, sometimes excitatory effects of these GABA-receptors can be explained by a change in the polarity of the Cl-conductance, like Usami *et al.* [8] suggest, or whether there are different ions acting on the labyrinthine postsynaptic membranes will have to be clarified by means of further intracellular studies. The sensitivity to picrotoxin is the reason why the GABA-receptors can be influenced so well clinically. Peripheral labyrinthine vertigo, including motion sickness can therefore be treated causally and successfully with the $GABA_A$-receptor antagonist picrotoxin [4].

Acknowledgement

We should especially like to thank Elfriede Brauneis for preparing the manuscript.

References

1. Bormann J (1988) T.I.N.S. 11: 112–116
2. Felix D and Ehrenberger K (1982) Acta Otolaryngol. 93: 101–105.

3. Felix D and Ehrenberger K (1985) In: Drescher DG (ed.) Auditory Biochemistry. Thomas, Springfield, USA, pp. 68–79.
4. Ehrenberger K, Benkoe E and Felix D (1982) Acta Otolaryngol. 93: 269–273.
5. Meza G, Carabez A and Ruiz M (1982) Brain Research 241: 151–161.
6. Meza G and Hinojosa R (1987) Hearing Research 28: 73–85.
7. Usami S, Igarashi M and Thompson GC (1987a) Hearing Research 30: 19–22.
8. Usami S, Igarashi M and Thompson GC (1987b) Brain Research 417: 367–370.
9. Flock A and Lam DM (1974) Nature 249: 142–144.
10. Annoni JM, Cochran SL and Precht W (1984) J. Neurosci. 4: 2106–2116.
11. Guth SL and Norris CH (1984) Exp. Brain Res. 56: 72–78.
12. Vega R, Soto E, Budelli R and Gonzalez-Estrada MT (1987) Hearing Research 29: 163–167.
13. Klinke R (1986) Hearing Research 22: 235–243.
14. Akoev GN and Andrianov GN (1989) In: Ottoson D (ed.) Progress in Sensory Physiology 9. Springer-Verlag, Berlin, Heidelberg, New York, London, Paris, Tokyo, pp. 53–95.
15. Engström H and Engström B (1981) In: Gualtierotti T (ed.) The Vestibular System: Function and Morphology. Springer-Verlag, New York, Heidelberg, Berlin, pp. 3–37.
16. Goldberg JM and Fernandez C (1971) J. Neurophysiol. 34: 635–660.
17. Walsh BT, Miller JB, Gacek RR and Kiang NY-S (1972) Int. J. Neurosci. 3: 221–235.
18. Ehrenberger K, Felix D and Wyss U (1979) Acta Otolaryngol. 87: 472–476.
19. Goldberg JM and Fernandez C (1980) J. Neurophysiol. 43: 986–1025.
20. Flock A (1971) In: Lowenstein WR (ed.) Handbook of Sensory Physiology I., Principles of Receptor Physiology. Springer-Verlag, Berlin, pp. 396–441.
21. Schwarz DWF, Schwarz IE and Hu K (1989) J. Otolaryngol. 18: 28–31.
22. Linas R and Precht W (1969) Exp. Brain Res. 9: 16–21.
23. Highstein SM and Backer R (1985) J. Neurophysiol. 54: 370–384.
24. Sala I. (1965) Acta Otolaryngol. Supp. 197: 1–34.
25. Precht W. (1974) In: Kornhuber HH (ed.) Handbook of Sensory Physiology VI/1. Springer-Verlag, Berlin, Heidelberg, New York, pp. 221–236.
26. Bormann J and Clapham DE (1985) Proc. Natl. Acad. Sci. USA 82: 2168–2172.
27. Keller EL (1976) Exp. Brain Res. 24: 459–471.

Address for correspondence: Klaus Ehrenberger, First E.N.T.-Department, University of Vienna, Lazarettgasse 14, A-1090 Vienna, Austria.

GABA uptake inhibitors: Possible use as anti-epileptic drugs

A. Schousboe[a], P. Krogsgaard-Larsen[b], O.M. Larsson[c], S.F. Gonsalves[d], R.E. Harbaugh[d] and J.D. Wood[e]

[a]PharmaBiotec Res. Center, Dept. of Biochem. A, Panum Inst., University of Copenhagen, DK-2200 Copenhagen N, Denmark

[b]Departments of Organic Chemistry and [c]Biology, Royal Danish School of Pharmacy, DK-2100 Copenhagen Ø, Denmark

[d]Departments of Surgery and Pharmacology, Dartmouth-Hitchcock Med. Center, Hanover, NH 03756, U.S.A.

[e]Department of Biochemistry, University of Saskatchewan, Saskatoon, Saskatchewan S7N OWO, Canada

Abstract

Using cultures of neurons and astrocytes and a variety of structurally restricted analogues of GABA the substrate specificity of the neuronal and glial high affinity GABA carriers has been investigated. A number of GABA analogues which preferentially inhibit astroglial GABA uptake have been identified and subsequently tested for anticonvulsant activity in different models of chemoconvulsions in rats. It has been demonstrated that the two GABA analogues 4,5,6,7-tetrahydroisoxazolo[4,5-*c*]pyridin-3-ol (THPO) and 5,6,7,8-tetrahydro-4H-isoxazolo[4,5-*c*]azepin-3-ol (THAO) act as anticonvulsant agents and the possibility that compounds of this nature may be potentially interesting as new anti-epileptic drugs is discussed.

Introduction

Inhibitory neurotransmission processes in the central nervous system are to a very large extent mediated by the amino acid gamma-aminobutyrate (GABA) which has a largely hyperpolarizing action on neurons [1]. Inactivation of GABA is brought about by high affinity transport either into presynaptic GABAergic nerve endings or astroglial cells surrounding the synapse [2,3]. Since the fate of GABA is dependent upon the cellular location of the uptake it is important for proper function of GABAergic synapses that uptake of GABA into these different, cellular compartments is well controlled [4]. GABA which is taken up into the nerve endings may be re-utilized as a neurotransmitter [5] whereas that taken up into astrocytes is metabolized and no longer available for neurotransmission purposes [6]. Based on investigations of uptake rates for GABA into neurons and astrocytes it has been estimated [7] that approximately 20% of synaptically released GABA will be taken up into surrounding astrocytes. Based on these assumptions there has been substantial interest in a detailed characterization of the uptake sites for GABA in neurons and astrocytes [8]. This review will give an account of some of these studies and evidence will be presented that compounds which selectively block astroglial GABA uptake may act as anticonvulsant agents.

Table 1. Inhibition of neuronal and glial GABA uptake by GABA analogues of restricted conformation.

GABA analogue	IC_{50} (μM)		Ki (μM)	
	Neuron[a]	Glia[c]	Neuron[b]	Glia[c]
(*R*)-nipecotic acid	70	30	11	15
Guvacine	100	25	31	28
N-methyl-nipecotic acid	300	70	74	94
Cis-4-OH-nipecotic acid	200	10	53	148[d]
SKF-89976 A (DPB-Nip.)	—	—	1	2
SKF-100330 A (DPB-Guv.)	—	—	5	4
THPO	>5000	300	—	550
THAO	>5000	500	—	600
N-DPB-THPO	—	—	38	26
N-DPB-THAO	—	—	9	3

[a] Neuronal uptake of GABA into mini-prisms of cerebral cortex
[b] Cultured neurons from cerebral cortex
[c] Cultured astrocytes
[d] indicates a non-competitive inhibition. In all other cases competitive inhibition was observed.
Results are from Schousboe *et al.* [11,12], Larsson *et al.* [13,14] or from unpublished work of E. Falch, O.M. Larsson, P. Krogsgaard-Larsen and A. Schousboe.

Characterization of neuronal and glial GABA uptake

In a series of papers [8–14] the structure activity relationship of a number of GABA analogues with regard to inhibition of neuronal and glial GABA uptake has been reported. Some of the results of these studies are summarized in Table 1. It is evident that a large number of GABA analogues derived from the lead structure of nipecotic acid [15] are potent inhibitors of both uptake systems although few, if any, of this class of compounds exhibit selectivity with regard to inhibition of the two uptake systems. It should, however, be noted that the derivative 4-OH-nipecotic acid was found to inhibit neuronal GABA uptake in a competitive fashion whereas glial GABA uptake was inhibited non-competitively [13]. In spite of this, 4-OH-nipecotic acid was found to be transported into astrocytes with GABA inhibiting the uptake in a mixed competitive/non-competitive manner.

Of a series of bicyclic isoxazoles two compounds, 4,5,6,7-tetrahydro-isoxazolo-[4,5-*c*]pyridin-3-ol (THPO) and 5,6,7,8-tetrahydro-4H-isoxazolo[4,5-*c*]azepin-3-ol (THAO) were found to preferentially inhibit astroglial GABA uptake [12]. THPO which has been shown to act as a competitive inhibitor of astroglial GABA uptake [12] surprisingly is not transported into astrocytes by a carrier mediated mechanism as shown by the finding (Table 2) that the tissue/medium ratio of ^{3}H-THPO in astrocytes after incubation with the compound is independent of the external concentration of THPO. The tissue/medium ratio obtained is compatible with an equal distribution of THPO intra- and extracellularly since the ratio equals the intracellular water space which is about 4 $\mu l \times mg^{-1}$ [16].

Table 2. Distribution ratios (intra/extracellularly) for THPO in astrocytes incubated in different concentrations of ^{3}H-THPO

Concentrations of THPO (μM)	Distribution ratio (μl × mg^{-1})
5	5.9 ± 0.8
50	3.7 ± 0.8
500	5.4 ± 0.4
1000	4.9 ± 0.5

Astrocytes were incubated for 5 min in media containing ^{3}H-THPO in the concentrations indicated. The radioactivity in the cells after the incubation was expressed relative to that of the medium. Values are averages ± S.E.M. of 5 experiments. Unpublished experiments of O.M. Larsson and A. Schousboe.

In an attempt to improve the ability of some of these GABA analogues to penetrate the blood-brain-barrier a series of 4,4-diphenyl-3-butenyl (DPB) derivatives of nipecotic acid [17] and THPO [9] has been synthesized. As seen from Table 1, these DPB derivatives are generally more potent than the respective parent amino acids as inhibitors of high affinity GABA uptake but they do not exhibit significant selectivity with regard to inhibition of the uptake systems in neurons and astrocytes respectively. Due to the fact that the DPB-derivative of nipecotic acid acts as a competitive inhibitor of neuronal and glial GABA uptake it was expected that DPB-nipecotic acid would be transported by the carrier. Using ^{3}H-labelled DPB-nipecotic acid it was, however, shown [14] that DPB-nipecotic acid is not transported by the carrier but enters the cells very efficiently by diffusion through the plasma membrane, a process that appears to be facilitated by the relatively high degree of lipophilicity of this compound.

Anticonvulsant activity of THPO

Using ^{3}H-THPO it has been shown that THPO penetrates the blood-brain-barrier in mice only poorly, whereas in chicks this penetration is much better [18]. In accordance with this finding it has not been possible to show any pharmacological action of THPO in mice after intramuscular injection [18,19], whereas in chicks THPO protects against light induced convulsions [19] as well as isonicotinic acid hydrazide (INH) induced convulsions [18]. If, on the other hand, THPO is given to rats intracerebroventricularly (i.c.v.) it has been found to protect against both INH and pentylenetetrazol (PTZ) induced seizures [20–23]. As seen from Table 3, 4-OH-nipecotic acid also protected against PTZ seizures, but only at very high doses. The GABA receptor agonist [24] muscimol was the only other GABA analogue which was found to protect the animals against these two types of seizures. The neuronal GABA uptake inhibitor [25] 2,4-diaminobutyric acid (DABA) also was found to protect against PTZ seizures but it had no effect against

Table 3. Effects of GABA mimetics on INH-induced generalized motor seizures and PTZ-induced seizures.

Treatment	Dose (μg, i.c.v.)	INH seizure latency	Maximal PTZ seizures	
			% protected	% survived
CSF	—	36.2 ± 2.5	5	20
THPO	100	48.7 ± 6.0[a]	0	33
	300	46.8 ± 3.5[a]	88[a]	100[a]
Cis-4-OH-nipecotic acid	30	31.6 ± 5.7	17	33
	300	33.2 ± 4.5	33[a]	50
DABA	1500	35.4 ± 3.7	92[b]	92[b]
Muscimol	0.1	40.1 ± 2.5	29[a]	71[b]
	1.0	104.0 ± 9.1	43[b]	86[b]

Drugs or mock CSF vehicle were infused i.c.v. 30 min prior to INH (822 mg/kg, i.v.) or i.v. bolus injection of PTZ (25 mg/kg). The latency (min ± S.E.) to convulsion is indicated for the number of animals tested. Significance of differences for INH seizures compared with CSF-treated group (control values pooled from 3 independent groups) is indicated by letters ([a]$P<0.05$, [b]$P<0.001$). Percentages (PTZ seizures) reflect protection against tonic forelimb extension and death. Control groups were pooled for statistical analysis. Letters in this group indicate significance of differences compared with CSF control by chi-square statistic ([a]$P<0.05$, [b]$P<0.01$). From Gonsalves *et al.* [23].

INH induced seizures. It should, however, be stressed that DABA, as previously reported by Meldrum *et al.* [21], showed proconvulsant activity (Table 4). Of the four different GABA analogues acting on respectively GABA receptors (muscimol), neuronal GABA uptake (DABA), glial GABA uptake (THPO) or on both uptake systems (4-OH-nipecotic acid), THPO was found to be the most promising anticonvulsant compound (Table 4). In this context it may be of interest that also the other bicyclic isoxazole acting as a glial GABA uptake inhibitor, THAO, has been found recently to protect rats against INH and PTZ induced seizures after i.c.v. injection [26]. Moreover, comparing toxic side effects of THPO and THAO

Table 4. Semiquantitative summary of antiseizure effects of GABA mimetics

Treatment	Seizure model		Proconvulsant activity
	Max PTZ	INH	
THPO	++++	+	No
Cis-4-OH-nipecotic acid	0	0	No
DABA	++++	0	Yes
Muscimol	0	++++	Yes

The antiseizure effects detailed in Table 3 are summarized. For maximal PTZ seizures, only compounds protecting at least 50% of animals against the tonic extensor component were considered anticonvulsant. Degree of anticonvulsant activity is indicated as follows: + = >25% increase over CSF control; ++ = >25%, ≤50% increase; +++ = >50%, ≤100% increase; ++++ = >100% increase. Proconvulsant activity was recorded as present or absent. From Gonsalves *et al.* [23].

Table 5. Effect of THPO and glycine on synaptosomal levels of glutamate and GABA

	Amino acid content (nmol × mg^{-1})		
Treatment	Glu	GABA	Glu + GABA
Control	40.3 ± 0.7	20.7 ± 0.6	61.0 ± 1.2
THPO	36.9 ± 1.4	22.6 ± 0.3	59.6 ± 1.6
Glycine	39.6 ± 0.8	23.2 ± 0.7[a]	62.8 ± 1.4
THPO + glycine	34.1 ± 0.9[b]	25.5 ± 0.6[b]	59.6 ± 1.4

Values are means ± S.E.M. for 4–6 animals either non-treated (controls) or injected intramuscularly with 2.0 mmol/kg of THPO and/or 10 mmol/kg of glycine 60 min, respectively 45 min before decapitation and subsequent preparation of synaptosomes, Wood *et al.* [28]. Asterisks indicate statistically significant differences from the control ([a]$P<0.05$; [b]$P<0.001$). From Wood *et al.* [28].

in the rats, it was quite clear that THAO was less toxic than its lower ring homologue, THPO [26].

Effects of glycine

It has been observed that simultaneous administration of glycine and THPO to mice enhances the anticonvulsant activity of THPO [27]. In an attempt to explain this synergistic action of glycine which clearly does not reflect facilitation of uptake of THPO into the brain [27], Wood *et al.* [28] investigated the effect of glycine and THPO on amino acid levels in nerve endings isolated from rats which had received THPO intramuscularly alone or in combination with glycine. It was found that THPO plus glycine elevated synaptosomal GABA levels more than either THPO or glycine alone compared to control values (Table 5). Moreover, it

Table 6. Effect of THPO and glycine on GABA-transaminase activity in brain homogenates

Addition (mM)	GABA-T activity (nmol × min^{-1} × mg^{-1})	Inhibition (%)
Control	81.7 ± 1.0	—
THPO (0.1)	80.2 ± 1.5	2.1 ± 0.6
THPO (0.5)	77.8 ± 1.0	5.9 ± 0.2
Glycine (0.5)	81.2 ± 0.6	0.4 ± 1.5
Glycine (2.5)	79.2 ± 1.4	2.9 ± 0.8
THPO (0.1) + Glycine (0.5)	80.7 ± 0.7	0.3 ± 0.9
THPO (0.5) + Glycine (0.5)	76.3 ± 0.7	6.8 ± 0.6
THPO (0.5) + Glycine (2.5)	76.8 ± 0.6	6.4 ± 0.5

GABA-T activities were determined in the absence and presence of drugs as described by Wood *et al.* [31]. Values are means ± S.E.M. of 5–8 experiments.
Unpublished results of J.D. Wood, P. Krogsgaard-Larsen and A. Schousboe.

was found that glycine in combination with THPO decreased glutamate levels correspondingly so that the sum of glutamate and GABA remained unaltered compared to control animals [28]. Since glycine only marginally interfered with GABA uptake into synaptosomes it was suggested that possibly the activity of the GABA degradating enzyme, GABA-transaminase might be affected by THPO or glycine. As shown in Table 6, THPO alone inhibited GABA-T from whole brain only marginally, and this inhibitory effect could not be enhanced by glycine, which on itself was without effect. The possibility still exists that the activity of the GABA synthesizing enzyme glutamate decarboxylase may be affected by THPO and glycine. Such an action would be compatible with the recent report that a correlation seems to exist between the activity of glutamate decarboxylase and the synaptosomal GABA content [29]. This latter possibility remains, however, to be demonstrated. Another explanation of this peculiar action of glycine may be an action of glycine on either GABA or glycine receptors. Such a mechanism of action may be supported by the demonstration that glycine in a synergistic fashion facilitates the anticonvulsant action of GABA receptor agonists [30].

Conclusions

It has been convincingly demonstrated that astrocytes actively participate in the processes which are responsible for maintenance of a synaptic level of GABA at which GABAergic neurotransmission is optimized. Any imbalance between neuronal and glial high affinity GABA transport is likely to disturb the inhibitory tonus of the central nervous system, a condition which may lead to seizure activity. Due to the suggestion that the GABA carriers in neurons and astrocytes exhibit differences with regard to the active conformation of the GABA molecule with respect to the carrier, it has been possible to design GABA analogues which preferentially inhibit astroglial GABA uptake. Such compounds have proved to be able to protect experimental animals against seizure activity induced chemically or by other stimuli. It appears that the compounds THPO and THAO may have two important characteristics in common: 1) They are reasonably selective for the glial GABA carrier so that neuronal reuptake and reutilization of GABA is not prevented; and 2) they are relatively weak inhibitors, which will allow the inactivating mechanisms to function partially. Recent studies of the effects of some of the very potent blockers of GABA transport have indicated that drugs with this profile have undesired side effects (C. Bræstrup, personal communication). It can be concluded from the present study that weak, selective inhibitors of astroglial GABA uptake are of potential interest as anti-epileptic drugs. Therefore, research related to this should be given high priority in the search for new anti-epileptic agents.

References

1. Curtis DR and Johnston GAR (1974) Ergb. Physiol. 69: 97–188.
2. Schousboe A (1981) Int. Rev. Neurobiol. 22: 1–45.
3. Schousboe A (1982) In: Pfeiffer SE, (ed.) Neuroscience Approached through Cell Culture. CRC Press, Boca Raton, Florida. Vol. 1, pp. 107–141.
4. Schousboe A (1979) GABA-Biochemistry and CNS Functions, In: Mandel P and DeFeudis FV (eds.) Adv. Exp. Med. Biol. Plenum Press, New York, Vol. 123, pp. 219–237.
5. Gram L, Larsson OM, Johnsen AH and Schousboe A (1988) Epilepsy Res. 2: 87–95.
6. Schousboe A, Larsson OM, Drejer J, Krogsgaard-Larsen P and Hertz L (1983) In: Hertz L, Kvamme E, McGeer EG and Schousboe A (eds.) Glutamine, Glutamate and GABA in the Central Nervous System. Alan R. Liss, Inc. New York pp. 297–315.
7. Hertz L and Schousboe A (1987) In: Vernadakis A, Privat A, Lauder JM, Timiras PS and Giacobini E (eds.) Model Systems of Development and Aging of the Nervous System. M. Nijhoff Publ. Comp., Boston, pp. 19–31.
8. Krogsgaard-Larsen P (1980) Mol. Cell. Biochem. 31: 105–121.
9. Krogsgaard-Larsen P, Falch E, Larsson OM and Schousboe A (1987) Epilepsy Res. 1: 77–93.
10. Schousboe A, Krogsgaard-Larsen P, Svenneby G and Hertz L (1978) Brain Res. 153: 623–626.
11. Schousboe A, Thorbek P, Hertz L and Krogsgaard-Larsen P (1979) J. Neurochem. 33: 181–189.
12. Schousboe A, Larsson OM, Hertz L and Krogsgaard-Larsen, P (1981) Drug Develop. Res. 1: 115–127.
13. Larsson OM, Krogsgaard-Larsen P and Schousboe A (1985) Neurochem. Int. 7: 853–860.
14. Larsson OM, Falch E, Krogsgaard-Larsen P and Schousboe A. (1988) J. Neurochem. 50: 818–823.
15. Krogsgaard-Larsen P and Johnston GAR (1975) J. Neurochem. 25: 797–802.
16. Pasantes-Morales H and Schousboe A (1988) J. Neurosci. Res. 20: 505–509.
17. Yunger LM, Fowler PJ, Zarevics P and Setler PE (1984) J. Pharmacol. Exp. Ther. 228: 109–115.
18. Schousboe A, Hjeds H, Krogsgaard-Larsen P and Wood JD (1986) J. Neurochem. 47: 758–763.
19. Wood JD, Johnson DD, Krogsgaard-Larsen P and Schousboe A (1983) Neuropharmacology 22: 139–142.
20. Krogsgaard-Larsen P, Labouta IM, Meldrum B, Croucher M and Schousboe A (1981) In: Morselli PL, Lloyd KG, Löscher W, Meldrum B and Reynolds EH (eds.) Neurotransmitters, Seizures and Epilepsy pp. 23–33, Raven Press, New York.
21. Meldrum BS, Croucher MJ and Krogsgaard-Larsen P (1982) In: Okada, Y and Roberts E (eds.) Problems in GABA Research from Brain to Bacteria. Excerpta Medica, Amsterdam, pp. 182–191.
22. Croucher MJ, Meldrum BS and Krogsgaard-Larsen P (1983) Europ. J. Pharmacol. 89: 217–228.
23. Gonsalves SF, Twitchell B, Harbaugh RE, Krogsgaard-Larsen P and Schousboe A (1989) Epilepsy Res. 4: 34–41.
24. Krogsgaard-Larsen P, Johnston GAR (1978) J. Neurochem. 30: 1377–1382.
25. Iversen LL and Kelly JS (1975) Biochem. Pharmacol. 24: 933–938.
26. Gonsalves SF, Twitchell B, Harbaugh RE, Krogsgaard-Larsen P and Schousboe A (1989) Eur. J. Pharmacol. 168: 265–268.
27. Seiler N, Sarhan S, Krogsgaard-Larsen P, Hjeds H and Schousboe A (1985) Gen. Pharmacol. 16: 509–511.
28. Wood JD, Krogsgaard-Larsen P and Schousboe A (1988) Neurochem. Res. 13: 917–921.
29. Lidén E, Karlsson L and Sellstrom A (1987) Neurochem. Res. 12: 489–493.
30. Seiler N and Sarhan S (1984) Gen. Pharmacol. 15: 367–369.
31. Wood JD, Russell MP, Kurylo E and Newstead JD (1979) J. Neurochem. 33: 61–68.

Address for correspondence: Dr. A. Schousboe, PharmaBiotec Res. Center, The Neurobiology Unit, Dept. of Biochemistry A, Panum Inst., Univ. of Copenhagen, DK-2200 Copenhagen N, Denmark.

Enzymatic depletion of rat blood tryptophan *in vivo* and its consequences – rapid depletion of brain serotonin and perturbation of sleep/waking patterns

Katsuji Takai, Eiko Nakamaru, Akira Kanda, Yoshiki Kamiyama, Takaaki Kawashima and Hidefumi Yoshii

Department of Biochemistry and Nutrition, School of Health Sciences, Faculty of Medicine, The University of Tokyo, Tokyo 113, Japan

Abstract

Rapid and extensive depletion of a brain neurotransmitter, serotonin (5-HT), has been achieved *in vivo* with rats by intraperitoneal administration of tryptophan side chain oxidase I (TSO I) from *Pseudomonas* (for TSO; Kanda A *et al.* and Nakamaru E *et al.*, these proceedings).

TSO I entered the circulation, degraded tryptophan specifically, and, at maximum doses, decreased its level to 1% of the control within 1 h. As brain tryptophan, a 5-HT precursor, declined following the change in blood, the brain 5-HT started to decrease, and more than 90% was depleted at around 5 h. In the whole brain level, no decrease of catecholamines was observed and the change in amino acid pattern was, if any, modest. Under the conditions above, the 5-HT depletion was maintained for up to 20–30 h and then returned to normal as TSO activity disappeared from the circulation. Time course, extent, and duration of depletion were TSO-dose dependent.

On these bases, we started the analyses of the metabolic and physiological responses towards this perturbation. The assessments of local turnovers and contents of 5-HT, catecholamines, and their metabolites by *in vivo* microdialysis and microdissection, respectively, indicated that the rates of decreases in 5-HT turnover were comparable in most of brain regions so far tested, except striatum, and the local 5-HT content virtually paralleled the local 5-HT turnover, which reportedly reflects the 5-HT neuron activity *in situ*. Local responses of catecholamine systems were observed but variable depending on the regions.

When brain activities upon 5-HT depletion were monitored by cortical brain wave, circadian rhythm of sleep/waking states was lost, and, unlike *p*-chlorophenylalanine(PCPA)-induced insomnia, a hitherto undescribed pattern, the alternations of a slow spindle wave and a fast desynchronized wave at 1–2 min intervals, predominated. We tentatively suggest that this pattern is a prototype of sleep/waking cycle manifested by the brain free from regulation of 5-HT.

Introduction

Brain serotonin (5-HT) neurons appear to be a unique 'open system' that plays a 'mass control' of higher order brain functions. In fact, 5-HT neurons originate almost exclusively in the brain stem, ramify repeatedly, distribute densely throughout the brain (Fig. 1), and end up at the termini with few synaptic contacts, containing, in some of them, other neurotransmitters [1–3]. A high molecular degeneracy is now clear for 5-HT receptors, mutually distinguishable by the second messenger and ion channel systems to which they couple, and regional distributions in the

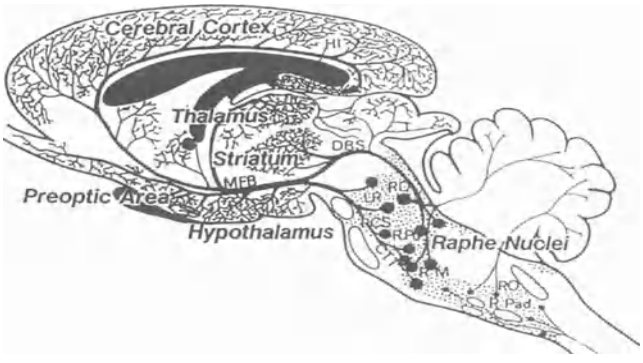

Fig. 1. Projection of 5-HT neurons in rat brain ([3] modified).

brain [4,5]. Such structural and functional premises for brain 5-HT issues *per se* may suggest that the brain 5-HT system is likely prescribed as a modulator of intrinsic functions of each brain region and, consequently, higher order functions of the whole brain; 5-HT and its congeners have been assessed to induce or modulate the core of animal behaviour, a highly coordinated set of responses [6]. Dynamic aspects of this widespread system as a whole are thus of central importance. Classical electrophysiology demonstrated a state-dependent and drug-sensitive autofiring of 5-HT cell bodies (raphe nuclei) [7], but its relationship with activities of the termini is still ambiguous.

In this context, the search for the metabolic perturbation of brain 5-HT system is crucial to assess the functional roles of 5-HT in the brain. To this end, *p*-chlorophenylalanine(PCPA), a tryptophan hydroxylase inhibitor arresting 5-HT synthesis, has been applied *in vivo* and has provided most of the biochemical bases for brain 5-HT issues, but one disadvantage is that PCPA was not specific [8].

In the present study, as a new perturbant, we applied *in vivo* to rats a crystalline preparation of an enzyme termed tryptophan side chain oxidase I (TSO I) (Fig. 2) [9–11] which acts on tryptophan, a 5-HT precursor, by the reaction below, and, *via* a rapid enzymatic depletion of blood tryptophan, 90% of brain 5-HT was depleted after several hours [12]. Detailed accounts of this approach are described followed by regional metabolic changes and physiological responses concurrent with the

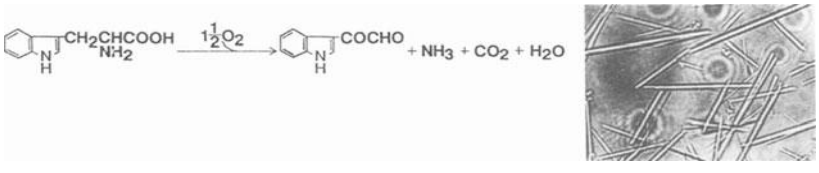

Fig. 2. TSO-catalyzed degradation of tryptophan (upper), and photomicrograph of crystalline TSO I from *Pseudomonas* (right).

brain 5-HT depletion, as assessed by *in vivo* microdialysis and microdissection, and the recording of cortical brain waves, respectively.

Experimental procedures

TSO I was purified from *Pseudomonas* essentially as described [11] with modifications to permit a rapid and g-order purification [13]. Male Sprague Dawley rats weighing 250–300 g (S.L.C., Japan) were kept in a chamber maintained at 24°C and humidity of 55% under a lighting schedule of LD 12:12 (0800–2000). They were deprived of food but not water overnight before and during the experiments. Blood samples were withdrawn from the tail vein with heparinized capillaries. The assay of TSO activity was performed for plasma as described [11]. Upon tryptophan determination [14] after TSO I injection, tips of capillaries were immersed before sampling in an aliquot of 1 M KCN (a TSO inhibitor) to avoid tryptophan depletion *in vitro*. The whole brain was dissected after decapitation and extracted by homogenization with a Polytron homogenizer in perchloric acid (PCA) containing EDTA and $Na_2S_2O_5$ [15] at −5°C, or else, the frozen brain was subjected to microdissection of nuclei and brain regions as described [16], followed by extraction in the same cocktail as above. Amino acid analysis was performed as described [17]. 5-HT, catecholamines, and their precursors and metabolites were analyzed by ion-pair reversed phase HPLC coupled with electrochemical detector (ECD) [15].

In vivo microdialysis was performed for free moving rats essentially as described [18,19] with probes (1–3 mm) stereotaxically installed according to the coordinates described [20]; brain Ringer solution was perfused at a rate of 1–3 μl/min, and the dialysates were injected on line to an HPLC system (Eicom, Kyoto) at 20-min intervals. Sleep/waking phases of rats were analyzed by polygraphic recordings of electroencephalogram of cerebral cortex (ECoG), electromyogram (EMG), and electroopthamogram (EOG), essentially as described [21].

Results and Discussion

After intraperitoneal administration of TSO I (20 units), the enzyme entered the circulation and exhibited activity *in situ*. Blood tryptophan decreased to 1–2% of the normal after 1 h, remained at 0.5–1% level for the ensuing 20–30 h, and then returned to normal as TSO activity disappeared with a half life of 0.5 day from the blood stream (Fig. 3A). Rate, extent, and duration of the tryptophan depletion were well correlated with the dose of TSO I (1–20 units). Analysis of the blood free amino acids showed that the depletion was specific for tryptophan.

Tryptophan in the whole brain responded sensitively to the changes in blood tryptophan (Fig. 3B). It fell to about 10% of the control after 1–2 h, remained at this level for the ensuing 20–25 h, and then returned to normal after 48 h as blood tryptophan was recovered, suggesting that the turnover of tryptophan in the brain

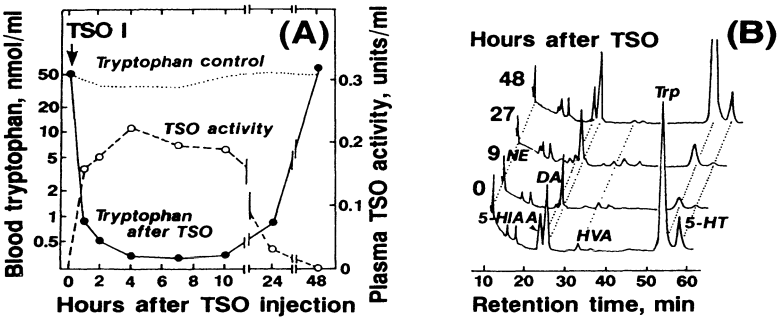

Fig. 3. (A) Time courses of plasma TSO activity and blood tryptophan concentrations after intraperitoneal injections of TSO I (20 units) or saline (control). (B) Ion-pair HPLC/ECD chromatograms of the whole brain extracts obtained before (0 h) and 9, 27, and 48 h after injection of TSO I (20 units). NE, norepinephrine; DA, dopamine; HVA, homovanillic acid; 5-HIAA, 5-hydroxyindoleacetic acid; Trp, tryptophan. (amplitude, arbitrary).

was very active and almost in an equilibrium with blood tryptophan. The pattern of other amino acids including amino acid transmitters, was essentially maintained in the whole brain level. 5-HT in the whole brain began to decrease within 1 h, reached the minimum level (10% of the control) at around 5 h, and maintained this level for 24 h followed by recovery after 48 h as brain tryptophan returned to normal. 5-HIAA, a main 5-HT metabolite, followed 5-HT (Fig. 3B). These results demonstrated unequivocally the very rapid turnover of brain 5-HT and the almost absolute dependence on its precursor, tryptophan, in the circulation. Despite such an extensive perturbation of brain 5-HT, catecholamines and their metabolites remained unaffected (Fig. 3B), raising an issue of the metabolic independence of catecholamine from 5-HT in the whole brain level.

Thus, the depletion of brain 5-HT induced by enzymatic depletion of its precursor *in vivo*, was shown to be rapid, specific, extensive, and readily reversible.

On these bases, we started the analyses of the regional metabolic changes and physiological responses concurrent with this perturbation. Upon *in vivo* microdialysis of brain regions, the amounts of dialyzable 5-HIAA, which represented the local 5-HT turnover and reportedly related to the activity of 5-HT neurons *in situ* [19], responded sensitively to the perturbation (Fig. 4). In the region including *raphe dorsalis* (cell bodies of 5-HT neurons), 5-HT turnover started to decrease almost without lag time and rapidly ($t_{1/2}$ = 1.5–2 h) declined to 5–10% of the control after 5 h. In the cingulate cortex, after 1 h or more of lag time, 5-HT turnover decreased with $t_{1/2}$ of 2–3 h. In striatum, after 2 h of silent period, 5-HT turnover abruptly ($t_{1/2}$ = 20 min) fell to almost nil, under the conditions. Decrease in regional 5-HT contents assessed by microdissection paralleled those of turnovers, irrespective of specific contents of 5-HT (or density of 5-HT neurons) ranging up to 2 orders of magnitude (Fig. 4), suggesting that the individual 5-HT neuron might exhibit essentially similar response to the precursor depletion in this study. These and additional results so far indicated that the rates of decrease in

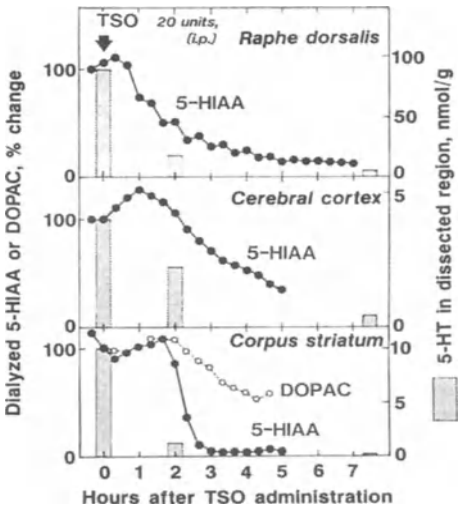

Fig. 4. In vivo microdialysis and microdissection of 3 brain regions after TSO I injection. (DOPAC, dihydroxyphenylacetic acid).

5-HT turnover were in a range of $t_{1/2}$ of 1.5–3 h in most of brain regions, values close to those of 5-HT and 5-HIAA ($t_{1/2}$ = 2 h) in the whole brain, except in striatum. Evaluation of distinction in lag time and $t_{1/2}$ values, and a unique response of striatum, remained to be clarified. Since $t_{1/2}$ obtained under arrest of 5-HT synthesis may likely be related to rates of turnover of each region in steady state, the issue of "synchronization" or "*in situ* regulation" of brain 5-HT turnover were invoked. We are, tentatively, in favor of synchronization prescribed by neuronal 5-HT contents with modulation by local mechanisms. Despite a modest response of catecholamine metabolism in the whole brain, regional turnover of DA, as assessed by dialyzable DOPAC and HVA, clearly decreased in striatum (Fig. 4), where its transient strictly synchronized with that of 5-HT, suggesting a tight interplay of these two systems. Other types of responses, mirror image or no effect, were also shown elsewhere.

The achievement of the brain 5-HT depletion in this study prompted us to apply this to crucial but unsolved issues of 5-HT and sleep. Classical hypothesis for 5-HT as a sleep-inducing substance, has been extensively modulated [22]. However, a concept that brain 5-HT depletion induces insomnia, based on PCPA-experiments, appears to survive as yet.

In the present study, 2–3 h after administration of TSO I (20 units), rats lost vigilance. Analyses of polygraphic recordings demonstrated that the pattern of daytime sleep (Fig. 5A, left) collapsed at around 3 h after TSO I injection (Fig. 5A, right), the timing of the onset of decreases in brain 5-HT contents and turnovers (Fig. 2A and 2B). Thereafter, as the perturbation of 5-HT system reached the maximum extent, the alternations of a synchronized slow wave and desynchro-

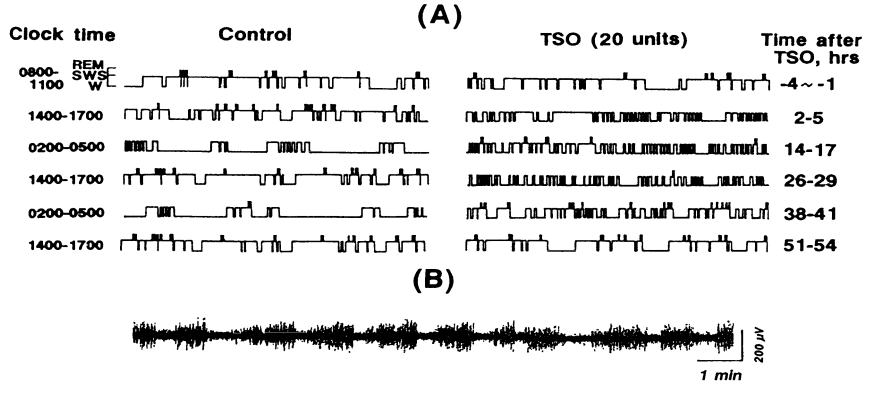

Fig. 5. (A) Partial somnograms after administrations of TSO I (20 units) (right) and saline (control, left). Injections were performed at 1200. Partial somnograms are presented for 3 h each in daytime (1400–1700) and the corresponding nocturnal period (0200–0500) up to 51–54 h after TSO I injection. (B) ECoG predominated 5–30 h after TSO injection. Time lapse, left to right.

nized fast wave at 1–2 min intervals, but not insomnia, predominated (Fig. 5A *right,* 14–29 after TSO injection; Fig. 5B, an expanded ECoG recording). The slow and fast waves were almost indistinguishable from the normal sleep spindles (7–8 Hz) and the fast wave in normal waking state, respectively. In each cycle, incidence of sleep spindles and their amplitude gradually increased in about 1 min, and, within a few msec, they collapsed to fast waves, strictly in time with a weak but clear monoclonic muscle twitch. Light sonic stimuli also collapsed the slow to fast waves and the response showed habituation, indicating that the rats were not comatose but retained the integrities of sensory system and its central processing. This pattern prevailed for ensuing 30 h, the period of extensive perturbation of 5-HT system. During the course of experiments, circadian rhythm was clearly lost, the REM sleep disappeared in daytime but, unlike the case with PCPA, reappeared at night, and the total time of sleep showed no marked change on daily basis (Fig. 5A), suggesting the individual mechanisms of sleep phases were not impaired. On the foregoing bases, we tentatively suggest that the new pattern (Fig. 5B) is a prototype of sleep/waking cycle manifested by the brain free from regulation by 5-HT. It is tempting to speculate that 5-HT may modulate the time cues responsible for switching of sleep and consciousness.

In this study, we achieved a rapid, extensive, specific, and reversible depletion of brain 5-HT, by taking advantage of the mechanism inherent to the brain, rather than impairment of enzyme or receptor. It is clear that this perturbation provides the means to clarify the crucial issues of synchronization and local regulation of 5-HT system, and interplays with other neurons. It may also be useful for assignments of 5-HT neurons and 5-HT receptors, their dynamics, and for those of coexistence with other transmitters, and even the rate of axonal flow may be taken into consideration. Reexamination of "5-HT and sleep issues" is the best target for

the study of 'mass control' of brain functions; among a number of approaches, the searches for a one-minute clock in the depth of brain, biochemical bases for maintaining the 'short sleep/waking cycle', and other types of biorhythms affected by this perturbation, may be crucial for the next step.

References

1. Steinbusch HWM (1981) Neuroscience 6: 557–618.
2. Beaundet A and Descarries L (1987) In: Steinbusch HWM (ed.) Monoaminergic Neurons; Light Microscopy and Ultrastructure. John Wiley, New York, pp. 265–313.
3. Baumgarten HG and Schlossberger HG (1984) In: Schlossberger HG, Kochen W, Linzen B and Steinhart H (eds.) Tryptophan and Serotonin Res. de Gruyter, Berlin, pp. 173–188.
4. Hartig PR (1989) Trends Pharmacol. Sci. 10: 64–69.
5. Osborne NN and Hamon M (eds.) (1988) Neuronal Serotonin. John Wiley, New York.
6. Soubrie P (1988) in ref. [5], pp. 255–270.
7. Fornal CA and Jacob BL (1988) in ref. [5], pp. 305–346
8. Koe BK and Weissman A (1966) Pharmacol. Exp. Ther. 154: 499–516.
9. Takai K, Ushiro H, Noda Y, Narumiya S, Tokuyama T and Hayaishi O (1977) J. Biol. Chem. 252: 2648–2656.
10. Takai K (1980) Dev. Biochem. 16: 103–115.
11. Takai K and Hayaishi O (1987) Methods Enzymol. 142: 195–217.
12. Takai K, Yasui H, Yoshii H and Sasai Y (1986) In: Bender DA, Joseph MH, Kochen W and Steinhart H (eds.) Prog. Trp. Serotonin Res. 1986. de Gruyter, Berlin, pp. 75–77.
13. Kanda A, Nakamaru E and Takai K, unpublished results.
14. Inoue S, Tokuyama T and Takai K (1983) Anal. Biochem. 132: 468–486.
15. Wagner J, Vitali P, Palfreyman MG, Zraika M and Huot S (1982) J. Neurochem. 38: 1241–1254.
16. Parkovitz M and Brownstein MJ (1988) Maps and Guide to Microdissection of the Rat Brain. Elsevier, New York.
17. Bohlen P (1983) Methods Enzymol. 91: 26–36.
18. Ungelstedt U (1984) In: Mardsen CA, (ed.) Measurement of Neurotransmitter Release *In Vivo*. John Wiley, New York, pp. 81–105.
19. Knott PJ (1988) in ref. [5], pp. 93–127.
20. Paxinos G and Watson C (1986) The Rat Brain in Stereotaxic Coordinates. Academic Press, New York.
21. Timo-Iaria C, Negrao N, Schmidek WR, Hoshino K, Lobato de Menzes CE and Leme da Rocha T (1970) Physiology and Behavior 5: 1057–1062.
22. Koella WP (1988) in ref. [5], pp. 153–170.

Relationships between plasma tryptophan and brain tryptophan, and consequences on CNS serotonin metabolism in the exercising rat

Francis Chaouloff

Laboratoire de Pharmacologie, INSERM U7, CHU Necker E.M., 75015 Paris, France

Abstract

The present paper will review the consequences of physical exertion (treadmill running) on CNS serotonin (5-hydroxytryptamine, 5-HT) synthesis and metabolism in the rat with regard to the relationships between plasma and brain tryptophan (TRP), i.e. 5-HT precursor. Trained rats were run for 1 h or 2 h and compared to trained rats that were left to rest during identical periods of time. The results indicate that exercise increases the portion of plasma TRP that is unbound to albumin (free TRP) without affecting that of plasma total (free plus albumin-bound) TRP. Exercise-induced lipolysis was found to be the determinant of the rise in plasma-free TRP inasmuch as free fatty acids displace TRP from its binding to albumin. These changes were associated with minor or no changes in the plasma levels of the amino acids that compete with TRP for entry into the brain. Moreover, the intrinsic kinetics of the transport system that allows TRP (and other neutral amino acids) to enter into the brain were found to be unaffected by exercise. These peripheral modifications were associated with a marked rise in brain TRP which, in turn, led to an increase in 5-HT metabolism. However, the rise in brain 5-HT synthesis and metabolism was found to be associated with a partial inhibition of tryptophan hydroxylase activity, thus rendering a key role for the increase in precursor availability. Indeed, pharmacological experiments led with an inhibitor of 5-HT synthesis revealed a region-dependent alteration in tryptophan hydroxylase activity. Inasmuch as CNS 5-HT is involved in mood regulation, it is important to appreciate the extent to which the above related exercise-induced changes in 5-HT metabolism are involved in the purported psychological benefit of physical exertion.

Introduction

It is now more than twenty five years since Eccleston *et al.* [1] reported that the administration of tryptophan (TRP), the precursor amino acid of serotonin (5-hydroxytryptamine, 5-HT), increases 5-HT synthesis. Indeed, nowadays it is well established that the rate limiting enzyme in the 5-HT pathway, namely tryptophan hydroxylase, is unsaturated with respect to its substrate TRP [2,3]. Such a property is of importance inasmuch as the rate of 5-HT synthesis (and in some circumstances that of 5-HT release) will be governed by changes in precursor availability within the serotonergic neuron. Thus, starvation [4] carbohydrate ingestion or insulin administration [5], and immobilization stress [6] both trigger increases in CNS TRP that are associated with significant rises in the rate of 5-HT synthesis. On the other hand, pharmacological and physiological situations that are known to

diminish the central level of TRP, e.g. valine administration [7] or streptozotocin-induced diabetes [8] slow down 5-HT synthesis. The above mentioned results emphasize the tight relationship between CNS TRP level and 5-HT synthesis; however, inasmuch as cerebral proteolysis is of weak importance and TRP is one of the so-called 'essential' amino acids, it is obvious that CNS TRP level (and 5-HT synthesis) will depend on the influx of TRP from the blood compartment.

The extraneuronal regulation of 5-HT synthesis

The amino acid TRP is unique since it is able to bind to the albumin molecule [9]. Then, the measurement of plasma (total) TRP includes the sum of a free portion (10%) and a protein-bound portion (90%). The equilibrium that pre-exists between the free and the bound forms of TRP is affected by lipolysis; thus, free fatty acids (FFA) are able to displace TRP from its binding to albumin [10]. As an example, fasting-induced lipolysis will promote an increase in plasma-free TRP and a decrease in plasma-bound TRP [4].

The absolute concentrations of plasma-free TRP and bound TRP depend on various factors among which the activity of the catecholaminergic systems [11] and the activity of hepatic tryptophan pyrrolase [12]. Thus, this latter enzyme is involved in the kynurenine pathway which allows the transformation of TRP into kynurenines and NAD(H). Inhibition or induction of tryptophan pyrrolase will respectively increase or decrease plasma TRP levels (and then brain TRP).

The entry of TRP into the brain compartment requires a stereospecific and saturable transporter [13] that is localized at the blood-brain barrier level. Indeed, TRP is not the sole amino acid to enter the brain by this means inasmuch as other neutral amino acids (such as valine, leucine, tyrosine...) share with TRP the latter transporter [7]. Consequently, such a common pathway will lead to a regulation of brain TRP level (and 5-HT synthesis) by these neutral amino acids. This is underlined in the case of macronutrients that are respectively characterized by high carbohydrate and high protein contents; thus, carbohydrate feeding triggers insulin release, that in turn lowers the blood level of the amino acids that compete with TRP for entry into the brain [5]. On the other hand, protein rich diets increase the blood level of the neutral amino acids, the lowest increase being that of TRP, so that the level of brain TRP will be decreased [7]. Lastly, it must be added that amino acid transport into the brain may be altered during situations that affect the transporter intrinsic kinetics and/or blood-brain barrier ultrastructure. Immobilization stress is such a situation since the brain influx of each of the neutral amino acids is increased in a manner that cannot be theoretically explained in terms of competition [14].

For a number of years, scientists have debated whether changes in plasma-free TRP or changes in plasma total TRP are responsible for the associated changes in brain TRP. Nowadays, it rather appears that, depending on the paradigm, either one or the other controls brain TRP level and then 5-HT synthesis. For instance, the

increase in plasma-free TRP is responsible for the rise in brain TRP that is measured in food-deprived animals [4] whereas, during immobilization stress, changes in plasma total TRP (and in the kinetics of transport into the brain) are actually those influencing the central level of TRP.

Plasma TRP and brain TRP during exercise

Rats were trained to run for 4–5 sessions before the final experiment. At that time, rats were divided into running (1 h or 2 h) and resting rats so that training did not have any influence on the biochemical parameters which were measured thereafter. Both plasma TRP levels, brain TRP, 5-HT and 5-hydroxyindoleacetic acid (5-HIAA, the metabolite of 5-HT) levels were estimated by HPLC-EC-UV [15].

Running was found to promote a marked time-dependent increase in the levels of plasma FFA and plasma-free TRP whilst plasma total TRP level remained unaffected [16]. The former changes were associated with marked increases in brain [16] and cerebrospinal fluid (CSF; 17) TRP levels. These results highlighted the possibility that exercise is a model in which changes in plasma-free TRP govern brain TRP levels. To confirm the latter hypothesis, rats were made to run for 2 h and plasma and brain levels of the neutral amino acids measured thereafter (in collaboration with the Department of Neurology of Pr. Curzon, MRC, London, U.K.). This study revealed that none of the amino acids that compete with TRP for entry into the brain were truly affected by exercise; in addition, with the exception of TRP and, to a lesser extent, threonine, the central level of the neutral amino acids remained constant [18]. The above mentioned results indicate that (i) exercise-induced lipolysis is responsible, by means of changes in plasma-free TRP, for the rise in brain TRP, (ii) exercise does not affect the intrinsic properties of the transporter that allows TRP (and other neutral amino acids) entry into the brain.

In another series of experiments, an attempt was made to study the short-term influence (1 h after the onset of running) of exercise on hepatic tryptophan pyrrolase activity. For that purpose, running rats were pretreated with the noradrenaline uptake inhibitor desipramine which inhibits the activity of tryptophan pyrrolase [19]. Indeed, such a treatment at the onset of running triggered important rises in both plasma-free TRP and plasma total TRP of the runners only [16]. These results suggest that exercise may, within a short delay, activate tryptophan pyrrolase activity, so that blockade of TRP transformation into kynurenine is able to increase the circulating levels of TRP.

Lastly, it is noteworthy that desipramine increased the transport of TRP into the brains of the runners, thus indicating that a high circulating level of catecholamines (e.g. running plus desipramine) facilitates TRP transport into the brain [16].

Consequences on central serotonergic metabolism

As mentioned above, running was found to increase CNS TRP levels. Logically, this rise in CNS TRP was found to be associated with significant increases in brain 5-HIAA [16], as well as in CSF 5-HIAA [17] levels. This variation indicates that brain TRP and serotonergic metabolism are increased during running. However, the comparison between the increases in brain (and CSF) TRP and the resulting changes in brain (and CSF) 5-HIAA levels show a discrepancy inasmuch as the latter increases were weaker than those predictable from the changes in precursor availability. In order to study the possibility that 5-HT synthesis and metabolism were respectively decreased and increased in the runners, rats were subjected to treatments known to increase brain TRP, 5-HT synthesis and metabolism (e.g. TRP loads or food deprivation). Analyses of the relationships between TRP levels and the sum of 5-HT plus 5-HIAA levels strongly suggested that 5-HT synthesis (i.e. TRP utilization toward 5-HT synthesis) was partially inhibited during running [20]. Taken together, these results suggest that running increases brain TRP at levels that would theoretically markedly increase 5-HIAA level, an index of 5-HT synthesis and metabolism. However, inasmuch as TRP transformation into 5-HT is partially inhibited during such a situation, the increase in 5-HIAA level is much lower than that predicted. Thus, if the increase in TRP is not sufficient to counteract and overpass such an inhibition of 5-HT synthesis and if exercise increases 5-HT metabolism, a decrease in 5-HT levels may be observed. Such a situation has been encountered following long-term training; thus, in rats trained for 8 weeks, an acute bout of exercise increased brain TRP and 5-HIAA levels only slightly whilst it significantly lowered that of 5-HT [21]. This result indicates that exercise partially inhibits 5-HT synthesis whilst it increases 5-HT utilization into 5-HIAA, and that depending on the magnitude of the effect of exercise on precursor availability, 5-HT level either remains unaltered or decreases. In summary, the increase in precursor availability would serve to prevent any depletion in neuronal 5-HT levels during running. This emphasizes the need to measure the effects of exercise on 5-HT release into the synapse; hence, it could be that the increased utilization of 5-HT into 5-HIAA is associated with an increased release of the amine. Interestingly, we have recently measured the regional consequences of a treatment that inhibits the transformation of 5-hydroxytryptophan (5-HTP, the product of tryptophan hydroxylase action) into 5-HT in short-term trained runner rats. We actually found that the running-induced increase in TRP was associated with an increased accumulation of 5-HTP in the midbrain (where serotonergic cell bodies are present), but not in the striatum nor in the hippocampus (where 5-HT terminals are numerous) [22]. This phenomenon could involve a feedback loop, i.e. end-product inhibition which is known to happen at the terminals but not at the level of the cell bodies [23,24].

Physical exercise and brain 5-HT: future trends

The above mentioned exercise-induced biochemical changes may be of interest if one is able to link the former to functional events. Indeed, the fact that central serotonergic activity is involved in various functions such as food intake or mood behaviors whilst on the other hand the latter are affected by exercise may be of future interest. As an example, we compared the anorectic potency of dextrofenfluramine, a 5-HT uptake inhibitor [25] in resting and running rats and found that dextrofenfluramine-induced hypophagia was much more pronounced in the runners [26]. This could indicate that 5-HT release is increased during running. Such an example illustrates the future possibilities of investigation in that field.

References

1. Eccleston D, Ashcroft GW and Crawford TBB (1965) J. Neurochem. 12: 493–503.
2. Friedman PA, Kappelman AH and Kaufman S (1972) J. Biol. Chem. 247: 4165–4173.
3. Hamon M, Bourgoin S, Artaud F and El-Mestikawy S (1981) J. Physiol. Paris 77: 269–279.
4. Knott PJ and Curzon G (1972) Nature 239: 452–453.
5. Fernstrom JD and Wurtman RJ (1972) Metabolism 21: 337–342.
6. Kennett GA and Joseph MH (1981) Neuropharmacology 2: 39–43.
7. Fernstrom JD and Wurtman RJ (1972) Science 178: 414–416.
8. Sadler E, Wyner M and Buterbaugh GG (1983) Res. Comm. Chem. Pathol. Pharmacol. 42: 37–50.
9. McMenamy RH and Oncley JL (1958) J. Biol. Chem. 233: 1436–1447.
10. McMenamy RH (1965) J. Biol. Chem. 240: 4235–4243.
11. Hutson PH, Knott PJ and Curzon G (1980) Biochem. Pharmacol. 29: 509–516.
12. Badawy AAB (1977) Life Sci. 21: 755–768.
13. Pardridge WM (1977) J. Neurochem. 28: 103–108.
14. Kennett GA, Curzon G, Hunt A and Patel AJ (1986) J. Neurochem. 46: 208–212.
15. Chaouloff F, Laude D, Mignot E, Kamoun P and Elghozi JL (1985) Neurochem. Int. 7: 143–153.
16. Chaouloff F, Elghozi JL, Guezennec Y and Laude D (1985) Br. J. Pharmacol. 86: 33–41.
17. Chaouloff F, Laude D, Guezennec Y and Elghozi JL (1986) J. Neurochem. 46: 1313–1316.
18. Chaouloff F, Kennett GA, Serrurier B, Merino D and Curzon G (1986) J. Neurochem. 46: 1647–1650.
19. Badawy AAB and Evans M (1981) Biochem. Pharmacol. 30: 1211–1216.
20. Chaouloff F, Laude D, Merino D, Serrurier B, Guezennec Y and Elghozi JL (1987) Neuropharmacology 26: 1099–1106.
21. Chaouloff F, Laude D, Serrurier B, Merino D, Guezennec Y and Elghozi JL (1987) Biogenic Amines 4: 99–106.
22. Chaouloff F, Laude D and Elghozi JL (1989) J. Neural Transm. 78: 121–130.
23. Hamon M, Bourgoin S and Glowinski J (1973) J. Neurochem. 20: 1727–1745.
24. Tappaz ML and Pujol JF (1980) J. Neurochem. 34: 933–940.
25. Garattini S, Mennini T, Bendotti C, Invernizzi R and Samanin R (1986) Appetite 7: 15–38.
26. Chaouloff F, Danguir J and Elghozi JL (1989) Pharmacol. Biochem. Behav. 32: 573–576.

Address for correspondence: Francis Chaouloff, Lab. Pharmacol., Grp Neuropharmacol., INSERM U7, CHU Necker–E.M., 156 rue de Vaugirard, 75015 Paris, France.

Influence of cerebral blood flow on tryptophan uptake into brain

Quentin R. Smith, Shinsuke Fukui, Peter Robinson and Stanley I. Rapoport

Laboratory of Neurosciences, National Institute on Aging, National Institutes of Health 10/6C103, Bethesda, MD 20892, U.S.A.

Abstract

The influence of protein binding on tryptophan uptake into brain was investigated at different flow rates in pentobarbital-anesthetized rats using the brain perfusion technique of Takasato *et al.*, (1984). The effective fraction of tryptophan that contributes to influx *in vivo* was found to exceed the free fraction measured *in vitro* and to vary inversely with flow rate over the physiologic range. The results suggest that blood flow, as well as competition and protein binding, may have a significant role in modulating tryptophan influx into brain.

Introduction

Serotonin synthesis within the central nervous system has long been known to be critically influenced by the brain concentration of precursor amino acid, L-tryptophan [1]. This dependence has stimulated considerable interest in the factors that regulate brain tryptophan, including plasma concentration and transport across the blood-brain barrier.

Tryptophan, like other large neutral amino acids, is taken up from plasma into brain by a saturable carrier at the brain capillary endothelium (i.e., the blood-brain barrier) [2]. This carrier has high affinity for at least 10 plasma neutral amino acids and is essentially saturated with amino acids as a group at normal plasma concentrations [3]. Consequently, influx for any given amino acid depends not only on the plasma concentration of the amino acid but on the plasma concentrations of all competitors. This relation was first summarized by Fernstrom and Wurtman [4] in 1972 as the 'plasma ratio', defined as $C_{\text{amino acid}}/\Sigma C_{\text{competitors}}$. More recently, kinetic constants (V_{max}, K_m) have been published for the blood-brain barrier neutral amino acid carrier that allow accurate prediction of influx rates over a wide range of plasma concentrations [3,5].

One issue that has generated significant controversy during the past 15 years is the contribution of albumin-bound tryptophan to tryptophan uptake into brain. Tryptophan is the only physiologic amino acid that binds significantly and reversibly to plasma proteins. Under normal conditions, 70–90% is bound to serum albumin [6]. Some studies have found that only free plasma tryptophan is available for uptake [7,8], whereas others suggest that essentially all (70–100%) plasma tryptophan contributes to influx into brain [9–12]. For the latter, it was originally

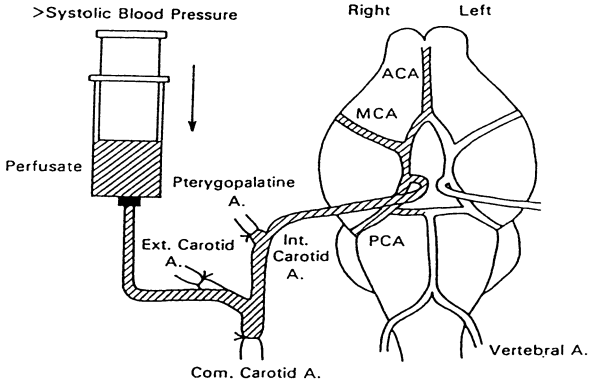

Fig. 1. Diagram of technique for perfusing the right cerebral hemisphere of the pentobarbital-anesthetized rat. In all experiments, the heart was stopped by severing the right and left ventricles just prior to the initiation of perfusion. (From ref. [16]).

proposed that the high transport affinity of the cerebrovascular neutral amino acid carrier essentially stripped tryptophan off albumin as it passed through the brain capillary [9,12]. More recently, Pardridge *et al.*, [13,14] have suggested that brain capillaries may enhance the dissociation of tryptophan from albumin through either the release of binding inhibitors or through the induction of a conformational change in the albumin molecule as a result of an interaction of albumin with the surface of the brain capillary cell membrane.

To evaluate this further, we measured the transport of [^{14}C]tryptophan and [^{3}H]leucine into brain in the absence and presence of albumin using a rat brain perfusion procedure (Fig. 1). Brains were perfused at different rates and with different fluids (whole blood, artificial plasma, serum, saline) to determine the effects of flow rate and fluid composition on uptake into brain. Results were analyzed with a model that incorporates rates of tryptophan binding and release from albumin, as well as blood flow and transfer across the blood-brain barrier [15]. The objectives were to determine 1) whether brain tryptophan uptake exceeds that predicted by the *in vitro* free fraction, 2) whether the magnitude of the difference is sensitive to flow rate and fluid composition, and 3) whether the difference can be explained by rapid rates of tryptophan dissociation and transport into brain.

Methods

Influx across the blood-brain barrier was measured using the *in situ* brain perfusion procedure of Takasato *et al.*, [16]. Pentobarbital-anesthetized rats were perfused at differing rates for 30 s with rat blood, serum, artificial plasma or saline containing

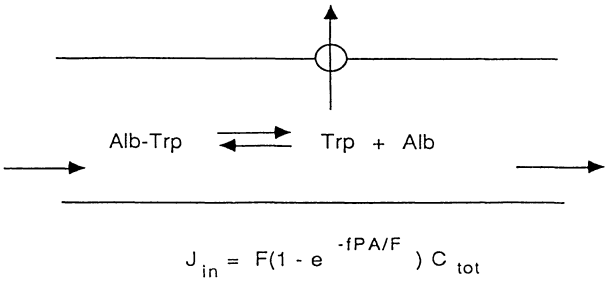

Fig. 2. Model for dissociation of tryptophan from albumin and transport into brain via the cerebrovascular neutral amino acid carrier. The equation gives the relation between influx (J_{in}) and flow (F), free fraction (f), cerebrovascular PA and total perfusate tryptophan concentration (C_{tot}). This equation assumes that the rate of dissociation is extremely rapid so that bound and free tryptophan are in equilibrium at all points in the capillary. PA can be calculated as described in reference [3].

L-[^{14}C]TRP and L-[^{3}H]LEU. In artificial plasma and saline perfusates, fatty acid-free bovine albumin was used instead of rat albumin. At the end of the perfusion, rats were killed by decapitation and radiotracer concentrations were determined in perfusate and brain. Results, after correction for residual intravascular activity and brain perfusate flow (F), were expressed as cerebrovascular permeability-surface area products (PA), and then an effective free fraction (f) *in vivo* was calculated as the ratio of PA's [(PA_{trp})/(PA_{leu})] in the presence of albumin divided by the ratio in the absence of albumin. This value was compared to the free fraction as measured *in vitro* at 37°C by equilibrium dialysis. All values were expressed as means ± S.E.M. for n = 3–6 animals.

Analysis based on calculated PA values assumes that rates of tryptophan dissociation and rebinding are rapid compared to brain capillary transit times. Use of [^{3}H]leucine as a second tracer facilitated comparisons by cancelling possible differences due to length of perfusion, capillary surface area and mean capillary amino acid concentration. Preliminary experiments demonstrated that the [(PA_{trp})/(PA_{leu})] ratio in the absence of albumin was independent of perfusion rate and perfusate amino acid composition. Such independence would be predicted based on theoretical grounds. The model of tryptophan dissociation and uptake into brain is illustrated in Fig. 2.

Results

The effective free fraction *in vivo* [f (*in vivo*)] for tryptophan uptake into parietal cortex equaled 0.53 ± 0.04 during perfusion with rat whole blood at the normal physiologic flow rate of 4.1×10^{-2} ml/s/g (2.4 ml/min/g). This value exceeded by greater than two fold the value measured *in vitro* by equilibrium dialysis (f (*in vitro*) = 0.25 ± 0.03). Variation of flow rate from 1.0- to 4.1×10^{-2} ml/s/g (0.6–2.4

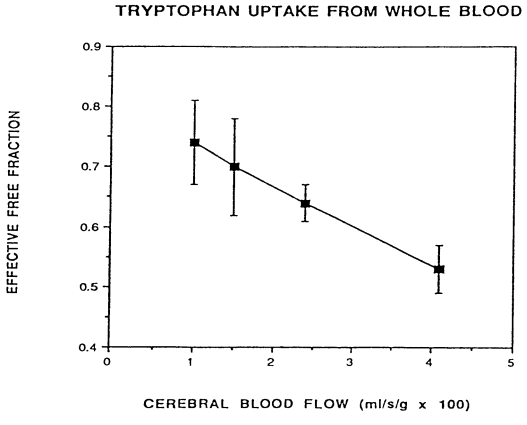

Fig. 3. Relation of effective free fraction *in vivo* for tryptophan to cerebral blood flow during perfusion of the rat brain with rat whole blood. Each point represents a mean ± S.E.M. for 3 animals.

ml/min/g) demonstrated an inverse linear relation between flow and f (*in vivo*) (Fig. 3). Best fit values of the slope and y-intercept of the regression equalled −6.93 g/s/ml and 0.81, respectively ($r=0.70$, $n=12$, $p<0.05$).

A similar flow dependence was observed using serum, plasma and saline perfusates. However, with these fluids, flow could be varied over a greater range because of their lower viscosity. With serum or plasma, f (*in vivo*) decreased from 0.56 ± 0.03 to 0.25 ± 0.02 as flow was increased from 0.3- to 10×10^{-2} ml/s/g (0.18–6.0 ml/min/g) ($p<0.01$). At the highest flow rates ($6–10 \times 10^{-2}$ ml/s/g), f (*in vivo*) differed minimally from the free fraction measured *in vitro* (range 0.18–0.25). There appeared to be no difference in available free fraction of tryptophan between rat serum and artificial plasma containing bovine serum albumin.

To determine whether the observed difference between f (*in vivo*) and f (*in vitro*) could be explained by rapid rates of tryptophan dissociation and transport into brain, transfer constants for brain uptake of tryptophan were calculated using the kinetic model of Robinson and Rapoport [15] which incorporates rates of binding and dissociation, blood flow and blood-brain barrier transport. Kinetic constants for uptake were taken from Smith *et al.* [3]. The results indicated that, even assuming instantaneous dissociation, predicted tryptophan uptake under normal physiological conditions (i.e., in the presence of normal plasma concentrations of amino acids) would differ minimally (<10%) from that calculated assuming contribution only from the free pool (no dissociation). Thus, a rapid rate of dissociation would not explain the observed greater uptake of tryptophan than that predicted by the *in vitro* free fraction.

Discussion

This study demonstrates that the effective fraction of plasma tryptophan that contributes to brain uptake exceeds the *in vitro* free fraction and that the magnitude of the difference varies with blood flow. The difference was greatest at low flow rates using blood perfusate and was least at high flow rates using saline or plasma perfusates. At the highest flow rates examined (10×10^{-2} ml plasma/s/g), the effective free fraction *in vivo* (0.25) differed minimally from that *in vitro* (0.18–0.25). Considering that cerebral blood flow in the awake rat ranges from 1.2–2.4 ml/min/g, the results predict that 50–65% of plasma tryptophan contributes to uptake under normal physiologic conditions. This value tallies well with a previous estimate (70–80%) obtained in pentobarbital-anesthetized rats using the brain uptake index technique [12,17].

The difference observed between f (*in vivo*) and f (*in vitro*) could not be explained by a rapid rate of tryptophan dissociation from albumin. Rapid dissociation could allow 'stripping' of bound tryptophan if the brain extraction of free tryptophan were sufficiently high to significantly deplete the free pool during a single pass through the brain vasculature. However, under normal physiologic conditions, the rate of transfer of free compound is too slow ($E<0.20$) to allow significant stripping from the bound pool. Thus, additional factors must be postulated. Pardridge et al., [13,14] have suggested that brain release of binding inhibitors or an induced conformational change in the albumin molecule may lead to a local increase in the free fraction of tryptophan in the brain capillary. If so, such changes might be detected by examining the influence of tryptophan on the uptake of another amino acid (i.e., through competitive inhibition). The flow dependence of F (*in vivo*) observed in this study would not be inconsistent with either the inhibitor or cell surface interaction hypotheses.

In summary, the results indicate that brain blood flow may have to be considered as well as plasma amino acid concentrations and brain capillary carrier kinetics in calculating estimates of tryptophan uptake into brain.

References

1. Fernstrom JD (1983) Physiol. Rev. 63: 484–546.
2. Oldendorf WH (1971) Am. J. Physiol. 221: 1629–1639.
3. Smith QR, Momma S, Aoyagi M and Rapoport SI (1987) J. Neurochem. 49: 1651–1658.
4. Fernstrom JD and Wurtman RJ (1972) Science 178: 414–416.
5. Hargreaves KM and Pardridge WM (1988) J. Biol. Chem. 263: 19392–19397.
6. McMenamy RH and Oncley JL (1958) J. Biol. Chem. 233: 1436–1447.
7. Bloxam DL, Tricklebank MD, Patel AJ and Curzon G (1980) J. Neurochem. 34: 43–49.
8. Sarna GS, Kantamaneni BD and Curzon G (1985) J. Neurochem. 44: 1575–1580.
9. Madras BK, Cohen EL, Messing R, Munro HN and Wurtman RJ (1974) Metabolism 23: 1107–1116.
10. Fernstrom JD, Hirsch MJ and Faller DV (1976) Biochem. J. 160: 589–595.
11. Yuwiler A, Oldendorf WH, Geller E and Braun L (1977) J. Neurochem. 28: 1015–1023.
12. Pardridge WM (1979) Life Sciences 25: 1519–1528.

13. Pardridge WM and Landaw EM (1984) J. Clin. Invest. 74: 745–752.
14. Pardridge WM (1987) Am. J. Physiol. 252: E157–E164.
15. Robinson PJ and Rapoport SI (1986) Am. J. Physiol. 251: R1212–R1220.
16. Takasato Y, Rapoport SI and Smith QR (1984) Am. J. Physiol. 247: H484–H493.
17. Pardridge WM (1983) Physiol. Rev. 63: 1481–1535.

Address for correspondence: Dr. Quentin R. Smith, Laboratory of Neurosciences, National Institute on Aging, National Institutes of Health, Bethesda, MD 20892, U.S.A.

Tyrosine and tryptophan analogues as MAO-inhibiting prodrugs

Michael G. Palfreyman[a], Ian A. McDonald[a], Monique Zreika[b], Jean-Noel Collard[b], Joseph Wagner[b], Philippe Bey[a] and Albert Sjoerdsma[a]

[a]Merrell Dow Research Institute, 2110 E. Galbraith Road, Cincinnati, OH 45215, U.S.A.
[b]Merrell Dow Research Institute, 16, rue d'Ankara, 67084 Strasbourg Cedex, Strasbourg, France

Abstract

(*E*)-ß-Fluoromethylene-*m*-tyrosine (FMMT) and (*E*)-ß-fluoromethylene-5-hydroxytryptophan (FM-5-HTP) are substrates of aromatic *L*-amino acid decarboxylase and yield the corresponding substituted tyramine and 5-hydroxytryptamine analogues which potently and irreversibly inhibit monoamine oxidase. In addition, the tyrosine analogue is a substrate for the neutral large amino acid transport system and is thereby concentrated in cerebral tissue. *In vivo*, FMMT is a potent inhibitor of MAO and this effect occurs predominantly in the brain. Such selectivity offers considerable therapeutic advantages.

A novel approach to achieve site specific enzyme inhibition is to design bioprecursors of mechanism-based enzyme inhibitors that are transported by the appropriate biosystem and metabolized to the actual inhibitor in the target sites. We have used this concept to design irreversible inhibitors of monoamine oxidase (MAO, EC 1.4.3.4, monoamine: O_2 oxidoreductase-flavin containing), the principal metabolizing enzyme in the important catecholamine and tryptophan pathways, according to the following Scheme:

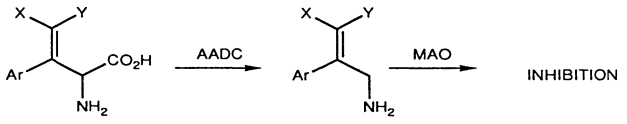

1 **2**

X and Y = H, Br, Cl, or F

Ar = 3-Hydroxyphenyl, or 5-hydroxy-3-indolyl

The first enzyme in both pathways, aromatic *L*-amino acid decarboxylase (AADC, EC 4.1.1.28) metabolizes the amino acid **1** to the amine **2** which, in turn, is a mechanism-based inhibitor of MAO. MAO oxidizes the allylamine moiety in **2** to produce an electrophilic species which convalently binds a nucleophilic residue

in the enzyme-active site leading to irreversible inactivation of the enzyme. Since AADC is a fairly selective enzyme, the choice of substitution on the aromatic nucleus of **1** was limited; in the present case we used either a phenol or hydroxy indole nucleus. We, and others, have published extensively on the AADC-substrate and MAO-inhibiting properties of (*E*)-ß-fluoromethylene-*m*-tyrosine (FMMT, MDL 72,394) [1–6]. This compound is an excellent substrate of AADC and the decarboxylated amine, (*E*)-ß-fluoromethylene-*m*-tyramine (MDL 72,392) is a very potent enzyme-activated irreversible inhibitor of MAO with preference for the MAO-A subtype [7]. The work described here shows that this concept can also be applied to an indole analogue. Furthermore, it is apparent that the above structural similarity of these analogues to the natural amino acids, *L*-dopa and *L*-tryptophan, respectively, allows them to exploit transport and distribution systems to their advantage. These 'secondary' consequences of modeling drugs on natural amino acids may help to explain the unique potency and/or selectivity of this class of compound.

Experimental procedures

Determination of MAO activity
MAO-A and MAO-B activities were determined using the selective substrates, 5-hydroxytryptamine and 2-phenethylamine, respectively; total MAO activity was determined with tyramine according to published methods [3,8,9].

Determination of monoamine and monoamine metabolite concentrations
The HPLC with electrochemical detection method [10] was used.

Purification of AADC and determination of the substrate properties of the prodrugs
Hog kidney enzyme was partially purified [11] to a specific activity of 50 nmole CO_2 liberated/min/mg protein with [1–^{14}C]-*L*-dopa as substrate. The amino acid analogues (5 mM) were incubated with 50 µl AADC at 37°C in the presence or absence of 50 µM *DL*-α-monofluoromethyldopa (MFMD, MDL 71,963), an irreversible inhibitor of AADC [12,13]. At various times aliquots were removed, acidified with 0.1 M $HClO_4$ containing 0.5% w/v EDTA and $Na_2S_2O_5$, and the indole analogues placed on an ultrasphere 1P-C_{18} (250 × 4.5 mm, 50 µM particle size) column in a modular HPLC system using a mobile phase A consisting of a 99/1 (v/v) mixture of 0.05 M NaH_2PO_4 and acetonitrile containing 5×10^{-3}M octane sulfonic acid (OSA), pH = 2.30, and mobile phase B consisting of a 60/40 (v/v) mixture of 0.05 M NaH_2PO_4 and acetonitrile containing 5×10^{-3}M OSA at pH = 3.0. Gradients were started with 75% A and 25% B for 5 min; followed by a linear gradient reaching 55% A and 45% B in 15 min and then final conditions held for 3 min before returning to initial conditions in 0.5 min, followed by a restabilization for 6.5 min. Flow-rate was 1.5 ml/min; 40°C.

Detection of indoles
Fluorescence with λ_{exc} = 300 nm and λ_{em} = 340 nm set up in series.

Detection of phenols
The phenolic compounds were determined by HPLC with U.V. detection as described by McDonald *et al.* [2].

Active transport of amino acids into the brain
Groups of rats (Male – Sprague-Dawley) were gavaged with 1 g/kg, p.o. leucine and thirty minutes later were injected intraperitonally with FMMT (0.5 mg/kg), FMMT (0.1 mg/kg) plus carbidopa (10 mg/kg) or saline (5 ml/kg). Four h later the rats were killed and MAO activity and monoamine concentrations determined in various tissues.

Results

(*DL*)-(*E*)-ß-Fluoromethylene-5-hydroxytryptophan (FM-5-HTP, MDL 73,095) and

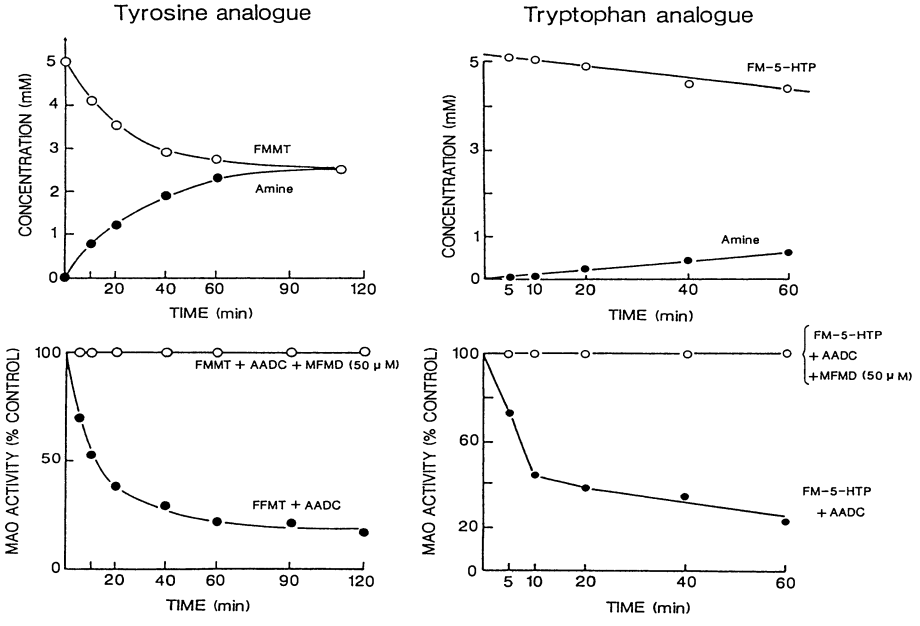

Fig. 1. Decarboxylation of FMMT and FM-5-HTP by hog kidney AADC and inhibition of MAO by the amine products. Amino acids (FMMT, Panel A, FM-5-HTP, Panel B at 5 mM) were incubated with AADC and aliquots removed at various times to determine formation of the corresponding amines and their ability to inhibit rat brain mitochondrial MAO. Incubations carried out in the presence of 50 μM MFMD (lower panels) showed no decarboxylation or inhibition of MAO.

(*DL*)-(*E*)-ß-fluoromethylene-*m*-tyrosine were both substrates for AADC and the respective decarboxylated products, (*E*)-fluoromethylene-5-hydroxytryptamine and (*E*)-ß-fluoromethylene-*m*-tyramine inhibited MAO (Fig. 1). The identity of (*E*)-ß-fluoromethylene-*m*-tyramine was confirmed by synthesis whereas the structure of the tryptamine analogue has not been rigorously verified. Its chromatographic behavior however is consistent with the proposed structure. Neither amino acid inhibited MAO in the presence of the AADC inhibitor (*DL*)-α-monofluoromethyldopa (MFMD, MDL 71,963). The rate of decarboxylation of the tyrosine substrate was considerably faster than that of the indole analogue (Fig. 1) consistent with the preferred catechol selectivity of AADC.

In vivo, FMMT is a potent inhibitor of MAO and small oral doses cause significant elevations in the brain of noradrenaline, dopamine, and serotonin and

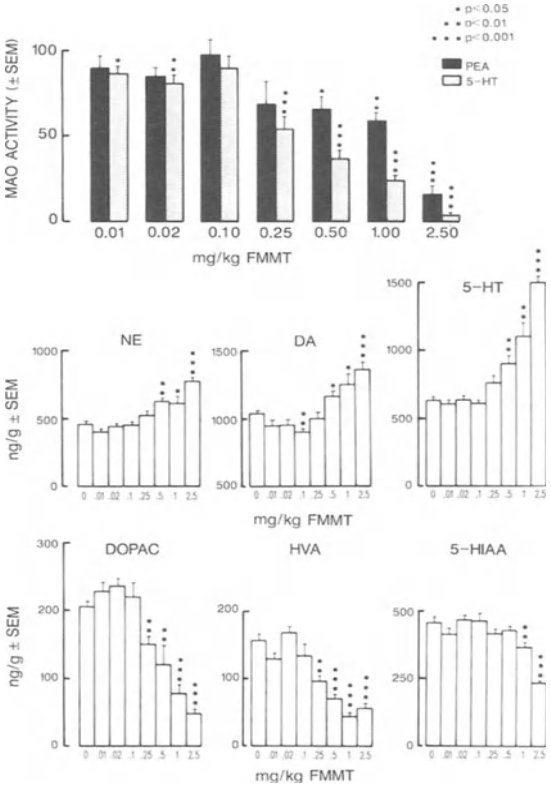

Fig. 2. Dose-response of effect of FMMT on rat brain MAO A and B and the concentration of monoamines and their metabolites. Animals were dosed orally and determinations made 18 h later. MAO A and B activities were determined with the selective substrates 5-HT and 2-phenethylamine (PEA), respectively.

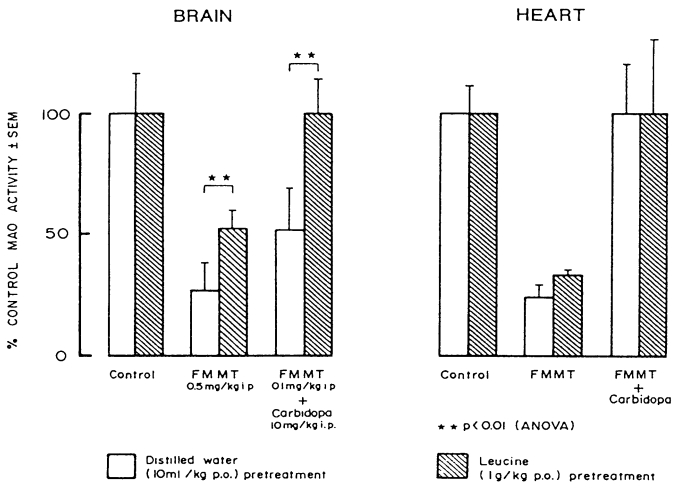

Fig. 3. Effect of leucine (1 g/kg, p.o.) on the MAO-inhibitory effect of FMMT with and without carbidopa. Rats were injected with leucine 30 min before FMMT and determinations made 4 h later. MAO activity shown is for the A enzyme only. Qualitatively similar effects were seen on the B enzyme (not shown).

decrease their deaminated metabolites (Fig. 2). Since only very small amounts of the synthetically challenging indole derivative have been made it has not been possible to investigate an *in vivo* effect in detail.

Pretreatment of rats with large oral doses of leucine to saturate the amino acid uptake carrier significantly reduced the MAO-inhibitory effect of FMMT in the brain, either administered alone or combined with carbidopa (Fig. 3). In contrast, in the heart (Fig. 3) and duodenum (data not shown) MAO inhibition was not attenuated. The data also indicate that FMMT produces little or no inhibition of MAO in the liver (data not shown) and that carbidopa co-administration blocks the MAO inhibitory effects of FMMT in the duodenum (not shown) and heart (Fig. 3) without reducing this effect in the brain. Pretreatment with leucine, while not affecting biogenic-amine concentrations in the brain *per se*, was able to attenuate the elevated concentrations produced by FMMT treatment (Table 1). Surprisingly, in view of the lack of effect on MAO activity, leucine pretreatment prevented the increase in noradrenaline concentrations in the heart (Table 1).

Discussion

MAO inhibitors have been used therapeutically in depression for over thirty years [14,16]. The initial enthusiasm for their efficacy in depression was soon tempered by concern over their side effects; in particular the risk of hypertensive crises

Table 1. Effect of leucine (1 g/kg, p.o.) on monoamine concentrations following FMMT treatment

Treatment	Brain NA ng/g ± S.E.M.	Brain 5HT ng/g ± S.E.M.	Heart NA ng/g ± S.E.M.
Control	344 ± 10	550 ± 18	769 ± 29
Leucine (1 g/kg)	368 ± 22	574 ± 46	727 ± 75
FMMT (0.5 mg/kg)	480 ± 30 (+40%)	857 ± 41 (+56%)	919 ± 78 (+20%)
FMMT (0.5 mg/kg) + Leucine (1 g/kg)	430 ± 9 (+25%)	662 ± 23 (+20%)	764 ± 59 (–)
FMMT (0.1 mg/kg) + Carbidopa (10 mg/kg)	455 ± 33 (+33%)	787 ± 47 (+43%)	1011 ± 85 (+31%)
FMMT (0.1 mg/kg) + Carbidopa (10 mg/kg) + Leucine (1 g/kg)	341 ± 22 (–)	589 ± 14 (–7%)	783 ± 61 (+2%)

Leucine administered orally 30 min before i.p. injection of FMMT or FMMT + carbidopa. Animals killed 4 h later. Percent change from control (H_2O p.o. followed by saline i.p.) shown in parenthesis.

associated with ingestion of tyramine-rich food such as cheese in patients taking MAO inhibitors. Tyramine, a substrate for MAO, releases noradrenaline from peripheral sympathetic nerves and causes vasoconstriction [17,18]. Thus, inhibition of MAO in organs such as the intestine, liver and vasculature would remove a critical protective barrier. On the other hand, the antidepressant efficacy of these inhibitors is most likely consequent on MAO inhibition in the brain [19]. Designing MAO inhibitors that exert their effect predominantly in the CNS is, therefore, a logical approach to limiting the risk of hypertensive interactions with tyramine-rich food. By utilizing the prodrug approach based on structural analogues of tyrosine and tryptophan we have exploited the potential to deliver these unnatural amino acids to the desired site with the enzyme and carrier systems that exist for the natural essential amino acids.

FMMT and FM-5-HTP are both substrates of AADC and not inhibitors as could have been anticipated on mechanistic grounds; both amino acids liberate potent MAO inhibitors. Surprisingly, however, FMMT is a much more effective inhibitor of the brain enzyme *in vivo* than can be rationalized purely on the basis of the MAO inhibitory potency of (*E*)-ß-fluoromethylene-*m*-tyramine. We feel that there are a number of factors which can contribute to this exceptional *in vivo* potency. Firstly, in the enzymatic cascade involved in biogenic amine synthesis, neuronal AADC is

essential for the formation of the active catecholamine and indoleamine neurotransmitters, dopamine and 5HT. Epinephrine and norepinephrine are formed by subsequent enzymatic conversion of dopamine in the same location. These amines are then predominantly metabolically inactivated by MAO. FMMT and FM-5-HTP, as substrates of AADC, will therefore be decarboxylated preferentially in close proximity to the intraneuronal pools of MAO, resulting in MAO inhibition and causing an elevation of the neurotransmitter concentrations. Secondly, the amino acid precursors of the monoamine neurotransmitters, *L*-tyrosine and *L*-tryptophan, are actively transported into the brain by the neutral large amino acid carrier that also transports leucine and is inhibited by 2-aminonorbornane-2-carboxylic acid [20]. Our data from experiments in which animals were treated with high doses of leucine support the notion that FMMT is also a substrate for the same carrier. Finally, Fagervall and Ross [6] have shown that the actual MAO inhibitor, (*E*)-ß-fluoromethylene-*m*-tyramine, is a substrate for the neuronal amine uptake system and that it is preferentially concentrated within noradrenergic and dopaminergic nerve endings. In the case of the tryptophan analog MDL 73,095, it is possible that (*E*)-ß-fluoromethylene-5-hydroxytryptamine will be a substrate for the serotonergic uptake system. These three properties of FMMT may also contribute to the brain selectivity of FMMT.

It is striking that doses of FMMT that substantially increase brain catecholamine and serotonin concentrations have little effect on liver MAO activity. Heart MAO activity is decreased, however, perhaps due to decarboxylation occurring in close proximity to MAO. Although leucine pretreatment did not prevent MAO inhibition in the heart, it was able to attenuate the increase in heart noradrenaline content. Co-administration of FMMT with the decarboxylase inhibitor carbidopa, on the other hand, prevented MAO inhibition in the heart without attenuating the elevation in noradrenaline concentrations. These observations could be explained in terms of the relative distribution of AADC, MAO and the neurotransmitters, and/or by the importance of the noradrenaline uptake systems. Noradrenaline in the heart is concentrated in the sympathetic nerve terminals whereas the mitochondrial enzyme MAO occurs in many cell types. A possible explanation for the apparent discrepancy between MAO inhibition and noradrenaline concentrations seen following FMMT treatment, therefore, is the likelihood that the sympathetic nerve endings can actively take up FMMT and (*E*)-ß-fluoromethylene-*m*-tyramine and that there is considerably more extraneuronal MAO than intraneuronal enzyme. Active uptake of FMMT into sympathetic nerves could be antagonized by leucine whereas passive uptake into other cardiac cells would not be. Unimpeded decarboxylation and MAO inhibition could then occur in areas outside of adrenergic neurons.

It is clear from the above that inhibition of AADC within sympathetic nerve endings should have prevented FMMT from increasing noradrenaline concentrations. However, carbidopa has probably not got access to this compartment of AADC since even very high doses are unable to cause a blockade of noradrenaline synthesis [13] or to prevent FMMT from elevating noradrenaline concentrations.

DL-α-Monofluoromethyldopa, on the other hand, does inhibit monoamine biosynthesis [13] and totally prevents FMMT from inhibiting MAO and elevating heart concentrations of noradrenaline [3]. It is, therefore, unlikely that carbidopa co-administration will bring substantial additional selectivity to the MAO inhibiting effects of FMMT, although it will certainly markedly enhance the bioavailability of this amino acid as both the gastro-intestinal and blood brain barriers have considerable AADC activity.

In conclusion, the MAO-inhibiting prodrugs, FMMT and FM-5-HTP have the potential to produce neuronally selective effects. The use of these compounds should be an effective means of treating depression and should be associated with a significantly reduced propensity to cause interactions with tyramine containing food. Preliminary results in man with FMMT support this contention [5,7].

Acknowledgements

The authors thank Francoise Dezeure for help with the leucine experiments and Mary Dooley for her skill in preparing the manuscript.

References

1. Palfreyman MG, McDonald IA, Zreika M and Fozard J (1983) Prog. Neuropsychopharmacol. and Biol. Psychiat. (Suppl.) Abs. 369.
2. McDonald IA, Lacoste JM, Bey P, Wagner J, Zreika M and Palfreyman MG (1984) J. Am. Chem. Soc. 106: 3354–3356.
3. Palfreyman MG, McDonald IA, Fozard JR, Mely Y, Sleight AJ, Zreika M, Wagner J, Bey P and Lewis PJ (1985) J. Neurochem. 45: 1850–1860.
4. McDonald IA, Lacoste JM, Bey P, Wagner J, Zreika M and Palfreyman MG (1986) Bioorg. Chem. 14: 103–118.
5. Palfreyman MG, McDonald IA, Bey P, Schechter PJ and Sjoerdsma A (1988) Prog. Neuropsychopharmacol. and Biol. Psychiat. 12: 967–987.
6. Fagervall I and Ross SB (1989) J. Neurochem. 52: 467–471.
7. Palfreyman MG, Zreika M and McDonald IA (1990) Tyrosine and tryptophan analogues as dual enzyme activated inhibitors of monoamine oxidase. In: Palfreyman MG, McCann PP, Lovenberg WM, Temple JG, and Sjoerdsma A (eds.) Enzymes as Targets for Drug Design. Academic Press, New York, pp. 139–156.
8. Zreika M, McDonald IA, Bey P and Palfreyman MG (1984) J. Neurochem. 43: 448–454.
9. Fozard JR, Zreika M, Robin M and Palfreyman MG (1985) Naunyn-Schmeid. Arch. Pharmacol. 331: 186–193.
10. Wagner J, Vitali P, Palfreyman MG, Zreika M and Huot S (1982) J. Neurochem. 38: 1241–1254.
11. Ribereau-Gayon G, Danzin C, Palfreyman MG, Aubry M, Wagner J, Metcalf BW and Jung MJ (1979) Biochem. Pharmacol. 28: 1331–1335.
12. Kollonitsch J, Patchett AA, Marburg S, Maycock AL, Perkins LM, Doldouras GA, Duggan DE and Aster SD (1978) Nature 274: 906–908.
13. Jung MJ, Palfreyman MG, Wagner J, Bey P, Ribereau-Gayon G, Zreika M and Koch-Weser J (1979) Life Sci. 24: 1037–1042.
14. Quitkin FM, Rifkin A and Klein DF (1979) Arch. Gen. Psychiatry 36: 749–760.

15. Robinson DS (1986) Psychopharm. Bull. 22: 12–15.
16. Jarrott B and Vajda FJE (1987) Med. J. Aust. 146: 634–638.
17. Blackwell B and Marley E (1966a) Br. J. Pharmacol. 26: 120–141.
18. Blackwell B and Marley E (1966b) Br. J. Pharmacol. 26: 142–161.
19. Murphy DL, Garrick NA, Aulakh CS and Cohen RM (1984) J. Clin. Psychiatry. 45: 37–43.
20. Christensen HN, de Cespedes C, Mandlogten ME and Ronquist G (1974) Ann. N.Y. Acad. Sci. 227: 355–379.

Altered glutamate metabolism in amyotrophic lateral sclerosis and treatment with branched chain amino acids*

Andreas Plaitakis

Mount Sinai School of Medicine, 1 Gustave L. Levy Place, New York, NY 10029, U.S.A.

Abstract

Recent studies have shown that a generalized defect in glutamate metabolism and widespread alterations in the central nervous system (CNS) levels of glutamate occur in amyotrophic lateral sclerosis, a disorder with a dismal prognosis. Present data support the hypothesis that altered presynaptic glutamatergic mechanisms, may be responsible for a neuroexcitotoxic cell loss in this disorder. In these glutamatergic mechanisms glutamate dehydrogenase (GDH) may play an important role, probably involved in the oxidation of transmitter glutamate.

We have accordingly reasoned that stimulation of GDH could increase the rate of oxidation of transmitter glutamate thus correcting the hypothesized malfunction of this amino acid in ALS. We have tested this hypothesis by performing a randomized, double-blind, placebo-controlled trial on 22 ALS patients using branched chain amino acids (BCAA) which can stimulate human brain GDH activity at physiological concentrations. During the one-year trial, patients treated with the BCAA showed a significant benefit as compared to control-treated group in terms of maintenance of extremity muscle strength and continued ability to ambulate.

Abnormal glutamate metabolism in ALS

Amyotrophic lateral sclerosis (ALS) is a progressive neurological disorder with a dismal prognosis characterized clinically by muscle weakness, wasting and spasticity and pathologically by degeneration of large motor neurons of the spinal cord, brain stem and/or motor cortex. Although the etiopathogenesis of the disease has not been fully understood, there is growing evidence that glutamate dysfunction may be involved in the neurodegeneration. Thus, glutamate levels have been shown to be elevated in the fasting plasma of ALS patients [1] and oral loading with monosodium glutamate resulted in plasma elevations which were greater and of longer duration in these patients as compared to controls [1].

These results, indicating the presence of a generalized defect in glutamate metabolism, were supported by additional studies showing that glutamate levels were decreased in areas of brain and spinal cord obtained at autopsy from ALS patients [2]. Since nerve tissue glutamate represents primarily the intracellular compartment (extracellular levels are relatively very low) and plasma levels reflect

* Supported by NIH Grants NS-16871 and NS-11631, The Clinical Center for Research in Parkinson's and Allied Diseases, and RR-71, Div. of Research Resources, General Clinical Research Center Branch.

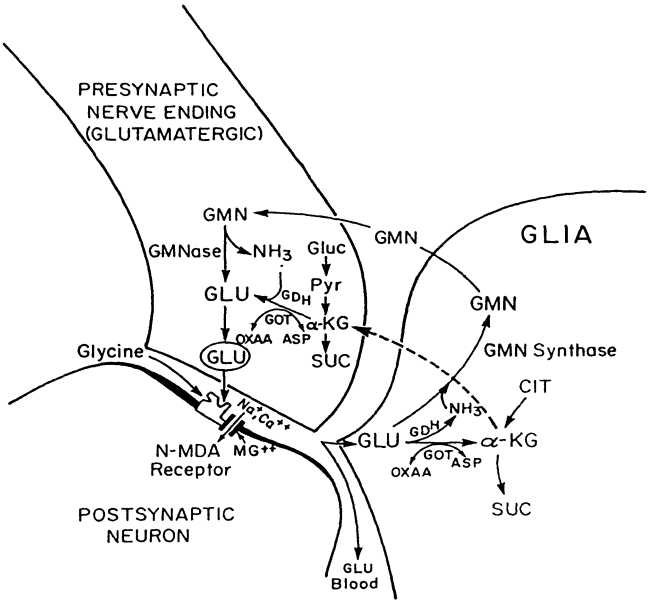

Fig. 1. Diagram showing a hypothetical glutamatergic synapse. Glutamate (GLU) released from the glutamatergic terminal during neurotransmission, is thought to bind to post-synaptic receptors, one of which, the N-methyl-D-aspartate (NMDA) receptor, is shown schematically. The NMDA receptor has been shown to mediate excitatory transmission by activating a Na^+ channel, which is also thought to be permeable to Ca^{++} and to be regulated by Mg^{++}.

Synaptic glutamate is thought to be inactivated by uptake, primarily into the surrounding astrocytes (GLIA) where it may be metabolized to α-ketoglutarate (α-KG) via glutamate dehydrogenase (GDH) or via glutamate oxaloacetate transaminase (GOT). Part of glutamate taken up by astrocytes may also be converted to glutamine (GMN) via glutamine synthase. Astrocytes may then supply the nerve terminal by glutamine and/or α-KG which can both serve as precursors of transmitter glutamate.

As described in the text, the hypothesized malfunction of synaptic glutamate in ALS may be due to 1) a defect in the uptake and/or metabolism of the transmitter (by astrocytes) or 2) increased release from the nerve terminals. Under such conditions of enhanced excitatory transmission, desensitization of the NMDA receptor may play an important role in protecting post-synaptic neurons. However, the presence of high glycine levels in the spinal cord and brain stem may prevent these adaptive processes leading to abnormal potentiation of excitatory transmission and selective degeneration of motor neurons. Glycine has been recently shown to potentiate glycinergic transmission by acting on a strychine-insensitive allosteric site of the NMDA receptor [5]. Glycine seems to increase the frequency of the NMDA receptor channel opening by accelerating the recovery of the receptor from glutamate-induced desensitization [20].

Since motor neurons has been shown to receive direct glycinergic innervation, release of glycine from glycinergic terminals may maintain high glycine concentrations in the vicinity of the NMDA receptor which in the presence of excessive synaptic glutamate may lead to temporal summation of post-synaptic potentials and abnormal enhancement of glutamatergic transmission [21] with resultant selective degeneration of motor neurons.

ASP = aspartate, GLUC = glucose, CIT = citrate, GMNase = glutaminase, OXAA = oxaloacetate, Pyr = Pyruvate, SUC = succinate.

concentrations present in the extracellular fluid, these changes have been suggested to result from an altered distribution between the intracellular and extracellular pools of glutamate [2]. A defect in the transport (and/or metabolism of transmitter glutamate) may occur (Fig. 1).

Enhanced synaptic glutamate may ultimately be responsible for degeneration of post-synaptic neurons (anterior horn cells) according to the neuroexcitotoxic hypothesis [3]. Although the defect in glutamate metabolism, as reflected in altered levels of this compound, was found to be present in all areas of brain and spinal cord studied, the neurodegeneration of ALS is known to be limited to motor neurons located in the ventral horns of spinal cord, brain stem and motor cortex. This selective involvement, occurring in the presence of a generalized metabolic abnormality, has been poorly understood but it may be related to the glycinergic innervation of motor neurons (Fig. 1). Glycine which is normally present in high concentrations in the spinal cord and brain stem [4] has been recently shown to potentiate excitatory transmission at the NMDA receptor [5].

Although we do not know the primary defect responsible for the above findings, the changes in glutamate levels suggest that altered pre-synaptic glutamatergic mechanisms may be involved in the pathogenesis of the disease. Glutamate, released from glutamatergic nerve terminals during neurotransmission, mediates its excitatory effect by acting on glutamate receptors present on post-synaptic neurons. Synaptic glutamate is thought to be inactivated by a high affinity uptake system which is energy dependent and which may operate primarily in the surrounding astrocytes [6]. (Fig. 1).

Glutamate taken up by glial cells is thought to be rapidly metabolized via two main pathways: The first involves formation of glutamine ('glutamine cycle') [7] which may then be transported back to the nerve terminal to serve as precursor of transmitter glutamate. The second involves oxidation via glutamate dehydrogenase or transamination via aspartate-oxaloacetate transaminase to α-ketoglutarate which in turn can be metabolized further through the Kreb's cycle to CO_2 and H_2O or could be transported to the nerve terminals also to serve as a precursor for transmitter glutamate [8].

As already indicated a defect in the high affinity uptake or metabolism of glutamate by glial cells may occur in ALS leading to excessive accumulation of synaptic glutamate and degeneration of post-synaptic neurons according to the neuroexcitotoxic hypothesis [3]. Therefore, a rational therapeutic approach to this disorder, will aim at attenuating the effect of enhanced synaptic glutamate. In this regard considerable interest has been generated in recent years by reports describing that specific antagonists of the NMDA receptor, can protect against neuroexcitotoxicity [9–11]. As to whether this approach can be used for the treatment of neurodegenerative disorders, is not certain at present. Of particular concern is the possibility that blocking excitatory transmission in ALS patients could result in increased muscle weakness and compromise of vital functions such as respiration. Another problem is posed by recent observation indicating that certain blockers of the NMDA receptor can be toxic to specific population of brain neurons [12].

Treatment of ALS with branched chain amino acids

Since the present evidence suggests altered pre-synaptic glutamatergic mechanisms in ALS, we have reasoned that modulation of glutamate metabolism may provide an alternative therapeutic approach to ALS. One strategy, we proposed, is to activate the enzyme glutamate dehydrogenase (GDH) which is thought to play a key role in transmitter glutamate metabolism. The enzyme is enriched in CNS regions receiving glutamatergic innervation where it seems to be localized in astrocytic processes [13]. Glutamate taken up by astrocytes in brain sections have been shown to induce GDH activity [14]. Moreover, cultured astrocytes have been observed to metabolize glutamate via GDH [15].

As such, stimulation of GDH could increase the rate of oxidation of transmitter glutamate thus correcting the hypothesized altered distribution of glutamate between intracellular and extracellular pools in ALS. Of the various agents that have stimulatory effect on GDH, the branched chain amino acids were felt to be mostly suitable for clinical use. L-leucine and to a lesser extent L-isoleucine can activate human brain GDH at physiological concentrations [16]. Because the administration of L-leucine results in a marked depression of the levels of the other two branched chain amino acids [17], L-isoleucine and L-valine, we have reasoned that in order to prevent deficiency of the latter, all three BCAA should be used in tandem.

To test whether administration of BCAA can be of potential benefit to ALS patients, we carried out a randomized, placebo-controlled trial involving 22 patients which lasted for one year [18]. Eleven of these patients received orally 3.0 grams L-leucine, 2.0 grams L-isoleucine and 1.6 grams L-valine in powdered form mixed thoroughly in dietetic jello or apple sauce, four times daily between meals. The other eleven patients received an equal amount of placebo powder (starch).

Clinical evaluations

The patients were examined at baseline and every three months afterwards without knowledge of what they received (double blind). Each of 13 limb muscle groups was evaluated on right and left sides as previously described [19] and summed to give a spinal score (normal power = 130) [19] Bulbar function was semiquantitated as previously described [19], giving a maximum score of 15. Most ratings were performed by the same examiner in individual patients; this method of clinical assessment has been shown to be reproducible.

Laboratory studies

Baseline blood chemistries and complete blood counts (CBC) were obtained. To assure bioavailability of the BCAA, an oral test dose of the above-described mixture or placebo was given after overnight fasting. Blood samples were drawn at

0, 60 and 120 minutes after dosing for multi-chemistries, CBCs and serum ammonia and amino acid levels.

Statistical analysis

The efficacy of treatment in each patient was assessed by computing the difference between the baseline and the scores obtained in each three month evaluation. Each three-month time period value was compared to the baseline value by using the paired t test for each group. In addition, each of the above scores (corrected for baseline values) was statistically compared for the two groups by the unpaired t test.

Repeated measures analysis of variance was calculated on the clinical scores for the time periods 0, 3, 6, 9 and 12 months for all patients having complete data. The same analysis was also done for the time periods 0, 3, 6 and 9 months only, as well as for 0, 3 and 6 months only.

The outcome of the study was evaluated using two criteria: 1) rate of decline in scores of each group and 2) continued ability to remain ambulatory at termination of the study. The proportion of success of the second criterion in each of the two groups was statistically compared using the chi-squared statistic and Fisher's exact test. For this analysis, we included all patients who completed the trial as well as those who, while under treatment, progressed to the point of wheelchair confinement (classified as failures) but did not complete one year on the trial either due to death or subsequent withdrawal. On the other hand, patients who withdrew while still ambulatory were excluded because they could not be classified as successes without having completed 12 months on observation.

Results and Discussion

As shown in Fig. 2A, which depicts the spinal scores obtained in all patients in each group three-month intervals, the placebo treated patients showed a rather linear decline in their functional status consistent with the natural history of the disease. In contrast, patients treated with the BCAA showed significantly better spinal scores than placebo-treated patients. Changes in the scores (values at the time points minus baseline values) were significantly worse in the placebo-treated than in the BCAA-treated patients (Fig. 2B).

Although the two groups of patients studied here were rather well matched, the favorable results obtained must be viewed cautiously because of the small sample size and because there is a substantial variation in the natural history of ALS.

Nevertheless, this pilot study is highly encouraging and may lead to finding a cure for this dreadful human disease. Further studies are clearly warranted. Should such studies confirm the results of this small trial, they will provide strong evidence favoring glutamatergic alterations as being primary to the disease process and as such they will advance our understanding of human neurodegenerations.

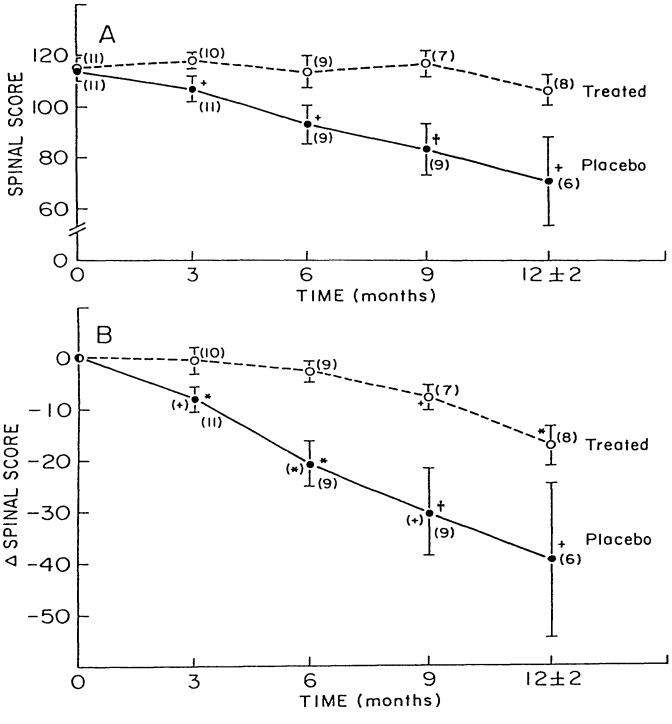

Fig. 2A. Spinal scores in the branched-chain amino acids (treated) and placebo groups. (N) is the number of patients who were clinically assessed at each time point as described in the Methods. The (N) decreased during the progress of the trial due to 1) death from the disease or severe disability precluding a visit to the clinic, 2) withdrawal from the study and 3) occasionally, non-compliance with the clinic appointments. Two amino acid treated patients could not attend the clinic at 12 months but they instead were evaluated at the 14th month of the trial. Values are means for each group ± S.E.M.

* denotes $p<0.02$, + denotes $p<0.05$ and ++ denotes $p<0.1$ of placebo compared to treated groups.

Fig. 2B. Comparison of spinal score difference from baseline (spinal score) for placebo and amino acid-treated (treated) groups. The difference was calculated by subtracting the baseline value from the value at each time point for each subject. Values are means ± S.E.M. Symbols without parentheses refer to comparisons with baseline values (using the paired t-test) and symbols in parenthesis refer comparisons between the placebo and the treated group at each time point (using the unpaired t-test). For explanation of symbols see Fig. 2A. Figure 2 is from reference [18].

References

1. Plaitakis A, Caroscio JT (1987) Ann. Neurol. 22: 575–579.
2. Plaitakis A, Constantakakis E and Smith J (1988) Ann. Neurol. 24: 446–449..
3. Olney JW, Ho OL and Rhee V (1971) Exp. Brain Res. 14: 61–70.

4. Aprison MH and Nadi NS (1978) In: Fonnum F (ed.) Amino Acids as Chemical Transmitters. Plenum Press, New York/London, pp. 531–570.
5. Johnson JW and Ascher P (1987) Nature 325: 529–531.
6. Balcar VJ, Borg J and Mandel P (1977) J. Neurochem. 27–28.
7. Bradford HF, de Belleroche JS and Ward HK (1978) In: Fonnum F (ed.) Amino Acids as Chemical Transmitters. New York, Plenum Press, pp. 367.
8. Shank RP and Campbell GL (1984) J. Neurochem. 42: 1162.
9. Choi DW (1988) Neuron 1: 623–634.
10. McDonald JW, Silverstein FS and Johnson MV (1987) Eur. J. Pharmacol. 140: 359–361.
11. Sonsalla PK, Nicklas WJ and Heikkila RE (1988) Science 243: 398–400.
12. Olney JW, Labruyere J and Price MT (1989) Science 244: 1360–1362.
13. Aoki C, Milner TA, Re Sheu K-FR, Blass JP and Pickel VM (1987) J. Neurosci. 7: 2214–2231.
14. Wolf G, Shünzel G and Rothe F (1986) Exp. Brain Res. 62: 659–662.
15. Hertz L and Schousboe A (1988) In: Kvamme E (ed.) Glutamine and Glutamate in Mammals. CRC Press, Boca Raton, Fl, U.S.A., Vol. II, pp. 39–55.
16. Plaitakis A and Shashidharan P (1988) Lancet II: 680–682.
17. Plaitakis A, Berl S and Yahr MD (1983) Neurology 33 (Suppl. 2): 78.
18. Plaitakis A, Smith J, Mandeli J and Yahr MD (1988) Lancet pp. 1015–1018.
19. Caroscio JT, Cohen JA, Zawodniak J *et al.*, (1986) Neurology 36: 141–145.
20. Mayer ML, Vyklicky L Jr. and Clements J (1989) Nature 338: 425–427.
21. Foster AC and Kemp JA (1989) Nature 338: 377–378.

Address for correspondence: Mount Sinai School of Medicine, Department of Neurology, 1 Gustave L. Levy Place, New York, NY 10029, U.S.A.

Tryptophan in the amelioration of drug-induced tardive dyskinesia*

H. Fisher, G.C. Wagner, L. Kozell, S.K. Johnson and R. Sandyk
Rutgers University, New Brunswick, New Jersey, U.S.A.

Introduction

The administration of 8 g L-tryptophan/day to an insomniac patient, suffering from tardive dyskinesia (TD), to promote sleep led to the discovery of an amelioration of the TD symptoms [1].

TD is currently believed to result from postsynaptic striatal and mesolimbic dopamine receptor supersensitivity caused by blockade of dopaminergic neurotransmission of neuroleptic drugs. The positive effect of tryptophan may be related to its precursor role in serotonin formation. In turn, serotonergic neurons have been shown to affect dopaminergic behavior [2].

The present studies were designed to 1) investigate the neurochemistry of dopamine and serotonin in neuroleptic-treated (haloperidol) rats and 2) to develop more readily quantifiable measurements of haloperidol-induced disruption of behavior in the rat model.

Experimental

Young (2 months old) and old (11 months) male Sprague-Dawley or Long-Evans rats were intramuscularly given 18 or 25 mg/kg haloperidol or vehicle. The injections were either single or double, 3 weeks apart. Tryptophan, in one study, was given as a diet supplement (0.3 vs 1.0% of diet) and in the water in a second study (as shown under results). Observations of spontaneous behavior were made 3 days after injections and weekly thereafter for side-to-side head movements. Locomotor performance was assessed at 10, 30, 100, 172, and up to 533 h post-injection. The assessment was carried out on a cloth-covered, rotating rod (15 cm circumference) operating at a speed of 12 revolutions/minute. Rats were first trained in a single session until they were able to remain on the rod for 60 seconds. They were then tested after treatment and the time on the rod measured with a stopwatch. At the end of each experiment the rats were sacrificed, the striatal region of the brain dissected and quickly frozen in liquid N_2. The tissue was analyzed by HPLC for dopamine, serotonin, and their metabolites DOPAC, HVA, and 5-HIAA.

* N.J. Agricultural Experiment Station Publication No. D–14101-3-90.

Results

In the first experiment where two levels of dietary tryptophan were fed in combination with injection of haloperidol (18 mg/kg), there was a significant reduction in head movement of rats receiving haloperidol together with the higher tryptophan level (Table 1). In the hypothalamus and caudate nuclei, haloperidol injection caused a significant increase in serotonin concentration, and the combination of haloperidol and 1% dietary tryptophan bordered on being significantly higher than the lower tryptophan-fed rats (Table 2).

The second experiment was designed to quantify the effect of haloperidol injection (25 mg/kg) on young and old Long-Evans rats' ability to negotiate a rotating rod (rotorod). Figure 1 shows that up to 10 h following haloperidol there is

Table 1. Head movement observations of haloperidol-injected rats fed 0.3% or 1.0% Tryptophan-containing diets[a]

Treatment Group	Head movement	
	None %	More than 1 %
0.3% L-Tryptophan	56	44
1.0% L-Tryptophan	50	50
Haloperidol[b] + 0.3% L-Tryptophan	21	79
Haloperidol + 1.0% L-Tryptophan[c]	50	50

[a] Rats observed by one observer on two separate occasions four weeks apart. Movements were scored as either none or more than 1 side-to-side head movement. The scores from the two separate observations were added and divided by 2 to give the mean score listed in the Table.

[b] Haloperidol, when administered to rats fed the lower (0.3%) tryptophan- containing diet, significantly ($p<0.05$) increased head movements.

[c] The higher (1) tryptophan intake, in conjunction with the haloperidol treatment, significantly ($p<0.05$) reduced the frequency of head movements in comparison with the haloperidol-treated group fed the lower level of tryptophan.

Table 2. Serotonin levels (μg/g) in hypothalamus and caudate nuclei of haloperidol-treated rats

	0.3% L-Tryptophan			1.0% L-Tryptophan	
Neurotransmitter	−	+	Haloperidol	−	+
Serotonin	0.57 ± .03[a]	0.77 ± .07[b]	Hypothalamus	0.55 ± .03[a]	0.96 ± .13[b]
Serotonin	0.29 ± .03[a]	0.43 ± .02[b]	Caudate nuclei	0.31 ± .01[a]	0.62 ± .02[b]

Within each row, values with different superscripts are significantly ($p<0.05$) different from each other.

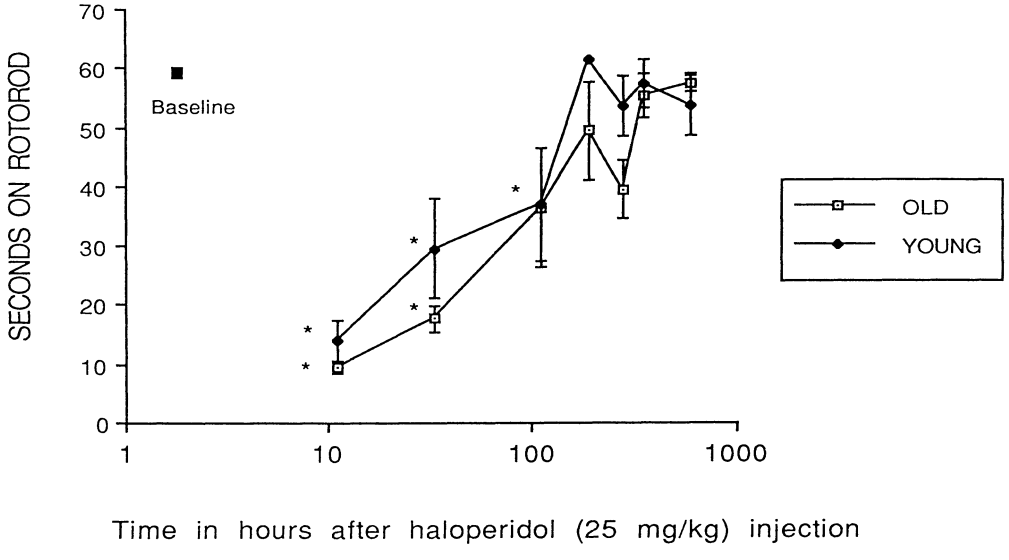

Fig. 1. Locomotor performance in young (2 months old) and aged (11 months old) Long-Evans rats after IM injection of haloperidol. N = 6/group, * sognificantly different ($p<0.01$) from baseline.

significant impairment in both young and old rats and the impairment is also significantly worse for the old compared with the young rats. The neurochemistry for this experiment (Table 3) showed a significant increase in dopamine for the haloperidol-treated old rats in comparison with all other groups.

The third experiment examined dopamine, serotonin, and their metabolites in the striatum of haloperidol-treated (25 mg/kg) young, Sprague-Dawley rats, up to

Table 3. Levels of striatal dopamine (DA) and its metabolites (μg/gram tissue) 30 days after 25 mg/kg haloperidol injection in young and aged Long-Evans rats

	Aged Veh (N=9)	Aged HAL (N=11)	Young Veh (N=9)	Young HAL (N=11)
DA	7±.78^{a}	11±.69^{b}	8±1.2	8±.96^{a}
DOPAC	.30±.02^{a}	.39±.03^{ab}	.48±.07^{b}	.35±.04^{ab}
HVA	.29±.03^{a}	.29±.02^{a}	.26±.02^{a}	.26±.03^{a}
DOPAC/DA	.04±.004^{a}	.04±.002^{a}	.06±.008^{b}	.04±.005^{ab}
HVA/DA	.04±.004^{a}	.03±.002^{b}	.03±.007^{ab}	.03±.003^{ab}

Mean values ± S.E. with different number superscripts within each row are significantly ($p<.05$) different from each other.

Table 4. Levels of striatal dopamine (DA) and its metabolites (μg/g tissue) after acute injections of 25 mg/kg of haloperidol (N=10/group)

	Control	1 hr	3 hr	10 hr	30 hr	100 hr
DA	11±.73	9±.58	8±.57[a]	10±.85	11±.68	12±.88
DOPAC	.62±.07	2.2±.16[a]	1.2±.12[a]	1.9±.21[a]	1.8±.15[a]	1.2±.11[a]
HVA	.46±.06	1.6±.13[a]	1.4±.10[a]	1.8±.19[a]	1.8±.17[a]	1.0±.13[a]
DOPAC/DA	.06±.01	.25±.02[a]	.16±.02[a]	.19±.01[a]	.18±.01[a]	.10±.01
HVA/DA	.04±.01	.18±.02[a]	.18±.02[a]	.17±.02[a]	.17±.02[a]	.08±.02

[a] significantly ($p<.05$) different from control.

100 h after drug injection. Dopamine concentrations decreased significantly by 3 h and recovered by 10 h following haloperidol injection. Both DA metabolites (DOPAC and HVA) increased sharply even after 1 h following haloperidol injection, indicating a large turnover rate of this neurotransmitter (Table 4). Serotonin concentration in the striatum also decreased significantly by 3 h following haloperidol injection and turnover rate as expressed by 5-HIAA/5-HT (Table 5).

The last experiment in this series was a repeat of the second experiment with young, Sprague-Dawley rats treated with vehicle and haloperidol, with or without tryptophan administered in the drinking water (172 mg/kg/day for the vehicle group and 161 mg/kg/day for the haloperidol rats). The animals were tested on the rotorod (Fig. 2) up to 244 h following haloperidol injection. As previously observed for the Long-Evans rats, haloperidol greatly reduced the time on the rotorod at 10 and 30 h post-injection. The tryptophan in conjunction with haloperidol had a further, significant effect in reducing the animals' balance on the rotorod. The tryptophan effect was particularly evident at 100 h, by which time the rats injected with haloperidol but given no tryptophan had already recovered to their baseline position.

Discussion

These experiments indicate that haloperidol, a neuroleptic drug associated with the development of tardive dyskinesia in humans, produces behavioral and locomotor

Table 5. Levels of striatal serotonin (5-HT) and its metabolites (μg/g tissue) after acute injections of 25 mg/kg of haloperidol (N=10/group)

	Control	1 hr	3 hr	10 hr	30 hr	100 hr
5-HT	.34±.03	.26±.02	.20±.01[a]	.24±.03[a]	.28±.03	.26±.04
5-HIAA	.29±.05	.34±.03	.31±.03	.27±.04	.30±.03	.23±.04
5-HIAA/5-HT	.80±.09	1.4±.11[a]	1.5±.14[a]	1.1±.04[a]	1.1±.05[a]	.80±.07

[a] significantly ($p<.05$) different from control.

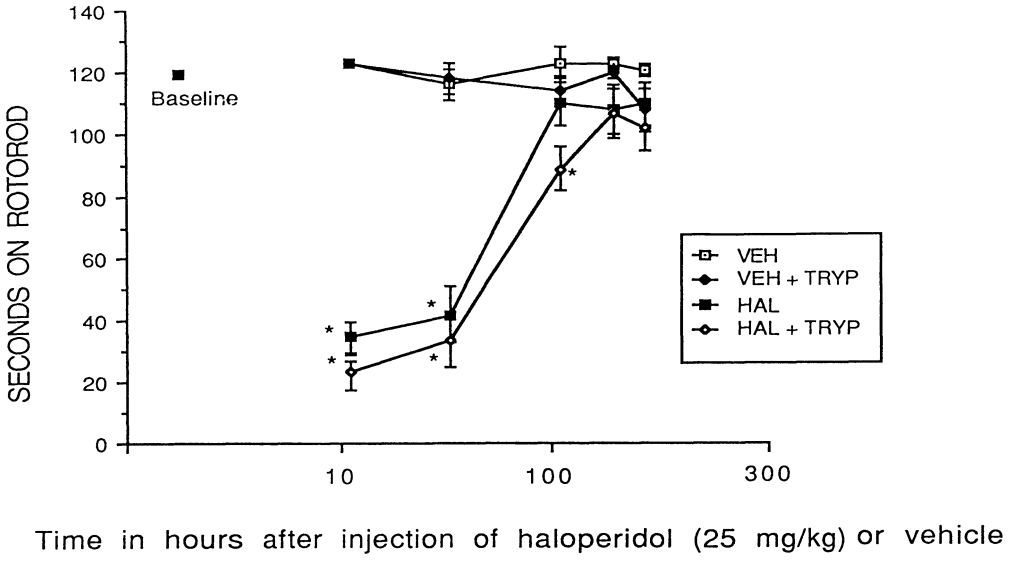

Fig. 2. Locomotor performance in young (2 months old) Sprague-Dawley rats after first injection of VEH or HAL. The TRYP groups received tryptophan in their drinking water. The HAL + TRYP groups consumed an average of 161 ± 3 mg/kg/day, while the VEH + TRYP groups consumed 172 ± 7 mg/kg/day. N = 15/group, * significantly different ($p<0.01$) from baseline.

abnormalities in rats, with older animals more severely affected in a rotorod balancing test than younger rats. Haloperidol causes changes in both dopamine and serotonin metabolism of the brain with evidence that dietary or water-added tryptophan can influence the effects on behavior and locomotor control of the drug. Further work is necessary to establish the mechanisms of the tryptophan-induced observations.

References

1. Sandyk et al. (1986) N. Engl. J. Med. 314: 1257.
2. Barbeau (1962) Can. Med. Assoc. J. 87: 802.

Biochemical and behavioural study of tryptophan administration to mice treated neonatally with 5,7-dihydroxytryptamine

E.F. Marshall, S. Dodds, E. Alderson and M. Leitch
Department of Psychiatry, University of Newcastle upon Tyne, U.K.

Anti-depressants have for many years been considered to function by modifying the serotonergic and noradrenergic concentrations in the central nervous systems and in particular in the synapses [1].

Recently, however, it has been demonstrated that some anti-depressants, in fact can alter receptor numbers in some areas of brain and modify receptor activated behaviour [3,7].

In a previous study, we demonstrated that a single dose of paroxetine, a specific 5-HT uptake blocker known to have anti-depressant activity, elicited an enhanced head twitch to receptor agonists which was diminished on chronic administration [6].

Furthermore, we demonstrated that compared with a single dose, chronic paroxetine decreased the number of head twitches observed in animals which had been subject to neonatal 5,7-dihydroxytryptamine(5,7-DHT), a treatment which specifically destroys in the long term, serotonin pathways in the central nervous system (unpublished observation). Thus it seems possible that paroxetine may not be acting by interfering simply with the reuptake of amine to increase its concentration in the synapse.

In this study, we consider the effects on head twitches of tryptophan administration which is known to increase the concentration of 5-HT in the brain by increasing the availability of the precursor.

Materials and Methods

Animals

Head twitches

Animals were injected with carbidopa (25 mg/kg i.p.) fifteen min before the administration of 5-HTP (100 mg/kg i.p.). Twenty min after the injection of the amino acid, the animals were placed in a box, allowed to customise themselves for five min and then the number of head twitches observed in the following five min were noted.

DHT treatment
Litters of mice (Barb-C) were injected with 5,7-DHT (200 mg/kg s.c.) or the vehicle, one h after desmethylimipramine (25 mg/kg s.c.), administered to protect the noradrenergic pathways. At the age of three weeks, all the DHT treated animals were tested for head twitches, as described below, to determine whether the neurotoxin administration had been successful. If there were less than ten head twitches in five min, the DHT injections were deemed to be unsuccessful.

Tryptophan treatment
One week later all animals were subject to administration of either tryptophan (60 mg/kg i.p.) or vehicle for a period of three weeks. Half the animals receiving the vehicle were administered tryptophan on the last day. For those animals receiving a single dose of tryptophan, separate groups were used for measuring the head twitches and for the biochemical assays. Those animals receiving chronic administration of tryptophan were tested for head twitches 48 h before the last injection of tryptophan. For the biochemical analyses, all animals were killed one h after the injection on day 21.

Biochemistry
On removal of the brain, it was immediately frozen in liquid nitrogen, various areas dissected out and maintained at −80 until homogenised in mobile phase. Aliquots were removed for protein assays. The tissue suspension was centrifuged at 12,000 g for 5 min, the supernatant placed into auto-analyser tubes for injection by 7125 injection valve (Rheodyne) fitted with a 20 μl loop. Separation was achieved using a 25 cm × 4.6 mm internal diameter stainless steel column (Spherisorb 5 ODS 2: Technicol) to which was fitted a precolumn filter (0.45 mm: Rheodyne). The analytical column was connected in series with an AMOR (Spark Holland) electrochemical detector (ECD), whose configuration requires that the mobile phase contains chloride ions. The mobile phase is detailed with a typical chromatogram for a standard and a brain sample in Fig. 1. Data is presented in relation to unit protein content, measured according to the method of Lowry *et al.* [5].

Statistical analysis
The data was analysed using analysis of variance and the significance of the difference between the means was determined by the student t-test.

Results

The DHT treated female animals exhibit significantly more head twitches than corresponding female controls (Fig. 2), whether treated with tryptophan or not. In addition, chronic tryptophan elicited a significantly greater number of head twitches than the corresponding controls for both DHT-treated females and untreated males.

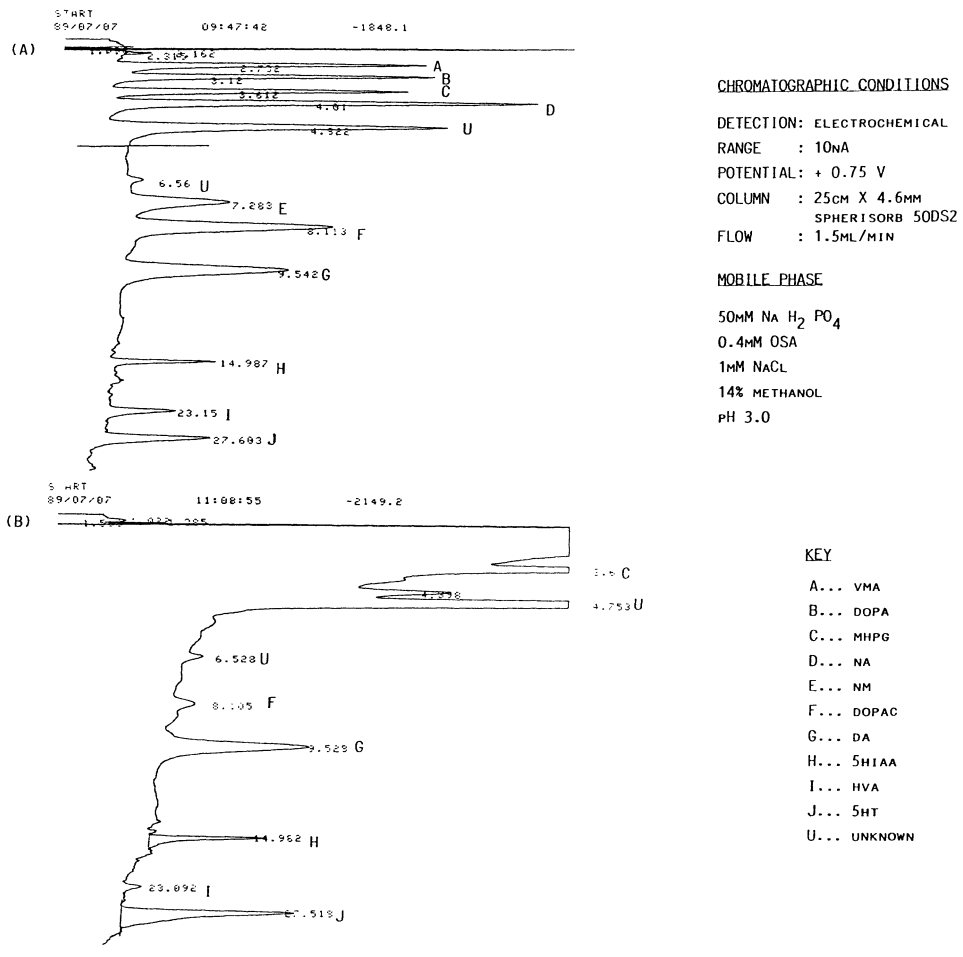

Fig. 1. (A) Chromatogram of a standard mixture (each 10 pM 20µl) in mobile phase. (B) Mouse hypothalamus.

In these three month old animals there are no significant differences in the 5-HT values of different areas of brain from control and DHT-treated animals (Table 1).

The effects of tryptophan on the levels of the precursor, 5-HT and 5-HIAA are presented in Fig. 3.

In the cortex of control animals, increasing the concentrations of TRY by 37% results in an almost threefold increase in the concentrations of 5-HT, with a small non-significant fall in 5-HIAA. On the other hand, in the DHT-treated animals the concentration of TRY increased almost three times and the amine and its metabolite fell to almost immeasurable levels. Chronic tryptophan caused the ratio of 5-HIAA to 5-HT to fall to the same level in both controls and treated animals.

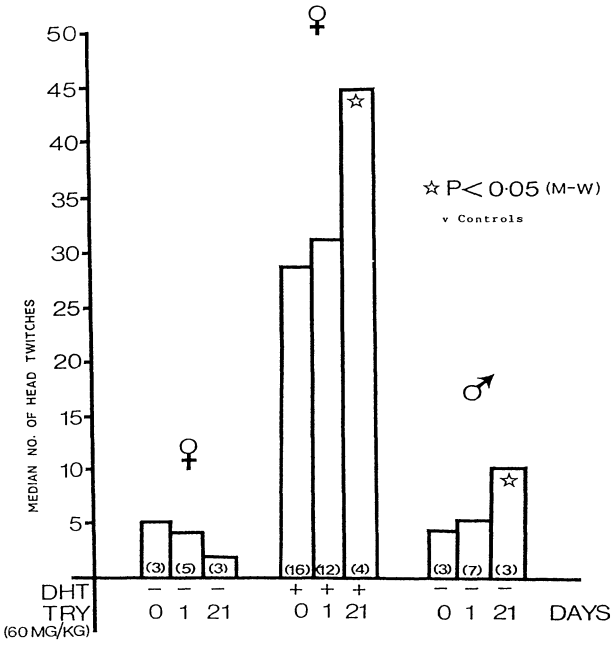

Fig. 2. Head twitch response after single or chronically administered trytophan (60 mg/kg i.p.) to control female and male mice, and female mice neonatally treated with DHT. Numbers in brackets represent sample size.

In the median raphe, the increases in TRY were of the same order as in the cortex for both control and DHT-treated animals, and the increase in control 5-HT was again almost threefold. However, control 5-HIAA increased significantly by more than 250%, and in the DHT brains 5-HT and 5-HIAA both increased by approximately 50%. These values were both less than the corresponding control, though not significantly so. The ratio of 5-HIAA to 5-HT increased in the controls, but there was no change in the DHT-treated animals.

Table 1. 5-HT levels in brain areas from control and DHT treated mice (age 4 months)

	Control	DHT
Cortex	33.3 ± 7.0 (6)	34.3 ± 15.0 (3)
Dorsal raphe	86.0 ± 9.8	105.2 ± 24.9
Median raphe	58.8 ± 15.2	75.7 ± 13.4
Striatum	38.4 ± 10.0	45.5 ± 16.6
Hypothalamus	79.5 ± 8.2	116.0 ± 5.0

Values represent pmole 5-HT/mg protein with numbers in brackets, the sample sizes.

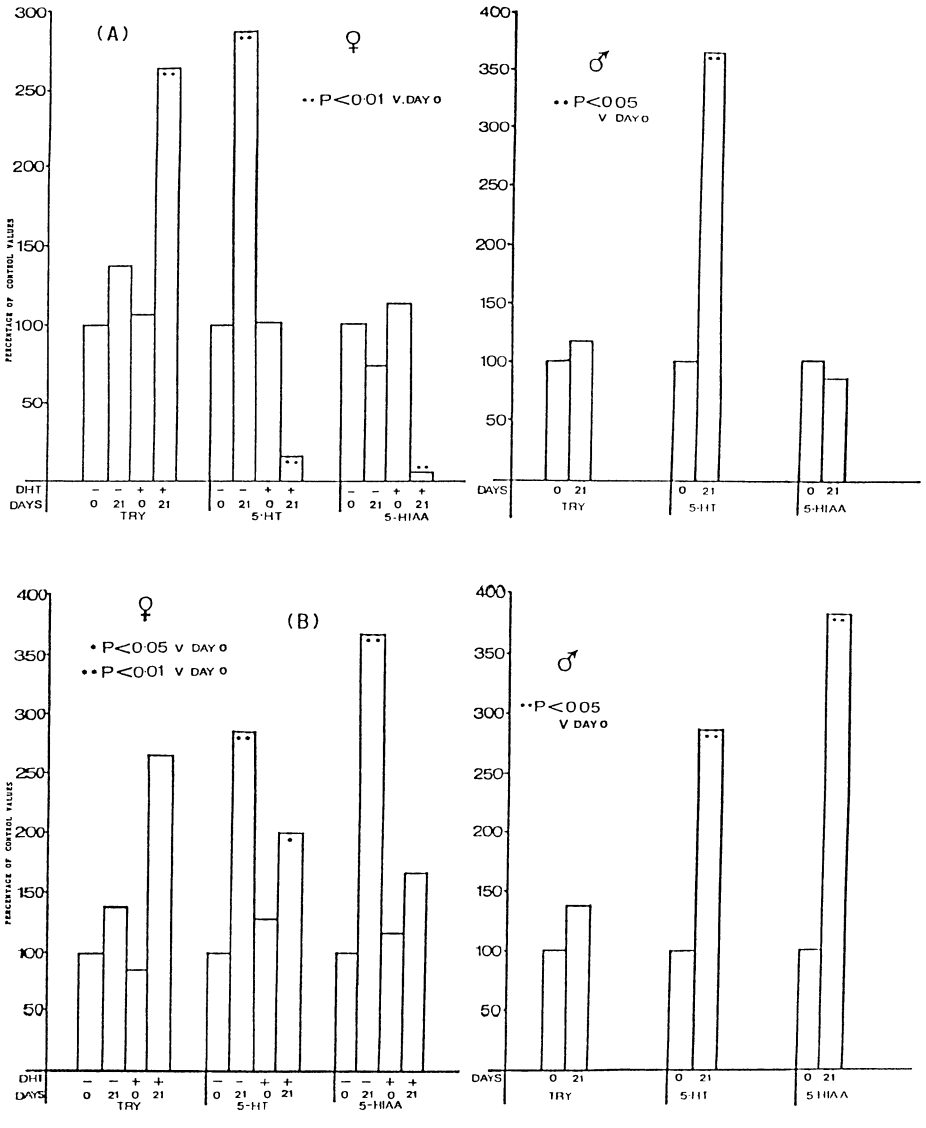

Fig. 3. (A) Effect of chronic tryptophan (60 mg/kg 21 day i.p.) on serotonin metabolism in the cortex of male and female mice. (B) Effect of chronic tryptophan (60 mg/kg 21 day i.p.) on the serotonin metabolism in the median raphe of male and female mice.

The pattern of changes in serotonin metabolism in male animals occasioned by tryptophan was similar to those observed in female controls.

Discussion

Despite the significantly increased head-twitch response in males chronically treated with tryptophan, over the male controls and against the female animals, the increase is not profound in comparison to the changes observed in the DHT-treated animals. Furthermore, there are no changes in the biochemistry of the chronically treated males, compared with the females, which could be associated with this small increase in head-twitch numbers. The lack of pronounced effect of tryptophan either as a single or chronic administration is in complete contrast to the effects of paroxetine [5] in which the number of head twitches after a single dose of paroxetine increased above controls by ten times and despite a decrease in number after chronic treatment the value remained four times higher than controls. Such results would tend to confirm the suggestion by Grahame-Smith [2] that tryptophan requires to be accompanied with a monoamine oxidase inhibitor to increase functionally available serotonin.

The increased number of head-twitches in the DHT-treated animals is in agreement with previous studies [6], and perhaps reflects increased numbers of receptors. However, the fact that 5-HT values have not altered after DHT treatment is unexpected. Our previous study indicated that 5-HT concentrations in the cortex was significantly reduced after DHT treatment after 4 weeks. These animals, however, are four months old. No previous study suggests that neurotransmitter levels return to normal with age. This may be another example of 5-HT receptor numbers not being related to 5-HT concentrations [4].

In any event, the lack of effect of DHT on control 5-HT and 5-HIAA levels suggest that there is no longer much damage to the storage sites and that turnover has returned to normal. The pronounced effect of administering tryptophan to these DHT-treated animals, however, indicates that the serotonergic pathways have not completely returned to normal. In the cell body region, chronic tryptophan has led to only a small increase in 5-HT with a similar increase in 5-HIAA suggesting no change in turnover whereas in the control animals the ratio of 5-HIAA to 5-HT has increased, almost two-fold. It can still not be stated that DHT has damaged the storage sites for 5-HT in the cellbody region. The lack of increased synthesis of 5-HT in tryptophan-loaded DHT might suggest that the uptake of tryptophan is somehow inhibited.

In the cortex of DHT treated animals, the loss of 5-HT and its metabolite, after chronic tryptophan suggest that there has been an irreplaceable release of 5-HT which is not observed in the control animals. Such a loss in 5-HT availability if it were to be observed in a projection area associated with head-twitching would be more consistent with an increased receptor activity. However, chronic paroxetine does not exercise such sweeping changes in serotonin metabolism in comparable areas of brain, and yet does allow increases in head-twitching to emerge both in control and DHT-treated animals.

Green *et al.* [3] suggested that head-twitching was a measure of hind-brain serotonergic activity. We are not able to confirm this suggestion but because of the

lack of correlation of head-twitching with 5-HT levels in animals not subject to tryptophan treatment, we cannot conclude that the increased receptor activity in DHT-treated animals after chronic tryptophan is a consequence of decreased 5-HT activity in the cortex. Clearly, it is necessary to investigate the levels of 5-HT and 5-HT turnover in other regions of high nerve-ending density.

Acknowledgements

The authors wish to thank Beecham Pharmaceuticals, Harlow, for the support which enabled them to undertake these studies. They also thank Yvonne Rutherford and Katherine Reed for secretarial and graphical assistance.

References

1. Baldessarini RJ (1975) The Basis for Amine Hypothesis in Affective Disorder. Arch. Gen. Psych. 32: 1087–1093.
2. Grahame-Smith DG (1971) Studies In Vivo on the Relationship between Brain Tryptophan, Brain 5-HT Synthesis and Hyperactivity in Rats Treated with a Monoamine Oxidase Inhibitor and L-Tryptophan. J. Neurochem. 18: 1053–1066.
3. Green AR, O'Shaughnessy K, Hammond M, Schachter M and Grahame-Smith DG (1983) Inhibition of 5-Hydroxytryptamine Mediated Behaviour by the Putative 5-HT^2 Antagonist Pirenperone. Neuropharmacol. 22(5): 573–578.
4. Lau C, Pylypiw A and Ross RL (1985) Development of Serotonergic and Adrenergic Receptors in the Rat Spinal Cord: Effects of Neonatal Chemical Lesions and Hyperthyroidism. Developmental Brain Res. 19: 57–66.
5. Lowry H, Roseburgh NJ, Farr AL, Randall AJ (1951) Protein Measurement with the Folin Reagent. J. Biol. Chem. 193: 265–275.
6. Marshall EF, Nelson DR, Johnson AM and Thomas DR (1988) Desensitisation of Central 5-HT^2 Receptor Mechanisms after Repeated Administration of the Antidepressant, Paroxetine. J. Psychopharmacology 2: 162.
7. Peroutka and Snyder (1980) Long Term Anti-Depressant Treatment Decreases Spiroperidol-Labelled Serotonin Receptor Binding. Science 210: 88–90.

New potent excitatory amino acids and marked potentiation of glutamate responses: Pharmacology of conformationally restricted glutamate analogues

M. Ishida and H. Shinozaki

The Tokyo Metropolitan Institute of Medical Science, 3-18-22, Honkomagome, Bunkyo-ku, Tokyo 113, Japan

Abstract

Eight isomers of α-(carboxycyclopropyl)glycine (CCG) which are conformationally restricted analogues of glutamate, demonstrated a large variety of depolarizing activities in the newborn rat spinal motoneurone. From these compounds, novel potent *N*-methyl-D-aspartic acid (NMDA) type agonists and some pharmacologically active compounds were found. The (2*R*,3*S*,4*S*) isomer of CCG (D-CCG-II) was a NMDA-type agonist and was much more potent than NMDA. The (2*S*,3*R*,4*S*) isomer of CCG (L-CCG-IV) is an L-glutamate analogue with a folded form and activates significantly NMDA-type receptors, leading to a conclusion that a preferred conformation of L-glutamate for activating NMDA-type receptors is a folded form. All D-isomers activated NMDA-type receptors. After a single application of the (2*S*,3*S*,4*R*) isomer of CCG (L-CCG-III), excitatory responses to L-glutamate were markedly enhanced. This enhancement lasted for more than several hours without a further application of L-CCG-III. Thus, CCG isomers would be expected to provide useful information about elucidating the function of the glutamate receptor.

Introduction

It is reasonable to assume that molecules of an acyclic transmitter such as glutamate have different conformations, and are capable of fitting to the different types of receptors. Therefore, glutamate is supposed to be able to bind to different subtypes of glutamate receptors: kainate-, quisqualate- and NMDA-type receptors. However, the interaction of glutamate with its receptors is not well understood with respect to their preference for particular conformers of the glutamate molecules. At present, there is no way to determine directly the conformation of transmitter molecules activating their receptors. The only possible technique to analyze the active conformations of transmitter molecules is by chemical modification of agonists and the characterization of the different actions of the various analogues.

cis- and *trans*-L-CCG have been isolated from young fruits of the plant, *Aesculus parviflora* and *Blighia sapida* [1]. Both natural CCGs cause a depolarization of neurones in the dorsal horn of the rat spinal cord when administered iontophoretically [2]. CCG is a conformationally restricted glutamate analogue in which the cyclopropyl group fixes the glutamate chain in an extended or folded form. Therefore, CCG would be expected to be a good compound for the analysis

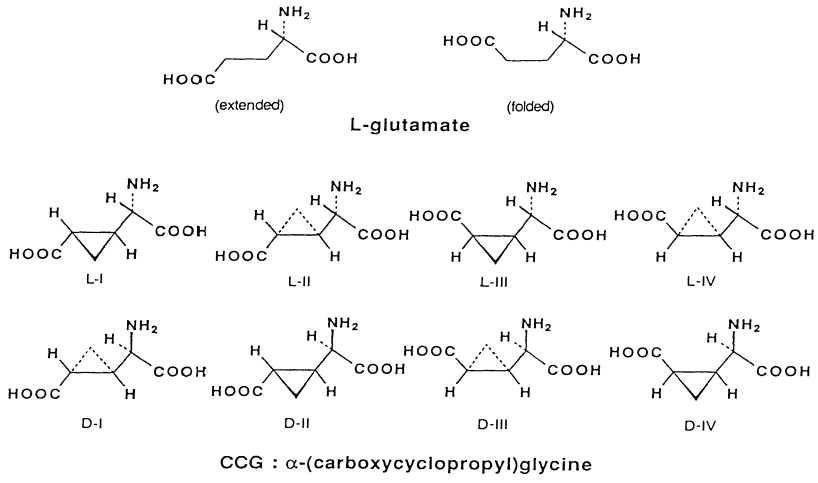

Fig. 1. Chemical structures of L-glutamic acid and all eight diastereomers of CCG.

of active conformations of glutamate molecules. The glutamate molecule is relatively flexible, and the carbon chain of glutamate is able to conform completely with that of CCG. CCG has eight stereoisomers theoretically (Fig. 1). Some of these CCG isomers would be expected to provide information about the interaction of glutamate molecules with excitatory amino acid receptor subtypes, and are thus potentially valuable compounds for analyzing mechanisms of the physiological function of glutamate. Ohfune *et al.* [3,4] synthesized several isomers of CCG expecting that these compounds would provide useful information about the active conformations of glutamate molecules. In the present paper, we examined the actions of eight conformational variants of CCG on the isolated newborn rat spinal cord. We are especially interested in the potent NMDA-like actions and marked potentiation of glutamate responses of these isomers.

Methods

The methods used for electrophysiological experiments in the isolated newborn rat spinal cord [1–5-day-old Wistar rats (N = 82)] were essentially similar to those described previously [5–8]. Under ether anaesthesia, the lumbar-sacral spinal cord was isolated, hemisected sagittally and placed in a 0.15 ml bath perfused at a fixed flow rate of 6 ml/min with artificial cerebrospinal fluid (in mM: NaCl 138.6, KCl 3.4, $CaCl_2$ 1.26, $MgCl_2$ 1.0, $NaHCO_3$ 21.0, NaH_2PO_4 0.58, glucose 10.0) which was oxygenated with a gas mixture of 95% O_2 and 5% CO_2. In most cases, $MgCl_2$ was replaced with NaCl to determine the excitatory activity of NMDA-type

agonists. The potential changes generated in the motoneurones were recorded extracellularly from the L_3-L_5 ventral root with a suction electrode. The tip of the suction electrode was a glass capillary, whose inner diameter fitted tightly with the recorded ventral roots in order to enhance the isolation impedance, which severely affected recording of the responses. After selecting only those spinal cord preparations, which demonstrated polysynaptic reflexes of above 2 mV in amplitude in normal [Mg^{2+}(1 mM)-containing, TTX-free] saline, TTX (0.5 μM) was added to the bathing solution throughout the experiment to block spontaneous depolarization and indirect drug effects. Excitatory amino acids and other test compounds were applied to the preparation either by perfusion or by brief-pulse injection into the perfusion system. The temperature of the perfusing fluid was kept at 27°C.

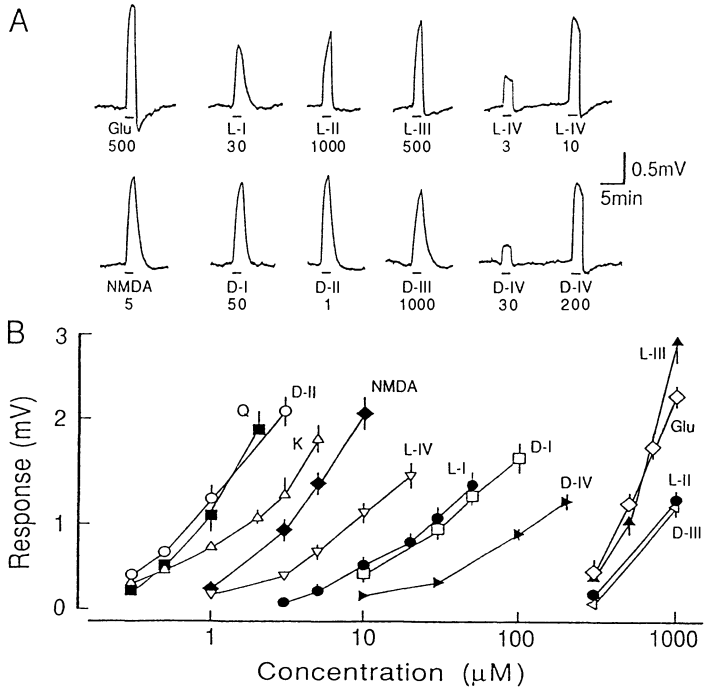

Fig. 2. A: Sample records of responses to eight CCG isomers, L-glutamate and NMDA. The responses to each excitatory amino acid were recorded from the ventral root extracellularly in Mg^{2+}-free, TTX-(0.5 μM) containing solution. Numerals under each response represent the concentrations (μM) of test compounds, which were added to the bathing solution for a period (2 min) indicated by horizontal bars. All records were obtained from the same preparation. B: The concentration-response relationships of eight stereoisomers of CCG and representative excitatory amino acids. All test samples were added to the bathing solution for a period of 2 min. Peak amplitudes of responses were plotted against concentrations of agonists. Vertical bars represent S.E.M. (N at least 4). Q: quisqualic acid, K: kainic acid, Glu: L-glutamic acid, L-I, L-II, L-III, L-IV: L-CCG-I, II, III, IV, D-I, D-II, D-III, D-IV: D-CCG-I, II, III, IV.

Results

A large variety of depolarizing activities of CCGs

When eight CCG stereoisomers (see Fig. 1) were added to the bathing solution for 2 min duration, all CCG isomers demonstrated a depolarization of the spinal motoneurones with a variation in their excitatory activity. Figure 2A represents sample records of responses to CCGs, L-glutamate and NMDA. These depolarizing responses were generally reproducible. D-CCG-II seemed to be the most potent among the CCG isomers when compared in terms of peak amplitudes of their responses at a certain concentration. L-CCG-IV also demonstrated a relatively high depolarizing activity, but it was less potent than D-CCG-II. Responses to the (2*S*,3*S*,4*S*) isomer of CCG (L-CCG-I), L-CCG-IV and the (2*R*,3*S*,4*R*) isomer of CCG (D-CCG-IV) were not maintained but gradually declined despite the presence of these agonists. The decrease in amplitudes of the responses to these CCGs during their application appears to be due to the desensitization of receptors for excitatory amino acids. This decline was observed even in small amplitudes of the responses. In the case of responses to L-glutamic acid, which also demonstrated such a decrease, small amplitude of responses did not decline during its application. The decay of tails of responses to L-CCG-I, D-CCG-II, III, NMDA and kainic acid was relatively slower than that of other agonists such as quisqualic acid, L-glutamic acid and L-CCG-IV.

Several factors, such as desensitization of receptors, equilibrium constants of agonist-receptor complexes and differences in rates of uptake of agonists, would affect the peak amplitude of depolarizing responses. Therefore, the peak amplitude sometimes varied in accordance with the duration of application of agonists, so it is technically difficult to determine the relative potency of excitation induced by CCGs. For the experiment shown in Fig. 2B, peak amplitudes of responses were plotted against the concentrations of excitatory agonists, which were added to the perfusing fluid for a period of 2 min. In passing, the order of the depolarizing activity in the case of 10 s application was as follows: L-quisqualic acid (300), D-CCG-II (200), L-CCG-IV, L-kainic acid (100), NMDA (40), D-CCG-IV (10), L-CCG-I (6), the (2*R*,3*R*,4*R*) isomer of CCG (D-CCG-I) (3), L-glutamate (1), L-aspartic acid, L-CCG-III (0.6), the (2*S*,3*R*,4*R*) isomer of CCG (L-CCG-II) (0.3), the (2*R*,3*R*,4*S*) isomer of CCG (D-CCG-III) (0.1), numerals in parenthesis showing a approximate relative activity [L-glutamate (1 mM) = 1].

Pharmacological classification of responses to CCGs

In order to clarify which type of the glutamate receptor subtype is activated by these CCG isomers, actions of some antagonists of excitatory amino acids were examined on responses to CCG isomers. At present, highly specific antagonists for kainate- and quisqualate-type receptors are not yet available in electrophysiological studies, but it is possible to block effectively the actions of NMDA-type

agonists without appreciable actions on responses to non-NMDA-type agonists. Mg^{2+} primarily acts by blocking the NMDA ion channel in a voltage-dependent manner [9–11], and D(−)-2-amino-5-phosphonovaleric acid (APV), 3-[(±)-2-carboxypiperazin-4-yl]propyl-1-phosphonic acid (CPP) and (+)-5-methyl-10,11-dihydro-5H-dibenzo[a,d]cyclohepten-5,10-imine maleate (MK-801) and some other compounds are known to selectively reduce the NMDA response [12–14]. When the Mg^{2+} free solution was changed to one containing Mg^{2+} (1 mM) to test the NMDA-type depolarizing activity, responses to L-CCG-IV and all stereoisomers of D-CCG (2 μM – 1 mM) were markedly reduced, in spite of the fact that the response to L-CCG-I (0.1 mM) was not so sensitive to Mg^{2+}. Depolarizing responses to L-CCG-III still remained in the presence of Mg^{2+} to some extent, suggesting that L-CCG-III activated the NMDA-type receptor, but was not a pure NMDA-type agonist.

Furthermore, effects of relatively high concentrations of NMDA-type antagonists were examined. APV completely abolished responses to NMDA (10 μM). D-CCG-II (2 μM), III (1 mM) and IV (0.2 mM) in concentrations of 50 100 μM. Residual amplitudes of responses to L-CCG-IV (10 μM) and D-CCG-I (0.1 mM) seemed negligible in the presence of 100 or 200 μM APV, but they still remained in almost equal amplitude even at higher concentrations of APV. Peak amplitudes of responses to L-CCG-III (1 mM) were reduced by APV (100 μM) to about 30% of the control. Responses to L-CCG-I (30 μM) and II (1 mM) were slightly reduced by APV (100 μM) and the degree of a decrease in amplitudes of the L-CCG-I responses varied from one preparation to the other. In the presence of APV (100 μM), responses to kainic acid and quisqualic acid were hardly affected. Fig. 3 represents sample records of responses to L-glutamate, NMDA, and representative CCGs in the presence of high concentrations of APV (50, 100 and 200 μM). After the preparation was exposed to MK-801 (2 μM) for more than 30 min, responses to L-CCG-IV (10 μM). NMDA (20 μM) and D-CCG-II (5 μM) gradually decreased in a use-dependent manner, while the responses to kainate (3 μM) and quisqualate (2 μM) remained almost unchanged. Amplitudes of responses to L-glutamate were reduced to about 85% of the control. A slight decrease in peak amplitudes of responses to L-CCG-I (0.1 mM) was sometimes observed.

Neither strychnine (10 μM) nor picrotoxin (10 μM) affected the depolarization induced by D-CCG-II and L-CCG-IV. The above results suggest that L-CCG-IV and all stereoisomers of D-CCG preferentially activate NMDA-type receptors. Furthermore, the actions of CPP on the depolarization induced by D-CCG-II and L-CCG-IV were examined. CPP is a potent and selective competitive antagonist for the NMDA-type receptor [13]. CPP (1–10 μM) markedly reduced the amplitude of responses to both D-CCG-II and L-CCG-IV. The effects of CPP in concentrations less than 100 μM were fully reversible upon washout. When the relationship between the agonist concentration and the peak amplitude of responses was examined in the presence of CPP (2, 5, 10 μM), the dose-response curve of D-CCG-II, L-CCG-IV and NMDA shifted in an almost parallel manner. The pA_2 values were 5.99 ± 0.08 (N=4), 5.90 ± 0.03 (N=4) and 5.86 ± 0.04 (N=4)

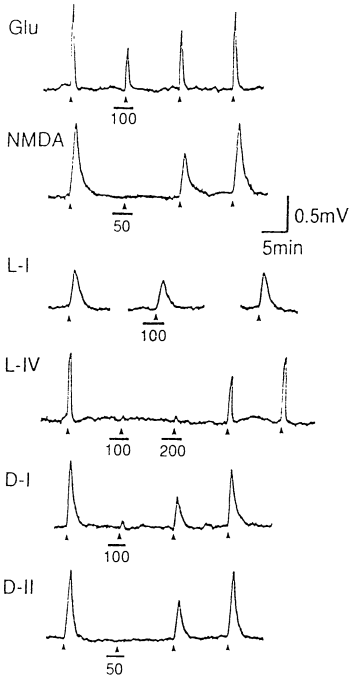

Fig. 3. Sample records of depolarizing responses to NMDA, L-glutamate and representative CCGs in the absence and presence of APV. Numeral under each response represents the concentration (μM) of APV, which was added to the bathing solution for a period indicated by horizontal bars. L-Glutamate (0.5 mM), NMDA (10 μM), L-CCG-I (30 μM), L-CCG-IV (10 μM), D-CCG-I (0.1 mM) and D-CCG-II (2 μM) were added at a mark point for a period of 30 s at a fixed interval of 10 min except L-CCG-I which was applied at an interval of 20 or 30 min.

for CPP versus D-CCG-II, L-CCG-IV and NMDA, respectively. In all cases the pA_2 values were not significantly different from 6.0.

Marked potentiation of glutamate responses by L-CCG-III

As shown above, L-CCG-III caused depolarization of newborn rat spinal motoneurones. In addition to its own depolarizing action, it caused marked potentiation of responses to L-glutamate and L-aspartate. After a single application of L-CCG-III (1 mM, 10–15 s), the preparation was thoroughly washed by the normal bathing solution, and the response was restored very quickly. When the periodic addition of L-glutamate to the bathing solution was resumed without simultaneous application of L-CCG-III, the amplitude of the responses to glutamate was markedly enhanced (Fig. 4A). In addition, the decline in amplitude probably due to receptor desensiti-

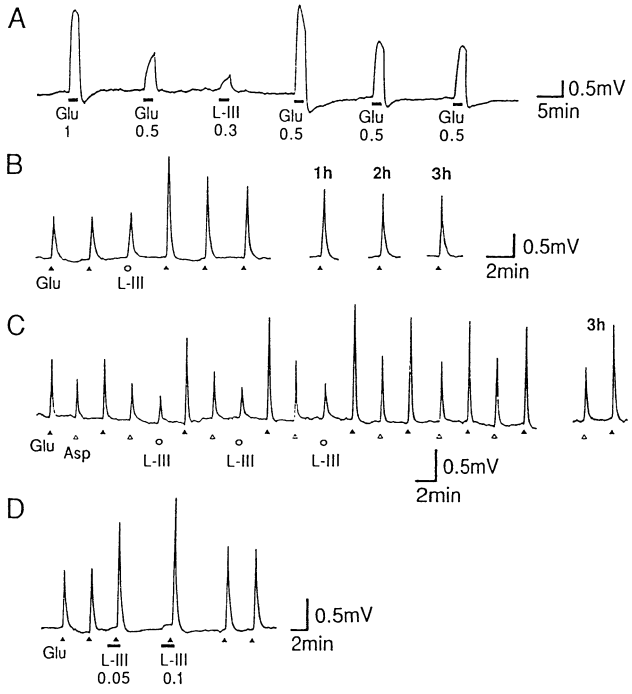

Fig. 4. A: Marked potentiation of responses to L-glutamate after a single application of L-CCG-III. L-Glutamate or L-CCG-III was added to the perfusing fluid for a period of 2 min. Numerals under each response represent concentrations (mM) of compounds. B: The long-lasting potentiation of the glutamate response after a single application of L-CCG-III. L-Glutamate (1 mM) was periodically added to the perfusing fluid for a period of 10 s. L-CCG-III (1 mM) was only once added to the perfusing fluid for a period of 15 s. C: Marked potentiation of responses to L-glutamate and L-aspartate after repetitive addition of L-CCG-III (1 mM, 10 s). L-Glutamate (▲, 1 mM) and L-aspartate (Δ, 1 mM) were alternatively added to for a period of 10 s. D: Potentiation of the glutamate response after simultaneous application of L-CCG-III and L-glutamate. L-CCG-III (50 and 100 μM) was added simultaneously with L-glutamate (1 mM, 10 s) for a period indicated by horizontal bars.

zation was observed during the application of L-glutamate, in striking contrast to the control response. The potentiation of the glutamate response lasted for a period of more than several hours without a further application of L-CCG-III (Fig. 4B). Responses to L-aspartate were also enhanced by L-CCG-III in a similar manner to L-glutamate. Figure 4C demonstrates that the potentiation of responses to L-glutamate or L-aspartate is reinforced by repeated application of L-CCG-III. The above case is one example of the effects observed after a single application of L-CCG-III. However, marked potentiation is observed even when both L-glutamate and L-CCG-III are simultaneously added to the bathing solution (Fig. 4D). In this case, the minimum effective concentration of L-CCG-III to cause the potentia-

tion seemed to be significantly less than 50 μM. At low concentrations of L-CCG-III, the potentiation did not continue for a long time, in spite of the fact that the response amplitude was considerably augmented at the first stage. Other isomers of CCG did not demonstrate such potentiation of responses to L-glutamate or L-aspartate. When L-glutamate and L-aspartate were applied in relatively high and low concentrations, L-CCG-III (1 mM) did not augment significantly the responses to them, but in dose ranges where log-log plots of responses to them against the concentration represent an almost straight line, L-CCG-III significantly augmented these responses, as if the dose-response curve was shifted to the left in a parallel manner.

We examined the responses to a variety of amino acid excitants which were affected by L-CCG-III. Responses to L-glutamate, D- and L-aspartate, L-cysteic acid and L-CCG-III were potentiated by L-CCG-III (1 mM), but those to kainic acid, quisqualic acid, NMDA, D-glutamate, L-CCG-I, IV, D-CCG-I, II and IV were hardly affected by L-CCG-III.

To test whether the potentiation of glutamate responses is directly related to the L-CCG-III-evoked depolarization, the potentiation was examined under the conditions where the depolarization was extremely reduced by Mg^{2+}, CPP and 6,7-dinitroquinoxaline-2,3-dione (DNQX). DNQX has both competitive and non-competitive antagonist actions at excitatory amino acid receptors [15,16]. The responses to L-glutamate (1 mM) were slightly reduced by changing from the Mg^{2+}-free to Mg^{2+} (1 mM)-containing normal solution, but the marked potentiation of glutamate responses was still observed after application of 1 mM L-CCG-III even in the Mg^{2+}(1 mM)-containing solution. When CPP (10 μM) or DNQX (0.1 mM) was added to the bathing solution in combination with L-CCG-III (1 mM) in order to reduce markedly peak amplitude of responses to L-CCG-III, glutamate responses were markedly augmented after the application of L-CCG-III. Even when both CPP (10 μM) and DNQX (20 μM) were simultaneously added to the bathing solution in order to reduce furthermore the L-CCG-III response, the marked potentiation was still observed, and the duration of potentiation remained unchanged.

Uptake inhibitors and L-CCG-III

As a possible mechanism for the potentiation, it is reasonable to assume that L-CCG-III blocks an uptake of excitatory amino acids from the vicinity of their receptors by the surrounding neurones and glia [17]. Some amino acids, such as D(+)- and L(−)-*threo*-3-hydroxyaspartate, dihydrokainic acid and L-cysteic acid, have been known to inhibit the uptake of glutamate and aspartate in the mammalian central nervous system [18–20]. So, we compared the actions of L-CCG-III and these uptake inhibitors on the potentiation of the glutamate response. Both D(+)- and L(−)-*threo*-3-hydroxyaspartate caused a slight depolarization of the rat spinal motoneurone to a similar degree, but the L(−)-isomer was superior to the D(+)-isomer in causing the potentiation of the glutamate response. L(−)-*threo*-3-

Hydroxyaspartate (1 mM) augmented the response to L-glutamate (1 mM) in a very similar manner to L-CCG-III. However, its duration of action was considerably shorter than that of L-CCG-III (1 mM), demonstrating that L-CCG-III was more potent than L(−)-*threo*-3-hydroxyaspartate. In the case of *threo*-3-hydroxyaspartate, both L- and D-isomers demonstrate an inhibitory effect on uptake of L-glutamate or L-aspartate, although the L-isomer is approximately twice as potent as the D-isomer with respect to the uptake of either L-glutamate or L-aspartate [21]. However, in contrast to L-CCG-III, D-CCG-III hardly affected the responses to these excitatory amino acids. Dihydrokainate and L-cysteic acid were weak agonists in the isolated rat spinal motoneurone, and they did not affect the response to L-glutamate or L-aspartate.

The spinal reflex evoked by the electrical stimulation (duration 100 μs, 10 V, at an interval of about 1 min) of dorsal root (L_4 or L_5) was hardly affected by the one-shot application of L-CCG-III (1 mM) or L(−)-*threo*-3-hydroxyaspartate (1 mM). When L-CCG-III was added to the bathing solution for a period of 3 min in a concentration of 0.1 mM, potentiation of the spinal reflex was not observed.

Discussion

Eight isomers of L- and D-CCG were synthesized in an attempt to gain some insight into possible conformations of L-glutamate molecules during activation of each glutamate receptor subtype. They demonstrated a large variety of depolarizing activity in the newborn rat spinal motoneurone. As a result, it was found that all D-isomers and a folded form of L-CCG (L-CCG-IV) preferentially activated NMDA-type receptors. Although L-CCG-I, II and III activated more than one receptor type (mixed type agonists), L-CCG-I preferentially activated non-NMDA-type receptors and L-CCG-III activated mainly NMDA-type receptors. L-CCG-II was not so potent. Binding assays of CCG isomers using labelled CPP in the rat hippocampal neurone have supported our present results (Kawai and Ishihara, unpublished observation). Binding studies with labelled NMDA antagonists have yielded affinities of a range of antagonists for the receptor that correlate closely with those calculated from the results of electrophysiological studies [22–24]. The structure of L-CCG-IV, as mentioned above, mimics very closely the folded conformation of L-glutamate, therefore, it seems reasonable to assume that the active conformation of the L-glutamate at the NMDA-type receptor is a folded form.

It is of great interest that all D-isomers of CCG, which include both the folded and extended forms, cause a depolarization due to activation of NMDA-type receptors in the isolated rat spinal cord. Of the compounds we examined on the isolated rat spinal cord, D-CCG-II is one of the most potent NMDA-type agonists. While D-CCG-II and L-CCG-IV are potent NMDA-type agonists, there is no apparent structural similarity between them. As shown in Fig. 1, the cyclopropyl ring of CCGs fixes their carbon chains in extended or folded forms close to those adopted by L-glutamate. L-CCG-IV corresponds to a folded form of L-glutamate

from the point of view of its configuration as well as conformation, on the other hand, D-CCG-II corresponds to an extended form of glutamate in its conformation but not in configuration. The polar functional groups of D-CCG-II and L-CCG-IV, which are probably binding sites with the receptors, never accurately superimpose. The carbon chain of aspartate is one atom shorter than that of glutamate and the ionisable groups of aspartate and NMDA cannot match those of glutamate. The NMDA-type receptor might have high affinity for substrates with the D-configuration by unknown mechanism. The conformational arrangement of the D-isomer when it interacts with receptors remains to be solved [25].

Glycine in micromolar concentrations has been reported to augment the excitatory action of NMDA in cultured cortical and diencephalic neurones [26]. This potentiation is insensitive to strychnine, and seems to be one of the characteristic properties of the NMDA response in the mammalian central nervous system. Since D-CCG-II and L-CCG-IV were shown in the present study to be potent NMDA-type agonists, we examined the action of glycine on responses to these agonists in the isolated rat spinal cord, but we were unable to demonstrate that superfusion with glycine (1 μM – 1 mM) facilitated significantly depolarizations evoked by CCG-isomers in strychnine-containing (0.01 mM) solution. This is interpreted to mean that the endogenous levels of glycine were already maximal for this effect in the isolated rat spinal cord. In order to demonstrate potentiation of the NMDA-type response by glycine in the rat spinal cord, other experimental conditions would be required [27].

In addition to the depolarizing activity of CCGs, a folded isomer of L-CCG (L-CCG-III) potentiated markedly responses to L-glutamate and aspartate. Other CCG isomers did not demonstrate such potentiation. In contrast to L-CCG-IV, which possessed potent depolarizing activity, L-CCG-III showed considerably lower depolarizing activity despite the fact that it has a similar folded structure to L-CCG-IV, and the configurations at ß and γ-carbon atoms are the only difference between them. Activation of the NMDA-type receptor and the potentiation of the response to L-glutamate are certainly differentiated by the steric role of the cyclopropyl group of CCG. In spite of the fact that the depolarization evoked by L-CCG-III is mainly due to the activation of the NMDA-type receptor, the potentiation of response to L-glutamate does not seem to be directly related to the activation of NMDA-type receptors.

One may consider some possibilities for the mechanism underlying the potentiation of the glutamate response, such as inhibition of uptake of agonists from the synaptic environment, an increase in transmitter release, changes of properties of receptors which might be related to glutamate neurotoxicity, and so on. It is also worth considering whether the potentiation in our case is similar to the glycine-induced potentiation of the NMDA response [26]; however, according to binding assays on hippocampal neurones, it seems unlikely that L-CCG-III binds to the glycine receptors (Kawai and Ishihara, unpublished observation). It would seem more plausible that L-CCG-III blocks the uptake process for excitatory amino acids, because it is generally accepted that re-uptake from the extracellular space is

the process whereby transmitter amino acids are removed from the vicinity of their receptors and thereby inactivated. There is some evidence to suggest that active uptake is partially responsible for their removal from the synaptic environment. In the present study, neither dihydrokainate nor L-cysteic acid potentiated responses to L-glutamate or L-aspartate. So far in our studies on the isolated rat spinal cord, only *threo*-3-hydroxyaspartate and L-CCG-III enhanced the response to L-glutamate and aspartate. According to Johnston *et al.* [20], under conditions where *threo*-3-hydroxyaspartate had little or no effect on the spontaneous firing rate of neurones in the cat spinal cord, excitation induced by the administration of L-glutamate was clearly potentiated. Responses to kainic acid, quisqualic acid, NMDA and D-glutamate were hardly affected by L-CCG-III in the present study. L-Glutamate, D-aspartate and L-cysteate are able to utilize the glutamate transport system efficiently, but D-glutamate, NMDA, and kainic acid are poor substrates for the glutamate transport system [28]. It was of great interest that the response to several compounds, which were believed to be taken up from the vicinity of their receptors, was often enhanced by L-CCG-III and/or *threo*-3-hydroxyaspartate in the isolated rat spinal cord. Although the potentiation of the glutamate response by L-CCG-III might be due to the inhibition of the uptake process, the reason for the extremely long duration of the potentiation is a question to be solved. Further investigation will be required in order to validate or negate a causal relationship between the potentiation of the glutamate response and the inhibition of the uptake of excitatory amino acids.

Neuronal damage is supposed to be aggravated by the potentiation of responses to L-glutamate [29], and may be related to the activation of NMDA-type receptors [30,31]. Since L-CCG-III significantly potentiates the glutamate response for a long time, it is possible that L-CCG-III may provide useful information about glutamate neurotoxicity. In addition, the long-term potentiation (LTP) in hippocampal neurones has for a long time captured the imagination of neuroscientists as a model with which to probe the cellular mechanisms of learning and memory in the mammalian brain. Many researchers are interested in the relationship between NMDA-type receptors and LTP [32]. Although the present data were obtained in the rat spinal cord, the actions of CCG-isomers are expected to be similar in other regions of the mammalian central nervous system. Whatever the mechanism for the potentiation of the glutamate response, L-CCG-III is expected to be useful as a pharmacological tool for analyzing the mechanisms underlying glutamate's transmitter functions [33].

Acknowledgements

The authors wish to thank Drs. Y. Ohfune and K. Shimamoto for their generous gift of CCG compounds. MK-801 was a gift from Merck, Sharp and Dohme. This work was supported in part by a Grant in Aid for Scientific Research from the Ministry of Education, Science and Culture of Japan.

References

1. Fowden L, Smith A, Millington DS and Sheppard RC (1969) Phytochem. 8: 437–443.
2. McLennan H, Hicks TP and Liu JT (1982) Neuropharmacol. 21: 549–554.
3. Kurokawa N and Ohfune Y (1985) Tetrahedron Lett. 26: 83–84.
4. Yamanoi K, Ohfune Y, Watanabe K, Li PN and Takeuchi H (1988) Tetrahedron Lett. 29: 1181–1184.
5. Ishida M and Shinozaki H (1988) Brain Res. 473: 193–197.
6. Ishida M and Shinozaki H (1988) Brain Res. 474: 386–389.
7. Shinozaki H and Ishida M (1988) In: Kanazawa I (ed.) Neurotransmitters: Focus on Excitatory Amino Acids. Excerpta Medica, Tokyo, pp. 17–30.
8. Shinozaki H, Ishida M, Shimamoto K and Ohfune Y (1989) Brain Res. 480: 355–359.
9. Ault B, Evans RH, Francis AA, Oakes DJ and Watkins JC (1980) J. Physiol. (London) 307: 413–428.
10. Mayer ML, Westbrook GL and Guthrie PB (1984) Nature 309: 261–263.
11. Nowak L, Bregestovski P, Asher P, Herbert A and Prochiantz A (1984) Nature 307: 462–465.
12. Davies J, Francis AA, Jones AW and Watkins JC (1981) Neurosci. Lett. 21: 77–81.
13. Davies J, Evans RH, Herrling PL, Jones AW, Olverman HJ, Pook P and Watkins JC (1986) Brain Res. 382: 169–173.
14. Wong EH, Kemp JA, Priestley T, Knight AR, Woodruff GN and Iversen LL (1986) Proc. Natl. Acad. USA 83: 7104–7108.
15. Birch PJ, Grossman CJ and Hayes AG (1988) Eur. J. Pharmac. 151: 313–315.
16. Honoré T, Davies SN, Drejer J, Fletcher EJ, Jacobsen P, Lodge D and Nielsen F (1988) Science 241: 701–703.
17. Watkins JC and Evans RH (1981) Ann. Rev. Pharmacol. Tox. 21: 165–204.
18. Balcar VJ and Johnston GAR (1972) J. Neurochem. 19: 2657–2666.
19. Johnston GAR, Kennedy SME and Twitchin B (1979) J. Neurochem. 32: 121–127.
20. Johnston GAR, Lodge D, Bornstein JC and Curtis DR (1980) J. Neurochem. 34: 241–243.
21. Balcar VJ, Johnston GAR and Twitchin B (1977) J. Neurochem. 28: 1145–1146.
22. Olverman HJ, Jones AW and Watkins JC (1984) Nature: 307: 460–462.
23. Olverman HJ, Monaghan DT, Cotman CW and Watkins JC (1986) Eur. J. Pharmacol. 131: 161–162.
24. Watkins JC, Evans RH, Mewett KN, Olverman HJ and Pook P (1987) In: Hicks TP, Lodge D and McLennan H (eds.) Excitatory Amino Acid Transmission. Alan R. Liss, pp. 19–26.
25. Watkins JC and Olverman HJ (1987) Trends Neurosci. 10: 265–272.
26. Johnson JW and Ascher P (1987) Nature 325: 529–531.
27. Fletcher EJ and Lodge D (1988) Eur. J. Pharmacol. 151: 161–162.
28. Stallcup WB, Bulloch K and Baetge E (1979) J. Neurochem. 32: 57–65.
29. McBean GJ and Roberts PJ (1985) J. Neurochem. 44: 247–254.
30. Rothman SM and Olney JW (1987) Trends Neurosci. 10: 299–302.
31. Finkbeiner S and Stevens CF (1988) Proc. Natl. Acad. Sci. 85: 4071–4074.
32. Collingridge GL and Bliss TVP (1987) Trends Neurosci. 10: 288–293.
33. Shinozaki H, Ishida M, Shimamoto K and Ohfune Y (1989) Br. J. Pharmacol. 98: 1213–1224.

Address for correspondence: H. Shinozaki, The Tokyo Metropolitan Institute of Medical Science, 3-18-22, Honkomagome, Bunkyo-ku, Tokyo 113, Japan.

The neurotoxic effects of kainic acid on photoreceptors and retinal pigment epithelium

Jintana Sattayasai[a] and David Ehrlich[b]

[a]Department of Pharmacology, Faculty of Medicine, Khon Kaen University, Khon Kaen 40002, Thailand

[b]Department of Anatomy, Monash University, Clayton, Victoria 3168, Australia

Abstract

In this study we examine the dose-response and time-response relationship of chick photoreceptors and retinal pigment epithelium following intraocular injection of kainic acid. Young white leghorn × black australorp chicks received a 10 µl, intraocular injection of either 5, 10, or 60 nmol KA in distilled water, brought to pH 7 with NaOH. Birds were killed at either 30 min, 1 h, 2 h, 6 h, 16 h, 24 h, 48 h or 96 h after treatment. Exposure to 5 nmol kainic acid, at all times, did not alter the appearance of either photoreceptors or pigment epithelium. Swelling of photoreceptor outer segments was observed at 10 nmol kainic acid, 1 h after exposure. The swelling was maximal at 6 h and persisted throughout the duration of the experiment. In contrast, increased evidence of disc shedding, as demonstrated by increased phagosomes in the pigment epithelium, was maximal at 30 min after exposure, and did not continue after 16 h.

Introduction

Over a number of years, our laboratory has investigated the effects of excitatory amino acids, kainic acid (KA), quisqualic acid (QUIS) and *N*-methyl-D-aspartic acid (NMDA), on the retina of chicks. Following exposure to the excitotoxins, a distinct pattern of neurotoxicity becomes evident for each of the compounds. For instance, KA selectively lesions bipolar, amacrine and ganglion cells; NMDA lesions mainly amacrine cells; QUIS lesions amacrine and horizontal cells [1–3]. All of the above neurotoxic effects are dose dependent and irreversible. However, one class of retinal cell, the photoreceptor, can be damaged by excitotoxins in a reversible manner [3,4]. Examination of this effect might provide information about the mechanism of action of excitatory amino acids. In addition, the role of the pigment epithelium during exposure to the neurotoxin has not been adequately assessed.

Evidence of disc shedding by rod and cone outer segments has been amply documented in a wide selection of vertebrate animals [5–9]. The apical tip of the photoreceptor outer segment is periodically detached, or 'shed', and phagocytized by the adjacent retinal pigment epithelial cell [10] in order to balance the continuous assembly of new disc membranes [11]. Several lines of evidence suggest that local factors within the eye play a fundamental role in controlling rhythmic disc shedding [12–16].

Recently, Greenberger and Besharse [17] reported that excitatory amino acids also induce massive rod photoreceptor disc shedding in frog eyecup maintained *in vitro*. Studies of the chick retina [4] also confirmed the effects of excitotoxins, KA and QUIS but not NMDA, on the outer segment disc. Whether the excitotoxins stimulate disc shedding specifically is still unknown. In this study we have examined the toxic effects of KA on the outer segment of disc morphology in relation to disc shedding.

Materials and Methods

Two-day old white leghorn × black australorp chicks obtained from local hatchery were lightly anaesthetized with ether and then given a single intraocular injection of either 5, 10 or 60 nmol KA in distilled water brought to pH 7 with NaOH. Control birds received 10 µl of distilled water. Injections were made within 10 s and the needle was left in place for a further 15 s. There were 4 retinae in each treatment condition. Birds were killed with an overdose of ether at either 30 min, 1 h, 2 h, 6 h, 16 h, 24 h, 48 h or 96 h after treatment. All the animals were killed during the period of 6–10 h after the onset of light which has been reported to have less phagocytotic activity of pigment epithelium [9].

The eyes were removed and hemisected. The posterior halves after removing the vitreous humour were immersed overnight at 4°C in a fixative consisting of 5% glutaraldehyde-3% paraformaldehyde in 0.1 M cacodylate buffer, pH 7.4. Using the pecten as a reference line, small pieces of retina were dissected out from the nasal areas and processed for electron microscopy [3]. Ultra thin sections were cut with a glass knife, stained with lead citrate prior to examination under electron microscope.

Results and Discussion

Examination of the outer segments from control retinae (Fig. 1A) revealed the orderly arrangement of the discs encircled by pigment epithelial processes containing pigment granules. The pigment epithelium contained many mitochondria and myeloid bodies (Fig. 1B). The phagosomes were imperceptible observed within the pigment epithelium.

Retinae at various times after a single intraocular injection of 5 nmol KA exhibited no morphological changes on the outer segment discs (Figs. 1C, D). The pigment epithelium was also comparable to control.

Examination of retinae 30 min, 1 h, 2 h, 6 h, 16 h, 24 h, 48 h and 96 h after a single intraocular injection of either 10 or 60 nmol KA (Figs. 2A–F) revealed major changes in the ultrastructure of the outer segment discs and the phagosome content in the pigment epithelium.

The swelling and distortion of the outer segment discs were first observed at 1 h after the injection and became much more severe at 6 h survival. More than half of

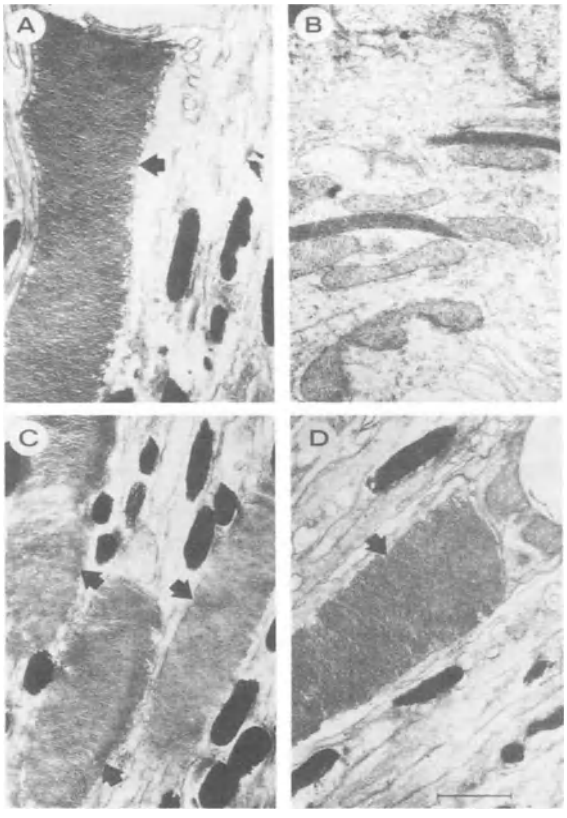

Fig. 1. Electron micrographs showing, A: photoreceptor outer segment from control retina. Note the orderly flattened sac structure (arrow) of the outer segment discs. B: pigment epithelium from control retina. Phagosomes could hardly be found during a period of 6–10 h after the onset of light. C & D: photoreceptor outer segments from retinae at 2 h (C) and 6 h (D) following a single intraocular injection of 5 nmol KA. Note the outer segment discs (arrows) appeared comparable to control. Bar = 1 μm.

the photoreceptor outer segments was affected and it seemed not localized to only either rods or cones. However, within the affected outer segment, small patches of normal discs were still present. The swollen discs gradually recovered after 16 h of injection and, at 4 d survival after 10 nmol KA, many outer segments appeared normal.

The number of phagosomes in the pigment epithelium was dramatically increased within 30 min after injection of either 10 or 60 nmol KA (Fig. 2D) and numerous numbers of phagosomes were still present up to 2 h survival. Both small and large size phagosomes were observed suggesting that they derived from both cones and rods [9]. Surprisingly, although the outer segment was still swollen at 6 h survival, the pigment epithelium appeared normal and phagosomes could hardly

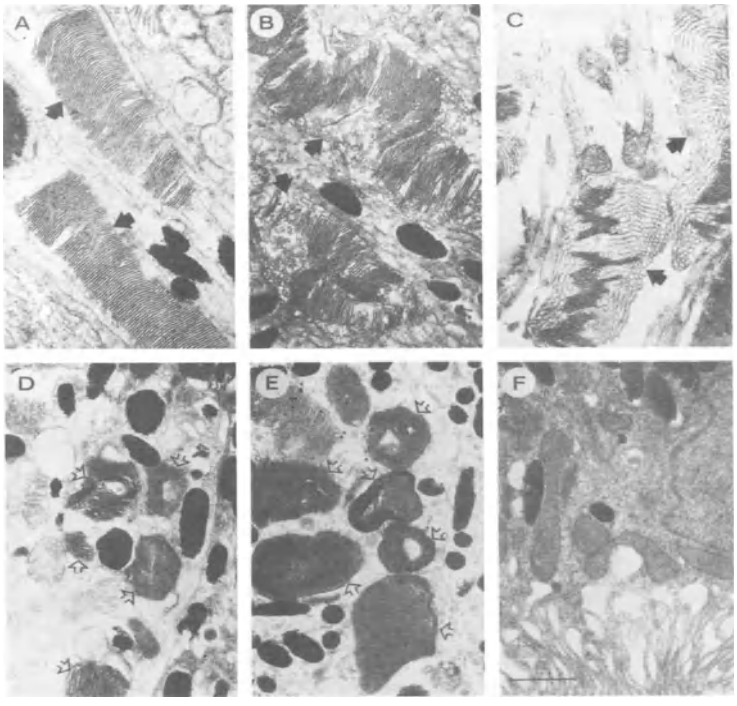

Fig. 2. Electron micrographs of the outer segments at 30 min (A), 1 h (8) and 6 h (C) and pigment epithelium at 30 min (D), 1 h (E) and 6 h (F) from the retinae received a single intraocular injection of 10 nmol KA. Note the normal appearance of outer segment discs appeared swollen and disorganized after 1 h (arrow in B) and 6 h (arrow in C) survival. Phagosome number (open arrows in D and E) was increased dramatically following 30 min (D) and 1 h (E) of injection. However, no phagosome could be observed after 6 h survival (F). Bar = 1 μm.

be observed (Fig. 2F). These changes were also evident after a single intraocular injection with 60 nmol KA, but were most severe.

The present study revealed that KA at doses higher that 5 nmol/eye increased photoreceptor disc shedding in chickens *in vivo*. Furthermore, our results also confirmed the neurotoxic effects of KA on the photoreceptor outer segments [4].

It is interesting that following treatment with 5 nmol KA, which exhibited its neurotoxic effects mainly on bipolar cells [1], there was no increase in phagosome number. In contrast at 10 nmol amacrine cells as well as photoreceptors were also affected, and there was an increase in disc shedding. Our results therefore suggest that postreceptoral neurons are unlikely to have a role in disc shedding.

A similar pattern of time-relationship of KA-induced increase in disc shedding has been observed with the high dose of KA. The increase in disc shedding reached its maximum within 30 min after injection and the membrane digestion completed

within 16 h. The rapid onset of these effects suggest a direct effect of KA on the induction of shedding of the discs.

The ultrastructural changes in the outer segments, following treatment with KA appear to be observed after the phase of disc shedding and persists through the experimental period (96 h), although many of the discs seem to recover, especially with lower dosages. The absence of phagosomes within the pigment epithelium while the outer segment discs were swollen suggests that there might be 2 distinct mechanisms responsible for both the increase in disc shedding and the neurotoxic effects on the disc structure. It is interesting to note that in frog, increase in disc shedding is not necessarily accompanied by swelling of the disc [17].

Any explanation of our results must, however, take into account the finding that excitatory amino acid can induce photoreceptor disc shedding, although the level might far exceed the normal light-evoked response [9]. It is possible that the excitatory amino acid, which is maximally released in the dark might be an important component of the disc shedding at the onset of the dark, whereas melatonin is responsible for the disc shedding at the onset of the light [14].

In conclusion, we have shown that KA can induce the increase in disc shedding and also has the neurotoxic effects on the outer segment discs. Although these effects have been observed at the same dose of KA in this study, the dose-response and time-response relationship suggest that the two processes may be independent.

References

1. Sattayasai J, Rogers LJ and Ehrlich D (1985) Neurosci. Lett. 54: 277–281.
2. Sattayasai J and Ehrlich D (1987) Exp. Eye Res. 44: 523–535.
3. Sattayasai J and Ehrlich D (1987) Invest. Ophthalmol. Vis. Sci. 28: 106–117.
4. Sattayasai J, Zappia J and Ehrlich D (1989) Vis. Neurosci. 2: 237–245.
5. Anderson DH and Fisher SK (1976) J. Ultrastruct. Res. 55: 119–141.
6. Basinger S, Hoffman R and Matthes M (1976) Science 194: 1074–1076.
7. La Vail MM (1976) Science 194: 1071–1074.
8. Young RW (1977) J. Ultrastruct. Res. 61: 172–185.
9. Young RW (1978) Invest. Ophthalmol. Vis. Sci. 17: 105–116.
10. Bok D and Young RW (1979) In: The Retinal Pigment Epithelium. Harvard Univ. Press, Cambridge, pp. 148–174.
11. Young RW (1976) Invest. Ophthalmol. 15: 700–725.
12. La Vail MM and Ward PA (1978) Invest. Ophthalmol. Vis. Sci. 17: 1189–1193.
13. Tamai M, Teirstein P, Goldman A, O'Brian P and Chander G (1978) Invest. Ophthalmol. Vis. Sci. 17: 558–562.
14. Hollyfield JG and Basinger SF (1978) Nature 274: 794–796.
15. Teirstein PS, Goldman AI and O'Brien PJ (1980) Invest. Ophthalmol. Vis. Sci. 19: 1273–1298.
16. Besharse JC, Terrill RO and Dunis DA (1980) Invest. Ophthalmol. Vis. Sci. 19: 1512–1517.
17. Greenberger LM and Besharse JC (1985) J. Comp. Neurol. 239: 361–372.

Address for correspondence: Jintana Sattayasai, Department of Pharmacology, Faculty of Medicine, Khon Kaen University, Khon Kaen 40002, Thailand.

CSF amino acids in childhood epilepsy

R.F. Goldsmith, J.W. Earl, R.A Ouvrier, P. Procopis and A.M. Cunningham*

Departments of Biochemistry and Neurology, The Children's Hospital, Camperdown, N.S.W., Australia

Introduction

Gamma-aminobutyric acid (GABA) is a major inhibitory neurotransmitter in mammalian brain and alterations in GABAergic function have been postulated to underlie seizure pathogenesis [1,2]. Studies of the GABA content of surgically removed epileptogenic foci have produced varying results with both elevated and low concentrations reported [3–5]. However, there is substantial evidence from experimental and clinical studies that CSF GABA concentrations may reflect central GABAergic activity [6,7]. Although the synthesis, metabolism and distribution of GABA in brain compartments is complex the CSF may provide an accessible means with which to study and follow changes in CNS neurotransmitters. Information on other CSF amino acids in epilepsy [8,9] is limited but it may be the balance between the excitatory amino acids, aspartic and glutamic acids, and inhibitory mechanisms that is important in seizure propensity. We are studying the concentration of GABA and other amino acids in the CSF of children with a variety of seizure disorders and febrile convulsions.

There is animal data to support the idea that low levels of CSF GABA may occur in generalized seizure states [10] and may indeed be correlated with seizure excitability [11]. Animal models have provided a valuable means with which to follow the effects of anticonvulsant therapy on seizures and CSF GABA levels. In particular, drugs which are believed to exert their major action through facilitation of GABA-mediated synaptic transmission, such as valproate and benzodiazepines, have been of interest and, in general, the results support a correlation between therapy and increased CSF GABA [11,12].

Studies of CSF GABA in humans have reported low concentrations in children with infantile spasms [13], idiopathic epilepsy [14], febrile convulsions [15] and in adults with various seizure states [16]. The newer GABA-mimetics certainly appear to be effective as anticonvulsants [16,17]. Advances in our understanding of the neurochemical basis of seizure disorders will provide more rational and appropriate therapy for the individual and allow the design of new anticonvulsants.

The ethical constraints concerning the collection of CSF in paediatric patients have meant that 'control' groups are often pyrexic patients undergoing lumbar

* Present address: Department of Molecular Biology and Genetics, The Johns Hopkins University School of Medicine, Baltimore, MD 21205, U.S.A.

puncture to exclude the diagnosis of meningitis. Many variables are known to alter the baseline chemical composition of CSF – in particular circadian rhythms, diet, medications, ventriculospinal concentration gradients and the effect of fever is unknown [18]. All these factors must be considered when planning studies and evaluating results. In addition, marked artifactual increases in neurotransmitter amino acids, especially GABA, occur rapidly at room temperature and during sample handling [19].

We have utilized a standardized collection and handling protocol [20] to minimize these effects and as a 'control' group used a group of healthy children undergoing elective myelography to exclude the diagnosis of spinal dysraphism. We report the concentration of GABA and 23 other amino acids in the CSF of children with a variety of seizure disorders, febrile convulsions and pyrexial illnesses and compared them with this group of control patients.

Methods

Twenty three amino acids including GABA were measured by a reverse phase high performance chromatography technique as previously reported [20]. In brief, 60 µl of CSF was mixed with 10 µl of internal standard. 20 µl of this mixture was then reacted with 120 µl of o-phthalaldehyde and the OPA-amino acids were then separated on a 5 µ C-18 reversed phase column using propionic acid-phosphate methanol-acetonitrile-water buffers. A run time of 65 min was needed to separate the amino acids. 5-hydroxyindole acetic acid (5-HIAA) and homovanillic acid (HVA) were measured on a reversed phase system using electrochemical detection.

Patients

The study group was comprised of 140 children aged 1 month to 15 years. They were subdivided into 5 categories:

1. 30 'normal' controls – children undergoing myelography as part of a diagnostic workup to exclude spinal abnormalities and who were subsequently shown to have normal CSF flow, cytology and chemistry and negative viral and bacterial cultures.
2. 31 children with a fever of unknown origin (PUO) who had a normal CSF examination and negative viral and bacterial cultures of CSF.
3. 21 children presenting acutely to hospital after suffering a fever-associated convulsion who underwent lumbar puncture to exclude meningitis as a cause of the fever.
4. A group of 23 children with idiopathic epilepsy, 6 of whom had infantile spasms, 9 had Lennox Gastaut syndrome and 8 with intractable seizures of uncertain origin.
5. A miscellaneous group of 35 children who underwent lumbar puncture as part of diagnostic evaluation. These children had a variety of clinical conditions such as spinal defects, optic neuritis, ataxia and miscellaneous neuropathies.

Results and Discussion

GABA concentrations and age

The mean CSF GABA concentration in the control group was 109 (± 39) nmol/L. This was similar to the mean concentration in the miscellaneous group 104 (± 58) nmol/L.

There was a significant correlation between age and GABA concentration in these two groups ($r = 0.28$, $p<0.02$). However an analysis of the data showed a wide variation in GABA concentrations in children under 4 years of age with one-third of children in this age group having a GABA concentration below 60 nmol/L (Fig. 1).

Febrile convulsions and pyrexia

CSF GABA concentrations were decreased in pyrexia the mean value in 31 patients being 79 (± 55) nmole/L. The values in patients having experienced a

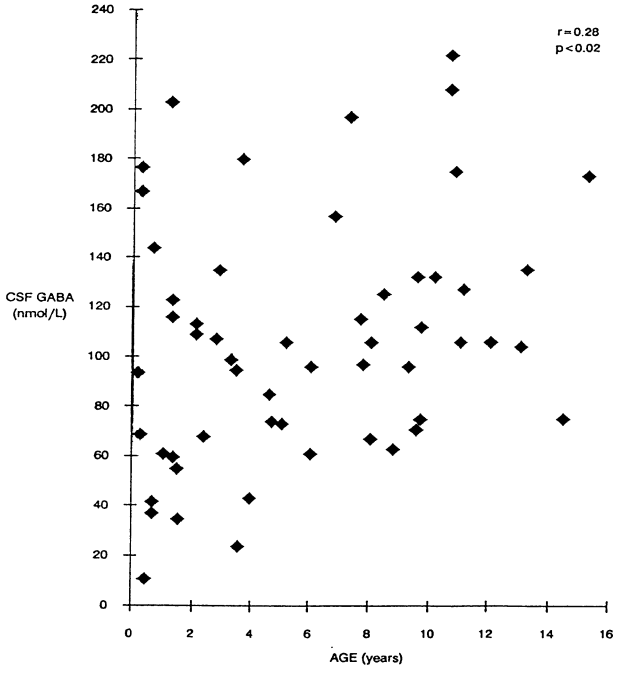

Fig. 1. The relationship between patient age in years and CSF GABA concentration (nmol/L) for the control and the miscellaneous study group. There is a trend for GABA to increase with age ($r = 0.28$, $p<0.02$).

Table 1. CSF neurotransmitter concentrations

		GABA nmol/L	Aspartic acid µmol/L	Glutamic acid µmol/L
Control group	n = 30	109 ± 39	0.48 ± 0.26	0.56 ± 0.22
PUO	n = 31	79 ± 55[a]	0.63 ± 0.46	0.77 ± 0.35[a]
Febrile convulsion	n = 21	68 ± 36[b]	0.44 ± 0.21	0.58 ± 0.38
Idiopathic epilepsy:				
Infantile spasms	n = 7(6)	29 ± 17[b]	0.24 ± 0.09[b]	0.48 ± 0.26
Lennox Gastaut	n = 10(9)	78 ± 37[b]	0.25 ± 0.12[b]	0.51 ± 0.27
Other generalized seizures	n = 8	44 ± 19[b]	0.26 ± 0.12[b]	0.44 ± 0.22

[a]$p<0.02$; [b]$p<0.001$; n = number of samples; (n) = number of patients.
Comparison between neurotransmitter concentrations in the control group and those in children with fever of unknown origin (PUO), febrile convulsions and idiopathic epilepsy. GABA concentration was measured before and after initiation of therapy in one patient with infantile spasms and one with Lennox Gastaut syndrome. In both cases GABA concentrations rose after treatment.

febrile convulsion were even lower, the mean value in 21 such patients being 68 (± 36) nmol/L (Table 1 and Fig. 2).

The low GABA concentration in pyrexia is suggestive that this may be a predisposing factor resulting in young children having febrile convulsions. Our data shows that young age itself is associated with low GABA concentrations, as is pyrexia alone. In combination, the diminished GABAergic inhibitory influences may underlie seizure occurrence in the young febrile child.

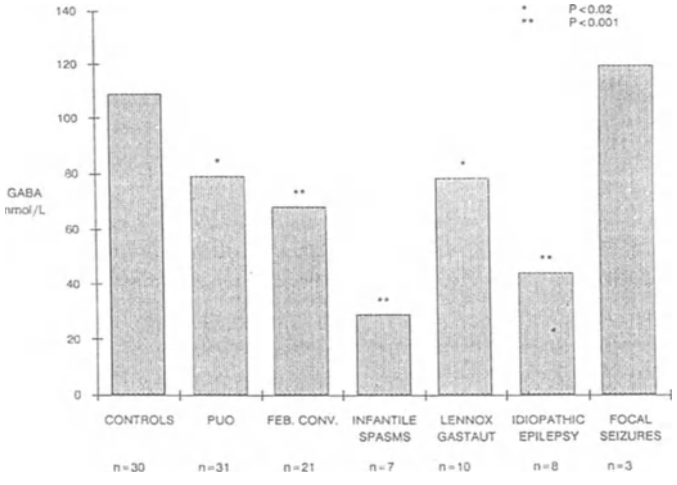

Fig. 2. CSF GABA concentration in the control group and various patient groups studied.

The concentrations of several other amino acids were significantly different in children with pyrexial illnesses when compared to control values. The basic amino acids lysine, arginine and ethanolamine were significantly reduced and phenylalanine was increased, often to three times normal values (Table 2). This 'fever pattern' was also seen in febrile children with meningitis, particularly bacterial meningitis, where concentrations of arginine sometimes dropped to 1.2 μmol/L and phenylalanine rose to 49.3 μmol/L.

These findings emphasize the importance of including children with a febrile illness as a separate group in any study of CSF amino acids. The tendency in the past has been to use these children as controls, but the significant differences found in this study suggest that these children are not valid control patients.

Generalized epilepsy

Turning to epilepsy, CSF GABA concentration was significantly lower in generalized forms of childhood epilepsy than in age matched controls but was not low in a small number of patients with focal seizures (Fig 2). The latter finding would be

Table 2. CSF Amino acid concentrations (μmol/L)

	Control group	PUO	Febrile convulsion	Idiopathic epilepsy
	n = 30	n = 31	n = 21	n = 25
Asparagine	5.5 ± 1.5	5.5 ± 1.9	5.1 ± 1.2	6.7 ± 1.8[a]
Serine	23.5 ± 5.7	27.0 ± 9.4	25.9 ± 9.4	31.7 ± 9,5[b]
Histidine	11.9 ± 2.8	10.3 ± 4.7	9.0 ± 4.6	12.7 ± 7.1
Glutamine	431.0 ± 187.6	429.0 ± 113	358.0 ± 92	525.0 ± 155
Glycine	5.1 ± 1.5	6.8 ± 3.5	5.9 ± 2.3	6.3 ± 2.4
Threonine	17.9 ± 4.1	16.0 ± 7.7	13.2 ± 3.2[b]	22.1 ± 7.3[a]
Arginine	18.6 ± 3.6	14.5 ± 4.2[b]	13.5 ± 4.4[b]	17.8 ± 4.2
Alanine	18.1 ± 4.7	17.6 ± 6.8	21.3 ± 5.8	23.7 ± 8.7[b]
Taurine	4.5 ± 0.6	4.1 ± 1.4	4.6 ± 2.0	5.1 ± 2.1
Tyrosine	8.6 ± 2.3	7.8 ± 3.2	8.2 ± 2.9	11.9 ± 7,3[a]
AABA	2.1 ± 0.7	2.4 ± 1.3	2.6 ± 1.1	2.9 ± 1.2[a]
Valine	11.9 ± 3.9	14.1 ± 7.3	12.0 ± 3.9	14.3 ± 7.8
Ethanolamine	7.1 ± 2.0	5.1 ± 1.9	5.6 ± 3.3	9.2 ± 11.2
Tryptophan	2.3 ± 0.5	2.4 ± 1.3	2.1 ± 0.7	2.3 ± 1.1
Phenylalanine	7.6 ± 1.62	13.2 ± 6.0[b]	14.1 ± 9.5[b]	8.4 ± 2.9
Isoleucine	4.3 ± 1.2	4.4 ± 1.8	3.9 ± 1.6	5.3 ± 2.1
Leucine	10.4 ± 2.2	11.0 ± 4.3	10.9 ± 3.9	11.8 ± 4.2
Ornithine	5.8 ± 1.4	6.1 ± 2.4	4.9 ± 2.3	7.9 ± 3.5[a]
Lysine	14.4 ± 4.5	10.1 ± 4.5[b]	8.9 ± 3.6[b]	16.6 ± 7.2

[a] $p<0.01$; [b] $p<0.001$.

CSF amino acid concentrations in children with fever of unknown origin (PUO), febrile convulsions and idiopathic epilepsy compared to a control group of children.

consistent with the normal brain tissue GABA concentration found in patients undergoing surgical resection of an epileptogenic focus for intractable partial seizure disorders [21].

The lowest GABA concentration was found in children with infantile spasms. This is in agreement with the study of Loscher and Siemes, 1985 [14] who reported low CSF GABA concentration in infantile spasms and unmedicated patients with generalized tonic clonic seizures.

Of the 22 other amino acids assayed several were significantly different from control values (Tables 1 and 2). Aspartic acid concentration was low in children with idiopathic epilepsy, a somewhat surprising finding. However it is in agreement with the study of Crawford and Chadwick, 1987 [9]. Glutamic acid concentration was not low in our patients but was high in febrile children who were not experiencing seizures. Indeed in the PUO group there was a significant negative correlation between GABA and glutamic acid concentrations ($r = -0.40$, $p<0.01$). Thus we hypothesize that this amino acid profile, with a high glutamic acid concentration in the presence of a low GABA concentration may actually provide some protection against fitting, hence these young children present with high fevers but not febrile convulsions.

In the group of generalized idiopathic seizures significant elevations of serine and alanine were found. These increases were not associated with high protein concentration, a common cause of high amino acid concentrations in CSF. CSF serine concentration has been shown to be increased in infants [8] and we have found this also, but there did appear to be a further increase in the epileptic group.

CSF HVA and 5-HIAA were not significantly different in either generalized epilepsy or febrile convulsions.

Conclusions

In the light of these findings the following provocative postulates may be made:

1. The low concentrations of GABA in CSF may be directly related to the much higher prevalence of seizures in infancy and early childhood.
2. Fever, which by some unknown mechanism, further reduces low concentrations of central nervous system GABA in young children, decreases the natural inhibitory defences of the brain resulting in the phenomenon of febrile convulsions.
3. The potential usefulness of anticonvulsants exerting this action via GABA mediated pathways, such as valproate, might be evaluated by assaying CSF GABA concentrations after a standard dosage regime.

The following questions remain to be answered:

1. What is the source of the 'fever pattern' i.e. low basic amino acids, arginine and lysine in combination with high phenylalanine concentrations, and does this contribute to the phenomenon of febrile convulsions?

2. What is the significance of the *low* aspartic acid concentration in children with idiopathic epilepsy in view of the fact that aspartic acid is an *excitatory* amino acid? CSF aspartic and glutamic acid concentrations are markedly low compared to serum concentrations. Is this a reflection of a localized metabolic pool or active transport mechanism? What does the concentration of CSF amino acids signify about the overall neurotransmitter state of the brain?

Much work needs to be done in the study of CSF amino acid concentrations in children with the use of appropriate proper control groups, good analytical techniques and suitable sample collection and storage. All CSF collected should be analyzed for the presence of cells and protein concentration, both of which may contribute to artifactually high aspartic and glutamic acid concentration and due attention must be paid to this in any analysis of patient data.

References

1. Meldrum BS (1979) In: Krogsgaard-Larsen P, Scheel-Kruger J and Kofod H (eds.) GABA, Neurotransmitters, Pharmocochemical, Biochemical and Pharmocological Aspects. Copenhagen, Murksgaard, pp. 390–405.
2. Loscher W and Schwark WS (1985) Brain Res. 339: 146–150.
3. Van Gelder NM, Sherwin AL and Russmussen T (1972) Brain Res. 40: 385–393.
4. Perry TL and Hanson S (1981) Neurology 31: 872–876.
5. Schmidt D, Cornaggia C and Loscher W (1984) In: Fariello RG et al. Neurotransmitters, Seizures and Epilepsy II. Raven Press, NY, pp. 275–283.
6. Enna SJ, Wood JH and Snyder SH (1977) J. Neurochem. 28: 1121–1124.
7. Bohlen P, Huot S and Palfreyman MG (1979) Brain Res. 167: 297–305.
8. Spink DC, Snead OC, Swan JW and Martin DL (1988) Epilepsia 29: 300–306.
9. Crawford PM and Chadwick DW (1987) Epilepsy Res. 1: 328–338.
10. Loscher W and Schwartz-Porsche D (1986) J. Neurochem 46: 1322–1325.
11. Loscher W (1982) J. Neurochem. 38: 293–295.
12. Loscher W and Schmidt D (1987) J. Neurochem. 49: 152–157.
13. Ito M, Mikawa H and Snyder SH (1984) Neurology 34: 235–238.
14. Loscher W and Siemes H (1985) Epilepsia 26: 314–319.
15. Rating D Siemes H and Loscher W (1983) J. Neurol. 230: 217–225.
16. Wood JH, Hare TA, Glaeser BS, Ballenger JC and Post RM (1979) Neurology 29: 1203–1208.
17. Hammond EJ and Wilder BJ (1985) Clin. Pharmacol. 8: 1–12.
18. Hare TA, Grossman MH, Wood JH, Glaeser BS and Manyam NVB (1980) Brain Res. Bull. 5(2): 725–729.
19. Ferraro TN, Manyam BV and Hare TA (1983) J. Neurochem. 41: 1057–1065.
20. Goldsmith RF, Earl JW and Cunningham AM (1987) Clin. Chem. 33: 1736–1740.
21. Sherwin AL and van Gelder NM (1986) Adv. Neurol. 44: 1011–1032.

Regulation of amino acid uptake into astrocytes: One way to modulate neuronal activity

Elisabeth Hansson[a] and Lars Rönnbäck[a,b]

[a]Institute of Neurobiology and [b]Department of Neurology, University of Göteborg, Göteborg, Sweden

Abstract

Astrocytes express receptors for monoamine and amino acid neurotransmitters and neuropeptides, uptake carriers for at least amino acid neurotransmitters and enzymes for transmitter catabolism. Recent data indicate interactions between second messengers for neuropeptide and monoamine receptors. Stimulation of α_1 and ß adrenoceptors leads to changes in the uptake capacity of glutamate and GABA into the cells while 5-hydroxytryptamine (5-HT) and α_2 receptor stimulation was ineffective. The aspartate uptake was not affected by any of the monoamine receptor agonists used. With regard to the anatomy of the cells with processes extending into synaptic regions and also establishing contacts with vessels and the brain surface, the astrocytes might supervise and regulate synaptic transmission. In addition, astrocytes seem to express somewhat different properties in various brain regions, suggesting a specificity concerning at least some functions in various neuronal systems.

A hypothesis based on experimental results partly from our laboratory, suggests that astrocytes can control, regulate and probably modulate synaptic transmission and thereby neural activity. If this hypothesis is correct, then specific effects on these cells might be a new way to restore dysfunction of the nervous system e.g. in epilepsy.

Introduction

A complex network of stimulatory and inhibitory neurons and feedback loops is considered responsible for the unique capacity of the central nervous system (CNS) to take in, work upon, accumulate and leave information. In addition to neurons, glial cells constitute a major cell population. Astrocytes, comprising up to 50% of the cell number in the cerebral cortex of higher mammals, can be divided into the two morphologically different types fibrillar and protoplasmic. The protoplasmic astrocytes extend long processes to the blood vessel walls on one hand, and to synaptic regions on the other. The cells are arranged in a network (syncytium) with gap junctions between the processes [1]. They can be depolarized but no action potential is formed [2].

From experiments using dissociated primary cultures from immature rat brain, astrocytes are known as metabolically active with a prominent protein synthesis [3]. Proteins are also secreted to the extracellular medium [4]. The cells express a large number of receptors for neurotransmitters [5–8] and uptake carriers for at least some amino acid neurotransmitters [9]. The cells also synthesize enzymes for neurotransmitter catabolism [8].

Interestingly, late research has demonstrated the presence of interactions between different classes of receptors [e.g. 10–13] and second messenger systems (e.g. cyclic AMP and the inositolphosphate system) [14]. Interactions have also been demonstrated to exist between monoamine receptors (α and ß) and uptake carriers (for GABA and glutamate) [15]. In this paper we will show further data on the specificity of such uptake regulation by monoamine receptor stimulation. We will also present a hypothesis where astrocytes actively participate in neuronal integration.

Materials and Methods

Cultures

Primary astroglial cultures were made from neonatal rat cerebral cortex (Sprague-Dawley strain, A-lab, Sweden), cultivated for 14 days in a humidified atmosphere [16].

Uptake studies

Transport studies were performed after transferring the cultures into serum-free Eagle's MEM for one hour. The isotopes were from NEN, Boston, Mass., U.S.A., and the cold transmitters, agonists and antagonists were from Sigma Fine Chemicals, St. Louis, U.S.A. 1.0 mCi/ml L-[2,3-^{3}H]-glutamate (20.4 Ci/mmol) plus L-glutamate in a concentration range of 1×10^{-7}–3.5×10^{-4} M were added to the incubation medium for the glutamate experiments. 1.0 mCi/ml γ-[2,3-^{3}H(N)]-aminobutyric acid (GABA; 40.1 Ci/mmol) plus GABA in a concentration range of 1×10^{-7}–3.5×10^{-4} M were added to the incubation medium for the GABA experiments, and 5×10^{-5} M aminooxyacetic acid (AOAA) was supplied to inhibit γ-aminobutyric acid transaminase (GABA-T). 1.0 mCi/ml L-[2,3-^{3}H]-aspartate (14.9 Ci/mmol) plus L-aspartate in a concentration range of 1×10^{-7}–3.5×10^{-4} M were added to the incubation medium for the aspartate experiments.

The incubation period was 4 min at 37°C. The procedure has been described in detail by Hansson *et al* [9]. The agonists, 5-HT, phenylephrine (α_1-agonist), clonidine (α_2-agonist) and isoproterenol (ß-receptor agonist) were added in graded concentrations, 10^{-7}, 10^{-6}, 10^{-5}, and 10^{-4} M 15 sec. before the aspartate, glutamate or GABA transport experiments. Ketanserin was used as a 5-HT antagonist, prazosin as an α_1-antagonist, yohimbine as an α_2-antagonist and propranolol as a ß-receptor antagonist. The V_{max} and K_m values were calculated using a Lineweaver-Burk plot. Protein determinations were made according to Lowry *et al.* [17] with bovine serum albumen as standard.

Results

The V_{max} and K_m values obtained for glutamate, GABA and aspartate uptake are shown in Table 1. In the presence of the α_1 agonist phenylephrine there was an increased active uptake (V_{max}) of glutamate while ß-adrenoceptor activation caused a slight inhibition of the glutamate uptake (Table 2) and a stimulation of the GABA uptake (Table 3). There were no changes in the K_m values. The uptake rates of GABA and glutamate were not affected by 5-HT or the α_2-receptor agonist clonidine. The active uptake of aspartate was unaffected by the presence of any of the monoamine receptor agonists used in this study.

Table 1. Kinetic constants of ^{3}H-L-glutamate (Glu), ^{3}H-GABA and ^{3}H-L-aspartate (Asp) uptake into primary astroglial cultures from newborn rat cerebral cortex

	K_m (µM)	V_{max} (nmol·mg prot^{-1}·min^{-1})
Glu	21.9 ± 4.5	6.28 ± 1.85
GABA	4.4 ± 0.7	0.014 ± 0.003
Asp	10.4 ± 6.2	0.19 ± 0.09

Mean ± S.E.M. of 3 experiments with 3 Petri dishes in each.

Table 2. ^{3}H-L-glutamate uptake, (Glu), V_{max} (nmol·mg prot^{-1}·min^{-1}) was measured after preincubation with the α_1-agonist phenylephrine (phe) and the ß-agonist isoproterenol (iso).

10^{-6} M phe	8.5 ± 1.3
10^{-5} M phe	12.0 ± 2.1[b]
10^{-4} M phe	14.5 ± 2.3[b]
10^{-6} M iso	3.3 ± 1.3[a]
10^{-5} M iso	1.5 ± 0.3[a]
10^{-4} M iso	8.4 ± 0.9

Values are means ± S.E.M. of 3 experiments with 3 Petri dishes in each.
Statistical evaluation: Student's t-test.
[a] $p<0.05$ compared to control.
[b] $p<0.01$ compared to control.

Table 3. ^{3}H-GABA uptake, V_{max} (pmol·mg prot^{-1}·min^{-1}) was measured after preincubation with the ß-agonist isoproterenol (iso)

10^{-7} M iso	38.1 ± 2.9[b]
10^{-6} M iso	35.7 ± 8.9[b]
10^{-5} M iso	22.4 ± 5.3
10^{-4} M iso	23.0 ± 11.3

Values are means ± S.E.M. of 3 experiments with 3 Petri dishes in each.
Statistical evaluation: Student's t-test.
[a] $p<0.05$ compared to control.
[b] $p<0.01$ compared to control.

Discussion

The K_m and V_{max} values for the amino acid neurotransmitters are at a similar level to those observed in earlier studies, although the kinetic parameters for the aspartate uptake were lower than earlier observed [9]. From the present results it can be concluded that the uptake rates of glutamate and GABA are influenced by the stimulation of α_1 and ß adrenoceptors. There was some specificity since 5-HT and α_2 agonists did not affect the uptake rates, nor was the aspartate uptake influenced by any of the monoamine receptor agonists used.

The anatomy of an astrocyte is interesting as one cell has contact with synaptic regions and thus one cell possibly registers the synaptic activities, i.e.
- the release of transmitter from the presynaptic terminal
- the transmitter activity in the synaptic space
- the electrical activation of the postsynaptic membrane.

In addition there are indications suggesting that astrocytes are to some extent specialized in different brain regions [11, 18–22]. By the expression of receptors, uptake carriers and interaction between these systems, astrocytes might supervise, control, facilitate and partly regulate synaptic transmission in many synaptic regions. Thus, when there is a prominent stimulation or inhibition in one synaptic region, the cells might communicate with and modify the pre- or postsynaptic membranes in another. If such a modifying capacity of astrocytes upon neuronal activity exists, it might prevent uncontrolled spreading of electrical activity as in epilepsy.

Acknowledgements

This study was supported by grants from the Swedish Medical Council (project No. 12X-06812), Torsten and Ragnar Söderberg's Foundation and the Swedish Fund for Scientific Research without Animal Experiments.

References

1. Peters A, Palay SL and Webster H de F (eds.) (1976) In: The Fine Structure of the Nervous System: The neurons and supporting cells. Saunders, Philadelphia.
2. Kimelberg HK (1983) Cell Molec. Neurobiol. 3: 1–16.
3. Hansson E and Rönnbäck L (1983) Neurochem. Res. 8: 375–388.
4. Hansson E and Rönnbäck L (1985) J. Neurosci. Res. 14: 479–490.
5. Evans T, McCarthy KD and Harden TK (1984) J. Neurochem. 43: 131–138.
6. Murphy S and Pearce B (1987) Neurosci. 22: 381–394.
7. Van Calker D, and Hamprecht B (1980) In: Fedoroff S and Hertz L (eds.) Advances in Cellular Neurobiology, Vol. 1. Academic Press, New York, pp. 31–67.
8. Hansson E (1988) Progr. Neurobiol. 30: 369–397.
9. Hansson E, Eriksson P and Nilsson M (1985) Neurochem. Res. 10: 1335–1341.
10. Rougon G, Noble M and Mudge AW (1983) Nature 305: 715–717.

11. Chneiweiss H, Glowinski J and Prémont J (1985) J. Neurochem. 44: 779–786.
12. Niehoff DL and Mudge AW (1985) EMBO J. 4: 317–321.
13. Hansson E and Rönnbäck L (1988) Neuropharmacol. 27: 295–300.
14. Hansson E, Simonsson P and Alling C (1990) Interactions between Cyclic AMP and Inositolphosphate Signalling Transduction Systems in Astrocytes in Primary Culture. Neuropharmacology, in press.
15. Hansson E and Rönnbäck L (1989) Life Sciences 44: 27–34.
16. Hansson E, Rönnbäck L, Persson LI, Lowenthal A, Noppe M, Alling C and Karlsson B (1984) Brain Res. 300: 9–18.
17. Lowry OH, Rosebrough NJ, Farr AL and Randall RJ (1951) J. Biol. Chem. 193: 265–275.
18. Burgess SK, Trimmer PA and McCarthy KD (1985) Brain Res. 335: 11–19.
19. Cholewinski AJ and Wilkin GP (1988) J. Neurochem. 51: 1626–1633.
20. Cholewinski AJ, Hanley MR and Wilkin GP (1988) Neurochem. Res. 13: 389–394.
21. Schousboe A and Divac I (1979) Brain Res. 177: 407–409.
22. Hansson E (1986) Neurochem. Res. 11: 759–766.

Address for correspondence: Dr. Elisabeth Hansson, Institute of Neurobiology, University of Göteborg, P.O. Box 33 031, S-400 33 Göteborg, Sweden.

Probing glycine interactions at the *N*-methyl-D-aspartate receptor with the ^{22}Na flux assay

L.M. Pullan*

CNS Diseases Research, Searle, St. Louis, MO 63198, U.S.A.

Abstract

N-Methyl-D-aspartate (NMDA) stimulated ^{22}Na flux from rat hippocampal slices has previously been used to explore the NMDA receptor complex. The pharmacology correlates well with NMDA sensitive [^{3}H]-glutamate receptor binding and with excitotoxicity preventable by 2-amino-7-phosphonoheptanoate (AP7). Reported here is the modest enhancement by glycine and the reversal by glycine of kynurenic acid inhibition of NMDA stimulated sodium flux. Glycine does not alter inhibition by 2-amino-7-heptanoate and possibly appears to enhance the effect of phencyclidine. The reversal of kynurenic acid inhibition by glycine is strychnine insensitive. The rank order of potency for reversal of kynurenic acid inhibition is glycine > D-serine > L-serine > L-alanine. The kynurenic acid inhibition of NMDA stimulated sodium flux appears noncompetitive in the absence of added glycine, but competitive in the presence of 100 μM glycine. Schild plot analysis is consistent with a theoretical model where kynurenic acid acts both as a competitive antagonist to NMDA and at a second site from which it is displaced by glycine. Thus kynurenic acid illustrates the complication of either non-selectivity or a possible allosteric interactions of the glycine antagonists with the NMDA competitive agonist recognition site.

Introduction

Responses at the *N*-methyl-D-aspartate (NMDA) excitatory amino acid receptor complex are modulated allosterically by glycine [1]. However, the selectivity of ligands at the glycine site remains unclear. Ligands such as kynurenic acid, 1-hydroxy-3-aminopyrrolidone-2 (HA-966), and 7-Cl-kynurenic acid, originally identified as noncompetitive NMDA antagonists [2–4], have recently been described as glycine antagonists [5–7]. The inhibition by these agents of responses to NMDA is reversible by the addition of agonists for the glycine recognition site such as glycine or D-serine. However, the reversal of inhibition by glycine or D-serine may mask some inhibition of NMDA responses due to actions at the NMDA recognition site. Selectivity of glycine antagonists for the glycine site is yet to be fully explored.

This report describes the modulation of NMDA stimulated sodium flux from rat hippocampal slices by the endogenous agonist glycine and the endogenous antagonist kynurenic acid and demonstrates through Schild plot analysis the competition of kynurenic acid with glycine and with NMDA. The pharmacology in NMDA

* Currently at ICI Pharmaceuticals Group, ICI Americas Inc., Wilmington, DE 19897, U.S.A.

stimulated sodium flux has previously been found to correlate well with NMDA sensitive [^{3}H]glutamate receptor binding and with excitotoxicity preventable by 2-amino-7-phosphonoheptanoate (AP7) [8,9]. Portions of this report have appeared previously [10].

Methods

The assay of the stimulation of sodium flux was as previously described [9]. All reagents were reagent grade. Briefly, 4 slices (325 μM thick) of hippocampus from 30–45 day old male Sprague-Dawley rats were placed into a sieve in oxygenated physiological medium (124 mM NaCl, 5 mM KCl, 1.24 mM $MgSO_4$, 2 mM $CaCl_2$, 10 mM glucose, 26 μM Tris HCl, pH 7.3). After 30 min the sieve was transferred into oxygenated physiological medium containing 2 μCi of radioactive ^{22}NaCl (New England Nuclear, Boston, Massachusetts) for 30–45 min. The slices were then washed by transferring the sieve every 30 s through a series of 8 tubes, each containing 1 ml of nonradioactive physiological buffer with 1.7 μM tetrodotoxin. Tubes 9–12 were used to establish a basal rate of flux for each sample. Tubes 13–16 contained the agonist, antagonist or agonist with antagonist. Controls contained only physiological buffer. Each determination had at least three replications. The radioactivity in each tube and in the slices at the end of the experiment was measured in a gamma counter.

An index of total stimulated flux above basal, I, summed the agonist stimulated flux in tubes 13–16 where:

$$I = \sum_{t = 6.5}^{8} \frac{(R_t - R_c)}{R_c}$$

R_c is the mean basal flux rate for the two tubes just prior to the tubes containing agonist. The flux rate R_t (the relative change in content of ^{22}Na per min at time t) was defined as:

$$R_t = \frac{C_{t-0.5} - C_t}{C_{t-0.5} \times 0.5}$$

where C_t is the content of radioactivity of the sample at time t and $C_{t-0.05}$ is the content 0.5 min earlier. The percent of control was then expressed as the percent of the index of total stimulated sodium flux to that produced by 100 μM NMDA. The two-tailed t-test was used to compare pairs of conditions.

Dose-response curves for NMDA were constructed with various concentrations of glycine and kynurenic acid. Dose ratios were defined as the EC_{50} values for NMDA in the presence and absence of kynurenic acid. Schild plot lines, log(dose ratio −1) versus log([kynurenic acid]), were constructed for no glycine, 100 μM glycine and 400 μM glycine using independent linear least squares regression.

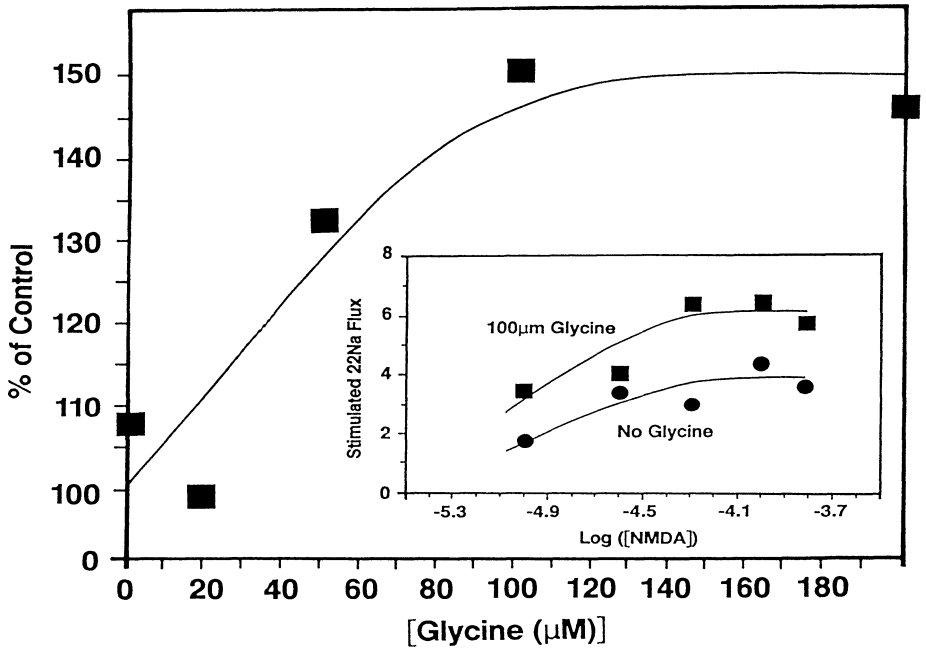

Fig. 1. Glycine enhances NMDA stimulated sodium flux from rat hippocampal slices. The enhancement by glycine of NMDA stimulated sodium flux is concentration dependent with a maximal enhancement of approximately 50% above 100 μM glycine. The data is expressed as a percent of the control flux stimulated by 100 μM NMDA in the absence of added glycine. Each point represents the mean of three experiments each containing 5 replicates. There was no effect of glycine on the basal flux. Inset: The enhancement by glycine appears to be non-competitive in that the maximal response to NMDA is increased.

Results

The enhancement of NMDA stimulated sodium flux by glycine is concentration dependent with a maximal enhancement of approximately 50% above 100 μM, and it appears noncompetitive in that the maximal response to NMDA is increased (Fig. 1). In a separate series of experiments (Fig. 2), NMDA stimulated sodium flux is enhanced by 100 μM glycine (127 ± 7% of NMDA alone, $p<0.05$). Glycine does not alter the inhibition by D-AP7 of NMDA stimulated sodium flux. NMDA (100 μM) with 100 μM D-AP7 gives 34 ± 10% ($p<0.05$) of the flux seen with NMDA alone, and the addition of 100 μM glycine results in 32 ± 8% ($p<0.05$) of the flux seen with NMDA alone. Glycine may enhance the inhibition by phencyclidine (PCP), although the differences here are not statistically significant. PCP (100 μM) added to the NMDA gives 27 ± 7% ($p<0.05$) of the flux with NMDA

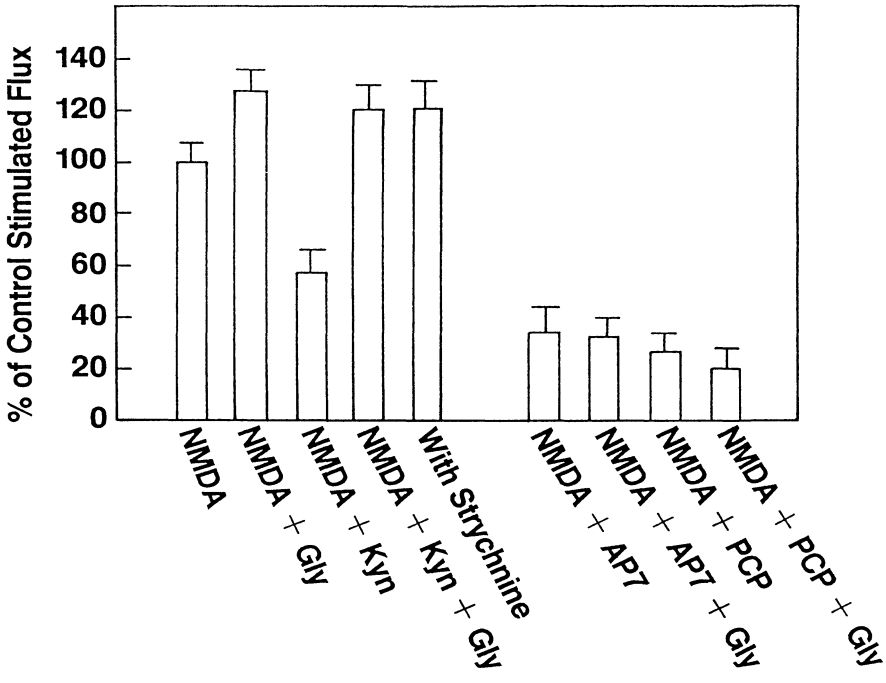

Fig. 2. The effects of glycine and kynurenic acid appear to be at least partially mediated via the glycine recognition site. The data is expressed as a percent of the control flux stimulated by 100 μM NMDA in the absence of added glycine. Each bar represents the mean ± SEM of three experiments, each containing five replicates. The enhancement by glycine was significantly different from the control of NMDA alone as determined at the 95% confidence level by a two-tailed t-test. Also statistically significant was the inhibition by kynurenic acid (Kyn), the reversal by glycine of the kynurenic inhibition, the inhibition by AP7 and the inhibition by PCP. Not statistically significant was the effect of strychnine, nor the effect of glycine on the inhibition by AP7 or PCP.

alone, while 100 μM glycine, 100 μM PCP and 100 μM NMDA results in 20 ± 8% of the flux seen with NMDA alone.

The inhibition by 100 μM kynurenic acid (57 ± 7% of that seen with NMDA

Table 1. The EC_{50} values for the reversal of inhibition by 100 μM kynurenic acid of sodium flux stimulated by 100 μM NMDA. Each value was determined from logit-log fit of the dose-response curve, averaging the values for three experiments

	EC_5 (μM)
Glycine	30
D-Serine	43
L-Serine	100
L-Alanine	>100

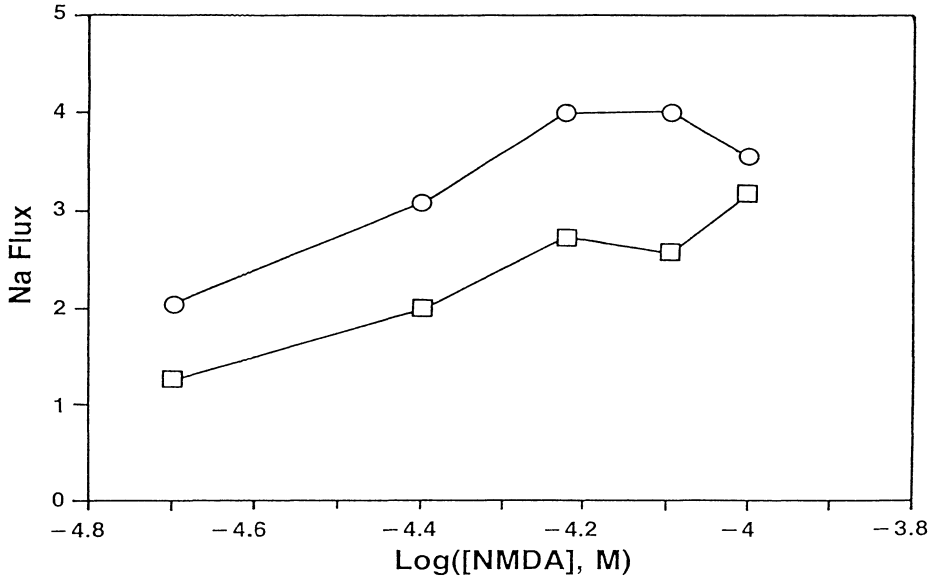

Fig. 3. The inhibition by 100 μM kynurenic acid (squares) of sodium flux stimulated by 100 μM NMDA (circles) appears noncompetitive. Each point represents the mean of five replicates. The data is expressed as an index of total agonist stimulated flux above basal.

alone, $p<0.05$) is reversed by 100 μM glycine or D-serine to give stimulated flux of 120 ± 10% ($p<0.05$) (Fig. 2). The reversal by glycine is strychnine (1 μM) insensitive, resulting in flux of 121 ± 9% of NMDA alone. As tabulated in Table 1, the rank order of potency for reversal of kynurenic acid inhibition is glycine (EC_{50} = 30 μM)>D-serine (EC_{50} = 43 μM)>L-serine (EC_{50} = 100 μM)>L-alanine (EC_{50}>100 μM). Kynurenic acid inhibits NMDA stimulated sodium flux in an apparently insurmountable manner, reducing the maximal response (Fig. 3).

A Schild plot (Fig. 4) of kynurenic acid antagonism of NMDA stimulated sodium flux in the absence of exogenous glycine results in a slope of 0.6 ± 0.1 ($r = 0.99$), not consistent with competitive inhibition. A Schild plot for kynurenic acid on NMDA in the presence of 100 μM glycine gives a slope of 1.0 ± 0.3 ($r = 0.90$). At 400 μM glycine, the slope is 1.9 ± 0.2 ($r = 0.98$).

Discussion

We report here the enhancement by glycine of NMDA stimulated sodium flux from rat hippocampal slices. The enhancement is modest, presumably due to endogenous glycine in this preparation. More substantial exploration of receptor interactions is possible with the glycine antagonist inhibition of NMDA stimulated sodium flux.

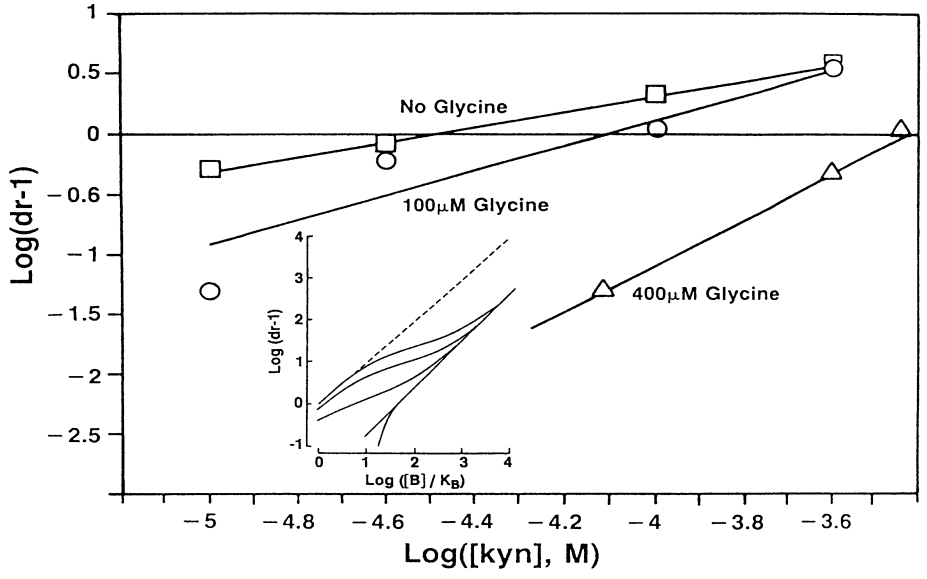

Fig. 4. A Schild plot of kynurenic acid against NMDA stimulated sodium flux with no glycine (squares), 100 μM glycine (circles), and 400 μM glycine (triangles). Each line was constructed with independent linear least squares regression from EC_{50} values from NMDA dose-response curves from three experiments each containing five replicates. Inset: A theoretical Schild plot for competitive antagonism complicated by the presence of an antagonist 'removal' site as adapted from Kenakin [11]. The various curves reflect different ratios of affinities of the antagonist for the 'removal' site and the agonist recognition site where function is assayed.

The reversal by glycine agonists of inhibition of NMDA stimulated sodium flux is strychnine insensitive. The effect of glycine is specific to the glycine site of the NMDA receptor complex in that the inhibition of ligands competitive (D-AP7) and non-competitive (PCP) to the NMDA receptor complex are not reversed. Indeed, glycine may enhance (not statistically significantly) the inhibition by PCP, as might be predicted from the enhancement by glycine of [^{3}H](+)-5-methyl-10,11-dihydro-5H-dibenzo[a,d]cyclohept-5,10-imine maleate (MK-801) binding [11]. The reversal by glycine of kynurenic acid inhibition of NMDA stimulated sodium flux is mimicked by other glycine agonists with a rank order of potency of glycine > L-serine > D-serine > L-alanine.

Kynurenic acid inhibition of NMDA stimulated sodium flux appears insurmountable, presumably due to inhibition predominantly through the allosteric glycine site of the NMDA receptor complex. To probe if, in addition to interactions at the glycine site, kynurenic acid interacts with the NMDA competitive recognition site, Schild plots were done using NMDA as the varied agonist. (Schild plots against glycine would presumably reflect primarily the competitive interaction of

kynurenic acid at the glycine site.) No effort is made to use the Schild plot to determine affinity at either site since kynurenic acid affects both sites simultaneously and agonists at both sites are present at unknown endogenous concentrations.

A Schild plot of kynurenic acid against NMDA in the absence of exogenous glycine gives a slope of 0.6 ± 0.1, apparently not competitive. However, the addition of glycine can shift the inhibition of kynurenic acid to a form apparently consistent with competition with NMDA. Addition of 100 μM glycine results in a slope of 1.0 ± 0.3, classically defining competitive inhibition and suggesting that saturation of the glycine site results in the competition of kynurenic acid for the NMDA site.

The Schild plots of kynurenic acid against NMDA in the presence of 0, 100, and 400 μM glycine resemble the theoretical curves for various ratios of affinities of the antagonist for the agonist recognition site and a second site [12]. Kenakin drew a calculated plot (see inset Fig. 4) for an antagonist which interacts not only at an agonist recognition site but also at an antagonist 'removal site'. Each curve reflects the theoretical Schild plot for a different ratio of the affinity of the antagonist for the agonist recognition site (where function is being assayed) and for a removal site for the antagonist. (The removal site can be a second site for the antagonist resulting in a lower free concentration of the antagonist). Curvature of Schild lines is most pronounced at low dose ratios, and the theoretical curves contain portions with varying slopes. At higher dose ratios the theoretical curves straighten.

Thus it appears we have mimicked the theoretical Schild curves expected for a competitive antagonist which also acts at a second site. By altering the concentrations of glycine, a competing ligand for the 'removal site', we have produced the expected series of curves for various ratios of affinities of the antagonist for its two sites. The apparent slopes we obtained are at low dose-ratios and reflect the lower nonlinear portions of the theoretical curves of Kenakin. Adding glycine to saturate the glycine site shifts the curve for kynurenic acid inhibition of the NMDA response. The addition of glycine lowers the apparent affinity of kynurenic acid for the glycine site and steepens the Schild plot curve for the effect of kynurenic acid against NMDA. These results are consistent with a model where kynurenic acid acts both as a glycine antagonist and as a competitive antagonist to the NMDA site. Kynurenic acid has also been characterized as an antagonist against kainate/quisqualate actions [4]. The broad spectrum of antagonism, the efficacy of kynurenic acid against hypoxic damage [13], and the speculation of possible involvement of the related kynurenines in Huntington's Disease [14] makes kynurenic acid interesting.

Glycine antagonists described to date lack specificity for the glycine site. 7-Cl-kynurenic acid may be the antagonist most selective for the glycine site (EC_{50} 0.56 μM) but also has some affinity (EC_{50} 169 μM) at the NMDA site [7]. Presumably the structural similarity of the glycine and glutamate recognition sites makes it difficult to design a ligand truly selective for the glycine or glutamate recognition site of the NMDA receptor complex. 6-Cyano-7-nitroquinoxaline-2,3-

dione (CNQX) was originally described as a non-NMDA antagonist [15], then found to be a glycine antagonist [16]. Addition of D-serine or glycine converted the inhibition by CNQX of the NMDA response from apparently non-competitive to NMDA to competitive to NMDA [17]. However, CNQX may also interact with the NMDA recognition site directly. Lester *et al.*, [18] report that CNQX inhibits the binding of the NMDA competitive antagonist [^{3}H]3-(2-carboxypiperazine-4yl)-propyl-1-phosphonic acid (CPP). Thus CNQX reflects the lack of specificity of current glycine antagonists.

There may also be necessary reciprocal allosteric coupling of the glycine and glutamate recognition sites on the complex. Kessler *et al.*, [19] reported that glutamate agonists increased (modestly) [^{3}H]glycine binding. They also found that glutamate antagonists inhibited [^{3}H]glycine binding. Verdoorn *et al.* [16] reported a reduction by CNQX in the NMDA EC_{50} although statistical significance was not found. The analysis of CNQX against the glycine site also revealed complexity. CNQX appeared to give a mixed competitive-noncompetitive block of the glycine site, reducing the apparent potency of glycine as well as reducing the maximal response [16].

The glycine recognition site of the NMDA receptor complex may be similar to the benzodiazepine site on the gamma-aminobutyric acid (GABA) receptor complex, with a spectrum of responses possible from agonist to inverse agonist. 7-Cl-kynurenic acid has already been suggested as a possible inverse agonist [7]. Thus the description of glycine antagonists, such as kynurenic acid as described here, with kinetically competitive NMDA actions may be the opening a Pandora's box of complications.

References

1. Johnson JV and Ascher P (1987) Glycine Potentiates the NMDA Response in Cultured Mouse Brain Neurons. Nature 325: 529–531.
2. Ganong AH and Cotman CW (1986) Kynurenic Acid and Quinolinic Acid Act at NMDA Receptors in the Rat Hippocampus. J. Pharmacol. Exp. Ther. 236: 293–300.
3. Watkins JC and Olverman HJ (1987) Agonists and Antagonists for Excitatory Amino Acid Receptors. Trends Neurosci. 10: 265.
4. Perkins MN and Stone TW (1982) An Iontophoretic Investigation of the Actions of Convulsant Kynurenines and their Interactions with the Endogenous Excitant Quinolinic Acid. Brain Res. 247: 18–187.
5. Watson GB, Hood WF, Monahan JB and Lanthorn TH (1988) Kynurenate Antagonizes Actions of *N*-Methyl-D-aspartate through a Glycine-sensitive Receptor. Neurosci. Res. Commun. 2: 169–17.
6. Fletcher EJ and Lodge D (1988) Glycine Reverses antagonism of *N*-Methyl-D-aspartate (NMDA) by 1-Hydroxy-3-aminopyrrolidone-2 (HA-966) but not by D-2-Amino-5-phosphonovalerate (D-AP5) on Rat Cortical Slices. Eur. J. Pharmacol. 151: 161–162.
7. Kemp JA, Foster AC, Leeson PD, Priestley T, Tridgett R, Iversen LL and Woodruff GN (1988) 7-Chlorokynurenic Acid is a Selective Antagonist at the Glycine Modulatory Site of the *N*-Methyl-D-aspartate Receptor Complex. Proc. Natl. Acad. Sci. USA 85: 6547–6550.
8. Pullan LM, Olney JW, Price MT, Compton RP, Hood WF, Michel J, and Monahan JB (1987) Excitatory Amino Acid Receptor Potency and Subclass Specificity of Sulfur-containing Amino Acids. J. Neurochem. 49: 1301–1307.

9. Pullan LM (1988) Receptor Specific Inhibition of *N*-Methyl-D-aspartate Stimulated ^{22}Na Flux from Rat Hippocampal Slices by Phencyclidine and Other Drugs. Neuropharmacology 27: 493–497
10. Pullan LM and Cler JA (1989) Schild Plot Analysis of Glycine and Kynurenic Acid at the *N*-Methyl-D-Aspartate Excitatory Amino Acid Receptor. Brain Res. (accepted).
11. Reynolds IJ, Murphy SN and Miller RJ (1987) ^{3}H-labelled MK-801 binding to the excitatory amino acid receptor complex from rat brain is enhanced by glycine. Proc. Natl. Acad. Sci. USA 84: 7744–7748.
12. Kenakin TP (1987) Pharmacologic Analysis of Drug-Receptor Interaction. Raven Press, N.Y., pp. 205–244.
13. Andine P, Lehmann A, Ellren K, Wennber E, Kjellmer I, Nielsen T and Hagberg H (1988) The Excitatory Amino Acid Antagonist Kynurenic Acid Administered after Hypoxic-Ischemia in Neonatal Rats Offers Neuroprotection. Neurosci. Letts. 90: 208–212.
14. Schwarcz R, Foster AC, French ED, Whetsell WO Jr and Kohler C (1984) Excitotoxic Models for Neurodegenerative Disorders. Life Sci. 35: 19–32.
15. Drejer J and Honoré T (1988) New Quinoxalinediones Show Potent Antagonism of Quisqualate Response in Cultured Mouse Cortical Neurons. Neurosci. Lett. 87: 104–108.
16. Verdoorn TA, Kleckner NW and Dingledine R (1989) *N*-Methyl-D-aspartate/glycine and Quisqualate/Kainate Receptors Expressed in *Xenopus* Oocytes: Antagonist Pharmacology. Mol. Pharmacol. 35: 360–368.
17. Birch PJ, Grossman CJ and Hayes AG (1988) 6,7-Dinitroquinoxaline-2,3-dion and 6-Nitro,7-cyano-quinoxaline-2,3-dion Antagonise Response to NMDA in the Rat Spinal Cord via an Action at the Strychnine-insensitive Glycine Receptor. Eur. J. Pharmacol. 156: 177–180.
18. Lester RAJ, Quarum ML, Parker JD, Weber E and Jahr CE (1989) Interaction of 6-Cyano-7-nitroquinoxaline-2,3-dione with the *N*-Methyl-D-aspartate Receptor-associated Glycine Binding Site. Mol. Pharmacol. 35: 565–570.
19. Kessler M, Terramani T, Lynch G and Baudry M (1989) A Glycine Site Associated with *N*-Methyl-D-aspartic Acid Receptors: Characterization and Identification of a New Class of Antagonists. J. Neurochem. 13: 1319–1328.

Regulation of breathing, glycine, and other neurotransmitter amino acids in brain and cerebrospinal fluid during respiratory acidosis and ammonia infusion*

R.E. Dutton[a,b], P.M. Stein[c,], P.J. Feustel[b,c], G.D. Renzi[d], P.M. Renzi[a,d], V.E. Shih[a] and H. Kazemi[a]**

[a]*Pulmonary Unit and Neurology Service, Massachusetts General Hospital, Boston, MA, U.S.A.*
[b]*Biomedical Engineering Department, Rensselaer Polytechnic Institute, Troy, NY, U.S.A.*
[c]*Albany Medical College, NY, U.S.A.*
[d]*University of Montreal, P.Q., Canada*

Abstract

The ventilatory response and amino acid levels in dog brain and cerebrospinal fluid (CSF) were determined after one hour of respiratory acidosis at a narcotic level of 25–35% CO_2, balance O_2, that raised $PaCO_2$ greater than 24 kPa, lowered pH of arterial blood to 6.66 ± 0.03 and pH of cisternal cerebrospinal fluid to 6.70 ± 0.03. Ventilation was 36 ± 4 liters/min (room air normal <5 liters/min). Cerebral brain tissue obtained by craniotomy was analyzed for amino acids by ion exchange liquid chromatography. Induced respiratory acidosis resulted in significant ($P<.05$) elevations of brain glycine, leucine, and lysine. Brain glutamate decreased and glutamine increased, but GABA did not significantly change. During hypercapnia, CSF leucine, lysine and serine significantly increased, and appeared to follow brain glycine levels. Intravenous ammonia infusion during hypercapnia did not alter brain NH_3 or amino acid levels, but shifted the CO_2 response to a point where ventilation decreased with increasing $PaCO_2$. These results suggest that the neurotransmitters glycine and glutamate participate in physiological alterations that impair the ventilatory response during CO_2 narcosis. In this study, ventilation was not depressed below room air control levels. However, the ventilatory response curve was greatly reduced in terms of the ratio 'ventilation-per-kPa increase in partial pressure of carbon dioxide' at $PaCO_2$ 24 kPa as compared to that normally observed at $PaCO_2$ 7 kPa.

Introduction

The excitatory amino acid neurotransmitters, aspartate and glutamate, increase neuronal discharge when experimentally applied to respiratory neurons in the medulla [1]. Phrenic nerve output is increased when an inhibitor to gamma-aminobutyric acid (GABA) is applied by means of pledgets on the surface of the medulla in the region of the ventral superficial chemoreceptive tissue [2]. When these neurotransmitter amino acids are delivered to the region of the medulla by means of ventriculocisternal perfusion, glutamate increases ventilation and GABA depresses ventilation [3]. This also occurs when glutamine synthesis is blocked by inhibition of glutamine synthetase [4]. The present study was undertaken to

* This work was supported by USA National Institutes of Health Grants HL-12564 & GM 15426.
** Present address: Premeon Division of Medtronic, Inc., Brooklyn Center, MN, U.S.A.

determine whether attenuation of the ventilatory response to anesthetic levels of inhaled carbon dioxide, expressed as the ratio of minute ventilation to arterial carbon dioxide tension (ventilation per kPa $PaCO_2$), is correlated with a reduction of excitatory and an elevation of depressant endogenous amino acid neurotransmitters in the brain.

Parenteral administration of glycine in man induces an elevation of blood ammonia and appears to depress the ventilatory response to inhaled carbon dioxide, expressed as ventilation per kPa $PaCO_2$ [5]. Since elevation of ammonia levels results in rapid formation of glutamine from the citric acid cycle component, alpha-ketoglutarate, and in the process depletes the intermediate neurotransmitter amino acid, glutamate [6]; we also studied the influence of experimental elevations of ammonia in blood, brain and cerebrospinal fluid, induced by ammonia infusion, on neurotransmitter amino acid concentrations in brain and cerebrospinal fluid.

Cisternal cerebrospinal fluid (CSF) was obtained for analysis of endogenous levels of amino acid neurotransmitters in order to determine whether any CSF amino acid levels might serve as an index of amino acid neurotransmitter levels in the brain. Lactate content of blood, CSF, and brain was determined to assess its contribution to the acid-base status during the study.

Methods

Six control animals were anesthetized with sodium pentobarbital (25–35 mg/kg). During surgical preparation and prior to institution of CO_2 anesthesia, 20 test animals received balanced anesthesia consisting of intravenous Na methohexital (6–8 mg/kg) and fentanyl citrate (5–6 μg/kg), supplemented with 80% nitrous oxide, 20% oxygen, by inhalation. The animals in this study were mongrel dogs weighing 17–32 Kg. Carbon dioxide anesthesia was then induced with 20–35% CO_2, balance oxygen, adjusted to raise $PaCO_2$ to 19–34 kPa, and was maintained for one hour. In one group of test animals, an isotonic ammonium chloride solution buffered with sodium bicarbonate to pH 7.4 was administered in an amount that raised blood ammonia four times normal level. Ventilation was measured by means of a J-valve and 13.5 liter spirometer (total equipment dead space 270 ml). Naloxone (1 mg) was administered intravenously to counteract any residual effect of fentanyl, and measurement of ventilation was repeated. Cerebrospinal fluid was obtained by needle aspiration from the cisterna magna. Cortical brain tissue was obtained by craniotomy. Control animals breathed room air for one hour following surgical preparation, at which time arterial blood was sampled for blood gases, pH, ammonia, and lactate determinations.

Cerebrospinal fluid was prepared for amino acid analysis by deproteinization with 40 mg of sulfosalicylic acid/ml and addition of an equal volume of 16% $HClO_4$. The sample was centrifuged at 10,000 g for 15 min at 4°C and the supernatant was frozen at −85°C until analyzed. Whole brain was homogenized with 9 ml of 3% sulfosalicylic acid/gram of brain tissue for 15 min in a blender

prechilled to 4°C, and was frozen at −85°C until analyzed. For analysis, an aliquot of the supernatant of brain homogenate or cerebrospinal fluid was brought to pH 2.2 with saturated lithium hydroxide solution and filtered through 0.2 μm filters. The samples were analyzed for amino acid content by high pressure liquid chromatography (Beckman 119CL Amino Acid Analyzer) with a lithium gel matrix in the separation column. Arterial blood gases and pH were measured in a Radiometer blood gas analyzer. Ammonia content of cerebrospinal fluid, brain, and blood was measured by a modification of the Conway diffusion technique [7]. In 20 animals lactic acid content of blood, cerebrospinal fluid and brain was determined by an enzymatic technique (Biodynamics bmc lactate reagent set, Indianapolis, IN) [8].

Student's unpaired and paired t-tests were used for statistical analysis of the results, with significance accepted at the 95% confidence level ($p<.05$).

Results

Arterial ammonia increased from 153 ± 31 μg/dl to 640 ± 125 μg/dl and cerebrospinal fluid ammonia from 47 ± 24 μg/dl to 363 ± 61 μg/dl without significantly raising brain ammonia levels (control 987 ± 112 μg/100 g wet weight, hypercapnia 2,120 ± 312 μg/100 g wet weight, and hypercapnia plus NH_3 infusion 1,655 ± 259 μg/100 g wet weight).

Mean ventilation during carbon dioxide anesthesia was 1.4 ± 0.2 l/min/kg. This was not significantly different from a mean ventilation of 1.3 ± 0.2 l/min/kg in

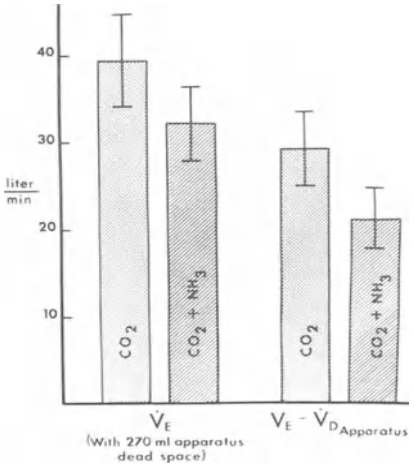

Fig. 1. Spontaneous minute ventilation (liters) during hypercapnia (n=10) and hypercapnia plus ammonia infusion (n=13). Correction for apparatus dead space reduces total ventilation, but does not reflect total ventilatory effort of the respiratory system under these study conditions.

animals receiving ammonia infusion during carbon dioxide anesthesia. Figure 1 presents ventilation in liters per minute (V_E). In the range of inspired 20% to 35% carbon dioxide, which produced $PaCO_2$ levels between 18.8 kPa to 33.6 kPa, ventilation decreased at a rate of 0.055 l/kg/kPa. This is expressed by the formula:

$$V_E = 2.913 - PaCO_2\ (0.055 \pm 0.026)\ \text{l/kg/kPa}. \quad P<.05,\ R=.42\ (n=23) \qquad (1)$$

The slope for animals receiving ammonia infusion during carbon dioxide anesthesia was:

$$V_E = 3.503 - PaCO_2\ (0.075 \pm 0.028)\ \text{l/kg/kPa}. \quad P<.05.\ R=.62\ (n=13) \qquad (2)$$

The slope for V_E versus $PaCO_2$ for animals breathing CO_2 alone was not significantly different from zero. The significant decrease in slope for CO_2 plus ammonia infusion suggests that ammonia shifts the CO_2 response curve to the right past its peak at these high levels of P_{CO2} whereas ventilation was approximately at its peak at comparable levels of P_{CO2} in the absence of an infused ammonia load.

There was no significant change in ventilation after administration of naloxone. Mean P_{CO2} was elevated to 29.1 ± 5.1 kPa, mean pH was 6.56, and mean PO_2 was greater than 36.5 kPa during CO_2 anesthesia. There were no significant differences in blood gases or pH between CO_2 anesthesia alone and CO_2 anesthesia plus ammonia infusion. The inspired CO_2:O_2 gas mixture raised mean $PaCO_2$ to 27.7

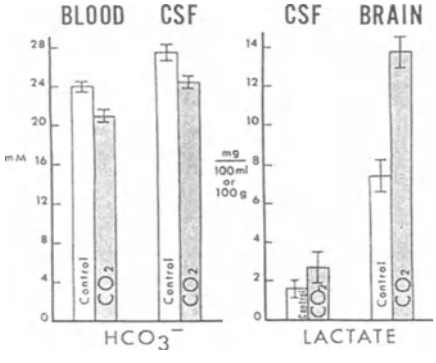

Fig. 2. Sodium bicarbonate levels (mM/l) in blood and cerebrospinal fluid during control room air breathing and during all hypercapnic experiments combined. Lactate levels in cerebrospinal fluid (mg/dl) and brain (mg/100 g wet weight) during control room air breathing and during all hypercapnic experiments combined.

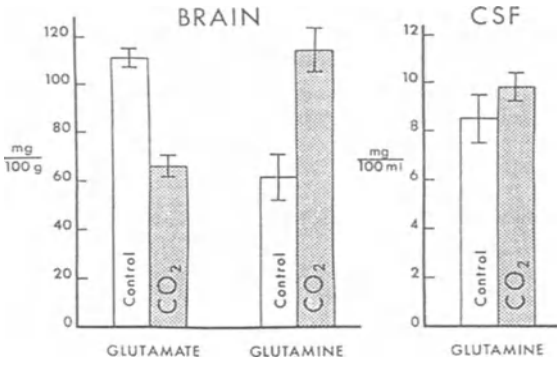

Fig. 3. Brain concentrations of glutamate and glutamine during control (n=10) and all hypercapnia experiments combined (n=21). The differences from control were significantly different (P<.05). Cerebrospinal fluid (CSF) glutamine was not significantly different from control during hypercapnia.

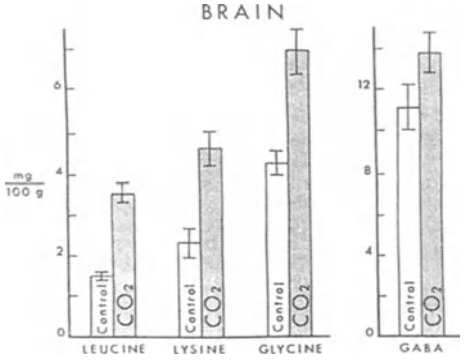

Fig. 4. Brain concentrations of leucine, lysine and glycine during control (n=10) and all hypercapnia experiments combined (n=21). The increases during hypercapnia were significantly different from control (P<.05).

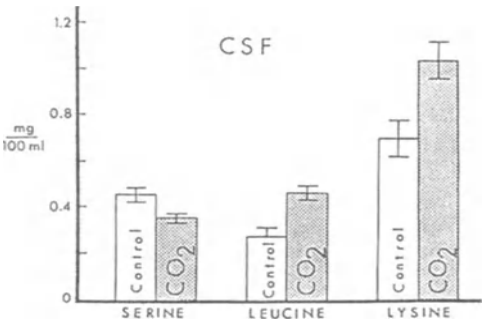

Fig. 5. Cerebrospinal fluid concentrations of serine, leucine and lysine during control (n=8) and all hypercapnia experiments combined (n=20). These differences were statistically significant (P<.05).

kPa, raised mean Pa_{O2} to 45.1 kPa, and lowered mean pH to 6.65. All mean values were significantly different from control values. Both blood and cerebrospinal fluid bicarbonate were significantly reduced during inhalation of CO_2 (Fig. 2). Lactate concentration was significantly higher in brain than in cerebrospinal fluid in all experimental groups. No significant difference between mean brain lactate concentrations resulted from ammonia infusion during CO_2 anesthesia, but both were significantly higher than control (Fig. 2).

Brain concentration of the excitatory amino acid, glutamate, significantly decreased during CO_2 anesthesia, and brain concentration of the inhibitory amino acid, glycine, significantly increased (Figs. 3,4). Concomitant changes in other brain amino acids were significant increases in glutamine, leucine, and lysine (Figs. 3,4). In cerebrospinal fluid the only changes in amino acid concentration from control were small, but significant, increases in leucine and lysine, and a decrease in serine (Fig. 5).

Discussion

There is a markedly attenuated ventilatory response to carbon dioxide, measured in terms of minute ventilation per kPa increase in P_{CO2}, during CO_2 anesthesia. Potential causes for this reduced sensitivity to CO_2 are impaired chemoreceptor input to the medullary respiratory center, or impaired respiratory center motor output to the respiratory muscles. Biochemical events that may lead to these changes include acidosis, hyperammonemia, an increase in brain concentration of

depressant amino acid neurotransmitters, and a decrease in brain concentration of excitatory amino acid neurotransmitters.

In the present study an induced elevation of blood ammonia four times the control level and an elevation of cerebrospinal fluid ammonia four to six times control levels caused no change in mean minute ventilation from that induced by carbon dioxide inhalation alone. However, regression analysis suggests that ventilation was at its peak in animals receiving CO_2 anesthesia alone, but was already declining from its peak at comparable levels of $PaCO_2$ with an added ammonia load. Since the brain ammonia levels were not significantly different, it remains a possibility that the fourfold increase in arterial blood ammonia was decreasing the ventilatory response to a rising PCO_2 by decreasing peripheral chemoreceptor input to the respiratory center.

Reduced levels of the excitatory neurotransmitter amino acids, glutamate and aspartate, and elevated brain concentrations of the depressant neurotransmitter amino acids, GABA and glycine, have been observed in rats exposed to acute and chronic elevation of inspired CO_2 concentrations [9]. At similar levels of inspired CO_2 in dog medulla, reduced levels of glutamate and aspartate were observed, but GABA also decreased instead of increased and there were no changes in glycine or taurine [10]. The present study of acute exposure to higher levels of CO_2 than those used by Weyne *et al.*, [9] and Dutton *et al.*, [10] reveals depression of glutamate and elevation of glycine in the dog. However, gamma-aminobutyrate again was not significantly changed. The directional changes in glutamate and glycine are consistent with amino acid neurotransmitter attenuation of neural output by neurons in the respiratory center or attenuation of central chemoreceptor input to the respiratory center neurons during severe acidosis induced by narcotic levels of inspired carbon dioxide.

The absence of a change in ventilation following administration of naloxone indicates that there was no residual effect of the opiate derivative, fentanyl after one hour of carbon dioxide anesthesia. lt also indicates that there was no endogenous endorphin influence on ventilation during hypercapnia in these grown animals. This finding is consistent with evidence in adult man that endogenous endorphins do not influence ventilation during hypoxia [11,12], but does not rule out a role for suppression of ventilation by endorphins in the fetus [13].

References

1. Toleikis J, Wang L and Boyarsky L (1979) J. Neurosci. Res. 4: 225–235.
2. Yamada KA, Norman WP, Hamosh P and Gillis RA (1982) Brain Res. 248: 71–78.
3. Chiang CH, Pappagoanopoulos P, Hoop B and Kazemi H (1986) J. Appl. Physiol. 60: 2056–2062.
4. Hoop B, Systrom DM, Shih VE and Kazemi H (1988) J. Appl. Physiol. 65: 1099–1109.
5. Renzetti AD Jr., Harris B and Bowen J (1961) J. Appl. Physiol. 16: 703–708.
6. McIlwain H (1966) Biochemistry of the Central Nervous System. Little Brown and Co., Boston, 3rd ed. p. 373.
7. Searcy RL, Reardon JE and Foreman JA (1967) Am. J. Med. Tech. 33: 15–20.

8. Gutmann I and Wahlefeld AW (1974) In: Bergmeyer HU (ed.) Methods of Enzymatic Analysis. Academic Press Inc., New York, 2nd English Edition, p. 1465.
9. Weyne J, Van Leuven F, Kazemi F and Leusen I (1970) J. Appl. Physiol.: Resp. Environ. Exercise Physiol. 44: 333–339.
10. Dutton RE, Feustel PJ, Dutton EH, Szema A, Shih VE, Renzi PM and Renzi GD (1988) In: Karczewski WA, Grieb P, Kulesza J and Bonsignore G (eds.) Control of Breathing During Sleep and Anesthesia. Plenum Press, New York, pp. 149–153.
11. Kagawa S, Stafford MJ, Waggener TB and Severinghaus JW (1982) J. Appl. Physiol. 52: 1030–1034.
12. Simon PM, Pope A, Lahive K, Steinbrook RA, Schwartzstein RM, Weiss JW, Fencl V and Weinberger SE (1989) Am. Rev. Respir. Dis. 139: 134–138.
13. Moss IR, Denavit-Saubie M, Eldridge FL, Gillis RA, Herkenham M and Lahiri S (1986) Federation Proc. 55: 2133–2147.

Role of GABA-mediated neurotransmission in seizures of El mice

Masatoshi Ito, Haruo Hattori, Yukiyoshi Shirasaka, Hideo Tsuda and Haruki Mikawa

Department of Pediatrics, Faculty of Medicine, Kyoto University, Kyoto 606, Japan

Abstract

Of the common antiepileptic drugs, diazepam was most effective in controlling the seizures of El mice. There was a significantly higher number and lower affinity of [^{3}H]muscimol binding sites in those El mice stimulated to produce convulsions and unstimulated El mice than in ddY mice. The basal and GABA stimulated [^{3}H]flunitrazepam (FNP) binding sites and the GABA concentration in the brains of El mice did not differ from those of ddY mice. GABA-induced chloride ion influx into the brain microsac was greater in stimulated El mice than in unstimulated El mice and ddY mice. However, in autoradiographic studies, [^{3}H]FNP bindings of stimulated El mice were significantly lower in the parietal cortex, hippocampus CA4, and dentate gyrus granular layer than in those of unstimulated El mice and ddY mice. In the hippocampus CA3 and amygdala of stimulated El mice, the bindings were also fewer than in ddY mice. In El mice following provoked convulsions, there were no temporary changes in [^{3}H]muscimol binding and [^{3}H]FNP binding with or without GABA stimulation in the whole brain. The GABA concentration in the brains of El mice increased immediately after a seizure and returned to the control value within 60 min. GABA-induced chloride ion influx 20 min after a convulsion was less sensitive than in the preconvulsive state or 60 min after a convulsion. In conclusion, changes of GABA-induced chloride ion influx and [^{3}H]FNP binding in autoradiography in stimulated El mice are due to repeated convulsions. In these assays, endogenous benzodiazepine receptor agonists which were increased and released by repeated seizures may be retained. The functional state of GABA-mediated neurotransmission in El mice is also changed by single convulsions. There was no deficit of GABAergic neurons in El mice, but GABA-mediated neurotransmission played an inhibitory role in the seizures of El mice.

Introduction

El mice are genetic animal models of epilepsy in which seizures are induced by postural stimulation [1–3]. The susceptibility to seizures of this strain increases with age. They begin to develop convulsions after stimulation 5–7 weeks after birth and become more sensitive to stimulation as they grow older. At about 15 weeks of age, most mice develop tonic-clonic convulsions when stimulated. When they are not stimulated, most of these mice do not have seizures [2,3].

The major inhibitory neurotransmitter in mammalian brains, γ-aminobutyric acid (GABA), exerts its effect by increasing postsynaptic membrane permeability to chloride ions [4,5]. GABA-A, benzodiazepine, and picrotoxin receptors, as well as a chloride ionophore, are thought to form a 'supramolecular complex' in post-synaptic membranes. Impairment of GABAergic function is related to seizures in various animal models [6,7] and in human epilepsy [8,9].

To investigate the role of GABA-mediated neurotransmission in the seizures of El mice, we tested the effects of phenobarbital, valproic acid and diazepam, which are thought to enhance GABA-mediated inhibition [10,11] and other common anticonvulsants. We also studied high affinity [^{3}H]muscimol and [^{3}H]flunitrazepam (FNP) binding, GABA concentration in whole brains of El mice, GABA-induced chloride ion influx into the brain 'microsac', and [^{3}H]FNP binding by a quantitative autoradiographic technique.

Materials and Methods

Animals

The El mice used in these experiments were of the 80th to 95th generations of an inbred strain. The El mice were stimulated once a week from the age of 4 weeks. Briefly, each mouse was taken out of its cage, placed on a metal mesh, and observed for 3 min. Then the mouse was tossed 15 cm into the air 30 times, or until a seizure occurred. The El mice subjected to these postural stimuli which have 14–18 repeated convulsions are called 'stimulated mice'. Unstimulated El mice were not tossed and did not develop convulsions, and ddY strain mice (the strain from which El mice were produced and which are not susceptible to postural stimuli) were used as controls. To evaluate the effects of given drugs or vehicles, the severity of the seizures was scored as follows; 5, tonic-clonic convulsion occurring on the metal mesh; 4, myoclonus occurring on the metal mesh; 3, tonic-clonic convulsions provoked by being tossed up 1–15 times; 2, tonic-clonic, convulsions provoked by being tossed up 16–30 times; 1, myoclonus or squealing provoked by being tossed up 30 times; 0, no convulsive behavior displayed. With this scoring system, half effective doses (ED_{50}) were determined.

Drug administration

Sodium valproate, phenytoin and diazepam were injected intraperitoneally in El mice 30 min before the stimulation procedure; phenobarbital, carbamazepine and ethosuximide were injected 60 min before stimulation. As a control, vehicles were injected in the same way. Because the mice were excitable and easily developed convulsions, they were lightly anesthetized with diethylether for 20 sec when drugs or vehicles were injected intraperitoneally. The anesthesia did not affect the convulsions of El mice.

[^{3}H]Muscimol binding

Membranes were prepared by the method of Enna and Snyder (1977) [12]. Binding assays for the high-affinity sodium-independent [^{3}H]muscimol receptor were performed by a modification [2] of the filtration assay method of Williams and Risley (1979) [13].

[^{3}H]FNP binding

Membranes were prepared and binding assays were performed by a modification [2] of the method of Horton *et al.* (1982) [14].

GABA concentration

The brains were removed rapidly (within 30 sec) and placed in a beaker of methanol precooled to approximately −80°C on dry ice and acetone. The GABA content was determined by a modification [16] of the [^{3}H]muscimol radioreceptor assay of Bernasconi *et al.* (1980) [15].

In vitro *chloride ion influx assay*

The membrane 'microsac' for the chloride influx study was prepared by the method of Harris and Allan (1985) [17] with minor modifications [18].

Quantitative autoradiography of [^{3}H]FNP binding sites

Mice were decapitated and the brains were removed rapidly, immersed in isopentane cooled in an acetone-dry ice bath, stored within a few minutes and embedded in ice-cooled Tissue Tek II OTC compound (Miles) on microtome chucks. These samples were stored at −70°C until the day of experiment. Coronal sections (10 μm) from 7 regions (6 slices adjacent to each region) were cut from each animal at −20°C in a cryostat microtome (Tissue-Tek II, Miles) and thaw-mounted tissue sections were transferred to an ice cold desiccator for 2 h under vacuum, then stored overnight at −20°C.

The slide-mounted tissue sections were brought to 0°C under vacuum, then preincubated for 60 min with ice-cold isotonic buffer (50 mM Tr is-HCl, 250 mM NaCl, pH 7.4 at 0°C). The preincubated tissue slices were rinsed once in 50 mM Tris HCl buffer, then rapidly dried with a cold stream of air in a cold room at 0–4°C. In the cold room, the slices were incubated for 60 min at 0°C with a 150 μl 'bubble' of 1 nM [^{3}H]FNP prepared in the same isotonic buffer. Non-specific binding was determined in the adjacent sections in the presence of 1 μM clonazepam. To terminate the reaction and reduce non-specific binding, the slices were rinsed rapidly in 50 mM Tris-HCl buffer (pH 7.4 at 0°C) for 15 sec four times, then dipped into ice-cold double distilled water to remove residual salts. Sections were then dried as rapidly as possible under a cold stream of air, brought to room temperature under vacuum for 2 hr and stored longer than overnight in a desiccator.

Labeled tissue sections from mice were exposed to [^{3}H]Ultrafilm (Amersham) in a light-proof X ray cassette for 2 weeks at 4°C. After exposure, the films were developed (Fuji HiRenfix, 4 min, 20°C), washed with water (30 min), and dried at room temperature. The optical density of the autoradiogram was quantified with an

automatic image analyzer and densitometer connected to an IBM Computer (The MCID System, Imaging Research Inc.). Optical density readings were made from several sections according to the area of interest, and the mean value was recorded. The optical density was converted into fmol [^{3}H]labeled ligand bound/mg of wet tissue with the use of microscales (American Radiolabeled Chemicals Inc.) for tritium as standards, and non-specific binding was subtracted.

Results

Prevention of seizures by common antiepileptic drugs

The seizure scores were reduced dose-dependently by the administration of phenobarbital, sodium valproate, diazepam, phenytoin, carbamazepine and ethosuximide (Fig. 1). The ED_{50} values were 15, 175, 0.4, 40, 60 and 260 mg/kg for phenobarbital, sodium valproate, diazepam, phenytoin, carbamazepine and ethosuximide, respectively.

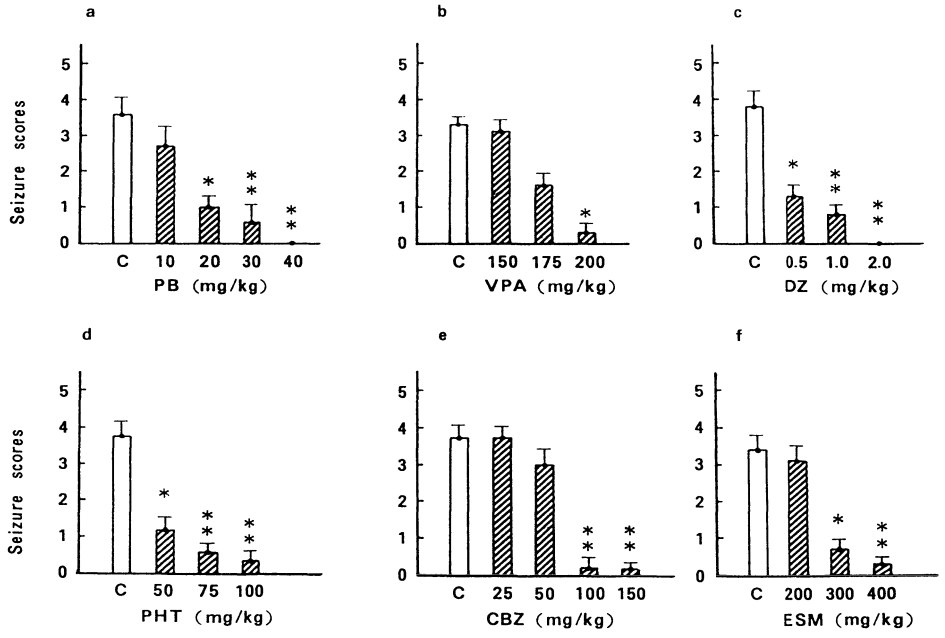

Fig. 1. Effects of common antiepileptic drugs in seizures of El mice. Seizure scores are mean ± S.E. (n = 10–20). C, control; PB, phenobarbital; VPA, sodium valproate; DZ diazepam; PHT phenytoin; CBZ, carbamazepine; ESM, ethosuximide. Statistical significance was determined by the two-tailed Student's t-test. A single asterisk indicates $p<0.05$ and double asterisks $p<0.001$ vs controls.

Muscimol binding

The affinity of high-affinity [^{3}H]muscimol binding sites was lower, but the number was larger in stimulated and unstimulated El mice than in ddY mice (Table 1). Neither K_D nor B_{max} values differed significantly between stimulated and unstimulated El mice.

[^{3}H]FNP binding and GABA concentrations

The K_D and B_{max} values of [^{3}H]FNP binding did not differ significantly among stimulated and unstimulated El mice and ddY mice (Table 1). Exogenous GABA increased the [^{3}H]FNP binding in El and ddY mice. The maximum stimulation by GABA did not differ significantly between El and ddY mice (40.4 ± 2.1% increase in stimulated El mice, 39.1 ± 2.8 in unstimulated El mice and 42.1 ± 2.5 in ddY mice; [^{3}H]FNP 1.1 nM). There were no significant differences in endogenous GABA concentrations among stimulated and unstimulated El and ddY mice.

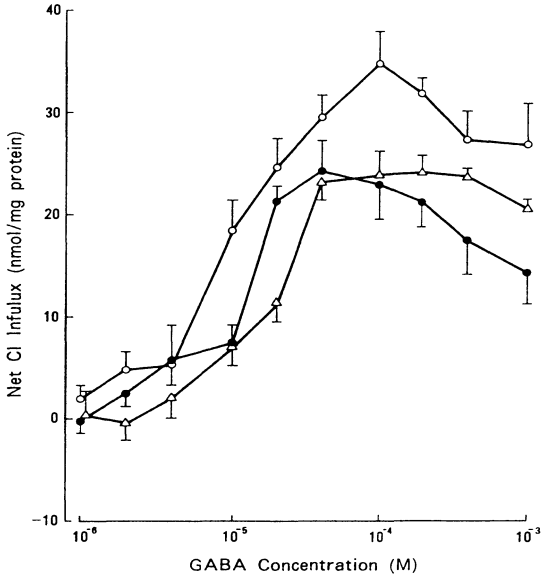

Fig. 2. Effect of increasing concentrations of GABA on chloride ion influx into brain microsac in stimulated (○) and unstimulated (△) El mice, and ddY (●) mice. Values represent the means ± S.E. from 8 separate experiments. These data were analyzed by a two-way repeated measure analysis of variance. There is one between-group factor (mouse group) and one within-group factor (GABA concentration). There were significant main effects on the mouse group ($p<0.01$) and on GABA concentration ($p<0.01$). The stimulated El mice had significantly greater sensitivity to GABA than the unstimulated El mice and ddY mice ($p<0.01$). There was no significant difference in sensitivity between unstimulated El mice and ddY mice.

Table 1. [^{3}H]Muscimol and [^{3}H]flunitrazepam binding to crude membrane fractions from the brains and GABA concentrations in the brains of stimulated and unstimulated El mice and ddY mice. N = number of animals. Data are means ± S.E. One-way analysis of variance was used to test for statistical significance. If there was a significant difference ($p<0.05$), the groups were compared by the least significant difference method

Mouse strain	[^{3}H]Muscimol binding			[^{3}H]FNP binding			GABA concentration	
	n	K_D (nM)	B_{max} (pmol/mg protein)	n	K_D (nM)	B_{max} (pmol/mg protein)	n	(μmol/g tissue)
El(stimulated)	5	1.96 ± 0.14[a]	1.73 ± 0.09[b]	4	3.53 ± 0.17	1.51 ± 0.04	10	1.81 ± 0.06
El(unstimulated)	5	1.87 ± 0.08[b]	1.70 ± 0.08[b]	4	3.26 ± 0.10	1.53 ± 0.02	7	1.77 ± 0.09
ddY	5	1.46 ± 0.07	1.32 ± 0.07	4	3.53 ± 0.25	1.42 ± 0.08	10	1.78 ± 0.05

[a]$p<0.01$ vs ddY mice, [b]$p<0.001$ vs ddY mice.

Table 2. Specific [^{3}H]flunitrazepam binding in autoradiography of stimulated and unstimulated El mice and ddY mice. N = number of animals. Dentate Gra., dentate gyrus granular layer. Data are mean ± S.E. One-way analysis of variance was used to test for statistical significance. If there was a significant difference ($p<0.05$), the groups were compared by the least significant difference method

Brain region	[^{3}H] FNP binding		
	El (stimulated) n = 6	El (unstimulated) n = 9	ddY n = 6
Parietal cortex	128.7 ± 2.7[a,b]	147.0 ± 5.4	157.3 ± 7.7
Hippocampus			
CA3	115.1 ± 2.4[a]	128.1 ± 5.7	143.7 ± 7.8
CA4	111.3 ± 3.1[a,b]	133.7 ± 4.5	139.9 ± 10.4
Dentate Gra.	85.3 ± 2.1[a,b]	103.4 ± 3.7	102.5 ± 5.1
Amygdala	128.0 ± 3.7[a]	138.0 ± 5.2	155.5 ± 7.3

[a]$p<0.05$ vs ddY mice, [b]$p<0.05$ vs unstimulated mice.

Chloride ion influx

The basal chloride influx, measured in the absence of added GABA, was not significantly different in the three groups of mice. GABA-induced chloride ion influx was concentration-dependent. There was significantly greater sensitivity to GABA in stimulated El mice than in unstimulated El mice and ddY mice (Fig. 2).

[^{3}H]FNP binding in autoradiography

The specific binding in stimulated El mice was significantly lower in the parietal cortex, hippocampus CA4 and dentate gyrus granular layer than in ddY mice and unstimulated El mice (Table 2). In the hippocampus CA3 and amygdala, the binding was significantly lower in stimulated El mice than in ddY mice. In these regions, however, [^{3}H]FNP binding in unstimulated El mice tended to be intermediate between that in stimulated El mice and that in ddY mice. There were no significant differences between specific [^{3}H]FMP binding in unstimulated El mice and that in normal ddY mice.

Changes in stimulated El mice during one hour after a provoked convulsion

The number of [^{3}H]muscimol and [^{3}H]FNP binding sites and the effect of GABA stimulation on [^{3}H]FNP binding were not affected by provoked convulsions (Table 3). The GABA concentration increased significantly 1 min after a provoked convulsion, remained high up to 45 min and returned to the control value by 60 min (Fig. 3). There were no significant changes in basal chloride influx 20 min after a convulsion. GABA-induced chloride influx 20 min after a convulsion was less sensitive than in the preconvulsive state or 60 min after a convulsion (data not shown).

Table 3. The effect of a provoked convulsion on [^{3}H]muscimol and basal and GABA-stimulated [^{3}H]flunitrazepam binding to crude membrane fractions from the brains of El mice. The concentrations of [^{3}H]muscimol and [^{3}H]flunitrazepam were 1.0 nM and 1.1 nM, respectively. The effect of GABA stimulation on [^{3}H]flunitrazepam binding is shown as a percent increase compared with respective controls. n = number of animals. Data are mean ± S.E. One-way analysis variance was used to test for statistical significance. There was no significant difference.

Time after a convulsion (min)	[^{3}H]Muscimol binding		[^{3}H]FNP binding		GABA (50 μM) stimulation on [^{3}H]FNP binding	
	n	(fmol/mg protein)	n	(fmol/mg protein)	n	(% increase)
Control	10	603 ± 16	7	357 ± 6	4	40.9 ± 3.3
1	4	575 ± 16	5	366 ± 17	5	35.9 ± 3.0
10	4	615 ± 20	5	363 ± 10	5	35.5 ± 2.0
20	4	621 ± 36	5	353 ± 17	5	41.8 ± 3.3
30	4	582 ± 22	5	338 ± 9	5	41.0 ± 2.3
45	4	584 ± 18	5	365 ± 10	5	35.2 ± 2.0
60	4	622 ± 17	5	361 ± 11	5	36.1 ± 3.4

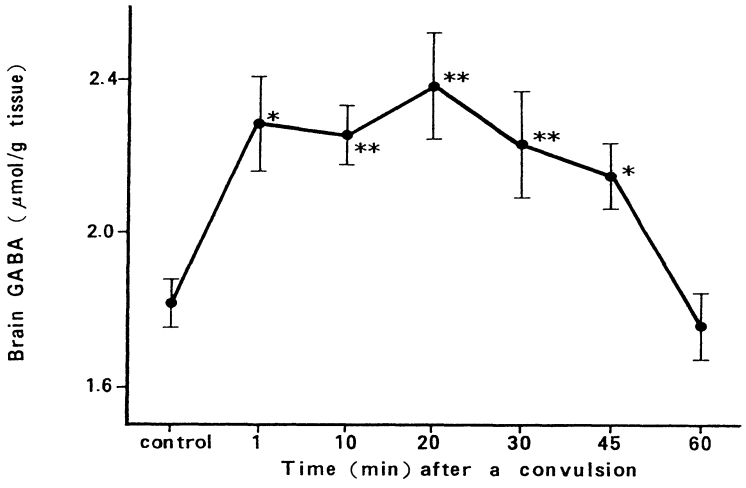

Fig. 3. Brain GABA concentrations in stimulated El mice at various times after a convulsion. Values are the means ± S.E. from 7–10 animals. Statistical significance was determined by the two-tailed Student's t-test. A single asterisk indicates $p<0.01$, and double asterisks $p<0.001$ vs controls.

Discussion

Phenobarbital, valproate and diazepam are believed to act through enhancing the GABAergic neuron system [10,11]. These drugs were relatively more potent in treating seizures in El mice than other drugs such as phenytoin, carbamazepine and ethosuximide. Diazepam was effective against seizures of El mice at the dose used to treat human epilepsy, while the other anticonvulsants were effective at doses several times those used clinically.

In this study, there was a significantly higher number and lower affinity of [^{3}H]muscimol binding sites in El mice than in ddY mice. The difference in [^{3}H]muscimol binding sites in El mice does not seem to be related to the repeated convulsions because unstimulated El mice which did not develop convulsions, also showed the same difference in [^{3}H]muscimol binding. Therefore, the difference in [^{3}H]muscimol binding may be due to a genetic difference between these two strains of mice. Because high affinity GABA-A sites do not seem to be coupled with chloride channels [10], the functional significance of the increased high affinity [^{3}H]muscimol binding is not clear. It may be unrelated to the seizures in El mice.

GABA-induced chloride ion influx into brain microsacs was greater in stimulated El mice than in unstimulated El mice and ddY mice. This increased sensitivity may be due to the effect of repeated convulsions, because the GABA-

induced chloride ion influx in unstimulated El mice was not significantly different from that in control ddY mice. Moreover, ddY mice that were stimulated from the age of 4 weeks by the same procedure as that performed in El mice showed no increase of sensitivity to GABA (data not shown). It is well established that direct blocking of GABA function causes seizures and that augmentation of GABA function can protect against seizure activity [19]. Thus increased GABAergic function in stimulated El mice may reflect an inhibitory compensation for excitability in the brain, even when it fails to prevent convulsions.

Autoradiographic studies showed less [^{3}H]FNP binding in the parietal cortex, hippocampus CA4 and dentate gyrus granular layer than in ddY mice and unstimulated El mice. In the hippocampus CA3 and amygdala, binding was also less than in ddY mice. The number of [^{3}H]FNP bindings in these regions in unstimulated El mice tended to be between that in stimulated El mice and that in ddY mice. These regions are highly involved in the seizures of El mice. Decreased [^{3}H]FNP binding is probably due not to genetic differences between El and ddY mice, but to the effects of repeated convulsions, since there were no significant differences observed between unstimulated El mice and ddY mice.

A high concentration of GABA down-regulates GABA/ benzodiazepine receptor complexes and lowers [^{3}H]FNP bindings in cultured neurons [20,21]. Thus, it is possible that the decreased [^{3}H]FNP binding observed in this study may represent down-regulation of GABA/benzodiazepine receptor complexes due to the repeated release of GABA following convulsions. However, [^{3}H]muscimol and [^{3}H]FNP binding in whole brain specimens showed no decrease in well washed synaptic membranes, and GABA-induced chloride influx was increased in stimulated El mice. Therefore, GABA and benzodiazepine receptors do not seem to be down-regulated.

There are many endogenous substances which interact with benzodiazepine receptor binding, such as GABA and endogenous benzodiazepine receptor ligands [22–25]. The GABA content in El mice one week after the last provoked convulsion was not significantly different from that in ddY mice, and 60 min preincubation appeared to remove most of the effects of endogenous GABA. Therefore, our results seemed to have little relation to the GABA content. Niznik *et al.* (1984) [26] reported that unwashed membranes showed decreased [^{3}H]FNP binding in kindling models, while well-washed membranes had the same binding as the controls. These findings suggest the possibility of changes in endogenous benzodiazepine receptor inhibitors. It is possible that the decreased [^{3}H]FNP binding observed in stimulated El mice is due to remaining endogenous benzodiazepine receptor ligands which are increased and released by repeated seizures.

Most of the candidates for endogenous ligands of central benzodiazepine receptor are inverse agonists and have proconvulsant activity. Therefore, increased endogenous ligands in the parietal cortex, hippocampus CA3, CA4, dentate gyrus granular layer and amygdala nuclei may be related to the generation of paroxysmal discharges in stimulated El mice. The increased sensitivity of GABA receptors may be compensation for this hyperexcitability. If the residual endogenous ligand

is an agonist, such as N-desmethyldiazepam [25], this phenomenon may be directly related to the increased GABA-mediated inhibitory function against seizures in El mice. This hypothesis is further supported by the fact that GABA-stimulated [^{3}H]FNP binding was not increased in well-washed membrane preparations in stimulated El mice, but GABA-induced chloride ion influx was increased. Membrane preparations for GABA-induced chloride ion influx were not well washed, so it is possible that endogenous benzodiazepine receptor agonists were retained and affected GABA receptor sensitivity.

There were no temporal changes of [^{3}H]muscimol and [^{3}H]FNP bindings in the brains of El mice after a provoked convulsion, while the GABA concentration in the brains of El mice increased following provoked convulsions. A rapid temporary change in the brain GABA concentration after a provoked seizure in El mice may cause a refractory period by elevating the seizure threshold. Although the elevated seizure threshold returned to normal after 45 min, the GABA concentration in the brains was still elevated. This indicates that the increase in the seizure threshold is not related simply to an increase in brain GABA concentration.

GABA-induced chloride influx was significantly decreased 20 min after a convulsion, and it returned almost to the preconvulsion state 60 min after the convulsion. After a convulsion, the release of GABA to synaptic clefts may increase temporarily. GABA receptor desensitization occurs rapidly after GABA exposure [27–29]. These findings suggest that this temporarily decreased sensitivity of GABA-induced chloride influx may be related to the desensitization phenomenon due to increased release of GABA.

In conclusion, changes of GABA-induced chloride ion influx and [^{3}H]FNP binding in autoradiography in stimulated El mice are secondary to repeated convulsions. In these assays, endogenous benzodiazepine receptor agonists which were increased and released by repeated seizures may be retained. The functional state of GABA-mediated neurotransmission in El mice is also changed by single convulsions. There was no deficit of GABAergic neurons in El mice, but GABA-mediated neurotransmission plays an inhibitory role in the seizures of El mice.

References

1. Imaizumi K and Nakano T (1964) Mouse News Letter 31: 57.
2. Hattori H, Ito M and Mikawa H (1985) Eur. J. Pharmacol. 119: 217–223.
3. Ochi J, Ito M, Okuno T and Mikawa H (1988) Epilepsia 29: 91–96.
4. McBurney RH and Barker JL (1978) Nature 274: 596–597.
5. Nistri A, Constanti A and Krynjevic K (1980) In: Pepeu G, Kuhar MJ and Enna SJ (eds.) Advances in Biochemical Psychopharmacology. Raven Press, New York, Vol. 21, pp. 81–90.
6. Wood JD (1975) In: Kerkut GA and Phillis JW (eds.) Progress in Neurobiology. Pergamon Press, New York, pp. 78–95.
7. Olsen RW, Wamsley JK, McCobe RT, Lee RJ, Lomax P and Seyfried JN (1986) In: Nistico G, Morselli PL, Lloyd KG, Fariello RG and Engel J Jr. (eds.) Neurotransmitters, Seizures, and Epilepsy III. Raven Press, New York, pp. 279–291.
8. Van Gelder NM, Sherwin AL, Rasmussen T (1972) Brain Res. 40: 385–393.

9. Lloyd KG, Munari G, Bossi L and Morselli PL (1984) In: Fariello RG, Morselli PL, Lloyd KG, Quesney LF and Engel J Jr. (eds.) Neurotransmitters, Seizures and Epilepsy II, Raven Press, New York, pp. 285–293.
10. Olsen RW (1982) Ann. Rev. Pharmacol. Toxicol. 22: 245–277.
11. Gale K (1984) In: Fariello RG, Morselli PL, Lloyd KG, Quesney LF and Engel J Jr. (eds.) Neurotransmitters, Seizures, and Epilepsy II. Raven Press, New York, pp. 57–80.
12. Enna SJ and Snyder SH (1977) Mol. Pharmacol. 13: 442–453.
13. Williams M and Risley EA (1979) J. Neurochem. 32: 713–718.
14. Horton RW, Prestwich SA, Meldrum BS (1982) J. Neurochem. 39: 864–870.
15. Bernasconi R, Bittiger H, Heid J and Martin P (1980) J. Neurochem. 34: 614–618.
16. Ito M, Mikawa H and Taniguchi T (1984) Neurology 34: 235–238.
17. Harris RA and Allan AM (1985) Science 228: 1108–1109.
18. Yu O, Ito M, Chiu TH and Rosenberg HC (1986) Brain Res. 399: 374–378.
19. Olsen RW, Snowman AM, Lee R, Lomox P and Wamsley JK (1984) Ann. Neurol. 16 (Suppl.): s90–97.
20. Maloteaux JM, Octave JN, Gossuin A, Laterre C, Trouet A (1987) Eur. J. Pharmacol. 144: 173–183.
21. Tehrani MHJ and Barnes EM Jr. (1988) Neurosci. Lett. 87: 288–292.
22. Chiu TH and Rosenberg HC (1979) Eur. J. Pharmacol. 56: 337–345.
23. Guidotti A, Forchetti CM, Corda MG, Konkel D, Bennett CD and Costa E (1983) Proc. Natl. Acad. Sci. USA 80: 3531–3535.
24. Ferrero P, Guidotti A, Conti-tronconi B and Costa E (1984) Neuropharmacol. 23: 1359–1362.
25. De Robertis E, Pena C, Palandini AC and Medina JH (1988) Neurochem. Int. 13: 1–11.
26. Niznik HB, Burnham WM and Kish SJ (1984) J. Neurochem. 43: 1732–1736.
27. Ben-Ari Y, Krynjević K and Reinhardt W (1979) Can. J. Physiol. Pharmacol. 57: 1482–1486.
28. Thalmann RH and Hershkowitz N (1985) Brain Res. 219–233.
29. Krynjević K (1981) in GABA and Benzodiazepine Receptors (Costa E, DiChihara G and Gessa GL (eds.) Raven Press, New York, pp. 111–120.

Address for correspondence: Masatoshi Ito, Department of Pediatrics, Faculty of Medicine, Kyoto University, 54 Kawahara-cho, Shogoin, Sakyo-ku, Kyoto 606, Japan.

The kainic acid model of human temporal lobe epilepsy: The superiority of intra-amygdaloid injection versus other application routes

Michael L. Berger[a], Karl Vass[b], Hans Lassmann[b] and Oleh Hornykiewicz[a]

[a]Institute of Biochemical Pharmacology and [b]Neurological Institute, University of Vienna, Vienna, Austria

Abstract

To evaluate the significance of the kainic acid (KA)-induced seizure/brain damage syndrome as an animal model for temporal lobe epilepsy, we compared behavioural and histopathological consequences of intra-amygdaloid (i.am.), intracerebroventricular (i.c.v.) and systemic application of the toxin. I.am. injection of 5 ng KA in conscious freely moving rats via chronically implanted guide cannulas resulted in typical limbic motor seizures in 6 out of 16 rats. Seizures were of short duration, and all rats appeared normal one hour after the injection. Seizure response increased to 70% responding animals with the KA dose raised to 8–15 ng; at this dose range, some animals developed *status epilepticus*, resulting in neuronal damage in hippocampal CA_1 and CA_3 sector; in rats undergoing only transient seizure attacks, no brain damage could be detected. I.C.V. injection of 200 ng KA induced severe and selective neuronal damage in the hippocampal CA_3-sector, even in cases with only mild motor seizures. Systemic injection of 10 mg/kg KA induced limbic motor seizures culminating in 11 out of 12 rats in behavioural *status epilepticus*, with variable histopathological consequences. We conclude that for the study of endogenous pathophysiological processes involved in the generation of *status epilepticus* and seizure induced brain damage, the i.am. injection of very low KA doses offers several advantages over the other application techniques described. I.C.V. injection of KA, on the other hand, is a powerful means to destroy CA_3 pyramidal cells, with no detectable damage to other neurons if the induction of *status epilepticus* is avoided.

Introduction

Kainic acid (KA) is a cyclic analogue of the major excitatory neurotransmitter glutamic acid and is the prototype agonist for the KA-subtype of glutamate receptors. Compared with the other major receptor subtype, the NMDA-receptor, which participates in more delicate electric gating phenomena probably representing the molecular mechanisms of learning, KA receptors seem to mediate straightforward excitatory actions of glutamic acid, maintaining a ground level of neuronal activity. In this article, we describe the epileptogenic action of KA and illustrate that i.am. injection of KA [1] is superior to other application routes as an animal model of human temporal lobe epilepsy, reproducing behavioural and histopathological features with high accuracy. We also discuss the limited usefulness of KA as a selective lesioning tool.

Experimental procedures

Animals

Male Sprague Dawley rats were obtained from Forschungsinstitut fur Versuchstierzucht, Himberg, Austria, and housed 2 rats per cage, with food pellets (Altromin®, Dr. Marek & Co., Vienna) and water *ad libitum*, artificial lights on from 6 a.m. to 6 p.m. They were used for experiments at an age of 3–4 months, weighing around 400 g.

Intracerebral injections

For injection of KA into the amygdala or the lateral ventricle of freely moving rats, guide and injection cannulas were prepared from polyimid coated fused silica capillaries as used in gas chromatography (outer diameters 300 and 170 µm, respectively; Scientific Glass Engineering, Ringwood, Vic., Australia). Their preparation and use has been extensively described elsewhere [2]. According to the rat brain atlas of König and Klippel [3], guide cannulas were stereotaxically (David Kopf apparatus) directed to the following injection points: A 4.38, L 4.0, V 3.3 (5 ng KA/0.32 µl, amygdala, 17 rats); A 5.78, L 1.8, V 2.0 (200 ng KA/1.0 µl, dorsal part of lateral ventricle, 8 rats); and A 3.43, L 3.8, V 2.2 (200 ng KA/1.0 µl, ventral horn of lateral ventricle, 7 rats). Guide cannulas ended 1.0 mm above the injection point, with the exception of injections into the ventral horn of the lateral ventricle (2.5 mm). In 12 rats, 10 mg/kg KA were injected systemically, by the intraperitoneal (i.p.) route.

Behaviour

The unrestrained and fully conscious rats were observed continuously during and after the injection for at least 1 h. The chronology of limbic seizure behaviour was continuously protocolled; these notes were later transformed to 'behaviograms', using a single-letter code (see legend to Fig. 1) developed for this purpose and described in detail elsewhere [5].

Fig. 1. Short-lasting limbic seizures in 6 out of 17 conscious, freely moving rats injected with 5 ng KA into the left amygdala. KA was injected in a volume of 0.32 µl artificial CSF (corresponding to a concentration of 73 µM KA), over a time period of 2–3 min. One-letter code for behaviour: • (dot), wet dog shakes (not all indicated); g, grooming; s, salivation; c, contraversive flexion (sometimes with right forelimbs clonus); o, barrel rotation (more intense expression of c, with falling of the animal around its own axis); M, mastication; 3,4,5, stage 3, stage 4, stage 5 limbic seizure attack, respectively [4]; !!, behavioural *status epilepticus* (i.e. continuous stereotype movements accompanied by mastication and salivation, negatively defined by absence of wet dog shakes and grooming behaviour). All animals described in this Fig. reassumed spontaneously resting position within 40–90 min.

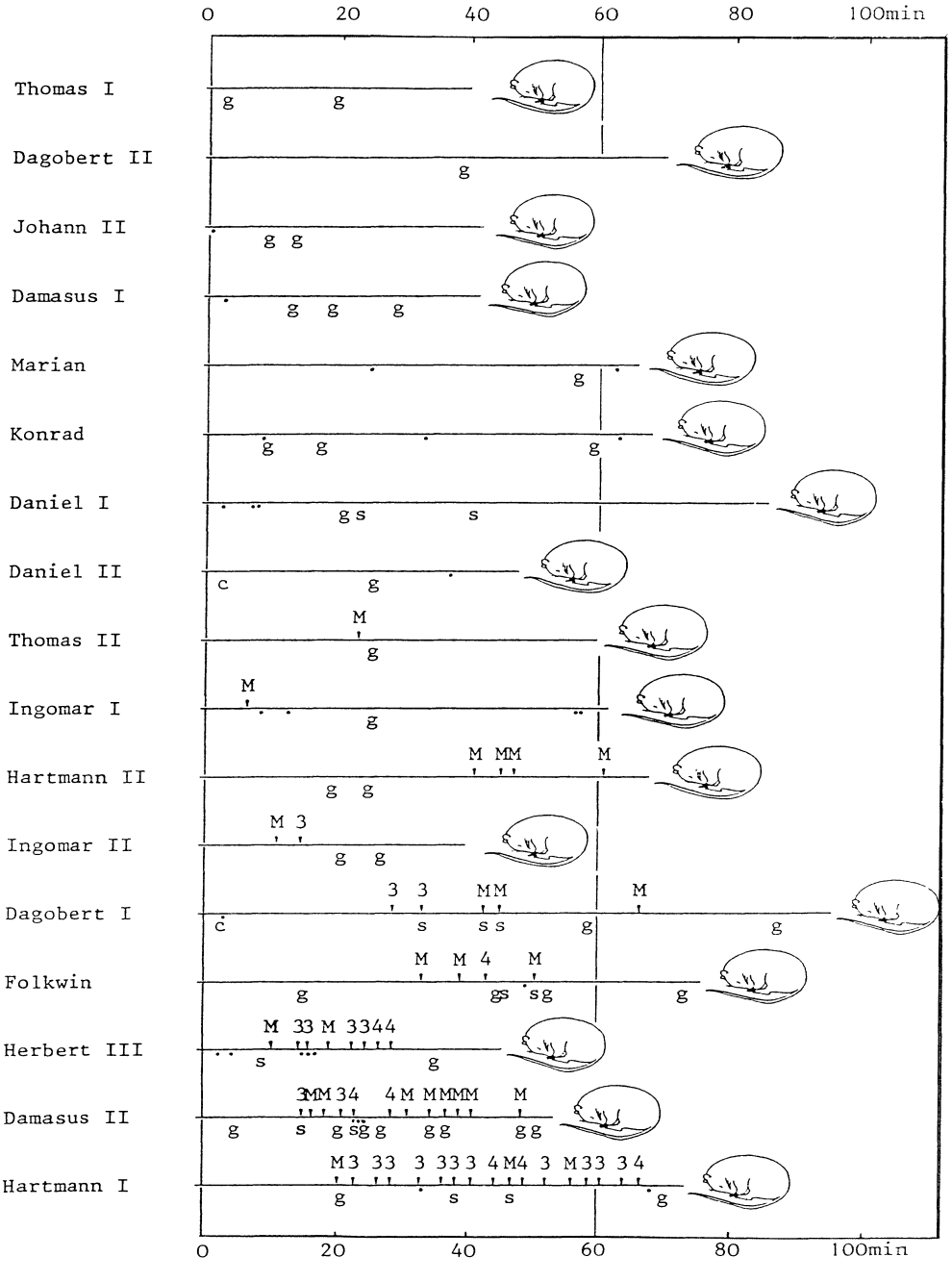
0
20
40
60
80
100min
Thomas I
Dagobert II
Johann II
Damasus I
Marian
Konrad
Daniel I
Daniel II
Thomas II
Ingomar I
Hartmann II
Ingomar II
Dagobert I
Folkwin
Herbert III
Damasus II
Hartmann I

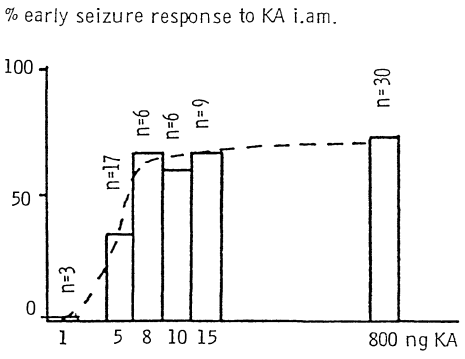

Fig. 2. Dose response relationship of limbic seizures induced within 40 min after intra-amygdaloid injection of KA. The criterion for early positive seizure response was the occurrence of at least one stage 3 attack (mastication + clonus of neck or one forelimb) within 40 min after onset of injection.

Histology

One to 14 d after the KA-injection, rats were deeply anesthetized (3 ml/kg equithesine) and perfused through the heart with saline followed by 4% paraformaldehyde in 0.1 M phosphate buffer, pH 7.4. Brains were removed and processed for examination of histopathological changes, using conventional staining techniques, as described elsewhere [5].

Results and Discussion

Injections of KA into the rat amygdala

KA injected into the amygdala of conscious rats induces limbic motor seizures in a dose-dependent manner (Fig. 2). After i.am. injection of 5 ng KA, 6 out of 17 rats exhibited at least one stage 3 attack (Fig. 1) and returned spontaneously to normal behaviour within maximally 90 min. After somewhat higher doses (8–15 ng), 3 out of 19 injected rats did not recover spontaneously but developed behavioural *status epilepticus* [5]. With a still higher KA dose (800 ng), the fraction of animals expressing seizures during the first 40 min after the injection did not increase further; however, with some delay, practically all rats developed seizures and most of them also *status epilepticus*.

Animals recovering from limbic motor seizures spontaneously within 40–80 min induced by i.am. injection of low KA doses (≤15 ng) never showed any seizure-related histopathological abnormalities in the brain. However, after permanent seizures (behavioural *status epilepticus*) of at least 10 min duration, spotted

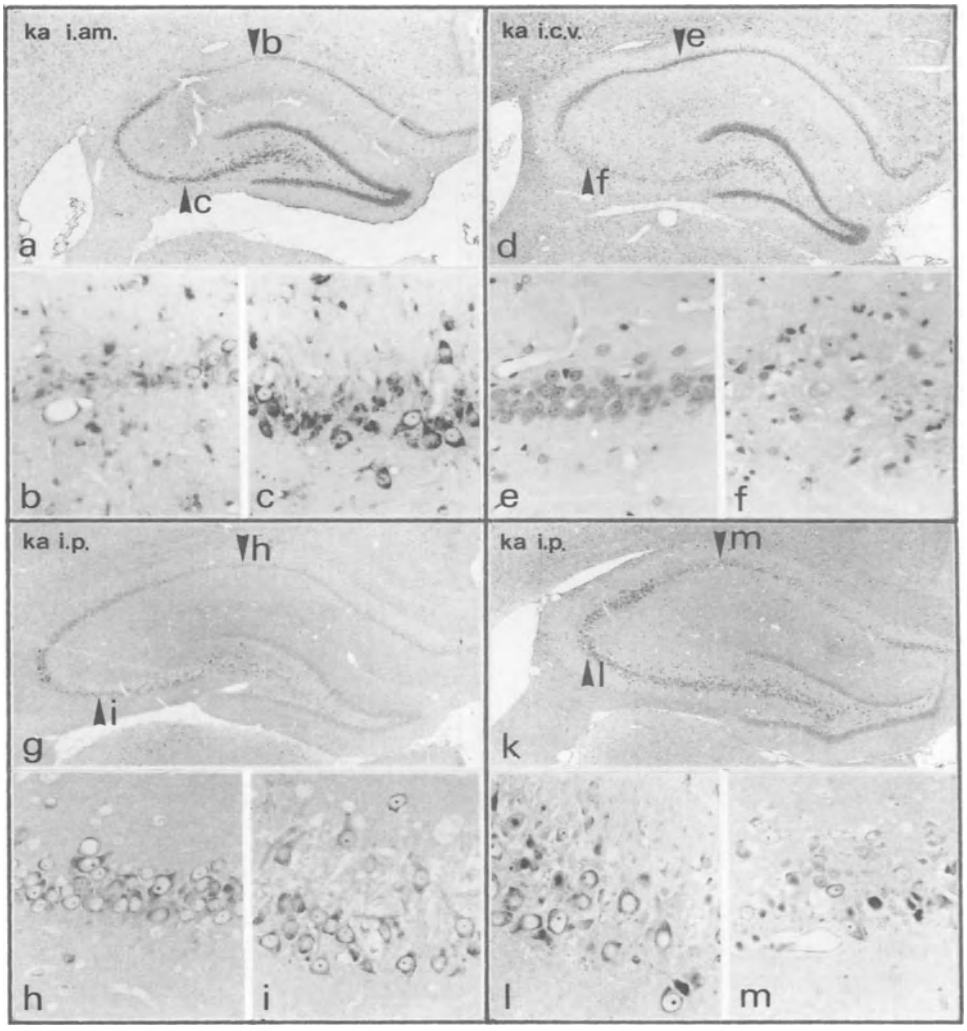

Fig. 3. Histopathological changes in hippocampal formation after KA application by different routes. Fixed brains were paraffin-embedded and 5 μm sections stained by hematoxylin/eosin; *a–c*, spotted type of neuronal damage distributed over CA_1 (b) and CA_3 (c) sector after 30 min *status epilepticus* induced by i.am. injection of 15 ng KA (case A2 contralateral hippocampus, 6 d survival, taken from a previous study, [5]); *d–f*, selective elimination of CA_3 pyramidal cells (f) after i.c.v. injection of 200 ng KA (case Ca14, 3 d survival); *g–m*, early (g–i) and mature (k–m) neuronal damage, 6 h and 2 d, respectively, after 30 min *status epilepticus*, induced by systemic injection of 10 mg/kg KA (cases Johannes II and Fridolin I, respectively). Magnification × 26 (a,d,g,k) and × 260 (b,c,e,f,h,i,l,m).

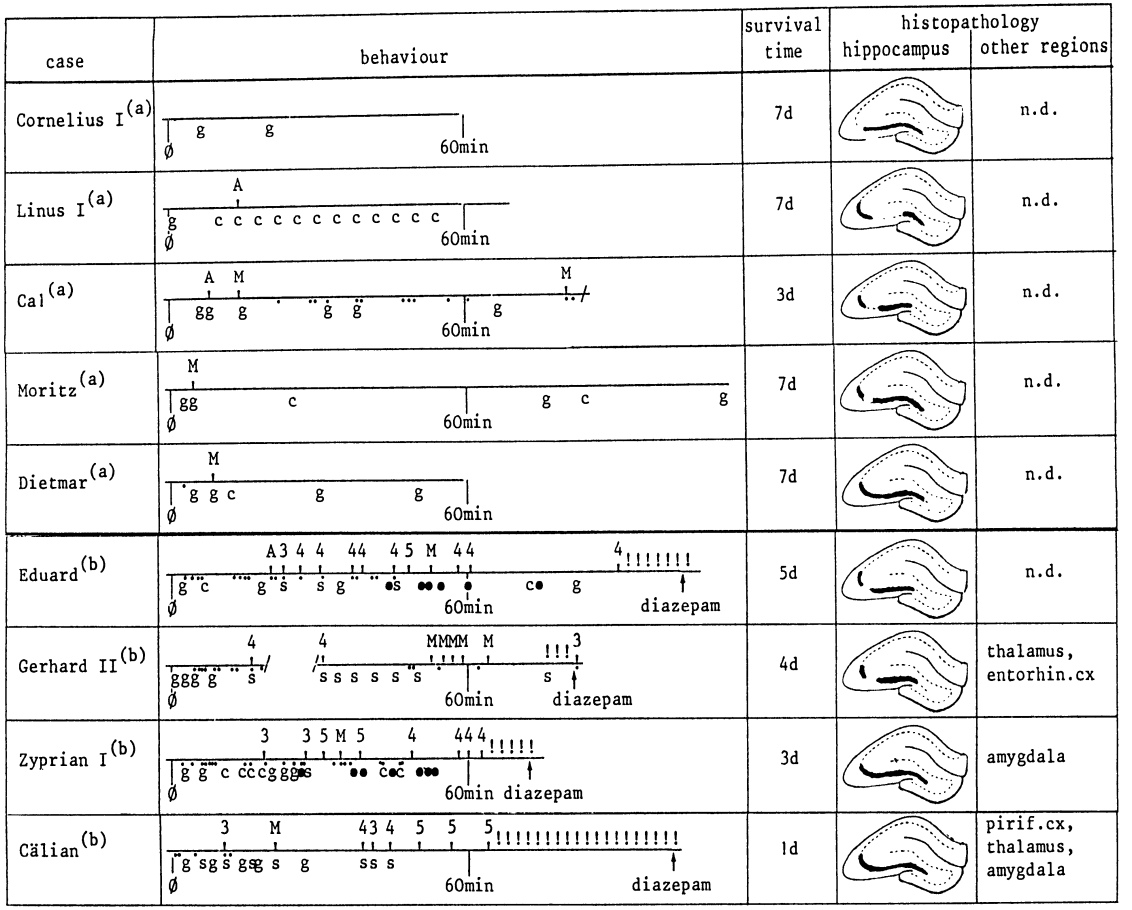

Fig. 4. Limbic seizure behaviour after injection of 200 ng KA into the left lateral ventricle of freely moving rats, with schematic illustration of resulting damage in ipsilateral hippocampus. (a), injection into dorsal part of lateral ventricle; (b), injection into deep ventral part of lateral ventricle. One-letter code for limbic seizure behaviour is described in legend to Fig. 1. A, atypical tonic attack. Diazepam was administered i.p. (10 mg/kg, repeatedly for up to 24 h); n.d., not detectable.

neuronal damage was observed in the hippocampus (Fig. 3a), interestingly not limited to the CA_3 sector, which is characteristically and selectively affected after i.c.v. injections of higher KA-doses (see below).

Injection of KA into the lateral ventricle

The behavioural outcome of i.c.v. injections of 200 ng KA was variable. Limbic motor seizures were not always observed, and *status epilepticus* developed in 9 out of 15 rats injected, including all 7 rats injected into the ventral horn of the ventricle, probably reflecting direct activation of the amygdaloid complex. Severe neuronal damage in the hippocampal CA_3 sector (Fig. 3d) was induced independently of the occurrence of *status epilepticus* (Fig. 4). In many cases, the destruction of CA_3 pyramidal cells was not complete, sparing islands of healthy appearing neurons (Fig. 4). In some of the animals which developed *status epilepticus* we observed additional damage in other limbic brain regions such as the entorhinal cortex, the piriform cortex, the amygdala, midline thalamic nuclei and in the hippocampal CA_1 sector.

Systemic injection of KA

In rats the most commonly used method to induce limbic motor seizures by KA is systemic application of about 10 mg/kg KA. Seizure histories of 12 cases are depicted in Fig. 5. Limbic motor seizures appeared with a time-lag of 40–70 min. From experiments with radio-labelled KA it is known that the toxin crosses the blood brain barrier (BBB) only very slowly [6]. However, once overt motor seizures developed, they usually progressed rapidly to behavioural *status epilepticus*, sometimes even immediately. The reason for this rapid progression might be a gradual opening of the BBB during seizure activity [7], with blood levels of KA still high. In most of these cases, patches of neuronal damage were found evenly distributed over CA_1 and CA_3, with damage appearing earlier in CA_3 (Fig. 3g) than in CA_1 (Fig. 3k). Additional damage was found in the lateral septum, the midline nuclei of the thalamus and occasionally in the piriform cortex.

The use of KA as a selective lesioning tool

In the late 1970s, KA has been used extensively as a tool to induce axon-sparing lesions in various brain sites (see [8] for contemporary overview), notably in the striatum. However, the hippocampal CA_3 pyramidal cells exhibit such a high susceptibility to the toxin [9] that it is almost impossible by conventional techniques to induce lesions in other parts of the brain without affecting this hippocampal subregion (see e.g. [10,11]). Thus, for such extrahippocampal lesions the use of KA is not advisable. On the other hand, KA seems ideally suited for the selective and almost complete elimination of CA_3 pyramidal cells. A high degree of selectivity is achieved by injecting 200 ng KA into one lateral ventricle.

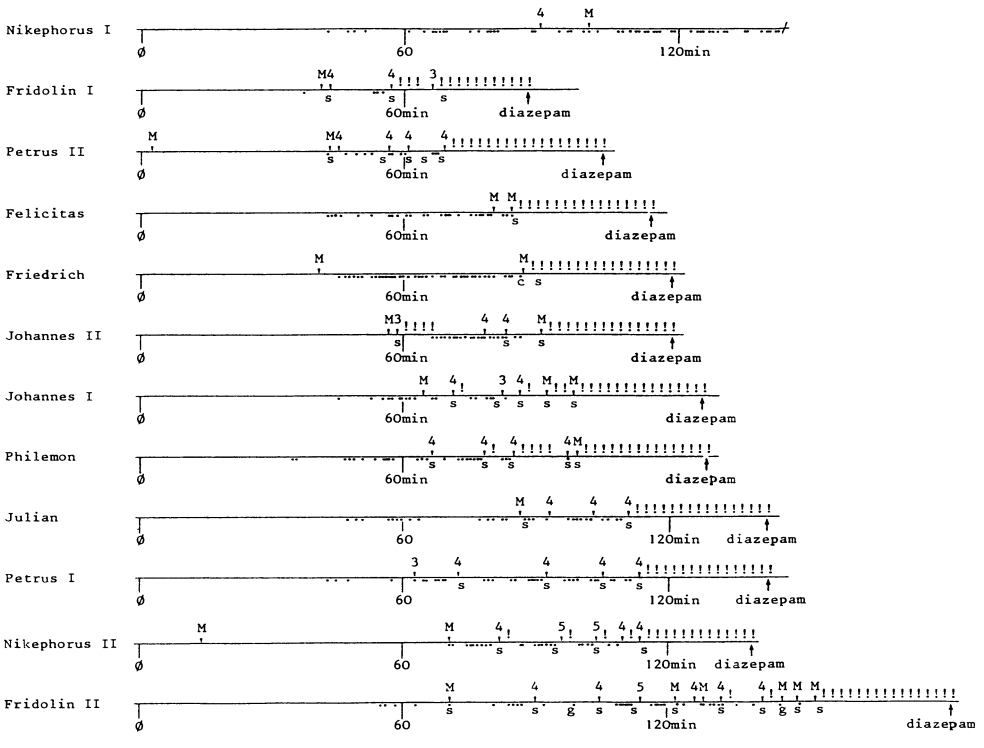

Fig. 5. Limbic seizure behaviour after systemic injection of 10 mg/kg KA. One-letter code for limbic seizure behaviour is described in legend to Fig. 1. Diazepam was administered i.p. (10 mg/kg, repeatedly for up to 24 h). For histopathological changes, see Fig. 3, g–m.

Although we performed these injections in conscious freely moving rats, we observed in many cases no or only mild motor expression of limbic seizures; nevertheless, those cases exhibited severe CA_3 histopathology (see Fig. 4), underlining the fact that with this type of KA application neuronal damage is not dependent on prolonged motor seizure activity (compare also [12]). On the contrary, prolonged seizure activity in this context should rather be regarded as an unwanted side effect, eventually resulting in neuronal damage at additional seizure sensitive sites. Thus, it is advisable to interfere with motor seizure expression once isolated seizure attacks have occurred by i.p. injection of diazepam (10 mg/kg), before the evolution of *status epilepticus*. From the cases presented in Fig. 4 it is evident that it is impossible to predict the degree of CA_3 lesion from the behavioural sequelae, making histological verification indispensable.

Which application technique of KA is the most useful for an animal model of temporal lobe epilepsy?

The acute clinical phenomenology of temporal lobe epilepsy is characterized by partial attacks of short duration, *status epilepticus* representing an exceptional and rare complication. Only i.am. injections of low KA doses reproduce this clinical behaviour with some accuracy. Concerning histopathological consequences, the hippocampus is the most susceptible brain region in both the human disease as well as all KA models described here. In post mortem as well as *ex vivo* material from patients suffering from temporal lobe epilepsy, often both the CA_1 (Sommer sector) and the CA_3 pyramidal cells (end folium) are affected [13]. However, in many other patients no hippocampal damage can be detected. Thus, the nearly complete destruction of exclusively CA_3 pyramidal cells by i.c.v. injection of KA reflects human pathology to a lesser degree than spotted type of neuronal damage distributed over CA_1 and CA_3 after *status epilepticus* induced by systemic KA injection or by i.am. injection of low KA doses. However, the greatest advantage of i.am. injection of low KA doses lies in the regionally strictly confined and transient action of KA sufficient to induce the seizure syndrome. In the other KA models described here, the whole brain is flooded with KA for considerable time periods, since the elimination of KA from rat brain seems to proceed slowly [14]. After i.am. injection of a low KA dose excitation of amygdaloid neurons, maintained beyond a critical duration, apparently triggers endogenous mechanisms which progress to permanent seizures, depending on pathophysiological processes rather than on the continued presence of sufficient KA in brain tissue (compare [15]). These processes are now amenable to pharmacological studies, with minimal interference by exogenously applied unphysiologic substances.

Acknowledgement

We thank Dr. R. Schmid for providing polyimid coated fused silica capillaries, Ing. H. Reither for surgery, and W. Krivanek for typing the manuscript. Supported by the Austrian Science Research Found, project P 5647.

References

1. Ben-Ari Y, Lagowska S, Tremblay E and Le Gal La Salle G (1979) Brain Res. 163: 176–179.
2. Berger ML, Reither H, Schmid RW and Lassmann H (1989b) J. Neurosci. Meth. 27: 225–234.
3. König JFR and Klippel RA (eds.) (1976) The Rat Brain, A Stereotaxic Atlas of the Forebrain and Lower Parts of the Brainstem. Krieger, Huntington, New York.
4. Racine R (1972) Electroenceph. Clin. Neurophysiol. 23: 281–294.
5. Berger ML, Lassmann H and Hornykiewicz O (1989a) Brain Res. 489: 261–272.
6. Berger ML, Lefauconnier J-M, Tremblay E and Ben-Ari Y (1986) In: Schwarcz R and Ben-Ari Y (eds.) Excitatory Amino Acids and Epilepsy. Plenum Publ. Corp., New York, pp. 199–209.

7. Ruth RE (1984) Epilepsia 25: 259–268.
8. McGeer EG, Olney JW and McGeer PL (eds.) (1978) Kainic Acid as a Tool in Neurobiology. Raven Press, New York.
9. Nadler JV, Perry BW and Cotman CW (1978) Nature 271: 676–677.
10. Nitsch C and Hubauer H (1986) Neurosci. Lett. 64: 53–58.
11. Fibiger HC and Atmadja S (1983) In: Fuxe K, Roberts P and Schwarcz R (eds.) Excitotoxins. MacMillan Press, London, pp. 271–279.
12. Sater AS and Nadler JV (1987) Neurosci. Lett. 84: 73–78.
13. Margerison JH and Corsellis JAN (1966) Brain 89: 499–530.
14. Nadler JV, Shelton DL, Perry BW and Cotman CW (1980) Life Sci. 26: 133–138.
15. McIntyre D, Nathanson D and Edson N (1982) Brain Res. 250: 53–63.

Excitatory amino acids control the gastric function in the rat

Y. Gotoh, M. Ishida and H. Shinozaki

The Tokyo Metropolitan Institute of Medical Science, 3-18-22, Honkomagome, Bunkyo-ku, Tokyo 113, Japan

Abstract

Systemic administration of excitatory amino acids, such as glutamic acid, kainic acid, quisqualic acid and *N*-methyl-D-aspartic acid (NMDA), depressed the spontaneous gastric motility of the rat in a dose-dependent manner. Their minimum effective doses were considerably low except glutamate, being much less than 1 mg/kg. Specific NMDA antagonists such as 3-[(±)-2-carboxypiperazin-4-yl]propyl-1-phosphonic acid (CPP), DL-2-amino-7-phosphonoheptanoic acid (APH) and (+)-5-methyl-10,11-dihydro-5H-dibenzo[a,d]-cyclohepten-5,10-imine maleate (MK-801) increased the spontaneous gastric motility in a dose-dependent manner and prevented the NMDA-evoked depression of the gastric motility. On the other hand, kynurenate, 6,7-dinitroquinoxaline-2,3-dione (DNQX) and 6-cyano-7-nitroquinoxaline-2,3-dione (CNQX) decreased the spontaneous gastric motility. Baclofen markedly stimulated the spontaneous gastric motility, and NMDA markedly depressed the baclofen-induced gastric motility, suggesting that the site of action of NMDA on the gastric motility may be distal from that of baclofen. Under the action of hexamethonium or chlorisondamine, bethanechol markedly stimulated the gastric motility, but CPP and MK-801 had little effect upon it. After treatment with atropine, responses to NMDA blockers were hardly observed. Similar results were obtained after vagotomy. These results suggest that excitatory amino acids serve the gastric function possibly via a central action.

Introduction

Glutamate (unless otherwise specified, L-glutamate) is believed to be an excitatory neurotransmitter in the mammalian central nervous system (CNS), and many glutamate analogues cause a depolarization of most mammalian central neurones. Direct actions of these amino acids upon various neurones have been well documented [1,2]. The pharmacological effects observed after systemic injection of excitatory amino acids or their antagonists have also been studied extensively in order to validate that glutamate serves a variety of physiological functions through activation of excitatory amino acid receptors, which have been brought into focus as potential pharmacological sites of actions. Receptors for excitatory amino acids have been divided into three subtypes based on their selectivity towards the agonists; kainate, quisqualate and NMDA [3]. Although highly specific antagonists for kainate- and quisqualate-type receptors are not yet available, actions of specific NMDA antagonists, such as CPP, D-2-amino-5-phosphonovaleric acid (APV), APH and MK-801 are widely documented. Pharmacological studies on neurotransmitters need essentially both agonists and specific antagonists. Thus,

studies on glutamatergic functions, in particular, with reference to the NMDA-type receptor, have been able to be performed in detail, because of widespread availability of specific NMDA antagonists.

Recently, it has been reported that glutamate affects some essential physiological functions, such as central cardiovascular regulation [4–8], respiration [9], motor functions [10–16], contractile function of the small intestine [17,18] and so on. The presence of functional receptors for excitatory amino acids outside the CNS of mammals has also been demonstrated [17–20]. In the course of studies on the actions of several compounds which block responses to glutamate in the mammalian CNS, we have noticed that glutamate exerts widespread influence upon the physiological functions of the rat internal organs. In particular, the gastric motility of the rat was markedly depressed by systemic administration of excitatory amino acids. The brain can exert on the gastrointestinal tract via the parasympathetic and sympathetic outflows [21], but little is known about their neuropharmacology. In the present paper, we describe the pharmacology of the gastric motility in the rat with regard to excitatory amino acids.

Materials and Methods

In situ *experiments*

Adult male Wistar rats (N = 195) weighing 275–375 g, were deprived of food but allowed free access to water for about 24 h prior to the experiment. The abdomen was opened to about 2 cm by midline section under urethane anaesthesia (1.2 g/kg s.c.). A small incision was made at the greater curvature of the fore-stomach about 10 mm from the limiting ridge, avoiding observable blood vessels in surrounding areas as much as possible. A small gastric balloon (2 cm in length, about 1 ml in volume) made of condom rubber was inserted into the stomach through the small incision. The rats were kept in a supine position on a heat-mat during the experiment. Fifteen to 30 min after the surgical operation, the balloon was filled with warm water (37°C) so that the overall gastric pressure could be kept within the desired levels. Intragastric pressure was measured by a transducer through a thin polyethylene tube (1.3 mm outer diameter) connected to the intragastric balloon and the output was displayed on a chart recorder through an amplifier. Some rats occasionally demonstrated a pause of the contraction for a while, and some rats showed extremely small amplitudes of the contraction. These animals were excluded from participation in the present study. When saline was injected into the rat in a volume of 0.2 ml per 100 g body weight, no apparent change in the spontaneous gastric motility was observed at all. The femoral vein was catheterized for the administration of drugs. Blood pressure was monitored continuously from the femoral artery, when necessary. In some rats, the role of the vagus in the response was assessed by sectioning the vagal trunks at the abdominal or cervical level and by atropine treatment.

In vitro *experiments*

The rats were sacrificed by cervical dislocation, and longitudinal and circular sections of the stomach fundus were prepared for *in vitro* examinations. Tissues were mounted in organ baths containing 10 ml of modified Tyrode solution of the following composition (mM): NaCl 16.9, $CaCl_2$ 1.8, KCl 2.68, NaH_2PO_4 0.3, $NaHCO_3$ 11.91, glucose 5.6. Tissue bath solutions were maintained at 37°C and equilibrated with 95% O_2 and 5% CO_2.

Results

Depression of the gastric motility induced by excitatory amino acids

The overall gastric pressure (tone) was set 5 cm H_2O by inflating the intragastric balloon with an appropriate amount of water. The stomach showed the superimposed rhythmic contractions with an amplitude of 10–30 cm H_2O and frequency

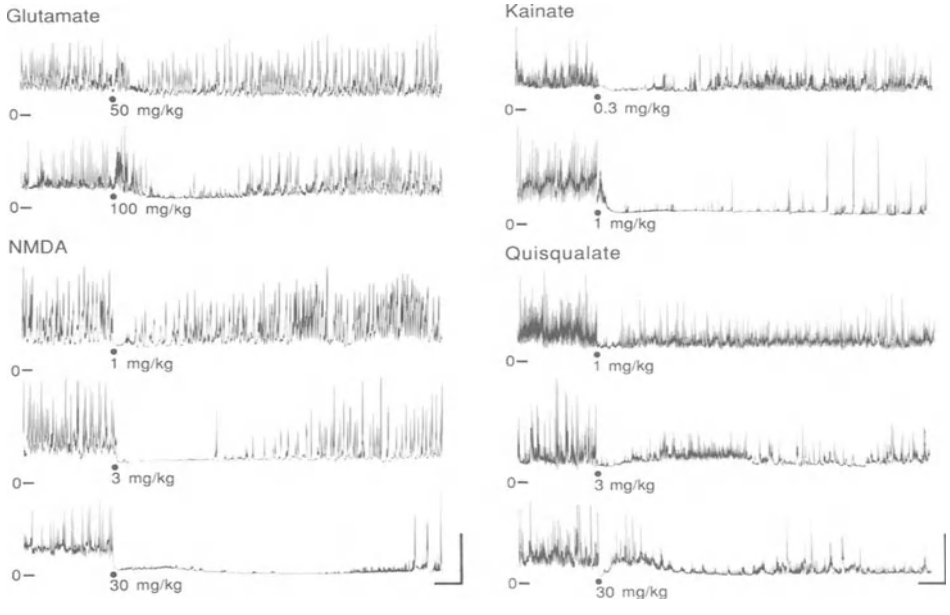

Fig. 1. Dose-dependent depression of the rat gastric motility caused by excitatory amino acids. The traces show representative responses to intravenous excitatory amino acids which are almost equivalent to the average. Dark points indicate the intravenous injection of each excitatory amino acid. The data were obtained from separated animals. Note that these excitatory amino acids reduce the gastric motility in a dose-dependent manner. The ground level of the overall gastric tone was shown under each trace. Calibration; 5 min, 10 cm H_2O.

of 1–5/min, which lasted in an almost constant manner for a considerably long time, although their frequency and amplitude of the gastric motility varied from one preparation to another. When glutamic acid (50–100 mg/kg, N = 6), NMDA (0.25–30 mg/kg, N = 68), kainic acid (0.1–1 mg/kg, N = 26) and quisqualic acid (0.3–30 mg/kg, N = 30) were intravenously given to the rat, the spontaneous gastric motility was obviously depressed in a dose-dependent manner. The onset of actions of these excitatory amino acids occurred within several minutes. Fig. 1 shows representative recordings of the spontaneous gastric motility depressed by these excitatory amino acids. There was no evident difference in mode of the depression among them, although there was a great difference in the effective dose range which was possibly due to different penetration into the blood brain barrier. In some rats the gastric tone increased slightly after the administration of relatively high doses of quisqualate. The minimum effective doses were less than 1 mg/kg, with the exception of glutamate which required a large dose of more than 50 mg/kg.

It was of great interest that NMDA showed a marked depression of gastric motility in considerably low concentrations, along with kainic acid and quisqualic acid. As mentioned above, specific NMDA blockers are now available for pharmacological studies, so examinations were performed mainly with regard to NMDA. After systemic injection of lower doses of NMDA, spontaneous rhythmic contractions with larger amplitudes but lower frequencies were sometimes observed, in particular, at the stage of recovery from the action.

Baclofen is known to stimulate the gastric function due to activation of the central γ-aminobutyric acid(GABA)ergic system [22–26]. Baclofen produces an increase in gastric motility by two vagally depressant mechanisms which reflect changes in activity in both the vagal fibres driving the intramural cholinergic neurones and those driving the non-cholinergic neurones [21]. A systemic injection of baclofen (2 or 4 mg/kg) markedly increased the gastric motility (Fig. 2). The onset was relatively rapid and the blood pressure was continuously decreased. When NMDA (1–4 mg/kg, N = 7) was intravenously given to the rat prior to the injection of baclofen (2 mg/kg i.v.) and vice versa, the baclofen-induced stimulation of the gastric motility was hardly observed. This indicates that systemic NMDA blocks the baclofen-induced stimulation of the gastric motility. When picrotoxin (1–2 mg/kg i.v., N = 3) and bicuculline (0.5–0.8 mg/kg i.v., N = 3) were injected to the rat, slight convulsions were observed and the blood pressure was slightly increased (10–20 mmHg), but they were not able to affect the inhibitory action of NMDA on the spontaneous gastric motility, suggesting that the gastric depression caused by NMDA is not related to GABAergic functions [27].

Stimulation of the gastric motility by specific NMDA blockers

CPP and APH are believed to be specific competitive antagonists of NMDA [28,29]. It is of great interest to examine the action of specific NMDA antagonists on spontaneous gastric motility. Doses of these NMDA antagonists were chosen by reference to those in the experiments of decerebrated rigidity rats where NMDA

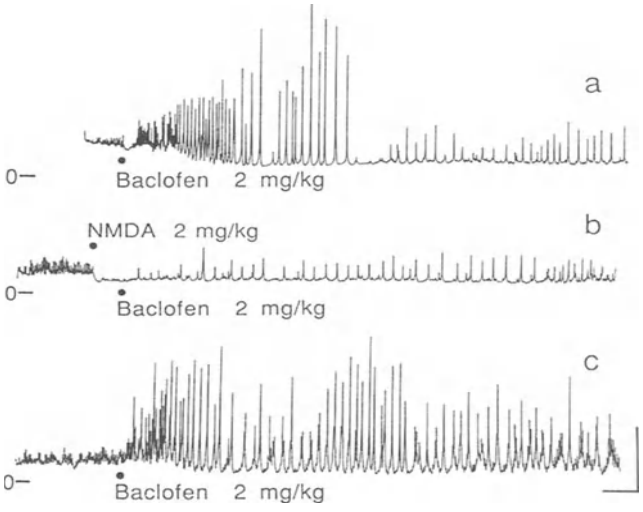

Fig. 2. Prevention by NMDA against the baclofen-induced gastric motility. The ground level of the gastric pressure was shown under each trace. a: Baclofen-induced stimulation of the spontaneous gastric motility. Baclofen was intravenously given at a dose of 2 mg/kg. b: Prevention of the baclofen-evoked gastric motility by NMDA. NMDA (2 mg/kg i.v.) was administered 4 min before injection of baclofen (2 mg/kg i.v.). c: Baclofen was applied 100 min after the administration of NMDA in b. Records in a, b and c were obtained from the same animal. Calibration; 5 min, 10 cm H_2O.

antagonists were intravenously given [13] and by other references [10,14]. Intravenous CPP in various doses (0.125–10 mg/kg, N = 40) increased the spontaneous gastric motility in a dose-dependent manner. Depression of the gastric motility was not observed even at a high dose of 10 mg/kg. The minimum effective dose was less than 0.25 mg/kg, demonstrating that the stimulant action of CPP on the gastric motility was more potent than the depressant action on decerebrate rigidity in terms of effective dose ranges in the rat [13], but was almost equal to that on seizures in DBA/2 mice [15]. The onset of the CPP action was within several minutes. CPP augmented the amplitude of the spontaneous gastric motility without affecting its frequency at the first stage of the action, but with a slight decrease in its frequency at the latter half of the action (Fig. 3). In the case of higher doses of CPP, say 10 mg/kg, an increase in amplitudes lasted for more than 2.5 h. APH (N = 10) also increased the gastric motility at doses greater than 10 mg/kg in a similar manner to CPP. Neither CPP nor APH caused a significant change in the blood pressure. Picrotoxin (2 mg/kg i.v., N = 2) hardly affected the CPP-evoked stimulation of the gastric motility.

Ketamine has been known to selectively reduce excitation of central mammalian neurones by NMDA [30]. Ketamine (0.5–2 mg/kg i.v., N = 9) slightly stimulated the spontaneous rhythmic motility like CPP and APH, and slightly increased the

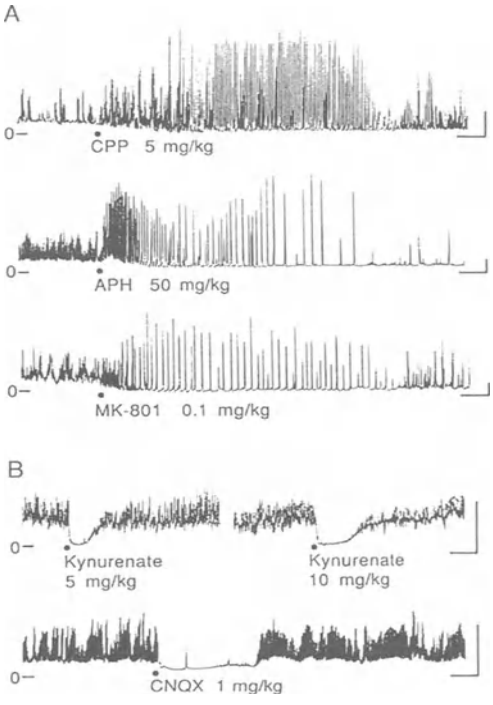

Fig. 3. A: An increase in the gastric motility induced by specific NMDA antagonists. CPP, APH and MK-801 were intravenously given to the rat in a dose indicated under each trace. The traces were obtained from different animals. B: Depression of the gastric motility by kynurenate and CNQX. Note that these antagonists sometimes decreased the gastric tone to a level less than the original pressure. Calibration; 5 min, 10 cm H_2O.

overall gastric pressure. The actions of ketamine did not last so much as that of CPP. Following doses of ketamine exceeding 5 mg/kg most rats died of respiratory arrest under the urethane anesthesia.

MK-801 is thought to act at the level of the NMDA receptor-associated ion channel and shows a marked use-dependence in its NMDA antagonist properties [31]. MK-801 (0.01–1 mg/kg i.v., N = 12) markedly stimulated the spontaneous gastric motility. The onset of its action was relatively rapid, being within 5 min, in striking contrast to that *in vitro* [31]. No significant change in the blood pressure was caused by MK-801 in this dose range. The stimulation of the gastric motility lasted for a relatively longer time than that of other specific NMDA antagonists. The characteristics of the stimulant action of MK-801 on the gastric motility was a large rhythmic contraction of the stomach with low frequencies (Fig. 3). The increase in amplitudes of the gastric contraction by MK-801 was dose-related.

If the NMDA-evoked depression of the gastric motility is due to activation of NMDA-type receptors, some specific NMDA blockers would prevent the depression caused by NMDA. After the administration of CPP (1–2 mg/kg i.v., N = 4), the NMDA-evoked decrease (NMDA: 2–4 mg/kg i.v.) in the gastric motility was almost completely prevented. Pretreatment with MK-801 (0.05–0.5 mg/kg i.v., N = 8) about 30 min before the administration of NMDA also prevented the NMDA-evoked decrease in the gastric motility. Quite similar results were obtained even when they were simultaneously given. These actions were in a dose-dependent manner.

Actions of kynurenate, DNQX and CNQX on the gastric motility

Kynurenate, CNQX and DNQX have been characterised as broad spectrum excitatory amino acid antagonists, although their mode of action on NMDA receptors is apparently different from that on non-NMDA receptors [32–34]. Kynurenate, CNQX and DNQX are competitive antagonists at non-NMDA receptors, although they do not distinguish between the receptors for quisqualate and kainate [35]. In addition, they reduce the maximum response to NMDA, indicating an unsurmountable antagonist. Kynurenic acid (2–10 mg/kg i.v., N = 8). DNQX (0.5–1 mg/kg i.v., N = 4) and CNQX (1–2 mg/kg i.v., N = 2) significantly depressed the spontaneous gastric motility in striking contrast with specific NMDA antagonists (Fig. 3B). Dimethylsulfoxide (DMSO), which was used as a solvent of these antagonists, slightly increased the spontaneous gastric motility in a concentration of 25%.

Effects of vagotomy and ganglion blockers

In order to get information about whether the decrease in the gastric motility by NMDA was due to activation of the central or peripheral NMDA-type receptor,

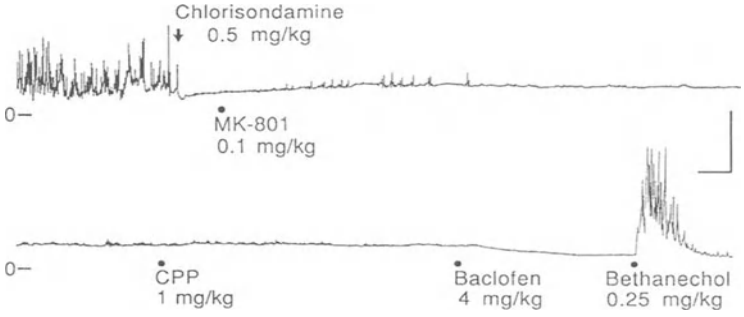

Fig. 4. Actions of MK-801, CPP, baclofen and bethanechol on the gastric motility after intravenous administration of chlorisondamine. Only bethanechol stimulated the gastric motility under the action of chlorisondamine. Calibration; 5 min, 10 cm H_2O.

effects of NMDA antagonists were examined under actions of ganglionic blocking agents, which might result in atony of the gastrointestinal tract. When chlorisondamine or hexamethonium, a ganglion blocker, was intravenously given to the rat at a dose of 0.1–0.5 mg/kg (N = 5) or 20 mg/kg (N = 2), respectively, the spontaneous gastric motility was considerably depressed with a marked decrease in the blood pressure (about 50 mmHg at a dose of 0.5 mg/kg) and the depression of the gastric motility lasted for more than 2 h. At this stage, CPP (1–5 mg/kg i.v., N = 3). MK-801 (0.1 mg/kg i.v., N = 2) and baclofen (2–4 mg/kg i.v., N = 2) did not stimulate the gastric motility at all, but bethanechol (0.25 mg/kg i.v., N = 2) markedly stimulated it (Fig. 4). In the case of stimulant action of bethanechol, the overall gastric pressure, which was set at 5 cm H_2O at the beginning of the experiment, was markedly increased with normal sizes of rhythmical contractions. This seems to be a characteristic feature of actions of compounds which act peripherally. When MK-801 (0.1 mg/kg) was intravenously administered 20 min before the administration of chlorisondamine (0.1 mg/kg i.v.), chlorisondamine completely depressed the MK-801 evoked spontaneous gastric motility and no rhythmical contraction was observed.

Atropine (1 mg/kg i.v., N = 6) decreased considerably the over-all gastric pressure and the superimposed rhythmic contractions, but some rats showed still the rhythmic contraction. Similar results had been obtained in the anaesthetized ferret (36]. CPP (5–10 mg/kg i.v., N = 4). under the action of atropine, hardly stimulate the gastric motility, but NMDA (4 mg/kg i.v., N = 6) completely abolished the contraction. Similar results were obtained after the surgical vagotomy at the abdominal or cervical level.

In vitro *experiments*

Moroni *et al.* [17] demonstrated that NMDA caused a contraction of the longitudinal ileal muscle which appeared to be mediated by the myenteric cholinergic neurones, and Luzzi *et al.* [18] confirmed that L-glutamate-induced ileal contraction was in some way dependent upon an action on the myenteric cholinergic neurones due to activation of NMDA-type receptors in the guinea-pig myenteric plexus. Therefore, it is necessary to examine whether the NMDA-evoked depression of the spontaneous gastric motility is due to direct or subsequent activation of the peripheral NMDA-type receptor, although above results strongly suggested that the depression of the gastric motility seems to be due to activation of central NMDA-type receptors. Isolated strips of longitudinal and circular gastric muscles were hardly affected by the addition of glutamate, NMDA, kainate, and quisqualate in concentrations up to 1 mM in a Mg-free solution. Magnesium ions (0.5 mM) also did not affect the contractions at all. Acethylcholine induced marked contraction of both longitudinal and circular muscles in concentrations less than 0.2 mM, and norepinephrine (0.1 mM) caused a relaxation of both muscles. However, excitatory amino acids did not affect the contraction or relaxation at all in concentrations up to 1 mM. MK-801 (0.01 mM) had no effect the contraction of the gastric muscle *in vitro*.

Discussion

The results from this study demonstrate that excitatory amino acids depress the spontaneous gastric motility in the rat. Their inhibitory actions on the gastric motility were in a dose-dependent manner. It is of great interest that specific NMDA antagonists *per se* stimulated the spontaneous gastric motility. As to NMDA blockers, it is so far known that systemic administration of these antagonists depresses epileptic seizures in DBA/2 mice [15]. It is generally believed that, under 'normal' conditions NMDA receptors contribute very little [37,38] because magnesium ions primarily act by blocking the NMDA ion channel in a voltage-dependent manner [39–41]. Peripheral NMDA receptors have also demonstrated similar pharmacological properties to central receptors [18]. However, in the present study, NMDA depressed the gastric motility even under 'normal' conditions of the urethane anesthetized rat where a considerable amount of magnesium ions were present, and specific NMDA antagonists, such as CPP, APH and MK-801, *per se*, stimulated the spontaneous gastric motility of the rat. These experimental results might support the hypothesis that NMDA receptors contribute under the ordinary conditions, possibly as a result of depolarization due to activation of other types of glutamate receptors or other transmitter systems.

It seems reasonable to divide the NMDA blockers concerned pharmacologically into three groups: competitive antagonists such as CPP, APV and APH [28,29]; non-competitive antagonists which block specifically the NMDA response, such as MK-801 and ketamine [30,31]; and mixed-type antagonists which are non-competitive NMDA antagonists but depress the responses to kainate and quisqualate in a competitive manner, such as kynurenic acid, CNQX and DNQX [32–35]. In the present examination the former two groups demonstrated stimulation of the spontaneous gastric motility in the rat, but the latter depressed it. These results are of great interest, because these data indicate that non-NMDA receptors act differently from the NMDA-type receptor in controlling the gastric function, although both kainate and quisqualate abolish or markedly reduce the spontaneous gastric motility like NMDA. It is reasonable to expect that the gastric motility should be much more stimulated by the mixed-type antagonist than by specific NMDA antagonists, because most receptors for excitatory amino acids should be hardly activated in the presence of the mixed-type antagonist which blocks both kainate- and quisqualate-type receptors as well as the NMDA-type receptor. There is no denying a possibility that the mixed-type antagonist exerts additional actions on the CNS. In our preliminary experiments, the mixed-type antagonist stimulated the micturition contractions of the rat urinary bladder, while specific NMDA antagonists depressed vesical micturition contractions (unpublished observations). Opposite but united actions of NMDA antagonists on the stomach and the bladder are of great interest. Further studies will be required to establish the pharmacology of the gastric or vesical motility.

Under actions of ganglionic blockers such as hexamethonium and chlorisondamine, NMDA antagonists hardly stimulated the spontaneous gastric motility,

suggesting that they act at a central site to stimulate the vagal outflows to the stomach. In addition, excitatory amino acids hardly affected the contraction of gastric muscles *in vitro*, and surgical and chemical vagotomy supported the central action of excitatory amino acids on the gastric motility. Recently, the presence of peripheral receptors for excitatory amino acids has been reported [17,18], but their action on the intestine was excitatory. NMDA-induced stimulation of these peripheral receptors caused a contraction of the longitudinal ileal muscle which appeared to be mediated by the myenteric cholinergic neurones [17]. In addition, it was reported that binding sites for the excitatory amino acid are associated with the perikarya of vagal afferent neurones and that these receptors undergo axonal transport in the peripheral vagal trunks [20]. Therefore, as a point to be considered, there is a problem whether NMDA at least in part acts peripherally, although the present examination strongly suggests that the inhibition of the gastric motility by NMDA or excitatory amino acids is via a central action.

In many cases there is a positive relationship between the gastric secretion and motility. In the case of systemic injection of baclofen, both the gastric secretion and motility were stimulated via a central action [22–26]. On the other hand, metoclopramide prefers to activate the gastric motility rather than the gastric secretion [42]. In our preliminary experiments, CPP stimulates markedly the gastric secretion in the rat, but NMDA did not always decrease the gastric acidity in low doses. As for the ability of excitatory amino acids to control the gastric secretion, further studies will be required. In any case, it is confirmed that excitatory amino acids play a key role in controlling the gastric function in the rat.

Acknowledgement

This work was supported in part by a Grant-in-Aid for Scientific Research from the Ministry of Education, Science and Culture of Japan. MK-801 was a gift of Merck, Sharp and Dohme.

References

1. Hicks TP, Lodge D and McLennan H (1987) Excitatory Amino Acid Transmission. Neurol. Neurobiol., Vol. 24, Alan R. Liss, Inc., New York.
2. Cavalheiro EA, Lehmann J and Turski L (1988) Frontiers in Excitatory Amino Acid Research. Neurol. Neurobiol. Vol. 46, Alan R. Liss, Inc., New York.
3. Cotman CW and Iversen LL (1987) Trends in Neurosci. 10: 263–265.
4. Reis DJ, Granata AR, Perrone MH and Talman WT (1981) J. Auton. Nerv. Syst. 3: 321–334.
5. Granata AR and Reis DJ (1983) Brain Res. 259: 77–93.
6. Willette RN, Barcas PP, Krieger AJ and Sapru HN (1983) Neuropharmacology 22: 1071–1079.
7. Guyenet PG, Filtz TM and Donaldson SR (1987) Brain Res. 407: 272–284.
8. Kubo T and Kihara M (1988) Brain Res. 451: 366–370.
9. Foutz AS, Champagnat J and Denavit-Saubie M (1988) Neurosci. Lett. 87: 221–226.

10. Croucher MJ, Collins JF and Meldrum BS (1982) Science 216: 899–901.
11. Shinozaki H and Hirate K (1986) Jap. J. Pharmac. 41: 7–14.
12. Shinozaki H, Hirate K and Ishida M (1987) Neuropharmacology 26: 9–17.
13. Shinozaki H, Ishida M and Gotoh Y (1989) Neuropharmacology 28: 593–598.
14. Turski L, Meldrum BS, Turski WA and Watkins JC (1987) Eur. J. Pharmac. 136: 69–73.
15. Chapman AG, Meldrum BS, Nanji N and Watkins JC (1987) Eur. J. Pharmac. 139: 91–96.
16. Shinozaki H (1988) Prog. Neurobiol. 30: 399–435.
17. Moroni F, Luzzi S, Franchi-Micheli S and Zilletti L (1986) Neurosci. Lett. 68: 57–62.
18. Luzzi S, Zilletti L, Franchi-Micheli S, Gori AM and Moroni F (1988) Br. J. Pharmac. 95: 1271–1277.
19. Yoneda Y and Ogita K (1986) Brain Res. 383: 387–391.
20. Lewis SJ, Cincotta M, Verberne AJM, Jarrott B, Lodge D and Beart PM (1987) Eur. J. Pharmac. 144: 413–415.
21. Andrews PLR, Bingham S and Wood KL (1987) J. Physiol. 388: 25–39.
22. Goto Y and Debas HT (1983) Dig. Dis. Sci. 28: 56–60.
23. Goto Y, Hollinshead JW and Debas HT (1984) Am. J. Surg. 147: 159–163.
24. Goto Y, Tache Y, Debas H and Novin D (1985) Life Sci. 36: 2471–2475.
25. Andrews PLR and Wood KL (1986) Br. J. Pharmac. 89: 461–467.
26. Wood KL, Addae JI, Andrews PLR and Stone TW (1987) Neuropharmacology 26: 1191–1194.
27. Williford DJ, Ormsbee III HS, Norman W, Harmon JW, Garvey III TQ, Dimicco JA and Gillis RA (1981) Science 214: 193–194.
28. Perkins MN, Stone TW, Collins JF and Curry K (1981) Neurosci. Lett. 23: 333–336.
29. Davies J, Evans RH, Herrling PL, Jones AW, Olverman HJ, Pook P and Watkins JC (1986) Brain Res. 382: 169–173.
30. Anis NA, Berry SC, Burton NR and Lodge D (1983) Br. J. Pharmac. 79: 565–575.
31. Wong EHF, Kemp JA, Priestley T, Knight AR, Woodruff GN and Iversen LL (1986) Proc. Natl. Acad. Sci. USA 83: 7104–7108.
32. Jahr CE and Yoshioka K (1986) J. Physiol. 370: 515–530.
33. Evans RH, Evans SJ, Pook PC and Hunter DC (1987) Br. J. Pharmac. 91: 531–537.
34. Honore T, Davies SN, Drejer J, Fletcher EJ, Jacobsen P, Lodge D and Nielsen FE (1988) Science 241: 701–703.
35. Birch PJ, Grossman CJ and Hayes AG (1988) Eur. J. Pharmac. 151: 313–315.
36. Andrews PLR and Scratcherd T (1980) J. Physiol. 302: 363–378.
37. Collingridge GL and Bliss TVP (1987) Trends Neurosci. 10: 288–293.
38. Collingridge GL, Herron CE and Lester RAJ (1988) J. Physiol. 399: 301–312.
39. Ault B, Evans RH, Francis AA, Oakes DJ and Watkins JC (1980) J. Physiol. 307: 413–428.
40. Mayer ML, Westbrook GL and Guthrie PB (1984) Nature 309: 261–263.
41. Nowak L, Bregestovski P, Ascher P, Herbet A and Prochiantz A (1984) Nature 307: 462–465.
42. Jacoby HI and Brodie DA (1967) Gastroenterology 52: 676–684.

Address for correspondence: H. Shinozaki, The Tokyo Metropolitan Institute of Medical Science, 3-18-22, Honkomagome, Bunkyo-ku, Tokyo 113, Japan.

Interfering with glutamatergic neurotransmission by means of MK-801 administration discloses the locomotor stimulatory potential of other transmitter systems in rats and mice*

Maria Carlsson and Anders Svensson

Department of Pharmacology, University of Göteborg, Göteborg, Sweden

Abstract

Previous work in our laboratory has shown that the selective, non-competitive NMDA antagonist MK-801 [(+)-5-methyl-10,11-dihydroxy-5H-dibenzo(a,d)cyclohepten-5,10-imine] causes a pronounced locomotor stimulation in monoamine-depleted mice. The present paper describes the remarkable behavioural effects obtained in monoamine-depleted *mice* when MK-801 is combined with either the α-adrenergic agonist clonidine, or the dopaminergic agonist apomorphine, or the muscarinic antagonist atropine. In addition, the behavioural effects of MK-801 and the competitive NMDA antagonist DL-2-amino-5-phosphonovaleric acid (AP-5) and their interactions with clonidine in monoamine-depleted *rats* are reported. The results are discussed in relation to 1) the pathophysiology of schizophrenia, with emphasis on the glutamate hypothesis of schizophrenia and 2) implications for the treatment of Parkinson's disease.

Introduction

Previous work in our laboratory has shown that the selective, non-competitive NMDA antagonist MK-801 [(+)-5-methyl-10,11-dihydroxy-5H-dibenzo(a,d)cyclohepten-5,10-imine; 1] causes a pronounced locomotor stimulation in monoamine-depleted mice [2,3]. From this finding it can be inferred that: 1) Dopamine (DA) is not indispensable for initiation and generation of locomotion 2) Central glutamatergic systems exert a powerful inhibitory influence on locomotion 3) Central glutamatergic and catecholaminergic systems are functionally opposed with regard to locomotion – possibly this antagonistic interaction takes place within the striatum, in analogy to the presumed cholinergic/dopaminergic antagonism within this structure [4].

The present paper describes the remarkable behavioural effects obtained in monamine-depleted *mice* when MK-801 in a low dose, which does not *per se* affect motor activity, is combined with either 1) a high dose of the α-adrenergic agonist clonidine or 2) a low (subthreshold) dose of the dopaminergic agonist apomorphine or 3) a high dose of the muscarinic antagonist atropine. In addition, the behavioural effects of MK-801 and the competitive NMDA antagonist DL-2-amino-5-phosphonovaleric acid (AP-5) and their interactions with clonidine in monoamine-depleted *rats* are reported.

* Parts of this paper have previously been published in J. Neural Transm. (1989) 77: 65–71.

The results are discussed in relation to 1) the pathophysiology of schizophrenia, with emphasis on the glutamate hypothesis of schizophrenia [5], and 2) implications for the treatment of Parkinson's disease.

Experimental procedures

Animals

Male albino mice of the NMRI strain (20–30 g) and male Sprague-Dawley rats (160–180 g) were purchased from ALAB, Sollentuna.

Drugs

Idazoxan (Reckitt & Colman) was dissolved in distilled water. Reserpine (Ciba-Geigy), yohimbine HCl (Sigma), prazosin HCl (Pfizer) and clozapine (Wander) were dissolved in a few drops of glacial acetic acid and 5.5% glucose solution. α-Methyl-paratyrosine methylester HCl (α-MT; Sigma), apomorphine HCl (Sandoz), clonidine HCl (Boehringer Ingelheim), atropine sulfate (Aldrich) and ketamine HCl (Sigma) were dissolved in physiological saline. DL-2-amino-5-phosphonovaleric acid (AP-5; Sigma) was dissolved in 1.0 M NaOH before being diluted to final volume with physiological saline; the solution was adjusted to neutral pH by adding a few drops of 1.0 M HCl. MK-801 ([(+)-5-methyl-10,11-dihydroxy-5H-dibenzo(a,d)cyclohepten-5,10-imine] hydrogen maleate), generously supplied by Dr GN Woodruff at the MSD laboratories, England, was dissolved in physiological saline in an ultrasonic bath. All drugs were injected i.p., except atropine which was given s.c. and AP-5 which was given ICV. In mice all drugs were given in a volume of 10 ml/kg, except reserpine which was administered in a volume of 20 ml/kg. In rats the injection volume was 5 ml/kg.

ICV surgery

Polyethylene cannulae were implanted into each lateral ventricle under chloral hydrate (400 mg/kg i.p.) anaesthesia according to a technique described previously [6]. The rats were allowed one week's recovery before the experiment was performed. 20 µl of vehicle or AP-5 was injected into each ventricle.

Experimental equipment

In mice, the model for measuring motor activity consisted of a circular track, 5 cm wide and 1 meter in circumference, the inner and outer walls being transparent plastic cylinders, 15 and 25 cm high, respectively. The number of turns (meters) the animal covered in 30 min was registered manually or by means of IR detectors. In rat motor activity was measured by means of a 'M/P 40 Fc Electronic Motility

Meter' (Motron Products, Stockholm) with 40 photoconductive sensors (5 rows × 8, centre-centre distance 40 mm). Two h after the animals had been injected with reserpine and throughout the experiment the ambient temperature was held at 28°C (mice) or 27°C (rats).

Statistics

Mann-Whitney U-test was used throughout for comparisons between groups.

Results

Mouse

Interaction between MK-801/ketamine and clonidine in monoamine-depleted mice
Neither 1 mg/kg of MK-801, nor 2 mg/kg of the α-adrenergic agonist clonidine administered separately significantly affected locomotion, but the combined treatment caused a dramatic enhancement of motor activity (Fig. 1a). This effect was effectively antagonized by the α_2-adrenergic blockers idazoxan and yohimbine, as well as by the 'atypical' neuroleptic clozapine (data not shown here, see instead ref. 3). When another less potent, non-competitive NMDA antagonist, i.e. ketamine, was combined with clonidine a similar, though less forceful, synergism was observed (Fig. 1b). The mice receiving either MK-801 or ketamine in combination with clonidine had an 'energetic' appearance, albeit running or walking in a stilty, swaying fashion, moving along the track in essentially one and the same direction during the entire test period.

Interaction between MK-801 and apomorphine in monoamine-depleted mice
Also when MK-801 (1.5 mg/kg) was administered together with a subthreshold dose (0.1 mg/kg) of the DA receptor agonist apomorphine a clear-cut synergism

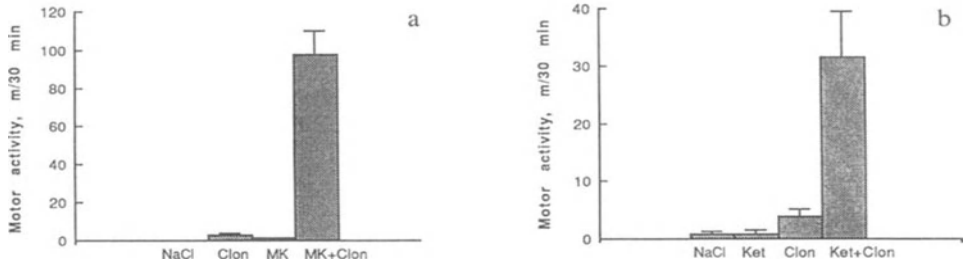

Fig. 1. Effects of MK-801 (1 mg/kg i.p.; **a**) or ketamine (50 mg/kg i.p.; **b**) in combination with clonidine (2 mg/kg i.p.) on motor activity in monoamine-depleted mice. Reserpine (10 mg/kg i.p.) was administered 18 h and α-MT (250 mg/kg i.p.) 30 (**a**) or 60 (**b**) min prior to MK-801/ketamine treatment. Clonidine was administered immediately before the registration of motor activity started, i.e. 60 min after MK-801/ketamine treatment. Motor activity was registered during 30 min. Shown are the means ± S.E.M. N = 6–11 (**a**) and 3–8 (**b**). *$p<0.02$ vs. the other groups. These data are in part from ref. 3.

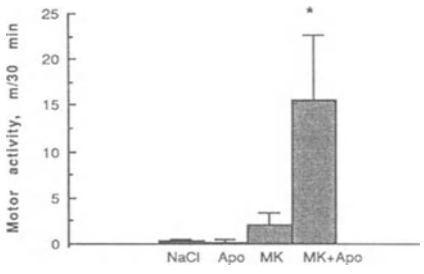

Fig. 2. Effects of MK-801 (1.5 mg/kg i.p.) in combination with apomorphine (0.1 mg/kg i.p.) on motor activity in monoamine-depleted mice. Reserpine (10 mg/kg i.p.) was administered 18 h and α-MT (250 mg/kg i.p.) 30 min prior to MK-801 treatment. Apomorphine was administered immediately before the registration of motor activity started, i.e. 60 min after MK-801 treatment. Motor activity was registered during 30 min. Shown are the means ± S.E.M. N = 9–11. *p<0.02 vs. the other groups. These data are from ref. 3.

was observed, although the effects were less dramatic than following the MK-801/clonidine treatment (Fig. 2).

Interaction between MK-801 and atropine in monoamine-depleted mice

Atropine *per se*, even in doses as high as 80 and 120 mg/kg (not shown) could not reverse the akinesia induced by reserpine and α-MT treatment. However, when atropine (40 mg/kg) was combined with 1 mg/kg of MK-801, a pronounced stimulation of motor activity was observed (Fig. 3). Similarly to the mice receiving MK-801 in combination with clonidine, the mice treated with MK-801 and atropine moved along the track in essentially one and the same direction, but they differed considerably from the former in appearance. Thus, whereas the MK-801/clonidine-treated animals had a stilty gait, their bodies lifted high above the

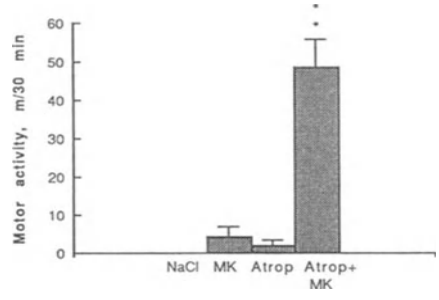

Fig. 3. Effects of MK-801 (1 mg/kg i.p.) in combination with atropine (40 mg/kg s.c.) on motor activity in monoamine-depleted mice. Reserpine (10 mg/kg i.p.) was administered 18 h, α-MT (250 mg/kg i.p.) 60 min and atropine 30 min prior to MK-801 treatment. Motor activity was registered during 30 min starting 60 min after MK-801 administration. Shown are the means ± S.E.M. N = 3–14. **p<0.01 vs. the other groups.

ground, the mice treated with atropine and MK-801 displayed crawling, lizard-like movements, their bodies flat against the ground.

Rat

MK-801-induced activation in monoamine-depleted rats

MK-801 (0.1 mg/kg i.p.) given to rats pretreated with reserpine and α-MT (10 and 250 mg/kg i.p. administered 18 h and 60 min, respectively, prior to MK-801) induced a behavioural activation in animals placed in an open field, starting about 30 min after the MK-801 injection and lasting for 30–60 min. The MK-801-treated rats explored the surroundings spontaneously but tended to get stuck in corners and displayed a certain degree of ataxia. In contrast to the feeble response evoked in control animals, touching and handling the MK-801-treated animals resulted in a clear-cut stimulation of locomotion. In contrast to the results obtained in the open field, MK-801-treated rats placed in motility meters did not display increased locomotion (see below).

With increasing doses of MK-801 (0.5–5 mg/kg i.p.) there was a dose-related decrease in muscle tonus and disappearance of the reserpine-induced hunch-back. In addition, spontaneous locomotion, as well as locomotion induced by tactile stimuli, decreased with increasing doses and the righting reflex was weakened. This picture of general anaesthesia lasted for about four h (data not shown).

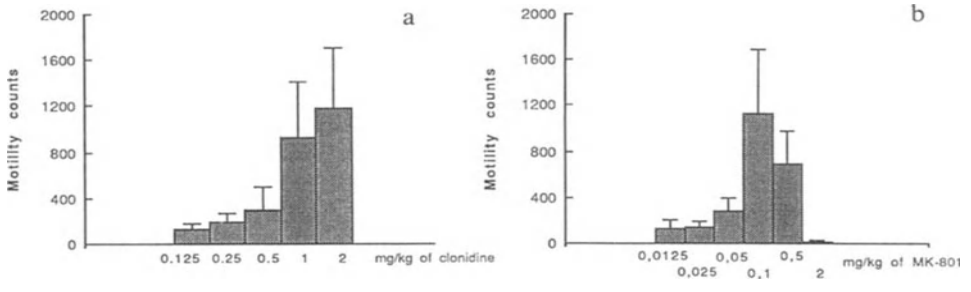

Fig. 4. a) Effects of varying doses of clonidine combined with 0.1 mg/kg of MK-801 on motor activity in monoamine-depleted rats. Reserpine (10 mg/kg i.p.) was administered 16 h and α-MT (250 mg/kg i.p.) 60 min prior to MK-801 treatment. Clonidine was given 20 min after MK-801 treatment. Motor activity was registered for 90 min beginning 10 min after clonidine treatment. Shown are the means ± S.E.M. N = 3–4. There was a significant correlation between clonidine dose and motility counts ($r = 0.59$, $p<0.01$). b) Effects of varying doses of MK-801 combined with 2 mg/kg of clonidine on motor activity in monoamine-depleted rats. Reserpine (10 mg/kg i.p.) was administered 7 h and α-MT (250 mg/kg i.p.) 60 min prior to MK-801 treatment. Clonidine was given 20 min after MK-801 treatment. Motor activity was registered for 90 min beginning 10 min after clonidine administration. Shown are the means ± S.E.M. N = 4. There was a significant positive correlation between dose of MK-801 in the range 0.0125–0.1 mg/kg and motility counts ($r = 0.54$, $p<0.03$) and a significant negative correlation between dose of MK-801 in the range 0.1–2 mg/kg and motility counts ($r = -0.59$, $p<0.05$).

Dose-response studies with clonidine and MK-801 in monoamine-depleted rats
When MK-801 was combined with clonidine a marked enhancement of motor activity was registered in the motility meters. Clonidine in doses ranging from 0.125 to 2 mg/kg was administered to rats receiving a fixed dose of MK-801 (0.1 mg/kg.). The dose-response curve did not plateau, even at the highest doses (Fig. 4a); thus 2 mg/kg of clonidine may not be a supramaximal dose with regard to locomotor stimulatory effect. On the other hand, when a dose-response study with MK-801 was conducted against a fixed dose (2 mg/kg) of clonidine, a bell-shaped response curve was obtained, the anaesthetic effects of MK-801 prevailing over the activational effects in higher doses (Fig. 4b).

Interaction between MK-801/AP-5 and clonidine in monoamine-depleted rats
When MK-801 (0.1 mg/kg) and clonidine (2 mg/kg) were administered separately, no enhancement of motor activity was registered in the motility meters. In contrast, when the two drugs were combined, a pronounced enhancement of motor activity was observed. Part of the time the animals walked around close to the walls of the motility meter box. However, most of the time the rats were stuck in the corners, displaying intensive and compulsive jumping and rearing behaviour, sometimes until complete exhaustion, as if attempting to escape from the box (Fig. 5a). A striking feature when placed in an open field were their attempts to force obstacles instead of walking around them.

The stimulatory effect on motor activity induced by the MK-801/clonidine treatment was antagonized by the α_2-antagonist idazoxan as well as by the 'atypical' neuroleptic clozapine, but it was not significantly decreased by the α_2-adrenoceptor antagonist yohimbine or the α_1-adrenoceptor antagonist prazosin. However, both the yohimbine-treated and the prazosin-treated groups were *qualitatively* affected. For instance, the yohimbine-treated rats spent relatively more time walking than jumping compared to controls and the prazosin-treated animals exhibited a greater degree of ataxia than controls (Fig. 5b).

The competitive NMDA receptor antagonist AP-5 induced a certain degree of locomotor stimulation when administered alone, and this effect was markedly potentiated by coadministration of clonidine. Similarly to the MK-801/clonidine-treated animals, the AP-5/clonidine-treated rats exhibited intensive jumping and darting behaviour of a highly bizarre appearance, reminiscent of a rabbit's way of jumping. Muscular hypotension and loss of the righting reflex were observed also after AP-5 administration, particularly after higher doses (Fig. 5c).

Discussion

The present study has shown that administration of NMDA antagonists to monoamine-depleted mice and rats promotes locomotion and discloses the activational potential of other transmitter systems, as illustrated by the marked synergism produced when the NMDA antagonists MK-801 or AP-5 were combined with an

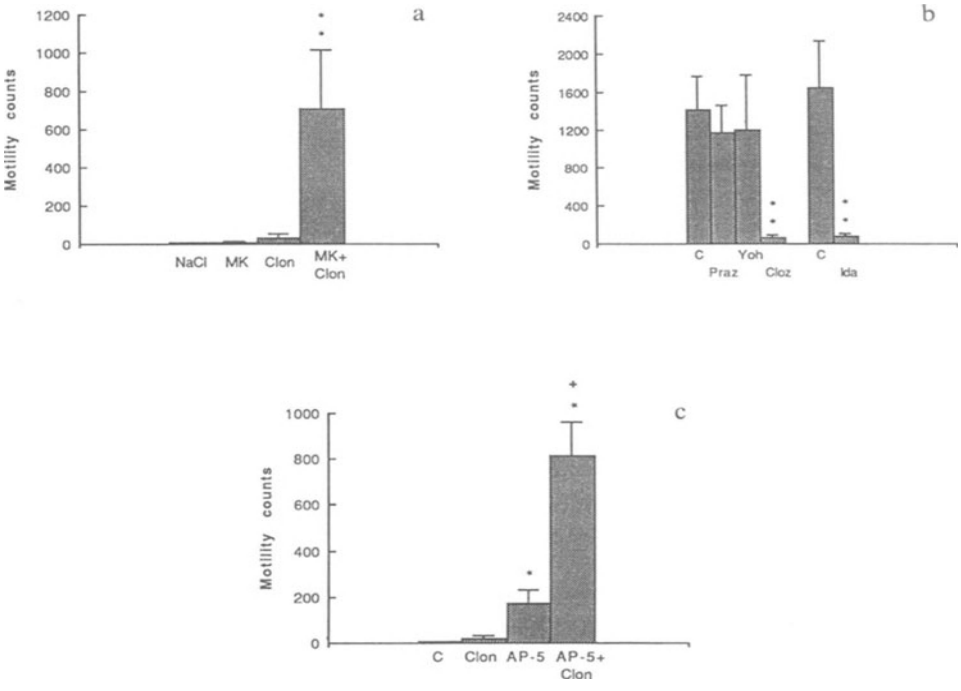

Fig. 5. a) Effects of MK-801 in combination with clonidine on motor activity in monoamine-depleted rats. Reserpine (10 mg/kg i.p.) was administered 16 h and α-MT (250 mg/kg i.p.) 60 min prior to MK-801 (0.1 mg/kg i.p.) treatment. Clonidine (2 mg/kg i.p.) was administered immediately before the registration of motor activity started, i.e. 30 min after MK-801 treatment. Motor activity was registered during 90 min. Shown are the means ± S.E.M. N = 3–8. **p< or = 0.01 vs. the other groups. b) Effects of different catecholaminergic blockers on the locomotor-stimulatory effects of MK-801 + clonidine in monoamine-depleted rats. Reserpine (10 mg/kg i.p.) was administered 16 h and α-MT (250 mg/kg i.p.) 60 min prior to MK-801 treatment. Prazosin (1 mg/kg i.p.), yohimbine (12 mg/kg i.p.) and clozapine (20 mg/kg i.p.) were administered 30 min and idazoxan (10 mg/kg i.p.) 60 min prior to clonidine treatment. Motor activity was registered during 90 min beginning 10 min after the clonidine injection, except in the idazoxan experiment in which the registration of motor activity began 50 min after clonidine administration. Shown are the means ± S.E.M. N = 5–8. **p<0.01 vs. controls (C). c) Effects of AP-5 in combination with clonidine on motor activity in monoamine-depleted rats. Reserpine (10 mg/kg i.p.) was administered 18 h and α-MT (250 mg/kg i.p.) 60 min prior to AP-5 (0.05 mg in 40 µl ICV) treatment. Clonidine (2 mg/kg i.p.) was administered immediately after the AP-5 administration. Motor activity was registered during 30 min beginning 5 min after clonidine treatment. Shown are the means ± S.E.M. N = 3–4. *p<0.05 vs. controls (= C = vehicle ICV + saline i.p.). +p<0.025 vs. AP-5.

adrenergic or a dopaminergic agonist, or a muscarinic antagonist. Thus, it appears that central glutamatergic systems exert a powerful inhibitory influence on locomotion. Suppressing this inhibitory force by MK-801 treatment results in a pronounced potentiation of the locomotor stimulatory effects of i.a. catecholaminergic

agonists. This postsynaptic effect, in conjunction with the presynaptic, i.e. catecholamine-releasing, effects of MK-801 may explain its outstanding locomotor stimulatory effects in intact animals, firstly described by Clineschmidt *et al.* [7].

Corticofugal projections seem to be essentially glutamatergic [8]. Thus, administration of a glutamatergic antagonist like MK-801 might produce a 'pharmacological decortication'. In fact, there is an interesting parallel between the behavioural effects obtained in mouse and rat in this study, by pharmacologically decreasing the telencephalic influence on subcortical structures by means of MK-801 administration, and the effects previously observed in the cat following removal of the cerebral hemispheres [9]. In both cases locomotion is stimulated, the animals tend to walk incessantly and they do not turn and change direction when encountering an obstacle, thus bumping into walls and getting stuck in corners. Possibly this bizarre behaviour results from activation of brainstem locomotor programs.

Another possibility is that the locomotor stimulatory effects caused by NMDA antagonist administration depends mainly on an action within the striatum. Such a notion is supported by the observation that application of AP-5 into the anterodorsal striatum results in behavioural stimulation, i.e. increased locomotion, rearing and sniffing [10]. Conceivably the marked synergism between NMDA antagonists on one hand and catecholaminergic agonists and atropine on the other also takes place within the striatum. Future experiments with topical drug application in discrete brain regions will hopefully shed light on this issue. Local drug application may also be helpful when attempting to understand why the anaesthetic actions are more pronounced with an agent like ketamine whereas with MK-801 the activational effects prevail. Could it be that ketamine predominantly interferes with glutamatergic transmission in sensory afferents and thalamocortical pathways, whereas MK-801 preferentially decreases glutamatergic transmission within the striatum? Are we dealing with subtypes of NMDA receptors?

In mice the pronounced synergism between MK-801 and clonidine was effectively antagonized by both yohimbine, idazoxan and clozapine, but not by prazosin, indicating the involvement of an α_2-adrenergic mechanism [3]. In rat, on the other hand, idazoxan and clozapine, but not yohimbine or prazosin, antagonized the clonidine effect. This may suggest that a different population of α_2-adrenoceptors are involved in the interaction with MK-801 in rat, as compared to mouse. Alternatively, non-adrenergic receptors may be involved [11–13]. Interesting in this context is a study showing that MK-801 potentiated the effects of noradrenaline-induced depolarization of motoneurons in isolated immature spinal cord preparations [14]. This paper and our results suggest that MK-801 may potentiate noradrenergic transmission at a postsynaptic level.

Implications for the pathophysiology of schizophrenia

In the last few years there has been a growing interest in the interaction between DA and glutamate in the striatum. Kornhuber and Kornhuber, among others, have

hypothesized that dopaminergic nigrostriatal fibers mediate a presynaptic inhibitory influence on striatal glutamate release via D_2 receptors located on the terminals of corticostriatal neurons [15]. They have also suggested that the therapeutic effect of neuroleptics might be brought about by strengthening glutamatergic transmission within the striatum. However, dopaminergic nigrostriatal neurons do not seem to *tonically* inhibit striatal glutamatergic transmission under normal conditions [15]; it then follows that if the therapeutic effect of neuroleptics in schizophrenia is achieved by increasing glutamatergic transmission, a hyperactive DA system, leading to a *secondary* deficiency in glutamatergic transmission in this disease must be postulated. However, Kornhuber and coworkers have suggested that schizophrenia might be caused by a *primary* deficiency in central glutamatergic transmission. Moreover, it should be kept in mind in this context that the physiological significance [16], and even the existence [17], of D_2 receptors on the terminals of corticostriatal neurons have been questioned.

According to another viewpoint there are, apart from the D_2 receptors located on the terminals of corticostriatal neurons mediating inhibition of glutamate release, NMDA receptors located on terminals of mesostriatal neurons mediating inhibition of DA release [18]. This hypothesis, which attempts to explain i.a. the NMDA antagonist-induced activation of dopaminergic neurons, has at least two weak points: 1) Why should an excitatory transmitter like glutamate be expected to *inhibit* DA release 2) How can two neuronal systems making axo-axonic synaptic contact and with mutually inhibitory actions be expected to work in a physiologically meaningful way?

Why is it then that blockade of NMDA receptors causes activation of dopaminergic neurons? One possibility is that inhibition of glutamatergic transmission in the striatum, a region with a high density of NMDA receptors, leads to a decreased firing in the GABAergic striatonigral neurons, in turn resulting in a decreased inhibition of impulse flow in the nigrostriatal DA neurons and hence an increased dopaminergic transmission in the striatum.

A third way of looking at the DA/glutamate interaction within the striatum involves the notion of a corticostriatothalamocortical negative feedback loop, serving to protect the cortex from an overload of information and hyperarousal [19]: Excitatory corticostriatal (glutamatergic), inhibitory striatothalamic (GABAergic) and excitatory thalamocortical pathways provide the anatomical substrate for a negative feedback loop. The thalamus might be looked upon as a filter for sensory input, and activation of the corticostriatothalamic loop would serve to close this filter. Conversely, activation of another neuronal system, namely the mesostriatal dopaminergic pathway would yield opposite effects, i.e. a widening of the filter, hence increasing the flow of information from the outer world to the cortex. An advantage with this hypothesis from a morphological point of view is that it does not require the assumption that dopaminergic and glutamatergic terminals make direct synaptic contact. Hence, it is in line with morphological data indicating 1) that axo-axonic synapses are rare or non-existent in the striatum [17] and 2) that corticostriatal/thalamostriatal glutamatergic and nigrostriatal dopa-

minergic neurons make synaptic contact with a common third neuron, i.e. with the dendritic spines pertaining to a GABAergic neuron [20]. Thus the corticostriatal glutamatergic and nigrostriatal dopaminergic systems may operate independently of one another on the local level, sharing a common target neuron or final endpoint, influencing the state of the thalamic 'filter' in opposite directions.

Interesting in this context is the present observation that locomotion was elicited in the MK-801-treated rat in the open field, and, most conspicuously, following tactile stimulation, but not in the motility meter (i.e. when deprived of sensory stimulation). An interesting parallel is the cat with lesioned caudates which is set in motion, exhibiting exaggerated treading movements, solely following sensory stimulation [9].

A currently held belief is that the NMDA antagonist-induced behavioural activation depends on enhanced catecholamine release. Accordingly, it has been suggested that a putative glutamate deficiency may cause schizophrenia by increasing dopaminergic tone [18]. However, our experiments show that NMDA antagonists can cause behavioural stimulation via a *catecholamine-independent* mechanism. Partly on the basis of this finding, partly on the basis of the above described 'filter hypothesis', we propose that schizophrenia induced by a primary glutamate deficiency can emerge regardless and independently of central dopaminergic tone. The notion of a glutamate deficiency as the primary cause of schizophrenia has previously been expressed by Kim *et al.* [5] (see above).

As has previously been suggested [2,18,19], an NMDA agonist acting either at the glutamate receptor or at an allosteric site of the receptor complex might be an interesting therapeutic alternative in schizophrenia. If the glutamate hypothesis of schizophrenia is correct this could then be regarded as a kind of 'substitution therapy'. Moreover, our results with MK-801 in rodents suggest that decreased glutamatergic transmission results in an increased activational power of other transmitter systems. Thus, just as DA receptor blockers are effective in schizophrenia, it is possible that manipulation with adrenergic and/or cholinergic transmission may be beneficial. Noteworthy in this context is the observation that the 'atypical' neuroleptic clozapine effectively antagonized the pronounced behavioural stimulation produced by MK-801/clonidine treatment, probably due to blockade of α_2-adrenoceptors [3]; it is well known that clozapine is clinically effective in a subgroup of therapy-resistant schizophrenics. Also interesting in this context, in view of the pronounced synergism between MK-801 and atropine, is a report showing beneficial effects of physostigmine in the treatment of PCP-induced psychosis [21].

Implications for the treatment of Parkinson's disease

Could a substance like MK-801 (or perhaps preferably an orally active competitive NMDA antagonist) be used in the treatment of Parkinson's disease? Considering the pharmacological similarity to phencyclidine (PCP), how great are the risks for psychotic side effects and abuse? Is catecholamine release a prerequisite for brain

reward and is the liability to abuse PCP related to activation of catecholaminergic neurons?

If brain reward mechanisms are intimately linked to catecholamine release (in the ventral striatum) the risk for abuse might be minimal in Parkinson's disease, at least in later stages when the degeneration of catecholaminergic neurons is extensive. Possibly it is also in this late phase, when the patient no longer responds to conventional pharmacological therapy, that an NMDA antagonist might be an important therapeutic alternative.

Considering the powerful synergism between on the one hand MK-801 and clonidine/apomorphine/atropine on the other, observed in the present study, an interesting clinical approach might be to combine an NMDA antagonist with a catecholaminergic agonist or a muscarinic antagonist, in order to achieve an optimal therapeutic effect and a minimum of side effects.

Acknowledgements

The present study was supported by grants from MFR (155), Stiftelsen för Gamla Tjänarinnor, Syskonen Svenssons Fond, Kerstin and Bo Pfannenstills Stiftelse and Lundbecks Fond. We wish to thank Dr GN Woodruff (MSD) for generously supplying MK-801. The excellent technical assistance of Kirsten Sönniksen is also gratefully acknowledged. Finally we wish to thank research engineer Stellan Ahl for constructing the IR detectors used to quantify motor activity in the present study.

References

1. Wong EHF, Kemp JA, Priestley T, Knight AR, Woodruff GN and Iversen LL (1986) Proc. Natl. Acad. Sci. USA 83: 7104–7108.
2. Carlsson M and Carlsson A (1989) J. Neural Transm. 75: 221–226.
3. Carlsson M and Carlsson A (1989) J. Neural Transm. 77: 65–71.
4. Bartus TB, Dean RL and Flicker C (1987) In: Meltzer HY (ed.) Psychopharmacology. The Third Generation of Progress. Raven Press, New York, pp. 219–232.
5. Kim JS, Kornhuber HH, Schmid-Burgk W and Holzmüller B (1980) Neurosci. Lett. 20: 379–382.
6. Garcia-Sevilla JA, Ahtee L, Magnusson T and Carlsson A (1978) J. Pharm. Pharmacol. 30: 613–621.
7. Clineschmidt BV, Martin GE, Bunting PR and Papp NL (1982) Drug Develop. Res. 2: 135–145.
8. Cotman CW and Monaghan T (1987) In: Meltzer HY (ed.) Psychopharmacology. The Third Generation of Progress. Raven Press, New York, pp. 197–210.
9. Villablanca JR, Marcus RJ and Olmstead CE (1976) Exp. Neurol. 52: 389.
10. Schmidt WJ and Bury D (1988) Life Sci. 43: 545–549.
11. Bylund DB (1988) TIPS 9: 356–361.
12. Wikberg JES (1989) Pharmacology & Toxicology 64: 152–155.
13. Martin CM, Brodde O-E, Schnepel B, Behrendt J, Tschada R, Motulsky HJ and Insel PA (1988) Molecular Pharmacology 35: 324–330.
14. Childs AM, Evans RH and Watkins JC (1988) Eur. J. Pharmacol. 145: 81–86.

15. Kornhuber J and Kornhuber ME (1986) Life Sci. 39: 669–674.
16. Stoof JC, De Boer T, Sminia P and Mulder AH (1982) Eur. J. Pharmacol. 84: 211–214.
17. Hattori T and Fibiger C (1982) Brain Res. 238: 245–250.
18. Deutsch SI, Mastropaolo J, Schwartz BL, Rosse RB and Morihisa JM (1989) Clin. Neuropharmacol. 12: 1–13.
19. Carlsson A (1988) Neuropsychopharmacology 1: 179–186.
20. Freund TF, Powell JF and Smith AD (1984) Neuroscience 13: 1189–215.
21. Castellani S, Giannini AJ and Adams PM (1982) Am. J. Psychiatry 139: 508–510.

Address for correspondence: Maria Carlsson, Department of Pharmacology, Box 33031, S-400 33 Göteborg, Sweden.

Glutamate and aspartate in corticofugal neurons: A combined immunocytochemical and tracing study

Rosario Giuffrida[a] and Aldo Rustioni[b]

[a]Institute of Human Physiology, University of Catania, Cittá Universitaria, I-95125 Catania, Italy
[b]Department of Cell Biology and Anatomy, University of North Carolina, Chapel Hill, NC 27599-7090, U.S.A.

Abstract

In this study immunostaining for glutamate (Glu) and aspartate (Asp) was tested in cortical neurons with projections to dorsal column nuclei (DCN). To this purpose, peroxidase immunocytochemistry was combined with the retrograde transport of a tracer injected in the DCN. At cortical level, retrograde labeling was found in pyramidal neurons of layer V of contralateral motor (MI), somatosensory I (SI) and somatosensory II (SII) areas. Cortico-DCN neurons immunopositive for Glu were 60–70% in MI and SI, 50–60% in SII. Similar percentages were obtained using the Asp antiserum. In experiments where both antisera were simultaneously visualized, percentages of immunopositive cortico-DCN neurons increased up to 85–95%; from these observations it is concluded that a fraction (about 30%) of cortico-DCN neurons was immunostained by the two antisera, and the majority (about 60%) was revealed by either one antiserum. These findings, combined with those obtained in previous studies on other cortical projections, are consistent with observations by several experimental approaches other than immunocytochemistry, and support a role for Glu and Asp as neurotransmitters in corticofugal pathways.

Introduction

Activation of the cerebral cortex can induce excitatory and inhibitory influences on neurons of several subcortical structures [see 1 for review]. Cortically-induced excitatory effects may occur at latencies compatible with a monosynaptic linkage [2], suggesting that an excitatory neurotransmitter is used by corticofugal neurons. Several lines of research indicate glutamate (Glu) and aspartate (Asp) as major excitatory neurotransmitters in corticofugal pathways [3–11]. Immunocytochemical techniques have contributed in the last years to the identification of neurons containing detectable concentrations of neurotransmitters in the central nervous system. Neurons accumulating Glu in their cell body were first visualized by Ottersen and Storm-Mathisen by means of an antiserum against Glu conjugated to a carrier protein [12]. Antisera for Glu- and Asp-conjugates were obtained in other laboratories [13–17], and attempts to identify glutamergic neurons have been also carried out raising antisera against glutaminase, which may be involved in the synthesis of the transmitter pool of Glu [18,19].

Results obtained using these antisera consistently indicate the cerebral cortex as a structure particularly rich in Glu- and Asp-immunopositive neurons. A more

detailed analysis of these neurons within sensorimotor areas has revealed that they are mostly pyramidal neurons with uneven laminar distribution [20,21]. They are not present in layer I and are more concentrated in layers III, V and VI, where most corticofugal neurons are located.

The occurrence of Glu- and Asp-immunoreactivity in projection neurons of the sensorimotor cortex has been investigated in a series of experiments in which immunocytochemistry was combined with tracing techniques [22–24]. In this paper we report on immunoreactivity for Glu and Asp in cortical projections to the dorsal column nuclei (DCN) of rats.

Materials and Methods

Colloidal gold-labeled enzymatically inactive horseradish peroxidase conjugated to wheat germ agglutinin (WGA-apoHRP-Au; 25) was pressure-injected (up to 0.5 µl) under barbiturate anesthesia in DCN of adult Sprague-Dawley rats (150–250 g). After two to three days the animals were perfused with 4% paraformaldehyde in phosphate buffer (0.1 M, pH 7.4), preceded by either 4% carbodiimide in the same buffer or physiological saline. Brains were left for overnight postfixation in 4% paraformaldehyde and subsequently cut in serial coronal sections which were stored, in groups of ten consecutive, in phosphate buffer.

Visualization at the light microscope of the tracer was obtained by silver enhancement of the retrogradely transported gold particles, as described by Basbaum and Menétrey [25]. Thirty to forty µm-thick sections, regularly alternated with thinner (15–20 µm) sections, throughout the rostrocaudal extent of the contralateral hemisphere, were mounted and counterstained with thionin. Their inspection was useful to identify the cytoarchitectonic features of the cortical areas [26,27] where DCN-projecting neurons were mainly located. The thinner sections through cerebral cortex containing the densest population of cortico-DCN neurons, as determined after the enhancement of the tracer, were processed free-floating for immunocytochemistry following a protocol previously described [24]. In synthesis, the sections were incubated with a) the primary antiserum (Glu and Asp, at dilution of 1:10,000 to 15,000 and 1:5,000 to 10.000, respectively, in Tris-buffered saline) for 12–15 h; b) the secondary biotinylated antiserum (goat anti-rabbit, 1:200); c) the avidin-biotinylated peroxidase complex (1:100); d) a solution of 3,3' diaminobenzidine tetrahydrochloride in Tris buffer, as chromogen to visualize the peroxidase activity. Rinses before, between and after the immunocytochemical steps were made in Tris-buffered saline. Antisera employed here were raised in rabbits against Glu and Asp conjugated with hemocyanin by glutaraldehyde. Their characterization is described in a paper by Hepler *et al.* [15]. Only experiments where the tracing procedures and the immunostaining were satisfactory were considered for quantitative analysis. Immunopositive and immunonegative cortico-DCN neurons were computed on *camera lucida* drawings of 10–20 sections from each experiment.

Results and Discussion

Injections of WGA-apoHRP-Au in the DCN led to retrograde labeling in pyramidal neurons of layer V of contralateral motor (MI), somatosensory I (SI) and somatosensory II (SII) cortex [28]. In these areas, three populations of neurons were observed (Fig. 1,2): a) neurons immunostained but not retrogradely labeled,

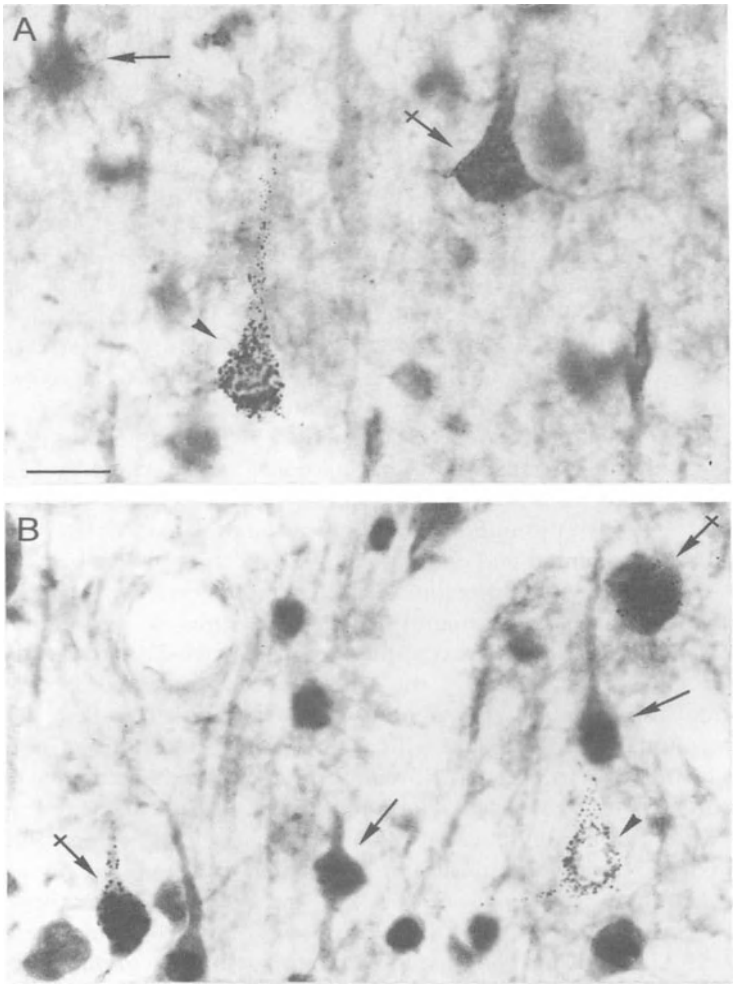

Fig. 1.

Figs. 1 and 2. Photomicrographs from layer V of the sensorimotor cortex of rats processed with antisera for glutamate (A) or aspartate (B), after the injection of the tracer at the bulbar level (Fig. 1) or in the cervical spinal cord (Fig. 2). Cortico-DCN neurons (Fig. 1) and corticospinal neurons (Fig. 2) are identified by the

characterized by the diffuse reddish-brown immunoproduct over the perikaryon, the apical dendrite and initial portions of the basal dendrites; b) neurons retrogradely labeled but immunonegative, characterized by the presence of black silver grains (bright in dark field) over a blank cell body; c) neurons retrogradely labeled and immunostained, in which both types of labeling occurred. The tracer employed was particularly suitable in combination with immunocytochemistry because of its

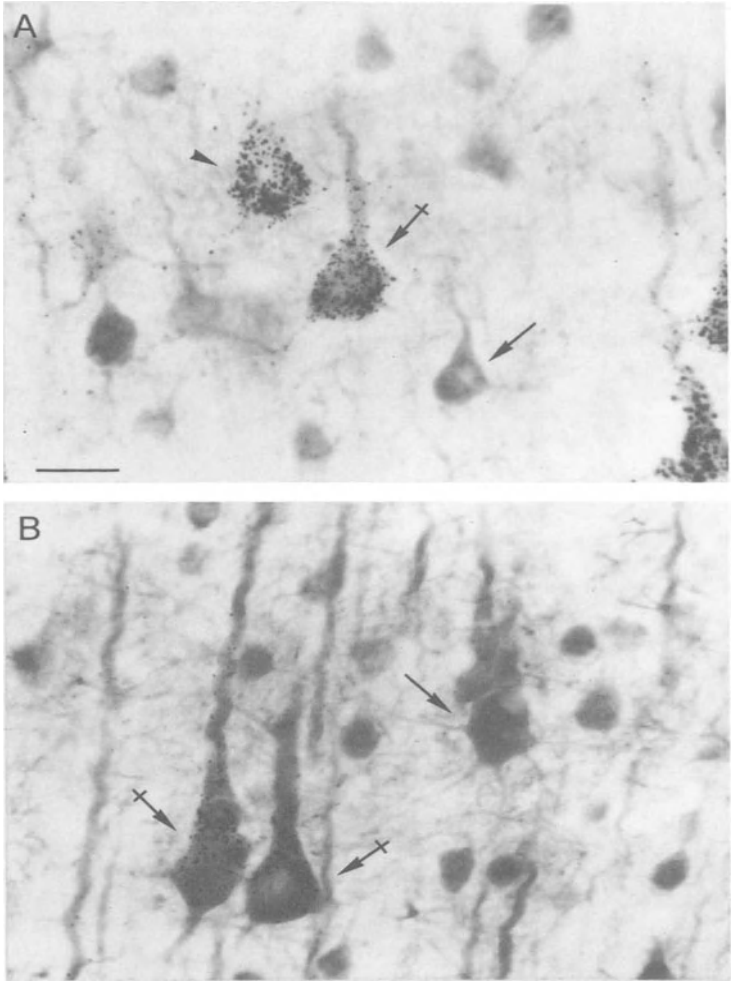

Fig. 2.

presence of black silver grains over the cell body. Three types of neurons are visible: 1) immunopositive only (arrows), 2) labeled only by the retrograde transport of the tracer (arrowheads), 3) immunopositive and retrogradely labeled (tailed arrows). Calibration: 20 μm.

stability and easy visualization, especially when observed in dark field or polarized light.

In experiments R660 and R662 a large population of cortico-DCN neurons was immunostained by the Glu-antiserum. Percentages in Table 1 show that more than a half of cortico-DCN neurons contain high levels of Glu with some differences in the different cortical areas. Higher percentages are in MI and SI (58–65%), and slightly lower in SII (53–65%). These experiments indicate that not all cortico-DCN neurons display intense Glu immunoreactivity. In two other experiments (R691, R692), in addition to Glu-antiserum, an antiserum for Asp was tested. Percentages of Asp-immunopositive cortico-DCN neurons in each of the three cortical areas were similar to those obtained for Glu-immunopositive ones (Table 1). Similar results were observed for corticospinal neurons where Glu- and Asp-immunopositive neurons (Fig. 2) were found in similar percentages [24]. This is not surprising, however, given the similarity between the two pathways: both of them originate from pyramidal neurons of the same cortical layer of the same

Table 1. Percentages of immunostained neurons out of the sample of cortico-DCN neurons (n) in layer V of MI, SI and SII of rats with injection of WGA-apoHRP-Au in contralateral DCN. Percentages of cortico-DCN neurons stained with only glutamate or aspartate are listed in GLU and ASP columns, respectively. Percentages of cortico-DCN neurons by both antisera, mixed together, are listed in GLU+ASP column

		GLU		ASP		GLU+ASP	
		%	n =	%	n =	%	n =
R660	MI	60	(63)				
	SI	65	(91)				
	SII	53	(47)				
R662	MI	58	(60)				
	SI	62	(77)				
	SII	55	(56)				
R691	MI	65	(125)	63	(161)		
	SI	69	(235)	72	(219)		
	SII	50	(131)	55	(137)		
R692	MI	67	(169)	68	(136)		
	SI	69	(282)	70	(297)		
	SII	60	(108)	59	(91)		
R701	MI	64	(187)	62	(162)	93	(212)
	SI	60	(245)	66	(261)	92	(232)
	SII	53	(98)	56	(117)	85	(122)
R702	MI	59	(195)	70	(183)	93	(181)
	SI	61	(216)	63	(250)	94	(229)
	SII	56	(115)	57	(139)	84	(159)

areas; moreover, a considerable amount of cortico-DCN projections is provided by collaterals of corticospinal tract fibers [29].

The similarity in the percentages of Glu- and Asp-immunopositive neurons raises the possibility that: a) the same populations of neurons are revealed by either antiserum, and b) the failure to immunostain all the cortico-DCN neurons with Glu- or Asp-antiserum results from incomplete penetration of the antibodies through the thickness of the tissue. These issues were dealt with in experiments R701 and R702, in which some sections were incubated with a mixture of both antisera. In these sections the percentages of immunopositive neurons increased to 92–94% in MI and SI, and to 84–85% in SII. These percentages are considerably higher than those obtained, in the same experiments, when the sections were incubated with Glu- or Asp-antiserum alone (Table 1). These observations demonstrate that most cortico-DCN neurons which are not stained by the antiserum for one amino acid are stained by the other. It remains possible that lack of immunostaining of the residual small percentage of cortico-DCN neurons resulted from: a) incomplete penetration of the antibodies, b) loss of immunoreactivity during the tissue treatment before immunocytochemical steps and c) undetectable concentrations of any of the two amino acids. In immunocytochemical runs for somatostatin, substance P, cholecystokinin in the present experiments, cortico-DCN neurons did not stain for any of these substances. However, in colchicine-treated cats, Conti *et al.* [30] have been able to demonstrate some tachykininpositive pyramidal neurons in somatosensory cortex; whether or not these neurons also contain excitatory amino acids in their perikarya remains to be ascertained.

From the analysis of the percentages obtained from all the experiments, using the Glu- and Asp-antisera singularly or mixed (Fig. 3), it appears that at least a fraction of cortico-DCN neurons is stained by both antisera (about 30%), and that the majority (about 60%) is selectively marked by only one. Similar results, although with lower percentages of double-immunostained neurons, were obtained in a colocalization study [20], by comparing adjacent thin paraffin sections, immunostained for Glu and Asp, alternatively; data of that study, however, refer to the entire neuronal population of cortical strips through the somatosensory cortex of rats; neurons were not identified as to their projection. From these considerations three classes of corticofugal neurons can be identified: two classes containing only Glu or Asp, respectively, and a third class containing both. Similar evidence was provided in a parallel series of experiments aimed at immunocytochemical characterization of corticospinal neurons [24], by using two distinguishable chromogens for the visualization, in the same sections, of the two antisera. In addition, it was shown that corticospinal neurons stained by both Glu- and Asp-antisera had a soma size significantly larger than those stained by only one antiserum. Whether a similar situation exists for cortico-DCN neurons remains to be established by appropriate double-immunostaining experiments.

Neurons immunopositive for Glu and Asp are detectable in other parts of the central nervous system besides the cerebral cortex, e.g. along ascending pathways (cuneothalamic, thalamocortical neurons) [31] or descending systems (rubrospinal,

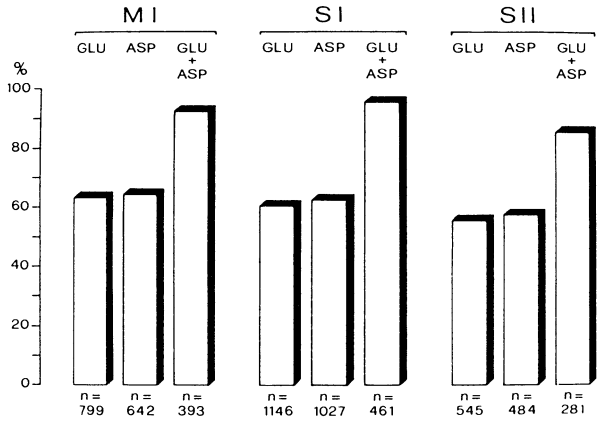

Fig. 3. Histograms of percentages of immunostained cortico-DCN neurons. Data are gathered from all the experiments listed in Table 1. For each cortical area percentages refer to immunostaining for glutamate (GLU), aspartate (ASP) or a mixture of both antisera (GLU+ASP) in populations of cortico-DCN neurons (n =). Note the similarity of percentages of Glu- and Asp-immunopositive neurons, and the higher percentages of (Glu+Asp)-immunopositive neurons.

vestibulospinal neurons; unpublished observations). Since the Glu- and Asp-antisera do not cross-react, to any significant degree, with Asp and Glu, respectively, two possibilities may explain why neurons are stained by both antisera: either the two amino acids are indeed colocalized in the same neurons, or the two antibodies cross-react for another substance, presumably an oligopeptide, not yet identified, and present in these neurons.

The present findings provide evidence in favor of acidic amino acids as neurotransmitters in corticofugal pathways. In particular, this immunocytochemical demonstration of Glu and Asp in DCN-projecting cortical neurons matches with electrophysiological data by Stone [7,8], showing a blockade of cortical excitation induced with antagonists of excitatory amino acids on neurons activated by pulses of Glu or Asp, in DCN as well as in other subcortical structures. Supporting results were also obtained by Rustioni and Cuénod after injections of D-^{3}H-Aspartate [32] in the cuneate nucleus of rats; in those experiments it was found that the retrograde transport of this transmitter-related compound, selectively uptaken by glutamergic and/or aspartergic endings, labeled layer V neurons of sensorimotor cortex, out of a number of structures projecting to DCN. A small decrease of Glu uptake has been shown by Young *et al.* [10,11] in DCN of cats and monkeys after ablation of sensorimotor areas; that in DCN it occurs in smaller degree than in other subcortical territories such as the thalamus or the spinal cord, it is likely related to the sparse cortico-DCN innervations, when compared with the corticothalamic or the corticospinal projections. Finally, post-embedding immunocytochemistry at the electron microscope has revealed specific immunostaining for

Glu in terminals within DCN [33]; many of these Glu-positive terminals can be identified as primary afferents, but several others, for their size and shape, are presumably corticofugal terminals.

Activation of sensorimotor cortex can also induce inhibitory effects on the activity of neurons of DCN [2], (see references in 1). Gamma-amino butyric acid (GABA) is considered the neuromediator responsible for inhibitory effects on DCN neurons [34]. Neither in these experiments, nor in other studies on different corticofugal pathways, a projection neuron in the sensorimotor areas was ever stained by antisera for GABA or glutamic acid decarboxylase (GAD), a selective marker for GABA-synthetizing neurons. If one assumes that corticofugal neurons use an excitatory neurotransmitter, GABAergic interneurons should mediate the cortically-induced inhibition. This hypothesis has been supported by immunocytochemical studies [35,36] which show, within DCN of rats and cats, a population of GAD-immunopositive neurons which, for their soma size and apparent lack of extrinsic projections, are most likely interneurons.

Efforts to establish that amino acids, particularly glutamate, are involved as neurotransmitters in corticofugal pathways are necessary steps toward the treatment, with receptor antagonists [37], of pathological effects on subcortical mechanisms consequent to cerebral ischemia.

References

1. Brodal A (1981) Neurological Anatomy, Oxford University Press, New York – Oxford.
2. Giuffrida R, Sapienza S and Sanderson P (1985) Somatosens. Res. 2: 237–247.
3. Fagg GE and Foster AC (1983) Neuroscience 9: 701–749.
4. Fonnum F (1984) J. Neurochem. 42: 1–11.
5. Mayer ML and Westbrook GL (1987) Progr. Neurobiol. 28: 197–276.
6. Potashner SJ, Dymczyk L and Deangelis MM (1988) J. Neurochem. 50: 103–111.
7. Stone TW (1976) J. Physiol. (London) 257: 187–198.
8. Stone TW (1979) Br. J. Pharmacol. 67: 545–551.
9. Streit P (1984) In: Jones EG and Peters A (eds.) Cerebral Cortex, Vol. 2. Plenum Press, New York, pp. 119–143.
10. Young AB, Bromberg MB and Penney JB (1981) J. Neurosci. 1: 241–249.
11. Young AB, Penney JB, Danth GW, Bromberg MB and Gilman S (1983) Neurology 33: 1513–1516.
12. Ottersen OP and Storm-Mathisen J (1984) J. Comp. Neurol. 229: 374–392.
13. Aoki E, Semba R, Kato K and Kashiwamata S (1987) Neuroscience 21: 755–765.
14. Campistron G, Buys RM and Geffard M (1986) Brain Res. 365: 179–184.
15. Hepler JR, Toomim CS, McCarthy KD, Conti F, Battaglia G, Rustioni A and Petrusz P (1988) J. Histochem. Cytochem. 36: 13–22.
16. Madl JE, Beitz AJ, Johnson RL and Larson AA (1987) J. Neurosci. 7: 2639–2650.
17. Madl JE, Larson AA and Beitz AJ (1986) J. Histochem. Cytochem. 34: 317–326.
18. Donoghue JP, Wenthold RJ and Altschuler RA (1985) J. Neurosci. 5: 2597–2608.
19. Kaneko T, Urade Y, Watanabe Y and Mizuno N (1987) J. Neurosci. 7: 302–309.
20. Conti F, Rustioni A and Petrusz P (1987) In: Hicks TP, Lodge D and Mc Lennan H (eds.) Excitatory Amino Acids Transmission. Alan R. Liss, New York, pp. 169–172.
21. Conti F, Rustioni A, Petrusz P and Towle AC (1987) J. Neurosci. 7: 1887–1901.

22. Giuffrida R and Rustioni A (1988) In: Bentivoglio M and Spreafico R (eds.) Cellular Thalamic Mechanisms. Elsevier, Amsterdam, pp. 311–320.
23. Giuffrida R and Rustioni A (1989) Exp. Brain Res. 74: 41–46.
24. Giuffrida R and Rustioni A (1989) J. Comp. Neurol. 288: 154–164.
25. Basbaum AI and Menétrey D (1987) J. Comp. Neurol. 261: 306–318.
26. Donoghue JP and Wise SP (1982) J. Comp. Neurol. 212: 76–88.
27. Zilles K and Wree A (1985) In: Paxinos G (ed.) The Rat Nervous System, Vol. 1. Academic Press, Sydney, pp. 375–415.
28. Giuffrida R, Sanderson P, Sapienza S and Albe-Fessard D (1986) Neurosci. Lett. Suppl. 26: S343.
29. Bentivoglio M and Rustioni A (1986) J. Comp. Neurol. 253: 260–276.
30. Conti F, Fabri M, Abdullah L and Manzoni T (1988) Neurosci. Abstr. 14: 717.
31. Rustioni A, Battaglia G, De Biasi S and Giuffrida R (1988) In: Bentivoglio M and Spreafico R (eds.) Cellular Thalamic Mechanisms. Elsevier, Amsterdam, pp. 271–296.
32. Rustioni A and Cuénod M (1982) Brain Res. 236: 143–155.
33. De Biasi S and Rustioni A (1988) Neurosci. Abstr. 14: 485.
34. Rustioni A and Weinberg RJ (1989) In: Björklund A, Hökfelt T and Swanson LW (eds.) Handbook of Chemical Neuroanatomy, Vol. 5. Integrated Systems of the CNS, Part II Somatosensory System. In press.
35. Barbaresi P, Spreafico R, Frassoni C and Rustioni A (1986) Brain Res. 282: 305–326.
36. Rustioni A, Schmechel DE, Cheema S and Fitzpatrick D (1984) Somatosens. Res. 1: 329–357.
37. Albers GW, Goldberg MP and Choi DW (1989) Ann. Neurol. 25: 398–403.

Address for correspondence: Dr. Rosario Giuffrida, Institute of Human Physiology, University of Catania, Citta' Universitaria, Viale A. Doria, 6, I-95125 Catania, Italy.

The role of excitatory and inhibitory amino acids in the integration of respiratory and cardiovascular functions

Jyoti Mitra, Jeffrey L. Overholt and Neil S. Cherniack

Department of Medicine, Case Western Reserve University, School of Medicine, Cleveland, OH 44106, U.S.A.

Abstract

In order to assess the role of GABA and glutamate in the ventrolateral medulla on vasomotor and respiratory responses, bicuculline (BIC), a GABA receptor antagonist, and kynurenic acid (KYN), a glutamate receptor antagonist, were microinjected into the rostroventrolateral (RVL) and caudoventrolateral medulla (CVL) while recording blood pressure (BP) and phrenic nerve activity (PNA). Experiments were carried out in urethane-anesthetized, paralyzed and artificially ventilated male Sprague-Dawley rats with carotid sinus nerves and vagi sectioned. Following microinjection of BIC (1 and 5 nmol) into the RVL, BP rose without any significant changes in either PNA or the PNA response to increased inspired CO_2 (5% CO_2 in 95% O_2). When a similar dose of BIC was injected into the CVL, BP fell but PNA and the PNA response to CO_2 were again unaltered. Microinjection of KYN (5 and 10 nmol) in the RVL, on the other hand, did not alter either BP or PNA. When KYN was microinjected into the CVL, however, BP increased while both PNA and the PNA response to higher CO_2 were strongly depressed. These results suggest that in the RVL and CVL regions, GABA may be essential for the regulation of vasomotor tone, but not for the respiratory drive. In contrast, in the CVL region, glutamate may be involved in the mediation of both the vasomotor and respiratory drive and thus the CVL may be one of the sites where vasomotor and respiratory responses are integrated.

Introduction

A large number of studies in several animal species have shown that the ventrolateral medulla of the brain plays an important role in the regulation of respiratory and cardiovascular functions [1–3]. Both excitatory and inhibitory amino acids have been implicated as putative neurotransmitters for these functions [4–13]. We, as well as others, have reported that the application of GABA, glutamate and their analogues to the ventral medullary surface (VMS) have profound effects on systemic blood pressure and breathing [11,14–16]. In general, GABA depresses both BP and respiration, while glutamate stimulates them. Several anatomical structures lie beneath the medullary surface and thus it was not clear from these studies which structures were responsible for the physiological responses. Since respiratory and vasomotor neurons are found in these regions, in our present study we assessed whether these same regions are also involved in modifying respiration and whether glutamate and GABA are involved in the regulatory process. Hence, in these experiments we microinjected glutamate and GABA antagonists into the RVL and CVL regions and simultaneously recorded both respiration and blood pressure.

Methods

Twelve Sprague-Dawley (male) rats were anesthetized with urethane (1.3 mg/kg, i.p.). A femoral artery and vein were cannulated for monitoring blood pressure and for the systemic injection of saline respectively. Animals were tracheotomized for artificial ventilation. The phrenic nerve was isolated unilaterally (usually the left) and prepared for recording mass electrical activity. Vagi and sinus nerves were isolated and sectioned to eliminate the effects of inputs from peripheral chemo and baroreceptors on phrenic nerve activity and blood pressure which might confound the interpretation of the results. The animal was placed in the prone position and its head was fixed in a stereotaxic apparatus at 45°. The dorsal surface of the lower brainstem was exposed by a limited occipital craniotomy. At the end of the surgery the animal was paralyzed with pancuronium bromide (0.6 mg/kg i.v.) and ventilated artificially with a small animal ventilator (Harvard Instrument). The body temperature was maintained at 37°C with a servo-controlled heating blanket. All experiments were performed while the animals breathed 100% O_2. Phrenic nerve response to CO_2 inhalation (5% CO_2 in 95% O_2) was tested during each experiment. Mass electrical activity of the phrenic nerve was recorded from a lateral approach using a stainless steel bipolar hook electrode. The nerve signal was amplified with an AC coupled amplifier (Grass Instruments, Quincy MA, Model PJ 511) having bandpass filter settings of 30–3000 Hz. Phrenic nerve activity was full-wave rectified and the rectified signal was processed by a moving averager (Charles Ward Enterprises, Philadelphia, PA) using a time constant of 100 msec.

Microinjection of the antagonists (kynurenic acid and bicuculline) were made bilaterally in each animal in the RVL and CVL (approached from the dorsal surface of the medulla) using a microdrive operated pressure injection system connected to a fine cannula (ID 50 μm, OD 75 μm). The volume of injection was kept constant (50 nl) and delivered over a period of one min. To assess dose response relationships at each injection site, two different doses of the same agent were injected. The time between successive injections at the same site was at least 15 min. It has been our experience that microinjection of a chemical agent more than twice at the same spot in the medulla often gives unreliable results. Control microinjection of artificial cerebrospinal fluid were performed for each experiment.

The approximate stereotaxic coordinates for the RVL (1.8–2.2 mm rostral, 1.5–2.0 mm lateral from the obex and 2.5–3.0 mm deep from the dorsal surface) and CVL (0.2–0.8 mm rostral, 1.6–2.0 mm lateral to the obex, 2.5–3.0 mm deep from the dorsal medulla) were obtained from Paxinos and Watson's atlas [21]. We used the following technique to identify the CVL and RVL. Using a semi-micro concentric stimulating electrode (Rhodes Medical Instruments, California), we first searched for the site in the medulla which had the lowest electrical stimulus threshold (stimulus duration (0.2 ms) and frequency (50 Hz) were kept constant, only the stimulus intensity was varied) for BP changes. For example, to locate the CVL region, we lowered a stimulating electrode in the vicinity of the target area obtained from the stereotaxic atlas. Next, we located the spot which had the lowest

threshold (usually 100 μA) for lowering BP by at least 15 mmHg and the coordinates were noted. We then inserted the microinjection cannula at this location. The same procedure was used to identify the RVL except that we searched for a site where stimulation raised BP by 15 mmHg. Kynurenic acid, xanthurenic acid and bicuculline methiodide were dissolved in artificial CSF (pH of the solutions was adjusted to 7.3) and used for microinjection.

At the end of each experiment a 1% solution of Fast Green dye in physiological saline was injected through the same needle at the same site. The brains were then fixed by intravascular perfusion with 10% formalin, removed and 15 μm sections of the medullary areas of interest were cut with a vibrotome and mounted on microscope slides. Sections were then stained with Thionin and compared with the atlas of Paxinos and Watson [21] to identify the injection sites.

Data analysis

Inspiratory peak phrenic nerve activity was measured using levels during expiration as a baseline. At least ten breaths were measured during a control period, averaged and expressed in arbitrary units. Phrenic nerve activity in response to CO_2 (PNA) were then expressed as percent change of control (Test-Control/Control). Statistical analysis was performed using the two-tailed Student's t-test for paired data. The criterion for statistical significance was $P<0.05$. Data is expressed as the mean ± standard error of the mean (SEM), n = 12 animals.

Results

The effects of microinjection of bicuculline (BIC) and kynurenic acid (KYN) in the RVL on phrenic nerve activity (PNA) and blood pressure (BP)

Bilateral injections of BIC in the RVL (1 and 5 nmol) significantly increased BP without any significant change in the amplitude of PNA. In six of the animals, however, there was a small increase in the rate of phrenic discharge (with the 5 nmol dose) which was not statistically significant. In addition, the increase in phrenic amplitude in response to 5% CO_2 inhalation was not different after BIC injection relative to controls.

The injection of KYN (5 and 10 nmol) in the RVL had little effect either on BP or phrenic amplitude. In five animals, however, immediately after the 10 nmol injection, BP decreased transiently by approximately 10 mmHg from control levels but returned to the baseline within two min. The phrenic response to 5% CO_2 inhalation was also not altered. Fig. 1 summarizes the effect of BIC and KYN injection in the RVL on BP, PNA and the PNA response to CO_2.

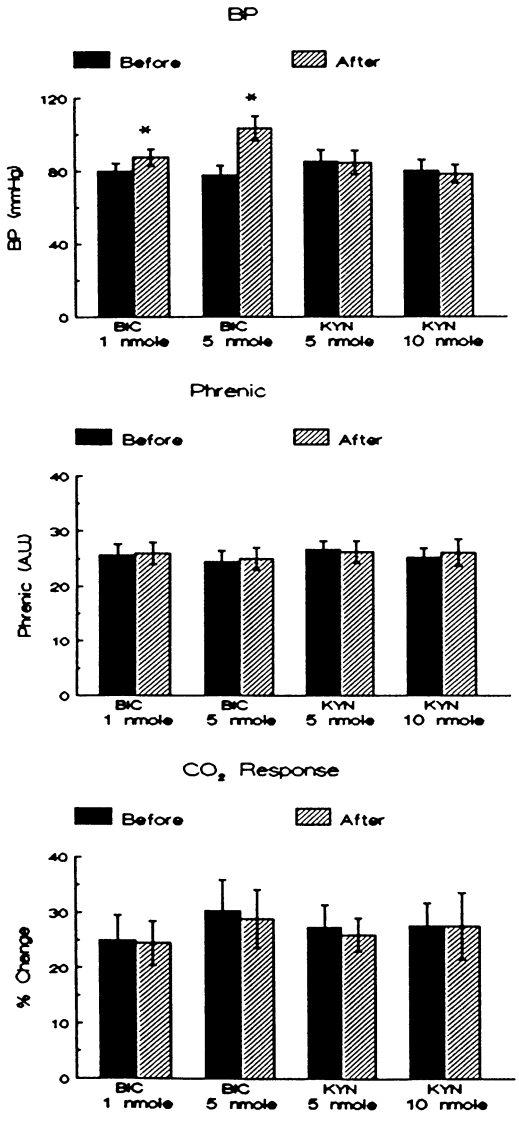

Fig. 1. Blood pressure (BP), phrenic nerve activity (Phrenic) and the phrenic nerve response to CO_2 (CO_2 Response) before and after microinjecting different doses of bicuculline and kynurenic acid in the rostroventrolateral medulla (RVL). Data is expressed as mean ± SEM (n = 12 animals), asterisk represents statistical significance ($P<0.05$).

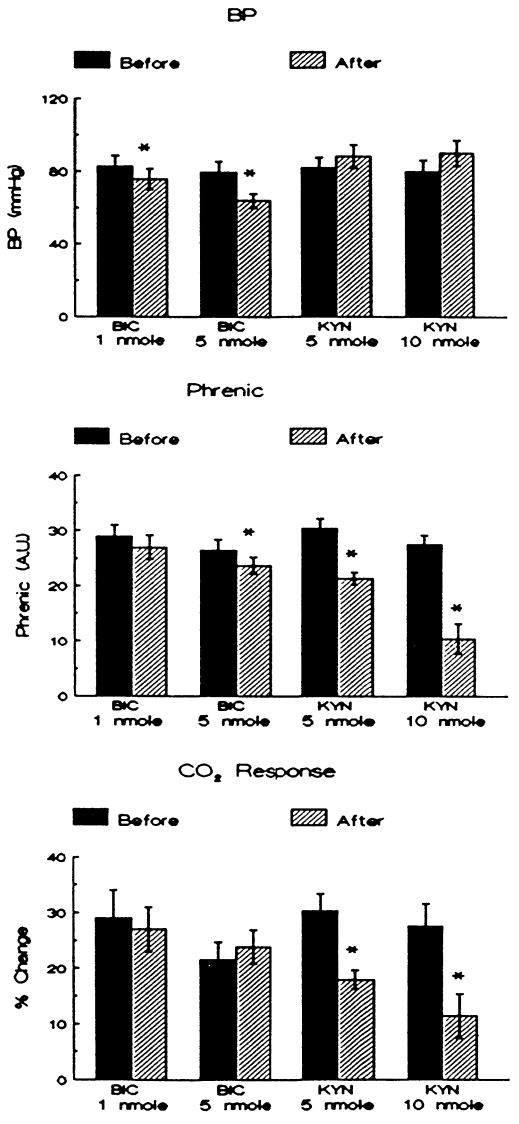

Fig. 2. Blood pressure (BP), phrenic nerve activity (Phrenic) and the phrenic nerve response to CO_2 (CO_2 Response) before and after microinjecting different doses of bicuculline and kynurenic acid in the caudoventrolateral medulla (CVL). Data is expressed as mean ± SEM (n = 12 animals), asterisk represents statistical significance ($P<0.05$).

The effects of microinjection of BIC and KYN in the CVL on PNA and BP

The injection of BIC in the CVL (1 and 5 nmol) significantly lowered BP in a dose dependent manner and transiently depressed phrenic amplitude at the higher dose. Phrenic amplitude returned to the control level in about five min, while the effect on BP lasted for about 10 min. BIC did not alter the phrenic response to 5% CO_2 inhalation.

On the other hand, KYN injection (5 and 10 nmol) in the CVL caused a significant depression of PNA and an increase in BP in a dose dependent manner. BP returned to control levels in about 8 ± 2 min while the depression of PNA continued for about 20 ± 5 min. Moreover, three animals became apneic with the 10 nmol dose and phrenic activity did not return even after one hour. In addition, the augmentation of phrenic amplitude in response to 5% CO_2 inhalation was attenuated substantially in all animals. The animals that became apneic did not respond to CO_2 inhalation. There was an increase in the rate of phrenic discharge in only two animals with the depression of phrenic amplitude (by 5.0 and 7.0% respectively). Figure 2 summarizes the effects of CVL injections of BIC and KYN on BP, PNA and the PNA response to CO_2.

In contrast, xanthurenic acid (an inactive KYN analogue, 10 nmol) was ineffective in altering phrenic amplitude when injected at the same site, although there was a small increase in BP (before 83.0 ± 5.0, after 87.0 ± 6.0 mmHg, $P>0.05$) which returned to control levels in about two min.

Discussion

There are two functionally distinct regions which lie beneath the surface of the ventrolateral medulla, a rostroventrolateral (RVL) and a caudoventrolateral (CVL) region. These two regions play an important role in the regulation of arterial blood pressure [17–20]. The CVL is believed to be a vasodepressor area. The RVL, on the other hand, is believed to be a vasopressor area and may be tonically inhibited by the CVL and GABA may be involved in this inhibition. Therefore, the primary aims of this study were to assess whether the putative neurotransmitters GABA and glutamate are involved in the regulation of vasomotor and respiratory responses in the CVL and RVL regions of the VMS and to compare the responses elicited from these regions.

In the present experiments, we found that in the RVL the GABA receptor antagonist BIC increased BP in a dose dependent manner without any significant effect on PNA or the PNA response to CO_2 This suggests that, at least in the RVL region, the inhibitory influence of GABA is greater on vasomotor than on respiratory neurons. On the other hand, BIC in the CVL lowered BP and only transiently depressed PNA. Moreover, the PNA response to higher CO_2 remained intact. These findings indicate that in the CVL as in the RVL, GABA plays a more important role in the regulation of vasomotor than of respiratory responses.

KYN, when injected in the RVL, had no effect on PNA and transiently lowered BP by about 10 mmHg, suggesting that glutamate may not play an important role in the RVL in the regulation of tonic vasomotor and respiratory drive. When KYN was microinjected in the CVL, however, it had a marked depressive effect on PNA and increased BP. KYN also attenuated the PNA response to higher CO_2 This suggests that, at least in the CVL region, some of the respiratory and vasomotor neurons are regulated by a glutamate pathway. This is consistent with our previous findings in the cat which showed that glutamate analogues stimulated breathing and lowered the apneic threshold when applied superficially to the VMS and this stimulatory effect on respiration was obtained from a more restricted region on the VMS (intermediate area) than the vasomotor responses [14].

We have previously shown that in the rat it is possible to dissociate respiratory and vasomotor responses using focal surface cooling of the VMS. Respiratory responses could be inhibited by cooling an area situated between the hypoglossal rootlets and the first cervical nerve, whereas the vasomotor responses had a wider distribution [22]. The present results are consistent with this finding since surface projections from the CVL region partly overlap the VMS region which blocked respiration when cooled [22].

These results also confirm reported observations by others that GABA receptors in the ventral medulla may be involved in the regulation of vasomotor tone [8,20] and that GABA may be involved as an inhibitory transmitter in the CVL [8,10,23]. Our results showed that KYN injected in the CVL depressed the CO_2 response markedly in a dose dependent manner and caused some animals to become apneic. Moreover, KYN also raised BP when injected in the CVL region which suggests that at least in part, both respiratory drive and vasomotor responses use glutamate pathways in this structure and may be one of the regions where these two responses are integrated. The vasomotor responses to CVL injection of KYN also agree well with the recent findings of Kubo and Kihara [24]. They injected the NMDA antagonist 2-amino-5-phosphonovalerate (APV) in the CVL and showed an increase in BP as well as an inhibition of the depressor and bradycardic responses to aortic nerve stimulation. Kubo and Kihara concluded that the NMDA receptor system may be involved in tonic vasodepressor control in the rat CVL. In our experiment we used kynurenic acid which blocks all three types of glutamate receptor subtypes, and thus the specific subtype involved in vasomotor and respiratory regulation in the CVL remains a topic for future studies.

Our results are consistent with recent anatomical studies of this area which have identified projections from the *nucleus tractus solitarius* (NTS) of the dorsal medulla to the RVL and CVL [25]. Although the function of these projections has not been fully established, Urbanski and Sapru [10,26] and Willette *et al.* [27] have identified two sympathoexcitatory pathways from the NTS, one to the RVL and the other to the CVL. The injection of KYN in the CVL increased BP in a dose dependent manner and this would suggest that we may have interfered with the tonically active glutamate vasomotor pathway from the NTS to the CVL. On the other hand, KYN in the RVL had little effect on BP, suggesting that under normal

circumstances glutamate input to this structure may not be tonically active. Furthermore, microinjection of xanthurenic acid (an inactive analogue of KYN) in the CVL did not reproduce the effect of KYN and suggests that this response is not due to nonspecific or toxic effects.

We have shown that in the CVL as in the RVL GABA is more important in the tonic regulation of vasomotor than of respiratory responses, depressing BP in the RVL while elevating BP in the CVL. Glutamate analogs, on the other hand, may have strong effects on both respiratory (excitatory) and vasomotor (inhibitory) responses but only in the CVL. These results suggest that there is a tonically active glutamate vasomotor pathway within the CVL, possibly originating in the NTS [10,26,27] but that a putative glutamate pathway from the NTS to the RVL may not be tonically active. We conclude that both GABA and glutamate are involved in the regulation of vasomotor and respiratory responses elicited from the VMS, perhaps by acting on excitatory pathways from the NTS, and furthermore, that these responses can be dissociated anatomically and neurochemically.

Acknowledgement

This research was supported by NIH Grant HL-25830.

References

1. Schlaefke ME (1981) Rev. Physiol. Biochem. Pharmacol. 90: 171–244.
2. Bruce EN and Cherniack NS (1987) J. Appl. Physiol. 62: 389–402.
3. Millhorn DE and Eldridge F (1986) J. Appl. Physiol. 61: 1249–1263.
4. Foutz AS, Champagnat J and Denavit-Saubie M (1988) Neurosci. Lett. 87: 221–226.
5. Champagnat J, Denavit-Saubie M, Moyanova S and Rondouin G (1982) Brain Res. 237: 351–365.
6. Taveira da Silva AM, Hartley B, Hamosh P, Quest JA and Gillis RA (1987) J. Appl. Physiol. 62: 2264–2272.
7. Lawing WL, Millhorn DE, Bayliss DA, Dean JB and Trzebski A (1987) Brain Res. 435: 322–326.
8. Willette RN, Krieger AJ, Barcas PP and Sapru HN (1983) J. Pharmacol. Exp. Therap. 226: 893–899.
9. McCrimmon DR, Smith JC and Feldman JL (1989) J. Neurosci. 9: 1910–1921.
10. Urbanski RW and Sapru HN (1988) J. Auton. Nerv. Syst. 25: 181–193.
11. Yamada KA, McAllen RM and Loewy AD (1984) Brain Res. 297: 175–180.
12. Howe PRC (1985) J. Auton. Nerv. Syst. 12: 95–115.
13. Schmid K, Böhmer G and Gebauer K (1989) Neurosci. Lett. 99: 305–310.
14. Mitra J, Prabhakar NR, Overholt JL and Cherniack NS (1987) Brain Res. Bull. 18: 681–684.
15. Gatti PJ, Taveira da Silva AM, Hamosh P and Gillis RA(1985) Brain Res. 330: 21–29.
16. McAllen RM, Neil JJ and Loewy AD (1982) Brain Res. 238: 65–76.
17. Ross CA, Ruggiero DA, Joh TH, Park DH and Reis DJ (1983) Brain Res. 273: 356–361.
18. Ross CA, Ruggiero DA, Joh TH, Park DH and Reis DJ (1984a) J. Comp. Neurol. 228: 165–185.
19. Ross CA, Ruggiero DA, Park DH, Joh TH, Sved AF, Fernandez-Pardal J, Saavedra JM and Reis DJ (1984b) J. Neurosci. 4: 474–494.
20. Ruggiero DA, Meeley MP, Anwar M and Reis DJ (1985) Brain Res. 339: 171–177.
21. Paxinos G and Watson C (1986) The Rat Brain in Stereotaxic Coordinates, 2nd ed. Academic Press, New York.

22. Mitra J, Prabhakar NR, Overholt JL and Cherniack NS (1988) Respir. Physiol. 35–48.
23. Sun MK and Guyenet PG (1985) Am. J. Physiol. 249: R672–R680.
24. Kubo T and Kihara M (1988) Brain Res. 451: 366–370.
25. Ross CA, Ruggiero DA and Reis DJ (1985) J. Comp. Neurol. 242: 511–534.
26. Urbanski RW and Sapru HN (1988) J. Auton. Nerv. Syst. 23: 161–174.
27. Willette RN, Barcas PP, Krieger AJ and Sapru HN (1984) J. Pharmacol. Exp. Ther. 230: 34–39.

Address for correspondence: Dr. Jyoti Mitra, Department of Medicine, Pulmonary Division, Case Western Reserve University, 2074 Abington Road, Cleveland, OH 44106, U.S.A.

2,3-Dihydroxy-6-nitro-7-sulphamoyl-benzo(f)quinoxaline, a selective non-*N*-methyl-D-aspartate excitatory amino acid receptor antagonist, has neuroprotective properties in a model of transient global ischaemia

Malcolm J. Sheardown, Elsebet Ø. Nielsen, Joergen Drejer and Tage Honoré

AIS Ferrosan, CNS Division, Sydmarken 5, DK-2860 Soeborg, Denmark

Abstract

NBQX (2,3-Dihydroxy-6-nitro-7-sulphamoyl-benzo(f)quinoxaline) was found to be a potent and selective ligand for quisqualate and kainate receptors.

Furthermore, it is a selective antagonist of non-NMDA responses in the rat neocortex, and of AMPA and kainate evoked neurotoxicity in cultured neurones.

NBQX (30 mg/kg) given pre and post or just post ischaemia, to Mongolian gerbils having received 5 min bilateral carotid artery occlusion, produced a clear neuroprotective effect. This is the first *in vivo* demonstration of a selective quisqualate/kainate antagonist showing neuroprotective properties.

Excitatory amino acid (EAA) neurotransmission in the central nervous system is mediated by at least three subtypes of receptor i.e. *N*-methyl-D-aspartate (NMDA), kainate and quisqualate receptors [1]. Recently, with the discovery of the quinoxalinediones, a new series of selective non-NMDA receptor antagonists [2], it has become possible to study the pharmacology of non-NMDA receptors, and to investigate the therapeutic potential of non-NMDA receptor blockade. Here we present data showing the effects of a highly potent and selective non-NMDA receptor antagonist 2,3-Dihydroxy-6-nitro-7-sulphamoyl-Benzo(F)quinoxaline (NBQX) on delayed neuronal cell death following a period of transient global ischaemia.

Experimental procedures

Binding experiments were performed at 0–4°C with extensively washed rat cortical membranes [3]. The displacement of [^{3}H] AMPA (α-amino-3-hydroxy-5-methyl-4-isoxazole propionic acid), [^{3}H] kainate, and [^{3}H] CPP (3-(2-carboxy-piperazine-4-yl propyl-1-phosphonic acid) binding by MNQX was studied using methods previously described [3–5].

Rat neocortex slices (cingulate cortex – *corpus callosum*) were prepared as described by Harrison and Simmonds [6] and the experimental procedures were as described by Sheardown [7].

In vitro neurotoxicity data was obtained using cerebral cortical interneurones cultured from 15 day old mouse embryo cortices [8]. Cells were incubated for 3 h in the control buffer plus either AMPA (20 μM), kainate (50 μM) or NMDA (100 μM). Cell survival was measured by addition of 3 μM (100 μl) 3-(4,5-Dimethyl-thiazolyl-2)-2,5-diphenyl-tetrazolinbromide (MTT) and the E570 measured, the figure obtained being proportional to the number of living cells.

Transient global ischaemia was produced in Mongolian gerbils (60–70 g, males) anaesthetized with 2% halothane in 70% nitrous oxide and 30% oxygen.

The common carotid arteries were occluded for 5 min and the animals were allowed to recover for 4 days. The animals were re-anaesthetized, decapitated and the brains quickly removed and frozen in powdered dry ice. Coronal sections (20 μM) were taken through the brain at the level of the hippocampus and stained with cresyl violet and hematoxylin-eosin. The brain sections were rated for neuronal damage in the hippocampus, using a rating scale from 0 (undamaged) to 3 (total damage of CA_1). NBQX (30 mg/kg) was administered intraperitoneally 5 and 15 min before occlusion and 5 after or 30, 40 and 55 min after occlusion.

Results

NBQX displaced [^{3}H] AMPA binding with an IC_{50} value of 0.15 μM, the IC_{50} values for displacement of [^{3}H] kainate and [^{3}H] CPP binding were 4:8 μM and

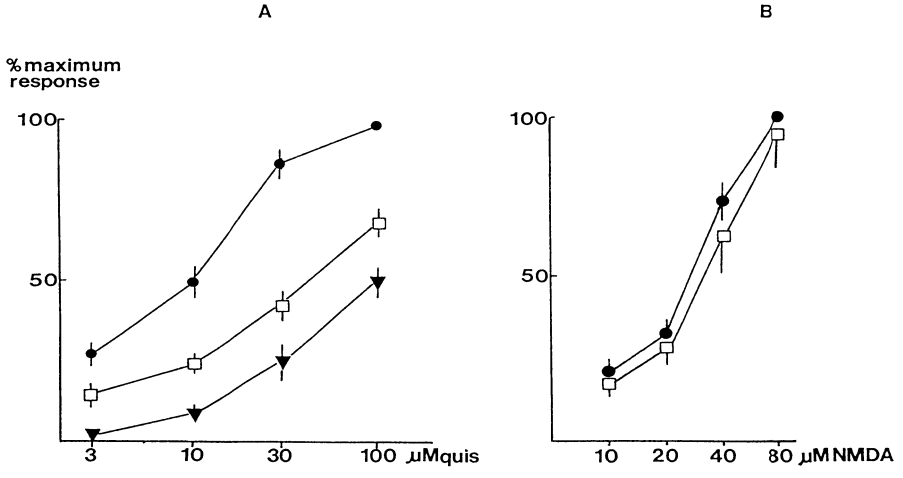

Fig. 1. NBQX selectively antagonizes quisqualate responses in rat neo-cortex slices.
A) effect of NBQX on quisqualate (quis) evoked depolarization of rat cingulate cortex slices, closed circles represent control quis responses, open squares plus NBQX 0.3 μM, closed triangles NBQX 1.0 μM.
B) effect of NBQX on NMDA evoked depolarization of rat cingulate cortex slices, closed circles represent control NMDA responses, open squares plus NBQX 30 μM. In both graphs, ordinate = percentage maximum response, abscissa = log concentration agonist, in both graphs n = 7–10.

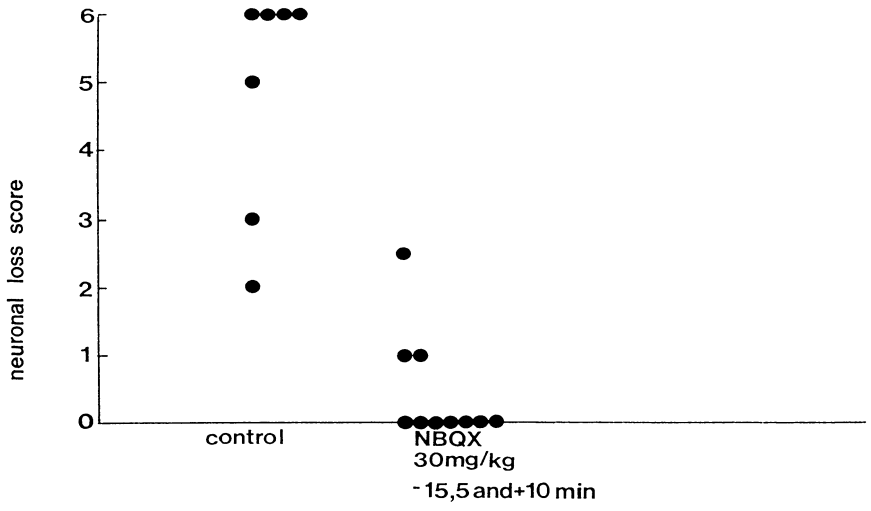

Fig. 2. NBQX administered before and after ischaemia has neuroprotective effects. Scattergram, showing NBQX (30 mg/kg) administered 5 and 15 min before and 10 min after ischaemia produces a protection against delayed neuronal cell death of hippocampal CA_1 neurones 4 days after a 5 min period of global ischaemia in mongolian gerbils. Each dot represents the sum total neuronal cell loss score from both hippocampi of one animal.

greater than 90 μM respectively. Furthermore, NBQX was inactive in inhibiting cortical [^{3}H] glycine binding up to a concentration of 100 μM (data not shown).

In the rat neocortex slice NBQX produced significant blockade of quisqualate evoked depolarization at 0.3 and 1.0 μM whilst a concentration of 30 μM had no effect on NMDA responses (Fig. 1). Furthermore, whilst NBQX at a concentration of 10 μM produced a 100% protection against AMPA and kainate toxicity, this concentration produced no protection against NMDA evoked toxicity in cultured cortical interneurones (data not shown). NBQX when administered at 30 mg/kg either 15 and 5 min before and 5 min after or 30, 40, and 55 min after carotid occlusion, produced a highly significant protection against the delayed cell death of CA_1 hippocampus neurones ($P = 0.008$ and 0.02 respectively using the Wilcoxon rank sum test) (Figs. 2 and 3).

Discussion

The data shows that NBQX is a specific ligand for non-NMDA EAA receptors, with no binding activity at CPP or glycine sites. Furthermore, NBQX is a specific antagonist of non-NMDA receptor responses in the rat neocortex up to a concentration of 30 μM and has no protective effect against NMDA neurotoxicity in cultured mouse neo-cortex neurones.

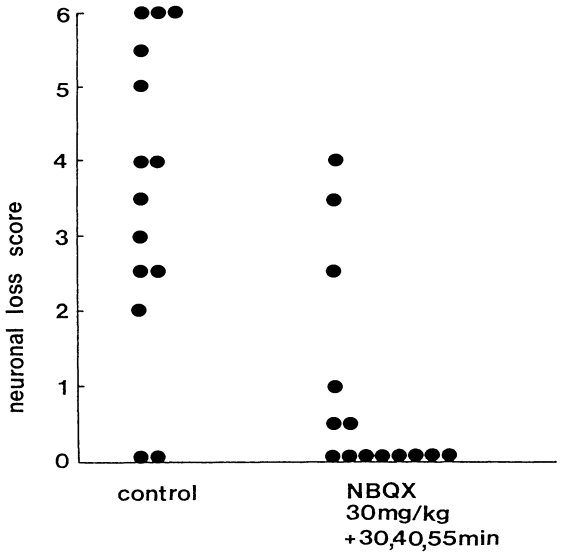

Fig. 3. NBQX administered after ischaemia has neuroprotective effects. NBQX (30 mg/kg) administered 30, 40, and 55 min after ischaemia gives protection against delayed cell death in the Mongolian gerbil. Details of figure as for Fig. 2.

This compound when given a) before and after or b) after temporary bilateral carotid occlusion in the Mongolian gerbil, produced a clear protection of hippocampal CA_1 neurones from the delayed neuronal cell death seen in this model of global ischaemia. Given the above data and that the compound is inactive at GABA, acetylcholine, 5-HT, noradrenergic, dopamine and opiate binding sites (Honoré, unpublished), the protection observed is probably due to non-NMDA receptor blockade. As such this is the first *in vivo* demonstration of neuroprotective activity by a non-NMDA EAA receptor antagonist.

Interestingly Garthwaite and Garthwaite [9] have shown in rat hippocampal slices that concentrations of 6-cyano-7-nitro-quinoxaline-2,3-dione (CNQX) selective for quis and kainate responses will give protection against quisqualate-evoked dark cell degeneration only if present after the quisqualate insult. This suggested that delayed neuronal damage can be produced by activation of non-NMDA EAA receptors.

The post ischaemic neuroprotective effects of NBQX in the gerbil suggest that an event mediated by non-NMDA EAA receptors plays a key role in the delayed cell death observed in models of transient global ischaemia. Thus, selective non-NMDA EAA receptor antagonism may prove to be an important therapy in the treatment of cerebral ischaemia.

References

1. Watkins JC and Evans RH (1981) Ann. Rev. Pharmacol. Toxicol. 21: 165–204.
2. Honoré T, Davies SN, Drejer J, Fletcher EJ, Jacobsen P, Lodge D and Nielsen FE (1988) Science 241: 701–703.
3. Honoré T and Nielsen M (1985) Neurosci. Lett. 54: 27–32.
4. Honoré T, Drejer J and Nielsen M (1986) Neurosci. Lett. 65: 47–52.
5. Honoré T, Drejer J, Nielsen M, Watkins JC and Olvermann HJ (1987) Eur. Pharmacol. 136: 137–138.
6. Harrison NL and Simmonds MA (1985) R. & J. Pharmacol. 84: 381–387.
7. Sheardown MJ (1988) Eur. J. Pharmacol. 148: 471–474.
8. Drejer J, Honoré T and Schousboe A (1987) J. Neurosci. 7: 2910–2916.
9. Garthwaite G and Garthwaite J (1989) Neurosci. Lett. 99: 113–118.

2-Amino-5-phosphonovaleric acid and nimodipine improve post-ischemic changes of brain antioxidative enzyme activities only when given together

Danica B. Stanimirović[a], Lidija Ivanović[a], Dejan Micić[b], Bogdan M. Djuričić[b], Jovan Savić[a] and Bogomir B. Mršulja[b]

[a]Institute of Experimental Medicine, Military Medical Academy, Belgrade, Yugoslavia
[b]Institute of Biochemistry, School of Medicine, Belgrade, Yugoslavia

Abstract

The effects of nimodipine, selective blocker of L-type of 'voltage-dependent' Ca^{2+} channels and 2-amino-5-phosphonovaleric acid (APV), selective antagonist of NMDA-receptors, both after single and combined administration were studied on the survival rate and activities of superoxide dismutase, glutathione reductase and Na,K-ATPase in the gerbil cerebral cortex, basal ganglia and hippocampus after 15 min of bilateral ischemia and 96 h of recirculation. Survival rate was improved in all treated groups (80%) compared to untreated (34%), but without differences among different treatments. But, while single therapy with each drug has only minor or moderate effects, combined therapy with both drugs attains successful recovery (or protection) of the enzyme activities, especially expressed on the cell antioxidative enzymes (superoxide dismutase and glutathione reductase) and membrane-incorporated enzymes (Na,K-ATPase). Thus, administration of APV and nimodipine in common exerts an increased effect on biochemical recovery and/or membrane protection after brain ischemia.

Introduction

Increase in intraneuronal free calcium concentration over a physiological range has been postulated as a crucial event in promotion of ischemic cell death, leading to certain harmful biochemical events: neurotransmitter release, activation of phospholipases and consequent stimulation of membrane phospholipid breakdown, release of free fatty acids, enhanced production of free radical species, activation of protein kinases etc. [1–3]. Membrane depolarization in the first minute of ischemia opens 'voltage-dependent' Ca^{2+} channels, the L-types of which are responsible for the main Ca^{2+} flux through neuronal membrane on account of their high conductance and slow inactivation [4,5]. Uncontrolled neurotransmitter release occurs upon the enhancement of cytosolic Ca^{2+} concentration [6]. Among released neurotransmitter, excitatory amino acids (glutamate, aspartate) express neurotoxic properties, to which is attributed a role in hippocampal susceptibility to ischemic damage [7,8]. Two types of ionic dependance of glutamate neurotoxicity have been distinguished: Na^{+}-mediated early toxicity and delayed toxicity related to Ca^{2+} influx [9,10]. Available data suggest that NMDA receptor-activated channels

may be the predominant route mediating glutamate-induced toxic Ca^{2+} influx and neuronal injury [11]. Other routes for Ca^{2+} entry may contribute to increase of free cytosolic Ca^{2+}, e.g. (a) Na^+/Ca^{2+} exchange that might operate in reverse under conditions of elevated Na^+; (b) other types of 'voltage-dependent' Ca^{2+} channels; (c) passive influx through membrane pores; and (d) Ca^{2+} mobilization from intracellular stores, but they seem to play only secondary roles [2].

Support for the importance of L-channel-mediated influx is provided by the experimental findings that organic Ca^{2+} channel blockers may reduce hypoxic-ischemic injury *in vivo* [12–14]. Similar beneficial effects have been found for systemically administered NMDA receptor antagonists in animal models of both local and global brain ischemia [15,16]. However, none of these single drugs is capable to completely prevent elevation of cytosolic Ca^{2+} during ischemia, or to completely abolish neurologic or metabolic consequences of brain ischemia.

The objective of the present study was to investigate the effect of the combined therapy with two drugs acting simultaneously on two major routes of calcium entry, on the survival rate and biochemical changes after complete ischemia in gerbils.

Materials and Methods

Experiments were performed on adult Mongolian gerbils of both sexes (60–70 g b.w.). All animals were subjected to 15 min of brain ischemia or sham operation and 4 days of recirculation. Drugs were injected after ischemia and during the period of recirculation. Ischemia was produced by bilateral common carotid occlusion, as described elsewhere [17]. Experimental animals were divided into seven experimental groups as follows: controls (sham-operated) (I); animals which received nimodipine diluted in 24% ethanol (1 mg/kg b.w., i.p.) repeatedly every 12 hours during four days (II); group which received 2-amino-5-phosphonovalerate (APV) (4 mg/kg b.w., i.p.) diluted in sterile water every 12 hours during four days (III); animals which were subjected to ischemia and recirculation (IV); animals subjected to ischemia and recirculation and treatment with nimodipine (NIMO) started immediately after removing the carotid clips and repeated every 12 hours during four days (V); ischemic animals treated with APV every 12 hours during four days (VI); and, ischemic animals treated with NIMO and APV in combination, by separate injections every 12 hours during four days of recirculation (VII). There were 5–8 animals in each group. Survival rate during four days of post-ischemia was noted in untreated and differently treated groups. Animals were sacrificed by decapitation, and cortex, basal ganglia and hippocampus were dissected at cold. Crude mitochondrial fraction was separated by differential centrifugation in 0.25 M sucrose [18]. Enzymes were solubilized by hyposmotic disruption in deionized water (1 h at 4°C). Protein content was measured according to Lowry *et al.* [19].

In the extracts (crude mitochondrial fraction) of brain structures, activities of superoxide dismutase, glutathione reductase, and Na,K-ATPase were measured.

Superoxide dismutase (EC 1.15.1.1; SOD) activity was measured as an inhibition of epinephrine autoxidation at 480 nm [20]. Kinetics was followed in a 50 mM sodium carbonate buffer, pH 10.2, containing 0.1 mM EDTA, after addition of 10 mM epinephrine. Incubation of samples with 0.8 mM KCN during 24 h at room temperature, resulted in inhibition of the activity of about 10%, meaning prevalence of mitochondrial (Mn-SOD) enzyme in prepared samples. Unit of the enzyme was expressed as the amount which causes 50% inhibition of epinephrine autoxidation.

Glutathione reductase (EC 1.6.4.2; GR) activity was determined in 100 mM Tris-HEPES buffer, pH 7.4) containing 1 mM NADPH, 1 mM EGTA and 10 mM oxidized glutathione. Reaction was started by the sample addition and stopped after 15 min with 1 M HCl, which destroys NADPH. Fluorescence of formed $NADP^+$ was measured after treatment with 6 M NaOH at 340/460 nm [21].

Na,K-ATPase (EC 3.6.1.3; ATPase) activity was determined as the difference of total ATPase activity assayed in the presence of 5 mM Mg^{2+}, 120 mM Na^+ and 20 mM K^+, and Mg^{2+}-ATPase activity, assayed in the presence of 5 mM Mg^{2+} and 1 mM ouabain. Reaction was measured in 50 mM Tris-HCl buffer, pH 7.4 after addition of ATP (1 mM) [17].

Statistical analysis (analysis of variance-ANOVA) followed by the least squares difference comparison between groups was performed and $p<0.05$ is considered significant.

Results

Survival rate (percentage of survived animals) in ischemic-untreated and differently treated groups is presented in Table 1. Treatment with each single drug improved post-ischemic survival rate: nimodipine from 34% to 83% and APV from 34% to 67%. Combined treatment with both drugs had a similar effect as treatment with nimodipine alone. No statistical difference among different treatments concerning survival was observed.

Table 1. Postoperative daily survival rate (percent of surviving animals) following ischemia in untreated and differently treated groups

Group	Day 1	Day 2	Day 3	Day 4
Untreated (n=35)	71%	57%	46%	37%
NIMO (n=8)	83%	83%	83%	83%
APV (n=8)	83%	67%	67%	67%
NIMO+APV (n=8)	100%	100%	83%	83%

Table 2. Enzyme activities in the control group(s)

Enzyme		Cortex	Basal ganglia	Hippocampus
SOD	(I)	465.3 ± 16.4 (6)	661.8 ± 29.4 (5)	494.5 ± 37.2 (5)
	(II)	ND	ND	ND
	(III)	467.9 ± 29.2 (5)	646.4 ± 28.9 (5)	503.3 ± 27.9 (5)
GR	(I)	11.75 ± 1.61 (7)	15.39 ± 0.89 (5)	16.98 ± 1.28 (5)
	(II)	10.92 ± 1.27 (4)	14.93 ± 1.14 (5)	ND
	(III)	11.51 ± 1.04 (5)	14.87 ± 1.22 (5)	15.19 ± 0.95 (5)
Na,K-	(I)	71.78 ± 7.36 (5)	86.98 ± 7.24 (4)	160.77 ± 9.29 (5)
ATPase	(II)	76.80 ± 6.66 (5)	86.11 ± 5.83 (5)	ND
	(III)	80.82 ± 8.82 (4)	89.89 ± 9.44 (4)	200.95 ± 23.33(4)

Activities are expressed: for SOD as units/mg prot; for GR as μmol $NADP^+$/mg prot/hr; for Na,K-ATPase as nmol Pi/mg prot/min. ND-not done. Group marks are explained in the text.

Administration of vehicle (24% ethanol), nimodipine dissolved in 24% ethanol, as well as APV to control groups in the same manner as to experimental groups, did not influence activity of the investigated enzymes (Table 2). Thus, enzyme activity in the untreated sham-operated group was accepted (and presented) as a reference control value.

Mitochondrial superoxide dismutase (Mn-SOD) activity in the prepared crude mitochondrial fraction of brain tissue represented 85–90% of total-SOD activity, hence only total-SOD was presented and assumed as mitochondrial. After ischemia of 15 min and 4 days of recirculation SOD activity was depressed to 53%, 59% and 66% of control value in the forebrain cortex, basal ganglia and hippocampus, respectively. Only combined treatment with nimodipine and APV achieved normalization of SOD activity in the cortex, while no differences were observed among the treatments in the basal ganglia and hippocampus. All treatments showed significant recovery of the enzyme activity compared to ischemic-untreated group (Fig. 1).

Glutathione reductase (GR) activity shows regional differences in the brain of control animals – high activity in the basal ganglia and hippocampus and low activity in the forebrain cortex (Table 2). Depression of the GR activity in all three brain regions examined was present four days after complete brain ischemia, being the most expressed in the basal ganglia. After APV administration slight recovery was observed in the cerebral cortex and basal ganglia, but complete normalization in the hippocampus. Treatment with nimodipine failed to influence disturbed activity of GR. Combined treatment resulted in complete normalization of GR activity in all three regions examined (Fig. 2).

Na,K-ATPase activity suffered great disturbances during post-ischemic period. Nearly double increases of the enzyme activity were observed in all brain regions examined at fourth day of recirculation. Nimodipine treatment even enhanced this increase, while APV treatment tended to decrease enzyme activity, which was

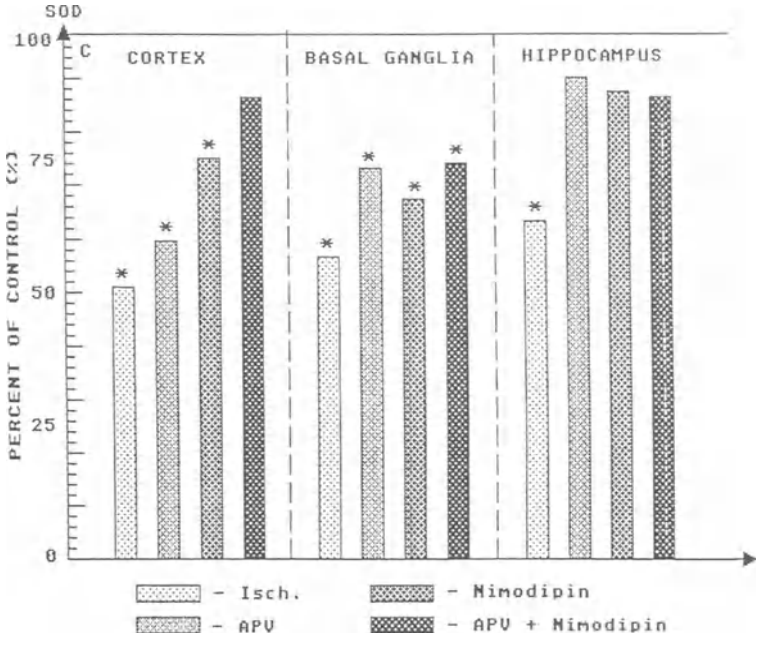

Fig. 1. Superoxide dismutase activity in the gerbil brain after 15 min ischemia and 96 h of recirculation (Isch.) and after application of different drug-treatments during the postischemic period. *- statistically significant difference to control values (C) (ANOVA; $p<0.05$).

still about 170% of control range. Treatment with both drugs normalized Na,K-ATPase activity in the cortex and hippocampus, while in the basal ganglia it was 81% of control value (Fig. 3).

Discussion

During and following cerebral ischemia, cerebral physiology and metabolism are severely deranged. Several sources suggest that excessive intracellular accumulation of calcium, provoked by the cell depolarization in the early phase of cerebral ischemia, could be a critical event in the pathogenesis of cell injury [2,3]. Membrane structures in the brain are 'target' tissues for events promoted by calcium [2,22]. Thus, the therapeutic prevention or limitation of the intracellular calcium increase during ischemia could prevent or diminish its jeopardizing effects on the cell membrane and organelle function.

Since the calcium entry in the neurons is mediated through several routes, each of them acting in the functional connection with the others, blockade of only one route is obviously insufficient to prevent calcium influx in the cell. Harris *et al.*

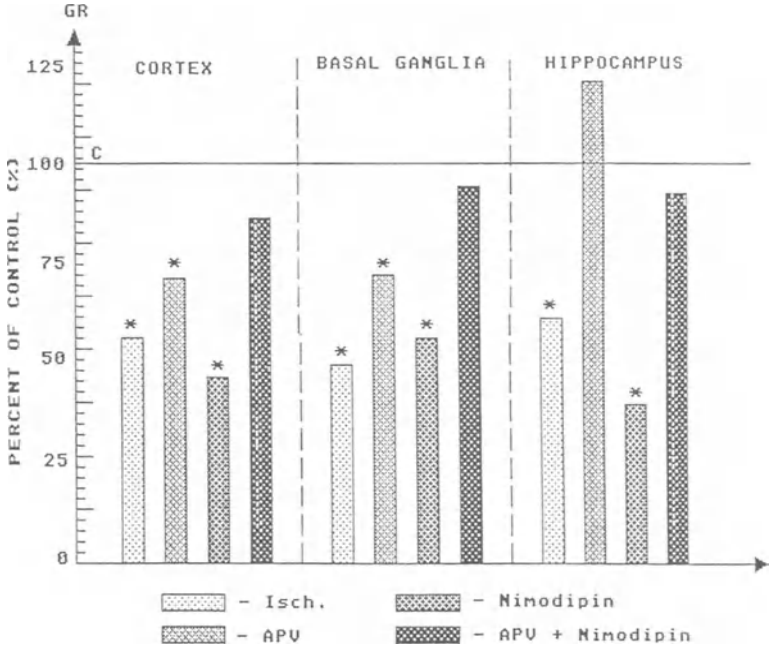

Fig. 2. Glutathione reductase activity in the gerbil brain after 15 min ischemia and 96 h of recirculation (Isch.) and after application of different drug-treatments during the postischemic period. *- statistically significant difference to control values (C) (ANOVA; $p<0.05$).

[12] have shown that nimodipine preloading does not stop the movement of calcium into ischemic cells which suggests that the main route of calcium movement is not through the slow channels. Recent findings [7,11] support the view that Ca^{2+} channels connected with NMDA-type of the excitatory amino acid receptors, activated by the excess of glutamate released during ischemia [23] are responsible for the predominant Ca^{2+} influx. Nevertheless, the initial event necessary for the promotion of neurotransmitter (excitatory amino acids) release is depolarization-stimulated opening of the 'voltage-dependent' calcium channels [1]. Released glutamate could increase cytosolic calcium levels not only through the action on the NMDA-receptors, but also by inducing excitatory cell depolarization, thus opening 'voltage-dependent' calcium channels [11].

Both nimodipine, an organic blocker of 'voltage-dependent' calcium channels and APV, a selective antagonist of NMDA-receptors have been shown to exert beneficial effects in therapy of brain ischemia [13–16]. In our study, both drugs were administered repeatedly after ischemia, with the intention to mimic the clinical situation, and were found to improve survival rate after bilateral carotid occlusion in gerbils. However, no differences were found among therapy with each

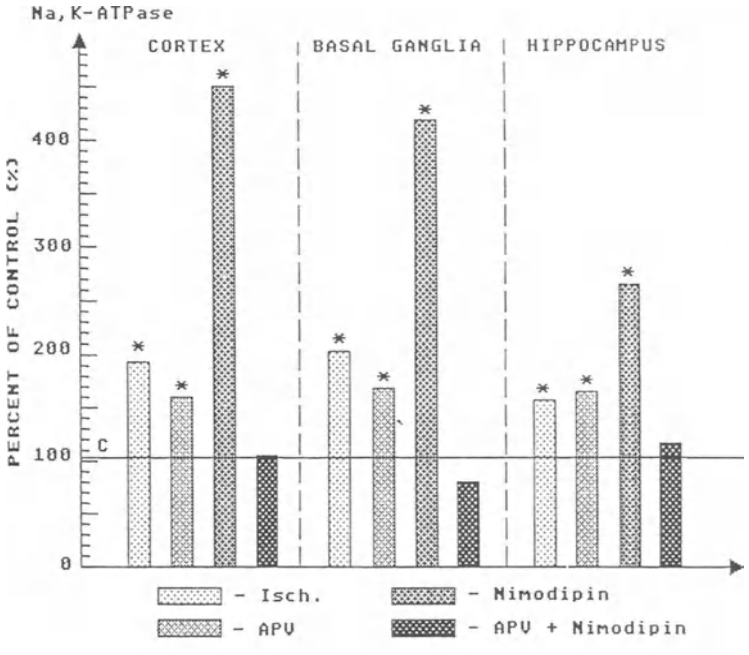

Fig. 3. Na,K-ATPase activity in the gerbil brain after 15 min ischemia and 96 h of recirculation (Isch.) and after application of different drug-treatments during the postischemic period. *- statistically significant difference to control values (C) (ANOVA; $p<0.05$).

single drug and with both drugs in common concerning survival rate. On the other hand, combined treatment exerts beneficial effect on biochemical recovery, preventing fluctuations in the enzyme activity.

One of the primary events promoted by the re-establishment of circulation in the ischemic brain is oxygen conversion in active free radical species such as superoxide radical, hydroxyl radical, singlet oxygen etc. and subsequent initiation of the chain free radical reactions (which is supported, or even started by the calcium action on membrane phospholipids). Thus adequate response of the brain antioxidative system is essential for protection against lipid peroxidation of neuronal membranes [22,24]. Superoxide dismutase activity is deeply depressed in the post-ischemic period in all three brain regions (Fig. 1), as well as glutathione reductase activity (Fig. 2), representing cell inability to neutralize free radicals and peroxides [25,26]; only combined treatment with nimodipine and APV was able to completely normalize glutathione reductase activity in all examined brain regions, and superoxide dismutase activity in the cortex and hippocampus. Therapy with APV alone showed beneficial effect on these enzymes only in the hippocampus. Improved capacity of brain antioxidative system upon the therapeutic intervention offers better protection against free radical damage to brain membranes.

Intact membrane phospholipid environment is necessary for the function of membrane-incorporated enzymes (e.g. Na,K-ATPase). Endogenous phospholipases activated by increased intracellular calcium and burst production of free radicals in post-ischemia lead to disturbance of membrane composition and fluidity, influencing function of membrane-bound enzymes [25]. Effects of nimodipine treatment on the Na,K-ATPase activity, membrane-bound enzyme representing ionic pump, point at deepening of membrane derangement, which is not in agreement with its presumed anticalcium properties. APV treatment showed a slight tendency to normalize Na,K-ATPase activity, while combined treatment both with nimodipine and APV returned Na,K-ATPase activity to the control levels. This membrane-protective effect of combined therapy corresponds well to the improvement of antioxidative system capacity for free radical quenching.

As our results indicate, repeated therapy with nimodipine and APV in combination during the post-ischemic period, improve not only survival rate, but also investigated biochemical parameters. This effect is especially marked on the Na,K-ATPase activity, which will aid faster resolution of brain edema, as well as membrane function restitution. After combined therapy, glutathione reductase is also normalized as well as superoxide dismutase activity in the cortex and hippocampus. Similar results were obtained in our laboratory when combined therapy with nimodipine and propentophylline was applied (unpublished).

Although at the present moment it is not possible to accuse one or more distinct events or reactions to be the final 'deciding' cause of ischemic neuronal death, we can, more or less, recognize some of them. However, it is evident that the complexity of biochemical changes, rather than only one or few of them, is responsible for the decision whether cells will die or not. Thus, it could be reasonable to direct therapeutic intervention toward more than one element of the biochemical cascade developed during cerebral ischemia and recirculation. Our results support this assumption; combined therapy with nimodipine and APV, acting at the same final point, e.g. prevention of calcium-induced deleterious events, but also exhibiting their own specific actions, exerts an intensified effect on biochemical recovery and membrane protection after brain ischemia.

References

1. Harris JR, Symon L, Branston MN and Bayhan M (1981) J. Cereb. Blood Flow Metab. 1: 203–209.
2. Siesjo BK (1981) J. Cereb. Blood Flow Metab. 1: 155–185.
3. Siesjo BK and Wieloch T (1985) In: Plumm F and Pulsinelli W (eds.) Cerebrovascular Diseases. Raven Press, New York, pp. 187–200.
4. Campbell PK, Leung TA and Sharp HA (1988) TINS 11: 425–430.
5. Tsien WR, Lipscombe D, Madison VD, Bley RK and Fox PA (1988) TINS 11: 431–438.
6. Smith JS and Augustin JG (1988) TINS 11: 458–464.
7. Rothman MS and Olney WJ (1986) Ann. Neurol. 19: 105–111.
8. Benveniste H, Jorgensen BM, Diemer HN, Hansen JA (1988) Acta Neurol. Scand. 76: 529–536.
9. Rothman MS (1986) Adv. Exp. Med. Biol. 203: 687–695.
10. Choi WD (1987) J. Neurosci. 7: 369–379.

11. Choi WD (1988) TINS 11: 465–469.
12. Harris JR, Branston MN, Symon L, Bayhan M and Watson A (1982) Stroke 13: 759–766.
13. Steen AP, Newberg AL, Milde HJ and Michenfelder DJ (1983) J. Cereb. Blood Flow Metab. 3: 38–43.
14. Barnett HG, Bose B, Little RJ, Jones CS and Friel TH (1986) Stroke 17: 884–890.
15. Meldrum B (1985) Clin. Sci. 68: 113–122.
16. Simon PR, Swan HJ, Griffiths T and Meldrum SB (1985) Science 226: 850–852.
17. Mrsulja BB, Ueki Y and Lust DW (1986) Matab. Brain Disease 1: 205–220.
18. Gurd JW, Jones LR, Mahler HR and Moore WJ (1974) J. Neurochem. 22: 281–290.
19. Lowry OH, Rosebrough NJ, Farr AL, Randall RJ (1951) J. Biol. Chem. 193: 952–958.
20. Sun M and Zigman S (1978) Anal. Biochem. 90: 81–89.
21. Lowry OH and Passonneau JV (1974) A Flexible System of Enzymatic Analysis. Academic Press, New York.
22. Kogure K, Arai H, Abe K and Nakano M (1985) In: Kogure K, Hossman K-A, Sisjo BK and Welsh FA (eds.) Progress in Brain Research, Volume 61. Elsevier Science Publishers, Amsterdam, pp. 237–259.
23. Fonnum F (1984) J. Neurochem. 42: 1–11.
24. Yashuda H, Shimada O, Nakajima A and Asano T (1981) J. Neurochem. 37: 934–937.
25. Mitchell BJ and Russo A (1987) Br. J. Cancer 55: 96–104.
26. Stanimirovic D, Djuricic MB and Mrsulja BB (1988) Metab. Brain Disease 3: 293–296.

Address for correspondence: Danica Stanimirovic, Institute of Experimental Medicine, Military Medical Academy, Crnotravska 17, 11000 Belgrade, Yugoslavia.

Astroglial ablation by the glutamate analogue gliotoxin α-aminoadipic acid prevents 1-methyl-4-phenyl-1,2,3,6-tetrahydropyridine-induced nigrostriatal neuronal death*

M. Takada[a,b], Z.K. Li[a], T. Hattori[a] and S.T. Kitai[b]

[a]*Department of Anatomy, University of Toronto, Toronto, Ontario M5S 1A8, Canada*
[b]*Department of Anatomy and Neurobiology, The University of Tennessee Memphis, Memphis, TN 38163, U.S.A.*

Abstract

The pyridine derivative 1-methyl-4-phenyl-1,2,3,6-tetrahydropyridine (MPTP) is a potent neurotoxin which selectively destroys nigrostriatal dopamine neurons, producing neurological symptoms relevant to parkinsonism (idiopathic Parkinson's disease). MPTP exhibits dopaminergic neurotoxicity to humans, monkeys, cats and rodents. The oxidative conversion of MPTP to 1-methyl-4-phenylpyridine (MPP^+) is responsible for the generation of its neurotoxicity. This metabolism is mediated by monoamine oxidase B, which in the *substantia nigra pars compacta* (SNc) is localized specifically in astroglia. Employing various combinations of intra-SNc injections of MPTP and the glutamate analogue gliotoxin L-alpha-aminoadipic acid (L-α-AA), we examined both the dose- and time-dependent effects of selective astroglial ablation on MPTP-induced nigrostriatal neuronal death in the rat. Varying nigrostriatal cell loss was assessed primarily by the aid of fluorescent retrograde axonal tracing. Treatment with MPTP alone caused tremendous nigrostriatal cell loss, while intra-SNc co-injections of MPTP and L-α-AA conferred protection against MPTP neurotoxicity in a dose-dependent fashion. A similar protective action was also exerted by L-α-AA injected just prior to or 1 day before MPTP administration. However, the protective effect of L-α-AA was considerably reduced 3 days after pretreatment. Remarkably, MPTP-induced nigrostriatal cell loss was even enhanced rather than attenuated 7 days following L-α-AA pretreatment. Thus, our data provide clear morphological evidence for the critical importance of the presence of astroglia in the onset of MPTP neurotoxicity.

Introduction

The compound 1-methyl-4-phenyl-1,2,3,6-tetrahydropyridine (MPTP) is increasingly being recognized as a crucial neurotoxin which induces irreversible neurological symptoms similar to idiopathic parkinsonism. MPTP causes selective degeneration of nigrostriatal dopamine neurons in humans [12,27], monkeys [4,28], cats [48–50], and mice [3,14,16,54]. Recently, both *in vivo* [13,53] and *in vitro* [35,37,46] studies have also reported that high concentrations of MPTP exhibit a certain neurotoxicity to rats. It now appears indisputable that the oxidative metabolism converting MPTP to 1-methyl-4-phenylpyridine (MPP^+) is a critical step for the manifestation of the dopaminergic neurotoxic effect [7,29,32].

* This was supported by the Medical Research Council of Canada.

This active metabolite is produced by the catalysis of monoamine oxidase B (MAO-B) [8], which in the *substantia nigra pars compacta* (SNc) is localized specifically in astroglial cells [31,42,56]. Although two recent *in vitro* studies [20,43] have indeed implicated astroglia in the conversion of MPTP to MPP^+, the commitment of MPTP-induced nigrostriatal neuronal death to astroglia has not directly been tested yet.

Considerable evidence from both *in vivo* [15,39,40,52] and *in vitro* [21,22] experiments has previously shown selective toxicity of alpha-aminoadipic acid (α-AA), a six-carbon chemical analogue of glutamate, to astroglia. These studies have indicated that the toxin displays no degenerative effects on all the other cell types in the central nervous system, including neurons, oligodendroglia, microglia and endothelial cells. In addition to the cellular specificity, comparison of the D- with L-isomer of α-AA has revealed remarkable stereospecificity [15,21,22,39,52]; the latter is the only isomer effective on the production of selective gliotoxicity. Furthermore, our recent work [53] has provided evidence that a combination of retrograde axonal tracing and intracerebral MPTP injections is a successful tool to identify morphologically MPTP-induced destruction of nigrostriatal dopamine neurons in the rat. In the present paper, fluorescent retrograde axonal tracing following various combinations of intra-SNc injections of MPTP and L-α-AA, was employed in the rat to examine whether the presence of astrocytes is indeed a prerequisite to the generation of MPTP neurotoxicity. We report here the varying effects (in both dose- and time-dependent manners) of selective astroglial ablation on the precipitation of MPTP-induced nigrostriatal neuronal death.

Experimental procedures

Under sodium pentobarbital anesthesia (65 mg/kg, i.p.), adult male albino rats (Wistar, 250–300 g) were positioned in a David Kopf stereotaxic apparatus. Various combinations of unilateral injections of MPTP (Aldrich, MPTP-hydrochloride) and L-α-AA (Sigma) were made into the SNc. Either or both of MPTP (25 μg) [53] and L-α-AA (ranging from 10 to 50 μg) [52] were dissolved in 4 μl of 0.05 M phosphate buffer (pH 7.4), and each solution was infused into 2 different rostrocaudal portions of the SNc through a 10-μl Hamilton microsyringe. In order to avoid physical damage to the SNc, the injection needle was placed somewhat dorsally to the nucleus and the drug-containing solution was slowly delivered over 20 min. Thus, in 2 needle penetrations, the unilateral SNc of each rat received total doses of 50 μg of MPTP and/or 20–100 μg of L-α-AA. On the contralateral side, symmetrical vehicle (0.05 M phosphate buffer) injections into the SNc were usually carried out to serve as control.

First, injections of MPTP alone were made for the estimate of its dopaminergic neurotoxicity yielded by the dose of 50 μg. Second, the dose-dependent effects of L-α-AA on MPTP neurotoxicity were examined by co-injecting increasing doses (20, 40, 60, 80, and 100 μg) of L-α-AA and 50 μg of MPTP. Third, the

time-dependent effects of L-α-AA (the dose of 80 μg which had afforded maximal protection) on MPTP neurotoxicity were investigated by varying the time interval between the gliotoxin and neurotoxin injections; L-α-AA was injected just prior to or 1, 3, 7 days before MPTP administration. Additionally, co-injections of 50 μg of MPTP and 80 μg of the D-isomer of α-AA were made to test the stereospecificity of the gliotoxin.

Three weeks following the final drug injection, a fluorescent retrograde tracer, True blue (TB, 0.4 μl of a 5%, aqueous suspension), was stereotaxically deposited bilaterally into the core of the striata through a 1-μl Hamilton microsyringe. After a survival of 4 days, the animals were deeply reanesthetized and transcardially perfused with 300 ml of 10% formalin in 0.1 M phosphate buffer (pH 7.4). The brains were removed immediately, saturated with 25% sucrose in the same buffer at 4°C overnight, and then cut serially into coronal sections of 40 μm thickness on a cryostat. Every second section through the SNc was kept, while every fourth section containing the striatal TB injection site was kept. The sections were mounted onto clean slides and observed with a Leitz fluorescence microscope. An ultraviolet filter providing excitation light of approximately 360 nm wave-length was used to examine the blue-emitting TB-positive cells. In each case, the extent of striatal TB was verified and the number of retrogradely labeled nigrostriatal cells was counted throughout the SNc on both sides. The number of TB-labeled cells on the drug-injected side was expressed as a percentage (the mean ± S.E.M. for 8 rats) of that on the vehicle-injected (contralateral) side.

In some cases (especially in animals administered with MPTP alone or MPTP 7 days after L-α-AA pretreatment), the SNc-containing sections were Nissl-stained with Cresyl violet and/or processed for tyrosine hydroxylase (TH) immunohistochemistry to confirm cell degeneration. According to the peroxidase-antiperoxidase (PAP) technique of Sternberger [51], the sections were incubated in rabbit antisera against TH (Eugene) for 48 h at 4°C, followed by goat anti-rabbit IgG (Cappel, 1:50 dilution) for 4 h at room temperature. Then, after incubation with rabbit PAP (Dako, 1:50 dilution) overnight at 4°C, the sections were reacted in 0.05 M Tris buffer (pH 7.6) containing 0.05% diaminobenzidine (Sigma) and 0.01% H_2O_2 for 5–10 min at room temperature.

Results

The data showing the dose- and time-dependent effects of L-α-AA on MPTP-induced nigrostriatal cell loss are summarized in Table 1 and Fig. 1, respectively. Retrogradely labeled SNc cells were examined on both sides following TB injections which symmetrically involved the major portions of the bilateral striata. In each case, the striatal TB injection produced intense retrograde perikaryal labeling in the SNc on the control side infused with vehicle. Thus, a large number (approximately 120–140 cells per section) of TB-positive cells were constantly found over the full size range of the SNc on this side (Fig. 2a). Conversely,

Table 1. Dose-dependent effects of L-α-AA on MPTP neurotoxicity

α-AA (μg)	MPTP[a] alone –	Co-injection of MPTP[a] and L-α-AA					Co-injection of MPTP[a] and D-α-AA
		20	40	60	80	100	80
%[b]	19.5±4.0	35.4±8.3	59.0±4.8	73.2±5.8	85.0±4.2	83.8±6.1	17.2±3.9

[a]A total dose of 50 μg of MPTP was administered into the unilateral SNc in each case.
[b]The number of retrogradely labeled nigrostriatal cells on the drug-injected side is expressed as a percentage of that on the control (contralateral) side infused with vehicle. Each number represents the mean ± S.E.M. for 8 rats.

intra-SNc MPTP administration drastically decreased the number of SNc cells retrogradely labeled from the striatum. The density of TB-containing cells in the SNc injected with 50 μg of MPTP was only 19.5 ± 4.0% of control (Fig. 2b).

Co-injections of L-α-AA and MPTP resulted in conspicuous protection against MPTP-induced nigrostriatal cell loss in a dose-dependent fashion. The number of TB-labeled SNc cells was increased by the injection of increasing quantities of the

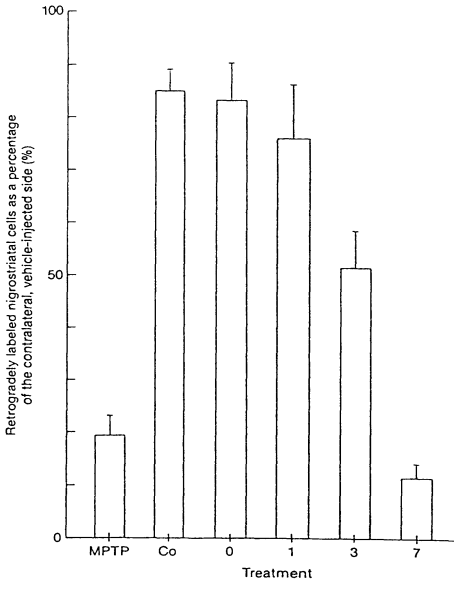

Fig. 1. Time-dependent effects of L-α-AA on MPTP neurotoxicity. Total doses of 50 μg of MPTP and/or 80 μg of L-α-AA were administered into the unilateral SNc with different time intervals. The numbers of retrogradely labeled SNc cells on both sides following TB injections symmetrically involving the major portions of the bilateral striata were compared. Data are expressed as percentages of the control (contralateral) side infused with vehicle. Each bar represents the mean ± s.e.m. for 8 rats ($P<0.05$). MPTP, MPTP treatment alone; Co, Co-injection of MPTP and L-α-AA; 0, 1, 3, 7, L-α-AA pretreatment just prior to, or 1, 3, 7 days before MPTP administration, respectively.

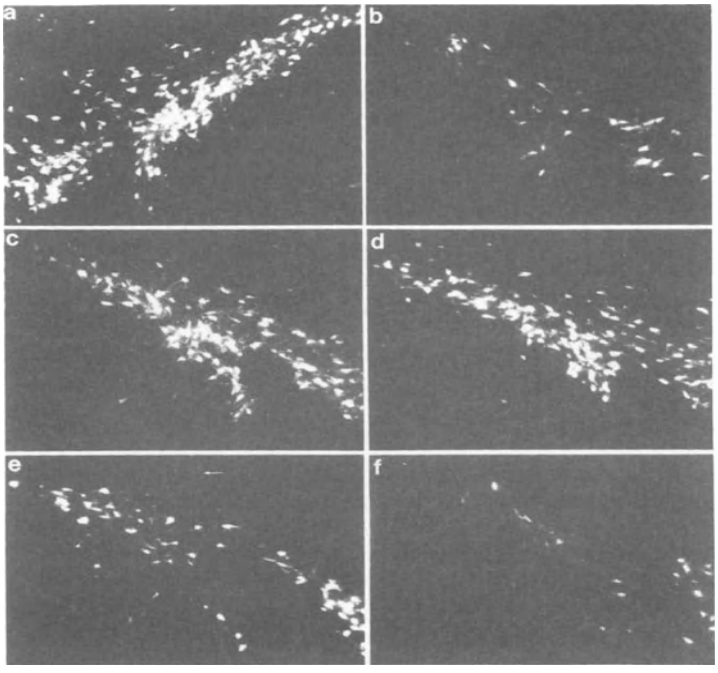

Fig. 2. Photomicrographs of retrogradely labeled SNc neurons following TB injections into the striatum. Intra-SNc administration of 50 μg of MPTP and/or 80 μg of L-α-AA was made with different time intervals. a: the SNc on the control side infused with vehicle. b–f: the SNc on the experimental side administered with MPTP and/or L-α-AA. b, MPTP treatment alone; c, co-injection of MPTP and L-α-AA; d, e, f, L-α-AA pretreatment 1, 3, 7 days before MPTP administration, respectively. All the pictures show almost the same level of the SNc. An arrow in e indicates an injection needle track. a–f, ×80.

gliotoxin, which afforded maximal protection at the dose of 80 μg (Table 1). Thus, after co-injecting MPTP (50 μg) and 80 μg of L-α-AA, a multitude of SNc cells (as many as 85.0 ± 4.2% of control) were labeled with TB retrogradely transported from the striatum (Fig. 2c). In remarkable contrast, the same dose (80 μg) of the D-isomer of α-AA did not display any protective effects on dopaminergic neurotoxicity of MPTP (50 μg); in comparison with the control side, only 17.2 ± 3.9% of SNc cells contained TB (Table 1).

Subsequently, in a second series of experiments, the time-dependent effects of L-α-AA (the dose of 80 μg which had produced maximal protection) on MPTP-induced nigrostriatal cell loss were examined (Fig. 1). Pretreatment with L-α-AA just prior to or 1 day before MPTP administration appeared to prevent nigrostriatal cells from degenerating. Thus, in both cases TB-labeled cells were evident in the SNc (Fig. 2d). However, such protection against MPTP neurotoxicity by L-α-AA was considerably attenuated in the SNc with MPTP administration 3 days following L-α-AA pretreatment; the number of TB-containing nigrostriatal cells went

down to 51.4 ± 7.2% of control (Fig. 2e). Interestingly, intra-SNc MPTP administration 7 days after L-α-AA pretreatment enhanced rather than reduced its dopaminergic neurotoxicity. Thus, more nigrostriatal cell loss occurred in this case than in the case of MPTP treatment alone (11.5 ± 2.6% compared with 19.5 ± 4.0% of TB-positive cells of control) (Fig. 2f).

In some cases (especially in animals administered with MPTP alone or MPTP 7 days after L-α-AA pretreatment), Nissl-staining and/or TH immunohistochemistry were performed to verify SNc cell loss caused by MPTP. Tissue from these animals showed a marked decrease in (Nissl-stained and/or TH-immunoreactive) cell number in the SNc as compared with the control side, and surviving cells largely overlapped TB-labeled ones (not illustrated). Additionally, many of these animals progressively lost body weight and manifested discernible abnormalities in ambulatory/rotational behavior.

Discussion

The selective gliotoxic effect of L-α-AA, a six-carbon chemical analogue of glutamate, has previously been shown both *in vivo* [15,39,40,52] and *in vitro* [21,22]. Upon systemic administration to the infant mouse, L-α-AA causes glial lesions in the arcuate nucleus of the hypothalamus and retina [39,40]. *In vitro* treatment of the dissociated postnatal mouse cerebellum with the toxin results in a rapid nuclear and cytoplasmic swelling of astroglia [21]. Furthermore, L-α-AA which is selectively taken up by astroglia and probably kills the cell following its intracellular accumulation, affects astrocytes only [22]. We have also demonstrated that similar astroglia-specific lesions in the rat can be produced by the stereotaxic intracerebral injection of L-α-AA [15,52]. The present model system is the first to postulate the use of L-α-AA as a tool for selective astroglial ablation.

There has been a controversy over the vulnerability of the rat brain to MPTP. The relatively slower metabolism rate (i.e. inefficient conversion) of MPTP and/or the considerably shorter biological half life (i.e. insufficient retention) of MPP^+, may issue part of factors in the lesser sensitivity of the rat to MPTP as compared with monkey or mouse [26]. Also, ^{3}H-MPTP binding sites are concentrated in the SNc and striatum in the human brain, whereas these regions have substantially fewer binding sites in the rat brain [25]. In fact, MPTP causes behavioral impairments (possibly due to striatal dopamine depletion) in the rat without distinct nigrostriatal lesions [3,9,45], although MPP^+ is extremely toxic to rat dopamine neurons [1,3,18,37,46,47]. However, recent available evidence has revealed that high concentrations of MPTP itself elicit a certain neurotoxicity to rat SNc cells (to a lesser extent ventral tegmental area and dorsal raphe cells as well) both *in vivo* [13] and *in vitro* [35,37,46]. We have also provided anatomical evidence, with the aid of retrograde axonal tracing, that the same large amounts as used in the present study of MPTP administered directly (but not systemically) into the SNc or medial forebrain bundle (MFB), are toxic to rat nigrostriatal neurons [53]. Moreover, our

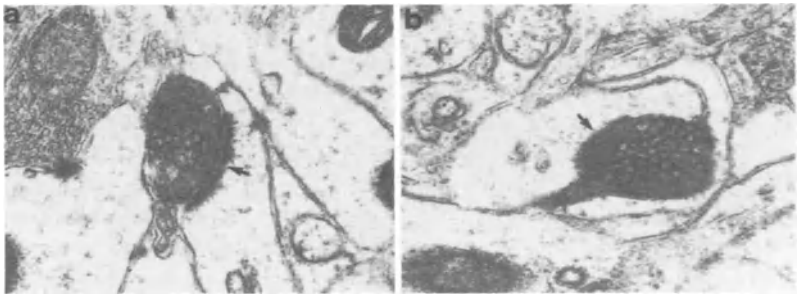

Fig. 3. Photomicrographs showing dark type degeneration of asymmetrical nigrostriatal terminal boutons 2 days after multiple intra-MFB injections of MPTP. a,b, ×16,000.

intra-MFB injections of MPTP resulted in conspicuous degeneration of striatal terminal boutons (Fig. 3).

It is obvious that MPTP is oxidized to the major active metabolite, MPP^+, by MAO-B [8], which is localized predominantly in astrocytes [31,42,56] and serotonergic neurons [31,38,55,56] in the brain. These histochemical studies have also pointed out that dopamine cells in the SNc fail to possess MAO-B, thus suggesting that nigrostriatal neurons themselves do not display the capacity to oxidize MPTP to MPP^+. Therefore, it is most likely that astroglia in the SNc region must be involved in converting MPTP to MPP^+ for the onset of its dopaminergic neurotoxicity. Indeed, two recent *in vitro* experiments [20,43] have indicated a critical role of astroglia in the generation of MPTP neurotoxicity. Cultured astrocytes take up H-MPTP [20] and promote the conversion of MPTP to MPP+ [43]. Moreover, high-affinity binding sites for ^{3}H-MPTP correspond to the localization of MAO-B (virtually ^{3}H-pargyline binding) [2,41]. Our recent investigation [5] has also shown heavy glial labeling as well as neuronal labeling in the SNc area following intraventricular injections of ^{3}H-MPTP. In the present study, fluorescent retrograde axonal tracing after various combinations of intra-SNc injections of MPTP and L-α-AA, has been employed to examine the effects of selective astroglial ablation on MPTP-induced nigrostriatal neuronal death. Our results clearly demonstrate that L-α-AA confers protection against MPTP in a dose-dependent manner. MPTP-induced loss of retrogradely labeled nigrostriatal cells is dramatically reduced by increasing doses of the gliotoxin. However, it may be a little puzzling that L-α-AA is strikingly protective when co-administered with MPTP. One would presume that some time would be required for the toxic effects of this compound to almost completely disable astroglia to mediate the conversion of MPTP to MPP^+. To our knowledge, no other actions of L-α-AA to prevent MPTP neurotoxicity via some different mechanism have hitherto been intimated. At present, it is most reasonable to understand that L-α-AA-induced glial dysfunction might occur so promptly as to obstruct the oxidative metabolism of MPTP. Additionally, co-injections of MPTP and the D-isomer of α-AA fail to afford any preventive effects.

This stereospecificity of the gliotoxin is in full agreement with previous reports [15,21,22,39,52].

Furthermore, our combined intra-SNc injections of both drugs with different time intervals indicate the peculiar time-dependent effects that L-α-AA exerts over MPTP. L-α-AA pretreatment just prior to or 1 day before MPTP administration, favors conspicuous protection against MPTP. Conversely, the neurotoxic potency of MPTP is considerably restored 3 days after L-α-AA pretreatment, and is finally even enhanced rather than attenuated by the gliotoxin pretreated 7 days before MPTP administration. Thus, as compared with the case of MPTP treatment alone, more severe loss of cells retrogradely labeled from the striatum occurs in the SNc. Our previous findings on the fine structural changes after the intracerebral injection of L-α-AA [15,52] might account for this reversed phenomenon. Tremendous invasion of reactive astrocytes starting 3 days after the gliotoxin injection, indicative of the recovery of astroglial function, reaches its peak 7 days after the injection [15,52]. A large number of these recruited astrocytes may accumulate excessive MAO-B to oxidize more efficiently MPTP to MPP^+, which even destroys surviving nigrostriatal cells under the toxic environment produced by regularly administered MPTP.

To date, attempts to reduce or prevent MPTP neurotoxicity have been focussed on the interference, by specific inhibitors, with MAO-B function or dopamine transport system, both of which are believed to be instrumental for the generation of its toxic effect. Indeed, MAO-B inhibitors (including pargyline and deprenyl) prevent the conversion of MPTP to MPP^+ [8,32], and administration of these inhibitors prior to MPTP treatment is protective against MPTP neurotoxicity as well [10,17,30,35,36]. Moreover, the fact that dopamine uptake inhibitors (including mazindol and amfonelic acid) protect against striatal dopamine depletion [33,44] and dopaminergic cell loss [46] caused by MPP^+, supports the notion that the uptake system of MPP^+ into dopaminergic neurons is responsible for selective neurotoxicity of MPTP [24].

There continues to be a great deal of debate regarding the primary site of action of MPTP/MPP^+ on nigrostriatal neurons. While many investigators believe that the major active site is at the level of SNc cell bodies, some argue that the compound first acts at the striatal terminal field and consequentially affects parent cells via retrograde axonal transport [48] or simply retrograde degeneration [19]. The present data showing that astroglial ablation at the SNc level prevents nigrostriatal cell loss following intra-SNc MPTP injections [53], stand in favor of the former idea, even though the latter cannot thoroughly be excluded. In fact, our recent autoradiographic study [6] has successfully demonstrated the capability of MPTP (eventually MPP^+) to be taken up by nigrostriatal terminals and transported retrogradely to SNc cell bodies. Furthermore, SNc cell elimination resulting from intrastriatal [23] or intra-MFB [53] MPTP infusion supports a role for retrograde degeneration. Astroglial ablation at the SNc or striatal level prior to systemic MPTP administration would be strategic in determining definitively its primary active site.

We have now elucidated a pronounced involvement of astroglia in the precipitation of MPTP-induced nigrostriatal neuronal death *in vivo*. The presence of astroglia must be instrumental in the mediation of drug-induced parkinsonism. The eminent role of astroglia seems peculiar to this major brain disease as yet, and the link between the cell and other types of neurodegenerative disorders remains a mystery. In this context, we have previously reported that L-α-AA also protects against kainic acid neurotoxicity in the rat striatum [15]. However, the possible functional relationship of astroglia to kainic acid-induced striatal cell death, which duplicates Huntington's chorea [11,34], still remains elusive. Thus, astroglia may subserve a so-far-unappreciated role in the brain's defense mechanism against neurotoxic insults.

References

1. Altar CA, Heikkila RE, Manzino L and Marien MR (1986) Eur. J. Pharmacol. 131: 199–209.
2. Bocchetta A, Piccardi MP, Del Zompo M, Pintus S and Corsini GU (1985) J. Neurochem. 45: 673–676.
3. Bradbury AJ, Costall B, Domeney AM, Jenner P, Kelly ME, Marsden CD and Naylor RJ (1986) Nature 319: 56–57.
4. Burns RS, Chiueh CC, Markey SP, Ebert MH, Jacobowitz DM and Kopin IJ (1983) Proc. Natl. Acad. Sci. U.S.A. 80: 4546–4550.
5. Campbell KJ, Takada M and Hattori T, submitted for publication.
6. Campbell KJ, Takada M, Nishihama MS and Hattori T, submitted for publication.
7. Castagnoli NJr, Chiba K and Trevor AJ (1985) Life Sci. 36: 225–230.
8. Chiba K, Trevor A and Castagnoli N Jr. (1984) Biochem. Biophys. Res. Commun. 120: 574–578.
9. Chiueh CC, Markey SP, Burns RS, Johannessen JN, Pert A and Kopin IJ (1984) Eur. J. Pharmacol. 100: 189–194.
10. Cohen G, Pasik P, Cohen B, Leist A, Mytilineou C and Yahr MD (1984) Eur. J. Pharmacol. 106: 209–210.
11. Coyle JT and Schwarcz R (1976) Nature 263: 244–246.
12. Davis GC, Williams AC, Markey SP, Ebert MH, Caine ED, Reichert CM and Kopin IJ (1979) Psychiat. Res. 1: 249–254.
13. Golden GT, Fariello RG, Ferraro TN, DeMattei M and Reyes PF (1986) Soc. Neurosci. Abstr. 12: 757.
14. Hallman H, Olson L and Jonsson G (1984) Eur. J. Pharmacol. 97: 133–136.
15. Hattori T and Takada M (1985) Soc. Neurosci. Abstr. 11: 1195.
16. Heikkila RE, Hess A and Duvoisin RC (1984) Science 224: 1451–1453.
17. Heikkila RE, Manzino L, Cabbat FS and Duvoisin RC (1984) Nature 311: 467–469.
18. Heikkila RE, Nicklas WJ and Duvoisin RC (1985) Neurosci. Lett. 59: 135–140.
19. Herkenham M, Little MD, Johannessen JN, Yang S-C, Markey SP and Bankiewicz K (1987) Soc. Neurosci. Abstr. 13: 712.
20. Hess A, Bretschneider A, Sullivan T and Adamo PJ (1985) Soc. Neurosci. Abstr. 11: 428.
21. Huck S, Grass F and Hatten ME (1984) Neuroscience 12: 783–791.
22. Huck S, Grass F and Hortnagl H (1984) J. Neurosci. 4: 2650–2657.
23. Imai H, Nakamura T, Miyashita N, Nishi K and Narabayashi H (1988) Soc. Neurosci. Abstr. 14: 9.
24. Javitch JA, D'Amato RJ, Strittmatter SM and Snyder SH (1985) Proc. Natl. Acad. Sci. USA 82: 2173–2177.
25. Javitch JA, Uhl GR and Snyder SH (1984) Proc. Natl. Acad. Sci. U.S.A. 81: 4591–4595.
26. Johannessen JN, Chiueh CC, Burns RS and Markey, SP (1985) Life Sci. 36: 219–224.

27. Langston JW, Ballard P, Tetrud JW and Irwin I (1983) Science 219: 979–980.
28. Langston JW, Forno LS, Rebert CS and Irwin I (1984) Brain Res. 292: 390–394.
29. Langston JW, Irwin I, Langston EB and Forno LS (1984) Neurosci. Lett. 48: 87–92.
30. Langston JW, Irwin I, Langston EB and Forno LS (1984) Science 225: 1480–1482.
31. Levitt P, Pintar JE and Breakefield XO (1982) Proc. Natl. Acad. Sci. U.S.A. 79: 6385–6389.
32. Markey SP, Johannessen JN, Chiueh CC, Burns RS and Herkenham MA (1984) Nature 311: 464–467.
33. Mayer RA and Heikkila RE (1985) Soc. Neurosci. Abstr. 11: 428.
34. McGeer EG and McGeer PL (1976) Nature 263: 517–519.
35. Mytilineou C and Cohen G (1984) Science 225: 529–531.
36. Mytilineou C and Cohen G (1985) J. Neurochem. 45: 1951–1953.
37. Mytilineou C, Cohen G and Heikkila RE (1985) Neurosci. Lett. 57: 19–24.
38. Nakamura S and Vincent SR (1986) Neurosci. Lett. 65: 321–325.
39. Olney JW, de Gubareff T and Collins JF (1980) Neurosci. Lett. 19: 277–282.
40. Olney JW, Ho OL and Rhee V (1971) Exp. Brain Res. 14: 61–76.
41. Parsons B and Rainbow TC (1984) Eur. J. Pharmacol. 102: 375–377.
42. Pintar JE, Levitt P, Salach JI, Weyler W, Rosenberg MB and Breakefield XO (1983) Brain Res. 276: 127–139.
43. Ransom BR, Kunis DM, Irwin I and Langston JW (1987) Neurosci. Lett. 75: 323–328.
44. Ricaurte GA, Langston JW, DeLanney LE, Irwin I and Brooks JD (1985) Neurosci. Lett. 59: 259–264.
45. Sahgal A, Andrews JS, Biggins JA, Candy JM, Edwardson JA, Keith AB, Turner JD and Wright C (1984) Neurosci. Lett. 48: 179–184.
46. Sanchez-Ramos J, Barrett JN, Goldstein M, Weiner WJ and Hefti F (1986) Neurosci. Lett. 72: 215–220.
47. Sanchez-Ramos JR, Michel P, Weiner WJ and Hefti F (1988) J. Neurochem. 50: 1934–1944.
48. Schneider JS (1987) In: Carpenter MB and Jayaraman A (eds.) The Basal Ganglia II: Structure and Function-Current Concepts, Advances in Behavioral Biology, vol. 32. Plenum Press, New York, pp. 405–413.
49. Schneider JS and Markham CH (1986) Brain Res. 373: 258–267.
50. Schneider JS, Yuwiler A and Markham CH (1986) Exp. Neurol. 91: 293–307.
51. Sternberger LA (1979) In: Immunocytochemistry, 2nd edn., John Wiley & Sons, Inc., New York.
52. Takada M and Hattori T (1986) Histol. Histopath. 1: 271–275.
53. Takada M, Li ZK and Hattori T (1987) Neurosci. Lett. 78: 145–150.
54. Wallace RA, Boldry R, Schmittgen T, Miller D and Uretsky N (1984) Life Sci. 35: 285–291.
55. Westlund KN, Denney RM, Kochersperger LM, Rose RM and Abell CW (1985) Science 230: 181–183.
56. Westlund KN, Denney RM, Rose RM and Abell CW (1988) Neuroscience 25: 439–456.

Address for correspondence: Dr. Masahiko Takada, Department of Anatomy, University of Toronto, Medical Sciences Building, Toronto, Ontario M5S 1A8, Canada.

Infant rats exposure to aspartate and glutamate: Neuroendocrinopathies and structural analysis of brain damage*

Jorge F. Rodriguez-Sierra[a], Stephanie R. Burns[a], Robert A. Earl[b], Bobbie L. Schneider[c] and Barbara J. Morley[c]

Departments of [a]Anatomy and [b]Pathology, University of Nebraska Medical Center, Omaha, NE 68105, U.S.A.

[c]Boys Town National Institute, Omaha, NE 68131, U.S.A.

Abstract

The acidic amino acids Aspartate (Asp) and Glutamate (Glu) appear to be excitatory neurotransmitters in the central nervous system (CNS). In addition to their neurotransmission roles, these compounds can produce neurotoxic effects, supposedly by an excitoxic mechanism. The most striking example of this effect is seen in the developing CNS of rodents. If rodents are exposed to either, exogenously administered, amino acid during the first days of life, there is a very specific pattern of the CNS that encompasses the degeneration of the retina and optic nerve and destruction of a large portion of the arcuate nucleus of the hypothalamus. When these animals grow to adulthood, they exhibit disorders of the endocrine system: reduced endocrine organs, obesity, and a slight hyperprolactinemia. Some of these disorders can be explained by the absence of a control mechanism from the arcuate nucleus of the hypothalamus to the pituitary. An unexplainable item is that prenatal Glu or Asp does not lead to the endocrinopathies described above. Yet we find that both compounds cross readily the placenta and move into the circulation of the fetus. Our ultrastructural results suggest that Glu acts in a different manner than Asp at the level of the hypothalamus. We find that the pattern of brain damage after Glu is more widespread than that seen with Asp. Yet Asp treatment seems to be more debilitating in terms of the extent of the endocrinological pathologies. We suggest that the differences observed between prenatal and postnatal treatments and the differences observed between the two amino acids represent a difference in the development of the receptor systems in the hypothalamus of the developing mammal.

Introduction

Acidic amino acids are considered the major excitatory neurotransmitters in the central nervous system (CNS). Much has been learned from their study as neurotransmitters and about the role of the multiple receptor family subserving these molecules. Yet, two of the dicarboxylic amino acids have been reported to be neurotoxic: glutamate almost 30 years ago [1] and aspartate for a shorter period of time [2,3].

We have previously reported that exposure to glutamate results in stunting of growth, obesity and a number of endocrinopathies [4]. Some of these disorders of

* This work was partially supported by funds from the NIH (HD-13219 to J.F. R.-S.) and by the Electron Microscopy Facility of Boys Town National Institute.

the endocrine system are expressed by a severe reduction in the size of the endocrine organs as well as by severe alterations in the physiology of the organism. There is an attenuation of pulsatile LH release [5], a change in the sensitivity of the pituitary to gonadotropin releasing hormone (GnRH) [6] and a loss of estradiol cytosol receptors in the mediobasal hypothalamus [7] as a result of the neuronal cell loss in this region [8].

The mechanism of action for the neurotoxicity appears to be related to the excitatory effects of these amino acids on postsynaptic receptors, although the entire mechanism is still unclear. The present series of experiments were conducted to compare the neurotoxicity of glutamate and aspartate in the mediobasal hypothalamus, to determine whether prenatal exposure results in neurotoxicity, and to investigate the effects of these amino acids on the lining of the walls of the third ventricle.

Materials and Methods

Animals

Sprague-Dawley rats (Simonsen Labs, Gilroy, CA) were used for breeding of the litters used in all the studies. Animals were maintained in a controlled light schedule (lights on from 05:00 to 19:00 h daily). Rat chow and water were available *ad libitum*. Litters were culled to 7–8 pups on the day after birth (Day 1). Some animals were injected subcutaneously with either l-monosodium glutamate (MSG) or l-monosodium aspartate (ASP) at a dose of 4 mg/g body weight to pups on days 1, 3, 5, 7, and 9 postnatally. Animals were weaned on day 21 of age and maintained 2 rats/cage. Control animals received normal saline of equal volume as the treated rats.

Body weights and organ weights

Body weights were recorded every 5 days for all rats. Animals treated with MSG were sacrificed at 60 days of age and animals treated with ASP were sacrificed at 40 days of age. At the time of sacrifice their gonads, adrenals and pituitary glands removed, trimmed of fat, and weighed.

Prenatal treatment

Pregnant rats exposed to 4 mg/g body weight of MSG or ASP on the third trimester of pregnancy were aborted. If MSG dosage was reduced to 3 mg/ml then pregnancy went to term. Some rats were sacrificed at 19 days of gestation and maternal and fetal serum collected and frozen until assayed for serum glutamate concentrations.

Scanning electron microscopy

Some animals were sacrificed, perfused intracardially with normal saline, followed by 2.5% glutaraldehyde 4% paraformaldehyde in 0.1 M cacodylate buffer (pH 7.4). The brains were removed and after trimming to expose the third ventricle, post-fixed for an additional hour. The brains were then osmicated (1% OsO_4 in sodium cacodylate buffer for 1 h) and washed in cacodylate buffer three times. The tissue was then dehydrated in a graded ethanol series and critically-point dried, mounted in aluminum stubs and sputter-coated with gold. The specimens were examined in a Jeol 848 Scanning electron microscope at 10 kV.

Glutamate analysis

Plasma glutamate concentrations were determined by amino acid analysis using DC-6 cation exchange resin, lithium citrate buffers, and a post-column ninhydrin reactor as previously described [9]. The samples were first deproteinized by mixing 0.100 ml of plasma with 0.050 ml of 12% sulfosalicylic acid in 1.5 ml micro centrifuge tubes. After 15 min, 0.050 ml of 0.8 M lithium citrate buffer (pH 4.24) was added, the tubes vortexed, and then centrifuged at 20,000 × g for five min. Fifty to 150 µl of the clear supernatant were loaded on the amino acid analyzer.

Results

The animals treated with MSG had lighter body weights than control animals throughout our experiment (see Fig. 1). Similar results were obtained for animals treated with aspartate (see Fig. 2). Regardless of sex or age, MSG- or ASP-treated rats were always stunted in their growth and despite their lower body weights, their bodies' composition was significantly greater in fat than that of controls.

The endocrine organs of ASP-treated animals showed a severe reduction in size of the gonads, adrenals and pituitary gland when compared to littermate controls (see Fig. 3). Similar effects were noted with MSG-treated animals (see Fig. 4). In several cases, one of the testes of the ASP-treated rats had never descended and remained in the abdominal cavity.

Prenatal exposure to ASP or MSG resulted in no differences between the treated animals and the control groups in terms of their body weights, endocrine organ weights, or any other signs of neuroendocrinological anomalies. We measured the serum concentration of Glutamate in the maternal and fetal circulation of animals treated with MSG to determine whether the molecule finds its way into the fetal circulation. We found that by the earliest time measured (15 min) the concentration of serum glutamate was significantly elevated in both the maternal and fetal circulation (see Fig. 5). Although the glutamate appears to clear more rapidly in the fetus than in the mother, there is no question that the glutamate finds its way into the fetal circulation and presumably to the brain.

Fig. 1. Body weights of male and female rats treated neonatally with MSG (4 mg/g body weight, sc). Note that control animals were significantly heavier than the MSG-treated animals of either sex throughout the entire period.

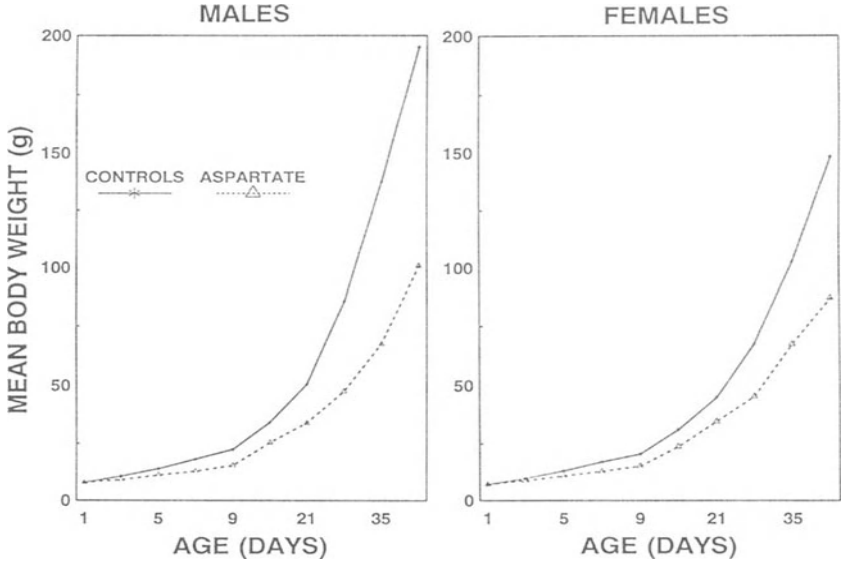

Fig. 2. Body weights of male and female rats treated neonatally with ASP (4 mg/g body weight, sc). Note that ASP animals were always lighter than the littermate controls.

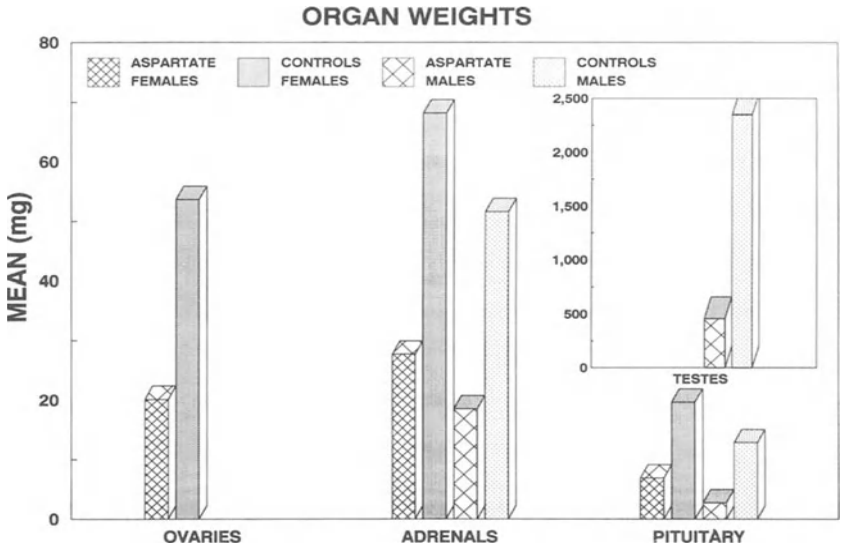

Fig. 3. Endocrine organ weights of rats treated neonatally with ASP. All differences are statistically significant ($p<0.001$) between experimental and control groups.

Upon analysis of the brains of MSG- and ASP-treated rats we noticed that the ependymal cell layer of the third ventricle at the level of the arcuate nucleus of the

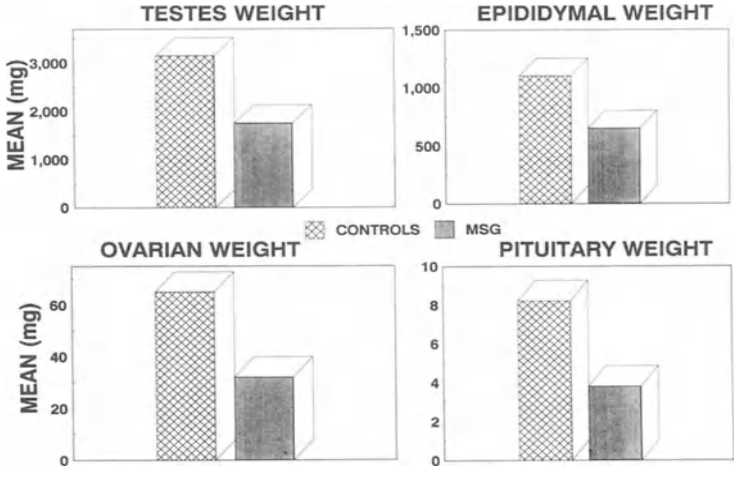

Fig. 4. Endocrine organ weights of rats treated neonatally with MSG. All differences are statistically significant ($p<0.001$) between experimental and control groups.

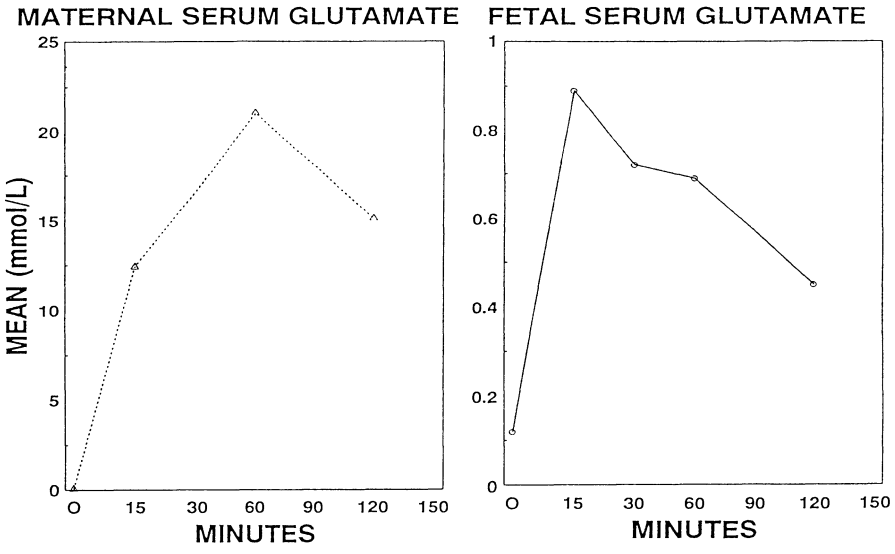

Fig. 5. Maternal and fetal serum glutamate concentrations at 17 days of pregnancy before and after a single injection of MSG (3 mg/g body weight, i.p.).

hypothalamus appeared disrupted (see Fig. 6). Notice that the neurons have been exposed after denudation of a large area of ependymal cells. That the effect is selective to this region of the brain is clear if we examine an area dorsal to that of Fig. 4, the ependymal region of the epithalamus in the same animal, which appears normal (see Fig. 7).

Discussion

Exogenous exposure to MSG or ASP during neonatal life in rats results in severe neuroendocrine disruptions. The sequelae of the pathology appears to be that excitoxic effects in the arcuate nucleus of the hypothalamus result in the loss of several neurotransmitter and neurohormonal systems (particularly dopamine, growth hormone releasing hormone, ß-endorphin, and possible other neuronal systems). The loss of these neurons appear to effect the normal development of the pituitary gland cells and in turn affecting the target organs of the pituitary gland. Of course, we cannot rule out the possibility that MSG or ASP act directly on some of the target tissues (like the ovaries) to affect their normal function.

We noticed that exposure to ASP appeared to be more debilitating to the animals than exposure to MSG. The mortality rate of the pups was higher, the endocrine anomalies appeared to be more severe (i.e. the incidence of cryptorchidism was

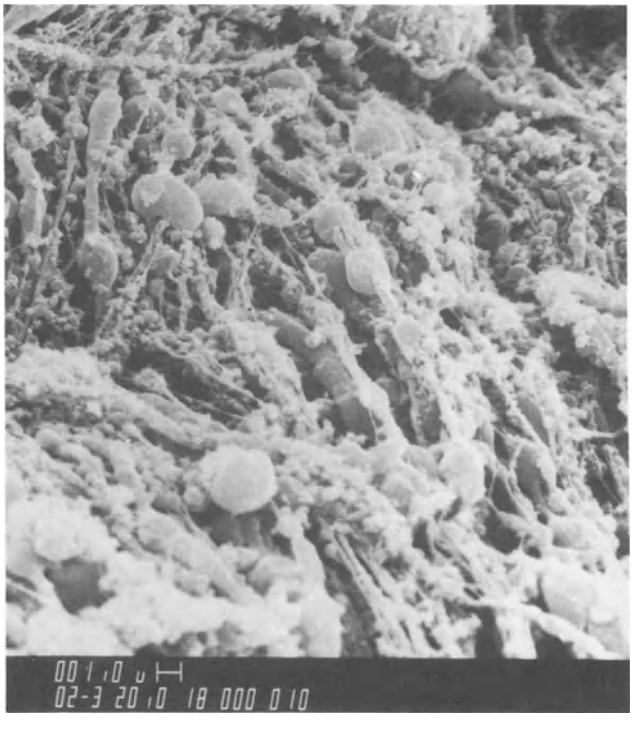

Fig. 6. Scanning electron micrograph of the lateral wall of the third ventricle at the level of the middle portion of the arcuate nucleus of the hypothalamus. Note the severe erosion of the ependymal walls and the exposure of neurons and axons that normally underlie this eroded layer.

greater). It is possible that the two amino acids are producing effects that appear to be similar, but they are acting via separate receptor systems and thus we see some subtle differences between the effects of the two compounds. It is also possible that the amino acids have different affinities for the receptors and the differences are a result of differences in the dissociation of the amino acids to the receptors.

We failed to see any effect of either amino acid when administered prenatally. This was surprising, as it had been reported that these compounds affected the innervation of the area postrema if administered prenatally [10]. Yet we found no somatic, endocrine or brain lesion effects in any of the animals that we tested. When we injected either MSG or ASP to a 17-day pregnant rat we could see that there was a significant elevation in the concentrations of the amino acids in the fetal circulation that mirrored the effects seen in their maternal blood. Thus, the placenta does not appear to be blocking the passage of these compounds into the fetal circulation. We feel that a possibility for the differences between prenatal vs. postnatal exposure is that the receptor system for the amino acids has not developed sufficiently before birth in the hypothalamic area to produce the neurotoxic effects.

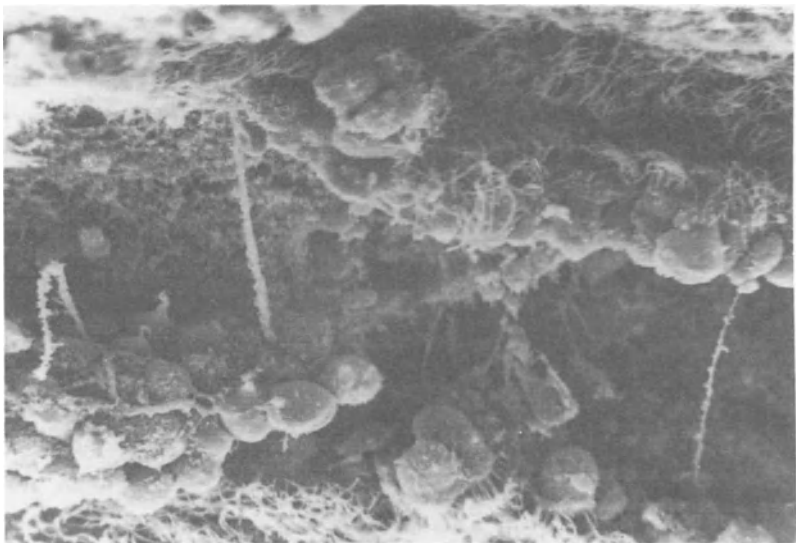

Fig. 7. Scanning electron micrograph of the dorsal portion of the third ventricle of the same animal shown in Fig. 6. This area is just above the habenular complex and it is possible to see portions of the choroid plexus in the field. Note that the ependymal layer appears intact and that it covers the neuronal parenchyme. A few axons are seen traversing the ventricular wall, but the neuronal soma lies deep below the ependymal wall.

We have noticed in previous studies that the lining of the ventricles of MSG-treated animals appeared to be disrupted. Our findings that portions of the ependymal layer are selectively destroyed by the treatment suggest that the acidic amino acids are acting on these cells as well as on the neurons. In fact, denudation of the ependymal layer would facilitate the penetration of the molecules into the neuronal parenchyme and thus increase the possibility for neurotoxicity. We are at a loss to explain the specificity for different regions of the ependymal layer. The mediobasal hypothalamic region of the ependymal layer shows differences from other regions of the third ventricle in terms of type of cilia, formation of blebs, and other structural characteristics of these cells. Surprisingly, we found a lesser effect of ASP than MSG on the denudation of the ependymal layer; despite the more severe physiological effects that we had noticed with ASP than with MSG.

Our results suggest that despite some similarities there is the possibility that MSG and ASP are acting via separate mechanisms or by modification of the same mechanism. There appears to be a major change in the sensitivity of the hypothalamus to the administration of exogenous acidic amino acids that coincides with the birth of the animal. Whether this change is due to a development of the receptor system remains to be determined.

References

1. Potts AM, Modrell RW and Kingsbury C (1960) Am. J. Ophthal. 50: 900–905.
2. Pizzi WJ, Tabor JM and Barnhart JE (1978) Pharmacol. Biochem. Behav. 9: 481–485.
3. Olney JW and Ho OL (1970) Nature 227: 609–610.
4. Rodriguez-Sierra JF, Sridaram R and Blake CA (1980) Neuroendocrinology 31: 228–235.
5. Sridaran R, Rodriguez-Sierra JF and Blake CA (1981) Proc. Soc. Exp. Biol. Med. 168: 38–44.
6. Dada MO, Rodriguez-Sierra JF, Clough RW, Garner LL and Blake CA (1985) Endocrinology 116: 246–251.
7. Rodriguez-Sierra JF, Blaustein JD, Blake CA, Clough RW and Elias KA (1982) Exp. Brain Res. 48: 272–278.
8. Rodriguez-Sierra JF and Morley BL (1985) Neuroendocrinology 41: 427–431.
9. Bensen JV, Gordon MJ and Patterson JA (1967) Anal. Biochem. 18: 228–240.
10. Toth L, Karcsu S, Feledi J and Kreutzberg GW (1987) Acta Neuropathol. (Berl.) 75: 16–22.

Address for correspondence: Jorge F. Rodriguez-Sierra, Department of Anatomy, University of Nebraska Medical Center, 42nd and Dewey Avenue, Omaha, NE 68105, U.S.A.

GYKI 52466, an inhibitor of spinal reflexes is a potent quisqualate antagonist

Istvàn Tarnawa, Ingemar Engberg and John A. Flatman

Institute for Drug Research, Budapest, Hungary
Institute of Physiology, University of Aarhus, Denmark

Abstract

GYKI 52466 is a 2,3-benzodiazepine compound, which inhibits spinal reflexes in cats. Contrary to the classical benzodiazepines (e.g. diazepam), GYKI 52466 does not potentiate the inhibitory action of gamma-amino butyric acid, but seems to affect excitatory processes in the spinal cord directly.

We have investigated the effect of GYKI 52466 on excitatory transmission and on the effect evoked by iontophoretic application of various excitatory amino acids in rat somatosensory cortex slices.

The neuronal depolarizations caused by iontophoretic application of glutamate, quisqualate and kainate were dose dependently depressed by adding 10–50 μM GYKI 52466 to the perfusing medium, whereas *N*-methyl-D-aspartic acid (NMDA) responses were unaffected. Further, the excitatory postsynaptic potentials (EPSPs) evoked by stimulation of the *corpus callosum* were inhibited by both perfusion- and iontophoretic application of GYKI 52466.

The maximum depression of the EPSPs was by about 80%. Quisqualate responses were similarly reduced, whereas glutamate responses were less affected.

In conclusion, GYKI 52466 appears to be a selective blocker of excitatory responses mediated by non-NMDA receptors. Our results also indicate that these receptors play a substantial role in the generation of postsynaptic potentials in the somatosensory cortex.

Introduction

Glutamate and aspartate are known as major excitatory transmitters in different parts of the central nervous system. There are at least two basically different subclasses of receptors, relaying the actions of these neurotransmitters: the NMDA and non-NMDA (quisqualate/kainate) receptors, named after their characteristic agonists, respectively [1]. Several specific NMDA receptor antagonists are available, and some are being tested as putative therapeutic drugs [2–4] These antagonists are valuable research tools in studies of modulatory or plastic phenomena in the brain [5]. Non-NMDA antagonists exist, but most of them are rather weak and unspecific with the exception of a few quinoxaline-derivatives, like 6-cyano-7-nitroquinoxaline-2,3-dione (CNQX) [6–8]. CNQX is able to block non-NMDA receptor mediated excitation at low micromolar concentrations. It also has an effect on the NMDA receptors, inhibiting the potentiating effect of glycine at these sites [9]. As CNQX is not able to cross the blood-brain barrier, it is not suitable in investigations of excitatory processes in the central nervous system, *in vivo*. Thus, there is a need for an antagonist which can be used *in vivo*.

We are reporting here the specific non-NMDA receptor antagonistic effect of a new compound, 1-(amino-phenyl)-4-methyl-7,8-methylendioxy-5H-2,3-benzodiazepine (GYKI 52466).

This drug has a central muscle relaxant action: it is able to inhibit spinal reflexes when administered intravenously (0.2–4 mg/kg) or intraduodenally (2–16 mg/kg) in cats. It is also effective against various chemically induced seizures and electroshock, in rats [10].

Although GYKI 52466 is similar to the classical 1,4-benzodiazepines (e.g. diazepam) in its chemical structure and also in some of its pharmacological actions, a comparison of their effects on spinal root potentials recorded from the dorsal and ventral roots following the stimulation of a peripheral nerve in spinal cats, suggests basically different mechanisms of actions: While 1,4-benzodiazepines primarily act via a potentiation of the inhibitory action of gamma-amino butyric acid [11], GYKI 52466 seems to affect excitatory processes in the spinal cord directly [12].

In our present study, we have investigated the effect of GYKI 52466 on electrically evoked EPSPs and on the effect evoked by iontophoretic application of various excitatory amino acids in rat somatosensory cortex slices.

Materials and Methods

Preparation and maintenance of neocortex slices

400 μm coronal slices were prepared from the brain of 150–170 g rats by a vibrotome. The area used roughly corresponded to the primary somatosensory cortex. The slices were stored in HEPES buffered solution until transferred to a Haas-type interface chamber for electrophysiological investigations. The chamber was continuously perfused at 3 ml/min with a solution containing (in mM): 126 NaCl; 1.8 KCl; 1.25 KH_2PO_4; 1.3 $MgSO_4$; 26 $NaHCO_3$; 2.4 $CaCl_2$; 10 glucose. Temperature was regulated at about 34°C.

Recording techniques

The recording and iontophoresis electrodes were arranged in a twin micromanipulator system [13]. A single microelectrode was first positioned at the recording site in the middle of the gray matter (layer IV-V) for intra- or extracellular recording. A 7-barrel iontophoresis electrode was then advanced to a desired position close to the first electrode (intertip distances usually 40–100 μm).

For intracellular recording the single electrode was filled with 3M KCl or 4M KAc; for extracellular with 1M NaCl. Some barrels in the iontophoretic electrode could also be used for extracellular recording.

Amplified signals were digitally processed by a Datalab 4000 computer system. Averaged evoked responses were stored on tape and recorded by an X-Y recorder

for illustration. Slow changes in DC level were continuously monitored by a strip chart recorder.

Stimulation

The white matter beneath the site of the recording electrode was stimulated. Pulses of 1–5 V amplitude and 0.2 ms duration were delivered through a glass insulated bipolar platinum electrode. Stimulation frequency was 0.1, rarely 0.2 per second. In most of the cases, the stimulation was just subthreshold for evoking spiking.

Drug applications

Amino acids (Na-glutamate 0.5 M; quisqualate 50 mM; kainate 50 mM; NMDA 50 mM) were iontophoresed in cycles (typically for 5–10 sec with a 1/min repetition rate), 52466 (10 mM) was ejected continuously, for several minutes. Current applications (8–100 nA) were usually (but not always) balanced by opposite current delivered through a NaCl barrel of the 7-barrel electrode array to reduce coupling.

When bath-applied, GYKI 52466 (HCl salt, synthesized by Dr. Jenö Körösi and coworkers at the Institute for Drug Research, Budapest) was usually added to the perfusing medium in a concentration range of 10–50 μM. 2-Amino-7-phosphono-pentanoic acid (APV) (Cambridge Research Biochemicals) or ketamine (Richter) were applied at 30–50 μM and 10–50 μM, respectively. Drug applications were started after a stabilization period, when the responses evoked by electrical or chemical stimulation had reached a stable level.

Results

Inhibition of amino acid effects by bath-applied GYKI 52466

Iontophoretic application of quisqualic acid caused a depolarization as revealed by intracellular recording (Fig. 1). The depolarization soon reached a plateau, frequently with excessive firing at the top. Recording the extracellular focal potential [14,15] near the site of the iontophoresis revealed a gradually developing negative potential shift in the DC level (up to 10 mV), well representing the course of neuronal depolarization (Fig. 2).

At 20 and 50 μM concentrations, GYKI 52466 caused a slowly developing reduction of responses (10 experiments). The time-course of the effect can easily be studied in Fig. 2. The inhibition appeared after about five min and tended to reach a saturation after 30 min. The recovery was also slow and not complete even after 60 min.

In a few experiments (n = 3), when kainate was studied, a very similar effect of GYKI 52466 could be observed.

On the contrary, GYKI 52466 up to 100 μM concentration did not inhibit NMDA-induced responses in 5 out of 6 experiments. Fig. 1 shows an experiment,

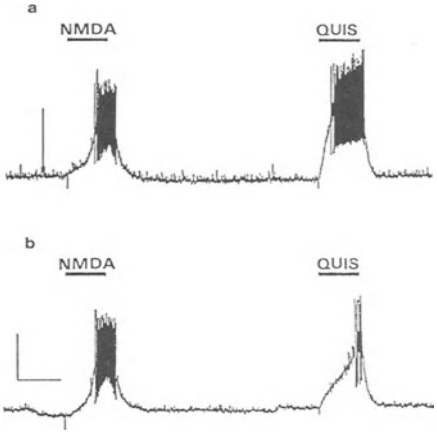

Fig. 1. Selectivity of GYKI 52466 action on NMDA- and quisqualate responses. Membrane potential records from a neurone in layer IV-V of the rat neocortex. NMDA (13 nA) and quisqualate (18 nA) were applied by alternating iontophoretic ejections every minute. Two samples of the continuous recording are shown: (a) control and (b) after 20 min with the addition of 20 μM of GYKI 52466 to the perfusion medium. The depolarization and firing caused by NMDA are both unchanged, whereas the quisqualate depolarization is much slower and barely reaches firing threshold after GYKI 52466 application. It should be noted that quisqualate had stronger actions than NMDA in the control.
Calibration: 10 mV; 10 sec.

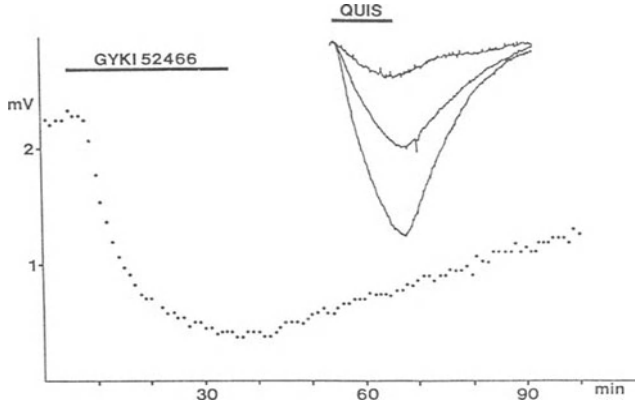

Fig. 2. Depression of quisqualate-evoked responses by GYKI 52466. The inserted records to the right show negative field potentials evoked by 5 sec iontophoretic applications of 20 nA quisqualate in a rat neocortex slice. Bottom record: control; top: after 30 min perfusion with 50 μM GYKI 52466 in the medium; middle: after 60 min washout. The plot shows the timecourse of the action.

when quisqualate and NMDA were alternately iontophoresed. A clear-cut inhibition of quisqualate responses by GYKI 52466 was found while NMDA responses were not altered.

Responses evoked by glutamate were also inhibited by GYKI 52466 but the block was only partial (not illustrated). When quisqualate and glutamate were iontophoresed alternately, we found a more pronounced effect on quisqualate responses than on glutamate responses. The rest of the depolarization caused by glutamate could be effectively blocked by the NMDA receptor blocker APV (30 or 50 μM).

Inhibition of EPSPs by bath application of GYKI 52466

EPSPs evoked by stimulation of the white matter under the recorded area were also blocked by GYKI 52466 in 10 cells (Fig. 3). Applying the drug to the perfusing medium at 50 μM, 80–85% inhibition of the intracellularly recorded EPSPs could be achieved. Only a small part of the remaining component of the EPSP could be inhibited by 50 μM ketamine (a non-competitive NMDA antagonist), suggesting the possible contribution of other transmitters than excitatory amino acids in the response.

The time course of the effect of GYKI 52466 was very much the same as in the case of inhibition of iontophoretic quisqualate evoked responses, i.e. maximum inhibition was seen after 30 min perfusion with GYKI 52466 and the recovery was rather slow.

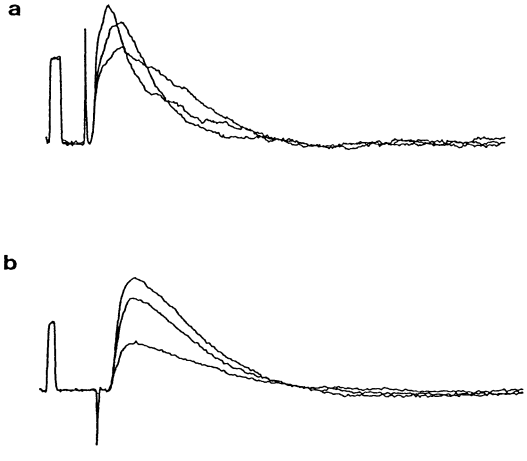

Fig. 3. Depression of EPSPs by GYKI 52466. Averaged records of EPSPs evoked by *corpus callosum* stimulation in two neurons in layer IV-V in the rat neocortex. Membrane potential varied little around −70 mV in both cases. Top records: controls; bottom: (a) after 15 min perfusion with 10 μM GYKI 52466, (b) after 14 min perfusion with 20 μM GYKI 52466; middle traces: recovery of the responses. Calibration pulses: (a) 5 mV; 5 ms, and (b) 5 mV; 2 ms.

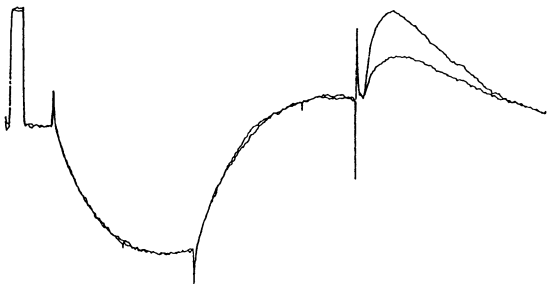

Fig. 4. The EPSP depression by GYKI 52466 is not due to a change in membrane conductance. The two records (each represents an average of 8 responses) are taken before and after a 15 min perfusion with 50 μM of GYKI 52466. They show two conductance measuring pulses (0.2 nA; 55 ms) superimposed followed by two EPSPs. The EPSP is reduced by at least 50%, but the conductance is completely unchanged. Calibration pulses: 5 mV; 5 ms.

In some experiments the duration of the EPSP was increased although its amplitude was decreased (Fig. 3A). This suggests that an inhibitory component of the evoked postsynaptic potential was also blocked.

It was found, that even deeply depressed responses could be restored by increasing the iontophoretic current or stimulus intensity, respectively.

To find out whether GYKI 52466 has an effect on passive membrane properties which could explain the decrease in responses, hyperpolarizing current pulses were applied through the recording electrode. Although in some cases, there occurred a very slight, inconsistent change in the membrane conductance (probably due to a small alteration in the membrane potential sometimes found with GYKI 52466 application), this could not be responsible for the substantial decrement in responses. Fig. 4 shows an experiment, where a 15 min perfusion of 50 μM GYKI 52466 caused about 60% inhibition of the evoked EPSP but no change in the conductance pulse. In two experiments, where the effect of the drug was studied on antidromically activated spikes, the spike threshold was not affected by 50 μM GYKI 52466.

Iontophoretic application of GYKI 52466

GYKI 52466 is not easy to iontophorese. A maximum 10 mM concentration inside the iontophoretic electrode could only be reached at a pH lower than 3. Thus, when the drug was ejected, a precipitation might have occurred at physiological pH, where the solubility is much lower.

Another complication was that GYKI 52466 must be iontophoresed as a cation. The excitatory amino acids are ejected as anions. Therefore, the ejected amino acids may be sucked up by the current in the GYKI 52466 barrel when this is activated, which would simulate a drug antagonism. Thus quantitative data were difficult to obtain.

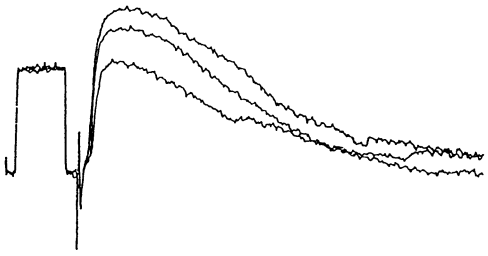

Fig. 5. Depression of EPSPs by iontophoretically applied GYKI 52466. EPSPs evoked in a neocortical cell by *corpus callosum* stimulation were depressed by 10 min iontophoretic application of 33 nA GYKI 52466. Averaged records are superimposed. Top trace: control; bottom: during iontophoretic application of GYKI 52466; middle: recovery after 13 min. Calibration pulses: 5 mV; 10 ms.

However, iontophoresis of GYKI 52466 gave a reduction of quisqualate and glutamate responses, which outlasted the current-effect with a gradual recovery during about 10 min, clearly indicating a pharmacological action.

The effect on stimulus-induced EPSPs was investigated in a few experiments. We found a rapid depression of the EPSP (Fig. 5), again with a recovery phase of about 10 min. The effectiveness of the drug was rather variable, probably reflecting the fact that we were not always close to the synaptic areas where the cell received most of its excitatory input.

Discussion

GYKI 52466 strongly decreased the neuronal depolarization induced by iontophoretically applied quisqualate or kainate and partially decreased glutamate responses, while the remaining glutamate effect was sensitive to the NMDA blocker, APV. NMDA responses were not inhibited by GYKI 52466. Thus, GYKI 52466 can be regarded as a specific blocker of non-NMDA (quisqualate/kainate) type excitatory amino acid receptors in the rat neocortex. Similarly to CNQX, however, GYKI 52466 does not make any difference between quisqualate and kainate receptors.

The blocking effect of GYKI 52466 could be surmounted by increasing the stimulus strength or the iontophoretic current, respectively, while in case of stronger stimuli or iontophoretic currents, a higher GYKI 52466 dose was necessary to achieve the same inhibition, suggesting a competitive antagonism. A systematic study of dose-response characteristics is to be done in the future, but it is not very easy to do in iontophoretic experiments, where the agonist concentration is rather difficult to relate to the ejected charge.

The slow onset and recovery can probably be explained by the high lipid solubility of the drug. Diffusibility of the drug inside the slice seemed to be dependent on the physical condition of the slice, the onset of the effect being more

delayed in older slices. Kinetic parameters were rather variable in different experiments.

The potency of GYKI 52466 is about 10 times weaker than that of the well known non-NMDA blocker CNQX [8], but since it passes the blood brain barrier, it is a much better research tool for studying excitatory processes in the central nervous system. GYKI 52466 at 0.5–4 mg/kg i.v. is able to block the spinal monosynaptic reflex in cats [12], suggesting a major role of non-NMDA receptors in this process. It also has an anticonvulsant effect in different rodent models [10], although its actions on higher brain functions seem to be somewhat weaker than its actions in the spinal cord.

Our results confirm the important role of non-NMDA receptors in transmitting excitation in the somatosensory cortex. 80–85% of intracellularly recorded EPSPs could usually be blocked by 50 μM GYKI 52466. The block is dose-dependent in the range of 10–50 μM. Part of the remaining potential was APV (NMDA receptor blocker) sensitive. In some experiments, when a pronounced inhibitory component contributed in shaping the EPSP, it was found, that even low doses of the drug was able to inhibit that component, similar to what has been found by Andreasen *et al.* [16] in the hippocampus. The most probable explanation of the effect on the EPSPs is, that the excitation on inhibitory interneurons is mediated by an activation of non-NMDA receptors and are blocked by GYKI 52466.

Acknowledgements

We gratefully acknowledge the technical assistance of Mrs. Jette Sandgaard and Mr. Finn Marquard.

References

1. Watkins JC and Olverman HJ (1988) In: Lodge D (ed.) Excitatory Amino Acids in Health and Disease. John Wiley and Sons Ltd, London, pp. 13–45.
2. Meldrum BS (1985) Clinical Sci. 68: 113–122.
3. Lechmann J, Meldrum BS, Chapman AG, Hutchinson A, Tsai C and Wood PL (1988) Eur. J. Pharmacol. 154: 89–93.
4. Woodruff GN, Foster AC, Gill R, Kemp JA, Wong EHF and Iversen LL (1987) Neuropharmacology 26: 903–909.
5. Collingridge GL and Bliss TVP (1987) NMDA receptors – their role in long-term potentiation. Trends Neurosci. 10: 288–293.
6. Drejer J and Honoré T (1988) Neurosci. Lett. 87: 104–108.
7. Honoré T, Davies SN, Drejer J, Fletcher EJ, Jacobsen P, Lodge D and Nielsen FE (1988) Science 241: 701–703.
8. Blake JF, Braun MW and Collingridge GL (1988) Neurosci. Lett. 89: 182–186.
9. Kessler M, Baudry, M. and Lynch G (1989) Brain Res. 489: 377–382.
10. Berzsenyi P, Tarnawa I, Farkas S and Andràsi F (1988) Pharmacol. Res. Commun. 20 (Suppl. 1): 139–140.

11. Haefely W and Polc P (1983) In: Malick JB, Enna SJ and Yamamura HI (eds.) Anxiolytics. Raven Press, New York, pp. 113–145.
12. Tarnawa I, Farkas S, Berzsenyi P, Pataki A and Andrasi F (1989) Eur. J. Pharmacol. 167: 193–199.
13. Engberg I, Källström Y and Marshall KC (1972) Acta Physiol. Scand. 84: 4A–5A.
14. Flatman JA and Lambert JDC (1979) J. Neurosci. Meth. 1: 205–218.
15. Lambert JDC, Flatman JA and Jahnsen H (1981) J. Neurosci. Meth. 3: 311–315.
16. Andreasen M, Lambert JDC and Skovgaard Jensen M (1989) J. Physiol. 414: 317–336.

Address for correspondence: I. Tarnawa, Institute for Drug Research, P.O. Box 82, H-1325 Budapest, Hungary.

Ifenprodil and SL 82.0715 antagonize the effects of NMDA via a polyamine-sensitive modulatory site

Christopher J. Carter, Jean-Paul Rivy, Françoise Thuret, Kenneth G. Lloyd and Bernard Scatton

Synthélabo Recherche (L.E.R.S.), Biology Department, 31 Avenue Paul Vaillant Couturier, 92220 Bagneux, France

Abstract

Ifenprodil and SL 82.0715 are non-competitive NMDA antagonists with cytoprotective ability in animal models of cerebral ischaemia. However, their mechanism of action in relation to the various sites on the NMDA receptor (recognition, channel or glycine) is obscure. A further modulatory site on the NMDA receptor, responsive to spermine and spermidine has recently been proposed. In this study, we have investigated the possible interaction of ifenprodil and SL 82.0715 with this polyamine modulatory site. The polyamines spermine and spermidine (0.1–100 μM) increase the binding of ^{3}H-CPP and ^{3}H-TCP to rat brain membranes. These effects are antagonized by micromolar concentrations of ifenprodil and SL 82.0715. In contrast, MK-801 or 7-chlorokynurenate had no effect on the polyamine-induced increase in ^{3}H-CPP binding. Spermine and spermidine (10–1000 μM) also potentiate the effects of NMDA on cyclic GMP production in immature rat cerebellar slices (maximal increase 400 and 160%, respectively). Neither polyamine stimulated cyclic GMP production in the absence of NMDA. Spermine (100 μM and 1 mM) reversed the inhibitory effects of ifenprodil but not of MK-801, CPP or kynurenate on this NMDA receptor mediated response. The present data support the existence of a polyamine modulatory site within the NMDA receptor complex, and suggest that ifenprodil and SL 82.0715 are antagonists at this site.

Ifenprodil and SL 82.0715 are potent non-competitive *N*-methyl-D-aspartate (NMDA) antagonists [1] which have proven cytoprotective ability in animal models of focal ischaemia [2]. However, their site of action within the NMDA receptor complex has so far proved difficult to define. These compounds potently antagonize the effects of NMDA on cyclic GMP production in immature rat cerebellar slices but are relatively weak displacers of the NMDA channel ligand ^{3}H-TCP, although they do antagonize the glutamate-induced increase in ^{3}H-TCP binding [1]. Unlike other non-competitive NMDA antagonists (e.g. MK-801) they also partially displace the NMDA recognition site ligand ^{3}H-CPP at micromolar concentrations [1]. Neither ifenprodil nor SL 82.0715 (100μM) displace strychnine-insensitive ^{3}H-glycine binding to cortical homogenates [3] thus excluding a possible interaction with the glycine modulatory site within the NMDA receptor. Although, ifenprodil and SL 82.0715 antagonize the depolarizing effects of NMDA on spinal neurones in culture, such activity is hard to detect in electrophysiological perfusion models (for instance the isolated hemisected rat spinal cord) [1].

In vivo, these two compounds are potent cytoprotective agents in focal ischaemia [2] whereas much higher doses are needed to demonstrate anticonvulsant activity [4]. Ifenprodil and SL 82.0715 are not behavioural stimulants, nor do they generalize to phencyclidine in drug discrimination studies [4,5].

These *in vitro* and *in vivo* data suggest that the potent non-competitive NMDA antagonist properties of these compounds cannot be explained in terms of any of the three pharmacological sites so far characterized within the NMDA receptor complex (recognition, channel or glycine sites).

Recently, a fourth site has been described by Ransom and Stec [6], who showed that the polyamines spermine and spermidine were able to increase the binding of the NMDA channel ligand ^{3}H-TCP to washed rat brain membranes. As neither polyamine displaced ^{3}H-CPP or ^{3}H-glycine, these effects were likely to be mediated by a distinct modulatory site within the NMDA receptor complex.

We have recently reported that both ifenprodil and SL 82.0715 antagonize the polyamine-induced increase in ^{3}H-TCP binding in rat cortical membrane preparations [7] and here provide further evidence that ifenprodil and SL 82.0715 antagonize the effects of NMDA via interaction with this polyamine modulatory site.

Experimental procedures

^{3}H-TCP binding

Adult rat brains (minus cerebellum and brainstem) were homogenized in 30 volumes ice-cold Tris HCl (50 mM, pH 7.7) and centrifuged for 20 min at 40,000 g. The pellet was resuspended in the same volume of buffer containing 0.5% Triton X-100 and recentrifuged as before. The pellet was resuspended in the same volume of 5 mM Tris HCl (pH 7.7) centrifuged for 20 min at 40,000 g, and resuspended in 15 volumes of this buffer. Membranes were frozen at −20°C before use. For the binding assay, thawed membranes were centrifuged at 40,000 g for 20 min and resuspended at a final protein concentration of 1 mg per ml. The incubation medium contained 0.5 mg membrane protein in 1 ml, 5 mM Tris HCl (pH 7.7) containing 0.1 mM EDTA, and 2.5 nM ^{3}H-TCP (41 Ci/mmole, CEA France) as well as varying concentrations of test compounds. After 1 hr incubation at 25°C, the membranes were recovered by vacuum-filtration on polyethylenimine (0.05%) soaked Whatman GF/B filters, followed by 3 washes with 3.5 ml cold buffer. Specific binding was defined by 10 μM unlabelled TCP. Results are expressed as pmoles ^{3}H-TCP bound per mg protein and are the mean of triplicate assays.

^{3}H-CPP binding

Rat cerebral cortices were homogenized in 15 volumes ice-cold 0.32 M sucrose (pH 7.0) and centrifuged for 10 min at 1,000 g. The supernatant was centrifuged at

17,000 g for 20 min and the resulting pellet lysed with 40 volumes of distilled water. The membranes were incubated at 38°C for 30 min, recentrifuged for 10 min at 50,000 g and washed twice by resuspension in 40 volumes of distilled water and centrifugation for 10 min at 50,000 g. The pellet was stored frozen at −80°C. For the binding assay, the thawed pellet was suspended in 25 vols, 50 mM Tris HCl (pH 7.4) centrifuged at 50,000 g for 10 min and resuspended in the same volume of buffer. The incubation buffer contained 500 µl of this suspension, 500 µl, 50 mM Tris HCl (pH 7.4), 15 nM ^{3}H-CPP (20 Ci/mmol, Tocris Neuramin, UK) and varying concentrations of test compounds. Specific binding was defined with 1 mM CPP. After incubation for 25 min at 25°C, the tubes were centrifuged (20,000 g, 1 min) and the supernatant aspirated. The pellets were washed twice in 1 ml distilled water, and radioactivity in the pellet determined by liquid scintillation spectrometry. Results are expressed in pmoles ^{3}H-CPP bound per mg protein and are the mean of triplicate assays.

NMDA-induced cGMP production in immature rat cerebellar slices

Cerebellar slices (400 × 400 µm) from 8-day-old rats were incubated for 2 hr at 37°C in oxygenated (95% O_2-5% CO_2) Krebs buffer (millimolar: NaCl, 118; KCl, 4.7; $CaCl_2$, 2.5; $MgSO_4$, 1.19; KH_2PO_4, 1.18; $NaHCO_3$, 25 and glucose, 11, pH 7.4), with changes of buffer every 30 min. Slice aliquots (≈ 200 µg of protein) were then transferred to tubes containing 400 µl of this buffer; the tubes were resealed under O_2-CO_2 at this and subsequent additions, and incubated in a shaking water bath at 37°C. Test compounds were added in a volume of 50 µl of Krebs' buffer followed 5 min later by addition of specified concentrations of NMDA, also in 50 µl of Krebs' buffer. The incubation was terminated after a further 5 min by the addition of 50 µl of 44 mM EDTA, and by immersion of the tubes in a boiling water bath for 4 min. After ultrasonic homogenization of the slices, the tubes were centrifuged for 20 min at 10,000 g. Cyclic GMP levels in aliquots of the supernatant were assayed with a radioimmunoassay kit (Amersham, Buckinghamshire, U.K.). The pellet was dissolved in 200 µl of 0.5 M sodium hydroxide and protein levels were assayed by the method of Lowry *et al.* [8]. The results are presented as the mean with S.E.M. of assays in triplicate, and data are expressed in pmoles of cyclic GMP per mg of protein.

Results

In the presence of L-glutamate (10 µM) (open channel conformation), both spermine and spermidine (0.1–100 µM) increased the binding of ^{3}H-TCP to well-washed rat brain membranes in a concentration dependent manner (Fig. 1). This effect was *not* observed in the absence of added L-glutamate (not shown). Ornithine and putrescine (100 µM) were ineffective in this model. Both ifenprodil and SL 82.0715 (0.1–10 µM) inhibited the potentiating effects of the polyamines

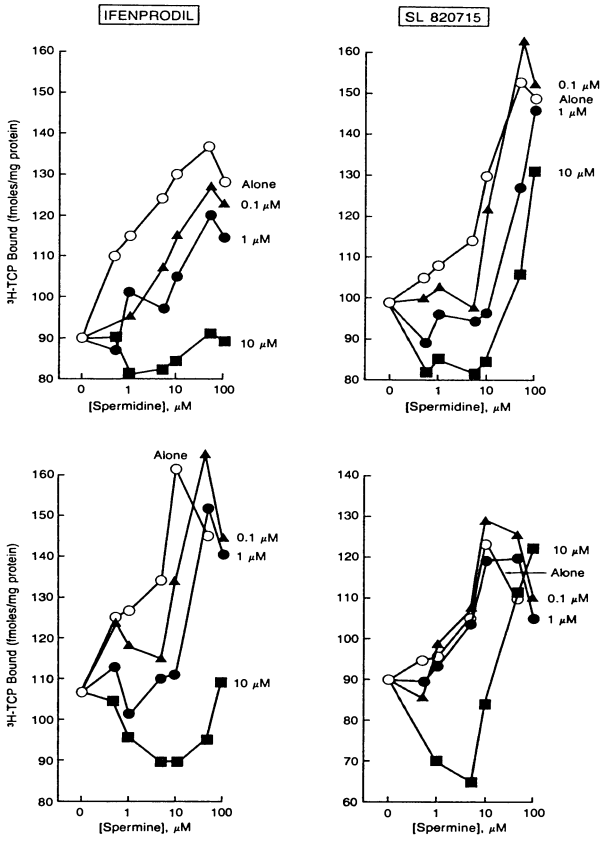

Fig. 1. The effects of spermidine and spermine on ^{3}H-TCP binding in the presence of glutamate (10 μM) and the antagonism of the spermidine induced increase in ^{3}H-TCP binding by ifenprodil or SL 82.0715. Data points are the means of triplicate determinations. Standard errors were less than 10% of the mean, and have been omitted for the sake of clarity. To the right of each curve is the corresponding concentration of ifenprodil or SL 82.0715.

on ^{3}H-TCP binding and at these concentrations did not significantly displace ^{3}H-TCP in the absence of added polyamine (Fig. 1).

Spermine and spermidine (1–100 μM) also increased the binding of ^{3}H-CPP to rat brain membranes in a concentration-related manner, spermine being the most effective agent (Fig. 2). No effect was observed with putrescine or ornithine (100 μM). The effects of spermine and spermidine were both antagonized by ifenprodil (0.1–10 μM) and SL 82.0715 (1–100 μM) (Fig. 2). Neither the NMDA channel blocker MK-801 (100 μM) nor the modulatory glycine site antagonist 7-chloro-kynurenate (100 μM) had any affect on the polyamine-induced increase in ^{3}H-CPP binding (not shown).

Scatchard analysis of the effects of spermine (100 μM) on ^{3}H-CPP binding

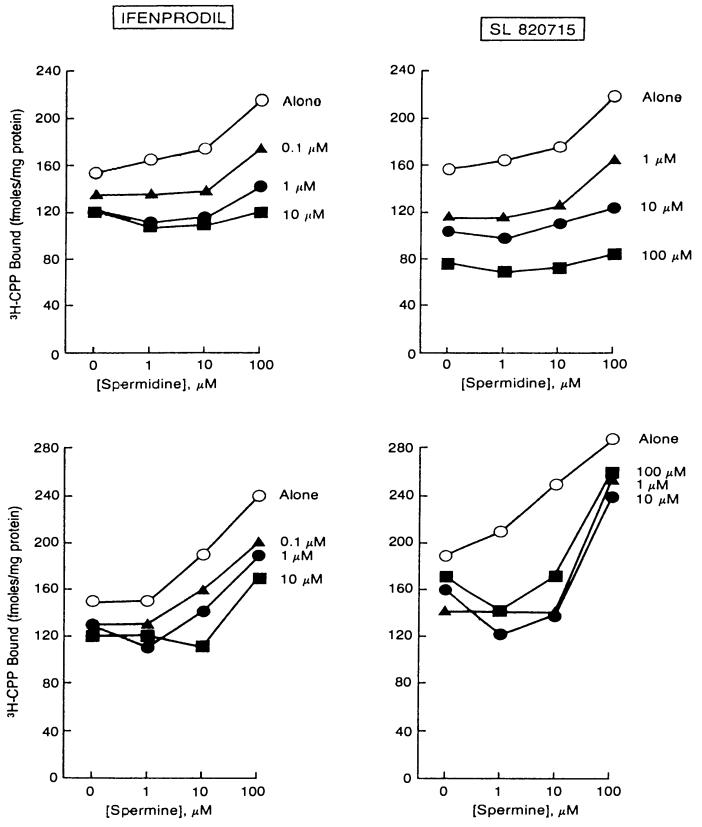

Fig. 2. The effects of ifenprodil (0.1–10 μM) and SL 82.0715 (1–100 μM) on the increase in ^{3}H-CPP binding to rat cortical membranes induced by spermidine or spermine (1–100 μM). Data points are the mean of triplicate determinations with standard errors of less than 10% of the mean. To the right of each curve is the corresponding concentration of ifenprodil or SL 82.0715.

showed a decrease in K_d (from 79.9 to 47.9 nM) with no change in B_{max} (control = 4.4; +spermine = 4.3 pmoles per mg protein).

In immature rat cerebellar slices, spermine and spermidine (10–1000 μM) did not affect basal cyclic GMP levels but both enhanced the maximal effects of NMDA (80–160 μM) on cyclic GMP production (Fig. 3). Spermine was the most effective agent (E_{max} = 400% at 1 mM) (Fig. 3). In the absence of added polyamine, ifenprodil inhibited the effects of NMDA (80 μM) on cGMP production with an IC_{50} of 0.4 μM (Fig. 4). The inhibition curve for ifenprodil was shifted to the right by increasing concentrations of spermine, and in the presence of 1 mM spermine ifenprodil no longer antagonized the effects of NMDA. In contrast, spermine (1 mM) had no effect on the inhibitory potencies of MK-801, CPP or kynurenate in this model (Fig. 4).

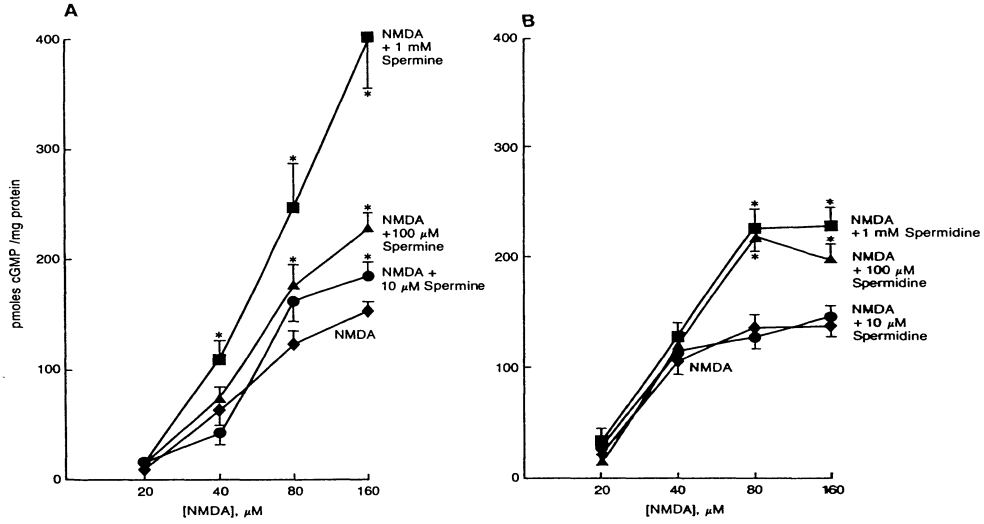

Fig. 3. The effects of spermine and spermidine (10–1000 μM) on the increase in cGMP levels produced by NMDA (20–160 μM) in immature rat cerebellar slices. Data points are the mean ± S.E.M. of assays in triplicate. *$p<0.05$ compared to the effects of NMDA alone.

Discussion

These results confirm and extend the data of Ransom and Stec [6], suggesting that the NMDA receptor is endowed with a second modulatory site responsive to the endogenous polyamines spermine and spermidine. These agents increase the affinity of the NMDA receptor for ^{3}H-CPP, and enhance the stimulatory effects of glutamate on ^{3}H-TCP binding. (Preliminary experiments suggest that this effect may also be mediated via an increase in the affinity for glutamate, as both spermine and spermidine reduce the EC_{50} of glutamate as a stimulator of ^{3}H-TCP binding). Ornithine and putrescine, the amino acid and polyamine precursors of spermidine and spermine do not increase ^{3}H-CPP or ^{3}H-TCP binding. The effects of spermidine and spermine on strychnine-independent ^{3}H-glycine binding are also negligible at physiological concentrations.

That these interactions have functional consequences was also shown by the ability of spermine and spermidine to increase the effects of NMDA on cGMP production in immature rat cerebellar slices. Neither polyamine stimulated cGMP production *per se*.

The neuroprotective non-competitive NMDA antagonists ifenprodil and SL 82.0715 appear to be antagonists at the polyamine modulatory site, as revealed in the binding studies, and also by the ability of spermine to overcome the inhibitory effects of ifenprodil on the NMDA induced increase in cerebellar cGMP produc-

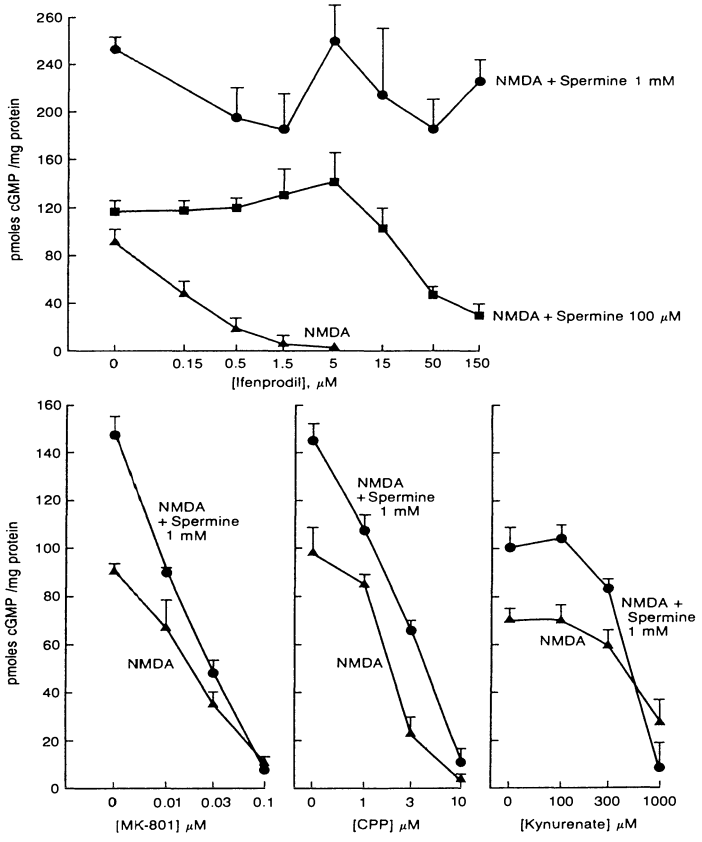

Fig. 4. The effects of spermine (100–1000 μM) on the inhibitory effects of ifenprodil, MK-801, CPP or kynurenate on the NMDA (80 μM) evoked increase in cGMP production in immature rat cerebellar slices.

tion. It is important to note that neither MK-801 nor 7-chlorokynurenate antagonized the effects of the polyamines on ^{3}H-CPP binding, and that spermine did not reverse the inhibitory effects of CPP, MK-801 or kynurenate on the NMDA-induced increase in cerebellar cGMP levels. The proposal that ifenprodil antagonizes the effects of NMDA via a polyamine modulatory site is further supported by binding studies using ^{3}H-ifenprodil as a ligand which have revealed a high affinity binding site in rat brain membranes sensitive to spermine and spermidine [9].

Ifenprodil and SL 82.0715 are potent neuroprotective agents in models of focal ischaemia ([2,10] Scatton *et al.*, this symposium), for example providing 50% cortical protection following middle cerebral artery occlusion in the mouse at doses of 7.0 and 1.1 mg/kg i.p., respectively. NMDA antagonists acting at the recognition site or the NMDA channel (CPP or MK-801) show similar potency in anticonvulsant and cytoprotective models [4,10]; in contrast, as compared to their

anti-ischaemic activity, much higher doses of ifenprodil or SL 82.0715 are needed to provide anticonvulsant effects following electroshock-induced seizures in the mouse [4]. Furthermore, those compounds produce no overt signs of behavioural stimulation following systemic administration, and do not generalize to phencyclidine in drug discrimination studies [4,5]. These data may suggest a differential involvement of the polyamines in different types of NMDA related behavioural or cytotoxic events. It is equally possible that linkage of the polyamine modulatory site to the NMDA receptor shows regional variations.

Polyamine metabolism is altered in the ischaemic brain, where there is a large increase in ornithine decarboxylase activity, the enzyme involved in the initial step of polyamine synthesis [11–13]. This is associated with an increase in the tissue levels of putrescine, whereas the tissue levels of spermidine or spermine are either unchanged or decreased [14–16]. Obviously, further studies are required to define the intra- vs extracellular profile of these polyamine changes in brain ischaemia. While intracellular polyamines play an important role in neuronal growth and differentiation, exogenously applied polyamines are neurotoxic to neurons [17,18]. It is therefore tempting to suggest that during ischaemia, the NMDA receptor (presumably overstimulated by the large quantities of glutamate and/or aspartate that accumulate in the extracellular space) [19] becomes subject to excessive feed-forward activation by polyamines. The antagonistic effects of ifenprodil and SL 82.0715 at the polyamine modulatory site could well account for at least part of the potent neuroprotective effects of these compounds.

In conclusion, our data support the existence of a polyamine-sensitive modulatory site within the NMDA receptor complex. Ifenprodil and SL 82.0715 are antagonists at this novel modulatory site. The effectiveness of ifenprodil and SL 82.0715 as cytoprotective agents in ischaemia suggests that this modulatory site may be an important target for the development of anti-ischaemic drugs.

References

1. Carter CJ, Benavides J, Legendre P, Vincent JD, Noel F, Thuret F, Lloyd KG, Arbilla S, Zivkovic B, MacKenzie ET, Scatton B and Langer SZ (1988) J. Pharm. Exp. Ther. 247: 1222–1232.
2. Gotti B, Duverger D, Bertin J, Carter CJ, Dupont R, Frost J, Gaudilliere B, MacKenzie ET, Rousseau J, Scatton B and Wick A (1988) J. Pharm. Exp. Ther. 247: 1211–1221.
3. Carter CJ, Rivy JP, Thuret F, Lloyd KG and Scatton B (1989) Am. Soc. Neurosci. abstract no. 133.8, p. 326.
4. Perrault G, Morel E, Sanger DJ and Zivkovic B, (1989) Br. J. Pharmacol. 97, suppl.: 580P.
5. Jackson A and Sanger D (1988) Psychopharmacology 96: 87–92.
6. Ransom RW and Stec NL (1988) J. Neurochem. 51: 830–836.
7. Carter CJ, Rivy JP and Scatton B (1989) Eur. J. Pharmacol. 164: 611–612.
8. Lowry OH, Rosebrough NJ, Farr AL and Randall (1951) J. Biol. Chem. 193: 265–275.
9. Schoemaker H, Allen J and Langer SJ (1989) Am. Soc. Neurosci., abstract no. 86.12, p. 200.
10. Benavides J, Gotti B, Dubois A, MacKenzie ET, Scatton B and Theraulaz M (1989) J. Cereb. Blood Flow Metab. 9 (1): S748.
11. Dempsey RJ, Maley BE, Cowen D and Olson JW (1988) J. Cereb. Blood Flow Metab. 8: 843–847.

12. Dienel GA, Cruz NF and Rosenfeld SJ (1985) J. Neurochem. 44: 600–610.
13. Kleihues P, Hossmann KA, Pegg AG, Kobayashi K and Zimmermann V (1975) Brain Res. 95: 61–73.
14. Paschen W, Hallmayer J and Mies G (1987) Neurochem. Pathol. 7: 143–156.
15. Paschen W, Hallmayer J and Rohn G (1988) Acta Neuropathol. 76: 388–394.
16. Paschen W, Schmidt-Kastner R, Djuricic D, Meese C, Linn F and Hossmann KA (1987) J. Neurochem. 49: 35–37.
17. Gilad GM and Gilad VH (1987) In: Model Systems in Neurotoxicology: Alternative Approaches to Animal Testing. Alan Liss Inc., pp. 193–206.
18. Anderson DJ, Crossland J and Shaw GG (1975) Neuropharmacology 14: 571–577.
19. Benveniste H, Drejer J, Schousboe A and Diemer NH (1984) J. Neurochem. 43: 1369–1374.

Address for correspondence: Bernard Scatton, Synthélabo Recherche (L.E.R.S.), Biology Department, 31 Avenue Paul Vaillant Couturier, 92220 Bagneux, France.

Therapeutic potential of the atypical non-competitive NMDA receptor antagonists, ifenprodil and SL 82.0715, in ischaemic cerebrovascular diseases

Bernard Scatton[a], Jesùs Benavides[a], Bernard Gotti[a] and Eric T. MacKenzie[b]

[a]Synthélabo Recherche (L.E.R.S.), Biology Department, 31 Avenue Paul Vaillant-Couturier, 92220 Bagneux, France

[b]CNRS UPR 16, Cycéron B.P. 5027, Bd. Becquerel, 14021 Caen Cédex, France

Abstract

The neuroprotective potential of ifenprodil and SL 82.0715, two non-competitive NMDA antagonists, the mechanism of which is related to a blockade of the polyamine regulatory site, has been evaluated in experimental paradigms of focal cerebral ischaemia in the rat, cat and mouse. When first administered 30 min after middle cerebral artery occlusion in the rat, SL 82.0715 (1 and 10 mg/kg p.o.) reduced by 34 and 48%, respectively the consolidated volume of infarction, as assessed histologically. Ifenprodil and SL 82.0715 (0.3–3 mg/kg i.v.) administered as a perfusion over 3 h after occlusion of the feline middle cerebral artery reduced the volume of infarcted tissue (measured 4 days after occlusion) in a dose-related manner by 25 to 42%. The administration of SL 82.0715 (10 mg/kg i.p.), 5 min, 6 h, 18 h after middle cerebral artery occlusion in the mouse and then twice a day until sacrifice evoked a decrease of similar magnitude (ca. 60–70%) in the volume of the infarction and in the proliferation of ω_3 (peripheral type benzodiazepine) binding site levels (an index of reactive gliosis). A significant diminution of cortical ω_3 sites was still noted when the first administration was delayed until 3 h post-occlusion. The overall consistency of these results in animal models of stroke strongly suggest that ifenprodil and SL 82.0715 are of potential value in the treatment of ischaemic cerebrovascular diseases.

Brain ischaemia, and the consequent neuronal damage, occur as a result of diverse pathological conditions that have in common a reduction of cerebral blood flow and nutrient delivery to the brain. The most frequent cause of cerebral ischaemia in humans is that occasioned by the thrombotic or embolic occlusion of a major cerebral artery (stroke) but cerebral ischaemia can also result from other causes e.g. anaesthetic accident, brain trauma, vasospasm or cardiac arrest.

The clinical and economic importance of ischaemic cerebrovascular diseases has prompted considerable research efforts in an attempt to understand the basic mechanisms of ischaemia-induced neurodegeneration and to develop stroke-related pharmacotherapies. Accumulating evidence indicates that a not inconsiderable fraction of postischaemic neuronal degeneration is a delayed, calcium-dependent phenomenon mediated by *N*-methyl-D-aspartate (NMDA) receptors and mainly caused by an overactivity of excitatory amino acid transmitter systems [1–4]. Stated simply the glutamate hypothesis of ischaemic neurotoxicity supposes that

the large quantities of glutamate and aspartate that accumulate in, and around the ischaemic zone (as a result of proteolysis, increased neuronal release and leaking of these aminoacids, impaired glial and neuronal uptake or cell lysis) open cation permeable, NMDA receptor-gated channels which results in increased intracellular calcium concentrations with cell death as a consequence [1].

The NMDA receptor complex is a complicated molecular entity consisting of a recognition site, a cationic channel highly permeable to calcium [5] and modulatory (stimulatory) glycine [6] and polyamine [7] sites whose activation facilitate NMDA mediated transmission. The opening of the NMDA receptor-gated channel is strictly controlled by magnesium ions whose blockade can be relieved by depolarization of the neurones [8]. The understanding of the pathological importance of the NMDA receptor complex has prompted the search for antagonists, a search that has been pursued over the last decade [9] and has led to the identification of a number of compounds that act at the various sites in the NMDA receptor complex. Phosphonate analogues of carboxylic acids (e.g. CGS 19755) [10] are potent competitive antagonists at the NMDA recognition site, whereas the dissociative anaesthetic agents, phencyclidine and ketamine, as well as TCP and MK-801 are use-dependent blockers of the NMDA associated cationic channel [11]. Glycine antagonists e.g. kynurenate, 7-chlorokynurenate [12], 1-aminocyclobutane-1 carboxylate [13] or indole 2-carboxylic acid [14] have also been identified.

Evidence has recently been provided that the phenylethanolamines, ifenprodil and SL 82.0715, antagonize the effects of NMDA via a blockade of the polyamine-sensitive regulatory site located in the NMDA receptor complex [7]. This aspect is discussed extensively in our companion paper (Carter *et al.*, this meeting). Here, we review the existing evidence that ifenprodil and SL 82.0715 are potent neuroprotective agents in experimental paradigms of focal cerebral ischaemia (induced by occlusion of the middle cerebral artery) in the rat, cat and mouse. For purposes of comparison, the tissue sparing effects of reference NMDA antagonists on infarction size have also been evaluated in parallel. In this study, the extent of infarction was assessed either histologically or by measuring the increase in the density of ω_3 (peripheral type benzodiazepine binding) sites, a reflection of the glial reaction and macrophage invasion of the ischaemic brain tissue [15].

Materials and Methods

Experiments were performed on male Fischer 344 rats, adult male and female cats (1.8–2.5 kg) and male Swiss mice (18–22 g).

Focal cerebral ischaemia in the rat

Anaesthesia was induced with 4% halothane in O_2 and maintained with 1.5% halothane in O_2 via a face mask. The left middle cerebral artery was thermocoagulated proximal to the origin of the lenticulostriate arteries by the technique of

Tamura *et al.* [16] as modified by Duverger and macKenzie [17]. SL 82.0715-HCl was administered p.o. 30 min, 18, 24 and 46 h after the middle cerebral artery occlusion (MCAO). TCP was injected i.p. 30 min before the occlusion. Control rats received the vehicle (saline solution) alone. Two days after the surgical intervention, the rats were again anaesthetized with 2% halothane and perfused with heparinized saline and a fixative (40% formaldehyde-glacial acetic acid-absolute methanol 1:1:8) over a period of 8 min. The animals were decapitated, the brains removed, postfixed in paraffin and coronal sections (15 μm thick) were cut throughout the rostrocaudal extent of the brain. The sections were then stained, by a method combining haemalun and phloxine B. The infarcted surface was measured by planimetry at different coronal levels as described previously [18]. The total volume of infarction was determined by the integration of the surfaces of the 10 chosen sections and the distances between them.

Focal cerebral ischaemia in the cat

Anaesthesia was induced with a mixture of 3.5% halothane in air. After the placement of an endotracheal cannula, muscular relaxation was achieved by the administration of gallamine (5 mg/kg i.v.). The cats were then placed on positive pressure ventilation and anesthesia was maintained with a mixture of N_2O-O_2 (3:1). The middle cerebral artery was occluded with a silver Cushing clip using the retro-orbital approach of Sundt and Waltz [19].

Five min after MCAO, an i.v. perfusion of ifenprodil, SL 82.0715 or vehicle was started and continued over the subsequent 3 hr. At the end of the infusion, the cats were ventilated with air until recovery of spontaneous respiration. Four days after the occlusion, the cats were anaesthetized with pentobarbital (37.5 mg/kg i.v.) and the brain was fixed *in vivo* by the intracarotid perfusion of 10% formalin. The brain was removed, and postfixed in paraffin. Brain sections were taken and stained with haemalun and eosin. The infarcted volume was measured as described above for the rat.

Focal ischaemia in the mouse

Mice were anaesthetized with chloral hydrate (500 mg/kg i.p.). The middle cerebral artery was then coagulated by bipolar diathermy according to Gotti *et al.* [20]. Sham-operated mice were subjected to a simple exposure of the middle cerebral artery. Drugs were injected i.p. 5 min, 6 h and 18 h following coagulation and then twice a day until sacrifice.

Four days following occlusion, mice were decapitated and the brains of those destined for autoradiography of ω_3 sites were frozen in isopentane (–45°C) and stored at –80°C until they were processed for sectioning and autoradiography with the specific ω_3 site ligand ^{3}H-PK 11195 as previously described [21]. Sections adjacent to those used for autoradiography were stained with haemalun and eosin. For conventional binding experiments in cortical membranes, the ipsilateral and

contralateral cortices were removed frozen on dry ice and stored at −80°C until assayed for ω_3 binding using ^{3}H-PK-11195 as a ligand [21].

Results

Focal ischaemia in the rat

SL 82.0715 (1 and 10 mg/kg p.o.) administered 30 min, 18, 24 and 46 h after the induction of ischaemia reduced the consolidated infarction volume (assessed histologically 2 days after the surgical intervention) by 34 and 48%, respectively (Table 1). This tissue-sparing effect was most pronounced in the centre and caudal extremity of the infarction volume (Fig. 1). In a group of rats pretreated with a single dose of TCP (1 mg/kg i.p.), a significant decrease (−27%) in infarction volume was also noted (Table 1). This decrease was distributed throughout the rostrocaudal extent of the infarction (Fig. 1) [18].

Focal ischaemia in the cat

Ifenprodil (1–3 mg/kg i.v.) administered as a perfusion over 3 h after occlusion of the feline middle cerebral artery reduced the volume of the infarcted tissue

Table 1. Effects of SL 82.0715, ifenprodil and reference NMDA antagonist on the volume of ischaemia-induced infarction after middle cerebral artery occlusion in the rat, cat and mouse

Species	Treatment	Dose (mg/kg)	Infarcted volume (mm^3)	Δ%
Rat	Vehicle		110.6 ± 8.8	
	SL 82.0715	1 (p.o.)	76.3 ± 5.8[a]	−34
	"	10 (p.o.)	63.0 ± 6.9[b]	−48
	Vehicle		95.6 ± 6.7	
	TCP	1 (i.p.)	70.2 ± 4.7[b]	−27
Cat	Vehicle		1895 ± 119	
	Ifenprodil	1 (i.v.)	1440 ± 149[a]	−24
	"	3 (i.v.)	1100 ± 132[b]	−42
	Vehicle		1848 ± 136	
	SL 82.0715	1 (i.v.)	1529 ± 206	−17
	"	3 (i.v.)	1184 ± 249[a]	−36
Mouse	Vehicle		27.9 ± 4.6	
	SL 82.0715	10 (i.p.)	10.4 ± 3.8[a]	−63

Results are means with S.E.M. of data obtained on 6–13 animals per group. [a]$p<0.05$, [b]$p<0.01$ vs respective controls (Duncan's test).

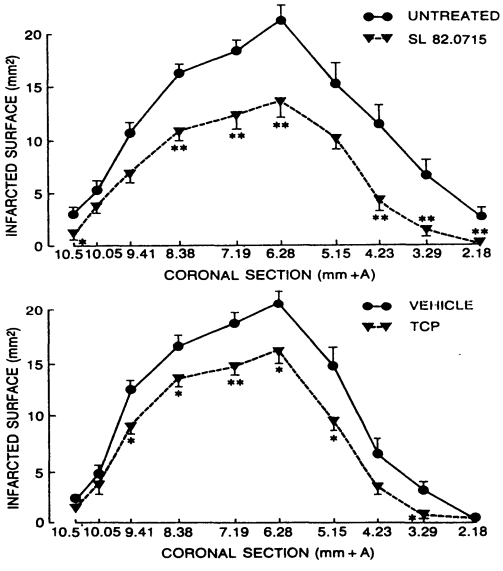

Fig. 1. Rostrocaudal extent of infarcted surface area (taken over 10 coronal sections) in groups of SL 82.0715- and TCP-treated rats compared to vehicle treated control groups. Results are means with S.E.M. of data obtained on 10 rats per group. *p<0.05; **p<0.01 vs relative controls (Duncan's test).

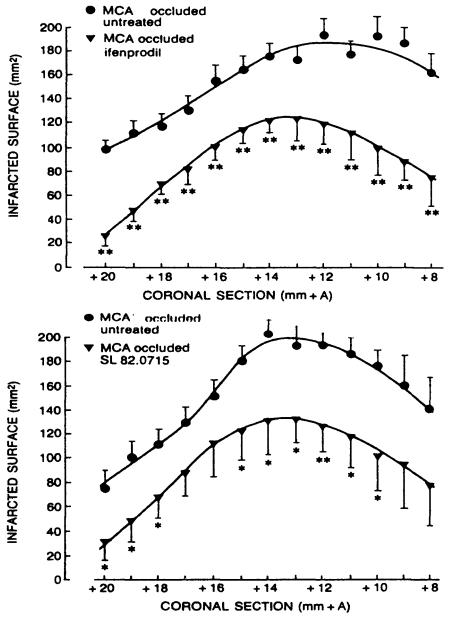

Fig. 2. Surface area of infarcted tissue at 18 coronal sections in SL 82.0715-treated, ifenprodil-treated and control cats. *P<0.05: **p<0.01 vs respective controls (Duncan's test). Results are means with S.E.M. of data obtained on the number of cats shown in parentheses. MCA, middle cerebral artery.

(assessed histologically 4 days after occlusion) in a dose-related manner (Table 1, Fig. 2). At the highest dose, a 42% reduction of infarcted volume was noted, essentially in cortical tissue. In an identical protocol, SL 82.0715 (3 mg/kg i.v.) reduced infarction size to approximately the same extent as that obtained with ifenprodil at the same doses (Table 1, Fig. 2). As with ifenprodil, the tissue-sparing effects of SL 82.0715 were the most pronounced in cortical, rather than striatal tissue [18].

Focal cerebral ischaemia in the mouse

The unavoidable sequelae of ischaemic insults are glial reaction and macrophage invasion secondary to the neuronal loss [22]. Fibrillary astrocytes and macrophages are richly endowed with ω_3 (peripheral type benzodiazepine) binding sites in comparison with healthy neuropil [23]. We have recently demonstrated that the

measurement of cortical ω_3 site densities provides an accurate and reliable index for the detection and quantification of ischaemic brain lesions following middle cerebral artery occlusion in the mouse [20]. Therefore, we have used this marker to assess the neuroprotective effects of SL 82.0715 and ifenprodil and for comparison of various NMDA receptor antagonists in this model of focal cerebral ischaemia [21].

The administration of SL 82.0715 (10 mg/kg i.p.) 5 min, 6 h and 18 h after the occlusion and then twice a day until sacrifice caused a diminution of the infarcted cortical surface at all coronal levels studied (Figs. 3,4). The infarcted volume (computed from the rostrocaudal integration of the infarcted surfaces) was reduced by 63% (Table 1). The reduction in the infarcted volume was paralleled by a decrease in ω_3 site densities. In sections adjacent to those used for stereometric reconstruction, the distribution of ω_3 sites faithfully reflected the tissue-sparing activity of SL 82.0715 (Fig. 3). Quantitative autoradiographic studies demonstrated that the percentage decreases in binding densities in the whole hemisphere (–68%) or in the cortex (–59%) were of the same magnitude as the reductions in the infarcted volume. In further experiments in which ω_3 site levels were measured in cortex homogenates from similarly occluded mice, the reduction in ω_3 site levels (–72%) elicited by SL 82.0715 (10 mg/kg i.p.) was again similar to that seen autoradiographically (in fmol/mg protein : control 304 ± 10; occlusion 556 ± 19; occlusion + SL 82.0715 376 ± 14*, *$p<0.05$ vs control). Ifenprodil was inactive when the standard administration schedule was employed (data not shown);

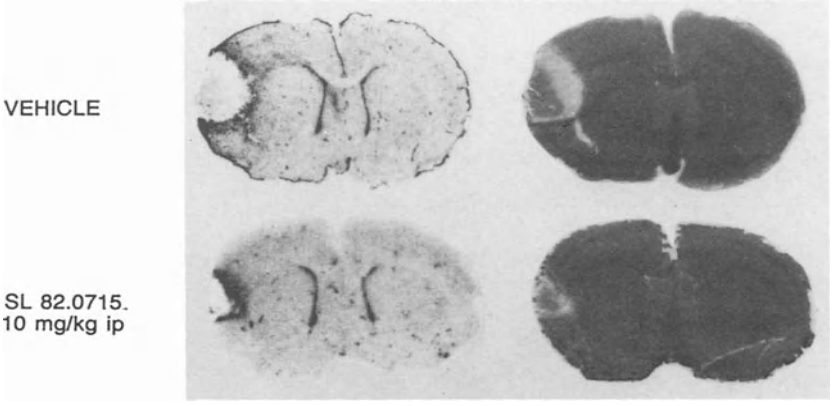

Fig. 3. Infarcted surface area (right) and increase in ω_3 site density (left) in vehicle and SL 82.0715-treated mice following middle cerebral artery occlusion.

For autoradiography, brain sections were incubated in the presence of 1 nM ^{3}H-PK 11195 and apposed to tritium-sensitive film. The adjacent, frozen sections were post-fixed and stained with haemalun and eosin. Note that the increase in ω_3 sites is mainly concentrated in the border of the infarction.

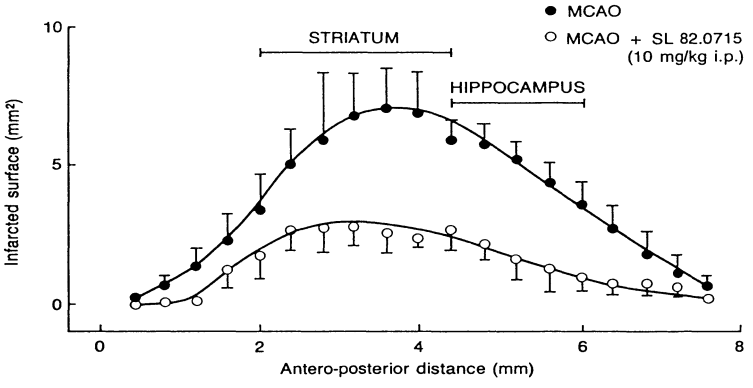

Fig. 4. Rostrocaudal extent of infarcted surface area (taken over 20 coronal sections) in groups of SL 82.0715- and vehicle-treated mice following middle cerebral artery occlusion. The surface of the ischaemic lesion was measured in haemalun and eosin stained serial sections. Symbols represent the mean ± S.E.M. of data obtained on 5 mice per group.

however, when the initial frequency of administration was increased (injection every 90 min for the first 6 h, then injected at 12 h, followed by the standard protocol), a significant protective effect (−58%) was observed at 10 mg/kg i.p. (Table 2).

The constant tissue sparing effect of SL 82.0715 allowed the examination of the window of therapeutic opportunity (the maximal delay between occlusion and treatment which would give a meaningful reduction in infarct volume). A significant diminution (−24%) of cortical homogenate ω_3 site density was still noted when the first administration of SL 82.0715 (10 mg/kg i.p.) was delayed until 3 h post-occlusion (in fmol/mg tissue: sham 14.9 ± 0.5; occlusion 24.6 ± 0.7; occlusion + SL 82.0715 21.6 ± 0.6*, *$p<0.05$ vs occlusion alone). Moreover, the protective

Table 2. Relative potency of NMDA receptor antagonists at preventing the ischaemia-induced augmentation of cortical ω_3 site densities in the mouse

Drug	ED_{50} (mg/kg i.p.)	Maximal protection (%)
MK-801	0.2	93
SL 82.0715	1.1	72
TCP	1.6	56
Ifenprodil	7	58
CGS 19755	≈ 10	46
Dextromethorphan	≈ 30	46
Kynurenate	260	58

Drugs were administered i.p. 5 min, 6 h, 18 h after middle cerebral artery occlusion and then twice a day until sacrifice (4 days post-occlusion). Relative increases in ω_3 sites were calculated in comparison to non occluded mice. ED_{50} = dose preventing by 50% the increase in ω_3 site levels.

effect of SL 82.0715 was enhanced by repeated treatment for the first 36 h but not thereafter (not shown).

Based on the histological, autoradiographic and homogenate binding results obtained with SL 82.0715 we studied the neuroprotective effects of several competitive and non-competitive NMDA receptor antagonists. When administered according to the standard protocol, these drugs reduced ω_3 site levels in cortical homogenates from middle cerebral artery occluded mice, with the following rank order of potency; MK-801>SL 82.0715>TCP>CGS 19755>dextromethorphan>-kynurenate (Table 2).

Discussion

Experimental models of focal cerebral ischaemia manifesting a temporary or permanent ligature of a major cerebral artery resemble the clinical situation of stroke after an embolic or thrombotic occlusion. The present study demonstrates that SL 82.0715 and ifenprodil substantially reduce infarction size (by 36 to 72%) in feline, rat and murine brain when administered *after* MCAO. SL 82.0715 was active in this model in the rat, when given post-occlusion by the *oral* route. The overall consistency of these results between animal models of stroke strongly suggest that SL 82.0715 and ifenprodil are of potential value in the treatment of ischaemic cerebrovascular diseases.

While SL 82.0715 and ifenprodil displayed a similar neuroprotective activity in cats subjected to focal cerebral ischaemia, SL 82.0715 was more potent than ifenprodil in the mouse model of MCAO. This differential potency probably relates to the rapid metabolism of ifenprodil in rodents [18], also explaining the high initial frequency of administration of ifenprodil needed to demonstrate its cerebroprotective activity in mice.

Focal ischaemia in mice appears to result in progressive neuronal death as the first administration of SL 82.0715 can be delayed up to 3 h and still produce a detectable reduction in ω_3 site density. However, this critical period seems to be limited as if the first administration is delayed by more than 6 h, then no significant neuroprotection could be evidenced in this experimental model. These results indicate that there is a certain 'window of opportunity' for a successful therapeutic intervention in the few hours that follow the initial infarction. Whether this progressive neuronal death in focal ischaemia is aetiologically the same as the delayed neuronal death of global ischaemia [12,24] is a question that remains to be answered.

Studies with SL 82.0715 in MCAO mice suggest that the cytoprotective effects obtained with compound administrations during the first 36 h post occlusion cannot be markedly enhanced by subsequent administration of the compound. This observation, together with the above mentioned 'therapeutic window' suggest that there is both a minimal time lapse to initiation of therapy and a maximum treatment period for optimal reduction in infarction volume after stroke.

The pivotal role played by excitatory amino acid neurotransmitters in the neuronal death induced by a variety of neuropathological states is supported by a growing body of experimental evidence (see ref. 4 for review). The potent neuroprotective effects of ifenprodil, SL 82.0715 and other NMDA receptor antagonists (irrespective of their site of action within the NMDA receptor complex) in focal ischaemia in rats, cats and mice adds to the accumulating evidence that NMDA receptors are involved in the pathogenesis of ischaemia-induced neuronal damage. The most potent and effective compound in the MCAO mouse model was the NMDA channel blocker MK-801 which afforded an almost complete protection (93%) at 1 mg/kg i.p., followed by SL 82.0715, TCP, ifenprodil, CGS 19755, dextromethorphan and kynurenate (Table 2). The fact that the efficacy of these compounds in focal ischaemia in the mouse correlates well with their potency as NMDA antagonists *in vivo* [25] strongly supports the causal relationship between NMDA receptor blockade and neuroprotection. Moreover, these results indicate that not only blockade of the NMDA-associated channel (by MK-801, TCP) but also blockade of the NMDA recognition site (by CGS 19755), the glycine site (by kynurenate) or the polyamine modulatory site (by SL 82.0715, ifenprodil) are effective means of cytoprotection. An obvious advantage of the latter three classes of compounds is that they lack the now recognized psychostimulant effects of the blockers of the NMDA receptor operated channel. Indeed, ifenprodil, SL 82.0715, CPP, CGS 19755 and kynurenate do not display noticeable behavioural stimulant effects in animals [26]. Moreover, ifenprodil and SL 82.0715 do not generalize to phencyclidine in rats [27] and are not psychotomimetic in man.

In conclusion, the present data indicate that SL 82.0715 and ifenprodil (which block NMDA mediated transmission by interacting with the polyamine regulatory sites located in the NMDA receptor complex) provide an effective neuroprotection in feline, rat and murine models of focal cerebral ischaemia. As these compounds are devoid of behavioural dissociative properties, they hold considerable promise for the prevention and treatment of cerebrovascular accidents.

References

1. Choi DW (1987) J. Neurosci. 7: 369–379.
2. Choi DW (1989) T.I.N.S. 11: 465–469.
3. Rothman SM and Olney JW (1986) Ann. Neurol. 19: 105–111.
4. Scatton B and Carter C (1989) Circ. Métab. Cerveau 6: 185–210.
5. Ascher P and Nowak L (1987) T.I.N.S. 10: 284–288.
6. Johnson JW and Ascher P (1987) Nature 325: 529–531.
7. Carter C, Rivy JP and Scatton B (1989) Eur. J. Pharmacol. 164: 611–612.
8. Nowak L, Bregestovski P, Ascher P, Herbet A and Prochiantz A (1984) Nature 307: 462–465.
9. Watkins JC and Olverman HJ (1987) T.I.N.S. 10: 265–272.
10. Murphy DE, Hutchison AJ, Hurt SD, Williams M and Sills MA (1988) Br. J. Pharmacol. 95: 932–938.
11. Kemp JA, Foster AC and Wong EHF (1987) T.I.N.S. 10: 294–298.

12. Kemp JA, Foster AC, Leeson PD, Priestley T, Tridgett R, Iversen LL and Woodruff GN (1988) Proc. Natl. Acad. Sci. USA 85: 6547–6550.
13. Hood WF, Sun ET, Compton RP and Monahan JB (1989) Eur. J. Pharmacol. 161: 281–282.
14. Huettner JE (1989) Science 243: 1611–1614.
15. Dubois A, Benavides J, Peny B, Duverger D, Fage D, Gotti B, Mackenzie ET and Scatton B (1988) Brain Res. 445: 77–90.
16. Tamura A, Graham DI, MacCulloch J and Teasdale GM (1981) J. Cereb. Blood Flow Metab. 1: 53–60.
17. Duverger D and MacKenzie ET (1988) J. Cereb. Blood Flow Metab. 8: 449–461.
18. Gotti B, Duverger D, Bertin J, Carter CJ, Dupont R, Frost J, Gaudilliere B, MacKenzie ET, Rousseau J, Scatton B and Wick A (1988) J. Pharmacol. Exp. Ther. 247: 1211–1221.
19. Sundt TM and Waltz AG (1966) Mayo Clin. Proc. 41: 159–168.
20. Gotti B, Benavides J, Dubois A, MacKenzie ET, Scatton B and Theraulaz M (1989) J. Cereb. Blood Flow Metab. 9: S258.
21. Benavides J, Dubois A, Duverger D, Gotti B, MacKenzie ET and Scatton B (1989) J. Cereb. Blood Flow Metab. 9: S140.
22. Dollman CL (1986) In: Davis, R.L. and Robertson, D.M. (eds.) Textbook of Neuropathology. Williams and Wilkins, pp. 117–137.
23. Benavides J, Gotti B, Dubois A, MacKenzie ET, Scatton B and Theraulaz M (1989) J. Cereb. Blood Flow Metab. 9: S748.
24. Petito CK, Feldmann E, Pulsinelli WA and Plum F (1987) Neurology 37: 1281–1286.
25. Carter C, Benavides J, Legendre P, Vincent JD, Noel F, Thuret F, Lloyd KG, Arbilla S, Zivkovic B, MacKenzie ET, Scatton B and Langer SZ (1988) J. Pharmacol. Exp. Ther. 247: 1222–1232.
26. Perrault G, Morel, E, Sanger DJ and Zivkovic. B (1989) Br. J. Pharmacol. 97, suppl.: 580P.
27. Jackson A and Sanger DJ (1988) Psychopharmacology 96: 87–92.

Address for correspondence: Bernard Scatton, Synthélabo Recherche (L.E.R.S.), Biology Department, 31 Avenue Paul Vaillant-Couturier, 92220 Bagneux, France.

Synthesis and neuroexcitatory activity of new kainoids

Kimiko Hashimoto and Haruhisa Shirahama

Department of Chemistry, Faculty of Science, Hokkaido University, Sapporo 060, Japan

Abstract

Stereoselective synthesis of a phenyl kainoid, (2S,3S,4S)-3-carboxymethyl-4-phenyl proline was achieved starting from a commercially available *trans*-4-hydroxy-L-proline. Oxidation of the protected 4-hydroxy proline with *t*-butyl hypochlorite afforded a 1-dehydro proline derivative which was subjected to double bond rearrangement to 2-dehydro-compound by the protection of the imino group with ethyl chloroformate. The bromoacetal of the 2-dehydro-4-hydroxyproline underwent radical cyclization reaction smoothly employing tributyltin hydride. The reaction was completely stereoselective and quantitatively to give a 3-(ß-oxoethyl)-4-hydroxy proline derivative whose configuration of C2 was arranged to 2S by treatment with a base and the glutamate skeleton was assembled in the proline ring. After adjustment of the functional groups, above obtained proline derivative was treated with lithium diphenyl cuprate to yield stereoselectively (2S,3S,4S)-3-hydroxyethyl-4-phenyl proline derivative which was converted to the phenyl kainoid. This synthetic method is undoubtedly applicable to prepare various kainoids. Neuroexcitatory activity of the newly obtained aromatic kainoid (3-carboxymethyl proline with an aromatic substituent at C4) in the isolated rat spinal cord was listed. Pyridonyl and methoxyphenyl kainoids were most potent, and phenyl and pyridyl kainoids were as active as kainic acid itself. Pyridine oxide as a substituent reduced activity. The conformation of pyrrolidine rings and γ-carboxyl groups of various aromatic kainoids were also discussed.

Introduction

Naturally occurring kainoids (Fig. 1), such as kainic acid **1**, domoic acid **2**, acromelic acids A **9**, and B **10**, cause a marked depolarization of the mammalian central nervous systems and the invertebrate muscle fiber. Because of their powerful excitatory activity and neurotoxicity, these compounds have been used as useful tools in the field of neuroscience research [1]. Among these kainoids, acromelic acids A and B, the toxic principles of the poisonous mushroom, exhibit the most potent activity in the rat spinal cord *in vitro*, and a demand for supply of these acids to laboratories is rapidly increasing [2,3]. However supply from nature is difficult owing to the rare occurrence of the mushroom and its difficult cultivation. Chemical syntheses of the acids were already achieved by us [4] and other two groups [5,6], but ours was for the structural determination and others also were not satisfactory for the preparation of rather large quantities. We planned therefore the development of the new synthetic method. The new method should be useful for supply of the excitatory reagents and convenient for the preparation of sorts of kainoids (3-carboxymethylproline with various substituents at C4). Neuroexcitatory activity of the kainoid was previously demonstrated to depend on the

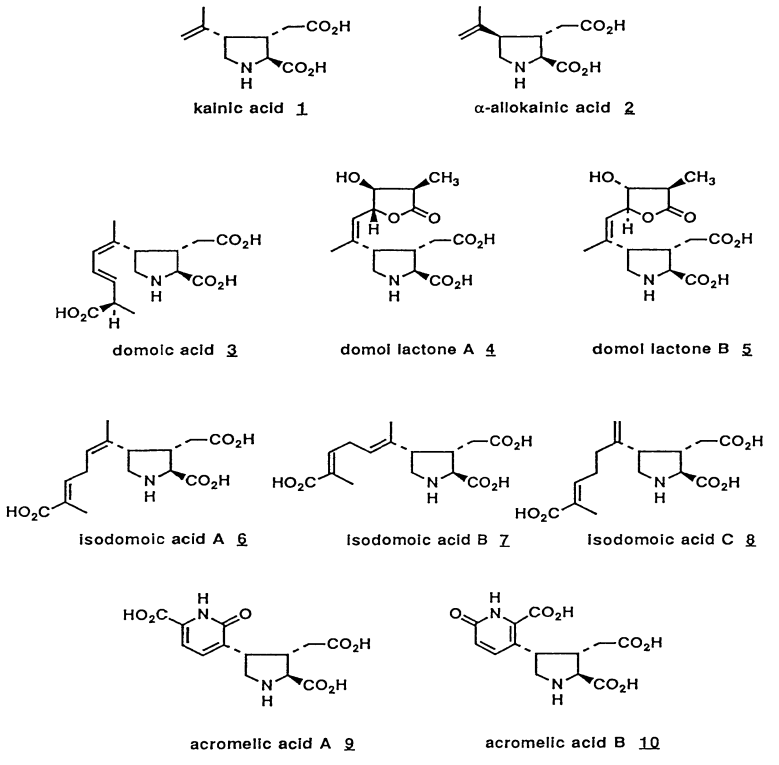

Fig. 1. Naturally occurring kainoids.

nature of the substituents at C4 [7–10]. For this purpose the most rational synthesis was probably simple introduction of various substituents at C4 of 3-carboxymethylproline. Furthermore, the synthesis should be stereoselective since the configuration of substituents on the proline nucleus of kainoids was undoubtedly

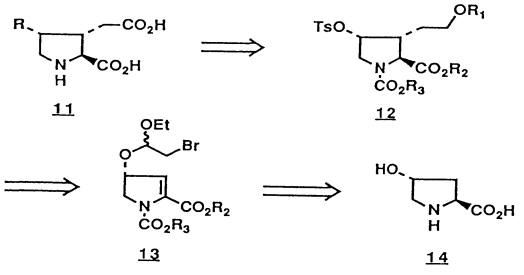

Fig. 2. Retrosynthesis of kainoids.

important for activity. *trans*-4-Tosyloxyproline was known to undergo stereoselective substitution reaction by means of a lithium diphenyl cuprate to give rise to *trans*-4-phenylproline with retention of the configuration at C4 [11]. Stereoselective introduction of a carboxymethyl group at C3 was probably possible using 4-hydroxy group as a handhold through a 2-dehydro-compound. We chose *trans*-4-hydroxy-L-proline as a starting material which was commercially available (Fig. 2). The reaction was successfully achieved and a phenyl kainoid was obtained. We would also like to discuss neuroexcitatory activity of new kainoids.

Experimental procedures

Synthesis of a new member of kainoid

The imino, carboxyl and hydroxyl groups of *trans*-4-hydroxy-L-proline **14** were successively protected to afford **15** ((1) 2-(*t*-butoxycarbonyloxyimino)-2-phenylacetonitrile (BocON) (2) benzyl chloride (3) *t*-butyldimethylsilyl chloride (TBDMSCl)) (Fig. 3). Treatment of **15** with trifluoroacetic acid (TFA) in dichloromethane gave N-deprotected compound, which was then allowed to react with *t*-butyl hypochlorite followed by dehydrochlorination with triethyl amine to give pyrroline derivative **16** [12,13]. Reprotection of imino group and simultaneous double bond isomerization occurred when **17** was made to react with ethyl chloroformate using pyridine as a base. Under the neutral condition desilylation of **17** with tetrabutyl ammonium fluoride (TBAF) in THF gave alcohol which was converted to α-bromoacetal by Stork's method, that is, alcohol was made to react with 1,2-dibromoethyl ethyl ether and N,N-dimethylaniline as a base to give **18** [14]. Radical cyclization reaction smoothly proceeded by the use of tributyltin hydride in the existence of 2,2'-azobisisobutyronitrile (AIBN) in refluxing benzene to give five-membered ring products **19** in quantitative yield. The cyclized products **19**, which were mixtures of stereoisomers of C2 and acetal carbon, were exposed to isomerization reaction by 1,8-diazabicyclo(5.4.0)undec-7-ene (DBU) in toluene to afford desired configurational isomer at C2. Jones' oxidation of lactol yielded lactone **20**. In the existence of ester, lactone was reduced to alcohol with sodium borohydride, and then the resulting primary alcohol was protected as a silyl ether and the secondary one was tosylated. Tosylate **21** was exposed to hydrogenolysis to remove benzyl ester under the neutral condition followed by desilylation with TBAF to afford key intermediate **23**. Tosylate **23** was allowed to react with lithium diphenylcuprate at room temperature in diethyl ether and THF to yield the desired compound as a single product, which was isolated as a methyl ester **24**. Alcohol **24** was converted to amino acid as a following sequence of reactions. (1) Oxidation of alcohol to carboxylic acid with pyridinium dichromate (PDC) in dimethylformamide (DMF) (2) esterification followed by hydrolysis of esters and carbamate (Fig. 3).

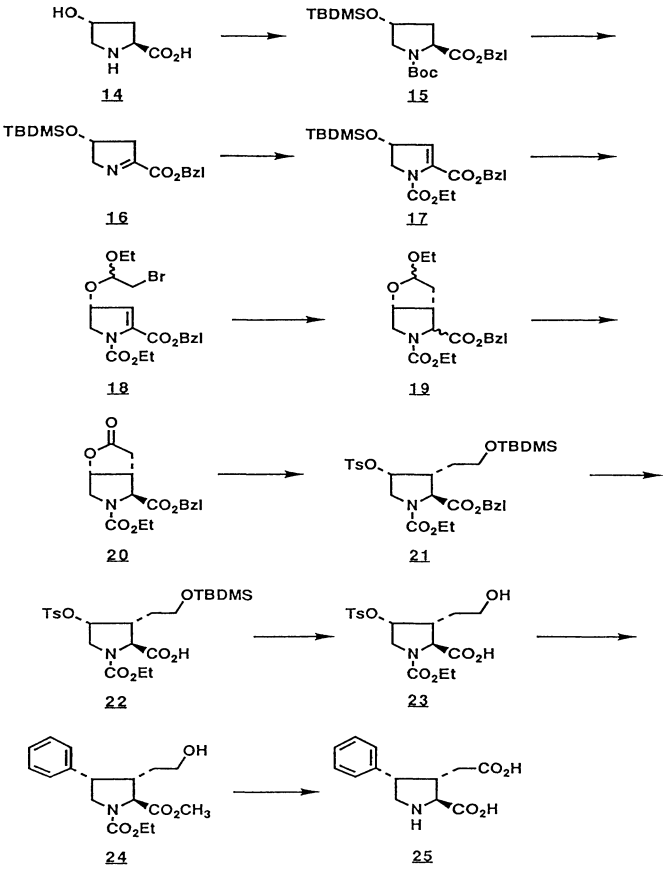

Fig. 3. Synthetic scheme of new kainoid.

Neuroexcitatory activity

Synthetic compounds were applied to electrophysiological experiment in the isolated newborn rat spinal cord in the same method as described in reference 2.

Results and Discussion

For the synthesis of basic skeleton, (2S,3R,4R)-3-carboxymethyl-4-hydroxyproline, introduction of a carboxymethyl group was achieved through intramolecular radical cyclization of (4R)-2-dehydro-4-hydroxyproline bromoacetal derivative (**18** to **19**). A double bond in a proline nucleus was introduced by *t*-butyl hypochlorite induced dehydrogenation of the C-N bond of proline derivative (**15**)

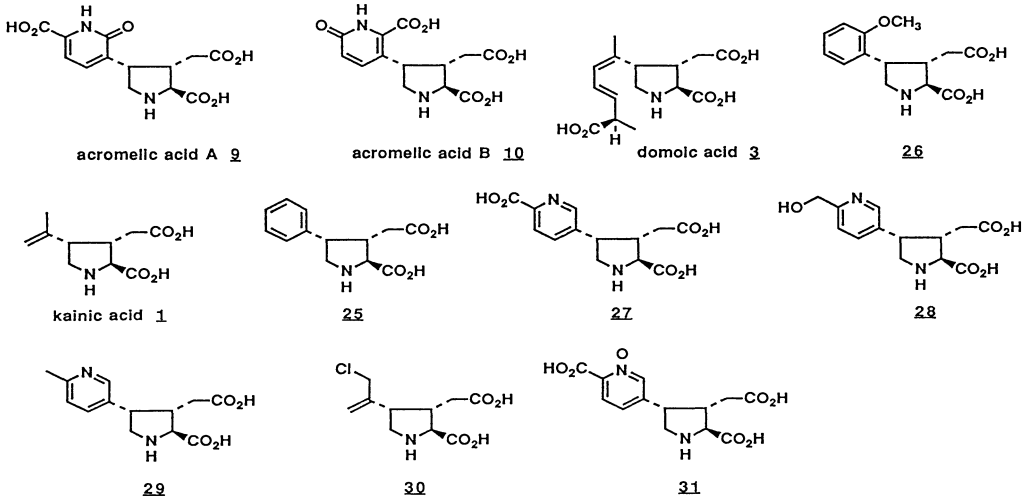

Fig. 4. Structure and neuroexcitatory activity in the rat spinal cord.

The C-N double bond of the proline was replaced to next C-C bond when the imino group was protected as an ethyl carbamate by treatment with ethyl chloroformate. The radical cyclization reaction, a new bond formation between the carbon bearing bromine atom of the acetal and the C3 carbon of the proline ring, was smoothly accomplished by treatment with tributyltinhydride in the presence of 2,2'-azobis-isobutyronitrile (AIBN). The reaction was completely stereoselective and the desired 3,4-*cis*-substituted pyrrolidine was singly and quantitatively obtained. The key reaction, substitution with lithium diphenylcuprate a C4 of (2S,3R,4R)-N-ethoxycarbonyl-3-hydroxyethyl-4-tosyloxyproline **23**, was successfully carried out with perfect retention of configuration. Starting from a commercially available *trans*-4-hydroxy-L-proline, two necessary substituents at C3 and C4 were beautifully assembled with splendid stereoselectivity. The present synthesis should be applicable to synthesize other kainoids with various substituents at C4 of proline ring.

On the newly synthesized phenyl kainoids, neuroexcitatory activity in the isolated rat spinal cord was estimated. Results were summarized in Fig. 4. The phenyl and pyridyl kainoids (**25**, **27**, **28** and **29**) were as active as kainic acid itself and pyridonyl, dienyl and methoxyphenyl kainoids (**9**, **10**, **3** and **26**) were most active. The potentiation was probably due to π-system on C4 of kainoid and the higher density of π-electron was accountable for the higher activity. The low activity of chloropropenyl and pyridine oxide kainoids (**30** and **31**) was presumably responsible to low density of π-electron caused by the electronegative substituents

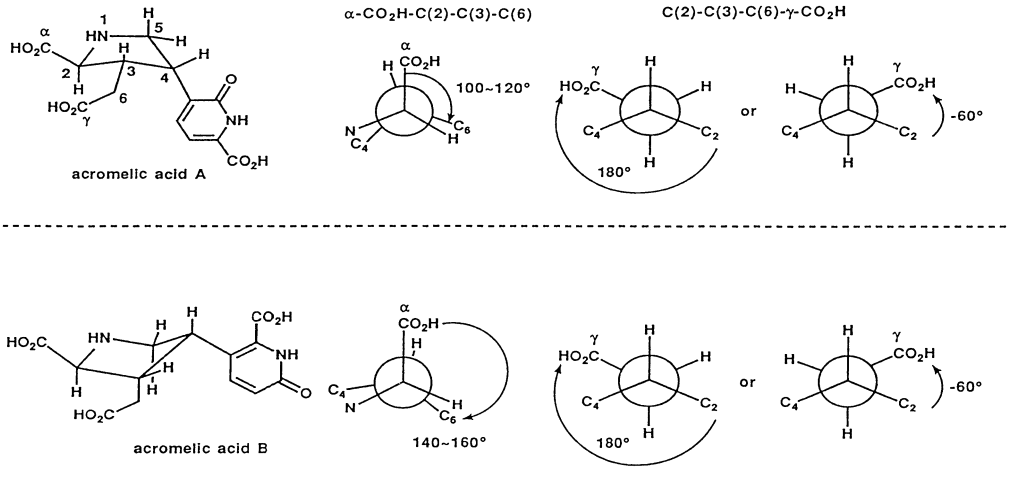

Fig. 5. Conformation of acromelic acids A and B.

on the isopropenyl and the pyridine groups. The X-ray crystallographic analysis of kainic acid **1** [15] and the ^{1}HNMR studies of kainic acid, domoic acid and acromelic acids A and B showed that the π-systems on C4 were perpendicular to the proline ring. The direction of the plane of π-system against pyrrolidine ring might be important. Accounting for the coupling constants among vicinal protons around the pyrrolidine ring, the conformation of the pyrrolidine seemed to be grouping two types, kainic acid and acromelic acid B group and domoic acid and acromelic acid A group. Newly synthesized kainoids, phenyl, methoxyphenyl, and pyridyl derivatives were in between. The conformation of the glutamate moiety of the various kainoids was evidently so important that many experiments for the study on the conformation-activity relationship about glutamate were performed. The ^{1}HNMR spectra revealed that all the kainoids depicted in Fig. 5 probably kept a fixed conformation because the methylene protons next to γ-carboxyl group showed AB type signals. The coupling constants showed that the dihedral angle of α-CO_2H-C(2)-C(3)-C(4) was 100≈120° (for acromelic acid A type) or 140≈160° (for acromelic acid B type) and that of C(2)-C(3)-C(4)-γ-CO_2H was 180 or −60° (Fig. 5). The pyrrolidine ring and the C4 substituents of kainoids clearly played a roll to fix the glutamate conformation so as to bind properly to the glutamate receptor. These studies on the structure-activity relationships should hold promise for designing novel kainic acid congeners which may exhibit characteristic neuroactivity.

Acknowledgement

We are very grateful to Drs. H. Shinozaki and M. Ishida (Tokyo Metropolitan Institute for Medical Science) for the estimation of neuroexcitatory activity and valuable discussion.

Added in proof

Neuroexcitatory activity of the methoxy phenyl kainoid **26** was found several times more potent than acromelic acid A (**9**), after all. So, the results summarized in Fig. 4 should be revised as follows:

26>9>10=3>1=25=27=28=29>30>>31.

Classification of the confirmation of **26** was found to be corrected in consequence of detailed NMR analysis. The class of **26** should be the acromelic acid A class.

References

1. Shinozaki H (1988) Prog. Neurobiol. 30: 399–435 and references cited therein.
2. Ishida M and Shinozaki H (1988) Brain Res. 474: 386–389.
3. Shinozaki H, Ishida M and Okamoto T (1986) ibid. 399: 395–398.
4. Konno K, Hashimoto K, Ohfune Y, Shirahama H and Matsumoto T (1988) J. Am. Chem. Soc. 110: 4807–4815.
5. Baldwin JE and Li C-S (1988) J. Chem. Soc., Chem. Commun. 261–263.
6. Takano S, Iwabuchi Y and Ogasawara K (1987) J. Am. Chem. Soc. 109: 5523–5524.
7. Shirahama H, Konno K, Hashimoto K and Matsumoto T (1988) Neurotox '88: Molecular Basis of Drug and Pesticide Action, Chapter 9: 105–122.
8. Takeuchi H, Watanabe K, Nomoto K, Ohfune Y and Takemoto T (1984) Eur. J. Pharmacol. 102: 325–332.
9. Conway GA, Park JS, Maggiora L, Mertes MP, Galton N and Michaelis EK (1984) J. Med. Chem. 27: 52–56.
10. Goldberg O, Luini A and Teichberg VZ (1980) Tetrahedron Lett. 21: 2355–2358.
11. Thottathil JK and Moniot JL (1986) ibid 27: 151–154.
12. Hansler J (1981) Liebigs Ann. Chem. 1073–1088.
13. Hansler J and Schmidt U (1979) ibid: 1881–1889.
14. Stork G and Mook R Jr. (1983) J. Am. Chem. Soc. 105: 3720–3722.
15. Nitta I, Watase H and Tomiie Y (1958) Nature 181: 761–762.

Address for correspondence: Haruhisa Shirahama, Department of Chemistry, Faculty of Science, Hokkaido University, Sapporo 060, Japan.

Immunocytochemical localization of glutamate, GABA and glycine in the human retina

Svend Davanger, Ole P. Ottersen and Jon Storm-Mathisen
Anatomical Institute, University of Oslo, Karl Johansgt. 47, N-0162 Oslo 1, Norway

Abstract

The amino acids glutamate, GABA and glycine, putative neurotransmitters in the mammalian retina, were localized immunocytochemically in the human eye. The posterior two thirds of an eye were immersion-fixed in a mixture of glutaraldehyde and paraformaldehyde in sodium phosphate buffer. Semithin sections of the retina were obtained after osmication, dehydration and embedding in an epoxy resin. Strong glutamate-like immunoreactivity (PAP method) was observed in ganglion cells and processes including axons in the nerve fiber layer, in the perikaryal cytoplasm and processes of many bipolar cells, and in round structures probably representing rod spherules in the inner plexiform layer. Numerous structures in the inner and outer plexiform layers were moderately labeled, as were photoreceptor inner segments and perikaryal cytoplasm (rods stronger than cones), and some bipolar and amacrine cells. Glutamate immunoreactivity could not be detected in Müller cells. Strong GABA-like immunoreactivity appeared in many amacrine cells, varicosities in the inner plexiform layer and small cells in the ganglion cell layer, and a few cells resembling ganglion cells. Strong glycine-like immunoreactivity was seen in varicosities in the inner plexiform layer, and moderate to strong immunoreactivity in populations of both amacrine and bipolar cells. Glycine immunostaining was occasionally seen in small cells of the ganglion cell layer.

Introduction

The retina is an extension of the CNS, and contains most, if not all, putative neurotransmitters found elsewhere in the brain, including the neuroactive amino acids. The retina has a unique, layered organization that facilitates identification of neuronal structures. Unlike other parts of the human CNS, the retina can be obtained intact at surgery for immediate fixation.

An excitatory amino acid appears to be the transmitter of both photoreceptors and bipolar cells, thus providing the 'straight-through' pathway for sensory information in the retina, ending on the ganglion cells. Thus glutamate has been regarded as the main transmitter candidate in photoreceptors (review: [1–3]). It is also proposed as neurotransmitter in some bipolar cells [4] and in some amacrine [4,5] and ganglion cells [3,4,6]. However, until now little evidence directly demonstrating the presence of glutamate in these cells has been provided (but see [7]).

Inhibitory amino acids, on the other hand, seem to be more involved in restricting the stimuli (i.e. directional selectivity, or red/green contrast) to which ganglion cells respond [3]. Substantial evidence supports γ-amino butyric acid (GABA) as transmitter of several classes of amacrine cells in vertebrates [1].

Likewise, glycine is a strong transmitter candidate of other classes of mammalian amacrine cells. Glycine is also accumulated to various extents in bipolar, horizontal and interplexiform cells, and GABA has been reported to be present in horizontal cells and interplexiform cells of several species. Both GABA [8–17] and glycine [18–22] have been localized in retinal cells by immunocytochemical methods.

Most of these investigations, however, focused on either glutamate, GABA or glycine separately. The present study aims to provide more insight into the comparative distribution of these amino acids in the human retina. To this end we have applied antisera raised against glutaraldehyde-fixed glutamate, GABA or glycine to consecutive semithin sections of the human retina.

Experimental procedures

Anti-glutamate (no. 13), anti-GABA (no. 25) and anti-glycine (no. 31) sera were obtained, purified, tested and used as described previously [23–28]. Briefly, rabbits were immunized against glutamate, GABA or glycine by repeated injections with the amino acid conjugated to protein by glutaraldehyde (mixed with adjuvant). Crude immune sera were purified by adsorption to carrier protein that, after being conjugated to agarose beads, had been reacted with glutaraldehyde, alone or in the presence of an amino acid other than that used for immunization.

The human (male, age 39) retina was obtained from the posterior two thirds of an eye removed for malignant melanoma (the pathological process was located in corpus ciliare and did not affect the areas of the retina investigated). The tissue was fixed in a freshly prepared mixture of 2.5% glutaraldehyde and 1.0% (para)formaldehyde in 0.1 M sodium phosphate buffer (pH 7.4, room temperature), within two minutes after the interruption of blood supply. (During the two minutes, the eye was excised, immersed in the fixative and cut open.)

Parts of the retina were osmicated, dehydrated and embedded in Durcupan (ACM, Fluka) as described before [29]. Semithin (0.5 μm) sections were mounted on gelatinized slides and processed with antiserum (anti-glutamate 1:1000, anti-GABA 1:150 or anti-glycine 1:100) before immunoreactivity was visualized by the PAP method, essentially as described by [30]. To eliminate possible unspecific staining, fixation complexes of glutaraldehyde (G) and an amino acid were added to the diluted antisera 18 h before incubation (the anti-glutamate serum was made to contain 100 μm aspartate-G, the anti-GABA serum 300 μm glutamate-G and the anti-glycine serum 300 μm ß-alanine-G). Additional control for staining specificity was provided by incubating semithin test sections (containing 6 different amino acids fixed by glutaraldehyde to rat brain macromolecules [29], together with the retinal sections (see insets in Fig. 2); and by adding fixation complexes (of glutaraldehyde and the amino acid against which the serum was raised) to the antiserum before incubation.

Results

Glutamate

All layers of the retina contained cell structures that were immunoreactive for glutamate (Figs. 1A and 2A). Virtually all ganglion cells (perikarya and dendrites), along with axons in the nerve fiber layer, were heavily stained. Staining of the same intensity was seen in perikaryal cytoplasm and processes of many bipolar cells, and, particularly, in what appeared to be rod terminal spherules in the outer plexiform layer. The inner plexiform layer also contained strongly immunoreactive varicosities. In the perifoveal region, occasional cells (similar to ganglion cells in size, shape and immunostaining characteristics) located within the inner plexiform layer were immunopositive. Moderate immunoreactivity appeared in photoreceptor inner segments (rods more strongly stained than cones) and perikarya, in cone pedicles, in some bipolar cells and in many amacrine cells. However, in the perifoveal retina the immunoreactivity of rods approached that of ganglion cells (Fig. 1A). Most structures in the inner and outer plexiform layers were moderately labeled, apart from the strongly stained processes mentioned above. Müller cell processes close to the corpus vitreum and capillary endothelium displayed insignificant immunoreactivity, i.e., staining intensity similar to that found in sections incubated with the anti glutamate serum in the presence of glutamate-G. In all immunoreactive cells, the nuclei showed weaker staining than the cytoplasm. This difference in staining intensity seemed to be more pronounced in photoreceptors and bipolar cells than for amacrine and ganglion cells.

GABA

In contrast to glutamate immunoreactivity, that of GABA was not widely distributed along the radial extent of the retina (Figs. 1B and 2B). Strong (or moderate) staining was seen in many amacrine cells (roughly 25–60% of the amacrines, the percentage in the perifoveal regions being larger than in more peripheral parts). Most of the cells were located near the outer margin of the inner plexiform layer. Also, a subpopulation of cells in the ganglion cell layer, the majority, but not all, of which was located adjacent to the inner plexiform layer, was strongly immunoreactive. Judged by their size and location, most of them seemed to be displaced amacrine cells, but some could not be distinguished from ganglion cells on the basis of size and morphology (however they were less glutamate immunoreactive than the other cells in this location, see below). Rarely, cells of similar size and staining characteristics as amacrine cells were observed within the inner plexiform layer. This layer was densely packed with strongly GABA immunoreactive varicosities. Scattered immunopositive punctate structures were also present both in the outer plexiform layer, and in the nerve fiber layer. Staining of cytoplasm was stronger than staining of the nucleus in immunopositive cells.

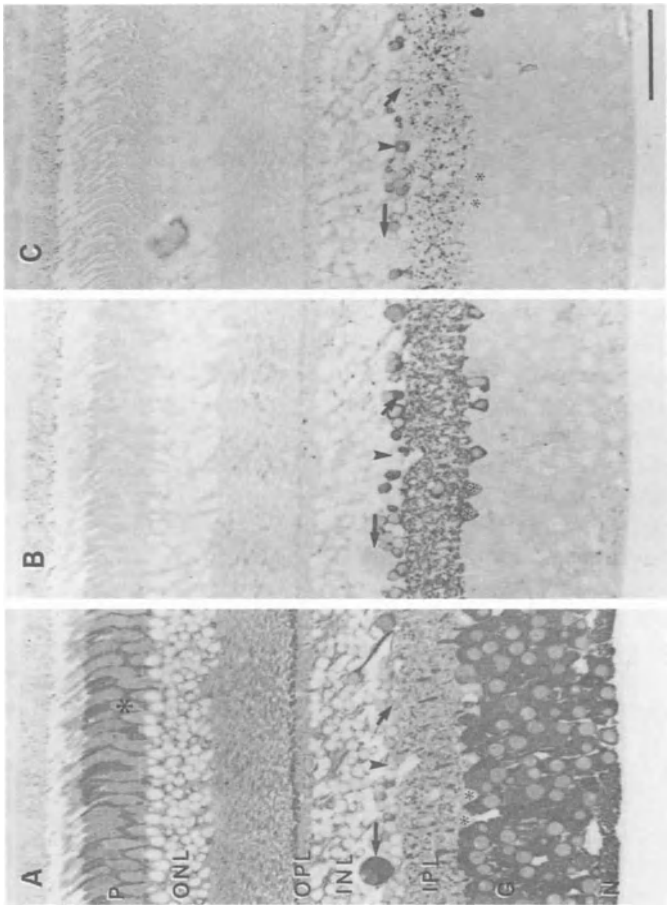

Fig. 1. Consecutive (0.5 μm) sections of human retina, perifoveal region. The sections show immunoreactivity for glutamate (A), GABA (B) and glycine (C), as visualized by the PAP method. P = photoreceptor layer, ONL = outer nuclear layer, OPL = outer plexiform layer, INL = inner nuclear layer, IPL = inner plexiform layer, G = ganglion cell layer, N = nerve fiber layer. Glutamate-like immunoreactivity (A) is strongly concentrated in ganglion cells, the nerve fiber layer, structures in the IPL, and in probable rod spherules of the OPL. Photoreceptor inner segments and perikarya, cone and rod perikarya, and some bipolar and amacrine cells show moderate staining intensity, though cone inner segments (large asterisk) somewhat less than rod inner segments. Large, displaced ganglion cell (long arrow) stained for glutamate does not show GABA- or glycine-immunoreactivity. B shows strong staining for GABA in many amacrine cells (near the outer margin of the IPL), in varicosities in the IPL, and in small cells of the ganglion cell layer. These cells, judged as displaced amacrines, were not stained for glutamate or glycine (small asterisks). Short arrow marks GABA-immunoreactive amacrine cell very weakly stained for glycine or glutamate. Moderate to intense glycine staining (C) is seen in some amacrine cells in the INL, and in varicosities in the IPL. Note glycine immunopositive amacrine cell (arrowhead), which is not stained for GABA and only weakly for glutamate. (Note that the dark punctate structures outside the photoreceptor layer belong to the pigment epithelium; they are not immunoreactive). Bar 50 μm.

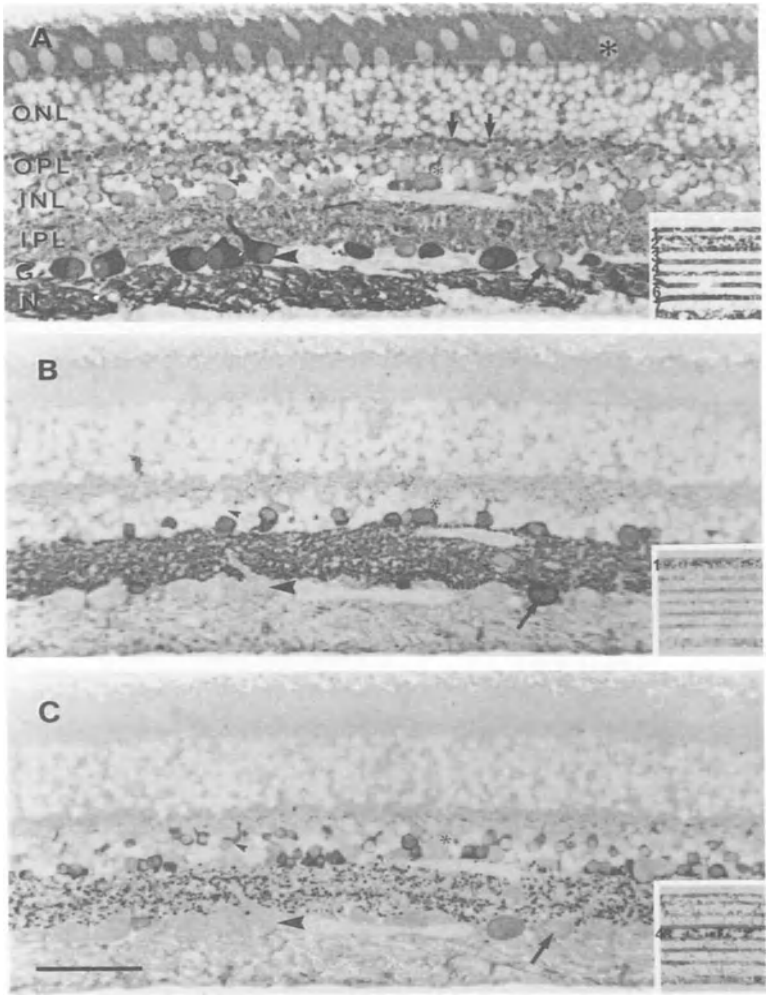

Fig. 2. Consecutive sections (0.5 μm) of human retina, peripheral region. Immunoreactive staining for glutamate (A), GABA (B) and glycine (C) is seen. Labeled structures correspond to staining shown in Fig. 1. Note though, that glycine-immunoreactive bipolar cells (small arrowhead) are seen (C). Rod spherules are also in this region strongly stained for glutamate (short arrows). Both rod and cone inner segments are moderately stained, but cones (large asterisk) clearly weaker than rods. Large arrowhead marks strongly glutamate-immunoreactive ganglion cell which is immunonegative for GABA and glycine. The same applies to bipolar cells strongly stained for glutamate (small asterisk). The ganglion cell layer contains a large cell (long arrow) that is heavily labeled by the anti-GABA serum, but it is only moderately (in A) or weakly (in C) stained for glutamate or glycine. Small arrowhead denotes a glycine immunoreactive bipolar cell without detectable labeling for GABA or glutamate. *Insets* show test sections incubated together with the retinal sections. Layers 1–7 are amino acids fixed by glutaraldehyde to rat brain macromolecules and embedded in resin, between layers of brain tissue (as spacers). 1 = GABA, 2 = glutamate, 3 = taurine, 4 = glycine, 5 = none (glutaraldehyde alone), 6 = aspartate, 7 = glutamine. Note selective staining of the respective amino acid conjugates. Bar = 50 μm.

Glycine

Moderate to heavy glycine-like immunoreactivity (Figs. 1C and 2C) appeared in a subpopulation of amacrine cells (about 30–45%, the higher percentage being found peripherally, i.e., the reverse of what was seen for GABA), located adjacent to the outer margin of the inner plexiform layer. Quite a few moderately to intensely stained bipolar cells were also seen, particularly in the peripheral region. The inner plexiform layer contained heavily labeled varicosities, though these were not as densely packed as in sections treated with the anti-GABA serum. A few cells in the ganglion cell layer were moderately to strongly stained. Also the anti-glycine serum produced more heavy labeling of the cytoplasm than of the nucleus.

Colocalization of immunoreactivities

Three separate areas of the retina (two from the perifoveal region, one from the peripheral region) were examined for colocalization of the amino acids in question. Each area extended for about 300 μm along the equator of the eye. The areas comprised 75 GABA immunoreactive and 78 glycine immunoreactive cells, in addition to the many glutamate immunoreactive cells.

Some of the cells stained for glutamate (a minority of the total) were also stained for GABA or glycine. The majority of cells stained for GABA or glycine also showed glutamate immunoreactivity (mostly moderate). A few cells were immunoreactive for both GABA and glycine. However, none of the cells seemed to be *strongly* stained by more than one antiserum. In the following we will present a few quantitative data on the extent of amino acid colocalization.

Of the strongly glutamate immunoreactive cells, only 1 (an amacrine cell) was stained for GABA; and only 3 (2 bipolar cells and 1 ganglion cell) were stained for glycine.

Of the cells strongly immunoreactive for GABA, 15 (amacrine cells) were stained for glutamate, and 3 (amacrines) were labeled by the anti glycine serum. One GABA-positive cell with the size and localization of a ganglion cell, was also labeled by the anti glutamate serum.

Of the cells strongly immunoreactive for glycine, 15 (9 amacrine and 6 bipolar cells) were stained for glutamate, while 4 cells (amacrines) were GABA immunoreactive. Of the latter cells, 1 also showed immunoreactivity for glutamate. This was the only cell that was immunoreactive for all three amino acids.

Discussion

The three different antisera employed have been purified and thoroughly tested earlier (see **Experimental procedures**). They have proved to be highly useful tools for neurochemical investigation of the CNS [27,31] including the retina [7,11,20].

To assure specific immunoreactivity in the present experiments, both positive and negative control procedures were implemented. The test sections incubated together with the retinal sections were significantly stained only in the layers containing glutamate-, GABA- and glycine-conjugates, respectively, whereas layers containing fixation products of other amino acids were not stained (see Fig. 2). On the other hand, absorption of the specific antibodies by glutaraldehyde treated glutamate, GABA or glycine, respectively, prevented staining of retina as well as of test sections (not shown).

For identifying glutamatergic neurons at the histological level, two different marker systems have traditionally been used: high-affinity uptake of glutamate, as demonstrated by L-[^{3}H]glutamate [5,32] or D-[^{3}H]aspartate [5,32,33] autoradiography, and high levels of the glutamate synthesizing enzymes, aspartate aminotransferase (L-aspartate: 2-oxoglutarate aminotransferase, AATase) [4,5,34] or glutaminase, as demonstrated immunocytochemically [35,36]. The activity of the uptake systems, and, particularly, the levels of the synthesizing enzymes bear an uncertain relation to the transmitter identity. Thus an enrichment of AATase may be related to high metabolic rate rather than to the synthesis of transmitter glutamate [37]. Glutamate immunocytochemistry, as used in the present report, permits a direct demonstration of glutamate, but the results obtained must be interpreted with caution since 'metabolic' glutamate is visualized along with transmitter glutamate. One previous report exists of immunocytochemical demonstration of endogenous glutamate in the turtle retina [7] showing a similar distribution of immunoreactivity as that presented here.

The presence of glutamate-like immunoreactivity in photoreceptors in our material is in accordance with the finding that both rods and cones accumulate glutamate in human retina [5]. However, we observed stronger staining of rods than of cones. Accordingly, others have reported that D-[^{3}H]aspartate [38] and L-[^{3}H]glutamate [39] label rods much more intensely than cones in human material. As for higher-order retinal neurons, we found many bipolar cells to be markedly labeled, and moderate labeling occurred in what seemed to be amacrine cells and some bipolar cells. Correspondingly, AATase immunoreactivity has been demonstrated in both amacrine and bipolar cells in man [5] as well as in monkey [4]. The identity of the retinal ganglion cell transmitter has been difficult to establish [6] but glutamate has been proposed as a likely candidate in some species [2]. For example, in the monkey, glutamate (and aspartate) are enriched in the innermost layer of the retina [40]. Further, D-[^{3}H]aspartate has been found to accumulate in about 5 to 10% of the ganglion cells of pigeon, guinea pig and rabbit [33]. The presence of AATase in retinal ganglion cells has been observed in monkey [4]. Evidence pertaining to this question has also been supplied by studies on the pigeon retino-tectal pathway: optic nerve stimulation markedly increased the content of glutamate (and aspartate) in perfusates from the optic tectum [41]; following intra-tectal or intra-vitreous injection of D-[^{3}H]aspartate, radioactivity migrated either retrogradely or anterogradely, respectively [42]; and, after retinal ablation, the concentration of glutamate (and aspartate) decreased in the superficial

part of the tectum which receives direct retinal input [43]. Our material shows strong glutamate-like immunoreactivity in a large majority of cells in the ganglion cell layer, as well as in fibers of the nerve fiber layer. This may suggest that human ganglion cells are glutamatergic; alternatively, the strong staining may simply reflect an enrichment of metabolic glutamate.

Some of the neurons stained for glycine or GABA in our preparations were also moderately immunoreactive for glutamate. The glutamate in these cells may probably represent a metabolic pool in neurons. Due to the multiple roles of glutamate in addition to that of a neurotransmitter (intermediary metabolite, protein synthesis), the presence of even a high perikaryal concentration of glutamate cannot be taken as proof that it functions as transmitter in the neurons in question. However, in axons and terminals the transmitter pool can be expected to be concentrated relative to the metabolic pool. Thus terminals of putative glutamatergic neurons in the cerebellum [29,44,45] and the hippocampus [44,45] have been shown to be more strongly glutamate immunoreactive (as judged by a quantitative immunogold procedure) than non-glutamatergic terminals. Our finding of high glutamate immunoreactivities in the rod spherules suggests that glutamate may play a transmitter role in these terminals. The high glutamate content in ganglion cell axons represents similar evidence.

The cellular localization of GABA in the retina has been investigated by autoradiographic demonstration of uptake sites for [^{3}H]GABA [46–48], uptake and binding sites for [^{3}H]muscimol [13,49,50] (this $GABA_A$-receptor ligand is also a substrate of a GABA uptake system), and by immunocytochemical demonstration of the synthesizing enzyme glutamic acid decarboxylase (GAD) [12,51–53]. Several authors have reported immunocytochemical localization of GABA in cells of the retina, but apparently only one group has utilized human material [11,12]. The present results show good correspondence with these studies on both GAD and GABA in human retina. Thus we find GABA-like immunoreactivity in cells of both the inner plexiform and the ganglion cell layers, as well as in the neuropil of the inner plexiform layer. Most of the cells seem to be amacrine or displaced amacrine (in the ganglion cell layer) cells. However, some GABA-immunoreactive cells in the ganglion cell layer could not be distinguished from ganglion cells by size and morphology. One cannot exclude the possibility that these, and a few scattered cells (not shown) of the same size and shape as amacrine cells located in the middle or inner part of the ganglion cell layer, are ganglion cells, and that the immunopositive punctate structures in the nerve fiber layer are crossectioned axons. GABA-immunoreactive ganglion cells have been reported in rabbit [14] and rat [54]. Contrary to Agardh, Ehinger and Wu [12] we did not see any GABA immunoreactive horizontal or bipolar-like cells, although the puncta in the outer plexiform layer stained for GABA may be terminals of such cells (alternatively, they may originate from interplexiform cells). Neither did our material show any GABA-immunoreactive structures with the location of photoreceptor terminals (outer half of the outer plexiform layer), as has been reported in monkey [9,55].

No enzyme marker exists for transmitter glycine, which until recently could only be demonstrated indirectly by autoradiography after [^{3}H]glycine uptake. The last few years, however, immunocytochemical procedures for demonstration of glycine have been applied to the retina of cat [18,19] larval tiger salamander [22] and monkey [21], but not in man.

We found immunoreactivity for glycine in a population of inner nuclear layer cells lying adjacent to the inner plexiform layer, resembling amacrine cells, in some bipolar cells, in varicosities of the inner plexiform layer, and in a small number of cells (moderately to strongly labeled) in the ganglion cell layer. The latter cells mostly appeared to be displaced amacrine cells, though a few were of a size and shape resembling ganglion cells. Corresponding findings were made by Hendrickson *et al.* [21]. In monkey retina, they found glycine-like immunoreactivity in amacrine cells, bipolar cells, structures of the inner plexiform layer and in cells of the ganglion cell layer.

References

1. Massey SC and Redburn DA (1987) Prog. Neurobiol. 28: 55–96.
2. Voaden MJ (1988) In: Kvamme E (ed.) Glutamine and Glutamate in Mammals. CRC Press, Boca Raton, Florida, Vol. II, pp. 71–88.
3. Daw NW, Brunken WJ and Parkinson D (1989) Ann. Rev. Neurosci. 12: 205–225.
4. Mosinger JL and Altschuler RA (1985) J. Comp. Neurol. 233: 255–268.
5. Brandon C and Lam DMK (1983) Proc. Natl. Acad. Sci. USA 80: 5117–5121.
6. Ehinger B (1982) In: Bradford HF (ed.) Neurotransmitter Interaction and Compartmentation. Plenum Press, New York and London, pp. 691–717.
7. Ehinger B, Ottersen OP, Storm-Mathisen J and Dowling JE (1988) Proc. Natl. Acad. Sci. USA 85: 8321–8325.
8. Hendrickson A, Ryan M, Noble B and Wu JY (1985) Brain Res. 348: 391–396.
9. Nishimura Y, Schwartz ML and Rakic P (1985) Brain Res. 359: 351–355.
10. Agardh E, Bruun A, Ehinger B and Storm-Mathisen J (1986) Invest. Ophtalmol. Vis. Sci. 27: 674–678.
11. Agardh E, Bruun A, Ehinger B, Ekström P, van Veen T and Wu JY (1987) J. Comp. Neurol. 258: 622–630.
12. Agardh E, Ehinger B and Wu JY (1987) Histochemistry 86: 485–490.
13. Ball AK (1987) J. Comp. Neurol. 255: 317–325.
14. Yu BCY, Watt CB, Lam DMK and Fry KR (1988) Brain Res. 439: 376–382.
15. Pourcho RG and Goebel DJ (1988) Brain Res. 447: 164–168.
16. Chun MH and Wässle H (1989) J. Comp. Neurol. 279: 55–67.
17. Wässle H and Chun MH (1989) J. Comp. Neurol. 279: 43–54.
18. Pourcho RG and Goebel DJ (1985) Brain Res. 348: 339–342.
19. Pourcho RG and Goebel DJ (1987) J. Neurosci. 7(4): 1189–1197.
20. Storm-Mathisen J, Ottersen OP and Davanger S (1986) Soc. Neurosci. Abstr. 12(2): 771.
21. Hendrickson AE, Koontz MA, Pourcho RG, Sarthy PV and Goebel DJ (1988) J. Comp. Neurol. 273: 473–487.
22. Yang CY and Yazulla S (1988) J. Comp. Neurol. 272: 343–357.
23. Storm-Mathisen J, Leknes AK, Bore A, Vaaland JL, Edminson P, Haug FMS and Ottersen OP (1983) Nature 301: 517–520.
24. Dale N, Ottersen OP, Roberts A and Storm-Mathisen J (1986) Nature 324: 255–257.

25. Ottersen OP, Storm-Mathisen J, Madsen S, Skumlien S and Strømhaug, J (1986) Med. Biol. 64: 147–158.
26. Storm-Mathisen J and Ottersen OP (1986) In: Panula P, Päivärinta H and Soinila S (eds.) Neurochemistry: Modern Methods and Applications. Alan R Liss, New York, pp. 107–136.
27. Ottersen OP and Storm-Mathisen J (1987) Trends Neurosci. 10: 250–255.
28. Ottersen OP, Davanger S and Storm-Mathisen J (1987) Exp. Brain Res. 66: 211–221.
29. Ottersen OP (1987) Exp. Brain Res. 69: 167–174.
30. Somogyi P, Hodgson AJ, Smith AD, Nunzi MG, Gorio A and Wu JY (1984) J. Neurosci. 4: 2590–2603.
31. Ottersen OP (1989a) Anat. Embryol. 180: 1–15.
32. Taxt T and Storm-Mathisen J (1984) Neuroscience 11: 79–100.
33. Ehinger B (1981) Exp. Eye Res. 33: 381–391.
34. Altschuler RA, Mosinger JL, Harmison GG, Parakkal MH and Wenthold RJ (1982) Nature 298: 657–659.
35. Ross CD, Bowers M and Godfrey DA (1987) Brain Res. 401: 168–72.
36. Kaneko T and Mizuno N (1988) J. Comp. Neurol. 267: 590–602.
37. Bolz J, Thier P and Brecha N (1985) Neurosci. Lett. 53: 315–320.
38. Lam DMK and Hollyfield JG (1980) Exp. Eye Res. 31: 729–732.
39. Bruun A and Ehinger B (1974) Exp. Eye Res. 19: 435–447.
40. Berger SJ, McDaniel ML, Carter JG and Lowry OH (1977) J. Neurochem. 28: 159–163.
41. Canzek V, Wolfensberger M, Amsler U and Cuénod M (1981) Nature 293: 572–574.
42. Cuénod M, Beaudet A, Canzek V, Streit P and Reubi JC (1981) In: DiChiara G and Gessa GL (eds.) Glutamate as a Neurotransmitter. Raven Press, New York, pp. 57–68.
43. Fonnum F and Henke H (1982) J. Neurochem. 38: 1130–1134.
44. Somogyi P, Halasy K, Somogyi J, Storm-Mathisen J and Ottersen OP (1986) Neuroscience 19: 1045–1050.
45. Ottersen OP (1989b) J. Chem. Neuroanat. 2: 57–66.
46. Lam DMK and Steinman L (1971) Proc. Natl. Acad. Sci. USA 68: 2777–2781.
47. Marshall J and Voaden MJ (1975) Vision Res. 15: 459–461.
48. Yazulla S, Studholme KM and Wu JU (1986) J. Comp. Neurol. 244: 149–162.
49. Yazulla S and Brecha N (1980) Invest. Ophtal. Vis. Sci. 19: 1415–1426.
50. Agardh E and Ehinger B (1982) J. Neurol. Trans. 54: 1–18.
51. Brandon C, Lam DMK and Wu JY (1979) Proc. Natl. Acad. Sci. USA 76: 3557–3561.
52. Brandon C (1985) Brain Res. 344: 286–295.
53. Mariani AP and Caserta MT (1986) J. Neurocytol. 15: 645–655.
54. Caruso DM, Owczarzak MT, Goebel DJ, Hazlett JC and Pourcho RG (1989) Brain Res. 476: 129–134.
55. Nishimura Y, Schwartz ML and Rakic P (1986) Nature 320: 753–756.

Contribution of glial cells and of aspartate aminotransferase for amino acid neurotransmitter metabolism in rat brain *in vivo*

Ragnhild E. Paulsen, Anne Helen O. Bakkelund and Frode Fonnum

Norwegian Defence Research Establishment, Division for Environmental Toxicology, P.O. Box 25, N-2007 Kjeller, Norway

Abstract

The effects of fluorocitrate, a selective gliotoxin, and amino-oxyacetic acid, an inhibitor of pyridoxal phosphate-dependent enzymes (including the aminotransferases), on the K^+-evoked release of glutamate and γ-aminobutyric acid (GABA) were studied during microdialysis of neostriatum in anesthetized rats. K^+-evoked (100 mM) release of glutamate and GABA during microdialysis was Ca^{2+}-dependent, and reflected therefore release from the transmitter pools. K^+-evoked release of glutamate and especially GABA increased temporarily (peaking at 2 h) after local treatment with fluorocitrate (1 nmol) *in vivo*, compared to control. This suggests that astrocytes contribute significantly to the inactivation of neuronally released glutamate and GABA by uptake processes. Following at least 7 h of fluorocitrate treatment the release of glutamate decreased below control, concomitant with a decreased efflux of glutamine. This indicates that astrocytes supply precursors to transmitter amino acids. Treatment with amino-oxyacetic acid gave a decreased K^+-evoked release of both glutamate and GABA, suggesting an involvement of aspartate aminotransferase in the synthesis of transmitter glutamate *in vivo*.

Introduction

Glutamate and γ-aminobutyric acid (GABA) are the major excitatory and inhibitory neurotransmitters, respectively, in the central nervous system [1–3]. It is therefore of importance to know the precise sequence of reactions leading to the synthesis and inactivation of transmitter glutamate and GABA. Numerous previous studies have been devoted to these mechanisms, leading to the formulation of the concept of the glutamine cycle [4]. This cycle consists of glutamate and GABA inactivation by uptake into astrocytes and a completely counterbalanced transport of glutamine from the astrocytes back to the neurons, where glutamine is converted to glutamate and GABA. Strong experimental support to this concept is the demonstration of a selective localization of glutamine synthetase in astrocytes [5]. In addition, it was recently demonstrated that the activity of aspartate aminotransferase, which is high in some glutamergic neurons [6] is crucial for the releasable pool of glutamate both in cultured cerebellar granule cells [7] and in slices from some brain areas [8]. However, conclusive evidence for the quantitative significance of the different metabolic processes is still lacking, at least *in vivo*.

The object of the present study was to investigate *in vivo* the involvement of glial cells for inactivation of transmitter glutamate and GABA, the importance of *de*

novo synthesis of glutamine in astrocytes as a precursor for the transmitters, and finally, the participation of aspartate aminotransferase in the synthesis of the transmitter pool of glutamate. By using brain microdialysis, we have studied the effect of fluorocitrate, a compound which blocks energy-dependent processes in astrocytes and spares neurons [9], and amino-oxyacetic acid, which blocks pyridoxal phosphate requiring reactions including the aspartate aminotransferase reaction [10,11]. K^+-evoked release of glutamate and GABA was measured, since it has been demonstrated that K^+-evoked release reflects release from the transmitter pool [12].

Experimental procedures

Materials

Adult male Wistar rats (300–400 g) were used throughout the study. All chemicals were commercially available. Dialysis probes were prepared in our laboratory according to the design described by Sandberg *et al.* [13]. The length and the outer diameter of the probe was 2.5 mm and 0.3 mm, respectively, and the molecular-weight cut-off was 3000.

Brain dialysis

Rats were anesthetized with 1.25 g/kg of urethane i.p. and remained under anesthesia for the duration of the experiment. The rats were premedicated with atropine sulfate (0.3 mg/kg) to prevent bradycardia. The body temperature was kept at 38°C by means of a Harward body temperature controller. Following induction of anesthesia, the rats were placed in a Kopf stereotaxic frame with the incisor bar set at −3.3 mm, according to the atlas of Paxinos and Watson [14]. Microinjection of drugs and implantation of microdialysis probes into both neostriata were at the coordinates anteroposterior with respect to the bregma of +1.0 mm, lateral with respect to the midline suture of ±3.0 mm, and dorsoventral with respect to the dura of −5.0 mm.

The probes were perfused at 3.0 µl/min with Krebs-Ringer bicarbonate solution (pH 7.4) of the following composition (in mM, [13]): NaCl, 122.0; KCl, 3.0; $MgSO_4$, 1.2; KH_2PO_4, 0.4; $NaHCO_3$, 25.0; and $CaCl_2$, 1.2. The perfusate was collected in 15-min fractions. For every third fraction, the buffer was replaced by a modified Krebs-Ringer bicarbonate solution containing 100 mM K^+ with a corresponding reduction of the Na^+ content. The change in the buffers during the microdialysis experiments was done by liquid switches (Carnegie Medicin, Stockholm, Sweden).

In experiments with fluorocitrate (Sigma, St. Louis, MO, U.S.A.), one microliter of a 1 mM solution of the drug in 0.9 % NaCl was microinjected on one side during 4 min prior to implantation of the dialysis probes. The buffer to the neostriatum

previously injected with fluorocitrate contained 0.5 mM fluorocitrate to maintain inhibition. In experiments with amino-oxyacetic acid, 10 mM of the drug was present in the buffer from fraction 10 to fraction 15 on one side. The contralateral sides constituted the control groups.

Amino acid analyses

Aliquots of the dialysates (20 µl) were mixed with *o*-phthaldialdehyde reagent and analyzed for amino acid content by the method of Lindroth and Mopper [15] as modified by Sandberg and Corazzi [16] as previously described [9].

Statistics

Statistical analyses were performed by the Sign test, as indicated in the figure legends.

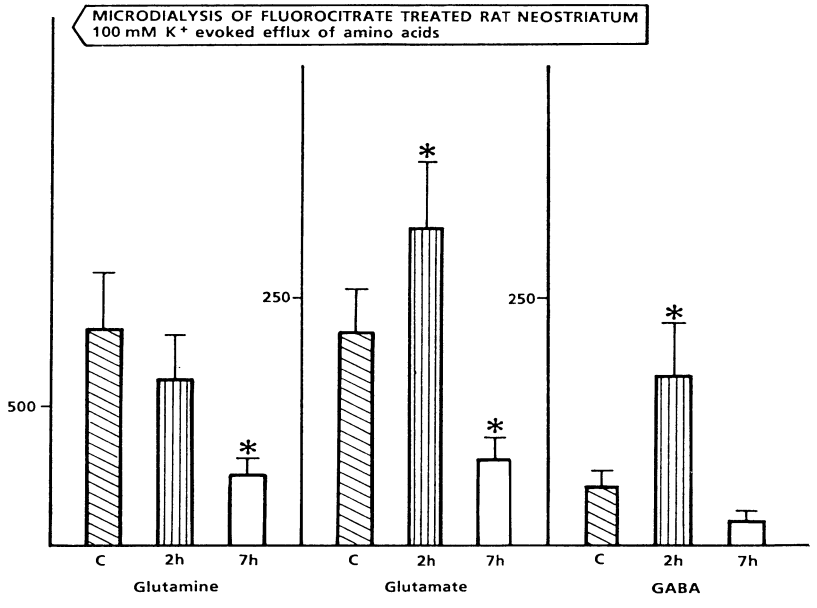

Fig. 1. Microdialysis of fluorocitrate-treated rat neostriatum. For every third 15 min fraction the basal Krebs-Ringer bicarbonate solution (3 mM K^+) was replaced by a solution containing 100 mM K^+ (K^+-evoked fraction). The vertical axis shows amino acid levels given as pmol/15 min fraction. Three fractions are shown in the figure: control K^+-evoked fraction in untreated (contralateral) neostriatum (C); K^+-evoked fraction at 2 h after fluorocitrate (1 nmol) microinjection (2 h); and K^+-evoked fraction at 7 h after fluorocitrate microinjection (7 h). The Krebs-Ringer bicarbonate solution for the neostriatum previously injected with fluorocitrate contained 0.5 mM fluorocitrate to maintain inhibition. The results are mean ± S.E.M. of 5 animals. *$p<0.05$, Sign test, when comparing the treated neostriatum with its contralateral neostriatum at 2 h and 7 h, respectively.

Results

The contents of glutamine, glutamate and GABA in the dialysate of rat neostriata treated with fluorocitrate (1 nmol) followed by a long-term perfusion with fluorocitrate (0.5 mM) are shown in Fig. 1. The fractions shown (containing 100 mM K^+) represent release from the transmitter pool, since it has been demonstrated that the increased efflux of glutamate and GABA following 100 mM K^+ is Ca^{2+}-dependent [12]. The release of transmitter glutamate, and in particular that of GABA, were higher than the control value at the start of the fluorocitrate treatment. This increase peaked at 2 h, which is shown in Fig. 1. The K^+-evoked release of glutamate decreased below the control value following at least 7 h of fluorocitrate treatment, concomitant with a decreased glutamine efflux (Fig. 1). A more detailed analysis of the time-dependent changes in amino acid efflux during microdialysis following fluorocitrate treatment has previously been shown [12].

Figure 2 shows the release of glutamate and GABA during depolarization with 100 mM K^+, following treatment with the aminotransferase inhibitor amino-oxyacetic acid (10 mM). Following 90 min of amino-oxyacetic acid treatment the K^+-evoked release of both glutamate and GABA decreased, by 67 and 72%, respectively, compared to the control values, with no concomitant decrease in the glutamine efflux.

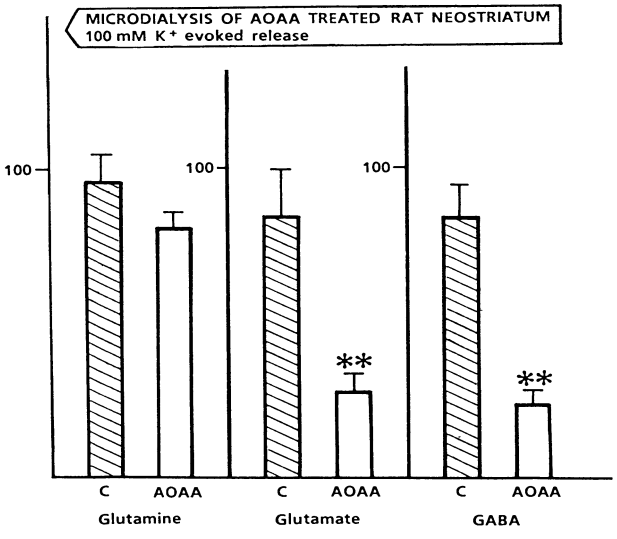

Fig. 2. Microdialysis of amino-oxyacetic acid (AOAA)-treated rat neostriatum. For every third 15 min fraction the basal Krebs-Ringer bicarbonate solution (3 mM K^+) was replaced by a solution containing 100 mM K^+ (K^+-evoked fraction). AOAA (10 mM) was present in the buffer in fractions 10 to 15. The vertical axis shows amino acid levels in K^+-evoked fractions given as the ratio (in percent) between fractions 18 and 19 in untreated (contralateral) neostriatum (C) and AOAA-treated neostriatum (AOAA). Data are mean ± S.E.M. values from 7 rats. **$p<0.01$, Sign test.

Discussion

Neostriatum of rat exhibits a large Ca^{2+}-dependent K^+-evoked release of glutamate and GABA during microdialysis, which could be used to study the size of the transmitter pool *in vivo* [12].

Fluorocitrate acts selectively in astrocytes by blocking the tricarboxylic acid cycle at the aconitase step [9,17], and inhibits thereby energy-dependent glial processes. Exposure to fluorocitrate increased temporarily the K^+-evoked release of both glutamate and GABA. Later the release of glutamate decreased below control. The increase is consistent with an important role of astrocytes in the inactivation of both glutamate and GABA by uptake processes following their release from nerve terminals. Further, the later decrease in the release of transmitter glutamate adds evidence to the concept of glially derived precursors to the transmitter pool of amino acids. A major precursor candidate synthesized in astrocytes *in vivo* is glutamine, since it decreased concomitantly with the decreased release of glutamate. A strong support to this finding is a severe decrease in the release of glutamate and GABA during microdialysis following specific inhibition of the glutamine synthetase in astrocytes by methionine sulfoximine [12]. The importance of glutamine as a precursor has earlier been established in several *in vitro* models [18,19].

Amino-oxyacetic acid was introduced early as a specific inhibitor of GABA metabolism, since in low concentrations it inhibits GABA transaminase [20]. In higher concentrations, however, it also inhibits other pyridoxal phosphate-dependent enzymes, like aspartate aminotransferase [11]. In the present investigation exposure to amino-oxyacetic acid in a high concentration led to a decreased release of glutamate and GABA, with no change in the efflux of glutamine. The inhibition of glutamate release caused by amino-oxyacetic acid suggests an important role of aspartate aminotransferase in the maintenance of the transmitter pool of glutamate, as has earlier been suggested *in vitro* after exposure of cells and slices to amino-oxyacetic acid [7,8]. In cerebellar granule cells it was suggested that glutamate produced by the action of phosphate activated glutaminase is not directly introduced into the transmitter pool, but is transaminated inside the mitochondria to 2-oxoglutarate by aspartate aminotransferase, transported into the cytoplasm as 2-oxoglutarate, and finally, undergoing a second transamination by aspartate aminotransferase to transmitter glutamate [7]. Our present results indicate that this may be the case also in rat neostriatum *in vivo*. One should keep in mind, however, that amino-oxyacetic acid is an inhibitor of several pyridoxal phosphate-dependent enzymes in this concentration. In addition, the aspartate aminotransferase reaction is an essential component of the malate-aspartate shuttle, which is necessary for the reoxidation of cytosolic NADH, and thereby the energy status of the cell [11]. The present study showed a decrease in the release of GABA following amino-oxyacetic acid treatment, consistent with the fact that the enzyme responsible for GABA synthesis, glutamic acid decarboxylase, which is pyridoxal phosphate-dependent [21] was also inhibited. In slices, however, there was an increase in the

evoked release of GABA in different brain areas, caused by the inhibitory action of amino-oxyacetic acid on GABA transaminase [8].

References

1. Krnjevic K (1970) Nature 228: 119–124.
2. Fonnum F (1984) J. Neurochem. 42: 1–11.
3. Fonnum F (1987) In: Meltzer HY (ed.) Psychopharmacology: The Third Generation of Progress. Raven Press, New York, pp. 173–182.
4. Van den Berg CJ, Matheson DF and Nijenmanting WC (1978) In: Fonnum F (ed.) Amino Acids as Chemical Transmitters. Plenum Press, New York, pp. 709–723.
5. Norenberg MD and Martinez-Hernandez A (1979) Brain Res. 161: 303–310.
6. Altschuler RA, Neises GR, Harmison GG, Wenthold RJ and Fex J (1981) Proc. Natl. Acad. Sci. USA 78: 6553–6557.
7. Palaiologos G, Hertz L and Schousboe A (1988) J. Neurochem. 51: 317–320.
8. Kihara M and Kubo T (1989) J. Neurochem. 52: 1127–1134.
9. Paulsen RE, Contestabile A, Villani L and Fonnum F (1987) J. Neurochem. 48: 1377–1385.
10. Smith SB, Briggs S, Triebwasser KC and Freedland RA (1977) Biochem. J. 162: 453–455.
11. Kauppinen RA, Sihra TS and Nicholls DG (1987) Biochim. Biophys. Acta 930: 171–178.
12. Paulsen RE and Fonnum F (1989) J. Neurochem. 52: 1823–1829.
13. Sandberg M, Butcher SP and Hagberg H (1986) J. Neurochem. 47: 178–184.
14. Paxinos G and Watson C (1982) The Rat Brain in Stereotaxic Coordinates, Academic Press, Sydney.
15. Lindroth P and Mopper K (1979) Anal. Chem. 51: 1667–1674.
16. Sandberg M and Corazzi L (1983) J. Neurochem. 40: 917–921.
17. Clarke DD, Nicklas WJ and Berl S (1970) Biochem. J. 120: 345–351.
18. Bradford HF, Ward HK and Thomas AJ (1978) J. Neurochem. 30: 1453–1459.
19. Hamberger A, Chiang GH, Nylen ES, Scheff SW and Cotman CW (1979) Brain Res. 168: 513–530.
20. van Gelder NM (1966) Biochem. Pharmacol. 15: 533–539.
21. Miller LP, Walters JR and Martin DL (1977) Nature 266: 847–848.

Address for correspondence: Ragnhild E. Paulsen, Norwegian Defence Research Establishment, Division for Environmental Toxicology, P.O. Box 25, N-2007 Kjeller, Norway.

Role of polyamines (spermine and spermidine) in mediating cerebral electrical activity and behaviour in rabbits

Paola Bo, Andrea Giorgetti, Claudia Camana, Lorenza Montalbetti and Faustino Savoldi

Neurological Institute 'C. Mondino', University of Pavia, Via Palestro 3, 27100 Pavia, Italy

Abstract

The eegraphic and behavioural changes induced by the administration of polyamines (spermine and spermidine) were studied in rabbits. Spermine and spermidine were administered at different doses (200–400 γ) into the mesencephalic ventricle (i.c.v.) both as a bolus and in constant perfusion (60 min. duration). We also studied the effects of methamphetamine (M.A.) in a group of rabbits pretreated with spermine and spermidine 200–400 γ i.c.v. as bolus. Spermine caused a dose-related cortical synchronization associated with a partial sedation; spermidine induced cortical synchronization at a low dose without any behavioural changes while at higher dose (after perfusion) cortical desynchronization with an arousal behavioural pattern. The possible interaction of these substances with mesolimbic dopaminergic system is discussed on the basis of their potential neuroleptic action.

Introduction

It has recently been hypothesized [1] that polyamines (spermine and spermidine) may play a role in modulating central dopaminergic pathways. This hypothesis arose from the structural similarities between polyamines and neuroleptic drugs [2]. Spermine and Spermidine, injected bilaterally into the nucleus accumbens, counteracted the hyperactivity induced by amphetamine injected into the same nucleus, in rats. When these substances were injected unilaterally into the rat corpus striatus they failed to cause any asymmetries or active circling behaviour either spontaneously or in the presence of apomorphine [1]. These authors suggested a selective action of polyamines on mesolimbic dopamine behaviour. The interest of the study of these substances lies in their possible involvement in the pathophysiology of mental disorders.

In order to increase our understanding of the mechanism of action exerted by polyamines, we studied their effects on cerebral electrical activity (EEG and quantified EEG analysis) and on behaviour, in rabbits. The interactions between polyamines and methamphetamine (M.A.) were also verified.

Experimental procedure

A total of 70 New Zealand white rabbits (2.8–3.0 kg) was used, all from the same breeding stock and fed according to a standard diet. All the animals were prepared according to the Monnier and Gangloff sterotaxic method [3] for EEG recording. The following cerebral structures were examined: motor cortex (MC), sensori-motor cortex (SC) and Cornu Ammonis dorsale (CAd). The experiments were carried out after 6 h. The occurrence of slow wave and spindle activity was evaluated both in basal conditions and after administration of drugs, as parameters of cortical synchronization. During the experiments, quantitative EEG analysis (QEEG) (by means the fast Fourrier transform) was carried out by means of a NOVA 4/C 16-bit computer (DATA GENERAL). The power density spectrum (PDS) and the power relative to each frequency band (0.15–3.70; 3.70–7.20; 7.20–12.20; 12.20–20.20; 20.20–38.46 Hz bands) were computed. During monitoring of the EEG, the animals were held in a specially designed hammock which facilitated behavioural observation. Groups of at least 5 rabbits received the following substances: spermidine (200–400 γ) and spermine (200–400 γ) solved in 0.2 ml of artificial liquor and administered into the mesencephalic ventricle (i.c.v.) (Monnier and Hatt's technique) both as a bolus and in constant perfusion (60 min duration). The animals that received the bolus were monitored for 1 h in basal conditions and for 2 h after administration of spermine and spermidine. The animals submitted to perfusion of the substances were monitored for 1 h in basal conditions, for 1 h during perfusion and for 1 h after perfusion. M.A. (2 mg/kg i.v.) was administered to two groups of animals pretreated 15 min before: one with spermine and the other with spermidine 200–400 γ i.c.v. as bolus. These groups of animals were monitored for 1 h in basal conditions and for 2 h after the administration of M.A..

Changes QEEG, against pre-drug values, were statistically analysed using the ANOVA test. Significance values are shown in Tables 1 and 2. All the experiments were carried out in accordance with the 'Guiding Principles in the Care and Use of Animals' of the American Physiological Society.

Results

Control groups did not show any significant change in the parameters considered after both bolus and perfusion of vehicle alone. Control rabbits presented an EEG pattern, shown in Fig. 1A, which characterizes their wakefulness-sleep state.

Spermidine

Bolus

Administration of spermidine (200 γ) induced on cortical recordings, with a latency of 10–15 min., an increase in slow waves and spindle activity (synchronized EEG pattern). On hippocampal recordings, concomitantly with the periods of cortical

Table 1. ANOVA: Significance values of analysis of variance (ANOVA) related to motor cortex-sensory motor cortex (Cortex) and Cornu Ammonis dorsale (CAd). Administration of spermidine and spermine 200 γ as bolus and perfusion

	Cortex			
	Spermidine 200 γ		Spermine 200 γ	
	Bolus	Perf	Bolus	Perf
PDS	p<.05	p<.01	p<.05	–
B1	p<.01	p<.05	p<.01	–
B2	p<.01	p<.01	p<.01	–
B3	p<.05	p<.01	–	–
B4	–	p<.01	–	–
	CAd			
	Spermidine 200 γ		Spermine 200 γ	
	Bolus	Perf.	Bolus	Perf.
PDS	p<.01	p<.01	p<.01	p<.01
B1	p<.01	p<.01	–	p<.01
B2	p<.01	p<.01	–	p<.01
B3	p<.01	p<.01	p<.01	p<.01
B4	p<.01	–	p<.05	p<.01

Table 2. ANOVA: Significance values of analysis of variance (ANOVA) related to motor cortex-sensory motor cortex (Cortex) and Cornu Ammonis dorsale (CAd). Administration of spermidine and spermine 400 γ as bolus and perfusion

	Cortex			
	Spermidine 400γ		Spermine 400 γ	
	Bolus	Perf.	Bolus	Perf.
PDS	p<.01	–	p<.05	p<.01
B1	p<.01	–	p<.05	–
B2	p<.01	p<.05	–	p<.01
B3	p<.01	p<.01	–	p<.01
B4	p<.01	p<.01	–	p<.01
	CAd			
	Spermidine 400 γ		Spermine 400 γ	
	Bolus	Perf.	Bolus	Perf.
PDS	p<.01	p<.01	p<.05	–
B1	p<.01	p<.01	p<.01	–
B2	p<.01	p<.01	–	p<.01
B3	p<.01	p<.05	p<.01	–
B4	p<.01	p<.01	p<.01	–

synchronization, the rhythmic theta activity disappeared: the electrical activity was represented by irregular frequencies of lower voltage than in basal condition (see Fig. 2A).

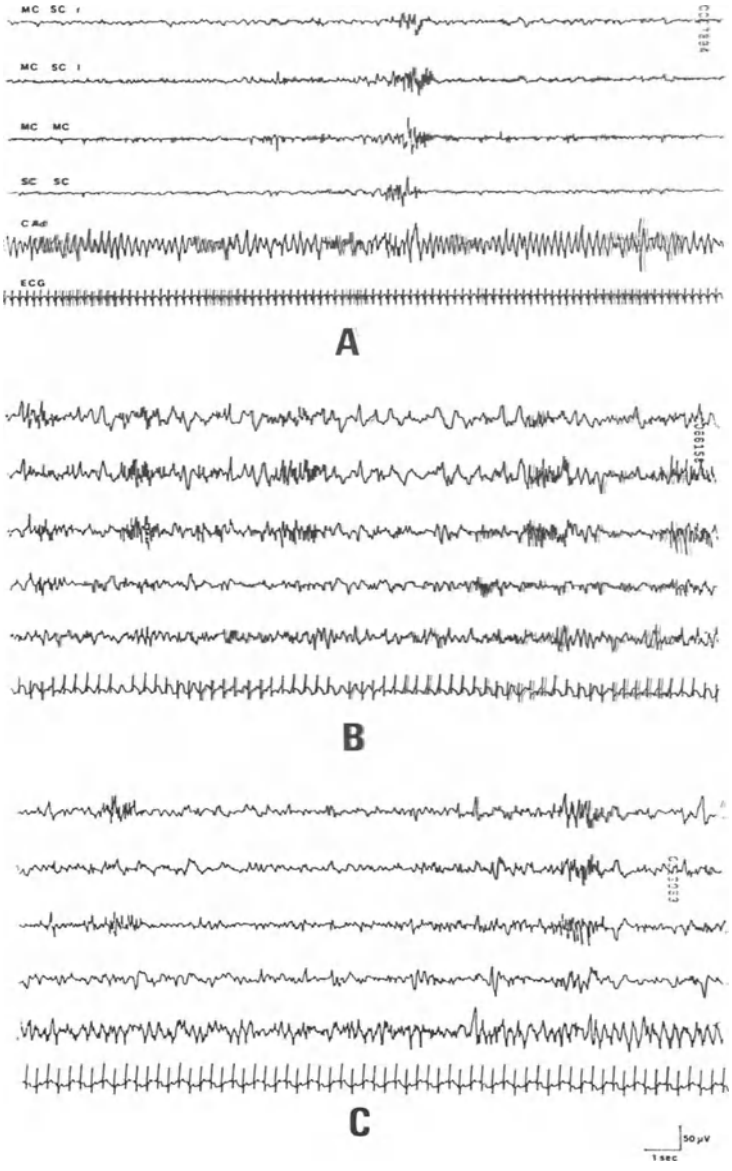

Fig. 1. A: sample of typical basal EEG tracings; B: sample of EEG tracings 20 min after perfusion of spermidine 200 γ; C: sample of EEG tracings after perfusion of spermine 200 γ.

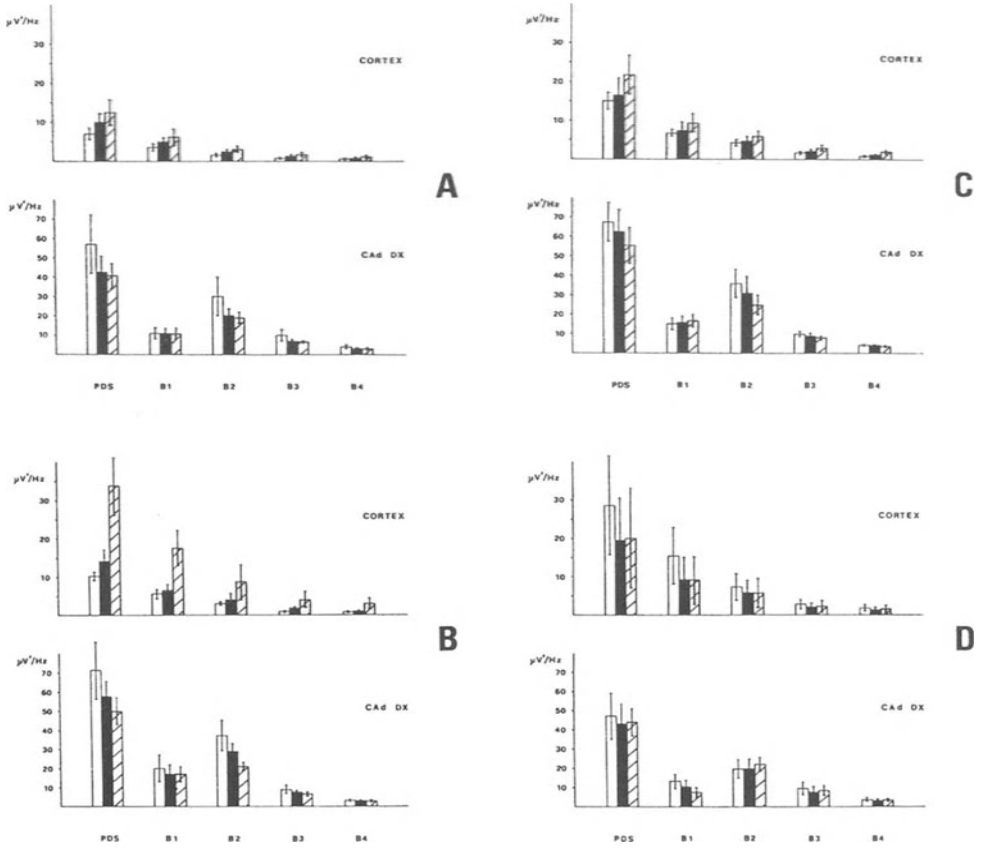

Fig. 2. Changes in the power density spectrum (PDS), 0.15–3.7 Hz band (B1); 3.7–7.2 Hz band (B2); 7.2–12.2 Hz band (B3); 12.2–20.2 Hz band (B4); on cortical and hippocampal (CAd) recordings. Spermidine (A) and spermine (C) administered as a bolus (200 γ): ❑ basal; ■ 1 h and ▨ 2 h after administration. Spermidine (B) and Spermine (D) administered by constant perfusion (200 γ): ❑ basal; ■ during perfusion and ▨ 1 h after perfusion.

Administration of spermidine 400 γ i.c.v. induced EEG modification similar to that obtained with the lower dose on cortex recordings. On hippocampal recordings there was an increase in slower frequencies of higher amplitude. Quantified EEG analysis confirmed visual reading of the recordings (see Fig. 3A).

Perfusion

In this group of animals the main changes were observed after perfusion of 200 γ (1 h observation). The modifications induced were similar to those obtained after bolus, but more evident (see Fig. 1B for EEG tracings and Fig. 2B for QEEG).

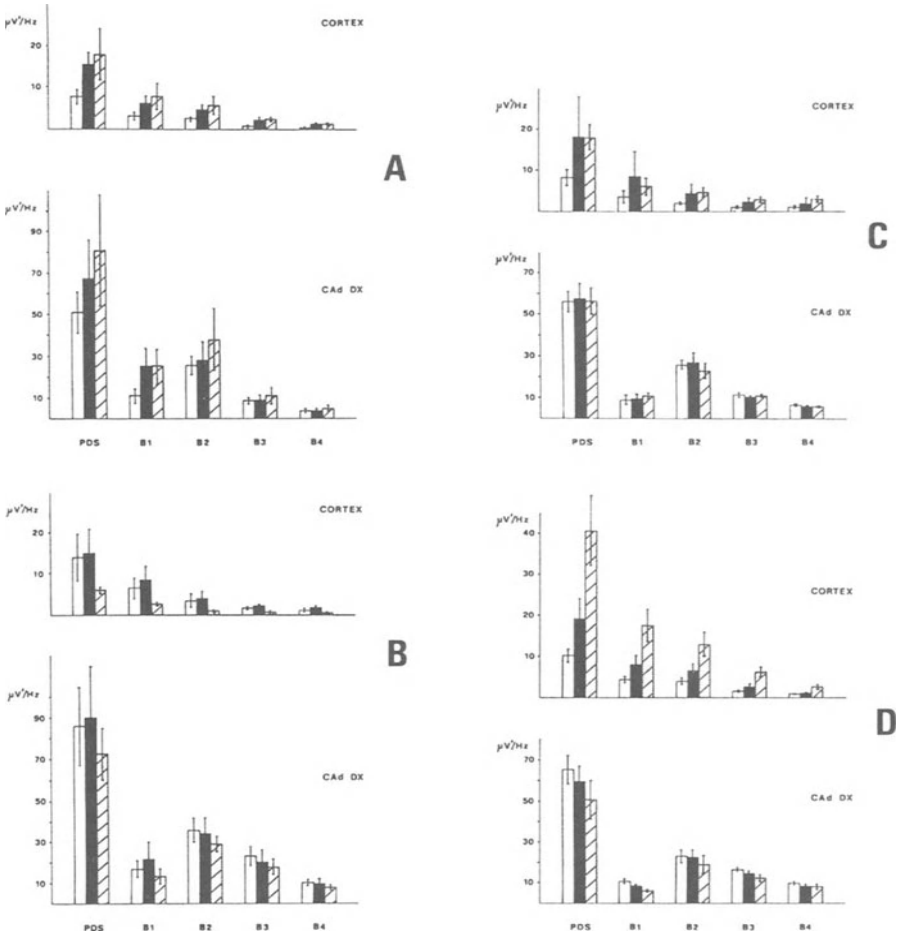

Fig. 3. Quantified EEG analysis as in Fig. 2. Spermidine (A) and spermine (C) administered as a bolus (400 γ): ❑ basal; ■ 1 h and ▨ 2 h after administration. Spermidine (B) and spermine (D) administered by constant perfusion (400 γ): ❑ basal; ■ during perfusion and ▨ 1 h after perfusion.

Perfusion of 400 γ induced a marked EEG cortical desynchronization which started on average at the 30th min of perfusion and lasted the whole hour following perfusion.In particular EEG analysis on cortex showed a significant decrease in PDS and in all frequency bands (Fig. 3B).

The animals treated with 200 γ by perfusion did not exhibit the gross behaviour, normally present in basal condition, and they were not reactive to external stimuli. No specific behaviour was observed in the other 3 groups.

Spermine

Bolus

Spermine 200 γ induced an increase in periods of cortical synchronization which were spontaneously interrupted by periods of cortical desynchronization.

Spermine 400 γ as bolus caused an EEG pattern analogous to that obtained with spermine 200 γ i.c.v. as bolus, but of higher degree.

On cortex after the administration of 200 γ, spectral analysis showed a significant increase in the delta activity (B1) and in PDS and on hippocampus a significant decrease in PDS and in the frequency band corresponding to fast theta activity (see Fig. 2C–3C). Similar findings were observed after 400 γ. No behavioural changes were noted in the animals.

Perfusion

Spermine 200 γ did not induce significant changes in EEG and QEEG, on cortical recordings (Fig. 1c). On hippocampal recordings we noted that during the periods of cortical desynchronization, the fast rhythmic theta activity was substituted by a more irregular activity of lower voltage.

Spermine 400 γ as perfusion induced an important EEG cortical synchronization which reached a remarkable degree during the hour following perfusion.

Spectral analysis confirmed these findings (see Figs. 2D–3D). Spermine 400 γ by perfusion induced behavioural sedation. No specific behaviour was noted in the other groups examined. Statistical study (ANOVA) related to EEG spectral analysis is shown in Tables 1 and 2.

Polyamines plus M.A.

M.A. (2 mg/kg i.v.) alone induced EEG cortical desynchronization and stereotyped dopaminergic behaviour typical of this animal species (Fig. 4A), which lasted 90 min on average. The pretreatment with spermidine (200 γ as bolus) did not modify the EEG cortical desynchronization but was able to inhibit behavioural activation (Fig. 4B). The pretreatment with spermine 200 γ did not show any significant change in EEG and behaviour (Fig. 4C).

The pretreatment with spermine 400 γ as bolus inhibited the stereotypes induced by M.A., which were evident only during the first 10–15 min; spermidine 400 γ completely inhibited stereotypes.

Discussion

The data obtained during our experiments were not homogeneous. The effects induced by these substances are time-related and depend on the type of administration (bolus or perfusion). Perfusion caused changes of a higher degree.

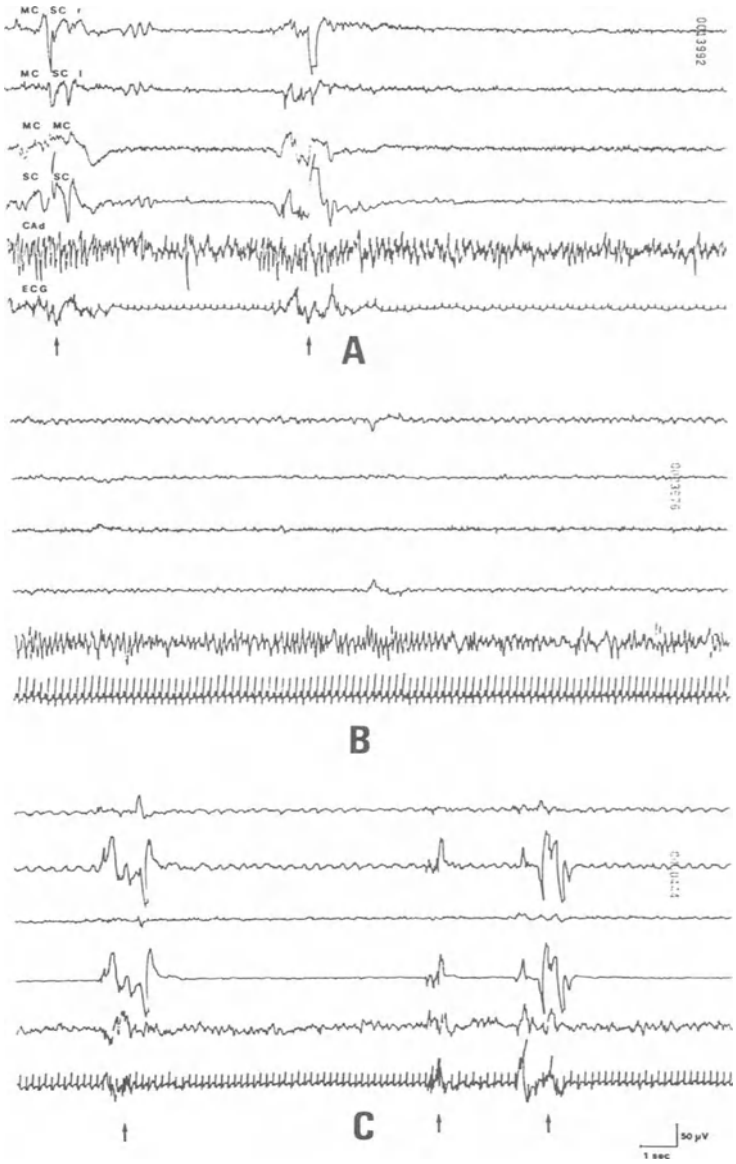

Fig. 4. A: sample of typical EEG tracings after the administration of M.A. (2 mg/kg), note EEG activation and artefacts (↑) due to the stereotyped behaviour induced by the drug. B: sample of EEG tracings after the administration of M.A. (2 mg/kg) in rabbits pretreated with spermidine (a bolus of 200 γ i.c.v.), note EEG activation but not artefact due to stereotyped behaviour. C: sample of EEG tracings after the administration of M.A. (2 mg/kg) in rabbits pretreated with spermine (a bolus of 200 γ i.c.v.), note that spermine was not able to interact either with EEG activation or with stereotyped behaviour (↑) induced by M.A.

In the attempt to explain our varying results, the following problems should be considered.

First, polyamines are injected into the mesencephalic ventricle and have then to reach the specific cerebral structures by diffusion. This fact could explain the latency needed to show eegraphic and behavioural effects.

A second consideration to keep in mind is the metabolic cycle of polyamines, in the brain, which is rather complex [4]. Other authors have suggested an interconversion of spermine and spermidine and of spermidine and putrescine, in brain [5,6].

The discrepancies encountered during our experiments could be ascribed to different steps in the metabolic cycle of polyamines. Moreover, Koenig *et al.* [7] suggested that polyamines in CNS may play a role in the mobilization of intracellular calcium and in the resulting stimulation of neurotransmitter release. It has been suggested [8] that the Ca-mediated release of D-aspartate may in part be regulated by biogenic polyamimes. D-Aspartate is an excitatory amino-acid; nevertheless, we obtained EEG desynchronization only with the higher doses and after perfusion.

On the other hand, it has been hypothesized [2] that polyamines may act on C.N.S. with a mechanism of action similar to that exerted by neuroleptic drugs. Hirsch *et al.* [1] demonstrated that polyamines act in the modulation of dopaminergic mesolimbic activity.

The EEG and behavioural patterns (EEG synchronization and behavioural sedation) obtained after the administration of spermine and spermidine at low dose are similar to those obtained by the administration of 'classic' neuroleptics, for instance haloperidol [9,10].

Further support for this hypothesis is the antagonism exerted by these polyamines on the behavioural syndrome induced by M.A. assessed in our experiments. As we obtained, at certain doses, EEG and behavioural patterns similar to those induced by 'classic' neuroleptics, we can hypothesize that these polyamines could act on the central nervous system by blocking D1-D2 receptors [11].

In one of our previous studies we found that both D1 (SCH 23390) and D2 (raclopride) antagonists and haloperidol (as reference drug) are able to antagonize the behavioural effects but not EEG desynchronization induced by methamphetamine [11].

Analogous results have been obtained by pretreatment with spermidine 200–400 γ and spermine 400 γ: the former completely counteracted the behavioural effects induced by methamphetamine, and the latter almost completely.

This experimental model proved to be reliable in the neurophysiological studies of polyamines. However, the mechanism involved and the potential biochemical consequences of the complex interrelations between polyamines need further investigation before a better evaluation of their significance can be made.

References

1. Hirsch SR, Richardson-Andrews R, Costall B, Kelly ME, de Belleroche J and Naylor RJ (1987) Psychopharmacology 93: 101–104.
2. Richardson-Andrews R (1983) Med. Hypotheses 11(2): 157–166.
3. Monnier M and Gangloff H (1961) Atlas for Stereotaxic Brain Research. Elsevier Publishing Company, Amsterdam.
4. Pegg AE (1988) Cancer Res. 48(4):759–774.
5. Seiler N (1973) In: Russel DH (ed.) Polyamines in Normal and Neoplastic Growth. Raven Press, New York, pp. 137–156.
6. Seiler N (1980) Physiol. Chem. Physics 12: 411–429.
7. Koenig H, Goldostone AD and Lu CY (1983) Biochem. Biophys. Res. Commun. 116(3): 1039–1048.
8. Bondy SC and Walker CH (1986) Brain Res. 371(1): 96–100.
9. Arrigo A, Savoldi F and Tartara A (1982) Symp. Int. Haloperidol. Triperidol. Milan, 157–175.
10. Ongini E, Caporali MG, Bo P, Camana C, Savoldi F (1988) Symposia in Neuroscience. Liviana Press, Padova, 139–148.
11. Bo P, Ongini E, Giorgetti A and Savoldi F (1988) Neuropharmacology 27: 799–805.

Address for correspondence: Dr. Paola Bo, Neurological Institute 'C. Mondino', Via Palestro 3, 27100 Pavia (PV), Italy.

Regulation of cortical and striatal dopamine and acetylcholine release by glutamate mechanisms assayed *in vivo* with microdialysis: *in situ* stimulation with kainate-, quisqualate- and NMDA-receptor agonists

M. Herrera-Marschitz, M. Goiny, H. Utsumi, S. Ferre, T. Guix and U. Ungerstedt

Department of pharmacology, Karolinska Institutet, Stockholm, Sweden

Abstract

Cortical and striatal dopamine and acetylcholine were measured in samples collected during microdialysis using Ringer or Ringer and kainic acid, quisqualic acid or *N*-methyl-D-aspartate as perfusion medium. In the striatum, kainic acid (10^{-5}–10^{-3} M) increased dialysate dopamine (DA) in a dose dependent manner, while decreasing acetylcholine (ACh). In the cortex, kainic acid decreased DA, but increased ACh. Quisqualic acid and *N*-methyl-D-aspartate (10^{-3}–10^{-4} M) moderately increased striatal DA, but increased ACh by more than 300%. The present results are in agreement with the idea of an excitatory regulation of striatal DA release by a glutamatergic pathway, with cell bodies located in the cortex and axons impinging on the ipsilateral DA terminals. It is probable that glutamate terminals have a stimulatory action on ACh neurons as well, since ACh was increased by NMDA and quisqualic acid, while DA release was only moderately increased.

Introduction

There is evidence that striatal dopamine (DA) release is presynaptically modulated by a glutamatergic cortical input (see [1–3]). In the caudate of the push-pull cannulated cats [4], as well as in striatal slice preparations in rats [5], glutamate stimulates DA release. It was proposed [4], that the DA stimulation produced by glutamate reflected direct axonal interactions between cortical glutamatergic and mesencephalic dopaminergic afferents, since the stimulating effect of L-glutamate was still observed in the presence of tetrodotoxin. This hypothesis has received support from biochemical and histochemical studies showing direct intrastriatal axonal interactions between cortico-striatal projections and mesencephalic-tyrosine hydroxylase-like terminals [6,7]. However, the majority of the striatal afferents from the cortex and the mesencephalon make axodendritic synaptic contacts with striatal neurons [8], giving a basis for polysynaptic loops including γ-aminobutyric acid (GABA) and/or acetylcholine (ACh) neurons, by which cortical glutamate neurons could also modulate striatal dopamine release. There is now evidence that the excitatory action of glutamate is conveyed by multiple receptors, which have been pharmacologically differentiated and characterized, i.e.

N-methyl-D-aspartate (NMDA)-, quisqualate- and kainate-receptors. All these receptors are found in the striatum (see reference [9]), but appear located on different cells or associated with different synapses, thereby related to different functions. For example, it has been shown that, in the cat caudate, cortically evoked monosynaptic excitatory postsynaptic potentials (EPSPs) are mediated by kainate or quisqualate, but not by NMDA receptors [10]. The present results obtained with microdialysis [11] show that, in the striatum, *in situ* kainic acid (KA) stimulation increases DA but decreases ACh. In contrast, in the cortex, KA increases ACh but decreases DA. Quisqualic acid and NMDA mainly stimulate striatal ACh.

Experimental procedures

Microdialysis

Male Sprague-Dawley rats weighing around 500 g were anaesthetized with halothane and placed in a David Kopf stereotaxic frame. The anaesthesia was maintained by free breathing into a mask fitted over the nose of the rat (1.0–1.5% of halothane maintained by an air flow of 1.5 l/min). Two microdialysis probes (CMA 10, Carnegie Medicin AB, Stockholm, Sweden) (dialysing length = 4 mm; diameter = 0.5 mm) were implanted: one diagonally into the left fronto-parietal cortex (coordinates, according to Zilles [12] atlas B 1.7, L −1.5, V 5.0; inserted with a 40° angle from vertical in the coronal plane); the other vertically into the lateral portion of the corpus of the left striatum (coordinates: B 0.7, L −3.5, V 7.5). The microdialysis probes were perfused with Ringer (147 mmol Na^+, 2.3 mmol Ca^{2+}, 4 mmol K^+ and 155.6 mmol Cl^-, pH 6.0), Ringer containing 10 μM neostigmine (Sigma, St. Louis, Mo, U.S.A.) and Ringer containing neostigmine and KA, quisqualic acid or NMDA (Sigma) as well. A constant flow of 2 μl/min was maintained with a microdialysis pump (CMA 100, Carnegie Medicin AB). Changes in the perfusion medium were performed by using a liquid switch (CMA 110, Carnegie Medicin AB), which made it possible to shift instantaneously syringes containing different perfusion media without introducing air into the system. Samples (40 μl) were collected in 300 μl Eppendorf tubes, containing 10 μl of 1 M perchloric acid if assayed for catecholamines. On completion of the dialysis experiment, the brain was rapidly dissected out and stored in 10% formaldehyde for confirmation of the location of the dialysis probes.

Biochemistry – HPLC assays

DA and metabolites were assayed in 20 min fractions on a reverse phase ion-pair High Performance Liquid Chromatography (HPLC) system (BAS, West Lafayette, IN, U.S.A.) with electrochemical detection (for details see [13]). ACh and Ch were determinated in 10 μl aliquots using a column-reactor system (BAS). ACh and Ch

were first separated on a polymeric column using a sodium phosphate buffer containing 1 mM sodium octanesulfonate as ion-pairing reagent. An enzymatic post column reactor with immobilized acetylcholinesterase and Ch oxidase converted ACh and choline to hydrogen peroxide and betaine. Hydrogen peroxide was electrochemically detected at a platinum electrode held at 500 mV (vs Ag/AgCl) (for details see [14]).

Statistics

DA and ACh are expressed as the concentrations found in the perfusates. Means and standard errors of the means (SEM) have been calculated. All statistical comparisons were made against cortical or striatal values obtained for the immediately precedent sampling period. Differences between the means were tested by Student's t-test for replicated data. A level of $P<0.05$ for the one tail test was considered critical for assigning significant statistical differences.

Results

Figure 1a,b,c shows striatal DA levels detected in 20 min perfusion fractions under Ringer (0–80 min period), Ringer + neostigmine (80–160 min period) and Ringer + neostigmine + KA (10^{-5}–10^{-3} M; pH>6.5) (160–400 min period) conditions. Striatal DA was dose-dependently increased by *in situ* KA. In contrast, cortical DA was decreased by *in situ* KA stimulation (>70%).

Figure 2a,b,c shows striatal ACh levels detected before and after KA stimulation. *In situ* KA stimulation induced a dose-dependent decrease in ACh levels. At the dose of 10^{-4} M, KA produced a short lasting 35% decrease of striatal ACh, while after the dose of 10^{-3} M striatal ACh decreased by 43% and did not reverse to control levels. At the doses of 10^{-5} and 10^{-4} M (Fig. 2a,b), cortical KA produced a significant increase in striatal ACh. In the cortex, KA produced a dose-dependent increase in ACh, which was already >70% at the dose of 10^{-5}M. *In situ* quisqualic acid (10^{-3}–10^{-4} M) stimulation produced a moderate increase in striatal DA (25–70%), while striatal ACh was increased by more than 300%. NMDA (10^{-4} M) produced a 25% increase in striatal DA, but a 400% increase in striatal ACh.

Discussion

The present *in vivo* microdialysis experiments give evidence that glutamate can modulate striatal DA transmission, since KA, a selective agonist for kainate type of glutamate receptors, produced, after *in situ* administration, a dose-dependent increase in striatal DA. The quisqualate receptor agonist, quisqualic acid, and the NMDA receptor agonist, NMDA were less effective in increasing striatal DA release. The action of KA on striatal DA release appeared specific, since striatal

ACh levels were instead decreased by KA. Furthermore, NMDA and quisqualic acid produced increase of striatal ACh levels. In the cortex, KA produced a decrease in cortical DA, which, at low doses, was paralleled by an increase in cortical ACh.

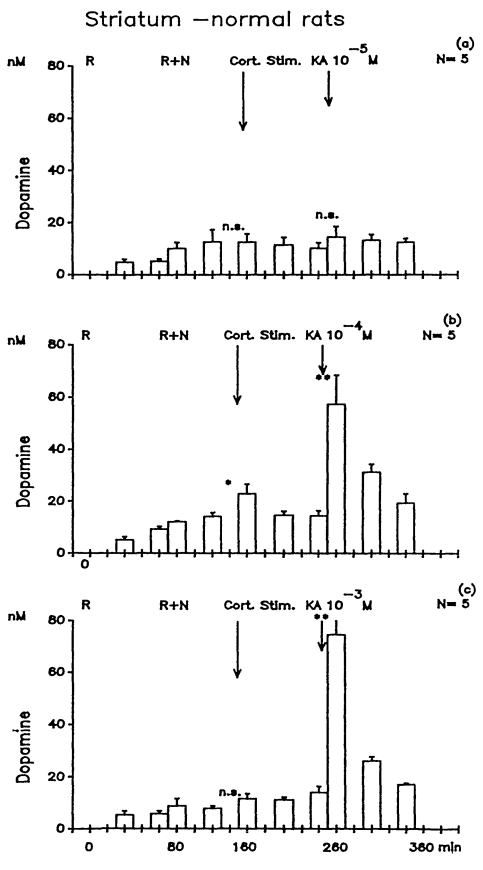

Fig. 1a,b,c. Means of dopamine levels in samples collected by microdialysis from the left striatum of normal adult rats. R (Ringer) is used as perfusion medium. N (neostigmine) is included 80 min after the implantation time. KA (kainic acid) is included 260 min after the implantation time. Cort. stim. = cortical stimulation. Abscissa: time (min) after the implantation of the microdialysis probe; ordinate: concentration of dopamine (nM). Vertical lines show standard errors of the means. Comparisons have been tested with Student's t-test against the values of the adjacent sampling fraction. * = P<0.05; ** = P<0.01.

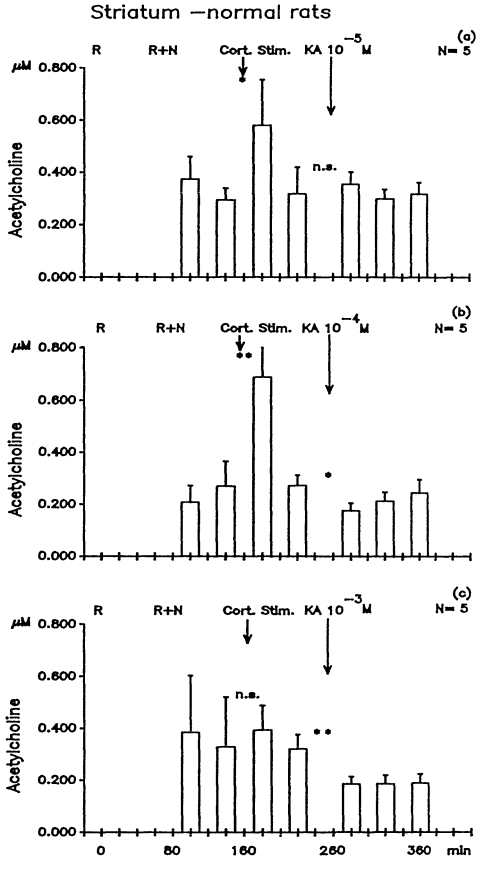

Fig. 2a,b,c. Means of acetylcholine levels in samples collected by microdialysis from the left striatum of normal adult rats. Abscissa: time (min) after the implantation of the microdialysis probe; ordinate: concentration of acetylcholine (μM). See also legend of Fig. 1.

The present results are in agreement with the idea of an excitatory regulation of striatal DA release by a glutamatergic pathway, with cell bodies located in the cortex and axons impinging on the ipsilateral DA terminals [4,5]. The stimulation produced by KA on striatal DA supports the hypothesis of direct axonal interactions between cortical glutamate and striatal DA terminals [6,7]. The parallel decrease observed in striatal ACh may represent a secondary effect due to the DA release. It is probable that glutamate terminals have a tonic stimulatory action on ACh neurons as well, since ACh levels were increased by NMDA and quisqualic acid, while DA release was only moderately increased. It is probable that the ACh increase produced by NMDA, and also by quisqualic acid, exerts in turn a stimulatory effect on DA terminals. Indeed, Carter *et al.*, [15] have presented results of a trans-striatal dialysis study, suggesting that while both NMDA and kainate receptor stimulations are responsible for a glutamate-evoked liberation of striatal DA, the stimulation produced by NMDA receptors may be conveyed by a polysynaptic loop since it is fully blocked by atropine and tetrodotoxin. The increase in striatal DA following cortical KA stimulation is in agreement with the observation that intracortical KA stimulation produces, dose-dependently, contralateral rotation which is inhibited by the DA antagonist, *cis*-(Z)flupentixol [16–18]. It is probable, however, that the main action of cortical stimulation is on striatal ACh release, since, at low doses, cortical stimulation produced a strong striatal ACh increase, but slight or no increase in striatal DA.

Acknowledgements

This study was supported by grants from the Medical Research Council (K88-21P-08154-02B; B89-14X-08669), Karolinska institutet fonder, The Swedish Medical Society, Loo och Hans Ostermans fond, Carnegie Medicin AB. The authors would like to thank Ms Monica Karlsson for excellent secretarial assistance.

References

1. Cheramy A, Romo R, Godeheu G, Baruch P and Glowinski J (1986) Neuroscience 19: 1081–1090.
2. Romo R, Cheramy A, Godeheu G and Glowinski J (1986a) Neuroscience 19: 1079–1086.
3. Romo R, Cheramy A, Godeheu G and Glowinski J (1986b) Neuroscience 19: 1091–1099.
4. Giorguieff MF, Kemel ML and Glowinski J (1977) Neurosci. Lett. 6: 73–77.
5. Roberts PJ and Sharif NA (1978) Brain Res. 157: 391–395.
6. Roberts PJ, McBean GJ, Sharif NA and Thomas ER (1982) Brain Res. 235: 83–91.
7. Bouyer JJ, Park DH, Joh TH and Pickel VM (1984) Brain Res. 302: 267–275.
8. Somogyi P, Bolam JP and Smith AD (1981) J. Comp. Neurol. 195: 567–584.
9. Cotman CW, Monaghan DT, Ottersen OP and Storm-Mathisen J (1987) TINS 10: 273–280.
10. Herrling PL (1985) Neuroscience 14: 417–426.
11. Ungerstedt U, Herrera-Marschitz M, Jungnelius U, Ståhle L, Tossman U and Zetterström T (1982) In: Tsukada Y, Shomori T, Tsukada Y and Woodruff GM (eds.) Advances in Dopamine Research, Advances in the Biosciences. Pergamon Press, Oxford, pp. 219–231.

12. Zilles K (1985) The Cortex of the Rat: A Stereotaxic Atlas. Springer, Berlin, p. 121.
13. Reid M, Herrera-Marschitz M, Hökfelt T, Terenius L and Ungerstedt U (1988) Eur. J. Pharmacol. 147: 411–420.
14. Maysinger D, Herrera-Marschitz M, Carlsson A, Garofalo L, Cuello AC and Ungerstedt U (1988) Brain Res. 461: 355–360.
15. Carter CJ, L'Heureux R and Scatton B (1988) J. Neurochemistry 51: 462–468.
16. Herrera-Marschitz M, Goiny M and Ungerstedt U (1988a) Acta Physiol. Scand. 132: 5.
17. Herrera-Marschitz M, Utsumi H, Goiny M and Ungerstedt U (1988b) Psychopharmacology 96: 25.
18. Herrera-Marschitz M, Goiny M, Utsumi H and Ungerstedt U (1989) Neurosci. Lett. 97: 266–270.

Address for correspondence: Mario Herrera-Marschitz, Department of Pharmacology, Karolinska Institutet, Box 60 400, S-104 01 Stockholm, Sweden.

Section III
Pharmacology/Physiology

Effect of arginine-aspartate on free amino acid levels in various brain regions and pituitary of stressed rats

Francesca R. Patacchioli, M. Assunta Di Cesare, M. Adelaide Micci and Luciano Angelucci

Institute of Pharmacology II, Medical Faculty, University of Rome 'La Sapienza', I-00185 Rome, Italy

Abstract

The effects of stress and arginine-aspartate treatment on brain and pituitary free amino acid levels were investigated.

Chronic oral treatment with arginine-aspartate reduced the rat adrenocortical stress response to 3 h of cold exposure or to a pure psychological stressor (novel environment). This buffering effect on stress response has been studied in relation to changes in free amino acids levels in the pituitary, in the whole brain and in various brain regions (hippocampus, hypothalamus, frontal cortex).

ALA, GLU and GABA were especially increased in the hippocampus of stressed rats, GLU and ASP in the hypothalamus, TYR and GLU in the frontal cortex. In the pituitary of stress exposed rats ARG and PHE were decreased and TRP increased.

Pre-treatment with arginine-aspartate counteracted many of the area-selective modifications observed in free amino acids levels of stressed rats.

In conclusion, it is suggested that changes in brain and pituitary free amino acids content might be the basis for the reduction of the adrenocortical stress response following arginine-aspartate treatment in the rat.

In this report a slightly modified HPLC method for the determination of the amino acids in brain tissue, utilizing pre-column derivazation with Dns-Cl, is also described.

Introduction

Stressful events provoke several neurochemical and hormonal variations which are controlled in different ways since the stress response can be displayed by different patterns. The mechanisms by which hypothalamus-pituitary-adrenal axis (HPAA) stress response is regulated are often explained by reference to monoaminergic and endocrine systems (for review see Ref. [1]).

Since evidence for a function of brain free amino acids as metabolic intermediates and neurotransmitters has been accumulating in recent years [2,3], it seemed interesting to evaluate brain and pituitary free amino acids level in stress-exposed rats.

Arginine is an amino acid known to produce various effects on the endocrine system, as those reported for growth hormone, insulin and glucagon [5,6], and the role of aspartic acid as neurotransmitter has been established [7]. Furthermore, oral administration of arginine-aspartate in the rat is able to stimulate protein phos-

phorylation in discrete brain regions [8], and by autoradiography, Blanquet and Laparra have demonstrated the selective accumulation of arginine-aspartate at the level of the rat pituitary and adrenal [9]. This peculiar localization may point to a specific action of arginine-aspartate on the hormonal activity of the hypothalamo-pituitary-adrenal axis.

On this basis, we have studied the effect of arginine-aspartate on the rat adrenocortical stress response in relation to the levels of free amino acids: a) in whole brain; b) in the hippocampus and hypothalamus, brain structures involved in the modulation of the adrenocortical stress response [10,11]; c) in the frontal cortex, where an increase in protein phosphorylation following arginine-aspartate treatment has been demonstrated [7]; d) in the pituitary, where arginine-aspartate after systemic administration highly concentrates [9].

In this report a modification of the method, previously described by Wiedmeier *et al.* [4], for the determination of brain free amino acids, utilizing pre-column derivatization with Dansyl-chloride (Dns-Cl), is reported. A special emphasis has been placed to increase sensitivity and improve resolution of selected amino acids that have been identified as acting as neurotransmitters.

Materials and Methods

Animals

Male Wistar rats, 3-month-old (300–330 g) with food and water available *ad libitum* and kept under a 12 h dark/light cycle, were used.

All experiments were performed between 9.00 and 12.00 a.m.

Stress procedures

Cold stress

Rats were exposed at 4°C for 3 h in a refrigerated room in individual cages, and killed by decapitation immediately at the end of this period.

Psychic stress

Rats were transferred into a novel cage and a novel room for 1 min, then returned to the home cage and killed 15 min later.

Treatment

Arginine-aspartate (Chinoin S.p.A., Milan-Italy) was dissolved in saline and administered orally by a gastric probe at a dose of 750 mg/kg of body weight for 5 days or at a dose of 2 g/Kg of body weight for 8 days. The animals were sacrificed 3 h after the last administration.

Corticosterone assay

Trunk blood samples were centrifuged at 1,500 × g, plasma removed and stored at −20°C until corticosterone content assay.

Plasma corticosterone was measured by a competitive binding assay using corticosterone binding globulin (CBG) from pregnant women, as previously described [13].

Tissue preparation

The brain was rapidly removed and dissected into frontal cortex, hypothalamus, hippocampus following the guidelines of Gispen *et al.* [14], quickly frozen on dry ice, and kept at −70°C until assayed.

HPLC conditions

The high performance liquid chromatograph (Kontron Instruments, Milan-Italy) consisted of two M420 pumps with an automatic gradient programmer M491, an autosampler M460 with a 1–40 µl sample loop. Fluorescence was detected using a fluorimetric detector SFM 25, coupled with a micro-flow cell. The apparatus was controlled by a computer system (Data System 450).

Pre-packed C 18 reversed-phase column (Supelco, 5 µm, 250 × 4.9 mm) maintained at 25°C, with a oven controller M480, was used for separation.

The mobil phase consisted of two solutions, with the flow being switched from one solution to the other in a step gradient manner. Solution 'A' was made up of 4 mM acetate buffer, adjusted to pH 4.25 and tetrahydrofuran (95:5). Solution 'B' consisted in acetonitrile: Tetrahydrofuran (90:10). The mobil phase was begun at a flow rate of 1.0 ml/min at 10% B and increased to 40% B over 30 min, at which time an isocratic hold lasting 15 min was instituted. At the end of the isocratic period, B was increased to 100% over 3 min and maintained at 100% for an additional 12 min. The column was then re-equilibrated with A:B (90:10) for 30 min.

Sample preparation

Each brain tissue was extracted twice by homogenization in ice-cold 80% ethanol (10 ml/g of tissue).

Protein content was measured according to Lowry *et al.* [15]. Pooled supernatants were evaporated to dryness in a vortex evaporator (Buchler Instruments, Searle-U.S.A.). The residue was dissolved in Titrisol buffer, pH 8.0 (Merck) immediately before the derivatization reaction with Dns-Cl (Merck).

Standards stock solutions were prepared by dissolving the appropriate amount of various amino acids (Sigma) in Titrisol buffer to yield a 5–10 mM concentration. Appropriate volumes of each amino acid were mixed together and brought to the final reaction volume with Titrisol buffer.

Samples, standards and samples containing internal standards for each amino acid were derivatizated together by Dns-Cl reagent (6 mg/ml acetone), at pH 9.0–9.2. After an overnight incubation, the reaction was stopped by adding Titrisol buffer (0.8 ml). Tubes were then centrifuged to remove any precipitate and 20 µl of the supernatant injected into the column.

The reaction remained stable for at least 72 h, which is very useful when an automatic sample injector is utilized.

Computation

The amino acid concentration was calculated using a standard curve for each amino acid, generated by determining in triplicate the peak area ratio between three different amounts of each amino acid, and considering the area of the standard alone and that of sample + standards.

All data were tested for homogeneity of Variance by Bartlett's test and analyzed by ANOVA, followed by Duncan's New Multiple Range test [16].

Results

Figure 1 shows a chromatogram of a standard mixture of amino acids Dns-derivatizated as described in the Materials and Methods section. Each peak represents 120 pmoles of the amino acid at 1/3 of the maximal sensitivity of the fluorimeter.

Calibration curves prepared for each of the amino acids showed a quite good linearity over a 10-fold concentration range (35–350 pmoles), which bracketed the concentrations observed in tissue extracts. Linear regression lines, used to calculate concentrations, had correlation values (r) of 0.98–0.99 for each amino acid. Precision was determined by analysing on 4 different days standard solutions containing 200 pmoles of each amino acid. Means ± S.E.M. of the calculated peak area ratios (Response Factor) were as follows: asparagine (ASN) 9.65 ± 0.16, glutamine (GLN) 7.18 ± 0.08, serine (SER) 7.37 ± 0.50, aspartate (ASP) 17.19 ± 2.46, glutamate (GLU) 11.72 ± 0.10, glycine (GLY) 3.94 ± 0.06, arginine (ARG) 3.22 ± 0.05, alanine (ALA) 4.65 ± 0.06, gamma amino-butyric acid (GABA) 2.25 ± 0.02, phenylalanine (PHE) 2.32 ± 0.07, tryptophan (TRP) 2.77 ± 0.01, tyrosine (TYR) 39.03 ± 0.96.

Figure 2 shows a chromatogram obtained from injection of an extract of rat hypothalamus, corresponding to 0.5 mg of brain tissue. Although some unidentified peaks were apparent, they were minor and eluated at times different from those of the standard mixture. Moreover, to evaluate the yield of the derivatization reaction, an internal standard mixture was utilized for each sample.

In one series of experiments we have studied the effect of a 5-day oral treatment with 750 mg/kg/day on the adrenocortical stress response to a 3 h cold exposure.

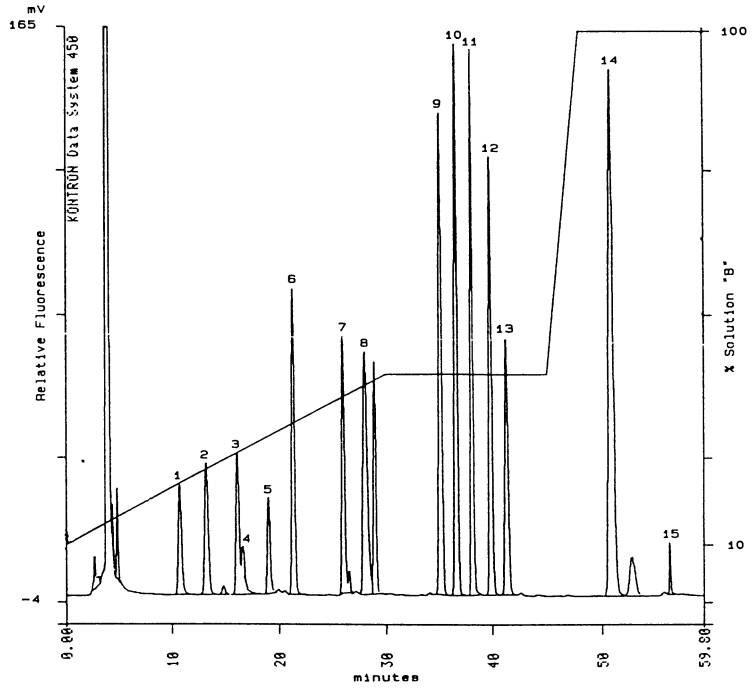

Fig. 1. A chromatogram showing the relative fluorescence and retention time of a standard mixture of amino acids after Dns-derivatization. Key to numbers: 1 ASN; 2 GLN; 3 SER; 4 ASP; 5 GLU; 6 GLY; 7 ALA; 8 ARG; 9 DNS-AMIDE; 10 GABA; 11 PHE; 12 TRP; 13 LEU + ILEU; 14 LYS; 15 TYR. For separation procedure, see *Materials and Methods.*

As reported in Table 1, treatment with arginine-aspartate did not modify basal plasma corticosterone concentration measured three h after the last administration, whereas it significantly reduced the adrenocortical stress response to cold-exposure.

In these animals whole brain free amino acids were measured (Table 2). Cold-stress induced a significant reduction of GABA and ASP levels. Treatment

Table 1. Plasma corticosterone levels (μg/100 ml) of male Wistar rats treated for 5 days with arginine-aspartate (750 mg/kg/day, per os), in basal condition and after 3 h of cold-exposure

Saline-treated, unstressed	1.85 ± 0.73
Saline-treated, stressed	28.83 ± 7.64[b]
Arginine-aspartate treated, unstressed	2.22 ± 0.42
Arginine-aspartate treated, stressed	14.41 ± 3.63[ac]

Mean values ± S.E. of 6 animals. [a] $p<0.05$, [b] $p<0.01$, respectively vs saline-treated unstressed group; [c] $p<0.05$ vs saline-treated stressed. ANOVA, followed by Duncan's New Multiple Range test.

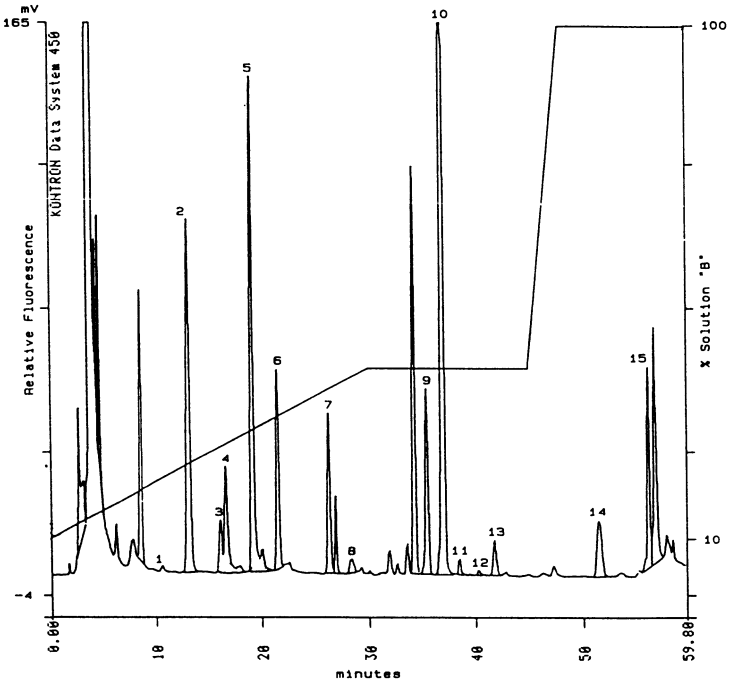

Fig. 2. An extract of rat hypothalamus, chromatographed after Dns-derivatization, without internal standard. Key to numbers as in Fig. 1.

with arginine-aspartate did not essentially modify the brain content of the free amino acids, but reversed the stress-induced changes in the levels of GABA and ASP, and induced a parallel increase in ALA and GLY concentration in stress-exposed rats.

Table 2. Brain free amino acids levels (nmoles/g fresh tissue) in male Wistar rats treated for 5 days with arginine-aspartate (750 mg/kg/day, per os), in basal condition and after 3 h of cold exposure

Amino acid	C	S	T	T+S
GABA	1800 ± 82	1562 ± 90[a]	1929 ± 145	2338 ± 225[ab]
ALA	841 ± 46	758 ± 54	876 ± 46	1105 ± 120[ab]
GLU	7374 ± 303	6698 ± 499	7534 ± 413	8660 ± 559[ab]
ASP	3122 ± 184	2552 ± 106[a]	3287 ± 182	3775 ± 326[ab]
GLY	1109 ± 69	985 ± 68	1218 ± 85	1575 ± 166[ab]
ARG	3409 ± 112	3498 ± 207	3473 ± 170	3977 ± 280[ab]

Mean values ± S.E. of 6 animals. C, saline-treated unstressed; S, saline-treated stressed; T, arginine-aspartate treated unstressed; T+S, arginine-aspartate treated for 5 days and stressed immediately after the last administration. [a] $p<0.05$ vs C; [b] $p<0.05$ vs S. ANOVA, followed by Duncan's New Multiple Range test.

Table 3. Plasma corticosterone levels (μg/100 ml) of male Wistar rats treated for 8 days with arginine-aspartate (2 g/kg/day, per os), in basal condition and 15 min after 1 min exposure to a novel environment

Saline-treated, unstressed	5.12 ± 1.51
Saline-treated, stressed	13.23 ± 2.69[a]
Arginine-aspartate treated, unstressed	3.84 ± 0.63
Arginine-aspartate treated, stresses	8.5 ± 1.61[a]b

Mean values ± S.E. of 6 animals. [a] $p<0.05$ vs saline-treated unstressed group; [b] $p<0.05$ vs saline-treated stressed group, ANOVA, followed by Duncan's New Multiple Range test.

In order to investigate the above preliminary results in more depth, a second series of experiments was performed aimed at studying the effect of a 8-day oral treatment with 2 g/kg/day of arginine-aspartate on the adrenocortical response to a pure psychological stressor (novel environment), so avoiding the physical component of the cold stress procedure. Furthermore, free amino acids were measured in discrete brain regions, to establish whether the stress-induced modifications of free amino acids, and the neurochemical effects of arginine-aspartate treatment, had a regional distribution.

As expected, 15 min after the exposure to a novel environment a significant increase in plasma corticosterone concentration was found (Table 3). Treatment with arginine-aspartate did not modify the basal activity of the hypothalamo-pituitary-adrenal axis, as shown by the level of plasma corticosterone measured 3 h after the last administration (Table 3). However, arginine-aspartate was able to significantly prevent the stress-induced increase in plasma corticosterone level, thus confirming the limiting effect on the stress response observed in the experiment reported in Table 1.

In these animals free amino acids levels were measured in the hippocampus (Fig. 3), hypothalamus (Fig. 4), frontal cortex (Fig. 5) and pituitary (Fig. 6).

As shown in Fig. 3, psychological stress was characterized by a statistically significant increase of ALA content (+24%). Moreover a tendency to an increase for ASP (+18.8%), GLU (+14.8), GABA (+17.8) and PHE (+14.5%) and a tendency to a decrease for TYR (−20.7%) was also detected.

Chronic arginine-aspartate treatment induced a significant increase (+15.8%) of ARG content in the hippocampus as well as of TRP (+24.5%), which was not very far from a statistical level (Fig. 3). Pre-treatment with arginine-aspartate induced an increase of GABA (+32%, $p<0.05$), ASN (+33.7%, $p<0.05$), GLN (+33%, $p<0.05$), GLY (+76%, $p<0.01$), and TRP (+69%, $p<0.01$) in the hippocampus of stress exposed rats (Fig. 3).

The 8-day oral treatment with 2 g/kg of arginine-aspartate induced a statistically significant increase of ARG content (+32%) as well of GLU (+39%) in the hypothalamus (Fig. 4). Moreover a 35% decrease of TRP level and, as shown in Fig. 4, an increase of hypothalamic GLU content (+24%) in psychological-stress exposed rats was also found. Pre-treatment for 8 days with arginine-aspartate was

able to significantly counteract some of the stress-induced changes in free amino acids hypothalamic content, as for GLU and PHE.

In the frontal cortex (Fig. 5), treatment with arginine-aspartate did not substantially modify the free amino acids levels. The stress-exposure produced an important increase in TYR content, which was completely blocked ($p<0.001$) by 8-day treatment with arginine-aspartate (Fig. 5). In treated and stressed rats an increase in frontal cortex ARG content was also found.

In the pituitary of rat chronically treated with arginine-aspartate (Fig. 6), a significant increase in the levels of GLN (+25.7%), GLU (+16.6%), ARG (+24%), ALA (+36%), GABA (+40%), PHE (+31%), TRP (+42%) and TYR (+38%) were

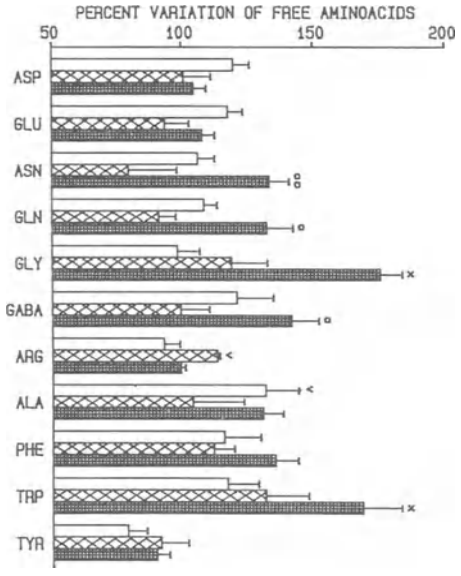

Fig. 3. Percent variations ± S.E. versus saline-treated rats (n=6) of free amino acids in the hippocampus. Open columns: Saline-treated, stressed; crossed columns: Arginine-aspartate-treated, unstressed; filled columns: Arginine-aspartate-treated, stressed. Control values (nmoles/mg protein) of free amino acids in saline treated group, referred as 100%: ASP 458 ± 44; GLU 1268 ± 103; ASN 363 ± 38; GLN 181 ± 27; GLY 4 ± 0.3; GABA 190 ± 20; ARG 7 ± 0.7; ALA 85 ± 7; PHE 207 ± 37; TRP 0.68 ± 0.1; TYR 18 ± 2. v $p<.05$ vs Saline-treated, unstressed; x $p<0.05$ vs Saline-treated, stressed; o $p<0.05$ and oo $p<0.01$ vs Arginine-aspertate-treated, unstressed (ANOVA, followed by Duncan's New Multiple Range test).

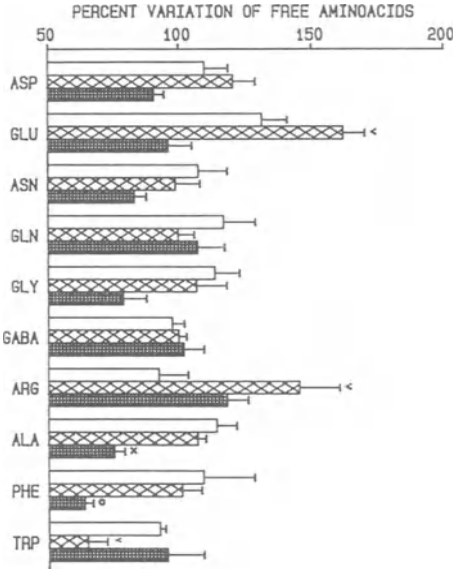

Fig. 4. Percent variations ± S.E. versus saline-treated rats (n=8) of free amino acids in the hypothalamus. Open columns: Saline-treated, stressed; crossed columns: Arginine-aspartate-treated, unstressed; filled columns: Arginine-aspartate-treated, stressed. Control values (nmoles/mg protein) of free amino acids in saline treated group, referred as 100%: ASP 305 ± 44; GLU 416 ± 12; ASN 111 ± 10; GLN 135 ± 13; GLY 28 ± 2; GABA 207 ± 7; ARG 3 ± 0.3; ALA 26 ± 3. PHE 0.93 ± 0.2; TRP 2 ± 0.5. v $p<0.05$ vs Saline-treated, unstressed; x $p<0.05$ vs Saline-treated, stressed; o $p<0.05$ vs Arginine-aspartate-treated, unstressed (ANOVA, followed by Duncan's New Multiple Range test).

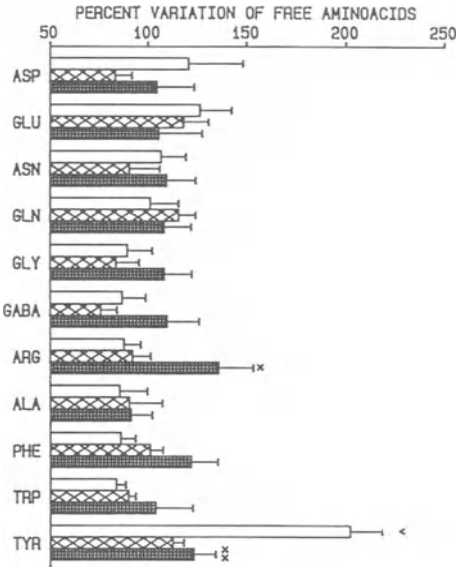

Fig. 5. Percent variations ± S.E. versus saline-treated rats (n=6) of free amino acids in the frontal cortex. Open columns: Saline-treated, stressed; crossed columns: Arginine-aspartate-treated, unstressed; filled columns: Arginine-aspartate-treated, stressed. Control values (nmoles/mg protein) of free amino acids in saline-treated group, referred as 100%: ASP 202 ± 20; GLU 859 ± 82; ASN 277 ± 65; GLN 147 ± 25; GLY 23 ± 4 ; GABA 170 ± 28; ARG 4 ± 0.7; ALA 75 ± 11; PHE 148 ± 9; TRP 0.85 ± 0.04; TYR 4 ± 0.65. v $p<0.001$ vs Saline-treated, unstressed; x $p<0.05$ and xx $p<0.001$ vs Saline-treated, stressed; oo $p<0.001$ vs Arginine-aspartate-treated, unstressed (ANOVA, followed by Duncan's New Multiple Range test).

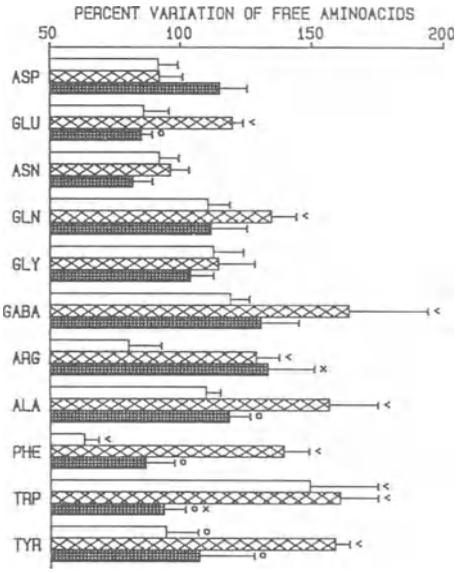

Fig. 6. Percent variations ± S.E. versus saline-treated rats (n=6) of free amino acids in the pituitary. Open columns: Saline-treated, stressed; crossed columns: Arginine-aspartate-treated, unstressed; filled columns: Arginine-aspartate-treated, stressed. Control values (nmoles/mg protein) of free amino acids in saline-treated group, referred as 100%: ASP 582 ± 45; GLU 741 ± 62; ASN 682 ± 54; GLN 525 ± 39; GLY 76 ± 11; GABA 10 ± 0.56; ARG 20 ± 1; ALA 83 ± 11; PHE 16 ± 2; TRP 1 ± 0.09; TYR 22 ± 3. v $p<0.05$ vs Saline-treated, unstressed; x $p<0.05$ vs Saline-treated, stressed; o $p<0.05$ vs Arginineaspartate-treated, unstressed (ANOVA, followed by Duncan's New Multiple Range test).

detected. As also shown in Fig. 6, in the same animals an increase in TRP (+32%) and a significant decrease in PHE levels (−37%) was found. Such modifications were reversed by arginine-aspartate pre-treatment.

Discussion

The HPLC method described by Wiedmeier *et al.* [4], which has been modified here for the mobile phase concentration, for the incubation buffer and for the

careful control of the operating conditions exerted by computer, permits the separation of many of the Dns-derivatives of amino acids contained in brain and pituitary extracts. The levels of amino acids reported in this study for whole brain tissues and brain areas were similar to those recently reported [17,18]. Quite new, we found an outstandingly lower level of GABA in the pituitary compared to the brain tissue.

Chronic oral administration of arginine-aspartate in the rat reduced the adrenocortical stress response to a 3 h cold exposure and to a pure psychological stressor.

The effect of stress from cold-exposure on whole brain amino acid concentrations reported in this paper was substantially in agreement with the findings of other researchers, who used different types of stress procedures [19,20].

It is difficult to discuss in an unitary way the data, reported in their completeness, on the effect of psychological stress on various brain regions. Mechanisms of psychological stress response are neurally mediated through specific neuromodulators and neurotransmitters [21], (for a review see Ref. [1]). At each regulatory level along the HPAA several regulatory mechanisms can be encountered, with the interaction of neurotransmitters, neuropeptides and peripheral hormones, thus ensuring an integration in the brain. The net effect on adrenocortical secretion is resulting from the above multiple interactions of stimulatory and inhibitory nature.

In this paper we have demonstrated stress-induced changes in the levels of free amino acids. A distinct pattern of tendential or statistically significant variations has been found for several amino acids after stress. ALA, GLU and GABA were increased especially in the hippocampus, GLU and ASP in the hypothalamus, TYR and GLU in the frontal cortex. In the pituitary, ARG and PHE were decreased and TRP increased. The concentration of free amino acid in the pituitary was analyzed considering the close functional link between neurotransmitter-neurohormonal systems in the brain and the pituitary activity. The knowledge of regional changes of free amino acids concentrations after stress suggested, better than whole brain measurement the indication of a possible physiological involvement of the various identified amino acids, and the demonstration of their connection with the effect of arginine-aspartate treatment.

Oral administration of arginine-aspartate modified free amino acids concentrations especially in the pituitary, suggesting that exogenous amino acids can change not only the level of the same amino acids, but also the availability of others, possibly through metabolic pathways. However, pre-treatment with arginine-aspartate counteracted some area-selective modifications in free amino acid levels in the psychological stress-exposed rats.

The changes in brain and pituitary free amino acids reported in this paper might account for certain of the pharmacological effects of arginine-aspartate administration [5,6], including changes in protein phosphorilation [9].

Finally, it would appear that changes in the concentration of brain and pituitary amino acids, especially those precursor of neurotransmitters, constitute a mechanism of arginine-aspartate action in the reduction of stress response.

Acknowledgements

We would like to thank Mr. M. Comuzio for his helpful technical assistance.

References

1. Keller-wood ME and Dallman MF (1984) Endocrinol. Rev. 5: 1-24.
2. Fonnum F (1984) J. Neurochem. 42: 1-11.
3. Hawkins RA and Mans AM (1983) In: Handbook of Neurochemistry, Plenum Press, New York, 3: 259-294.
4. Wiedmeier VT, Porterfield SP and Hendrich CE (1982), J. Chnomatagr. 231:4110-417.
5. Franchimont P, Campistrom G, Creuzet MH, Gros J and Luyckx A (1984) Arch. Intl. Pharmacoyn. 287: 161-468.
6. Franchimont P, Luyckx A, Campistrom G and Gros J (1979) Therapie 34: 641-647.
7. Nadler JW, White WF, Vaca KW, Perry BW and Cotman (1978) J. Neurochem. 31: 147-155.
8. Cehovich G (1983) C.R. Acad. Sci. Paris 298: 207-212.
9. Blanquett P and Lapana J (1968) La Semaine des Hopitaux 10: 648-647.
10. Angeluci L, Valeri P, Palmery M, Patachioli FR and Catalani A (1980) Biochem. Psychopharmacol. 21: 394-395.
11. Casady RL and Taylor AN (1976) Neroendocrinology 20: 68-78.
12. Confonti N and Feldman S (1978) Neroendocrinology 22:1-7.
13. Murphy BEP (1967) J. Clin. Endocrinol. 27: 955-973.
14. Gispem WH, Schotman P and De Kloet ER (1972) Neroendocrinology 9: 285.
15. Lowy OH, Rosenbrough NJ, Farr AL and Randall RJ (1951) J. Biol. Chan. 183: 265-275.
16. Winear BJ (1982) Statistical Principles in Experimental Design. McGraw-Hill-Kogakusha, Tokyo.
17. Wison WE, Hudson PM, Karamatsu T, Walsh TJ, Tilson HA, Hong JS, Mavenport RR and Thompson M (1986) Neurotoxicology 7: 655-669.
18. Hikal AH, Lipe GW, Slikker W Jr., Scallet AC, Ali SF and Newport GD (1988) Life. Sci. 42: 2029-2035.
19. Eroglu L, Binjildiz P and Atamer-Simsek S (1980) Psychopharmacology 70: 187-189
20. Weyne J, Leuven FV, Kazemi H and Leusen I (1979) J. Appl. Physiol. 44: 333-339.
21. Patacchioli FR, Alemà S, Cigliana G, Maccari S, Micci MA and Angelucci L (1988) Pharmacol. Res. Commun. 20: 293-294.

Address for correspondence: Dr. Francesca Romana Patacchioli, Institute of Pharmacology II, Medical Faculty, University of Rome 'La Sapienza', Piazza Aldo Moro 2, I-00185 Rome, Italy.

Effects of L-tyrosine and L-tryptophan on the cardiovascular and endocrine system in humans

Hendrik Lehnert[a], Juergen Beyer[a] and Dirk H. Hellhammer[b]

[a]Third Medical Clinic, Department of Endocrinology and Metabolism, University of Mainz, F.R.G.
[b]Department of Clinical and Physiological Psychology, University of Trier, F.R.G.

Introduction

Brain catecholamine and serotonin neurons are intimately involved in a number of relevant physiological functions such as cardiovascular regulation, neuroendocrine output from the anterior pituitary (e.g. ACTH, prolactin), regulation of behavior (e.g. aggression, sleep, locomotor and sexual behavior), mood or appetite control [1–5]. The modification of transmitter synthesis and release appears to be remarkably correlated with the subsequent physiological changes observed. While there are numerous pharmacological approaches that affect the respective neurotransmitter products (i.e. the catecholamines dopamine, noradrenaline and adrenaline and the indoleamine serotonin), one particular attractive (while specific) approach is the administration of a precursor amino acid. It is thus a prerequisite for the physiological and possibly therapeutical properties of the precursor amino acids L-tyrosine and L-tryptophan that they affect synthesis and release of their transmitter product. For the understanding of the nature of the different physiological responses some of the neurochemical mechanism guiding the transmitter synthesis need to be briefly described.

The synthesis of brain serotonin depends on the availability of the large neutral amino acid L-tryptophan that is hydroxylated to 5-1-hydroxytryptophan and subsequently decarboxylated to yield serotonin. The rate-limiting enzyme tryptophan hydroxylase has a Michaelis-constant of approximately $2–3 \times 10^{-5}$ M with tetrahydrobiopterin used as a cofactor [6] and thus approximates normal brain tryptophan concentrations of about $1–5 \times 10^{-5}$ M. Therefore, the enzyme is not saturated under normal circumstances and an increased availability of brain tryptophan will lead to an enhanced synthesis of brain serotonin [7].

The availability of tryptophan to the central nervous system is further enhanced, when the amino acid is administered along with a high-carbohydrate meal. This is based on the finding that the carbohydrate-induced insulin secretion will lead to an uptake of those large neutral amino acids into striated muscle tissue that compete with tryptophan for transport across the blood brain barrier. Thus, as an index of tryptophan availability for brain serotonin synthesis a ratio of serum tryptophan to amino acids with comparable affinity for the cerebrovascular transport sites is

calculated (i.e. tyrosine, valine, phenylalanine, leucine and isoleucine). This ratio will be referred to as amino acid ratio. Tryptophan can be bound to serum albumin and is thus not subject to transport into the striated muscle cells. The albumin binding of tryptophan can be further enhanced by the insulin-induced dissociation of non-esterified fatty acids from albumin [8]. Both free and albumin-bound tryptophan can cross the blood brain barrier because of the high affinity of the transport molecule. Thus, the capacity of tryptophan to bind to albumin is important for prevention of striated muscle uptake and transport across the blood brain barrier. These mechanisms explain the clinically most relevant dependency of brain serotonin synthesis on the availability of tryptophan, the amino acid ratio and the composition of a previous meal.

While brain serotonin synthesis is affected by the availability of tryptophan already in a controlled state, the precursor dependency of catecholamine synthesis in the brain is coupled to the firing rate of the tyrosine hydroxylase (TOH) containing neuron. A large number of studies have clearly demonstrated, that a supplementation of L-tyrosine does not augment the synthesis of catecholamines under basal conditions, while an enhanced neuronal activity will increase synthesis and release of dopamine and noradrenaline following tyrosine application [9]. Therefore, experimental maneuvers such as psychological stress or pharmacological manipulations to enhance TOH activity are mandatory for L-tyrosine administration to affect catecholamine synthesis [10–12]. The mechanism that couples a catecholaminergic neuron's firing frequency to its precursor responsiveness involves phosphorylation of the tyrosine hydroxylase protein [13]. Thereby, the enzyme's affinity for its cofactor is enhanced and it becomes independent of end-product inhibition but dependent on the availability of tyrosine [14]. It also follows, that tyrosine supplementation does not affect brain catecholamine synthesis under basal conditions (in the quiescent state).

Much of our work has focussed on the physiological and possibly therapeutical effects of L-tyrosine and L-tryptophan in both animals and humans. We have principally investigated the state-dependent biological properties of these precursor amino acids and will briefly summarize some of our findings on the human cardiovascular and endocrine system.

Cardiovascular effects of L-tryptophan and L-tyrosine in humans

In animal experiments we were able to show that the administration of a drug regimen designed to enhance brain serotonergic neurotransmission, namely the immediate 5-HT precursor 5-hydroxytryptophan in conjunction with a peripheral decarboxylase inhibitor and MAO blockade, significantly decreased sympathetic outflow to the heart and vasculature [3,15,16]. In particular, while cerebrospinal fluid 5-HT and 5-HIAA were increased, blood pressure and heart rate were decreased. The ventricular fibrillation threshold was elevated indicating myocardial protection. Very likely, the neuroanatomical basis for this effect is the dense

innervation of sympathetic preganglionic neurons by bulbospinal serotoninergic neurons that originate in the raphe nuclei [17].

We then decided to investigate the cardiovascular, endocrine and behavioral effects of L-tryptophan in conjunction with two different diets (high-protein vs. high-carbohydrate diet) in humans [18–20]. In this study, 42 essential hypertensive patients were enrolled in a placebo-controlled, randomized and double-blind trial. After a wash-out phase, they received either tryptophan (50 mg/kg) or placebo for three weeks at 8 a.m.; in the first week, they ingested it together with a standard meal, in the second and third week either with a high-protein or high-carbohydrate meal in an intra-group cross-over design. Analysis of serum amino acids, plasma renin activity, serum aldosterone and cortisol was performed. At the end of the four week trial, blood pressure was significantly lower in the tryptophan than in the placebo group (Fig. 1). The subgroup analysis in the tryptophan-treated patients demonstrated a trend towards lower blood pressure levels in those patients, who received a carbohydrate-rich meal first as compared with those receiving a protein-rich meal first. Serum concentrations of tryptophan were increased significantly with no differences between the subgroups receiving the amino acid. Accordingly, a marked elevation in the plasma amino acid ratio in the groups receiving L-tryptophan was found, that was further enhanced when the patients ingested tryptophan together with a high-carbohydrate meal. Following a protein meal alone, the amino acid ratio was found to be significantly lower than following a high-carbohydrate meal alone (Fig. 2). Furthermore, a significant inverse correlation was observed between the ratio and blood pressure levels that suggests to us that carbohydrate intake may augment the tryptophan-mediated drop in blood pressure.

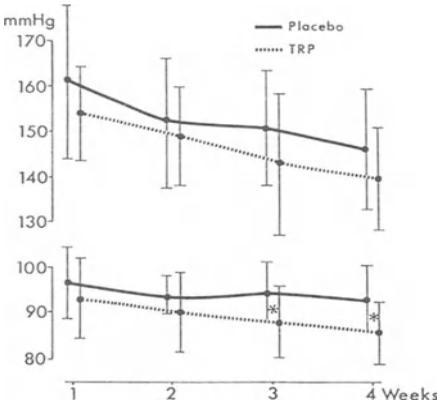

Fig. 1. Effects of oral intake of L-tryptophan (50 mg/kg) on blood pressure in essential hypertensives.

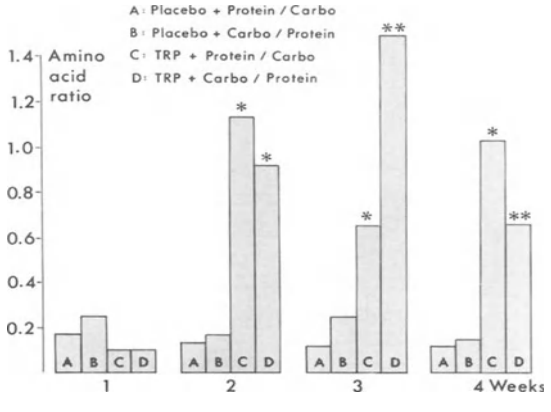

Fig. 2. Serum amino acid ratio following intake of L-tryptophan and various diets.

Although the involvement of brain serotonin in cardiovascular regulation is discussed very controversially, the results of this study are in accordance with a number of animal studies demonstrating depressor effects of brain serotoninergic neurons and in particular of L-tryptophan [21–24]. In addition, one human study found an acute effect of tryptophan on blood pressure in hypertensive patients [25]. The study on the antihypertensive effects of L-tryptophan in spontaneously hypertensive rats [23] clearly suggested that L-tryptophan acted by enhancing the serotonin release from the presynaptic neuron, since tryptophan's effects could be augmented by co-administration of fluoxitene, a presynaptic serotonin reuptake-blocker. Our data in summary suggests that tryptophan acts through a decrease in sympathetic nervous system activity to lower blood pressure. In addition, it is suggested that the serum amino acid ratio is of potential predictive relevance.

In a number of studies, the antihypertensive properties of L-tyrosine were investigated in the animal model with unequivocal results. Thus, a dose-dependent lowering of arterial blood pressure following peripheral or central application of L-tyrosine was found in different rat models of hypertension, e.g. spontaneously hypertensive rats (SHR) or DOCA salt rats [26–29]. Concurrently, increases of the norepinephrine metabolite MHPG sulfate in brain stem of spontaneously hypertensive rats (SHRs) was found following intraperitoneal injection of L-tyrosine [26].

Vice versa, the administration of tyrosine to rats made hypotensive by hemorrhagic shock significantly increased blood pressure, an effect likely mediated by enhanced peripheral (adrenomedullary) secretion of catecholamines [30]. These data thus apparently confirm that the blood pressure affecting properties of tyrosine are closely related to the state of the animal, i.e. to the starting blood pressure values. While tyrosine administration has little or no effect in normotensive rats, it lowers blood pressure in hypertensive rats presumably by augmenting norepinephrine synthesis and release in relevant brain stem areas, for example, *locus coeruleus* [31], and increases blood pressure in experimentally hypotensive rats.

So far, only sparse data are available in human essential hypertension; one controlled study was performed for two weeks in patients with mild essential hypertension and no effects of tyrosine were observed on blood pressure, heart rate and plasma norepinephrine levels, indicating that the administration of tyrosine has no beneficial effect at least in the patients studied [32]. We have recently concluded a controlled trial (3×1 g of tyrosine) for a period of 10 weeks in a cross-over design and obtained data that favor a similar interpretation.

These observations also clearly suggest that the experimental design and in particular the state of the organism is crucial to the outcome and implications of such experiments. We have thus decided to investigate the effects of both tyrosine and tryptophan in young borderline hypertensives. Borderline hypertensives represent a subgroup of patients with typical cardiovascular features, namely elevated systolic and normal to mildly elevated diastolic blood pressure levels with a high risk to develop stable hypertension. Their blood pressure values are between 140 and 160 mmHg (systolic BP) and/or 90 and 95 mmHg (diastolic BP). In

addition, strong hemodynamic reactions are observed during various stressful tasks such as mental challenge or cold pressure test. The rational for this study was to investigate whether a stress-induced increase in blood pressure is sensitive to precursor amino acid application.

A group of 15 male students who were previously identified as suffering from borderline hypertension were studied under three different, randomly applied conditions. For this purpose they received either 5 g of tyrosine, tryptophan or placebo and were exposed to a stressful task consisting of mental arithmetics for 15 minutes under continuous noise distraction of 90 dB. While the baseline blood pressure levels were similar for all three conditions, the stress-induced increase in systolic blood pressure was significantly attenuated in the tyrosine group when compared with tryptophan and placebo. Additionally, the higher the starting blood pressure, the more pronounced was tyrosine's antihypertensive effect [33]. Thus, while we did not observe an effect of tryptophan on blood pressure behavior in a stressful task, tyrosine appears to be beneficial in stress-induced blood pressure increases only.

Endocrine effects of L-tyrosine, L-tryptophan and macronutrient intake in humans

A number of hormonal effects are associated with the administration of L-tryptophan and little doubt exists that the intravenous application of L-tryptophan stimulates growth hormone and prolactin secretion in human subjects [34,35]. On the other hand little, if any, effect on the secretion of these hormones is observed following oral intake. The effects on ACTH release are even more inconsistent, with stimulatory [36] and inhibitory [37] modes of action described, although the majority of data supports a stimulatory effect on the hypothalamic-pituitary-adrenal axis in humans. Also in favor for a stimulatory role of the brain serotoninergic system is the finding that the spontaneous release of CRF from incubated hypothalami was stimulated by serotonin in a dose-dependent fashion and that this effect was antagonized by methysergide [38,39]. In addition, central serotoninergic neurons appear to stimulate aldosterone secretion both *in vivo* and *in vitro* and serotonin antagonists have been shown to decrease serum aldosterone concentrations in patients with idiopathic hyperaldosteronism [40].

In our study of essentially hypertensive patients, we did not find data robust enough to suggest a relationship between tryptophan intake and cortisol or aldosterone secretion, but our data did suggest a negative correlation between the amino acid ratio and plasma renin activity with renin activity being even significantly lower following intake of tryptophan and carbohydrates as compared to tryptophan and proteins. Since renin secretion can be promoted by activation of ß-adrenoceptors, lowering of plasma renin activity might indicate a reduction in sympathetic nervous tone.

Similarly, tryptophan intake had no major effect on serum cortisol concentrations, while independent of tryptophan intake the carbohydrate diet clearly appeared to lower serum cortisol levels. Episodic hormone secretion has to be considered, especially since we took only single blood samples, but these data are in accordance with findings from a recent study that investigated the effects of different diets on cortisol concentrations in normal men. Consistently lower concentrations of cortisol were found during the high-carbohydrate diet than during the high-protein diet with parallel changes in the level of the cortisol binding globulin [41]. It appears possible that alterations in hormone binding globulins reflect the intrahepatic effects of dietary factors on synthesis and degradation of liver-derived factors.

In another study we administered oral tryptophan and tyrosine (5 g each) to normal men and did not find a significant effect of tryptophan administration on prolactin and TSH secretion, while there was a minor increase in growth hormone levels. Similarly, tryptophan did not affect the TRH- or metoclopramide (MCP)-stimulated prolactin secretion. Very consistently though, a significant increase of basal levels of prolactin and TSH following intake of L-tyrosine with differential effects on the stimulated levels of these hormones was observed [42]. When stimulated with TRH and MCP following tyrosine administration, the prolactin surge was clearly attenuated when compared with tryptophan and placebo (Fig. 3). This effect on prolactin stimulation apparently was not due to elevated basal prolactin levels, since no correlation was found between basal and stimulated levels. The tuberoinfundibular dopaminergic system is thus a highly attractive model for studying the short-term regulation of prolactin secretion by modifying dopaminergic activity. It has been shown in normal rats that tyrosine injection does not change serum prolactin concentrations [43], while it reduces prolactin secretion in chronically reserpinized rats [44], i.e. under circumstances of neuronal activa-

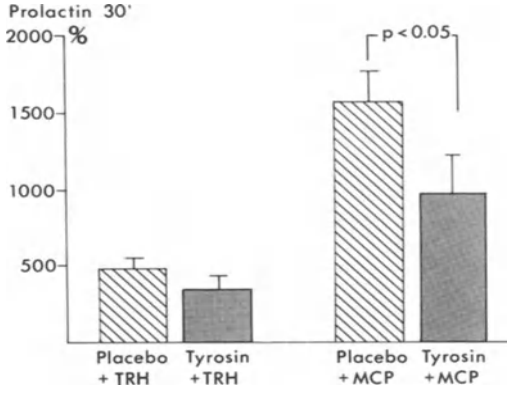

Fig. 3. Prolactin concentrations following injection of TRH and metoclopramide (MCP) in conjunction with tyrosine or placebo administration.

tion. Moreover, it was found that tyrosine injection increases DOPA production in the median eminence following intracerebral injection of ovine prolactin, a treatment that selectively enhances the activity of TIDA neurons.

Thus, since prolactin regulates its own secretion by stimulation of the TIDA system, tyrosine may act to amplify the inhibitory effects of dopamine. On the other hand, the TRH stimulated TSH secretion was further enhanced by tyrosine administration, suggesting an enhanced TRH release (which would also explain the increase in basal prolactin levels).

As demonstrated recently, tyrosine's effects on anterior pituitary hormone secretion appear to be mediated through central alpha-1 adrenoceptors. This has been shown in humans, where the combined administration of tyrosine and an alpha-2 antagonist enhanced ACTH secretion [45]. On the other hand, during stressful maneuvers in animals, tyrosine administration acted to decrease the stress-induced ACTH and corticosterone secretion presumably through augmented hypothalamic turnover, while under basal conditions a strong negative correlation was found between hypothalamic adrenaline levels and pituitary ACTH content [46]. Thus, the regulation of the HPA axis also appears to be subject to state-dependent control of precursor availability.

Conclusion

We have presented a number of examples for relevant physiological effects of the precursor amino acids L-tryptophan and L-tyrosine in humans. The differential influence on synthesis and release of their transmitter products, that have been experimentally found to depend on the state of the organism, are reflected in the various cardiovascular and endocrine responses described. We do not yet know, whether and if so, effective clinical interventions can be tailored based on these findings. Clearly though, the effects of micronutrients such as precursor amino acids on physiological systems and their promotion by macronutrients have to be considered for diagnostic (i.e. probing a specific neurotransmitter deficiency) and therapeutic approaches.

References

1. Wurtman RJ (1987) Integr. Psychiatry 5: 226–257.
2. Fernstrom JD (1983) Physiol. Rev. 63: 484–545.
3. Lehnert H, Lombardi F, Raeder EA, Lorenzo AV, Verrier RL, Lown B and Wurtman RJ (1987) J. Cardiovasc. Pharmacol. 10: 389–397.
4. Spring B, Chiodo J and Bowen DJ (1987) Psychol. Bull. 102: 234–256.
5. Lehnert H, Reinstein DK, Strowbridge BW and Wurtman RJ (1984) Brain Res. 303: 215–223.
6. Tong JH and Kaufmann S (1975) Biol. Chem. 250: 4152–4158.
7. Fernstrom JD and Wurtman RJ (1971) Science 173: 149–152.
8. Madras BK, Cohen EL, Messing R, Munro HN and Wurtman RJ (1974) Metabolism 23: 1107–1116.

9. Milner JD and Wurtman RJ (1986) Biochem. Pharmacol. 35: 875–881.
10. Reinstein DK, Lehnert H, Scott NA and Wurtman RJ (1984) Life Sci. 34: 2225–2231.
11. Sved A and Fernstrom JD (1982) Life Sci. 29: 743–748.
12. Roth RH, Morgenroth VA and Salzman PM (1975) Naun. Schmiedeb. Arch. Pharmacol. 289: 327–334.
13. El Mestikaway S, Glowinski J and Hamon M (1983) Nature 302: 830–832.
14. Lovenberg W, Ames MM and Lerner P (1978) In: Lipton MA, DiMascio A and Killam AF (eds.) Raven Press, New York, pp. 247–259.
15. Lehnert H, Lombardi F, Verrier RL, Lown B and Wurtman RJ (1983) J. Am. Coll. Cardiol. 1: 606.
16. Raeder EA, Berger R, Kenet R, Kiely JP, Lehnert H, Cohen RJ and Lown B (1987) J. Appl. Cardiol. 2: 283–300.
17. Bowker RM, Steinbusch HW and Coulter JD (1979) Brain Res. 211: 412–417.
18. Lehnert H, Beyer J, Heismann I, Siekermann H, Schmidt H, Ullrich K and Vetter H. Akt. Ernaehr. 13: 1–5.
19. Lehnert H, Beyer J, Hellhammer DH, Gutberlet I, Ullrich K and Vetter H. Submitted.
20. Lehnert H, Beyer J, Cloer E, Gutberlet I and Hellhammer D (1989) Neuropsychobiology 21:84–89.
21. Kuhn DM, Wolf WA and Lovenberg W (1980) Hypertension 2: 243–255.
22. Echizen K and Freed CR (1982) J. Pharmacol. Exp. Ther. 220: 579–584 (1982).
23. Sved AF, v. Itallie CM and Fernstrom JD (1982) J. Pharmacol. Exp. Ther. 221: 329–333.
24. Fregly MJ, Lockley OE, van der Voort J, Sumners C and Henley WN (1987) Can. J. Physiol. Pharmacol. 65: 753–764.
25. Feltkamp H, Meuer KA and Godehardt E (1984) Klin. Wschr. 62: 1115–1119.
26. Sved AF, Fernstrom JD and Wurtman RJ (1979) Proc. Natl. Acad. Sci. 76: 3511–3514.
27. Yamori Y, Fujiwara M, Horie K and Lovenberg W (1980) Eur. J. Pharmacol. 68: 201–204.
28. Bresnahan MR, Hatzinikolaou P, Brunner HR and Gavras H (1980) Am. J. Physiol. 239: H206–211.
29. Bossy J, Guidoux R, Milon H and Wuerzner HP (1983) Ztschr. Ernaehrwiss. 22: 45–49.
30. Conlay LA, Maher T and Wurtman RJ (1981) Science 212: 559–560.
31. Lehnert H, Maher T, Yokogoshi H and Wurtman RJ (1985) J. Hypertension 3: 412.
32. Sole MJ, Benedict CR, Myers MG, Leenen FHH and Anderson GH (1985) Hypertension 7: 593–596.
33. Diebschlag U, Lehnert H, Reche A, Warnecke W, Hellhammer D and Beyer J (1988) Acta Endocrinol. 120 (suppl. 1): 257.
34. Cowen PJ, Gadhvi H, Goseden B and Kolakowska T (1985) Psychopharmacology 86: 164–169.
35. Winokur A, Lindberg NO, Lucki I, Philipps J and Amsterdam JW (1986) Psychopharmacology 88: 213–219.
36. Modlinger RS, Schonmuller JM and Arora SP (1980) J. Clin. Endocrinol. Metabol. 50: 360–363.
37. Woolf PD and Lee L (1977) J. Clin. Endocrinol. Metabol. 45: 123–133.
38. Buckingham JC and Hodges JR (1977) J. Physiol. (Lond.) 272: 469–479.
39. Holmes MC, Renzo GD, Becford U, Gillham B and Jones MT (1982) J. Endocrinol. 93: 151–160.
40. Shenker Y, Gross MB and Grekin RJ (1985) J. Clin. Invest. 76: 1485–1490.
41. Anderson KE, Rosner W, Khan M, New M, Pang S, Wissel P and Kappas A (1987) Life Sci. 40: 1761–1768.
42. Lehnert H, Beyer J, Czernik C, Schneider KP, Schrezenmeir J and Krause U (1988) Akt. Ernaehr. 14: 41–43.
43. Donoso AO, Bishop W, Fawcett CP, Krulich L and McCann SM (1971) Endocrinology 89: 774–784.
44. Sved AF, Fernstrom JD and Wurtman RJ (1979) Life Sci. 25: 1293–1300.
45. Al-Damluji S (1988) J. Endocrinol. 119: 5–14.
46. Lehnert H, Beyer J, Reinstein DK, Richardson UI and Wurtman RJ (1988) Res. Exp. Med. 189: 289–293.

Address for correspondence: Dr. Hendrik Lehnert, Third Medical Clinic, University of Mainz, Langenbeckstr. 1, 65 Mainz, F.R.G.

Therapeutic basis for congenital hyperammonemia: The role of amino acids and their transport systems in ureogenesis in the primary culture of adult rat hepatocytes

Masayoshi Nagao[a], Toshihiko Mori[a], Yoshinori Kuniya[b] and Kazuhiko Oyanagi[a]

[a]Department of Pediatrics, Sapporo Medical College, Sapporo 060, Japan
[b]Division of Pediatrics, Sapporo Teishin Hospital, Sapporo 060, Japan

Abstract

The urea cycle enzyme deficiencies are the most common genetic causes of hyperammonemia in children and the clinical and biochemical features of respective diseases have been reported. However, the mechanism regulating ureogenesis has not been well clarified at the cellular level. We studied the relationship between urea synthesis and the transport of amino acids using the primary culture of hepatocytes from adult rats. The ammonia detoxication and urea synthesis were affected by the amino acids of urea cycle intermediates. The concentration of ammonia in the incubation medium containing ornithine, aspartate and arginine (2 mM) decreased more than it did in the medium with any other amino acids. But when glutamine was added to the medium, elimination of ammonia from the medium was inhibited. The rates of urea synthesis were high when these amino acids were added to the medium. When the hepatocytes were incubated in the medium containing 1 mM ammonium chloride, the transport activity of system-A mediated amino acid (MeAIB) did not change compared with the control level. The uptake of system-L mediated amino acid (BCH) increased slightly.

Glutamine uptake was decreased to about 60% of the control level. However, the transport activity of ornithine was increased to a maximum (four times the control) after 4 h of incubation with ammonia, and then decreased gradually to twice the control level. The activity of ornithine transcarbamylase was induced to twice the control at the same time. These results indicate that the amino acids of urea cycle intermediates, especially ornithine, can be the short-time regulator of ureogenesis through their transport processes.

Introduction

The liver is the most important organ for amino acid metabolism and plays a significant role for the disposal of ammonia. Catabolism of amino acids results in the production of free ammonia, which is toxic to the central nervous system. Ammonia is detoxified to urea through a series of enzyme reactions known as the urea cycle, which occurs primary in the liver [1]. Many reports on congenital hyperammonemia have been compiled and the clinical and biochemical features of the respective diseases have been ascertained [2]. However, the mechanism regulating ureogenesis and ammonia detoxication has not been well clarified. Many investigators have attempted to determine the factors involved in the regulation of ureogenesis. The close relationship between the hepatic levels of urea

cycle enzymes and the extent of urea excretion has been investigated [3,4]. In hepatic amino acid metabolism, recent evidence suggests that amino acid transport into liver cells is the rate limiting step for further metabolism [5]. Saheki *et al.* [6] reported that the level of urea synthesis varies with the concentration of urea cycle intermediates. That is, the increase of urea formation is accompanied by an increase of acetylglutamate, ornithine and citrulline in the liver. So we have attempted to clarify the role of amino acids and their transport process in the ureogenesis. Recent studies have indicated that primary cultured hepatocytes isolated by the collagenase perfusion method retain many liver functions [7]. Therefore it seems appropriate to use these cultured hepatocytes for the studies on ureogenesis. The present paper describes studies of the biosynthesis of urea, the metabolism of ammonia and the transport of amino acids, using the primary culture of hepatocytes from adult rats.

Materials and Methods

Materials

The materials used for cell isolation and culture were as reported previously [7]. Insulin and dexamethasone were obtained from Sigma, St. Louis, MO. Aprotinin was from Bayer, Leverkusen.

Collagenase for cell isolation was from Wako Pure Chemicals, Osaka. Radioisotope labeled amino acids, [^{14}C]-methyl-2-amino isobutyric acid (MeAIB), [^{14}C]-2-aminobicyclo-[2,2,1]-hepatane-2-carboxylic acid (BCH), [^{14}C]-ornithine, [^{14}C]-arginine, [^{14}C]-lysine and [^{14}C]-glutamine were purchased from New England Nuclear, Boston, MA, U.S.A.

Animals

Adult male Wistar rats were purchased from Hokkaido Experimental Animals, Sapporo, weighed about 150 g to 200 g and maintained on laboratory chow.

Isolation and monolayer culture of adult rat hepatocytes

Adult rat hepatocytes were isolated from male Wistar rats by the *in situ* perfusion method reported as previously [8]. The isolated cells were plated at near confluent density (4×10^5 cells/cm^2) and grown as monolayers in Williams medium E (WE) with 5% calf serum, 10^{-9} M dexamethasone and 10^{-9} M insulin in 2-cm diameter of Linbro multiwell plastic dishes coated with collagen type I. Five hours after seeding, the medium was changed to WE containing 5 U/ml aprotinin [9], 10^{-9} M dexamethasone and 10^{-9} M insulin. This medium change was carried out once every day.

Measurement of amino acid uptake

The uptake of amino acid in hepatocytes attached to the culture dish was measured by the method of Kletzien *et al.* [10]. The plate was rinsed with 10 to 15 ml of warm (37°C) Hanks'-Hepes salt solution (Hanks' balanced salt solution minus glucose at pH 7.4 with 20 mM Hepes buffer). This was followed by incubation in 1.0 ml of Hanks' complete-Hepes solution (8 mM glucose added to Hanks'-Hepes salt solution) at 37°C containing radiolabeled amino acid (0.2 mM, 0.1 μCi/ml) for the various length of time (30 sec, 1 min, 2 min, 5 min and 10 min). Incubation was terminated by aspirating the medium and rinsing the cells several times with phosphate buffered saline (PBS). Cells were digested in 0.5 N NaOH and aliquots of the digest were taken for the protein determination and liquid scintillation counting. [^{3}H]-insulin was used for the determination of the extracellular trapping. The data were corrected for the extracellular trapping and expressed as pmoles of amino acids/mg protein/30 seconds.

Assay procedure

Urea synthesis and ammonia detoxication by the hepatocytes were determined as follows. After 24 h of culture in serum free WE, the hepatocytes were washed with PBS, then incubated for 12 h in Hanks'-Hepes salt solution (1.0 ml) containing 1 mM ammonium chloride and further addition of various amino acids. Samples of incubation media were taken and the amount of urea formed was measured by the method of Ceriotti and Spandrio [11]. The results were expressed as μmoles of urea formed per mg of cellular protein. The concentration of ammonia in the incubation medium was assayed by the indophenol method [12]. The enzyme activity of ornithine transcarbamylase (E.C.2.1.3.3.) was measured by the method of Schimke *et al.* [4]. Cellular protein was measured by the method of Lowry *et al.* [13].

Results

Urea synthesis from ammonium chloride in primary cultured hepatocytes

To test the effect of ammonium chloride on urea synthesis in primary cultured hepatocytes, the concentrations of urea and ammonia in the incubation media were determined after incubation of the cells in Hanks'-Hepes salt solution containing 1 mM ammonium chloride for 12 h (Fig. 1). The intrinsic synthesis of urea and ammonia by the hepatocytes was excluded from the results. The concentration of ammonia decreased rapidly to less than 0.5 mM after 12 h of incubation and the hepatocytes produced urea from ammonia chloride gradually with time. It is confirmed that the primary cultured hepatocytes have the ability to synthesize urea from ammonium chloride as observed *in vivo* [6].

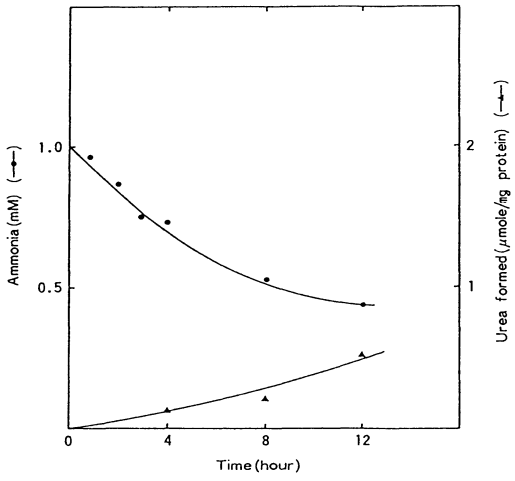

Fig. 1. Changes in the concentration of ammonia and urea during the culture of hepatocytes. Hepatocytes were cultured in Hanks'-Hepes salt solution containing 1 mM ammonium chloride for 12 h. Samples of incubation media were taken and the concentrations of ammonia and urea were measured at the indicated times. ●, ammonia; ▲, urea.

Effects of amino acids on urea synthesis from ammonium chloride

It is accepted that urea synthesis *in vivo* requires a supply of amino acids as the source of the urea cycle intermediates and energy metabolism [14]. We have examined the effects of various amino acids on urea synthesis using primary cultured hepatocytes. The results are shown in Figs. 2 and 3. The same batch of hepatocytes was used under each condition to allow for direct comparisons. Each amino acid was added at the concentration of 2 mM in Hanks'-Hepes salt solution containing 1 mM ammonium chloride. The rates of urea synthesis were high when the amino acids of urea cycle intermediates (ornithine, aspartate and arginine) were added to the media. Lysine also stimulated urea synthesis. Though glutamine inhibited the elimination of ammonia from the medium, it increased urea synthesis in the majority of the amino acids tested. The concentrations of ammonia in the incubation media containing urea cycle intermediates decreased more than they did in the medium with any other amino acids.

Changes of amino acid transport activity

We examined the effects of ammonia on the cellular transport activity of amino acids (Table 1). After 12 h of culture in Hanks'-Hepes salt solution containing 1 mM ammonium chloride, transport activity was assayed as mentioned above. To monitor the transport activity of system-A we used methyl-2-aminoisobutyric acid (MeAIB) a nonmetabolizable alanine analog. The transport activity of system-L

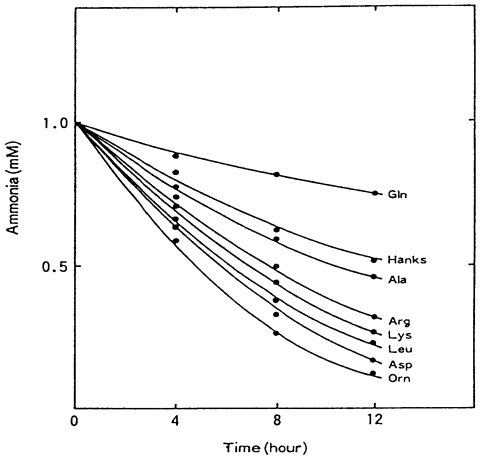

Fig. 2. Effects of various amino acids on the changes in ammonia concentration during the culture of hepatocytes. Various amino acids were added at a concentration of 2 mM in Hanks'-Hepes salt solution containing 1 mM ammonium chloride. The concentration of ammonia was measured at the indicated times. Changes of ammonia concentrations in the incubation media without amino acids were also measured (Hanks).

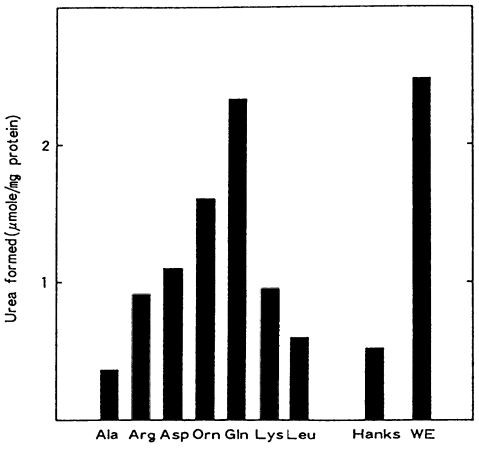

Fig. 3. Effects of various amino acids on urea synthesis in cultured hepatocytes. Various amino acids were added at the concentration of 2 mM in Hanks'-Hepes salt solution containing 1 mM ammonium chloride. The concentration of urea was measured after 12 h of incubation. Urea synthesis in the incubation medium without amino acids (Hanks) and in WE containing 1 mM ammonium chloride (WE) are also shown.

was assayed using the nonmetabolizable analog 2-aminobicyclo-[2,2,1]-hepatane-2-carboxylic acid (BCH). We further analyzed the transport activity of ornithine, arginine, lysine and glutamine. The uptake of MeAIB by hepatocytes cultured in ammonia-containing medium was approximately the same level as the control. The uptake of BCH by hepatocytes increased slightly compared with the control level.

Table 1. Effects of ammonia on amino acid uptake

	Amino acid uptake (pmoles/mg protein/ 30 sec)	
Substrate	NH_4Cl	Control
MeAIB	116.4 ± 3.3	113.1 ± 8.7
BCH	81.5 ± 9.5	62.7 ± 1.8
Ornithine	194.3 ± 5.5	102.4 ± 4.8
Arginine	174.5 ± 4.2	124.4 ± 3.3
Lysine	342.8 ± 3.0	212.9 ± 7.5
Glutamine	225.9 ± 5.8	426.1 ± 13.3

Uptake of amino acids was measured as described under *Materials and Methods*. The results are the mean ± S.D. of three experiments.

The transport activity of ornithine increased to twice that of the control cells. In addition, those of arginine and lysine were apparently stimulated. However the uptake of glutamine decreased to about 60% of the control levels.

Ornithine transport and ornithine transcarbamylase activity

We have indicated that urea synthesis from ammonium chloride in hepatocytes is stimulated by adding amino acids of urea cycle intermediates to the medium. At the same time, the membrane transport of these amino acids is activated. In particular, ornithine had the most stimulating effect on urea synthesis in these amino acids. We therefore measured the rate of ornithine transport and ornithine transcarbamylase (OTC) activity during the time of incubation with ammonia. The uptake of ornithine increased rapidly more than three times the control level after 4 h of incubation, then it decreased gradually to twice the control (Fig. 4). The time course of OTC activity is shown in Fig. 5. When ammonium chloride was added to the medium at a final concentration of 1 mM, OTC activity was induced gradually, reaching twice the control after 12 h of incubation. However, OTC activity in control hepatocytes was approximately constant over this period.

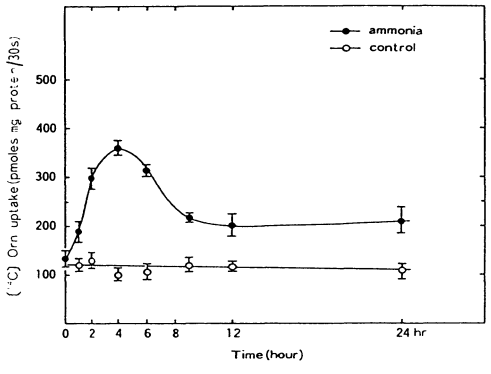

Fig. 4. Effects of ammonia on the time course of ornithine transport in cultured hepatocytes. The time course of ornithine uptake was measured in the hepatocytes cultured in the incubation medium containing 1 mM ammonium chloride (●, ammonia). The uptake of ornithine in the incubation medium without ammonia is also shown (○, control) The values are the mean ± S.D. of three experiments.

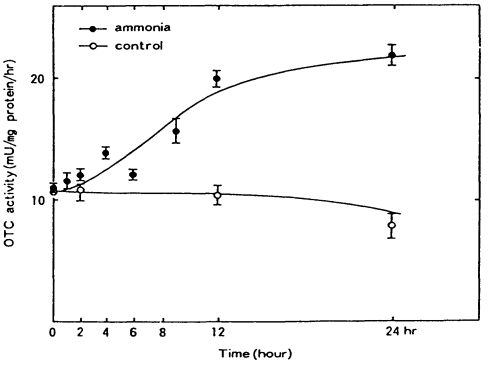

Fig. 5. Changes of ornithine transcarbamylase (OTC) activity in the hepatocytes. OTC activity in the hepatocytes cultured in ammonia-containing medium was measured (●, ammonia). Control values were obtained in the hepatocytes cultured in the incubation medium without ammonia (○, control). The results are the mean ± S.D. of three experiments.

Discussion

The experiments described in this paper were designed to clarify some aspects of the regulation of ureogenesis. In addition to urea cycle enzymes, the transport processes of amino acids are important in urea synthesis. Transport across the plasma membrane or mitochondrial membrane is not usually considered, but it is the first step by which amino acid is committed to further metabolism. It is not well known how the amino acid transport systems are concerned in the regulation of urea synthesis in the liver. It is reported that urea synthesis is regulated by the amounts of amino acids transported to the liver [6]. When the serum level of ammonia increases and a great deal of ammonia is transported to the liver, it is expected that the role of amino acids in the urea synthesis and ammonia disposal might be greater.

The present data indicated that amino acids of urea cycle intermediates (ornithine, aspartate and arginine) stimulated urea synthesis and ammonia removal much more than the other amino acids did. Arginine is known as one of the regulators of ureogenesis [1]. It stimulates the activity of *N*-acetylglutamate synthetase (NAGS) which synthesizes the allosteric activator of CPS, *N*-acetylglutamate [15]. It is also accepted that the synthesis of carbamylphosphate is the rate limiting step for ureogenesis, and arginine can be the key substrate. However, Cohen *et al.* [17] reported that ornithine could be the regulator of ureogenesis. We also observed that the ornithine content of liver *in vivo* increased on injection of ammonium chloride [14]. The present data using the primary culture of adult rat hepatocytes indicated that the urea synthesis was stimulated by ornithine. Therefore we had an interest in the ornithine transport and OTC activity in the hepatocytes loaded with high concentration of ammonia. In the range of physiological concentration of ammonia in the medium (0–50 μM), synthesis of urea in hepatocytes was saturated at the endogenous concentration of ornithine (0.11 ± 0.02 mM, unpublished data). When the hepatocytes were incubated in a high concentration of ammonia (1 mM), the rate of ornithine transport was accelerated to twice the control. This suggests that the intracellular concentration of ornithine was increased to amplify the urea cycle. It may be that ornithine transport at the mitochondrial membrane is stimulated at the same time. OTC activity was also increased to about twice the control at the same time. The mechanism of OTC induction in cultured hepatocytes is suggested to be substrate induction [18], the increase of ornithine and carbamyl phosphate.

The inhibition of glutamine transport is another important aspect in the regulation of amino acid transport. Free ammonia released from tissue was synthesized to glutamine and metabolized to urea in the liver. However, when the concentration of ammonia in the extracellular space was high, glutamine transport into hepatocytes was suppressed. We often observed that the serum concentration of glutamine was consistently high in patients with congenital hyperammonemia. The suppression of glutamine uptake by hepatocytes may account for some part of this.

Our results indicated that amino acids of urea cycle intermediates, especially ornithine, play an important role in the regulation of urea synthesis. With high concentrations of ammonia in the extracellular space, the synthesis of urea in the hepatocytes is determined by the supply of ornithine to the cells. This is in keeping with the phenomenon that the ornithine transport at the plasma membrane and OTC activity are activated. It is also suggested that the transport processes of amino acids must be taken into consideration as the short time regulator of ureogenesis. We are now attempting to clarify the molecular mechanism of the regulation of amino acid transport using our culture system.

References

1. Brown GW and Cohen PP (1959) J. Biol. Chem. 234: 1769–1780.
2. Walser M (1983) In: Stunbury JB, Wyngaarden JB, Fredrichson DS, Goldstein JL and Brown MS (eds.) The Metabolic Basis of Inherited Disease. McGraw-Hill Book Company, New York. pp. 402–438.
3. Schimke RT (1962) J. Biol. Chem. 237: 1921–1930.
4. Schimke RT (1962) J. Biol. Chem. 237: 459–470.
5. Shotwell MA, Kilberg MS and Oxender DL (1983) Biochim. Biophys. Acta. 737: 267–284.
6. Saheki T, Ohkubo T and Katsunuma T (1977) J. Biochem. 82: 551–560.
7. Tanaka K, Sato M, Tomita Y and Ichihara A (1978) J. Biochem. 84: 937–946.
8. Seglen PO (1976) Methods Cell. Biol. 13: 29–83.
9. Nakamura T, Asami O, Tanaka K and Ichihara A (1984) Exp. Cell Res. 154: 81–91.
10. Kletzien RF, Pariza MW, Becher JE, Potter VR and Butcher FR (1976) J. Biol. Chem. 251: 3014–3020.
11. Ceriotti G and Spandrio L (1963) Clin. Chim. Acta. 8: 295–299.
12. Chaney AL and Marbach EP (1973) Clin. Chem. 18: 1162–1169.
13. Lowry OH, Rosebrough BJ, Farro AC and Randall RJ (1951) J. Biol. Chem. 183: 265–275.
14. Saheki T, Ohkubo T and Katsunuma T (1978) J. Biochem. 84: 1423–1430.
15. Sigesada K and Tatibana M (1971) J. Biol. Chem. 246: 5588–5595.
16. Glasgow AM, Orloff S, Mukherjee A, Butler EJ and Schulman JD (1977) Pediatr. Res. 11: 456–463.
17. Cohen NS, Cheung CW, Kyan FS, Jones EE and Raijman L (1982) J. Biol. Chem. 257: 6898–6970.
18. Piearson DL, Cox SL and Gilbert BE (1977) J. Biol. Chem. 252: 6464–6470.

Address for correspondence: Dr. Masayoshi Nagao, Department of Pediatrics, Sapporo Medical College, Sapporo 060, Japan.

Local delivery of liposome-encapsulated proline analogue prevents pulmonary hypertension in the rat*

George J. Poiani, James M. Sumka, Carol A. Tozzi, Wei-Chi Liao and David J. Riley

Division of Pulmonary and Critical Care Medicine, Department of Medicine, University of Medicine and Dentistry of New Jersey – Robert Wood Johnson Medical School, New Brunswick, NJ 08903, U.S.A.

Department of Medicine, Lyons Veterans Administration Medical Center, Lyons, NJ 07939, U.S.A.

Abstract

Analogues of proline prevent collagen accumulation in some models of experimental fibrosis but they are toxic if administered chronically. We studied whether local administration of the proline analogue *cis*-4-hydroxy-L-proline (cHyp) to a vascular bed undergoing collagen accumulation in response to hypertension is effective in preventing the hemodynamic and biochemical change of hypertension. Adult rats were exposed to hypoxia (10% O_2) for 3 days to produce pulmonary hypertension; treated groups were given a single intravenous injection of liposome-encapsulated cHyp (200 mg/kg) prior to hypoxic exposure and controls were given 'empty' liposomes. Blood pressure was 15 ± 1 in controls vs. 10 ± 1 mmHg in treated ($p<0.05$, n=8); hydroxyproline content was 88 ± 5 in controls and 68 ± 8 μg/vessel in treated ($p<0.05$, n=8). Injection of 200 mg/kg of cHyp alone was ineffective. These results show that cHyp delivered in liposomes partially prevents the rise in blood pressure and the accumulation of collagen in the pulmonary artery. Local delivery of proline analogues at sites undergoing collagen accumulation may prevent fibrosis and reduce systemic toxicity.

Introduction

Proline analogues inhibit collagen production in tissues with rapid rates of collagen synthesis by interfering with post translational processing of procollagen α-chains [1]. The incorporation of *cis*-4-hydroxy-L-proline (cHyp) into nascent pro-α chains results in formation of non-helical procollagen which is degraded intracellularly [1] and is secreted more slowly than helical procollagen into the extracellular matrix [2]. This interference occurs in tissues undergoing rapid collagen synthesis such as pulmonary arteries following induction of hypertension [3]. In this model, exposure to hypoxia causes constriction of small pulmonary arteries, and chronic hypertension develops from sustained vasoconstriction and structural changes in blood vessel walls [4]. These structural changes consist of a

* This work was supported by U.S. Public Health Service Grants HL24264 and HL07467, the Barbara Wallace Cornwall Respiratory Research Laboratory, the John M. Kent Pulmonary Fibrosis Fund, the American Heart Association/New Jersey Affiliate and the Medical Research Service of the Veterans Administration.

proliferation of smooth muscle cells and connective tissue accumulation which thicken the wall and narrow the lumen of central pulmonary arteries thereby sustaining elevated blood pressure [5].

We have previously shown that twice daily injections of 'free' cHyp subcutaneously for 3 weeks ameliorates development of pulmonary hypertension in rats exposed to hypoxia [3]. Because chronic treatment with cHyp causes toxicity in adult rodents [6], we studied whether local delivery of cHyp encapsulated in phospholipid vesicles (liposomes) could lower the effective dose of cHyp and prevent the hemodynamic alterations associated with collagen accumulation in hypertensive pulmonary arteries. We found that this antifibrotic agent delivered locally in liposomes is effective, reduces the dose of drug and causes sustained suppression of collagen accumulation in hypertensive blood vessels.

Methods

Animals

Six-week-old male Sprague-Dawley rats (Crl:CD[SD]BR) weighing 185–205 g (Charles River Breeding Laboratories, Wilmington, MA) were maintained in a holding area one wk prior to study, randomly allocated to treatment groups, and fed food and water *ad libitum*. Control animals were pair-fed to the experimental animals to maintain equivalent body weights [3].

Exposure conditions

Four animals were placed in a polycarbonate chamber measuring $51 \times 41 \times 22$ cm, and humidified gas (10% O_2, 90% N_2) flowed into the chamber at a rate of 400 ml/min. Gas samples were analyzed electrometrically (model BM53MK2, Radiometer, Copenhagen, Denmark); PO_2 ranged from 74–80 Torr and PCO_2 from 3–5 Torr. Control animals, maintained under similar conditions, breathed ambient air. The chambers were opened once daily for 10 min to clean, weigh and feed the animals.

Liposome preparation

Small unilamellar, positively charged liposomes were prepared by reverse phase evaporation using the method of Szoka and Papahadjopoulos [7] as modified by Turrens and associates [8]. A stock solution containing 97.5 mg L-α-dipalmitoyl lecithin, 24.2 mg cholesterol and 9.6 mg stearylamine in a molar ratio of 14:7:4 was dissolved in 5 ml of chloroform and 50 mg cHyp in 2.5 ml phosphate-buffered saline (PBS), pH 7.4, was added. The mixture was sonicated (model W-385, Heat Systems-Ultrasonics. Inc. Farmingdale, NY) at a power output of 7 for 1 min at 10°C. The mixture was converted to a homogeneous, slightly viscous milky

emulsion, and the volume was reduced in a rotary evaporator under vacuum (400 Torr) at 25°C. When the emulsion became viscous and did not pool in the flask, 1.25 ml PBS was added, and evaporation was continued at 49°C until the odor of chloroform was no longer detected and a free flowing turbid suspension was present. The suspension was kept at 4°C overnight, centrifuged at 100,000 × g for 35 min at 4°C, and recentrifuged after suspending the pellet in 6.5 ml PBS. Prior to injection, the pellet was suspended in 2.5 ml PBS (40 μmol phospholipid/ml), filtered (0.22 μm filter), and passed serially through 18, 25 and 30 gauge needles.

Characterization of liposomes

Liposome diameter was determined by a fluorescent activated cell sorter (Coulter Epic 753 Dye Laser System, Coulter Electronics, Hialeah, FL) using latex beads as size markers and was 0.10–0.22 μm. Encapsulation efficiency, estimated from percent entrapment of 10 μCi [^{14}C]proline, was 51 ± 6% (n=5) and remained constant during storage at 4°C for 21 days.

Hemodynamic measurements and heart weight

Mean right ventricular pressure was measured by a catheter placed in the right ventricle of anesthetized rats (50 mg/kg pentobarbital intraperitoneally) using a pressure transducer (model P23Db, Statham Instruments, Oxnard, CA) and recorded (model SP-2006, Statham Instruments) after the animal had breathed room air for 20 min to eliminate the tonic response to hypoxia [4,9]. After sacrifice by abdominal aorta transection, hematocrit and ratio of ventricular weights were measured as previously described [9]. The position of the catheter was confirmed at autopsy.

Biochemistry

Main pulmonary artery (9 mm in length) was excised [3] and analyzed for total protein and hydroxyproline contents. Tissue was hydrolyzed in 6N HCl at 118°C for 48 h, diluted 1:10 in water, and a 0.1 ml aliquot was assayed for total protein by the ninhydrin method [10] using leucine as standard and hydroxyproline by a colorimetric method [11]. Results of triplicate measurements were expressed as content per vessel.

Experimental protocols

Four treatment protocols were used for groups of 5–10 rats exposed to hypoxia (Fig. 1). Single injections of empty liposomes were given prior to exposure to hypoxia and served as a negative control. Single injections of 200 mg/kg or 100 mg/kg of cHyp in liposomes were given prior to hypoxic exposure. A third group was given a single intravenous injection of free cHyp prior to hypoxic exposure. A

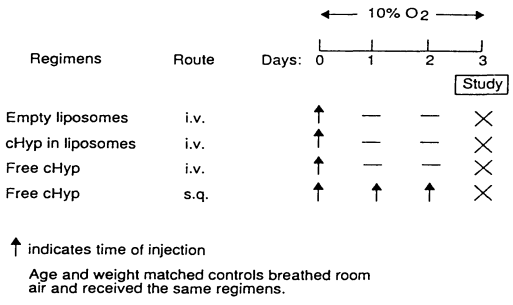

Fig. 1. Experimental protocol. Groups of animals were injected with *cis*-hydroxy-L-proline (cHyp) in either the free form or encapsulated in liposomes. Controls were given empty liposomes. Groups were given single injections of liposomes or twice daily injections of free cHyp and were studied 3 days after hypoxic exposure.

fourth group was given free cHyp subcutaneously twice daily during the 3 day exposure to hypoxia; this group served as a positive control. For all groups, effects on right ventricular pressure, ratio of ventricular weights, hematocrit and protein and hydroxyproline contents of the main pulmonary artery were assessed. Air-breathing animals were studied prior to exposure and at 3 days. Benzocaine anesthesia was applied to the penis, and an intravenous injection into the dorsal vein was given as a bolus using a 30 g needle over 5 sec. The volume injected (approximately 450 μl) contained 18 μmol of phospholipid. Free cHyp (500 μl) was administered subcutaneously or intravenously. Empty liposomes were given by intravenous injection while mean right ventricular pressure was continuously monitored to determine whether the injection acutely affected right ventricular pressure.

Statistical analysis

Mean ± S.E.M. from each group were obtained and analyzed by one-way ANOVA [12,13] followed by Duncan's post-hoc test [14]. Non-parametric data (animal survival) were analyzed by a continuity adjusted Chi-square analysis with Yates correction [12,15]. A p value of 0.05 was considered significant.

Results

Animals

Body weight prior to injection was 198 ± 4 g (n=81), and there were no differences in final body weights (190–202 g) among the groups. In control animals 25 of 26 (96%) survived while 47 of 55 (85%) of hypoxic animals survived (χ^2 = 18.7,

$p<0.05$). One control animal died following pentobarbital anesthesia. Eight deaths in hypoxic animals, occurring during the first day of exposure, were distributed as follows: 1 animal treated with saline; 2 treated with empty liposomes; 2 treated with cHyp in liposomes; and 3 treated with free cHyp. Survival was similar in hypoxic animals injected with saline (8 of 9, 89%) and with liposomes (23 of 27, 87%) ($\chi^2 = 0.4$, NS).

Acute injection of liposomes

Mean right ventricular pressure increased from 9.5 ± 0.3 to 10.9 ± 0.3 mmHg (n=5) ($p<0.05$) between 0 and 2 min of injection of 450 µl of liposomes containing cHyp but was normal after 2 min. Injection of 450 µl saline under the same conditions had no effect on blood pressure (9.4 ± 0.2 vs. 9.7 ± 0.2 mmHg, n=4).

Hemodynamic and biochemical measurements

On day 3 mean right ventricular pressure, hematocrit, and the ratio of the ventricular weights were increased in hypoxic animals injected with empty liposomes (Fig. 2), indicating development of pulmonary hypertension, secondary polycythemia and right ventricular hypertrophy. Treatment with free cHyp given subcutaneously twice daily ameliorated the rise in blood pressure, partially prevented the increase in hematocrit and prevented the development of right ventricular hypertrophy (Fig. 2). The single dose of 200 mg/kg cHyp in liposomes was as effective as the

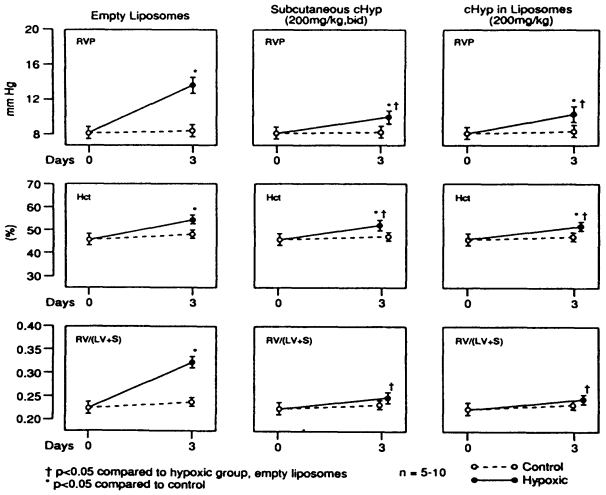

Fig. 2. Effect of treatment regimens on hemodynamic measurements and hematocrit. Groups of animals were studied prior to study (day 0) or 3 days after exposure to 10% O_2 (hypoxic) or air (control). Data point indicates mean; bracket, SEM. Abbreviations: RVP, mean right ventricular pressure; hct, hematocrit; RV/(LV+S), ratio of weights of cardiac ventricles.

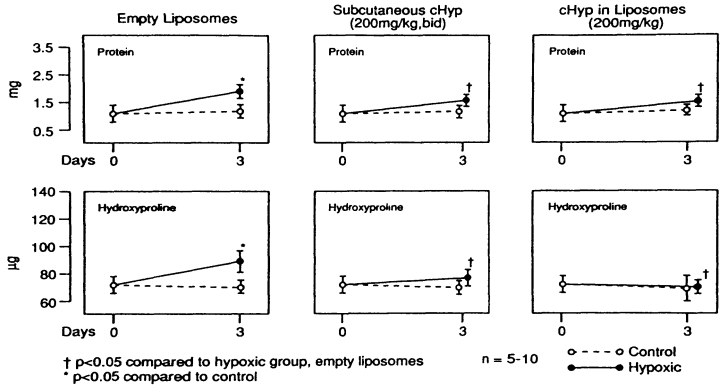

Fig. 3. Effect of treatment regimens on protein and collagen contents of pulmonary artery for same groups as in Fig. 2. Format and abbreviations same as Fig. 2.

multiple subcutaneous doses (Fig. 2). Both regimens of 200 mg/kg twice daily subcutaneously for 3 days and a single intravenous dose of 200 mg/kg in liposomes were equally effective in preventing collagen and protein accumulation (Fig. 3). The single intravenous injection of free 200 mg/kg cHyp and a dose of 100 mg/kg cHyp in liposomes had no effect in reducing right ventricular pressure or ventricular hypertrophy (Fig. 4) or preventing protein and collagen accumulation (Fig. 5). These data suggest that delivery of cHyp in single doses intravenously using liposomes is more effective than free cHyp and that the effective dose of a single injection of cHyp in liposomes is between 100 and 200 mg/kg.

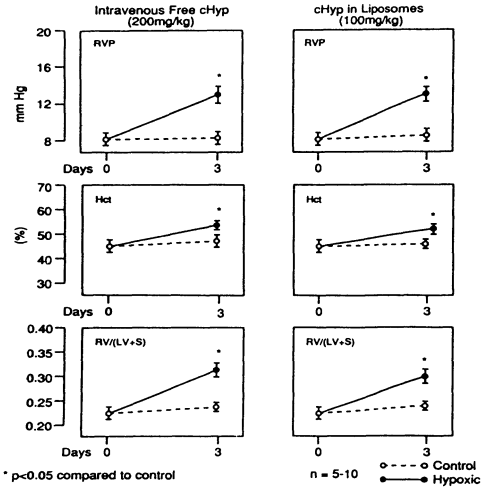

Fig. 4. Effect of treatment regimens on hemodynamic measurements and hematocrit. Format and abbreviations same as Fig. 2.

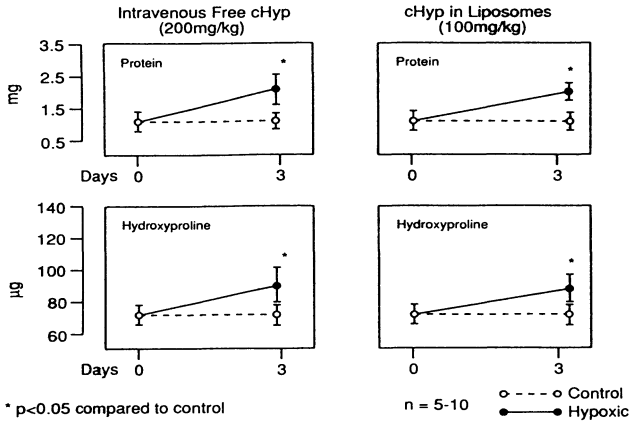

Fig. 5. Effect of treatment regimens on protein and collagen contents of pulmonary artery for same groups as in Fig. 4. Format and abbreviations same as Fig. 2.

Discussion

Collagen is the most abundant protein in vertebrates [16] and comprises one third of the dry weight of pulmonary arteries [9]. Collagen biosynthesis is similar to that of other proteins but involves unique post-translational modifications. For example, hydroxylation of prolyl and lysyl residues is essential for normal triple helical structure and cross-linking of collagen [16]. If post-translational processing of pro-α chains is inhibited, nonhelical procollagen forms which is degraded by intracellular proteases and is secreted at a reduced rate as a non-functional protein [17]. The incorporation of proline analogues such as cHyp, *cis*-4-fluoroproline, *cis*-4-bromoproline, 3,4-dehydroproline and azetidine-2-carboxylic acid into nascent pro-α chains prevents extracellular accumulation of collagen [18]. Through distortion of bond angles and steric hindrance among polypeptide chains, proline analogues inhibit folding of pro-α chains into a stable triple helix [1]. Some agents affect other metabolic steps: 3,4-dehydroproline reduces prolyl hydroxylase activity [1], and cHyp interferes with translation of procollagen mRNA [19]. Since collagen contains abundant imino acids compared to other proteins, proline analogues are relatively specific for inhibiting collagen production. Agents such as colchicine and corticosteroids which affect collagen deposition are less specific in their action.

The antifibrotic activity of cHyp is most effective in tissues undergoing rapid rates of collagen synthesis such as the pulmonary artery during early adaptation to high blood pressure after exposure to hypoxia. The rate of collagen synthesis in hypertensive pulmonary arteries is maximal during the first few days of hypoxic exposure [20,21]. One stimulus for increased collagen synthesis appears to be

distension of the main pulmonary artery by mechanical tension as demonstrated in isolated segments of rat pulmonary artery [22]. We have previously shown that cHyp injected twice daily subcutaneously ameliorates development of early [19] and chronic hypoxic pulmonary hypertension by inhibiting vascular collagen accumulation and the associated thickening of pulmonary arterioles [3]. In this study, we found that a single dose of 200 mg/kg cHyp in liposomes was as effective as 6 subcutaneous injections of 200 mg/kg cHyp in preventing development of pulmonary hypertension, right ventricular hypertrophy and vascular collagen accumulation in rats exposed to 3 days of hypoxia. We have also demonstrated that treatment with cHyp of animals with 'remodeled' hypertensive pulmonary arteries prevents further hemodynamic and structural changes of hypertension [23]. These studies support the concept that vascular collagen production contributes to the development and progression of pulmonary hypertension.

Proline analogues have been used to inhibit collagen production in other models of organ fibrosis. Azetidine-2-carboxylic acid administered to rats with experimental cirrhosis [24] and schistosomiasis [25] prevents hepatic collagen accumulation and improves liver function. Treatment with cHyp prevents lung fibrosis from hyperoxia [26] and bleomycin [27] in rodents and reduces formation of flexor tendon adhesions [28] and neuronal scars in rats [29]. A determinant of the efficacy of proline analogues is the nature of the fibrotic injury. For example, cHyp does not inhibit collagen synthesis in dermal granuloma induced by polyvinyl sponge implants in rats [30] and fails to inhibit lung collagen accumulation in silica-induced pulmonary fibrosis in hamsters [6].

A potential limitation of long-term use of proline analogues is that the drug might inhibit collagen biosynthesis in normal organs such as bone since the rate of collagen synthesis may be greater in these tissues than the fibrotic tissue. Effective use of proline analogues may be possible if treatment is limited to the period of rapid collagen synthesis and is selectively delivered to the sites of active fibrosis. Our study has demonstrated that it is possible to deliver antifibrotic agents to tissue undergoing rapid accumulation of collagen and prevent the pathophysiologic consequences of fibrosis. We hypothesize that the liposomes containing cHyp are taken up by endothelial cells and cHyp is released locally over 3 days in the blood vessel walls to inhibit the synthesis of collagen by vascular smooth muscle cells. The other major sites of deposition of liposomes containing cHyp are the liver, spleen and kidney, organs with relatively low rates of synthesis of collagen. Although we showed that a lower dose of cHyp was effective if administered in liposomes, our study does not establish that this regimen results in less drug toxicity. Future studies using long-term treatment will be useful to determine whether systemic toxicity is reduced by local injection of liposome-encapsulated antifibrotic agents.

Acknowledgements

We thank Carol L. Ruppert and Angel Santiago for technical assistance and Marcella Spioch for secretarial assistance.

References

1. Uitto J and Prockop DJ (1975) In: Popper M and Becker K (eds.) Collagen Metabolism in the Liver. Stratton Intercontinental Medical Book Corp., New York, pp. 139–148.
2. Kao WW, Prockop DJ and Berg RA (1979) J. Biol. Chem. 254: 2234–2243.
3. Kerr JS, Ruppert CL, Tozzi CA, Neubauer JA, Frankel HM, Yu SY and Riley DJ (1987) Am. Rev. Respir. Dis. 135: 300–306.
4. Reid LM (1986) Chest 89: 279–288.
5. Jones R, Langleben D and Reid LM (1985) In: Said SI (ed.) The Pulmonary Circulation and Acute Lung Injury. Futura Publishing Co., Mount Kisco, New York, pp. 137–188.
6. Geismar LS, Kerr JS, Trelstad RL and Riley DJ (1988) Toxicology 53: 331–344.
7. Szoka F and Papahadjopoulos D (1978) Proc. Natl. Acad. Sci. U.S.A. 75: 4194–4198.
8. Turrens JF, Crapo JD and Freeman BA (1984) J. Clin. Invest. 73: 87–95.
9. Kerr JS, Riley DJ, Frank MM, Trelstad RL and Frankel HM (1984) J. Appl. Physiol.: Respirat. Environ. Exercise Physiol. 57: 1760–1766.
10. Moore S and Stein WH (1948) J. Biol. Chem. 176: 367–388.
11. Kivirikko KI, Laitinen O and Prockop DJ (1967) Anal. Biochem. 19: 249–255.
12. SAS User's Guide: Statistics (1982) SAS Institute, Inc., Caney, N.C., pp. 119–137.
13. Winer BJ (1971) Statistical Principles in Experimental Design, 2nd Ed. McGraw-Hill, New York, pp. 210–218.
14. Duncan DB (1975) Biometrics 31: 339–359.
15. Ferguson GA (1966) Statistical Analysis in Psychology and Education. McGraw-Hill, New York, pp. 206–207.
16. Prockop DJ, Kivirikko KI, Tuderman L and Guzman NA (1979) N. Engl. J. Med. 301: 13–23.
17. Uitto J, Hoffman H-P and Prockop DJ (1975) Science 190: 1202–1204.
18. Fuller GC (1981) J. Med. Chem. 24: 651–658.
19. Poiani GJ, Tozzi CA, Belsky SA, Berg RA and Riley DJ (1988) Am. Rev. Respir. Dis. 137: A390.
20. McKenzie JC and Klein RM (1983) Blood Vessels 20: 283–294.
21. Poiani GJ, Tozzi CA, Yohn SA, Pierce RA, Belsky SA, Berg RA, Yu SY, Deak SB and Riley DJ (1990) Circ. Res. 66: 968–978.
22. Tozzi CA, Poiani GJ, Harangozo AM, Boyd CD and Riley DJ (1989) J. Clin. Invest. 84: 1005–1012.
23. Poiani GJ, Tozzi CA, Choe JK, Yohn SE and Riley DJ (1990) J. Appl. Physiol., in press.
24. Rojkind M (1973) J. Clin. Invest. 52: 2451–2456.
25. Dunn MA, Rojkind M, Warren KS, Hait PK, Rifas L and Seifter S (1977) J. Clin. Invest. 59: 666–674.
26. Riley DJ, Berg RA, Edelman NH and Prockop DJ (1980) J. Clin. Invest. 65: 643–651.
27. Riley DJ, Kerr JS, Berg RA, Ianni BD, Pietra GG, Edelman NH and Prockop DJ (1981) Am. Rev. Respir. Dis. 123: 388–393.
28. Bora FW, Lane JM and Prockop DJ (1972) J. Bone Jt. Surg. 54A: 1501–1508.
29. Pleasure D, Bora FW, Lane J and Prockop DJ (1974) Exp. Neurol. 45: 72–78.
30. Dayan D and Shushan S (1982) Cell Molec. Biol. 28: 217–219.

Address for correspondence: George J. Poiani, M.D., Department of Medicine, Lyons Veterans Administration Medical Center, Lyons, NJ 07939, USA.

Analogues to glutamine in clinical practice

Jan Wernerman[a,d], Folke Hammarqvist[b], Alexandra von der Decken[c] and Erik Vinnars[d]

[a]*Department of Anesthesiology and Intensive Care, Huddinge University Hospital, Karolinska Institute, Stockholm, Sweden*

[b]*Department of Surgery, St Göran's Hospital, Karolinska Institute, Stockholm, Sweden*

[c]*The Wenner-Gren Institute for Experimental Biology, University of Stockholm, Stockholm, Sweden*

[d]*Department of Anesthesiology and Intensive Care, St Göran's Hospital, Karolinska Institute, Stockholm, Sweden*

Trauma is accompanied by a negative nitrogen balance and a loss of skeletal muscle proteins [1]. The changes in muscle protein metabolism are characterized by a decrease in protein synthesis [2] and a depletion of intracellular free glutamine [3]. These alterations are not prevented by postoperative TPN including conventional amino acid solutions.

Glutamine is the most abundant free amino acid in skeletal muscle [5]. Today commercial available amino acid solutions do not contain glutamine for pharmaceutical reasons. Addition of glutamine to postoperative TPN after elective abdominal surgery prevents the negative whole body nitrogen balance (Fig. 1) and attenuates the the decline of muscle protein synthesis and of muscle free glutamine [6]. Addition of a dipeptide containing glutamine to postoperative TPN is even reported to leave the intracellular concentration unaltered on the 3rd day following surgery [7]. Ornithine-alpha-ketoglutarate added to postoperative TPN also results in a maintained nitrogen balance (Fig. 1), a prevention of the decrease in muscle protein synthesis, and a less pronounced decline in intracellular free glutamine in skeletal muscle [8–10]. The common determinant is the carbon skeleton of glutamine – alpha-ketoglutarate. It was hypothesized that addition of alpha-ketoglutarate to postoperative TPN could mimic the results obtained by provision of glutamine or ornithine-alpha-ketoglutarate. This would also present a possibility to provide glutamine-equivalents into commercial available amino acid solutions in a cheap and convenient way.

Metabolically healthy patients (n=21) undergoing elective cholecystectomy served as a reproducible trauma model, used in several recent studies [2,6,8,10,11]. They were given postoperative TPN including 135 kcal and 0.2 g N per kg body weight and 24 h. Percutaneous muscle biopsies were taken before surgery and on the third postoperative day. One group of the patients (n=9) were randomized to receive an addition of alpha-ketoglutarate (0.136 g per kg bw and 24 h) to their intravenous nutritional support. The other patients (n=12) served as controls. Urine was collected in 24 h portions and the nitrogen balance was calculated.

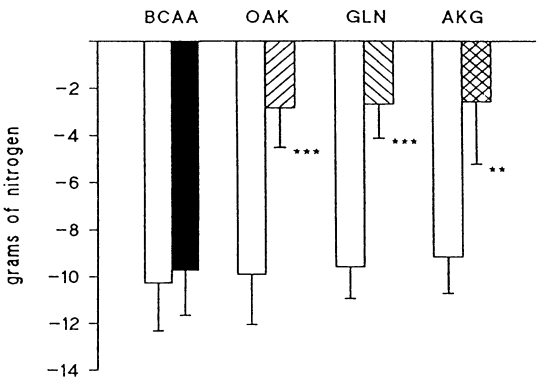

Fig. 1. Cumulated nitrogen balance during 3 days immediately following elective abdominal surgery. Patients were given conventional TPN (controls, oben bars) or an isocaloric and isonitrogenous TPN supplemented with branched chain amino acids, BCAA [11], ornithine-alpha-ketoglutarate, OAK [8], glutamine, GLN [6], or alpha-ketoglutarate, AKG**,*** indicate significantly different nitrogen balance as compared to the respective control group, $p<0.01$ and $p<0.001$. Fig. from [13].

The muscle tissue specimens were used to estimate muscle protein synthesis by determination of the concentration and size distribution of ribosomes [12] and to measure the intracellular concentrations of free amino acids [5]. As compared to the controls receiving an isocaloric and isonitrogenous TPN without addition of alphaketoglutarate the alpha-ketoglutarate group showed:

a) no negative nitrogen balance (-2.6 ± 2.7 g versus -9.9 ± 1.8 g, $p<0.01$, Fig. 1),
b) no decrease in muscle protein synthesis ($6.9 \pm 6.9\%$ versus $25.3 \pm 4.6\%$, $p<0.05$),
c) an attenuation of the decline in muscle free glutamine ($19.1 \pm 3.4\%$ versus $38.0 \pm 7.4\%$ $p<0.05$).

The results compare well with those obtained when postoperative TPN is supplemented with glutamine or ornithine-alpha-ketoglutarate. The hypothesis that alpha-ketoglutarate, the carbon skeleton of glutamine, is the critical substance in protein substance after trauma gains support from these data. Future investigations futher exploring the alpha-ketoglutarate hypothesis are advocated.

References

1. Cuthbertson DP (1931) The distribution of Nitrogen and Sulphurin the Urine during Conditions of Increased Catabolism. Biochem. J. 25: 236–244.
2. Wernerman J, von der Decken A and Vinnars E (1986) Protein Synthesis in Skeletal Muscle after Abdomnial Surgery: The Effect of Total Parenteral Nutrition. JPEN 10: 578–582.
3. Vinnars E, Bergström I and Fürst P (1975) Influence of the Postoperative State on the Intracellular Free Amino Acids in Human Muscle Tissue. Ann. Surg. 182: 665–671.
4. Vinnars E, Holmström B, Schildt B, Odeback A-C and Fürst P (1983) Metabolic Effects of Four Intravenous Nutritional Regimens in Patients Undergoing Elective Surgery. II. Muscle Amino Acids and Energy-rich Phosphates. Clin. Nutr. 2: 3–11.

5. Bergström I, Fürst P, Norée L-Oand Vinnars E (1974) Intracellular Free Amino Acid Concentrations in Human Muscle Tissue. J. Appl. Physiol. 36: 690–697.
6. Hammarqvist F, Wernerman I, Ali MR, von der Decken A and Vinnars E (1989) Addition of Glutamine to Total Parenteral Nutrition After Elective Abdominal Surgery Spares Free Glutamine in Muscle, Counteracts the Fall in Muscle Protein Synthesis, and Improves Nitrogen Balance. Ann. Surg. 209: 455–461.
7. Stehle P, Zander I, Mertes N, Albers S, Puchstein Ch, Lawin P and Fürst P (1989) Effect of Parenteral Glutamine Peptide Supplements on Muscle Glutamine Loss and Nitrogen Balance after Major Surgery. Lancet i: 231–233.
8. Wernerman J, Hammarqvist F, von der Decken A and Vinnars E (1987) Ornithine Alpha-ketoglutarate Improves Skeletal Muscle Protein Synthesis as Assessed by Ribosome Analysis and Nitrogen Balance Postoperatively. Ann. Surg. 206: 120–124.
9. Leander U, Fürst P, Vesterberg K and Vinnars E (1985) Nitrogen Sparing Effect of Ornicetil in the Immediate Postoperative State: Clinical Biochemistry and Nitrogen Balance. Clin. Nutr. 4: 43–51.
10. Hammarqvist F, Wernerman I, Ali MR and Vinnars E (1990) Effects of an Amino Acid Solution Enriched with either Branched Chain Amino Acids or Ornithine-alpha-ketoglutarate on the Postoperative Intracellular Amino Acid Concentration of Skeletal Muscle. Br. J. Surg. 77: 214–218.
11. Hammarqvist F, Wernerman I, von der Decken A and Vinnars E (1988) The Effect of Branched Chain Amino Acids upon Postoperative Muscle Protein Synthesis and Nitrogen Balance. Clin. Nutr. 7: 171–175.
12. Wernerman I, von der Decken A and Vinnars E (1985) Size Distribution of Ribosomes in Biopsy Specimens of Human Skeletal Muscle during Starvation. Metabolism 34: 665–669.
13. Hammarqvist F (1989) Intravenous Amino Acid Supply after Trauma: The Effects of Glutamine on Muscle Protein Metabolism. Thesis, Karolinska Institute, Stockholm, Sweden.

Address for correspondence: Jan Wernerman MD PhD, Department of Anesthesiology and Intensive Care, St Göran's Hospital, S-112 82 Stockholm, Sweden.

Effect of amino acids and their analogues on renal function

Aldo Claris-Appiani, Baroukh M. Assael, Amedea S. Tirelli, Graziella Cavanna, Caterina Funari, Caterina Tempesti and Fabiola Terzi

Clinica Pediatrica II, Universitá di Milano, Milano, Italy

Abstract

Renal hemodynamics (Cinutest, CPAH) were measured in 5 volunteers (23–28 years of age), before and after each of the following 1-week regimen: a) low protein diet as 50% of usual intake (LPD); b) LPD + 0.6 g/kg of a mixture of essential and non essential amino acids (AAmix); c) LPD + 0.6 g/kg of branched chain amino acids (BCAA); d) LPD + 0.15 g/kg of essential amino and Keto acid supplement (EAKA). LPD induced a decrease in renal plasma flow (RPF) without GFR variation; this finding was annulled when LPD was supplemented either with AAmix or EAKA, suggesting that EAKA used as supplement of LPD in chronic renal disease could counterbalance the low-protein induced reduced glomerular hemodynamic load. BCAA tended to antagonize the LPD renal effects: these data were partially inconsistent with the renal vasoconstriction we previously observed during BCAA infusion in normal man.

Introduction

It is known that an oral protein or an i.v. amino acid load increases the glomerular filtration rate (GFR) and renal plasma flow (RPF) [1–2]. However some differences exist between the single or the single classes of amino acids about their effects on renal function. We have demonstrated that branched chain amino acids have a lesser stimulatory effect on GFR and cause a renal vasoconstriction after prolonged infusion [3]. The low protein diet is known to decrease GFR, RPF and intraglomerular pressure: this mechanism may explain how protein restriction can modify the course of progressive renal injury [4,5]. This study was undertaken to assess, in normal subjects, if the renal low protein induced hemodynamic changes were maintained with the addition to hypoproteic regimen of: a) branched-chain amino acids (BCAA) in dosage equivalent to 50% of usual nitrogen intake; b) essential amino/keto acids at the dose usually proposed to supplement protein intake in chronic renal failure [6].

Methods

Five normal volunteers (3 female), 23–28 years of age, were submitted to the study. Their average usual protein intake had been assessed for seven days twice before the beginning of the study with daily dietary records. Based on this we prepared a low

protein prescription consisting on 50% of the usual intake and with 75% as high biological value proteins. The diet was isocaloric and salt intake was unrestricted.

Experimental design

A cross over design was used consisting of four 7-day periods: 1) low protein diet (LPD) 0.4–0.5 g/kg; 2) LPD + a mixture of essential and nonessential amino acids (AAmix) equivalent to 50% of usual nitrogen intake (0.6–0.65 g/kg); 3) LPD + BCAA equivalent to 50% of usual nitrogen intake (0.6–0.65 g/kg); 4) LPD + essential amino/keto acids (EAKA) (Ketosteril Fresenius) 150 mg/kg.

Dietary compliance was controlled with daily dietary record analyzed by a dietist and daily urinary nitrogen excretion.

On the morning of the 1st and the 7th day of each period blood determination of electrolytes, BUN, Hct and albumin and renal clearances studies were performed. The periods were separate by 1–3 months to avoid any carry over effects. Before each period the normal diet was assessed by a 7-day dietary record.

At 9 a.m., with the subjects fasting, an i.v. priming dose followed by a constant infusion of Inutest (Laevosan-Gesellschaft, Linz, Austria) and PAH (Monico, Italy) were given at rates calculated to reach a steady state concentrations of 20 mg/dl for Inutest and 2 mg/dl for PAH. During an equilibration period of 1 h the subjects were given oral water (20 ml/kg) to induce abundant diuresis. Urine losses were replaced by corresponding volumes of water and by constant infusion of 0.45% saline (500 ml/h). After the 1 h equilibration period two consecutive 20-minute urine sample were collected by spontaneous voiding and three blood samples during each 20 minute period were drawn. The average value for Inutest and PAH clearances during the two periods was considered to represent GFR and RPF respectively.

Plasma and urinary Inutest and PAH were determined as previously described [2]. Filtration Fraction was given by FF=GFR/RPF.

The significance of differences between the pre- and post-regimen renal functional data was analyzed by the Wilcoxon Signed Rank Test for paired samples or by the Student's t test for paired data, for each regimen period. The mean intra-subject coefficient of variation of basal GFR and RPF in these 5 subjects repeated 4 times was 10% and 5.5% respectively.

Results

General data of the subjects are shown in Table 1. There was no change in weight, hematocrit (Hct), serum albumin and daily sodium excretion. Serum urea and urinary nitrogen excretion were lower than pre regimen values after LPD and after LPD + EAKA. The BCAA and AAmix regimens did not vary these parameters.

Table 2 shows the renal hemodynamic data pre and post each period. LPD period induced a significant decrease of RPF with increase of FF (because GFR did

Table 1. Nutritional data of the 5 subjects, before and after each regimen (Mean(SD))

		serum urea (mg/dl)	urinary nitrogen excretion (mg/kg/day)	Hct %	urinary sodium excretion (mmol/100 mlGF)
LPD	before	41(7)	148(19)	43.6(3)	.19(.1)
	after	24(6.5)[a]	85(13)[a]	43.6(2)	.18(.1)
AAmix	before	31(3.4)	131(15)	42(4.4)	.22(.04)
	after	28(8.2)	144(26)	41.6(1.5)	.15(.07)
BCAA	before	32(5)	132(14)	40.7(3)	.2 (.05)
	after	26(6)	116(24)	41.3(3)	.19(.05)
EAKA	before	35(5)	151(47)	41.6(2)	.15(.04)
	after	21(7)[a]	79(19)[a]	41.6(2.5)	.15(.03)

[a]$p<0.01$ vs before regimen.

Table 2. Renal hemodynamics before and after each regimen (Mean(SD))

		GFR (ml/min/1.73m^2)	RPF (ml/min/1.73m^2)	FF (%)
LPD	before	112(23)	556(123)	20.7(1)
	after	109(16)	473(117)[a]	23.9(5.5)[a]
AAmix	before	130(19)	503(133)	21.3(3.7)
	after	148(28)	475(89)	21.2(2.7)
BCAA	before	100(9.4)	554(118)	18.7(4)
	after	103(10.5)	503(92)	21.5(6)
EAKA	before	108(9)	513(102)	20.9(1.5)
	after	110(8)	522(108)	21.0(3)

[a]$p<0.01$ vs before regimen.

not vary). BCAA tended to decrease RPF also not significantly. Neither RPF nor GFR changed after any other regimen.

Figure 1 depicts the mean percentage variation of RPF induced by each regimen, compared with the mean intra-subject coefficient of variation (MCV) of each basal RPF. Only LPD caused a significant modification (decrease) of RPF versus MCV.

Discussion

In these normal subjects the 1-week LPD resulted in a lowering of the RPF without variation in GFR and then with an increase of FF. Previous reports [7,8] showed a parallel fall of RPF and GFR: however in these works the LPD had been prolonged for 3 weeks. This finding may suggest that the LPD induced RPF modification takes place earlier than the GFR decrease.

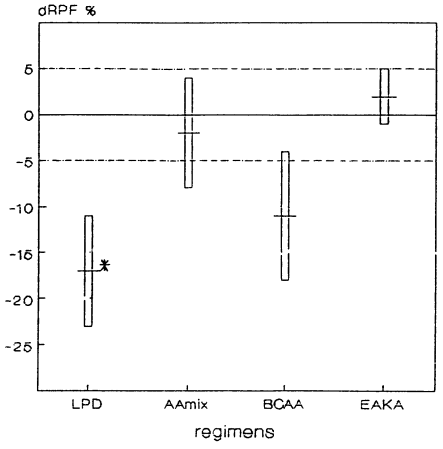

Fig. 1. The mean percentage variation of RPF after each regimen, compared to the mean intra-subject coefficient of variation (MCV) (dotted line) of basal RPF *p<0.01 vs. MCV.

As expected the addition of AAmix reversed the effects of the LPD on renal hemodynamics. However we were surprised to observe the addition of a low supplement of EAKA could also abolish the fall in RPF induced by protein restriction. This finding could not be attributed to a different nitrogen metabolism since the decrease of urinary nitrogen excretion and of serum urea was similar in both LPD and LPD + EAKA. Meisinger *et al.* [9] had actually shown that EAKA supplement of a LPD caused a significant hyperfiltration in uremic rats. When the supplement was only with keto acids they did not observe hyperfiltration; they concluded that the amino acids given were the potentially hperfiltrating part of the supplement. The data suggests that the effects of dietary prescriptions in renal failure, aimed at reducing the glomerular hemodynamic load, could be annulled by EAKA supplement. This is in line with the report of Hirshberg *et al.* [10], demonstrating that a mixture of essential amino and keto acids did not exert a protective effect against glomerular sclerosis in azotemic rats fed high-protein diets.

BCAA partially antagonized the renal hemodynamic effects seen after LPD. This was surprising since we observed that BCAA infusion induced a decrease in RPF in normal volunteers [3]. Thus the results of our two studies seem in part inconsistent and could be accounted for the different dose used (higher rate of intravenous infusion) and route of administration.

References

1. Hostetter T (1986) Human Renal Response to a Meat Meal. Am. J. Physiol. 250: F613–18.
2. Claris Appiani A, Assael AM, Tirelli A, Cavanna G, Corbetta C and Marra G (1988) Proximal Tubular Function and Hyperfiltration during Amino Acid Infusion in Man. Am. J. Nephrol. 8: 96–101.

3. Claris Appiani A, Assael BM, Tirelli A, Cavanna G and Marra G (1988) Lack of Glomerular Hemodynamic Stimulation after Infusion of Branched Chain Amino Acids. Kidney. Int. 33: 91–94.
4. Brenner BM, Meyer T and Hostetter TH (1982) Dietary Protein Intake and the Progressive Nature of Kidney Disease. N. Engl. J. Med. 307: 652–659.
5. Nath KA, Kren SM and Hostetter TH (1986) Dietary Protein Restriction in Established Glomerular Capillary Pressure in Progressive Glomerular Disfunction. J. Clin. Invest. 78: 1199–1205.
6. Lucas PA, Meadows JH, Roberts D and Coles G (1986) The Risks and Benefits of a Low-protein Essential Amino Acid-Keto Acid Diet. Kidney. Int. 29: 995–1003.
7. Pullman TN, Alving AS, Dern R and Landowne M (1954) The Influence of Dietary Protein on Specific Renal Functions in Normal Man. J. Lab. Clin. Med. 44: 320–332, 1954.
8. Viberti G, Bognetti E, Wiseman M, Dodds R, Gross J and Keen (1987) Effect of Protein Restricted Diet on Renal Response to a Meat Meal in Humans. Am. J. Physiol. 253: F388–393.
9. Meisinger E, Gretz N and Strauch M (1988) Influence of Amino acid and Keto acid Supplements on Hyperfiltration in Uremic Rats. Contr. Nephrol. 60: 152–158.
10. Hirshberg R, Cohen A and Kopple JD (1988) Effects of Keto Acid Supplements on Renal Function and Histology in Azotemic Rats Fed High-protein Diets. Am. J. Nephrol. 8: 50–56.

Address for correspondence: A. Claris Appiani, Clinica Pediatrica II, Via Commenda 9, 20122 Milano, Italy.

Modulation of protein synthesis in a cell-free system from rat brain by Cerebrolysin* during development and aging

A. Piswanger, B. Paier and M. Windisch

Institute of Zoology, Department of Metabolic Physiology, University of Graz, Austria

Abstract

We performed a series of experiments to examine the influence of Cerebrolysin, a drug produced by enzymatic hydrolysis of brain protein, consisting of small peptides and free amino acids (100 mg/kg/d), a peptide-enriched derivative (PEP) (1 mg/kg/d) and an amino acid mixture (AAM) (0,01 mg/kg/d), analogous to the amino acid fraction of Cerebrolysin, on protein synthesis of rat brains.

Group A was treated from the 1st to the 7th day of life and sacrificed after the 28th day. Group B (also 28 days old), group C (4 months old) and group D (24 months old) received daily subcutaneous injections for 7 days prior to killing. Saline-injected rats served as controls. The protein content, the amino acid content and pattern of the postmitochondrial tissue extract showed neither a significant dependence upon pretreatment nor upon age.

Compared to the adult control rats (C), the young rats (A,B) showed an increased (+77%, +50%), the old rats a decreased (–26%) leucine incorporation. Cerebrolysin attenuated the differences between adult and young, and abolished that between adult and old rats. AAM and PEP decreased these differences, producing a relatively uniform pattern of protein synthesis in all groups.

In group C there were no significant differences in leucine incorporation due to treatment. In group A and group B we could observe a modest treatment-dependent decline in protein synthesis. In contrast, AAM, Cerebrolysin and PEP significantly elevated protein synthesis (+21%, +31%, +78%) in group D.

Introduction

Development and aging are common phenomena in living animals and men. They are related to a lot of metabolic and biochemical changes in every cell. Aging of the brain results in alterations of learning and memory processes as well as in changes of social behaviour. On the other hand, early brain development is characterized by extremely high rates of energy requirement, due to intensive anabolic metabolism. Disturbances in the period of postnatal brain development will result in serious mental disease.

Since it has been emphasized that peripherally administered peptides can influence CNS events, either after permeation of the blood-brain barrier [1] or by several mechanisms not involving direct BBB transfer [2], a possible role of brain peptides in the treatment of some mental and neurological disorders as well as in

* Produced by EBEWE, Austria.

optimizing normal CNS functions can be suggested. In previous studies the influence of the peptide-amino acid derivative Cerebrolysin on brain metabolism of developing and aging brain has been investigated [3] showing significant improvement of glucose metabolism. Results published by other laboratories [4] indicated drug effects on brain protein synthesis. Paier [5] demonstrated clear effects of Cerebrolysin on learning behaviour in rats of different ages. The aim of the present study was to elucidate the effects of Cerebrolysin on brain protein synthesis in accordance with behavioural experiments. The differentiation of actions of the peptide-and amino acid-fraction of Cerebrolysin was of special interest.

Material and Methods

Male and pregnant female Sprague-Dawley rats have been derived from the Versuchstierzuchtanstalt Himberg, Austria. All animals were housed in small groups in a room controlled for temperature, and having a daily photoperiod of 14 h light. Each animal had free access to water and was fed *ad libitum* on pellets (Fa. Tagger, Graz, Austria). Group A: 28-day-old male and female rats, treated from 1st to 7th day of life. Group B: 28-day-old male and female rats, treated from 21st to 27th day of life. Group C: 4-month-old male rats, treated for 7 days prior to killing. Group D: 24-month-old male rats, treated for 7 days prior to killing.

Rats were pretreated with: Cerebrolysin, a drug produced by enzymatic hydrolysis of brain protein, consisting of small peptides (15%; <10 kDa) and free amino acids (85%) (100 mg/kg body weight/day); PEP, a peptide-enriched derivative of Cerebrolysin (1 mg/kg body weight/day), consisting of 75% small peptides and 25% free amino acids; AAM, an amino acid mixture, with an amino acid pattern analogous to Cerebrolysin (0.01 mg/kg body weight/day). The stock solutions were diluted with 0.9% sodium chloride and injected subcutaneously once a day. The dosage used was the most effective dosage of the drugs in passive avoidance learning experiments [5]. Saline injected rats served as controls.

All chemicals used were analytical grade. L-U-^{14}C-leucine (342 mCi/mmol) was obtained from the Radiochemical Centre, Amersham, U.K., ATP, GTP, creatine phosphate and creatine kinase from Boehringer Mannheim, G.F.R., and all other chemicals from Merck, G.F.R.

We used a method that has been published by Schotman and Allaart [6] to obtain a postmitochondrial supernatant (PMS), active in cell-free protein synthesis. 0.04 ml PMS were added to the incubation medium, containing (final concentrations): 50 mM Tris-HCl, pH 7.6, 200 mM KCl, 12 mM $MgCl_2$, 6 mM ß-mercaptoethanol, 0.5 mM ATP, 0.1 mM GTP, 6.25 mM creatine phosphate and creatine kinase (0.025 mg/ml). After preincubation at 37°C for 5 min under gyrotory shaking, the incorporation period was started by addition of 2 µCi ^{14}C leucine. The final incubation volume was 200 µl. After 30, 60 and 120 min, aliquots of 60 µl were taken and mixed with 1 ml icecold 0.3 mM perchloric acid (PCA) and 50 µl bovine

serum albumin (10 mg/ml). The precipitate was centrifuged at 1000 g for 5 min, and the resulting pellet was washed with 1 ml 0.3 M PCA containing 1 mM leucine, at 0°C and homogenized ultrasonically (Branson sonifier-B15P). Subsequently, the pellet was incubated with 0.5 M PCA at 90°C for 20 min. The pellet was washed again with 0.3 M PCA followed by methanol-ether (1:1) and ether successively. The resulting protein residue was thoroughly dried, solubilized in 200 µl 1 M NaOH for several h, and later neutralized with 4 M HCl. Radioactivity was determined by mixing 200 µl solution with 5 ml Hydroluma (Baker) and counting in a liquid scintillation counter (Packard CA 1900) applying automated quench correction by external standard ratio method. The protein content of the PMS was measured according to Lowry *et al.* [7].

The amino acids of the postmitochondrial tissue extract were determined with an amino acid analyzer (Aminoquant, Hewlett Packard).

Statistical analysis of data was done using a non-parametric test according to Kruskal and Wallis [8].

The study was performed in conformity with the GLP-regulations of U.S.A., Japan and OECD.

Results

The protein content, the amino acid content and the amino acid pattern of the postmitochondrial tissue extract showed neither a significant dependence upon pretreatment nor upon age. *In vitro* brain protein synthesis of control rats showed a clear age dependence (Fig. 1). Highest levels have been measured in young

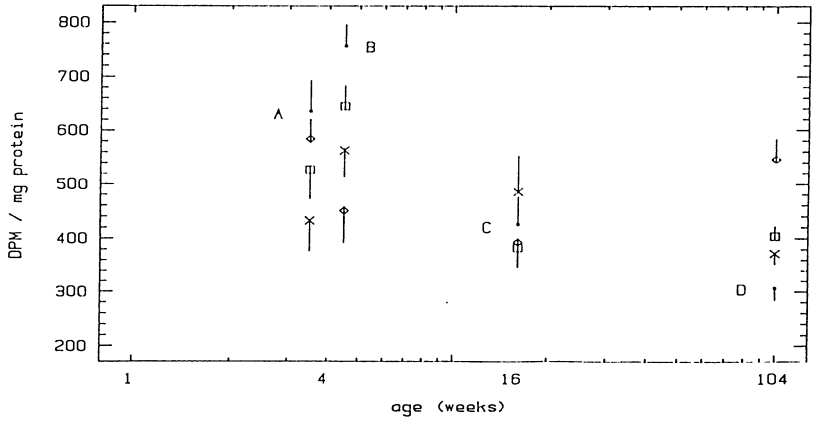

Fig. 1. Age dependent incorporation of [^{14}C] leucine by the PMS at 120 min of incubation due to pretreatment with saline solution (■), Cerebrolysin (❑), PEP (◊) or AAM (X) for 7 days. Bars represent mean ± S.E.M. of at least 10 incubations. Significant differences ($p<0.05$): AAM vs. NaCl in group A; PEP and AAM vs. NaCl in group B; PEP, Cerebrolysin and AAM vs. NaCl in group D.

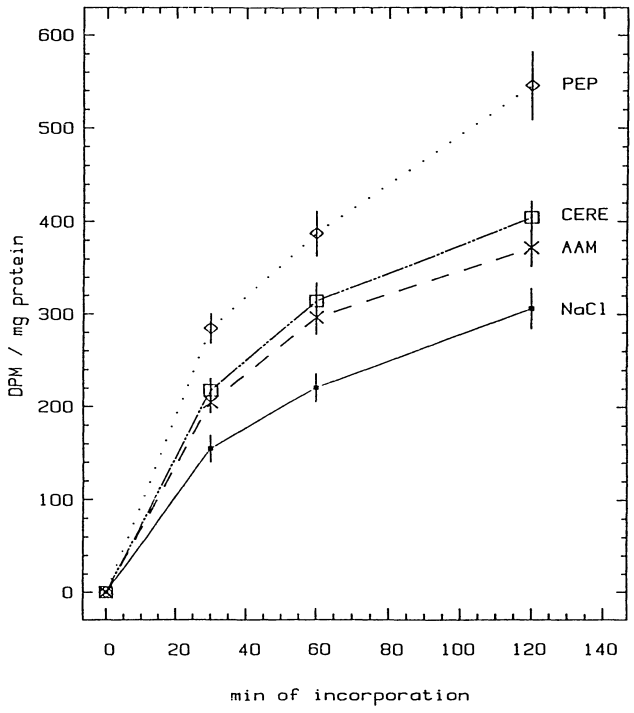

Fig. 2. Time curve of the incorporation of [^{14}C] leucine by the PMS of 104-week-old rats at 0, 30, 60 and 120 min of incubation. Pretreatment with saline solution, Cerebrolysin, PEP or AAM for 7 days. Bars represent mean ± S.E.M. of at least 12 incubations. All values show significant differences ($p<0.05$) compared to saline-pretreated rats.

animals (group A and group B), a significant decline has been detected in the adult rats (–44%: $p<0.001$) and there is a further decrease in the old ones (–59%; $p<0.001$). The greatest leucine incorporation has been obtained in the control rats of group B. Drug treatment decreased the brain protein synthesis in group A and group B. In comparison to the control results AAM decreased the leucine incorporation significantly in group A and B ($p<0.05$), PEP only in group B ($p<0.01$). Adult rats show a uniform pattern of protein synthesis – there are no drug effects at all. In group D – the 24-month-old rats – drug administration results in a significant stimulating effect. Cerebrolysin and AAM increased leucine incorporation to an extent of +31% ($p<0.001$) and +21% ($p<0.05$) respectively. PEP nearly doubled the rate of synthesis (+78%; $p<0.001$) compared to controls. This result is also significantly different from those obtained from Cerebrolysin and AAM animals ($p<0.01$). Figure 2 shows the time course of leucine incorporation in postmitochondrial brain extracts from the old rats.

Discussion

Protein synthesis in the mammalian brain is known to undergo significant changes during maturation and aging. Highest rates could be measured in foetal and neonatal animals. After early postnatal development there is a permanent decrease. In rat brain, Goldspink [9] demonstrated a decline of protein synthesis of 24% from the 20th foetal day to the 3rd postnatal week, and a further drop of 78% to the 105th week of life. Similar results have been shown by Dunlop [10] and Dwyer *et al.* [11]. All of these studies have been done *in vivo*. Although we have used an *in vitro* system, the same age dependence was measured in control rats. This result is in accordance with the findings in previous studies of oxidative metabolism of aging rat brain [3].

An explanation of the drug effects in the two different groups of 28 day-old rats is difficult. In group A (Fig. 1) only AAM application shows an effect, decreasing the rate of protein synthesis. In behavioural tests using the same experimental schedule, Paier [5] found significant improvement of passive avoidance learning in rats treated with Cerebrolysin, PEP or AAM from the first to the seventh day of life. We have to remember that in group A there is a period of 3 weeks between the end of treatment and the experiment and obviously there are long-lasting effects of Cerebrolysin and PEP on behaviour but not on protein metabolism. The effect of AAM, however, not only in this study, but also in the work of Paier [5] remains inexplicable, because of the extremely low effective dosage, which will not be able to change the serum concentration of amino acids and in this way alter brain amino acid levels significantly [12]. There are no authors at all who have used AAM in this low dosage and higher doses are reported to be inactive [13].

In animals treated from the 21st to the 27th day of life (group B) the reason for the action of PEP treatment could be explained by metabolic active peptides, like some fragments of ACTH, vasopressin analogues and so on. In contrast, Paier [5] could not find any effects of treatment on behaviour in this group.

In both groups it could not be distinguished if the decline in leucine incorporation is the result of a general inhibition of protein synthesis or energy metabolism, or if it shows an acceleration of brain development indicating that the rate of anabolic metabolism and protein synthesis measured in the brain of young rats is comparable to those of adult ones. In previous metabolic studies, done in our laboratory, using these drugs we could prove an organ-specific, stimulating effect of Cerebrolysin and PEP on oxygen consumption [14]. So inhibition of protein synthesis seems to be improbable.

Experiments testing drug actions immediately after treatment of newborn rats, not older then 7 days, should be performed to get information about these contradictory results.

The finding that there are no drug dependent effects in group C, the healthy adult rats, indicates that it is impossible to detect small changes in protein synthesis using this *in vitro* system, although administration of Cerebrolysin or PEP always resulted in pronounced changes of glucose and oxidative metabolism [15] and

learning behaviour [5]. This discrepancy may imply that measured rates of leucine incorporation reflected chiefly synthesis of structural proteins. A treatment with Cerebrolysin for 14 days shows a slight, but non-significant increase in cerebral protein (+10.1%) [15].

The reduction of protein synthesis in old age may be only the first step in a series of complex events which culminate in geriatric cognitive dysfunctions. The decline in rate of brain protein synthesis is correlated with a progressive fall in the ribosomal activity and content [9]. Also Fando and Wasterlain [16] found brain polyribosome profiles demonstrating an age-related decline in heavy aggregates with a concomitant increase of monosomes. Histological studies in rats pretreated with Cerebrolysin showed an enhanced number of polysomes in neurons [17]. Wenzel *et al.* [18] investigated Cerebrolysin in explantate cultures of the hippocampus and found an increase in number of membrane-bound ribosomes and polysomes. This high ratio of membrane-bound ribosomes respectively polysomes to monosomes pointing to an enhancement in protein synthesis is in good correlation with our results in aged rats. Furthermore there is an absolute decrease in polyribosomal aggregates and synthesis of messenger-like RNA as a result of hypophysectomy [19,20]. Since Cerebrolysin as well as PEP contains peptides up to a molecular weight of 10,000, obtained by hydrolysis of brain protein, an action of these components is plausible – similar to the effects of ACTH-like peptides on protein synthesis [21].

AAM also increases leucine incorporation (+21%), but this is inexplicable at present. No evidence explaining the action of such a low dose of amino acids is reported in current literature.

References

1. Banks W and Kastin AJ (1987) Life Sci. 41: 1319–1338.
2. Meisenberg G and Simmons WH (1983) Life Sci. 32: 2611–2623.
3. Windisch M and Piswanger A (1985b) Arzneim. Forsch-Drug Res. 35: 1225–1227.
4. Wenzel J, Stender G and Duwe G (1981) J. Hirnforsch. 22: 629–683.
5. Paier B (1989) Dissertation 'Wirkung von Cerebrolysin, eines Peptidkonzentrates und einer Peptidfreien Synthetischen Aminosäurelösung auf Lernen und Gedächtnis von Ratten', Karl-Franzens-University of Graz, Austria.
6. Schotman P and Allaart J (1981) J. Neurochem. 37: 1349–1352.
7. Lowry OH, Rosebrough NJ, Farr AL and Randall RJ (1951) J. Biol. Chem. 193: 265–275.
8. Kruskal WH and Wallis WA (1952) J. Amer. Statist. Ass. 47: 583–621.
9. Goldspink DF (1988) J. Neurochem. 50: 1364–1368.
10. Dunlop DS (1983) In: Lajtha A (ed.) Handbook of Neurochemistry, 2nd ed. Plenum Press, New York – London, Vol. 5, pp. 25–63.
11. Dwyer BE, Fando JL and Wasterlain CG (1980) J. Neurochem. 35: 746–749.
12. Glaeser BS, Maher TJ and Wurtman RJ (1983) J. Neurochem. 41: 1016–1021.
13. Trojanova M, Karasek F, Pruzkova V and Mourek J (1976) Physiol. Bohemoslov. 25: 319–323.
14. Windisch M and Piswanger A (1985a) Arzneim. Forsch-Drug Res. 35: 87–89.
15. Windisch M and Piswanger A (1985c) Arzneim. Forsch-Drug Res. 35: 1353–1356.
16. Fando JL and Wasterlain CG (1980) Neurochem. Res. 5: 23–33.

17. Sommer H and Quandt J (1973) Schweiz. Arch. Neurol., Neurochirurg. Psychiat. 112: 372–385.
18. Wenzel M, Wenzel J, Grosse G, Lindner G, Kirsche W and Matthies H (1977) J. Hirnforsch. 18: 357–371.
19. Gispen WH, De Wied D, Schotman P and Jansz HS (1970) J. Neurochem. 17: 751–761.
20. Gispen WH and Schotman P (1970) In: De Wied D and Weijnen JAWM (eds.) Pituitary, Adrenal and the Brain, (Progress in Brain Research, Vol. 32). Elsevier, Amsterdam, pp. 236–244.
21. Brown IR and Cosgrove JW In: Lajtha A (ed.) Handbook of Neurochemistry, 2nd ed. Plenum Press, New York–London, Vol. 5, pp. 1–24.

The antispastic effect of L-threonine

Kui-Chung Lee[a], Victor Patterson[a], Geraldine Roberts[b] and Elisabeth Trimble[b,c]

Departments of [a]Neurology and [b]Clinical Biochemistry, Royal Victoria Hospital, Belfast, U.K.
[c]Department of Chemical Pathology, Queen's University, Belfast, U.K.

Introduction

Spasticity is a part of the upper motor neurone syndrome in which there is a velocity-dependent increase in tone. It is easy to recognise but much more difficult to treat successfully. Despite the recent advance of intrathecal baclofen treatment [1] the need for a new oral antispastic agent still exists as conventional therapy is often limited by side-effects [2]. Glycine is an important inhibitory neurotransmitter in the spinal cord, [3] and it is diminished in the ventral gray matter of animals with spasticity [4]. Glycine, however crosses the blood-brain barrier poorly, and a possible precursor L-threonine has been used as treatment [5,6]; threonine crosses the blood-brain barrier more easily and may be converted to glycine by the enzyme serine hydroxymethyltransferase [7]. Systemic administration of L-threonine increases spinal cord glycine in rats [8]. In previous open studies, L-threonine has been given to patients with spasticity in doses ranging from 1.5 to 3 g/day. The lower dosage was ineffective but 3 g/day produced a modest effect. We therefore decided to test the antispastic effect of L-threonine by using higher doses than previous studies. We also monitored neurochemical changes by measuring CSF glycine and L-threonine during the different phases of the study.

Patients and Method

Six patients were recruited for the single-blind, open-label, crossover study (three with multiple sclerosis and three with spinal cord injury), and informed consent was received from each patient.

These patients were recruited after a baseline period of four weeks. During the baseline period three assessments of muscle tone were performed to ensure that the greatest variation was less than 20% of the mean of these measurements. No patient was rejected because of excessive fluctuation in spasticity. Treatment with L-threonine using 3 g/day and 6 g/day was then given in two two-week periods to each patient. The dosages were allocated in a random order to the two treatment periods, blinded to the examiner. Capsules were taken on an empty stomach, at 8 am, 2 pm, and just before bedtime. After treatment, the patients were followed up

Table 1. Ashworth scale

1. No increase in tone
2. Slight increase in tone giving a 'catch' when the limb was moved in flexion or extension
3. More marked increase in tone but limb easily flexed
4. Considerable increase in tone – passive movement difficult
5. Limb rigid in flexion or extension

for four weeks or until spasticity had returned to within 20% of the baseline. A washout period was not used between treatment periods.

We assessed increased muscle tone with the Ashworth Scale [9] (Table 1). Factors that could influence muscle tone were controlled as much as was possible. All examinations were carried out in a standardised manner. For the purpose of our study, we devised a spasticity score which was the composite score of the six passive movements rated highest by the Ashworth Scale. Spasticity scores for each patient were gathered twice weekly throughout the study including the follow-up period. Side-effects were sought at each visit.

Functional status was monitored by the Barthel Index (range of scores 0–20) [10], Kurtzke Disability Status Scale and Functional Systems [11]. Measurements were carried out at baseline and at the end of each treatment period.

In order to study the neurochemical effect of L-threonine, three lumbar punctures were performed on each patient. CSF was gathered at baseline and before the end of each treatment period. The procedure followed an overnight ten hour fast and was performed two hours after the morning dose of L-threonine. Blood was also drawn at the time of the lumbar puncture for assay of plasma threonine and glycine.

For accurate analysis of CSF amino acids, proper processing is important and we adhered strictly to the recommendations of Perry and Jones [12]. This meant immediate preparation for storage once the specimens were collected. CSF was separated by high speed centrifugation at a rate of 15,000 rpm and the supernatant was then removed and stored at −70°C until the time of analysis. Measurement of amino acids was carried out by an automated amino acid analyser (Biotronik LC 5001).

The different scores were recorded on specially designed forms. Results of all six patients were plotted on line charts. Different line charts were used for spasticity scores, Barthel Index scores, and CSF glycine and threonine. Means were calculated for measurements of various study phases. These were then represented on a histogram. Comparison with baseline was also expressed in terms of percentage improvement. We further analysed results of each treatment period with baseline by using paired-t tests [13].

Results

Figure 1 contains line charts for spasticity scores, Barthel Index, and plasma and CSF amino acid levels in different phases of the study. Muscle tone decreased during treatment with both 3 g/day and 6 g/day dosages. Mean improvements with treatment were 25% (3 g/day) and 23% (6 g/day) by comparing each period with

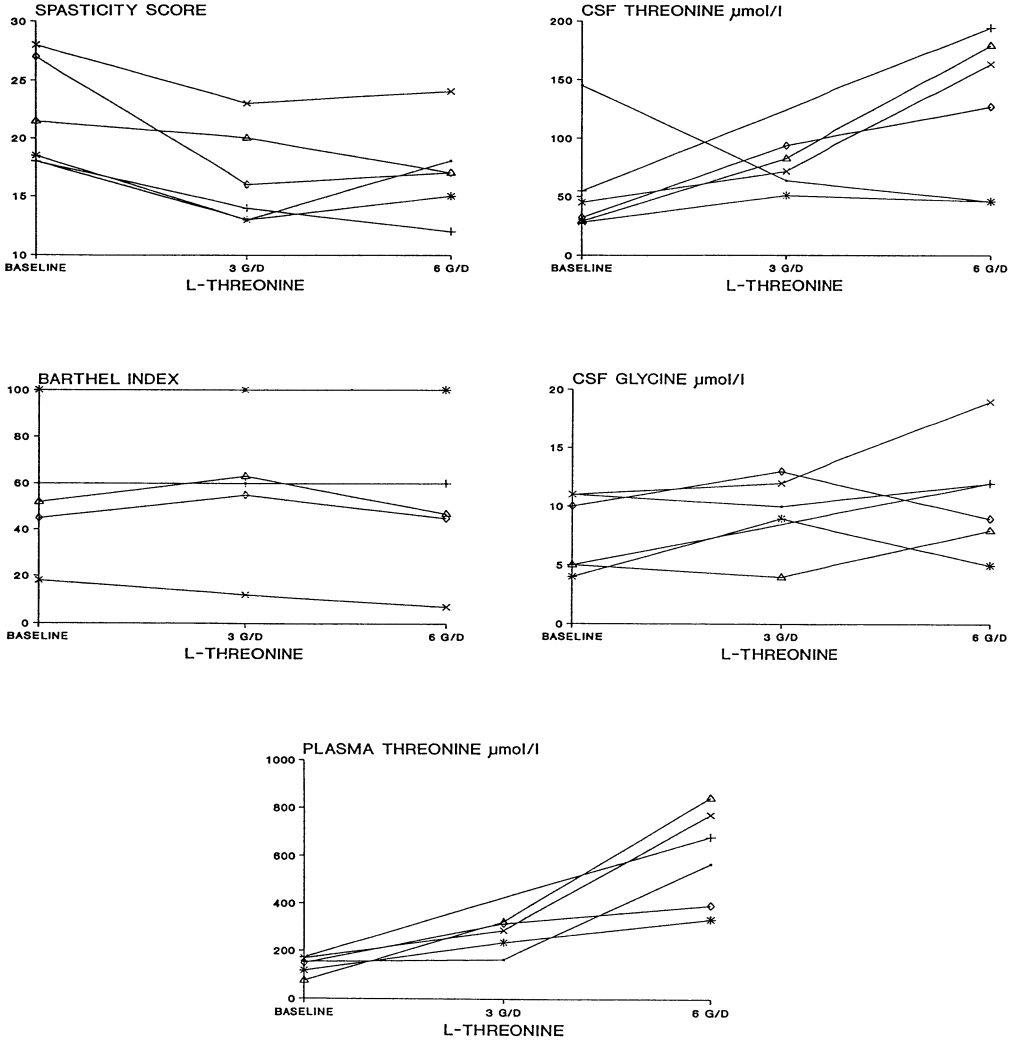

Fig. 1.

baseline. Paired-t tests showed significant improvement with 3 g/day ($p = 0.009$) and 6 g/day ($p = 0.018$) treatment. There was no difference between the two dosages.

Plasma and CSF threonine rose in a dose-dependent fashion with L-threonine. These changes were found to be significant at the 5% level. Plasma and CSF glycine did not change in any significant way. The Barthel Index and Kurtzke Scales failed to detect any functional improvement in patients with decreased tone.

Side-effects associated with treatment were infrequent. One patient reported headaches within a few days of starting therapy, and in another subjective stiffness and spasms grew worse.

Discussion

We have shown that L-threonine reduces muscle tone in the patients studied without appreciable side-effects at doses of 3 g/day and 6 g/day. No treatment difference was found for the two dosages used. The onset of clinical response was noted one week after starting L-threonine and once therapy was finished, tone returned to the baseline level within several days.

The Ashworth Scale which was used in this study, has become an established tool for measuring spasticity in clinical trials. In a separate study, we have verified its reliability [14]. There was no detectable change in the functional status, a finding similar to other studies of antispastic therapy [2]. This is hardly surprising since spasticity is not the only impairment in these patients and usually coincides with upper motor neurone weakness. A reduction in tone without the return of power and dexterity is unlikely to result in functional recovery [15]. It has also been suggested that disability scales may not be a sensitive index of functional improvement [16].

The dose-dependent rise in plasma and CSF levels of L-threonine during treatment confirmed that patients were taking the prescribed medication and there was good penetration of the blood-brain barrier by this amino acid. We were however unable to show any significant change in CSF glycine level during L-threonine supplementation. Our failure to do so could be due to several reasons. Firstly, it is possible that L-threonine has increased spinal cord glycine without detectable CSF changes. Secondly the timing of CSF sampling may be important. We performed our lumbar punctures two hours after the ingestion of L-threonine capsules, but it was unclear whether this matched any potential rise in CSF glycine level. Thirdly we used a standard technique of amino acid analysis which might not be sensitive enough for its purpose. At such low glycine level (<20 μmol/l), it is associated with a high coefficient of variation (30%). The present study therefore neither confirms nor denies a small increase in glycine resulting from threonine administration and other more accurate methods of analysis are being explored at present. Lastly, the antispastic action of this amino acid may not involve glycinergic pathways at all.

In recent years, amino acids have seen an increasingly important role in the treatment of neurological disorders. The postsynaptic inhibitory action of glycine has been extensively studied using iontophoresis [17]. In animals with spinal spasticity, glycine led to tone improvement together with a rise of this amino acid in the gray matter of the spinal cord [18]. There is abundant evidence for glycine as an inhibitory neurotransmitter and it seems to have an important role in muscle tone control.

We have demonstrated in a preliminary study the antispastic effect of L-threonine and confirmed the results of previous open studies. We did not find any difference between dosages of 3 g and 6 g per day. This agent should now be investigated in a double-blind trial. Its efficacy should also be compared with baclofen. Although our study showed only modest effect with L-threonine in reducing muscle tone, the use of amino acid and development of glycinergic agents represents a new and potentially important approach to the treatment of spasticity.

References

1. Penn RD and Kroin JS (1987) Long-term Intrathecal Baclofen Infusion for Treatment of Spasticity. J. Neurosurg. 66: 181–185.
2. Hattab JR (1980) Review of European Clinical Trials with Baclofen. In: Feldman RG, Young RR and Koella WP (eds.) Spasticity: Disordered Motor Control. Year Book, Chicago, pp. 71–85.
3. Young AB and MacDonald RL (1983) Glycine as a Spinal Cord Neurotransmitter. In: Davidoff RA (ed.) Handbook of the Spinal Cord. Marcel Dekker, New York, pp. 1–43.
4. Davidoff RA, Shank RP, Graham LT, Aprison MH and Werman R (1967) Is Glycine a Neurotransmitter? Nature 214: 680–681.
5. Nader TMA, Growdon JH, Maher TJ and Wurtman RJ (1987) L-Threonine Administration Increases CSF Glycine Levels and Suppresses Spasticity. Neurology 37(1): 125.
6. Barbeau A, Roy M and Chouza C (1982) Pilot Study of Threonine Supplementation in Human Spasticity. Can. J. Neurol. Sci. 9(2): 141–145.
7. Bridgers WF (1968) Serine Transhydroxymethylase in Developing Mouse Brain. J. Neurochem. 15: 1325–1328.
8. Maher TJ and Wurtman RJ (1980) L-Threonine Administration Increases Glycine Concentrations in the Rat Central Nervous System. Life Sci. 26: 1283–1286.
9. Ashworth B (1964) Preliminary Trial of Carisoprodol in Multiple Sclerosis. Practitioner 192: 540–542.
10. Mahoney FI and Barthel DW (1965) Functional Evaluation: The Barthel Index. Md. State Med. J. 14: 61–65.
11. Kurtzke JF (1965) Further Notes on Disability Evaluation in Multiple Sclerosis, with Scale Modifications. Neurology 15: 654–661.
12. Perry TL and Jones RT (1961) The Amino Acid Content of Human Cerebrospinal Fluid in Normal Individuals and in Mental Defectives. J. Clin. Invest. 40: 1363–1372.
13. Armitage P and Berry G (1987) Statistical methods in medical research. Blackwell Scientific, Oxford, pp. 93–140.
14. Lee KC, Carson L, Kinnin E and Patterson VH (1989) The Ashworth Scale: a Reliable and Reproducible Method of Measuring Spasticity. Neurology 39(1): 143.
15. Burke D (1988) Spasticity as an Adaptation to Pyramidal Tract Injury. In: Waxman SG (ed.) Advances in Neurology Vol. 47, Functional Recovery in Neurological Disease. Raven Press, New York, pp. 401–422.

16. Skilbeck CE, Wade DT, Langton-Hewer R and Wood VA (1983) Recovery after stroke. J. Neurol. Neurosurg. Psychiatry 46: 5–8.
17. Curtis DR, Hosli L and Johnston GAR (1967) Inhibition of Spinal Neurones by Glycine. Nature 215: 1502–1503.
18. Smith JE, Hall PV, Galvin MR, Jones AR and Campbell RL (1979) Effects of Glycine Administration on Canine Experimental Spinal Spasticity and the Levels of Glycine, Glutamate, and Aspartate in the Lumbar Spinal Cord. Neurosurgery 4(2): 152–156.

Address for correspondence: Dr. V. Patterson, Department of Neurology, Royal Victoria Hospital, Belfast BT12 6BA, Northern Ireland.

Effectiveness of taurine in protecting biomembrane against oxidants

Ikuo Koyama, Katsu Nakamori, Tomomi Nakamura and Yasuo Ozawa

Department of Pharmaceutical Research, Taisho Pharmaceutical Co., Ltd., 403 Yoshino-Cho 1-Chome, Ohmiya-shi, Saitama 330, Japan

Abstract

We examined the effect of taurine and other antioxidants on erythrocytes following HOCl treatment under neutral conditions in phosphate buffer. At low HOCl:erythrocyte ratios, HOCl attacked the membrane of the erythrocytes causing gradual lysis, but hemoglobine was not oxidized. The lysis may be mainly due to the decomposition of free amino groups of membrane components into their respective aldehydes, and the degradation of peptide links. Taurine inhibited the lysis of HOCl-treated erythrocytes more effectively when the concentration was increased, and it appears that a complete inhibition of the lysis was attained at the highest concentration, 160 mM. Taurine may remove the chlorine in the membrane components thereby producing monochlortaurine (TauNHCl). In our study, TauNHCl was produced by the effect of taurine on HOCl-treated sepharose gel. In the case of the HOCl-treated erythrocytes, the yield of TauNHCl was so low that the amount of TauNHCl could not be exactly determined with the DPD (N'N-diethyl-p-phenyl-enediamine) method. The oxidation of intracellular components such as GSH (glutathione) by TauNHCl might result in the reduction of the amount of TauNHCl. But it is apparent that a small amount of TauNHCl was yielded. Further, taurine was the most effective inhibitor of the lysis compared with other amino acids such as glycine, α-alanine, and ß-alanine.

These results suggest that taurine could be effective in protecting the biomembrane against oxidants such as HOCl.

Introduction

It is well known that there is a high concentration of taurine in the retina, a tissue where various oxidants are generated photolytically and enzymatically [1,2], and in neutrophils, cells that enzymatically produce oxidants during the phagocytic process [3]. Taurine may have a significant role in protecting neutrophils against oxidative attack by acting as a trap for hypochlorous acid (HOCl) [4]. Wright *et al.* reported the role of taurine as a scavenger of oxidized chlorine in biological systems [5]. Some amino acids were reported to be membrane-stabilizing substances which inhibited the lysis of rabbit erythrocytes perturbed by chlorpromazine [6]. Taurine may also be a membrane-stabilizing substance. It has been reported that taurine may be effective in healing corneal damage caused by HOCl which is used to disinfect water in swimming pools [7]. In this study we examine the effectiveness of taurine in protecting biomembranes against HOCl, using erythrocytes as a model.

Experimental section

Materials

Taurine was synthesized in our laboratory. L-Glycine, L-α-alanine, L-ß-alanine, Sodium Hypochlorite Solution (NaClO), and N,N-Diethyl-p-phenylene-diamine Sulfate (DPD) were purchased from WAKO Pure Chemical Industries. Sepharose gel (EAH Sepharose^R gel 4B) was purchased from Pharmacia LKB. These and other chemicals used were reagent grade commercial products.

Cells

Fresh blood from a healthy Beagle dog was drawn into heparinized tubes. Red blood cells were then separated by centrifugation at 2,000 rpm for 5 min and washed three times with 40 mM phosphate buffered isotonic saline solution (pH 7.4, PBS). The packed cells were then diluted with PBS to make a red blood cell suspension of 4×10^8 cells/ml. This erythrocyte suspension was used as the stock solution for the experiments.

HOCl-treated erythrocytes

The amount of oxidized chlorines (HOCl) in NaClO solution was determined using the DPD method [8].

1 ml of varying concentrations of NaClO was added to 1 ml of erythrocyte suspension (4×10^8 cells/ml) in a test tube at 4°C. After 5 seconds, 2 ml of 80 mM taurine solution was added to the test tube to remove free HOCl from the suspension. These erythrocytes were then separated by centrifugation at 2,000 rpm for 5 min and washed once with PBS. The washed erythrocytes were then diluted with PBS to make HOCl-treated erythrocyte suspensions of 4×10^8 cells/ml and 4×10^7 cells/ml.

HOCl-treated sepharose gel

1 ml of sepharose gel with from 7 μmol to 11 μmol of free amino groups was used. The sepharose gel was washed three times and diluted by ten times with PBS. 1 ml of varying concentrations of NaClO was added to 1 ml of the sepharose gel suspension in a test tube at 4°C. After 1 min of treatment, 2 ml of 80 mM taurine solution was added to the test tube to remove free HOCl from the suspension. HOCl-treated sepharose gel was then separated by centrifugation at 2,000 rpm for 5 min and washed three times with PBS. HOCl-treated sepharose gel was diluted with PBS to produce the same sepharose gel concentration as that before the HOCl-treatment.

Quantitative determination of hemolytic behavior

HOCl-treated erythrocytes (4×10^7 cells/ml) were incubated with varying concentrations of taurine and other amino acids or without them over a 4 h period at 37°C. HOCl-induced hemolytic behavior was assayed by measuring the absorbance of released hemoglobine at 416 nm.

Determination of the removed chlorine (TauNHCl) from HOCl-treated sepharose gel and erythrocytes

2 ml of HOCl-treated erythrocyte suspension (4×10^8 cells/ml) or HOCl-treated sepharose gel suspension was incubated with 2 ml of PBS and 4 ml of varying concentrations of taurine over a 4 h period at 4°C.

The amount of removed chlorine (TauNHCl) in the supernate was determined using the DPD method and by measuring the absorbance of TauNHCl at 250 nm.

Result and Discussion

Figure 1 shows the time-dependent lysis of HOCl-treated erythrocytes. At a high concentration of HOCl, 423 μM, the erythrocytes caused rapid lysis, but hemo-

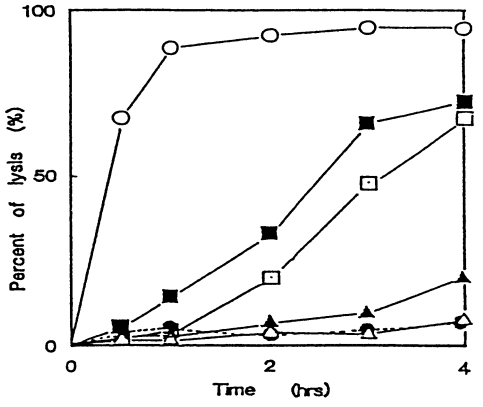

Fig. 1. Time-dependent lysis of HOCl-treated erythrocytes. The erythrocytes (10^7 cells/ml) treated with varying concentrations of NaClO solution were incubated at 37°C.
Key: Δ; 0 mM HOCl (final concentration), ●; 70 μM HOCl, ▲; 105 μM HOCl, □; 140 μM, ■; 213 μM, ○; 423 μM HOCl.

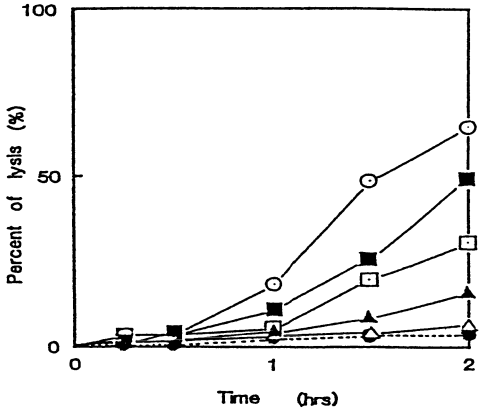

Fig. 2. Effect of taurine on inhibition of a HOCl-induced lysis. HOCl-treated erythrocytes (10^7 cells/ml) were incubated at 37°C in PBS with varying concentrations of taurine. Intact erythrocytes were incubated at 37°C in PBS as the control. Concentration of HOCl in NaClO solution used in HOCl treatment was 140 μM.
Key: ○; 0 mM taurine, ■; 5 mM taurine, □; 20 mM taurine, ▲; 40 mM taurine, Δ; 160 mM taurine, ●; control.

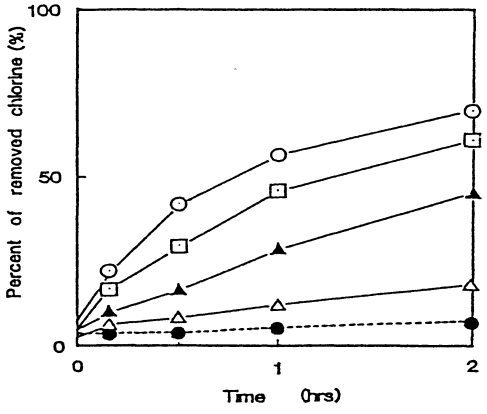

Fig. 3. Effect of taurine on removing the chlorine from HOCl-treated sepharose gel. HOCl-treated sepharose gel was incubated with varying concentrations of taurine at 37°C. Concentration of HOCl in NaClO solution that was used in HOCl-treatment was 2.8 mM. Percentage of removed chlorine was calculated from absorbance of TauNHCl at 250 nm.
Key: ●; 0 mM taurine (final concentration), Δ; 10 mM taurine, ▲; 20 mM taurine, ❑; 40 mM taurine, ○; 80 mM taurine.

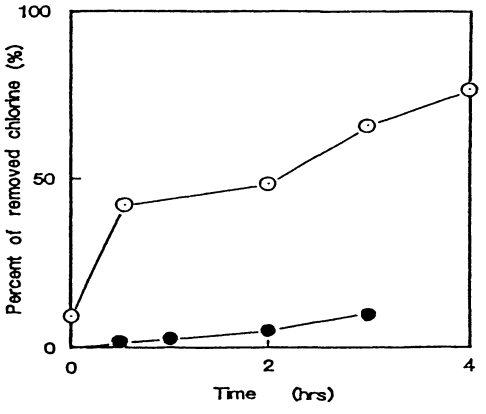

Fig. 4. Effect of taurine on removing the chlorine from the HOCl-treated sepharose gel and erythrocytes. HOCl-treated sepharose gel and erythrocytes (10^8 cells/ml) were incubated in PBS with 160 mM taurine. Concentration of HOCl in NaClO solution that was used in HOCl-treatment was 0.7 mM. Percentage of removed chlorine was calculated by determination of the amount of TauNHCl using the DPD method.
Key: ○; HOCl-treated sepharose gel, ●; HOCl-treated erythrocytes.

globine was not oxidized. HOCl could not pass through the membrane without encountering N-compounds and other substances that react with HOCl. At a concentration of HOCl lower than 213 μM, HOCl attacked the membrane of the erythrocytes, causing gradual lysis. This lysis may be mainly due to the gradual decomposition of free amino groups of membrane components into their respective aldehydes, and the gradual degradation of peptide links. The lipid peroxidation of the membrane may also be responsible for the lysis.

The effect of Taurine, a known scavenger of oxidized chlorine in biological systems on HOCl-induced lysis is shown in Fig. 2. Taurine inhibited the lysis of HOCl-treated erythrocytes more effectively when the concentration was increased, and complete inhibition of the lysis was attained at the highest concentration, 160 nM. Taurine is thought to stabilize the membrane of erythrocytes perturbed by HOCl.

It has been reported that taurine was found to extract the chlorine from a N-chloramine, such as a monochloroarginine [4]. Figure 3 shows the effect taurine has on removing the chlorine from HOCl-treated sepharose gel. Since the amount of amino groups in the sepharose gel was greatly in excess of HOCl, a part of each amino group was oxidized by HOCl thereby producing monochloroamine groups (-NHCl). Taurine removed the chlorine in the monochloroamino groups more

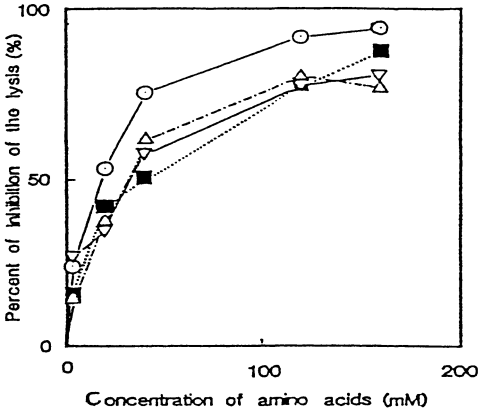

Fig. 5. Effect of various amimo acids on inhibiting a HOCl-induced lysis. HOCl-treated erythrocytes (10^7 cells/ml) were incubated in PBS with various amino acids at 37°C. Concentration of HOCl in NaClO solution that was used in HOCl-treatment was 0.7 mM.
Key: ○; taurine, ■; glycine, Δ; α-alanine, ∇; ß-alanine.

effectively when the concentration of taurine was increased. Fig. 4 shows that the yield of TauNHCl in the case of the HOCl-treated erythrocytes was much lower than that in the case of the HOCl-treated sepharose gel. The oxidation of intracellular components such as GSH by TauNHCl might result in the reduction of TauNHCl. But it is apparent that a small amount of TauNHCl was yielded.

Some amino acids such as glycine, lysine, and aspartic acid, have been reported to be membrane stabilizing substances which inhibit the lysis of rabbit erythrocytes perturbed by chlorpromazine [6]. Taurine may also be a membrane-stabilizing substance. Figure 5 shows the effect of various amino acids on the inhibition of a HOCl-induced lysis. The concentrations of taurine, α-alanine, ß-alanine and glycine required for 50% inhibition of the lysis of erythrocytes (hemolysis) were 18, 30, 34 and 40 mM respectively. Taurine was the most effective inhibitor of lysis compared with the other amino acids. This result suggests that taurine is an effective membrane-stabilizing substance more than other amino acids. Further, taurine may remove the chlorine in the membrane components more effectively than other amino acids.

These results suggest that taurine could be effective in protecting the membrane against oxidants such as HOCl.

References

1. Pasantes-Morales H, Klethi J, Leydig M and Mandel P (1972) Brain. Res. 41: 494.
2. Orr HT, Cohen AI and Lowry OH (1976) J. Neurochem. 26: 609.
3. Klebanoff SJ and Clark RA (1978) The Neutrophil: Function and Clinical Disorders. North Holland Publishing Company, Amsterdam.

4. Grisham MB, Tefferson MM, Melton DF and Thomas EL (1984) J. Biol. Chem. 259(16): 10404–10413.
5. Wright CE, Lin TT, Lin YY, Sturman JA and Gaull GE (1985) Taurin: Biological Actions and Clinical Perspectives. Alan R. Liss, Inc., pp. 137–147.
6. Takeuchi Y, Yamaoka Y, Morimoto Y and Kaneko I (1989) J. Pharm. Sci. 78(1): 3–7.
7. Yoshimura H, Shoji J and Kitano S (1989) N. Ganka Kiyou, in press.
8. A.P.N.A., A.W.W.A., W.P.C.F. (1975) Standard Method for the Examination of Water and Wastewater, 14th ed. Washington, pp. 329–332.

The effect of substance L on glucose mediated cross links of collagen in the diabetic KK mouse

G. Lubec, B. Bartosch, R. Mallinger, D. Adamiker, H. Höger and J. Gialamas

Departments of Paediatrics and Electron Microscopy, University of Vienna, Vienna, Austria
Institute of Versuchstierzucht, Himberg, Austria

Abstract

Genetically diabetic mice (KK) were given 50 mg/kg body weight/day substance L, a nontoxic basic amino acid, and compared to control diabetic mice without treatment. The oral administration of the compound was started at the age of 8 months and the animals were sacrificed at 12 months. No adverse effects were observed in animals given the substance L. Total food consumption, drinking water intake and body weight were comparable between the groups. Nonenzymatic glycosylation of serum proteins and hemoglobin was not significantly different in the groups. Renal pathological lesions in the control diabetic mice showed glomerular mesangial expansion and on electron microscopy thickened glomerular basement membranes with a mean thickness of 3,540 ± 301 Å. Treated animals showed significantly less mesangial crescents and thinner glomerular basement membrane thickness of 2,651 ± 199 Å ($p<0.01$). The experimental animals showed in addition a lower mean kidney weight. Glomerular but not tubular proteinuria was reduced in the treated group. Basement membrane collagen type IV isolated from kidneys of experimental animals was more soluble in acidity, showed a lower degree of cross linking as evaluated by SDS-polyacrylamide gel electrophoresis and lower glycosylation induced fluorescence. We therefore conclude that there is a benefit of substance L treatment to diabetic renal changes. We suggest that this positive effect was due to the inhibition of glucose mediated abnormal cross linking of collagenous structures by interaction of substance L with reactive carbonyl residues of glycosylation adducts of collagen.

Introduction

It is well known and documented that glucose mediated cross links play an important role in the pathogenesis of diabetic long term complications [1,2]. Glucose mediated cross links of collagen lead to insolubility and accumulation of collagenous material in the extracellular matrix, which in turn represents basement membrane thickening in micro- and macroangiopathy. Brownlee and coworkers reported the positive effect of aminoguanidine on glucose mediated cross links of collagen [3]. This important observation forced the basis to search for substances with the aforementioned activity, but without the high toxicity of this hydrazine compound.

A compound was found and figured out with the aminoguanidine group as nucleophilic residue and a nontoxic carbon skeleton and named substance L. Based on the experiments of Brownlee we tested the aminoguanidine-like activity of our compound *in vivo* on diabetic renal changes.

Materials and Methods

Animals

Twenty-eight KK mice (supplied by Prof. L. Herberg, Düsseldorf, F.R.G. and bred by the Institut für Versuchstierzucht, Himberg, Austria) were used in the experiments. At the onset of the study animals were 8 months old, they were sacrificed at 12 months. They were kept under a day/night rhythm at 23°C. They had free access to mouse cake, the control group also to tap water. The experimental group was fed a solution containing a daily dosage of substance L 50 mg/kg body weight/day orally. At the start and the end of the study body weight was taken and the fluid and food uptake calculated. The kidney weight was taken at sacrifice.

Histological examinations

The protocol of Lee [4] was followed for histological examinations of kidney sections and the evaluation of mesangial pathology was performed semiquantitatively according to Lee (0 through 4+).

Electron microscopy

The determination of basement membrane size and electron microscopical details are given in a previous publication [5].

For comparison of groups the Student's t test was applied. For nonenzymatic glycosylation of serum proteins the Fructosamin® kit (Hoffmann-La Roche) was used. Total glycosylated hemoglobin was measured by affinity chromatography after a standard procedure (Isolab). Collagen type IV was isolated from kidneys according to the protocol given by Dixit [6]. Collagen solubility in acetic acid was determined according to the method given by Bailey [7]. SDS-polyacrylamide gel electrophoresis (8%) for the characterization of collagen and the selectivity of urinary proteins was performed according to the method of Lämmli [8].

Fluorescence spectroscopy of isolated collagen was determined after the method published by Monnier and coworkers [9]. Proteinuria was measured by the Bradford method [10] and related to creatinine which was measured by a standard Jaffe technique.

Results

At the start of the experiment the body weight of animals in the non-treated group was 29 ± 4.2 g in the experimental panel 30.2 ± 5.1, the difference being non significant. At the end of the study at sacrifice the body weights were 64.5 ± 14.1 g in the experimental group versus 61.9 ± 13.8 in the control group. No statistical significance could be calculated.

The fluid and food uptake did not differ significantly in the groups either.

The kidney weights at sacrifice, however, were significantly different ($p<0.001$) with 171 ± 15.4 in the experimental and 201 ± 18.3 in the control group.

Light microscopical results

The non-treated controls showed diffuse widening and thickening of the mesangial region due to increased mesangial matrix material. The experimental animals displayed substantially less mesangial expansion and were clearly distinguishable from the controls. The relative degree of glomerular mesangial thickening was in controls 3.3 ± 0.2 and in the experimental mice 2.1 ± 0.2. A statistically significant lower degree was found in the Student's t test, with the probability of $p<0.001$.

Electron microscopy

Electron microscopical determination of the peripheral glomerular basement membrane width showed a significantly lower thickening in treated mice: 2,651 ± 199 Å, in contrast to non-treated diabetics with a thickness of 3,540 ± 301 ($p<0.001$, Fig. 1).

Nonenzymatic glycosylation

Fructosamin kit

The panel of non-treated mice showed mean values of 4.0 ± 0.9 µmol/l morpholinofructose in serum, the experimental group presented 3.7 ± 1.1 µmol/l – no significant difference was observed ($p<0.12$).

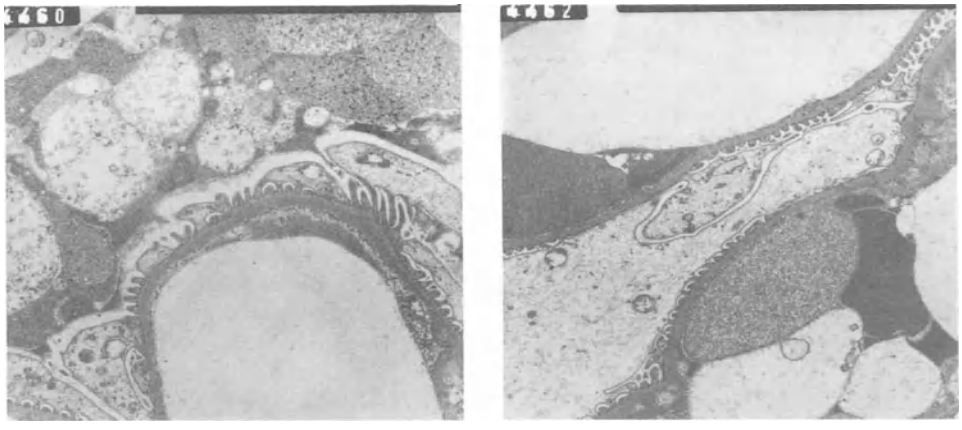

Fig. 1. Electron microscopical results of kidney sections: A photomicrograph of a kidney section of a treated (right) and a control (left) animal.

Total glycosylated hemoglobin
Total glycosylated hemoglobin was 8.9 ± 2.1 in the control group versus 7.2 ± 2.3 in the experimental group. No statistical significance could be shown.

Collagen type IV
Collagen type IV eluted from mouse kidneys in the experimental group based upon hydroxyproline determination revealed 11.2 ± 3.7 mg collagen per 100 mg of kidney protein versus 12.9 ± 4.2 mg collagen/100 mg. No statistical difference could be found.

Collagen solubility experiments

Acid salt soluble collagen was eluted from homogenized kidneys. From kidney of treated animals 4.7 mg collagen/100 mg kidney weight (dry) ± 0.2 was eluted versus 2.6 ± 0.4 mg collagen/100 mg kidney weight from non-treated controls. By Student's t test a significant increase in acid salt solubility in the treated group could be found ($p<0.001$).

SDS-polyacrylamide gel electrophoresis

On SDS-polyacrylamide gel electrophoresis the high molecular weight pattern dominated in pepsin digested extracted collagen of non-treated mouse kidneys. There was a visible shift in the pattern toward low molecular weight peptide patterns in the substance L treated kidney collagen preparations.

Fluorescence spectroscopical results were clearly different from isolated collagen of treated (absorbance 0.145 ± 25) versus non-treated (0.263 ± 41) animals ($p<0.01$).

Proteinuria was quantitatively not different in the groups (1400 µg/mg creatinine ± 189 in the non-treated versus 1290 ± 295 µg/mg creatinine in the treated panel. As evaluated by scanning of SDS-polyacrylamide gel electrophoresis however, there was a significant shift of albuminuria: in the non-treated group albuminuria counted for 55 ± 11 of urinary proteins, in the treated group for 35 ± 8% only ($p<0.01$).

Discussion

In previous experiments (to be published) we found that aminoguanidine could be replaced *in vitro* by substance L concerning the effect on glucose mediated cross links of collagen. Based upon these observations we started an *in vivo* study on spontaneously diabetic KK mice. They develop hyperinsulinemia several months after birth and first signs of glomerulopathy as mesangial proliferation and thickening of the glomerular basement membrane (GBM), thus forming a suitable and reliable model for therapy studies [11]. The animals were under the same metabolic control enabling the comparison of groups: fructosamine and total glyco-

sylated hemoglobin did not differ. The glomerular basement membrane consists mainly of collagen type IV [12] which becomes nonenzymatically glycosylated in the diabetic state. This leads to severe biochemical and biophysical changes: accumulation of collagenous material in the extracellular matrix, thickening of the GBM by increased synthesis and decreased catabolism. The major pathognomonic mechanism seem to be the abnormal glucose mediated cross linking of collagens [7] which renders the collagenous structures highly insoluble, a phenomenon easily to be observed *in vitro* and *in vivo*. In our study we could find a positive effect of substance L on glucose mediated cross links: on SDS-polyacrylamide gel electrophoresis the high molecular weight material reflecting cross linked collagen was less pronounced in contrast to non-treated controls. Solubility of collagen extracted from the kidneys of experimental animals was significantly increased, confirming the electrophoretical data of reduced abnormal cross linking.

The findings of decreased fluorescence of collagen isolated from the kidney are presenting the interaction of substance L with the glycosylation adducts on collagen leading to quenched absorption by the reaction (Fig. 2). This decrease in fluorescence reflecting the 'browning reaction' of proteins must not be interpreted as reduced nonenzymatic glycosylation.

As found on SDS-polyacrylamide gel electrophoresis of urinary proteins the glomerular (albumin) pattern was reduced in treated animals. The lack of differences between treated and non-treated groups expressed by non-different total proteinuria can be explained by the administration of the basic amino acid-substance L: it is well known and dated that the administration of amino acids leads

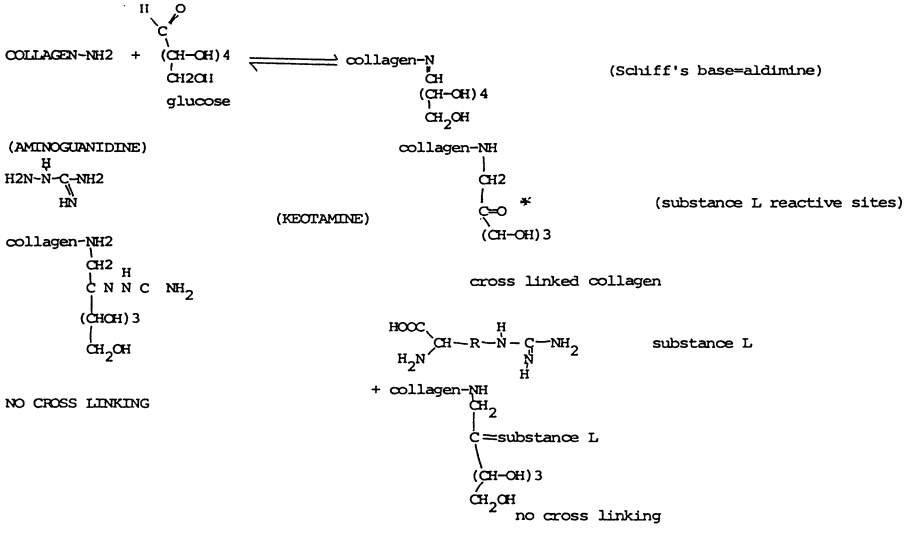

Fig. 2. Scheme of the reaction mechanism of substance L with nonenzymatic glycosylation adducts.
* the reactive carbonyl being blocked by amino residues.

to increased low molecular weight proteinuria due to inhibited tubular reabsorption, to name but ß-2-microglobulin [13]. The improvement of glomerular proteinuria in the treated animals could be explained by interactions of the highly positive charges of the basic amino acid with the charge barrier of acid glycosyaminoglycans in the GBM. The positive effect on diabetic renal changes is confirmed by the reduction of kidney weight in the treated group despite comparable body weight of the two panels. Electron microscopical data are in congruence with a positive effect revealing significantly reduced GBM thickness in the treated animals and semiquantitative data on mesangial proliferation as given by Lee [4] underline the action of the compound given. Studies with this substance are under way in other models like the BB rat, streptozotocin rats, db/db mice and first results are promising.

References

1. Rosenblom AL, Silverstein JH, Riley W, Lezotte DC, Richardson K and McCallum M (1981) N. Engl. J. Med. 305: 191–194.
2. McMillan DE and Cook SL (1981) Diabetologia 21: 303.
3. Brownlee M, Vlassara H, Kooney A, Ulrich P and Cerami A (1986) Science 232: 1629–1633.
4. Lee SM (1982) Diabetologia 22: 349–353.
5. Lubec G, Kitz K and Adamiker D (1979) Renal Physiol. 2: 79–82.
6. Dixit SN (1979) FEBS Lett. 106: 379–384.
7. Kent MH, Light ND and Bailey AJ (1985) Biochem. J. 225: 745–752.
8. Lämmli UK (1970) Nature 227: 680–687.
9. Monnier VM, Kohn RR and Cerami A (1984) Proc. N. A. S. (U.S.A.) 81: 583–587.
10. Bradford A (1976) Anal. Biochem. 72: 248–252.
11. Diani AR, Sawada GA, Zhang NY, Wyse BM, Connell CL, Vidmar TJ and Connell MA (1987) Blood Vessels 24: 297–303.
12. Lubec G (1983) Renal Physiol. 7: 61–62.
13. Mogensen CD and Solling K (1977) Scand. J. Clin. Lab. Invest. 37: 447–486.

Address for correspondence: G. Lubec, Department of Pediatrics, University of Vienna, Währinger Gürtel 18, A-1090 Vienna, Austria.

Hemodynamic effects of the renin inhibitor CP-80,794 in several species

William R. Murphy, Ronald T. Wester, Robert L. Rosati, Dennis J. Hoover, Irene M. Purcell, Joseph T. MacAndrew, Teresa M. Schelhorn, Donald E. Wilder, Andrew H. Smith and William F. Holt

Departments of Metabolic Diseases and Medicinal Chemistry, Pfizer Central Research, Eastern Point Road, Groton, Connecticut 063403, U.S.A.

Abstract

CP-80,794 is a potent, modified dipeptide inhibitor of human renin (*in vitro*, IC_{50} = 0.7 ± 0.1 nM). Inhibitory potency (IC_{50}) against plasma renin of guinea pigs, dogs and monkeys ranges from 0.3 to 0.7 nM allowing for evaluation of blood pressure lowering in these species. *In vivo* studies were performed in Na^+-depleted animals to render mean arterial pressure (MAP) renin-dependent. CP-80,794 at 3 mg/kg i.v. in conscious guinea pigs maximally depresses MAP ≈30 mmHg (captopril-like effect) for at least 2.5 h. In conscious marmoset monkeys CP-80,794 at 1 mg/kg i.v. maximally depresses MAP (≈20 mmHg) for more than 1 h. Cardiac output and heart rate are not affected by CP-80,794 suggesting that the fall in MAP involves only a change in vascular resistance (up to 40%). Orally at 30 mg/kg CP-80,794 reduces MAP for ≈2.5 h in conscious guinea pigs and for ≈3 h in cynomolgus monkeys. In marmoset monkeys 10 mg/kg p.o. of CP-80,794 decreases MAP ≈20 mmHg for more than 5 h. CP-80,794 does not affect MAP in guinea pigs, cynomolgus monkeys, or marmosets on normal sodium diets. Additionally, in renin-dependent hypertensive rats, CP-80,794 dose-dependently decreases blood pressure. In summary, the data on blood pressure lowering in several species are consistent with CP-80,794 acting through inhibition of renin.

Introduction

Renin is an aspartyl protease formed in the kidney and released into the circulation in response to factors such as decreased renal perfusion pressure/blood pressure (e.g. from hemorrhage or sodium/plasma volume depletion). Renin cleaves a liver-derived substrate, angiotensinogen, to form the decapeptide angiotensin I (AI). In the lung and other vascular sites, angiotensin converting enzyme (ACE) hydrolyzes a dipeptide from the carboxyl terminus of AI to form angiotensin II (AII). This octapeptide is capable of potent blood pressure elevating effects as a result of its direct vasoconstrictor activity to increase peripheral vascular resistance. AII indirectly raises blood pressure by stimulating the synthesis and release of aldosterone by adrenal glomerulosa cells to promote renal tubular and intestinal uptake of sodium and water, resulting in expansion of the extracellular fluid volume [1].

The important role of the renin-angiotensin system (RAS) in blood pressure regulation and electrolyte balance has been demonstrated by angiotensin convert-

ing enzyme (ACE) inhibitors. Pharmacological interruption of the RAS by ACE inhibition has proven to be effective in the treatment of hypertension and congestive heart failure. However, inhibiting ACE not only affects the RAS, but several other enzyme systems and this has raised questions concerning alternative mechanisms through which blood pressure may be lowered, and the side effects related to ACE inhibition. In contrast, inhibition of the very selective enzyme renin constitutes a RAS-specific approach to the treatment of hypertension [2]. One of the problems in the past with renin inhibitors, however, is that they have generally been primate specific and have lacked oral blood pressure lowering activity. We report here experiments concerning the biological activity of CP-80,794, a potent inhibitor both of primate renin and renin of several non-primate species. Identification of this compound has allowed for the evaluation of the cardiovascular effects of inhibition in species in addition to monkeys (e.g., rats, guinea pigs, hamsters, and dogs).

Methods

The blood pressure lowering effect of CP-80,794 (isopropyl N-[*N*-(4-morpholinocarbonyl)-L-phenylalaninyl-S-methyl-L-cysteinyl]-2-(*R*)-hydroxy-3(*S*)-amino-4-cyclo-hexybutanoate) was examined in four species: guinea pig, marmoset monkey, cynomolgus monkey, and the rat. In the guinea pig, marmoset monkey, and cynomolgus monkey sodium depletion was used as a means of stimulating the renin-angiotensin system, thus making blood pressure renin-dependent. In the rat, CP-80,794 was evaluated in an aortic coarctation model, which is a renin-dependent form of hypertension.

The IC_{50} represents the concentration of CP-80,794 that inhibited 50% of the normal generation of angiotensin I (AI) in a plasma sample. The generation of AI was measured using a plasma renin activity (radioimmunoassay) kit (Clinical Assays). The radioimmunoassay (RIA) kit was also used to measure the effects of CP-80,794 on plasma renin activity (PRA) in the cynomolgus monkey. To determine IC_{50}s, known concentrations of drug were added to plasma samples to generate a standard curve from which the IC_{50} was determined. Samples were incubated at 37°C for 3 h. A sample of plasma without drug was kept at 4°C and 37°C to control for background generation of AI (4°C) and to establish the maximal generation of AI at 37°C. At the end of the incubation 0.1 ml of sample was added to the antibody-coated tube along with 1 ml of ^{125}I-labeled AI solution and the samples were incubated for 18–20 h at 4°C. After removal of the radioactivity, samples were counted to determine the amount of AI generation. Guinea pig and marmoset monkey samples were incubated at 37°C for 2 h and rat samples for 1 h at 37°C. Determination of an IC_{50} for hog renin was performed by measuring AI generated by purified hog renin (Sigma Chemicals) added to rat plasma.

Guinea pigs (300 to 500 g) were placed on low sodium chow (Purina Laboratories) for a period of 2 weeks; at least three times during this period Lasix (furosemide, Hoechst-Roussel Pharmaceuticals) was given at a dose of 2 mg/kg, i.m., to accelerate sodium loss. Guinea pigs were anesthetized with 10 mg/kg xylazine (Haver, Bayvet Division of Miles Laboratories, Inc.), s.c., and 80 mg/kg ketamine HCl (Parke-Davis), i.m. The right common carotid artery was cannulated using PE 50 tubing (Clay-Adams) for the direct measurement of arterial blood pressure. A left jugular vein was catheterized for i.v. compound administration. Catheters were tunneled subcutaneously and exteriorized to the interscapular region of the animal's back. Guinea pigs were allowed to recover from surgery overnight. On next day CP-80,794 was given i.v. or p.o. in a vehicle consisting of 5% ethanol and 9.5% Emulphor in water. Cardiac output studies in the guinea pig were performed in anesthetized animals using thermodilution techniques (Cardio-Max II, Columbus Instruments).

Marmoset monkeys (≈250–350 g) were placed on a low sodium diet (BioServ, 0.02–0.04% sodium) for a period of 2 weeks. Animals were given Lasix (10 mg/kg, i.m.) at least three times during the second week of dietary sodium restriction. Marmosets were sedated with 16 mg/kg, i.m., ketamine HCl and intubated with an infant feeding tube. Anesthesia was induced with halothane. The right common carotid artery was cannulated using PE 50 tubing (Clay-Adams) for the measurement of arterial blood pressure. For intravenous dosing studies a left jugular vein was also catheterized. Catheters were tunneled subcutaneously and exteriorized to the interscapular region of the animal's back. On the following day, conscious marmosets were restrained in plexiglass chairs for the experiments. CP-80,794 was administered i.v. in a lipid emulsion (Intralipid, 10% lipid emulsion) plus (5%) ethanol; 0.1% methylcellulose was used as the drug carrier in the oral efficacy studies.

The oral efficacy of CP-80,794 in cynomolgus monkeys was examined in animals prepared with vascular access ports (VAP) to measure arterial pressure. The catheter of the VAP was advanced through the right carotid artery into the aorta and the VAP was secured subcutaneously between the shoulder blades. Experiments were performed after the animals had fully recovered from surgery (at least 1 month post-operative). Sodium depletion was accomplished by placing the animals on a low sodium diet (BioServ) for a period of 10 days and administering Lasix (2 mg/kg, i.m.) 4–5 times during this period. Animals were placed in a restraining chair, and arterial pressure was monitored via a Huber point needle inserted through the skin into the port septum. CP-80,794 was administered in 0.1% methylcellulose.

Renin-dependent hypertension was produced in male Sprague-Dawley rats (300–350 g) by coarctation of the aorta [3]. Rats were anesthetized with sodium pentobarbital (60 mg/kg), and the aorta was approached by a midline abdominal incision. The aorta was ligated between the renal arteries using 5-O silk suture, the incision was closed and the animals were allowed to recover. Three days later rats were re-anesthetized (60 mg/kg, sodium pentobarbital) and a femoral vein and

artery were cannulated. The catheters were then tunneled subcutaneously to exit in the interscapular region of the back. The following day rats were placed in small plexiglass restraining cages for the study. After a control period, CP-80,794 was infused i.v. for 15 min and the average fall in MAP was determined. With cessation of the i.v. infusion MAP rapidly returned to control levels in the rats. The animals were allowed approximately 60 min to stabilize before subsequent infusions of the renin inhibitor.

Arterial blood pressure for all studies was measured with Statham P23 ID pressure transducers and recorded on a Grass Model 7D physiograph. After establishing a stable control arterial pressure, CP-80,794 was administered i.v. or p.o. (gavage) and the effect on blood pressure was followed. Effects of the compound were monitored until blood pressure had returned to approximately pre-drug control levels. The i.v. and p.o. dosing vehicles had no effect on MAP. At the end of each experiment, animals were given an angiotensin-converting enzyme (ACE) inhibitor (captopril, 1 mg/kg i.v. for all species, except the cynomolgus monkey which received 15 mg/kg, p.o.) to determine the degree to which blood pressure had become renin-dependent. The sodium depletion regime was unsuccessful if animals did not respond to the ACE inhibitor and such animals were excluded from the study. Statistical comparisons were performed using a paired Student's t-test and the procedure outlined by Dunnet [4] for multiple comparisons with a single control.

Results

The IC_{50}s of CP-80,794 in human plasma and in the plasma of several other species are shown in Table 1. CP-80,794 possesses a similar level of inhibitory potency for plasma renin of different primates (IC_{50} = 0.5 nM against cynomolgus monkey renin, 0.6 nM against marmoset monkey renin, and 0.7 nM against human renin). The *in vitro* renin inhibitory activity of CP-80,794 was greatest against guinea pig renin (IC_{50} = 0.3 nM), and the value for dog (IC_{50} = 0.7 nM) and hamster renin

Table 1. Inhibition of plasma renin by CP-80,794 in the plasma of different species.

Species	IC_{50} (nM) ± S.E.M. CP-80,794
Human	0.7 ± 0.1 (n = 32)
Cynomolgus	0.5 ± 0.1 (n = 6)
Marmoset	0.6 ± 0.2 (n = 7)
Guinea pig	0.3 ± 0.1 (n = 6)
Dog	0.7 ± 0.2 (n = 6)
Hamster	0.9 ± 0.1 (n = 6)
Hog (rat substrate)	3.3 ± 0.3 (n = 6)
Rat	85.0 ± 7.0 (n = 6)

(IC_{50} = 0.9 nM) was similar to primate values. This suggested that the guinea pig could be used as a model for studying the cardiovascular effects of renin inhibition in a non-primate model. Compared to its activity in the primate, CP-80,794 was 5-fold less active against porcine renin (3.3 nM). CP-80,794 was 100-fold less potent against rat plasma renin (IC_{50} 85 nM).

Efficacy studies to evaluate the blood pressure lowering effects of CP-80,794 were performed in the guinea pig, two primate species (marmoset monkey and cynomolgus monkey) and in the rat. CP-80,794 administered to conscious, sodium-deficient guinea pigs by the i.v. and oral routes produces significant blood pressure lowering. As shown in Fig. 1, a dose of 0.3 mg/kg promotes an immediate and profound depression of MAP. The maximal depression of blood pressure at this dose is 18.6 ± 3.8 mmHg (mean ± S.E.M.) from a resting MAP of 57.2 ± 1.7 mmHg (normal baseline blood pressure for guinea pigs). However, the duration of the blood pressure lowering effect was short-lived, and in less than half an hour post-drug the blood pressure had returned to control levels. Increasing the dose of CP-80,794 to 1 mg/kg produced a similar absolute fall in MAP as observed above, but the duration of blood pressure lowering effect was increased to approximately one hour. Increasing the dose to 3 mg/kg, i.v., produced a more profound effect; the absolute fall in MAP was 28.6 ± 3.9 mmHg. This effect was equivalent to that produced by a maximally effective dose of captopril in the animals. Blood pressure remained at this level for nearly 30 min before beginning to return toward pre-drug levels. Two and one half hours later, the effect had waned and blood pressure had essentially returned to control levels. Higher doses of the renin inhibitor were not studied in this species; it is speculated that although the absolute fall in blood pressure would be equivalent to the 3 mg/kg dose, the duration of effect would be longer.

Studies were performed in the guinea pig to determine whether changes in vascular tone or cardiac performance caused the blood pressure lowering effect of CP-80,794. Cardiac output, arterial pressure and heart rate were examined in anesthetized guinea pigs at an intravenous dose of 1 mg/kg of CP-80,794. Cardiac output before drug was 71.5 ± 7.9 ml/min (n = 6); 10–15 min after giving 1 mg/kg

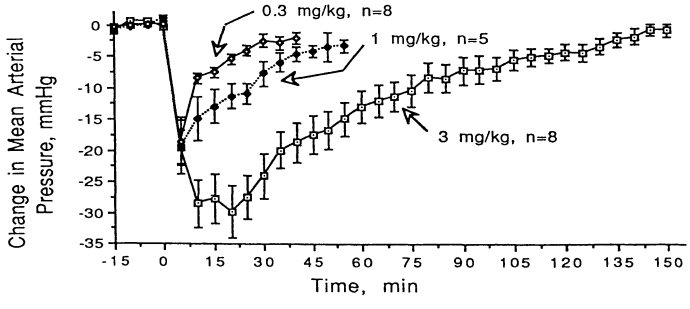

Fig. 1. The effect of intravenously administered CP-80,794 on blood pressure in conscious, sodium-depleted guinea pigs.

of CP-80,794 cardiac output (CO) showed a slight, but not significant increase to 76.3 ± 10.8 ml/min. MAP in the guinea pigs fell from 38 ± 2.2 to 26.5 ± 1.7 mmHg ($p<0.01$). Control TPR (total peripheral resistance) in the study was 0.56 ± 0.05 mmHg/ml/min. The administration of 1 mg/kg of CP-80,794 to the guinea pigs produced a highly significant change in TPR. Total peripheral resistance fell to 0.37 ± 0.04 mmHg/ml/min ($p<0.001$) after drug, which represents a 34% reduction. Importantly, this indicates that CP-80,794 produces its effects on blood pressure through changes in TPR and not through changes in CO. An additional 4 mg/kg of CP-80,794 for a total of 5 mg/kg ($n = 4$) produced no significant changes in MAP and CO; TPR was calculated as 0.41 ± 0.06 mmHg/ml/min. Heart rate in the guinea pigs was unchanged throughout the study (i.e., as for ACE inhibitors no reflex tachycardia was observed); the control heart rate was 212 ± 10 bpm (beats/min). After 1 mg/kg of CP-80,794 heart rate was 209 ± 9 bpm, and after 5 mg/kg 198 ± 11 bpm.

The oral efficacy of CP-80,794 was also evaluated in the guinea pig. Shown in Fig. 2 is the effect of a 30 mg/kg oral dose of CP-80,794 in the guinea pig. The baseline MAP of the guinea pigs in this study was 57.1 ± 1.3 mmHg. CP-80,794's effect on blood pressure after oral gavage at this dose was slower in onset and not of the magnitude seen with intravenous dosing. The maximal decrease in MAP occurred 50 min post-dose with an absolute fall in MAP of 11.2 ± 2.6 mmHg. From this point MAP slowly recovered with time; the experiment was concluded approximately 3 h after administering CP-80,794. The change in MAP was significant at the 60 ($p<0.05$) and 120 ($p<0.01$) min time points as compared to control, but the change in MAP was not statistically significant at 180 min after drug.

CP-80,794 was administered i.v. and p.o. to conscious, sodium-depleted marmoset monkeys. At an i.v. dose of 3 μg/kg, there was a modest fall in MAP with the duration of effect lasting less than 15 min (Fig. 3). Although the blood pressure lowering effect was not significant at a dose of 3 μg/kg in conscious marmosets, it

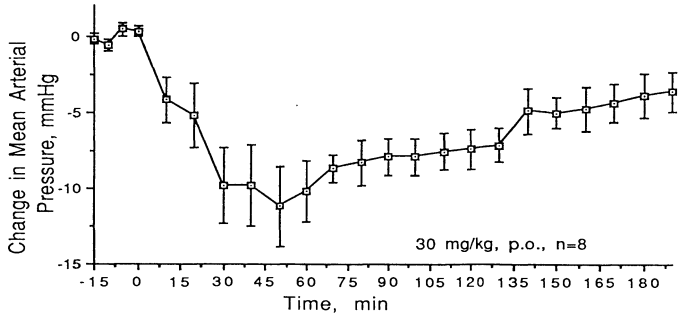

Fig. 2. Effect of a 30 mg/kg oral dose of CP-80,794 on blood pressure in conscious, sodium-depleted guinea pigs.

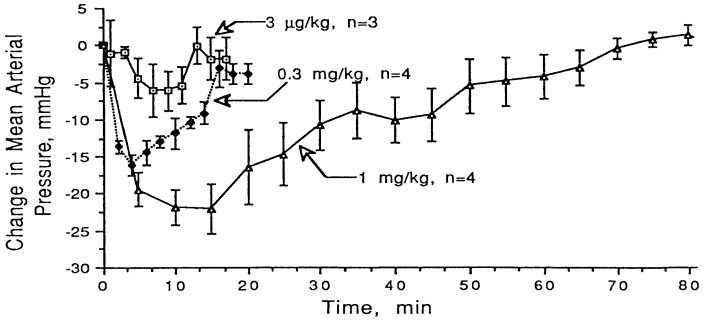

Fig. 3. Effect of intravenous CP-80,794 on blood pressure in conscious, sodium-depleted marmoset monkeys.

is highly significant ($p<0.01$) 5 min after i.v. administration of CP-80,794 at 0.3 mg/kg. CP-80,794 at an i.v. dose of 1 mg/kg produced a peak reduction in blood pressure of 22.0 ± 3.4 mmHg; the fall in MAP was equivalent to that produced by a maximally effective i.v. dose of captopril. Although significant at earlier time points at this dose, blood pressure lowering was not significantly different from the pre-drug levels 40 min after compound administration. CP-80,794 administered orally to the marmosets at a dose of 10 mg/kg (Fig. 4) produced a peak effect on blood pressure similar to that resulting from a 1 mg/kg i.v. dose of CP-80,794 (i.e., 20–25 mmHg). The effect on blood pressure was long-lasting; MAP had not fully returned to control levels when the study was stopped 330 min post-drug.

To further understand the effects of renin inhibition in primates, oral efficacy studies with CP-80,794 were also performed in cynomolgus monkeys. The relatively large size of these monkeys compared to marmosets (i.e., 3 kg versus 300 g)

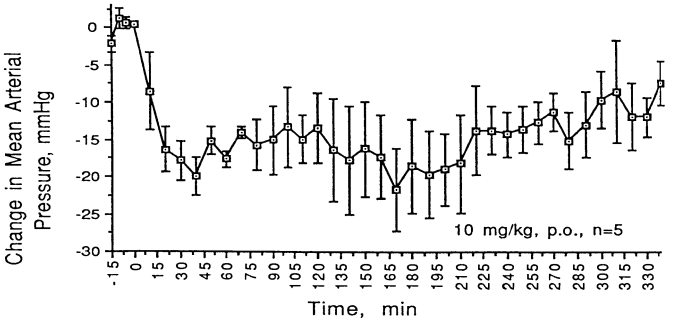

Fig. 4. Effect of CP-80,794, 10 mg/kg p.o., on mean arterial pressure in conscious, sodium-depleted marmoset monkeys.

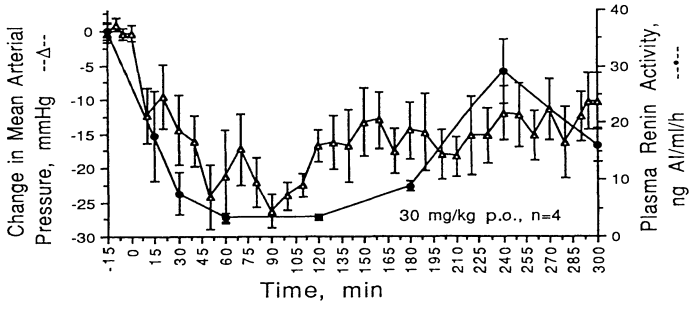

Fig. 5. The effects of oral CP-80,794, 30 mg/kg, on blood pressure (left axis) and plasma renin activity (right axis) in conscious, sodium depleted cynomolgus monkeys.

meant that sequential plasma samples could be collected over the course of the study to examine the relationship between PRA and blood pressure. As shown in Fig. 5 (left axis) a 30 mg/kg (p.o.) dose of CP-80,794 produced a maximal fall in blood pressure of 26.3 ± 2.4 mmHg which occurred at 90 min after drug; the control MAP for these animals was 109 ± 5.2 mmHg. MAP slowly recovered from its nadir remaining approximately 15 mmHg below the baseline MAP value for the next several hours. Five hours post-drug, blood pressure was still approximately 10 mmHg below baseline. Captopril (15 mg/kg, p.o.) at the end of the study produced an additional 25 mmHg decrease in MAP; 15 min after captopril MAP was 35.3 ± 4.6 mmHg lower than initial control levels, indicating what one should expect from complete inhibition of plasma renin in this species.

PRA was also measured at several time points during the course of the study. As shown in Fig. 5 (right axis), the effects of CP-80,794 on PRA and blood pressure closely paralleled each other over the course of the study. Baseline PRA was 36.4 ± 1.6 ng AI/ml/h in these sodium-depleted cynomolgus monkeys. After drug, PRA and MAP fell in unison during the first hour. Sixty minutes after the 30 mg/kg oral dose of CP-80,794, PRA had decreased to 3.4 ± 0.8 ng AI/ml/h, its lowest point. This represents over a 90% reduction in PRA compared to control levels. As the effect of the compound waned and blood pressure began to recover, there was a corresponding increase in PRA. PRA values were statistically ($p<0.05$) different from control from 60 to 240 min after oral administration of CP-80,794.

The studies described so far have involved only normotensive animals, but there was also interest in ascertaining the blood pressure lowering effects of CP-80,794 in hypertensive animals. CP-80,794 was evaluated in a renin-dependent model of hypertension, a rat coarctation model which involved ligation of the aorta between the renal arteries. The baseline mean arterial pressure of the animals used in the study was 171.6 ± 2.3 mmHg (n = 8). Because CP-80,794 is rapidly eliminated by the rat and is far less active against rat renin (IC_{50} = 85 ± 7 nM), the renin inhibitor was administered by i.v. infusion. CP-80,794 was administered at three infusion rates as shown in Fig. 6. CP-80,794 produced a dose-dependent reduction in MAP

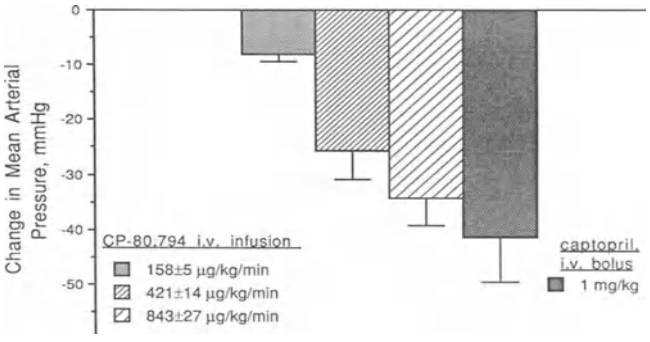

Fig. 6. The blood pressure lowering effect of intravenously infused CP-80,794 in a renin-dependent rat hypertension model. Hypertension was produced through coarctation of the aorta between the kidneys.

that was highly significant ($p<0.01$) at all three infusions. Infusion of CP-80,794 at 158 µg/kg/min decreased MAP by 8.1 ± 1.5 mmHg from control MAP in the rats. The 421 ± 14 µg/kg/min infusion produced a fall in MAP of 25.8 ± 4.9 mmHg. MAP decreased by 34.4 ± 4.9 mmHg at the highest infusion rate of 843 ± 27 µg/kg/min. Blood pressure rapidly returned to control upon terminating each infusion. Captopril at the end of the study decreased MAP by 41.3 ± 8.3 mmHg compared to the pre-captopril blood pressure (see Fig. 6). The captopril response was taken as the maximal MAP lowering effect attainable in this renin-dependent model by blockade of the renin-angiotensin system. Based on this response the infusion rate of CP-80,794 that produces half of the maximal blood pressure lowering effect was calculated as 480 µg/kg/min.

Discussion

CP-80,794 is a potent inhibitor of plasma renin in several different species. The compound is unusual in that it possesses sub-nanomolar potency against guinea pig, hamster, canine, marmoset monkey, cynomolgus monkey, and human renin, and <100 nM potency against rat renin. Many of the renin inhibitors in the literature are highly primate specific, exhibiting significantly less activity against the renin of species such as the dog and rat [5–7]. This presents a problem because the dog and rat are the species commonly used in hypertension research. A few renin inhibitors do demonstrate activity against dog and rat renin [8–10], which allows for evaluation in these species; the use of a primate model is the only means of evaluating the primate specific compounds. CP-80,794's activity across species lines allowed for the cardiovascular evaluation of the renin inhibitor in guinea pig and rat models, in addition to the primate models. This appears to be the first report of a renin inhibitor lowering blood pressure in the guinea pig. Furthermore, it

suggests that guinea pig renin is more like human renin than is rat renin; thus the guinea pig can serve as a small animal model to replace the rat when one is interested in investigating the effects of renin inhibition.

CP-80,794 is effective in lowering blood pressure after i.v. and oral administration in conscious, sodium-depleted guinea pigs and marmoset monkeys. The compound was also found to be effective orally in another primate species, the cynomolgus monkey. Intravenously, CP-80,794 produces a similar degree of blood pressure lowering in both the guinea pig and marmoset monkey models. At a dose of 0.3 mg/kg the absolute fall in blood pressure was similar in both models (15–20 mmHg), as was the short duration of the response (<30 min). Increasing the dose to 1 mg/kg i.v. produced a fall in MAP of approximately 20 mmHg in both species; again the duration of the response was similar in the two species with blood pressure returning to baseline within approximately 60 min. With respect to oral efficacy, there appear to be clear differences between the conscious, sodium-depleted guinea pig, marmoset monkey and cynomolgus monkey models. A 30 mg/kg oral dose of CP-80,794 in the guinea pig produces only a modest depression of blood pressure with a duration of effect lasting approximately 180 min. An equivalent oral dose of CP-80,794 in the cynomolgus monkey produces a peak depression of MAP over twice that observed in the guinea pig and with a total duration of effect lasting for more than 300 min. A difference in the degree of sodium depletion is not suspected as a factor since a maximal dose of the ACE inhibitor captopril, or CP-80,794 produces a similar absolute fall in MAP (25–30 mmHg) in both species.

The blood pressure lowering effect of CP-80,794 by the oral route was greater in the marmoset monkey as compared to the guinea pig or cynomolgus monkey. A 10 mg/kg oral dose of CP-80,794 in the marmoset produced a rapid decline in MAP, with the major effect on blood pressure occurring within 20 min after dosing. MAP remained at that level for approximately $3^1/2$ h before beginning a slow increase toward control levels; MAP had not fully recovered when the study was ceased at 340 min. By comparison 30 mg/kg of CP-80,794 (p.o.) in the guinea pig produced only a modest effect on MAP. The fact that the *in vitro* and i.v. activities of CP-80,794 are similar in the two species suggests that the compound is less well absorbed in the guinea pig. The oral efficacy of CP-80,794 in the cynomolgus monkey was intermediate between that observed in the guinea pig and the marmoset. A 30 mg/kg oral dose of CP-80,794 in the cynomolgus monkey produced a depressor response of magnitude and duration similar to that of 10 mg/kg of CP-80,794 (p.o.) in the marmoset monkey. CP-80,794 given at 10 mg/kg in the cynomolgus had no significant effects on MAP. Thus, oral CP-80,794 is more efficacious in the marmoset compared to the cynomolgus monkey. A conclusion that can be drawn from these studies is that pharmacokinetic parameters (including the contribution of oral absorption) of a renin inhibitor can vary widely between species, and that comparisons concerning the oral activity of renin inhibitors may not be predictable across species lines.

CP-80,794 does not have significant effects in animals whose blood pressure has not been made renin-dependent. CP-80,794 at 3 mg/kg, i.v., in guinea pigs fed a normal sodium diet produced only a slight, transient effect on MAP; in sodium-depleted guinea pigs, the same dose decreased MAP by 30 mmHg and took several hours to recover. In addition, the compound had no significant effects on blood pressure in the marmoset (1 mg/kg,i.v.) or the cynomolgus monkey (30 mg/kg, p.o.). This suggests that in these short term studies the blood pressure lowering activity of CP-80,794 results only from renin inhibition. Interestingly, there have been reports concerning renin inhibitors which are effective in lowering blood pressure in sodium-replete animals. A-62198 has been reported to lower MAP with nearly equal effect in sodium-replete and -depleted anesthetized cynomolgus monkeys [5]. Maruyama *et al.* [11] recently reported that KRI-1314 produces the same magnitude of effect on MAP in replete and depleted marmoset monkeys after a single 30 mg/kg oral dose, or after chronically administering the compound to animals for a period of 2 weeks. It has not been determined if these observations are related to renin inhibition or some other effect of the compound on blood pressure.

A reduction in MAP can be accomplished by reducing either TPR (total peripheral resistance) or cardiac output. A reduction in cardiac output is not a desirable means by which to reduce blood pressure; thus CP-80,794 was evaluated for its effects on cardiac output. CP-80,794 at 1 mg/kg, i.v., in the guinea pig maintained CO while producing a dramatic fall in MAP which resulted in a significant decrease in TPR (34%). CP-80,794's effect on MAP occurs through a reduction in TPR due to a reduction in circulating levels of the potent vasoconstrictor AII. Increasing the dose of CP-80,794 to 5 mg/kg produced no further changes in MAP, CO, or TPR. Heart rate was not affected by CP-80,794 in any of the *in vivo* efficacy studies. In spite of significant decreases in MAP produced by CP-80,794, there was no evidence of a reflex tachycardia. The lack of reflex tachycardia has been consistently noted with other renin inhibitors [5,6,10].

The effect of CP-80,794 on plasma renin activity and blood pressure closely paralleled each other in the cynomolgus monkey. After the oral administration of CP-80,794, MAP and PRA declined in a parallel fashion during the experiments. The maximal blood pressure lowering effect occurred approximately 60 min post-drug, and this corresponded to the maximal fall in PRA. The suppression of PRA was not absolute at this point; PRA at 60 min was 3.4 ± 0.8 ng AI/ml/h, which was approximately 90% of the control value. As blood pressure began to increase in the animals there was also a corresponding increase in PRA. Not all renin inhibitors exhibit this relationship between PRA and MAP. Several renin inhibitors have been reported to cause a total suppression of PRA in sodium-deficient animals at doses without effects on blood pressure. Only when the renin inhibitors are given in excess of a dose producing total suppression of PRA are the effects on blood pressure observed [8,10,12]. However, other compounds are similar to CP-80,794 with respect to the relationship between PRA and MAP [7,13]. Therefore, the relationship between PRA and MAP may be specific to each particular

renin inhibitor. An explanation for the dissociation between PRA and MAP may lie in the renin compartments being reached by an inhibitor. Inhibitors which show a dissociation between PRA and blood pressure may fully affect circulating renin at low plasma concentrations, but the effects on MAP only occur at higher plasma levels when the concentration of inhibitor begins to increase in key tissue compartments. The data reported here demonstrate a strong relationship between the blood pressure lowering effect of CP-80,794 and a reduction in PRA. At this time we have no information concerning blood pressure lowering and inhibition of tissue renin by CP-80,794. Work remains to be performed to explain the relationship between PRA and blood pressure lowering with renin inhibition.

The ability of a renin inhibitor to lower blood pressure in a sodium-deficient, normotensive animal may not ensure that it will be effective in the treatment of hypertension. Renin inhibitors are being developed primarily as antihypertensive agents (although inhibition of the renin angiotensin system by ACE inhibitors has been effective in the treatment of congestive heart failure) and demonstrating the effectiveness of CP-80,794 in a hypertension model was necessary [2]. Because CP-80,794 is active against rat renin, a rat coarctation model was chosen to evaluate the compound's antihypertensive effects. As shown in Fig. 6, CP-80,794 produced a dose-dependent effect on blood pressure lowering in this hypertension model. The fall in MAP at the highest dose was similar to that produced by a maximally effective dose of the ACE inhibitor captopril.

In summary, CP-80,794 is a potent *in vitro* inhibitor of renin in several species. CP-80,794 lowers blood pressure in the guinea pig, marmoset monkey, and cynomolgus monkey when given by the oral route, and in a manner consistent with it acting solely as a renin inhibitor. CP-80,794 was also effective in reducing MAP in a renin-dependent model of hypertension (rat coarctation model). The compound is without effect on heart rate and cardiac output. Blood pressure lowering appears to be the result of vasodilatory activity that is expressed as a result of interruption of the renin-angiotensin cascade. The high degree of potency against the renins of different species means that CP-80,794 can be utilized in a variety of different animal models to examine the contribution of renin in regulating blood pressure in different physiologic and pathophysiologic states. This will in turn lead to a more complete understanding of the renin-angiotensin system (and its different components) in cardiovascular and renal homeostasis.

References

1. Vallotton MB (1987) TIPS 8: 69–74.
2. Greenlee WJ (1987) Pharm. Res. 4: 364–374.
3. Fernandes M, Onesti G, Weder A, Dykyj R, Gould AB, Kim KE and Swartz C (1976) J. Lab. Clin. Med. 87: 561–567.
4. Dunnett CW (1964) Biometrics 20: 482–491.
5. Kleinert HD, Martin D, Chekal M, Young G, Rosenberg S, Plattner JJ and Perun TJ (1988) J. Pharm. Exp. Ther. 246: 975–979.

6. Pals DT, Thaisvongs S, Lawson JA, Kati WM, Turner SR, DeGraaf GL, Harris DW and Johnson GA (1986) Hypertension 8: 1105–1112.
7. Wood JM, Gulati N, Forgiarini P, Fuhrer W and Hofbauer KG (1985) Hypertension 7: 797–803.
8. Blaine EJ, Schorn TW and Boger J (1984) Hypertension 6(I): I-111–I-118.
9. Mento PW, Holt WF, Murphy WR and Wilkes BM (1989) Hypertension 13: 741–748.
10. Wood JM, Criscione L, de Gasparo M, Buhlmayer P, Rueger H, Stanton JL, Jupp RA and Kay J (1989) J. Cardio. Pharm. 14: 221–226.
11. Maruyasu K, Moro M, Murakami M, Etoh Y, Kubota T and Ikeda S (1989) Jap. J. Pharm. 49: Suppl. 214 P.
12. DeForrest JM, Waldron TL, Oehl RS, Scalese RJ, Free CA, Weller HN and Ryono DE (1989) J. Hyperten. 7(2): 515–519.
13. Miyazaki M, Etoh Y, Iizuka K and Toda N (1989) J. Hyperten. 7(2): 525–527.

Address for correspondence: William R. Murphy, PhD, Department of Metabolic Diseases, Pfizer Central Research, Eastern Point Road, Groton, Connecticut 06340, U.S.A.

Phosphatidylserine: Preclinical basis for a therapeutic approach to the aging brain

A. Zanotti, M.G. Nunzi, F. Milan, D. Guidolin and G. Toffano

Fidia Research Laboratories, Via Ponte della Fabbrica 3/A, 35031 Abano Terme (PD), Italy

Abstract

In rats, chronic oral phosphatidylserine (BC-PS) administration (50 mg/kg) prevented age-induced atrophy of the cholinergic neuronal population in the septal complex and restored spatial behaviour in aged impaired animals. The effects of BC-PS could be related to its pharmacological action on neuronal membranes and neurotransmission and forms a rational basis for the therapeutic use of BC-PS in treating cognitive deterioration associated with pathological aging.

Introduction

Aging is characterized by a decay of learning and memory function. Neurochemically, a decrease of cholinergic and monoaminergic neurotransmission, among others, occurs both in normal and pathological aging. In particular, the degree of cognitive deficits in Alzheimer's Disease and related disorders has been correlated with morphological alterations and loss of cholinergic markers in basal forebrain nuclei, hippocampus and neocortex [1,2]. Based on this evidence, treatments capable of increasing cholinergic function have been suggested to be potentially useful in relieving clinical symptoms of dementia [3]. Brain cortex phosphatidylserine (BC-PS), a pharmacologically active phospholipid [4], counteracts age-related changes in the central nervous system of rodents. BC-PS increases Na^+/K^+ATPase activity [5], normalizes the membrane cholesterol to phospholipid molar ratio [6] and restores the electrically stimulated release of acetylcholine (Ach) in cortical slices [7]. Moreover, BC-PS prevents loss of dendritic spines in the CA_1 region of the hippocampus [8]. These dendritic spines receive synaptic contacts from cholinergic fibers originating in the basal forebrain and have been proposed as a substrate for information storage [9]. We investigated the effects of BC-PS administration on structural deterioration of the cholinergic neurons of the basal forebrain and on spatial memory in aged rats. Spatial learning in rodents is, in fact, dependent upon structural and functional integrity of the septo-hippocampal cholinergic system [10].

Experimental procedures

Animals in this study were male Sprague-Dawley rats (Charles River, Italy), maintained on 12 h light: 12 h dark cycle, with access to drinking water and food *ad libitum*. An aqueous suspension of BC-PS was given to the rats in place of the drinking water. The concentration of the phospholipid was adjusted throughout the course of the treatment, in order to ensure an average daily intake of 50 mg/kg BC-PS per rat. For morphological analysis BC-PS was administered from the age of 15 months to sacrifice. In the behavioural study, BC-PS administration started 1 week after screening and lasted until the end of behavioural testing.

Brains of young-adult (4 month), aged (27 month) and aged-matched BC-PS-treated rats, were processed for choline acetyltransferase (ChAT) immunocytochemistry. After perfusion with a mixture of aldehydes (4% paraformaldehyde and 0.05% glutaraldehyde in 0.1 M sodium phosphate buffer, pH 7.4), the brains were cut on a Vibratome. The sections through the septal complex (medial septum and diagonal band) were incubated with a monoclonal antibody to ChAT (Boehringer, Type I), and were then processed for peroxidase-antiperoxidase immunocytochemistry. The sections were mounted on glass slides, reacted with 2% OsO_4 and processed by standard procedures for light microscopic observation.

For morphometric analysis of ChAT-immunoreactive neurons, three parameters were considered: number of ChAT-positive cells, area covered by all immunoreactive profiles (somata and neuronal processes) and somatic cross-sectional area. Morphometric analysis was carried out by means of a computerized image analysis system (IBAS, Kontron, Zeiss). The sections analyzed contained the greatest extension of the medial septum and diagonal band. For each animal the mean of the sections was considered. Differences across the animal groups were tested by means of the Student's t test.

For assessment of spatial memory, young-adult (5 month) and old (21–24 month) rats were tested in the Morris Water Maze [11] using a large pool (150 cm in diameter) with a submerged circular platform positioned in one of 4 quadrants defined by the cardinal points. Rats could locate the platform only by use of the many extramaze spatial cues available. The rats were trained in 2 blocks of 4 trials each, every day of each test week, i.e. at screening and after 7 and 12 weeks of treatment (week 7 and week 12).

After the last trial of week 7, the rats were submitted to a single spatial probe trial (platform was removed from the pool) for evaluation of searching behaviour.

The swim path and latency to the hidden platform were automatically recorded. Old impaired rats were selected based on a mean escape latency in the screening test above the 99% confidence limit of the young-adult group, and then assigned to the treatment groups. The remaining old rats constituted the old non-impaired group.

Results

The morphometric immunohystochemical study shows regressive changes in the cholinergic neuronal population of forebrain nuclei of old rats. The cholinergic cell number is markedly decreased in aged animals with respect to young subjects (−19.6%, $p<0.01$), suggesting a high vulnerability of the cholinergic cells to age-related compromising processes. Similarly, the area covered in the sections by all immunoreactive structures decreases significantly in old untreated rats as compared to young controls (−41%, $p<0.05$). This is consistent with the reduction in soma size of ChAT-positive neurons observed in the aged group of animals with respect to young rats (−18.5%, $p<0.05$). No statistically significant differences in the above reported parameters are found between old BC-PS-treated rats and young animals (Fig. 1).

Behavioural performance in the Morris Water Maze indicates that a subpopulation of old rats is impaired in the acquisition of the spatial task. Mean escape latencies of young, old non-impaired, old impaired control and old impaired BC-PS treated rats to reach the hidden platform are shown in Fig. 2. The performance of old impaired control rats does not change throughout testing and continues to be significantly different from that of young and old non-impaired rats. In contrast, treatment with BC-PS improves the performance of old impaired rats at both retesting weeks, as shown by the significant decrease in escape latencies as compared to screening.

The searching behaviour of rats of all groups (i.e. the ability to use spatial cues to locate the platform in the pool) was evaluated in the probe trial by counting the intersections (annulus entries) of the swim path with a platform-sized nominal annulus at the center of each quadrant, defining a possible platform location. While

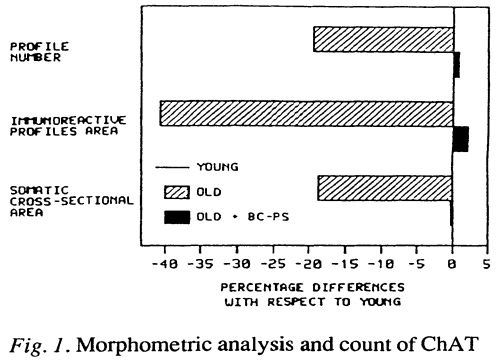

Fig. 1. Morphometric analysis and count of ChAT positive neurons in the basal forebrain of old untreated and old BC-PS-treated rats. Values are expressed as percentage difference with respect to the values found in young 4-month-old rats, assumed as baseline (young = 0).

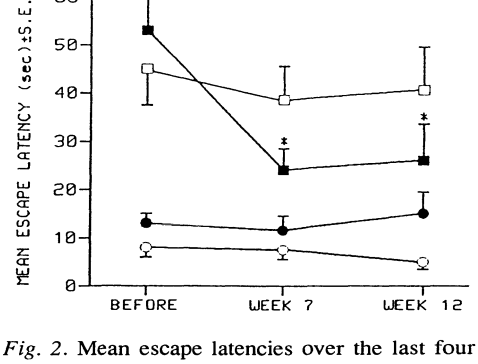

Fig. 2. Mean escape latencies over the last four trial blocks during screening (before), week 7 and week 12 for young (0, n=8), aged non-impaired (●, n=8), aged impaired control (□, n=17) and aged impaired treated (■, n=11) rats. *$p<0.01$ vs before treatment, by Dunnett's test.

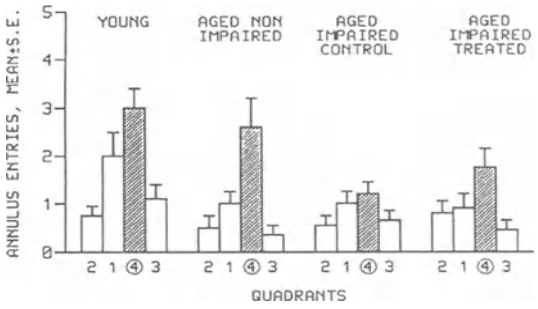

Fig. 3. Mean number of annulus entries four young, aged non-impaired, aged impaired control and aged impaired treated rats during the single 'spatial probe' trial. 1=NE quadrant, 2=NW quadrant, 3=SW quadrant, 4=SE quadrant. During training the platform was located in the center of quadrant No. 4 (solid ring).

old impaired control rats do not show any spatial bias towards the training quadrant, the searching behaviour of old impaired BC-PS-treated rats is focused on the previous platform location, similar to young and old non-impaired rats (Fig. 3).

Discussion

Atrophy of cholinergic neurons and loss of ChAT-immunoreactivity in the septal complex of aged rats may be regarded as a structural-neurochemical correlate of the reduction in neuronal activity in the septo-hippocampal projection in old age. The age-related impairment in spatial behaviour shown in this as well as other studies [12] is likely dependent, at least in part, upon such deterioration. Cholinergic septal graft into the hippocampal formation consistently improves spatial learning and memory in aged rats by an atropine-sensitive mechanism [12].

The capability of BC-PS to restore impaired spatial behaviour may thus be related to its effects on cholinergic neuronal atrophy. Recovery of cholinergic function after BC-PS administration is also supported by the BC-PS-induced increase of ACh release from electrically stimulated cortical slices in aged rats [7]. Given the relevance of synaptic renewal to cognitive functions, the beneficial effects of BC-PS on age-associated memory decay may reflect improved interneuronal septo-hippocampal connectivity [8].

As to the mechanism(s) of action, BC-PS administration counteracts age-related changes in membrane structure and function [5,6]. These effects may be factors relevant in old age to renewal and maintenance of synaptic connections since synaptic function has a major role in stabilization of synaptic sites. Maintenance of trophic degree of cholinergic neurons in old age is also consistent with the finding that serine phospholipids interact synergistically with nerve growth factor (NGF) [13]. Interestingly, intracerebral infusion of NGF can reverse the cholinergic cell body atrophy and improve spatial memory in behaviourally impaired aged rats [14].

Based on the experimental results and the cholinergic hypothesis of geriatric memory dysfunction, we feel justified in recommending clinical testing of BC-PS for the treatment of pathological brain aging.

References

1. Ball MJ (1977) Acta Neuropathol. 37: 111–118.
2. Perry EK, Tomlinson BE, Blessed G, Bergman K, Gibson PH and Perry PH (1978) Br. Med. J. 2: 1457–1459.
3. Bartus RT, Dean RL, Beer B and Lippa AS (1982) Science 217: 408–417.
4. Toffano G and Bruni A (1980) Pharmacol. Res. Commun. 12: 829–845.
5. Calderini G, Bellini F, Bonetti AC, Galbiati E, Guidolin D, Milan F, Nunzi MG, Rubini R, Zanotti A and Toffano G (1987) Clin. Tri. J. 24: 9–17.
6. Calderini A, Aporti F, Bellini F, Bonetti AC, Rubini R, Teolato S, Xu C, Zanotti A and Toffano G (1985) In: Horrocks LA, Kanfer JN and Porcellati G (eds.) Phospholipid in the Nervous System. Raven Press, New York, pp. 11–19.
7. Pedata F, Giovanelli L, Spignoli G, Giovannini MG and Pepeu G (1985) Neurobiol. Aging 6: 337–339.
8. Nunzi MG, Milan F, Guidolin D and Toffano G (1987) Neurobiol. Aging 8: 501–510.
9. Fifkova E and Van Harreveld A (1977) J. Neurocytol. 6: 211–230.
10. Becker JT, Walker JA and Olton DS (1980) Brain Res. 200: 307–320.
11. Morris R (1984) J. Neurosci. Methods 11: 47–60.
12. Gage FH and Björklund A (1986) J. Neurosci. 6: 2837–2847.
13. Bruni A, Bigon E, Boarato E, Mietto L, Leon A and Toffano G (1982) FEBS Lett. 138: 190–192.
14. Fischer W, Wictorin K, Björklund A, Williams LR, Varon S and Gage FH (1987) Nature 329: 65–68.

Suppressive effects of dexamethasone on the availability of L-tryptophan and tyrosine to the brain of healthy controls

C. Leclercq, F. Christiaens, M. Maes, E. Suy and B. Minner

The Psychiatric Center, Abdijstraat 2, 3751 Munsterbilzen, Belgium

Abstract

In the past, decrements in the availability of L-tryptophan (L-TRP) and tyrosine were found in the serum of major depressed patients. The reductions in L-TRP were reportedly linked to an augmented escape of cortisol to dexamethasone suppression. Recently, it was shown that a cortisol suppression dose of dexamethasone significantly decreased the availability of L-TRP in rats. In order to elucidate the effects of a cortisol suppression dose of dexamethasone on the disposal of L-TRP and tyrosine in man, the authors examined L-TRP, tyrosine and the sum of five competing amino-acids (CAA) both before and after administering 1 mg dexamethasone p.o. in 34 normal controls. We found that dexamethasone significantly reduced L-TRP, ($p<10^{-5}$), the L-TRP/CAA ratio ($p<10^{-5}$) and tyrosine ($p<10^{-5}$). It is suggested that these reductions in L-TRP and tyrosine availability caused by dexamethasone could modify the serotonergic and noradrenergic control over the hypothalamic-pituitary-adrenal axis during the dexamethasone suppression test.

Introduction

A functional deficit in the serotonergic [1,2] and noradrenergic [3,4] neurotransmission in the brain, disorders in the corticotropin-releasing-factor.

(CRF)/adrenocorticotropic hormone (ACTH) /cortisolaxis [5–8] and a reduced (total) L-tryptophan (L-TRP) availability to the brain [9–11] were repeatedly reported in major depressed patients.

The CRF/ACTH/cortisolaxis is partly regulated via noradrenergic and serotonergic inputs. Noradrenaline exerts an inhibitory control over CRF [12,13]. Serotonin has probably a dual effect on the axis it stimulates CRF [12,14] and it could enhance the negative feedback of corticosteroids on CRF and ACTH [15]. Brain serotonin and noradrenaline metabolism are partly determined by the availability of their precursors, i.e. respectively L-TRP and tyrosine in the plasma [16,17]. The ratios of both amino acids to the sum of those amino acids known to compete for the same cerebral uptake mechanism (CAA) are used as an index of the availability of both amino-acids to the brain [16–18]. One of the most commonly applied probes to evaluate the function of the CRF/ACTH/cortisolaxis in depression, is the 1 mg dexamethasone suppression test (DST). However, we have found that the availability of L-TRP and tyrosine in the plasma of 34 normal controls were markedly reduced after treatment with 1 mg dexamethasone. Consequently, we can

Table 1. Amino acid levels before and after treatment with 1 mg dexamethasone

	Pre DEX levels	Post DEX levels	F statistic	p value
L-TRP	58.6 (± 7.1)	49.5 (± 8.2)	50.8	0.0000
Valine	265.1 (± 45.8)	256.3 (± 36.2)	3.05	0.08
Leucine	127.4 (± 20.2)	122.3 (± 18.8)	5.19	0.02
Phenylalanine	63.7 (± 8.4)	67.6 (± 8.0)	7.02	0.01
Tyrosine	65.4 (± 12.0)	52.6 (± 9.7)	49.4	0.0000
Isoleucine	7.5 (± 11.7)	61.4 (± 10.3)	15.81	0.0006

hypothesize that if this dexamethasone dose is capable of reducing the availability of both amino acids to the brain, it could concomitantly alter the serotonergic and noradrenergic control over the CRF/ACTH axis.

Patients and Methods

The subjects were 34 normal controls i.e. staff-members (18 females, 16 males; average age 33 + 13.2 years). The amino acids (L-TRP, tyrosine, valine, leucine, isoleucine and phenylalanine) were determined on two consecutive days. On day 1, a fasting (>12 h) blood sample was taken at 8.00 a.m.. The same day, 1 mg dexamethasone (orally) was ingested at 11.00 p.m. and the next day a second blood sample was drawn at 8.00 a.m.. The assay of the amino acids was carried out by means of liquid chromatography [19].

Results and Discussion

Table 1 lists the effects of the treatment with 1 mg dexamethasone on the amino-acids. There was a significant suppressant effect for dexamethasone on L-TRP, tyrosine, leucine, and isoleucine. Phenylalanine was significantly increased by dexamethasone administration. The circulating levels of valine were not affected. Both the ratio L-TRP/CAA_1 (i.e. tyrosine + valine + leucine + isoleucine + phenylalanine) and the ratio tyrosine/CAA_2 (i.e. L-TRP + valine + leucine + isoleucine + phenylalanine) were significantly reduced after dexamethasone.

Thus, treatment with 1 mg dexamethasone reduces the L-TRP and tyrosine availability to the brain. These effects are presumably caused by an induction of L-TRP pyrrolase [20] and tyrosine aminotransferase [21] the major L-TRP and tyrosine degrading enzymes.

Acknowledgement

This investigation was supported in part by Eli Lilly Benelux.

References

1. van Praag HM (1979) In: Obiols J (ed.) Biological Psychiatry Today. Elsevier/North Holland Biomedical Press, New York.
2. Charney DS, Henninger GR and Sternberg DE (1982) Arch. Gen. Psychiatry 41: 359–363.
3. Schildkraut JJ (1978) In: Lipton M (ed.) Psychopharmacology: A Generation of Progress. Raven Press, New York, pp. 1223–1234.
4. Bunney WE (1975) Psychopharmacol. Commun. 1: 599–609.
5. Carroll BJ (1980) In: van Praag HM (ed.) Handbook of Biological Psychiatry, Part III. Marcel Dekker, New York, pp. 179–193.
6. Maes M, De Ruyter M, Hobin P and Suy E (1986) J. Affect. Disord. 10: 207–214.
7. Maes M, De Ruyter M, Hobin P and Suy E (1986) J. Affect. Disord. 11: 165–172.
8. Maes M, Minner B and Suy E (1989) J. Affect. Disord. 17: 39–46.
9. DeMyer MK, Shea PA, Nendric HC and Yoshimura NN (1980) Arch. Gen. Psychiatry 38: 642–646.
10. Maes M, De Ruyter M, Hobin P and Suy E (1987) Psychiatr. Res. 21: 323–335.
11. Maes M, De Ruyter M and Suy E (1987) Biol. Psychiatry. 22: 177–188.
12. Lal S and Martin JB (1980) In: van Praag NM (ed.) Handbook of Biological Psychiatry, Part III. Marcel Dekker, New York, pp. 101–167.
13. Ganong WF (1984) In: Brown GM (ed.) Neuroendocrinology and Psychiatric Disorder. Raven Press, New York, pp. 133–143.
14. Martin JB and Reichlin S (1987) In: Clinical Neuroendocrinology. Davis Company FA, Philadelphia, pp. 159–200.
15. Nuller JL and Ostroumova JL (1980) Acta Psychiatr. Scand. 61: 169–177.
16. Fernstrom JD, Larin F and Wurtman J (1973) Life Sci. 13: 517–524.
17. Gibson CJ and Wurtman RJ (1978) Life Sci. 22: 1399–1406.
18. Moller SE, Reisby N, Ortmann J, Elley J and Krautwald O (1981) J. Affect. Disord. 3: 231–244.
19. Turnell D and Cooper J (1982) Clin. Chem. 28: 527–531.
20. Badawy AA-B (1977) Life Sci. 21: 755–768.
21. Stanley JC, Fisher MJ and Pogson CI (1985) Biochem. J. 228: 249–255.

Therapeutic effects of taurine and vit-E in retinitis pigmentosa

H. Pasantes-Morales[a], O. Quesada[a], M. Zertuche[b], J.A. Paczka[b], A. Santos[b], M. De Regil[b] and H. Quiroz[b]

[a]Instituto de Fisiología Celular, Universidad Nacional Autónoma de México, Mexico City, México
[b]Hospital de la Asociación para Evitar la Ceguera, A.C. Mexico City, Mexico

Abstract

The effect of a treatment with taurine (1.2 g per day) and tocopherol (800 mg per day) was examined in 39 subjects affected with retinitis pigmentosa. Two main parameters of visual function. i.e. visual field size and visual acuity, were examined after 12, 24 and 30 months of treatment. The average changes in visual field area as compared to initial values were +5.6%, −18.3% and −26.9% in 12, 24 and 30 months, respectively. Some genetic groups responded more favorably to the treatment than others: in the autosomal recessive group, changes in the visual field area were +23%, −12.5%, −20.6%; in patients with Usher's syndrome, +8.3%, +4.3%, −11%; in the X-linked group −8.9%, −20.9%, −27% and in the simplex cases, +0.1%, −35%, −57%. The autosomal dominant group has been followed during 12 months so far and a decrease of 3.5% was observed. Since the estimated average decrease of visual field area is 15%–17% of the remaining visual field per year, the taurine-tocopherol treatment appears beneficial in some groups. The visual acuity increased 63% in average in 48 subjects examined. The highest number of patients with increases in visual acuity was found in the autosomal dominant group (90%), followed by patients with Usher's syndrome (80%). In the autosomal recessive group, 60% of patients showed increases in visual acuity and in the simplex and the X-linked groups, increases in this parameter were found in 50% and 36% of subjects, respectively. A beneficial effect of treatment with taurine and tocopherol seems to be exerted in patients of both autosomal groups and of Usher's syndrome.

Introduction

Retinitis pigmentosa (RP) is a group of separate, genetically determined visual disorders of unknown etiology, in which progressive degeneration of rods and cones is accompanied by migration of pigment-containing cells into the retina [1,2]. There are at least three genetic forms of RP: autosomal dominant, autosomal recessive and X-linked recessive. The Usher's syndrome includes an heterogenous set of diseases including typical RP. Simplex form of RP comprises cases in which appropriate investigations have excluded a recognized pattern of inheritance. The autosomal dominant form is characterized by a later onset and the slowest rate of visual deterioration whereas the X-linked cases exhibit the fastest rate of visual loss and the autosomal recessive form shows an intermediate rate of visual impairment. The clinical syndrome of RP is characterized by night blindness and loss of peripheral vision due to photoreceptor degeneration, particularly of rods. A large proportion of RP patients showed a markedly reduced ERG and in advanced stages of the disease, this response is usually lost [3,4].

In this study, the effect of combined administration of taurine and tocopherol (TT) was examined on the progression of visual field size and visual acuity in 39 subjects with typical RP, distributed in the three genetic types, in the simplex form and the Usher's syndrome. The rationale for the trial of taurine and tocopherol as possible therapeutic agents in RP, stems from observations of a marked protective effect of these compounds on rod structure *in vitro* and *in vivo*. Taurine protects rod outer segments from injury caused by intense illumination [5], by oxidation [6] or by increased ionic permeability [7]. Tocopherol also exerts a marked protective action on photoreceptor structure altered by oxidation [8]. Taurine and tocopherol preserve cell viability, preventing ion overload and swelling in human lymphoblastoids exposed to agents causing membrane lipid peroxidation [9]. The mechanism of these protective actions is unknown, but may be related to an antioxidant effect or to a stabilizer action on cell membranes. *In vivo*, taurine and tocopherol are implicated in the maintenance of normal structure and function of photoreceptors, since a decrease in their physiological levels leads to disorganization of photoreceptor structure and visual dysfunction [10–12]. Although taurine and tocopherol are most probably unrelated to the etiology of RP, they could exert a protective action on photoreceptors affected by the disease, increasing their viability and limiting the deleterious effect on photoreceptor membranes of degradation products known to generate autopropagated membrane lipid peroxidation.

Taurine and tocopherol have been administered to patients with various diseases, at large concentrations and no adverse effects have been reported [13–15].

Subjects and Methods

Patients recruitment

Patients were recruited at the Hospital de la Asociación Para Evitar la Ceguera, in Mexico City. Prior to enrollment in the study, an orientation session was held with each patient. The nature and purposes of the study were discussed and patients were informed about the innocuousness of the treatment. Written informed consent was required for enrollment.

Patient eligibility and exclusion criteria

Patients were selected according to the following criteria: 1) Typical RP 2) aged between 14–50 years 3) Visual acuity of 1/10 or better, 4) kinetic visual fields larger than 10° as measured with the IV 4e stimulus and 5) No surgical eye history nor any ophthalmological disease other than RP. Individuals showing systemic conditions possibly affecting the eye, or unusual forms of RP were excluded of the study.

Medical and ophthalmic examinations

Detailed family histories and medical histories were elicited from patients and genetic assignment was performed by trained personnel. Patients underwent complete ophthalmic evaluations to establish the baseline visual functions. The evaluation included measurement of best corrected visual acuity using the Snellen chart, fundus photography and fluorescein angiography. Visual fields were evaluated by Goldman perimetry using the IV 4e test stimulus moving from periphery to center. The baseline and successive determinations of visual field size were performed by the same person in order to avoid external variability [16]. Areas of responsive regions were digitized and integrated in a graphics program. Results are expressed in mm^2.

Electroretinograms were recorded in a Ganzfeld test system with a bipolar ERG-Jet contact lens electrode placed on the topically anesthetized cornea, after pupil dilation. ERG's were elicited under photopic and scotopic conditions in response to 1 Hz flashes of white bright light (30 ft/lambert) and to intensity attenuated ($>10^{-3}$ ft/lambert) blue light flashes, respectively.

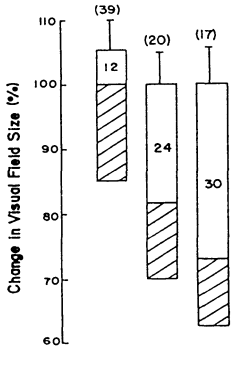

Fig. 1. The effect of TT treatment during 12, 24 or 30 months, on the change in visual field size of patients with RP from all genetic groups, simplex cases and patients with Usher's syndrome. The white bars represent the change (increase or decrease) in percentage over the baseline measurement (100%). The dashed part of the bar represents the expected decrease according to the average rate of loss reported in Massof and Finkelstein [17]. Results are the means ± S.E.M. of the number of subjects indicated in parenthesis.

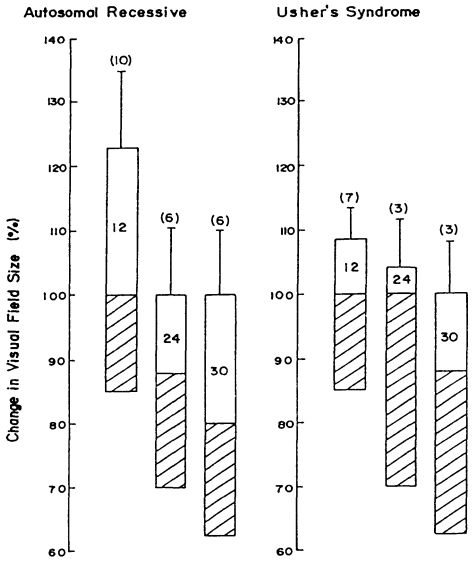

Fig. 2. The effect of TT treatment during 12, 24 or 30 months on the change in visual field size of patients with RP of the autosomal recessive type and with Usher's syndrome. Expression of results is as described in Fig. 1. Results are the means ± S.E.M. of the number of subjects indicated in parenthesis.

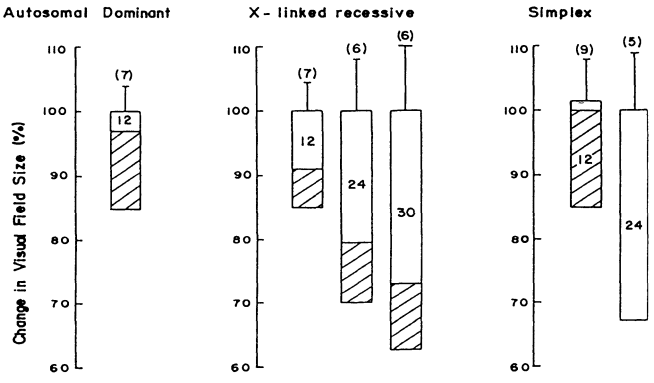

Fig. 3. The effect of TT treatment during 12, 24 or 30 months on the change in visual field size of patients with RP of the autosomal dominant type. X-linked recessive type and simplex type. Expression of results is as described in Fig. 1. Results are the means ± S.E.M. of the number of subjects indicated in parenthesis.

Treatment

Patients received a daily dose of 1.2 g of taurine and 800 mg of -tocopherol. Both compounds were given orally as half the daily dose every 12 h.

Results

Patients included in this study corresponded to the three genetic types of RP, to the Usher's syndrome and to simplex cases, distributed as follows: autosomal domi nant, 7; autosomal recessive, 11; X-linked recessive, 7; simplex, 8; Usher's syndrome, 8. Not all patients in the group were recruited at the same time and they were incorporated in the study only when all the baseline visual functions had been determined. This is the reason for the different number of patients included in the treatment intervals, i.e. n = 39 for 12 months of treatment, n = 20 for 24 months and n = 17 for 30 months.

Visual field size

Figure 1 shows the average change in visual field size in all patients after 12, 24 and 30 months of TT treatment. The change in visual field size was compared to that reported in the study of Massof and Finkelstein [17] (dashed bars), in which an average decrease of 15%–17% of the remaining visual field size per year was found in 154 patients. After 12 months of treatment, an increase of 5.6% on average, was observed in the group of 39 patients. A decrease in visual field size of 18.3% was observed after 24 months of treatment and a reduction of 26.9% after

Table 1. Changes in visual acuity in RP patients after 6–12 months of treatment with TT

Genetic type	Change			n	% of n showing increase
	Decrease	No change	Increase		
Autosomal dominant	1	1	13	15	90%
Usher's syndrome	1	1	8	10	80%
Autosomal recessive	1	2	5	8	60%
Simplex	5	3	8	16	50%
X-linked recessive	5	4	5	14	36%

Visual acuity was evaluated with the Snellen chart.

30 months of treatment. The change in visual field size after TT treatment evaluated in the different genetic types is shown in Figs. 2 and 3. In the autosomal recessive group, an increase in average of 23% was observed after 12 months of treatment and decreases of 12.5% and 20.6% after 24 and 30 months, respectively (Fig. 2). The autosomal dominant group has been followed during 12 months so far, and an average change of −3.5% was observed during this period (Fig. 3). In the group of Usher's syndrome, an average increase of 8.3% was observed after 12 months of treatment and the increase persisted after 24 months, 4.3%; after 30 months a slight decrease of 11% was observed in this group (Fig. 2). In the X-linked recessive group and the simplex group, average decreases in the visual field size were observed at all the times examined: 8.9%, 20.9% and 27% after 12, 24 and 30 months respectively, for the X-linked group and 0.1%, 35% and 52% for the simplex group (Fig. 3).

Visual acuity

The progress in visual acuity was followed in 63 patients after 6–12 months of TT treatment. From this number of patients 20% showed decreases in visual acuity of 2 lines in average, 17% had no changes and 63% had increases from 0.5 to 4 lines, as shown in Table 1. From a group of patients receiving placebo, 80% showed no changes in visual acuity (not shown).

When the effect of TT treatment on visual acuity was examined in the different genetic types, it was observed that the largest improvement occurred in the autosomal dominant group, in which 90% of patients exhibited increases in visual acuity. In the Usher's syndrome group, 80% of patients showed increases in visual acuity, from 1 to 4 lines. The autosomal recessive and the simplex groups showed increases in 60% and 50% of patients, respectively and in the X-linked recessive group only 36% of patients showed increases in visual acuity. No adverse effects were observed or reported by patients throughout the treatment.

Discussion

Retinitis pigmentosa is a progressive degenerative disease in which most parameters of visual function decline with time. In a study by Berson and coworkers [4] on the natural course of RP in 92 patients, changes in visual acuity, visual field size, dark-adaptation threshold and electroretinogram were examined over a three year interval. The full field electroretinogram was found to decline significantly in 77% of patients with detectable responses at the beginning of the study. The visual acuity and dark adaptation threshold remained stable. From the 92 patients, 26% showed decreases in visual acuity, 71% showed no change and 3% exhibited increases in this parameter. These results agree with other studies [1,2] and clearly contrast with the results of the present study in which a large proportion of patients (62%) showed increases in visual acuity, sometimes higher than 3–4 lines.

With respect to visual field size, in the study of Berson *et al.* [4] the rate of visual field loss was calculated as 4.6% of the remaining visual field area per year. In the study of Massof and Finkelstein [17], the average rate of visual field loss was found to be similar in all genetic types and occurs according to an exponential decay with an average time constant of 4–4.5 years. That means that, on average, patients lose 50% of the remaining field area every 4–4.5 years. The average rate of loss is 15% to 17% per year, of the remaining visual field area. In comparison with these studies, the TT treatment seems to have some beneficial effect, particularly in the autosomal recessive group and the Usher's syndrome group and, to a lesser extent, in the autosomal dominant group. These three groups were also those having the best response to TT regarding visual acuity. The reason for these different responses of the genetic types of RP to the TT is unclear at present.

In a study by Reccia *et al.* [18], taurine was administered to 7 patients in daily doses of 2 g orally and 1 g intravenously during one month and then of 3 g orally from the 2nd up to the 12th month. This treatment did not result in any noticeable improvement of the visual functions examined. It should be noted, however, that in terms of visual field size, all patients had no detectable or very small visual field areas [18]. According to the rationale for the TT treatment, no improvement in visual field size is expected, since the treatment would provide, at the best, a protection to remaining visual cells. The increase in visual field size observed in some subjects in the present study may result from a stabilizer effect on cells with different stages of injury but still viable. Beneficial effects of TT treatment on visual acuity might be related to an action on macular vision resulting from the improvement of macular edema which is often associated with RP. It is also possible that taurine has a beneficial effect directly on visual acuity, since taurine deficiency has been shown to impair visual acuity in infant primates [19]. The results of the present study, showing some stabilizing effects of TT treatment in the course of visual field loss and visual acuity in some groups of RP although preliminary, are encouraging and warrant further investigations. A double-blind, randomized, placebo controlled study in 40 patients is now in progress.

Acknowledgements

This work was supported in part by grants from the Programa Universitario de Investigación en Salud (PUIS) to H.P.M. We thank Ms Yolanda Díaz de Castro for typing the manuscript.

References

1. Heckenlively JR (1988) Retinitis Pigmentosa. J.B. Lippincott Company, Philadelphia.
2. Pagon RA (1988) Surv. Ophtalmol. 33: 137–177.
3. Pruett RC (1983) Trans. Am. Ophtalmol. Soc. 81: 693–735.
4. Berson EL, Sandberg MA, Rosner B, Birch DG and Hanson AH (1985) Ann. J. Ophtalmol. 99: 240–251.
5. Pasantes-Morales H, Ademe RM and Quesada O (1981) J. Neurosci. Res. 6: 337–348.
6. Pasantes-Morales H and Cruz C (1985) Brain Res. 330: 154–157.
7. Pasantes-Morales H, López-Escalera R and Díaz-Macedo M (1989) In: Redburn DA and Pasantes-Morales H (eds.) Extracellular and Intracellular Messengers in the Vertebrate Retina. Neurology and Neurobiology. Alan R. Liss Inc., New York, Vol. 49, pp. 87–104.
8. Farnsworth CC and Dratz EA (1976) Biochim. Biophys. Acta 443: 556–570.
9. Pasantes-Morales H, Wright CE and Gaull GE (1985) Biochim. Pharmacol. 34: 2205–2207.
10. Hayes KC, Carey RE and Schmidt SY (1975) Science 188: 949–951.
11. Schmidt SY, Berson EL, Watson G and Haung C (1977) Invest. Ophtalmol. Vis. Sci. 16: 673–682.
12. Robison WG, Kuwabara T and Bieri JG (1981) Retina 2: 263–281.
13. Mutani R, Bergamini L and Durelli L (1978) In: Barbeau A and Huxtable R (eds.) Taurine and Neurological Disorders. Raven Press, New York, pp. 359–373.
14. Takahashi R and Nakane Y (1978) In: Barbeau A and Huxtable R (eds.) Taurine and Neurological Disorders. Raven Press, New York, pp. 375–385.
15. Muller DPR, Lloyd JK and Wolff OH (1985) J. Inherited Metab. Dis. 8: 88–92.
16. Ross DF, Fishman GA, Gilbert LD and Anderson RJ (1984) Arch. Ophtalmol. 102: 1004–1010.
17. Massof RW and Finkelstein D (1987) In: Zrenner E, Krastel H and Gorbel HN (eds.) Research in Retinitis Pigmentosa. Advances in the Biosciences. Pergamon Journal Ltd., London, Vol. 62, pp. 29–58.
18. Reccia R, Pignalosa B, Grasso A and Campanella G (1980) Acta Neurologica (Naples) 35: 132–136.
19. Neuringer M and Sturman J (1987) J. Neurosci. Res. 18: 597–601.

Address for correspondence: Dr. H. Pasantes-Morales, Instituto de Fisiología Celular, Apartado Postal 70-600, 04510 Mexico D.F., Mexico.

Treatment of Leukemia 1210 intravenous transplants with tumor modifiers, redoubt cytotoxics and minor tranquilizers*

Mario Gosalvez, Mariaflor Blanco, Mercedes Bueno and Rosa Balaguer**
Servicio de Bioquimica Experimental, Clinica Puerta de Hierro, 28035 Madrid, Spain

Abstract

Analysis by sequential video microscopy of HeLa cell colonies treated with the tumor cell reverse modifier thioproline further characterizes the modified cells as having a series of benign social patterns some of which refer to cell mobility. It has preliminarily identified the less malignant cell fraction as the thioproline sensitive compartment of the cultures.

The administration of thioproline and its analogue 2-amino-thiazoline to intravenously transplanted mouse Leukemia 1210 affords partial tumor rejections when Quelamycin and Quemycin, two possible redoubt cytotoxics, and bromazepam and medazepam, two minor tranquilizers, are given in combination. This protocol represents a dual strategy cancer reversal addressed to both the malignant and less malignant tumor compartments.

Introduction

A number of reports have appeared proposing, for thioproline and its analogue 2-amino-thiazoline, a new type of anticancer agency [1–9], which has been denominated tumor cell reverse modification [4,9].

In this communication data is presented on sequential video microscopy of HeLa cell cultures treated with thioproline in an attempt to find the cell fraction sensitive to modification. It is preliminarily identified as the less malignant cell compartment.

In a dual approach to the malignant and less malignant compartments, mice Leukemia 1210 intravenous transplants were treated with low doses of thioproline, 2-amino-thiazoline, Quelamycin, Quemycin, bromazepam and medazepam. Quelamycin and Quemycin are two ferric derivatives of the cytotoxic antibiotic doxorubicine designed to have as targets the anoxic and the phagocytic tumor redoubts [10–12]. Bromazepam and medazepam are two new potent derivatives of the minor tranquilizer diazepam for which was proposed an enhancing effect on thioproline [13]. The combined protocol obtained a significant increase in mean survival time in spite of a late beginning of the treatment and the use of low doses of each drug.

* Supported by Grant 82-1475 from Comisión Asesora de Investigación Cientifica y Tecnica, Spain.
** Rosa Balaguer received a fellowship from the Fundación Cientifica de la Asociación Española contra el Cancer.

Materials and Methods

Thioproline modification of HeLa cells

HeLa cells (69 chromosomes at the peak of chromosomal distribution) were obtained indirectly from the repository of The American Type Culture Collection (Rockville, MD, U.S.A.). Experiments were done from the 6th to the 20th passage in monolayer tissue culture. All cultures were stationary with Costar plastic support for cell growth. For cell dispersion a five minute washing with 0. 25% trypsin solution at room temperature was carried out. The incubation of cells was done at 37°C in 5% CO_2 air atmosphere.

L-thioproline (Sigma Co., U.S.A.) was prepared as a sodium salt (pH 7) dissolved in single distilled non-deionized water. It was sterilized by filtration to be added upon preparation.

The thioproline modification protocol for HeLa cells is as follows. HeLa cell suspensions obtained by trypsinization of very confluent cultures in stationary phase are seeded at a density of 4×10^3 cells/cm^2 in 75 cm^2 Costar flasks. As growth supporting medium the Eagle Minimum Essential medium with Hanks salts (HMEM) is used, supplemented with 10% donor calf serum, 1% non essential amino acids and 1% glutamine plus antibiotic mixture (Flow Laboratories, U.K). The volume of medium is maintained at 0.4 ml/cm^2 of culture surface and the pH adjusted to near 7. The medium is changed at day 1 and 4 from the seeding and all the following days. To obtain modified cultures 0.33 mM thioproline is included in the exchange medium of days 1,4,5 and 6 [9].

Sequential video microscopy of modified HeLa cells

Video recording microscopy of the thioproline treated and untreated HeLa cell cultures described above was done in an Olympus IM inverted microscope with thermostatically controlled culture incubator (5% CO_2-Air Atmosphere). The microscope was equipped with an Hitachi CCTV video camera and a Panasonic 8050 time sequence recording system and monitor. Analysis of video films was done visually, noting and calculating events and behaviors for four days (8 h video time) of culture (1 to 5), focusing single colonies (4 cells at the beginning) all the time. Microscope magnification was 200 X. Several colonies from control and treated cultures were studied.

Combined treatment of Leukemia 1210 intravenous transplants

Preparation of Leukemia 1210 intravenous transplants

Deep-frozen suspensions of mice Leukemia 1210 cells were obtained from the repository of the American Type Culture Collection. The cells were given two passages in suspension culture (RPMI medium, 10% Horse serum) and then were injected intraperitoneally in DBA/2 mice. Nine days later ascites fluid was col-

lected from the mice and transplanted intraperitoneally again. From the second ascites passage, 1×10^6 cells in 0.1 ml saline were injected by the tail vein into black inbred hybrid mice ($D2B6F_1$) (Female, 17 grams of weight). Said procedure resulted in mice which developed leukemic infiltrates mainly in the spleen and liver and all died three weeks later.

The transplants and their controls were housed in 25 cm plastic cages, 3 animals per cage, each animal separated from the other by plastic dividers (three corridors). Water and pellet diet was allowed *ad libitum* to each mice. Mice, cages, dividers and diet were obtained from Panlab. S.A. Barcelona.

Combined treatments

Groups of six transplanted mice were treated intraperitoneally from the 3rd to the 20th day after the injection of the cells with various combinations of thioproline, 2-amino-thiazoline, bromazepam, medazepam, Quelamycin and Quemycin. Control animals received the solvents alone. The exact dose, day and moment of the day at which each compound was administered is indicated in the results section. Each experimental group consisted at least of 18 mice.

Preparation of drugs

The redoubt cytotoxic drugs, tumor modifiers and minor tranquilizers were prepared and injected as follows.

Quelamycin was injected through a millipore sterile filter upon its synthesis from commercial doxorubicin and ferric iron. A vial of 10 mg of the lyophilized pharmaceutical preparation of doxorubicin used in the clinics (Farmitalia Carlo Erba, Barcelona) is dissolved in 5 ml of distilled water. Then drop by drop under stirring 0.46 ml of a 3% solution of ferric chloride (6 water molecules) (Merck, W. Germany) was added. The complex is then neutralized drop by drop to pH 6 with 0.1 N NaOH adjusting the final volume to 10 ml. This procedure yields Quelamycin, (triferric doxorubicin) [10,14], at a concentration of 1 mg per ml (doxorubicin equivalent) ready to be injected into the mice.

Quemycin was formed in the following manner. First Quelamycin is prepared as above. Then 50 mg in powder of very pure low molecular weight inulin (Merck) is added and stirred. The Quelamycin-inulin mixture is heated rapidly to 50°C by immersion in a boiling water bath. Then it is cooled rapidly to 5°C in a ice bath and filtered by millipore for injection. With this procedure, Quemycin, [12] (a micro-colloidal association of doxorubicin, iron and inulin forming irregular, quasi spherical particles averaging 20 nano meters in diameter) is formed at a concentration of 1 mg/ml (doxorubicin equivalent). The uninjected Quelamycin or Quemycin solution is discarded.

Very pure 2-amino-2-thiazoline HCl was obtained from The Walter Reed Institute, (Washington, U.S.A.) and was injected diluted in distilled water after millipore filtration. Sodium thioproline (pH 6) was prepared with NaOH in single distilled non-deionized water departing from L-thiproline (Sigma). Bromazepam and medazepam were obtained from Hoffmann-La Roche A.G., Basle, Switzer-

land, and were first diluted at high concentration in ethanol and afterwards in water. After preparation, the compounds were injected rapidly through millipore sterile filters and the leftover solutions were discarded.

Results

Sequential video microscopy of modified HeLa cells

The observation of video films of thioproline treated HeLa cell cultures in a general view shows that there are colonies totally insensitive to modification and there are others that soon degenerate and detach. The only hint of prospective thioproline sensitivity at 24 h after seeding, time of the first addition of thioproline, is the size of the colony and the size of its cells. Usually, selecting colonies with four slightly bigger cells increases the possibility of filming modification. The modification consists in the stopping or slowing of cell division when the cells reach a certain level of approximation to other cells, while changing to an irregular form of bigger size.

Upon detailed analysis of the video films, sequence by sequence, the duration of the mitotic and intermitotic time of each cell can be quantified, their type of movement and their speed defined, and the approximate area of the cells can be

Table 1. Number of cells and mitoses, mitotic times, size and migratory characteristics of a colony modified by thioproline

Cell Parameter	Control	Modified
Initial number of cells	4	4
Final number of cells	27	16
Total number of mitoses	20	8
Average mitotic time	41 min	162 min
Average intermitotic time	21 h	40 h
Percentage of cells with a given size		
<400 square microns	1%	0%
400–800 square microns	69%	14%
800–1,200 square microns	30%	52%
>1,200 square microns	0%	44%
Percentage of cells with a given type of movement		
With Zig-Zag movement	9.3%	81.7%
With linear movement	90.6%	17.2%
Percentage of cells with a given velocity		
<2 microns/h	66.6%	41.3%
2–5 microns/h	33.3%	24.3%
5–20 microns/h	0%	20.7%
>20 microns/h	0%	13.8%

Table 2. Migratory characteristics of thioproline modified cells of different sizes.

Characteristics of cell movement	Approximate cell area (microns square)				
	400–800		800–1200		>1200
	C	M	C	M	M
Linear Movement	91%	25%	90%	33%	10%
Zig-Zag Movement	9%	75%	10%	66%	90%
Centrifugal direction	82%	75%	80%	54%	50%
Centripetal direction	18%	25%	20%	26%	50%
With velocity					
2–5 microns/h	43%	0%	20%	26%	20%
5–20 microns/h	0%	0%	0%	26%	20%
>20 microns/h	0%	75%	0%	17%	10%

C = Control; M = Modified.

estimated. For those measurements, both the monitor clock and a transparent reticula calibrated in microns that is placed over the monitor screen, are used. Table 1 compares a typical colony fully modified by thioproline with a typical control colony with respect to number of cells, number of mitoses, mitotic time, intermitotic time, cell size, cell speed and the percentage of cells with linear or zig-zag movement.

The treated colony, in comparison with the control colony, has a lower growth yield constituted by bigger and quicker cells that preferentially move in zig-zag. The lower growth yield is due mainly to longer intermitotic times. The changes appear in the treated colonies as early as the second day after the initiation of treatment and, as said before, do not occur upon cell contact but on reaching a certain approximation.

A curious characteristic of the changes in migratory behavior of the treated cells is the direction, centrifugal or centripetal, with which the cells migrate with respect to the center of the colony. While in the control colonies most cells move centrifugally, in the treated colonies the number of cells moving centripetally is increased, and these are mostly the bigger cells. Migratory characteristics with respect to cell size are shown in Table 2 for the same typical colonies analyzed in Table 1.

In the control colonies, the smaller cells have the shortest mitotic and intermitotic times and always show linear movement, centrifugal direction and velocity of less than 2 μ/h. The ranges of mitotic time and intermitotic time observed in control colonies are from 30 to 50 min and from 18 to 24 h, respectively. However in modified colonies, these ranges are from 150 to 180 min and from 30 to 55 h, respectively. Conversely, it is observed that the bigger cells have the longer mitotic and intermitotic times and as it is seen more frequently in modified colonies always show zig-zag movement, centripetal direction and velocity higher than 2 μ/h. In

Table 3. Percentage of malignant, less malignant and benign cell characters related to movement in a colony modified by thioproline

Malignant character	Control colony	Modified colony	Control colony	Modified colony	Benign character
Centrifugal direction with linear movement at less than 2 microns per h of speed	21.2%	0%	3%	27%	Centripetal direction with zig-zag movement at more than 2 microns per h of speed
Centrifugal direction at less than 2 microns per h	51.5%	17.2%	6%	27.6%	Centripetal direction at more than 2 microns per h
Centrifugal direction	81.8%	51.7%	18.2%	48.3%	Centripetal direction

these colonies, it is not rare to see cells that do not divide at all. These associations of characters permit the estimation in each colony of the percentage of cells with more or less, malignant, less malignant and benign characters. Table 3 depicts those percentages in the same colonies studied in Table 1 and Table 2.

The data of Table 3 clearly indicates that the modification by thioproline produces a decrease in malignant cells and an increase in less malignant and benign cells. Additionally, Table 3, together with the data of Table 1 and Table 2, further characterizes the cell modification induced in HeLa cells by thioproline reported elsewhere [4,9], with parameters related to direction and speed of cell movement associated with cell size and rate of cell division. On the other hand the analysis presented preliminarily suggests that the main cell fraction sensitive to thioproline is the less malignant compartment of the cultures.

Combined treatment of Leukemia 1210 intravenous transplants

Attempts to treat tumors with thioproline should include the administration of cytotoxics addressed to the malignant cell compartments which were not sensitive to thioproline.

Such a dual strategy cancer reversal was attempted in intravenous Leukemia 1210 transplants using as cytotoxics, Quelamycin and Quemycin, two derivatives of doxorubicin designed for anoxic and phagocytic tumor redoubts, respectively [10–12]. First, in a series of pilot experiments, it was found that the combination of thioproline and 2-amino thiazoline with Quelamycin and Quemycin was more effective than either type of drugs alone. It was also found that a substantial increase in survival time was obtainable even starting treatment at day 3 after transplant and using very low doses of the compounds if the tumor modifiers plus

Table 4. Combined treatment of intravenous Leukemia 1210 transplants at selected moments of mice general motor activity

Compound and dose (micrograms/Kg)	Day and hour of administration	Experimental group	Mean survival time
Thioproline (1,500)	from 3rd to 12th 4.30 PM	Only solvents	22 days
Aminothiazoline (750)	from 11th to 20th 4. 30 PM	TP,AT,BR,MD	27 days
Quelamycin (2,500)	3,4,7,8,11,12,15, 16,19 and 20 5.30 PM		
Quemycin (2,500)	3,4,7,8,11,12,15, 16,19 and 20 5.30 PM	QL,QM	23 days
Bromazepam (0.0003)	3,5,7,9,11,13,15 and 17 5. 30 PM		
Medazepam (0.0003)	4,6,8,10,12,14, 16 and 18 5.30 PM	TP,AT,QL,QM,BR and MD	43 days

the redoubt cytotoxics were giving in combination with very low doses of bromazepam and medazepam, two potent derivatives of the minor tranquilizer diazepam for which has been proposed and enhancing effect on thioproline [13].

A simple procedure for these combined protocols is for example to administer at 4.30 p.m. the tumor modifiers, first thioproline for 9 days and then 2-aminothiazoline for other 9 days. The redoubt cytotoxics however are given jointly at 5.30 p.m. in groups of two days separated by groups of two days in which are given the very low doses of bromazepam and medazepam, also at 5.30 p.m.

Table 4 presents an experiment of this type indicating doses, days of administration and increase in mean survival time in the different experimental groups compared. It is clearly shown that the tumor modifiers plus tranquilizers or the redoubt cytotoxics given alone are totally ineffective at these low doses while the combination shows marked antitumor activity.

Discussion

Our studies on sequential video microscopy further characterize the thioproline modification and also begin to define several types of cell compartments in HeLa cell cultures according to the number of cell malignant and benign characters. However it is not yet possible to identify with certainty the precise cell fraction

which is best amenable to thioproline modification. It appears clear that the less malignant cells, those with slightly bigger size and longer mitotic and intermitotic time are in general more frequently modifiable but more extensive studies are deemed necessary to define percentages and subcompartments.

If it were possible to extrapolate from cell cultures to the *in vivo* situation, the treatment of tumors with thioproline should require the concomitant treatment of the malignant cell fractions. The preliminary results presented using intravenous Leukemia 1210 transplants encourages efforts in such direction. It is possible that protocols of this type could represent a dual strategy, addressed to both the malignant and less malignant compartments that could validate the early expectations of the cancer reversal field.

References

1. Brugarolas A and Gosalvez M (1982) Preliminary Clinical Results with Norgamem (thioproline) and Revercan (2-amino-2-thiazoline): The First Inducers of Reverse Transformation. Recent Results in Cancer Research 80: 346–350.
2. Diaz Gil JJ and Trilla C (1982) Disminución de la Velocidad de Crecimiento de Celulas HeLa Causada por Tioprolina (Tp) y 2-Amino-tiazolina (2-AT). Efecto de la L-Prolina. Revista Española de Oncologia 29: 615–621.
3. Parks RC, Jones T, Banks AR and Hessek E (1981) Thioproline: An Inhibitor of Chemical Carcinogenesis. Neoplasm 29: 535–537.
4. Gosalvez M (1983) Thioproline and the Reversal of Cancer. The Lancet, May 14, p. 1108.
5. Pine MJ, Mirand EA, Ambrus JL and Bock FG (1983) Antitumor Studies of 2-Amino-2-thiazoline and Other Tumor Modifying Agents. Journal of Medicine 14: 433–449.
6. Grier RL (1984) Pilot Study on the Treatment with Thioproline of 24 Small Animals with Tumors. Am. J. Vet. Res. 45: 2162–2166.
7. Garcia Cañero R, Lopez-Alarcón L, Veloso JJ and Guijarro MC (1988) Effect of L-Thioproline on the Progression and Events of the Cell Cycle of HeLa Cells. Int. J. Cancer 41: 859–862.
8. Lopez-Alarcón L and Guijarro MC (1988) Incremento en los Niveles de Beta-2-microglobulina en Cultivos de Celulas Tumorales por Tratamiento con Thioprolina. Oncologia IX: 283–286.
9. Gosalvez M et al. (1989) Reverse Modification of Cancer Cells in Tissue Culture by Treatment with Thioproline. Submitted to Cancer Research (May).
10. Gosalvez M, Blanco MF, Vivero C and Valles F (1978) Quelamycin. A New Derivative of Adriamycin with Several Possible Therapeutic Advantages. Eur. J. Cancer 14: 1185–1190.
11. Cortes-Funes H, Brugarolas A and Gosalvez M (1980) Quelamycin: A Summary of Phase I Clinical Trials. Recent Results in Cancer Research 74: 210–216.
12. Gosalvez M (1987) Eradication of Advanced Leukemia by Sequential Combination of Cancer Reversing Agents, Tumor Redoubt Targeted Cytotoxics and Pineal Gland Modulators. International Workshop on 'The Pineal Gland and Cancer'. University of Tübingen, Tübingen, W. Germany (Sept).
13. Gosalvez M (1982) On the Irreproducibility of Thioproline. Biomedicine and Pharmacotherapy 36: 387–388.
14. Kozlowsky H, Dravent K, Scyszuk H and Gosalvez M (1982) Mossbauer, Magnetic and Thermogravimetric Studies on Adriamycin Ferric Complexes. Inorganica Chemica Acta 66: 189–192.

Oral treatment with branched-chain amino acids in 10 cases of hepatic encephalopathy: Dose finding, pharmacokinetics and therapeutic response

Günter Fondalinski[a], Peter Jürgens[a], Andreas Reymann[b] and Martin Schulz[c]

[a]Allgemeines Krankenhaus St. Georg, I. Medizinische Abteilung, Lohmühlenstr. 5, D-2000 Hamburg 1, F.R.G.

[b]Universitäts-Krankenhaus Eppendorf, Abteilung Allgemeine Pharmakologie, Martinistr. 52, D-2000 Hamburg 20, F.R.G.

[c]Arzneimittelinformationstelle der Bundesvereinigung Deutscher Apothekerverbände – ABDA, Beethovenplatz 1–3, D-6000 Frankfurt 1, F.R.G.

Abstract

Amino acid kinetics and psychometric parameters were studied in 10 patients with portosystemic encephalopathy (grade I–II) after oral branched-chain amino acid (BCAA) supplementation.

BCAA kinetics were established in healthy volunteers on a defined diet and in patients after a single oral dose (Leu 2.6 g, Ile 1.7 g, Val 1.7 g): Patients readily absorbed BCAA (peak plasma levels, 40 min, % of basal concn.: Leu 490, Ile 620, Val 360; controls: Leu 450, Ile 620, Val 320).

A significant elevation of plasma BCAA concentrations was observed over a period of 3 h; plasma aromatic amino acid (AAA) levels significantly decreased 1 h after BCAA intake (minimum, % of basal: Tyr 75% at 4 h, Phe 62% at 3 h). Patient BCAA/AAA ratio, used as therapeutic index, was maintained above 3 for at least 4 h.

Based on this, patients received a total amount of 0.3 g/kg b.w. BCAA daily, divided into 5 doses (1st day loading dose 150%) or placebo for 5 days. Treatment improved the BCAA/AAA ratio (mean minimum prior to next dose 2.9, range 1.6–5.1; placebo 1.5, range 0.8–2.4).

There were no adverse effects in patients' reports or in extended clinical biochemistry screening. EEG analysis revealed a slight improvement with regard to both dominant and mean dominant frequency in verum groups. Performance improved in psychometric arrays testing practical intelligence (digit symbol, number connection) or attention. Effects on psychomotor functions (aiming, line tracing, tapping, steadiness) were not consistently significant vs. training effects in the crossover design.

Results show that 5 daily doses of oral BCAA substantially ameliorate the BCAA/AAA imbalance. Whether beneficial effects on EEG and psychometric scores could be enhanced by higher BCAA supplementation or longer treatment remains to be studied.

Introduction

Branched-chain amino acids (BCAAs) have been recommended in the treatment of advanced liver cirrhosis and hepatic encephalopathy. Beneficial effects are expected in consideration of a) patients' low plasma BCAA content, b) augmented permeability of the blood brain barrier for neutral amino acids facilitating the influx of aromatic amino acids to the brain [1] and c) an imbalance in brain

neurotransmitter synthesis presumably including the production of false neurotransmitters [2].

Controversial evidence on effects of intravenous and oral BCAA supplementation have been found in clinical trials with marked variation in study design and on patients suffering from different grades of hepatic encephalopathy [3,4].

We investigated the effect of five-day oral BCAA supplementation in patients suffering from hepatic encephalopathy grade I–II [5] after initial pharmacokinetic studies for dose-finding.

Parameters measured included patients' plasma amino acid levels, EEG frequency spectra and performance in an array of psychometric tests.

Methods

Participants

Single dose pharmacokinetics were established in 7 healthy volunteers (5 female, 2 male; age 21–38) and in 7 patients (4 female, 3 male, age 33–58). Effects of sustained BCAA treatment was studied in 10 patients (3 female, 7 male, age 35–63) over a period of 5 days. Control subjects were within 15% limits of normal body weight (according to the Broca Index) and were asymptomatic in both physical examination and in routine clinical chemical screening. Patients included in both studies showed conclusive clinical evidence of portal hypertension caused by liver cirrhosis and hepatic encephalopathy (grade I-II, according to [5]) as well as typical changes in extended clinical chemistry analysis. Patients were in a stable metabolic state, including normal blood glucose and plasma kreatinine levels. Medication (diuretics, lactulose, oral neomycin) was unchanged for at least 14 days before the beginning of and during studies.

Criteria for exclusion from the study were clinical signs of ascites or edema, acute progression of the disease, signs of withdrawal, sedative medication (e.g. clomethiazole, benzodiazepines) or unrelated additional disease.

Informed consent was obtained from all participants and the study has been approved by the local medical ethics committee.

Single dose pharmacokinetics

Subjects fasted overnight and received a standard breakfast (350 ± 50 kcal; protein 5 ± 1%, carbohydrate 46 ± 2%, fat 49 ± 2%) as part of a defined diet (1 g protein, 30 ± 5 kcal/kg b.w. per day) during the test period.

At 8.00 a.m. BCAA were applied as a single oral dose (Leu 2.6 g, Ile 1.7 g, Val 1.7 g) in the form of two tablets of a commercial preparation (Bramin Hepa^{R}, Pfrimmer, Erlangen F.R.G.) at breakfast. Venous blood samples were obtained immediately before breakfast and during the next 24 h at intervals as indicated under results.

Five day treatment

Throughout the study, patients received a standard hospital diet that consisted of 14 ± 2% protein (i.e. less than 1 g protein/kg b.w.), 40 ± 3% carbohydrates, and 46 ± 4% fat amounting to a caloric intake of equal to or less than 30 kcal/kg b.w. depending on patients' acceptance. The actual daily food intake was monitored by weighing leftover food components. Patients were assigned to two groups by randomization and underwent a three day pre-study observation phase, during which all basic biochemical and haematological parameters were monitored. Reference data for psychometric tests and EEG valuation were obtained on the third day of the pre-study observation phase. In study phase I, one group of patients received BCAA in the form of powderized chocolate-flavoured tablets suspended in water according to the following regimen: 4 doses of BCAA at 8.00 a.m., 11.30 a.m., 3.00 p.m., 6.30 p.m (each dose mg/kg b.w.: Leu 33, Ile 21, Val 21) and twice this dose at 10.00 p.m. amounting to a total BCAA supplement of 450 mg/kg b.w. on the first day. For the next 4 days, therapy was continued with individual doses reduced to 67% (daily intake of 300 mg BCAA/kg b.w.). The second group of patients received a placebo preparation of the same flavor and galenic composition with casein replacing BCAA. After 5 days, under strict observation of the single blind conditions, groups were switched in medication for the study phase II commencing for another 5 days. All medication was taken by patients in the presence of medical staff. In addition, compliance was checked according to [6]: Vitamin B_6 3‰ (w.w.) had been added to both verum and placebo preparations and compliance was checked by daily measurement of urinary 4-pyridoxic acid excretion.

During the pre-study period and both study phase I and II, venous blood samples were obtained daily before breakfast and before the first BCAA intake. Additional venous blood samples were obtained at the third day of the pre-study phase and the last day of both study phases. Patients' urine was collected and analyzed in 24 h increments throughout.

Analytical procedures

Clinical chemistry parameters were obtained via standard methods within hospital facilities. Plasma amino acid concentrations were measured as described previously [7]. In brief, after precipitation of proteins according to Hamilton and van Slyke [8], amino acids were determined by photometric determination (multichrome M analyzer, Beckman AG, Munich, F.R.G) subsequent to separation by ion exchange chromatography using a digital integrator.

Electroencephalogram

Visual assessment of EEG frequency patterns [9] was conducted by one investigator (G.F.) before breaking patient coding.

Psychometric tests

Practical intelligence was assessed by a subtest of the Wechsler Adult Intelligence Series (WAIS), the Digit Symbols [10], the Multiple Choice Vocabulary Test [11] and the Number Connection Test [12]. Psychomotor functions were evaluated with the Motor Performance Test Battery, a mechanized version of pencil-and-paper based tests measuring Fleishman factors of motor skill [13], i.e. aiming, line tracing, tapping, steadiness. Speed and accuracy of reaction were tested with the Vienna Reaction Time Apparatus [4], mnestic functions (visual retention time) as well as attention under stress were measured using the Attention Stress Test as described elsewhere [4].

Statistical evaluation

Data are shown as means giving variation as the standard error of the mean (S.E.), the range (minimum and maximum value observed), or the 99% confidence limits according to the t-distribution as indicated. The significance of differences between means was evaluated using the paired or unpaired t-test, one-way or two-way analysis of variance, as appropriate.

Results

Single dose pharmacokinetics of oral BCAA

This part of the study was conducted in order to find approximate criteria for single oral dose requirements and dosing intervals in sustained oral BCAA supplementation. Plasma levels of valine, isoleucine, leucine, as well as of the aromatic amino

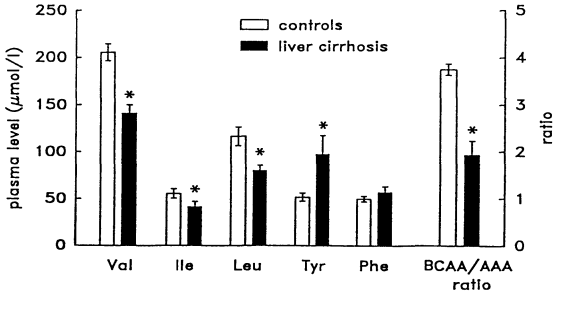

Fig. 1. Pre-study plasma amino acid status of participants. Plasma levels of the BCAAs valine, isoleucine, leucine, and the AAAs tyrosine and phenylalanine as well as for the resulting BCAA/AAA ratio [Val+Leu+Ile]/[Phe+Tyr] are given for healthy controls (n = 7) as opposed to patients suffering from hepatic encephalopathy with portal hypertension (n = 7). Means ± S.E., * = $p<0.05$ according to unpaired two-tailed t-test evaluation.

acids tyrosine and phenylalanine were determined in both healthy subjects and patients following a single oral dose applied in the morning during breakfast.

The pre-treatment baseline values for plasma amino acid levels in both patients and controls are shown in Fig. 1. Blood samples were obtained immediately before BCAA application and show the typical pattern of disease-related plasma-amino acid imbalance in patients as compared to controls: The BCAA/AAA ratio in patients, referred to as a therapeutic index, is decreased by half as a consequence of both lowered BCAA levels and increased tyrosine and phenylalanine plasma contents. Statistical details of plasma amino acid imbalance in patients are referred to in Fig. 1. Obvious diurnal rhythms do not affect the pattern of BCAA/AAA imbalance in the absence of BCAA medication (day-profile studies, results not shown).

Changes in plasma amino acid contents following the oral BCAA application (Leu 2.6 g, Ile 1.7 g, Val 1.7 g) are given in Fig. 2. Despite of different baseline – plasma levels (Fig. 1), BCAAs were readily absorbed in both patients and controls (Fig. 2). As soon as after 20 min, i.e. at the first measurement following the ingestion of BCAA tablets, valine, isoleucine, and leucine plasma contents had increased to manifolds of the baseline concentrations ($p<0.01$ each) in both groups. Peak plasma levels were observed by 40 min and BCAA elevation had ceased after

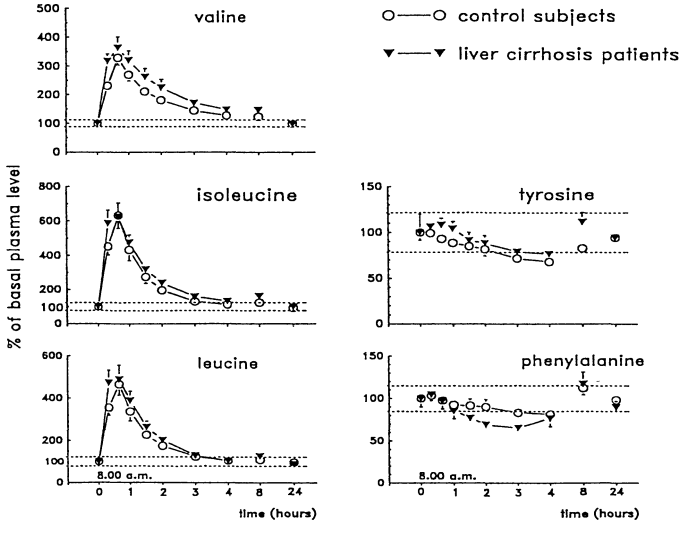

Fig. 2. Pharmacokinetics of oral BCAA and response of AAA levels. Changes in plasma contents of the BCAAs valine, isoleucine, leucine (panels on the left) and the subsequent decrease in levels of the AAAs tyrosine and phenylalanine (panels on the right) are shown for healthy controls (n = 7) and hepatic encephalopathy patients (n = 7) on a relative basis in order to allow for direct comparison of slopes. Percentage values refer to pre-study baseline levels (time=0; for absolute values comp. Fig. 1). Dashed lines indicate the 99% confidence limit for these basal conditions. Means ± S.E. (included in symbols where not shown).

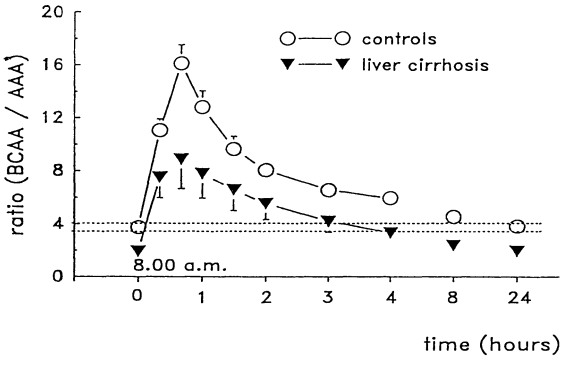

Fig. 3. BCAA/AAA ratio after BCAA ingestion. Subsequent to the complex changes in plasma amino acid composition due to oral intake of a single dose of BCAA, the BCAA/AAA ratio [Val+Leu+Ile]/[Phe+Tyr] is elevated in both hepatic encephalopathy patients and healthy controls. Values are calculated from data given in Fig. 1 and Fig. 2. Dashed lines denote the 99% confidence limits for the BCAA/AAA ratio in untreated control persons. Means ± S.E. (included in symbols where not shown), n = 7 each.

a period of 4 h, with the exception of valine, which was still significantly elevated in the patient group at 8 h after BCAA intake.

Subsequent to the increase in BCAA plasma levels following oral supply, AAA levels decreased (Fig. 2). In the patient group, with a 1-h delay, plasma tyrosine concentrations decreased quite slowly with statistically significant differences from pre-treatment conditions at last assay (4 h post application).

Phenylalanine plasma levels however, were lowered significantly by 90 min, with the most pronounced decrease found at 3 h. The impact of these changes in plasma amino acid contents on the BCAA/AAA ratio as the therapeutic index is shown in Fig. 3.

Coinciding with the maximum rise in plasma BCAAs (Fig. 2), peak values for the BCAA/AAA ratio were observed in both patients and controls at 40 min after BCAA ingestion. However, 4 h after intake, when BCAA levels were about to return to normal, BCAA/AAA ratios in both patients and controls were still elevated significantly compared to their respective pre-treatment values. The late effect on the BCAA/AAA ratio was due to the delayed lowering of AAA plasma levels towards the late phase in BCAA distribution and elimination. In patients, the BCAA/AAA ratio was restored from subnormal values by 20 min and could be kept above the lower margin of healthy control baseline levels (see Fig. 3, dashed lines) for a period of 4 h.

Plasma amino acid levels during sustained BCAA treatment

Patients were randomly assigned to two groups, observed for three days without treatment, received BCAA or casein placebo divided into 5 daily doses for 5 days (see methods), and then switched treatment in the single-blind crossover design.

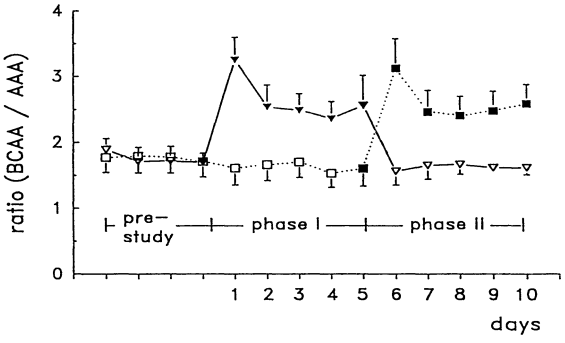

Fig. 4. Sustained BCAA intake and patients' BCAA/AAA ratio. The figure shows the BCAA/AAA ratio [Val+Leu+Ile]/[Phe+Tyr] in two groups of hepatic encephalopathy patients during a 3 day pre-study observation phase, during oral BCAA treatment (filled symbols), or receiving casein placebo (open symbols) in a single blind crossover design. Data were calculated from plasma amino acid concentrations obtained at 8.00 a.m. before the first application of the day and thus represent minimum values in treatment groups. Means ± S.E. (included in symbols where not shown), n = 5 each.

During the pre-study observation phase, no significant differences were observed between study groups with regard to clinical and laboratory parameters, food intake or urinary nitrogen excretion. Both groups had uniform characteristics with regard to plasma levels of BCAA (n = 10, mean ± S.E; μmol/l: Val 126 ± 7 Ile 44 ± 3, Leu 68 ± 4) and of AAA (μmol/l: Tyr 88 ± 8, Phe 52 ± 3). The BCAA/AAA ratio of either group during the pre-study observation phase is included in Fig. 4.

It is further shown in Fig. 4 that oral BCAA treatment substantially improved the BCAA/AAA ratio in both study groups according to crossover. Data shown in Fig. 4 were calculated from plasma amino acid assays conducted at 8.00 a.m. in the morning prior to the first daily dose of either BCAA or placebo and 10 h after application of the last medication of the preceding day. Thus, on the day after receiving the loading dose of a total of 450 mg/kg BCAA in both verum phases, the remaining minimum improvements in patients' BCAA/AAA ratios were from below 2 to values above 3. For the next four days, BCAA intake was reduced to 67% of the loading dose. Accordingly, BCAA/AAA ratio minima in the morning amounted to values around 2.5 ($p<0.05$ vs. placebo in both phases, two-way analysis of variance). In both study groups, improvement of BCAA/AAA ratios – as measured at 8.00 a.m. – remained quite stable during these four days of the treatment phases. Day profiles of BCAA/AAA ratios during BCAA or casein placebo medication in both collectives are summarized in Fig. 5. The ratio responds to BCAA application at daytime with a rise from its lowest value in the morning to a mean minimum value (before next BCAA dose) of about 3 in the afternoon in all patients studied. During placebo medication, there is virtually no diurnal variation in pathologic BCAA/AAA ratios ranging from 1.5 to 1.6.

Patients plasma levels of valine, isoleucine and leucine were elevated parallel to the BCAA ration in day-profile assays (n = 10, mean ± S.E.; μmol/l, 8.00 a.m.

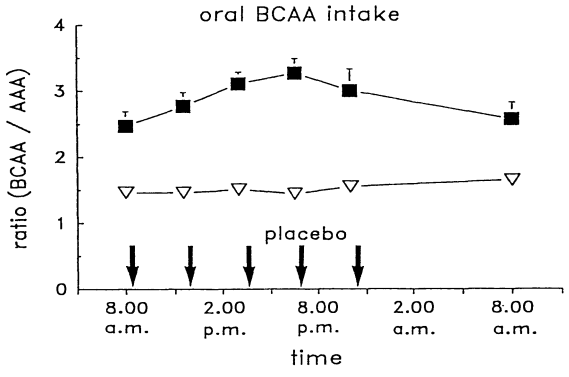

Fig. 5. Five daily doses of BCAA and patients' BCAA/AAA ratio. The figure summarizes day profiles of BCAA ratios in patients receiving five daily doses (time of application indicated by arrows) of either BCAA (filled squares) or casein placebo (open inverse triangles) at the 5th day of the respective study phase (see Fig. 4). Means ± S.E. (included in symbols in placebo group), n = 10 each.

vs. 6.30 p.m.: Val 184 ± 15 vs. 272 ± 14, Ile 49 ± 4 vs. 101 ± 8, Leu 84 ± 9 vs. 150 ± 13) whereas little variation was observed in casein placebo groups, who had amino acid plasma levels as shown for patients in Fig. 1 (particular results not shown). As in single dose pharmacokinetics, lowered AAA levels in treatment groups substantially contributed to improvement of patients' BCAA/AAA ratio. In AAA day profiles at the fifth day of medication, BCAA intake had slightly lowered both tyrosine and phenylalanine (plasma levels in BCAA groups, % of placebo, Tyr mean 72%, range 63–83%, $p<0.05$, Phe mean 88%, 71–99%, not significant).

Therapeutic response

In the pre-study phase, 5 patients had symptoms according to grade I hepatic encephalopathy (5) including intellectual dysfunction, psychomotoric and neuromuscular disturbances (e.g. tremor, difficulties with handwriting), and 5 patients were classified as grade II hepatic encephalopathy showing pronounced disorientation, confusion, or drowsiness.

Frequency analysis of patients' EEGs were performed within the pre-study observation phase (nonfocal changes in 2 patients) and at the fifth day of either medication term. In two patients EEG recordings were not evaluated because of initial beta wave dominance. BCAA treatment increased dominant frequency (pre-study: mean 8.9/s, range 8–10/s) in 5/8 patients and had no effects in 3/8 patients. Under casein placebo, increase (1/8) and decrease (1/8) were observed once compared to pre-study dominant frequency. BCAA treatment improved values calculated for mean dominant frequency in 7/8 patients (n = 8, mean, S.E.; 1/s: pre-study 9.1 ± 0.3; BCAA 9.8 ± 0.3; placebo 9.2 ± 0.3, $p<0.05$, paired t-test). Evaluation of scores in the psychometric test arrays was done under consideration of training effects due to repeated testing within 11 days. The data for BCAA and

placebo group test performance are expressed as changes in test scores of patients receiving either BCAA or placebo for five days, compared to scores obtained immediately before this period (i.e. in the pre-study phase or under alternate medication). For obvious reasons, both BCAA and placebo results expressed this way will include improvement due to training.

Practical intelligence was tested with the Digit Symbol Test and the Number Connection Test. In pre-study testing, patients assigned 24.2 ± 3.8 digits to corresponding symbol within the test period of 90 seconds. Improvement subsequent to BCAA intake was marginally superior to effects due to training alone after casein placebo (BCAA +4.4 ± 0.8; placebo +3.0 ± 0.3, $p < 0.05$). More pronounced were effects on the time score in the Number Connection Test (pre-study: 67.4 ± 5 9 s), where BCAA-treated patients were significantly faster than in prior testing (−13.3 ± 5.5 s, $p<0.05$) but placebo (−2.8 ± 4.7 s) was without effect.

Improvement in the Attention Stress Test (mean time required pre-study: 414 ± 54 s) also was superior in BCAA groups compared to patients tested in the casein placebo phase (−64 ± 24 s vs. −26 ± 22 s, $p<0.05$).

Psychomotor functions were tested using an array of tests (see methods). Beneficial effects of BCAA supplementation were found on patients' steadiness. Patients held a metal probe inserted into a hole, with the fails (touching the wall) and time of such incorrect positioning recorded (pre-study, mean fails 24 ± 6 / duration 0.77 ± 0.27 s). In the BCAA phase, significantly less fails (−21 ± 13) of possibly shorter duration (−0.14 ± 0.09 s) were recorded in patients, whereas test performance appeared to decline during placebo phases (mean fails +25 ± 18 / duration +0.19 ± 0.12 s).

In a number of additional tests on psychomotor function (aiming, line tracing, tapping), as well as on mnestic functions (visual retention time), beneficial effects of BCCA intake were not significant in statistical analysis. The reaction time, measured using visual and auditory signals, appeared to be unaffected throughout the study.

Discussion

Results of this work relate to the increasing number of clinical investigations into the use of BCAA in the therapy of nutritional support and of correcting metabolic derangements induced by liver cirrhosis. Beneficial effects of BCAA in the treatment of hepatic encephalopathy are not unequivocally acknowledged [3]. Clinical studies have been performed with BCAA infusion therapy as well as with oral BCAA supplements (for ref. see [3,14,15]).

With regard to the considerable incidence of hepatic encephalopathy and the large number of out-patients with subchronic disease, oral BCAA application would be superior to infusion therapy in terms of safety, patients' convenience, and expense. However, besides disagreement on the therapeutic benefits of BCAA

infusions [16,18], reports on oral BCAA treatment of hepatic encephalopathy patients have been particularly controversial [3,4,19].

We therefore addressed BCAA pharmacokinetics after oral treatment. Bioavailability from the oral BCAA preparation was not impaired in hepatic encephalopathy patients as compared to healthy controls. Absorption occurred rapidly and undisturbed in liver cirrhosis patients, with peak levels after a period of 40 min. Apparent plasma half-life of the BCAA elevation was within the range of 1 to 2 h. For the patient group, these data comply well with previous reports on leucine and isoleucine [20], or punctual data obtained 1 h post application [21]. There were no obvious differences in BCAA kinetics between patients and controls. This is in agreement with BCAA infusion studies [22], reporting normal plasma clearance, BCAA decay constantly after infusion stop, and distribution volumes for all BCAA in cirrhosis patients as compared to healthy controls.

In the present study as in others [21], patients' initially elevated plasma AAA levels slowly decreased after medication, presumably due to a partial reconstitution of protein synthesis subsequent to BCAA supplementation [23]. The decrease in plasma AAA contributed to the improvement in patients' subnormal BCAA/AAA ratio, and prolonged the effect of medication. The BCAA/AAA ratio was reconstituted to values within the physiological range for a period of 4 h.

The schedule for sustained oral BCAA treatment was designed with the following intentions:

A) Application of a loading dose to fill in patients' chronic BCAA deficits on the first day treatment. Results show that the initial rise in the BCAA/AAA ratio could not be maintained during subsequent treatment, thus questioning this objective.

B) Division of BCAA supplementation into five daily doses, according to time courses observed in initial pharmacokinetic studies. Day profiles on the fifth day of medication show that plasma BCAA/AAA contents could be kept at or near physiological levels this way.

C) Extra late night BCAA supplement, with twice the usual dose of BCAA applied at 10.00 p.m. to cover the longer interval until next morning. As a result, a significant improvement from plasma amino acid imbalance (as compared to placebo) could be maintained until the following morning.

Results show that profound and constant improvements in patients' plasma amino acid imbalance can be obtained by oral BCAA intake. Compared to steady-state pharmacokinetics of infusion therapy, reconstitution of patients' BCAA/AAA imbalance to physiological values was not entirely satisfactory. Restoration of patients' BCAA plasma levels to values above the lower physiological level did not cover the entire treatment period, and the BCAA/AAA ratio, though markedly improved compared to placebo, remained at subnormal values in particular in early morning assays. As BCAA levels in the intracellular compartment fill up fast and decrease much slower than in plasma [24], prolonged steady state infusion kinetics for BCAA are of doubtful relevance in grade 1 to 2 hepatic encephalopathy.

We conclude that intervals of oral BCAA supplementation should not exceed 4 h during the day. A 10-h interval at night for patients' convenience may be tolerable.

Pharmacokinetics indicate, that further approximation of physiological amino acid plasma levels in hepatic encephalopathy patients via oral supplementation could be expected by dividing the daily supplement into still more doses rather than increasing the single dose.

Therapeutic benefits of oral BCAA supplementation vs. casein placebo could be detected in both EEG frequency analysis and psychometric tests. Test performance in tests improved in assays of practical intelligence and attention. Beneficial effects on psychomotor function were less pronounced, as only patients' tremor (Steadiness test) responded significantly to BCAA treatment, whereas an array of additional tests did not. Mnestic functions and reaction time were not affected at all.

Within this preliminary study of short duration, the recovery of patients from the profound hepatic encephalopathy – associated alterations in central nervous system neurotransmission [25] could not be expected. However, pharmacokinetic findings and the therapeutic effects shown here encourage further testing of oral BCAA treatment in hepatic encephalopathy for prolonged periods and on a larger scale.

References

1. James JH and Fischer JE (1981) Pharmacology 22: 1–7.
2. Fischer JE and Baldessarini RJ (1971) Lancet II: 76–80.
3. Alexander WF, Spindel E, Harty RF and Cerda JJ (1989) Am. J. Gastroenterol. 84: 91–96.
4. Egberts EH, Schomerus K, Hamster W and Jürgens P (1985) Gastroenterology 88: 887–895.
5. Schenker S and Hoyumpa AM (1984) Hosp. Pract. 9: 99–121.
6. Udenfried S (1962) Fluorescence Assay in Biology and Medicine. Academic Press, New York, London, pp. 252–263.
7. Jürgens P, Dolif D and Fondalinski G (1978) Klin. Ernähr. 5: 3–15.
8. Hamilton PB and van Slyke DD (1943) J. Biol. Chem. 150: 231–250.
9. Laidlaw J, Read AE (1963) Clin. Sci. 24: 3–5.
10. Wechsler D (1964) Die Messung der Intelligenz Erwachsener, 3rd Ed., Huber, Bern, Stuttgart.
11. Lehrl S (1977) Mehrfachwahl-Wortschatz-Intelligenztest MWT-B, Straube, Erlangen.
12. Conn HO (1977) Am. J. Dig. Dis. 22: 541–550.
13. Fleishman EA (1962) A Factor Analysis of Psychomotor Abilities. J. Exp. Psychol. 46: 95–105.
14. Wahren J, Denis J, Desurmont P, Eriksson LS, Escoffier J-M, Gauthier AP, Hagenfeldt L, Michel K, Opolon P, Paris J-C and Veyrac M (1983) Hepatology 3: 475–480.
15. Gerok W (1984) Therapiewoche 34: 49–62.
16. Cerra FB, Cheung NK, Fischer JE, Kaplowitz N, Schiff ER, Dienstag JL, Bower RH, Mabry CB, Leevy CM and Kierman T (1985) J. Parent Nutr. 9: 288–295.
17. Michel H, Borries P, Aubin JP, Pomier-Layarques G, Bauret P and Bellet-Herman H (1985) Liver 5: 282–289.
18. Kanematsu T, Koyanagi N, Matsumata T, Kitano S, Takenaka K and Sugimachi K (1988) Surgery 104: 482–488.
19. Fiaccadory F, Elia GF, Lehndorff H, Merli M, Pedretti G, Riggio O and Capocaccia L (1988) In: Soeters PB, Wilson JHP, Meijer AJ and Holm E (eds.) Advances in Ammonia Metabolism and Hepatic Encephalopathy. Elsevier, Amsterdam, pp. 489–497.
20. Schauder P (1985) J. Lab. Clin. Med. 106: 701–707.
21. Eriksson LS and Wahren J (1982) In: Capocaccia L, Fischer JE and Rossi-Fanelli F (eds.) Hepatic Encephalopathy in Chronic Liver Failure. Plenum Press, New York, pp. 287–299.
22. Marchesini G, Bianchi GP, Vilstrup H, Checchia GA, Patrono D and Zoli M (1987) J. Hepatol. 4: 108–117.

23. Marchesini G, Zoli M, Dondi C, Bianchi G, Cirulli M and Pisi E (1982) Hepatology 2: 420–425.
24. Montanari A, Simoni I, Vallisa D, Trifiro A, Colla R, Abbiati R, Borghi L and Novarini A (1988) Hepatology 8: 1034–1039.
25. Rossi-Fanelli F, Cascino A, Strom R, Cardelli-Cangiano P, Ceci F, Muscaritoli M and Cangiano C (1987) Prog. Neurobiol. 28: 277–301.

Oral glutathione increases hepatic glutathione and prevents acetaminophen toxicity

Juan R. Viña[a], Federico V. Pallardo[b], Tadayasu Furukawa[c] and Jose Viña[b]

[a]Department of Biochemistry and Molecular Biology, University of Valencia, Valencia, Spain
[b]Department of Physiology, University of Valencia, Valencia, Spain
[c]Tokyo Research Laboratories, Kyowa Hakko Kogyo, Tokyo, Japan

Abstract

Administration of oral glutathione (GSH) increases hepatic GSH levels in fasted rats, in mice treated with GSH depletors such as diethylmaleate and in mice treated with high doses of paracetamol. An increase in hepatic GSH levels after administration of oral GSH does not occur in animals treated with buthionine suphoximine, an inhibitor of GSH synthesis. Administration of oral GSH leads to an increase in the concentration of L-cysteine, a precursor of GSH, in portal blood plasma. Oral administration of L-methionine to fasted rats produced a significant decrease of hepatic ATP, but not in fed rats. Administration of N-acetyl-cysteine or GSH did not affect the hepatic ATP levels. The results show that the oral intake of GSH is a safe and efficient form of administration of its constituent amino acids in cases when GSH synthesis is required to replete hepatic GSH levels.

Introduction

The availability of L-cysteine is the rate-limiting factor for GSH synthesis [1]. Attempts to increase the hepatic levels of GSH have focussed on the administration of L-cysteine or L-methionine [1], N-acetyl cysteine (NAC) [2], or 2-oxothiazolidine carboxilate [3] which are all precursors of L-cysteine. However, in some circumstances these substances have undesirable side effects [4–6]. Parenteral GSH cannot be used to increase intracellular GSH levels because free GSH does not enter the cells [7].

Other procedures are difficult and not easily available [8,9]. In contrast with parenteral GSH, dietary GSH has proved effective in reversing the age-associated decline in immune responsiveness in mice [10]. However, direct evidence that oral GSH, which is a natural and non-toxic substance [11], serves to increase the intracellular levels of GSH in cells was lacking.

We have studied the ability of oral GSH to replenish hepatic GSH in three different circumstances known to deplete the levels of hepatic GSH: 1. Fasting [12,13]; 2. Pretreatment with diethyl maleate [14]; and 3. Paracetamol overdosage [15].

Materials and Methods

Animals

Wistar rats 4–5 months of age or Swiss mice 2–3 months of age were used.

Some mice were injected intraperitoneally with diethylmaleate (1 g (5 mmol)/kg body weight) or with paracetamol (0.9 g/kg body weight).

Precursors for hepatic GSH synthesis were methionine (1 gr (6.7 mmol)/kg body weight, N-acetylcysteine (1 gr (6.1 mmoles)/kg body weight or GSH (1 gr (3.26 mmol)/kg body weight). These precursors were given orally through a cannula under light diethylether anaesthesia.

Determination of metabolites

Metabolites were always measured in freeze-clamped tissues. GSH, method of Racker [16]. ATP method by Lamprecht & Trautschold [17], glycogen by the method of Kepker & Decker [18] and L-cysteine method described by Gaitonde [19].

Statistics

See Viña *et al.*, [20].

Results

Effect of oral GSH on the levels of hepatic GSH in 48 h fasted rats

Fasting for 48 h decreases the levels of hepatic GSH [12]. The concentration of GSH found in fed rats was 5.7 (SE 0.4) μmol/g (fresh weight) (n 6) and this value

Table 1. Effect of oral methionine, N-acetylcysteine (N-Ac-cys) or glutatione (GSH) on the concentrations of hepatic GSH in 48 h starved rats

	Hepatic GSH level (μmol/g fresh wt)			
Oral Treatment	Control (6) Mean ± SE	Methionine (5) Mean ± SE	N-Ac-cys (5) Mean ± SE	GSH (4) Mean ± SE
Period after treatment (h)				
2.5	3.1 ± 0.2	5.9[a] ± 0.3	3.4 ± 0.4	5.8[a] ± 0.2
10	3.0 ± 0.1	4.9[a] ± 0.3	5.4[a] ± 0.3	4.2[a] ± 0.3
24	3.1 ± 0.2	5.2[a] ± 0.2	5.9[a] ± 0.3	7.0[a] ± 0.3

Mean values with their standard errors; no of observations in parentheses. The animals were killed at the indicated period after treatment. Hepatic GSH concentration in fed rats was 5.7 ± 0.4) (n 6) μmol/g. Mean values were significantly different from control values: [a]$p<0.05$ + 9 g Sodium chloride/l.

Table 2. Effect of oral methionine and glutatione (GSH) on hepatic ATP concentrations in fed and 48 h fasted rats

	Hepatic ATP (μmol/g fresh wt)			
Oral treatment...	Period after treatment (h)	Saline[a] Mean ± SE	Methionine Mean ± SE	GSH Mean ± SE
Fed Rats	2.5	1.9 ± 0.1(3)	1.7 ± 0.1(6)	2.7[b] ± 0.1(6)
	10	2.0 ± 0.1(9)	1.6[b] ± 0.1(4)	2.1 ± 0.2(5)
	24	1.7 ± 0.1(6)	————	1.1[b] ± 0.2(5)
Fasted Rats	2.5	1.2 ± 0.1(5)	0.7[b] ± 0.1(5)	1.3 ± 0.2(4)
	10	1.0 ± 0.2(6)	0.7 ± 0.1(5)	1.3 ± 0.3(4)
	24	1.4 ± 0.2(4)	0.6[b] ± 0.1(4)	1.6 ± 0.2(4)

Mean values with their standard errors; no. of observations in parentheses. The animals were killed at the indicated period after treatment. Mean values were significantly different from control values: [a] ± 9 g Sodium chloride/l, [b]$p<0.05$.

fell to 3.6 (SE 1.4) μmol/g fresh weight (n 8) in fasted animals. Table 1 shows that oral administration of GSH significantly increases the levels of hepatic GSH of 48 h fasted rats to values similar to those found in fed controls. Table 2 shows that oral administration of L-methionine induced a depletion of hepatic ATP only in fasted rats.

Effect of oral GSH on the levels of hepatic GSH after the administration of diethylmaleate

Table 3 shows that oral administration of GSH, methionine or N-acetyl cysteine promotes GSH synthesis in liver after depletion with diethylmaleate. GSH replen-

Table 3. Effects of oral glutathione (GSH), methionine or N-acetylcysteine (N-Ac-cys) on hepatic GSH concentrations in mice treated with diethyl maleate (DEM)

	Hepatic GSH (μmol/g fresh wt)			
Oral treatment...	DEM	DEM plus methionine	DEM plus N-Ac-cys	DEM plus GSH
Period after treatment (h)	Mean ± SE	Mean ± SE	Mean ± SE	Mean ± SE
2.5	1.4 ± 0.1(8)	5.8[a] ± 0.3(6)	6.4[a] ± 0.2(4)	2.3[a] ± 0.1(6)
10	2.7 ± 0.2(6)	7.5[a] ± 0.5(6)	7.7[a] ± 0.2(5)	7.0[a] ± 0.2(5)
24	4.4 ± 0.2(4)	6.6[a] ± 0.2(5)	4.4[a] ± 0.2(5)	5.2[a] ± 0.1(6)

Mean values with their standard errors; no. of observations in parentheses. The animals were killed at the indicated period after treatment. Mean values were significantly different from control values: [a]$p<0.05$.

ishment is slower when GSH is given as a precursor than with the other two compounds used.

Protection against paracetamol hepatotoxicity by oral GSH

Table 4 shows that oral GSH partially prevented the fall in GSH levels after treatment of mice with paracetamol.

It was reported that paracetamol overdosage promotes glycogen depletion [21]. We have confirmed this observation and found that when paracetamol was administered together with oral GSH the hepatic glycogen levels were always higher than those found in animals treated with paracetamol alone. A good indication of hepatic cellular damage is the leakage of cytosolic enzymes to blood plasma. Table 4 shows that oral GSH prevented the increase in alanine amino transferase activity in plasma subsequent to paracetamol administration. Furthermore, 24 h after administration of paracetamol all six mice had died. However, when paracetamol was given together with oral GSH 67% of the mice had

Table 4. Protection against paracetamol toxicity (900 mg/kg body weight) afforded by glutathione (GSH), methionine or N-acetylcysteine (1 g/kg body weight)

Period after treatment (h)	GSH (μmol/g fresh wt) Mean ± SE	Glycogen (μmol of glucose equivalent/ g fresh wt) Mean ± SE	AAT (International Units) Mean ± SE
Paracetamol			
2.5	0.9 ± 0.1(16)	43 ± 3(11)	27 ± 2(5)
10	1.7 ± 0.2(6)	4 ± 1(4)	1503 ± 123(5)
24	100% of the mice injected had died (6)		
Paracetamol + GSH			
2.5	1.4[a] ± 0.1(11)	16[a] ± 3(6)	14[a] ± 1(5)
10	5.6[a] ± 0.3(6)	46[a] ± 9(6)	21[a] ± 1(5)
24	5.7 ± 0.3(6)	86 ± 9(5)	28 ± 4(5)
Paracetamol + N-acetylcysteine			
2.5	2.5[a] ± 0.2(6)	4[a] ± 1(6)	19[b] ± 3(5)
10	5.8[a] ± 0.2(6)	88[a] ± 9(6)	49[a] ± 16(5)
24	7.0 ± 0.4(4)	132 ± 14(4)	21 ± 31(5)
Paracetamol + Methionine			
2.5	2.9[a] ± 0.2(6)	38 ± 3(6)	18[a] ± (4)
10	4.4[a] ± 0.2(7)	27[a] ± 2(7)	34[a] ± 3(3)
24	7.8 ± 0.3(5)	118 ± 14(4)	33 ± 6(4)

Mean values with their standard errors; no. of observations in parentheses. The animals were killed at the indicated period after treatment. AAT, alanine aminotransferase (E.C. 2.6.1.2.). Mean values were significantly different from control (paracetamol alone) values: [a]$p<0.05$. The values found in untreated mice were: GSH: 5.7 (SE 0.4),(n 6); Glycogen: 99(SE 17),(n 6) and AAT: 28(SE 3),(n 6).

survived. N-acetyl cysteine and methionine had similar protective effects against paracetamol overdose. It is worthwhile to emphasize that no animals died except in the group treated 24 h with paracetamol alone as stated above.

Requirement of GSH synthesis to explain the increase in hepatic GSH after oral administration of GSH

The effect of oral GSH on the hepatic concentration of GSH could be due to: 1) a direct absorption of the tripeptide from the intestine which could be transported via the portal vein and taken up by the liver or 2) a degradation to the constituent amino acids by the combined action of -glutamyl transpeptidase (E.C. present in intestinal brush border cells) and intestinal dipeptidases. In this case the free amino acids could be absorbed from the intestine and be taken up by the liver. This requires active GSH synthesis by the liver.

The first hypothesis is unlikely because GSH itself does not enter the hepatocytes [7]. Thus, we tested the second hypothesis, i.e. that GSH is converted to its constituent amino acids in the intestine and that these are transported to the liver where active GSH synthesis is promoted. Since the availability of cysteine is a rate-limiting step for GSH synthesis in liver [12], the concentration of cysteine was measured in portal blood plasma of 48 h fasted rats, one hour after the administration of oral GSH (1 g (3.26 mmol)/kg body weight), the concentration of cysteine in their portal blood plasma was 0.21 (SE 0.05) (n 14).

Rats were treated with diethylmaleate their hepatic GSH level fell to 1.6 (SE 0.6) μmol/g (n 4), but when rats pretreated with diethylmaleate were given oral GSH (3.26 mmoles/kg body weight) their hepatic GSH concentration was increased, as expected, to a value of 3.8 (SE 1.0) μmol/g (n 4). When rats treated with diethylmaleate were administered 3.26 mmoles/kg body weight of oral GSH and 5 μmol/kg body weight of buthionine sulfoximine an inhibitor of GSH synthesis [22], their hepatic GSH concentration was 0.21 ± 0.15 μmol/g (n=4). The fact that in the presence of an inhibitor of GSH synthesis administration of oral GSH does not serve to increase the levels of hepatic GSH, shows that the increase in hepatic GSH levels after the administration of oral GSH is dependent on active GSH synthesis.

Thus, an explanation for the effectiveness of oral GSH in increasing the hepatic levels of GSH is that oral GSH is converted to its constituent amino acids by the concerted action of glutamyl transferase and of intestinal dipeptidases. The increase in hepatic GSH after oral GSH administration requires active GSH synthesis in liver.

Acknowledgements

We thank Mrs. J. Belloch and Miss E. Gascó for their excellent technical assistance. This work was supported by grants F.I.S.S. 87/1415, C.I.C.Y.T. DEP-483 to J.V. and C.A.I.C.Y.T. 0888–84 to J.R.V.

References

1. Vale JA, Meredith TJ and Goulding R (1981) Archives Internal Medicine 141: 394–396.
2. Prescott LF, Park J, Ballantyne A, Adriaenssens P and Proudfoot AT (1977) Lancet 2: 432–434.
3. Williamson JM and Meister A (1981) Proceedings of the National Academy of Science U.S.A. 78: 936–939.
4. Olney JW, Ho OL, Rhee V and Schainker B (1972) Brain Research 45: 309–313.
5. Viña J, Romero FJ, Saez GT and Pallardó FV (1983b) Experientia 39: 164–165.
6. Hardwick DF, Applegarth DA, Cockcroft DM, Ross PM and Calder RJ (1970) Metabolism 19: 381–391.
7. Hahn R, Wendel A and Flohé L (1978) Biochimica et Biophysica Acta 539: 324–337.
8. Wendel A (1983) International Journal of Clinical Pharmacological Research 3: 443–447.
9. Puri RN and Meister A (1983) Proceedings of the National Academy of Science U.S.A. 80: 5258–5260.
10. Furukawa T, Meydani SN and Blumberg JB (1987) Mechanisms of Ageing and Development 38: 107–117.
11. Sakamoto Y, Higashi T and Tateishi N (1983) In: Glutathione: Storage, Transport and Turnover in Mammals. Japan Scientific Societies Press, Tokyo and VNU Science Press, Utrecht, pp. 1–202.
12. Tateishi N, Higashi T, Shinya S, Naruse A and Sakamoto Y (1974) Journal of Biochemistry (Tokyo) 75: 93–103.
13. Viña J, Hems R and Krebs HA (1978) Biochemical Journal 170: 627–630.
14. Boyland E and Chasseaud LF (1967) Biochemical Journal 104: 95–102.
15. Mitchell JR, Thorgeirsson SS, Potter WZ, Jollow DJ and Keiser H (1974) Clinical Pharmacology and Therapeutics 16: 676–684.
16. Racker E (1951 Journal of Biological Chemistry 190: 685–696.
17. Lamprecht W and Trautschold I (1979) In: Bergmeyer HU (ed.) Methods of Enzymatic Analysis. Academic Press, New York, pp. 2101–2110.
18. Keppler D and Decker K (1979) In: Bergmeyer HU (ed.) Methods of Enzymatic Analysis. Academic Press, New York, pp. 1127–1131.
19. Gaitonde MK (1967) Biochemical Journal 104: 627–633.
20. Viña JR, Puertes IR, Rodriguez A, Sáez GT and Viña J (1987) Journal of Nutrition 117: 533–538.
21. Hinson JA, Mays JB and Cameron AM (1983) Biochemica, Pharmacology 32: 1979–1988.
22. Griffith OW and Meister A (1979) Journal of Biologica, Chemistry 254: 7558–7560.

Address for correspondence: Dr. José Viña, Department of Physiology, Faculty of Medicine, Avenida Blasco Ibáñez 17, 46010 Valencia, Spain.

Syntheses of thymopoietins and their immunological effects: Relationship of amino acid sequence to immunological activity

Takashi Abiko and Hiroshi Sekino

Kidney Research Laboratory, Kojinkai, 1–6, Tsutsujigaoka 2-chome, Miyagino-ku, Sendai 980, Japan

Abstract

Peptides and fragment analogs of the thymopoietin (TP) family have been synthesized using conventional synthesis in solution and tested for immunological effects on the impaired lymphocytes of uremic patients. These studies indicate that the Arg-residue of the sequence 32 to 36 of thymopoietin II is necessary for restoring activity of E-rosette formation on reduced E-rosette formation in uremic patients and the shortest peptide fragment of thymopoietin II (thymopentin), Arg-Lys-Asp-Val-Tyr, increased the activity of E-rosette-forming cells similarly to the longer chain of thymopoietin fragments containing thymopentin in their sequences. The synthetic human thymopoietin (hTP) showed restorative effect on the impaired T-lymphocyte activity of uremic patients as well as the synthetic two other synthetic thymopoietins, bovine thymopoietin I (bTP-I) and bovine thymopoietin II (bTP-II). However, the restoring activity of the synthetic bovine thymopoietin III (bTP-III or bovine splenin) was lower than that of the synthetic bTP-I. A synthetic analog of human splenin (hSP), [Glu^{34}]hSP showed an enhancing effect on the reduced B-lymphocytes of uremic patients.

Introduction

Thymus is an endocrine organ which regulates and development, differentiation and maturation of T-lymphocytes and controls the immune systems [1].

Bovine thymopoietins I (bTP-I) and II (bTP-II) are two closely related polypeptides isolated from bovine thymus [2]. These purified polypeptides subsequently proved to be active in induction of early T-cell differentiation, inhibition of B-cell differentiation, and modulation of mature lymphocytes [3,4]. The complete amino acid sequence of bTP-II was determined [5], and the biological activity was shown to reside in fragment 29-41 by chemical synthesis [6]. Subsequently the pentapeptide (TP-5), corresponding to residues 32–36 of bTP-II was shown to retain the biological activity of bTP-II and thus probably corresponds to a biologically active site of the parent molecule [7].

bTP-I and bTP-II are composed of 49-amino-acid residues [3]. Then thymopoietin III (bovine splenin, bSP) was isolated from bovine spleen [8]. The only structural difference in active site between splenin and thymopoietins I and II, both of bovine origin, is the substitution of Glu^{1} for Asp at position 34. bSP and bovine splenopentin (bSp-5) corresponding to amino acids 32–36 of bSP induce both T- and B-precursors [9].

```
                1                   5                  10                  15
bTP-II      H-Pro-Glu-Phe-Leu-Glu-Asp-Pro-Ser-Val-Leu-Thr-Lys-Glu-Lys-Leu-Lys-Ser-Glu-

bSP(bTP-III) H-Pro-Glu-Phe-Leu-    -Asp-   -Ser-              -Glu-

hTP         H-Gly-Leu-Pro-         -Val-   -Ala-              -Gln-

hSP         H-Gly-Leu-Pro-Lys-     -Val-   -Ala-              -Gln-
              20                  25                  30                  35
bTP-II      Leu-Val-Ala-Asn-Asn-Val-Thr-Leu-Pro-Ala-Gly-Glu-Gln-Arg-Lys-Asp-Val-Tyr-Val-

bSP(bTP-III)              -Asn-                           -Gln-       -Glu-

hTP                       -Gly-                           -Met-       -Asp-

hSP                       -Asn-                           -Met-       -Ala-
                  40                  45                  49
bTP-II      Glu-Leu-Tyr-Leu-Gln-Ser-Leu-Thr-Ala-Leu-Lys-Arg-OH

bSP(bTP-III)                  -His-           -Leu-Lys-Arg-CH

hTP                           -His-           -Leu-His-OH

hSP                           -Ser-           -Glu-His-OH
```

Fig. 1. Complete amino acid sequences of bTP-II, bSP, hTP and hSP. Within the active site region (32–36), bTP-II and hTP are identical, but bSP and hSP differ at position 34 (Glu and Ala, respectively).

In 1987, Audhya *et al.* [10] reported the isolation of human thymopoietin (hTP) and splenin (hSP) from human thymus and spleen respectively. The complete amino acid sequences of purified hTP and hSP were determined and the two molecules were shown to be 48-amino-acid polypeptides differing at four positions [10]. The pentapeptide active site of thymopoietin (positions 32–36) is the same in hTP and bTP, but position 34 in the active site of hSP has changed from Glu in hSP to Ala in hSP.

Syntheses of fragments and fragment analogs of bTP-II

Syntheses of fragments and fragment analogs of bTP-II were described in the preceding papers [11–15]. As an example of synthetic routes for bTp-II fragments and fragment analogs, we describe here the synthesis of the octadecapeptide fragment [15] corresponding to positions 32 to 49 of the amino acid sequence of bTP-II in Fig. 2.

As illustrated in Fig. 2, amino acid derivatives bearing protecting groups, i.e., Arg(NO_2)-OBzl, Lys(Z), Z-Arg(NO_2), Glu(OBzl) and Asp(OBzl), which could be removed by treatment with hydrogen fluoride were used. Hydroxy groups of Ser, Thr and Tyr residues were not protected. The above protecting groups survive mostly intact under careful TFA treatment for removal of the Boc group, employed as temporary α-amino protecting group. As shown in Fig. 2, three peptide subunits, Boc-Gln-Ser-Leu-Thr-Ala-Leu-Lys(Z)-Arg(NO_2)-OBzl, Boc-Val-Glu-(OBzl)-Leu-Tyr-Leu-NHNH-Troc and Z-Arg(NO_2)-Lys(Z)-Asp(OBzl)-Val-Tyr-NHNH-Troc, served as building blocks for the construction of the full sequence corresponding to positions 32 to 49 of bTP-II. First, the C-terminal octapeptide, Boc-Gln-Ser-Leu-Thr-Ala-Leu-Lys(Z)-Arg(NO_2)-OBzl, was synthesized by the

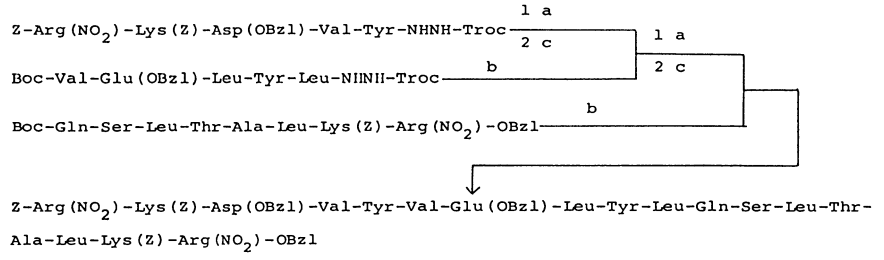

Fig. 2. Synthetic route to protected bTP-II fragment 32–49. a) Zn-AcOH; b) TFA-anisole; c) azide.

stepwise elongation method. The protected heptapeptide ester, Boc-Ser-Leu-Thr-Ala-Leu-Lys(z)-Arg(NO_2)-OBzl, was prepared stepwise by the HOBT-DCC procedure starting from Boc-Lys(Z)-Arg(NO_2)-OBzl. After the TFA-anisole treatment of Boc-Ser-Leu-Thr-Ala-Leu-Lys(Z)-Arg(NO_2)OBzl, the resulting heptapeptide ester was condensed with Boc-Gln-ONp to give the protected octapeptide, Boc-Gln-Ser-Leu-Thr-Ala-Leu-Lys(Z)-Arg(NO_2)-OBzl. Next, in order to prepare the peptide hydrazides containing Asp(OBzl) and Glu(OBzl), these two fragments were synthesized starting with Troc-$NHNH_2$. First, Boc-amino acid was condensed with Troc-$NHNH_2$ by the HOBT-DCC procedure. Then, the two fragments, Boc-Val-Glu(OBzl)-Leu-Tyr-Leu-NHNH-Troc and Arg(NO_2)-Lys(Z)-Asp(OBzl)-Val-Tyr-NHNH-Troc, were synthesized stepwise by the HOBT-DCC procedure and the Boc groups of intermediates were removed by treatment with TFA-anisole prior to the next coupling reaction.

The three fragments thus obtained were assembled successively according to Fig. 2 by Rudinger's azide procedure. The Troc group of Z-Arg(NO_2)-Lys(Z)-Asp(OBzl)-Val-Tyr-NHNH-Troc was removed by treatment with Zn dust in AcOH and DMF to give Z-Arg(NO_2)-Lys(Z)-Asp(OBzl)-Val-Tyr-$NHNH_2$. The Boc group of Boc-Val-Glu(OBzl)-Leu-Tyr-Leu-NHNH-Troc was removed by usual TFA-anisole treatment and the corresponding free base was condensed with Z-

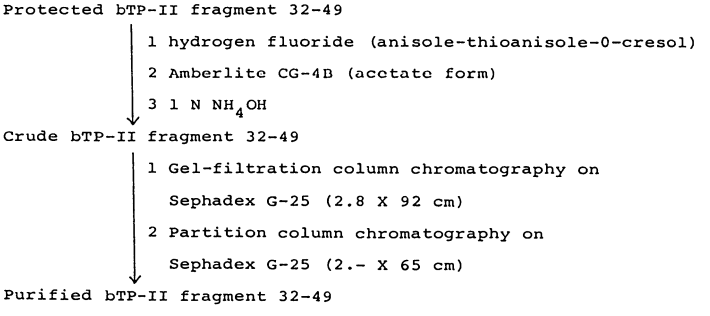

Fig. 3. Deprotection and purification of bTP-II fragment 32–49.

Arg(NO_2)-Lys(Z)-Asp(OBzl)-Val-Tyr-$NHNH_2$ by the azide procedure to yield Z-Arg(NO_2)-Lys(Z)-Asp(OBzl)-Val-Tyr-Val-Glu(OBzl)-Leu-Tyr-Leu-NHNH-Troc, which was purified by column chromatography on silica gel with DMF and MeOH (1:3). Next, after removal of the Troc group of Z-Arg(NO_2)-Lys(Z)-Asp(OBzl)-Val-Tyr-Val-Glu(OBzl)-Leu-Tyr-Leu-NHNH-Troc by treatment with Zn dust in AcOH and DMF, the resulting decapeptide hydrazide, Z-Arg(NO_2)-Lys(Z)-Asp(OBzl)-Val-Tyr-Val-Glu(OBzl)-Leu-Tyr-Leu-$NHNH_2$, was condensed with H-Gln-Ser-Leu-Thr-Ala-Leu-Lys(Z)-Arg(NO_2)-OBzl by the azide procedure to yield Z-Arg(NO_2)-Lys(Z)-Asp(OBzl)-Val-Tyr-Val-Glu(OBzl)-Leu-Tyr-Leu-Gln-Se-Leu-hr-Ala-Leu-Lys(Z)-Arg(NO_2)-OBzl, which was purified by silica gel column chromatography with BuOH and DMF (3:1).

The protected octadecapeptide ester thus obtained was treated with hydrogen fluoride, in the presence of anisole-thioanisole-o-cresol (1:1:1, V/V) to suppress side reaction of Tyr, to remove all protecting groups. The deblocked peptide was precipitated by adding dry ether, and converted to the corresponding acetate on Amberlite CG-4B (acetate form), then treated with 1 N NH_4OH at pH 10 for 30 min. The latter treatment was performed because of the reversible N $\rightarrow$ O shift at the Thr and Ser residues during the hydrogen fluoride treatment.

Finally, the product was purified by gel-filtration on Sephadex G-25 using 2% AcOH, followed by partition column chromatography on Sephadex G-25 according to Yamashiro [16]. The octadecapeptide thus obtained was found to be homogeneous by paper chromatographies in two different solvent systems. Its purity was further assessed by amino acid analyses of both hydrolysates and aminopeptidase digest. Amino acid analyses of both hydrolysates gave molar rarios in good agreement with the expected values.

Synthetic procedures for the other fragments and fragment analogs of bTP-II were also described in the preceding papers [11–14].

Effect of the synthetic peptide fragments and fragment analogs of bTP-II on low E-Rosette-forming lymphocytes of patients with cell mediated immunodeficiency

Effect of our peptides were tested on the low E-rosette-forming lymphocytes from patients with cell-mediated immunodeficiency.

Results of these synthetic peptides suggest that the Arg-residue of 32 position of bTP is required for restoring activity of low E-rosette-forming cells [11–15]. bTP-5 corresponding to amino acids 32–36 of bTP, the shortest fragment, increased the activity of E-rosette-forming cells similar to the longer chain of thymopoietin fragments including bTP-5 in their sequences [11–15].

Syntheses of bTP-I, bTP-II, bSP, hTP and [Glu^{34}]hSP

bTP-I [17], bTP-II [18], bTP-III (bSP) [19], hTP [20] and [Glu^{34}]hSP [21] were synthesized by a conventional solution method to study on immunological effect

Table 1. Effect of bTP-II fragments and fragment analogs on low E-rosette-forming cells of uremic patients with impaired cellular immunity

peptides	increasing effect on low E-rosette-forming cells[a]
1 H-Arg-Lys-Asp-Val-Tyr-OH	+ +
2 H-Lys-Asp-Val-Tyr-OH	–
3 H-Asp-Val-Tyr-OH	–
4 H-Val-Tyr-OH	–
5 H-Val-Lys-Asp-Val-Tyr-OH	–
6 H-Lys-Lys-Asp-Val-Tyr-OH	–
7 H-Arg-Lys-Glu-Val-Tyr-OH	+
8 H-Arg-Lys-Asp-Val-Tyr-OMe	–
9 H-Lys-Asp-Val-Tyr-Val-Gln-Leu-Tyr-Leu-OH	–
10 H-Arg-Lys-Asp-Val-Tyr-Val-Gln-Leu-Tyr-Leu-OH	+ +
11 H-Glu-Gln-Arg-Lys-Asp-Val-Tyr-OH	+ +
12 H-H-Val-Thr-Leu-Pro-Ala-Gly-Glu-Gln-Arg-Lys-Asp-Val-Tyr-OH	+ +
13 H-Arg-Lys-Asp-Val-Tyr-Val-Glu-Leu-Tyr-Leu-Gln-Ser-Leu-Thr-Ala-Leu-Lys-Arg-OH	+ + +

[a] + = active; + + + > + + > +; – = inactive.

on impaired T- and B-lymphocytes from uremic patients with cell-mediated immunodeficiency.

We describe here the solution synthesis of hTP (20) as an example of our solution syntheses of thymopoietin series [17–21].

Our synthetic route to hTP is illustrated in Fig. 4, which shows the ten fragments selected as building blocks to construct the entire amino acid sequence of hTP. The

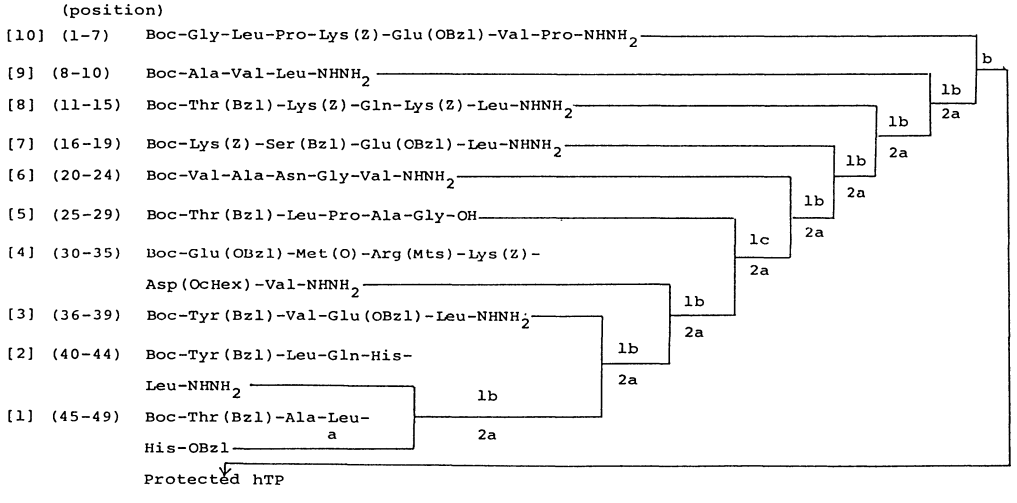

Fig. 4. Synthetic route to protected hTP. a) TFA-anisole; b) azide; c) HOSu-WSCI.

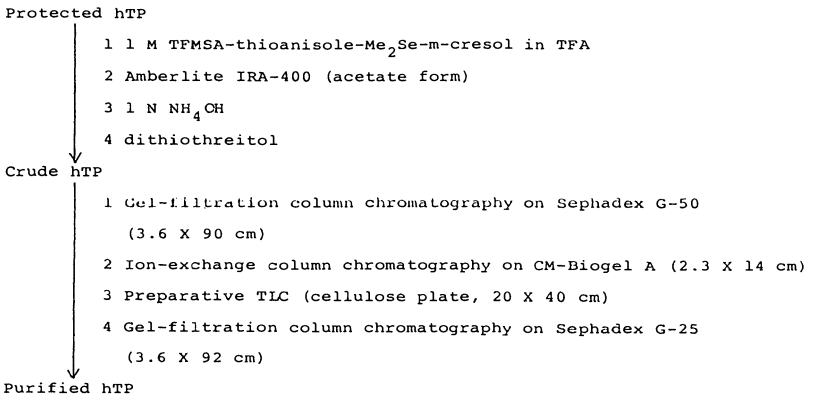

Fig. 5. Deprotection and purification of hTP.

Boc group, removable by TFA, was adopted as a temporary N^{α}-protecting group for every intermediate.

In the present synthesis, the thioanisole-mediated TFMSA deprotecting procedure was employed, i.e. Lys(Z), Glu(OBzl), Thr(Bzl), Ser(Bzl), Tyr(Bzl), Asp(OHex) and Arg(Mts). The Met residue was reversibly protected as its sulfoxide in order to prevent partial S-alkylation during the N^{α}-TFA deprotection as well as partial air oxidation during the synthesis. Asp(OcHex) was employed to minimize aspartimide formation during the synthesis of Asp-containing peptide. N^{α}-Deprotection with TFA was performed in the presence of anisole, prior to each condensation reaction as usual. The substituted hydrazine, Troc-$NHNH_2$, was employed for preparation of fragments containing the Asp(OcHex) or Glu(OBzl) residue. This Troc group is known to be cleaved by Zn in AcOH without affecting other functional groups. Throughout the syntheses of these intermediates and fragments, the purity of every fragment and intermediate was checked by TLC, elemental analysis and amino acid analysis. The ten fragments were assembled successively by the azide procedure and the HOSu-WSCI procedure according to the routes illustrated in Fig. 4. The amount of the acyl component in each fragment condensation was increased from 1.5 to 4 eq as the chain elongation proceeded. The solubility of protected intermediates in DMF decreased remarkably with chain elongation. Consequently, mixtures of DMF-DMSO had to be employed for the subsequent condensation reactions. Some of the intermediates were purified by gel-filtration on Sephadex LH-60 using DMF as the eluant. Throughout this synthesis, Ala or Gly was taken as the diagnostic amino acid in acid hydrolysis. By comparison of the recovery of Ala or Gly with those of newly incorporated amino acids, satisfactory incorporation of each fragment in each condensation reaction was confirmed. In the final step of the synthesis, the protected octatetradecapeptide ester was treated with 1 M TFMSA-thioanisole in TFA in the presence of m-cresol and Me_2Se. m-Cresol was used as an additional scavenger to suppress a side reaction i.e., O-sulfation of Tyr residues. Me_2Se was employed to facilitate acidic

cleavage of protecting groups. The deprotected peptide was next precipitated with peroxide-free ether, converted to the corresponding acetate with Amberlite IRA-400 (acetate form) and then treated with 1 N NH_4OH to reverse a possible N $\rightarrow$ O shift at Ser and Thr residues. The Met(O) residue was reduced back to Met in two steps, firstly with thioanisole and Me_2Se during the above acid treatment, and secondly with dithiothreitol during incubation of the deprotected peptide. The reduced product was purified by gel-filtration on Sephadex G-50, followed by ion-exchange column chromatography on a CM-Biogel A column with linear gradient elution using ammonium acetate buffer, followed by preparative TLC. Desalting on Sephadex G-25 gave a fluffy powder, which exhibited a single spot (ninhydrin- and Sakaguchi-positive) on TLC in two different solvent systems and on paper electrophoresis. The peptide also exhibited a single peak on HPLC. Homogeneity of the synthetic hTP was further ascertained by amino acid analysis, after 6 N HCl hydrolysis and enzymatic digestion.

The other four peptides related to thymopoietins and splenins, bTP-I [17], bTP-II [18], bSP [19] and [Glu^{34}]hSP [21] were also synthesized in the similar manner as described for the preparation of hTP [20].

Effect of the synthetic bTP-I, bTP-II, hTP and [Glu^{34}]hSP on impaired T- and B-lymphocytes of uremic patients with immunodeficiency

Immunological effect of these synthetic peptides was tested on impaired T- and B-lymphocytes from uremic patients with immunological deficiency. Results suggest that bTP-I, bTP-II and hTP which share the same active site (Arg^{32}-Lys-Asp-Val-Tyr^{36}-) within their molecules exhibited the same restoring activity on impaired T-lymphocytes of uremic patients [17,18,20]. However, the synthetic bSP which has Glu residue at position 34 in place of Asp exhibited lower activity than that of bTP-I [19]. The synthetic [Glu^{34}]hSP showed enhancing activity on the reduced percentage of B-lymphocytes of uremic patients [21]. However, the synthetic hTP had no effect on the reduced percentage of B-lymphocytes of uremic patients under the same conditions [21].

Results

A series of fragments and fragment analogs related to bTP-II were prepared [11–15]. Thymopoietin fragments which share the same active site corresponding to residues 32–36 of TP within their molecule were shown to have restoring effects on T-lymphocyte deficiency [11–15].

Our synthetic bTP-I, bTP-II and hTP which also share the same active site corresponding to residues 32–36 of TP within their molecules seemed to have restoring effects on impaired T-lymphocytes [17,18,20] However, bTP-III (bSP) which has Glu residue at position 34 instead of Asp exhibited lower activity than that of bTP-I [19].

Table 2. Effect of the synthetic bTP-I, bTP-II, bSP, hTP and [Glu^{34}]hSP on the impaired PHA stimulation of T-lymphocytes and the reduced percentage of B-lymphocytes of uremic patients

Peptides	Restoring effect on the impaired PHA stimulation of T-lymphocytes	Increasing effect on the reduced percentage of B-lymphocytes
bTP-I	active	N.D.
bTP-II	active	N.D.
bSP (bTP-III)	weak	N.D.
hTP	active	inactive
[Glu^{34}]hSP	N.D.	active

N.D.: Not done.

On the other hand, our synthetic [Glu^{34}]hSP showed restoring effect on the reduced percentage of B-lymphocytes of uremic patients [21]. However, our synthetic hTP showed no restoring effect on the reduced percentage of B-lymphocytes of uremic patients under the same conditions [21]. Other research group emphasized that bTp-III (bSP) or SP-5 acts on differentiation of B-lymphocytes [9]. These results seemed to suggest that these differences of immunological activities must be ascribed to the single amino acid substitution that distinguishes the TP-5 pentapeptide from SP-5.

References

1. Davis AJS (1969) Transplant Rev. 1: 43; Stutman O (1969) Transplant Proc. 644: 615.
2. Goldstein G (1974) Nature (London) 247: 11.
3. Basch RS and Goldstein G (1974) Proc. Natl. Acad. Sci. USA 71: 1474.
4. Basch RS and Goldstein G (1975) Ann. N.Y. Acad. Sci. 249: 290.
5. Schlesinger DH and Goldstein G (1975) Cell 5: 361.
6. Schlesinger DH, Goldstein G, Scheid MP and Boyse EA (1975) Cell 5: 367.
7. Goldstein G, Scheid MP, Boyse EA, Schlesinger DH and Van Wauwe J (1979) Science 204: 1309.
8. Audhya T, Schlesinger DH and Goldstein G (1981) Biochemistry 20: 6195.
9. Goldberg EH, Goldstein G, Haiman DB and Boyse EA (1984) Transplantation 38: 52.
10. Audhya T, Schlesinger DH and Goldstein G (1987) Biochemistry 84: 3545.
11. Abiko T, Kumikawa M and Sekino H (1979) Chem. Pharm. Bull. 27: 2233.
12. Abiko T, Onodera I and Sekino H (1980) Chem. Pharm. Bull. 28: 2507.
13. Abiko T, Onodera I and Sekino H (1981) Chem. Pharm. Bull. 29: 2322.
14. Abiko T and Sekino H (1981) Chem. Pharm. Bull. 29: 3320.
15. Abiko T and Sekino H (1982) Chem. Pharm. Bull. 30: 3271.
16. Yamashiro D (1964) Nature (London) 201: 76.
17. Abiko T and Sekino H (1985) Chem. Pharm. Bull. 33: 1583.
18. Abiko T and Sekino H (1987) Chem. Pharm. Bull. 35: 2016.
19. Abiko T, Shishido H and Sekino H (1986) Chem. Pharm. Bull. 34: 2133.
20. Abiko T and Sekino H (1988) Chem. Pharm. Bull. 36: 2506.
21. Abiko T and Sekino H (1989) Chem. Pharm. Bull. 37: 391.

Effect of L-tryptophan on the blood pressure of patients with mild to moderate essential hypertension

J. Robert Cade, Melvin J. Fregly and Malcolm Privette

Departments of Medicine and Physiology, College of Medicine, University of Florida, Gainesville, FL 32610, U.S.A.

Abstract

Seventeen patients (13 male and 4 female), ranging in age from 21 to 69 years, with mild to moderate essential hypertension were studied. Blood pressures (supine) were measured weekly for 4 weeks (control period) while the patients were off all medication. Medical histories, physical examinations, chest X-ray, liver function test, complete hemogram, urinalysis, plasma creatinine concentration, creatinine clearance, and a Zung Depression Test were carried out on each patient at the end of the control and treatment periods. Following completion of the control period, treatment with tryptophan began for 8 weeks. Because of differences in dose and schedule, it was necessary to analyze blood pressures of individuals by regression analysis (blood pressure vs dosage of tryptophan). The results indicate that 9 of 16 patients had a significant ($p<0.05$–0.01) reduction in mean arterial pressure during the 8 weeks of treatment, as assessed by a significant correlation coefficient. In these cases, blood pressure declined linearly with increasing doses of tryptophan. One patient was dropped from the study during the sixth week because of non compliance with therapy. There were no significant adverse effects of therapy. Body weight was not affected significantly by treatment. The results of this study, while of short duration and a limited number of patients, suggest that chronic treatment of mild to moderate hypertension with L-tryptophan, alone or in combination with other antihypertensive drugs, holds promise as a naturally occurring antihypertensive compound.

Introduction

Studies have been carried out in our laboratories which demonstrated that chronic dietary administration of the neutral amino acid, L-tryptophan, can attenuate the development of deoxycorticosterone acetate (DOCA)-induced, renal-induced, and spontaneous (genetic) (SHR) hypertensions in rats without significantly affecting either their food intake or body weight [1–3]. Others have shown that similar treatment attenuated the development of hypertension in Dahl salt sensitive rats [4].

Chronic treatment with tryptophan was also accompanied by an improved renal concentrating ability following a 24 h dehydration in both DOCA-and renal-induced hypertensions and by an attenuation of cardiac hypertrophy in DOCA-, renal and Dahl-induced hypertensions [2–4]. These latter effects may not be due to tryptophan per se, but may be secondary effects related to the fact that the treated animals were protected against a rise of blood pressure. In addition, we have shown that chronic treatment with L-5-hydroxytryptophan, the immediate precursor of serotonin, protects against the development of DOCA-induced hypertension [5].

Thus, there is now ample evidence to show that chronic dietary treatment with L-tryptophan provides significant protection against the development of DOCA-, renal, spontaneous and Dahl-induced hypertensions in rats.

In addition to the studies described above in which hypertensive rats were treated with tryptophan, the effect of chronic treatment with L-tryptophan on the blood pressure of 17 patients with mild to moderate essential hypertension was also studied. Lehnert and Beyer [6] recently reported a significant reduction in both systolic and diastolic blood pressures of patients with mild to moderate hypertension when treated for 3 to 4 weeks with tryptophan (50 mg/kg).

Methods

Those participating in this 8 week study were patients whose hypertension was untreated when they were referred to the clinic and whose diastolic blood pressure was greater than 90, but less than 118 mm Hg. The blood pressures of these patients were measured weekly until diastolic pressure was constant within a range of 10 mm Hg (usually within 4 weeks) (Control period). A second group of patients was also studied. The group consisted of patients on medication whose hypertension was poorly controlled; i.e., diastolic blood pressure was greater than 95 but less than 105 mm Hg. In this group of patients, all medication was stopped and they were observed at weekly intervals until their diastolic blood pressures stabilized within a 10 mm Hg range (usually within 4 weeks). Thus, a total of 17 patients (13 male and 4 female) participated in this study. Upon admission to the study, medical histories and physical examinations were carried out on each of the patients. Blood pressure was measured in the supine position after 20 minutes of rest in a dimly lighted room by means of a mercury column sphygmomanometer. The fifth Karothoff sound was used as an approximation of diastolic pressure. In addition, a chest X-ray, a liver function test, complete hemogram (including hematocrit, hemoglobin, red and white blood cell counts, differential blood cell count), urinalysis, plasma, creatinine concentration, creatinine clearance and a Zung Depression Test were carried out on each patient.

At the end of the control period, treatment with L-tryptophan began. The dosage and schedule during the first two weeks of treatment varied among the patients beginning with 0.5 g TID (1.5 g/day) in 3 patients and 0.5 g TID + hs (2.0 g/day) in 11 patients while 1 patient received 1.0 g TID (3.0 g/day) and two others received 1.0 g TID + hs (4.0 g/day). During the third through the fifth week, 4 patients received 0.5 g TID + hs; 6 received 1.0 g TID, while the remaining 6 received 1.0 g TID + hs. During the sixth through the eighth week, 4 patients received 0.5 g TID + hs while the remaining 13 patients received 1.0 g TID + hs. Each patient was seen at weekly intervals for 3 weeks to ascertain the effectiveness of the medication. Age, sex, race and other characteristics of the 17 patients participating in this study are given in Table 1.

Table 1. Some characteristics of patients participating in the study

Patient	Male or female	Race	Age (Yr)	Body Wt. (Pounds)		Initial reclining BP (mm Hg)		Response to Tryptophan Treatment[a]	
				Initial	Final	Syst.	Diast.	Syst.	Diast.
1. R.C.	M	W	45	192	193	141	97	0.09	0.76[c]
2. H.U.	M	W	65	173	175	148	94	0.22	0.17
3. S.B.	F	W	49	149	143	151	99	0.40	0.35
4. L.H.	M	W	65	189	189	155	102	0.19	0.75[c]
5. J.B.	M	W	65	195	195	140	93	0.69[b]	0.85[c]
6. D.O.	F	W	55	165	166	153	107	0.30	0.78[c]
7. S.J.	M	W	36	187	187	167	102	0.33	0.38
8. T.R.	M	W	21	151	152	141	96	0.68[b]	0.50
9. M.W.	F	B	38	165	165	134	92	0.70[c]	0.45
10. D.S.	M	W	53	160	160	196	118	0.77[c]	0.47
11. R.S.	M	W	29	178	177	152	99	0.12	0.22
12. J.J.	F	B	38	202	204	167	105	0.28	0.38
13. M.C.	M	W	54	183	184	155	93	0.39	0.55[d]
14. L.C.	M	B	30	184	190	136	96	0.28	0.18
15. C.P.	M	W	69	238	238	150	100	0.39	0.25
16. W.S.	M	B	59	158	158	175	106	0.63[b]	0.45
17. M.D.	M	W	55	155	150	158	99	0.74[c]	0.66
Mean:			49	178	178	154	100		

[a]Correlation coefficient of relationship between blood pressure and dose of tryptophan administered.
[b]Significant ($p<0.06$).
[c]Significant ($p<0.01$).
[d]Dropped from study.

Results

The results of this study show that the reclining blood pressure of the patients remained elevated and relatively constant throughout the 4 weeks they were off all drugs (Fig. 1). Since the schedule of doses differed for most patients treated with tryptophan, the data of individual patients were subjected to a regression analysis. Thus, both reclining systolic and diastolic blood pressures of J.B. (Fig. 2) decreased during the course of treatment as the dose of tryptophan increased. When a regression of reclining blood pressure (systolic and diastolic) versus dosage of tryptophan (g/day) administered was calculated, there was a significant ($p<0.05$, systolic; $p<0.01$, diastolic) correlation, with a negative slope for both diastolic and systolic blood pressures (Fig. 3) indicating that these blood pressures declined as dosage of tryptophan increased. A similar response of blood pressure to administration of tryptophan occurred in patient M.D. (Fig. 4). This patient was followed for 4 additional weeks after treatment with tryptophan ceased and no other medication was given. The average blood pressure during these four weeks is

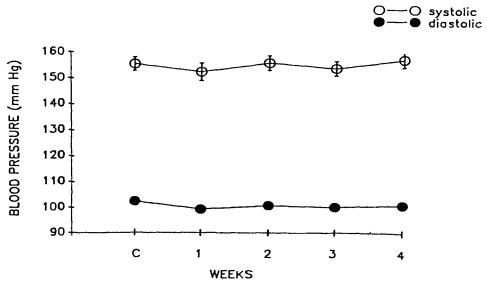

Fig. 1. Reclining systolic and diastolic blood pressures of the 17 patients during a 4 week period off all antihypertensive medications and prior to treatment with tryptophan. 'C' represents the first blood pressure measurement. Additional measurements were made at weekly intervals thereafter. One standard error is set off at each mean. Standard errors for diastolic pressures are smaller than the size of the symbols.

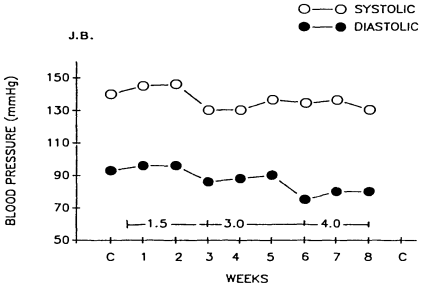

Fig. 2. Reclining systolic and diastolic blood pressures of patient J.B. prior to, and during, treatment with tryptophan. The doses (g/day) and duration of treatment with each dose are shown at the bottom of the figure. 'C' represents the mean systolic and diastolic blood pressures measured during the four week control period.

shown as the last point in the figure and is designated 'C' on the abscissa (Fig. 4). Both diastolic and systolic blood pressures increased in the absence of treatment

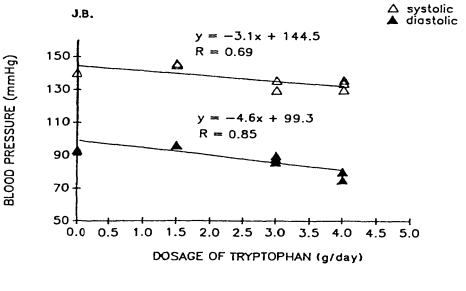

Fig. 3. Regression analysis of reclining systolic and diastolic blood pressures of patient J.B. versus dose of tryptophan administered. The equation and correlation coefficient of each regression are shown in the figure.

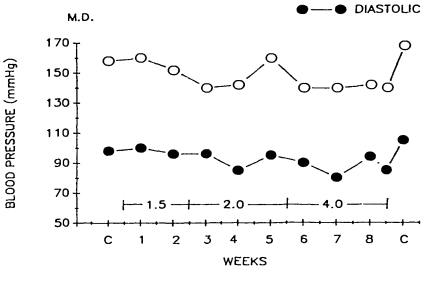

Fig. 4. Reclining systolic and diastolic blood pressures of patient M.D. prior to, and during, treatment with tryptophan. The doses (g/day) and duration of treatment with each dose are shown at the bottom of the figure. The first 'C' in the figure represents the mean systolic and diastolic blood pressures measured during the four week control period. The final 'C' represents the mean systolic and diastolic blood pressures measured during a four week period when tryptophan was withdrawn.

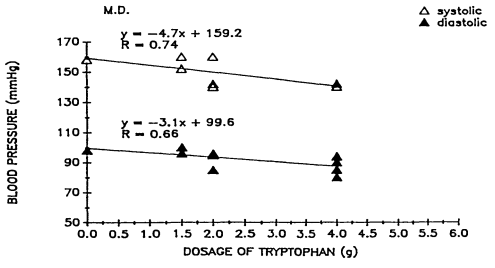

Fig. 5. Regression analysis of reclining systolic and diastolic blood pressures of patient M.D. versus dose of tryptophan administered. The equation and correlation coefficient of each regression are shown in the figure.

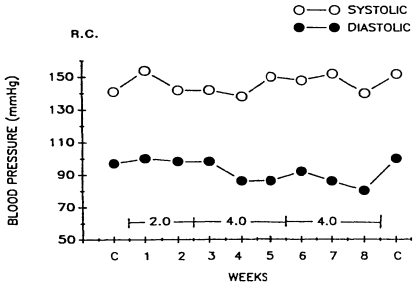

Fig. 6. Reclining systolic and diastolic blood pressures of patient R.C. prior to (first 'C'), during, and after (final 'C') treatment with tryptophan. The doses (g/day) and duration of treatment with each dose are shown at the bottom of the figure.

indicating that tryptophan had exerted an antihypertensive effect. A regression of blood pressure versus dosage of tryptophan administered is shown for this patient (M.D.) in Fig. 5. There is again a significant ($p<0.01$, systolic; $p<0.05$, diastolic; correlation between both blood pressures and daily dose of tryptophan administered. Again, the slopes of the regressions were negative, indicating that these blood pressures declined as dose of tryptophan increased.

A slightly different response was observed in patient, R.C. (Fig. 6). This patient received only two doses of tryptophan (2.0 and 4.0 g/day). As observed in Fig. 6, 2.0 g/day had no effect on blood pressure. When treated with 4.0 g/day (beginning week 3), diastolic blood pressure declined. Again, when treatment ceased and no other drugs were administered, the average blood pressure for the four weeks off drugs increased ('C' on abscissa of Fig. 6), again indicating that tryptophan had exerted an antihypertensive effect. The regression of blood pressure versus dose of

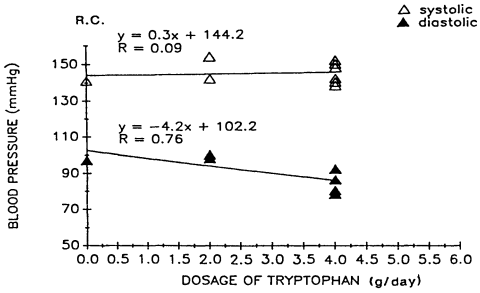

Fig. 7. Regression analysis of reclining systolic and diastolic blood pressures of patient R.C. versus dose of tryptophan administered. The equation and correlation coefficient of each regression are shown in the figure.

tryptophan (g/day) (Fig. 7) revealed a significant ($p<0.01$) correlation between diastolic blood pressure and daily dose of tryptophan. In contrast, systolic blood pressure was unaffected. Since the diastolic blood pressure reflects peripheral vascular resistance (an increase of which is the primary cause of hypertension), the significant decline in diastolic blood pressure with increasing dose of tryptophan is physiologically and medically significant since it signifies a reduction peripheral vascular resistance.

Although the data for only three of the 17 treated patients are given here for brevity of discussion, it can be stated that 9 of the 16 patients treated with tryptophan had a significant ($p<0.05$–<0.01) decrease in mean arterial blood pressure during the 8 weeks of treatment (Table 1). One patient was dropped from the study during the sixth week because of non compliance with therapy. Two additional patients were partially responsive [correlation coefficients of the relationship between blood pressure (systolic and diastolic) versus dose of tryptophan = 0.40 to 0.60, and six (correlation coefficients = 0.10 to 0.39), including the non-compliant patient, were unresponsive.

There were no significant adverse effects of therapy. Liver function tests (including SGOT, SGPT, alkaline phosphatase, total and indirect bilirubin and serum albumin) during treatment were unchanged from those made prior to treatment in all patients. Comparison of chest X-rays taken before administration of tryptophan with those taken after 7 to 8 weeks of treatment showed no change in either lungs or heart. Routine urine analysis, plasma creatinine concentration and creatinine clearance were also unaffected by treatment with tryptophan. Body weight was not affected significantly by treatment (Table 1).

Discussion

The results of these studies are of considerable interest since they reveal that humans with mild to moderate hypertension of unknown etiology may benefit from chronic treatment with tryptophan. In this respect, the rat appears to be a good model for the human since hypertension was also attenuated in these animals by chronic dietary treatment with tryptophan. Of additional importance is the fact that tryptophan is a naturally occurring compound which had no significant side effects at the doses used. Thus, tryptophan would appear to provide an important option to treat patients with mild to moderate hypertension without subjecting them to the undesirable side effects inherent in most of the currently used antihypertensive drugs.

A question naturally arises regarding potential mechanisms by which tryptophan exerts its antihypertensive effect. In the case of the rat, studies carried out in our laboratories showed that chronic infusion with L-5-hydroxytryptophan prevented the development of DOCA-induced hypertension [5]. Since L-5-hydroxytryptophan is the immediate precursor of serotonin (5-HT) and cannot be converted to tryptophan, it may be assumed that increased formation of either serotonin or its metabolites mediates the antihypertensive properties of both tryptophan and L-5-

hydroxytryptophan. Indeed, studies carried out in our laboratories showed an increased turnover of serotonin in the brains of rats treated chronically with tryptophan [2]. In addition, recent evidence suggests that centrally produced serotonin may stimulate serotonergic receptors on spinal catecholaminergic neurons located in the descending bulbospinal pathways to induce vasodilation of peripheral resistance vessels and reduction of blood pressure [7]. An additional possibility suggested by the recent publication of Teichberg *et al.* [8] is that tryptophan can inhibit the transport of sodium across the wall of the gut. This could limit the amount of sodium absorbed and thus, in part at least, mediate the antihypertensive effect of tryptophan. This possibility requires testing.

Reduction of blood pressure was not the result of a loss in body weight of the patients (Table 1). We did not measure the cardiac output of any of the patients and cannot state whether a reduction in cardiac output may have played a role in the reduction of blood pressure.

It is difficult to state reasons for the failure of 6 of the patients to respond to treatment with tryptophan. Several of them manifested an unusual amount of nervousness and anxiety. Although we do not at present have evidence to associate anxiety with failure to respond, we are currently measuring urinary catecholamines of patients treated with tryptophan to assess this possibility in our second ongoing clinical trial.

While we have not tested whether patients with more severe hypertension would benefit from treatment with tryptophan, a clinical trial in which tryptophan is administered alone, and in combination with other selected antihypertensive drugs, is planned.

References

1. Fregly MJ and Fater DC (1986) Clin. Exp. Physiol. Pharmacol. 13: 767–776.
2. Fregly MJ, Lockley OE, van der Voort J, Sumners C and Henley WN (1987) Can. J. Physiol. Pharmacol. 65: 753–764.
3. Fregly MJ, Sumners C and Cade JR (1989) Can. J. Physiol. Pharmacol. 67: 656–662.
4. Lark L, Witt P, Becker K, Studzinski W and Weyhenmeyer JA (1988) Neurosci. Abst. 14: 974.
5. Fregly MJ, Lockley OE and Sumners C (1987) J. Hypertension. 5: 621–628.
6. Lehnert H and Beyer J (1989) Proc. Int. Study Group For Tryptophan Research, ISTRY '89. Baltimore, MD, p. S39.
7. Ramirez AJ, Giarcovich SS and Enero MA (1986) J. Hypertension 4(Suppl. 1): S47–S49.
8. Teichberg S, Wapnir RA, Zdanowicz M, Roberts B, Ribeiro H.DaC. Jr. and Lifshitz F (1989) Lab. Invest. 60: 88–101.

Address for correspondence: Dr. Melvin J. Fregly, Department of Physiology, Box J274, University of Florida, College of Medicine, Gainesville, FL 32610, U.S.A.

Excitatory amino acid antagonists and memory: Effect of drugs acting at *N*- methyl-D-aspartate receptors in learning and memory tasks*

Jolanta Parada-Turska and Waldemar A. Turski

Department of Pharmacology, Medical School, Jaczewskiego 8, PL-20090 Lublin, Poland

Abstract

The role of *N*-methyl-D-aspartate (NMDA) receptors in memory processes was examined using Y-shaped maze and step-through passive avoidance task in mice. In the Y-maze, the total number of arm entries which represents locomotor activity, and alternation behavior thought to reflect working memory, were measured. CGS 19755 (*cis*-4-phosphonomethyl-2-piperidine-carboxylate) and CPP (3-((±)-2-carboxy-piperazin-4-yl)-propyl-1-phosphate), competitive NMDA antagonists, influenced neither locomotion nor spontaneous alternation of mice. In contrast, non-competitive NMDA antagonist MK-801 ((+)-5-methyl-10,11-dihydro-5H-dibenzo(a,d)cycloheptan-5,10-imine maleate) dramatically enhanced the total number of arm entries and reduced alternation behavior. NMDA had no effect on MK-801-induced enhancement of locomotor activity and impairment of alternation. These results suggest that NMDA dependent processes are not preferentially involved in the mechanisms of working memory.

In the passive avoidance task, mice were trained to avoid dark compartment entry. CPP, CGS 19755 and MK-801 reduced acquisition when administered before training. NMDA antagonized the effect of CPP, CGS 19755 and MK-801. CPP and MK-801 did not affect retention when administered immediately after training or before retention testing. NMDA had no effect on retention at high-intensity shock, but facilitated retention at low-intensity shock.

These findings suggest that NMDA antagonists may impair learning (storage) but have little or no effect on recall (retrieval) from long-term memory. Working memory appears to be unaffected by treatment with NMDA antagonists. NMDA may enhance animal performance in passive avoidance task.

Introduction

With the advent of compounds selectively blocking neurotransmission mediated by L-glutamate the question of their therapeutic use in clinical neurology has been raised repeatedly [1]. Preferential *N*-methyl-D-aspartate (NMDA) antagonists were detected to have neuroprotective, anticonvulsant, anxiolytic and muscle relaxant actions [2–7]. Such perspectives offer new therapeutic principles to treatment of stroke, epilepsy, anxiety and spasticity [8]. However, activation of NMDA receptors is also believed to be required for induction of long-term potentiation (LTP) which underlies information storage in the brain and may be critical for learning and memory [9,10]. Interference of excitatory amino acid (EAA) antagonists with such processes could disqualify their use in humans except in life-threatening situations [8].

* This research was supported by project grant from the Polish Academy of Sciences.

The purpose of this study was therefore to extend our knowledge of action of preferential antagonists at NMDA receptors in two animal models used to investigate learning and memory. CPP and CGS 19755 were used as representatives of competitive NMDA antagonists and MK-801 as a non-competitive NMDA antagonist [11–13]. The first model used, spontaneous alternation of mice in an Y-shaped maze, is regarded as a measure involving spatial working memory [14,15]. The second model employed, a step-through passive avoidance task, may give information about acquisition (learning) and recall (retrieval) which are components of long-term memory [16].

Materials and Methods

Animals

The experimental subjects were male albino Swiss S mice, 18–22 g in weight. The mice were maintained on a standard light-dark cycle with free access to chow pellets and water. The assignment of mice to experimental groups was random. Experimental groups consisted of 6–12 animals.

Spontaneous alternation in a Y-shaped maze

The mice were individually placed in the Y-maze (three compartments of $10 \times 10 \times 10$ cm) for 8 min. The total number of arm entries (locomotor activity) and the alternation behavior (defined as consecutive entries into all three arms without repetitions) expressed as percentage of the total arm entries were scored. Following each trial, the maze was placed on a new sheet of paper. In the Y-maze, mice tend to explore the maze systematically, entering each arm in turn [14,15]. The ability to alternate requires the mice to know which arms have already been visited. Therefore alternation behavior can be regarded as a measure involving spatial working memory [17].

Step-through passive avoidance task

The mice were placed in an illuminated box ($10 \times 13 \times 15$ cm) connected to a large dark box ($25 \times 20 \times 15$ cm) which was equipped with an electric grid floor. Entrance into the dark box was punished by an electric footshock (0.6 mA for 2 s; unscrambled DC current; impairment of acquisition or 0.1 mA for 2 s; facilitation of acquisition). On the next day (24 h), the same mice were placed in the illuminated box. Mice avoiding the dark compartment for over 60 s were considered as remembering the task. The retention was quantified as percentage of animals avoiding the dark compartment. The step-through passive avoidance task may give information about ability to acquire the task (learning) and to recall the task (retrieval) and may be regarded as a measure involving long-term memory [16].

Administration of test drugs before training may disrupt or improve learning by affecting acquisition and/or recall. Administration of test drugs immediately after training or before retention test may affect recall [16].

Drugs

N-Methyl-D-aspartic acid (NMDA), D-(-)-2-amino-7-phosphonoheptanoic acid (AP7), 3-((±)-2-carboxypiperazin-4-yl)-propyl-1-phosphonic acid (CPP), were obtained from Tocris (Buckhurst Hill, Essex, U.K.). (+)-5-Methyl-10,11-dihydro-5H-dibenzo(a,d)cycloheptan-5,10-imine maleate (MK-801) was obtained from Merck Sharp and Dohme (Harlow, Essex, U.K.). The drugs were brought into solution with a minimum quantity of 1 N NaOH and the final volume was made up with saline, with the pH being adjusted to 7.35 by adding 0.2 N HCl.

The performance of animals in the Y-shaped maze was measured 30 min after i.p. administration of drugs tested. The effect of drugs on acquisition of step-through passive avoidance task was assessed when training was performed 30 min after i.p. administration. The effect on recall was assessed when drugs were administered i.p. 30 min before retention test or immediately after the training.

Statistics

The analysis of the data was performed by means of the Student's t-test or χ^2-test.

Results

Y-Maze

The competitive antagonists at NMDA subtype of L-glutamate receptors, CGS 19755 and CPP, reduced locomotor activity of mice in the Y-maze (Table 1). In doses, which do not depress the locomotor activity both NMDA antagonists had no effect on alternation behavior (Table 1). High-dose treatment with CGS 19755 (4 mg/kg) and CPP (5 mg/kg) induced both sedation and impairment of alternation (Table 1).

The non-competitive NMDA antagonist MK-801 dose-dependently increased locomotor activity of mice (measured as a total number of arm entries) and impaired their alternation behavior in the Y-maze in doses ranging from 0.05–0.2 mg/kg (Table 1). At the dose of 0.4 mg/kg MK-801 induced severe ataxia which led to a reduction of locomotor activity and significant impairment of alternation (Table 1).

NMDA in doses of 10, 25 and 50 mg/kg had no effect on locomotor activity and alternation behavior (Table 1).

Table 1. Effect of NMDA and NMDA antagonists on spontaneous alternation behavior and total arm entries in an Y-shaped maze. Male albino Swiss S mice, 18–22 g in weight, were individually placed in the Y-maze for 8 min. The total number of arm entries (locomotor activity) and the alternation behavior (defined as consecutive entries into all three arms without repetition) expressed as percentage of the total arm entries were scored 30 min after i.p. administration of drugs tested. For antagonism testing, NMDA and respective antagonists were administered i.p. 30 min before the experiment

Treatment (mg/kg)	N	Total arm entries x ± SD	Alternation x ± SD
Solvent	9	35.4 ± 7.9	62.2 ± 9.2
CGS 19755			
1	8	38.5 ± 11.8	52.4 ± 8.1
2	7	28.6 ± 6.1	57.1 ± 10.0
4	8	20.4 ± 5.0[a]	47.2 ± 13.2[a]
CPP			
0.5	9	33.9 ± 11.8	62.6 ± 10.1
1	8	22.9 ± 8.7	61.7 ± 10.9
2.5	9	19.6 ± 5.9[b]	62.9 ± 6.2
5	8	19.3 ± 6.6[b]	46.0 ± 4.7[c]
MK-801			
0.05	7	36.6 ± 4.5	51.4 ± 11.0
0.1	8	51.0 ± 6.7[c]	43.2 ± 5.0[c]
0.2	9	76.7 ± 27.3[c]	42.4 ± 9.1[c]
0.4	6	22.8 ± 9.0	46.2 ± 11.1[a]
NMDA			
10	10	32.2 ± 10.6	60.0 ± 8.3
25	10	27.1 ± 8.0	60.8 ± 8.4
50	8	27.8 ± 11.2	60.1 ± 8.6
NMDA 50 + CGS 19755 4	11	25.5 ± 7.1	57.0 ± 8.6
NMDA 50 + CPP 5	7	25.1 ± 4.7	58.6 ± 6.4
NMDA 50 + MK-801 0.1	12	52.1 ± 12.5[c]	49.4 ± 9.2[b]

N = number of animals.
[a]$P<0.05$; [b]$P<0.01$ and [c]$P<0.001$ versus respective control values (Student's t-test).

Sedation and impairment of alternation induced by CGS 19755 (4 mg/kg) and CPP (5 mg/kg) were both antagonized by pre-treatment with NMDA (50 mg/kg) (Table 1). In contrast, NMDA (50 mg/kg) had no effect on increase in the locomotor activity and impairment of alternation in mice subjected to medium dose of MK-801 (0.1 mg/kg) (Table 1).

Table 2. Effect of CGS 19755, CPP, MK-801 and NMDA on retention of a passive avoidance task in mice. Male albino Swiss S mice, 18–22 g in weight, were individually placed in an illuminated box (10 × 13 × 15 cm) connected to a large dark box (25 × 20 × 15 cm) which was equipped with an electric grid floor. Entrance into the dark box was punished by an electric footshock (0.6 mA for 2 s). On the next day (24 h), the same mice were placed in the illuminated box. Mice avoiding the dark compartment for over 60 s were considered as remembering the task. The retention was quantified as percentage of animals avoiding the dark compartment. The effect of drugs on acquisition of step-through passive avoidance task was assessed when training was performed 30 min after i.p. administration

Treatment (mg/kg)		N	Latency to enter the dark box x ± SD (s)	Retention %
Solvent		12	12.5 ± 2.9	100
CGS 19755				
1		12	16.2 ± 7.6	91.7
2		12	17.5 ± 4.8	83.3
4		12	22.6 ± 8.5	58.3[a]
CPP				
1		12	18.1 ± 2.7	100
2.5		12	19.2 ± 6.7	91.3
5		12	19.6 ± 5.3	33.3[a]
MK-801				
0.05		12	22.0 ± 8.5	91.7
0.1		12	10.8 ± 3.7	58.3*
0.2		12	13.4 ± 3.3	8.3*
NMDA				
50		10	15.8 ± 4.0	100
NMDA	50			
+ CGS 19755	4	10	19.7 ± 5.4	90
NMDA	50		19.5 ± 7.7	100
+ CPP	5	12		
NMDA	50		11.3 ± 2.8	88.9
+ MK-801	0.1	9		
NMDA	50		17.4 ± 7.4	66.7
+ MK-801	0.2	12		

N = number of animals.
[a]$P<0.05$ versus respective control values (χ^2 test).

Table 3. Effect of CPP and MK-801 on retention of a passive avoidance task in mice. The effect of drugs on recall (retrieval) of step-through passive avoidance task was assessed when drugs were administered i.p. 30 min before retention test (24 h after training) or immediately after the training. For further details cf. Table 2

Treatment (mg/kg)	N	Latency to enter the dark box x ± SD (s)	Retention %
30 min before retention test			
Solvent	12	11.4 ± 2.7	100
CPP 5	12	15.4 ± 3.9	91.2
MK-801 0.2	12	13.0 ± 4.0	83.3
Immediately after training			
Solvent	12	13.2 ± 3.8	100
CPP 5	12	13.4 ± 4.3	100
MK-801 0.2	12	10.8 ± 2.6	100

N = number of animals.
[a]$P<0.05$ versus respective control values (χ^2 test).

Step-through passive avoidance

The acquisition of passive avoidance task measured with high-intensity shock was impaired by treatment with CGS 19755 (4 mg/kg), CPP (5 mg/kg) and MK-801 (0.1 and 0.2 mg/kg) 30 min before training (Table 2). Measurement of latencies to enter the dark box showed no effect of NMDA antagonists in this paradigm (Table 2). NMDA (50 mg/kg) affected neither latency to enter the dark box nor retention in mice subjected to high-intensity shock (Table 2). The impairment of retention induced by CGS 19755 (4 mg/kg), CPP (5 mg/kg) and MK-801 (0.1 and 0.2 mg/kg) was reversed by NMDA (50 mg/kg) (Table 2).

Administration of CPP (5 mg/kg) or MK-801 (0.2 mg/kg) 30 min before retention test or immediately after training had no effect on retention (Table 3).

Decrease in the shock-intensity reduced retention in a dose-related manner (Table 4). At 0.1 mA the retention reached only 16.7% (Table 4). In mice subjected to such low-intensity shock pretreatment with NMDA (50 mg/kg) 30 min before training considerably increased retention (Table 4).

Discussion

Analysis of action of NMDA-type of excitatory amino acid antagonists shows that compounds classified as competitive antagonists, CPP and CGS 17955, do not affect working memory in mice behaving in the Y-shaped maze. At dosages which do not affect motor behavior neither alternation nor activity of mice were affected. The non-competitive NMDA antagonist MK-801 increased locomotor activity of mice and reduced alternation behavior under similar experimental conditions. At

Table 4. Facilitation of retention of a passive avoidance task in mice by NMDA. The effect of NMDA on acquisition of step-through passive avoidance task was assessed when the drug was administered i.p. 30 min after the training. Entrance into the dark box was punished by a low-intensity shock (0.1 mA for 2 s)

Treatment (mg/kg)	N	Latency to enter the dark box x ± SD (s)	Retention %
Solvent			
0.6 mA	12	12.5 ± 2.9	100
0.4 mA	12	14.6 ± 4.1	83.3
0.1 mA	12	14.4 ± 3.8	16.7[a]
NMDA			
50; 0.1 mA	12	20.6 ± 7.5	47.1[b]

N = number of animals.
[a]$P<0.05$ versus control group punished with shock intensity of 0.6 mA for 2 s (x^2 test).
[b]$P<0.05$ versus control group punished with shock intensity of 0.1 mA for 2 s (x^2 test).

dosages which induced ataxia both types of antagonists reduced locomotor activity of mice.

The impairment of spatial working memory induced by MK-801 was resistant to treatment with NMDA although NMDA blocked motor impairment and decrease of locomotor activity induced by CPP and CGS 17955. NMDA had no effect on locomotor activity and alternation behavior in mice.

Our observations of action of non-competitive NMDA antagonists in the Y-shaped maze are similar to those reported by Morris and coworkers [18] in rats using the open field water-maze. In this experimental paradigm rats learned to search for the hidden platform and difference in the escape latency between the first and second trial of each day served as a measure of spatial working memory [18]. The administration of D-AP5 into the lateral ventricle did not impair working memory as measured by the duration of escape latency [18]. These findings indicate that working memory remains unaffected by compounds acting as competitive antagonists at NMDA receptors.

The impairment of spontaneous alternation behavior by MK-801 shows similarity to that induced by scopolamine in the Y-shaped maze. It is not clear at present which mechanism is responsible for the action of MK-801 on working memory. MK-801 has several actions apart from non-competitive blockade of NMDA receptors which include sympathomimetic properties and some interaction with benzodiazepine receptors [19]. We do not know at present to what extent such properties contribute to the observed effect of MK-801 on the spontaneous alternation in mice.

In the step-through passive avoidance task, in mice subjected to drug treatment prior to the training, impairment of retention was induced by both competitive and non-competitive NMDA receptor antagonists at dosages which did not impair motor performance. Post-training treatment with both types of antagonists had no

effect on retention. These findings may be therefore interpreted in terms of NMDA antagonists impairing learning performance (acquisition) and having little or no effect on retrieval (longterm memory). Administration of NMDA in mice subjected to low-intensity shock facilitated acquisition of the task. This finding may mean that NMDA or drugs increasing NMDA mediated transmission facilitate learning.

An impairment of learning performance in the water-maze by the competitive antagonist D-AP5 has been previously reported by Morris *et al.* [10]. In this study however D-AP5 did not affect visual discrimination learning [10]. MK-801 was also recently shown to impair learning in another passive avoidance paradigm [20]. On the other hand, Fagg *et al.* [21] showed that action of NMDA antagonists on learning is task-dependent. Similar to our experiments, this group observed impairment of learning performance in the water- and radial-maze in gerbils, and in dark-avoidance tasks in mice [21]. An enhanced retention was seen in the step-through shock-avoidance in mice [21].

In olfactory discrimination task in rats treated with D-AP5 the learning of low-intensity odors and long delays between trials (acquisition) was retarded, while retention of odors learned before the treatment remained intact [22]. In one-way active avoidance procedure D-AP5 rather facilitated than retarded acquisition of the task [22].

In summary, NMDA receptor antagonists disrupt acquisition but not recall of a step-through avoidance task. This may suggest that retrieval from long-term memory is left intact under treatment with NMDA antagonists, while learning (storage) may be affected. This observation is substantiated by beneficial effect of NMDA on acquisition of a step-through avoidance task. Since spontaneous alternation in the Y-shaped maze remains unchanged under treatment with competitive NMDA antagonists, we suggest that working memory was not altered.

An impairment of spontaneous alternation in Y-shaped maze by non-competitive NMDA antagonist MK-801 (by mechanism which is at present unclear), which may indicate disruption of working memory, may be used as a simple model to test ability of drugs to antagonize amnesia.

References

1. Meldrum BS (1985) Clin. Sci. 68: 113–122.
2. Simon RP, Swan JH, Griffith T and Meldrum BS (1984) Science 226: 850–852.
3. Wieloch T (1985) Science 230: 681–683.
4. Croucher MJ, Collins JF and Meldrum BS (1982) Science 216: 899–901.
5. Stephens DN, Meldrum BS, Weidmann R, Schneider C, Grützner M (1986) Psychopharmacology 90: 166–169.
6. Bennett DA and Amrick CL (1986) Life Sci. 39: 2455–2465.
7. Turski L, Schwarz M, Turski W, Klockgether T, Sontag K-H and Collins JF (1985) Neurosci. Lett. 53: 321–326.
8. Olney JW (1988) In: (Cavalheiro EA, Lehmann J and Turski L (eds.) Frontiers in Excitatory Amino Acid Research. Alan R. Liss, New York, pp. 589–596.

9. Artola A and Singer W (1987) Nature (Lond.) 330: 649–652.
10. Morris RGM, Anderson E, Lynch GS and Baudry M (1986) Nature (Lond.) 319: 774–776.
11. Lehmann J, Schneider J, McPherson S, Murphy DE, Bernard F, Tsai C, Bennett DA, Pastor G, Steel DJ, Boehm C, Cheney DL, Liebman JM, Williams M, and Wood PL (1987) J. Pharmacol. Exp. Ther. 240: 737–746.
12. Lehmann J, Hutchinson AJ, McPherson SE, Mondadori C, Schmutz M, Sinton CM, Tsai C, Murphy DE, Steel DJ, Williams M, Cheney DL and Wood PL (1988) J. Pharmacol. Exp. Ther. 246: 65–75.
13. Wong EHF, Kemp JA, Priestley T, Knight AR and Woodruff GN (1986) Proc. Natl. Acad. Sci. USA 83: 7104–7108.
14. Anisman H (1975) Pharmacol. Biochem. Behav. 3: 613–618.
15. Douglas RS and Isaacson RL (1965) Psychol. Rep. 16: 87–92.
16. Venault P, Chapouthier G, Prado de Carvalho L, Simiand J, Morre M, Dodd RH and Rossier J (1986) Nature (Lond.) 321: 864–866.
17. Sarter M, Bodewitz G and Stephens DN (1988) Psychopharmacology 94: 491–495.
18. Davies S, Butcher SP, Morris RGM (1988) In: Cavalheiro EA, Lehmann J and Turski L (eds.) Frontiers in Excitatory Amino Acid Research. Alan R. Liss, New York, pp. 385–392.
19. Clineschmidt BV, Martin GE and Bunting PR (1982) Drug Dev. Res. 2: 123–134.
20. Benvenga MJ and Spaulding TC (1988) Pharmacol. Biochem. Behav. 30: 205–207.
21. Mondadori C, Weiskrantz L, Buerki H, Petschke F and Fagg GE (1989) Exp. Brain Res. 75: 449–456.
22. Staubli U, Thibault O, DiLorenzo M and Lynch G (1989) Behav. Neurosci. 103: 54–60.

Section IV
Metabolism

A brief preliminary analysis of the biochemical data from patients who have attempted suicide

Elizabeth F. Marshall[a], F. Hassanyeh[a], S. Wright-Honari[a] and C.H. Ashton[b]

Departments of [a]Psychiatry and [b]Pharmacology, University of Newcastle upon Tyne, Newcastle upon Tyne, U.K.

Abstract

1. Part of a comprehensive survey, including biochemical, physiological and psychiatric assessment of patients who have attempted suicide – with a view to identifying repeat markers. Preliminary analysis of biochemical data obtained from 27 patients.
2. Twentytwo percent [6] of the sample attempted suicide again within eighteen months.
3. When all the data was examined there were no significant differences in any of the markers of serotonergic function between patients who repeated and those who did not repeat self-harm.
4. If the patients are classified according to their RDC rating, those suffering from major depression who repeated a suicide attempt had significantly lower plasma TRY and a lower ratio of TRY to HIAA.

Introduction

Self-poisoning has been defined as the intentional taking of a substance knowing it to be both excessive and potentially harmful [3]. Ten percent of routine medical admissions and up to 20% of emergency admissions are due to self-poisoning. In numerical terms, this constitutes upwards of 2,000 cases of self-poisoning a week in England and Wales, and involves considerable hospital costs [8]. Twenty percent of self-poisoners repeat their act within a year and 1–2% die as a result of suicide during that time, rising to 10% in subsequent years [9].

Prevention of suicide is believed to be potentially feasible in view of the number of suicides and attempted suicides consulting helping agencies shortly prior to their act [6]. Over 50% of self-poisoners and a similar percentage of suicides [11] make such contact with general medical services, with one third also seeing psychiatrists [1,10]. Yet, despite this apparent potential for intervention, the helping services have made little or no impact on the follow-up rates of suicide and attempted suicide.

A recent study of self-poisoning in Newcastle [7] reveals that 27% of these patients repeated their self-poisoning within 18 months and 2% committed suicide. None of the large number of clinical (psychiatric diagnosis, levels of depression, severity of self-poisoning act) and social variables noted at the original interview differentiated the repeaters from the non-repeaters. Thus a strategy aimed at

reducing the toll of suicide and self-poisoning must more accurately identify those who are at risk.

This presentation is part of a wider comprehensive study of biochemical, electrophysiological and psychiatric assessment of patients attempting suicide, aimed at determining factors predicting risk of repeated attempts to self-harm. It represents a brief preliminary analysis of the biochemical data in relation to the patient rating according to the research diagnostic questionnaire [12]. It does not anticipate or prejudice the final analyses, as blood samples are code-labelled on submission to the laboratory and biochemists and technicians remain blind to the assessment of the psychiatrist.

Methods

Patient samples

The subjects were 27 consecutive admissions (15 males, 12 females), who attempted suicide. They all met the exclusion criteria, which are that they should not have taken any substance known to interfere with the electrophysiological or biochemical measures included in this study. No patient was excluded on the grounds of diagnosis. The demographic details are presented in Table 1.

Clinical ratings

Patients were rated after completing the Research Diagnostic Questionnaire, and were assessed by the Montgomery Asberg Depression rating scale. The patients were interviewed initially within a few days of their attempted suicide and again within six weeks. Confirmation of repeated attempts to commit suicide were made through the General Practitioner.

Table 1. Details on patient sample

	Total		Male		Female	
	N	Age	N	Age	N	Age
Total	27 (16)	30 ± 5	15 (8)	37 ± 2	12 (8)	21 ± 3[a]
Repeat attempt	6 (5)	33 ± 4	5 (4)	35 ± 3	1 (1)	23
RDC classification						
Major depression	7/2 (3)	36 ± 5	4/1 (2)	40 ± 5	3/1 (1)	30 ± 4
Other disorder	13/4 (10)	31 ± 4	9/4 (6)	38 ± 3	4/0 (4)	18 ± 5[a]
No disorder	7/0 (3)	22 ± 5[a]	2/0 (0)	31 ± 5	5/0 (3)	19 ± 3

[a]$P<0.01$ v. male or v. major depression. For N_1/N_2 (N_3) N_1 = Total number in group, N_2 Number in the group who attempted repeat suicide and N_3 = Number in the group who have made a second visit. Age is the age (in years) for the total number in the group ± S.E.M.

Biochemistry

Blood was collected on the occasion of each interview. Aliquots of whole blood were taken for measures of 5HT [5] and MAO by a modification of the method of Campbell *et al.* [2]. Plasma samples were prepared for the measurement of tryptophan [5], 5-hydroxyindoleacetic acid and homovanillic acid [13], using high performance liquid chromatography with electrochemical detection.

Statistical analysis

The student t-test for significance of differences between mean values was adopted.

Results

The details of the patient sample are presented in Table 1. Of the twenty-seven patients assessed, six (22%) repeated an attempt at suicide, of whom five were men. This apparently high proportion of males in the repeat group was not significantly different from that in the total group. The males were significantly older than the females and where it was possible to carry out a statistical analysis this was true also for the patients having an RDC of major or other depression. However, no correlation of any of the biochemical parameters with age could be identified in this study.

The patients were tested on two occasions, if they agreed to return. The correlation for the biochemical parameters in the group of patients who visited twice is presented in Table 2. 5HT and TRY correlated strongly and 5HIAA and HVA did not. The full significance of these correlations will not become obvious until the study has accumulated a larger total and a larger number of repeat suicide attempts.

In Table 3 are detailed the mean values for the serotonin parameters according to whether they made a repeat attempt. They are subdivided according to their RDC rating. From Table 3, it is evident that for the group of patients classified as suffering from major depression, there were large differences in the levels of biochemical compounds between patients repeating or not repeating suicide at-

Table 2. Correlation (r) for biochemical parameters at visit A against visit B

	r.	N	P
5HT	0.73	12	<0.005
5-HIAA	–0.10	14	n.s
TRY	0.73	12	<0.005
HVA	–0.02	14	n.s.
MAO	0.29	14	n.s

N = Sample number; P = Significance of r.

Table 3. Measures of serotonin metabolism in patients attempting suicide, when values from two visits were included

	Major depression		Other disorder		No disorder	
	Repeat	No repeat	Repeat	No repeat	Repeat	No repeat
HT	261.9±191.2(4)	63.9±44.3(6)	101.6±54.5(6)	105.5±54.5(10)		107.6±45.0(10)
HIAA	7.3±3.4	3.8±3.1	12.0±16.1	8.3±14.9(12)	3.00(1)	7.3±8.2
TRY	5.5±2.5	10.0±2.5[b]	13.8±4.5	12.4±4.0(10)		10.8±3.1
HVA	10.8±7.5	5.6±1.6	6.9±4.2	6.3±2.9(12)	5.22	9.8±6.7
MAO	4.6±4.4	10.7±5.0[c]	6.2±3.5	6.7±4.2(12)	5.26	6.0±3.0
TRY/ HIAA	0.8±0.2	3.5±1.6[a]	3.0±3.4	3.2±2.2(10)		2.3±1.2

Values for HT, HIAA, HVA, represent μg/l and for TRY, mg/l ± S.E.M.
Values for MAO represent nmole phenylethylamine oxidised/ml blood/h ± S.E.M.
Numbers in brackets represent sample size.
[a]$P<0.02$ against repeat; [b]$P<0.05$ against repeat; [c]$P<0.1$ against repeat.

tempts. In the former group of patients, there are significantly lower values of TRY and in the ratio of TRY to HIAA. There is also a tendency for the monoamine oxidase values to be lower. However, these data include values obtained at both visits, and may over-emphasise the differences where there is a good correlation between first and second visits and envelop the differences where there is not. If the data from only the first visit is examined, the sample size becomes too small for statistical analysis to be applied. Nevertheless, the same tendencies can be noted as in Table 4.

Discussion

Of the patients in this study, the proportion who attempted suicide again within eighteen months compares well with that observed in a previous study [7]. Five of

Table 4. Measures of serotonin metabolism at the first visit of patients attempting suicide

	Major depression		Other disorder		No disorder	
	Repeat	No repeat	Repeat	No repeat	Repeat	No repeat
HT	209.9(2)	64.0±19.8(5)	112.0±33.5(4)	94.0±16.5(7)		93.2±19.2(6)
HIAA	7.0	3.8±1.4	5.5±1.2	10.7±6.4(8)		9.1±4.3
TRY	4.4	9.9±1.1	14.3±2.9	12.1±1.8(9)		10.8±1.4
HVA	13.3	5.6±0.7	4.5±0.9	6.6±1.0(8)		11.4±3.3
MAO	2.9	10.7±2.2	4.8±1.2	6.8±1.7(8)		5.8±1.3

Values for HT, HIAA, HVA, represent μg/l and for TRY, mg/l ± S.E.M.
Values for MAO represent nmole phenylethylamine oxidised/ml blood/h ± S.E.M.
Numbers in brackets represent sample size.

the six who repeated the attempt, had, in fact a history of previous self-harm. However, using this parameter as a dependent variable none of the biochemical measures separated out. The values of tryptophan in patients, having a major depression and who didn't repeat attempted suicide, are within the normal range [5] so the low values, observed in the patients of the group repeating suicide attempts, may be an indicator of reduced availability of the 5HT precursor, although, according to Wurtman [14], the real indicator should be the ratio of plasma tryptophan to the total plasma concentrations of the other large neutral amino acids. The reduced ratio of TRY to HIAA, apart from being a consequence of low TRY levels, may also reflect an increased turnover of the available 5HT.

In a previous study [5] we observed a tendency to higher plasma tryptophan concentrations in patients suffering from chronic depression than in normal controls. If the low plasma tryptophan values in this study are confirmed on completion, biochemical classification of some of the affective disorders may become a possibility.

Acknowledgements

The authors appreciate the support given by Newcastle Area Health Authority which enabled these studies to be carried out. The secretarial and graphical assistance given by Yvonne Rutherford and Katharine Reed is also appreciated.

References

1. Barraclough B, Bunch J, Nelson B and Sainsbury P (1974) A Hundred Cases of Suicide. Brit. J. Psychiat. 125: 355–373.
2. Campbell IC, Robinson DS, Lovenberg W and Murphy DL (1979) The Effects of Chronic Regimens of Clorgyline and Pargyline on Monoamine Metabolism in the Rat Brain. J. Neurochem. 32: 49–55.
3. Kessel N (1965) Self-poisoning. Brit. Med. J. 2: 1336.
4. Mann JJ, Stanley M, McBride A and McEwen BS (1986) Increased Serotonin-2 and ß-drenergic Receptor Binding in the Frontal Cortices of Suicide Victims. Arch. Gen. Psychiat. 43: 954–959.
5. Marshall EF, Kennedy WN, Eccleston D et al. (1987) Whole Blood Serotonin and Plasma Tryptophan Using High Pressure Liquid Chromatography with Electrochemical Detection. Biochem. Med. 37: 81–86.
6. Morgan HG (1981) Management of Suicidal Behaviour. Brit. J. Psychiat. 144: 320.
7. O'Brien G, Holton AR, Hurren K, Watt L and Hassanyeh F (1987) Acta, Psychiat. Scand. 75: 474–477.
8. Office of health economics (1981) Suicide and Deliberate Self-harm. HMSO.
9. Pallis DJ, Barraclough BM, Levey AB, Jenkins JS and Sainsbury P (1982) Estimating Suicide Risk among Attempted Suicides. Brit. J. Psychiat. 14: 37–44.
10. Robins E (1981) The Final Months. A Study of the Lives of 134 Persons who Committed Suicide. Oxford University Press.
11. Seager et al. (1965) Suicide in Bristol. Brit. J. Psychiat. 111: 919.
12. Spitzer RL and Endicott J (1978) Research Diagnostic Criteria. Arch. Gen. Psychiat. 35: 773–782.
13. Wright-Honari S, Marshal EF, Ashton CH and Hassanyeh F (1989) Estimation of Blood Plasma 5-Hydroxyindoleacetic Acid and Homovanillic Acid. Presented to the International Symposium on Serotonin, Florence 29th March–1st April 1989. Abstract p. 181.
14. Wurtman RJ (1983) Behavioural Effects of Nutrients. Lancet i: 1145–1147.

Metabolic tyrosine disorder in mink and PLP therapy of hereditary tyrosinemia

K. Christensen[a], P. Henriksen[b], K. Mortensen[c] and H. Sørensen[c]

[a]Department of Animal Genetics, Royal Veterinary and Agricultural University, 13, Bülowsvej, DK-1870 Frederiksberg C, Denmark

[b]National Veterinary Laboratory, 27, Bülowsvej, DK-1870 Frederiksberg C, Denmark

[c]Chemistry Department, Royal Veterinary and Agricultural University, 40, Thorvaldsensvej, DK-1871 Frederiksberg C, Denmark

Abstract

Tyrosinemia is a serious hereditary metabolic disorder in man. Various forms are known including tyrosinemia type I, which has been described to comprise defects related both to hepatic 4-hydroxyphenylpyruvate dioxygenase (EC 1.13.11.27) and other enzymes. In tyrosinemia type II defects at hepatic tyrosine aminotransferase (EC 2.6.1.5) are involved.

Three forms of hereditary tyrosinemia type II have been found in mink (*Mustela vison Schreb*). The disease may lead to death for animals with homozygotic recessive genes. Deficiency of hepatic tyrosine aminotransferase is found for all of the three different forms of this mink disease. This results in insufficient degradation and excretion of tyrosine and phenylalanine as well as their metabolites. The severity of the disease and the time of onset are characteristic differences among the three different forms of tyrosinemia type II.

The metabolism of tyrosine in normal and affected animals have been investigated by use of ^{14}C-L-tyrosine as precursor. The tracer technique combined with different analytical methods revealed that various tyrosine products are formed in other tissues and/or internal organs than the liver. Tyrosine products accumulated in diseased animals. In addition to tyrosine and phenylalanine the following products were found: 4-hydroxyphenyllactate, 4-hydroxyphenylacetate, 4-hydroxy-3-methoxyphenyllactate, *N*-acetyltyrosine, dopa and some other products from the normal metabolism of tyrosin.

Tyrosine aminotransferase isolated from mink liver has been investigated for clarification of the cause to tyrosinemia type II. Kinetics revealed that insufficient binding of the cofactor pyridoxalphosphate (PLP) to hepatic tyrosine aminotransferase is a likely cause of the disease. Dietary treatments of affected mink with PLP have been successful, as revealed from the data presented and discussed in this paper.

Introduction

Hereditary tyrosinemia in man was first described more than five decades ago [1]. An animal model was unknown until about one decade ago when tyrosinemia was found to occur as a simple autosomal recessive character in mink (*Mustela vison Schreb*) [2,3]. Various forms of tyrosinemia in man and three different forms of tyrosinemia in mink have now been described [4 and refs. cited therein].

Tyrosinemia is a complex metabolic disorder, but a common feature of all of the various forms of this disease is a blocked pathway of normal tyrosine catabolism

and/or excretion of tyrosine. As a result, prominent biochemical abnormalities expressed are high blood and urine levels of tyrosine and tyrosine metabolites [3,4 and refs. cited therein].

Reduced activity of hepatic 4-hydroxyphenylpyruvate dioxygenase (EC 1.13.-11.27) is a characteristic feature of tyrosinemia type I, and hepatic tyrosine aminotransferase (EC 2.6.1.5) is affected in tyrosinemia type II [4,5]. However, various features at the biochemical basis of tyrosinemia remain at present uncertain, and other variant forms of tyrosinemia and reasons for the disease have to be considered [4 and refs. cited therein].

Tyrosinemia type II in mink are considered as a model of human tyrosinemia type II [4–7]. Furthermore, the disease allows studies of unsolved problems concerning tyrosine metabolism and possibilities for treatment of the diseased animals. This communication describes investigations of tyrosinemia type II in mink, metabolism of tyrosine in the animals, studies of tyrosine aminotransferase in mink liver and effects of PLP therapy.

Experimental procedures

Animals

Mink used in this study were male and female standard black mink (*M. vison Schreb*). The animals were housed in mink farms [3,4] and fed a traditional mink diet [8]. Rats used in biochemical experiments were Wistar male rats [9].

Materials

Chemicals, solvents and reagents were of analytical-reagent grade purchased from Merck (West Germany), Sigma (U.S.A.), Bio-Rad (U.S.A.) and LKB Pharmacia (Sweden). Water was deionized and organic impurities were removed by use of Elgastat UHQ (Elga Ltd., Lane End, High Wycombe, Bucks., U.K.). Columns and column materials were purchased from Millipore Waters (U.S.A.) and LKB Pharmacia. The radiochemicals 1-^{14}C-4-hydroxyphenylpyruvate, L-(1-^{14}C)tyrosine and L-(U-^{14}C)tyrosine were from The Radiochemical Centre, Amersham, Bucks., (U.K.).

General methods and instrumentation

Methods and equipment used for the different types of analysis have been described previously; for amino acids, amines, carboxylic acids and other low molecular weight (LMW) compounds in [3,4,10–12] and for enzymes in [13,14]. CLC and CLC-MS were performed on per-trimethylsilylated (TMSi) compounds. HPLC were performed on the native compounds after group separation [10–12] or for urine and serum samples after treatment of 50–200 µl samples with an equal

volume of CCl_3COOH-H_2O (1:2) before centrifugation (3000 × g, 20°C). Radioactivity was counted in a 1217 Rackbeta Liquid Scintillation Counter (LKB Pharmacia, Sweden) and/or detected in autoradiography. Removal, treatment and storage of blood, urine and internal organs and tissues for clinics, pathology and biochemical experiments are described elsewhere [4].

Assays

The assays described before [4] for tyrosine aminotransferase and 4-hydroxyphenylpyruvate dioxygenase were used. Direct assays of crude soluble fractions of liver homogenates were in addition based on the enole-borate complex procedure for tyrosine aminotransferase [15] and the procedure based on 1-^{14}C-4-hydroxyphenylpyruvate for 4-hydroxyphenylpyruvate dioxygenase [16]. One unit (U) was defined as 1 μmol of substrate consumed or 1μmol of product formed under the assay conditions specified [4].

Protein determinations

The content of protein was determined by a modification of Lowry's method and by measuring the UV absorbance [13].

Preparation of crude extracts and pre-purifications

The procedures used for liver homogenization, extractions and pre-purifications of tyrosine aminotransferase and 4-hydroxyphenylpyruvate dioxygenase have been described elsewhere [4].

Purification and characterization of tyrosine aminotransferase

Sucrose-gradient-centrifugations were performed with a MSE superspeed 75 ultracentrifuge, 8 × 14 titanium swing out rotor, at 110,000 × g, 4°C, 48 h. Polycarbonate tubes were used for the sucrose-gradient-solution (12.5 ml) which was produced from 100 mM potassiumphosphate buffer (pH 7.3) containing 2.5 mM 2-ketoglutarate, 100 mM PLP and 13% (w/v) sucrose. The solutions were twice placed at −82°C, 16 h, then at 4°C, 10 h before 1 ml of sample (± 1 mg) was placed on the top of the gradient formed. After centrifugation the content of the tubes was removed from the bottom, collected in fractions of about 0.5 ml and tested for protein and enzyme activity. Purification and characterization of tyrosine aminotransferase were, furthermore, based on DEAE column chromatography, gelfiltration, PPLC techniques and electrophoresis including isoelectric focusing methods as described previously [13,14]. Kinetics were based on the above described assay containing varying amounts of substrates, products and PLP. Additional details concerning purification, characterization and kinetics of tyrosine aminotransferase will be presented elsewhere.

Dialysis and PLP – apoenzyme association

Production of the apoenzyme of tyrosine aminotransferase from mink liver was performed with a partially purified enzyme preparation (after ultracentrifugation and DEAE-column purification). Dialysis was performed against a potassium-phosphate buffer (10 mM, pH 7) containing phenylmethylsulfonylfluoride (PMSF; 0.1 mM), NaCl (0.9%), EDTA (1 mM) and 2-ketoglutarate (2.5 mM) during the day. 2-ketoglutarate was exchanged with L-Tyr (0.4 mM) during the night. After three days about 10% of the activity was still present, which means that it was not possible to remove all of the PLP. Alternatively other holoenzymes with tyrosine aminotransferase activity could have been present. Dialysis was also performed for 18 h with the above mentioned buffer + PLP in various concentrations for studies of the optimal PLP concentration.

Tracer experiments

Mink affected by the 'early type tyrosinemia type II' and normal mink of the same age (6 weeks) [3,4] were subcutaneously injected 15 μCi (U-^{14}C)-L-tyrosine dissolved in sodiumphosphate buffer (100 mM; pH 7.4) containing 0.9% NaCl. Blood and urine were removed from the animals which were killed after 4 h. The following organs were placed at –40°C: liver, heart, pancreas, lungs, thyroid/trachea, salivary gland, spleen, brain, kidneys, urinary bladder, eyes, eye-lids, skin/axillary region, skin/hind part, paws. Sections of the frozen tissues and organs were cut in 5 μm sections and used for autoradiography and biochemical investigations after extractions twice in 0.1 M HCl (Aq; 5 ml) + ethylacetate (EtAc; 5 ml), group separation, electrophoresis (HVE) and chromatography (PC, TLC) [4,11,12].

PLP therapy

Four mink affected by the 'intermediate type tyrosinemia type II', one with 'late type tyrosinemia type II' and four with the 'early type tyrosinemia type II' have been included in trials with pyridoxalphosphate PLP; vitamin B6) treatment of the disease. The animals were fed a traditional mink diet (*vide supra*) with additional PLP added (500 mg PLP per day per mink; 100 mg was used for three of the mink with the 'intermediate type tyrosinemia type II'). Blood and urine were collected for chemical analysis (*vide supra*) with two days interval in the first part of the period, then with seven days interval.

Results and Discussion

Hereditary tyrosinemia type II in mink

Three different forms of the disease have been found in mink [2–5]. Investigations of the genetics have been based on some few thousands of mink [3,4]. The diseases

Table 1. Segregation ratio for the litters in testcrossing of heterozygotes (Tt) and (Tt') for tyrosinemia type II. Calculations are based on a corrected 3:1 segregation as the expected numbers

	Tt × Tt	Tt × Tt'	Tt' × Tt'			
	TT + 2Tt + *tt*	TT + Tt + Tt' + *tt'*	TT + 2Tt' + *t't'*			
	Obs.	Exp.	Total	chi	p>	
tt early type	32	28.9	94	0.5	0.5	
	14	16.9	56	0.8	0.3	
tt' intermediate	28	31.6	96	0.6	0.3	
t't' late type	10	(9.3)	28	–	–	

T = normal gene; t and t' = tyrosinemia II genes.

are inherited as a simple autosomal recessive character due to homozygosity at a single locus, without indication of pleiotropic effect and linkage between genes [4]. The diseases may lead to death for animals with homozygotic recessive genes for the diseases, which seems to be caused by defects/deficiency in hepatic tyrosine aminotransferase [2–5]. With the symbol (T) representing the normal genes and (t) and (t') representing the genes for tyrosinemia II, genotypes of the following types (Table 1) were found in testcrossing of heterozygotes (Tt and Tt').

Clinics and histopathology

The symptoms and features of the disease indicate common reasons for the three forms [3,4], but the onset and severity of the symptoms are different (Table 2). Kits affected by the 'early type' (tt) died 2–4 days after onset of the symptoms, those affected by the 'intermediate type' (tt') died usually within 1–3 months after visible symptoms. Kits with the 'late type' (t't') were observed to have the same symptoms but less severe than for the 'intermediate type'. Details are described elsewhere [3,4].

Table 2. Time of onset of symptoms for mink kits affected by tyrosinemia type II

	Visible symptoms after birth	Additional time before dead
tt early type	ca. six weeks	2–4 days
tt' intermediate	ca. three months	1–3 months
t't' late type	ca. six months	? several months

Table 3. Concentrations (mM) of urea and creatinine in plasma of mink kits with tyrosinemia type II and values for normal kits of the same age in bracket

	Concentrations in plasma	
	mM urea	mM creatinine
tt early type	14–75	80–200
(normal)	(6–13)	(20–40)
tt' intermediate	47–56	120–250
(normal)	(13–29)	(20–50)
t't' late type	40–60	—
(normal)	(15–30)	—

Chemical-biochemical features of tyrosinemia type II

Mink affected by tyrosinemia type II, (tt), (tt') and (t't') have strongly elevated concentrations of urea and creatinine both in blood and urine. Results from analysis of blood samples from affected kits with clinical signs of the disease and normal kits including heterozygotes are shown in Table 3. The same trend with strongly elevated concentrations of urea and creatinine was found in urine from mink, when the mink was affected by tyrosinemia type II. However, these values were difficult to quantify owing to evaporation/concentration increase during collection of urine in open trays.

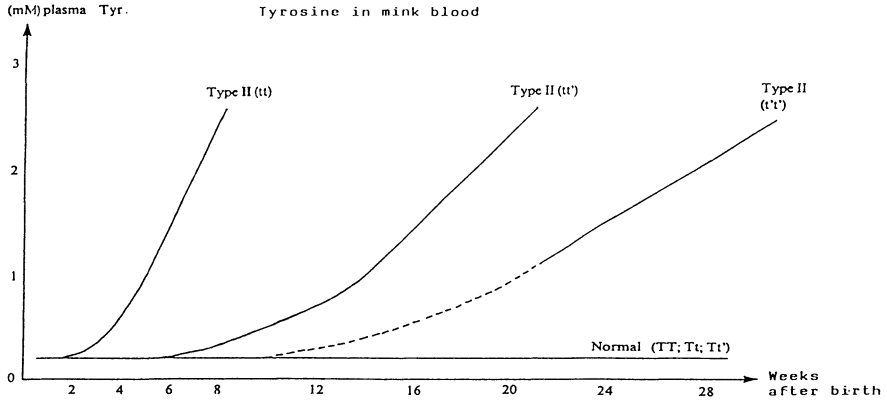

Fig. 1. Concentration of tyrosine in plasma of mink affected by the three different types of tyrosinemia II (Table 1).

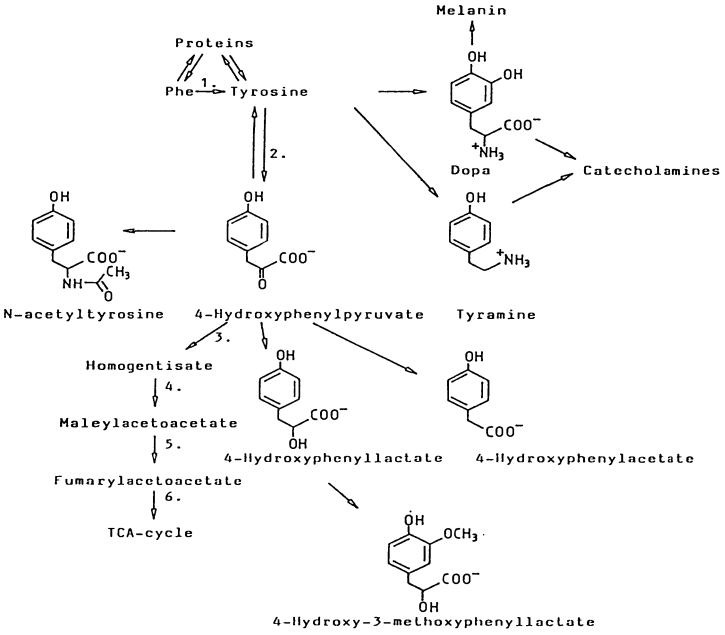

Fig. 2. Tyrosine metabolism in mink. Normal, catabolism of phenylalanine and tyrosine through the sequence catalyzed by the enzymes 1–6.: 1. Phenylalanine-4-monooxygenase (EC 1.14.16.1); 2. Tyrosine aminotransferase (EC 2.6.1.5); 3. 4-Hydroxyphenylpyruvate dioxygenase (EC 1.13.11.27); 4. Homogentisic acid 1,2-dioxygenase (EC 1.13.11.5); 5. Maleylacetoacetate isomerase (EC 5.2.1.2); 6. Fumaroylacetoacetase (EC 3.7.1.2). Tyrosinase catalyze the oxidation to 3,4-dihydroxyphenylalanine (Dopa) and Melanine.

Analysis of urine and plasma free amino acids [11] revealed that the disease especially affected the concentration of tyrosine [3,4]. Figure 1 shows the results obtained based on blood sample analyses by HPLC. It is revealed, that the disease can be detected long time before the first clinical signs appear (Table 2). Both the intermediate type (tt') and the late type (t't') have not elevated blood tyrosine concentration at the time when animals affected by the early type (tt) die (Fig. 1). Quantitation of levels of tyrosine and phenolic acids in urine and blood was carried out by HPLC (280 nm UV detection) after treatment with CCl_3COOH and/or group separation [11] as well as by GLC of TMSi derivatives. Identification was confirmed by PC, HVE and TLC [11,12], for some samples combined with the tracer experiments including autoradiography, and for some compounds by combined GLC-MS.

The experiments have shown, that affected animals with the high concentration of tyrosine in the blood also produce elevated concentrations in blood and urine of phenylalanine, 4-hydroxyphenylacetate, 4-hydroxyphenyllactate and 4-hydroxy-3-

Table 4. The activity of hepatic tyrosine aminotransferase (TAT) and hepatic 4-hydroxyphenylpyruvate dioxygenase (PHPPA) based on direct assays (see 'experimental procedures')

Mink No.	Age (days)	Plasma Tyr (mM)	TAT (U/g prot.)	PHPPA (U/g prot.)
1. normal	29	0.08	8.7	13.9
2. normal	28	0.09	1.7	13.0
3. early type (tt)	29	1.10	0.0	22.8
4. early type (tt)	28	0.43	0.0	15.0
5. normal	43	0.15	15.3	33.6
6. normal	45	0.20	5.9	40.6
7. early type (tt)	45	3.99	0.09	40.7
8. early type (tt)	45	4.81	0.02	47.4
9. early type (tt)	40	2.38	0.07	42.8

methoxyphenyllactate. In some cases *N*-acetyltyrosine, dopa and tyramine were also found in slightly elevated concentrations (Fig. 2). The possibility of an enzyme defect at 2. (TAT) or 3. (PHPPA) (Fig. 2) in the tyrosine catabolism was investigated by use of the direct assay (*vide supra*). The liver is the richest source of those enzymes, and results from determination of TAT- and PHPPA-activity in liver homogenates are shown in Table 4 for mink kits with the 'early type tyrosinemia II' and normal kits of the same age. Mink kits at an age of about six weeks with the early type tyrosinemia II (tt) had some TAT activity which could be a result of liver mitochondria aspartate aminotransferase. Otherwise, the results indicate that hereditary tyrosinemia type II involves a defect in hepatic tyrosine aminotransferase and not in 4-hydroxyphenylpyruvate dioxygenase.

Tracer experiments with ^{14}C-L-Tyr as precursor (*vide supra*) have revealed a fast metabolism (Fig. 2) and excretion of tyrosine and tyrosine metabolites from normal mink compared to that of mink with the 'early type tyrosinemia II' (Fig. 3).

Group separation of LMW-compounds in blood from the affected mink (tt) in the tracer experiment, followed by TLC, HVE, PC and autoradiography confirmed the occurrence of the metabolites discussed in connection with Fig. 2. The C_6-C_3 compounds accumulated do not seem to be a result of tyrosine metabolism in the liver through 4-hydroxyphenylpyruvate (Table 4). These compounds could more likely be formed by help of enzymes in other tissues and organs (Figs. 3 and 4).

Tyrosine aminotransferase has been isolated from mink liver, purified and characterized by use of the methods described in 'experimental procedures'. The preliminary results obtained have shown the enzyme has a dimer structure with MW 100,000–110,000 D and a monomer with MW of 45,000–55,000 D. Ultracentrifugation revealed especially appreciable amounts of monomer enzyme in liver of tyrosinemia type II affected mink. FPLC chromatofocusing and isoelectric focus-

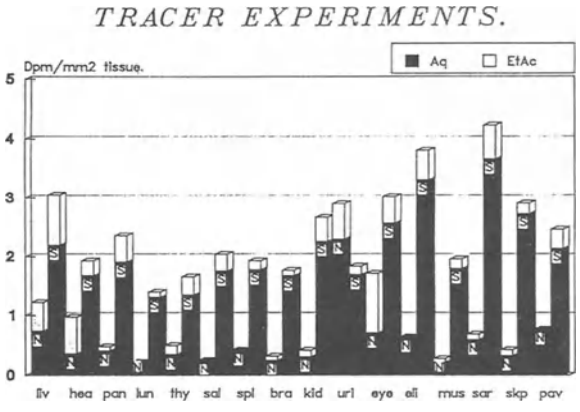

Fig. 3. (U-^{14}C)-L-Tyrosine tracer experiments with early type tyrosinemia II (tt; S) and a normal mink kit (N) of the same age (6 weeks). Results shown are for termination after 4 h, where the blood had 111 Dpm/µl for (S) and 9 Dpm/µl for (N). x-Axis symbols (three letters) for the different tissues and organs have the same sequence as the full names in 'experimental procedures'.

ing showed two enzyme peaks with pH determined to about 4.9 and 5.4, respectively. Mink hepatic tyrosine aminotransferase seems to be less stable than the corresponding enzyme from rat liver, especially if insufficient PLP was present in the applied buffer systems. With PLP present in the buffer systems, appreciable tyrosine aminotransferase activity was found in liver of mink affected by the intermediate type tyrosinemia II (tt'). Experiments with dialysis and kinetics revealed an optimum PLP concentration at 1–2 mM, and appreciable inhibition of the enzyme by glutamate and 4-hydroxyphenylpyruvate.

PLP therapy (see 'experimental procedures') of mink affected by the intermediate type (tt') and the late type (t't') resulted in a reduction of the tyrosine concentration in blood and urine, to a nearly normal level (Fig. 1). The time

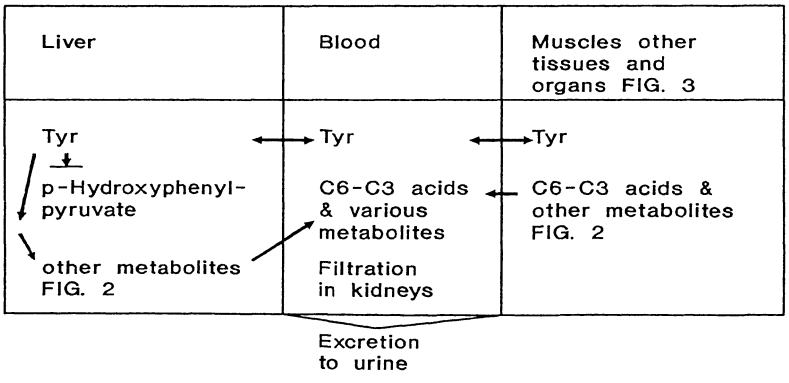

Fig. 4. Formation and excretion of tyrosine metabolites.

required was 1–2 months. After this period the clinical signs of tyrosinemia disappeared. The experiments were terminated for two minks (tt' and t't') after 6 months, for two minks (tt') the therapy was continued to about one year and for one mink (tt') the therapy was continued to about 18 months after start. The additional PLP was then removed from the diet fed to this 'healthy' (tt') mink. Increase in the blood tyrosine concentration was observed about one month later and during the next month all signs of tyrosinemia type II appeared. A diet with additional PLP was again used and it required, as originally, about 1–2 months to obtain an acceptable blood and urine tyrosine concentration and thereby also a healthy (tt') mink. The PLP therapy of mink with the early type tyrosinemia II (tt) was not successful; possibly owing to the relatively long time required (Table 2) for reduction of the blood tyrosine concentration. Experiments with PLP therapy of mink with the early type tyrosinemia II (Tables 1 and 2) could be of interest if the treatment starts when the blood tyrosine concentration increases over the normal value (Fig. 1). The doses of PLP required/used, where the therapy was successful, were in the range of 500 times the requirement for normal maintenance, and no adverse effects on the animals were found as a result of these high vitamin B6 doses. The physiologic basis for the effect of PLP is, however, unknown at present, and additional investigations on hepatic tyrosine aminotransferase are required.

Acknowledgements

Support from the Danish Medical Research Council and the Danish Fur Breeders Association is gratefully acknowledged.

References

1. Medes G (1932) Biochem. J. 26: 917–940.
2. Christensen K, Venge O and Sørensen H (1978) Proceeding of European Association for Animal Production: 29th annual meeting, Stockholm, June 5–7.
3. Christensen K, Fischer P, Knudsen KEB, Larsen S, Sørensen H and Venge O (1979) Can. J. Comp. Med. 43: 333–340.
4. Christensen K, Henriksen P and Sørensen H (1986) Hereditas 104: 215–222.
5. Christensen K and Sørensen H (1979) XIth International Congress of Biochemistry, Toronto, Canada, July 8–13.
6. Goldsmith LA, Thorup JM and Marsh RF (1981) Biochem. Genet. 19: 687–693.
7. Bjerg B, Christensen K, Henriksen P and Sørensen H (1986) Proceedings of NJF seminarium No. 110, Kuopio, Finland, September 9–11, pp. 96–109.
8. Henriksen P, Hillemann G, Mortensen K and Sørensen H (1987) Proceedings of 7th International Rapeseed Congress, Poznan, Poland, May 11–14, V(7): 1817–1824.
9. Bjerg B, Eggum BO, Jacobsen I, Otte J and Sørensen H (1983) J. Anim. Physiol. Anim. Nutr. 61: 227–244.
10. Bjerg B, Ebmeyer E, Eggum BO, Larsen T, Røbbelen G and Sørensen H (1988) Plant Breeding 101: 277–291.

11. Eggum BO and Sørensen H (1989) Chemistry and analysis of amino acids. In: Friedman M (ed.) Absorption and Utilization of Amino Acids. CRC Press, Boca Raton, Florida, vol. III, Chapter 17.
12. Eggum BO, Hansen NE and Sørensen H (1983) Amino acid precursors of biogenic amines. In: Friedman M (ed.) Absorption and Utilization of Amino Acids. CRC Press, Boca Raton, Florida, vol. III, chapter 5.
13. Børresen T, Klausen NK, Larsen LM and Sørensen H (1989) Biochim. Biophys. Acta, RPG 018581, in press.
14. Elnif J, Hansen NE, Mortensen K and Sørensen H (1988) Proceeding of Biology, Pathology and Genetics of Fur Bearing Animals. 4th International Scientific Congress in Fur Animal Production, Toronto, Canada, August 21–24, pp. 308–319.
15. Lin ECC, Pitt BM, Civen M and Knox WE (1958) J. Biol. Chem. 233(3): 668–673.
16. Lindblad B (1971) Clin. Chim. Acta 34: 113–121.

Tryptophan degradation in tumor cells undergoing rejection*

Ryotaro Yoshida, Osamu Takikawa and Akemi Habara-Ohkubo
Department of Cell Biology, Osaka Bioscience Institute, Suita 565, Japan

Abstract

The depletion of essential amino acid, tryptophan, caused by indoleamine 2,3-dioxygenase induction by IFN-γ *in vitro* is a mechanism of self-defense against inhaled microorganisms and tumor growth. In this communication, we report the mechanisms [cellular localization of the induced dioxygenase, characterization of the enzyme inducer(s) and identification of the types of host cells] of indoleamine 2,3-dioxygenase induction by *in vivo* tumor transplantation. After transplantation of tumor cells into the peritoneal cavity of various strains of mice, the enzyme was induced only when the tumor cells were being rejected from allogeneic animals, and no change was observed when the cells continued to grow in syngeneic animals. The enzyme was induced exclusively in the tumor cells undergoing rejection by factor(s), which was released through the interaction of allografted tumor cells with host cells. When the types of host cells infiltrating into transplantation loci were studied by flow cytometry, specific induction of cells bearing both Thy-1 antigen (a marker for T lymphocytes) and κ light chain of immunoglobulin (a marker for B lymphocytes) on their surfaces was observed only when the tumor cells were being rejected from allogeneic animals. The IDO inducer activity in the conditioned medium of cultured whole peritoneal exudate cells was completely neutralized by the addition of antibody against IFN-γ but not by antibody against IFN-α/ß. The concentration of IFN-γ in the medium was found to be 1–2 U/ml.

Introduction

When mice were treated with bacterial lipopolysaccharide (LPS), poly I·poly C or viruses, IFN-mediated indoleamine 2,3-dioxygenase (IDO) induction occurred exclusively in the host cells (alveolar interstitial cells) [1–6]. The *in vivo* substrate of IDO has been found to be the essential amino acid, tryptophan [7]. In several laboratories, it has been postulated that the depletion of tryptophan caused by IDO induction *in vitro* is physiologically significant in that the enzyme serves in the defense mechanism against microorganism and tumor growth [8–10]. Not only is tryptophan required for protein synthesis, but also it is necessary for the synthesis of the neurotransmitter (serotonin) and NAD. In fact, the omission of tryptophan from the growth medium of mouse LM cells or L1210 cells has been shown to produce growth arrest, presumably in G_1, which is reversible and which is attended by a partially synchronous growth upon restoration of tryptophan [11,12]. Therefore, it is interesting to speculate that depletion of the essential amino acid

* This work was supported in part by a research grant from the Sankyo Foundation of Life Science and by a Grant-in-Aid for Scientific Research from the Ministry of Education, Science and Culture, Japan.

tryptophan around virus- or parasite-infected cells and invading tumor cells are responsible for inhibiting their growth. In this communication, we report 1) that tryptophan degradation enzyme was dramatically induced in allogeneic or syngeneic tumor cells undergoing rejection, but not in host cells, 2) that the enzyme (or the antitumor state) was induced by factor(s) released through the interaction of allografted tumor cells with host cells, 3) that such factor was found to be IFN-γ, and 4) that we found specific induction of a novel murine lymphoid cell bearing both Thy-1 antigen (a marker for T lymphocytes) and κ light chain of immunoglobulin (a marker for B lymphocytes) on their surfaces only when the tumor cells were being rejected from the transplantation sites.

Experimental procedures

Chemicals

L-[ring-2-^{14}C]Tryptophan (36 Ci/mol) was purchased from Commissariat à l'Énergie Atomique, France, and was purified by column chromatography on Dowex 50W-X2 H^+ form)(0.5 × 1.0 cm) as described previously [13]. Catalase was a product of Boehringer Mannheim. Methylene blue, ascorbic acid, L-tryptophan and trypan blue were purchased from Wako Pure Chemicals, Osaka, Japan. Fetal calf serum (FCS) was obtained from HyClone Labs., Inc. (Logan, UT) and used after heat inactivation. All other chemicals were of reagent grade.

Animals

Male specific pathogen-free (SPF) BALB/c and C57BL/6 mice, weighing 25 ± 2 g, were purchased from Japan SLC, Shizuoka, Japan. Mice were raised under SPF conditions in an air-conditioned room at 25 ± 2°C and about 50% humidity at the Osaka Bioscience Institute, Suita, Japan.

Tumor cells

Meth-A cells were kindly provided by Dr. S. Muramatsu, Department of Zoology, Kyoto University Faculty of Science. 3LL cells were the generous gift of Dr. S. Sugino of the Department of Microbiology, Kyoto Prefectural University of Medicine. Meth-A cells and 3LL cells were maintained by weekly i.p. passage of 10^7 cells into BALB/c and C57BL/6 mice, respectively.

Antibodies

Monoclonal antibodies to mouse Thy-1.2 antigen [fluorescein isothiocyanate (FITC)-labeled] and immunoglobulin (Ig) κ light chain [phycoerythrin (PE)-labeled] were purchased from Becton Dickinson (Mountain View, CA).

Enrichment of peritoneal leukocytes and macrophages

Two or three mice (BALB/c or C57BL/6 strain) were sacrificed in each experiment at various time intervals after an intraperitoneal transplantation of Meth-A cells (3×10^6 cells/mouse). The peritoneal cavity was lavaged three times with 2.5 ml of cold Dulbecco's phosplate-buffered saline (PBS) without divalent cations, pH 7.4. After three times of washings and centrifugations at $10 \times g$ for 10 min at 4°C, a total of 3 supernatant fractions was collected and passed through a nylon cloth (71 μm mesh). The cell suspension was centrifuged at $300 \times g$ for 10 min at 4°C. The pellet was resuspended in an appropriate volume of incubation medium (PBS containing 2% FCS and 0.1% sodium azide) to give a concentration of 2×10^7 cells/ml.

Fluorescence-activated cell sorter analysis

Host cell-rich fraction (10^6 cells in 50 μl of incubation medium) was incubated at 4°C with the above-mentioned monoclonal antibodies in a total volume of 100 μl for 20 to 30 min. In double label experiments, the cells were stained first with the labeled antibody to mouse κ light chain of Ig followed by normal rat serum, and then incubated with the labeled antibody to mouse Thy-1.2 antigen. The reaction was terminated by the addition of cold incubation medium (2 ml/tube) and the mixture was centrifuged at $300 \times g$ for 10 min at 4°C. The supernatant was carefully aspirated, the pellet resuspended in the medium, and the cells were analyzed by flow cytometry with a fluorescence-activated cell sorter (FACStar) [Becton Dickinson, Mountain View, CA] using the 488 nm emission of the argon laser.

Cell number and viability

After the centrifugations and filtrations through a nylon cloth (71 μm mesh), the cell number was determined with a hemocytometer using turk solution (Kanto Kagaku, Japan). The viability of the cells was determined by trypan blue (Wako Chemicals, Japan) exclusion method.

Results and Discussion

Changes in IDO activities and tumor growth after transplantation of tumor cells

When Meth-A cells (3×10^6/mouse) were introduced i.p. into an allogeneic (C57BL/6) strain of mice, the growth of Meth-A cells began within 24 h after transplantation as in syngeneic animals, but the tumor cells ceased to grow on the 9th day (Fig. 1). Rapid elimination of the tumor cells from the peritoneal cavity commenced around the 12th day and on the 20th day none was found. The IDO

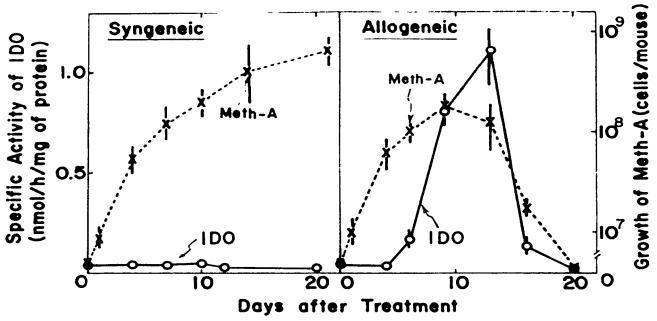

Fig. 1. IDO induction and growth of Meth-A cells in peritoneal cavity. Meth-A cells (3×10^6/mouse) were given i.p. to syngeneic (BALB/c)(left) or allogeneic (C57BL/6)(right) mice. At appropriate time intervals, peritoneal exudate cells were recovered as described in 'Experimental procedures'. Cell numbers (×) were determined with a hemocytometer. Each value represents the mean value ± SEM for five mice. The IDO activities (○) were determined as described in 'Experimental procedures'. Each value represents the mean ± SEM for five mice.

activity in the peritoneal exudate cells began to increase from the 6th day after transplantation and reached a peak (approximately 50-fold) on the 12th day. Thereafter, the enzyme activity rapidly decreased and was undetectable around 20th day. In the case of syngeneic (BALB/c) animals, however, the tumor cells continued to grow in the peritoneal cavity for 2 to 3 weeks without leukocyte infiltration and the mice died on day 12–16. The IDO activity in the peritoneal cells was almost undetectable and did not change significantly. Similar increase (approximately 150-fold) in IDO activity in the peritoneal exudate cells was observed by i.p. transplantation of 3LL cells (4×10^5 cells/mouse) into an allogeneic (BALB/c) strain of mice but not into syngeneic animals (C57BL/6 strain of mice) (data not shown).

IDO induction in transplanted syngeneic tumor cells which are undergoing rejection

When the syngeneic tumor (3LL) cells in a diffusion chamber were transplanted into the peritoneal cavity of C57BL/6 mice simultaneously with i.p. injection of allogeneic tumor (Meth-A) cells, the enzyme activity of syngeneic tumor cells in the diffusion chamber started to increase on day 9 after tumor transplantation, reached a maximum (approximately 30-fold) on day 11, and gradually decreased thereafter (Fig. 2). The time course was essentially the same as that observed with allografted Meth-A cells (Fig. 1). Under these conditions, the tumor cells in the diffusion chamber ceased to grow on day 11 and subsequently approximately 50% of the cells were rejected. These results suggest that the cytotoxicity for either syngeneic or allogeneic tumor cells was mediated by soluble factor(s) which are permeable through the filter membrane on the diffusion chamber.

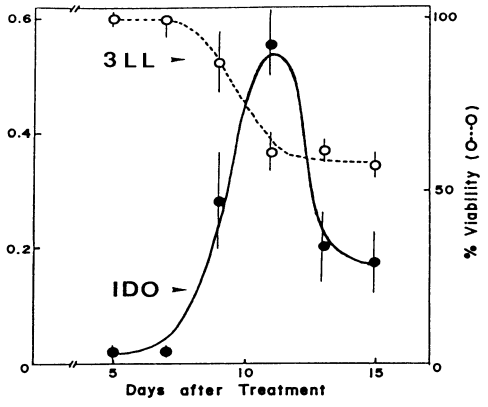

Fig. 2. Induction of IDO in the transplanted syngeneic tumor cells undergoing rejection. 3LL cells (2×10^5/0.15 ml) in a diffusion chamber were transplanted simultaneously with i.p. injection of Meth-A cells (2×10^6/mouse) into the peritoneal cavity of C57BL/6 mice. Cell viability (○) was determined with a hemocytometer. The IDO activity (●) was determined as described in Fig. 1. Each value represents the mean ± SEM for five mice.

The time course of enzyme induction in the allogeneic animals coincided well with that of the i.p. infiltration of small lymphoid cells. The localization of indoleamine 2,3-dioxygenase in the tumor cells was identified either by sedimentation under gravity and differential centrifugation or by complement-dependent lysis with specific antibodies against tumor and host cells (data not shown).

Appearance of Thy-1.2$^+$/κ$^+$ cells at the transplantation sites of allogeneic tumor cells

The types of host cells were studied by flow cytometry at various time intervals after the tumor (Meth-A cells) transplantation, and they were compared with those of tumor-transplanted syngeneic (BALB/c) strains of mice or untreated animals (BALB/c and C57BL/6 strains of mice). Specific induction of cells bearing both Thy-1 antigen (a marker for T lymphocytes) and κ light chain of immunoglobulin (a marker for B lymphocytes) on their surfaces was observed only when the tumor cells were being rejected from allogeneic (C57BL/6) animals (Fig. 3). The percentage of Thy-1.2$^+$/κ$^+$ cells gradually increased after tumor transplantation into allogeneic strains of mice, reaching a plateau (approximately 5-fold) on day 13, which was maintained at almost maximum level for a week. In the case of syngeneic animals, however, almost no change in the percentages of Thy-1.2$^+$/κ$^+$ cells in whole peritoneal exudate cells was observed, the tumor cells continued to grow, and the mice died on day 12–16.

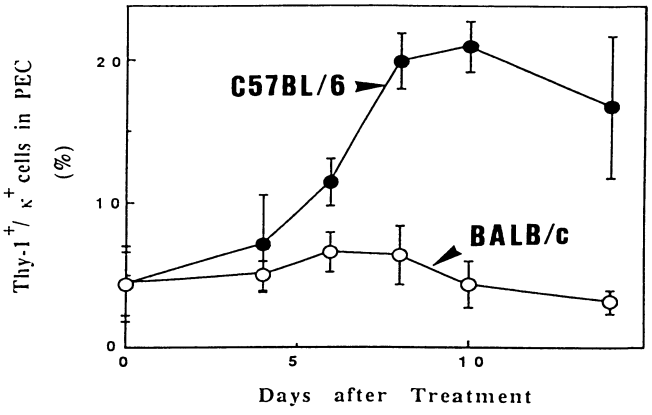

Fig. 3. Induction of Thy-1.2$^+$/κ$^+$ cells at transplantation loci of allogeneic tumor cells. Peritoneal exudate cells (host cell-rich) were harvested at various time intervals after an intraperitoneal transplantation of Meth-A cells (3×10^6/mouse). The percentages of Thy-1.2$^+$/κ$^+$ cells in whole peritoneal exudate cells were determined as described in 'Experimental procedures'. Each value represents the mean ± SD of 3 (day 0, day 4, day 6, and day 14), 5 (day 8) or 10 (day 10) experiments. ○, BALB/c; ●, C57BL/6.

IFN-γ is the soluble factor for IDO induction in allografted tumor cells

To assay the IDO inducing factor, we used a 35 mm special culture dish (Transwell™), which consisted of two wells divided vertically with a membrane (0.4 μm pore). Host cells, that infiltrated into the transplantation sites, were cultured in the

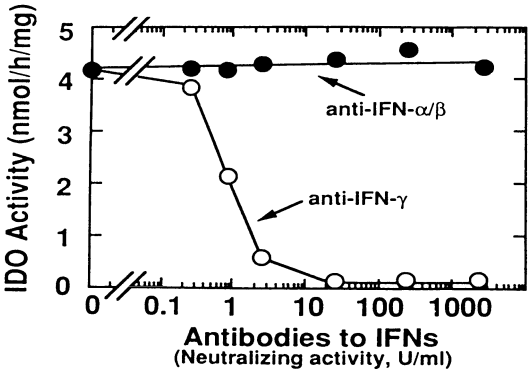

Fig. 4. Identification of IDO inducer that was released through the interaction of host cells with transplanted tumor cells. The conditioned medium containing IDO inducer was incubated with an antibody specific for IFN-α/β or IFN-γ at 37°C for 2 h, the antibody-treated medium was transferred to a new culture dish containing untreated Meth-A cells, and the IDO activity in the tumor cells was determined after 2-day culture. Each point represents the mean of duplicate determinations

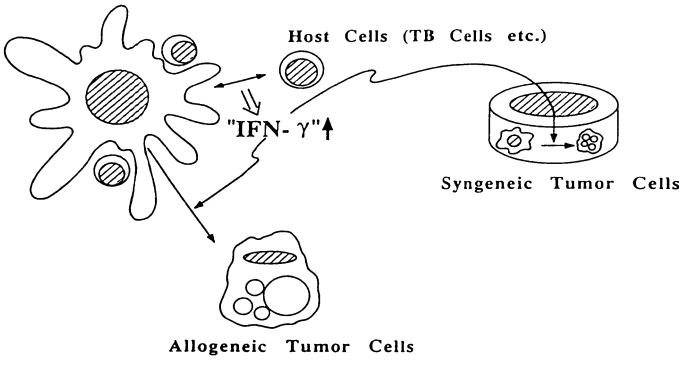

Fig. 5. Possible mechanisms of tumor rejection from transplantation loci.

upper well, and untreated Meth-A cells in the lower well. With this *in vitro* system, the IDO was induced in the tumor cells (lower well). The culture supernatants, obtained by centrifuging the culture media of the upper and lower wells, induced the IDO to essentially the same extent as that observed with the Transwell. The inducer activity in the conditioned medium was completely neutralized by the addition of antibody against IFN-γ but not by antibody against IFN-α/ß (Fig. 4). The concentration of IFN-γ in the 1 day-cultured medium with Transwell™ was found to be 1–2 U/ml based on the neutralization curve with the antibody. At this concentration, recombinant IFN-γ induced IDO in Meth-A cells to the same extent as that observed with the conditioned medium.

These results taken together indicate 1) that IFN-γ was released by the interaction of host cells (Thy-1.2$^+$/κ$^+$ cells etc.) with transplanted tumor cells, 2) that the released IFN-γ acted on not only allogeneic but also syngeneic tumor cells to induce IDO, and 3) that the depletion of essential amino acid tryptophan caused by IDO induction resulted in the rejection of tumor cells.

Acknowledgements

The authors are indebted to Dr. O. Hayaishi for his continued encouragement during this investigation. The authors also thank Ms. J. Sato and Ms. Y. Ogasawara for skillful technical assistance, and Ms. K. Hirata for aiding in the preparation of this manuscript.

References

1. Yoshida R and Hayaishi O (1978) Proc. Natl. Acad. Sci. USA 75: 3998–4000.
2. Yoshida R, Urade Y, Tokuda M and Hayaishi O (1979) Proc. Natl. Acad. Sci. USA 76: 4084–4086.

3. Yoshida R, Urade Y, Nakata K, Watanabe Y and Hayaishi O (1981) Arch. Biochem. Biophys. 212: 629–637.
4. Urade Y, Yoshida R, Kitamura H and Hayaishi O (1983) J. Biol. Chem. 258: 6621–6627.
5. Yoshida R, Oku T, Imanishi J, Kishida T and Hayaishi O (1986) Arch. Biochem. Biophys. 249: 596–604.
6. Yoshida R, Imanishi J, Oku T, Kishida T and Hayaishi O (1981) Proc. Natl. Acad. Sci. USA 78: 129–132.
7. Takikawa O, Yoshida R, Kido R and Hayaishi O (1986) J. Biol. Chem. 261: 3648–3653.
8. Takikawa O, Kuroiwa T, Yamazaki F and R Kido (1988) J. Biol. Chem. 263: 2041–2048.
9. Pfefferkorn ER (1984) Proc. Natl. Acad. Sci. USA 81: 908–912.
10. Byrne GI, Lehmann LK and Landry GJ (1986) Infect. Immun. 53: 347–351.
11. Brunner M (1973) Cancer Res. 33: 29–32.
12. Wooley PV, Dion RL and Vono VH (1974) Cancer Res. 34: 1010–1014.
13. Ohnishi T, Hirata F and Hayaishi O (1979) J. Biol. Chem. 252: 4643–4647.

Address for correspondence: Ryotaro Yoshida, Department of Cell Biology, Osaka Bioscience Institute, Suita 565, Japan.

A stimulatory effect of substrates for aromatic L-amino acid decarboxylase on insulin secretion in mice*

Per Lindström

Department of Histology and Cell Biology, University of Umeå, Umeå, Sweden

Abstract

L-5-Hydroxytryptophan raises serum insulin levels in mice. This can be explained by a potentiating effect of L-5-hydroxytryptophan on insulin release induced by different secretagogues in pancreatic ß-cells. Other substrates for aromatic L-amino acid decarboxylase also stimulate insulin release in isolated mouse pancreatic islets. The stimulatory effect can be coupled to increased turnover by the decarboxylase. L-5-Hydroxytryptophan does not stimulate insulin release in islets from hamsters and rats. The net effect of decarboxylase substrates on insulin release is probably the sum of a stimulatory effect of decarboxylation and an inhibitory effect of formed monoamines.

Introduction

It was observed early that the biogenic monoamine dopamine affects carbohydrate metabolism and induces hyperglycemia [1]. Correll *et al.* [2] studied rabbits and rats and found that 5-hydroxytryptamine (5-HT) also induced hyperglycemia. The exact nature and physiological relevance of the effects of biogenic monoamines on carbohydrate metabolism is still unsettled. Biogenic amines probably play a role in CNS regulation of food intake and glucose metabolism [3–6]. Glycogenolytic and gluconeogenic effects on the liver have been reported [7–9], but also hypoglycemia mediated through effects on the liver [10]. Amines have effects on fat tissue [11], the anterior pituitary [12], and the thyroid [13].

An early study indicating possible effects of 5-HT on insulin release was presented by Ui [14]. It was later found that 5-HT and dopamine inhibit glucose-induced insulin release [15,16]. This has been shown in many studies and the topic has been reviewed [cf. 17].

Pancreatic islets contain biogenic amines [18,19]. They also contain aromatic L-amino acid decarboxylase [20–22] but tyrosine hydroxylase, the rate limiting enzyme in amine synthesis, is found only in fetal islets and in some islet cells in adult animals [23,24]. Islets from adult animals do not form 5-HT from added L-tryptophan [25] but they rapidly accumulate biogenic amines when decarboxy-

* This work was supported by grants from the Swedish Medical Research Council (12X-7124), the Swedish Diabetes Association, and the Medical Faculty, University of Umeå.

lase substrates are added [25–28]. Several studies have shown that such pretreatment with decarboxylase substrates causes a reduced insulin secretory response in subsequent experiments [27,29–31]. One might assume that decarboxylase substrates would have the same effects as amines also in acute experiments. L-Dihydroxyphenylalanine (L-DOPA) inhibits insulin release [28,32]. However, we found that 5-HT and L-5-hydroxytryptophan (L-5-HTP) have opposite effects on insulin release in isolated mouse islets [31].

We have characterized this difference between the amine and its precursor amino acid in a series of papers with particular focus on the stimulatory effect of L-5-HTP [22,31,33–37]. The 'Results' section summarizes some of the main published findings. A stimulatory effect of L-5-HTP *in vivo* is demonstrated. It is also shown that there are species differences in the effect of L-5-HTP.

Experimental procedures

Animals and islet isolations

Obese hyperglycemic mice (Umeå *ob/ob*) and their lean littermates were from a local non-inbred colony. Female Sprague-Dawley rats were from ALAB Laboratory Services, Stockholm, Sweden and golden hamsters were from the Wenner-Gren Institute, Stockholm, Sweden. *In vivo* studies were performed in lean mice. Pancreatic islets from overnight fasted *ob/ob*-mice were isolated by free-hand microdissection [38]. Rat, hamster, and mouse islets were isolated by collagenase digestion [39,40] using collagenase from Worthington Biochemical Company, NJ, U.S.A.

Studies in vivo

Lean adult mice (22–28 g) were used. After overnight starvation, 100 mg/kg L-5-HTP + 150 mg/kg D-glucose was dissolved in sterile saline and injected into a tail vein (0.20–0.25 ml). Controls received glucose alone. Animals were killed by decapitation either immediately after the injection or after 2, 5, 15, 30, or 60 min. Serum was frozen and saved for insulin radioimmunoassay.

Insulin release in vitro

Groups of 2–3 *ob/ob*-mouse islets or 10 lean mouse, rat, or hamster islets were preincubated at 37°C in 1 ml Krebs-Ringer bicarbonate medium (O_2 + CO_2, 95:5) containing 1 mg/ml bovine serum albumin and 3 mM D-glucose. Preincubation time was 30 min. The islets were moved to new vials and incubated 60 min in 300 µl medium with glucose and test substances added as indicated. 5-Hydroxytryptamine and L-5-hydroxytryptophan were from Sigma Chemical Co., MO, U.S.A. Incubation media were saved for later insulin assay using mouse insulin as standard. *Ob/ob*-mouse islets were freeze-dried and weighed.

Decarboxylase activity

Aromatic L-amino acid decarboxylase activity was measured in homogenates from *ob/ob*-mouse, rat, and hamster islets. The method has been described in detail [22]. Islets were homogenized and a sample saved for determination of protein content [41]. The rest of the homogenate was diluted in Krebs-Ringer medium buffered with Hepes + NaOH to pH 7.40. The incubation medium contained 0.5 mM ascorbic acid, 1 mM glucose, 1 mg/ml bovine serum albumin, and 10 μM pyridoxal phosphate. The final concentration of homogenate was 10–30 μg protein/100 μl medium. L-3,4-Dihydroxyphenyl [1-^{14}C]alanine (200 GBq/mol, Amersham International plc, U.K.) was added to give a concentration of 0.1 mM and the homogenate was incubated for 60 min at 37°C. Incubation was arrested by adding 100 μl 0.1 M HCl. The $^{14}CO_2$ formed was trapped in 1 M KOH in an outer via and the radioactivity was measured by liquid scintillation spectrometry.

Results

5-Hydroxytryptamine (5-HT) inhibits glucose-induced insulin release in *ob/ob*-mouse islets but the precursor amino acid for 5-HT, L-5-hydroxytryptophan (L-5-HTP), potentiates the effect of glucose. This is shown in Fig. 1 (data taken from Ref. 31). L-5-HTP also potentiates insulin release induced by L-leucine, glibenclamide, D,L-glyceraldehyde, and K^+ [37]. Fig. 2 shows that L-5-HTP stimulates insulin release in mice *in vivo*. Already 2 min after injection, serum insulin was higher in the group receiving 100 mg/kg L-5-HTP + 150 mg/kg

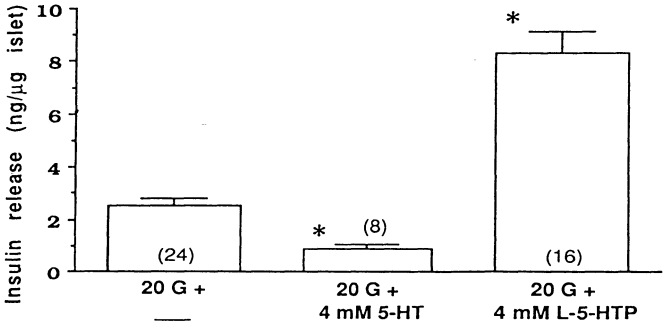

Fig. 1. Opposite effects of 5-hydroxytryptamine and L-5-hydroxytryptophan on glucose-induced insulin release in mouse pancreatic islets. Microdissected *ob/ob*-mouse islets were preincubated 30 min in basal medium with 3 mM D-glucose. They were then incubated 60 min at a stimulatory glucose concentration (20 mM, 20 G) and with 5-hydroxytryptamine (5-HT) or L-5-hydroxytryptophan (L-5-HTP) added as indicated. After incubation, islets were freeze-dried and weighed. Insulin release to the incubation medium is presented as means ± S.E. for the numbers of experiments given in parentheses. *P<0.01 when compared with 20 mM glucose alone (Student's t test for paired data).

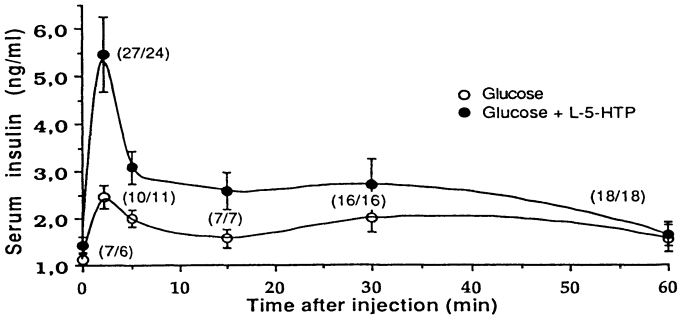

Fig. 2. Effect of L-5-hydroxytryptophan on serum insulin in mice. Lean mice were starved overnight. D-Glucose (150 mg/kg body weight) or D-glucose + L-5-HTP (100 mg/kg) was injected into a tail vein. Blood was collected by decapitation at various times after injection and serum insulin determined. Means ± S.E.M. for the numbers of experiments given in parentheses (glucose/glucose + L-5-HTP).

glucose ($P<0.001$ compared with mice receiving glucose alone). This effect of L-5-HTP *in vivo* lasted more than 30 min.

L-5-HTP is a good substrate for aromatic L-amino acid decarboxylase [42] and mouse islets contain high activity of this enzyme [22]. The decarboxylase blockers benserazide, α-monofluoromethyldopa, carbidopa, and NSD 1015, all inhibit the effect of L-5-HTP [34]. From this we concluded that the stimulatory effect of L-5-HTP on insulin secretion is coupled to decarboxylation [33,34]. Later studies showed that alternative metabolic pathways for L-5-HTP are probably not involved [36]. Two other substrates for the decarboxylase, *m*-tyosine and *o*-tyrosine, also potentiated glucose-induced insulin secretion but L-dihydroxyphenylalanine (L-DOPA) inhibited insulin release [34,37]. A synthetic decarboxylase substrate, E-ß-Fluoromethylene-*m*-tyrosine (MDL 72394) [43], has now been tested and was found to inhibit insulin release. *Ob/ob*-mouse islets incubated 60 min with 20 mM D-glucose released 1.33 ± 0.25 ng insulin/μg dry weight (n = 8). If 5 mM MDL 72394 was also added, the release was 0.60 ± 0.14 ng/μg ($P<0.005$ compared with 1.33 using Student's t test for paired data, n = 11). When islets were pretreated with 5 mM MDL 72394 during a 30 min preincubation, in subsequent incubations insulin release was 0.45 ± 0.07 ng/μg (n = 8) ($P<0.005$ compared with 1.33). Lower concentrations of MDL 72394 (0.1 and 1 mM) had no effect on insulin release.

It was of interest to see if a stimulatory effect of L-5-HTP on insulin release could also be observed in islets from other species. Fig. 3 shows that L-5-HTP potentiated glucose-induced insulin release in collagenase isolated islets from both obese hyperglycemic and lean mice. In contrast, L-5-HTP inhibited insulin release in islets from hamsters and had no effect in rat islets (Fig. 3). There are many possible explanations for this difference between species. Since the stimulatory effect of L-5-HTP is probably coupled to decarboxylation [33,34], the activity of the enzyme was measured in islets from mice, hamsters, and rats. The decarboxy-

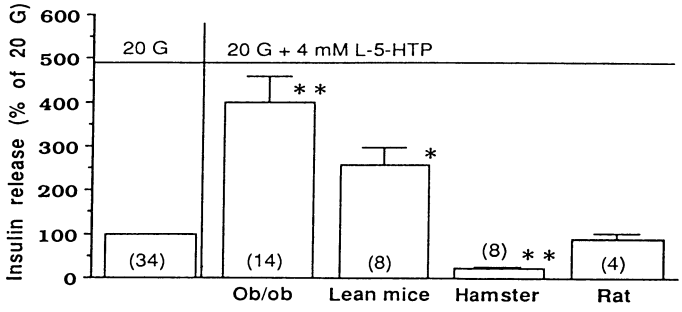

Fig. 3. Effect of L-5-hydroxytryptophan on glucose-induced insulin release in *ob/ob*-mouse, lean mouse, hamster, and rat pancreatic islets. Collagenase isolated islets were incubated 60 min with 20 mM D-glucose or 20 mM D-glucose + 4 mM L-5-HTP. Results are expressed as per cent of the insulin release obtained with 20 mM D-glucose alone in each individual experiment. Means ± S.E.M. for the numbers of experiments indicated. *P<0.02 and **P<0.005 when compared with 20 mM D-glucose alone (Student's t test for paired data).

lase activity was low in rat islets when compared with islets from mice and hamsters. Homogenates from *ob/ob*-mouse islets released 34.17 ± 3.52 (n = 8) nmol $^{14}CO_2$/mg protein when incubated with 0.1 mM ^{14}C-labelled L-DOPA. The decarboxylation rate was 29.41 ± 4.11 (n = 7) nmol/mg protein in hamster islet homogenates and 10.15 ± 1.72 (n = 4) nmol/mg protein in homogenates from rat islets (P<0.001 comparing 34.17 and 10.15, P<0.01 comparing 29.41 and 10.15).

Islets incorporate decarboxylase substrates and convert them to the corresponding amines [25,26,44]. The stimulatory effect of L-5-HTP on insulin release must therefore be the net result of a stimulatory effect of L-5-HTP and an inhibitory effect of 5-HT formed. Fig. 4 shows that pancreatic islets from hamsters are more sensitive than mouse islets to the inhibitory effect of 5-hydroxytryptamine.

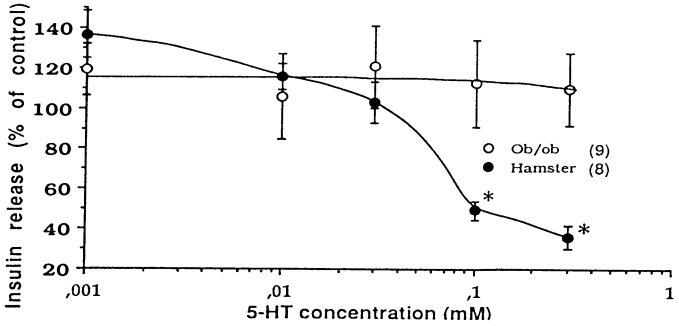

Fig. 4. Effect of 5-hydroxytryptamine on glucose-induced insulin release in *ob/ob*-mouse and hamster islets. Collagenase isolated islets were incubated 60 min with 20 mM glucose and different concentrations of 5-HT. Data are presented as per cent of the release in the presence of 20 mM D-glucose alone. Means ± S.E. *P<0.001 when compared with 20 mM D-glucose alone (paired data) and P<0.02 when compared with the corresponding values in *ob/ob*-mouse islets (independent observations).

Discussion

L-5-Hydroxytryptophan has a hypoglycemic effect in mice [45,46]. To a large extent, this effect may be caused by 5-HT accumulated in the liver [10]. Furman and Wilson [47] have shown that L-5-HTP induces a rise in serum insulin. We have found that L-5-HTP has only a small effect on insulin release in isolated mouse islets in the absence of other stimuli but strongly potentiates the effect of glucose and other secretagogues [31,37]. In support of a potentiating effect of L-5-HTP on glucose-induced insulin release and a role of insulin in the hypoglycemia response [47], it is here shown that L-5-HTP strongly increases serum insulin levels also when glucose is administered simultaneously. The highest value was obtained already two minutes after injection indicating that the effect of L-5-HTP *in vivo* is rapid.

L-5-HTP and other decarboxylase substrates potentiate the effect of several different insulin secretagogues with proposed different mechanisms of action [37]. It is therefore unlikely that L-5-HTP interacts with stimulus-recognition in the ß-cells. Decarboxylase substrates probably enhance some later step(s) in stimulus-secretion coupling or exocytosis. L-5-HTP has no effect on islet glucose metabolism [34] or glucose-induced changes in potassium fluxes (^{86}Rb) [48] but L-5-HTP stimulates islet ^{45}Ca uptake [31] and increases the alkalinization induced by glucose [49].

A number of amino acids and amino acid analogues stimulate insulin release. It cannot be excluded that the amino acid L-5-HTP is metabolized, and affects the ß-cells, by mechanisms other than decarboxylation. The finding that L-5-HTP and L-tryptophan potentiate glucose-induced insulin release through different mechanisms [36] argues against that possibility.

The decarboxylation product 5-hydroxytryptamine (5-HT) inhibits insulin release. The reason for the stimulatory effect of L-5-HTP is probably that increased turnover by aromatic L-amino acid decarboxylase potentiates the signal for insulin release remaining in the presence of 5-HT. This balance between a stimulatory effect of decarboxylation and an inhibitory effect of formed amines can be part of the explanation for the differences between species observed for the effect of L-5-HTP. When compared with islets from hamsters and rats, mouse islets show a high decarboxylase activity and a low sensitivity to 5-HT. The higher sensitivity of hamster islets to 5-HT is in accordance with Quickel *et al.* [50]. Dopamine is a strong inhibitor of insulin secretion in mouse islets, and this may explain why L-DOPA inhibits the effect of glucose [33].

The physiological role of the high decarboxylase activity in mouse islets is unclear. Islets do not form 5-HT from added tryptophan [25] and the serum content of decarboxylase substrates is probably low [51]. Decarboxylase inhibitors have no effect on glucose-induced insulin release (in the absence of decarboxylase substrates) in incubations for up to one hour [34]. We have data showing that insulin release is also not affected by prolonged inhibition of the decarboxylase in tissue culture (Lindström, in preparation).

m-Tyrosine potentiates insulin release induced by glucose [34] and L-leucine [37]. This effect is inhibited by decarboxylase blockers [37]. E-ß-Fluoromethylene-*m*-tyrosine (MDL 72394) is decarboxylated by aromatic L-amino acid decarboxylase in nerve endings into the corresponding *m*-tyramine [43]. E-ß-Fluoromethylene-*m*-tyramine is an inhibitor of monoamine oxidase [43]. We do not know if *m*- or *o*-tyramine have any effects on islets but *p*-tyramine inhibits insulin release [32]. We also do not know if islet cells take up and decarboxylate MDL 72394. However, one possible explanation for the opposite effects of *m*-tyrosine and MDL 72394 on insulin release could be that the tyramine formed from decarboxylation of MDL 72394 is accumulated in large amounts because of reduced metabolism through monoamine oxidase.

To summarize, increased turnover by aromatic L-amino acid decarboxylase stimulates insulin release in mouse islets. The net effect of decarboxylase substrates on insulin secretion is probably the sum of a stimulatory effect of decarboxylation and an inhibitory effect of formed amines. This balance between stimulatory and inhibitory effects may explain species differences in the effect of L-5-HTP and differences in the net effect of decarboxylase substrates.

Acknowledgements

E-ß-Fluoromethylene-*m*-tyrosine (MDL 72394) was a gift from Merrell Dow Research Institute, Strasbourg, France.

References

1. Hirai K and Gondo K (1927) Biochem. Zeitschr. 189: 92–100.
2. Correll JT, Lyth LF, Long S and Vanderpoel JC (1952) Am. J. Physiol. 169: 537–544.
3. Blundell JE (1979) In: Essman WB (ed.) Serotonin in Health and Disease, Vol 5. Spectrum Publications Inc., New York, pp. 403–450.
4. Leibowitz SF and Shor-Posner, G. (1986) Appetite 7 (suppl.): 1–14.
5. Rowland N and Stricker EM (1982) Physiol. Behav. 28: 271–277.
6. Arneric SP, Chow SA, Bhatnagar RK, Webb RL, Fischer LJ and Long JP (1984) Neuropharmacology 23: 137–147.
7. Levine RA, Pesch LA, Klatskin G and Giarman N (1964) J. Clin. Invest. 43: 797–809.
8. Schmidt MJ, Root MA and Hall JL (1983) Eur. J. Pharmacol. 90: 169–177.
9. Pernet A, Hammond VA, Blesa-Malpica G, Burrin J, Orskov H, Alberti KG and Johnston DG (1984) Eur. J. Clin. Pharmacol. 26: 23–28.
10. Endo Y (1985) Br. J. Pharmacol. 85: 591–598.
11. Yoshimura K, Hiroshige T and Itoh S (1969) Jpn. J. Physiol. 19: 176–186.
12. Smythe GA (1977) Clin. Endocrinol. 7: 325–341.
13. Melander, A. (1969) Acta Endocrinol. (Copenh.) 62: 565–576.
14. Ui M (1962) Endocrinol. Jpn. 9: 22–32.
15. Telib M, Raptis S, Schröder KE and Pfeiffer EF (1968) Diabetologia 4: 253–256.
16. Wong KK, Symchowicz S, Staub MS and Tabachnik IIA (1967) Life Sci. 6: 2285–2291.
17. Sundler F, Håkanson R, Lorén I and Lundquist I (1980) Invest. Cell Pathol. 3: 87–103.

18. Cegrell L (1968) Acta Physiol. Scand. suppl. 314: 1–60.
19. Bird JL, Wright EE and Feldman JM (1980) Diabetes 29: 304–308.
20. Lebovitz HE and Downs Jr. RW (1973) In: Usdin E (ed.) Frontiers in Catecholamine Research. Pergamon Press, New York, pp. 831–833.
21. Oie HK, Gazdar AF, Minna JD, Weir GC and Baylin SB (1983) Endocrinology 112: 1070–1075.
22. Lindström P (1986) Biochim. Biophys. Acta 884: 276–281.
23. Teitelman G, Lee JK and Alpert S (1987) Cell Tissue Res. 250: 435–439.
24. Teitelman G, Alpert S and Hanahan D (1988) Cell 52: 97–105.
25. Gylfe E, Hellman B, Sehlin J and Täljedal, I-B (1973) Endocrinology 93: 932–937.
26. Cegrell L, Falck B and Hellman B (1964) In: Brolin SE, Hellman B and Knutson H (eds.) The Structure and Metabolism of the Pancreatic Islets. Pergamon Press, Oxford, pp. 429–435.
27. Ericson LE, Håkanson R and Lundquist I (1977) Diabetologia 13: 117–124.
28. Tjälve H (1971) Acta Physiol. Scand. Suppl. 360: 1–122.
29. Boyd III AE, Lebovitz HE and Feldman JM (1971) J. Clin. Endocrinol. Metab. 33: 829–837.
30. Zern RT, Bird JL and Feldman JM (1980) Diabetologia 18: 341–346.
31. Lindström P and Sehlin J (1983) Diabetologia 24: 52–57.
32. Feldman JM, Boyd III AE and Lebovitz HE (1971) J. Pharmacol. Exp. Ther. 176: 611–621.
33. Lindström P (1982) Acta Biol. Med. Germ. 41: 1185–1190.
34. Lindström P and Sehlin J (1983) Endocrinology 112: 1524–1529.
35. Lindström P (1984) Acta Endocrinol. (Copenh.) 106: 248–253.
36. Lindström P and Sehlin J (1986) Mol. Cell. Endocrinol. 48: 121–126.
37. Lindström P and Sehlin J (1987) Acta Endocrinol. (Copenh.) 116: 21–26.
38. Hellerström C (1964) Acta Endocrinol. (Copenh.) 45: 122–132.
39. Moskalewski S (1965) Gen. Comp. Endocrinol. 5: 342–353.
40. Gotoh M, Maki T, Kiyoizumi T, Satomi S and Monaco AP (1985) Transplantation 40: 437–438.
41. Whitaker JR and Granum PE (1980) Anal. Biochem. 109: 156–159.
42. Lovenberg W, Weissbach H and Udenfriend S (1962) J. Biol. Chem. 237: 89–93.
43. Palfreyman MG, McDonald IA, Fozard JR, Mely Y, Sleight AJ, Zreika M, Wagner J, Bey P and Lewis PJ (1985) J. Neurochem. 45: 1850–1860.
44. Mahoney C and Feldman JM (1977) Diabetes 26: 257–261.
45. Lundquist I, Ekholm R and Ericson LE (1971) Diabetologia 7: 414–422.
46. Furman BL (1974) Br. J. Pharmacol. 50: 575–580.
47. Furman BL and Wilson GA (1980) Diabetologia 19: 386–390.
48. Lindström P and Sehlin J (1982) Biochim. Biophys. Acta 720: 400–404.
49. Lindström P and Sehlin J (1984) Biochem. J. 218: 887–892.
50. Quickel Jr. KE, Feldman JM and Lebovitz HE (1971) Endocrinology 89: 1295–1302.
51. Engbaek F and Magnussen I (1978) Clin. Chem. 24: 376–378.

Address for correspondence: Dr. P. Lindström, Department of Histology and Cell Biology, University of Umeå, S-901 87 Umeå, Sweden.

Polyamines in human lymphocytes

Sebastiano Colombatto, Barbara Fulgosi and Maria Angelica Grillo
Dipartimento di Medicina e Oncologia Sperimentale, Sezione di Biochimica, Università di Torino, Italy

Abstract

Human peripheral lymphocytes are able to synthesize and interconvert polyamines. Concanavalin A and calcium ionophore A23187 induce ornithine decarboxylase activity, whereas spermidine acetyltransferase (SAT) activity is not modified. *In vivo*, however, SAT activity is markedly modified, being increased in several pathological conditions. Polyamine concentration is increased in lymphocytes of patients with persistent generalized lymphadenopathy (PGL) and acquired immunodeficiency syndrome (AIDS).

Lymphocytes take up polyamines from the external medium with an energy dependent mechanism. Maximum uptake occurs with B cells, T cells being twentyfold less active. B cells also have a higher polyamine content and a higher SAT activity.

Introduction

Polyamines are organic cations. They are widely distributed in cells and essential for cell growth and differentiation [1]. Their synthesis starts from ornithine, which is formed from arginine by the action of arginase and then converted into putrescine by ornithine decarboxylase (ODC). Putrescine is transformed into spermidine, and afterwards into spermine in the presence of decarboxylated S-adenosylmethionine [formed by decarboxylation of S-adenosylmethionine by the action of S-adenosylmethionine decarboxylase (SAMDC)] and two different aminopropyl transferases.

Spermidine and spermine in turn can be acetylated by a cytosolic acetyl transferase (SAT) to N^1-acetyl derivatives. Polyamines are interconverted by oxidation on the part of polyamine oxidase (PAO), and terminally catabolised by diamine oxidase (DAO) (Fig. 1).

ODC, SAMDC and SAT are regulatory enzymes. ODC has been studied to the greatest extent. Its very rapid turnover rate means that its amount can be quickly modified by many stimuli, such as hormones and growth factors [2]. Moreover, its activity can be modified by induction of a high molecular weight inhibitor, called the ODC antizyme [3]. Post-translational modifications, namely phosphorylation [4] or transglutamination [5] have also been reported.

Polyamines are also present in blood, and their concentration is altered in many pathological conditions. They can be synthesized in lymphocytes, but here their regulation has only been extensively studied in beef or guinea pig cells. It has been shown that increase of ODC and SAMDC are early events in lymphocyte activa-

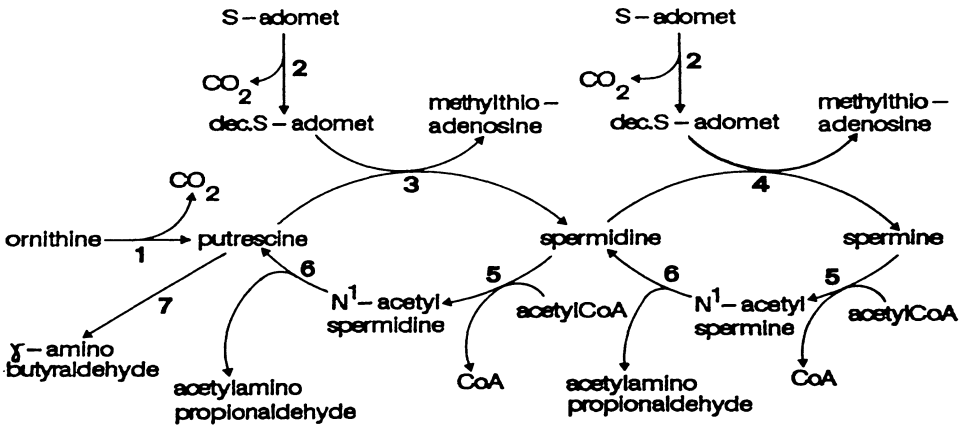

Fig. 1. Polyamine metabolism. 1. Ornithine decarboxylase; 2. S-adenosylmethionine decarboxylase; 3. spermidine synthase; 4. spermine synthase; 5. spermidine/spermine acetyltransferase; 6. polyamine oxidase; 7. diamine oxidase.

tion. Induction of ODC results from increases in both the level of ODC mRNA and the efficiency of its translation. The latter mode of control is due to an increase in the fraction of ODC mRNA associated with polysomes [6]. According to Otani *et al.* [7], both activation by diacylglycerol of Ca^{++}-activated phospholipid dependent protein kinase and a function dependent on calcium and calmodulin may be involved in induction of ODC in activated lymphocytes.

Other results by Otani *et al.* [8] suggest that a Ca^{++}-dependent pathway, other than that for protein kinase C, is essential for the induction of SAMDC, and that both a cAMP-dependent pathway and protein kinase C are involved in potentiation of the induction.

In bovine lymphocytes, SAT activity is also induced during lectin-activation, reaching its maximum after 48 h and already significant after 24 h [9]. Such induction occurs with two mechanisms: one dependent on protein kinase C, the other enhanced by cyclic AMP [10].

By contrast, in resting human lymphocytes ODC activity is very low. Putrescine and spermidine are known to inhibit ODC of lectin-stimulated lymphocytes. Inhibition is dependent on the continuation of protein synthesis, but does not require RNA synthesis [11].

Moreover, it has been shown that SAMDC is also active in resting conditions, and that spermidine can be transformed into putrescine via N^1-acetylspermidine. The diamine in turn may be further transformed into spermidine. Synthesis of new polyamines can occur during activation with lectins, but SAT activity is only modified later, so that the degradative enzymes appear to be of minor regulatory importance [12].

However, little is known about the mechanism of human lymphocyte polyamine regulation. We have therefore started to study the synthesis of polyamines and the mechanisms involved in the regulation of their concentration in human lymphocytes under normal and pathological conditions. Moreover, since cell polyamine concentration depends not only on synthesis, but also on transport into the cell from the external medium, we studied the mechanism of this transport into lymphocytes.

Experimental procedures

D,L-ornithine-1-^{14}C was obtained from New England Nuclear Co. (U.S.A.); ^{14}C-putrescine, ^{14}C-spermidine, ^{14}C-spermine, ^{14}C–acetylCoA from Amersham (U.K.); Ficoll-Hypaque from Pharmacia (Uppsala, Sweden) foetal calf serum, penicillin-streptomycin, RPMI 1640 with glutamine from Flow Laboratories (Irvine, U.K.); gentamicin from Schering (U.S.A.); Concanavalin A (Con A) and phytohemagglutinin (PHA) from Sigma (U.S.A.); Leu 4(CD3) and Leu 12 (CD19) MoAb and fluorescein-conjugated goat anti-mouse immunoglobulin from Becton and Dickinson (Mountain View, Ca., U.S.A.). α-difluoromethylornithine was a generous gift from the Centre de Recherche Merrell International (Strasbourg, France). All other chemicals were of analytical reagent grade.

Lymphocytes were prepared from human blood packs by Ficoll-Hypaque gradient centrifugation and washed several times. When cells were incubated with other compounds, they were suspended in RPMI 1640 (containing 10% foetal calf serum, penicillin (100 units/ml), streptomycin (100 μg/ml), gentamicin (50 μg/ml), counted and diluted to 2×10^6cells/ml. Four ml samples were placed in plastic Petri dishes and incubated at 37°C under 5% CO_2 in air in a humidified incubator. In some experiments foetal calf serum was replaced by human serum (with similar results).

T and B cell preparation

Suspensions depleted of macrophages by the adherence method were enriched in T cells by rosetting at 29°C [13]. Enriched B cell populations were obtained by collecting non-rosetting lymphocytes at the interface after density gradient centrifugation. In some experiments, non-rosetting populations were further purified by depletion of NK cells [14]. Purity of T cell and B cell preparations was determined by indirect immunofluorescence, using Leu 4 (CD3) and Leu 12 (CD19) MoAbs and fluorescein-conjugated goat anti-mouse immunoglobulin as the second layer. T cell preparations were always 90% pure; B cell preparations were 40% pure after rosetting and 70% pure after further purification. Cell viability was determined microscopically with trypan blue.

For polyamine assay, cells were treated with 0.2 M $HClO_4$; aliquots of the clear acid extract were dansylated overnight and polyamines were separated by HPLC according to Stefanelli *et al.* [15].

To measure SAT activity, cells were treated with Triton X-100 (5% final concentration). The supernatant obtained by centrifugation was used to measure enzyme activity according to Libby [16] by measuring the incorporation of (acetyl-1-^{14}C)acetylCoA into acetylspermidine. The incubation was 4 min at 30°C [17].

For the assay of ODC in cells in culture, the non-adherent cells were collected, washed with ice-cold phosphate saline solution (0.8% NaCl, 0.02% KCl, 0.115% Na_2HPO_4, 0.02% KH_2PO_4, at pH 7.2), resuspended in 0.7 ml of 0.15 mM Tris, at pH 7.2, containing 0.4 mM pyridoxal phosphate and 10 mM dithiothreitol. After freezing and thawing 3 times at –40°C, the suspension was centrifuged for 10 min at 3,000 rpm. 0.5 ml of the supernatant were added to 1 μCi of D,L-ornithine-1-^{14}C (48 mCi/mmol). $^{14}CO_2$ was collected during 60 min incubation at 37°C [18].

Polyamine uptake

After 15 h preincubation, radioactive putrescine, spermidine or spermine (0.1 μCi, 0.1 mM final concentration) was added and incubation continued for the desired time. For the radioactivity uptake assay, cells were collected by centrifugation, washed twice with cold phosphate-saline (pH 7.2) and extracted with 0.2 N $HClO_4$. After freezing and thawing, the samples were centrifuged and radioactivity measured in part of the supernatant. Another part was dansylated and processed by HPLC. To measure radioactivity of the separated polyamines, their corresponding peaks and that for N^1-acetylspermidine were collected and counted.

Protein was measured according to Lowry *et al.* [19].

Results

Polyamine metabolism in human lymphocytes

ODC activity is very low in resting lymphocytes. When they are cultured for 48 h in the presence of a lectin, it rises to a maximum at 21 h, but is again low at 48 h (Fig. 2), as reported by Korpela *et al.* [12]. The rate of ODC induction is much faster in bovine lymphocytes, rising to a maximum after only 11 h, followed by a fast decrease to normal values [20]. Calcium ionophore A23187 promotes activation of ODC activity in both guinea pig [21] and human lymphocytes (Table 1).

Table 1. Effect of ionophore A 23187 on lymphocyte ODC activity

Addition	Activity (pmoles/10^7 cells/h)
None	1409
A 23187	2527

Each value is the mean of duplicate experiments.

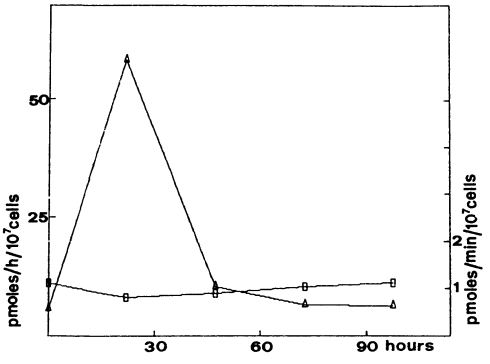

Fig. 2. Effect of a lectin on ornithine decarboxylase and spermidine acetyltransferase activity of human lymphocytes. Cells were cultured with phytohemagglutinin (10 µg/ml) for the time shown before measuring enzyme activity as described. Δ——Δ, ornithine decarboxylase activity (pmoles/h/10^7 cells); ❑——❑, spermidine acetyltransferase activity (pmoles/min/10^7 cells).

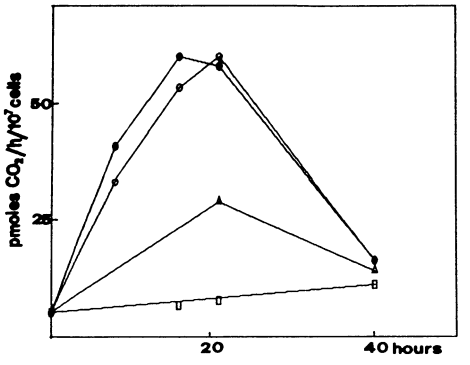

Fig. 3. Effect of selenite on ornithine decarboxylase induction by a lectin. Cells were cultured with phytohemagglutinin (10 µg/ml) in the presence or in the absence of selenite for the time shown before measuring enzyme activity as described. ○——○, PHA; ●——●, PHA and 3 µM selenite; ▲——▲, PHA and 12 µM selenite; ❑——❑, PHA and 60 µM selenite.

Selenite, which we had shown to promote an increase of ODC activity in chicken liver and a decrease in the bursa of Fabricius, was also tested. In lymphocytes in culture, the rate of ODC induction was enhanced by 3 µM selenite, but inhibited by 12 µM selenite (Fig. 3). The mechanism of this modification is not clear. In chicken spleen cells, we have shown [22] that propranolol, a ß-antagonist, partially counteracts the effect of selenite on ODC, showing that ß-receptors are involved. Participation of adrenergic receptors in the effect of selenite is also suggested by the desensitization offered by TPA, similar to that observed with epinephrine.

Table 2. Spermidine acetyltransferase activity in lymphocytes from normal subjects and subjects with various diseases

	Activity (pmoles/10^7 cells/min)
Normal subjects	1.13 ± 0.10 (14)
Psoriasis	2.00 ± 0.19 (8)[a]
Chronic lymphocytic leukemia B	3.41 ± 0.31 (6)[b]
Chronic lymphocytic leukemia T	2.93 ± 0.17 (4)[b]
Sézary syndrome	1.03 ± 0.12 (3)
Acute hepatitis (A and B)	3.74 ± 0.58 (7)[b]
PGL	3.19 ± 0.44 (6)[b]

In comparison with normal subjects p: [a]≤0.01; [b]≤0.001.

Table 3. Polyamines in mixed populations of lymphocytes from normal subjects and anti-HIV positive patients with PGL or AIDS

Subjects	No	Putrescine	Spermidine	Spermine
		pmoles/mg protein		
normals	10	191 ± 20	756 ± 52	1814 ± 138
PGL	12	294 ± 66	1906 ± 222	3894 ± 316
AIDS	16	805 ± 139	1751 ± 214	3648 ± 460

In contrast to bovine lymphocytes, SAT activity of human lymphocytes is not modified by culturing with a lectin (PHA) (Fig. 1) or in the presence of A 23187 (not shown).

As, in contrast with ODC, SAT is active in quiescent cells, it could be responsible for the marked modification in mononuclear cell spermine/spermidine ratio observed in a few patients [23]. SAT activity was therefore measured in normal lymphocytes and in those known to have an altered spermine/spermidine ratio (chronic lymphocytic leukemia) and in other diseases. The results are shown in Table 2. In subjects with psoriasis, SAT activity was markedly increased (+70%). ODC and SAMDC activities were not significantly altered, in contrast with the picture in the epidermis during psoriasis. A much higher increase in SAT activity was noted in chronic lymphatic leukemia T (+148%) and B (+189%) together with the greatest change in the spermine/spermidine ratio in one of these subjects (7.48 vs. 1.94.). SAT activity was unchanged in the Sézary syndrome (malignant proliferation of a subpopulation of T lymphocytes). Patients examined at the clinical onset of acute viral hepatitis (A and B), for which immunoregulatory defects have also been reported, displayed an even higher increase (+224%). Once again, ODC and SAMDC activities were not significantly altered. In lymphocytes from anti-HIV positive patients with persistent generalized lymphadenopathy (PGL) the activity was also markedly altered.

We have recently found that polyamines are also increased in mixed populations of lymphocytes of patients with antibodies against the immunodeficiency virus (HIV) and PGL. The modifications are similar for spermidine and spermine in

Table 4. Polyamine content in T and B lymphocytes

	Putrescine	Spermidine	Spermine
		pmoles/10^6 cells	
T cells	27 ± 9	65 ± 12	184 ± 7
B cell enriched preparation	59 ± 11	139 ± 20	338 ± 11

The data are the average of 4 different assays. Significance: $p \leq 0.1$ for putrescine; $p \leq 0.01$ for spermidine and spermine.

Table 5. Effect of Con A on ODC activity of T and B lymphocytes

Time in culture	Con A	ODC activity	
		T cells	B cells
		pmoles/10^7 cells/h	
21	–	7.8	19.4
48	–	17.4	5.3
21	+	22.5	51.5
48	+	44.1	32.0

Cells were cultured in the presence or in the absence of 10 μg Con A/ml before measuring ODC activity. Each value is the mean of duplicate experiments.

patients with overt AIDS, while putrescine is increased still further (4.2 vs 1.6 times) (Table 3). The mechanism of these modifications is under study.

Further experiments examining the distribution of polyamines and some enzymes involved in their metabolism in lymphocyte subpopulations, showed that polyamines are present in both B and, to a lesser extent, T cells (Table 4). ODC activity is present in both subsets. Con A increased ODC activity in both cases, though the rate of induction was higher in B cells (Table 5). Spermidine acetyltransferase activity is also more active in the B cells (average of three experiments 0.94 and 0.22 pmoles acetylspermidine formed/10^7 cells/min, respectively), where it is also differently regulated [24].

Polyamine uptake

Lymphocytes also take up polyamines from the external medium. This is an energy-dependent process as it is inhibited by 1 mM dinitrophenol. The effect

Table 6. Energy dependence of polyamine uptake by human lymphocytes. Effect of ionophore A 23187

Addition	Concentration	Uptake	
		spermidine	spermine
None		100	100
2,4-Dinitrophenol	1 mM	60	57
Ouabain	0.15 mM	48	40
Vanadate	1 mM	–	0
Amyloride	1 mM	–	0
A 23187	2 μM	100	–

Cells were incubated in the presence or absence of the inhibitors at the final concentration shown for 30 min; then ^{14}C-spermidine or ^{14}C-spermine (0.1 mM final concentration) was added and radioactivity taken up measured after 4 h.

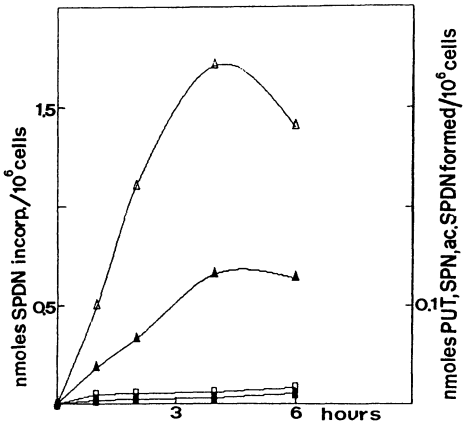

Fig. 4. Radioactive compounds in human lymphocytes incubated with ^{14}C-spermidine. Cells were incubated with 0.1 mM ^{14}C-spermidine for the time shown, then extracted with 0.2 M $HClO_4$. After dansylation, polyamines were separated by HPLC. Peaks containing the polyamines were collected and counted. ❑——❑, putrescine; Δ——Δ, spermidine; ■——■, spermine; ▲——▲, N^1-acetylspermidine.

promoted by ouabain, amyloride and vanadate, all inhibitors of Na^+/K^+ ATPase, shows that the transport is dependent on Na^+ (Table 6).

With 0.1 mM ^{14}C-spermidine, maximum radioactivity inside the cell is obtained after 4 h incubation. The subsequent slow decrease suggests that polyamines are excreted (Fig. 4).

When the rate of uptake is measured with B and T cell preparations, a twentyfold higher transport rate is measured with B cell enriched preparations. However, activity is much higher with the mixed population, suggesting that both B and T cells are necessary for maximum uptake (Table 7).

In non-T lymphocytes, the destiny of ^{14}C-spermidine taken up was followed during culture for 6 h. As shown in Fig. 5A, spermidine is actively taken up and a peak is reached in this experiment after 2 h, during which there is a sixfold increase of spermidine intracellular concentration. Afterwards, the concentration decreases. In the meantime, spermine concentration keeps decreasing, being probably catabolized (Fig. 5B). When radioactivity was measured in the same samples, a similar

Table 7. Uptake of spermidine by B and T lymphocytes

	Uptake (pmoles/10^6 cells/h)
T cells	15 ± 2
B cell enriched population	409 ± 79

The data are the average of 4 different assays.

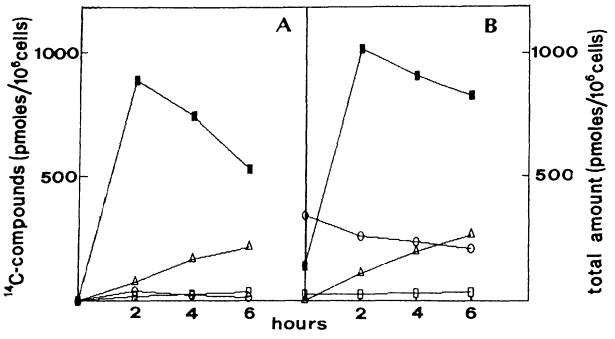

Fig. 5. Radioactive polyamines (A) and total polyamine content (B) in human non-T lymphocytes incubated with ^{14}C-spermidine. Cells incubated with 0.1 mM ^{14}C-spermidine for the time shown were extracted with 0.2 M $HClO_4$, dansylated and analysed by HPLC. Peaks containing the polyamines were collected and counted. ❑——❑, putrescine; ■——■, spermidine; ○——○, spermine; Δ——Δ, N^1-acetylspermidine.

pattern was observed for spermidine. Practically no radioactivity is accumulated in spermine, while it is in N^1-acetylspermidine, which is also accumulated.

Conclusions

It thus appears that human peripheral lymphocytes synthesize and interconvert polyamines, and also take them up from the external medium. Polyamine content is modified in pathological conditions, such as PGL and AIDS. Interestingly, polyamine concentration is higher in B cells, where higher values of thymidine and valine incorporation were also shown [25]. As the role of polyamines in nucleic acids and in protein synthesis is well known, their higher concentration can suggest their importance for the B lymphocytes in these pathways. Of the enzymes which participate in polyamine metabolism, spermidine acetyltransferase was also shown to be modified in several viral and non-viral diseases. Cells with more endogenous polyamines, moreover, also have a higher ability to take them up from the external medium. The function of this energy-dependent transport system is not known. Further experiments will show whether it is also modified in pathological conditions.

References

1. Pegg AE (1986) Biochem. J. 234: 249–262.
2. Bachrach U (1984) Cell Biochem. Funct. 2: 6–10.
3. Heller JS, Fong WS and Canellakis ES (1976) Proc. Natl. Acad. Sci. 73: 1858–1862.

4. Meggio F, Flamigni F, Guarnieri C and Pinna LA (1987) Biochim. Biophys. Acta 929: 114–116.
5. Russell DH (1981) Biochim. Biophys. Res. Commun. 99: 1167–1172.
6. White MW, Kameji T, Pegg AE and Morris DR (1987) Eur. J. Biochem. 170: 87–92.
7. Otani S, Matsui I, Kuramoto A and Morisawa S (1985) Eur. J. Biochem. 147: 27–31.
8. Otani S, Matsui-Yuasa I, Mimura-Shimazu Y and Morisawa S (1988) Eur. J. Biochem. 171: 509–513.
9. Matsui I, Otani S, Kuramoto A, Morisawa S and Pegg AE (1983) J. Biochem. 93: 961–966.
10. Matsui-Yuasa I, Otani S, Yukioka K, Goto H and Morisawa S (1989) Arch. Biochem. Biophys. 268: 209–214.
11. Kay JE and Lindsay VJ (1973) Biochem. J. 132: 791–796.
12. Korpela H, Hölttä E, Hovi T and Jänne J (1981) Biochem. J. 196: 733–738.
13. West WH, Cannon GB, Kay HD, Bonnard GD and Herberman RB (1977) J. Immunol. 118: 355–361.
14. Dianzani U, Massaia M, Pileri A, Grossi CE and Clement LT (1986) J. Immunol. 137: 484–490.
15. Stefanelli C, Carati D and Rossoni C (1986) J. Chromat. 375: 49–55.
16. Libby PR (1978) J. Biol. Chem. 253: 233–237.
17. Grillo MA (1983) In: Bachrach U, Kaye A and Chayen R (eds.) Advances in Polyamine Research. Raven Press, New York, pp. 321–330.
18. Jänne J and Williams-Ashman HG (1971) J. Biol. Chem. 246: 1725–1732.
19. Lowry OH, Rosebrough NJ, Farr AL and Randall RJ (1951) J. Biol. Chem. 193: 265–275.
20. Kakinuma Y, Hoshino K and Igarashi K (1988) Eur. J. Biochem. 176: 409–414.
21. Otani S, Matsui-Yuasa I, Hashikawa K, Kasai S, Matsui K and Morisawa S (1985) Biochim. Biophys. Res. Commun. 130: 389–395.
22. Colombatto S, Fasulo L and Grillo MA (1989) Int. J. Biochem. 21: 1197–1201.
23. Cooper KD, Shukla JB and Rennert OM (1978) Clin. Chim. Acta 82: 1–7.
24. De Agostini M, Colombatto S and Dianzani U (1986) In: Biomedical Studies of Natural Polyamines. Caldarera CM, Clò C and Guarnieri C (eds.) CLUEB, Bologna, pp. 229–232.
25. Hrabak A, Szabo MT and Antoni F (1985) Int. J. Biochem. 17: 113–117.

Modulation of amino acid-induced insulin and glucagon secretion by the hepatic vagus nerve in the rat

Katsuaki Tanaka, Shuji Inoue, Hajime Nagase and Yutaro Takamura

The Third Department of Internal Medicine, Yokohama City University School of Medicine, Urafune-cho, Yokohama 232, Japan

Abstract

The present study was carried out to examine the effect of the hepatic branch of the vagus nerve on the secretion of insulin and glucagon after intraperitoneal injection of L-arginine, L-alanine, and L-leucine in rats. Sectioning of the hepatic branch of the vagus nerve enhanced both plasma insulin and glucagon secretion compared to that in sham-operated (control) rats after intraperitoneal arginine. Sectioning of the hepatic branch of the vagus nerve enhanced plasma glucagon secretion after intraperitoneal alanine, and plasma insulin secretion after intraperitoneal leucine compared to that in sham-operated rats. The results suggest that the hepatic branch of the vagus nerve inhibits arginine-induced insulin and glucagon secretion, alanine-induced glucagon secretion, and leucine-induced insulin secretion. The existence of 'sensors' in the liver for arginine, alanine, and leucine is proposed as an explanation for the inhibition of the secretion of insulin and/or glucagon by the hepatic vagus nerve.

Introduction

Although a number of reports that vagal neural efferent pathways to the pancreatic islets modulate the secretion of insulin and glucagon have been published [1,2], afferent pathways which might affect this system have received little attention. Recently, Lee and Miller [3] demonstrated that acute sectioning of the hepatic vagus nerve caused an increase in plasma insulin concentrations and that electrical stimulation of the central end of the hepatic branch of the vagus nerve suppressed the concentration of plasma insulin compared to sham-stimulated controls. Sectioning of the celiac vagal branches to the pancreas abolished these changes. More recently, we found that intraperitoneal arginine enhanced both plasma insulin and glucagon concentrations more in hepatic-vagotomized than in sham-vagotomized rats [4]. Since the hepatic branch of the vagus nerve consists mostly of afferent fibers in the rat [5,6], we have advanced a working hypothesis that nerve sensors in the liver sense nutrient arginine and convey this information over afferent vagal nerves to the brainstem from which neural efferent pathways alter the secretion of insulin and glucagon. This hypothesis is supported by our recent electrophysiological proof [7] that arginine sensors exist in the liver and that administration of arginine into the portal vein causes a reflex inhibition of pancreatic vagus nerve activity.

It was reported that administration of amino acids besides arginine enhanced insulin and glucagon secretion [8,9]. The present study was designed to test the working hypothesis that afferent information in the hepatic vagus nerve for other amino acids besides arginine in the hepato-portal system influences insulin and glucagon release from the pancreas after amino acids stimulation.

Materials and Methods

Animals

Sixteen-week-old female Sprague-Dawley rats weighing 260–280 g were housed individually in wire-bottomed stainless steel cages and exposed to 12 h light-dark cycles at constant temperature (23 ± 2°C). The rats were allowed free access to laboratory chow and water except the night before the experiment. Three to 5 days before the experiment, the rats were handled frequently to keep experiment-associated stress to a minimum.

Surgery and cannulation

Three days before the experiment, surgery was performed under hexobarbital anesthesia (50 mg/kg body wt). Hepatic vagotomy was performed as previously described [4]. Sham vagotomy achieved the same surgical damage except sectioning of the vagus nerve. After surgery, a catheter [Silastic and polyethylene tubing (PE-50)] was inserted into the right atrium of the heart by the method of Steffens [10]. After cannulation, the rats were returned to their cages and allowed free access to food and water.

Experimental procedures

Three experiments were performed.

Experiment 1

Effect of hepatic vagotomy on plasma glucose, insulin, and glucagon concentrations after intraperitoneal arginine (1 g/kg body wt). Two groups of 8 animals each were prepared: 1) a group of hepatic-vagotomized rats, and 2) a group of sham-vagotomized (control) rats.

Experiment 2

Effect of hepatic vagotomy on plasma glucose, insulin, and glucagon concentrations after intraperitoneal alanine (0.5 g/kg body wt). Two groups of 6 animals

each were prepared: 1) a group of hepatic-vagotomized rats, and 2) a group of sham-vagotomized (control) rats.

Experiment 3

Effect of hepatic vagotomy on plasma glucose, insulin, and glucagon concentrations after intraperitoneal leucine (0.3 g/kg body wt). Two groups of 7 animals each were prepared: 1) a group of hepatic-vagotomized rats, and 2) a group of sham-vagotomized (control) rats.

Three days after the surgery, intraperitoneal amino acid tests were performed after 16 h overnight food deprivation. L-arginine solution (1 g/kg body wt), L-alanine solution (0.5 g/kg body wt), and L-leucine solution (0.3 g/kg body wt) were injected intraperitoneally in each experiment. For glucose and hormone determinations, 0.9 ml of blood was withdrawn from the right atrium through the cardiac catheter with a heparinized syringe before (0 min) and 5, 10, 15, 30, and 60 min after the injection and poured into a glass tube containing 1000 U of Trasylol. The blood samples were chilled in ice and plasma was separated immediately after the completion of the experiments. The plasma was stored at −80°C until the assay.

Assay

Glucose was measured in a Beckman glucose analyzer employing the glucose oxidase method. Immunoreactive insulin was measured by the modified double antibody method of Hales and Randle [11] using rat insulin as a standard (insulin assay kit, Amersham, Japan). Immunoreactive glucagon was measured by the method of Imagawa *et al.* [12] using a specific antiserum for pancreatic glucagon and porcine glucagon standards (Glucagon assay kit, Daiichi Radioisotope Labs., Japan).

Statistical analysis

Data were expressed as means ± SE. The Student's t-test was employed for statistical analysis. The level of significance was $p<0.05$.

Results

Experiment 1

There were no significant differences in the change of body weights between the two experimental groups three days after the operations (259.6 ± 5.1 g in hepatic-vagotomized rats, and 268.4 ± 11.1 g in sham-vagotomized rats). Plasma insulin and glucagon concentrations after intraperitoneal injection of arginine in hepatic-

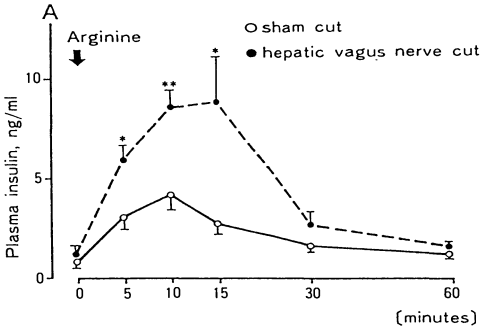

Fig. 1A. Time course of plasma insulin responses to i.p. arginine. Closed circles, hepatic-vagotomized rats; open circles, sham-vagotomized rats. Each point is mean ± SE, n=8. *p<0.05, **p<0.01 compared with sham-vagotomized rats.

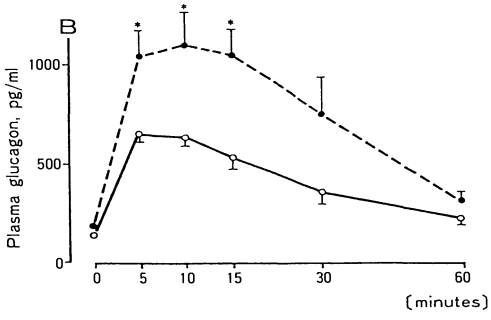

Fig. 1B. Time course of plasma glucagon responses to i.p. arginine. Closed circles, hepatic-vagotomized rats; open circles, sham-vagotomized rats. Each point is mean ± SE, n = 8. *p<0.05 compared with sham-vagotomized rats.

vagotomized and sham-vagotomized rats are shown in Fig. 1. Plasma glucose concentrations after arginine stimulation were slightly lower in hepatic-vagotomized rats than in sham-vagotomized rats, but there were no significant differences between the two groups (data not shown). Plasma insulin in hepatic-vagotomized rats resulted in a significant elevation at 5, 10, and 15 min as compared to that of sham-vagotomized rats at corresponding time (Fig. 1A). Plasma glucagon in hepatic-vagotomized rats resulted in a significant elevation at 5, 10, and 15 min compared to that of sham-vagotomized rats at corresponding time (Fig. 1B). There were no significant differences in the basal glucose, insulin, and glucagon concentrations between the two groups.

Experiment 2

Plasma insulin and glucagon concentrations after intraperitoneal injection of alanine in hepatic-vagotomized and sham-vagotomized rats are shown in Table 1. Plasma glucose concentrations after alanine stimulation were not significantly different between the two groups at any time (data not shown). There were no significant differences in plasma insulin concentrations at any time between the two groups. Plasma glucagon in hepatic-vagotomized rats resulted in a significant elevation at 10, 15, and 30 min compared to that of sham-vagotomized rats at corresponding time. There were no significant differences in the basal glucose, insulin, and glucagon concentrations between the two groups.

Experiment 3

Plasma insulin and glucagon concentrations after intraperitoneal injection of leucine in hepatic-vagotomized and sham-vagotomized rats are shown in Table 2.

Table 1. Effect of hepatic vagotomy on insulin and glucagon concentrations after intraperitoneal injection of alanine

	Time (minutes)					
	0	*5*	*10*	*15*	*30*	*60*
			Insulin (ng/ml)			
Sham-vagotomized rats	0.7 ± 0.1	1.1 ± 0.2	1.0 ± 0.3	1.2 ± 0.3	1.7 ± 0.6	0.9 ± 0.1
Hepatic-vagotomized rats	0.8 ± 0.2	1.2 ± 0.1	1.1 ± 0.2	1.0 ± 0.2	1.0 ± 0.2	1.2 ± 0.2
			Glucagon (pg/ml)			
Sham-vagotomized rats	90 ± 13	225 ± 18	206 ± 11	238 ± 32	202 ± 25	226 ± 99
Hepatic-vagotomized rats	76 ± 12	299 ± 51	350 ± 33[a]	388 ± 31[b]	360 ± 51[b]	413 ± 102

Values are means ± SE, n = 6.
[a]$p<0.01$; [b]$p<0.05$ compared with sham-vagotomized rats.

Table 2. Effect of hepatic vagotomy on insulin and glucagon concentrations after intraperitoneal injection of leucine

	Time (minutes)					
	0	*5*	*10*	*15*	*30*	*60*
			Insulin (ng/ml)			
Sham-vagotomized rats	1.2 ± 0.2	1.9 ± 0.2	3.0 ± 0.3	2.7 ± 0.4	1.9 ± 0.3	1.0 ± 0.2
Hepatic-vagotomized rats	1.1 ± 0.1	3.2 ± 0.3[b]	5.2 ± 0.7[b]	4.4 ± 0.6[a]	2.4 ± 0.4	1.4 ± 0.4
			Glucagon (pg/ml)			
Sham-vagotomized rats	116 ± 17	324 ± 41	280 ± 33	264 ± 41	244 ± 20	267 ± 15
Hepatic-vagotomized rats	109 ± 9	286 ± 46	273 ± 34	256 ± 30	267 ± 44	313 ± 56

Values are means ± SE, n = 7.
[a]$p<0.05$; [b]$p<0.02$ compared with sham-vagotomized rats.

Plasma glucose concentrations after leucine stimulation showed no significant differences at any time between the two groups (data not shown). Plasma insulin in hepatic-vagotomized rats resulted in a significant elevation at 5, 10, and 15 min compared to that of sham-vagotomized rats at corresponding time. There were no significant differences in plasma glucagon concentrations at any times between the two groups. There were no significant differences in the basal glucose, insulin, and glucagon concentrations between the two groups.

Discussion

We demonstrated that arginine, alanine, and leucine stimulation in hepatic-vagotomized rats is followed by a marked rise in circulating insulin and/or glucagon levels compared to those in sham-vagotomized rats.

The enhancement of insulin and glucagon secretion by arginine after hepatic vagotomy confirmed our previous study [4]. The results might be explained by the existence of neural arginine sensors in the liver, and hepatic vagal afferent fibers from arginine sensors might exert inhibition on the efferent pancreatic neuroendocrine system through brainstem centers after arginine stimulation. Hepatic vagotomy would remove this inhibition and would increase insulin and glucagon secretion from pancreatic islets. This concept is consistent with our recent electrophysiological proof [7] that arginine sensors exist in the liver and that administration of arginine into the portal vein causes a reflex inhibition of pancreatic vagus nerve activity.

The enhancement of insulin and/or glucagon secretion by alanine and leucine after hepatic vagotomy might also be explained by the existence of 'sensors' in the liver for alanine and leucine.

This explanation is based on the fact that there is behavioral and electrophysiological evidence for neural metabolic receptors in the liver [7,13–16]. Russek [17] suggested the existence of vagal glucoreceptors in the liver on the basis of behavioral studies. Niijima [14] found an inverse correlation between portal venous glucose concentrations and afferent hepatic vagal nerve activity. Niijima [15] further observed that injection of glucose into the portal vein increased efferent activity of the pancreatic vagus nerve in the guinea pig. Lee and Miller [3] demonstrated that intraperitoneal glucose enhanced plasma insulin less in hepatic-vagotomized than in sham-vagotomized rats.

The effect of hepatic vagotomy on amino acids-induced insulin secretion seemed to have an effect opposite to that on glucose-induced insulin secretion reported by Lee and Miller [3], since amino acids-induced insulin and/or glucagon secretion was enhanced by hepatic vagotomy. This difference was confirmed by electrophysiological studies that activity of hepatic vagal afferents reduced after intraportal glucose [14], on the other hand, increased after intraportal arginine [7]. In these circumstances, we may hypothesize that nerve sensors in the liver sense nutrient amino acids (arginine, alanine, and leucine) and convey this information

over afferent vagal nerves to the brainstem from which neural efferent pathways alter the secretion of insulin and glucagon. Regarding to alanine and leucine, electrophysiological studies are needed to clarify this possibility.

There may be another possibility that the enhancement of insulin and/or glucagon secretion by amino acids after hepatic vagotomy could be due to modulation of the liver metabolism of amino acids by the vagotomy, and consequently a high concentration of amino acids in hepatic-vagotomized rats would increase insulin and/or glucagon secretion. The explanation is based on the fact that vagal activation affects hepatic metabolism [18], and it is possible that hepatic-vagotomy may produce its effects by modulating the liver metabolism of amino acids. However, hepatic vagotomy did not alter plasma amino acids concentrations after intraperitoneal arginine, alanine, and leucine respectively (unpublished observation). Consequently, it is implausible that hepatic vagotomy modulates amino acids metabolism in the liver.

In conclusion, we might explain the results of the present study as follows: 1) The hepatic branch of the vagus nerve inhibits arginine-, alanine-, and leucine-induced insulin and/or glucagon secretion. 2) The existence of 'sensors' in the liver for alanine and leucine, as same as arginine-sensors [4,7], is hypothesized as an explanation for the inhibition of the secretion of insulin and/or glucagon by the hepatic vagus nerve.

References

1. Miller RE (1981) Endocrine Rev. 2: 471–494.
2. Woods SC and Porte D Jr. (1974) Physiol. Rev. 54: 596–619.
3. Lee KC and Miller RE (1985) Endocrinology 117: 307–314.
4. Tanaka K, Inoue S, Fujii T and Takamura Y (1986) Neurosci. Lett. 72: 74–78.
5. Adachi A, Niijima A and Jacobs HL (1976) Am. J. Physiol. 231(4): 1043–1049.
6. Magni F and Carobi C (1983) J. Auton. Nerv. Syst. 8: 237–260.
7. Tanaka K, Inoue S, Takamura Y, Jiang Z-Y and Niijima A (1986) Neurosci. Lett. 72: 69–73.
8. Assan R, Rosselin G and Dolais J (1967) Ann. Diabetol. Hôtel Dieu 7: 25–41.
9. Floyd JC Jr., Fajans SS, Conn JW, Knopf RF and Rull J (1966) J. Clin. Invest. 45: 1487–1502.
10. Steffens AB (1969) Physiol. Behav. 4: 833–836.
11. Hales CN and Randle PJ (1963) Biochem. J. 90: 620–624.
12. Imagawa K, Nishino T, Shin S, Uehara S, Hashimura E, Yanaihara C and Yanaihara N (1979) Endocrinol. Jpn. 26: 123–131.
13. Lautt WW (1980) Can. J. Physiol. Pharmacol. 58: 105–123.
14. Niijima A (1969) Ann. N.Y. Acad. Sci. 157: 690–700.
15. Niijima A (1977) In: Katsuki Y (ed.) Food Intake and Chemical Senses. Japan Scientific Societies Press, Tokyo, pp. 413–426.
16. Sawchenko PE and Friedman MI (1979) Am. J. Physiol. 236 (Regulatory Integrative Comp. Physiol. 5): R5–R20.
17. Russek M (1963) Nature (Lond) 197: 79–80.
18. Shimazu T (1967) Science 156: 1256–1257.

Address for correspondence: Dr. Katsuaki Tanaka, The Third Department of Internal Medicine, Yokohama City University School of Medicine, 3–46 Urafune-cho, Minami-ku, Yokohama 232, Japan.

Regulation of pancreatic amino acid transporters: Use of amino acids as probes for screening regional tissue metabolism in pancreatitis*

G.E. Mann

The Biomedical Sciences Division, King's College London, Campden Hill Road, London W8 7AH, U.K.

Abstract

Amino acid transport in the isolated perfused exocrine pancreas is mediated by at least four parallel transporters, exhibiting differential sensitivity to islet hormones, diabetes, fasting and dietary composition. Insulin and streptozotocin-induced diabetes stimulate amino acid influx via the Na^+-independent Systems asc (L-serine) and y^+ (L-lysine). Moreover, activation of transport by insulin is dependent upon extracellular Ca^{2+} and inhibited by somatostatin-14. Elevation of transport induced by diabetes may not be mediated by glucagon, as exogenous glucagon fails to stimulate transport. Although system L (L-phenylalanine) is unaffected by insulin and diabetes, fasting for 72 h activates transport and refeeding for 24 h restores transport to fed levels. Adaptive responses in the activities of systems L and y^+ induced by fasting and changes in dietary protein may involve changes in intracellular amino acid levels which are known to influence counter-transport. Elucidating the mechanisms regulating uptake and incorporation of amino acids into pancreatic enzymes is of clinical relevance, since ^{11}C-labelled amino acids are currently used as PET imaging probes for regional tissue metabolism in pancreatitis.

Introduction

Exocrine pancreatic acinar cells exhibit a high rate of protein synthesis and accumulate extracellular amino acids against a considerable gradient [1–4]. Specific receptors for gastrointestinal hormones have been identified in the basolateral membrane of the exocrine epithelium [5], and a pancreatic portal circulation conveying islet hormones directly to the exocrine cells [6] may provide another endocrine control mechanism for acinar cell nutrient transport, enzyme synthesis and secretion. Although secretagogues induce both coordinate and anticoordinate changes in individual enzyme levels [7,8], it remains uncertain whether changes in amino acid transport are associated with altered rates of enzyme synthesis or the premature activation of proenzymes in pancreatitis [9].

* Supported by research grants from the Medical Research Council (U.K.), British Counci/Spanish Government and ONO Pharmaceutical Co., Osaka, Japan. I gratefully acknowledge the collaboration of Drs P.S.R. Norman, M. Munoz, Y. Habara, P.W. Emery, I.C.H. Smith and S. Peran and Wellcome Trust (U.K.) BSc research students.

The research described here reviews our studies of the hormonal regulation of basolateral amino acid transporters in the mammalian exocrine pancreas. Application of rapid dual isotope dilution techniques to the isolated perfused rat pancreas has enabled us to discriminate unidirectional influx from efflux and cell metabolism [10–20]. The present results suggest that influx of extracellular amino acids is mediated by at least four basolateral transporters (Systems A, asc, L and y^+) with differing sensitivity to feeding, fasting, islet hormones and diabetes.

Materials and Methods

Isolation and perfusion of the pancreas in vitro

Pancreata were isolated from anaesthetized (60 mg/kg) Sprague Dawley rats (180–260 g) and perfused (1.8 ml/min) *in vitro* with a Krebs-Henseleit bicarbonate medium via the superior mesenteric and coeliac arteries with the portal vein as outlet [21]. Unlabelled amino acids were added to the control perfusate to characterise the specificity and kinetics of influx. Na^+-dependence of transport was studied by replacing NaCl and $NaHCO_3$ with buffered Trizma HCl. Effects of exogenous bovine insulin (100 μU/ml) and somatostatin-14 (250 pg/ml) were examined after perfusion of the isolated pancreas for 30 min with an amino acid-free solution containing the hormone(s), and then measuring transport in the presence of hormone(s).

Transport measurements using a dual isotope dilution technique

Rapid unidirectional amino acid uptake (15 s) was measured by comparing portal vein dilution curves for a tritiated amino acid and D-[^{14}C]mannitol (extracellular tracer) following an intra-arterial injection (100 μl/2 s) of both tracers [10–20]. Twenty-five to thirty sequential samples were connected from the portal vein over 45–60 s (see Fig. 1A). Tracer uptake was quantified in successive venous samples e.g. uptake = {1 − (L[^{3}H]amino acid/D-[^{14}C]mannitol)}. The fractional uptake (U_{max}), measured at different substrate concentrations, was then used to calculate unidirectional influx $v = [-F.In(1 - U_{max}).C_a]$, where C_a is the perfusate amino acid concentration and F the perfusion rate in ml/min per g pancreas wet weight.

Tracer amino acid efflux was studied after preloading pancreata with L-[^{3}H]-serine and D-[^{14}C]mannitol [22]. After 30 min cell loading, pancreata were perfused with an isotope-free solution and tracer washout was monitored continuously (100 μl samples for 15 min). The specificity of L-[^{3}H]serine efflux was characterised by injecting different unlabelled amino acids (100 mM, 100 μl in 2–3 s) into the arterial inflow during the 16 min washout phase.

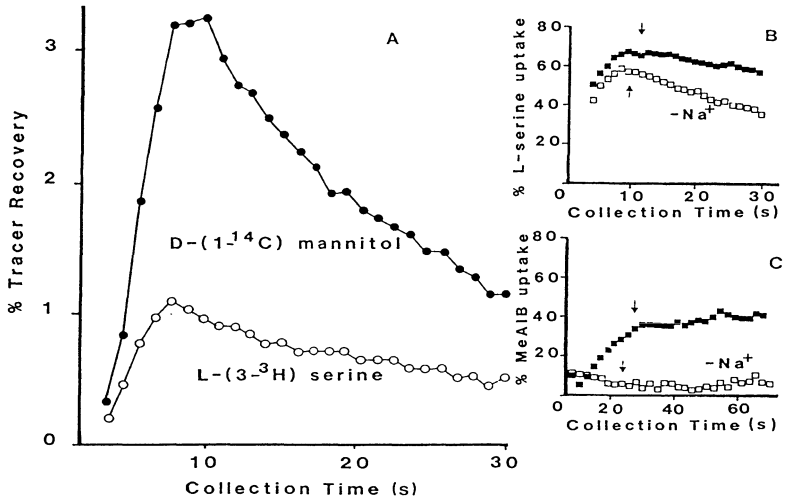

Fig. 1. Sodium dependence of amino acid uptake at the basolateral membrane of the exocrine pancreatic epithelium. A, paired venous concentration-time curves for L-[^{3}H]serine and D-[^{14}C]mannitol following a pulse arterial injection of both tracers. Tracer recoveries, expressed as a % of radioactive doses injected, are plotted versus the sampling time. B, time course of L-[^{3}H]serine uptake in the presence and absence of Na^+. C, 2-[^{14}C]MeAIB uptake in the presence and absence of Na^+. Taken from [15].

Kinetics of self- and cross-inhibition

Pancreata were perfused for 4 min with a given amino acid concentration (0.05 – 50 mM) before measuring rapid [^{3}H]amino acid uptake in the continued presence of substrate. Under these conditions tracer uptake serves as an index of unidirectional substrate transport. Kinetic constants presented in this study were estimated using a single Michaelis-Menten analysis revealing the lowest standard deviation of residuals.

Materials

Bovine insulin was purchased from Wellcome, Dartford, U.K., somatostatin-14 from Peninsula Laboratories, Merseyside, U.K. and unlabelled amino acids and other reagents from Sigma. Radioisotopes were obtained from either Amersham international plc, U.K. or NEN, Dreieich. F.R.G.

Results

Sodium dependence of amino acid transport via System A and asc

Figure 1A shows venous tracer dilution profiles for labelled L-serine and D-mannitol during a single circulation through the isolated pancreas. The lower

Table 1. Unidirectional uptake of nutrients at the basolateral membrane of the exocrine pancreatic epithelium

Substrate	Injectate (μmol/L)	% maximal uptake (15 s)	% Na^+-dependence
L-[3-^{3}H]alanine	0.4	59 ± 3	
L-[3-^{3}H]serine	2.8	64 ± 2	18 ± 2
2-[^{14}C]MeAIB	133	37 ± 2	81 ± 3
2-[^{3}H]glycine	1.0	21 ± 0.3	
L-[methyl-^{3}H]methionine	0.4	62 ± 7	
L-[4,5-^{3}H]eucine	0.2	55 ± 3	11 ± 5
L-[4-^{3}H]phenylalanine	1.0	71 ± 2	13 ± 6
L-[3,4-^{3}H]glutamine	50	71 ± 1	18 ± 5
L-[3,5-^{3}H]tyrosine	0.7	57 ± 3	
L-[G-^{3}H]tryptophan	3.8	11, 12	
L-[2,3-^{3}H]ornithine	50	45 ± 4	
L-[4,5-^{3}H]lysine	50	49 ± 2	
L-[2,3-^{3}H]arginine	50	56 ± 1	
L-[2,3-^{3}H]aspartic acid	2.0	11 ± 3	
D-[1-^{3}H]glucose	1.4	6 ± 1	
Methyl[^{3}H]choline	—	39 ± 5	
[^{3}H]folic acid	—	6 ± 1	

Rapid tracer uptakes (15 s) were measured in the isolated pancreata perfursed with an amino acid-free Krebs-Henseleit solution. Values denote the mean S.E. of measurements in 3 to 20 animals.

recovery of L-[^{3}H]serine reflects amino acid uptake at the basolateral membrane of the pancreatic epithelium. L-serine transport reached a maximum within 15 s and thereafter decreased with time due to tracer efflux (Fig. 1B). Unidirectional transport of L-serine was largely Na^+-independent, reminiscent of neutral amino acid transport via System asc [23]. By contrast. uptake of the System A specific analogue MeAIB was Na^+-dependent and accompanied by negligible efflux (Fig. 1C).

Our previous transport studies in the perfused rat pancreas revealed that amino acid influx was mediated by several basolateral transport systems: a Na^+-independent System asc selective for substrates of intermediate size [10]. a Na^+-dependent System A selective for small neutral substrates and MeAIB [10,12,17], a large neutral Na^+-independent System L [10,11] and a Na^+-independent System y^+ [18,19].

Table 1 summarizes unidirectional uptakes measured for neutral, basic and acidic amino acids, as well as, D-glucose, choline and folate. With exception of glycine, tryptophan and the acidic substrate aspartate, high uptakes were measured for neutral and cationic amino acids. Uptake for choline was significant, whilst folate uptake was low. At tracer concentrations uptake for D-glucose was negli-

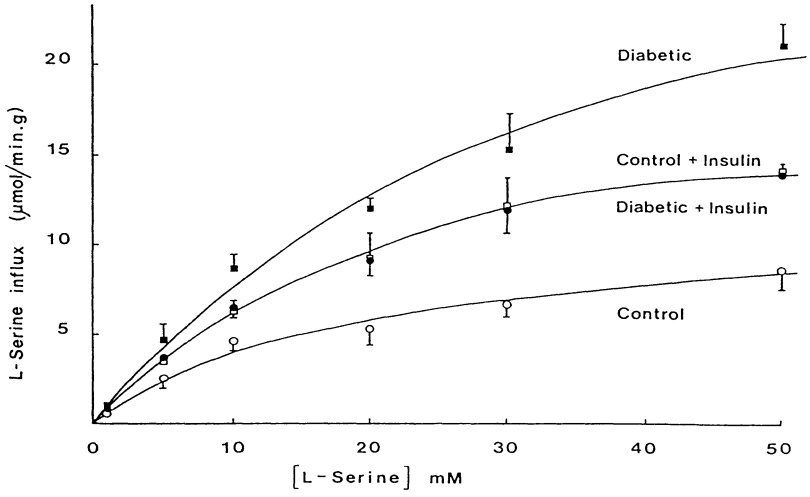

Fig. 2. Regulation of System asc activity by insulin (□,●) and streptozotocin-induced diabetes (■,●). Pancreata were isolated from normal and diabetic rats and perfused *in vitro*. L-serine transport (0.05–50 mM) was saturable and the rectangular hyperbolas were obtained using a single site, weighted Michaelis-Menten analysis. Data are the mean S.E. of determinations in 3–7 animals. Taken from [14].

gible, confirming that the exocrine pancreas appears to metabolize amino acids in preference to glucose [3].

Stimulation of System asc activity by streptozotocin-induced diabetes and insulin

Figure 2 illustrates the enhanced transport of L-serine via System asc in pancreata isolated from streptozotocin-diabetic rats [14]. In non-diabetic preparations perfusion with insulin stimulated L-serine transport, whereas insulin was found to partially downregulate the elevated transport activity induced by diabetes [14]. In the rat pancreas transport via System L appears to be insulin and diabetes insensitive [11]. As in the perfused liver [24], we were unable to detect stimulation of the System A specific analogue MeAIB. Our recent studies have confirmed that, as in cultured hepatocytes [25], insulin and streptozotocin diabetes activate System y^+ [26].

Regulation of System L activity by fasting and refeeding

As shown in Fig. 3, fasting for 72 h stimulated the V_{max} for L-phenylalanine transport via System L, whereas L-serine transport remained essentially unchanged (data not shown). After refeeding 72 h fasted animals for 24 h, kinetics of phenylalanine transport returned to values measured in fed animals [13]. Fasting

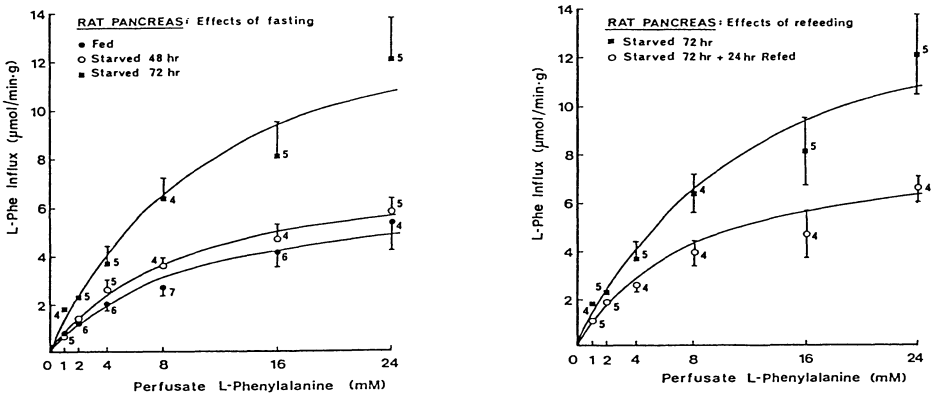

Fig. 3. Regulation of System L activity in pancreata isolated from fasted and refed rats. Unidirectional L-phenylalanine transport (1–24 mM) was measured in pancreata isolated from fasted (48 h, 72 h) and refed (24 h) rats. Rectangular hyperbolas are weighted for the reciprocal standard error at each mean influx value. Data are the mean S.E. of determinations in 4–7 animals and have been replotted from Fig. 2 and 3 in Mann *et al.* [13].

for 72 h also significantly elevated pancreatic concentrations of large neutral amino acids [27], suggesting that enhanced phenylalanine transport may have been mediated via exchange diffusion with intracellular substrates.

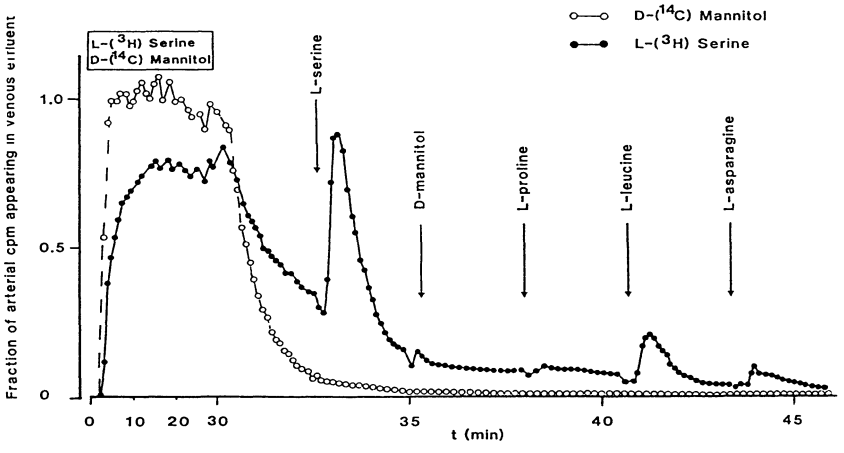

Fig. 4. Trans stimulation of L-serine efflux in the vascularly perfused rat pancreas. Portal vein tracer recoveries of L-[^{3}H]serine and D-[^{14}C]mannitol are shown during the loading (0–30 min) and washout (30–45 min) phases in a single experiment. During the washout phase the pancreas was challenged arterially with 100 mM bolus injections (arrows) of unlabelled L-serine, D-mannitol, L-proline, L-leucine and L-asparagine.

Trans-stimulation of amino acid efflux by vascular amino acids

In order to characterise the specificity of amino acid efflux, washout of L-[^{3}H]serine and D-[^{14}C]mannitol was followed for 15 min after preloading pancreata for 30 min with these tracers (Fig. 4). As previously reported [22], D-mannitol predominantly cleared from a fast exchanging compartment with a time constant of 0.68 ± 0.04 min. Although L-serine exhibited a similar fast phase of washout, a larger efflux occurred from a slowly exchanging pool with a time constant of 5.98 ± 0.46 min [22]. When preloaded pancreata were challenged successively with different unlabelled substrates during the washout phase, L-[^{3}H]serine (or ^{3}H metabolite) efflux was accelerated by L-serine, L-leucine and L-asparagine but unaffected by L-proline or D-mannitol. The substrates which most readily stimulated serine efflux paralleled those effective in accelerating efflux via System asc in horse erythrocytes [23]. In the pancreas System L, y+ and, to a lesser extent, System A also mediate exchange diffusion [22].

Modulation of System L activity after treatment with a synthetic protease inhibitor used in pancreatitis

Oral treatment with the protease inhibitor camostat mesilate is associated with pancreatic growth and enhanced enzyme secretion [28]. It is generally accepted

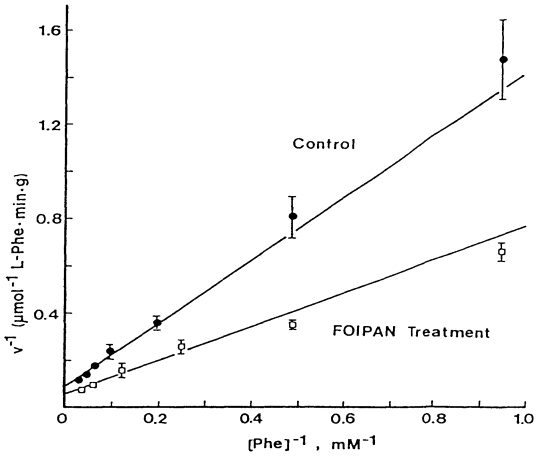

Fig. 5. Stimulation of System L activity following oral treatment with the synthetic protease inhibitor camostat mesilate. Rats were offered water ad libitum and received a single daily dose (200 mg/kg body wt) of camostat mesilate [N.N-dimethylcarbamoylmethyl-p-(p-guanidinobenzoyloxy) phenylacetate methanesulfonate, ONO Pharmaceutical Co., Japan] for 10 days via an orogastric tube. Pancreata were isolated from these rats and kinetics of L-phenylalanine transport were measured as described in legend to Fig. 3. Lineweaver-Burke analyses revealed that camostat significantly elevated the V_{max} for L-phenylalanine transport. Vertical lines denote S.E. of determinations in 4–11 perfused pancreata and if not indicated standard errors lie within the symbols. Data replotted from Fig. 1 in Mann and Munoz [20].

that release of cholecystokinin induced by such protease inhibitors mediates the trophic changes in the exocrine pancreas [29]. As shown in Fig. 5, treatment of rats with the synthetic protease inhibitor camostat mesilate markedly elevated the V_{max} for L-phenylalanine transport (20). In concurrent experiments transport rates for L-serine and L-lysine remained unaffected (data not shown).

Discussion

The studies reviewed here provide the first detailed description of basolateral amino acid transporters in the exocrine pancreas. Research from this laboratory has demonstrated that high rates of amino acid influx are mediated by at least four parallel basolateral amino acid transporters: a small neutral Na^+-independent System asc and a Na^+-dependent System A, a large neutral Na^+-independent System L and a cationic System y^+. Kinetic studies revealed that some of the identified transporters, particularly Systems A and L, exhibited marked overlapping specificities [10–12]. Although only Systems A and y^+ appear to be saturable within physiological plasma concentrations, it is worth noting that high rates of amino acid influx are always accompanied by significant efflux [10]. For certain amino acids efflux is mediated selectively via Systems A, asc or L [22].

Exocrine pancreatic insufficiency is not a common clinical manifestation of diabetes, however, several studies have reported that insulin-dependent diabetic patients have abnormal pancreatic secretory responses to cholecystokinin and secretin [6]. The difficulty of studying human pancreatic tissue has necessitated exocrine function to be evaluated in animals with experimental diabetes induced by B-cell toxins such as streptozotocin or alloxan. Our findings establish that transport activity of System asc is significantly stimulated in diabetes but, unlike observations in non-diabetic rats [14–16], bovine insulin downregulates the elevated transport induced by streptozotocin (Fig. 2).

In non-diabetic rats activation of System asc by insulin was found to be dependent upon extracellular Ca^{2+}, inhibited by somatostatin-14 and unaffected by ouabain, amiloride, monensin or the sulfhydryl blocker N-ethylmaleimide [14,15]. Paradoxically, release of endogenous rat insulin in response to a vascular glucose challenge did not stimulate System asc activity [16]. Lack of an effect with rat insulin may reflect the presence of efferent vessels leading from the islets of Langerhans directly into the systemic circulation [6], however, our results are consistent with an alternative hypothesis. If during a vascular glucose challenge insulin and somatostatin were co-released and conveyed to the exocrine pancreas via insulo-acinar portal vessels [6], it is conceivable that somatostatin inhibits the stimulatory actions of insulin on amino acid transport in the exocrine pancreas.

Fasting, refeeding, diabetes and changes in dietary composition result in adaptive responses in the synthesis and secretion of pancreatic enzymes [1,7,8] and intracellular amino acid concentrations [27]. In the exocrine pancreas amino acids undergo vigorous exchange diffusion [4], and hence altered intracellular amino

acid levels may modulate homo- or heteroexchange mechanisms. The selective stimulation of System L by fasting (and inhibition by refeeding) is paralleled by increases (and decreases) in pancreatic concentrations of large neutral amino acids [27]. These adaptive responses in the activity of select amino acid transporters may provide mechanism(s) by which influx of certain essential amino acids is increased to meet the demands of continued proteolytic and lipolytic enzyme synthesis in fasting. Recent studies in the pancreas have also shown that System L transport activity is inhibited following adaptation to a high or low carbohydrate diet [18] and stimulated following oral treatment with a synthetic protease inhibitor [20].

Currently an important diagnostic problem in nuclear medicine is tho need for an improved positron-labelled substrate for imaging pancreatic metabolism in disease. Although extensive animal studies have shown that radiolabelled amino acids are accumulated rapidly by the exocrine pancreas [1–3,10], few such studies have been performed in humans. In clinical trials the high transport rato for amino acids has been exploited by using [^{11}C]methionine as a pancreatic imaging agent (PET scanning) in chronic pancreatitis [30]. The isolated rat pancreas has evolved as a powerful animal model for exploring the mechanisms regulating adaptation of pancreatic amino acid transport, enzyme synthesis and secretion. Furthermore, our findings may be of relevance for the design and synthesis of a reliable positron-labelled amino acid for scanning pancreatic metabolism in diabetes and acute or chronic pancreatitis.

References

1. Case RM (1978) Biol. Rev. 53: 211–354.
2. Van Venrooij WJ, Poort C, Kramer MF and Jansen MT (1972) Eur. J. Biochem. 30: 427–433.
3. Danielsson A and Sehlin J (1974) Acta Physiol. Scand. 91: 557–565.
4. Clayman S and Scholefield PG (1969) Biochim. Biophys. Acta 73: 277–289.
5. Gardner JD and Jensen RT (1986) In: Go VLW (ed.) The Exocrine Pancreas: Biology, Pathobiology and Disease. Raven Press, New York, pp. 109–122.
6. Williams JA and Goldfine ID (1985) Diabetes 34: 980–986.
7. Dagorn J-C (1986) Biochemie 68: 329–331.
8. Wicker C, Puigserver A and Scheele GA (1984) Eur. J. Biochem. 139: 381–387.
9. Gyr K, Heitz PU and Beglinger C (1984) In: Kloppel G and Heitz PU (eds.) Pancreatic Pathology. Churchill Livingstone, London pp. 44–72.
10. Mann GE and Peran S (1986) Biochim. Biophys. Acta 858: 263–274.
11. Mann GE, Habara Y and Peran S (11986) Pancreas 1: 239–245.
12. Norman PSR and Mann GE (1986) Biochim. Biophys. Acta 861: 389–394.
13. Mann GE, Munoz M and Peran S (1986) Biochim. Biophys. Acta 862: 119–126.
14. Mann GE and Norman PSR (1984) Biochim. Biophys. Acta 778: 618–622.
15. Norman PSR and Mann GE (1987) J. Menbrane Biol. 96: 153–163.
16. Norman PSR, Habara Y and Mann GE (1989) Diabetologia 32: 177–184.
17. Norman PSR and Mann GE (1988) Biochim. Biophys. Acta 943: 541–546.
18. Munoz M, Emery PW, Peran S and Mann GE (1988) Biochim. Biophys. Acta 945: 272–280.
19. Mann GE, Munoz M and Peran S (1988) Alcohol 5: 101–115.
20. Mann GE and Munoz M (1988) Pancreas (paper in press).
21. Kanno T, Suga T and Yamamoto M (1976) Jpn. J. Physiol. 26: 101–115.

22. Mann GE, Norman PSR and Smith ICH (1989) J. Physiol. 416: 485–502.
23. Fincham DA, Mason DK and Young JD (1988) Biochim. Biophys. Acta 937: 184–194.
24. Kilberg MS and Neuhaus OW (1977) J. Supramol. Struct. 6: 191–204.
25. Handlogten ME and Kilberg MS (1984) J. Biol. Chem. 259: 3519–3525.
26. Mann GE and Munoz M (1988) J. Physiol. 406: 123P.
27. Mann GE, Smith SA, Norman PSR and Emery PW (1988) Pancreas 3: 67–76.
28. Ishikawa T and Kanno T (1988) Biomed. Res. 9: 287–304.
29. Goke B, Printz H, Koop J, Rausch U, Richter G, Arnold R and Adler G (1986) Pancreas 1: 509–515.
30. Syrota A, Dop-Ngassa M, Cerf M and Paraf A (1981) Gut 22: 907–915.

Address for correspondence: Dr G.E. Mann, Physiology, Biomedical Sciences Division, King's College London, Campden Hill Road, London W8 7AH, U.K.

Modulation of ovine lymphocyte function by leucine and leucine metabolites

Steven Nissen[a], Gail Kuhlman[a] and James A. Roth[b]

[a]Department of Animal Science, Iowa State University, Ames, IA 50011, U.S.A.
[b]Department of Veterinary Microbiology and Preventive Medicine, Iowa State University, Ames, IA 50011, U.S.A.

Introduction

Previous studies indicate that the oral supplementation of leucine (Leu) to sheep decreased serum antibody response to porcine red blood cells and decreased mitogen-stimulated lymphocyte blastogenesis, however, the first catabolic product of Leu, α-ketoisocaproate (KIC), enhanced the antibody response to porcine red blood cells and increased mitogen-stimulated lymphocyte blastogenesis [1–3]. It may be that KIC is altering the ratio of certain T-cell subsets in a manner that would enhance such immune responses, while Leu is altering the ratio of certain T-cell subsets such that antibody production and lymphocyte blastogenesis are lowered. The objectives of the studies reported here were: (1) to determine whether the oral administration of small doses of Leu and KIC can alter the proportions of circulating T-cell subsets in lambs, and (2) to determine if the effects of LEU and KIC are due to a direct effect of the compound or to another leucine metabolite.

Materials and Methods

Animals and diets

Twenty-one mixed-breed ram lambs were fed a basal diet *ad libitum* to which was added rumen protected Leu (n=7) or calcium-KIC (n=7) or limestone (control; n=7) [3]. These supplements were fed at a rate of approximately 3 g per lamb per day, which corresponds to approximately 5 mmol of LEU or KIC per total kg of diet.

Blood sampling and lymphocyte preparation

Animals were bled for lymphocyte blastogenesis assays and T-cell subset analysis 38,45 and 52 days after dietary treatments began. Isolated lymphocyte were cultured as described previously [4]. Unstimulated and mitogen stimulated cultures were assayed in triplicate.

Antibodies

Monoclonal antibodies, in the form of cell-free culture supernatants were obtained from Dr. M.R. Brandon, University of Melbourne, Parkville, Victoria, Australia. Additional properties of the antigens recognized by the monoclonal antibodies have been reviewed elsewhere [5–7]. Monoclonal antibodies SBU-T4, T8 and T19 were used in both experiments.

Immunofluorescent staining

Sheep lymphocytes (10^6) in 50 µl phosphate-buffered saline, 0.1% sodium azide (PBS/Az), 0.5% BSA were incubated for 30 min at 4°C with 50 µl monoclonal antibody culture supernatant. The cells were washed twice with PBS/Az by centrifuging at 150 × *g* for 15 min and incubated with 40 µl of FITC-RAM for 30 min at 4°C. Cells were washed 3 times with PBS/Az, resuspended in 200 µl 1% formalin and stored overnight at 4°C until analyzed by flow cytometric analysis. (Coulter Electronics, Hialeah, FA).

In vitro *addition of leucine and leucine metabolites*

Leucine, IVA, KIC and HMB were prepared in RPMI-media-1640 and passed through a 0.2 µm filter to assure sterility. Each metabolite was incubated with isolated lymphocytes as described above. The final concentration in the media was 10 mM.

Results

The lymphocyte blastogenic response to mitogens is summarized in Table 1. Feeding KIC resulted in significantly increased blastogenic response to PHA (KIC

Table 1. The effects of oral supplementation of LEU or KIC on lymphocyte blastogenesis and the percentage of T-lymphocyte subsets[1]

Diet	Mitogen added		Lymphocyte subset %		
	None[2]	PHA[2]	T4[3]	T8[3]	T19[3]
Control	700	18900[a]	18[a]	9[a]	18[a]
KIC	776	24870[b]	21[b]	10[a]	18[a]
LEU	730	16160[a]	18[a]	11[a]	15[b]
SEM[4]	92	1975	1	0.6	1.3

[1]Means are of 3 repeated measures. Means not sharing a common superscript letter are significantly different at $P<0.05$.
[2]Expressed as counts per min per 200.000 lymphocytes.
[3]Expressed as the percentage of peripheral lymphocytes stained by the specific monoclonal antibody.
[4]Pooled standard error of the mean from ANOVA.

Table 2. Effect of addition of Leu and Leu metabolites to PHA-stimulated cultures of normal ovine lymphocytes

Metabolite	Concentration	Percent change over no addition ± SEM	P <
Leucine	10 mM	−24 ± 5	0.01
Ketoisocaproate	10 mM	−8 ± 12	0.60
Isovalarate	10 mM	−17 ± 8	0.30
3-hydroxy 3-methyl butyrate	10 mM	+91 ± 12	0.01

All metabolites were added to the cultures at the time of the labeled thymidine was added.

vs control; $P<0.05$). Feeding Leu significantly decreased the blastogenic compared to KIC-fed animals ($P<0.05$) and tended to decrease lymphocyte blastogenesis when compared to controls. No changes were seen in background (unstimulated) blastogenesis.

Table 1 also summarizes the effects of feeding Leu or KIC on T-cell subset in sheep. KIC-fed animals had a significantly greater percentage of T4 cells when compared to control and Leu-fed animals ($P<0.05$). Leu-fed animals had a significantly lower percentage of T19 cells when compared to KIC-fed animals ($P<0.05$) and this number also tended to be lower than the control animals.

The effect of adding leucine metabolites on mitogen stimulated blastogenesis assays are shown in Table 2. The PHA-stimulated blastogenic response for lymphocytes cultured in the absence of metabolites was 29212 ± 2324 counts per min per 200,000 lymphocytes. When Leu was added to lymphocytes, a decrease in lymphocyte blastogenesis of approximately 25% over this control value was observed at 10 mM Leu. The next two metabolites in the Leu pathway, KIC and IVA, did not alter the mitogenic stimulation. HMB also significantly increased blastogenesis at approximately twofold.

Discussion

As reported in previous studies [3] mitogen stimulated lymphocyte blastogenesis was increased with KIC supplementation. In the case of KIC, the percentage of T4 cells was increased approximately 15% which could be responsible for the increase in blastogenesis and antibody production. In the case of Leu, the only observed change was a 17% decrease in T19 cells for which a function has not yet been described. The fact that these two compound affect two distinct T-lymphocyte subsets in opposing manners, may partially explain the mechanism of the contradictory effects that Leu and KIC exert on immune function.

From the *in vitro* additions of metabolites clearly indicate that the stimulatory effect of KIC on lymphocyte blastogenesis is not directly due to KIC itself. However, the metabolite HMB markedly stimulated blastogenesis may indirectly

be responsible for the effects of KIC seen *in vivo*. HMB is produced in the cytosol of liver by the action of KIC oxygenase [8]. Thus, KIC could act *in vivo* via conversion to HMB.

Conversely, Leu significantly suppressed lymphocyte blastogenesis *in vitro* thus suggesting suppressive effect of Leu on immune function *in vivo* could be due to a direct effect of Leu on lymphocyte function. Further studies will be necessary to document the importance of this observation and its relationship to Leu nutrition.

In conclusion, these data suggest that the dietary supplementation of KIC may increase blastogenesis and antibody production by increasing the number of T-helper lymphocytes, whereas Leu, decreases blastogenesis and antibody production by decreasing the number of T19 lymphocytes in the peripheral blood circulation. It appears the suppressive effect of leucine may due to a direct action on lymphocyte function whereas the KIC effect is likely mediated by the metabolite HMB.

References

1. Flakoll PJ, VandeHaar MJ, Kuhlman G, Roth JA and Nissen S (1987) Evaluation of Steer Growth, Immune Function and Carcass Composition in Response to Oral Administration of Ruminally Protected 2-ketoisocaproate. J. Anim. Sci. 65(Suppl 1): 476 (Abstr.).
2. Nissen S, Flakoll P and Roth J (1986) Enhanced Lymphocyte Blastogenesis by 2-Ketoisocaproate in Young Lambs. Fed. Proc. 45: 240 (Abstr).
3. Kuhlman G, Roth JA, Flakoll PJ, VanderHaar MJ and Nissen S (1988) Effects of Dietary Leucine, α-Ketoisocaproate and Isovalerate on Antibody Production and Lymphocyte Blastogenesis in Growing Lambs. J. Nutr. 118: 1564–1569.
4. Roth JA, Kaeberle ML and Hsu WH (1982) Effects of ACTH Administration on Bovine Polymorphonuclear Leukocyte Function and Lymphocyte Blastogenesis. Am. J. Vet. Res. 43: 412–416.
5. Mackay CR, Maddox JF and Brandon MR (1986) Three Distinct Subpopulations of Sheep T-Lymphocytes. Eur. J. Immunol. 16: 19–25.
6. Mackay CR, Maddox JF, Gogolin-Evens KJ and Brandon MR (1985) Characterization of Two Sheep Lymphocyte Differentiation Antigens, SBU-T1 and SBU-T6. Immunology 55: 729–737.
7. Maddox JF, Mackay CR and Brandon MR (1985) Surface Antigens, SBU-T4 and SBU-T8, of Sheep T-Lymphocyte Subsets Defined by Monoclonal Antibodies. Immunology 55: 739–748.
8. Sabourin PJ and Bieber LL (1982) Purification and Characterization of an α-Ketoisocaproate Oxygenase of Rat Liver. J. Biol. Chem. 257: 7460–7467.

Polyamine-derived post-translational modification of glutamine residues in intracellular proteins

Simone Beninati*

Laboratory of Cellular Development & Oncology, National Institute of Dental Research, National Institutes of Health, Bethesda, MD 20892, U.S.A.

Abstract

We present evidence for the covalent incorporation of polyamines into glutamine-containing proteins as the corresponding γ-glutamyl adducts. This novel type of post-translational protein modification has been investigated in human integuments. It is well known that the chemical stability of the insoluble protein components of skin and hair is attributable to a high degree of ε-(γ-glutamyl)lysine crosslinking arising from cellular transglutaminase activity. We found that urea-insoluble fractions obtained from human callus, nail and hair contain an additional type of crosslink formed through the polyamine spermidine. Further more, the precursors of the spermidine crosslinks, namely *mono*-(γ-glutamyl)spermidines, have been identified in the urea-soluble fraction of all the integuments under investigation. These data suggest that polyamines play a role in the assembly of the insoluble intracellular structures of human integuments through a transglutaminase-catalyzed post-translational modification of the precursor proteins.

Introduction

A rapid increase in polyamine concentrations and in the activity of the enzymes involved in their biosynthesis occurs in rapidly growing tissues. These changes usually precede, or are concomitant with, the increases in protein and nucleic acid content in the cell [1,2]. Both extracellular and intracellular levels of these amines may be regulated in response to the physiological and pathological status of the cell. Beside the gross control of the rate of their biosynthesis it is tempting to speculate that extracellular and intracellular compartmentation may be dependent on the binding with certain cellular components. Polyamines have been described to bind to cell membranes, nucleic acids and organelles. However, polyamines, being highly charged cations, exhibit non specific interactions that could be unrelated to their specific biological role.

The growing experimental interest in the metabolic reactions of putrescine, spermidine and spermine as substrates for a group of enzymes called transglutaminases has highlighted a new aspect of their metabolism, i.e., the post-translational modification of cellular proteins. In this regard the specificity of the protein modification is very high because only protein bound glutaminyl residues

* On leave from Department of Biology, II University of Rome (Tor Vergata), Rome, Italy.

are the acceptor sites of the reaction involved [3]. The specificity of the reaction may be considerable even among the proteins. Indeed the extent to which a particular glutaminyl residue is linked depends not only upon its accessibility and the environment of the residue on the protein surface, but also upon the structure of the amine substrate [4]. These properties should make the intracellular polyamine dependent post-translational modification of proteins very useful as a tool to explore the biological significance of polyamines. With the foregoing in mind we started to investigate this new aspect of polyamine metabolism. As a preliminary approach we assessed the presence of γ-glutamyl polyamine conjugates *in vivo* in rat liver [5] and in isolated hepatocytes [6]. Unforeseen difficulties encountered in the attempt to measure the levels of the new transformation products, i.e., *mono* and *bis*-(γ-glutamyl)polyamines, stimulated us to improve the existing analytical methods [7]. Furthermore, we have exploited the metabolic conversion of labeled putrescine in cell cultures.

The polyamine-dependent post-translational modification of proteins was monitored in exponentially growing and confluent CHO cells, in which transglutaminase activity and polyamine metabolism were manipulated by a series of drugs [8], and during the terminal differentiation of a primary culture of mouse epidermal cells [9]. Although the intracellular levels of γ-glutamylpolyamines were low, there was clear evidence for the existence of such derivatives in both cell cultures studied. Significantly higher values were observed in mouse keratinocytes than in CHO cells. It is noteworthy that γ-glutamylpolyamines were found to be a component of mouse epidermal cornified envelopes. This discovery prompted the systematic search for similar crosslinks in human integuments *in vivo*. Spermidine was determined in foot callus as a peptide-bound *bis*-(γ-glutamyl)derivative at levels in the range comparable to that of ε-(γ-glutamyl)lysine. Spermidine-dependent crosslinks in psoriasis were more abundant than those of ε-(γ-glutamyl)lysine [10].

The present report provides evidence for the occurrence of polyamine-derived post-translational modifications of glutamine residues of intracellular protein in human integuments (foot callus, nail and hair). The results strongly suggest that although the linkage of protein through polyamines, as well as those crosslinks by ε-(γ-glutamyl)lysine, occurs to a limited extent in intact cells, the stimuli arising from severe cell damage, cell death, terminal differentiation of epidermis or certain disease states might prime such a novel metabolic pathway.

Experimental procedures

Materials

Callus, nail and hair samples were collected from normal volunteers at National Institutes of Health (Bethesda, MD, U.S.A.). Other material and reagents have been described in previous publications [5,7].

Methods

Isolation of crosslinked proteins was performed by treatment of callus, nail and hair with 0.1 M Tris-HCl buffer, pH 8.5, containing 8 M urea, 1 mM EDTA, 10 mM dithiothreitol and 2% sodium dodecyl sulfate (extracting buffer). The human integuments were extracted by overnight stirring at 100°C, followed by centrifugation for 60 min at 10,000 × g. The pellet, which contained the crosslinked proteins, was washed with 0.1 M Tris-HCl buffer, pH 8.5, containing 1 mM each of putrescine, spermidine and spermine. The supernatant and washes were combined and the proteins were precipitated with cold 5% trichloroacetic acid.

Characterization and quantitation of the isopeptide ε-(γ-glutamyl)lysine and of γ-glutamylpolyamines was carried out by isolation of the compound that contains the bounds connecting the chains. The method employed was cleavage of the peptide bonds by exhaustive digestion with proteolytic enzymes and determination of the crosslinks by identification and measurement of γ-glutamylamines, which are resistent to proteolysis [11]. The techniques used in the analyses reported in these studies have all been described in detail elsewhere (see Ref. [5–10]) specific details for each experiment are given in the figure legends.

Protein was determined from amino acid analyses of the insoluble pellets.

Results

Table 1 shows the total amount of polyamines determined on the acid hydrolysate of human integuments. Putrescine levels were higher in nail than in the other integuments. In callus and hair the amounts of this diamine were about 9% of that of spermidine. In each of these integuments spermidine was the most abundant polyamine. Spermidine and spermine were found to be at about the same level in nail, whereas in callus and hair the amount of spermine was about 30% of that of spermidine.

The amounts of putrescine, spermidine and spermine in the insoluble fraction extracted from callus, nail and hair from normal individuals, as reported under

Table 1. Polyamine levels in human integuments

Integument	Polyamine		
	Putrescine	Spermidine	Spermine
	nmol/g wet tissue		
Callus	20.5 ± 2.7	278.0 ± 20.0	87.8 ± 6.7
Nail	244.5 ± 28.3	478.2 ± 56.3	355.6 ± 72.5
Hair	44.4 ± 8.3	544.5 ± 89.5	155.6 ± 37.2

Callus, nail and hair specimens were hydrolyzed in 6N HCl for 18 h at 110°C. The hydrolysates were analyzed for polyamines as reported [11]. Values are means of four determinations ± S.E.M.

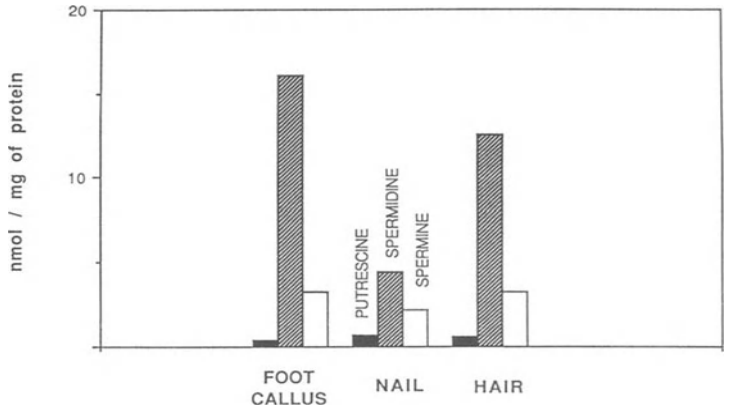

Fig. 1. Total putrescine, spermidine and spermine content of buffer insoluble fraction from foot callus, nail and hair. Determination of total polyamines was carried out performing the acid hydrolysis of the specimen in 6N HCl for 18 h at 110°C.

Experimental procedures are shown in Fig. 1. Spermidine level was found to be higher in foot callus (16.5 ± 2.5 nmol/mg of protein) than in the other integuments. In this tissue putrescine and spermine levels were lower than spermidine, at 0.6 ± 0.05 nmol/mg of protein and 3.5 ± 0.8 nmol/mg of protein, respectively. The levels of spermidine and spermine in nail were similar (4.5 ± 0.6 nmol/mg of protein and 3.2 ± 0.3 nmol/mg of protein, respectively). In hair the differences in the levels of the two polyamines, i.e., spermidine and spermine, were similar to that found in callus (spermidine: 13.5 ± 2.0 nmol/mg of protein; spermine 3.7 ± 0.5 nmol/mg of protein). As in callus, the concentration of putrescine found in nail and hair was quite low (nail: 0.9 ± 0.04 nmol/mg of protein; hair: 0.7 ± 0.05 nmol/mg of protein).

Figure 2 shows the level of γ-glutamylpolyamines found in the soluble fraction of the integuments examined. N^1- and N^8-(γ-glutamyl)spermidines and N^1-(γ-glutamyl)spermine were found in all the integuments under investigations. The amount of *mono*-spermidine derivatives was higher than that of *mono*-spermine derivatives. The levels of the spermidine derivatives were 1.9 ± 0.5 nmol/mg of protein (callus), 1.2 ± 0.2 nmol/mg of protein (nail) and 1.5 ± 0.4 nmol/mg of protein (hair). The spermine derivative was 0.5 ± 0.01 nmol/mg of protein (callus), 0.6 ± 0.01 nmol/mg of protein (nail) and 0.8 ± 0.04 nmol/mg of protein (hair). None of the digests contained *bis*-(γ-glutamyl)polyamines at detectable levels. When proteolytic digests of the buffer-insoluble fraction from callus, nail and hair were examined for γ-glutamylpolyamines, *bis*-(γ-glutamyl)spermidine was found at levels comparable to those of ε-(γ-glutamyl)lysine (Fig. 3). *Mono*-(γ-glutamyl-spermidines were seen in some digests of insoluble pellet from callus and nail, but

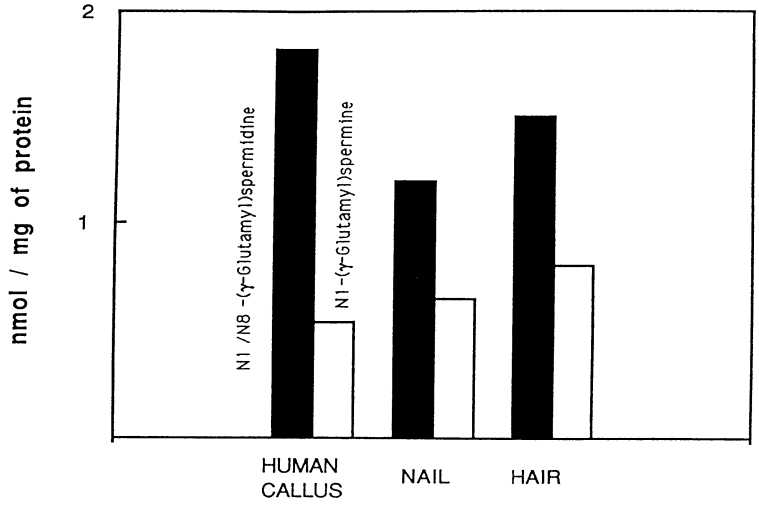

Fig. 2. γ-Glutamylpolyamine levels in buffer-soluble proteins from human integuments. The supernatant of the extraction reported under *Experimental procedures*, was dialyzed against water, treated with 5% trichloroacetic acid and centrifuged at 2,000 × g for 5 min. The trichloroacetic acid precipitate was extracted with anhydrous ethyl ether and lyophilized. Proteolytic digestion was carried out as previously reported [5].

only at trace levels. Trace levels of *bis*-(γ-glutamyl)spermine were observed in all the integuments examined (data not shown). When samples from the insoluble

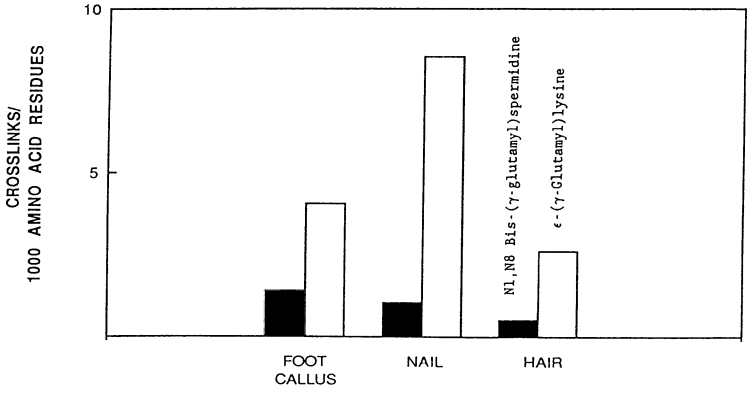

Fig. 3. Crosslink levels of buffer.insoluble proteins from specimens of foot callus, nail and hair. The pellet obtained after extraction with 0.1 M Tris-HCl buffer containing urea, dithiothreitol, EDTA and sodium dodecyl sulfate was lyophilized and digested as previously reported [5].

fraction of the extracted integuments were acid hydrolyzed and the polyamine content of the hydrolysates measured, in each case good correspondence was observed between the spermidine released by acid hydrolysis and the spermidine found in crosslink form (data not shown). This close agreement indicates that essentially all of the spermidine associated with the insoluble proteins is in the form of polyamine crosslinks and is further evidence for good quantitation of *bis*-(γ-glutamyl)spermidine. The comparison of the values presented in Fig. 3 shows that the level of the ε-(γ-glutamyl)lysine crosslinks in nail (8.6 ± 1.0 crosslink/1000 amino acid residues) is significantly higher than that in callus or hair (4.1 ± 0.6 and 3.6 ± 0.2 crosslink/1000 amino acid residues, respectively). The levels of *bis*-(γ-glutamyl)spermidine crosslink are lower: 1.5 ± 0.03 (callus), 1.0 ± 0.02 (nail) and 0.4 ± 0.01 (hair), expressed as crosslink/1000 amino acid residues.

Discussion

The present report provides unequivocal evidence for the occurrence in human integuments of an additional type of crosslink derived from the polyamine spermidine. This γ-glutamylspermidine crosslink, like the ε-(γ-glutamyl)lysine crosslink, is a product of transglutaminase catalytic activity. Despite their probable common enzymatic origin, however, these two linkages differ significantly in several respects. *Bis*-(γ-glutamyl)spermidine bonds have a more extended chemical structure that allows greater distance between the crosslinked protein chains and may provide chain attachments at positions unsuitable for crosslinking through ε-(γ-glutamyl)lysine bonds. Furthermore, in this type of crosslink the secondary amino group of the spermidine moiety remains unconjugated [12]. It thus may contribute to the net charge in the vicinity of this crosslink with an increase of the hydrophilicity of the protein(s) involved in the linkage.

The marked difference in chemical structure of the two crosslinks may suggest that different precursor conformations and interactions would serve as prerequisites for these crosslinks and therefore that the type of crosslinking may be more directly controlled by features of the macromolecular substrate than by enzyme specificity.

Identification of *mono*-(γ-glutamyl)derivatives of spermidine and spermine in urea extract of integuments may be useful in identification of some of the protein components of the crosslinked cell structures. The absence of γ-glutamylspermine crosslinks in all the integuments studied is in contrast to the previous finding that this polyamine is incorporated *in vitro* into ß-casein by guinea pig liver transglutaminase [13]. The absence of this spermine-derived crosslink may result from spermine compartmentation in the cell or from a rapid degradation of the direct precursor of the crosslink, i.e., *mono*-(γ-glutamyl)spermine. It is premature to speculate in detail as to why the spermidine-derived crosslinking is preferred in the irreversible hardening of the cellular structures of human integuments. A simple explanation is to assume that crosslink modulation follows a cycle of reactions in which *mono*-(γ-glutamyl)spermine is the substrate for a degradative metabolic step.

References

1. Tabor CW and Tabor H (1984) Annu. Rev. Biochem. 53: 749–790.
2. Pegg AE (1986) Biochem. J. 234: 249–262.
3. Folk JE (1980) Annu. Rev. Biochem. 49: 517–531.
4. Folk JE and Chung SI (1973) Adv. Enzymol. 38: 109–191.
5. Beninati S, Piacentini M, Argento-Cerú MP, Russo-Caia S and Autuori F (1985) Biochim. Biophys. Acta 41: 120–126.
6. Piacentini M and Beninati S (1988) Biochem. J. 249: 813–817.
7. Beninati S, Martinet N and Folk JE (1988) J. Chrom. 443: 329–335.
8. Beninati S, Piacentini M, Cocuzzi ET, Autuori F and Folk JE (1988) Biochim. Biophys. Acta 952: 325–333.
9. Piacentini M, Martinet N, Beninati S and Folk JE (1988) J. Biol. Chem. 263: 3790–3794.
10. Beninati S and Folk JE (1988) In: Zappia V and Pegg A (eds.) Progress in Polyamine Research. Plenum Publishing Corporation, New York, pp. 411–422.
11. Folk JE, Park MH, Chung SI, Schrode J, Lester EP and Cooper HL (1980) J. Biol. Chem. 225: 3695–3700.
12. Folk JE and Finlayson JS (1977) Adv. Prot. Chem. 31: 1–133.
13. Schrode J and Folk JE (1978) J. Biol. Chem. 253: 4837–4840.

Regulatory effects of thyroid hormones on amino acid metabolism in the brain: The influence of maternal hypothyroxinemia on brain biochemistry of adult rat progeny

Mark R. Pickard, Arun K. Sinha, Damiano Gullo*, Mohamed M. Khaled and Roger P. Ekins

Department of Molecular Endocrinology, University College and Middlesex School of Medicine, London W1N 8AA, U.K.

Abstract

The effects of maternal hypothyroxinemia during pregnancy on brain amino acid metabolism in adult rat progeny were investigated. Normal and partially thyroidectomised dams were mated and the progeny allowed to grow to adulthood. [U-^{14}C]Glutamate, [U-^{14}C]glucose and [4,5-^{3}H]leucine metabolism were determined in cerebral cortical slices, and enzymes associated with glutamate metabolism were assayed in cerebral cortical homogenates.

In the case of the thyroidectomised dam progeny, reductions were observed in the incorporation of radioactivity from [U-^{14}C]glucose into the following intracellular fractions: glucose/tricarboxylic acid intermediates (by 45%, $P<0.005$), CO_2 (by 33%), amino acids (by 48%, $P<0.01$) and protein (by 31%). Only minimal changes were observed in glutamate metabolism, as evidenced by tissue slice studies and enzyme activity measurements. Thus, *de novo* synthesis of amino acids from glucose is compromised in the experimental progeny, whereas glutamate catabolism is essentially unchanged.

Incorporation of [4,5-^{3}H]leucine into protein was depressed (by 20%) in experimental progeny, whereas accumulation of total intracellular radioactivity was unchanged. It is feasible therefore, that the synthesis of selected proteins/enzymes in amino acid metabolism is altered in adult progeny as a consequence of maternal hypothyroxinemia during pregnancy.

Introduction

Iodine deficiency is endemic to vast areas of the third world, with isolated pockets also present in Europe and the U.S.A. It has been estimated that as many as 1 billion people live in such areas and are therefore at risk from iodine deficiency disorders [1].

An increased incidence of sporadic 'neurological' cretinism is observed in offspring born in iodine-deficient regions. This condition is irreversible and is manifested in most severe cases by mental retardation, deaf-mutism, spastic diplegia and often strabismus [1,2]. Although the incidence of such overt 'neurological' cretinism is relatively small (10–15 % of total live births per year), much larger numbers of the population suffer from less visible, more insidious effects,

* Wellcome Trust research fellow from the Department of Endocrinology, University of Catania, Italy.

including psychomotor incompetence, cognitive dysfunction, low IQ, partial hearing loss and poor school performance [3,4].

Early field studies in Papua New Guinea demonstrated that the incidence of 'neurological' cretinism can be reduced by iodine administration to mothers [5]. For therapy to be completely successful, it must be initiated prior to conception, implying that the fetal damage occurs very early in pregnancy (most likely the first trimester), before the development of independent fetal thyroid function [5]. On the basis of these studies, it has often been suggested that the fetal damage results from an insufficiency of iodine per se, independent of its requirement in thyroid hormone synthesis [2,5]. However, a role for elemental iodine in brain development remains unproven. Rather, we believe that a decreased fetal supply of maternal thyroxine (T_4) may be largely responsible for the defects [6]. In iodine-deficient endemias, levels of maternal serum T_4 (total and free) are often below the normal range, whereas those of 3,5,3'-triiodothyronine (T_3) are normal or raised [7,8].

The role of thyroid hormones in the development of the central nervous system (CNS) has been studied in detail and extensively reviewed [9–12]. Almost all such investigations have been confined to the period following the establishment of independent fetal thyroid function, reflecting the hitherto widely-held belief that maternal thyroid hormones are neither available nor necessary for the development of the fetal CNS. In the last few years, we and others have shown with the aid of a rat model that thyroid hormones cross the placenta, are available to the fetal CNS in significant quantities in early pregnancy, and are localised in the fetal brain [13–17].

More recently, we showed that maternal hypothyroxinemia results in a wide range of biochemical deficits in brains of immature and adult rat progeny [15,18]. Apart from decreased DNA and total protein concentrations, we reported alterations in the activities of selected enzymes associated with parameters as diverse as synaptic function, myelin metabolism, calcium homeostasis, energy metabolism and lysosomal function [15,18]. In general, changes are often brain region-specific, and not all enzymes studied are affected by maternal hypothyroxinemia [15]. These findings are analogous to the selective dysfunctions observed in humans in the iodine-deficient regions.

In this communication, we have extended the above studies to include enzyme activities associated with glutamate metabolism. We also report on the effect of maternal hypothyroxinemia on glutamate metabolism, amino acid synthesis from glucose, and amino acid (leucine) uptake/incorporation into protein in tissue slices from cerebral cortex of adult progeny.

Materials and Methods

Materials

L-[1-^{14}C]Glutamic acid (specific activity 58 mCi/mmol), L-[U-^{14}C] glutamic acid (specific activity 280 mCi/mmol), D-[U-^{14}C]glucose (specific activity 270 mCi/mmol), L-[4,5-^{3}H]leucine (specific activity 70 Ci/mmol) and NCS tissue solubiliser were obtained from Amersham International (Aylesbury, Bucks, U.K.). Analytical grade cation exchange resin (AG 50W-X8, 20–50 mesh) was supplied by Bio-Rad (Watford, Herts, U.K.). All biochemicals were from Sigma (Poole, Dorset, U.K.). General laboratory chemicals were purchased from BDH Ltd. (Dagenham, Essex, U.K.) and were of AnalaR grade, whenever possible. Scintillation fluid was supplied by National Diagnostics (Aylesbury, Bucks, U.K.).

Animals

Partially thyroidectomised (parathyroid-intact) and control Sprague-Dawley rat dams were maintained on a standard small laboratory animal diet (iodine-sufficient) in the local animal house facilities. Blood samples were obtained from a tail vein prior to mating with normal males and the animals were allowed to give birth. Progeny were standardised to a litter size of six at birth and allowed to grow to adulthood. Food intake was found to be similar for both sets of dams and for both groups of progeny. Before sacrifice, age-matched progeny were normally weighed and, in certain cases, blood samples were collected. Brains were removed, weighed and cerebral cortices dissected on ice.

Tissue preparation

For enzyme assays, homogenates (10% w/v in 0.25 M sucrose) of cerebral cortex were prepared. For metabolic studies, tissue slices were prepared: the cerebral cortex was washed in Krebs Ringer phosphate buffer (KRP; composition: NaCl (118 mM), KCl (4.74 mM), $CaCl_2$ (1 mM), KH_2PO_4 (1.185 mM), $MgSO_4$ (1.185 mM) and sodium phosphate buffer pH 7.4 (16.15 mM)) and longitudinal free-hand slices were cut with a Stadie-Riggs blade (2 slices per hemisphere). Each slice was added to a separate flask containing the appropriate incubation medium (4°C).

Metabolic studies

For determination of glucose and glutamate metabolism, cortical slices were incubated in flasks containing either 0.125 μCi [U-^{14}C]glucose and 10 mM carrier glucose or 0.5 μCi [U-^{14}C]glutamate, 10 mM carrier glutamate and 0.1 mM glucose. A well containing a filter paper wick moistened with hyamine hydroxide was suspended in each flask to absorb liberated CO_2. Flasks were gassed with oxygen, tightly capped and then incubated at 37°C (or 4°C for controls) for 1 h. At

the end of the incubation procedure, flasks were chilled on ice and immediately processed.

For determination of leucine uptake and incorporation into protein, incubation medium consisted of 2 ml KRP containing 1 μCi [4,5-^{3}H]leucine, 2 mM carrier leucine and 10 mM glucose. Incubations were conducted as described above, except the CO_2 trapping wells were omitted.

Sample processing

Filter paper wicks were removed from the appropriate flasks and prepared for liquid scintillation counting (LSC). Tissue slices from all incubations were transferred to centrifuge tubes and pelleted (2000 g, 10 min, 4°C). Pellets were washed twice with 2 ml ice-cold incubation medium (minus radiotracer) and then homogenised in 2 ml water (4°C). Aliquots of homogenate were removed for determination of total accumulation of radioactivity and protein. The remainder of the sample was precipitated with an equal volume of 1 M perchloric acid and, after centrifugation (2000 g, 20 min, 4°C), the pellet was washed with 2 ml perchloric acid (0.2 M). Combined supernatants were neutralised and stored at −20°C, prior to further processing. For leucine and glucose experiments, insoluble material (protein) was extracted (twice) with chloroform:methanol (3:1; 2 ml) and the delipidated pellet was digested with NCS tissue solubiliser (0.2 ml). This was then prepared for LSC.

The perchloric acid-soluble material was neutralised with KOH and then passed through a 2 ml column of cation exchange resin (AG 50W-X8, hydrogen form). The columns were washed with five bed volumes of water and then eluted with five bed volumes of 1 M ammonia. Aliquots of the water wash (which contain glucose and tricarboxylic acid cycle intermediates) and ammonia eluates (amino acid fraction) were counted (LSC).

Enzyme assays

Glutamate decarboxylase (EC 4.1.1.15) activity was determined by assay of $^{14}CO_2$ release from [1-^{14}C]glutamate [19]. Glutamine synthetase (EC 6.3.1.2) was assayed by a colorimetric procedure [20]. In GABA transaminase (EC 2.6.1.19) assays, succinic semialdehyde formation from GABA was determined by reaction with 3,5-diaminobenzoate [21]. Glutamate dehydrogenase (EC 1.4.1.2) activity was determined by measurement of NADH oxidation in the presence of α-ketoglutarate and ammonia [22]. A malate dehydrogenase-coupled procedure [23] was used for aspartate aminotransferase (EC 2.6.1.1) assay.

Determination of thyroid hormones

Plasma total T_4 and T_3 were determined by 'in house' radioimmunoassay procedures.

Protein determination

Protein was assayed by a dye-binding procedure [24].

Statistical analysis

Statistical significance of the results was evaluated by the paired Student's t test. All results are expressed as mean ± standard error of the mean (S.E.).

Results

Thyroid hormone status of animals

Plasma total T_4 levels in thyroidectomised dams were severely reduced compared with normal dams: values (mean ± S.E., n = 5) were 13.5 ± 3.9 nM and 44.7 ± 9.1 nM, respectively ($p<0.02$). Plasma total T_3 levels were reduced to a lesser extent in thyroidectomised dams (0.84 ± 0.11 nM and 1.22 ± 0.16 nM, respectively), but this difference was not statistically significant.

In adult progeny (n = 8) from normal and thyroidectomised dams, both plasma total T_4 (37.3 ± 4.9 nM and 38.3 ± 6.2 nM, respectively) and total T_3 (1.07 ± 0.10 nM and 1.00 ± 0.13 nM) levels were similar. Thus, maternal hypothyroxinemia during pregnancy was without effect on the thyroid status of the progeny at adulthood.

Brain and body weights of adult progeny

The body weights of male progeny from thyroidectomised dams were increased by 23%, compared with control progeny ($p<0.02$; Table 1). The body weights of female experimental progeny were also increased, but by only 11%, and this difference was not statistically significant. No difference was apparent in brain weights of control and experimental progeny (Table 1).

Table 1. Body and brain weights of adult progeny from normal and thyroidectomised dams. Data are mean ± S.E. of ten animals

Sex	Dam type	Body weight (g)	Brain weight (g)
Male	Normal	471.0 ± 19.6	2.03 ± 0.07
	Thyroidectomised	578.8 ± 34.1[a]	2.07 ± 0.07
Female	Normal	286.4 ± 12.3	1.95 ± 0.06
	Thyroidectomised	316.1 ± 8.4	1.96 ± 0.03

[a]$p<0.02$; control progeny *versus* progeny of thyroidectomised dams, Student's t test.

Table 2. Specific activities of enzymes associated with glutamate metabolism in cerebral cortex from adult progeny of normal (N) and thyroidectomised (TX) dams

Enzyme	Specific activity	
	N-dam progeny	Tx-dam progeny
Glutamate decarboxylase	0.60 ± 0.07	0.55 ± 0.0
Glutamine synthetase	36.4 ± 3.1	33.1 ± 3.2
GABA transaminase	5.23 ± 0.22	4.85 ± 0.43
Aspartate aminotransferase	568 ± 34	520 ± 48
Glutamate dehydrogenase	41.4 ± 2.5	43.8 ± 5.6

Homogenates of cerebral cortex were prepared in 0.25 M sucrose and a variety of enzymes assayed as described in *Materials and Methods*. Activities (mean ± S.E. minimum of five animals) are expressed as nmol/mg protein/min. No significant differences were found between the two groups (Student's t test).

Enzyme activities associated with glutamate metabolism

The specific activities of a variety of enzymes associated with glutamate metabolism were assayed in homogenates of cerebral cortex from control and experimental adult progeny (Table 2). In thyroidectomised dam progeny, a slight increase (6%) in glutamate dehydrogenase activity was observed, whereas all other enzyme activities were decreased (by approximately 10%). None of the above changes were statistically significant.

Table 3. Glutamate metabolism in tissue slices of cerebral cortex from adult progeny of normal (N) and thyroidectomised (TX) dams

Fraction	Radioactivity	
	N-dam progeny	Tx-dam progeny
CO_2	4842 ± 443	4344 ± 453
Glucose/tricarboxylic acid intermediates	5178 ± 987	5200 ± 1198
Amino acids	6181 ± 372	6086 ± 909

Slices were incubated in KRP containing 10 mM [U-^{14}C]glutamate and 0.1 mM glucose at 37°C (or 4°C for controls). Liberated CO_2 was trapped in a well containing hyamine hydroxide. After 1 h, washed tissue was homogenised in water and then precipitated with perchloric acid. Neutralised soluble material was fractionated on a cation exchange column to yield glucose/tricarboxylic acid intermediate (water wash) and amino acid (ammonia eluate) fractions. Results (mean ± S.E. of six animals) represent radioactivity (dpm/mg protein) associated with the specified fractions after correction for control (4°C) values. No significant differences were found between the two groups (Student's t test).

Table 4. Glucose metabolism in tissue slices of cerebral cortex from adult progeny of normal (N) and thyroidectomized (TX) dams

Fraction	n	Radioactivity	
		N-dam progeny	TX-dam progeny
CO_2	6	666 ± 87	443 ± 55
Glucose/tricarboxylic acid intermediates	6	2105 ± 185	1155 ± 87[a]
Amino acids	4	268 ± 29	138 ± 12[b]
Protein	4	16 ± 2	11 ± 2

Slices were incubated in flasks with KRP plus 10 mM [U-^{14}C]glucose and a well containing hyamine hydroxide to trap CO_2. After 1 h at 37°C (or 4°C for controls), washed tissue was homogenised in water and protein precipitated with perchloric acid. The pellet was delipidated before counting. Neutralised soluble material was fractionated on a cation exchange column to yield glucose/tricarboxylic acid intermediate (water wash) and amino acid (ammonia eluate) fractions. Data (mean ± S.E.) represent radioactivity (dpm/mg protein) associated with the specified fractions, after correction for 4°C control values. The number of animals studied (n) is indicated.
[b]$p<0.01$, [a]$p<0.005$; control progeny versus progeny of thyroidectomised dams (Student's t test).

Glutamate metabolism in tissue slices

Glutamate metabolism in adult progeny was further evaluated by incubation of cerebral cortical slices with [U-^{14}C]glutamate (Table 3). No obvious difference was observed between control and experimental progeny with respect to labelling of the total amino acid pool or the glucose/tricarboxylic acid intermediate pool, whereas a slight (10%; not statistically significant) decrease was observed in the labelling of CO_2 in thyroidectomised dam progeny (Table 3).

Glucose metabolism in tissue slices

Glucose metabolism *in vitro* was studied by incubation of cerebral cortical slices with [U-^{14}C]glucose. Statistically significant reductions were observed for thyroidectomised dam progeny in the labelling of the glucose/tricarboxylic acid intermediate fraction (45%, $p<0.005$) and the total amino acid pool (49%, $p<0.01$) (Table 4). Although the reductions in label associated with the CO_2 and protein fractions of experimental progeny were also large (>30%), these differences were not statistically significant.

Leucine accumulation and incorporation into protein in tissue slices

Only a slight decrease was observed in total radioactivity in slices from thyroidectomised dam progeny, whereas a much greater (20%) reduction was observed in the labelling of the protein fraction (Table 5). This latter difference was not statistically significant.

Table 5. Leucine accumulation and protein incorporation in tissue slices of cerebral cortex from adult progeny of normal (N) and thyroidectomised (TX) dams

Fraction	Radioactivity	
	N-dam progeny	Tx-dam progeny
Total accumulation	12475 ± 530	11732 ± 606
Protein	244 ± 21	194 ± 13

Slices were incubated in KRP containing 2 mM [4,5-^{3}H]leucine and 10 mM glucose for 1 h at 37°C (or 4°C for controls). Washed tissue was homogenised in water and total radioactivity determined. Protein was precipitated with perchloric acid and the pellets were delipidated before counting. Results (mean ± S.E. of seven animals) represent radioactivity (dpm/mg protein) associated with the specified fractions after correction for 4°C control values. No significant differences were found between the two groups (Student's t test).

Discussion

In this study, we observed an increase in the body weight of adult progeny of thyroidectomised dams compared with offspring of normal dams. In the case of male progeny, the increase (23%, $p<0.02$) was greater than that for female progeny (11%, not statistically significant). Several other studies have also reported significant changes in body weight of progeny from severely hypothyroid [17] and hypothyroxinemic dams [25], but values were found to be decreased. The discrepancy may be related to the age of the progeny studied: in the latter reports, foetuses and suckling animals were investigated, whereas in the present study, adult animals were used. Although the reasons for the increase in body weight of adult progeny are not known, it should be mentioned that food intake in control and experimental progeny after weaning was similar.

Age differences also exist with respect to the effect of maternal thyroidectomy on the brain weight of the progeny. Brain growth of young progeny has been reported to be compromised as a consequence of maternal hypothyroidism [17] and hypothyroxinemia [25], whereas the brain weight of the adult progeny studied here appeared normal. Longitudinal studies are therefore required to clarify the effects of maternal thyroidectomy on both brain and somatic growth of progeny.

We have previously reported that maternal hypothyroxinemia during pregnancy results in a spectrum of biochemical changes in brains of young and adult progeny [15,18]. We have now extended these studies to include amino acid metabolism. Initial experiments revealed only slight changes in enzyme activities associated with glutamate metabolism, and this was subsequently confirmed by analysis of glutamate metabolism in cerebral cortical slices. Although none of the observed changes were statistically significant, a 10% reduction in the activity of glutamate decarboxylase is consistent with a 10% decrease in labelling of the CO_2 pool from [U-^{14}C]glutamate.

Cerebral cortical metabolism of glucose in progeny from thyroidectomised dams was severely affected. Incorporation of the glucose carbon skeleton into total amino acids was greatly reduced (by 48%, $p<0.01$) and it is not surprising therefore, that subsequent incorporation of radioactivity into protein also differed (decreased by 31%, but not statistically significant). In addition, glucose oxidation was depressed, as evidenced by a decrease in the labelling of the CO_2 fraction (by 33%, not statistically significant). Together, these findings indicate a decreased rate of turnover of glucose in the experimental progeny. Such a proposal is consistent with previous work in this laboratory demonstrating a reduction in the activity of lactate dehydrogenase in cerebral cortical homogenates from adult progeny [15]. However, since the findings in the present study were associated with a significant reduction in the labelling of the intracellular glucose/tricarboxylic acid intermediate fraction (by 45%, $p<0.005$), then the results may also be explained by a decrease in the size of the intracellular glucose pool, possibly mediated by impaired transport function. Direct measurement of the intracellular glucose pool in progeny from thyroidectomised dams should help clarify this issue.

Irrespective of the identity of the metabolic steps that are compromised in adult progeny, the above results indicate that *de novo* synthesis of amino acids from glucose is reduced, whereas amino acid catabolism (at least in the case of glutamate) is essentially unaffected. Such findings are consistent with the selective pattern of damage observed for other biochemical parameters in the CNS of adult progeny from thyroidectomised dams [15]. For example, in the case of acetylcholine metabolism, degradation (acetylcholine esterase activity) is impaired in cerebral cortex, whereas synthesis (choline acetyltransferase activity) is normal [15]. Since glutamate may serve as an important respiratory and metabolic substrate in the brain, it is possible that normal glutamate catabolism may alleviate the damage resulting from compromised glucose catabolism.

In an attempt to gain a better understanding of the mechanisms responsible for the above effects, we designed experiments to investigate protein synthesis in the experimental animals. Although labelling of the protein fraction from glucose was reduced in experimental progeny, it is difficult to draw firm conclusions since labelling of both the total glucose and the total amino acid pools was also affected. Therefore, cerebral cortical slices were incubated with radiolabelled leucine, under flooding conditions, and the total accumulation of ^3H and its incorporation into protein determined. Although total accumulation was similar in both types of progeny, protein incorporation was reduced by 20% in the experimental group. Although this decrease was not statistically significant ($0.1>p>0.05$), the coefficient of variation between slice preparations from different animals was high (approximately 20%). We believe, however, that this may represent a real result, based on previous measurements of enzyme activities in brains from adult progeny of thyroidectomised dams [15]; statistically significant degrees of change normally fall within the range 20–40%. Furthermore, not all enzyme activities studied are affected and, in a few cases, activities are actually increased.

The mechanisms by which maternal hypothyroxinemia during pregnancy result in compromised brain function in progeny are not understood. We have previously demonstrated that the thyroid hormones stimulate both glucose uptake and leucine incorporation into protein in neuronal cultures derived from fetal brain [26,27]. It is feasible, therefore, that a decreased supply of maternal T_4 during pregnancy will result in defects in these parameters in progeny. What is surprising though, is the fact that an altered pattern of metabolism is observed in the progeny at adulthood, despite their apparently normal thyroid status (as judged by total T_4 and total T_3 measurements). Thus, the effects we observe are irreversible.

Many workers have shown that hypothyroidism and hyperthyroidism exert deleterious effects on postnatal brain development [9–12]. These effects can normally be reversed by correction of the thyroid status of the animal, providing that this is performed early in development (before 10–14 postnatal days in the rat) [11]. Our results imply the existence of similar critical time period(s), with requirements for an adequate supply of (maternal) thyroid hormones, much earlier in development, most likely before the onset of independent fetal thyroid function (17.5 gestational days in the rat). If these developmental stages are missed, then subsequent correction of the thyroid status of the progeny will be without effect. Furthermore, the degree of dependence upon thyroid hormones and the timing of these critical periods may vary for different proteins. Although it has been reported that glutamate-metabolising enzymes are under thyroid hormone control in neural cell cultures systems and developing brain [28–32], these enzyme activities were apparently normal in adult progeny of thyroidectomised dams.

Work is currently in progress to investigate the effects of maternal hypothyroxinemia on the ontogenesis of amino acid metabolising systems in progeny, in order to ascertain the controlling influence of thyroid hormones on CNS cell types.

References

1. Hetzel BS (1983) The Lancet II: 1126–1129.
2. Pharoah POD, Delange F, Fierro-Benitez R and Stanbury JB (1980) In: Stanbury JB and Hetzel BS (eds.) Endemic Goiter and Endemic Cretinism. John Wiley and Sons, Inc., New York, pp. 395–421.
3. Ma T, Lu TZ, Tan YB and Chen BZ (1986) In: Kochupillai N, Karmarkar MG and Ramalingaswami V (eds.) Iodine Nutrition, Thyroxine and Brain Development, Tata McGraw-Hill, New Delhi, pp. 28–33.
4. Connolly KJ (1986) In: Kochupillai N, Karmarkar MG and Ramalingaswami V (eds.) Iodine Nutrition, Thyroxine and Brain Development. Tata McGraw-Hill, New Delhi, pp. 317–323.
5. Pharoah POD, Buttfield IH and Hetzel BS (1971) The Lancet I: 308–310.
6. Ekins R (1985) The Lancet I: 1129–1132.
7. Pharoah POD, Lawton NF, Ellis SM, Williams ES and Ekins RP (1973) Clin. Endocrinol. 2: 193–199.
8. Chopra IJ, Hershman JM and Hornabrook RW (1975) J. Clin. Endocrinol. Metab. 40: 326–333.
9. Ford DH and Cramer EB (1977) In: Graves GD (ed.) Thyroid Hormones and Brain Development. Raven Press, New York, pp. 1–18.
10. Nunez J (1984) Mol. Cell. Endocrinol. 37: 125–132.

11. Dussault JH and Ruel J (1987) Ann. Rev. Physiol. 49: 321–334.
12. Timiras P (1988) In: Meisami E and Timiras PS (eds.) Handbook of Human Growth and Developmental Biology. CRC Press, Inc., Boca Raton, Florida, Vol. 1(part C): pp. 59–82.
13. Woods RJ, Sinha AK and Ekins RP (1984) Clin. Sci. 67: 359–363.
14. Ekins RP, Sinha AK and Woods RJ (1986) In: Kochupillai N, Karmarkar MG and Ramalingaswami V (eds.) Iodine Nutrition, Thyroxine and Brain Development. Tata McGraw-Hill, New Delhi, pp. 222-245.
15. Ekins R, Sinha A, Ballabio M, Pickard M, Hubank M, Al Mazidi Z and Khaled M (1989) In: Delange F, Fisher DA and Glinoer D (eds.) Research in Congenital Hypothyroidism. Plenum Publishing Corporation, New York, pp. 42–60.
16. Obregon MJ, Mallol J, Pastor R, Morreale de Escobar G and Escobar del Rey F (1984) Endocrinology 114: 305–307.
17. Morreale de Escobar G, Pastor R, Obregon MI and Escobar del Rey F (1985) Endocrinology 117: 1890–1900.
18. Ruiz de Elvira MC, Sinha AK, Pickard M, Ballabio M, Hubank M and Ekins RP (1989) J. Endocrinol. 121: 331–335.
19. Nistico G, diGiorgio RM, de Luca G and Macaione S (1979) J. Neurochem. 33: 343–346.
20. Ward HK and Bradford HF (1979) J. Neurochem. 33: 339–342.
21. Maitre M, Ciesielski L, Cash C and Mandel P (1975) Eur. J. Biochem. 52: 157–169.
22. Chee PY, Dahl JL and Fahien LA (1979) J. Neurochem. 33: 53–60.
23. Wenthold RJ (1980) Brain Res. 190: 293–297.
24. Bradford MM (1976) Anal. Biochem. 72: 248–254.
25. Hubank M, Ballabio M, Sinha A, Gullo D, Bidey S, Bashir A and Ekins R (1986) Ann. Endocrinol. (Paris), (Abstract) 47: 48.
26. Pickard MR, Sinha AK, Gullo D, Patel N, Hubank M and Ekins RP (1987) Endocrinology 121: 2018–2026.
27. Gullo D, Sinha A, Ballabio M, Pickard M, Hubank M, Bidey S and Ekins RP (1987) Ann. Endocrinol. (Paris), (Abstract) 48: 79.
28. Pasquini JM, Kaplun B, Garcia Argiz CA and Gomez CJ (1967) Brain Res. 6: 621–634.
29. Garcia Argiz CA, Pasquini JM, Kaplun B and Gomez CJ (1967) Brain Res. 6: 635–646.
30. Ruel J and Dussault JH (1985) Dev. Brain Res. 21: 83–88.
31. Fernandez-Pastor JM, Morata P, Escobar MC, Fernandez-Pastor VJ and Morell M (1986) Rev. Esp. Fisiol. 42: 251–256.
32. Aizenman Y and de Vellis JM (1987) Brain Res. 406: 32–42.

Address for correspondence: Arun K. Sinha, Department of Molecular Endocrinology, University College and Middlesex School of Medicine, Mortimer Street, London W1N 8AA, U.K.

The biological importance of the formation of nitric oxide from L-arginine*

Richard M.J. Palmer and Salvador Moncada

Wellcome Research Laboratories, Langley Court, Beckenham, Kent BR3 3BS, U.K.

Abstract

Nitric oxide (NO) is synthesised from the terminal guanidino nitrogen atoms of L-arginine by the vascular endothelium, cytotoxic macrophages, neutrophils and brain synaptosomes. The enzyme(s) responsible are soluble, NADPH-dependent and require a divalent cation, which has been identified as Ca^{2+} in brain synaptosomes, and are inhibited by L-N^G-monomethyl arginine (L-NMMA). Endothelial NO plays a role in the control of vascular tone and of platelet-vessel wall interactions through activation of soluble guanylate cyclase. L-NMMA induces a hypertensive response *in vivo*, demonstrating the importance of endothelial NO synthesis in the maintenance of blood pressure. The synthesis of NO contributes to the cytotoxic properties of macrophages and may be involved in intercellular communication in the brain. The formation of NO is therefore a widespread transduction mechanism for the regulation of cell function and communication.

The discovery of the importance of the vascular endothelium in mediating relaxation of vascular tissue [1], by the release of a labile humoral factor, endothelium-derived relaxing factor (EDRF), led to the description of a number of properties of this substance and a great deal of speculation as to its identity [2]. Endothelium-derived relaxing factor relaxes vascular smooth muscle, inhibits platelet aggregation, causes disaggregation of aggregated platelets and inhibits platelet adhesion via activation of soluble guanylate cyclase and the resultant elevation of cGMP levels. It is labile (half-life 3–50 sec), inactivated by oxygen and superoxide anions (O_2^-) and is bound by haemoglobin. Furthermore, it is inactivated by some redox compounds through the generation of O_2^- [for review see 3].

Following the suggestion by both Furchgott [4] and Ignarro *et al.* [5] that EDRF might be NO, we studied the comparative pharmacology of EDRF on vascular strips and on platelets and demonstrated the release of NO from endothelial cells, vascular tissue and the isolated perfused Langendorff heart in amounts sufficient to account for the biological activity observed (for review see [3]). These and other studies showed that EDRF and NO were indistinguishable and therefore that a mammalian cell could synthesise NO.

More recently, we have shown by mass spectrometry that endothelium-derived NO is synthesised enzymically from the terminal guanidino nitrogen atoms of the amino acid L-arginine [6]. We have also characterised L-N^G-monomethyl arginine (L-NMMA) as an enantiomerically specific inhibitor of this pathway [7] and have

* This presentation was awarded the Ajinomoto Prize for the best oral communication of the congress.

partially characterised the enzyme responsible for the synthesis of NO in homogenates of porcine vascular endothelial cells. This enzyme is soluble, NADPH-dependent, requires a divalent cation, forms L-citrulline as a co-product and is inhibited by L-NMMA [8].

The identification of L-NMMA as an inhibitor of endothelial NO synthesis has allowed the study of the role of NO formation from L-arginine in the control of vascular tone. L-NMMA inhibits acetylcholine-induced endothelium-dependent vascular relaxation and release of NO from the perfused rabbit aorta, without affecting relaxations induced by nitroglycerin [9]. Furthermore, L-NMMA inhibits acetylcholine induced release of NO and fall in coronary perfusion pressure in the coronary circulation of the rabbit heart in vitro [10] indicating that the L-arginine: NO pathway is present in both conduit arteries and resistance vessels.

More significantly, L-NMMA induces an increase in mean arterial blood pressure and inhibits the hypotensive action of acetylcholine in the anaesthetised rabbit. These effects are enantiomer specific, reversed by L-arginine and are accompanied by a reduced release of NO from the perfused aorta from treated animals *ex vivo* [11]. This, together with the finding that L-NMMA causes similar vasoconstrictions in all vascular beds of the conscious rat studied to date [12], confirms the proposal that NO is the endogenous nitrovasodilator and suggests that a reduction in the synthesis of NO may contribute to the genesis of hypertension. The release of NO by the vascular endothelium may also play other regulatory roles in the cardiovascular system including modulating platelet function and leukocyte-vessel wall interactions. Whether NO also regulates vascular smooth muscle cell replication or cholesterol metabolism requires investigation.

A novel, L-NMMA inhibitable, L-arginine-dependent pathway has also been demonstrated in activated macrophages, which contributes to the cytotoxic activity of these cells [13,14]. This pathway results in the formation of L-citrulline and NO_2^- and NO_3^-, formed as a result of the breakdown of NO. The latter has recently been shown to be synthesised by these cells [15–17]. The cytotoxic effects of NO are thought to be mediated by inhibition of iron-containing enzymes in target cells, although NO may also regulate cGMP levels in cells with which the macrophage comes into contact.

The release of an NO-like material has also been detected in peritoneal neutrophils [18]. We have recently shown that this synthesis is inhibited by L-NMMA, in an enantiomerically specific manner, and this effect is reversed by L-arginine [19]. Furthermore, NO synthesis by these cells is enhanced by F-met-Leu-Phe (FMLP), which interacts with the O_2^- formed in response to FMLP in a manner which suggests that NO may modulate O_2^- levels [19].

In 1977, a low molecular weight activator of the soluble guanylate cyclase in brain synaptosomes, whose action was inhibited by haemoglobin, was described [20] and subsequently identified as L-arginine [21]. In view of this we investigated whether the brain contained the NO-forming enzyme and found that L-arginine was converted to L-citrulline with the concomitant synthesis of NO. This reaction was NADPH- and Ca^{2+}-dependent and inhibited by L-NMMA [22]. While this

work was in progress, Garthwaite *et al.* [23] reported that N-methyl-D-aspartate induced the release of an EDRF-like material from cerebellar cells. It is possible that many agents that induce the elevation of cGMP levels in the brain do so by activation of the L-arginine: NO pathway. The functional importance of this pathway in the brain remains to be established. It is possible that NO may act as a transmitter, may modulate transmitter release or may modulate the actions of other transmitters, or all three, through elevation of cGMP.

Furthermore, it is also possible that NO could be the non-adrenergic, non-cholinergic transmitter in the rat anococcygeus and the bovine retractor penis, since the response to nerve stimulation in both preparations can be inhibited by L-NMMA (J.S. Gillespie, personal communication).

Present evidence indicates that the L-arginine: NO pathway is widely distributed. The similarities between the systems from different sources are remarkable in that the enzymes are soluble, NADPH-dependent, divalent cation-dependent and are inhibited by L-NMMA. It is not possible, as yet, to tell whether they are the same enzyme or a system of isoenzymes. The latter is more likely since there are small variations in the potency of inhibitors in the different cells. For example L-canavanine inhibits macrophage [24] and neutrophil [19] NO synthesis without affecting the enzyme in the brain [22] or endothelium [8].

The precise enzymic mechanism for formation of NO from L-arginine, the mechanism of its activation and the source of L-arginine have yet to be established. In addition, the importance of this pathway in relation to other L-arginine-metabolising pathways also requires elucidation. Since the presence of the arginine: NO pathway has also been implicated in Kupffer cells [25] and in adenocarcinoma cells [26], we can postulate that this is a widespread transduction mechanism which contributes to the regulation of a variety of functions in different cells.

Nitric oxide is a potent activator of soluble guanylate cyclase and is probably the endogenous activator of this enzyme. It is also possible that NO may exert some of its effects by other mechanisms unrelated to activation of this enzyme. Nitric oxide is a nitrosating agent and since it is thought to activate soluble guanylate cyclase through an interaction with the iron atom in the haem of the enzyme and such an interaction also underlies its interaction with haemoglobin and the target enzymes in tumour cells, it is tempting to speculate that all the actions of NO are mediated through an interaction with transition metals.

The precise distribution of the L-arginine: NO pathway in the body remains to be systematically investigated. What is already evident is that the arginine: NO pathway serves a general regulatory function which, if altered, could contribute to the pathogenesis of a wide variety of diseases.

Acknowledgements

We wish to thank Mrs. G. Henderson and Mrs. E.A. Higgs for their assistance in the preparation of this manuscript.

References

1. Furchgott RF and Zawadzki JV (1980) Nature 288: 373–376.
2. Furchgott RF (1984) Ann. Rev. Pharmacol. Toxicol. 24: 175–197.
3. Moncada S, Radomski MW and Palmer RMJ (1988) Biochem. Pharmacol. 37: 2495–2501.
4. Furchgott RF (1988) In: PM Vanhoutte (ed.) Vasodilatation: Vascular Smooth Muscle, Peptides, Autonomic Nerves and Endothelium (1988) Raven Press, New York, 401–414.
5. Ignarro LJ, Burns RE and Wood KS In: PM Vanhoutte (ed.) Vasodilatation: Vascular Smooth Muscle, Peptides, Autonomic Nerves and Endothelium (1988) Raven Press, New York, 427–436.
6. Palmer RMJ, Ashton DS and Moncada S (1988) Nature 333: 664–666.
7. Palmer RMJ, Rees DD, Ashton DS and Moncada S (1988) Biochem. Biophys. Res. Commun. 153: 1251–1256.
8. Palmer RMJ and Moncada S (1989) Biochem. Biophys. Res. Commun. 158: 348–352.
9. Rees DD, Palmer RMJ, Hodson HF and Moncada S (1989) Br. J. Pharmacol. 96: 418–424.
10. Amezcua JL, Palmer RMJ, De Souza BM and Moncada S (1989) Br. J. Pharmacol. 97: 1019–1024.
11. Rees DD, Palmer RMJ and Moncada S (1989) Proc. Natl. Acad. Sci. USA 86: 3375–3378.
12. Gardiner S, Compton A, Bennett T, Palmer RMJ and Moncada S (1989) Br. J. Pharmacol. 98: 623P.
13. Hibbs JB Jr., Vavrin Z and Taintor RR (1987) J. Immunol. 138: 550–565.
14. Iyengar R, Stuehr DJ and Marletta M (1987) Proc. Natl. Acad. Sci. USA 84: 6369–6373.
15. Marletta MA, Yoon PS, Iyengar R, Leaf CD and Wishnock JS (1988) Biochemistry 27: 8706–8711.
16. Hibbs JB Jr, Taintor RR, Vavrin Z and Rachlin EM Biochem. Biophys. Res. Commun. 157: 87–94.
17. Stuehr DJ, Gross S, Sakuma I, Levi R and Nathan C (1989) J. Exp. Med. 169: 1011–1020.
18. Rimele TJ, Sturm RJ, Adams LM, Henry DE, Heaslip RJ, Weichman BM and Grimes D (1988) J. Pharmacol. Exp. Ther. 245: 102–111.
19. McCall TB, Boughton-Smith NK, Palmer RMJ, Whittle BJR and Moncada S (1989) Biochem. J. 261: 293–296.
20. Deguchi T (1977) J. Biol. Chem. 252: 7617–7619.
21. Deguchi T and Yoshioka M (1982) J. Biol. Chem. 257: 10147–10151.
22. Knowles RG, Palacios M, Palmer RMJ and Moncada S (1989) Proc. Natl. Acad. Sci. USA 86: 5159–5162.
23. Garthwaite J, Charles SL and Chess-Williams R (1988) Nature 336: 385–388.
24. Iyengar R and Marletta MA (1988) Biochemistry 27: 3096.
25. Billiar TR, Curran RD, Stuehr DJ, West MA, Bentz BG and Simmons RL (1989) J. Exp. Med. 169: 1467–1472.
26. Amber IJ, Hibbs JB, Taintor RR and Vavrin Z (1988) J. Leuk. Biol. 43: 187–192.

Effects of infusion of leucine and other essential amino acids on leucine metabolism in humans

W. Frederick Schwenk and Morey W. Haymond

Department of Pediatrics, Endocrine Research Unit, Mayo Clinic and Foundation, Rochester, MN 55905, U.S.A.

Abstract

Infusion of leucine intravenously in normal postabsorptive humans appears to stimulate leucine oxidation and non-oxidative leucine disappearance (an estimate of protein synthesis). However, estimates of leucine kinetics made during these studies are complicated because the pool being sampled is also being perturbed by the exogenous leucine infusion. Despite this problem, isotope dilution techniques using a radioactive tracer to measure the rate of appearance of an intravenous leucine infusion labeled with a stable tracer appear to be valid at least up to an infusion rate of 0.5 μmol of leucine·kg^{-1}·min^{-1}. Preliminary reports using other amino acid tracers during an exogenous leucine infusion suggest that leucine may not affect protein degradation until rates of leucine infusion are ≥1.0 μmol.kg^{-1}·min^{-1}.

Introduction

Numerous *in vitro* studies have suggested that the branched-chain amino acids, and in particular leucine, may modulate protein metabolism [1–5]. The mechanism by which this occurs is not completely understood but is thought to involve stimulation of protein synthesis at the level of peptide chain initiation and/or inhibition of protein degradation through lysosomal stabilization [5].

Because leucine and the other branched chain amino acids are reversibly and rapidly transaminated to their respective α-keto acids [α-ketoisocaproate (KIC) in the case of leucine] both *in vitro* and *in vivo* [6], it is unclear whether the anabolic effects of the branched-chain amino acids are mediated through the amino acids themselves or their α-keto acids.

The effects of the branched-chain amino acids on *in vivo* estimates of protein metabolism have recently been reviewed [5]. As is true with the *in vitro* data, the results are somewhat conflicting. If nitrogen balance is used as the primary experimental variable, infusion of leucine, KIC, or total parenteral nutrition enriched with branched chain amino acids has been reported to cause nitrogen sparing in most but not all reports [7–13].

Another approach to studying *in vivo* protein metabolism has been to assess the effects of the branched-chain amino acids on protein turnover by using isotope dilution techniques. In these studies, a labeled amino acid is infused intravenously to measure the rate of appearance and/or oxidation of a specific amino acid into the

plasma space. There appears to be agreement in the data from such studies that provision of leucine, either orally or intravenously, stimulates oxidation of leucine in normal volunteers [14–21]. However, when an infusion of leucine has been found to exert an anabolic effect, conflicting results have appeared concerning whether this effect occurs because of a decrease in protein degradation and/or an increase in protein synthesis [14,20–24]. The purpose of this report is to summarize some of the limitations of the mathematical model used in these isotope infusion studies, as well as to review the somewhat conflicting studies involving intravenous infusion of leucine in humans.

Modeling whole body amino acid metabolism during intravenous infusion of leucine

Studies investigating *in vivo* protein metabolism have often used isotopically labeled leucine as a tracer. Since leucine is an essential amino acid, its measured rate of appearance in the fasted state provides an estimation of protein degradation.

Measurements are usually made at substrate and isotopic 'steady state' – a time when the rate of appearance of leucine (Ra) is equal to its rate of disappearance (Rd). If breath collections are also carried out to estimate leucine oxidation (Ox), the rate of incorporation of leucine going into protein (NOLD) can be calculated as:

$$Rd = Ox + NOLD \tag{1}$$

At steady state, the rate of appearance of leucine into the plasma space (μmol/min) can be calculated by the Fick principle using the equation:

$$Ra = \frac{F}{SA} \tag{2}$$

where F (dpm/min) is the infusion rate of the isotopic tracer, and SA (dpm/μmol) is the plasma specific activity of the infused tracer. Use of the above equation – the so-called 'primary pool' model – assumes that all leucine derived from protein degradation enters the plasma space. However, leucine derived from proteolysis most likely enters the intracellular rather than the extracellular space. Thus, the intracellular leucine specific activity is probably lower than the plasma leucine specific activity. Since the only source of KIC is the intracellular transamination of leucine and the transamination of leucine and KIC is rapid and not rate limiting, the specific activity of plasma KIC during infusion of labeled leucine (or, conversely, the specific activity of plasma leucine during infusion of labeled KIC) may provide a more accurate indication of the intracellular leucine specific activity than the plasma specific activity of the infused tracer itself. Based on this assumption, we recently proposed an alternative method to assess 'total carbon leucine flux', which uses the same equation above (Equation 2), except that SA is the specific activity

of labeled KIC during labeled leucine infusion or the specific activity of labeled leucine during infusion of labeled KIC [25] – the so-called 'reciprocal pool model'. The reciprocal pool model has now been applied to a number of clinical states, including during infusion of unlabeled leucine [14] and appears to be more accurate than the traditional primary pool model [25].

During infusion of labeled and unlabeled leucine, the labeled leucine must trace the entry of unlabeled leucine entering intracellularly (from protein degradation) and intravenously (from the infusion). During infusion of unlabeled leucine along with simultaneous infusion of [4,5-^{3}H]leucine and [1-^{14}C]KIC, similar estimates of the total leucine rate of appearance were obtained with either isotope [14]. At the higher rate of infusion (1.0 μmol of leucine·kg^{-1}·min^{-1}), the traditional method of using the plasma leucine specific activity during infusion of labeled leucine ('primary pool model') underestimated the rate of leucine infusion [14].

In that previous study, about 10% of the leucine that was infused was administered as L-[5,5,5-$^{2}H_3$]leucine. (99% mole % enrichment, Merck, Sharp and Dohme, Pointe Claire-Dorval, Quebec, Canada). Analysis of the plasma [5,5,5-$^{2}H_3$]leucine and [5,5,5-$^{2}H_3$]KIC enrichments at steady state have now been completed using gas chromatography/mass spectrometry as previously described [26].

While isotopic tracers are usually used to assess rate of appearance of unlabeled substrate, one isotopic tracer can also be used to measure the rate of appearance of another [15]. If one is at steady state, Equation 2 can be utilized, except that 'SA' is now the ratio of one tracer to another. By including [$^{2}H_3$]leucine in our infusate, the simultaneously infused [^{3}H]leucine can be used to trace the rate of appearance of the [$^{2}H_3$]leucine. The results of such calculations during infusion of leucine at 0.47 and 0.94 μmol·kg^{-1}·min^{-1} are shown in Table 1. At the lower infusion rate (Group 2), the [^{3}H]leucine data accurately predicted the measured infusion rate of [$^{2}H_3$]leucine (pump infusion rate × concentration of [$^{2}H_3$]leucine). At the higher infusion rate, the estimated rate of [$^{2}H_3$]leucine was about 10% lower than the measured infusion rate, although this difference was not statistically significant.

Table 1. Rate of infusion of [5,5,5-$^{2}H_3$]leucine measured directly and estimated using [5,6-^{3}H]leucine

Group[a]	Total leucine infusion rate (μmol·kg^{-1}·min^{-1})	[5,5,5-$^{2}H_3$]leucine infusion rate (μmol·kg^{-1}·min^{-1})	
		Measured	Estimated (using [5,6-^{3}H] leucine)
Group 2 (n=5)	0.474 ± 0.044	0.047 ± 0.004	0.045 ± 0.003
Group 3 (n=5)	0.932 ± 0.019	0.093 ± 0.002	0.084 ± 0.004

[a] Groups are those described in reference 14.
All values mean ± SEM.

These data, along with our previously published study [14], confirm that up to 0.5 μmol of leucine·kg^{-1}·min^{-1}, both the primary and reciprocal pool models can be utilized to assess accurately an exogenous infusion of leucine. At rates of leucine infusion of 1.0 μmol·kg^{-1}·min^{-1} or more, the primary pool model may underestimate the exogenous infusion rate, at least when [^{3}H] leucine is infused. The explanation for this discrepancy is not clear but may be the result of a small systematic analytical overestimation of the specific activities or saturation of the transport of labeled and unlabeled leucine into and out of the intracellular space.

Summary of previous reports involving whole body estimations of protein metabolism during infusion of leucine

Table 2 summarizes five previous reports of the effect of intravenous leucine on whole body estimates of protein metabolism. In two studies involving infusion of labeled leucine [14,15], infusion of leucine intravenously increased leucine oxidation, except at the lowest dose of leucine infusion (0.16 μmol·kg^{-1}·min^{-1}). In our previous study [14], this increase in leucine oxidation appeared to be dose dependent over the range of 0 to 1.0 μmol·kg^{-1}·min^{-1}.

We also found that using the reciprocal pool model, intravenous infusion of leucine into normal subjects in the postabsorptive state had no effect on endogenous leucine appearance [14]. However, infusion of leucine affected amino acid metabolism since the concentration of total amino acids and essential amino acids

Table 2. Effects of an intravenous leucine infusion on protein metabolism *in vivo* in humans

Reference	Leucine infusion rate (μmol·kg^{-1}·min^{-1})	Isotopes employed	Conclusions		
			Protein degradation	Protein synthesis	Leucine oxidation
14	0.47, 0.94	[4,5-^{3}H]leucine [1-^{14}C]KIC	↔	↑	↑
15	0.16, 0.26	[4,5-^{3}H]leucine [1-^{14}C]KIC	↔	↔	↔,↑
22	?	[5,5,5-^{2}H$_3$]leucine [1-^{13}C]lysine	↔	?	?
23	0.25, 0.50, 1.00	[1-^{14}C]leucine [ring-2,6-^{3}H] phenylalanine	↔	?	?
24	2.50	[ring-^{2}H$_5$] phenylalanine [1-^{13}C]valine	↓	?	?

↓ = decrease, ↑ = increase, ↔ = no change, ? = not reported.

decreased ($p<0.05$ or better) during leucine infusion compared to saline controls (total amino acids: -26 ± 20, -110 ± 16, -155 ± 23 μM for saline infusion, and leucine infusions at 0.47 μmol·kg^{-1}·min^{-1}, and 0.94 μmol·kg^{-1}·min^{-1}, respectively). These results for leucine were also in contrast to two additional groups of normal volunteers who were infused with isoleucine or threonine for 3 h at ≈0.5 μmol·kg^{-1}·min^{-1}, where leucine kinetic and amino acid concentration changes were similar to saline controls.

In that study, the decrease in plasma amino acid concentrations during infusion of leucine appeared to be the result of a relatively greater rate of non-oxidative leucine disappearance (protein synthesis) when compared to the saline control and not an effect on proteolysis. In contrast, at lower rates of leucine infusion [15], no change in the non-oxidative rate of disappearance of leucine was observed when compared to saline controls.

Each of the studies discussed so far has a limitation in that conclusions are being drawn using leucine tracers during infusion of unlabeled leucine. To validate our conclusions that an infusion of leucine up to 1.0 μmol·kg^{-1}·min^{-1} does not seem to affect the exogenous leucine rate of appearance, additional studies have been carried out in normal subjects using [^{3}H] phenylalanine as a tracer. As we have reported in preliminary form [24], changes in phenylalanine flux before and after leucine infusion up to 1.0 μmol of leucine·kg^{-1}·min^{-1} were similar to changes in phenylalanine flux observed during a saline control.

Finally, there have been two other recent preliminary reports of studies involving infusion of leucine in normal humans where an amino acid tracer other than leucine was employed [22,23]. In the first of these two reports, an infusion of leucine at a rate not stated did not seem to affect lysine flux, while in the second an infusion of leucine at 2.5 μmol·kg^{-1}·min^{-1} decreased phenylalanine flux.

Taken as a whole, these five studies seem to suggest that leucine may not have an effect on protein degradation until more than 1.0 μmol of leucine·kg^{-1}·min^{-1} is infused. One might suggest that the higher leucine infusion rates may be stimulating insulin secretion; however, in none of these five studies has the leucine infusion seemed to stimulate insulin secretion as assessed by plasma insulin and C-peptide measurements. Finally, the total amount of leucine infused in our study [14] over 3 h was similar to the estimated total daily requirement of leucine in humans [16,17]; whether there is any physiologic significance to higher doses of infused leucine as used in the other studies is unclear.

The five studies discussed involve only infusion of leucine. Several authors have also investigated the acute effects of a balanced amino acid infusion on leucine metabolism [20,21]. In the first study, Gelfand infused leucine at 1.85 μmol·kg^{-1}·min^{-1} along with other amino acids for 4 h and found stimulation of leucine oxidation and protein synthesis and suppression of protein degradation. Similar findings were reported by Pacy infusing a solution containing leucine at 0.96 μmol of leucine·kg^{-1}·min^{-1}. Whether these disparate results are due to the inclusion of other amino acids along with the leucine or are due to use of a primary pool model of leucine metabolism at high infusion rates of leucine is unclear.

Summary

In vivo studies involving infusion of leucine intravenously appear to agree that leucine infusion can stimulate non-oxidative leucine disappearance (an estimate of protein synthesis). Estimates of leucine kinetics made during these studies are complicated because the pool being sampled is also being perturbed by the exogenous leucine infusion. Preliminary reports using other amino acid tracers suggest that leucine may not affect protein degradation until rates of leucine infusion are ≥ 1.0 $\mu mol \cdot kg^{-1} \cdot min^{-1}$.

Acknowledgements

This work was supported in part by National Institutes of Health Grants, DK 26989 and RR-585 and the Mayo Foundation. WF Schwenk was supported in part by the National Institutes of Health Grant DK-07352.

References

1. Buse MG and Reid SS (1975) J. Clin. Invest. 56: 1250–1261.
2. Mitch WE and Clark AS (1984) Biochem. J. 222: 579–586.
3. Fulks RM, Li JB and Goldberg AL (1975) J. Biol. Chem. 250: 290–298.
4. Mortimore GE, Poso AR, Kadowski M and Wert JJ Jr (1987) J. Biol. Chem. 262: 16322–16327.
5. May ME and Buse MG (1989) Diabet. Metab. 5: 227–245.
6. Harper AE, Miller RH and Block KP (1984) Ann. Rev. Nutr. 4: 409–454.
7. Mitch WE, Walser M and Sapir D (1981) J. Clin. Invest. 67: 553–562.
8. Sherwin RS (1978) J. Clin. Invest. 61: 1471–1481.
9. Freund H, Hoover HC Jr, Atamian S and Fischer JE (1979) Ann. Surg. 190: 18–23.
10. Daly JM, Mihranian MH, Kehoe JE and Brennan MF (1983) Surgery 94: 151–158.
11. Cerra FB, Upson P, Angelico R, Wiles C, Lyons J, Faulkenbach LA and Paysinger J (1982) Surgery 92: 192–199.
12. Cerra FB, Mazuki JE, Chute E, Nuwer N, Teasley K, Jolynn L, Shronts EP and Konstantinides FN (1984) Ann. Surg. 199: 286–291.
13. Sapir DG, Walser M, Moyer ED, Rosenshein NB, Stewart PM, Moreadith C, Imbembo AL and Munoz S (1983) Lancet 1: 1010–1014.
14. Schwenk WF and Haymond MW (1987) Am. J. Physiol. 253: E428–434.
15. Tessari P, Tsalikian E, Schwenk WF, Nissen SL and Haymond MW (1985) Am. J. Physiol. 249: E121–E130.
16. Meguid MM, Matthews DE, Bier DM, Meredith CN, Soeldner S and Young VR (1980) Am. J. Clin. Nutr. 43: 770–780.
17. Cortiella JC, Matthews DE, Hoen RA, Bier DM and Young VR (1988) Am. J. Clin. Nutr. 48: 998–1009.
18. Motil KJ, Matthews DE, Bier DM, Burke JF, Munro HN and Young VR (1981) Am. J. Physiol. 240: E712–721.
19. Sketcher RD, Fern EB and James WPT (1974) Br. J. Nutr. 31: 333–342.
20. Gelfand RA, Glickman MG, Castellino P, Loward RJ and De Fronzo RA (1988) Diabetes 37: 1365–1372.
21. Pacy PJ, Garrow JS, Ford GC, Merritt H and Halliday D (1988) Clin. Sci. 75: 225–231.

22. Nair KS, Matthews DE, Wee SL and Braiman T (1988) Clin. Res. 36: 358A.
23. Lecavalier L and Haymond MW (1988) Clin. Res. 36: 852A.
24. Nair KS, Schwartz RS and Wee SL (1989) Clin. Res. 37: 333A.
25. Schwenk WF, Beaufrere B and Haymond MW (1985) Am. J. Physiol. 249: E646–E65U.
26. Schwenk WF, Berg PJ, Beaufrere B, Miles JM and Haymond MW (1984) Anal. Biochem. 141: 101–109.

The use of amino acid based CAPD fluid in chronic renal failure

Gerald A. Young, John B. Dibble and Aleck M. Brownjohn
Renal Research Unit, General Infirmary, Leeds LS1 3EX, U.K.

Abstract

CAPD is a major treatment for end-stage renal disease. A dialysis fluid in the peritoneum, changed several times a day, uses glucose, an effective osmotic agent but which contributes to hyperlipidaemia and malnutrition. Amino acids have been investigated as an alternative to glucose in several short and long-term studies described in the literature. One to two % amino acids are maximally absorbed into blood after 2–4 h and decrease to initial concentrations after 6 h unless constituents are in excess e.g. phenylalanine and methionine. These changes and those for other metabolites are similar to a marked post-prandial effect. In several studies up to 12 weeks duration, one or two exchanges of 1% amino acids daily were well tolerated with modest nutritional improvement (e.g. in amino acids, transferrin or total body nitrogen), small decreases in hyperlipidaemia, with no clinical problems due to loss of appetite, increase in urea, overhydration or acidosis. Both these and less favourable studies suggest problems could occur with higher concentrations or multiple exchanges and also in unsuitable patients. Slight loss of ultrafiltration and increased protein losses into dialysate suggest a reversible effect on permeability. Our studies suggest that amino acid exchanges increase complement activation by the alternative pathway which with generation of prostaglandin E2, increases permeability. However, amino acids absorbed exceed all protein losses, although percentage utilisation is not known. Amino acid based fluids are unsuitable for patients on high protein or low calorie diets or those requiring more effective dialysis. Fluids containing increased buffering capacity and lower concentrations of certain amino acids are indicated.

Introduction

Continuous ambulatory peritoneal dialysis (CAPD) was first introduced in 1976 [1] and is now a major treatment for end-stage renal disease. During CAPD the peritoneum behaves as a semi-permeable membrane allowing 'uraemic' molecules to dialyse from the patient, and the presence of an osmotic agent in the dialysis solution, which is changed three or four times a day, maintains the intraperitoneal volume and ultrafiltrates excess fluid. Glucose, the usual osmotic agent, is used in several different concentrations and is cheap and effective but has been associated with hyperlipidaemia, obesity and other metabolic problems [2,3]. High glucose fluids may contribute to loss of appetite leading to a decrease in dietary protein [4]. If dietary intake is insufficient to meet requirements and compensate for the daily losses of about 1.2–3.4 g of amino acids and 5–15 g of protein into dialysate [5] then gradual depletion of body nitrogen is likely [6] (Fig. 1). About 40% of CAPD patients may have some degree of malnutrition [7] including decreases in some amino acids and proteins both in plasma and muscle [5], low plasma albumin [4]

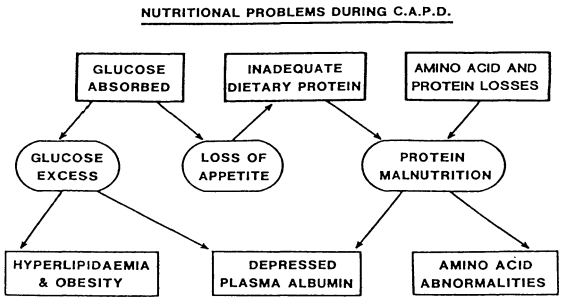

Fig. 1. The interrelated effects of glucose dialysis fluid and protein malnutrition.

and losses of muscle, fat and body weight (Fig. 1). Chemical and hormonal abnormalities of renal failure may contribute to protein energy malnutrition and complicate both the diagnosis and treatment.

Amino acids were first used as a supplementary osmotic agent in glucose based dialysis solutions to prevent amino acid losses during haemodialysis [8] and peritoneal dialysis [9,10]. These studies showed that the addition of amino acids reduced losses into the dialysate and maintained plasma concentrations. In 1979 Oreopoulis *et al.* [11] first suggested the use of amino acids to replace glucose as the osmotic agent during CAPD. Since that time there have been several short term studies that have confirmed amino acids as an effective osmotic agent with respect to ultrafiltration and the clearance of creatinine, urea and potassium [12–14]. The changes in osmolality that occur during dialysis with 1% amino acids are similar to those for 1.36% glucose [15] whereas those for 2% amino acids are similar to 4.25% glucose solutions [12].

An ideal amino acid based CAPD fluid in addition to functioning as an osmotic solution, should contain optimum concentrations to promote protein synthesis and

Table 1. Composition of 1% amino acid solution (Baxter '151')

	mg/l		mg/l	
Valine	1,260	Proline	540	
Arginine	970	Glycine	460	
Leucine	920	Serine	460	
Lysine (HCl)	860	Tryptophan	250	
Alanine	860	Tyrosine	60	
Isoleucine	770	Calcium chloride	260	(1.77 mmol/l)
Methionine	770	Magnesium chloride	150	(0.74 mmol/l)
Phenylalanine	750	Sodium lactate	3,920	(35 mmol/l)
Histidine	650	Sodium chloride	5,500	(94 mmol/l)
Threonine	590	pH	6.2	

avoid excesses of any constituents that would contribute to acidosis, toxicity, loss of appetite or effects on the peritoneal membrane. The first commercially available solution (Baxter Dianeal 151), which we have used in our own studies, contains 1% amino acids and provides 20 g/per 2 litre exchange (Table 1). This solution is high in branched-chain amino acids and low in glycine and alanine. Unlike earlier solutions acetate is not included and at pH 6.2, additions of sodium bicarbonate solution are not required. Calcium, magnesium and lactate composition were similar to Dianeal 1.36% glucose.

Our evaluations of '151' were made on eight patients with plasma albumin less than 35 g/l who had been on CAPD for at least four months and remained free from peritonitis. Details of this study have been described elsewhere [16]. Eight hour dialysis studies on fasting patients were carried out during a glucose exchange (1.36%) and on the following day when 1% amino acid fluid was substituted. Blood and dialysate samples were collected at 1,2,4,6 and 8 h (Fig. 2). After 6 h of a '151' exchange, 13% of the 15 amino acids remained and after 8 h 8% was left. As in several short term studies in adults the maximum rate of absorption occurred during the first 2–4 h when the concentration in plasma was maximal [12] although in children, maximal absorption probably occurs during the first hour [17,18]. During our glucose exchanges the small increase in plasma amino acids can be attributed to the standardised breakfast given after the start of each dialysis (20.5 g protein and 460 Kcal). At the end of each '151' exchange most amino acids had returned to their initial concentrations with the exception of branched-chain amino acids, methionine and phenylalanine which were between 150 and 250%. Methionine maintained the highest concentrations throughout each exchange, as in previous studies [12,17]. Amino acids in excess may be utilised or removed during subsequent glucose exchanges. However, any adverse effects of these amino acids

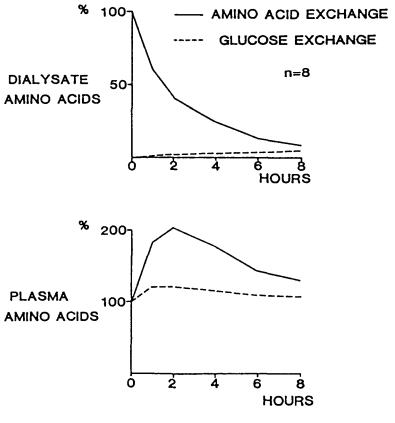

Fig. 2. Percentage of total amino acids remaining in the dialysis solution during 8 h dwell times. Changes in plasma during 'amino acid' and 'glucose' exchanges are expressed as a percentage of fasting concentrations.

particularly during multiple exchanges could be avoided in future solutions by the use of lower concentrations.

During '151' and glucose exchanges plasma glucose and insulin increased whilst growth hormone was suppressed. Similar observations were made in a previous study although the glucose response was greater during glucose exchanges whilst insulin and glucagon increases were greater during amino acids [15]. More detailed studies of changes during dialysis for free fatty acids, triglycerides, apolipoproteins and cholesterol have been described elsewhere [19].

In the first long-term study, 1% amino acid fluid was alternated with glucose exchanges for four weeks in patients eating less than 0.8 g/kg/day of dietary protein [20]. An improvement in nutritional status was indicated by increases in total body nitrogen and serum transferrin. In a later assessment [21] a similar regime over 12 weeks induced beneficial plasma amino acid concentrations although no other improvements in nutritional status occurred, probably because all seven patients were consuming a protein rich diet in excess of 1.2/kg daily. In a recent communication [22] a 1% amino acid solution was considered to be ineffective when infused overnight in five patients for six months probably due to low calorie intake or because they were not severely malnourished. Patients on overnight exchanges are likely to be calorie starved unless a meal or calorie supplement is given at the start of an exchange. In our study [16], eight patients received one exchange of 1% amino acid fluid daily and most were eating less than 1.2 g/kg daily. Nutritional improvements were modest but transferrin increased in all but one a patient who developed influenza. We did not observe any significant increases in albumin, IgG, IgA or prealbumin or fasting concentrations of individual amino acids although essential and total amino acids did increase. In a recent study using 1% amino acids over a six month period, improvements in nitrogen balance were observed [23].

A potential benefit of using one or more exchanges of amino acid based CAPD fluid is the reduction in the amount of glucose absorbed. The continual absorption of glucose during CAPD increases triglycerides, cholesterol and apolipoprotein B and promotes obesity. During our long term study we have not observed any significant decrease in triglycerides and glucose, non-esterified fatty acids or body fat [16,19] although cholesterol and apolipoprotein B decreased in seven of our patients on a constant calorie intake. There was a tendency for triglycerides to decrease in an earlier four week study [20] and both triglycerides and cholesterol significantly decreased in the recent six month assessment by Bruno *et al.* [23]. Further investigations are required, using constant calorie intakes, to establish whether amino acid-based fluids may have a role in the treatment of CAPD patients with a high risk of cardiovascular disease. Such a benefit is unlikely if additional calories are required to obtain maximum utilisation of amino acids.

In our study using a single exchange of '151', amino acids were tolerated well with no clinical acidosis, uraemia, loss of appetite or hydration problems. Similar observations were made in the previous studies using two exchanges per day but with 1% amino acid fluid of different composition [20,21]. However, certain potential problems would be evident if higher concentrations or multiple ex-

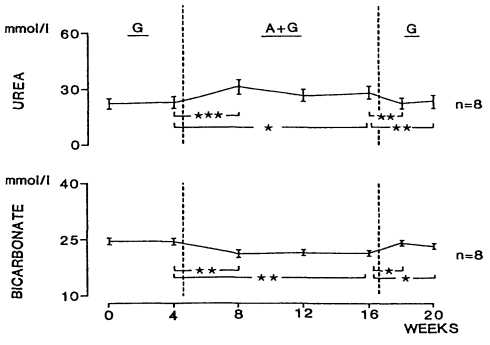

Fig. 3. Mean (± SE) for plasma urea and bicarbonate during the 20 week study period when either glucose (G) or amino acid (A) were used for the morning exchange. * $p<0.05$, ** $p<0.01$, *** $p<0.001$.

changes were used particularly if buffering was inadequate, utilisation poor or patients underdialysed.

In our study we incorporated control periods of four weeks when glucose exchanges only were used, both before and after 12 weeks of '151' exchanges. Urea increased significantly by 36% after four weeks of amino acids and subsequently decreased over the following eight weeks by 18% and returned to the initial concentration when glucose solution was resumed (Fig. 3). None of our patients had any clinical evidence of uraemia although urea could have increased to unacceptable concentrations if dietary intake had been high or if calorie intake was insufficient to allow optimum utilisation. Plasma bicarbonate decreased by 13% during amino acids but chloride was unaffected and there was no clinical evidence of acidosis. Potential problems of acidosis which might occur during multiple exchanges could be avoided by increasing the buffering capacity of the solution. Several biochemical changes which could be beneficial such as significant decreases in phosphate, sodium and potassium were reversed when glucose was restored [16].

During CAPD exchanges the osmolalities for both '151' and 1.36% glucose decreased comparably although the volume of dialysate recovered was lower for the amino acid based fluid [16]. A previous study in children also reported poor ultrafiltration suggesting that amino acids have a slight effect on the permeability of the membrane [17]. Such an effect was also suggested by increases in the absorption of amino acids and losses of proteins during the 12 weeks of '151'. The amounts of amino acid absorbed increased by a small but significant increment of 4% [24]. During glucose exchanges the daily losses of total protein, albumin, transferrin, prealbumin, α_1-acid glycoprotein and immunoglobulin were comparable to previous studies [25,26], but over 12 weeks of '151' the losses increased and decreased when glucose was restored. The clearance of all these proteins, expressed as dialysate to plasma concentration ratios (D/P) were increased at the start of '151' exchanges by an average of 18% and after 12 weeks by 34% [24]

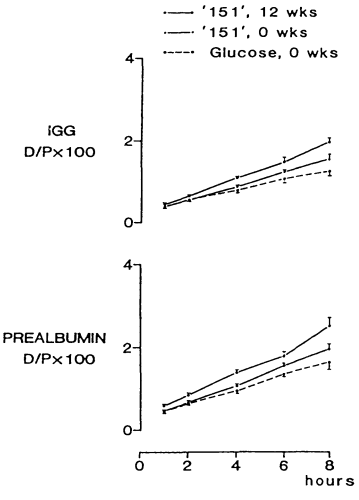

Fig. 4. Mean (± SE) dialysate to plasma concentration ratios (D/P) for IgG and prealbumin during dialysis with glucose at week 0 and amino acids at weeks 0 and 12.

(Fig. 4). An increased peritoneal loss of proteins which correlated with an increased generation of prostaglandin E2 was observed during single amino acid exchanges by Steinhauer *et al.* [27].

We are currently investigating factors contributing to the generation of prostaglandin E2 and increased permeability. We have measured complement fragments associated with the activation of complement by the alternative pathway, in both glucose and amino acid dialysates which were collected during our study and

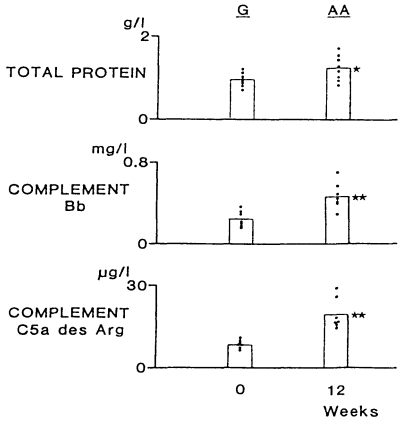

Fig. 5. Dialysate total protein, Bb fragment and C5a des Arg concentrations, before and after 12 weeks of single daily amino-acid exchanges. * $p<0.05$, ** $p<0.01$.

stored at −80°C. The increased protein losses which occurred into amino acid dialysate after twelve weeks, as compared with losses into glucose, were associated with increased amounts of complement Bb and C5a des Arg (Fig. 5). These studies suggest that the increased permeability during the use of amino acid based CAPD fluid is associated with the activation of complement by amino acids or their metabolites to produce C5a and the generation of prostaglandin E2. C5a and its des Arg metabolite increase the permeability of venules to plasma proteins and the prostaglandin increases the intravenular hydrostatic pressure by dilating arterioles [28,29].

The quantity of amino acids absorbed and retained daily from '151' fluid is greater than the losses of protein and amino acids in dialysate and urine, despite the progressive increase in permeability. About 16 g of amino acids are absorbed, of which 1 g is removed during the remaining exchanges of the day in addition to normal daily losses [16]. Most of this absorption occurs during the first 2–4 h of the exchange and we might expect utilisation for protein synthesis both in the liver and in muscle to be maximal during this period, or alternatively if conditions are unfavourable, for degradation to be greatest. The percentage utilisation in the absence of accurate nitrogen balance data or isotopic studies is unknown. However, if plasma concentrations during absorption are similar to those after oral intake the requirements for utilisation may be similar.

The future role of amino acid based CAPD fluid has yet to be established. Potential benefits are evident although the methods of evaluation, conditions for their use and the ideal composition require further investigation. In several studies where amino acid solutions have been ineffective or unfavourable the patients may have been receiving high protein intakes or insufficient calories, or need more effective dialysis or a solution of different composition. Patients who are able to eat more than 1.2 g/kg of dietary protein are unlikely to benefit from amino acids in dialysis fluid and those who are anorexic and malnourished due mainly to uraemia may require more effective dialysis. If malnutrition is due to nitrogen depletion and a good oral intake cannot be maintained, a favourable response to amino fluid is more likely. These patients may require additional calories both at the start and during the exchange to ensure maximum utilisation. The use of multiple exchanges and higher concentrations of amino acids in patients with severe malnutrition will require greater buffering capacity and lower concentrations of certain amino acids, particularly methionine and phenylalanine. Further investigations are necessary to establish the effects of higher concentrations of amino acids and their metabolites on appetite suppression and loss of ultrafiltration.

References

1. Popovich RP, Moncreif JW, Decherd JB, Bomar JB and Pyle WK (1976) ASAIO Journal 5: 64.
2. Ramos JM, Heaton A, McGurk JG, Ward MK and Kerr DNS (1983) Nephron 35: 20–23.
3. Young GA, Hobson SM, Young SM, Young JB, Hildreth B, Gibson J, Coltman SJ, Brownjohn AM and Parsons FM (1983) Lancet II: 1421.

4. Young GA, Young JB, Young SM, Hildreth B, Brownjohn AM and Parsons FM (1986) Nephron 43: 177–186.
5. Lindholm B and Bergstrom J (1986) In: Gokal R (ed.) Continuous Ambulatory Peritoneal Dialysis. Churchill Livingstone, Edinburgh, pp. 228–264.
6. Williams P, Kay R, Harrison J, McNeil K, Petitt J, Kelman B, Mendez M, Klein M, Ogilvie R, Khanna R, Carmichael D and Oreopoulos D (1981) Perit. Dial. Bull. 1: 82–87.
7. Oreopoulos DG, Izatt S, Anderson H, Bergstrom J, Lindholm B, Brownjohn A, Young G, Gibson J Hobson S, DeVecchi A, Scalamogna A, Kopple JD, Blumenkrantz J, DiChiro J, Gentile D, Nissenson A, Sakrani L, Nolph K, Khanna R, Prowant B, Twardowski Z, Algrim C, Martis L, Serkes K, Vonesh E and Zentz M (1989) Kidney Int. (Abstract) in press.
8. Young GA and Parsons FM (1966) Clin. Sci. 31: 299–307.
9. Gjessing J (1968) Lancet II: 812.
10. Jackson MA, Talbot S, Thomas DW and Lee HA (1979) Postgrad. Med. J. 55: 533–536.
11. Oreopoulos DG, Crassweller P, Katirtzoglou A, Ogilvie R, Zellerman G, Rodella H and Vas SI (1979) In: Legrain M (ed.) First International Symposium on CAPD. Excerpta Medica, Amsterdam, pp. 335–340.
12. Williams PF, Marliss EB, Harvey Anderson G, Oren A, Stein AN, Khanna R, Petitt J, Brandes L, Rodella H, Mupas L, Dombros N and Oreopoulos DG (1982) Perit. Dial. Bull. 2: 124–130.
13. Oreopoulos DG, Marliss EB, Harvey-Anderson G, Oren A, Dombros N, Williams P, Khanna R, Rodella H and Brandes L (1983) Perit. Dial. Bull. 3: S10–S12.
14. Lindholm B, Werynski A and Bergstrom J (1988) Artif. Organs. 12: 2–10.
15. Goodship THJ, Lloyd S, Mckenzie PW, Earnshaw M, Smeaton I, Bartlett K, Ward MK and Wilkinson R (1987) Clin. Sci. 73: 471–478.
16. Young GA, Dibble JB, Hobson SM, Tompkins L, Gibson J, Turney JH and Brownjohn AM (1989) Nephrol. Dial. Transplant 4: 285–292.
17. Hanning RM, Balfe JW and Zlotkin SH (1987) Am. J. Clin. Nutr. 46: 22–30.
18. Hanning RM, Balfe JW and Zlotkin SH (1987) J. Pediat. Gastroenterol. Nutr. 6: 942–947.
19. Dibble JB, Young GA, Hobson SM and Brownjohn AM (1990) Perit. Dial. Int. (in press).
20. Oren A, Wu G, Harvey Anderson G, Marliss E, Khanna R, Petitt J, Mupas L, Rodella H, Brandes L, Roncari DA, Kakis G, Harrison J, McNeil K and Oreopoulos DG (1983) Perit. Dial. Bull. 3: 66–73.
21. Pederson FB, Dragsholt C, Laier E, Frifelt JJ, Trostmann AF, Ekelund S and Paaby P (1985) Perit. Dial. Bull. 5: 215–218.
22. Dombros N, Prutis K, Tong M, Anderson H, Harrison J, Sombolos K, Digenis G and Oreopoulos DG (1989) Perit. Dial. Int. Abstract, pp. 556.
23. Bruno M, Bagris C, Marangella M, Rovera L, Cantallupi A and Linari F (1989) Kidney Int. 35: 1189–1194.
24. Young GA, Dibble JB, Taylor AE, Kendall S and Brownjohn AM (1989) Nephrol. Dial. Transplant. 4: 900–905.
25. Furst P, Bergstrom J and Lindholm B (1980) In: Legrain M (ed.) Continuous Ambulatory Peritoneal Dialysis. Excerpta Medica, Amsterdam, pp. 292–297.
26. Young GA, Brownjohn AM and Parsons FM (1987) Nephron 45: 196–201.
27. Steinhauer HB, Lubrich-Birkner I, Kluthe R and Schollmeyer P (1988) Fifth International Congress on Nutrition and Metabolism in Renal Disease (Abstract), pp. 163.
28. Williams TJ and Jose PJ (1981) J. Exp. Med. 153: 136–153.
29. Williams TJ and Peck MJ (1977) Nature 270: 530–532.

Address for correspondence: Dr G.A. Young, Scientific Director, Renal Research Unit, General Infirmary, Leeds LS1 3EX, U.K.

Is serum tryptophan a good indicator of CNS serotonin metabolism in chronic alcoholics with hepatopathy?

E. Baccino[a], J. Caroff[b], J.C. Bigot[a], J.F. Menez[a] and H.H. Floch[a]

[a]Biochemistry Department, Brest School of Medicine, 29285 Brest Cedex, France
[b]Physiology Department, Brest School of Medicine, 29285 Brest Cedex, France

Introduction

Due to the fact that tryptophan hydroxylase is not saturated under normal conditions, the concentration of brain tryptophan greatly influences the rate of serotonin synthesis in rat brain [1]. It is also widely admitted that, at least in rats, tryptophan is transported from the blood to the brain through a saturable uptake mechanism; large neutral amino-acids (principally phenylalanine, thyrosin, leucine, isoleucine and valine) compete with tryptophan for this transport. Therefore it makes sense that significant correlations between brain tryptophan and various serum variables (free tryptophan, total tryptophan, free tryptophan/competitors and total tryptophan/competitors) were reported [2]. Chronically intoxicated baboons and rats also showed a concomitant decrease in brain TRP and 5 HT concentrations and in the serum TRP/competitors ratio [3]. In humans the studies have been limited to the measurement of CSF tryptophan concentrations which reflect those of the brain [4]. In 1975 S.N. Young [4] seemed to confirm the findings previously done on animals by showing a positive relationship between total serum tryptophan and CSF tryptophan in control subjects. However, even if he didn't find any correlation in patients with advanced hepatic cirrhosis, some authors have kept on speculating about human alcoholism physiopathology on the basis of animal experiments [3].

The aim of our study was to confirm the results of Young and moreover to determine whether abstinence has any effect on them.

Patients and Methods

Fifteen males and one female of mean age 42.9 ± 5.8 years (m ± SD) entered the study; all were chronic alcoholics (more than 60 grams of ethanol per day for more than six months) with biological markers of alcoholism (γ GT, MCV) as well as clinical and biological (increased transminases, SGOT/SGPT > 1) evidence of liver damages. All of them were free of medication for at least 15 days before the study and didn't have any disease (psychiatric or organic) susceptible to interfere with

Table 1.

Serum	(m ± SEM) µmol/ml	CSF	(m ± SEM) µmol/ml	Correlation coefficients
Day 1 (n = 16)				
Total TRP	50.5 ± 3.7			NS
Free TRP	10.1 ± 1.3	TRP	1.94 ± 0.3	NS
Total TRP/competitors × 100	9.9 ± 2.1			NS
Free TRP/competitors × 100	2.3 ± 0.3			NS
Day 21 (n = 10)				
Total TRP	52.5 ± 4.9			r = 0.79 (p = 0.056)
Free TRP	10.7 ± 1.6	TRP	2.8 ± 1.3	r = 0.90 (p = 0.005)
Total TRP/competitors × 100	12.6 ± 2.6			NS
Free TRP/competitors × 100	2.2 ± 0.3			NS

serotonin metabolism. CSF and serum were collected at 9.00 a.m. after 12 h of bed rest and fasting. Correlation coefficients between CSF tryptophan and various serum variables (free tryptophan, total tryptophan, free tryptophan/large neutral amino-acids, total tryptophan/large neutral amino-acids) were calculated from samples collected within 24 h of admission and, in 10 of the patients, at day 21 of hospitalization. All the measurements were made by ion exchange chromatography (Biotronick LC 5000 amino acid analyser).

As shown in Table 1, there is no relationship between serum and CSF at day 1; at day 21 CSF tryptophan was correlated significantly and positively with the serum-free tryptophan; correlation between total serum tryptophan and CSF tryptophan almost reached significance (p = 0.056).

Discussion

Our results are consistent with those of Young in showing that in the immediate post intoxication phase (Young collected the samples after 3 days of hospitalization), tryptophan values in the serum do not reflect the CSF concentration. The reasons for these discrepancies are not known but a disorder of the blood brain barrier is suggested; such an abnormal transport across the blood brain barrier was previously demonstrated for large neutral amino-acids (increased) and the di-basic amino-acids (decreased) during hepatic encephalopathy [6]. Regarding our results at day 21, the situation seems to come back to normal even if the serum tryptophan/large neutral amino acids ratio still shows no correlation with CSF values. It is therefore tempting to assume that the impairment of the blood brain barrier is a transient disorder which recovers after abstinence. One explanation for this disorder could be the ethanol related changes in the lipid composition of the cell membranes which are known to disturb the uptake mechanisms and which also return to normal after a period of abstinence. In conclusion our results confirm that

in chronic alcoholics during intoxication, the serum tryptophan concentrations do not reflect the CSF values. It therefore becomes evident that no conclusion can be drawn from studying these values in order to evaluate the CNS serotonin metabolism; in this field it appears that the animal model even under various experimental conditions of intoxication is not a valid tool to explore the physiopathology of chronic human alcoholism. This discrepancy is possibly due to a transient disorder of the blood brain barrier in alcoholic patients which didn't show in experimental animals; the underlying mechanism has not clearly been explained yet and needs further investigations.

References

1. Fernstrom JD (1984) Tryptophan Availability and Serotonin Synthesis in Rat Brain: Effects of Experimental Diabetes. Progress in Tryptophan and Serotonin Research, pp. 161–172.
2. Curzon G and Sarna GS (1984) Tryptophan Transport to the Brain: Newer Findings and Older Ones Reconsidered. Progress in Tryptophan and Serotonin Research, Walter de Gruyter & Co., pp. 145–160.
3. Branchey L, Shaw S and Lieber CS (1981) Ethanol Impairs Tryptophan Transport into the Brain and Depresses Serotonin. Life Sciences, Vol. 29, pp. 2751–2755.
4. Beck O, Borg S and Sedvall G (1983) Tryptophan Levels in Human Cerebrospinal Fluid After Acute and Chronic Ethanol Consumption. Drug and Alcohol Dependence, Vol. 12, pp. 217–222.
5. Young SN, Lal S, Sourkes TL, Feldmuller F, Aronoff A and Martin JB (1975) Relationships Between Tryptophan in Serum and CSF, and 5-Hydroxyindoleacetic Acid in CSF of Man: Effect of Cirrhosis of Liver and Probenecid Administration. Journal of Neurology, Neurosurgery and Psychiatry, Vol. 38, pp. 322–330.
6. Sax NC, Talamini MA and Fischer JE (1985) Clinical Use of Branched-Chain Amino Acids in Liver Disease, Sepsis, Trauma and Burns. Arc. Surg., Vol. 121, pp. 358–366 .

Address for correspondence: E. Baccino MD, CHU A. Morvan, Service Sebileau, 5 Avenue Foch, 29285 Brest Cedex, France.

Effects of branched chain amino acids and ketoanalogues on brain branched chain and aromatic amino acids in experimental liver disease

Santiago Munoz[a], Marshall Stafford[a], Sharon Westerberg[a], Mackenzie Walser[b] and Willis Maddrey[a]

[a]Jefferson Medical College of Thomas Jefferson University, Philadelphia, Pennsylvania, U.S.A
[b]The Johns Hopkins School of Medicine, Baltimore, Maryland, U.S.A.

Abstract

Decreased plasma levels of branched chain amino acids (BCAA) and increased levels of aromatic amino acids (AAA) are often found in patients with liver disease. These abnormalities have been implicated in the pathogenesis of hepatic encephalopathy. In acute hepatic injury BCAA are often normal or slightly elevated and the ratio BCAA/AAA is decreased due largely to elevated AAA concentrations. We investigated the effects of infusing BCAA and their α-ketoanalogues (BCKA) on brain and plasma amino acid patterns of rats with either acute hepatitis or portal hypertension and shunting. Acute hepatitis (Gal-AH) was induced in Sprague-Dawley male rats with an intraperitoneal injection of D(+)galactosamine using standard techniques. Portal hypertension and portal systemic shunting (PHT) was surgically created by subcutaneous transposition of the spleen followed by complete portal vein ligation. Experimental and control groups of animals underwent a 3 h intravenous infusion of the following solutions: isotonic NaCl; BCAA; sodium salts of BCKA (Na-BCKA); ornithine salts of BCKA (Orn-BCKA). BCAA and BCKA were infused at 50% the recommended daily allowance. In addition, BCKA doses were increased by a factor of 0.5 based on previous experiments on the relative efficiency of BCKA for brain protein synthesis in rats with AH and PHT. Plasma and brain tissue levels of the individual BCAA and AAA were determined at the end of the infusions using a Beckman 6300 amino acid analyzer. Gal-AH and PHT rats had lower or similar BCAA/AAA ratios in plasma and brain tissue compared to control animals. Orn-BCKA but not Na-BCKA infusions were able to increase the plasma ratio in PHT rats. Conversely, in Gal-AH rats both BCAA and Na-BCKA infusions induced marked elevation of plasma BCAA/AAA ratio with Orn-BCKA having a lesser effect. Brain tissue of both PHT and Gal-AH rats had much lower BCAA/AAA than did plasma, due primarily to decreased amounts of BCAA in brain tissue. In PHT animals, Na-BCKA, BCAA and Orn-BCKA infusions induced similar elevations of the brain molar ratio with the latter producing the greatest effect. The molar ratio increased only slightly in brain tissue of Gal-AH animals when BCAA were infused. In contrast, the ratio markedly rose when BCKA, given as either Na or Orn salts, were administered. These results indicate that the response of brain BCAA/AAA to BCAA and BCKA infusions differs between rats with acute hepatitis and portal hypertension. Collectively taken our data suggests that in acute hepatic injury, the transport of BCAA into the brain may be impaired while BCKA are still effectively translocated into cells and transaminated to form the corresponding amino acids.

Introduction

Decreased levels of branched chain amino acids (BCAA) and increased levels of the aromatic amino acids (AAA) have been documented in the plasma of patients

with chronic liver disease by several investigators [1–4]. Furthermore, it has been suggested that these abnormalities may have a role in the pathogenesis of the syndrome of hepatic encephalopathy [5–7]. The amino acid pattern appears to differ between acute and chronic liver disease. Thus, in severe acute hepatitis in humans, the plasma levels of BCAA are generally normal or slightly increased whereas the ratio BCAA/AAA is decreased due largely to elevated levels of AAA [8].

Administration of BCAA-enriched mixtures have been reported to ameliorate hepatic encephalopathy although considerable controversy still exist on this issue [9–11]. The α-ketoanalogues of the branched chain amino acids have also been proposed as a rational therapy for both the encephalopathy and malnutrition that occurs in chronic liver disease [12,13]. We have previously shown that the keto-analogues of leucine and valine are effectively transaminated to the corresponding amino acids and utilized for protein synthesis even in the presence of liver disease [14,15]. We now report on the effects of pharmacologic doses of BCAA and branched chain ketoanalogues (BCKA) on the molar ratio of BCAA to AAA in two animal models of liver disease.

Material and Methods

Severe acute hepatitis (AH) was induced in 20 male Sprague-Dawley rats (160–260 g) by intraperitoneal injection of D(+)galactosamine hydrochloride (110 mg/100 g BW, Sigma Co., St. Louis, MO, U.S.A.) according to techniques reported elsewhere [15,16]. Animals were allowed *ad libitum* access to water and rat chow diet (Purina Rodent Lab Chow 5001, 23% protein). Seventy-two hours following the D(+)galactosamine injection, all animals underwent intravenous infusions of either BCAA, BCKA or NaCl according to the protocol described below.

Twenty male Sprague-Dawley rats weighing 230–310 g were anesthetized with ketamine HCl-acepromazine (Parke Davis, Morris Plains, NJ) and portal hypertension with portal systemic shunting was surgically created. Briefly, a subcutaneous transposition of the spleen and promotion of collateral neovascularization was initially performed. Seven to 10 days later, during a second laparotomy, complete and double ligation of the main portal vein was accomplished (Fig. 1). This rat model of portal hypertension and portal systemic shunting resulted in hyperammonemia, atrophy of the liver, encephalopathic behaviour and amino acid changes similar to those observed in the presence of liver disease. Experiments were performed 7–10 days later to allow for recovery.

Infusions

After an overnight fasting, animals were anesthetized and an intravenous polyethylene catheter was inserted and positioned at the level of the inferior vena cava

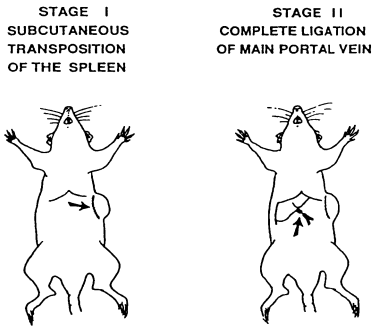

Fig. 1. A rat model of portal hypertension and portal systemic shunting was surgically created in two stages. After the second laparotomy, the animals exhibited abnormal behaviour, hyperammonemia, hepatic atrophy and decreased plasma and brain levels of branched chain amino acids.

(Intermedic tubing i.d. 0.58 mm, Fischer Scientific, Springfield, NJ). Solutions of amino acids and keto-analogues described below were infused over 3 h, 15 min (Infused volume: 5 ml. Rate of infusion: 0.026 ml/min) using a continuous infusion syringe pump (Sage Instruments, model 352, Cambridge, Mass.).

Groups of 4 or 5 rats with AH (Group I.A) or PHT (Group I.B) were infused with isotonic saline (total NaCl administered: 215 ± 1 mg). Additional animals with AH (Group II.A) or PHT (Group II.B) received a solution containing BCAA (leucine: 83 ± 1 mg; isoleucine: 61 ± 1 mg; valine: 67 ± 1 mg). The dose was designed to provide approximately 50% of the recommended daily allowance of each BCAA, based on a 14% protein, 20 g/day, growing rat diet [17]. Amino acids and sodium salts of BCKA were obtained from Sigma Co., St Louis, MO. Sodium salts of the branched chain keto-analogues were administered to rats with AH (Group III.A) and PHT (Group III.B). Doses of BCKA were also calculated to provide approximately 50 % of the recommended daily allowance for the corresponding amino acids. In addition, the amounts of BCKA were increased by a factor of 0.5 based on previous 'studies from our laboratory on the relative efficiency of leucine/ketoleucine and valine/ketovaline for protein synthesis in experimental liver disease [14,15]. α-ketoisocaproate (KIC), α-keto(B)methylvalerate (KMV) and α-ketoisovalerate (KIV) were infused in the amounts of 213 ± 1 mg, 157 ± 1 mg and 175 ± 1 mg respectively. Groups IV.A and IV.B consisted of animals with AH or PHT. Each received infusions of ornithine salts of BCKA in doses calculated in a similar manner as for Group III (ornithine-KIC: 367 ± 1 mg; ornithine-KMV: 270 ± 1 mg ; ornithine-KIV: 314 ± 1 mg). Sodium chloride (217 ± 1 mg) was given to these animals, and to those of groups I (control) and II, to correct for the sodium administered to Group III (see above).

After completion of the infusions, one hour was allowed for equilibration of BCAA and BCKA into the various body compartments. Rats were then sacrificed and whole brain and plasma samples were quickly obtained and freezed at −80°C. Brain tissue was subsequently prepared for amino acid analysis by weighing

Table 1. BCAA/AAA in acute hepatitis (A) and portal hypertension (B)

	Plasma	Brain
A.		
Hepatitis	2.8 ± 0.1	0.6 ± 0.02
controls	3.3 ± 0.1[a]	0.6 ± 0.02
B.		
Portal hypertension	3.7 ± 0.6	1.1 ± 0.2
Controls	2.9 ± 0.5	0.6 ± 0.1

[a]$p < 0.05$ compared to plasma of acute hepatitis. Means ± S.E.M.

aliquots of 250 ± 20 mg, pulverization in liquid nitrogen, homogeneization (BioHomogeneizer, Fischer Scientific, Springfield, NJ) and protein precipitation with 50% sulfosalicylic acid. Samples were filtered through a 0.2μ membrane filter and amino acids were determined using a Beckman 6300 Amino Acid Analyzer (Beckman, Palo Alto, CA) with a 50 μL loop.

Results

Rats with either acute hepatitis or portal hypertension and portal systemic shunting had lower or similar BCAA/AAA ratios in plasma and brain tissue when compared with animals without liver disease (Table 1). In addition, in both groups the concentrations of BCAA in brain were lower than plasma levels (20.4 and 28.7% of plasma values respectively) resulting in a markedly decreased brain BCAA/AAA molar ratios. The plasma molar ratio increased to the same extent after infusion of BCAA or Orn-BCKA in animals with either AH or PHT. However, Na-BCKA infused to PHT rats was not associated with an increase in plasma molar ratio. An additional difference between AH and PHT animals was the absence of effect on brain BCAA/AAA in rats with AH infused with BCAA. This solution resulted in a significant elevation of the brain molar ratio of PHT animals. The plasma and brain BCAA/AAA molar ratios in animals with acute hepatitis are shown in Fig. 2. Infusion of BCAA and Na-BCKA produced massive elevation of the ratio in plasma of rats with AH while Orn-BCKA did so to a lesser extent (non significant). In marked contrast to the plasma ratio, the brain molar ratio increased only slightly when BCAA were administered (0.64 v. 0.75). However, infusion of either sodium or ornithine salts of BCKA however significantly increased the brain molar ratios (0.64 v. 3.4 and 0.64 v. 4.1 respectively).

The BCAA/AAA ratios in plasma and brain tissue of animals with portal hypertension and shunting are shown in Fig. 3. BCAA and ornithine salts of BCKA, but not Na-BCKA, significantly elevated the molar ratio in plasma. In brain tissue, all three mixtures were associated with a significant increase in the molar ratio, with ornithine-BCKA having the greatest effect. BCAA and Na-BCKA increased the brain ratio to a similar extent.

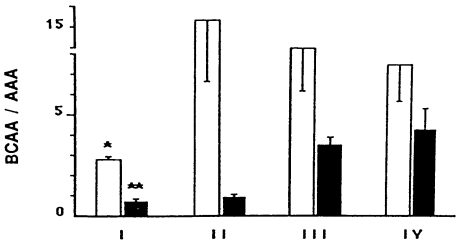

Fig. 2. Molar ratio of branched chain amino acids (BCAA) to aromatic amino acids (AAA) in plasma (❑) and brain tissue (■) of rats with D(+)galactosamine-induced acute hepatitis. Groups I to IV received intravenous infusions of NaCl (group I), BCAA (group II), Na-BCKA (group III) and ornithine-BCKA (group IV) as described in the text. Administration of BCAA and Na-BCKA resulted in elevation of plasma BCAA/AAA (*p<0.005). In brain tissue, sodium and ornithine salts of BCKA were associated with significant increases of the molar ratio (**p<0.001 and p<0.01 respectively).

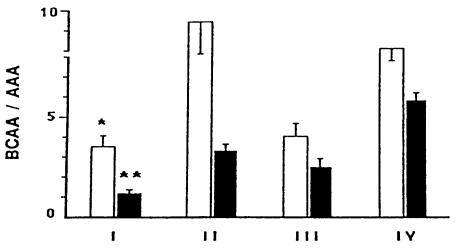

Fig. 3. Molar ratios of BCAA to AAA in plasma (❑) and brain tissue (■) of rats with portal hypertension and portal systemic shunting following intravenous administration of NaCl (group I), BCAA (group II), Na-BCKA (group III) and ornithine-BCKA (group IV) as described in the text. Infusion of BCAA and ornithine-BCKA significantly increased the plasma molar ratio in PHT rats (* p=0.02 and p=0.003 respectively). Administration of BCAA, Na-BCKA and ornithine-BCKA significantly increased the brain molar ratio in portal hypertensive rats compared to NaCl infused animals (**p<0.001). Ornithine salts of BCKA (group IV) caused marked elevation of brain BCAA/AAA (5.6 v. 1.1, p<0.001).

Discussion

The role of BCAA and AAA in the pathogenesis of hepatic encephalopathy is still controversial [18]. We have been interested in the use of the nitrogen-free analogues of the BCAA as a potential therapy for hepatic encephalopathy and malnutrition occurring in severe liver disease. The anticatabolic action of the leucine ketoanalogue, α-ketoisocaproic acid, may also be of benefit due to the increased catabolism found in cirrhosis [19–21]. Our experiments indicate that the BCAA/AAA ratios in brain tissue are substantially lower than those observed in plasma in agreement with the findings from other laboratories [22,23]. Both ornithine and sodium salts of BCKA significantly raised the brain molar ratio while BCAA did not. The ability of BCKA over BCAA to increase BCAA/AAA may be related to an impaired neuronal transport of the neutral amino acids in acute liver disease since abnormalities of the blood brain barrier have been found in acute hepatic failure [24]. In contrast, all three infused mixtures significantly increased the brain molar ratio in animals with portal hypertension and portal systemic shunting, with ornithine salts of BCKA having the greatest effect. In summary, we found that BCKA are be effectively transported into the brain and transaminated to form the corresponding amino acids in animals with acute hepatitis or portal hypertension

and shunting. Translocation of BCAA into neurons may be impaired in the presence of acute hepatic injury. In addition, these results indicate that the effect of exogenous BCAA and BCKA on the concentration of branched chain and aromatic amino acids differ between animals with acute hepatic damage and those with portal systemic shunting. Whether these biochemical changes, induced by administration of BCKA, have a neurophysiological or functional expression remains under study.

References

1. Morgan MY, Milson JP and Sherlock S (1978) Gut 19: 1068–1073.
2. McCullough AJ, Czaja AJ, Jones JD and Go VL (1981) Gastroenterology 81: 645–652.
3. Morgan MY, Marshall AW, Milson JP and Sherlock S (1982) Gut 23: 362–370.
4. Fischer JE, Funovics JM, Aguirre A, James JH, Keane JM, Wesdorp RIC, Yoshimura N and Westman T (1975) Surgery 78: 276–290.
5. James JH, Zipara V, Jeppsson B and Fischer JE (1979) Lancet 1: 772–775.
6. Munro HN, Fernstom JD and Wurtman RJ (1975) Lancet 1: 722–724.
7. Soeters PB and Fischer JE (1976) Lancet 2: 880–882.
8. Record CO, Buxton B, Chase RA, Curzon G, Murray-Lyon IM and Williams R (1976) Eur. J. Clin. Invest. 6: 387–394.
9. Maddrey WC (1985) J. Amer. Coll. Nut. 4: 639–650.
10. Horst D, Grace ND, Conn NO, Schiff E, Schenker S, Viteri A, Law D and Atterbury CE (1984) Hepatology 4: 279–287.
11. Freund H, Dienstag J, Leherich J, Yoshimura N, Bradford R, Rosen H, Atamian S, Slemmer E, Holryode J and Fischer J (1982) Ann. Surg. 196: 209–220.
12. Herlong HF, Maddrey WC and Walser M (1980) Ann. Intern. Med. 93: 545–550.
13. Walser M (1984) Clin. Sci. 66: 1–15.
14. Munoz S and Walser M (1986) Hepatology 6: 472–476.
15. Munoz S, Shotwell B and Maddrey WC (1987) Hepatology 7: 1043.
16. Record CO and Alberti KG (1973) Eur. J. Clin. Invest. 3: 130–135.
17. National Research Council (U.S.), Subcommittee on Laboratory Animal Nutrition. Nutrient Requirements of Laboratory Animals, 2nd rev. ed. Washington, Natl. Acad. of Sciences, 1972.
18. McCullough AJ, Mullen KD and Tavill AS (1983) Hepatology 3: 269–272.
19. Tischler ME, Desautels M and Goldberg AL (1982) J. Biol. Chem. 257: 1613–1621.
20. Marchesini G, Zoli M, Dondi C, Bianchi G, Cirulli M and Pisi E (1982) Hepatology 2: 420–425.
21. Marchesini G, Zoli M, Angiolini A (1981) Hepatology 1: 294–299.
22. Mans AM, Saunders SJ, Kirsch RE and Biebuyck JF (1979) J. Neurochem. 32: 285–292.
23. Peters JC and Harper AE (1985) J. Nutr. 115: 382–398.
24. Zaki AEO, Ede RJ, Davis M and Williams R (1984) Hepatology 4: 359–363.

Modulation by ligands of the phosphorylation state of phenylalanine 4-monooxygenase in intact hepatocytes

Anne P. Døskeland[a], Olav K. Vintermyr[b], Torgeir Flatmark[a], Richard G.H. Cotton[c] and Stein O. Døskeland[b]

[a]*Department of Biochemistry, The Preclinical Institutes, University of Bergen, Årstadveien 19, N–5009 Bergen, Norway*

[b]*Department of Anatomy, The Preclinical Institutes, University of Bergen, Årstadveien 19, N–5009 Bergen, Norway*

[c]*The Birth Defects Research Institute, Royal Children Hospital, Parkville, Victoria 3052, Australia*

Abstract

1. The rate of phosphorylation of phenylalanine hydroxylase was studied in isolated rat liver cells, preincubated with ^{32}Pi. The intracellular cAMP-kinase was activated either by a glucagon-stimulated increase of endogenous cAMP or by N^6-benzoyl-cAMP. The hydroxylase was isolated by immunoaffinity adsorption on anti-PAH(monoclonal)-Protein A- Sepharose and the ^{32}P incorporation measured by autoradiography.

2. When the intracellular concentration of free phenylalanine or chlorophenylalanine was increased (by preincubation of the cells with the relevant amino acid), the rate of phosphorylation of hydroxylase increased. The cellular response was in good agreement with the results obtained with the isolated enzyme (Døskeland AP, Døskeland SO, Øgreid D and Flatmark T (1984) J. Biol. Chem. 259: 11242–11248.)

3. Similarly, preincubation of the cells with the synthetic cofactor 2-amino-4-hydroxy-6,7-dimethyl-5,6,7,8-tetrahydropteridine ($DMPH_4$) also increased the rate of phosphorylation. This response is not observed with the isolated enzyme, and is most likely explained by 1) a cellular uptake of $DMPH_4$, 2) a displacement of the natural cofactor tetrahydrobiopterin (BH_4), bound to the hydroxylase, and 3) the fact that BH_4 is a negative effector in the phosphorylation of hydroxylase by cAMP-dependent protein kinase.

4. Stimulation of the hepatocytes with vasopressine moderately increased the phosphorylation of hydroxylase independently of $DMPH_4$ and phenylalanine. This is in agreement with previous observations on the Ca^{2+}/calmodulin stimulated phosphorylation of hydroxylase *in vitro* (Døskeland AP, Schworer CM, Døskeland SO, Chrisman TD, Soderling TR, Corbin JD and Flatmark T (1984) Eur. J. Biochem. 145: 31–37).

5. It is concluded that the cAMP-stimulated phosphorylation of hydroxylase is regulated by the concentration of both substrate and cofactor in intact hepatocytes.

Introduction

Phenylalanine 4-monooxygenase (phenylalanine hydroxylase; EC 1.14.16.1) is an oligomer composed of identical monomers (M_r = 50,000). One serine residue, Ser^{16} [1,2], is phosphorylated *in vitro* by both cAMP-kinase [3] and multifunctional Ca^{2+}/calmodulin kinase [4]. The rate of phosphorylation of the isolated enzyme by cAMP-kinase is increased by the substrate phenylalanine and decreased by the

natural cofactor, tetrahydrobiopterin (BH_4) at relevant physiological concentrations [5–7]. However, the phosphorylation by Ca^{2+}/calmodulin kinase was slightly inhibited by phenylalanine [4] and not significantly modulated by cofactor (Døskeland A, unpublished observation).

The purpose of the present study was to investigate whether the rate of phosphorylation of the hydroxylase was regulated by ligands (substrate, cofactor) also in the intact hepatocyte.

Experimental procedures

Preparation of hepatocytes

Hepatocytes were isolated from male Wistar rats (200 g) by *in vitro* collagenase perfusion, filtration and low speed centrifugation [8]. Cells were harvested by centrifugation (300 gav., 5 min), washed with and suspended in a low phosphate (0.1 mM) Krebs-Ringer bicarbonate buffer that contained 10 mM Hepes/NaOH pH 7.4. The medium was supplemented with 0.5% (w/v) bovine serum albumin and lactate/pyruvate at final concentrations of 5 mM.

Study of the phosphorylation state of the hydroxylase in hepatocytes

The carrier-free ^{32}Pi was added to the cell suspension (4×10^6 cells/ml) at a final activity of 100 μCi/ml. The cells were incubated at 37°C in a shaking water bath. The additives (kinase activators and substrates or cofactor of the hydroxylase) were dissolved in a low phosphate (0.1 mM) Krebs-Ringer buffer without bicarbonate, but supplemented with 20 mM Hepes/NaOH pH 7.4. Due to its low solubility, chlorophenylalanine (85 mM) was dissolved in alkaline solution. Due to its instability at neutral pH, 2-amino-4-hydroxy-6,7-dimethyl-5,6,7,8-tetrahydropteridine ($DMPH_4$) was kept in 0.1 M HCl in the presence of ascorbic acid until use. Right before addition of the effectors to the incubation medium, they were neutralized by the addition of HCl and NaOH.

Extraction of ^{32}P-hydroxylase from hepatocytes

The phosphorylation reaction was quenched by direct pelleting or pelleting after mixing with saturated ammonium sulphate (see also legend to Fig. 2), and rapid freezing of the pellet in liquid nitrogen. The pellet was homogenized immediately after removal from liquid nitrogen in 1 ml of ice-cold homogenization medium (50 mM NaH_2PO_4-NaOH, pH 7.0, containing 50 mM NaF, 10 mM EDTA, 1 mM EGTA, 0.1 mM AMP, 0.5 mM DTT, 1mM ATP, 1 mM benzamidine, 0.2 mM phenylmethylsulphonyl fluoride, 20 μg/ml leupeptine, 14 μg/ml pepstatine and 0.5 mg/ml soybean trypsin inhibitor). The cytosolic fraction of the homogenate was incubated with specific antibodies, [9,10] immobilized to protein A-Sepharose, and the immunoimmobilized hydroxylase eluted as described in the legend to Fig. 1.

Results and Discussion

Validation of the method used

As shown in Fig. 1, the eluate from the immunoaffinity beads contained one major radioactively-labelled band with a size (M_r = 50,000) corresponding to that of the subunit of the hydroxylase. The amount of phosphate incorporated was determined as the ratio between optical density of the laser-scanned autoradiogram and optical density of the silver-stained gel corresponding to the M_r = 50,000 band. There was an excellent correlation between the degree of blackening of the autoradiographic film and the radioactivity of the excised M_r = 50,000 band as determined by liquid scintillation counting.

The results were similar whether the intracellular phosphorylation was quenched by mixing the cell incubates with saturated ammonium sulphate or by immersion of the cell pellet into liquid nitrogen (Fig. 2).

The initial rate of phosphorylation after the addition of glucagon (Fig. 2) appeared linear with respect to time. This fact and the fact that similar maximum values of phosphate incorporation were obtained with high and moderate initial phosphorylation rates (Fig. 2) argued that the rate of dephosphorylation by phosphatases was modest and probably did not affect the determination of phosphorylation rates.

In order to verify that the specific radioactivity of ^{32}P-ATP remained constant during the period of study, the time course of incorporation of ^{32}Pi into cellular

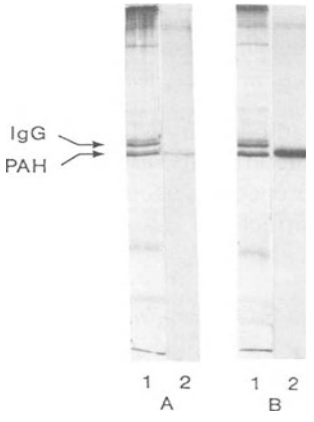

Fig. 1. Typical silver stained polyacrylamide slab gel and its corresponding autoradiogram.

PAH from ^{32}P-labelled hepatocytes was immunoadsorbed using monoclonal antibodies immobilized to protein A-Sepharose and eluted from the Sepharose beads with SDS. The eluate was subjected to PAGE. The gels were silver-stained for protein (lanes 1A,B), dried and subjected to radioautography (lanes 2A,B). The eluate was from cells incubated for 6 min with 5 mM phenylalanine in the absence (A) or presence (B) of 1 μM glucagon. The M_r = 52,000–53,000 doublet stained with silver corresponds to the heavy chain of IgG. The other major band (M_r = 50,000) corresponds to phenylalanine hydroxylase (PAH).

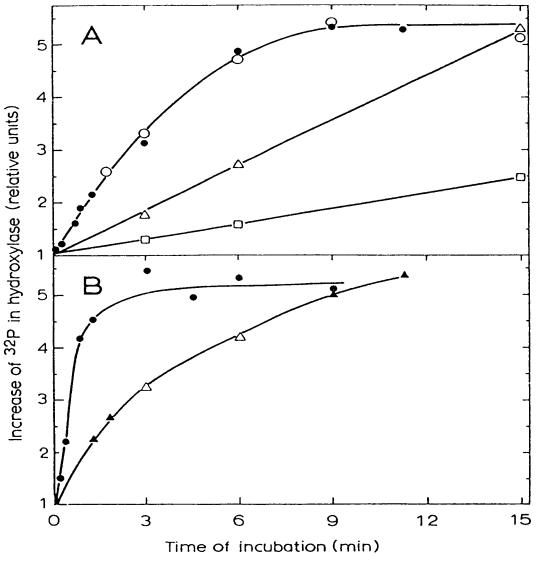

Fig. 2. Time course of the cAMP-dependent phosphorylation of hydroxylase in hepatocytes. Effect of chlorophenylalanine.

The figure shows the time course of incorporation of ^{32}P into hydroxylase as a function of time after addition of glucagon (o, ● ; final concentration 1 μM), 3.5 μM N^6-benzoyl-cAMP (Δ) or 0.35 μM N^6-benzoyl-cAMP (❑). Panel B shows the effect of adding 5 mM DL-*p*-chlorophenylalanine 3 min before the cAMP-elevating agents. The phosphorylation reaction was quenched either by rapidly pelleting the cells and plunging the tube with pellet into liquid nitrogen (open symbols) or by rapidly mixing the cells with saturated ammonium sulphate (filled symbols).

ATP was studied. The specific radioactivity of ATP increased nearly linearly up to 45 min and reached a steady state after about 60 min (Fig. 3) in accordance with earlier reports [11,12]. The presence of effectors (phenylalanine, chlorophenylalanine and $DMPH_4$) did not affect the rate of incorporation of ^{32}P into ATP (Fig. 3).

Modulation of the intracellular cAMP-stimulated phosphorylation of hydroxylase by substrate

Comparison of Fig. 2A and B shows that the hydroxylase was phosphorylated 3.5 to 4 times faster in hepatocytes exposed to 5 mM chlorophenylalanine in the medium. The rate of phosphorylation was enhanced to a similar range when the cells were preincubated with phenylalanine (Table 1). The degree of enhancement was similar whether the phosphorylation was activated by glucagon/forskolin/3-isobutyl-1-methyl-xanthine (IBMX) or by the cAMP analog N^6-benzoyl-cAMP (Fig. 2, Table 1). Glucagon/forskolin/IBMX increased the cAMP level more than

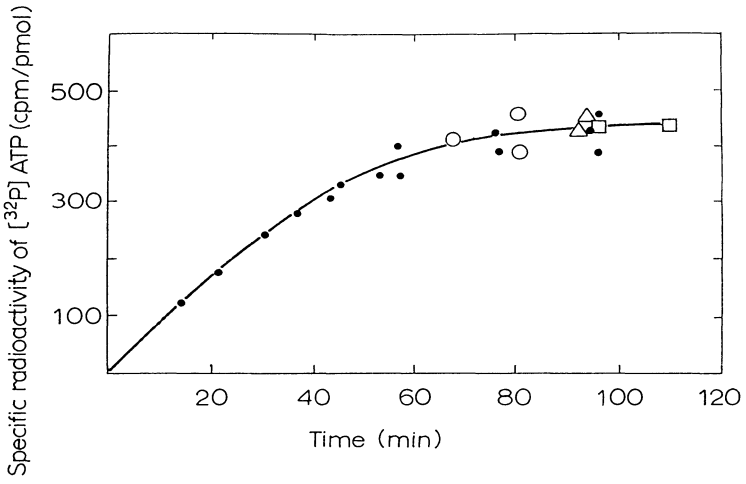

Fig. 3. The increase of specific radioactivity of hepatocyte ATP during preincubation with ^{32}Pi.

Hepatocytes were preincubated for various periods of time according to the standard protocol for the study of incorporation of ^{32}P into hydroxylase (●) or with 5 mM phenylalanine (O), 5 mM chlorophenylalanine (❑), or 1 mM $DMPH_4$ (Δ) for the last 12 min of the incubation. For the measurement of ATP, a 0.25 ml aliquot (10^6 cells) of the incubation was precipitated with 0.6 M perchloric acid (final concentration), the supernatant neutralized with $KHCO_3$/KOH, and subjected to high pressure liquid chromatography. The chromatographic separation was achieved at 20 °C on an anion exchanger (110 × 4.5 mm Partisphere 5 SAX, from Whatman) equipped with a 10 × 2 mm precolumn of pellicular silica (HC Pellosil from Whatman). The mobile phase (0.75 M potassium phosphate, pH 3.95) was pumped at a flow rate of 1.0 ml/min (1000 psi). The fractions containing ATP (t_R = 6.4) were collected and the radioactivity determined by liquid scintillation counting.

20-fold in 15 seconds (data not shown). Under the conditions used, 3.5 μM N^6-benzoyl-cAMP was almost half as potent as glucagon/forskolin/IBMX in stimulating hydroxylase phosphorylation. In isolated hepatocytes, 0.5 μM of N^6-benzoyl-cAMP achieves half-maximal phosphorylase activation, whereas 60 μM of N^6-benzoyl-cAMP is required to half-maximally induce mRNA for phosphoenolpyruvate carboxykinase in a hepatoma cell line, both of which are processes activated by cAMP-kinase [13]. The concentration of N^6-benzoyl-cAMP required to elicit hydroxylase phosphorylation was therefore in the range expected for a cAMP-kinase mediated process. We therefore conclude that phenylalanine and chlorophenylalanine enhanced the cAMP-kinase catalyzed phosphorylation of hydroxylase in the intact cell, as previously shown for the isolated enzyme [6].

Chlorophenylalanine enhances the phosphorylatability of the isolated enzyme by cAMP-kinase to the same extent as phenylalanine itself [6]. A similar effect of chlorophenylalanine was observed on the phosphorylation of the hydroxylase in isolated hepatocytes (Fig. 2, Table 1).

Both in the absence and presence of substrate or substrate analog, the maximal amount of ^{32}P incorporated in the hydroxylase of cells stimulated via the cAMP-

Table 1. Effect of ligands (phenylalanine, chlorophenylalanine, $DMPH_4$) on the rate of phosphorylation of phenylalanine hydroxylase in response to agents activating hepatocyte cAMP-kinase or Ca^{2+}/calmodulin-kinase

Kinase activator	Change in apparent phosphorylation rate due to:			
	–	Phenylalanine (5 mM)	Chlorophenylalanine (5 mM)	$DMPH_4$ (1 mM)
N^6-benzoyl-cAMP (3.5 μM)	1	4.1	3.7	2.3
Glucagon/Forsk./IBMX (1 μM/1μM/600 μM)	1[a]	4.0	3.6	2.6
Vasopressin (70 nM)	1[b]	1.0	n.d.	1.0

The apparent rate of phosphorylation of hydroxylase was determined from the slope of plots (like those shown in Fig. 2) of ^{32}P incorporation into hydroxylase as a function of time. The concentrations of effectors given refer to the final concentration in the suspension of cells. For further details, see legend to Fig. 2 and experimental procedure. The relative phosphorylation rate is the ratio between the rate in the presence and absence of effector. The values reported in the table were obtained by laser scanning of gels and autoradiograms at 633 nm. Similar results were obtained by scintillation counting. The band corresponding to the hydroxylase (M_r = 50,000) was excised from the gels. The slices were then incubated for 4 h in 1ml aqueous solution containing 2% (w/v) SDS. After addition of 8 ml insta-gel 2 (Packard), the samples were counted for radioactivity.

[a]The rate of phosphorylation of hydroxylase in the presence of the mixture of glucagon, forskolin and IBMX was as for glucagon alone (Fig. 2A)

[b]The rate of phosphorylation of hydroxylase in the presence of vasopressin was 13% of the rate with 1 μM glucagon (substrate and cofactor absent).

kinase system was about six times higher than that measured in unstimulated cells. A similar value of the maximal change in the state of phosphorylation of the hydroxylase has been reported by Garrison *et al.* [14], while Fisher and Pogson [15] found about three-fold increase.

Modulation of the intracellular cAMP-stimulated phosphorylation of hydroxylase by cofactor

The synthetic cofactor $DMPH_4$ is chemically more stable than the natural cofactor BH_4 and was added to the cell suspension in order to replace the natural cofactor from its binding site on the hydroxylase. The addition of $DMPH_4$ alone increased the rate of cAMP-stimulated phosphorylation more than two-fold (Table 1). In addition, $DMPH_4$ slightly further increased the effect observed with phenylalanine when added in combination with the amino acid (data not shown). We have shown that $DMPH_4$ can overcome the inhibitory effect of BH_4 on the cAMP-kinase catalyzed phosphorylation of isolated hydroxylase [16]. The mechanism of the $DMPH_4$ effect is therefore most probably a displacement of the natural cofactor, which inhibits the rate of hydroxylase phosphorylation by cAMP-kinase [6,7].

We conclude that $DMPH_4$ is able to penetrate the hepatocytes and displace the natural cofactor. Indirectly, this argues that a high proportion of the hydroxylase has bound natural cofactor and that the endogenous cofactor inhibits the cAMP-mediated phosphorylation in the intact hepatocyte. It is of interest that Milstien and Kaufman [17] found that addition of both natural cofactor and $DMPH_4$ to liver slices increased the phenylalanine metabolism in the slices.

Lack of effect of substrate and cofactor on the vasopressin-induced phosphorylation of hydroxylase

We finally studied whether ligands (substrate and cofactor of the hydroxylase) affected the vasopressin-stimulated phosphorylation of hydroxylase in the hepatocytes. The cells were incubated for 3 min with phenylalanine or $DMPH_4$ before stimulation with vasopressin. The rate of incorporation of ^{32}P into the hydroxylase was unaffected by the presence of either substrate or cofactor (Table 1).

The degree of stimulation of hydroxylase phosphorylation (50% increase after 6 min of incubation) was moderate, in accord with data from other groups [12,14]. The effect of vasopressin on hydroxylase phosphorylation in intact hepatocytes is probably mediated via the Ca^{2+}/calmodulin-dependent protein kinase [14], whose phosphorylation of the isolated hydroxylase was not stimulated by phenylalanine [4]. We therefore conclude that the lack of substrate-directed stimulation of the Ca^{2+}/calmodulin-kinase catalyzed phosphorylation of hydroxylase is true also in intact cells.

References

1. Wretborn M, Humble E, Ragnarsson U and Engstrøm L (1980) Biochem. Biophys. Res. Commun. 93: 403–408.
2. Ledley FD, Dillela AG, Kwok SCM and Woo SLC (1985) Biochemistry 24: 3389–3394.
3. Abita J-P, Milstien S, Chang N and Kaufman S (1976) J. Biol. Chem. 251: 5310–5314.
4. Døskeland AP, Schworer CM, Døskeland SO, Chrisman TD, Soderling TR, Corbin JD and Flatmark T (1984) Eur. J. Biochem. 145: 31–37.
5. Døskeland AP, Døskeland SO, Øgreid D and Flatmark T (1983) Fed. Proc. 42: 2193.
6. Døskeland AP, Døskeland SO, Øgreid D and Flatmark T (1984) J. Biol. Chem. 259: 11242–11248.
7. Phillips RS and Kaufman S (1984) J. Biol. Chem. 259: 2474–2479.
8. Ekanger R, Sand T, Øgreid D, Christoffersen T and Døskeland SO (1985) J. Biol. Chem. 260: 3393–3401.
9. Jennings IG, Russel RG McR, Armarego WLF and Cotton RGH (1986) Biochem. J. 235: 133–138.
10. Smith SC, McAdam WJ, Kemp BE, Morgan FJ and Cotton RGH (1987) Biochem. J. 244: 625–631.
11. Garrison JC, Borland MK, Florio VA and Twible DA (1979) J. Biol. Chem. 254: 7147–7156.
12. Pogson CI, Dickson AJ, Knowles RG, Salter M, Santana MA, Stanley JC and Fisher MJ (1986) Adv. Enzyme Regul. 25: 309–327.
13. Beebe SJ, Blackmore PF, Chrisman TD and Corbin JD (1988) Methods Enzymol. 159: 118–139.
14. Garrison JC, Johnsen DE and Campanile CP (1984) J. Biol. Chem. 259: 3283–3292.

15. Fisher MJ and Pogson CI (1984) Biochem. J. 219: 79–85.
16. Døskeland AP, Haavik J, Flatmark T and Døskeland SO (1987) Biochem. J. 242: 867–874.
17. Milstien S and Kaufman S (1975) J. Biol. Chem. 250: 4777–4781.

Address for correspondence: Anne P. Døskeland, Department of Biochemistry, Årstadveien 19, N–5009 Bergen, Norway.

Solubilization and functional reconstitution of the mitochondrial branched chain α-keto acid transporter*

Susan M. Hutson[a], Stewart K. Roten[a], Debra L. Oliveira[b] and Ronald S. Kaplan[b]

[a]*Department of Biochemistry, Bowman Gray School of Medicine, Wake Forest University, Winston-Salem, NC 27103, U.S.A.*

[b]*Department of Pharmacology, College of Medicine, University of South Alabama, Mobile, AL 36688, U.S.A.*

Abstract

The mitochondrial branched chain α-keto acid transporter has been solubilized from rat liver and heart mitochondria and its function reconstituted in phospholipid vesicles. The transporter was extracted from mitoplasts with Triton X-114 in the presence of exogenous cardiolipin and α-ketoisocaproate. Upon incorporation of this extract into asolectin vesicles, a p-chloromercuribenzoate-sensitive, protein-dependent transport of α-ketoisocaproate into the proteoliposomes has been demonstrated. Studies with covalent modification reagents indicate that the reconstituted carrier is substantially inhibited by sulfhydryl reagents as well as by the histidinespecific reagent diethyl pyrocarbonate. Thus the transporter appears to contain cysteine(s) and histidine(s) residues that are essential to the transport reaction mechanism. In conclusion, the extraction and functional reconstitution of the branched chain α-keto acid transporter represents an important first step towards purification and molecular characterization of this anion carrier.

Introduction

The branched chain α-keto acids (BCKAs) are products of the branched chain aminotransferase reaction. Recently, we have characterized a separate mitochondrial transport system for these α-keto acids [1]. This carrier catalyzes the transport of BCKA across the mitochondrial inner membrane; hence, it may play an important role in regulating accessibility of BCKAs to the BCKA dehydrogenase enzyme complex which is located in the mitochondrial matrix [2,3]. The kinetic properties of this transport system are consistent with transport of BCKA via proton symport and with an external pK for proton binding of 6.9 [1,2]. This is especially interesting, since there is evidence that mitochondrial BCKA oxidation can be regulated by pH changes within the physiological range [2,3]. Therefore, careful definition of the properties of this transporter will provide a better understanding of cellular branched chain amino acid metabolism. In this paper we report

* This work was supported by Grants DK34738 (S.M.H.) and GM38785 (R.S.K.) from the National Institutes of Health, United States Public Health Service, Bethesda, Maryland.

procedures which result in extraction and reconstitution of the functional BCKA transporter from rat liver and heart mitochondria.

Experimental procedures

Solubilization of the functional BCKA transporter

Rat liver mitochondria and mitoplasts were isolated from male Sprague Dawley rats employing the procedure described [4]. Heart mitochondria were prepared as described [2]. Frozen mitoplasts (approximately 40–45 mg protein) were thawed and then diluted with ice-cold Buffer A (final concentration 50 mM NaCl, 20 mM Hepes, 1 mM EDTA, pH 7.2; 5 mM KIC) to 30 mg protein/ml. The transporter was extracted by adding an equal volume of Buffer A + 6% Triton X-114 + 6 mg cardiolipin/ml to the mitoplast suspension. After 20 min at 4°C, the mixture was centrifuged at 138,000 × g for 45 min and the supernatant incorporated immediately into phospholipid vesicles.

Preparation of proteoliposomes

Asolectin vesicles were prepared in Buffer B (120 mM Hepes, 50 mM NaCl, 1 mM EDTA, pH 7.4) as described previously [4]. Proteoliposomes were then formed by the sequential addition of Buffer B (188 μl) and freshly isolated Triton X-114 extracted protein (0.25 ml) to the asolectin vesicles (0.53 ml). The vortexed mixture was frozen rapidly in liquid nitrogen. Immediately prior to assay, the proteoliposomes were thawed, sonicated, and prepared as described [4]. For preparation of liposomes without mitoplast protein, a detergent solubilization incubation was carried out with H-medium [4] instead of mitoplasts.

Measurement of pCMB-Sensitive KIC uptake

Aliquots (60 μl) of proteoliposomes were preincubated for 3 min at 30°C with either 6 μl of 10 mM pCMB (control) or with 6 μl of water (experimental). Transport was initiated by the addition of 12 μl of 1.62 mM [1-^{14}C]KIC (22,000 dpm/nmol), and was quenched by addition of 6 μl of pCMB to the experimental incubation or water to the control. Aliquots (60 μl) of each reaction mix were placed immediately onto separate Dowex-1 columns. Liposomes were eluted with Buffer B and intraliposomal [1-^{14}C]KIC was quantified using liquid scintillation counting. Protein was determined by the method of Kaplan and Pedersen [5].

Materials

All reagents for electrophoresis were purchased from Bio-Rad (Richmond, CA). Digitonin was from Calbiochem (LaJolla, CA). All other materials and reagents were obtained from Sigma (St. Louis, MO).

Results and Discussion

The aim of the present study was to develop extraction and reconstitution conditions that yielded an inhibitor-sensitive, protein-dependent transport of KIC into liposomes. As a starting point, the basic extraction and reconstitution conditions that Kaplan *et al.* [6] have used previously for other anion transporters were employed. Extraction was carried out with the nonionic detergent Triton X-114 (3%, v/v) in the presence of cardiolipin, conditions which extract several other mitochondrial anion transporters in functional form [4,6,7–9]. The results are presented in Fig. 1. Panel A shows that in the absence of preincubation with the sulfhydryl reagent pCMB, KIC was transported into proteoliposomes. When liposomes were formed with buffer instead of protein, KIC was not taken up into liposomes regardless of whether or not pCMB was present during the preincubation (see Fig. 1A).

Figure 1, Panel B, depicts the pCMB-sensitive transport of KIC into proteoliposomes as a function of time. Transport was linear for approximately 4 h and then reached a plateau at approximately 20 h. The inset shows that transport was also linear at earlier time points (<1 h). The reconstituted specific transport activity was 2.45 nmol/h/mg protein, and transport was nearly completely (>98%) abolished by preincubation with 1 mM pCMB. Similar results were obtained with heart mitochondrial extracts, however, considerably more activity was obtained in heart

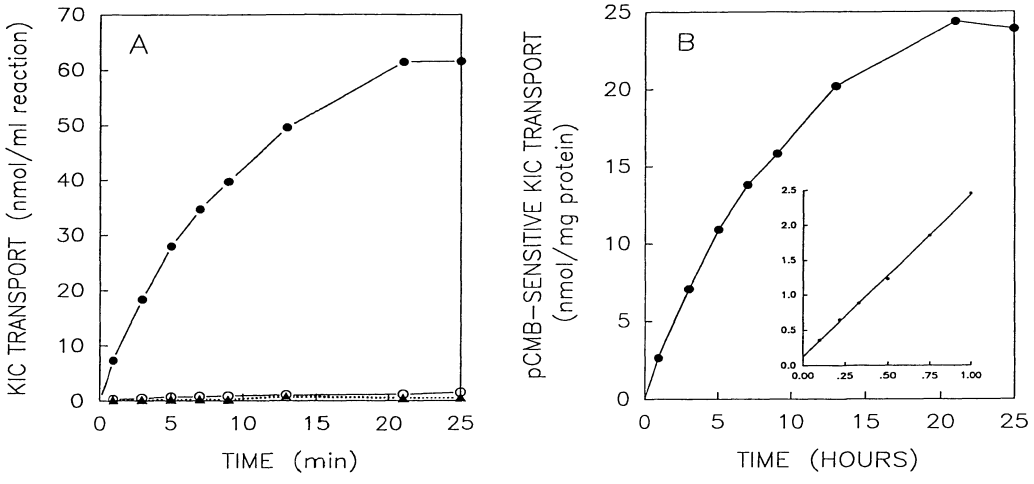

Fig. 1. Time dependence of BCKA uptake. Panel A, a plot of [1-^{14}C]KIC (0.25 mM) uptake into proteoliposomes with (○) and without preincubation with pCMB (●). Also shown is uptake of [1-^{14}C]KIC into liposomes prepared by addition of buffer rather than protein to asolectin vesicles, with (▲) and without (Δ) preincubation with pCMB (see Experimental Procedures). Panel B, a plot of the protein-catalyzed pCMB-sensitive [1-^{14}C]KIC uptake into proteoliposomes versus time (●). The inset depicts a linear regression analysis of transport data obtained at the earliest time points. Mean values from 3–6 experiments are presented.

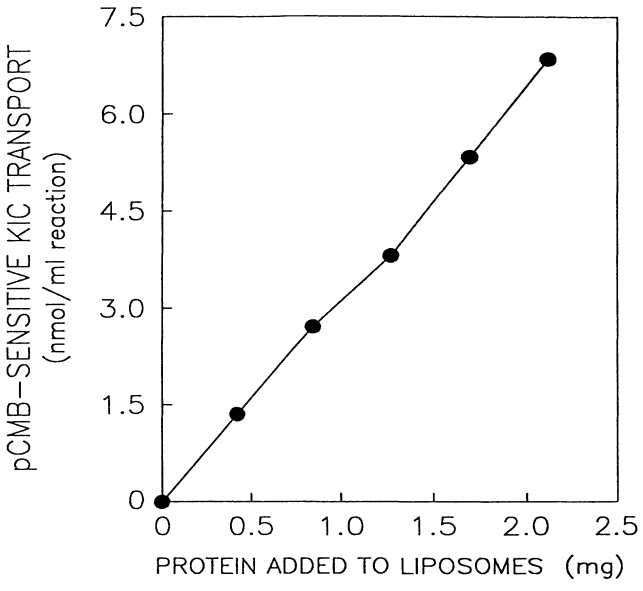

Fig. 2. Rate of pCMB-sensitive KIC uptake into proteoliposomes as a function of the amount of added Triton X-114 extract. Varying amounts of Triton X-114 solubilized protein from liver mitoplasts were added to preformed asolectin vesicles. The volume of the resulting proteoliposomes was maintained at 0.968 ml by adding varying volumes of the extraction buffer. Mean values from 6 experiments are presented.

(0.98 nmol/min/mg protein). These results demonstrate that we have achieved the first successful extraction of the reconstitutively active form of the mitochondrial BCKA transporter.

Experiments were conducted to examine the dependence of the observed pCMB-sensitive KIC transport rate on the amount of detergent-solubilized protein that was added to the liposomes. As depicted in Fig. 2, as increasing amounts of the Triton X-114 detergent extract were added, KIC transport increased in an approximately linear manner up to 3 mg protein, which was the largest quantity of protein tested. These results indicate that the reconstituted transport system did reflect the presence of the transport protein.

The SDS-polyacrylamide gel electrophoretic profile of the Triton X-114 mitoplast extract prior to its incorporation into asolectin vesicles is shown in Fig. 3. Numerous protein bands were visualized in addition to protein bands in the molecular mass range of 30–40 kDa where several other mitochondrial transport proteins have been shown to appear in this gel system [4,6,7].

Finally, Table 1 presents the effects of covalent labeling agents on the reconstituted BCKA transporter. These results provide the first demonstration that the

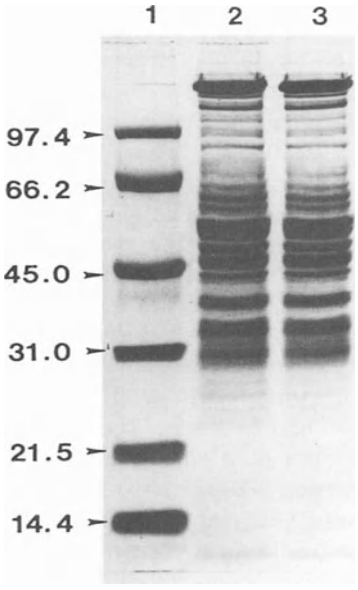

Fig. 3. Coomassie-stained SDS-polyacrylamide gradient gel electrophoretic pattern of the Triton X-114 solubilized BCKA transporter fraction. Proteins were run in a 4.5% polyacrylamide stacking gel followed by a highly resolving 14-20% gradient gel. Lane 1: 2.5 μg each of Bio-Rad SDS-PAGE low molecular weight standard proteins. Lanes 2 and 3: 25 μg of different preparations of the Triton X-114 solubilized BCKA transporter extract.

Table 1. Effect of protein labeling reagents on reconstituted activity of the BCKA transporter from rat liver mitochondria

Agent	Concentration (mM)	Inhibition of reconstituted KIC transport (%)
pCMB	1	100
Mersalyl	2	99 ± 1
α-Cyano-4-hydroxycinnamate	10	71 ± 2
N-Ethylmaleimide	2	45 ± 2
Diethyl pyrocarbonate	5	99 ± 1
N-Acetylimidazole	15	34 ± 2

Proteoliposomes were preincubated with the various agents for 3 min except for N-acetylimidazole where a 30 min preincubation was used. Following a 1 h transport incubation, reactions were terminated by addition of pCMB, and intraliposomal [1-^{14}C]KIC was measured as described under Experimental Procedures. In the absence of labeling agent, the mean rate of pCMB-sensitive transport was 2.49 nmol/h/mg of protein. Mean and standard errors from 3–5 separate experiments are presented.

transporter can be completely inhibited by sulfhydryl reagents such as pCMB and mersalyl. These findings are similar to observations with other mitochondrial anion transport proteins [4]. Less inhibition was observed with the sulfhydryl reagent N-ethylmaleimide. High concentrations of α-cyano-4-hydroxycinnamate, a sulfhydryl reagent that inhibits the pyruvate transporter at micromolar concentrations [7,10], were also inhibitory (71%). α-cyano-4-hydroxycinnamate is a partial inhibitor (60%) of KIC oxidation and transport in isolated mitochondria [1]. Interestingly, diethyl pyrocarbonate completely inhibited the reconstituted transporter which suggests that the transporter contains a histidine residue that is essential to the reaction mechanism. One possible candidate is the transporter's external proton binding site which has a pH of 6.9 [2]. Finally, a 34% inhibition was observed with N-acetylimidazole, a tyrosine-specific reagent. Taken together, these results provide the first information on the type of amino acid residues that appear to be essential for functioning of the BCKA transporter.

The successful solubilization and functional reconstitution of the BCKA transporter will now permit development of procedures for the purification of this transporter to essential homogeneity. While the identity of the BCKA transporter has been established kinetically [1,2], purification of the transport protein will provide the physical evidence for the existence of this transport system.

References

1. Hutson SM and Rannels SL (1985) J. Biol. Chem. 260: 14189–14193.
2. Hutson SM (1987) J. Biol. Chem. 262: 9629–9635.
3. Hutson SM (1986) J. Biol. Chem. 261: 4420–4425.
4. Kaplan RS and Pedersen PL (1985) J. Biol. Chem. 260: 10293–10298.
5. Kaplan RS and Pedersen PL (1985) Anal. Biochem. 150: 97–104.
6. Kaplan RS, Mayor JA, Oliveira DL and Johnston N (1989) In: Azzi A, Naleçz KA, Naleçz MJ and Wojtczak L (eds.) Anion Carriers of Mitochondrial Membranes. Springer-Verlag, New York, pp. 59–69.
7. Naleçz KA, Bolli R, Wojtczak L and Azzi A (1986) Biochim. Biophys. Acta 851: 29–37.
8. Stipani I and Palmieri F (1983) FEBS Lett. 161: 269–274.
9. Mende P, Huther F-J and Kadenbach B (1983) FEBS Lett. 158: 331–334.
10. Halestrap AP (1975) Biochem. J. 148: 85–96.

Address for correspondence: Dr. Susan M. Hutson, Department of Biochemistry, Bowman Gray School of Medicine, 300 South Hawthorne Road, Winston-Salem, NC 27103, U.S.A.

Regulation of branched chain amino acid catabolism in mammalian tissues: Characterization of the mitochondrial aminotransferase*

Reidar Wallin, Timothy R. Hall and Susan M. Hutson
Department of Biochemistry, Bowman Gray School of Medicine, Winston-Salem, NC 27103, U.S.A.

Introduction

The branched chain aminotransferase (BCAT) catalyzes the first step in catabolism of the three essential branched chain amino acids (leucine, isoleucine, valine). The second step is irreversible oxidative decarboxylation of the transamination products, the branched chain α-keto acids, catalyzed by the branched chain α-keto acid dehydrogenase multienzyme complex. It is the tissue distribution of these two enzymes that is largely responsible for the unique metabolism of this group of amino acids among different organs and tissues [1]. Because branched chain α-keto acid dehydrogenase, which is the first rate-controlling step in branched chain amino acid catabolism, is a mitochondrial matrix enzyme, the subcellular distribution of BCAT in a tissue can influence branched chain amino acid oxidation. In the present study the role of the mitochondrial and cytosolic aminotransferase(s) in regulating branched chain amino acid oxidation is discussed. Molecular characteristics and purification of the mitochondrial aminotransferase from rat heart are presented, and the relationship of this enzyme to the brain cytosolic enzyme is described.

Experimental procedures

Preparation of mitochondria and assays

Male Sprague-Dawley rats were used. Heart mitochondria were prepared as described [2] and brain cytosol [3]. Aminotransferase activity was measured at 37°C in 50 mM Hepes buffer, pH 7.8, which contained 50 μM pyridoxal phosphate, 5 mM DTT and 0.5 mg/ml bovine serum albumin as described by Hutson *et al.* [4]. The standard assay contained 1 mM [1-^{14}C]KIV and 12 mM isoleucine. A unit of enzyme activity was defined as 1 μmol valine formed/min at 37°C.

*This work was supported by Grant DK-34738 (SMH from the National Institutes of Health).

Purification of BCAT from rat heart mitochondria

For purification of BCAT, the mitochondrial suspension was diluted with deionized water (1:9, v/v) in the presence of 1 mM DIFP and sonicated for 5 min at 70% duty cycle using a Branson sonifier (Model 250). Subsequently, the mitochondrial suspension was centrifuged at 100,000 × g and the resulting supernatant used for purification. All buffers and solutions contained 1 mM DIFP and 1 mM DTT.
Briefly, the purification scheme consisted of the following steps:

Step 1: Ion-exchange chromatography
The supernatant was loaded onto a column of DEAE-cellulose (Whatman DE52) equilibrated with 10 mM potassium phosphate, pH 7.5, (buffer A). The aminotransferase was stepwise released from the column in buffer A containing 0.3 M NaCl.

Step 2: Hydroxylapatite chromatography
Retained proteins were eluted with a phosphate gradient ranging from 10 mM (buffer A) to 0.3 M potassium phosphate, pH 7.5. The enzyme eluted at 0.1 M phosphate.

Step 3: Ammonium sulfate precipitation
The BCAT containing fraction was mixed with an equal volume of saturated ammonium suliate (4°C). The supernatant contained the BCAT activity.

Step 4: Hydrophobic interaction chromatography using HPLC
The BCAT in 50% ammonium sulfate was chromatographed on a HYDROPORE HPLC column supplied by Rainin Instruments (Waburn, MA, U.S.A.). Retained proteins were eluted with a descending gradient of ammonium sulfate in 0.1 M phosphate buffer, pH 7.0. The BCAT eluted at 1 M ammonium sulfate.

Step 5: HPLC exclusion chromatography
The BCAT containing fraction was gel filtrated on Sephacryl S-100 in 0.1 M potassium phosphate buffer, pH 7.5.

Step 6: Discontinuous electrophoresis at pH 9.1 [5] and electroelution
Gel pieces containing BCAT were sliced from the tube gel and placed in an ISCO Model 1750 sample concentrator (Isco Inc., Lincoln, NE for electroelution.

SDS-PAGE

SDS-PAGE was carried out according to Laemmli [6] in 10% gels. Standard proteins used for molecular mass determinations were obtained from Bio-Rad (Richmond, CA)

Preparation of antiserum

Antiserum against the purified enzyme was raised in rabbits using standard immunization methods.

Immunoblotting

Proteins in SDS-PAGE gels were transferred to Immobilon P membranes (Millipore Corp., Bedford, MA, U.S.A.) for immunoblotting. The transfer was carried out as described recently [7] and immunoreactive protein bands were visualized as described [8].

Chemicals and reagents

The radioactive [1-^{14}C]KIV was synthesized from [1-^{14}C]valine (Amersham Corp., Arlington Heights, IL). PANSORBIN was obtained from Calbiochem (LaJolla, CA). Bovine serum albumin (essentially fatty acid-free, globulin-free) was obtained from Sigma (St. Louis, MO). All other reagents were reagent grade or better.

Results and Discussion

Since all of the other enzymes in branched chain amino acid catabolism are mitochondrial, the subcellular distribution of the BCAT determines the degree to which catabolism and anabolism of this group of essential amino acids is compartmentalized in tissues. Recently, we have shown that rat heart mitochondria have high BCAT activity and that the enzyme is located exclusively in the mitochondria in rat heart tissue [4]. The heart is an oxidative working muscle and, indeed, in

Table 1. Mitochondrial BCAT activity in selected rat tissues

Tissue	Mitochondrial BCAT activity relative to heart[a]	Mitochondrial activity
		total tissue activity (%)
Heart	1.0	104
Skeletal muscle	1.0[b]	—
Soleus	—	104
White gastrocnemius	—	30
Brain	0.2	26
Liver	0	0

BCAT was assayed in isolated mitochondria and tissue homogenates using 1 mM [1-^{14}C]KIV and 15 mM isoleucine as described [10].

[a]Heart mitochondrial BCAT activity was 71.7 ± 4.2 milliunits/mg mitochondrial protein (n = 8) [10].

[b]Mitochondrial activity did not vary with muscle type.

skeletal muscles with high red fiber content such as soleus, the aminotransferase appeared to be mitochondrial as in heart (see Table 1). However, in white gastrocnemius, which consists of about 91% fast-twitch white fibers [9], at least 70% of the enzyme appeared to be extramitochondrial [10] (see Table 1). In brain, which is known to have substantial extramitochondrial BCAT, mitochondrial activity was low relative to heart and only 26% of tissue activity was mitochondrial (see Table 1). On the other hand, little BCAT activity was detectable in liver [10], and none was found in the mitochondria. The differences in compartmentation of BCAT in different muscle types and tissues suggest that there are functional differences in the role of BCAT in these tissues.

In order to achieve a better understanding of the BCAT enzyme(s) in different organs and tissues, it is essential that these enzymes are purified for molecular characterization and detailed kinetic analysis. The purification scheme presented in the Experimental Procedures section represents the first purification of BCAT (EC 2.6.1.42) from rat heart mitochondria. The enzyme was purified from the 100,000 × g supernatant obtained after sonication and ultracentrifugation of isolated rat heart mitochondria.

The first two steps in the purification procedure consisted of ion-exchange and hydroxylapatite chromatography. In the first step, when a gradient of NaCl in the phosphate buffer was used for elution of the enzyme from the ion exchanger, only trace amounts of enzyme activity could be measured in column fractions. On the other hand, when the enzyme was stepwise eluted from the column with 0.3 M NaCl dissolved in buffer A, recovery of activity was >80%. Hydroxylapatite chromatography separated the enzyme from the main protein peak eluting from the column. These steps resulted in about a total 40-fold purification of the enzyme from the original mitochondria.

Hydrophobic interaction chromatography on HPLC, which was the next step in the procedure, was the key step, because it separated the BCAT enzyme from most of the contaminating proteins. This chromatography step usually resulted in a 4- to

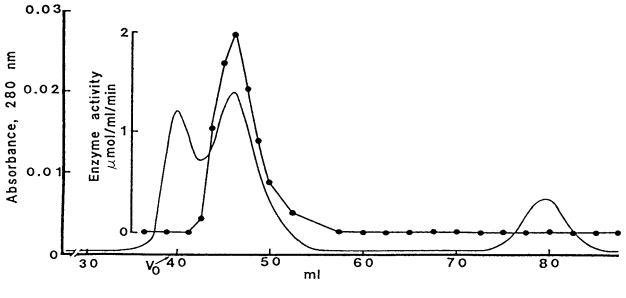

Fig. 1. HPLC size exclusion chromatography on Sephacryl S-100. Aliquots of 2 ml from the pooled enzyme containing fractions that eluted from the HYDROPHORE column were chromatographed on a Sephacryl S-100 column (50 × 1.6 cm). Enzyme activity was eluted with 0.1 M potassium phosphate buffer, pH 7.0, at a constant flow rate of 2 ml/min. V_0 indicates the void volume. Optical density at 280 nm (——); BCAT activity (•—•).

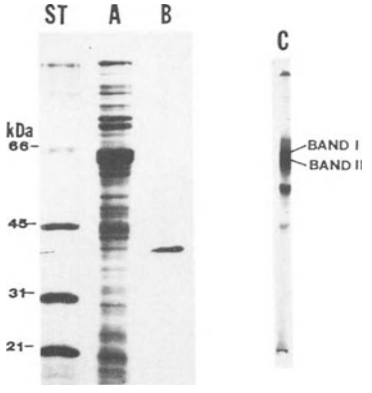

Fig. 2. SDS-PAGE and discontinuous electrophoresis of proteins. Prior to SDS-PAGE, all protein samples were boiled in the presence of 1% SDS and 5% mercaptoethanol. Lanes ST, A and B show SDS-PAGE of standard proteins, proteins in the mitochondrial 100,000 × g supernatant and the combined proteins in bands I and II after they were electroeluted from the discontinuous electrophoresis gel, respectively. Lane C shows a stained tube gel containing the proteins from the Sephacryl S-100 column after discontinuous electrophoresis at pH 8.9.

6-fold further purification of the enzyme. Next, size exclusion chromatography on a Sephacryl S-100 column separated the enzyme from ammonium sulfate and other low molecular weight contaminants as well as some contaminating proteins with higher molecular mass that eluted from the column with the void volume (see Fig. 1).

Five protein bands were apparent when the Sephacryl S-100 enzyme fraction was electrophoresed into 2.5 × 80 mm tube gels (see Fig. 2). The proteins in bands I and II contained the BCAT activity (see Fig. 2, lane C). After electroelution from the gel, both yielded one protein band of 43 kDa when mixed and subjected to SDS-PAGE (Fig. 2, lane B). These two proteins had the same specific enzyme activity and thus appeared to be enzyme isoforms which differed in electrical charge. In addition, both bands I and II showed identical substrate specificity after electroelution from the gel. Final purification was about 800-fold (average specific activity of 66) with a final recovery of 4%. Since the purified enzyme also eluted from the Sephacryl S-100 column with an apparent molecular weight of 50 kDa, we concluded from these data that the BCAT isolated from rat heart mitochondria is a single polypeptide with a molecular mass of 43 kDa.

On immunoblotting, antibodies raised against the purified enzyme did not recognize any proteins in the mitochondrial 100,000 × g supernatant other than a 43 kDa protein, and 98% of the BCAT activity was neutralized by the anti-serum (see Fig. 3). Brain was selected for comparison with heart, because in this tissue the aminotransferase is predominantly cytosolic [10,11] and thought to consist primarily of the Enzyme III form [11,12]. Rat heart has been reported to contain only the Enzyme I form of BCAT [11]. The antibodies did not recognize any protein present in cytosol from rat brain, and the brain enzyme activity in the cytosol eluted

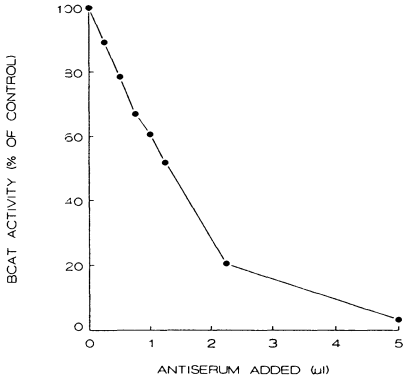

Fig. 3. Antibody neutralization of BCAT activity in rat heart mitochondrial 100,000 × g supernatant. The supernatant from the mitochondrial sonicate (500 µl, 1.05 mg protein/ml) was mixed with various concentrations of BCAT antiserum, and the mixtures were left on ice for 90 min. Controls contained pre-immune serum. Staphylococcus aureus protein A (Pansorbin) was then added to each sample (100 µl per 500 µl of sample) which was left on ice for another 45 min. The samples were centrifuged in an Eppendorf centrifuge at 14,000 × g for 10 min, and BCAT activity determined in the supernatant fraction.

from the Sephacryl S-100 column with an apparent molecular mass of 66 kDa, and the purified enzyme had a molecular weight of 66 kDa in SDS-PAGE.

Our data confirm earlier reports [13] which suggested the existence of different enzyme forms of BCAT. Indeed, the rat heart mitochondrial enzyme appears to be a polypeptide which is approximately 20 kDa smaller than the brain enzyme. Thus, in conclusion, purification of BCAT from rat heart mitochondria has provided the necessary tools for a more detailed investigation of the BCAT enzyme family.

References

1. Harper AE, Miller RH and Block KP (1984) Annu. Rev. Nutr. 4: 409–454.
2. LaNoue KF, Jeffries FM and Hand Radda GK (1986) Biochemistry 25: 7667–7675.
3. Booth RFG and Clark JB (1978) Biochem. J. 176: 365–370.
4. Hutson SM, Fenstermacher D and Mahar C (1988) J. Biol. Chem. 263: 3618–3625.
5. Davis BS (1964) Ann. NY Acad. Sci. 121: 404–427.
6. Laemmli UK (1970) Nature 227: 680–685.
7. Reiderer BM, Zagon IS and Goodman SR (1987) J. Neurosci. 7: 864–874.
8. Wallin R and Rannels SR (1988) Biochem. J. 250: 557–563.
9. Armstrong RB and Phelps RO (1984) Am. J. Anat. 171: 259–272.
10. Hutson SM (1988) J. Nutr. 118: 1475–1481.
11. Ichihara A (1985) In: Christen P and Metzler DE (eds.) Transaminases. John Wiley and Sons, New York, pp. 430–438.
12. Aki K, Yokojima A and Ichihara A (1969) J. Biochem. 65: 539–544.
13. Aki K, Ogawa K, Shirai A and Ichihara A (1967) J. Biochem. 62: 610–617.

Address for correspondence: Dr. Susan M. Hutson, Department of Biochemistry, Bowman Gray School of Medicine, 300 South Hawthorne Road, Winston-Salem, NC 27103, U.S.A.

Effect of ornithine on albumin and transferrin secretions in rat and human hepatocyte cultures

Gérard Lescoat[a], Noëlla Hubert[a] and Pierre Brissot[a,b]

[a]INSERM U 49, Unité de Recherches Hépatologiques, CHRU Pontchaillou, Rennes, France
[b]Clinique des maladies du foie, CHRU Pontchaillou, Rennes, France

Abstract

Immature and mature rat or human hepatocyte cultures and a human hepatoma cell line (Hep G2) were cultured in an arginine-free medium, supplemented or not with ornithine. In these different culture models, ornithine increases albumin and transferrin secretions. By using α-methyl ornithine, an inhibitor of ornithine decarboxylase, we demonstrate firstly that this effect of ornithine is mediated by polyamine production and secondly localized at a pretranslational level.

Introduction

The addition of amino acids, and particularly ornithine, to the perfusate solution of the isolated liver, increases albumin and urea synthesis [1,2]. This observation demonstrates that ornithine, the amino-acid precursor of polyamines and not incorporated into protein, is able to stimulate albumin secretion. The aim of the present work was to investigate the effect of ornithine on the secretion of two major proteins of the liver metabolism albumin and transferrin. For this purpose, immature or mature rat and human hepatocyte cultures as well as a human hepatoma cell line (Hep G2) were used.

We report here that ornithine enhances strongly albumin and transferrin secretions in the different hepatocyte culture models used. Moreover, the involved mechanism has a pretranslational origin and the polyamine pathway seems likely to be the primordial way of action of ornithine.

Materials and Methods

Cell isolation and cultures

Fetal or adult rat and neonatal human hepatocytes were isolated by using a collagenase solution according to procedures described elsewhere [3,4]. Fetal rat and neonatal human hepatocytes were isolated respectively from 19 day-old Sprague-Dawley rats and a non viable neonate. Adult hepatocytes were isolated

from a three month-old Sprague-Dawley male rat. After the enzyme dissociation, the hepatocytes were collected in Hepes buffer and centrifuged at low speed (150 × g) for 15 sec. Hepatocytes were washed twice with the same buffer, once with the selective medium and then tested for viability. The human hepatoma cell line (Hep G2) used in this study was maintained in our laboratory by subculture.

Hepatocytes were suspended in an arginine-free Eagle's medium containing 0.1% bovine albumin, 5 μg/ml bovine insulin and 10% fetal calf serum. For experimental procedure, the hepatocytes were plated in 10 cm^2 culture dishes. The medium was changed 3–4 h later and then every two days with an arginine-free Eagle's medium deprived of bovine albumin and fetal calf serum and supplemented with 10^{-7}M dexamethasone (Sigma). For experimental purpose, 0.18 mM L-ornithine hydrochloride (Sigma) was added to this defined medium on day 1 of culture.

Protein assay

In order to measure total protein per flask, the cultures were rinsed with a phosphate saline buffered solution (pH 7.4); then the cells were scraped and sonicated. The total protein of the cell lysate was measured by the method using the Bio-Rad reagent [5].

Albumin and transferrin assays

Culture media were collected every two days and stored at −20°C. Albumin and transferrin secretions were quantified by laser immunonephelometry [6]. Standard protein and culture media were mixed in appropriate dilutions of antiprotein antisera in NaCl 0.9% containing 4% polyethylene glycol. Light scatter was measured after 1 h incubation at room temperature.

Standard rat albumin or transferrin and antisera were from CAPPEL Laboratories (Cochranville, USA). The limit of sensitivity of the assay was about 2 μg/ml. Inter- and intra-assay variations did not exceed 10%. Albumin and transferrin secretions were expressed in μg/mg total protein.

Extraction of total RNA

On day 5 of culture, total RNA was extracted by the procedure of Glisin *et al.* [7] modified by Chirgwin *et al.* [8] and Raymondjean *et al.* [9]. For each experimental condition, adult rat hepatocytes from six 25 cm^2 flasks were pooled. The hepatocytes were washed and directly homogenized to a final concentration of 3% (W/V) in a mixture of 5 M guanidine thiocyanate, 5% 2-mercaptoethanol, 2% sarcosyl, 1 mM EDTA, pH 7, 0.1 M sodium acetate, pH 5.5. The homogenate was centrifuged at 1500 × g for 15 min at 20°C. The pellet was dissolved at 65°C for 5 min, in 10 mM tris-HCl pH 7.4, 1 mM EDTA pH 7, 1% sarcosyl. Total RNA was precipitated from the supernatant overnight with 0.1 volume of 2 M sodium acetate, pH 5.5 and

2.5 volumes of chilled ethanol at −20°C and collected by centrifugation. It was washed three times with ethanol and dissolved in water before storage in liquid nitrogen.

Northern blot hybridization assay

Twenty μg of total RNA were firstly dissolved in 25 μl of buffer containing 10 mM sodium phosphate, 2.2 M formaldehyde, 0.5 mM EDTA, 50% formamide and secondly heated at 65°C for 5 min. Then, 5 μl of a mixture containing 0.5% sodium dodecyl sulfate (SDS), 25% glycerol, 25 mM EDTA, 0.025% bromophenol blue were added to the solution of RNA. Electrophoresis of total RNA was carried out at 55 V for 6 h in 1.5% agarose gel in 10 mM phosphate buffer pH 7.4 containing 1.1 M formaldehyde. After electrophoresis, RNA was transferred onto a nitrocellulose filter (Amersham Hybond C) as described by Thomas [10]. After baking for 3 h at 80°C the filter was prehybridized at 65°C in 3 × Standard Saline Citrate (SSC) in the presence of 10 × Denhardt's reagent [11]. The hybridization was carried out for 18 h at 65°C in the same solution with the addition of 3×10^6 cpm/ml of albumin DNA probe [12], previously nick translated [13] with α^{32}P dCTP to a specific activity of at least 15×10^6 cpm/ml. The relative amounts of ALB mRNA sequences were measured in the different samples by densitometry.

Expression of the results

Albumin and transferrin secretions are expressed in a percentage of the values obtained with 1 day cultures. Each experimental point is the mean of triplicate cultures. Experiments were repeated three times.

Results

Albumin secretion

In the absence of ornithine, albumin secretion by fetal rat (Fig. 1a,b) and by neonatal human (Fig. 1c) hepatocytes decreased progressively from day 1 to day 7 of culture. The same phenomenon was observed in the human hepatoma cell line (Fig. 1d). When the cultures were maintained in the presence of 0.18 mM ornithine from day 1 to day 7, albumin secretion increased or was much more stable (Fig. 1a,b,c,d). The final result was a strong increase of albumin secretion when the hepatocytes and the human hepatoma cell line were maintained in the presence of ornithine (Fig. 1a,b,c,d).

Transferrin secretion

In the absence of ornithine, transferrin secretion decreased progressively from day 1 to day 7 of culture in the fetal or adult rat (Fig. 2a,b) and the neonatal human

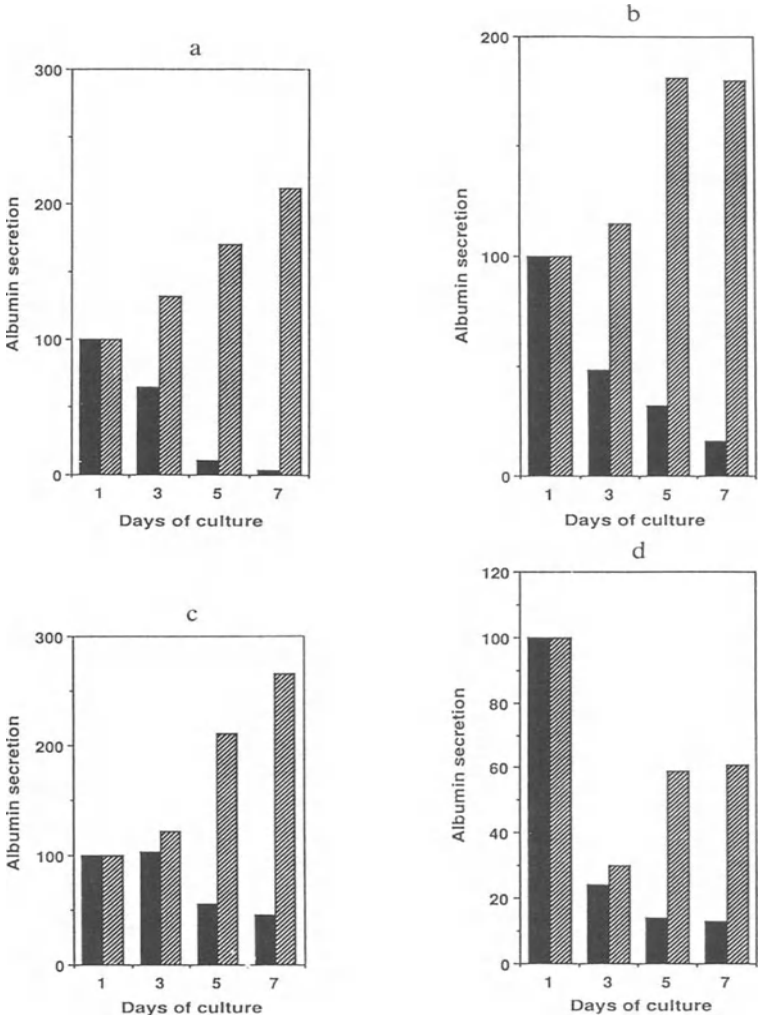

Fig. 1. Albumin secretion by fetal (a) or adult (b) rat, neonatal human (c) hepatocytes and a human hepatoma cell line (d) maintained in control conditions (■) or in the presence of 0.18 mM ornithine (▨) from day 1 to day 7 of culture. Albumin secretion is expressed in a percentage of the values obtained with 1 day cultures. Each experimental point is the mean of triplicate cultures.

(Fig. 2c) hepatocytes; the same was true for the human hepatoma cell line (Fig. 2d). When ornithine was present, transferrin secretion increased from day 1 to day 7 in the different hepatocyte culture models. It appeared that the addition of ornithine to the culture medium also increased transferrin secretion in the hepatocyte cultures, as well as in the human hepatoma cell line (Fig. 2a,b,c,d).

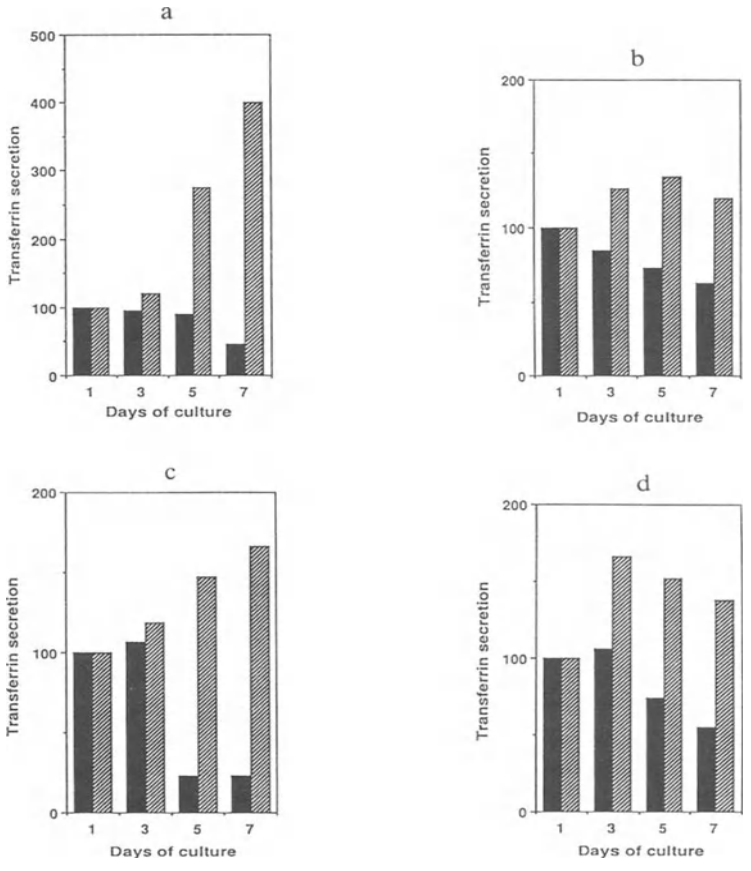

Fig. 2. Transferrin secretion by fetal (a) or adult (b) rat, neonatal human (c) hepatocytes and a human hepatoma cell line (d) maintained in control conditions (■) or in the presence of 0.18 mM ornithine (▨) from day 1 to day 7 of culture. Transferrin secretion is expressed in a percentage of the values obtained with 1 day cultures. Each experimental point is the mean of triplicate cultures.

Mechanism of action of ornithine

The addition of 0.18 mM ornithine increased albumin and transferrin secretions in the different hepatocyte culture models tested. However, the increased hepatocyte protein secretion observed in the presence of ornithine may be mediated by two possible ways; the production of arginine in the urea cycle or the polyamine pathway. To discriminate between these two ways, we blocked the biosynthesis of polyamines in adult rat hepatocyte cultures by the use of α-methyl ornithine, a potent inhibitor of ornithine decarboxylase. The addition of 3 mM α-methyl ornithine to the medium of the control cultures was without effect on albumin and transferrin secretions (Fig. 3a,b). However, the same concentration of α-methyl

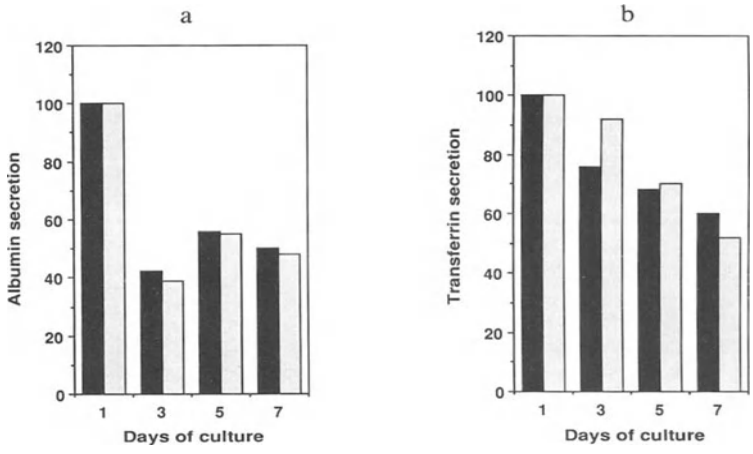

Fig. 3. Albumin (a) and transferrin (b) secretions by adult rat hepatocyte cultures maintained in the control conditions (■) or in the presence of 3 mM α-methyl ornithine (▩) from day 1 to day 7 of culture. Albumin and transferrin secretions are expressed in a percentage of the values obtained with 1 day cultures. Each experimental point is the mean of triplicate cultures.

ornithine abolished the effect of 0.18 mM ornithine on albumin and transferrin secretions as soon as day 5 of culture (Fig. 4a,b). Therefore, our results suggested that stimulation of albumin and transferrin secretions by ornithine was rather mediated by polyamine synthesis.

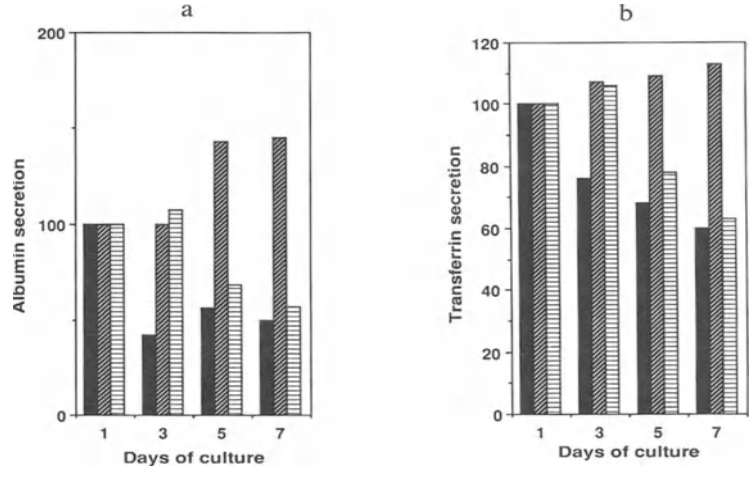

Fig. 4. Albumin (a) and transferrin (b) secretions by adult rat hepatocyte cultures maintained in the control conditions (■), in the presence of 0.18 mM ornithine (▨) or 0.18 mM ornithine plus 3 mM α-methyl ornithine (▤) from day 1 to day 7 of culture. Albumin and transferrin secretions are expressed in a percentage of the values obtained with 1 day cultures. Each experimental point is the mean of triplicate cultures.

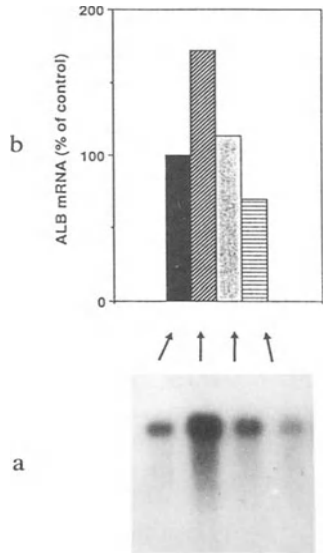

Fig. 5. Northern blot (a) and graphic representation of its densitometric scanning (b) of albumin mRNA concentrations in 5-day adult rat hepatocyte cultures maintained in the control conditions (■), in the presence of 0.18 mM ornithine (▨), 3 mM α-methyl-ornithine (▩) or 0.18 mM ornithine plus 3mM α-methyl-ornithine (▤). Data are given as a percentage of the control hepatocyte culture values.

In order to investigate the mechanism whereby ornithine stimulated hepatocyte protein secretion, we isolated total RNA from 5-day cultured adult rat hepatocytes maintained in the absence of ornithine, in the presence of 0.18 mM ornithine, in the presence of 3 mM α-methyl ornithine or in the presence of 0.18 mM ornithine plus 3 mM α-methyl ornithine. The relative amounts of albumin mRNA sequences, measured in the different samples by densitometry, were expressed in a percentage of the value measured in the control cultures. In our experimental conditions, albumin mRNA was increased by a factor 1.8 in the presence of ornithine (Fig. 5a,b). The addition of α-methyl ornithine to the medium of the control cultures was without effect on albumin mRNA level (Fig. 5a,b). However, in the presence of this drug, ornithine did not increase albumin mRNA level (Fig. 5a,b).

Discussion

The present studies concern the *in vitro* effects of ornithine on albumin and transferrin secretions by fetal or adult rat hepatocytes, neonatal human hepatocytes and a human hepatoma cell line. They demonstrate clearly that this amino-acid greatly increases their albumin and transferrin secretions. Moreover, the ornithine

effect appears to be localized at a pretranslational level as the mRNA level is also increased by the treatment.

The present data demonstrates that the addition of ornithine to an arginine deprived culture medium stimulates hepatocyte albumin and transferrin secretions. This result corresponds with previous observations showing that addition of ornithine to the perfusate solution of a rabbit liver favours aggregation of bound ribosomes and stimulates albumin secretion [2]. However, this effect of ornithine could be mediated by either of two possibilities, namely the production of arginine from ornithine in the urea cycle or the polyamine pathway catalyzed by ornithine decarboxylase. Indeed, in the perfused rabbit liver, arginine was as effective as ornithine [2]; moreover, polyamines and especially spermine, appeared to be potent stimulators of liver protein secretion [14]. By using α-methyl ornithine, it is possible to discriminate between the arginine and the polyamine pathway. In the presence of this known ornithine decarboxylase blocker [15], the increase in albumin and transferrin secretions observed in the presence of ornithine disappears. This result suggests that if the ornithine to polyamine pathway is blocked, ornithine does not increase albumin or transferrin secretion and supports the concept that in our hepatocyte cultures ornithine stimulation of albumin and transferrin secretions is mediated by polyamine synthesis. Our observations confirm the results of Oratz *et al.* [2] obtained in the perfused rabbit liver. Moreover, previous studies have demonstrated that polyamines stimulate many intermediate steps in protein synthesis *in vivo* and *in vitro* [16,17] and stabilize ribosomal structure and function.

In the present data, we also observe that induction of albumin secretion by ornithine is well correlated to a higher mRNA level. Moreover, when the ornithine effect is inhibited by α-methyl ornithine the increase in albumin mRNA level is no longer observed. Thus, our results demonstrate that ornithine regulates hepatocyte protein secretion at a pretranslational level.

In conclusion, the present results emphasize the role played by ornithine in the stimulation of albumin and transferrin secretions in different hepatocyte culture models. In our experimental conditions, this amino acid effect appears to be mediated by polyamine synthesis as demonstrated clearly by the use of α-methyl ornithine. Moreover, the ornithine effect is localized at a pretranslational level.

Acknowledgements

The authors are indebted to Mrs N. Pasdeloup for the technical assistance and acknowledge Mrs A. Saunier for preparing the culture medium and Mrs A. Vannier for typing the manuscript. We thank the Fondation Langlois for the support in the present work.

References

1. Rothschild MA, Oratz M and Schreiber SS (1974) Gastroenterology 67: 1200–1213.
2. Oratz M, Rothschild MA, Schreiber SS, Burks A, Mongelli J and Matarese B (1983) Hepatology 3: 567–571.
3. Guguen-Guillouzo C, Tichonicky L, Szajnert MF, Schapira F and Kruh J (1978) Biol. Cell. 31: 225–234.
4. Guguen-Guillouzo C, Tichonicky L, Szajnert MF and Kruh J (1980) In Vitro 16: 1–10.
5. Bradford MM (1976) Anal. Biochem. 72: 248–254
6. Ritchie RF (1975) In. Putman FW (ed.) The Plasma Proteins: Structure, Function and Genetic Control. Academic Press, New York, Vol. II, pp. 375–425.
7. Glisin V, Crkvenjakov R and Byus C (1974) Biochemistry 13: 2633–2637.
8. Chirgwin JM, Przybyla AE, Mac Donald RJ and Rutter WJ (1979) Biochemistry 18: 5294–5299.
9. Raymondjean M, Kneip B and Kruh J (1983) Biochim. Biophys. Acta, 741: 30–37.
10. Thomas PS (1980) Proc. Natl. Acad. Sci. USA 77: 5201–5205.
11. Andrews GK, Dziadek M and Tamaoki T (1982) J. Biol. Chem. 257: 5148–5153.
12. Sargent TD, Wu JR, Sala-Trépat JM, Wallace RB and Reyes AA (1979) Proc. Natl. Acad. Sci. USA 76: 3256–3260.
13. Rigby PW, Dieckmann, M, Rhodes C and Berg P (1977) J. Mol. Biol. 113: 237–251.
14. Choudhury I, Chaudhuri D, Kushari J and Mukerjea M (1984) Biol. Neonate 46: 209–214.
15. Mamont PS, Bohlen P, Mc Cann PP, Bey P, Schuber F and Tardif C (1976). Proc. Natl. Acad. Sci. USA 73: 1626–1630.
16. Cohen SS (1977) Cancer Res. 37: 939–942.
17. Duzendorpr U and Russell DH (1978) Cancer Res. 38: 2321–2324.
18. Tabor H and Tabor CW (1972) Adv. Enzymol. 36: 203–268.

Address for correspondence: Gérard Lescoat, INSERM U 49, Unité de Recherches Hépatologiques, CHRU Pontchaillou, 35033 Rennes Cedex, France.

Hormonal regulation of glycine metabolism*

John T. Brosnan, Markandeya Jois and Beatrice Hall

Department of Biochemistry, Memorial University of Newfoundland, St. John's, Newfoundland A1B 3X9, Canada

Abstract

The effects of several hormones on flux through glycine cleavage system (GCS) in rat liver was studied using isolated perfused liver, isolated hepatocytes and in mitochondria isolated from rats previously injected with glucagon. Glucagon (100 nM), epinephrine (1 μM), norepinephrine (1 μM), phenylephrine (10 μM) and vasopressin (100 nM) stimulated flux through GCS in perfused liver by two- to threefold. In isolated hepatocytes, the stimulation of flux by glucagon (0.01 to 1000 nM) was followed closely by increases in intracellular cyclic AMP concentration. Isolated mitochondria were exquisitely sensitive to submicromolar concentrations of free calcium. Mitochondria isolated from rats injected with glucagon 30 min before sacrifice showed 3–4 fold higher rates of decarboxylation of glycine than did mitochondria isolated from rats injected with saline when calcium was absent from incubation medium. Flux through GCS in mitochondria was also highly sensitive to the osmolarity of the medium; hypoosmotic conditions led to stimulation of the flux. The stimulation of the flux by calcium was dependent on medium osmolarity suggesting that the stimulation of flux by calcium may be mediated by changes in mitochondrial matrix volume.

Introduction

Large quantities of glycine are present in most parenteral solutions [1]. Attempts to use dipeptides in parenteral nutrition have also led to large intakes of glycine as glycyl peptides are preferred over other dipeptides due to longer half-lives of dipeptides with glycine at the N-terminal [2]. Thus there is an increasing need to understand the regulation of glycine metabolism. Hepatic glycine cleavage system (GCS) is the major route for glycine catabolism in mammals [3]. The enzyme system consists of four separate enzymes presented as an enzyme complex located in the inner mitochondrial membrane. The overall reaction catalysed by GCS is:

$$\text{glycine} + \text{NAD}^+ + \text{tetrahydrofolate} \rightarrow \text{CO}_2 + \text{NH}_3 + {}^5\text{N},{}^{10}\text{N methylene tetrahydrofolate} + \text{NADH} + \text{H}^+$$

The structure and mechanism of action of the four enzyme proteins have been studied in detail, but information regarding physiological control mechanism(s) is limited. We have recently shown that glucagon stimulates catabolism of glycine in

* Supported by grants from Medical Research Council of Canada.

isolated hepatocytes [4]. Studies presented here show that the flux through GCS is regulated by several hormones, by hormones known to act via cyclic AMP as well as by hormones known to act by increasing intracellular calcium concentration. The results also show that submicromolar concentrations of calcium stimulates flux through GCS in isolated mitochondria possibly by increasing mitochondrial matrix volume.

Materials and Methods

Materials

Collagenase was obtained from Boehringer-Mannheim (Dorval, Quebec, Canada) [1-^{14}C]Glycine was obtained from Dupont-New England Nuclear (Mississauga, Ontario). All other chemicals were of analytical grade.

Isolation and incubation of hepatocytes

Hepatocytes were isolated by collagenase perfusion of livers of fed rats weighing 200–250 g [4]. Incubation was carried out in a total volume of 2 ml of Krebs-Henseleit medium, gassed with O_2/CO_2 (95:5) at 37°C in 25 ml Erlenmeyer flasks. Flux through GCS was measured as described previously [4].

Liver perfusion

Livers of fed rats (150–250 g) were perfused without recirculation as described previously [5]. Perfusate contained Krebs-Henseleit buffer, 2.1 mM lactate, 0.3 mM pyruvate and 0.3 mM [1-^{14}C]glycine. Hormones were introduced into the perfusion line just before portal vein. $^{14}CO_2$ was released from 5 ml aliquots of perfusate samples collected under mineral oil by injecting the samples into 25 ml Erlenmeyer flasks containing 0.4 ml 1 N HCl and fitted with rubber stoppers. Plastic center wells containing 0.4 ml NCS tissue solubilizer were suspended through the rubber stoppers into the flasks. $^{14}CO_2$ was collected for 1 h and counted. Flux through GCS was calculated from $1^{14}CO_2$ released and the specific activity of [1-^{14}C] glycine infused.

Separation of hepatocytes from the medium and measurement of cAMP

Hepatocytes were separated from the incubation medium by centrifugal filtration through silicone oil (Dow Corning) of density 1.35 g/ml. The hepatocyte suspension, containing incubation medium and hepatocytes, was quickly transferred to a 1.8 ml Eppendorf centrifuge tube containing 0.15 ml of perchloric acid (30% w/v) overlaid with a 0.3 ml silicone oil and immediately spun at 8,000 × g for 10 seconds. The acid layer below the silicone oil layer, containing deproteinized

hepatocytes, was used for measurement of cyclic AMP. Cyclic AMP was measured by a competitive protein binding assay (TRK.432, Amersham) according to the instructions by the manufacturer.

Isolation and incubation of mitochondria

Mitochondria were isolated from livers of fed rats (150–250 g body wt.). The liver was homogenized in a medium containing 0.225 M mannitol, 0.075 M sucrose, 5 mM Hepes and 1 mM EGTA, pH 7.2. The homogenate was centrifuged for 10 min at 2,200 × g. The mitochondria were separated from the supernatant by centrifugation for 10 min at 8,200 × g. The pellet was washed twice, each time centrifuging at 8,200 × g. The final pellet was resuspended in isolation medium to give 30 to 40 mg mitochondrial protein/ml. Protein content was measured using a biuret procedure [6] using bovine serum albumin as standard. Mitochondria were incubated under state IV or state III (1 mM ADP) conditions in 25 ml Erlenmeyer flasks with constant agitation. The incubation medium contained 125 mM KCl, 10 mM MOPS, 7 mM Tris base, 2.5 mM potassium phosphate, 2.5 mM magnesium chloride, 5 mM NaCl, 5 mM [1-^{14}C]glycine, 1 mM EGTA and 0 to 0.95 mM $CaCl_2$ to give free Ca^{2+} concentration ranging from 0 to 2.88 μM. Preparations of solutions of EGTA and EGTA + $CaCl_2$ are described previously [7]. Concentration of free Ca^{2+} was calculated from the composition of the incubation medium by using a computerized programme (EQCAL, Biosoft, NJ). The absolute stability constants used were those given by Fabiato and Fabiato [8]. The flux through GCS was measured as described previously [4].

Results

We have previously shown that glucagon stimulates flux through GCS in isolated hepatocytes [4]. The stimulation could be mimicked by 0.1 mM dibutyryl cyclic AMP suggesting that the stimulation of flux by glucagon is mediated by an increase in intracellular cyclic AMP. Figure 1 shows results from experiments where intracellular concentration of cyclic AMP was measured directly in hepatocytes incubated with various concentrations of glucagon. The stimulation of flux through GCS by glucagon was followed closely by increase in cellular cyclic AMP levels induced by glucagon.

Figure 2 shows results from experiments conducted to examine the effects of several hormones on flux through GCS in perfused liver. Glucagon (100 nM), epinephrine (1 μM), norepinephrine (1 μM), phenylephrine (1 μM) and vasopressin (100 nM) all stimulated flux through GCS by 2–3 fold. Thus hormones which are known to exert their effects on liver by increasing cellular cyclic AMP as well as hormones known to act through increases in intracellular calcium levels stimulated flux through GCS.

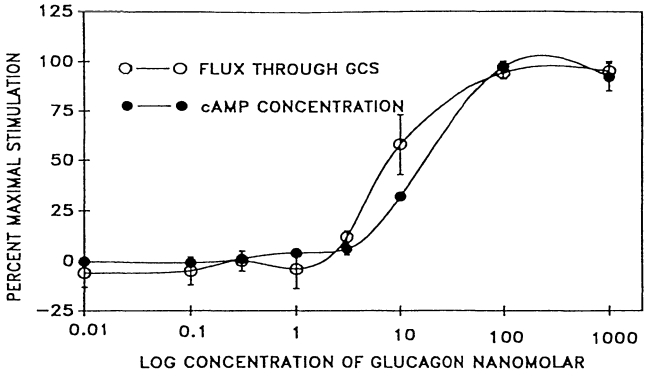

Fig. 1. Dose-response curves for stimulation of flux through GCS and cellular cyclic AMP levels by glucagon in hepatocytes. Details of isolation and incubation of hepatocytes are given in *Materials and Methods*. Incubation period was 30 min for measurement of flux through GCS and was 5 min for measurement of cyclic AMP. Results are expressed as mean ± S.E.M. of percent of maximal stimulation from 3 separate experiments.

We have demonstrated previously that mitochondria isolated from rats injected with glucagon 30 min prior to sacrifice show increased flux (50%) through GCS [4]. In these experiments calcium concentration in the medium was not controlled. Figure 3 shows data from experiments where stimulation flux through GCS by calcium was measured in mitochondria isolated from rats previously injected with glucagon (0.33 mg/100 g body wt. i.p., 30 min prior to sacrifice). Flux through GCS in mitochondria was highly sensitive to concentrations of calcium in the

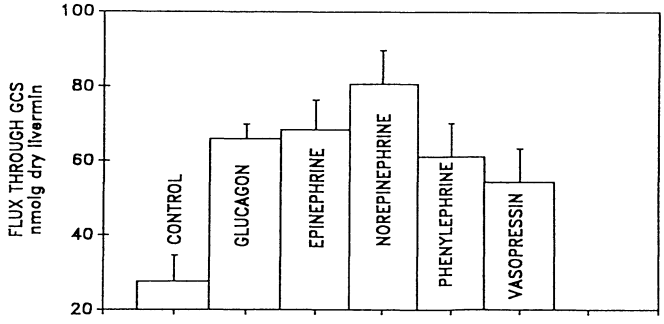

Fig. 2. Effect of hormones on flux through GCS in perfused liver. Livers from fed rats were perfused as described in *Materials and Methods* for 20 min before addition of hormone and 35 min after start of infusion of hormone into perfusion line. Results are expressed as mean ± S.E.M. (3–4 separate experiments) of flux during last 15 min of perfusion when a new steady state was reached. The final concentrations of hormones in the perfusate were glucagon, 100 nM; epinephrine, 1 μM; norepinephrine, 1 μM; phenylephrine, 10 μM; vasopressin, 100 nM.

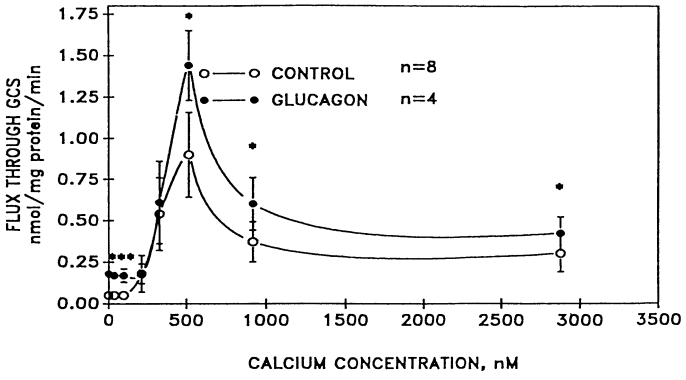

Fig. 3. Stimulation of flux through GCS by calcium in mitochondria isolated from rats previously injected with glucagon or vehicle. Experimental details are given in *Materials and Methods*. Results are expressed as mean ± S.E.M. n indicates number of separate experiments. * $P<0.05$ control vs glucagon.

range of 0.2 to 1 nM. Mitochondria isolated from glucagon treated rats exhibited increased flux through GCS; threefold higher flux when free calcium in the medium was less than 0.2 μM and 50% higher rates when free calcium in the medium was above 0.2 μM. Both types of mitochondria showed biphasic responses for stimulation by calcium when ADP was absent from the medium; when free calcium concentration in the medium was above 0.5 μM inhibition of the stimulated flux was observed (Fig. 4). Presence of ADP (1 mM) in the medium prevented such an inhibition. ADP also right-shifted the dose-response curve.

Several effects of hormones and calcium on mitochondria have been suggested to be mediated by increase in mitochondrial matrix volume [9]. Figure 5 shows that

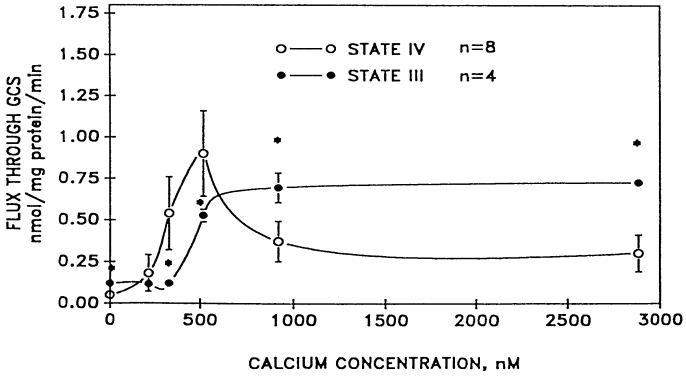

Fig. 4. Stimulation of flux through GCS by calcium in mitochondria incubated under state III or state IV conditions. Experimental details are given in *Materials and Methods*. Results are expressed as mean ± S.E.M. n indicates number of separate experiments. * $P<0.05$, state III vs state IV.

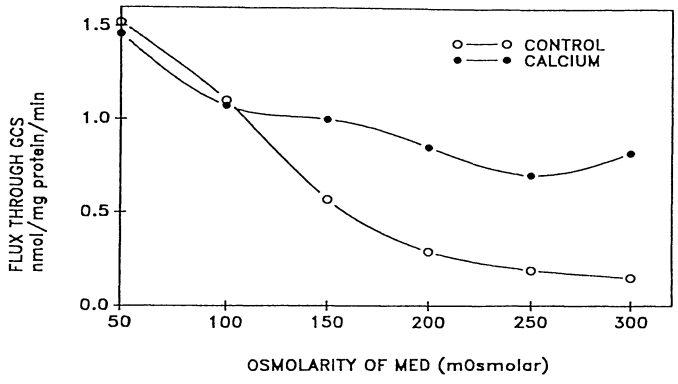

Fig. 5. Effect of changes in osmolarity of the medium on flux through GCS in mitochondria in presence and absence of 0.5 μM free calcium. Mitochondria were incubated under state III conditions as described in *Materials and Methods*. Osmolarity was changed by varying KCl concentration. Results from a typical experiment is presented.

the flux through GCS is highly sensitive to changes in the osmolarity of the medium. The stimulation of flux by calcium was evident only when osmolarity of the medium was above 100 mOsmolar.

Discussion

Hepatic glycine metabolism constitutes a major route of glycine catabolism and is primarily responsible for changes in circulating glycine concentration [3]. We have proposed that glucagon is involved in physiological regulation of glycine metabolism [4]. Studies presented here indicate that other hormones can also take part in this regulation. Glucagon is generally believed to act via increases in cyclic AMP although some groups have presented evidence that glucagon can mediate effects on metabolism independent of changes in cellular cyclic AMP levels [10,11]. That the stimulation of flux by glucagon can be mimicked by dibutyryl cyclic AMP [4] and that the stimulation of flux by glucagon is closely followed by increase in cellular cyclic AMP levels strongly suggest that glucagon mediates its effects on flux through GCS by increase in intracellular cyclic AMP levels. However the possibility that the effects of glucagon are mediated by calcium cannot be ruled out as both glucagon and cyclic AMP have been shown to elevate intracellular calcium levels [12,13].

α_1-Adrenergic agonists and vasopressin are known to exert their effects in liver by increasing the concentration of intracellular free calcium [14,15]. In isolated hepatocytes, these hormones increase intracellular free calcium concentration from resting values of 0.1–0.2 μM to about 0.6 μM. Present experiments show that these hormones stimulate flux through GCS in perfused liver and that isolated mito-

chondria are exquisitely sensitive to concentration of free calcium in the medium similar to the concentrations in hepatocytes stimulated with hormones. The reasons for the biphasic response of mitochondria incubated under state IV conditions to medium calcium is not known.

Evidence has been obtained, especially by Halestrap and coworkers, that intramitochondrial volume may play an important role in the regulation of liver mitochondrial metabolism by glucagon, α_1-adrenergic agonists and vasopressin [9]. Data presented here show that flux through GCS is extremely sensitive to changes in osmolarity of the medium and we postulate that calcium may stimulate flux through GCS by increasing intramitochondrial volume.

References

1. Stegink LD, Bell EF, Dabees TT, Andersen DW, Zike WL and Filer LJ Jr. (1983) In: Amino Acids: Metabolism and Medical Applications. Blackburn GL, Grant JP and Young VR (eds.), John Wright, PSG Inc., pp. 123–146.
2. Adibi SA (1987) Utilization of intravenously administered peptides: Influence of molecular structure. Contr. Ther. Clin. Nutr. 17: 69–90.
3. Kikuchi G (1973) Mol. Cell. Biochem. 1: 169–187.
4. Jois M, Hall B, Fewer K and Brosnan JT (1989) J. Biol. Chem. 264: 3347–3351.
5. Siess H (1978) Methods Enzymol. 52: 48–59.
6. Gornall AG, Bardwill CJ and David MM (1949) J. Biol. Chem. 177: 751–766.
7. Denton RM, Richards DA and Chin JG (1978) Biochem. J. 176: 899–906.
8. Fabiato AA and Fabiato F (1979) J. Physiol. Paris 75: 463–505.
9. Halestrap AP (1989) Biochim. Biophys. Acta 973: 355–382.
10. Corvera S, Huetra-Bahena J, Pelton JT, Hruby VJ, Trivedi D and Garcia-Sainz JA (1984) Biochim. Biophys. Acta 804: 434–441.
11. Wakelam MJO, Murphy GJ, Hruby VJ and Houslay MD (1986) Nature 323: 68–71.
12. Charest R, Blackmore PF, Berthon B and Exton JH (1983) J. Biol. Chem. 254: 8769–8773.
13. Sistare FD, Picking RA and Haynes RC (1985) J. Biol. Chem. 260: 12744–12747.
14. Williamson JR, Cooper RH, Joseph SK and Thomas AP (1985) Am. J. Physiol. 248: C203–C216.
15. Exton JH (1985) J. Clin. Invest. 73: 1753–1757.
16. Murphy E, Coll K, Rich TL and Williamson JR (1980) J. Biol. Chem. 255: 6600–6608.
17. Blackmore PF, Brumley FT and Exton JH (1982) J. Biol. Chem. 253: 4851–4858.
18. Thomas AP, Alexander J and Williamson JR (1984) J. Biol. Chem. 259: 5574–5584.

Treatment of congenital hyperammonemia with L-carnitine

Kazuhiko Oyanagi[a], Masayoshi Nagao[a], Yoshinori Kuniya[a], Toshihiko Mori[a] and Ichiro Matsuda[b]

[a]Department of Pediatrics, Sapporo Medical College, Kumamoto University Medical School, Sapporo 060, Japan

[b]Department of Pediatrics, Kumamoto University Medical School, Sapporo 060, Japan

Abstract

Carnitine status was evaluated in patients with congenital hyperammonemia caused by ornithine transcarbamylase (OTC) deficiency, carbamyl phosphate synthetase (CPS) deficiency, systemic carnitine deficiency and in identical twins who were born from a partially OTC-deficient mother. We found decreased free carnitine and increased acylcarnitine levels in the serum and in the liver tissues. The ratio of acyl/free carnitine was significantly elevated in both serum and liver tissues. After oral administration of L-carnitine (20–150 mg/kg/day) in the patient with congenital hyperammonemia, hyperammonemic episodes and metabolic acidosis disappeared and the ammonia level in the blood decreased significantly, accompanied by an increase in serum free carnitine levels.

Introduction

Carnitine is essential for the transport of long chain fatty acids across the inner mitochondrial membrane before ß-oxidation [1]. Carnitine metabolism is being closely followed from reports of carnitine deficiency arising from various etiologies [2,3]. The primary carnitine deficiency syndromes include systemic and myopathic forms.

Hyperammonemia in association with a carnitine deficiency has been well documented in cases of Reye syndrome and Reye-like syndromes [2–5], where some patients with OTC were included [5]. Carnitine-dependent mitochondrial enzymes are involved in the transport of fatty acids into the mitochondria and utilized through ß-oxidation for production of ATP [2,3]. Another function of carnitine is facilitation of the removal of accumulated toxic acyl-CoA from the mitochondrial matrix, with return of a normal free CoA level, after the conversion of carnitine to acyl-carnitine [2–4]. Therefore, severe carnitine deficiency may have untoward effects on mitochondrial function, including hyperammonemia [2,3], because ureagenesis is closely related to mitochondrial function [6], and the formation of N-acetyl-glutamate, an activator of carbamyl phosphate synthetase, might be reduced in CoA deficiency [2].

The purpose of the present paper is to describe the carnitine status in patients with congenital hyperammonemia and effectiveness of oral administration of L-carnitine for hyperammonemic attacks.

Table 1. Serum carnitine concentrations of patients with ornithine transcarbamylase (OTC) deficiency

Cases	Sex	Age	OTC activities (percent of controls)	Serum carnitine (n mole/ml)			
				Free	Acyl	Total	Acyl/Free ratio
1	M	28 days	not detectable	28.7	18.1	46.8	0.63
2	M	6 days	6%	36.8	28.8	65.6	0.78
3	M	3 months	9%	21.8	30.9	52.7	1.42
		3 years		17.3	27.2	44.5	1.57
4	M	3 months	15%	48.2	31.8	80.0	0.66
		6 years		38.7	35.6	74.3	0.92
5	F	9 years	17%	19.1	56.9	76.0	2.98
		10 years		6.3	30.5	36.8	4.85
6	F	30 years	45%	43.2	27.5	70.7	0.64
Controls							
Newborns (n =25)				33.9±7.5	15.2±7.8	49.5±11.5	0.46±0.26
1≈11 months (n = 51)				37.4±9.9	21.3±8.9	58.8±14.8	0.60±0.31
1≈10 years (n = 20)				59.6±11.7	29.7±12.6	80.8±20.5	0.55±0.16
Adults (n = 20)				53.5±13.0	28.6±10.1	78.0±9.7	0.60±0.30

M: male, F: female, n: number of cases.

Experimental procedures

Materials

Carnitine status was evaluated in patients with OTC deficiency, identical twins who were born from a partially OTC-deficient mother, CPS deficiency and systemic carnitine deficiency.

Patients with OTC deficiency

Clinical and biochemical findings of patients are shown in Table 1. The diagnosis of OTC deficiency was made on the basis of results of laboratory measurements of urea cycle enzymes in liver tissues. The activities of urea cycle enzymes other than OTC were within normal range.

Identical twins who were born from a partially OTC-deficient mother (case 6, in Table 1); the patients were male identical twins who were delivered at 34 weeks of gestation by Caesarean section. The birth weight of the first twin was 2110 g and that of the second twin was 2190 g. No abnormality was noted in the perinatal period. The family history included a male sibling who died of hyperammonemia in the neonatal period. OTC activity in his liver was not detectable (case 1, in Table 1). The diagnosis of partial OTC deficiency was made in the mother by the findings of decreased OTC activity in the tissue obtained by the liver biopsy. The first son

of her younger sister also died of episodes of hyperammonemia caused by OTC deficiency at 3 years of age (case 3, in Table 1). Since OTC deficiency is inherited as an X-linked trait, we started feeding the twins with low protein milk (0.5 g/kg/day initially, increased gradually to 2 g/kg/day) and monitoring the blood ammonia levels and urinary orotic acid excretion. The blood ammonia levels increased slightly for the first few days after birth, but urinary orotic acid was within normal range. Though protein intake was increased, the blood ammonia levels remained normal. But body weight gain of the twins was poor. On the 19th day after birth, they presented tachypnea, hypotonia, poor feeding and lethargy. Analyses of arterial blood gases indicated severe metabolic acidosis. Hence these clinical and laboratory findings suggested secondary carnitine deficiency, therapy with L-carnitine and sodium bicarbonate was started and clinical symptoms were immediately improved. During the attacks of severe metabolic acidosis, organic acids in urine were not detected.

Patient with CPS deficiency

The patient, a 53-day-old boy, was the first child of unrelated and healthy parents. He was born after an uneventful delivery with a birth weight of 3,358 g. At 21 days of age, a generalized tonic-clonic seizure developed. At 50 days of age, he again suffered from a seizure, with frequent vomiting, feeding difficulties and apathy. Blood ammonia level was elevated more than 400 μg/dl, and he was transferred to our hospital. On admission, the patient was comatose and did not respond to painful stimuli. Laboratory studies showed a mild metabolic acidosis and blood ammonia was elevated to 741 μg/dl (normal, <70 μg/dl). Analysis of urinary organic acids showed no abnormalities. CPS-1 activity in liver was 25.6% of control values (patient; 0.011 μmol product/mg protein/min, control; 0.043 ± 0.014). Therapy was started with L-arginine, sodium benzoate, essential amino acids, peritoneal dialysis and L-carnitine (20 mg/kg/day). After recovering from the hyperammonemic coma, he was put on a low-protein diet with oral administration of L-carnitine (20 mg/kg/day).

Patient with systemic carnitine deficiency

A new born female, the third child of unrelated parents was referred to our hospital because of persistent vomiting on the second day after birth. The birth weight was 3110 g. No abnormalities were noted at the birth. Though the blood ammonia level was 95 μg/dl on admission, it increased to 188 μg/dl after 6 h. Plasma and urine amino acid analyses were normal. Urinary organic acid excretion was within normal range. By administration of L-arginine (500 mg/kg), the blood ammonia level was immediately lowered to less than 100 μg/dl. So she was fed with protein restricting diet (1 g/kg/day initially, gradually increased to 2.5 g/kg/day) to prevent hyperammonemia. Though her blood ammonia levels were controlled below 70 μg/dl, she vomited occasionally and her body weight gain was poor. Elevation of blood ammonia level recurred from a month of age in spite of protein restricting diet. She presented tachypnea, hypotonia, poor feeding and lethargy at 2 months of

age. Laboratory findings indicated severe metabolic acidosis. Since the episode of illness, the patient was treated orally with L-carnitine (100 mg/kg/day). Clinical symptoms were immediately improved and acid-base balance of arterial blood gases was normalized. The family history included a male sibling (the second child) who died of acute respiratory failure with metabolic acidosis and hyperammonemia at one week old. Serum and urine amino acid analysis and urinary organic acids analysis revealed no abnormalities. A definite diagnosis had not been made until the birth and the episode of illness of the third child. Other members of the family, including both parents and the eldest brother, were healthy.

Methods

Free and acylcarnitine concentrations in serum and liver samples were measured by the method of McGarry and Foster [7]. Urea cycle enzymes in liver samples were measured by the method of Brown and Cohen [8]. N-acetylglutamate synthetase in liver was assayed by the method of Shigesada and Tatibana [9]. Carnitine palmitoyl-transferase in liver was measured by the method of Bieber *et al.* [10].

Results

Serum and liver carnitine concentrations in patients with OTC deficiency are shown in Tables 1 and 2. A reduction in free carnitine and an elevation of acylcarnitine in serum was evident in almost all the patients except case 6. The

Table 2. Hepatic carnitine levels in patients with ornitine transcarbamylase (OTC) deficiency

Cases	Liver tissue	Carnitine (nmol/mg NCP)			
		Free	Acyl	Total	Acyl/Free ratio
1	autopsy	3.25	3.15	6.41	0.97
2	autopsy	3.01	2.61	5.62	0.87
3	biopsy	5.91	2.82	8.73	0.32
	autopsy	2.86	1.85	4.71	0.65
4	autopsy	2.93	1.25	4.19	0.43
	biopsy	7.54	2.16	9.70	0.29
5	biopsy	5.68	3.91	9.59	0.69
	autopsy	3.26	1.65	4.91	0.51
6	biopsy	5.24	2.97	8.21	0.57
Controls					
Newborns	(n = 17)	4.10±1.12	1.61±0.25	5.71±1.55	0.42±0.25
1 month≈5 years	(n = 11)	5.16±0.60	2.24±0.56	7.40±0.85	0.45±0.21
>6 years	(n = 10)	9.34±1.20	2.03±0.35	11.37±0.69	0.24±0.21

NCP: Non Collagen Protein.

Table 3. Changes in serum carnitine levels in the patients after birth

Days after birth		Carnitine (nmol/ml)	
		Free	Total
At birth	(1)	17.7	36.6
	(2)	18.6	39.0
19 days	(1)	12.1	22.0
(metabolic acidosis)	(2)	13.0	20.8
21 days	(1)	264.0	352.0
(L-carnitine	(2)	161.0	340.8
150 mg/kg/day)			
42 days	(1)	49.0	75.5
(no therapy)	(2)	52.0	81.6
Control (n = 25)		33.9±7.5	49.1±11.5
Umbilical cord blood			
	(patients)	14.4	27.3
	(control, n=5)	21.3±2.9	38.6±7.2

The control values for serum carnitine were measured in the infants receiving usual formula milk. Control data are expressed as mean ± S.D.
(1) the 1st twin, (2) the 2nd twin.

ratio of acyl/free carnitine was elevated compared with control values. These findings were more prominent with increasing age in case 5. The free carnitine content of the liver tissue was reduced in all the tested patients and the acyl/free carnitine ratio was elevated.

Serum free carnitine of the twins who were given birth to by an OTC deficient mother was decreased at the time of birth and episode of metabolic acidosis. Total carnitine levels in the serum decreased to less than half of the control level at the acidosis in both cases (Table 3). Serum carnitine levels were normalized by oral administration of L-carnitine (150 mg/kg/day). They did not decrease after termination of the therapy (Table 3). The serum free carnitine concentrations in the mother of the twins during pregnancy were consistently lower than the control level. The data at delivery indicated a low free carnitine concentration and elevation of acyl/free ratio (Table 4). The carnitine content of the liver tissue of the mother was apparently below the control levels (Table 2, case 6).

Serum free carnitine level of patients with CPS deficiency was normal on admission, but markedly decreased 12 h later. This was accompanied by an increased ratio of acyl/free carnitine. After L-carnitine treatment (20 mg/kg/day), the serum free carnitine level was increased to normal levels (Table 5). Serum free carnitine levels determined at 35 days and 60 days after termination of the

Table 4. Changes of serum carnitine levels of the mother during gestation and after delivery

	Carnitine (nmol/ml)		
	Free	Total	Acyl/Free
Before gestation	27.8	45.5	0.64
Gestation 13 weeks	21.0	39.2	0.87
17 weeks	16.8	38.4	1.29
27 weeks	16.6	47.5	1.86
30 weeks	15.3	23.7	0.55
At delivery (34 weeks)	16.5	53.8	2.25
After delivery 1 week	27.0	36.5	0.35
2 weeks	26.8	49.0	0.83
4 weeks	43.2	70.7	0.64
Controls			
pregnant women (n=24)	27.1 ± 5.9	48.6 ± 13.5	0.80 ± 0.36
adults (n=34)	48.8 ± 4.2	63.4 ± 8.7	0.30 ± 0.16

Control values are expressed as mean ± S.D.

L-carnitine treatment were within normal values. However, at 7 months of age and while he was asymptomatic, his serum free carnitine level decreased again together with an increase of an acyl/free carnitine ratio. Oral administration of L-carnitine

Table 5. Serum carnitine concentrations of patient with CPS deficiency

	Serum carnitine (nmol/ml)			
	Free	Acyl	Total	Acyl/Free ratio
On admission	40.0	9.8	49.8	0.25
12 hours after admission	22.5	41.0	63.5	1.82
After termination of L-carnitine therapy				
35 days	35.7	22.7	58.4	0.64
60 days	37.7	10.6	48.3	0.28
5 months	11.5	16.5	28.0	1.44
3 months after L-carnitine therapy (20 mg/kg/day)	55.0	23.8	78.8	0.43
Controls, 1–11 months (n=51)	37.4 ± 9.9	21.3 ± 8.9	58.7 ± 14.8	0.60 ± 0.31

n: number of cases.

Table 6. Serum carnitine levels of the patient and her family members

Subject	Carnitine (nmol/ml)		
	Free	Total	Acyl/Free
Patient			
Before therapy			
at birth	18.0	32.5	0.81
2 months of age (metabolic acidosis)	3.3	20.3	5.15
After therapy			
3 months of age	36.8	93.0	1.53
Mother	35.2	63.4	0.80
Father	46.2	58.5	0.27
The 1st child (5 yr.)	43.0	80.2	0.87
The 2nd child a	9.6	17.8	0.85
Controls			
Newborn (n=25)	33.9 ± 7.5	49.1 ± 11.5	0.46 ± 0.26
1 yr – adult (n=51)	37.4 ± 9.9	58.7 ± 14.8	0.60 ± 0.31

Control values are expressed as mean ± S.D.
[a]The blood sample of the 2nd child was taken at the metabolic crisis.

(20 mg/kg/day) was initiated and continued. At 11 months of age, the blood ammonia levels of the patient were well controlled under the low protein diet with oral administration of L-carnitine and his body weight and motor development were normal.

Serum carnitine levels of patients with systemic carnitine deficiency were about half of the control level at birth. Serum free carnitine concentration decreased to 10% of the control and total carnitine concentration was less than half of the control level at the episode of acidosis. Ratio of acyl/free carnitine was very high (Table 6). After the carnitine therapy (100 mg/kg/day) for a month, both free and total carnitine levels increased to the normal range. Acyl/free ratio was also normalized. The level of the second child who had died at 7 days of age, was apparently decreased at the metabolic crisis. However, those of the parents and the eldest brother were within normal range (Table 6). Carnitine contents in liver tissue of patient were measured after 10 months of carnitine supplementation. Carnitine content of liver of patient was within normal level. Also carnitine content of liver of the second child was measured and both free and total carnitine contents decreased to quarter of control level (Table 7). When the patient became one year old, the amount of carnitine supplementation was reduced to one third of the prior dose (150 mg/kg/day → 50 mg/kg/day) for 7 days to test the effect of reduction of oral carnitine on serum carnitine levels. The free carnitine level decreased to 20% of the former values. The patient is now 2 years old and she is well controlled with

Table 7. Carnitine contents in liver tissues of patient and her brother

	Free carnitine (nmol/mg NCP)	Total
Patient (after therapy)	8.53	11.29
Brother[a]	1.73	2.08
Control infants (n=14)	7.02 ± 1.40	9.22 ± 1.94

[a]The carnitine content in the brother was measured in the tissue obtained at autopsy.
NCP: Non Collagen Protein.

oral administration of L-carnitine (100 mg/kg/day). Urea cycle enzyme activities and carnitine parmitoyltransferase activity were measured in the liver sample of her brother. All urea cycle enzymes and carnitine palmitoyltransferase were within normal range.

Discussion

Carnitine is essential for the transport of fatty acids into mitochondria where they undergo ß-oxidation. Another function of carnitine is the buffering of toxic acyl-CoA compounds [2]. Therefore, secondary carnitine deficiency can lead to deterioration of multiple mitochondrial processes and to biochemical abnormalities including hyperammonemia. Recently, carnitine deficiency secondary to a variety of genetic defect of intermediate metabolism or other disorders has been recognized [3].

Present study revealed that serum free carnitine levels in patients with OTC deficiency and CPS deficiency were apparently decreased accompanying an increase in the acyl/free carnitine ratio, and a decreased free carnitine content with elevated acyl/free carnitine ratio in the liver. These observations indicate that patients with OTC, CPS deficiency and hyperammonemic attacks had a secondary carnitine deficiency, as based on the criteria of Engel and Rebouche [2], Chalmers *et al.* [3], and Stumpf *et al.* [4]. Recently, Ohtani *et al.* [11] reported that urine acylcarnitine analysis revealed a large amount of acetyl carnitine and significant amounts of dicarboxylic acid derivatives in many of the patients with OTC deficiency, indicating some impairment of ß-oxidation and an increase in ω-oxidation of fatty acid.

Identical twins, who were born from partially OTC-deficient mother, developed clinical symptoms of carnitine deficiency during the neonatal period. It is speculated that the patients had been deficient in tissue carnitine storage in the fetal period, because serum levels of free carnitine in the mother were low during the gestation. The low levels of serum free carnitine in the umbilical cord blood and in the twins at birth support this speculation. The formula milk for treatment of congenital hyperammonemia produced in Japan contains little carnitine (4.5 ± 1.2

μmol/l, commercial formula 183.3 ± 29.0 μmol/l). It is probable that the carnitine deficient state was promoted by feeding with the formula in the present cases.

Systemic carnitine deficiency can be diagnosed by the determination of carnitine levels in serum and tissues. In the present case, serum carnitine levels were extremely low at the time of metabolic acidosis. In addition, serum and liver carnitine levels of the brother, who died of metabolic acidosis and hyperammonemia, were also decreased. Secondary carnitine deficiency due to organic acidemia was excluded since no abnormal metabolites were detected by the urinary organic acids analysis in both cases. Urea cycle enzymes in the liver of the brother showed normal activities. These results strongly suggest that the patient and her brother had the same metabolic disorder, systemic carnitine deficiency. Carnitine replacement therapy will not be effective to all patients with systemic carnitine deficiency but in our patient oral administration of L-carnitine (100–150 mg/kg/day) was effective for metabolic acidosis and ammonia disposal. The molecular mechanism of systemic carnitine deficiency has not been determined, but may be due to a defect in carnitine biosynthesis in this patient.

Though the mechanism of secondary carnitine deficiency is still unknown, treatment of L-carnitine is effective to prevent for hyperammonemia and metabolic acidosis.

References

1. Rebouche CJ (1986) Ann. Rev. Nutr. 6: 41–66.
2. Engel AG and Rebouche CJ (1984) J. Inher. Metab. Dis. 7(Suppl.): 38–43.
3. Chalmers RA, Roe CR, Stacey TE and Hoppel CL (1984) Pediatr. Res. 18: 1325–1328.
4. Stumpf DE, Parker WD and Angelini C (1985) Neurology 35: 1041–1045.
5. Matsuda I and Ohtani Y (1986) Pediatr. Neurol. 2: 90–94.
6. Stumpf DA and Parks JK (1980) Neurology 30: 178–184.
7. McGarry JD and Foster DW (1976) J. Lipid Res. 17: 277–281.
8. Brown GW and Cohen PP (1959) J. Biol. Chem. 234: 1769–1774.
9. Shigesada K and Tatibana M (1971) J. Biol. Chem. 246: 5588–5595.
10. Bieber LL, Abraham T and Helmrath T (1972) Anal. Biochem. 50: 509–518.
11. Ohtani Y, Ohyanagi K, Yamamoto S and Matsuda I (1988) J. Pediatr. 112: 409–414.

Characterization of glutamate transport in isolated adult rat heart cells

Ludger M. Dinkelborg, Rudolf J. Wiesner and Manfred K. Grieshaber

Institut für Zoologie, Lehrstuhl für Tierphysiologie, Heinrich-Heine-Universität, D-4000 Düsseldorf, F.R.G.

Abstract

Uptake of L-glutamate was studied in isolated adult rat heart myocytes in the presence and absence of oxygen. Normoxic incubation of cardiomyocytes with glutamate concentrations varying from 0.0625 to 0.33 mM led to an apparent K_m-value for glutamate of 0.18 mM. However, incubation of cardiomyocytes with glutamate concentrations up to 10 mM did not saturate glutamate uptake. We therefore assume that the high affinity glutamate carrier is saturated and further nonspecific transport mechanisms are responsible for the non-saturation kinetics. The initial glutamate uptake rate from the incubation medium, under normoxia, amounted to 24.3 ± 1.6 pmol min^{-1} mg^{-1} protein and increased under anoxia to 38.1 ± 3.8 pmol min^{-1} mg^{-1} protein. Even this increased glutamate uptake could not prevent a depletion of intracellular glutamate in anaerobic cardiomyocytes. Under reoxygenation glutamate increased again to control values with a rate of 930 pmol min^{-1} mg^{-1} protein within 15 min. Glutamate uptake from the incubation medium after reoxygenation amounted to 31.9 ± 2.5 pmol min^{-1} mg^{-1} protein. Therefore the glutamate uptake from extracellular space cannot be responsible for the rapid increase in intracellular glutamate concentration after reoxygenation. Cardiomyocytes must replenish glutamate by other mechanisms, e.g. intracellular proteolysis.

Introduction

The amino acid L-glutamate functions not only as a precursor for protein synthesis but also has a potential role in myocardial energy metabolism. Glutamate, as well as the corresponding 2-oxoacid 2-oxoglutarate are involved in the malate-aspartate cycle to transport reduction equivalents which originate in glycolysis and from oxidation of exogenous lactate, into the mitochondrial compartment [1]. Moreover glutamate deamination acts as an anaplerotic reaction to dampen fluctuations in the concentrations of citric acid cycle intermediates which are dependent upon the substrate supply to the heart [2]. In coronary artery disease, glutamate seems to be of additional importance. Previous studies have shown that hypoxia leads to a decrease in myocardial glutamate content [3–5] and ischaemia causes an augmented glutamate uptake from the blood [6–9]. Furthermore glutamate protects the isolated ischaemic or hypoxic myocardium [10–12]. Heart surgery has taken advantage of this beneficial effect using cardioplegic solutions enriched with this amino acid [13,14]. The enhanced extraction of glutamate from the blood in patients suffering from coronary artery disease may be the explanation for the

possibility of imaging ischaemic regions using L(^{13}N)-glutamate in positron scintigraphy [15–17].

Neither the mechanism of the observed augmented glutamate uptake from blood, nor the mechanism of its protective effect on the heart are as yet understood. Therefore we used isolated adult cardiomyocytes to study a) the underlying transport mechanism and b) its importance in hypoxia.

Experimental procedures

Cell preparation and incubation

Ca^{++}-tolerant myocytes were prepared from hearts of adult, male Wistar rats (300 g) by Langendorff perfusion with crude collagenase [for a detailed description see Ref. 18]. The preparations used in this study contained 85 ± 5 % of cells with the elongated, rod-shaped morphology of myocytes *in situ*, examined by light microscopy (n = 25). Cells were incubated in a gyratory water-bath shaker at 37°C in a physiological, phosphate-buffered saline (pH 7.4) containing NaCl (121 mM), KCl (5 mM), glutamine (0.7 mM), bovine serum albumin (2%, Fraction V, Boehringer, Mannheim, F.R.G.) and a complete mixture of amino acids and vitamins [18].

Oxygenated cells were incubated in open siliconized flasks with oxygen (100%), in a humidified chamber throughout the experiment. Anoxic cells were incubated in stoppered flasks flushed with humidified argon for 5 min. Before beginning of an uptake study isolated cardiac myocytes were incubated for 30 min under an oxygen or an argon atmosphere, respectively. The uptake studies were initiated by adding ^{14}C-glutamate in tracer concentrations to the medium. Under neither conditions did the percentage of rod-shaped cells change significantly during a 1 h incubation. The cell titer was approx 360,000 cells ml^{-1} equal to approx 3.2 mg of cellular protein ml^{-1}.

Extraction and fractionation of cells

Cells were simultaneously separated from the incubation medium and extracted in perchloric acid by centrifugation of 1 ml of cell suspension through 350 µl of bromododecane into 100 µl of 2 M $HClO_4$, using a Heraeus (Osterode, F.R.G.) microfuge [19].

Uptake assay

Transport of L-glutamate into myocytes was measured using 0.5 µCi ml^{-1} L-(^{14}C)-glutamate (specific radioactivity 5 nCi $nmol^{-1}$) and unless otherwise stated, L-glutamate concentration in the medium was 0.1 mM. The extracellular contamination of labeled glutamate in perchloric acid extracts was determined by two different approaches. In a first attempt we measured the amount of radioactivity in

perchloric acid extracts of myocytes, which was due to an extracellular contamination, by adding ^{3}H-sorbitol to the incubation medium. Samples of the incubation medium, as well as perchloric acid extracts were combusted (Packard Oxidizer, Mod. 306, Illinois, U.S.A.) and the resulting ^3H_2O and $^{14}CO_2$ were counted separately in a liquid scintillation counter. In a second attempt we measured the contamination by incubating the myocytes on ice, followed by the addition of labelled glutamate and immediate centrifugation of myocytes into the perchloric acid. The initial uptake rates for glutamate were calculated from data derived in the first 3 min of the individual uptake experiment, when uptake of glutamate was found to be linear with time.

Determination of metabolites, amino acids and protein

Extracts and deproteinized incubation media were neutralized using K_2CO_3 (2 M) in triethanolamine (0.5 M) [19]. ATP, phosphocreatine, lactate and glutamate were measured by standard enzymatic methods [20], by spectrophotometry (Kontron, Eching, F.R.G.) or fluorometry (Foci A 4, Farrand, New York, U.S.A.). Amino acids were measured using an automated amino acid analyzer (Liquimat III, Kontron, Eching, F.R.G.) and the specific radioactivity of glutamate was either measured using an on-line radioactivity monitor (Ramona, Isomess, Essen, F.R.G.) before ninhydrin derivatization, or by counting the radioactivity of extracts and media in a liquid scintillation counter (Beckmann, Irvine, U.S.A.).

Total cellular protein was estimated after dissolving the perchloric acid pellet in NaOH (1 M) by the method of Bradford [21] using bovine serum albumin as standard.

Materials

Amino acids, vitamins and enzymes were from Boehringer, Mannheim, F.R.G., Worthington Collagenase from Biochrom, Berlin, F.R.G. L-(U-^{14}C)-glutamate and D-(1-^{3}H(N))-sorbitol was purchased from New England Nuclear (Dreieich, F.R.G.). All other chemicals were obtained from Merck, Darmstadt, F.R.G.

Results

High energy phosphate content and lactate production

The ATP and phosphocreatine content of isolated myocytes was 18.8 ± 1.9 and 49.5 ± 4.1 nmol mg^{-1} protein, respectively (n = 4) which is in good agreement with the results of Dow *et al.* [22]. Lactate production was linear in anoxic incubations and amounted to 4.3 μmol h^{-1} mg^{-1} Protein (n = 4). This production rate is comparable to the maximal glycolytic flux measured in Langendorff perfused rat hearts [23].

For calculation of glutamate uptake by cardiomyocytes, the determination of contamination of perchloric acid extracts due to extracellular glutamate is necessary. The contamination determined with ^{3}H-sorbitol amounted to 1.3 ± 0.2 µl mg^{-1} protein (n = 8) and was slightly higher than the initial uptake of labelled glutamate. Therefore we measured the contamination by incubating myocytes with ^{14}C-glutamate on ice. Using this procedure a contamination of 0.9 ± 0.1 µl mg^{-1} protein (n = 20) was determined which is in fair agreement with 0.5 µl mg^{-1} protein as measured with (^{14}C)-polyethylenglycol [19]. Apparently sorbitol yields higher values than other extracellular space markers, a result which has been demonstrated by other investigators [24].

In order to assess the metabolism of glutamate the concentration and specific radioactivity of glutamate and all other amino acids was measured in cells and media. During the first 5 min of either normoxic or hypoxic incubation more than 95% of the radioactivity accounted for was glutamate. Thus the radioactive label of cells reflects glutamate uptake during the initial phase of incubation.

Concentration dependence of glutamate uptake

Figure 1 shows the dependence of the initial glutamate uptake rate from the extracellular glutamate concentration. Cardiomyocytes were incubated under oxygenated conditions with glutamate concentrations between 0.0625 and 0.33 mM. Initial uptake rates yield an apparent K_m-value of 0.18 mM and an apparent V_{max} of 50 pmol min^{-1} mg^{-1}. However, glutamate uptake with glutamate concentrations up to 10 mM did not reach saturation (Fig. 2). The glutamate concentration in rat blood amounted to 0.11 ± 0.02 mM (n = 3).

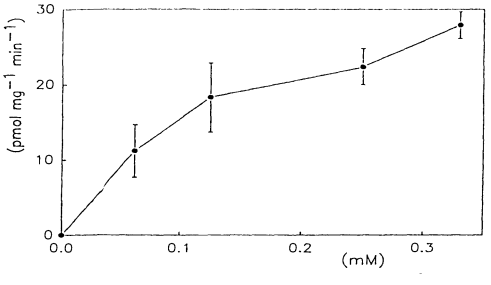

Fig. 1. Initial glutamate uptake rates (pmol min^{-1} mg^{-1} protein) versus glutamate concentration in the incubation medium (0.0625–0.33 mM) of normoxically incubated isolated adult rat heart cells (X ± S.D.; n=3).

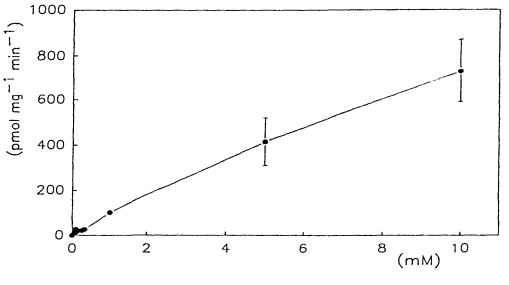

Fig. 2. Initial glutamate uptake rates (pmol min^{-1} mg^{-1} protein) versus glutamate concentration in the incubation medium (0.0625–10 mM) of normoxically incubated isolated adult rat heart cells (X ± S.D.; n=3).

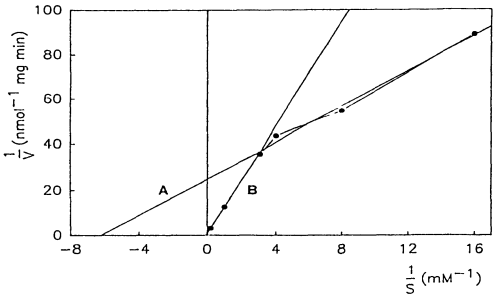

Fig. 3. Lineweaver-Burk-diagram of initial glutamate uptake rates of normoxic incubations of adult rat heart cells. A: 0.0625–0.33 mM glutamate, K_m = 0.18 mM; B: 0.33–10 mM glutamate, K_m = infinite (n=3).

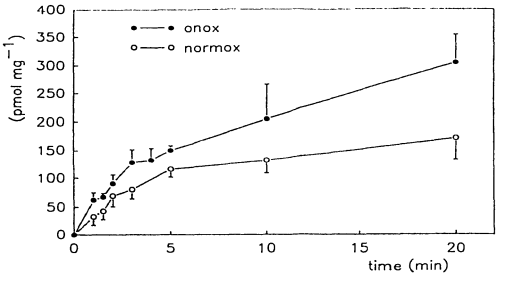

Fig. 4. Time course of L-glutamate uptake (pmol mg^{-1} protein) in normoxic and anoxic incubation of isolated adult rat heart cells. The glutamate concentration in the incubation medium was 0.1 mM. The initial uptake rate in normoxic incubations amounts to 24.3 ± 1.6 pmol min^{-1} mg^{-1} protein and in anoxic incubations 38.1 ± 3.8 pmol min^{-1} mg^{-1} protein. (X ± S.D.; n=3).

Oxygen dependence of glutamate uptake

The time courses of glutamate uptake by cardiomyocytes with or without oxygen is shown in Fig. 4. The initial uptake rate of glutamate under normoxia, amounted to 24.3 ± 1.6 pmol min^{-1} mg^{-1} protein and increased under anoxia to 38.1 ± 3.8 pmol min^{-1} mg^{-1} protein (n = 3).

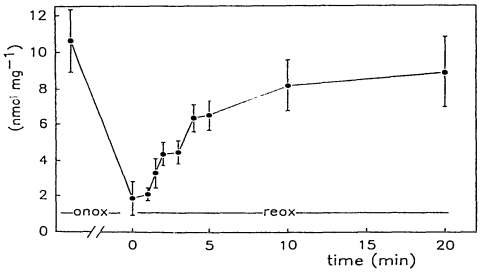

Fig. 5. Glutamate content (nmol mg^{-1} protein) of isolated adult rat heart cells during 30 min of anoxic incubation (anox) and subsequent reoxygenation (reox). The glutamate concentration in the incubation medium was 0.1 mM. The initial rate of intracellular glutamate increase was 930 pmol min^{-1} mg^{-1} protein. Note that the simultaneously measured glutamate uptake rate from the incubation medium amounted to 31.9 ± 2.5 pmol min^{-1} mg^{-1} protein (X ± S.D.; n=3).

Despite the increase of glutamate uptake in hypoxic cardiomyocytes the anaerobic metabolism leads to an intracellular depletion of this amino acid. Figure 5 shows the time course of glutamate depletion during 30 min of anoxia. Reoxygenation of cardiomyocytes leads to a rapid increase in glutamate content which reaches control values after 15 min. The initial velocity of glutamate repletion was 930 pmol min^{-1} mg^{-1} protein, but the simultaneously measured glutamate uptake from the incubation medium amounted to only 31.9 ± 2.5 pmol min^{-1} mg^{-1} protein.

Discussion

Although much is known about the uptake of neutral and basic amino acids in various cells and tissues, less information exists about transport of acidic amino acids (for Ref. see [25]). Knowledge of glutamate transport in heart is limited to those studies concerning the determination of arteriovenous differences of isolated perfused heart [3,4,6] or patients suffering from coronary artery disease [7,8,9]. This is surprising, since glutamate plays an important role in heart metabolism, especially in ischaemia. Myocardial oxygen deficiency, whether induced by hypoxia or ischaemia leads to a decrease of the intracellular glutamate content [3–5]. An augmented glutamate uptake from blood has been demonstrated in patients suffering from coronary artery disease [6–9]. ^{13}N-glutamate can therefore be used as a diagnostic means for imaging ischaemic heart regions using positron scintigraphy [15–17]. Moreover the provision of glutamate protects the ischaemic or hypoxic myocardium of isolated perfused hearts [10–12] and patients suffering from coronary artery disease [13,14].

The present study demonstrates that isolated adult rat heart cells are a suitable model for basic investigations of glutamate uptake in heart. Striated, non-working isolated heart muscle cells are characterized by a routine metabolism, therefore functional changes can be excluded. The ATP-content of cardiomyocytes in this study was stable throughout the experiment in oxygenated as well as in anoxic incubation, where anaerobic glycolysis accounts for ATP regeneration. Furthermore it is possible to distinguish glutamate uptake of cardiomyocytes from that of other cell types of the heart, e.g. endothelial or smooth muscle cells. The uptake of L-glutamate over a wide range of glutamate concentrations (0.0625 to 10 mM) leads to two apparent K_m-values, one of 0.18 mM and the other which was infinite (see Fig. 3). We conclude that the transport mechanism with the apparent K_m-value of 0.18 mM represents the high affinity glutamate carrier which is important under physiological conditions since glutamate concentration in the blood amounts to 0.11 ± 0.02 mM. The apparent K_m-value of the high affinity carrier is about 7 times higher than the apparent K_m-value of the system A transporter for neutral amino acids which has been determined to 1.3 mM by Walker *et al.* [24]. The second component of glutamate transport which cannot be saturated even at unphysiological high glutamate concentrations may be due to a non-specific uptake of glutamate by other amino acid transporters. Glutamate uptake via system A for

neutral short chain amino acids, or system L for amino acids with aromatic side chains has been reported [26]. Likewise the glutamate transporter of pulmonary endothelial cells is characterized by non saturation kinetics [27].

Cardiomyocytes are able to take up glutamate against a high concentration gradient. The initial glutamate uptake rate of oxygenated cardiomyocytes amounts to 24.3 ± 1.6 pmol min^{-1} mg^{-1} protein. The glutamate concentration in rat blood is 0.11 mM, whereas the calculated glutamate concentration in the cytosol of aerobic cardiomyocytes amounts to 7 mM [28]. Therefore the underlying mechanism for glutamate transport into the cell must be an active one. The motive power for this transport against the concentration gradient may be derived from the Na^+-gradient existing across the plasma membrane as described in cultured rat hepatocytes [29] or cultured human fibroblasts [30].

Anoxic incubation of cardiomyocytes leads to a rapid decrease in intracellular glutamate content which might be due to the depletion of cytosolic 2-oxoglutarate which stimulates cytosolic transamination of glutamate with pyruvate to alanine [28].

The initial uptake rate of anoxic cardiomyocytes which amounts to 38.1 ± 3.8 pmol min^{-1} mg^{-1} protein counteracts the decrease in intracellular myocardial glutamate content. This value for an increased glutamate transport in hypoxic cardiomyocytes corresponds well with the twofold increase of glutamate uptake in patients suffering from ischaemia due to coronary artery disease [7,9]. But the 1.6-fold increase of hypoxic glutamate uptake rate as compared to normoxic cells cannot compensate for the rapid utilization of glutamate.

The enhanced glutamate uptake of anaerobic cardiomyocytes may result from the decreased concentration gradient across the cell membrane due to intracellular glutamate depletion. Nevertheless cytosolic glutamate concentration of anaerobic cardiomyocytes amounts to 1 mM [28] and, therefore, transport of glutamate must still take place against a concentration gradient.

Reoxygenated cardiomyocytes reestablish the glutamate content rapidly at a rate of about 930 pmol min^{-1} mg^{-1} protein (Fig. 5). If all of the glutamate replenished was taken up from extracellular space, glutamate transport should be accelerated at least by a factor of 30 as compared to normoxic rates. The simultaneously measured initial glutamate uptake from the incubation medium after reoxygenation (31.9 ± 2.5 pmol min^{-1} mg^{-1} protein) accounted, however, for only 3.4% of the glutamate which appears inside the cell after reoxygenation. Although cardiomyocytes are able to respond to glutamate depletion caused by hypoxia with an augmented glutamate uptake from the medium, the glutamate content is primarily replenished by endogenous processes. Initial observations suggest that endogenous production of glutamate results from accelerated intracellular proteolysis.

Acknowledgements

This work was supported by the Deutsche Forschungsgemeinschaft, SFB 242. L.D. is a fellow of the Konrad-Adenauer-Foundation.

References

1. Safer B (1975) Circ. Res. 37: 527–533.
2. Gailis L and Benmouyal E (1973) Can. J. Biochem. 51: 11–20.
3. Taegtmeyer H (1978) Circ. Res. 43: 808–815.
4. Freminet A, Leclerc L, Poyart C, Huel C and Gentil M (1980) J. Physiol. (Paris) 76: 113–117.
5. Wiesner RJ, Rösen P and Grieshaber MK (1988) Biochem. Med. Metab. Biol. 40: 19–34.
6. Wiesner RJ, Deussen A, Borst M, Schrader J and Grieshaber MK (1989) J. Mol. Cell. Cardiol. 21: 49–59.
7. Mudge GH Jr., Mills RM Jr., Taegtmeyer H, Gorlin R and Lesch M (1976) J. Clin. Invest. 58: 1185–1192.
8. Brodan V, Fabian J, Andel M and Pechar J (1978) Basic Res. Cardiol. 73: 160–170.
9. Thomassen AR, Nielsen TT, Bagger JP and Henningsen P (1983) Clin. Science 64: 33–40.
10. Bittl JA and Shine KI (1983) Amer. J. Physiol. 245: H406–H413.
11. Pisarenko OI, Movikova EB, Serebuyakova LI, Tskitishvili OV, Ivanov VE and Studneva IM (1985) Pflügers Arch. 405(4): 377–384.
12. Choong YS, Gavin JB and Armiger LC (1988) J. Mol. Cell. Cardiol. 20: 1043–1051.
13. Rosenkranz E, Okamoto F, Buckberg GD, Robertson JM, Vinten-Johansen J and Bugyi HJ (1986) J. Thorac. Cardiovasc. Surg. 91: 428–435.
14. Bernard M, Menasche P, Canioni P, Fontanarava E, Grousset C, Piwnica A and Cozzone P (1985) J. Thorac. Cardiovasc. Surg. 90: 235–242.
15. Knapp WH, Helus F, Ostertag H, Tillmanns H and Kübler W (1982) Eur. J. Nucl. Med. 7: 211–215.
16. Krivokapich J, Keen RE, Phelps ME, Shine KI and Barrio JR (1987) Circ. Res. 60: 505–516.
17. Zimmerman R, Tillmanns H, Knapp WH, Helus F, Georgi P, Rauch B, Neumann F-J, Girgensohn S, Maier-Borst W and Kübler W (1988) J. Am. Coll. Cardiol. 11: 549–556.
18. Hohl C, Altschuld R and Brierley GP (1983) Arch. Biochem. Biophys. 221: 197–205.
19. Geisbuhler T, Altschuld RA, Trewyn RW, Ansel AZ, Lamka K and Brierley GP (1984) Circ. Res. 54: 536–546.
20. Bergmeyer HU (ed.) (1974) Methods in Enzymatic Analysis. Academic Press, New York.
21. Bradford MM (1976) Anal. Biochem. 72: 248–254.
22. Dow JW, Harding NGL and Powell T (1981) Cardiovasc. Res. 15: 549–579.
23. Rovetto MJ, Whitmer JT and Neely JR (1973) Circ. Res. 32: 699–711.
24. Walker EJ, Burns JH and Dow JW (1982) Biochim. Biophys. Acta 721: 280–288.
25. Lerner J (1987) Comp. Biochem. Physiol. 87B(3): 443–457.
26. Christensen HN (1979) Adv. Enzymol. Relat. Areas Mol. Biol. 41–101.
27. Steiger V, Deneke SM and Fanburg BL (1987) J. Appl. Physiol. 63(5): 1961–1965.
28. Wiesner RJ, Kreutzer U, Rösen P and Grieshaber MK (1988) Biochim. Biophys. Acta 936: 114–123.
29. Gebhardt R and Mecke D (1983) FEBS 161(2): 275–278.
30. Dall'Asta V, Gazzola GC, Franchi-Gazzola R, Bussolati O, Longo N and Guidotti GG (1983) J. Biol. Chem. 258(10): 6371–6379.

Amino acid determination of human intestinal mucosa obtained by endosopic biopsies

Günter Ollenschläger[a], Klaus Langer[b], Erich Roth[c], Hubert Schmitt[b], Matthias Schrappe-Bächer[a], Hans-Michael Steffen[a] and Bruno Allolio[a]

[a]Department of Internal Medicine II, University of Cologne, F.R.G.
[b]Research Institute for Experimental Nutrition, Erlangen, F.R.G.
[c]1st Surgical University Clinic, Department of Surgical Pathophysiology, Vienna, Austria

Abstract

In this study we describe a method which makes possible the determination of the free amino acids in biopsies of human gastrointestinal mucosa. Biopsies of duodenal or colonic mucosa were obtained from internal patients without histologically proven pathological processes of duodenum or colon during routinely performed gastrointestinal endoscopy. After shock-freezing in fluid nitrogen and lyophilization, the analysis of the extracts was performed by ion exchange chromatography. Standard deviations of the individual amino acid concentrations of 3 parallel specimens was 3–13% (except histidine: 19%). The sum of all amino acids without taurine was 61.9 (5.4) mmol/kg dry weight (mean, SD of 7 patients) in duodenal biopsies, and 82.9 (0.6) in colonic specimen; 50% (44%) of which consisted of aspartate and glutamate, and 14% (12%) of total essential amino acids. The relative amino acid pattern differed completely from the muscle pattern: aspartate was fourfold higher; glutamate, phenylalanine, glycine, valine, leucine, isoleucine about twofold higher. In contrast, glutamine amounted only to 4% (duodenum)/ 14% (colon) of muscle glutamine. The results obtained from duodenum were compared with that of HIV-positive patients (n=3). We found enhanced intracellular levels of serine and glutamate (150% of normal), glutamine (220%), valine (125%), and ornithine (410%). Amino acid analysis of endoscopically obtained mucosa biopsies might be helpful to monitor intestinal amino acid metabolism, as well as the effect of nutrition therapy in critically ill patients.

Introduction

The gastrointestinal tract plays a central role in the inter-organ exchange of nutrients, especially of amino acids (AA). It is not only the place, where substrates are digested, absorbed, and delivered to the bloodstream. The gut is also an organ, which actively metabolizes absorbed nutrients, and circulating substrates too. Because of their anatomic relationship, the gut and liver cooperate in the handling and processing of ingested nutrients; as well as in protecting the organism from unphysiological metabolite concentrations.

Recent studies have demonstrated that especially the intestinal metabolism of glutamine (GLN) is of great interest. This AA is the primary respiratory fuel of the intestinal mucosa [1], and there are evidences that morphological and functional integrity of this organ depend highly on sufficient amino acid availability, especially of glutamine [2].

Until now, the intracellular amino acid metabolism of the human gut has not been characterized exactly, because there was no routine method for the amino acid determination of the gastrointestinal mucosa available. In the following, we describe a procedure for the AA analysis of mucosal biopsies, obtained during routinely performed gastrointestinal endoscopies.

Experimental procedures

The intramucosal amino acid pattern was characterized in duodenal and colonic specimens and compared to the plasma amino acid pattern [3], as well as the muscular AA concentrations [4] of healthy volunteers.

Patients and endoscopy

Biopsies of duodenal and colonic mucosa were obtained with informed consent from 13 patients (5 females; 8 males; mean age: 53.8, SD 16.9 years), who had to undergo a gastrointestinal endoscopy because of abdominal pain (n=7), suspect of malignoma (n=3). anemia of unknown origin (n=1), diarrhea (n=2). The patients with diarrhea were HIV-positive (stage WR 5,6), and one subject with abdominal pain too: stage WR 4 of the Walter Reed Classification [3]. Two patients had lost more than 5% of their original body weight during the last 3 months as a consequence of anorexia. The endoscopies were done after a fast of at least 12 h between 08.30 and 13.00 hours. Before the endoscopy, a local anaesthesia of the pharynx with lidocaine (Xylocain® Spray, Astra Chemicals, Wedel, F.R.G) was obligatory; sometimes a premedication with 2.5–5 mg Midazolam (Dormicum®, Roche Inc., Basel, Switzerland) was necessary.

Biopsies were performed only in those patients, who needed a histological examination (Inst. of Pathology, Univ. of Cologne; head: Prof.Dr. Fischer). Specimens for amino acid analysis and for histology were taken from the same region. Histological changes, characteristic of unspecific slight duodenitis, were found in 5 cases. The results of the patients with slight duodenitis did not differ from those without it.

Analysis of intramucosal free amino acids

Specimen of the intestinal mucosa were shock-frozen by fluid nitrogen within 20 seconds, after the endoscopic biopsy had been performed. After a freezing time of 3 h, the biopsates were stored at −80°C.

After a storage period of less than 10 days, the wet weight was determined by weighing frozen specimen on a Cahn C 31 electrobalance (Cahn Instr. Inc., Cerritos, California, U.S.A.). Thereafter specimens were lyophilized over 4 h by use of a Lyovac GT 2 lyophilisator (Leybold-Heraeus GmbH, Köln) with an initial temperature of −65°C. The lyophilisate was weighed to obtain the dry weight, and

the AA were extracted at room temperature in a glass-homogenizer with 250 µl of a 30 g/l solution of sulfosalicylic acid in 0.1 mol/l lithium citrate buffer (adjusted with HCl to a final pH of 2.2) containing 5 g/l dithioethanol.

After centrifugation, specimens were analyzed by ion exchange chromatography in a Biotronik LC 5001 analyzer (Biotronik, München, F.R.G.). The glass column (400 × 3.2 mm i.d.) was packed with CK 10F-resin (Misubishi Chem. Ind. Ltd., Tokyo, Japan) to a height of 138 mm. The buffer flow rate was 0.42 ml/min. Lithium citrate buffers of different ion concentrations and pH's were used. The separation conditions were as follows: temp. 1: 36°C, 29.5 min; temp. 2/1: 42°C, 28 min; temp. 3/1: 63°C, 28.4 min; temp. 2/2: 42°C, 8 min; temp. 3/2: 63°C, 14.3 min; temp. 4: 74°C, 28 min. The time intervals were for buffer A (pH 2.93) 8.5 min, for buffer B (pH 3.15) 33 min, for buffer C (pH 3.36) 44.4 min, for buffer D (pH 3.75) 20.3 min, and for buffer E (PH 3.94) 30 min. The regeneration period was 8 min, at 74°C with 0.3 mol/l lithium hydroxide, and the equilibrium time with buffer A was 24.5 min. Amino acids were detected as reaction products with 20 g/l ninhydrin solution at a wavelength of 570 nm (proline 440 nm). The solution was made under nitrogen atmosphere with 7.5 parts ethylene glycol monomethyl ether and 2.5 parts 4 mol/l sodium acetate buffer, containing 0.1 g titanium chloride. For one analysis, the whole extract of one biopsy was necessary.

Calculations and statistics

The amino acid levels of an individual are the median intramucosal concentrations of three parallel biopsies. Values are expressed as means, medians and standard deviations of these medians; the concentrations are expressed as mmol/kg dry weight or as percent of the amino acid sum. Differences between duodenal concentrations of patients without HIV-infection (n=7) and with it (n=3), as well as colonic levels (n=3) were tested to be statistically significant by use of the U-test (Wilcoxon, Mann, Whitney). P values below 0.05 were considered to be significant.

Results

Table 1 lists the absolute concentrations of free amino acids in biopsies of the duodenum and the colon. The mean wet weight of the biopsies was 5.63 mg (SD: 1.3), and the dry weight 1.15 (0.26). The standard deviations of individual AA concentrations of 3 parallel specimen were between 3 and 13% (except histidine with 19%). We were not able to detect quantitatively relevant levels of asparagine, α-aminobutyrate, cystine, and tryptophan. We found significant differences between duodenum and colon, regarding the total AA concentration, as well as the AA pattern in absolute and relative terms. Whereas the absolute amounts of total EAA are nearly identical in duodenum, colon, as well as in muscle (9.7/ 8.3 / 8.8 mmol/kg d.w.), this is not the case with the relative pattern (% of total EAA). If

combined to 4 EAA-groups as recommended by Waterlow and Fern [5], the relative pattern of duodenum corresponds with that of the plasma (Table 4). In contrast, the EAA rank order of the colon resembles more to that of muscle: in these organs, lysine and threonine have higher levels than the BCAA. The difference

Table 1. Amino acid concentrations of intestinal mucosa biopsies (mmol/kg dry weight)

AS	Duodenum (n = 7) ME(SD)	Med.	Colon (n = 3) ME(SD)	Med.	p^a	Duod-HIV (n = 3) ME(SD)	Med.	p^b
TAU	23.7 (2.9)	21.7	13.3 (2.1)	14.7	***	28.6 (6.9)	32.2	
ASP	14.0 (1.5)	13.7	12.4 (1.6)	13.0		14.5 (5.4)	15.9	
THRE	1.17 (0.14)	1.1	1.43 (0.17)	1.5	*	1.43 (0.25)	1.4	*
SER	2.16 (0.27)	2.2	2.43 (0.29)	2.4		3.2 (0.85)	3.3	**
GLU	17.17 (1.76)	16.2	23.0 (0.5)	22.8	***	25.97 (7.56)	21.7	***
GLN	2.31 (0.6)	2.1	8.0 (0.3)	8.2	***	4.97 (1.96)	4.8	**
GLY	7.9 (1.3)	6.7	12.1 (1.0)	11.6	***	8.0 (3.16)	6.7	
ALA	4.64 (1.0)	4.3	10.6 (0.5)	10.9	***	5.17 (1.36)	5.9	
VAL	1.74 (0.1)	1.7	1.73 (0.26)	1.6		2.17 (0.29)	2.0	***
ILE	0.63 (0.15)	0.6	0.60 (0)	0.6		0.57 (0.06)	0.6	
LEU	1.84 (0.24)	1.7	1.33 (0.17)	1.4	***	1.47 (0.12)	1.4	*
TYR	0.78 (0.24)	0.7	0.50 (0)	0.5	**	0.47 (0.06)	0.5	**
PHE	0.68 (0.12)	0.7	0.50 (0.08)	0.5		0.73 (0.15)	0.7	
ORN	0.31 (0.09)	0.3	0.58 (0.17)	0.6	***	1.27 (0.57)	1.1	***
LYS	1.71 (0.27)	1.6	2.40 (0.16)	2.4	***	1.77 (0.40)	1.7	
HIS	0.66 (0.18)	0.6	1.10 (0.16)	1.1	***	0.90 (0.17)	1.0	
ARG	1.27 (0.42)	1.3	1.27 (0.12)	1.3		1.23 (0.46)	1.5	
Total w.out TAU	61.9 (5.4)	58.3	82.9 (0.55)	83.5	***	73.7 (19.5)	66.7	

p: [a]colon versus duodenum; [b]duodenum HIV-positive versus duodenum; *** <0.01; ** <0.025; * <0.05.
Abbr.: ME = Means; SD = Standard deviations.

Table 2. Rank order of relative amounts of free essential amino acids in duodenum, colon, muscle and plasma

AA	Duodenum		Colon		Muscle		Plasma	
	Rank	% total AA	Rank	% total AA	Rank	% total AA	Rank	% total AA
LEU	1	3.0	4	1.7	5	0.7	4	3.7
VAL	2	2.8	2	2.0	4	1.0	1	6.8
LYS	2	2.8	1	3.0	1	3.2	2	5.7
THRE	3	1.9	3	1.9	2	1.9	3	4.1
PHE	4	1.1	7	0.6	6	0.3	7	1.7
HIS	4	1.1	5	1.4	3	1.3	5	2.7
ILE	5	1.0	6	0.7	6	0.3	6	2.0
MET	6	0.5	8	0.4	7	0.2	8	0.7
Total ess.AA		14.2		11.7		8.9		27.4

of the total amino acid amount between duodenum and colon (62/83 mmol/kg d.w.) results primarily from glutamate, glutamine, glycine, and alanine; their concentrations are 5–6 mmol/kg d.w. each higher in colon than in duodenum.

The relative concentration of glutamate however is identical and amounts to 28% of total AA, which is twice the plasma level and three times the amount of the human muscle. Thus glutamate shows the highest level of all intracellular free amino acids in duodenum and colon, while glutamine holds only the fifth rank of

Table 3. Rank order of relative amounts of free non-essential amino acids in duodenum, colon, muscle and plasma

AA	Duodenum		Colon		Muscle		Plasma	
	Rank	% total AA	Rank	% total AA	Rank	% total AA	Rank	% total AA
GLU	1	27.8	1	28.2	2	10.4	9	1.5
ASP	2	22.6	2	16.1	6	2.9	11	0.3
GLY	3	12.8	3	14.3	5	4.2	3	6.8
ALA	4	7.5	4	13.5	3	9.0	2	10.2
GLN	5	3.7	5	10.1	1	53.1	1	18.0
SER	6	3.5	6	3.0	7	1.9	5	3.1
PRO	7	3.2	7	2.8	4	4.5	3	6.8
ARG	8	2.1	8	1.6	8	1.6	8	1.7
TYR	9	1.3	10	0.6	12	0.4	8	1.7
CIT	10	1.0	10	0.6	13	0.4	10	1.0
ORN	11	0.5	9	0.7	10	0.9	6	2.4
ASN					9	1.0	7	2.1
CYS					11	0.5	4	3.4
Total AA w.out TAU		61.9 mmol/kg dry		82.9		99.8 weight		2.95 nmol/l

Table 4. Relative amounts of free essential amino acids (% of total essential AA) in duodenum, colon, muscle and plasma

AA	Duodenum	Colon	Muscle	Plasma
BCAA	47.8	37.6	22.5	45.5
LYS+THR	33.1	41.8	57.3	35.8
PHE+MET	11.3	8.6	5.6	8.8
HIS	7.8	12.0	14.6	9.9

the NEAA with 4% of the duodenal and 10% of the colonic AA, which is 4/14% of the muscular concentration (Table 3).

Aspartate is the compound, which has the largest difference from plasma and muscle concentrations. Duodenal aspartate has nearly the same concentration as glutamate, and it occupies also the second rank in the colon. Glycine ranks third, and by this before alanine, which is in contrast to plasma and muscle.

The data of HIV+ subjects show much larger standard deviations than the results of the other patients. That is why they must be confirmed by further investigations. All HIV+ patients suffered from histologically proven duodenitis. The AA concentrations of two other patients with duodenitis, but without HIV-infection, did not differ from that of patients without duodenitis.

Discussion

Our results and especially the narrow standard deviations demonstrate, that the intracellular free amino acid pattern of the gastrointestinal mucosa can be characterized by analysis of mucosal biopsies. As far as we know, there is only one study in the literature, dealing with the same subject in men. Adibi and Mercer obtained specimens of the jejunal mucosa from 4 subjects using a biopsy capsule for the determination of 13 different free amino acids in the biopsies [6]. There are several disadvantages, which make this method useless for routine diagnosis, quite in contrast to our procedure: an X-ray control of the capsule site is necessary; an inspection of the region which is to be biopsied is not possible. Only 1 specimen can be obtained; and this is the prime problem: in order to interpret correctly the results of the biopsy analysis with respect to the patient's disease, a parallel sample has to be examined by a pathologist.

Our rank order of the mucosal amino acid concentration in the duodenum (Tables 2,3) is identical with Adibi's jejunal data [6]; although the absolute AA levels are not comparable because of the methodical differences between the two studies.

According to their varying physiological functions for amino acid and protein metabolism, the gut, muscle and blood plasma show different amino acid patterns. As an example, the highest relative portion of the essential amino acids can be seen

in the plasma, e.g. in the transport system for vital substrates, with a two- to threefold higher relative EAA concentration than in the gut/muscle.

Glutamine is the amino acid with the most pronounced concentration differences between the above-mentioned organs. Our investigation confirms the results from rat small intestine [1] and human jejunum [6], that the lowest concentrations of free glutamine are measured at the location of consumption, e.g. in the duodenum. The duodenal levels amount to only 4% of free muscle-GLN, and 15% of the liver concentrations [7]. Under physiological conditions, the intestinal glutamine levels depend predominantly on glutaminase activity of the tissue. The specific activity is similar in mucosa of duodenum, jejunum, and ileum, but much lower in stomach, cecum and colon of the rat [8]. From the higher GLN-levels of colonic mucosa (nearly fourfold higher than duodenum, Table 1) we deduce, that this is also a fact in man.

In contrast, skeletal muscle has the highest levels of free glutamine. It is the most important source of this amino acid and releases the compound for removal by other organ tracts during the post-absorptive state [9,10]

We now investigate, whether the GLN-availability for intestinal consumption is impaired as a result of enhanced systemic GLN-catabolism [11], of disturbed muscular synthesis [12], or of glutamine-deficient artificial nutrition [13], or not.

Next to glutamine, the intestinal levels of glutamate and aspartate differ most from muscular and plasma concentrations. These two compounds make up about 50% of all mucosal free amino acids, compared to 13%/1.8% in muscle/plasma.

Similar to the liver pattern [14], we found almost equimolar concentrations of aspartate and glutamate in the duodenum, but not in colonic biopsies. Thus, the enzymatic activities of the upper intestine are more likely to resemble the liver than the distal intestine, especially the activities of the glutamate dehydrogenase/ aspartate aminotransferase system [15].

Although glutamic acid is the major amino acid of all proteins [16], plasma levels increase only slightly after a protein-rich meal [6]. There are several mechanisms, which protect the organism from the toxic effects of a glutamate load [17,18]. First, glutamate is absorbed at a slower rate than other amino acids in man [19]. Second, after the ingestion of a protein rich diet, the amino acid is concentrated in the jejunum: in contrast to several other amino acids increased intracellular levels of the free amino acid can be measured [6]. Third, glutamate is released from the jejunum into the blood in only very small portions [8]. The formation of ammonium and alanine (substances rapidly metabolized by the liver), as well as of citrulline avoid the output of large quantities of intramucosal glutamate into the plasma [20]. It might be of interest to investigate, whether the enhanced plasma glutamate levels of patients with neoplastic diseases or HIV-infection [21] result from disturbances of these protective mechanisms.

Our results concerning the HIV-positive patients can only be regarded as preliminary, because of the very high standard deviations, compared to the other groups' data. Nevertheless, the glutamate levels are of predominant interest, because of our recent investigation, which shows HIV-positive patients of stage

WR 5,6 have significantly increased plasma glutamate levels [3]. On the other hand, the enhanced intraduodenal glutamine levels of the HIV-positive subjects lead to the assumption that the intracellular degradation of glutamine is likely to be disturbed in critically ill patients. It is now under investigation, whether this is correct or not.

Acknowledgements

The technical assistance of Heike Moll and Helga Golling is gratefully acknowledged. We wish to thank Ortrud Brand for valuable discussions.

References

1. Windmueller HG and Spaeth AE (1974) J. Biol. Chem. 249: 5070–5079.
2. Fox AD, Kripke SA, DePaula J, Berman JM, Settle RG and Rombeau JL (1988) J. Parent. Enter. Nutr. 12: 325–331.
3. Ollenschläger G, Jansen S, Schindler J, Rasokat H, Schrappe-Bächer M and Roth E (1988) Clin. Chem. 34: 1787–1789.
4. Roth E, Zöch G, Schulz F, Karner J, Mühlbacher F, Hamilton G, Mauritz W, Sporn P and Funovics J (1985) Clin. Chem. 31: 1305–1309.
5. Waterlow JC and Fern EB (1981) In: Waterlow JC and Stephen JML (eds.) Nitrogen Metabolism in Man. Applied Science Publishers, London, pp. 1–16.
6. Adibi SA and Mercer DW (1973) J. Clin. Invest. 52: 1586–1594.
7. Roth E, Mühlbacher F, Karner J, Hamilton G and Funovics J (1987) Metabolism 36: 7–13.
8. Windmueller HG (1982) Adv. Enzymol. 53: 201–237.
9. Marliss EB, Aoki TT, Pozefksy T, Most AS and Cahill GF (1971) J. Clin. Invest. 50: 814–817.
10. Felig P, Wahren J, Karl I, Cerasi E, Luft R and Kipnis DM (1973) Diabetes 22: 573–576.
11. Ollenschläger G, Roth E, Linkesch W, Jansen S, Simmel A and Mödder B (1988) Eur. J. Clin. Invest. 18: 512–516.
12. Roth E, Funovics J, Mühlbacher F, Schemper M, Mauritz W, Sporn P and Fritsch A (1982) Clin. Nutr. 1: 25–41.
13. Souba WW, Smith R and Wilmore DW (1985) J. Parent. Enter. Nutr. 9: 608–617.
14. Roth E, Mühlbacher F, Karner J, Steininger R, Schemper M and Funovics J (1985) Surgery 97: 436–442.
15. Kovacevic Z and McGivan JD (1983) Physiol. Rev. 63: 547–605.
16. Giacometti T (1979) In: Filer LJ (ed.) Glutamic Acid: Advances in Biochemistry and Physiology. Raven Press, New York, pp. 25–34.
17. Levey S, Harroun JE and Smyth CJ (1949) J. Lab. Clin. Med. 34: 1238–1248.
18. Kingsland PA, Kingsnorth A, Royle GT, Kettlewell MGW and Ross BD (1981) Br. J. Surg. 68: 234–237.
19. Adibi SA, Gray SJ and Menden E (1967) Am. J. Clin. Nutr. 20: 24–33.
20. Watford M, Lund P and Krebs HA (1979) Biochem. J. 178: 589–596.
21. Ollenschläger G, Karner J, Karner-Hanusch J, Jansen S, Schindler J and Roth E (1989) Scand. J. Clin. Lab. Invest., 49: 773–777.

Address for correspondence: Dr. Dr. med. Günter Ollenschläger, Klinik II und Poliklinik für Innere Medizin der Universität Köln, J. Stelzmann-Str 9, D-5000 Köln 41, F.R.G.

Taurine and osmoregulation: An assessment using *in vivo* and *in vitro* experimental systems

Howard Trachtman, Richard Del Pizzo and Stephen Futterweit

Department of Pediatrics, Division of Nephrology, Schneider Children's Hospital (Long Island Campus of the Albert Einstein College of Medicine), New Hyde Park, NY 11042, U.S.A.

Introduction

Taurine, 2-aminoethane sulfonic acid, is present in nearly all body tissues and frequently is the most abundant free amino acid in the cytosol [1]. In invertebrate marine species, taurine serves an osmoregulatory role to maintain cell volume constant in the face of fluctuations in environmental osmolality [2]. In mammals, there is also circumstantial evidence in favor of a cerebral osmoprotective function of taurine. It is known that the brain content of taurine varies in direct relationship to the serum Na^+ concentration in rats with chronic hyponatremia and hypernatremia [3,4]. In order to gain a more complete picture of the role of taurine in osmoregulation, we conducted the following experiments with two goals in mind;

1) to directly evaluate the importance of taurine in cerebral osmoregulation by studying the impact of dietary manipulation of brain taurine content on animal tolerance of chronic hypo- and hypernatremia. Cats were utilized in these experiments since their limited capacity to synthesize taurine and obligatory use of this amino acid in bile conjugation make them critically dependent on taurine administration in the diet [5];

2) to determine whether the contribution of taurine to cerebral osmoregulation during chronic hypo- and hypernatremia involves an adaptive increase in transmembrane taurine flux in brain synaptosomes. These are sealed, metabolically active, neuronal membrane fragments that can be used in *in vitro* assay systems to evaluate intrinsic changes in membrane function [6].

Methods

Chronic hyponatremia and hypernatremia regimens

Hyponatremia was produced in cats over a 48 h interval by injections of pitressin tannate in oil, 5 U/day, aqueous vasopressin, 5 U/day and 5% dextrose in water, 7.5% body weight/day. Hypernatremia was induced in the same species for 96 h by

complete water restriction for 24 h followed by daily injections of 1M NaCl designed to raise the serum Na^+ concentration to 180 mmol/L over the next 72 h. Animals were weighed daily and serum samples were obtained prior to and at completion of the regimen for measurement of electrolyte concentrations. At sacrifice, the brain and a specimen of muscle tissue were rapidly excised. The organs were analyzed for tissue water compartment sizes by drying to constant weight and using the chloride space as a marker of the extracellular water compartment [7]. The brain taurine content was measured after homogenization and deproteinizing the sample with perchloric acid.

In each condition of serum Na^+ concentration, two groups of cats were studied; 1) controls fed a standard, pelleted taurine replete diet; and 2) an experimental group fed a taurine-free, color-coded diet of similar consistency. The dietary pre-treatment phase lasted 12 weeks prior to the induction of hypo- or hypernatremia.

Taurine tranport in synaptosomes

These studies were conducted in rats fed standard rodent chow. Groups of rats were then made either hyponatremic or hypernatremic for 48 h according to the regimen described above. Normonatremic control rats that received sham injections were studied in parallel in all experiments. At the completion of the hypo- or hypernatremic interval, the animals were sacrificed by decapitation and the brains were rapidly removed and placed in an ice cold isolation medium containing (in mM): Sucrose 320, Tris-HCl 10, K-EDTA 1. The brains were minced and then homogenized in a Dounce homogenizer. Synaptosomes were isolated by sequential centrifugation and purification on discontinuous Ficoll gradients, as described by Fraser *et al.* [8]. Integrity and purity of the synaptosomes were verified by electron microscopy, release of LDH after incubation with Triton X-100, and measurement of rotenone-insensitive NAD(P)H dependent cytochrome c reductase activity.

Taurine transport was assessed after pre-equilibrating the synaptosomes with 150 mM KCl. Total taurine uptake was measured after 30, 60, 90, and 120 minutes in the presence of 100 μM taurine and an inward Na^+ gradient, using tracer amounts of ^3H-taurine and a rapid filtration technique. The ionic requirements of taurine transport were assessed by replacing external Na^+ and Cl^- with choline and gluconate, respectively. The addition of ß-alanine to the external medium was utilized to ascertain the role of the ß-amino acid transport system in taurine transport. Kinetic parameters of taurine uptake were determined by measuring specific taurine tansport after 60 minutes incubation in the presence of 10, 50, 100 and 250 μM taurine.

Statistical analysis

Data were analyzed using the t-test, analysis of variance and linear regression where appropriate and results were considered significant if the value of P was less than 0.05.

Results

The 12 week dietary preparation lowered cerebral taurine content from 1.8 ± 0.3 in control cats (N = 6) to 0.3 ± 0.1 μmol/g wet weight in the taurine deficient animals (N = 6). The hyponatremia regimen succesfully lowered the serum Na^+ concentration to 117 ± 2 and 110 ± 3 mmol/l in the taurine-replete and deficient cats, respectively. While none of the animals in either group died prior to completion of the observation period, control taurine replete animals were more lethargic and consumed less food. These clinical changes were reflected in a greater expansion of the cerebral intracellular water (ICW) compartment size in taurine-replete versus taurine-deficient cats, 355 ± 7 vs 309 ± 12 ml/100 g dry weight, $P<0.05$.

Dietary pre-treatment of the cats prior to production of chronic hypernatremia reduced brain taurine content from 9.5 ± 1.9 to 5.6 ± 1.9 μmol/g dry weight in control (N = 7) vs. experimental (N = 7) cats. The hypernatremia protocol elevated the serum Na^+ concentration to 177 ± 2 and 183 ± 4 mmol/l in the taurine-replete and taurine depleted groups, respectively. In these experiments, 5/7 taurine depleted cats failed to survive for the entire observation period and died within 36 h of onset of hypernatremia. In addition, three of these cats had generalized tonic-clonic seizures prior to their death. These findings contrasted markedly with the results in taurine-replete cats, among whom only one died and none had overt neurological dysfunction. The experimental taurine-deficient cats suffered significantly greater shrinkage of the cerebral ICW space, 353 ± 12 vs 484 ± 35 ml/100 g fat-free dry weight in the control taurine-replete animals ($p<0.05$).

In order to determine whether the use of taurine as a cerebral osmolyte during conditions of deranged serum osmolality involved alterations in transmembrane flux of this amino acid, we measured taurine uptake in synaptosomes isolated from rats with hyponatremia and hypernatremia of 48 h duration. Synaptosomes isolated from control rats or experimental animals with hyponatremia or hypernatremia had a similar ultrastructural appearance and internal volume and minimal contamination with mitochondria. The hyponatremia regimen lowered the serum Na^+ concentration to 100 ± 7 compared to 143 ± 1 mmol/l in control animals studied in parallel. Taurine uptake after 120 minutes incubation in synaptosomes was reduced from 5.87 ± 0.27 in controls to 5.24 ± 0.28 μmol/mg protein in hyponatremic rats, $p<0.01$. Substitution of external Na^+ and Cl^+ with choline and gluconate reduced total taurine uptake by 70 and 30%, respectively in control and experimental synaptosomes.

The 48 h hypernatremia protocol raised the serum Na^+ concentration from 140 ± 1 in controls to 167 ± 3 mmol/l in experimental rats. This manipulation resulted in an increase in total synaptosomal taurine uptake from 4.79 ± 0.21 in controls to 5.47 ± 0.32 μmol/mg protein in experimental rats, $P<0.001$. Ionic requirements for taurine transport were similar to those observed during hyponatremia with a 70 and 30% reduction in total taurine uptake by substitution of external Na^+ and Cl^+ by choline and gluconate, respectively. The addition of ß-alanine to the external medium reduced total taurine uptake by 30%. Kinetic analysis of specific taurine

uptake during hypernatremia indicated that the adaptive change in taurine uptake resulted from an increase in V_{max} from 0.107 ± 0.001 in controls to 0.121 ± 0.001 μmol/mg protein/minute in experimental rats ($P<0.02$), without any significant change in the Km of the transport system, 55 μM.

Discussion

The results of these experiments directly demonstrate that taurine is a cerebral osmolyte in the mammalian brain. Thus, dietary depletion of brain taurine content in cats resulted in an enhanced susceptibilty to cerebral cell contraction during hyperosmolal states and conferred protection against brain cell swelling under hypoosmolal conditions. While the changes in brain taurine content following the 12 week dietary pre-treatment phase appear to be disproportionate to the degree of change in brain ICW compartment size, this may be a consequence of partitioning of the brain taurine content in the grey or white matter during conditions of altered serum osmolality. This would result in a relatively larger contribution of taurine to the effective cytosolic osmolyte pool in critical areas of the brain. Further studies of brain taurine distribution during hyponatremia and hypernatremia are needed to clarify this point. An alternative explanation for taurine's osmoprotective effect may include a direct effect on the blood brain barrier to stabilize intercapillary tight junctions [9].

In earlier work work we have shown that exogenous administration of taurine analogues conferred protection against brain cell shrinkage during hypernatremic dehydration [10]. This suggested that the brain possesses the capability to modulate transmembrane taurine flux in response to perturbations in serum osmolality. Studies in marine invertebrate and vertebrate species have indicated that there are changes in osmolyte transport following perturbations in external osmolality [11]. The present studies confirm that there is a similar adaptive change in taurine uptake in the mammalian brain that parallels changes in serum Na^+ concentration. Modification of cerebral taurine transport represents an intrinsic adaptation of the cell membrane, since alterations in uptake are preserved in an *in vitro* system in which taurine transport is assayed under the conditions of a similar, controlled transmembrane Na^+ gradient. The requirement for external Na^+ and Cl^+ and the competitive inhibition achieved by adding ß-alanine to the external medium indicates that the adaptive change in taurine uptake is likely to involve the ß-amino acid carrier system [12]. Based on the kinetic studies performed in synaptosomes isolated under hypernatremic conditions, the increased transport is mediated by either an increase in the number or turnover rate of the ß-amino acid carrier system.

The importance of the changes in cerebral taurine transport to the adaptive alterations in brain taurine content can be estimated from a lower value of the increase in taurine uptake, the total brain protein content and the percentage of brain protein in synaptosomes. Calculations based on published data would suggest

that modulation of brain taurine transport is responsible for nearly 50% of the total change in brain taurine content in chronic hyponatremia and hypernatremia [3,4]. Alterations in transmembrane flux and release from subcellular storage sites are probably of equal importance in mediating the changes in cytosolic osmolyte concentrations in states of abnormal osmolality. Additional work is required to clarify the nature of the signal transduction mechanism that transmits alterations in serum osmolality to modulation of cellular handling of osmoprotective molecules.

References

1. Jacobsen JG and Smith LH Jr. (1968) Physiol. Rev. 48: 424–511.
2. Pierce SK (1982) Biol. Bull. 168: 405–419.
3. Thurston JH, Hauhart RE and Dirgo JA (1980) Life Sci. 26: 1561–1568.
4. Thurston JE and Hauhart RE (1987) Life Sci. 40: 2539–2542.
5. Sturman JA, Rassin DK, Hayes KC and Gaull GE (1978) J. Nutr. 108: 1462–1476.
6. Meiners BA, Speth RC, Bresolin N, Huxtable RJ and Yamamura HI (1980) Federation Proc. 39: 2695–2700.
7. Trachtman H, Barbour R, Sturman JA and Finberg L (1988) Pediatr. Res. 23: 35–39.
8. Fraser CL, Sarnacki P and Arieff AI (1985) J. Clin. Invest. 75: 2014–2023.
9. Gordon RE, Shaked A and Solano DF (1986) Amer. J. Pathol. 125: 585–600.
10. Trachtman H, DelPizzo R, Sturman JA, Huxtable RJ and Finberg L (1988) Amer. J. Dis. Child 142: 1194–1198.
11. Ziyadeh FN, Feldman GM, Booz GW and Kleinzeller A (1988) Biochim. Biophys. Acta 943: 43–52.
12. Kontro P and Oja SS (1978) Neuroscience 3: 761–765.

Role of amino acids in experimental intrahepatic cholestasis

B. Tuchweber, F. Guertin, I.M. Yousef, A.M. Weber and C.C. Roy

Departments of Nutrition, Pharmacology and Pediatrics, University of Montreal, Pediatric Research Center, Hôpital St. Justine, Montreal, Quebec, Canada

Abstract

Guinea pigs infused with amino acid-dextrose solution for 3 days developed intrahepatic cholestasis which is characterized by significant decrease in bile flow and bile acid secretion. The addition of taurine to the parenteral nutrition, exerted a beneficial effect against the cholestasis probably by influencing the hepatic bile acid uptake and secretion and by increasing bile acid independent flow.

Introduction

Total parenteral nutrition (TPN) has gained acceptance as a viable method in patients who need nutritional support. But, biliary and hepatic complications remain a threat, particularly during prolonged TPN in infants and children, as well as in adults [1,2]. Cholestasis is a complication often associated with TPN, and a number of factors appear to be responsible for its development [2]. They include immaturity of liver function, prolonged starvation, sepsis and infection, disease of lower intestinal tract and the microflora, gastrointestinal surgery in the neonate, as well as components and duration of the TPN.

Of the three macronutrients used in TPN, amino acids have attracted considerable attention. In clinical studies, the amino acids given intravenously were associated with cholestasis in a dose-related manner [3,4]. In animal studies, infusion of amino acid-dextrose or amino acid-dextroselipid solutions has resulted in cholestasis [5–7]. Moreover, using a liver perfusion system, it has been shown that single amino acids or amino acid mixtures can induce a dose-dependent cholestatic response [8–11].

Further studies in animals showed that amino acid imbalance may be a factor in the development of cholestasis. In rats, comparison of different amino acid mixtures indicated that animals treated with Travasol exhibited cholestasis, while those treated with Vamin did not [12]. The addition of serine (present only in Vamin) to the Travasol enhanced bile secretion markedly, suggesting that some amino acid(s) have greater potential than others to cause hepatobiliary disfunction.

Recent work indicated that taurine may have protective effects against a variety of toxic agents [13]. Of interest is the observation that taurine supplements in the diet

offers protection against lithocholic acid-induced cholestasis in Guinea pigs [14] as well as against cholestasis which follow the injection of the sulfated form [15].

Taurine feeding also resulted in increased activity of 7α-hydroxylase and HMGCoA reductase [16], and there are indications of enhanced availability of cholesterol (via lipoprotein uptake by the liver) [17] and increased bile acid secretion rate [16,18]. The enhancement of bile acid secretion rate maximum (SRm) probably results from facilitated excretion at the bile canalicular level, and can be accounted for only in part by a change of the bile acid conjugation pattern [18].

The present study aims at: 1) establishing a model of amino acid-induced cholestasis in Guinea pigs and studying its pathogenesis, and 2) testing whether the addition of taurine to the solution could have a beneficial effect against cholestasis.

Materials and Methods

Male Guinea pigs weighing 450–500 g were obtained from Charles River, Quebec, Canada and housed in a temperature controlled room (22°C) with alternative 12 h light-dark cycles. Animals were fed Guinea pig food *ad libitum* and had free access to water for one week prior to use in the experiment.

Under anesthesia (50 mg/kg ketamine hydrochloride, Ketalar, Parke Davis, Detroit, Mi), a central catheter was positioned in the superior *vena cava*, after its introduction into the right external jugular vein. The catheter was tunneled subcutaneously and threaded through a metal swivel which allowed free movement of the Guinea pigs, fitted with a harness.

Three groups of animals were fed parenterally. The first one was given saline solution and had access to Guinea pig food *ad libitum*, the second group received a TPN solution of the composition described in Table 1 without taurine, and the third group received TPN solution with taurine supplements. The solutions were delivered at a flow of 1.8 ml/h, and after 3 days of TPN, perfusion was stopped and animals were anesthetized. The common bile duct was cannulated, the gallbladder was ligated, and body temperature was maintained at 37°C by a temperature controlled heating lamp with a rectal probe. Bile was collected for 2 h in 15 min aliquots, and, at the end of collection, blood and liver collected for analysis.

Bile flow was determined gravimetrically, and total bile acids were measured enzymatically [19]. The pattern of biliary bile acids was measured by gas liquid chromatography [18] and the glyco- and tauro-conjugated biliary bile acids separated as described earlier [18]. Other biliary components were determined as indicated in previous work from this laboratory [12]. The plasma osmolality, as well as alanine aminotransferase, cholesterol, and protein contents were measured by the hospital's central laboratory.

Liver composition [12] and morphology [14] were also studied.

Table 1. Composition of TPN solution

	amount (per 100 ml)		
Crystalline amino acids (Travasol 10%)			80 ml
Essential amino acids		*Non-essential amino acids*	
L-leucine	620 mg	L-alanine	2.08 g
L-phenylalanine	620 mg	L-glycine	2.08 g
L-methionine	580 mg	L-arginine	1.04 g
L-lysine	580 mg	L-proline	0.42 g
L-isoleucine	480 mg	L-tyrosine	0.40 g
L-valine	460 mg		
L-histidine	440 mg		
L-threonine	420 mg		
L-thryptophane	180 mg		
Electrolytes			
Na	70 mEq/l		
K	60 mEq/l		
Mg	10 mEq/l		
acetate	150 mEq/l		
chlore	70 mEq/l		
phosphate	60 mEq/l		
bisulfite of Na	3 mEq/l		
Taurine			1.19 nmoles
Dextrose			29 g
Vitamins (MVI)			0.08 ml

Results and Discussion

The present study shows that amino acid-dextrose solutions for 3 days led to a significant decrease of bile flow. In the group receiving TPN supplemented with taurine, bile flow increased significantly (Fig. 1). Bile acid concentration in bile did not change significantly during the first h of bile collection. The bile secretion rate decreased significantly in TPN group and taurine supplements improved the bile acid output (Fig. 2).

Analysis of the correlations between bile flow and bile acid secretion rates indicated that, in the control group, there was a significant correlation between these parameters ($r = 0.68$). But TPN treatments affected the correlation between bile flow and bile acid secretion. The extrapolation of the correlation line to theoretical zero bile acid secretion rate permits the estimation of the bile acid independent fraction of the bile flow (BAIF). Figure 3 shows that the BAIF decreased with TPN, and that animals with taurine supplementation showed a BAIF closer to that of control animals. The slope of the correlation line, which gives an estimate of the choleretic potency of bile acids secreted, indicates that in TPN plus taurine, the bile flow is independent of bile acids.

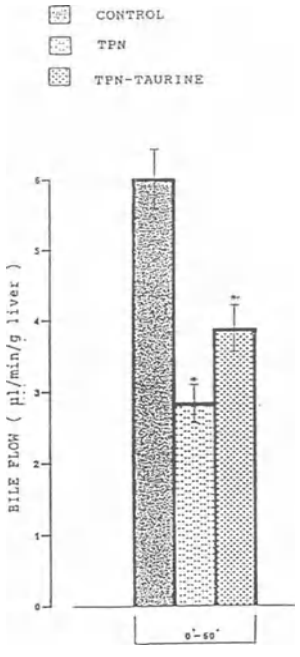

Fig. 1. Effect of TPN on bile flow.

Studies of bile acid metabolism (Table 2 and Fig. 4) showed that TPN did not modify bile acid distribution. Chenodeoxycholic acid and 7-Keto lithocholic acid

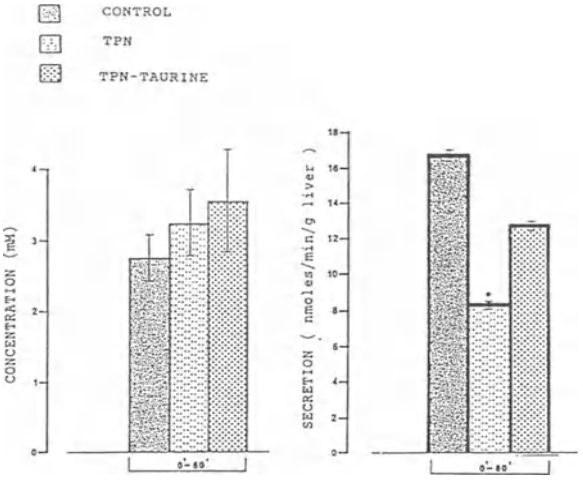

Fig. 2. Effect of TPN on bile acid concentration and secretion rate.

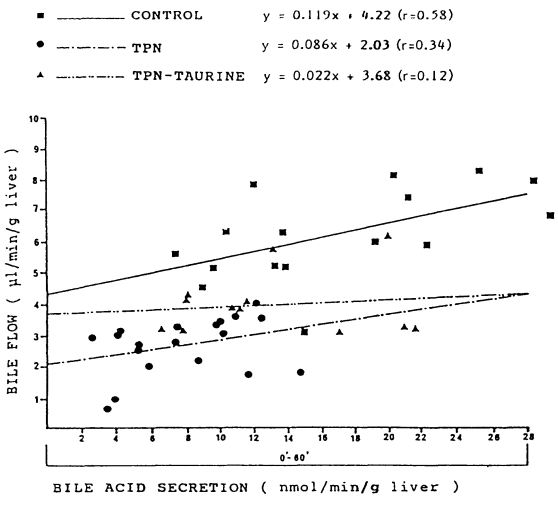

Fig. 3. Effect of TPN on the relation between bile flow and bile acid secretion.

were the major bile acids in Guinea pigs of all groups. The bile acid conjugation pattern indicated that taurine supplements led to an increase in tauroconjugates. As to other biliary components, concentrations of Na^+, K^+, and Cl^- remained unchanged in TPN groups. However, bicarbonate content decreased markedly in TPN groups and taurine restored this value close to normal. Bile osmolality was virtually similar in all groups.

Examinations of liver morphology and serum ALT indicated that TPN did not result in evident cellular damage (results not shown).

Several factors have been considered to explain the TPN-induced cholestasis. It was suggested that lack of oral feeding may influence bile formation. It could slow down the entero-hepatic cycle, thus favoring formation of cholestatic mono-

Table 2. Percent distribution of biliary bile acids

Bile acid	Saline (6)	TPN (6)	TPN-Taurine (5)
Deoxycholic acid	0.96 ± 0.22	1.71 ± 0.64	0.9 ± 0.30
Chenodeoxycholic acid	62.48 ± 5.87	59.32 ± 3.72	54.98 ± 3.2
Ursodeoxycholic acid	7.52 ± 1.61	4.18 ± 0.92	4.15 ± 0.12
7 Keto lithocholic acid	24.25 ± 4.90	29.33 ± 5.03	30.31 ± 3.29
Cholic acid	1.21 ± 0.17	0.37 ± 0.37	Not detected
Others[a]	6.83 ± 2.93	0.92 ± 0.43	7.28 ± 1.56[b]

[a]Unidentified peaks with retention time which do not correspond to bile acid standards available and which may represent keto bile acids.
[b]TPN-Taurine vs TPN $p<0.05$.

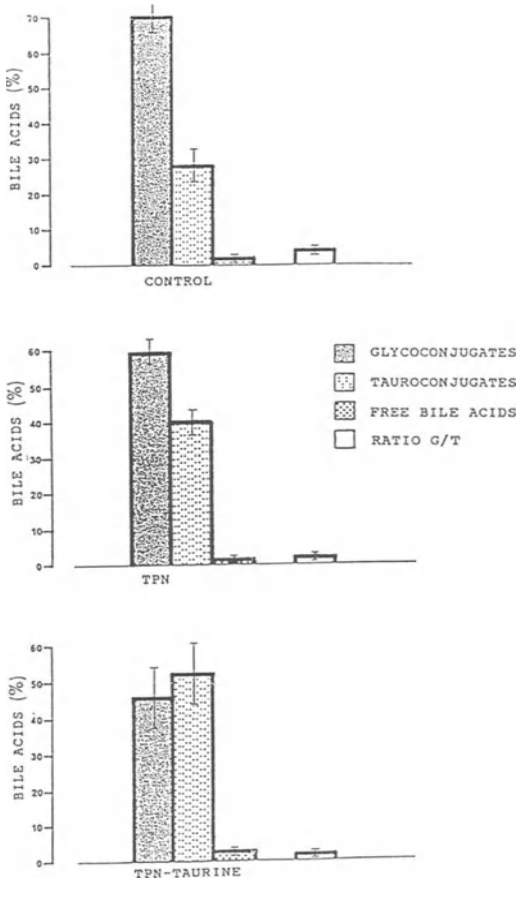

Fig. 4. Effect of TPN on bile acid conjugation.

hydroxy bile acids (e.g. lithocholic acid), but studies in rats showed that cholestasis associated with TPN was not changed by oral feeding [12]. Results of experiments in Guinea pigs not reported here indicate that amino acid-dextrose solutions infused for 2 h to fed animals resulted in cholestasis. Furthermore, a 24 h fasting period did not alter bile formation.

It has also been suggested that the infusion of hypertonic solutions can increase plasma osmolality, which in turn may inhibit bile secretion [19]. High osmolality can be ruled out as a factor in the development of cholestasis since in this study, plasma values remained unaltered.

The TPN appears to change the bile acid secretion in bile, and the defect may be at the level of bile acid uptake [20] and/or secretion. The BAIF, which is a major component of bile flow in the Guinea pig, is also influenced by the amino

acid-dextrose solution. The cholestasis may depend in part on the decreased secretion of Na^+ and Cl^- in bile, and, in particular, of bicarbonate. Bicarbonate is an important component of the BAIF [21], and, although the mechanisms of secretion have not been fully elucidated, a direct relationship has been established between choleresis induced by 7-Keto lithocholic acid and bicarbonate secretion [22]. Guinea pig bile contains a significant portion of this bile acid, which may partly explain the bicarbonate output. An additional and perhaps more important mechanism may be localised at the plasma membrane of the canaliculus, where an exchange of Cl^-bicarbonate has been described [23]. The TPN may alter such membrane exchange mechanism, but this hypothesis needs to be tested.

The significant finding of this study was the beneficial effect of taurine on bile formation. We can hypothesize that taurine exerts its effect by influencing the hepatic bile acid uptake and secretion, and by increasing the BAIF.

Acknowledgements

This work was done with the support of grants of the Medical Research Council of Canada.

References

1. Whitington PF (1985) Hepatology 5: 693–696.
2. Roy CC and Belli DJ (1985) Amer. College Nutrition 4: 651–660.
3. Vileisis RA, Inwood RJ and Hunt CE (1980) J. Pediatr. 96: 893–897.
4. Black DP, Suttle EA, Whitington PF et al. (1981) J. Pediatr. 99: 445–449.
5. Gimmon Z, Kelley RE, Simko V et al. (1982) J. Surg. Res. 32: 256–263.
6. Zahavi I, Shaffer ZA and Gall DC (1983) Gastroenterology (Abstract) 84: 1359.
7. King WWK, Boelhouwer RV, Kingsnorth AN et al. (1983) J. PEN 7: 443–446.
8. Preisig R and Rennert O (1977) Gastroenterology (Abstract) 73: 1240.
9. Perea A, Tuchweber B, Yousef IM (1987) Nutr. Res. 7: 89–99.
10. Graham MR, Tavill SA, Halpin TC et al. (1984) Hepatology 4: 69–73.
11. Meritt RJ, Sinatra FR and Henton DH (1982) Pediatr. Res. (Abstract) 16: 171A.
12. Belli D, Fournier LA, Lepage G et al. (1987) J. PEN 11: 67–73.
13. Gaull G (1986) J. Amer. Coll. Nutrition 5: 121–125.
14. Dorvil NP, Yousef IM, Tuchweber B et al. (1983) Am. J. Clin. Nutr. 37: 221–232.
15. Belli DC, Roy CC, Fournier LA et al. Amer. J. Physiol. (Submitted).
16. Bellentani S, Pecorari M, Cordoma P et al. (1987) J. Lipid Res. 28: 1021–1027.
17. Zouhair F, Stephan ZF, Lindsey S et al. (1987) J. Biol. Chem. 262: 6069–6073.
18. Belli D, Fournier LA, Lepage G et al. (1988) Ped. Research 24: 34–37.
19. Weber AM, Chartrand L, Doyon G et al. (1972) Clin. Chim. Acta 39: 524–531.
20. Chenderovitch J, Phocas E and Rautureau M (1963) Am. J. Physiol. 205: 863–867.
21. Blitzer BL, Ratoosh SL and Donovan CB (1983) Am. J. Physiol. 245: 6399–6405.
22. Hardison WGM and Wood CA (1978) Am. J. Physiol. 235: E158–E164.
23. Dumont M, Erlinger S and Uchman S (1980) Gastroenterology 79: 82–89.
24. Meier PJ, Knickelhein R, Moseley RM et al. (1985) J. Clin. Invest. 75: 1256–1273.

Physiological properties of 4-chlorotryptophan, a novel natural chloroamino acid

Akira Yoshida, Hideki Kamuro and Satoshi Nagaoka
Department of Agricultural Chemistry, Nagoya University, Nagoya 464, Japan

Introduction

4-Chlorotryptophan was first isolated from the extract of immature seeds of peas (*Pisum sativum*) by Marumo and Hattori [1] in 1970 as a possible precursor of 4-Chloroindoleacetic acid (Fig. 1). 4-Chloroindoleacetic acid is a plant growth hormone and its activity for pea seedlings is much stronger than that of indole acetic acid (auxin) which is a well known plant growth hormone. Recently the distribution of 4-chloroindoleacetic acid was further investigated in other species of peas and beans than *Pisum sativum*. Peas and beans are important and good protein sources for human life in the world. Therefore, the physiological properties of 4-chloroindole tryptophan was studied using rats. Tryptophan is not only a constituent of tissue proteins but it converts to niacin and serotonin in the body and has many important physiological roles.

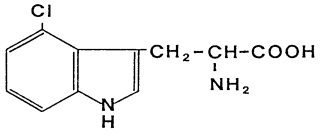

4-Chlorotryptophan

Fig. 1.

Materials and Methods

Male wealing rats of the Wistar strain weighing about 50 g were used for the experiments. The composition of the basal diet is as follows: Gelatin (20%) and casein (3%) were used as the protein sources to make a low tryptophan diet. L-Methionine (0.2%) and L-isoleucine (0.1%) were included in the basal diet so that only tryptophan was the limiting amino acid for the growth and nitrogen balance of rats. Dietary level of tryptophan in the basal diet was 0.039%. Corn starch and sucrose (2:1) were used as carbohydrate sources. Appropriate amounts of minerals and vitamins were also included in the basal diet. 4-Chlorotryptophan was generously supplied by Dr. S. Marumo of the Nagoya University, Japan.

Animals were divided into 4 groups 5 or 6 animals as a group and were fed the different experimental diets as follows: group 1, the basal diet (tryptophan: 0.039%); group 2, the basal diet plus 0.031% L-tryptophan (total dietary tryptophan: 0.07%); group 3, the basal diet plus 0.061% L-tryptophan (total dietary tryptophan: 0.10%) ; group 4, the basal diet plus 0.10% DL-4-chlorotryptophan. Except specified, diets and water were supplied *ad libitum*.

Tryptophan contents in diets, tissues and excreta were determined by the fluorometric method of Denkla and Dewey [2]. The wave length of the excitation and emission of fluorescence were 371 nm and 443 nm respectively. Similar method was used for the determination of 4-chlorotryptophan in the group of animals fed diet containing 4-chlorotryptophan. Emmission coefficient of 4-chlorotryptophan was 57.9% of tryptophan. The contents of 4-chlorotryptophan were calculated from the difference between basal and chlorotryptophan groups using the emission coefficient of the chlorotryptophan. Serotonin and 5-hydroxyindole acetic acid in brain were determined by the method of Thompson *et al.* [3].

Results and Discussion

Experiment 1: Comparison of tryptophan and 4-chlorotryptophan for the growth of rats

Rats were fed the four different experimental diets *ad libitum* for 6 days. The body weight of rats fed the basal diet (Trp: 0.039%) were almost maintained but slightly decreased (Table 1, Fig. 2). When the dietary level of tryptophan was elevated to 0.07% and 0.10%, the gains in body weight were also increased depending on the dietary level of tryptophan. On the other hand, the group of rats fed a diet containing 0.1% of 4-chlorotryptophan and 0.039% of tryptophan gradually lost their body weight during the experimental period. The results indicate that tryptophan can not be replaced by 4-chlorotryptophan for the growth

Table 1. Effect of dietary level of tryptophan and chlor-tryptophan on the gain in body weight and food intake

Groups	Gain in body weight g/6days	Food intake g/6days
1. Basal diet (Trp:0.039%)	-2.2 ± 2.7^{a}	38.8 ± 2.1^{a}
2. Diet 1 + 0.039%Trp (Trp:0.07%)	5.6 ± 2.2^{b}	51.2 ± 2.7^{b}
3. Diet 1 + 0.061%Trp (Trp:0.10%)	16.9 ± 2.6^{c}	61.8 ± 2.4^{c}
4. Diet 1 + 0.10%Cl-Trp	-9.2 ± 1.1^{d}	25.7 ± 2.2^{d}

Young male Wistar rats were fed the oxperimental diets containing various levels of tryptophan or chlor-tryptophan for 6 days *ad libitum*. Means within a column not followed by the same supperscript letters are significantly different ($p<0.05$).

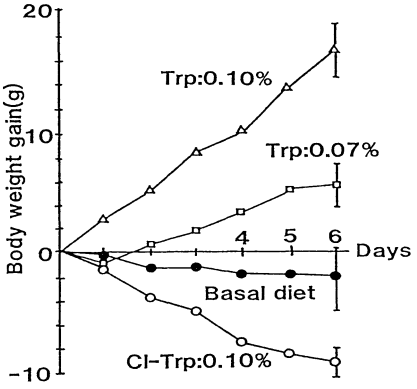

Fig. 2. Effect of dietary 4-chlorotryptophan on body weight gain of rats. Rats were fed either the basal diet (Trp: 0.039%), tryptophan supplemented diets (Trp: 0.07% and 0.10%) or chlorotryptophan diet (4-chlorotryptophan: 0.10%) *ad libitum* for 6 days.

of rats. Addition of 0.10% of 4-chlorotryptophan to the basal diet clearly showed an adverse effect. Thus, 4-chlorotryptophan has no nutritive value as tryptophan but showed growth retarding effect for rats. Food intake for 6 days of the basal diet group was 38.8 g and the food intake increased with each increase in dietary level of tryptophan. The addition of 0.10% of 4-chlorotryptophan significantly decreased the food intake of rats, that was 25.7 g for 6 days. The decrease of body weight of chlorotryptophan group may be due to the decreased food intake. Feces and urine of group 3 (Trp: 0.10%) and group 4(chlorotryptophan: 0.10%) were collected for day 1–3, and 4–6, and the excretions of tryptophan and chlorotryptophan were estimated (Table 2). The excretions of tryptophan or chlorotryptophan in feces were 1% or less and it was supposed that most of tryptophan or chlorotryptophan was absorbed from the gastrointestinal tract. On the other hand, though the urinary excretions of 0.10% tryptophan group were very small amounts, 1.1% for day 1–3, and 0.6% for day 4–6, fairly large amounts of chlorotryptophan were excreted from the animals fed the diet containing chlorotryptophan, they were 24.8% and 39.1% respectively. We did not determine the

Table 2. Fecal and urinary excretion of tryptophan and 4-chlorotryptophan[a]

	Fecal excretion		Urinary excretion	
	Day 1–3	Day 4–6	Day 1–3	Day 4–6
	% of intake		% of intake	
Tryptophan	0.37 ± 0.03	0.27 ± 0.03	1.7 ± 0.2	0.6 ± 0.3
Cl-Tryptophan	1.36 ± 0.09	0.37 ± 0.14	24.8 ± 3.7	39.7 ± 2.9

[a]Trp diet: 0.1%; Cl-Trp diet: Cl-Trp 0.1%, Trp 0.039%.

amounts of chlorotryptophan metabolized in the animal body and incorporated into tissue proteins. Nevertheless, it can be said that quite large amounts of absorbed chlorotryptophan were excreted into urine. The precise determination of chlorotryptophan by gas-liquid chromatography and mass-spectrometry is a complex procedure, and in this experiment the amounts of chlorotryptophan in urine were estimated from the difference of the values between the chlorotryptophan group and the tryptophan group using the specific emission coefficient for chlorotryptophan. It may be interesting to examine whether chlorotrypton incorporates into tissue proteins or not and also whether it can be metabolized or not.

Experiment 2: Comparison of tryptophan and 4-chlorotryptophan for the growth of rats in pair-feeding

In the next experiment, the body weight gains were compared with the same amount of food intake. In this pair-feeding experiment, three groups of rats were fed different experimental diets, the low tryptophan basal diet (Trp: 0.039%), tryptophan supplemented diet (Trp: 0.089%) and chlorotryptophan diet (4-chlorotryptophan: 0.03%, Trp: 0.039%). The group following the chlorotryptophan diet was fed *ad libitum* and the same amounts of other diets were supplied to the paired animals of the other groups. The rats from the chlorotryptophan group gradually lost their body weight and the body weight loss for 6 days was 13.5 g. The pair-fed rats of the other two groups also lost their body weight for the first 2–3 days, but later maintained the body weight (basal diet group) or somewhat recovered (Trp: 0.089% group). The loss of body weight for 6 days of the basal diet group was 7.2 g and that of the tryptophan supplemented group was 2.3 g. It was concluded that the loss of body weight of the chlorotryptophan group was partly due to the depression of food intake, although this is not the only reason as other toxic effects of chlorotryptophan would be involved in the mechanisms of body weight loss.

Experiment 3: Food selection of rats for tryptophan diet and chlorotryptophan diet

In the previous experiment, it was shown that the food intake of rats fed the chlorotryptophan diet significantly decreased accompanied by the body weight loss. 4-Chlorotryptophan does not show special flavor for man, and it is interesting to examine why rats do not eat adequate amounts of the diet containing 4-chlorotryptophan. A food selection experiment was carried out as follows. Two kinds of diet were prepared. One contained 0.10% of L-tryptophan, and the other contained 0.13% of 4-chlorotryptophan and 0.039% of L-tryptophan. After over night fasting, rats were allowed to select these two kinds of diets *ad libitum*, and food intake was determined. As indicated in Fig. 3, rats almost exclusively selected the tryptophan diet from the first hour and ate only very small amounts of the diet containing chlorotryptophan over a period of 24 h. Discrimination between the two diets was very rapid. Though rats might be able to discriminate the chlorotryp-

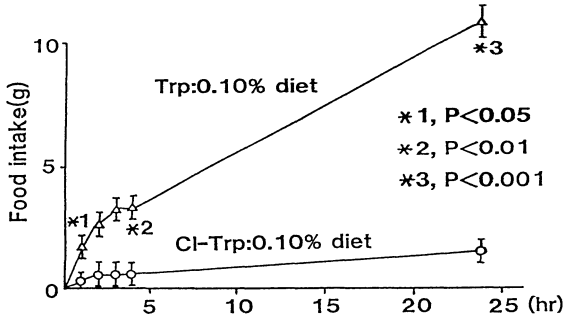

Fig. 3. Food selection of rats for tryptophan diet and chlorotryptophan diet. Rats were offered tryptophan diet (Trp: 0.10%) and chlorotryptophan diets (4-chlorotryptophan: 0.10%) together after overnight fasting and were given choices for these two diets.

tophan diet by flavor, there is possibility to cause rapid physiological changes by chlorotryptophan intake. If the rats were given a choice between two diets after feeding on the chlorotryptophan diet for several days, rats could not discriminate two diets, but total intake for 24 h were small. Thus 4-chlorotryptophan has a strong appetite depressing effect in small amounts.

Experiment 4: Effect of dietary chlorotryptophan on brain serotonin and its metabolite

Tryptophan is a precursor of serotonin and brain serotonin may have a regulatory role for food intake [4], 4-chlorotryptophan may affect the tryptophan and serotonin metabolism. Therefore, brain tryptophan concentration was determined after feeding rats the chlorotryptophan containing diet. The experimental diet contained 0.1% of 4-chlorotryptophan and 0.039% of L-tryptophan, whereas the control diet contained 0.1% of L-tryptophan. Animals were fed the experimental diets for five days and the serotonin and 5-hydroxyindoleacetic acid, a metabolite of serotonin, in the brain were determined. Both serotonin and 5-hydrovyindoleacetic acid concentrations in the brain were not significantly affected by the intake of 4-chlorotryptophan. It may be possible that serotonin contain some amounts of 4-chloroserotonin. This is remained for further study. Metabolism of 4-chlorotryptophan is not clear. 4-Chlorotryptophan may be a possible appetite depressant.

References

1. Marumo S and Hattori H (1970) Planta 90: 208–211.
2. Denkla WD and Dewey HR (1967) J. Lab. Clin. Med. 69: 160–169.
3. Thompson JH, Spezia CA and Agnulo M (1970) Experientia 26: 327–329.
4. Fenton JD and Wurtman RJ (1972) Science 178: 414–416.

Cardiac metabolism and clinical effects of glutamate in controls and patients with coronary artery disease

Anne Thomassen, Torsten T. Nielsen, Jens P. Bagger and Per Henningsen
Department of Cardiology, Skejby Sygehus, DK-8200 Aarhus N, Denmark

Abstract

Myocardial uptake of glutamate was greater in patients with coronary artery disease than in controls. Treatment with nitroglycerin, calcium antagonists or bypass surgery induced a decrease in glutamate utilization. During the early phase of acute myocardial infarction circulating levels of glutamate were low, whereas arterial levels and cardiac uptakes of glutamate rose after propranolol administration. Acute pretreatment with monosodium glutamate increased ischemic threshold during exercise and rapid atrial pacing in patients with angina pectoris. Glutamate had no haemodynamic effects.

Myocardial glutamate uptake was closely related to carbohydrate uptakes in basal fasting state. However, neither a bolus dose of insulin nor infusion of glucose did influence cardiac glutamate utilization despite pronounced increases of the consumptions of both glucose and lactate. Increased myocardial uptake of free fatty acids, induced by heparin, was accompanied by decreased uptakes of glucose, lactate and glutamate in controls but not in patients with ischemic heart disease. Administration of monosodium glutamate rapidly decreased arterial levels of free fatty acids and increased those of glutamate, glucose and insulin but lactate was unchanged. Myocardial uptakes of free fatty acids fell, whereas those of glutamate and glucose but not of lactate increased. The release of alanine rose.

The findings indicate specific adaptations and beneficial effects of myocardial glutamate uptake during ischemia. There is a substrate competition between glutamate and non-carbohydrate substrates. Glutamate stimulates myocardial glucose utilization partly through increased insulin secretion.

Myocardial glutamate uptake

Glutamate is the only naturally occurring amino acid demonstrated to have a positive arterio-venous difference across the human heart [1–3]. Myocardial uptake of glutamate is significantly higher in patients with coronary artery disease than in controls even in resting asymptomatic state (Fig. 1). A high regional myocardial extraction of N-13-glutamate in the areas with reduced blood flow was found by positron emission tomography [4,5]. Moreover, improvement of myocardial blood supply by treatment with nitroglycerin, calcium antagonists [6,7] or bypass surgery (unpublished data) is accompanied by a reduction of cardiac glutamate utilization (Fig. 2). Together, these findings suggest a specific adaptation of myocardial glutamate metabolism induced by chronic or repetitive ischemia.

Myocardial uptake of glutamate rises when arterial glutamate levels are increased both in controls (unpublished data) and in patients with coronary artery disease [8]. The fractional cardiac extraction ranges up to 90% of arterial glutamate

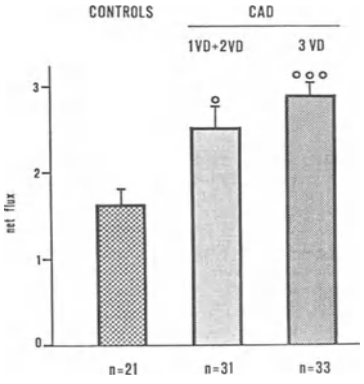

Fig. 1. Myocardial net uptake of glutamate (μmol/min) at resting state in controls and in patients with coronary artery disease of 1, 2 or 3 vessels. measured by aorto and coronary sinus catheterization.

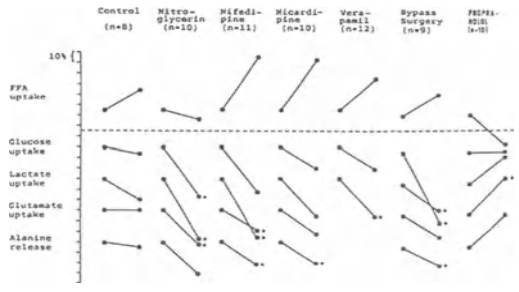

Fig. 2. Percentual changes in myocardial substrate exchanges at resting state in patients with coronary artery disease after acute intervention with antianginal drugs compared to no intervention (control) and before and 3 months after coronary bypass surgery. Measured by aorto and coronary sinus catheterization.

contents in patients with ischemic heart disease [3] suggesting an all most complete extraction and possibly insufficient supply of glutamate to certain areas. Therefore the very low plasma levels of glutamate, demonstrated during the early phase of acute myocardial infarction [9], may be inadequate to cover the requirements of the ischemic heart. On the other hand, the increased supply and cardiac uptake of glutamate seen after propranolol administration (Fig. 2) may be part of the well documented beneficial effects of this drug [8].

Cardioprotective effects of glutamate.

Perfusion with glutamate has been shown to improve the recovery of mechanical function after anoxia and/or ischemia in several animal experimental models [10–14]. To investigate whether administration of glutamate had any cardioprotective actions in man we performed 2 studies (unpublished data). In the 1st study each of 20 patients with stable angina pectoris and positive stress tests underwent 4 upright bicycle exercise tests in fasting state on 4 consecutive days. The 1st and 4th tests were performed without medication while the 2nd and 3rd tests were preceded by a low and high bolus dose of monosodium glutamate either 0.8 and 1.5 mg/kg body weight intravenously (10 patients) or 40 and 80 mg/kg orally (10 patients). Comparison of the 1st and 4th tests revealed good reproducibility of clinical, electrocardiographic and hemodynamic data. As seen in Fig. 3 glutamate pretreatment significantly increased total exercise time, time to and rate-pressure product at onset of ST-segment depression. Maximal ST-depression and the degree of chest pains at exercise stop were uninfluenced by glutamate. In

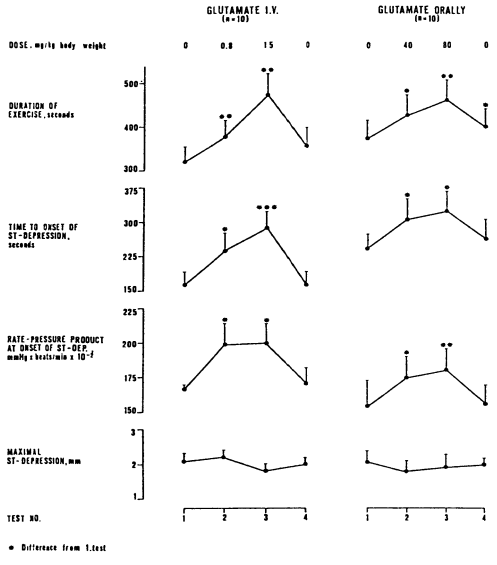

Fig. 3. Effect of monosodium glutamate on exercise tolerance in patients with stable angina pectoris. Intravenous doses were given 4 min before and oral doses 30 min before upright bicycle exercise test in fasting state on consecutive days.

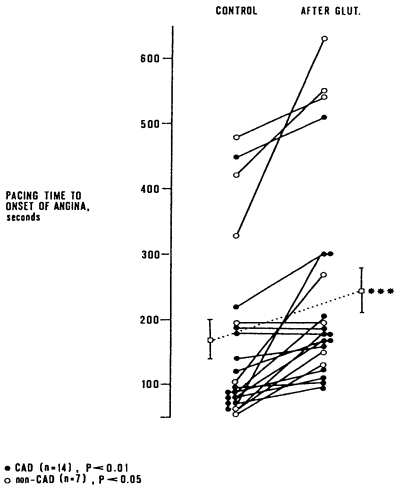

Fig. 4. Time to onset of angina pectoris during rapid atrial pacing before and after monosodium glutamate in patients with stable angina pectoris with or without coronary artery disease.

the second study 21 patients with stress induced chest pains each underwent 2 identical periods of rapid atrial pacing, 150 beats/min, with an interval of 45 min. The 1st pacing period was performed without premedication whereas the 2nd period was preceded by an intravenous bolus injection of either 1.2 or 2.5 mg/kg monosodium glutamate. Pacing time to onset of angina pectoris increased significantly after glutamate both in the patients with coronary artery disease (n=14) by an average of 54 seconds ($P<0.01$) and in those with normal coronary arteries (n=7) by 114 seconds ($P<0.05$) as seen in Fig. 4. In none of the studies did glutamate induce any hemodynamic changes at rest or at comparable workloads. These results suppose that augmented glutamate provision, through a metabolic mechanism, allows the human heart to reach higher levels of energy expenditure before coronary insufficiency develops.

Metabolic effects of glutamate

There are several ways by which glutamate may improve energy production and protect ischemic cardiac cells. Once inside the cell glutamate transaminates with puruvate forming alanine and α-ketoglutarate [15,16], which subsequently serve as fuel for aerobic and anaerobic Krebs cycle activity [16–18]. Energy production

from glutamate breakdown seems ,however to be very small [19]. The earlier demonstrated close relationship between myocardial uptake and release of alanine [2,3] supports the theory that glycolytically produced pyruvate is shunted to alanine instead of lactate, which may diminish the toxic lactate accumulation during ischemia [20]. Moreover glutamate is involved in the malate-aspartate shuttle [21] and may consequently be of importance for the maintenance of the increased myocardial breakdown of carbohydrates [22] observed in patients with coronary artery disease [3] and believed to be the major energy source in hypoxic conditions [20]. Increased glucose oxidation has been reported in isolated myocytes when glutamate is present as the second substrate [23]. We have previously demonstrated a tight relationship between myocardial uptake of glutamate and uptake of glucose and lactate in basal fasting state [3] and the drug-induced changes of myocardial glutamate utilization were accompanied by corresponding alterations of carbohydrate uptake (Fig. 4). However, neither treatment with insulin 2 U intravenously nor infusion with glucose (350 mg/min) influenced myocardial glutamate uptake despite inducing pronounced accelerations of cardiac glucose and lactate utilization rates [24,25]. On the other hand, increased myocardial uptake of free fatty acids induced by heparin 12.500 U intravenously was accompanied by significant reductions of myocardial uptakes of glucose, lactate and glutamate in controls but not in patients with coronary artery disease (unpublished data). The inhibitory effects of free fatty acids on cardiac glutamate utilization probably occurs at the Krebs cycle level as a similar inhibitory effect of acetoacetate has recently been demonstrated in rabbit heart [19]. The lack of a free fatty acid inhibition on cardiac carbohydrate and glutamate uptake in patients with ischemic heart disease may be explained from the altered substrate preference and hampered ß-oxidation in these patients [3]. These results suggest a substrate competition between glutamate and non-carbohydrate substrates in the mitochondria but do not fully explain the cardioprotective effects of exogenous glutamate.

To study the effect of exogenous glutamate on substrate availability and utilization in the human heart, a bolus of 1.2, 2.5 or 5.0 mg/kg body weight of monosodium glutamate was given to 27 patients during cardiac catheterization and metabolic data were obtained at 1,2,4,6,8,10,12,15,20 and 25 min after the injection (unpublished data). Arterial glutamate levels rose by 2.5–5 fold in a dose-related way. Regardless of dose, glutamate administration reduced arterial levels of free fatty acids by 25% ($P<0.001$); lactate by 13% ($p<0.05$) and alanine by 6% ($p<0.05$). Arterial glucose rose by 10% ($p<0.001$) and insulin threefold ($p<0.01$), while that of citrate was unchanged. Myocardial uptake of free fatty acids fell by 25% ($p<0.001$) whereas uptakes of glutamate and glucose rose by 60% ($p<0.001$) and 100% ($p<0.001$) respectively. Myocardial alanine release rose by 50% ($p<0.05$) whereas lactate exchanges were uninfluenced. In conclusion, glutamate administration changes substrate availability and utilization in human heart from free fatty acids towards glutamate and glucose. This effect is at least partly mediated by an increased insulin secretion. However, accumulation of lactate normally seen after

insulin administration [24] does not occur after glutamate probably due to a shunting of pyruvate into alanine production.

Acknowledgement

All our studies on myocardial glutamate metabolism in man were supported by grants from the Danish Heart Foundation and the Danish Medical Research Council.

References

1. Mudge GH, Mills RM, Taegtmeyer H, Gorlin R and Lesch M (1976) Alterations of Myocardial Amino Acid Metabolism in Chronic Ischemic Heart Disease. J. Clin. Invest. 58: 1185–1192.
2. Thomassen AR, Nielsen TT, Bagger JP and Henningsen P (1983) Myocardial Exchanges of Glutamate, Alanine and Citrate in Controls and Patients with Coronary Artery Disease. Clin. Sci. 64: 33–40.
3. Thomassen A, Bagger JP, Nielsen TT and Henningsen P (1988) Altered Global Myocardial Substrate Preference at Rest and During Pacing in Coronary Artery Disease with Stable Angina Pectoris. Am. J. Cardiol. 62: 686–693.
4. Knapp WH, Helus F, Ostertag H, Tillmanns H and Kübler W (1982) Uptake and Turnover of L-13N-glutamate in the Normal Human Heart and in Patients with Coronary Artery Disease. Eur. J. Nucl. Med. 7: 211–215.
5. Zimmermann R, Tillmanns H, Knapp WH, Helus F, Georgi P, Rauch B, Neumann FJ, Girgensohn S, Maier-Borst W and Kübler W (1988) Regional Myocardial Nitrogen-13 Glutamate uptake in Patient with Coronary Artery Disease: Inverse Post-Stress Relation to Thallium-201 Uptake in Ishemia J.A.C.C. 11: 549–556.
6. Thomassen A, Nielsen TT and Bagger JP (1985) Alterations in Myocardial Uptake of Glutamate and Release of Alanine after Propranolol, Nifedipine, and Glyceryl Trinitrate in Coronary Artery Disease. J. Cardiovasc. Pharmacol. 7: 394–400.
7. Thomassen A, Bagger JP, Nielsen TT and Henningsen P (1987) Metabolic, Hemodynamic and Symptomatic Effects of Nicardipine During Pacing-Induced Angina Pectoris. Am. J. Cardiol. 59: 219–224.
8. Nielsen TT, Bagger JP and Thomassen A (1986) Improved Myocardial Lactate Extraction after Propranolol in Coronary Artery Disease: Effected by Peripheral Glutamate and Free Fatty Acid Metabolism. Br. Heart. J. 55: 140–147.
9. Thomassen AR, Mortensen PT, Nielsen TT, Falstie-Jensen N, Thygesen K and Henningsen P (1986) Altered Plasma Concentrations of Glutamate, Alanine and Citrate in the Early Phase of Acute Myocardial Infarction in Man. Eur. Hear. J. 7: 773–778.
10. Rau EE, Shine KI, Gervais A, Douglas AM and Amos EC (1979) Enhanced Mechanical Recovery of Anoxic and Ischemic Myocardium by Amino Acid Perfusion. Am. J. Physiol. 236: H873–H879.
11. Lazar HL, Buckberg CD, Manganaro AM and Becker H (1980) Myocardial Energy Replenishment and Reversal of Ischemic Damage by Substrate Enhancement of Secondary Blood Cardioplegia with Amino Acids During Reperfusion. J. Thorac. Cardiovasc. Surg. 80: 350–359.
12. Bittl JA and Shine KI (1983) Protection of Ischemic Rabbit Myocardium by Glutamic Acid. Am. J. Physiol. 245: H406–H412.
13. Pisarenko OI, Solomatina ES, Studneva IM, Ivanov VE, Kapelko VI and Smirnov (1983) Protective Effect of Glutamic Acid on Cardiac Function and Metabolism During Cardioplegia and Reperfusion. Basic Res. Cardiol. 78: 534–543.

14. Rosenkranz ER, Okamoto F, Buckberg GD, Vinten-Johansen J, Robertson JM and Buggi H (1984) Safety of Prolonged Aortic Clamping with Blood Cardioplegia. Glutamate Enrichment in Energy-Depleted Hearts. J. Thorac. Cardiovasc. Surg. 88: 402–410.
15. Taegtmeyer H, Peterson MB, Ragavan VV, Ferguson AG and Lesch M (1977) De Novo Alanin Synthesis in Isolated Oxygen-Deprived Rabbit Myocardium. J. Biol. Chem. 252: 5010–5018.
16. Peuhkurinen KJ, Takala TES, Nuntinen EM and Hassinen IE (1983) Tricarboxylic Acid Cycle Metabolites During Ischemia in Isolated Perfused Rat Heart. Am. J. Physiol. 70 (Suppl. 1): 165–174.
17. Safer B and Williamson JR (1973) Mitochondrial-Cytosolic Interactions in Perfused Rat Heart. Role of Coupled Transamination in Repletion of Citric Acid Intermediates. J. Biol. Chem. 248: 2570–2579.
18. Sanborn T, Gavin W, Berkowitz S, Perille T and Lesch M (1979) Augmented Conversion of Aspartate and Glutamate to Succinate During Anoxia in Rabbit Heart. Am. J. Physiol. 237: H535–H541.
19. Taegtmeyer H and Russell RR (1987) Glutamate Metabolism in Rabbit Heart: Augmentation by Ischemia and Inhibition with Acetoacetate. J. Appl. Cardiol. 2: 231–249.
20. Neely JR and Morgan HE (1974) Relationship Between Carbohydrate and Lipid Metabolism and the Energy Balance of the Heart Muscle. Annu. Rev. Physiol. 36: 413–459.
21. Digerness SB and Reddy WJ (1976) The Malate-Aspartate Shuttle in Heart Mitochondria. J. Mol. Cell Cardiol. 8: 779–785.
22. Kobayashi K and Neely JR (1979) Control of Maximum Rates of Glycolysis in Rat Cardiac Muscle Circ. Res. 44: 166–175.
23. Burns AH and Reddy WJ (1978) Amino Acid Stimulation of Oxygen and Substrate Utilization by Cardiac Myocytes. Am. J. Physiol. 235: E461–E466.
24. Thomassen A, Nielsen TT, Bagger JP and Henningsen P (1989) Cardiac Metabolic and Hemodynamic Effects of Insulin in Controls and Patients with Coronary Artery Disease. Diabetes 38: 1175–1180.
25. Thomassen A, Nielsen TT, Bagger JP and Henningsen P (1989) Antianginal and Cardiac Metabolic Effects of Low Dose Glucose Infusion During Pacing in Patients with and without Coronary Artery Disease. Am. Heart. J. 118: 25–32.

Address for correspondence: Dr. Anne Thomassen, Department of Cardiology, Skejby Sygehus, DK-8200 Aarhus N, Denmark.

Changes in glutathione and cysteine levels after 2-oxothiazolidine-4-carboxylate administration in guinea pig tissues

Toshihiko Ubuka[a], Jun Ohta[a], Reiko Akagi[b], Hideo Nishina[a], Shigeko Yoshida[b] and Tazuko Taguchi[c]

[a]Department of Biochemistry, Okayama University Medical School, Okayama 700, Japan
[b]Faculty of Food and Nutrition, Okayama Prefectural Junior College, Okayama 700, Japan
[c]Faculty of Junior College, Mimasaka Women's University, Tsuyama 708, Japan

Abstract

Guinea pig liver and kidney contained 7.97 ± 0.51 and 2.87 ± 0.42 μmol/g wet weight of glutathione, respectively. These tissues contained 0.45 ± 0.05 and 0.69 ± 0.11 μmol/g tissue of free cysteine. We made an attempt to increase glutathione and cysteine levels in guinea pig tissues by administration of L-2-oxothiazolidine-4-carboxylic acid (OTCA), a derivative of L-cysteine. The intraperitoneal injection of 5 mmol of OTCA/kg of body weight produced the increase in liver glutathione level by 23% and 26% at one and two h after the administration, respectively. In the kidney, on the contrary, OTCA administration resulted in about 30% decrease in the glutathione level. A tendency of increase in cysteine level was observed in the kidney and brain, but not in the liver, after OTCA administration. The results show that OTCA has potential to increase liver glutathione level and glutathione may serve as the reservoir of cysteine in the liver.

Introduction

Glutathione is the most ubiquitous and abundant SH compound in animal tissues [1]. It has been proposed that one of the functions of glutathione is the reservoir of cysteine [2]. Williamson and Meister reported that 2-oxothiazolidine-4-carboxylic acid (OTCA) was cleaved by 5-oxoprolinase to produce S-carboxycysteine, which decarboxylated to cysteine, and that administration of OTCA into mice increased hepatic glutathione level [3]. During the course of our study on the transamination pathway of cysteine metabolism [4], it was suggested that cysteine metabolism in the guinea pig was somewhat different from that in the rat [5]. The present study was undertaken to examine the effect of OTCA administration [6] on glutathione and cysteine levels in guinea pig tissues.

Experimental procedures

Animals

Male guinea pigs of Hartley strain weighing 550–770 g were maintained on a laboratory diet, RC4, of Oriental Yeast Co., Tokyo, Japan.

Administration of OTCA and amino acid analysis

OTCA was obtained from Chemical Dynamics Corp., South Plainfield, NJ, USA. One molar solution of OTCA was neutralized with NaOH and intraperitoneally injected to guinea pigs at a dose of 5 mmol/kg of body weight. At the time indicated below, tissues were taken out, washed with cold saline, blotted and frozen in liquid nitrogen. Frozen tissues were homogenized with 3 volumes of 4% sulfosalicylic acid by a glass homogenizer, and the homogenates were centrifuged at 1,200 × *g* for 20 min. Glutathione and amino acids in the resulting supernatant were analyzed with a Hitachi KLA-5 amino acid analyzer [7]. Cysteine was determined with acidic ninhydrin reaction [8]. Statistical significance was evaluated by Student's *t* test.

Results

Contents of glutathione and sulfur-containing amino acids in guinea pig tissues

Table 1 summarizes the contents of glutathione, cysteine, and some sulfur-containing amino acids. Average glutathione contents in the liver and kidney were 7.97 and 2.87 μmol/g of wet weight, respectively. Oxidized glutathione was not detected. Guinea pig tissues contained considerable amounts of cysteine. On average, liver and kidney contained 0.45 ± 0.05 and 0.69 ± 0.11 μmol/g of cysteine, respectively. Heart, brain and blood also contained appreciable concentrations of cysteine.

In the present study, cysteine was determined with acidic ninhydrin reagent 2 [8] after dithiothreitol treatment of the tissue extracts. Therefore, the possibilities whether cysteine might be present as cystine or as mixed disulfides with gluta-

Table 1. Contents of glutathione, cysteine and related compounds in guinea pig tissues

	Concentrations (μmol/g or ml)				
Tissue	Glutathione	Cysteine	HCETC[a]	Taurine	Methionine
Liver	7.97 ± 0.51 (6)	0.45 ± 0.05 (5)	tr-0.29	0.78 ± 0.25 (6)	0.10 ± 0.03 (6)
Kidney	2.87 ± 0.42 (6)	0.69 ± 0.11 (5)	tr	6.81 ± 0.94 (6)	0.07 ± 0.03 (6)
Heart	1.90 ± 0.25 (4)	0.11 ± 0.02 (5)	–	21.70 ± 1.44 (4)	tr
Brain	1.45 ± 0.12 (4)	0.12 ± 0.01 (5)	–	2.66 ± 0.46 (4)	0.03 ± 0.01 (4)
Blood		0.14 ± 0.02 (5)	–	–	
Plasma		0.21 ± 0.03 (4)	–	–	
Erythr		0.06 ± 0.01 (4)	–	–	

Tissues taken were frozen in liquid nitrogen and homogenized with 3% sulfosalicylic acid. Glutathione and amino acids were determined with an amino acid analyzer. Cysteine was determined with acidic ninhydrin reaction. Results are expressed as mean ± SD. Numbers of animals are shown in parentheses. [a]Range is shown. tr: Trace amount.

Table 2. Glutathione, cysteine and taurine concentrations in guinea pig tissues after the intraperitoneal administration of L-2-oxothiazolidine-4-carboxylic acid

Tissue	Hours after the administration				
	0	1	2	3	4
	Glutathione (μmol/g wet weight, mean ± SD, n=4)				
Liver	8.18 ± 0.13	10.08 ± 0.80[a]	10.32 ± 1.23	9.71 ± 1.16[a]	9.07 ± 0.77
Kidney	2.32 ± 0.37	1.67 ± 0.25[a]	1.61 ± 0.45	1.56 ± 0.43[a]	1.55 ± 0.30[b]
Brain	1.11 ± 0.13	1.00 ± 0.14	0.99 ± 0.11	1.25 ± 0.26	1.25 ± 0.11
	Cysteine (μmol/g wet weight, mean ± SD, n=2)				
Liver	0.85 ± 0.17	0.85 ± 0.04	0.74 ± 0.01	0.74 ± 0.14	0.70 ± 0.23
Kidney	1.06	1.60 ± 0.26	1.63 ± 0.09	1.66 ± 0.62	1.47 ± 0.18
Brain	0.11 ± 0.02	0.15 ± 0.01	0.15 ± 0.05	0.17 ± 0.05	0.26 ± 0.02
	Taurine (μmol/g wet weight, mean ± SD, n=4)				
Liver	0.65 ± 0.15	0.59 ± 0.17	1.47 ± 0.60[a]	0.90 ± 0.20	1.26 ± 0.46
Kidney	4.30 ± 0.58	3.63 ± 0.59	3.85 ± 0.71	3.60 ± 0.67	3.69 ± 0.88
Brain	1.69 ± 0.15	1.41 ± 0.20	1.69 ± 0.14	1.83 ± 0.99	1.56 ± 0.18

Five mmol of L-2-oxothiazolidine-4-carboxylic acid/kg of weight was intraperitoneally injected to guinea pigs. At the time indicated, glutathione and taurine contents were determined with an amino acid analyzer, and cysteine with acidic ninhydrin reaction. Significantly different from the control (time 0): [a]$p<0.05$; [b]$p<0.025$.

thione or other thiol compounds were examined. The results of amino acid analysis with an amino acid analyzer revealed that cystine contents in tissue extracts were only trace amounts, and that liver and kidney extracts contained only trace amounts of two mixed disulfides: 3-mercaptolactate-cysteine mixed disulfide [S-(2-hydroxy-2-carboxyethylthio)cysteine] [9] and cysteine glutathione mixed disulfide [10,11]. Therefore, it was concluded that cysteine was present mostly in the free state in the guinea pig tissues.

Average taurine concentrations in the liver, kidney and heart were 0.78, 6.81 and 21.70 μmol/g wet weight, respectively. These values mean that the taurine content in the guinea pig liver is very low compared to those in kidney and heart. In general, taurine concentrations in guinea pig tissues are low compared to those in the rat tissues [12,13].

Changes of glutathione and cysteine concentrations in guinea pig liver and kidney after OTCA administration

Table 2 shows changes of glutathione concentrations in liver, kidney and brain after the intraperitoneal injection of 5 mmol of OTCA/kg of body weight. In the liver, glutathione level increased significantly by 23% and 26% at 1 and 2 h

after the administration, respectively. On the contrary, the kidney glutathione level decreased significantly by 28% one h after the OTCA administration, and this low value continued at least for 3 h. Glutathione contents in the brain did not significantly change by OTCA administration.

As shown in Tables 1 and 2, guinea pig tissues contained considerable amounts of cysteine. Table 2 shows the effect of OTCA administration on the tissue cysteine levels. Basic cysteine levels differed widely among guinea pigs used in the experiment shown in Table 2. Some guinea pigs exhibited unusually high values. Therefore, these values are not included in this table. In general, cysteine concentrations in the liver after OTCA administration fluctuated with no definite tendency, but those in the kidney exhibited a tendency to increase. Cysteine levels in the whole brain also tended to increase.

OTCA administration produced a significant increase in taurine concentration in the liver at 2 h after the injection. The values at 3 and 4 h after the administration were higher than those of the controls, but the differences were not statistically significant. Taurine concentrations in the kidney and brain exhibited no significant change.

Discussion

OTCA is a derivative of L-cysteine and is cleaved by 5-oxoprolinase. The product, S-carboxycysteine, decarboxylates non-enzymatically, and cysteine is produced [3]. When OTCA was intraperitoneally administered to mice that had been depleted of hepatic glutathione, the normal glutathione level was restored rapidly [3].

The present study shows that OTCA is a useful agent that increases the glutathione level in the guinea pig liver.

L-Cysteine may be metabolized through oxidation pathway (cysteinesulfinate pathway) and non-oxidation pathway (desulfuration pathway) [4]. Many studies, performed mostly in rats, show that L-cysteine is metabolized mainly through the oxidation pathway [14]. As shown in Table 1, the level of taurine, one of the main end products of the oxidation pathway, in the guinea pig liver is much lower than that in the rat liver [13]. Moreover, the cysteine levels were considerably high in guinea pig tissues (Table 1). These facts may suggest that oxidation pathway in the guinea pig liver is not as active as that in the rat liver.

We reported that guinea pig tissues exhibited very low activities of 3-mercaptopyruvate sulfurtransferase (EC. 2.8.1.2) [5]. This enzyme is a member of the transamination pathway of cysteine metabolism [4], which is one of the desulfuration pathways. The low activity of 3-mercaptopyruvate sulfurtransferase suggests that the activity of the transamination pathway is also low in the guinea pig liver.

These observations seem to suggest that cysteine metabolism in the guinea pig liver is not as active as that in the rat liver.

In the present study, OTCA administration increased the glutathione level in the guinea pig liver, but the cysteine level did not increase. This seems to agree with the proposal that glutathione functions as the reservoir of cysteine [2].

In the kidney, OTCA administration resulted in the decrease in the glutathione level and the increase in the cysteine level. The mechanism is not known at present, but it might be suggested that glutathione turnover in the kidney is accelerated by OTCA administration.

Acknowledgements

This work was supported in part by a Grant-in-Aid for Scientific Research from the Ministry of Education, Science and Culture of Japan and in part by a Grant-in-Aid for Medical Research from the Ministry of Health and Welfare of Japan.

References

1. Kosower NS and Kosower EM (1978) Intern. Rev. Cyt. 54: 109–160.
2. Higashi T, Tateishi N, Naruse A and Sakamoto Y (1977) J. Biochem. 82: 117–124.
3. Williamson JM and Meister A (1981) Proc. Natl. Acad. Sci. U.S.A. 78: 936–939.
4. Ubuka T, Ohta J, Akagi R, Hosaki Y, Ishimoto Y, Kiguchi S, Ikeda T and Ishino K, unpublished results.
5. Ubuka T, Hosaki Y, Nishina H and Ikeda T (1987) Physiol. Chem. Phys. Med. NMR. 19: 41–43.
6. Nishina H, Ohta J and Ubuka T (1987) Physiol. Chem. Phys. Med. NMR. 19: 9–13.
7. Hosaki Y, Nishina H and Ubuka T (1985) Acta Med. Okayama 39: 425–429.
8. Gaitonde MK (1967) Biochem. J. 104: 627–633.
9. Ubuka T, Kobayashi K, Yao K, Kodama H, Fujii K, Hirayama K, Kuwaki T and Mizuhara S (1968) Biochim. Biophys. Acta 158: 493–495.
10. Neish WJP and Rylett A (1963) Biochem. Pharmacol. 12: 913–918.
11. Ubuka T, Hosaki Y, Reiko A, Yoshida S and Taguchi T (1983) Ganryuaminosann (Sulfur Amino Acids) 6: 109–112 (in Japanese).
12. Jacobsen JG and Smith LH Jr (1968) Physiol. Rev. 48: 424–511.
13. Hays KC and Sturman JA (1981) Ann. Rev. Nutr. 1: 401–425.
14. Jocelyn PC (1972) Biochemistry of the SH Group. Academic Press, London, pp. 170–172.

Estimation of maternal fetal amino acid transport and alanine production in the fetus, with stable tracer L-[^{15}N]alanine and L-[^{15}N]valine

Aviva Lapidot, Towuanse S. Emudianughe and Bella Kalderon

Department of Isotope Research, Weizmann Institute of Science, 76 100 Rehovot, Israel

Abstract

A mixture of ^{15}N-labeled L-alanine and L-valine was infused at a constant rate into five rabbits with gestational age of 29–30 days. Steady state was achieved after 2 h of a prime dose-constant infusion. Maternal blood samples were taken during 3 h simultaneously with umbilical venous followed by arterial blood between 2–3 h. The ^{15}N enrichment of the umbilical vein alanine was 69% lower than simultaneously obtained form maternal vein. A further decrease of 42% in the umbilical arterial samples compared to umbilical venous plasma was determined. While valine ^{15}N enrichment showed umbilical venous blood 55% less than that of the maternal blood, no significant difference was found between umbilical venous and arterial plasma, although alanine and valine concentration in umbilical venous and arterial plasma were similar. A possible mechanism of alanine production in the fetus in utero is suggested.

Introduction

Fetal amino acid uptake seems to be unrelated to the concentration of amino acids in maternal blood [1]. The flux of amino acids across the placenta is poorly understood, but it is known that the placenta concentrates amino acids intracellularly and actively transports them to the fetus [1].

Restrictions in the use of radioactive tracers in healthy humans have prompted us to develop a convenient non-invasive stable isotope and gas-chromatography-mass spectrometry technique to determine the nitrogen-15 enrichment of plasma amino acids [2]. By the use of this method the rate of uptake of amino acids and the whole body pool of extracellular amino acids can be measured. This technique was applied to several human studies [3–5] including infants during the neonatal period. Recently dynamic aspects of glycine metabolism was measured in normotensive pregnant women and in hypertensive women with impaired fetal growth [6].

Alanine production in the human fetus in utero was recently reported by administration of ^{13}C-alanine to pregnant women [7]. The present study was designed to investigate alanine synthesis in the rabbit fetus in utero under isotopic steady state condition both at the maternal and fetus compartments. By using a mixture of ^{15}N labeled alanine and valine the sources of alanine and valine for the fetus at term gestation were examined.

Materials and Methods

[^{15}N]-alanine-[^{15}N]-valine mixture was synthesized from $(^{15}NH_4)_2SO_4$ (98% ^{15}N-enriched) as previously described [8] for microbial production of ^{15}N-glutamatic acid with some modification.

Animals and procedures

New Zealand albino rabbits with gestational age of 29–30 days (weighing 4–4.75 kg) were used in all experiments. The marginal veins in each ear were cannulated to allow tracer infusion through one ear vein while the other was used for repeated blood sample collection. A prime dose was administered followed by infusion of a mixture of [^{15}N]-alanine and [^{15}N]-valine at a rate of 30 μg/kg/min and 7.5 μg/kg/min respectively. The prime dose was 25% of the total infusion mixture. The tracers were dissolved in isotonic sterile saline and infused at a rate of 16 ml/h for a 3 h period. After 2 h of infusion the animals were anesthetized followed by abdominal section to expose utero. The utero was opened at the mid-line to allow the exposure of one fetus at a time. Maternal blood samples were taken at 0, 1, 2, 2.5 and 3 h, while umbilical venous samples followed by arterial blood samples were taken at 2, 2.5 and 3 h time points. A fetus was used for each of the time points and fetuses were taken with the placenta still intact.

Analytical procedures

Protein free plasma alanine and valine concentration and isotopic enrichments were determined by amino acid analyzer and by GC-MS, respectively, as previously described [4–7].

GC-MS measurements were performed on a Finnigan 4500 quadrupole GC-MS interfaced to an INCOS data system as previously described [9]. Measurements of isotopic abundance were made using computer controlled selected ion monitoring (SIM). The fragments m/z 140–141 and 168–169 of alanine and valine respectively, were analyzed using the EI mode. Statistical analyses were carried out using either the Student t test or the Anova one way analysis.

Results

Concentrations of alanine and valine in maternal and umbilical venous and arterial blood are presented in Table 1. Over the experimental period there were no significant changes in alanine concentrations (mean ± SD) within the sampling intervals in maternal, umbilical venous and arterial blood samples. Similar results were obtained for valine, suggesting that both amino acid concentrations were in steady state.

Table 1. Concentration of alanine and valine in maternal and fetal blood during 3 h of continuous infusion of alanine and valine mixtures

Time	0.0	2.0	2.5	3.0
Alanine				
(nmol/ml)	561.96±112.56	518.96±118.68[ab]	636.10±15.10[ab]	638.14±114.24[ab]
MV	(430.30–665.60)	(404.40–651.20)	(621.00–651.20)	(510.60–808.20)
UV	ND	1164.60±191.73[a]	1373.63±303.33[a]	1631.67±70.21[a]
		(998.30–1374.60)	(1150.90–1719.10)	(1550.90–1678.10)
UA	ND	1169.13±253.33[b]	1194.97±169.91[b]	1654±81.23[b]
		(911.30–1417.70)	(1045.20–1379.60)	(1563.20–1719.10)
Valine				
(nmol/ml)	284.73±67.32	288.53±31.24	337.87±11.87	320.93±26.21
MV	(229.20–359.60)	(270.00–324.60)	(325.30–348.90)	(300.20–350.40)
UV	ND	363.00±110.56	374.63±114.05	454.77±65.01
		(251.10–472.20)	(262.50–490.50)	(399.50–526)
UA	ND	321.60±90.75	352.56±109.00	421.5±46.60
		(231.30–412.50)	(352.20–461.60)	(369.2–458.60)

Results are means ± SD of at least 3 animals with ranges in parenthesis. MV = maternal venous blood; UV = umbilical venous blood; UA = umbilical arterial blood [a,b]$P \leq 0.001$ comparison of MV vs UV, MV vs UA.

Alanine concentration in the umbilical venous blood was significantly higher as compared with the simultaneously sampled maternal peripheral venous blood after 2 h of infusion (0.518 mM and 1.164 mM respectively). The increase of ≈2 fold alanine concentration in the U.V. compartment remained constant during the experimental period, while no significant changes could be found between alanine concentrations in the umbilical venous and umbilical arterial blood (Table 1). Valine concentration in the umbilical venous blood was slightly higher when compared with the simultaneously sampled maternal peripheral blood (0.363 mM and 0.288 mM respectively, after 2 h of infusion). No significant changes of valine concentrations were observed between simultaneous samples taken from the umbilical venous and arterial blood. The mean values of alanine and valine concentrations in the three compartments after 150 min infusion is depicted in Fig. 1.

Isotopic steady state was achieved in all compartments after 2 h of ^{15}N alanine and valine infusion and was maintained throughout the study. The ^{15}N enrichments of alanine and valine were compared in the maternal and umbilical blood during isotopic steady state in the maternal and fetal compartments (Table 2).

The ^{15}N enrichment of alanine in the umbilical venous (4.5% average sampling times of 2.0, 2.5 and 3.0 h) was 68.9 ± 2.4% lower than that simultaneously obtained from the maternal vein (14.49 ± 0.49%). The ^{15}N enrichment of alanine was further decreased by 42.01 ± 4.7% in the umbilical arterial samples (2.57 ±

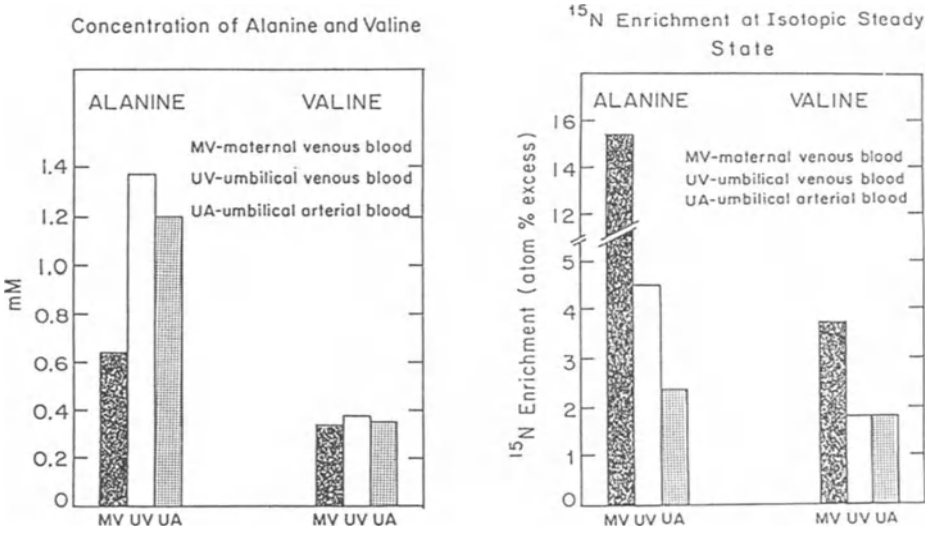

Fig. 1, 2. Alanine and valine concentration and ^{15}N enrichment in maternal and fetal plasma taken after 150 min of amino acids infusion. Five animals were studied, maternal venous plasma compared to umbilical venous and arterial plasma.

0.11%) as compared with umbilical venous blood samples. The ^{15}N enrichment of valine in the umbilical venous blood (1.7%, average sampling time of 2.0, 2.5 and 3.0 h) was 54.8 ± 6.3% lower than that of the maternal blood samples. However, only a slight decline in the ^{15}N enrichment of ^{15}N valine was detected in the umbilical arterial samples in comparison to that of the umbilical venous blood (≈4.5%).

Our results reveal a significant difference of alanine and valine dilution between the maternal venous and umbilical venous compartments, but only significant dilution of alanine was detected between the umbilical venous and arterial blood, indicating that alanine, but not valine, is endogenously produced by the fetus in utero.

Discussion

Amino acids are actively transported from the mother to the fetus across the placenta, providing exogenous source to the fetus [1]. It was also suggested that a significant amount of amino acids taken up by the sheep fetus is oxidized [10]. It was found that 42% of alanine flux in the human fetus is derived from endogenous sources [7]. With respect to amino acid concentration in maternal and umbilical blood, our results are in agreement with previous finding in fetal lamb [11] and in human [8], showing that the amino acid concentration, especially the neutral amino

Table 2. The enrichment of [^{15}N]alanine and [^{15}N]valine of maternal and fetal plasma

Time	2	2.5	3.0
Alanine (atom % excess)			
MV	13.91 ± 4.56 (10.98 – 19.16)	15.48 ± 5.81 (11.38 – 19.59)	14.09 ± 4.86 (11.09 – 19.69)
UV	4.24 ± 1.51 (3.50 – 5.98)	4.48 ± 0.084 (4.43 – 4.53)	4.75 ± 0.80 (3.95 – 5.56)
UA	2.62 ± 1.09 (1.87 – 3.86)[a]	2.35 ± 0.63 (1.90 – 2.79)[a]	2.74 ± 0.92 (2.01 – 3.78)[a]
$\frac{\text{UV-VA}}{\text{UV}}$ %	38.2	47.52	42.13
Valine			
MV	3.67 ± 0.68 (3.02 – 4.38)	3.66 ± 0.56 (3.12 – 4.25)	3.82 ± 0.49 (3.37 – 4.35)
UV	1.40 ± 0.07 (1.32 – 1.46)	1.84 ± 0.029 (1.81 – 1.86)	1.80 ± 0.08 (1.72 – 1.86)
UA	1.26 ± 0.15 (1.10 – 1.39)	1.84 ± 0.12 (1.77 – 1.99)	1.74 ± 0.39 (1.70 – 1.78)
$\frac{\text{UV-VA}}{\text{UV}}$ %	10	0	3

Results are mean ± SD of at least 3 animals with ranges in parenthesis after 5 h period of infusion of the amino acid mixtures. [a]$P<0.05$ comparison of UV vs UA; MV = maternal venous blood; UV = umbilical venous blood; UA = umbilical arterial blood.

acids are higher in the fetus than in the maternal blood. These data are consistent with the known active transport systems for alanine and valine in the placenta [1]. But changes in concentration in the maternal and fetal blood cannot provide data for amino acid production. This can be achieved only by isotopic techniques such as presented in the present study. From the different isotopic enrichments of ^{15}N alanine and ^{15}N valine in the maternal venous blood and umbilical venous blood the extent of alanine and valine dilution in the placenta was estimated. Alanine and valine were 3.2 and 2 fold diluted respectively across the placenta. This is the result of high turnover of proteins in the placenta.

The ^{15}N enrichment and concentration of alanine and valine remained constant (SD ± 10%) throughout the experimental period when fetuses were removed during the second and the third hours of amino acids infusion. Thus, the 42% lower ^{15}N enrichment of alanine in the umbilical arterial blood as compared with the umbilical vein, indicates endogenous production of alanine by the rabbit fetus in utero. In contrast to alanine, only a limited isotopic dilution (≈4%) of valine was

detected across umbilical circulation. These results indicate that the source for alanine endogenous production in the rabbit fetus is not from a release of free alanine derived from protein catabolism, since this would lead to a limited dilution of alanine similar to that of valine. Instead, our data revealed a preferable dilution of alanine in comparison to valine. The source of alanine production in the fetus is probably due to nitrogen transfer from catabolized amino acids to pyruvate by transamination. The hypothesis that amino acids are extensively catabolized in the fetal life was recently further supported by the observation of high rate of urea production in the fetal lamb [10]. Similar dilution of the labeled alanine across the umbilical circulation were obtained by the use of ^{13}C alanine in the human fetus at term gestation [7] and ^{15}N alanine in the rabbit fetus at term gestation in the present study. Our results further support the proposal that alanine is produced in the fetus to transfer nitrogen for urea synthesis in the liver.

Acknowledgements

We are grateful to Dr. Nava Nevo for technical assistance and to Dr. A. Gopher and M. Dorsman for the synthesis of the [^{15}N] L-alanine and [^{15}N] valine. T.S.E. is a recipient of Sir Charles Clore fellowship.

This work was partly supported by a grant from the Ministry of Science and Development of the National Council for Research and Development to A.L.

References

1. Yudilevich DL and Sveiry JH (1985) Biochem. Biophys. Acta 822: 169.
2. Nissim I and Lapidot A (1979) Am. J. Physiol. 6: E418.
3. Lapidot A and Nissim I (1980) Metabolism 29: 230.
4. Amir J, Reisner SH and Lapidot A (1980) Pediat. Res. 14: 1238.
5. Lapidot A, Nissim I, Sahklai M, Samuel R and Liberman U (1984) Clin. Sci. 66: 147.
6. Lapidot A, Hod M, Amir J et al. (1990) Hypertension (in press).
7. Gilfillian CA, Tserng K-Y and Kalhan SC (1985) Biol. Neonate. 47: 141.
8. Kahana Z and Lapidot A (1983) Anal. Biochem. 132: 160.
9. Kalderon B, Korman SA, Gutman A and Lapidot A (1989) Am. J. Phys. 257: E346.
10. Battaglia FC (1984) Am. J. Obstet. Gynecol. 148: 850.
11. van Veen LCP, Teng C, Hay Jr WW, Meschia G and Battaglia FC (1987) Metabolism 36: 48.

The evaluation of melatonin as a possible anti-stress hormone

R. Khan[a], S. Morley[a], S. Daya[b] and B. Potgieter[a]

[a]*School of Pharmaceutical Sciences, Rhodes University, Grahamstown, 6140, South Africa*
[b]*Department of Biochemistry, Rhodes University, Grahamstown, 6140, South Africa*

Abstract

Various stressful stimuli alter pineal melatonin production. It has recently been shown that melatonin counteracts the effects of acute stress on thymus weight via an opiatergic mechanism. A preliminary study done in our laboratory indicated that melatonin inhibited the effects of stress on the incidence of gastric ulceration. At the doses used in this preliminary study, the inhibitory effect of melatonin was not dose-dependent. This study was undertaken to evaluate a role for melatonin as a possible anti-stress hormone, and to examine if melatonin's inhibitory action on gastric stress ulceration is exerted via an opiatergic mechanism. We have found that at night, when the endogenous level of melatonin is high in rats, exposure to stressful stimuli results in a lower incidence of gastric ulceration than during the day. We have also found that small doses of melatonin inhibited gastric stress ulceration in a dose dependent manner. Administration of opiates, opiate antagonists and melatonin prior to the induction of stress yielded the following results: naloxone exacerbated stress lesion production in a dose dependent manner, and this effect was not antagonized by melatonin. Morphine also showed a dose dependent inhibition of lesion production. At the doses used in this study, melatonin does not appear to be acting via an opiatergic mechanism. The results of these studies suggest a role for melatonin in stress.

Introduction

Man is constantly exposed to stressful events that can cause biochemical and physiological changes that affect his homeostasis. Selye has defined stress as being "the nonspecific response of the body to any demand made upon it" [1]. This demand, created by the stressor on the body, initiates adaptive functions for readjustment, and for the re-establishment of normalcy.

The pineal gland secretes a hormone, melatonin, first identified in 1965 by Lerner and co-workers [2]. It has since been implicated in the functional activities of many organs, eg. the brain, adrenal glands, gonads, thyroid glands and smooth muscle [3].

Many studies have shown that stressful stimuli alter melatonin production [4–6]. Exposure of rats to restraint immobilization results in a fourfold increase in pineal melatonin production, indicating an activation of the melatonin biosynthetic pathway [4]. Miline has proposed that melatonin exerts an inhibitory influence on the adrenal-hypothalamo-pituitary axis, [7] while Romijn in his review suggested that the pineal gland acts as a tranquilizing organ [8].

Recently, Maestroni *et al.* reported that the administration of melatonin to rats could counter the effects of acute stress on thymus weight, and that this effect was mediated via an opiatergic mechanism [9]. We examined the effects of melatonin on the production of gastric stress lesions in rats, and found that melatonin clearly inhibits the formation of stress ulcers [10].

In 1977, Guilleman *et al.* showed that, in rats, ß-endorphin and ACTH are secreted simultaneously by the pituitary gland in conditions of acute stress [11]. This stirred much interest as to the role of the endorphins in stress. Many studies have since examined the role of the opiates and opiate antagonists in gastric stress pathology, [13–14] and contradiction exists as to their exact function.

This study was thus undertaken to examine a possible role for melatonin as an anti-stress hormone, and to investigate whether melatonin was acting via an opiatergic mechanism.

One of the peripheral changes indicative of stress is gastric ulceration [15]. Pare and Glavin [16] reviewed various restraining techniques extensively, and found that, alter starving rats for 12–24 h, prone restraint on a board, coupled with exposure to cold (4–7°C) for 3 h, resulted in a 100% incidence of gastric stress ulceration. This was in accordance with the findings of Senay and Levine, who concluded that the combination of stressors (cold and restraint) acted synergistically to rapidly produce gastric ulceration in starved rats [17].

This method of inducing stress was thus adopted, and further modified to reduce the exposure to stressful stimuli to only 2 h.

Materials and Methods

Animals

Inbred female rats of the Wistar strain housed five per cage and maintained in an automatically regulated lighting cycle of LD 12:12 were used in all studies. They were allowed access to a standard diet and water *ad libitum* prior to experimentation.

Drugs

Melatonin (Sigma) was dissolved in a vehicle containing 2% benzyl alcohol, 10% polysorbate 80, and 0.025% w/v citric acid, and made up to volume with distilled water.

Morphine SO4 (Labebethica) and Naloxone HCl (Sigma) were dissolved in sterile normal saline.

The required solutions and control vehicles were freshly prepared on the day of experimentation.

Stress

Rats were deprived of food for 24 h prior to restraint, but were allowed access to water *ad libitum*. They were then lightly anaesthetized with ether, injected with treatment drugs or control vehicles (see experiments) and restrained in the supine position on a wooden board, using adhesive tape. By this time the rats had already recovered from the ether anaesthesia. They were immediately transported to a cold room (4–6°C) where they remained for the duration of the stress procedure. During the daytime studies, the light intensity in the cold room was 600 lux, sufficient to inhibit endogenous melatonin synthesis. Two hours later, rats were removed from the cold room and sacrificed by neck fracture. Stomachs were rapidly dissected, cut along the greater curvature, rinsed in distilled water, and quickly pinned onto polystyrene boards. They were then examined for gastric lesions by an observer naive of treatment conditions. Total length of ulceration in mm to the nearest 0,1 mm was measured.

A previously described method, noting area of ulceration as a percentage of total stomach area, was used as an additional validation of results [10].

Experiments

1. The effect of small doses of melatonin on gastric stress ulcer formation

Melatonin was administered in doses of 100 μg, 250 μg, and 500 μg per kg body weight i.p. Control rats were treated with vehicle only.

2. The endogenous day/night response to stress

At night, endogenous melatonin levels are high [18]. Rats were injected with melatonin vehicle only, 3 h after lights off. They were then exposed to stress while being kept in the dark, and handled using a photosafe dim red light source. The results obtained were compared to light phase controls.

3. Effect of various doses of morphine on gastric stress ulceration

Rats were injected with vehicle or morphine (1 mg, 55 mg or 10 mg) per kg body weight i.p.

4. Effect of various doses of naloxone on gastric stress ulceration

Rats were injected with vehicle or naloxone (10 mg, 20 mg or 30 mg) per kg body weight i.p.

5. Effect of morphine and naloxone on gastric stress ulceration

Rats were injected with vehicle, morphine (10 mg/kg bw), melatonin (10 mg/kg bw), and morphine and melatonin (10 mg/kg bw each).

6. Effect of melatonin and naloxone on gastric stress ulceration.

Rats were injected with vehicle, melatonin (1 mg/kg bw), naloxone(12.5 mg/kg bw), and melatonin (10 mg/kg bw) plus naloxone(12.5 mg/kg bw).

Statistics

All data were statistically analysed using Students t-test or oneway analysis of variance followed by Scheffe's test for multiple range comparisons. All data are expressed as mean ± S.E.M. Except where indicated, n = 5.

Results

Experiment 1

Figure 1 clearly shows that, in the dark phase, when endogenous melatonin levels are high, the response to stress as manifested by gastric ulceration is significantly lower than that observed when compared to light phase controls. $t = 3.46$, $p<0.001$.

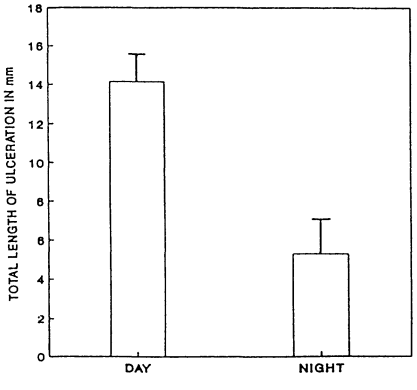

Fig. 1. The endogenous response to stress showing a significant reduction in lesion production. Day: n = 25 Night: n= 10, t = 3.46, p<0.001.

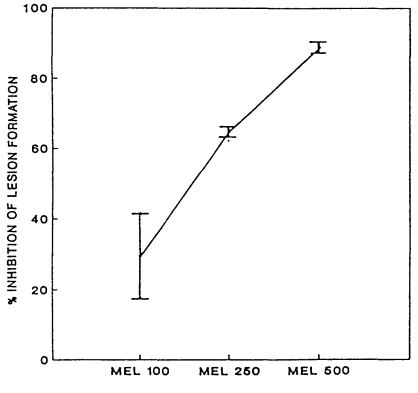

Fig. 2. Melatonin, at small doses, inhibits lesion formation. F(df = 19) = 6.73, p<0.01.

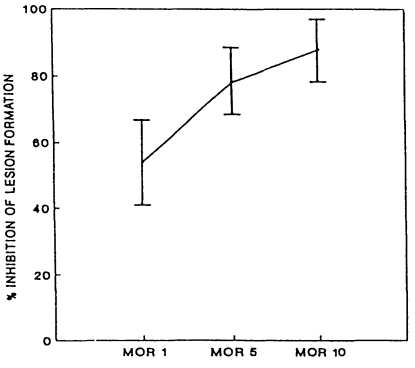

Fig. 3. Morphine inhibits stress lesion formation in a dose dependent manner. * = significantly different to control. F(df = 19) = 11.13, p<0.001.

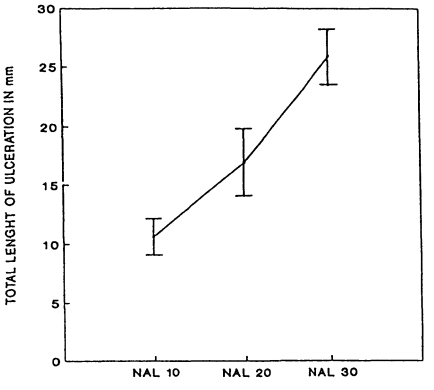

Fig. 4. Naloxone dose dependently exacerbates lesion production. F(df = 19) = 30.21, p<0.0001.

Experiment 2

At the low doses used in this study, melatonin has the ability to induce a dose dependent inhibition of gastric stress ulceration. A 500 μg dose of melatonin induces an 88.79% ± 0.04% inhibition of lesion formation. F(df = 19) = 6.73, p<0.005. (see Fig. 2)

Experiment 3

Morphine treatment resulted in a dose dependent inhibition of stress ulceration at the doses used in this study. F(df = 19) = 11.13, p<0.0005 (Fig. 3).

Experiment 4

Figure 4 shows that naloxone causes a dose dependent exacerbation of gastric stress ulcer production. Very severe ulceration covering a large area of the mucosa was noted at the higher doses of naloxone. F(df = 19) = 30.21, p<0.0001.

Experiment 5

Figure 5 summarizes the gastric stress data obtained, indicating that melatonin and morphine also cause an inhibition of stress lesion formation in rats, and a combination treatment shows no antagonism of this effect. F(df = 19) = 20.82, p<0.0001.

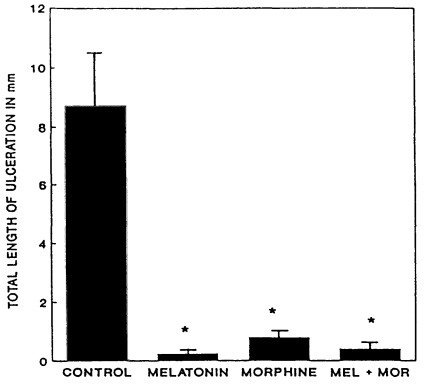

Fig. 5. A combination treatment of melatonin and morphine results in an inhibition of lesion formation. * = significantly different to control. F(df = 19) = 20.82, p<0.0001.

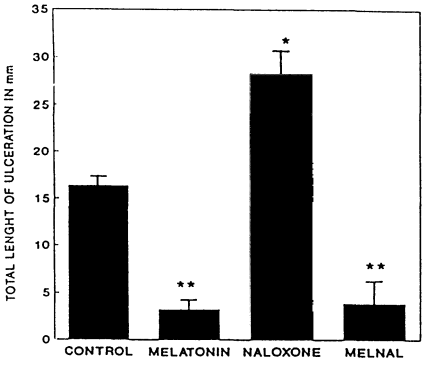

Fig. 6. Melatonin does not antagonize the exacerbating effect of naloxone on gastric stress ulcer production. * = significantly different to control. ** = significantly different to control and naloxone. F(df = 19) = 41.47, p<0.0001.

Experiment 6

Naloxone clearly exacerbates lesion formation, and melatonin significantly antagonized this effect indicating that the effect of melatonin on gastric lesion formation is not mediated via an opiatergic mechanism. (see Fig. 6) F(df = 18) = 41.47, p<0.0001.

Discussion

The role of melatonin in stress is not clear. Various studies have shown that exposure to stressful stimuli attenuates the melatonin biosynthetic pathway [4–6].

Dickson and Hasty [19] suggested that the pineal gland secretes a substance that acts at the hypothalamo-pituitary-adrenal axis to reduce the production or release of ACTH, thus exerting an inhibitory influence on the adrenal glands. Other authors suggested that together with the ovaries, the pineal gland plays a role in the modulation of adrenal steroidogenesis [20]. Rivest concluded that the primary function of the pineal gland in stress is to regulate the physiological reactions of defence or adaptation [21].

The most studied hormone released by the pineal gland is melatonin. In the above experiments, we have shown that small exogenous doses of this hormone act in a dose-dependent manner to inhibit the formation of one of the peripheral consequences of stress, gastric ulceration. Also, it is a well known fact that pineal melatonin synthesis undergoes a circadian rhythm, reaching peak levels in the dark phase of the cycle [18]. Rats stressed during this period show a secant reduction in

the severity of lesion formation. These results could very well implicate melatonin as a possible anti-stress hormone. Many studies have examined the effects of opiates and opiate antagonists on gastric stress pathology, and inconsistency in the results obtained is characteristic of the work done in this field. Some investigators [12,14] have found that the specific opiate antagonist, naloxone, decreases stress ulcer formation. Others have found that intraperitoneal or intracerebro-ventricular injections of morphine reduced gastric stress ulcer formation [13–15]. Our findings show that clearly, under these conditions of stress, morphine significantly inhibits, and naloxone exacerbates the production of gastric stress ulcers. This suggests that the release of endogenous opioids from the pituitary in stress serves as a protective mechanism for the body against the pathological consequences of such stimuli.

Of late, much work done by pineal researchers has centered around the interactions between the opioid system and the pineal gland. It has been suggested that the opiates require a modulation of the pineal gland for at least some of their actions [22]. There is evidence for the interaction between these systems in the immune system [23], cancer [24], and the mechanisms of analgesia in rats [25]. Melatonin has been shown to act via the opiate system to counter the effects of acute stress on thymus weight. However, under these conditions of stress and using these treatment doses, melatonin does not appear to acting via an opioidergic mechanism.

These interesting results clearly suggest a role for melatonin in stress. This hormone could be acting via a central mechanism, or perhaps even at a peripheral cellular level in the gastro-intestinal tract.

These findings require further work to attempt to elucidate the exact locus of melatonin's mode of action in stress.

Acknowledgements

This work was supported by grants from the Medical Research Council of South Africa and the Rhodes University Council to Prof. B. Potgieter and Dr. S. Daya.

References

1. Selye H (1974) Stress without Distress. Lippincott, Philadelphia, pp. 15–16.
2. Lerner AB, Casey JD, Takahashi Y, Lee TH and Moore W (1958) J. Am. Chem. Soc. 80: 2587.
3. Minneman KP and Wurtman RJ (1984) Life Sci. 17: 1189–1200.
4. Vaughan GM, Allen JP, Tullis W, Sackman JW and Vaughan MK (1978) Neurosc. Lett. 9: 83–87.
5. Tannenbaum MG, Reiter RJ, Vaughan MK, Troiani ME and Gonzalez-Brito A (1988) Cryobiology 25: 227–230.
6. Lynch HJ, Eng JP and Wurtman RJ (1973) Proc. Natl. Acad. Sci. 70: 227–230.
7. Miline R (1980) J. Neural. Trans. 47: 191–220.
8. Romijn HJ (1978) Life Sci. 23: 2257–2274.
9. Maestroni GJM, Conti A and Pierpaoli W (1988) Immunology 63: 465–470.
10. Khan R, Burton S, Morley S, Daya S and Potgieter B (1989) Experientia, in press.

11. Guilleman R, Vargo T, Rossier J, Minick S, Ling N, Rivier C, Vale W and Bloom F (1977) Science 197: 1367–1369.
12. Dai S and Chan MY (1983) Pharmacology 27: 180–184.
13. Ferri S, Arrigo-Reina R, Candeletti S, Costa G, Murari G, Speroni E and Scoto G (1983) Pharm. Res. Comm. 15: 409–419.
14. Del Tacca M, Bernadini C, Corsano E, Bertelli A and Roze C (1987) Int. J. Tiss. Reac. 10: 413–418.
15. Glavin GB, Kiernan K, Hnatowich MR and Labella FS (1986) Eur. J. Pharmacol. 124: 121–127.
16. Pare WP and Glavin GB (1986) Neurosci. Biobehav. Rev. 10: 339–370.
17. Senay EC and Levine RJ (1967) Proc. Soc. Exp. Med. 124: 1221–1223.
18. Axelrod J (1974) Science 184: 1341–1348.
19. Dickson KL and Hasty DL (1972) Acta. Endocrinol. 70: 438–444.
20. Ogle TF and Kitay J (1976) Endocrinology 39: 345–350.
21. Rivest R cited in Romijn R (1978) Life Sci. 23: 2257–2274.
22. Reiter RJ and Fraschini F (1987) In: Reiter RJ and Fraschini F (eds.) Advances in Pineal Reseach 2, John Libbey & Co. Ltd., London.
23. Maestroni GJM, Conti A and Pierpaoli W (1987) Clin. Exp. Immunol. 68: 384–391.
24. Eposti D, Lissori P, Tancini G, Barni S, Crispino S, Paolorossi F, Rovelli F, Cattaneo G, Eposti G, Lucini V and Frashihi F (1988) Cancer 62: 494–499.
25. Lakin ML, Miller CH and Winters WD (1981) Life Sci. 29: 2543–2551.

Role of glutathione metabolism in heavy metal poisoning

Kimiko Hirayama[a], Akira Yasutake[b] and Masayasu Inoue[c]

[a]Kumamoto University College of Medical Science, Japan
[b]National Institute for Minamata Disease, Japan
[c]Kumamoto University Medical School, Japan

Abstract

Effect of manipulation of GSH status on the *in vivo* fate of methylmercury (MeHg) was studied. Administration of butyl hydroxyanisole (BHA) (1 g/kg/day for 5 days) to C57BL female mice increased the glutathione (GSH) levels of liver, kidney, blood and plasma and accelerated the hepato-renal efflux of GSH. BHA also increased Hg levels significantly in urine and feces after oral administration of MeHgCl (5 mg/kg).

Male and female mice fed 7.5% protein diet (low protein diet) had lower hepatic GSH levels than animals fed 24% protein diet (normal protein diet). Urinary Hg excretion after oral administration of MeHgCl (5 mg/kg) markedly decreased in animals fed low protein diet (LPD). After 24 h of MeHgCl administration, animals were intraperitoneally injected with glutathione isopropylester (GSE); GSE restored urinary Hg excretion in mice fed LPD toward that in mice fed normal protein diet. These and other results suggest that glutathione status in liver and kidney might be the major factor for determining the rate of elimination of MeHg from a rodent.

Introduction

Glutathione (GSH) has important functions in the detoxification of a variety of hazardous compounds. One mechanism for detoxification is the conjugation of electrophilic compounds followed by elimination of the resulting metabolites in bile and urine. Recent studies of the sex difference in the fate of MeHg revealed that MeHg elimination correlated with the rate of hepato-renal efflux of GSH; Male mice having faster GSH efflux showed a higher rate of urinary Hg excretion [1] and were more resistant to MeHg toxicity than females with slower GSH efflux [2]. These facts drove us to speculate that the toxicity of MeHg might be modulated by manipulation of hepato-renal GSH efflux. Although administration of sulfur amino acids increased hepatic GSH in fasted animals, it failed to increase hepatic GSH in mice fed normal diet [3,4]. On the other hand, butyl hydroxyanisole (BHA) could elevate tissue GSH in mice fed normal diet [5]. Thus, BHA might be a useful agent for modulating the GSH status of animals fed normal diet.

Hepatic GSH levels in mice fed a low protein diet decreased by a mechanism which was inhibited by supplementing sulfur amino acids [4,6]. Thus, nutritional conditions, particularly those of sulfur containing amino acids and protein, are important for determining hepatic GSH status. Since glutathione-esters increased

hepatic GSH levels in fasted mice [7], glutathione isopropylester (GSE) is expected to affect the fate of MeHg. The present study describes the effect of BHA treatment, and low protein diet on the MeHg elimination.

Materials and Methods

Materials-MeHgCl and butyl hydroxyanisole (BHA) were purchased from Wako Chemical Co. (Osaka). Glutathione isopropylester (GSE) was a gift from Yamanouchi Pharmaceutical Co. MeHgCl was dissolved in highly purified water to give a concentration of 0.5 mg/ml. BHA was dissolved in olive oil to give a concentration of 0.2 g/ml. GSE was dissolved in saline. Casein-based diets supplemented as in Table 1 were purchased from Clea Co. (Japan).

Animals-C57/6NJcl male and female mice (8 weeks of age) were used in the present experiments. Unless otherwise stated, five mice were housed on corncob bedding in a clear plastic cage in an air-conditioned room maintained at 23 ± 2°C with a light-dark cycle of 12/12 h, allowed free access to laboratory chow (CE-2, Clea Japan) and water.

Effect of BHA on the fate of MeHg

Female mice were orally administered 0.1 ml of olive oil (vehicle) or BHA (1 g/kg/day) for 5 days. One day after the last injection, they were orally administered MeHgCl (5 mg/kg) and housed in metabolism cages (one mouse/cage). After collecting urine, and feces for 24 h, blood samples were collected from the caval vein under pentobarbital anesthesia. After perfusion with saline, tissues were excised. Hg levels of these specimens were determined according to the oxygen combustion-gold amalgamation method [8] using a Sugiyamagen Mercury Analyzer (Tokyo). GSH levels in blood, plasma, kidney and liver in mice treated with BHA or vehicle were determined by the method of Teitze [9]. Turnover rate of GSH in liver and kidney were determined by using L-buthionine sulfoximine [1].

Table 1. Composition of diets

Dietary protein	Normal protein 24.0%	Low protein 7.5%
Casein	29.3 g/100 g	8.8 g/100 g
Cornstarch	45.5	61.1
Corn oil	6.0	6.0
Cellulose	5.0	5.0
Vitamin mix	1.0	1.0
Mineral mix	7.0	7.0
α-Starch	1.0	1.0

Effect of low protein diet on the fate of MeHg

Male and female mice were fed either 24% (normal) or 7.5% (low) protein diet (Table 1) for 7 days. On day 6, they were orally administered MeHgCl (5 mg/kg), and urine and feces were collected for the following 24 h and their Hg levels were determined as described above. On day 6, hepato-renal GSH levels in mice fed normal (NPD) or low protein diet (LPD) were also determined as described above. In the separate experiment, male mice fed NPD or LPD were orally administered MeHgCl (5 mg/kg). At 24 and 36 h after MeHg administration, animals were intraperitoneally administered GSE (50 mg/kg) and urine and feces were collected for 24 h after GSE administration.

Statistical analysis-Statistical analysis of difference was calculated according to Student's t-test; the level of significance was put at $p<0.05$.

Results

Effect of BHA on the fate of MeHg

To study the effect of increased tissue GSH levels on the fate of MeHg, mice were treated with BHA. BHA markedly increased the GSH levels of liver, kidney, blood and plasma (Fig. 1). Half time of hepatic GSH was much longer in mice treated

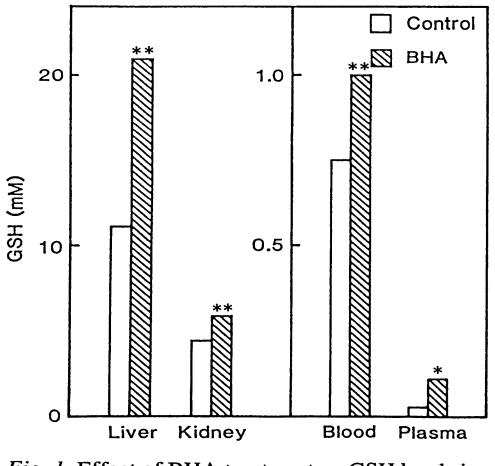

Fig. 1. Effect of BHA treatment on GSH levels in liver, kidney, blood and plasma. Female mice were orally administered BHA (1 g/kg/day for 5 days). One day after the last administration, GSH levels were determined. *Significantly different ($p<0.05$) from control; **Significantly different ($p<0.01$) from control; n=5.

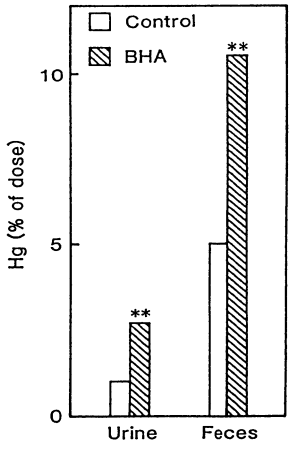

Fig. 2. Effect of BHA treatment on Hg excretion after administration of MeHg. Female mice were orally administered BHA (1 g/kg/day for 5 days). One day after the last injection, animals were orally administered MeHgCl (5 mg/kg) and urine and feces were collected for 24 h. **Significantly different ($p<0.01$) from control; n=5.

Table 2. Effect of BHA on tissue Hg levels[a] 24 h after administration of MeHgCl in female mice

	Control	BHA
Brain	0.59 ± 0.04	0.89 ± 0.06[a]
Liver	11.70 ± 0.27	9.71 ± 0.70[b]
Kidney	8.21 ± 0.57	8.29 ± 0.87
Blood	3.19 ± 0.21	2.37 ± 0.30[b]
Plasma	1.27 ± 0.09	1.05 ± 0.09[a]

Female mice were orally administered BHA (1 g/kg) for 5 days. One day after the last administration animals were orally administered MeHgCl (5 mg/kg). After 24 h, blood, plasma and tissue samples were determined for Hg. Values are expressed as mean ± SD (% of dose for tissues and μg/ml for blood and plasma), n=5; [a]Significantly different ($p<0.05$) from control; [b]Significantly different ($p<0.01$) from control.

with BHA (140 min) than in mice treated with vehicle alone (95 min), while half time of renal GSH remained unchanged. Finally, BHA markedly increased hepato-renal GSH levels and GSH efflux in liver (from 82.2 to 153.6 μmol/day/liver) and kidney (from 16.2 to 24.0 μmol/day/kidney). Excretion of Hg in urine and feces

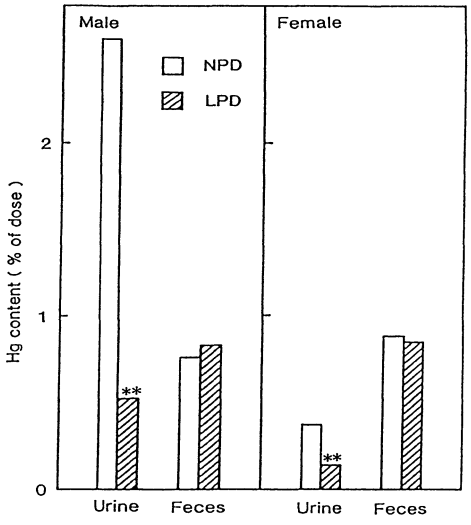

Fig. 3. Effect of low protein diet on Hg excretion after administration of MeHg. Male and female mice were fed normal (NPD) (24% protein) or low protein (LPD) (7.5% protein) diet for 7 days. On day 6, they were orally administered MeHgCl (5 mg/kg) and urine and feces were collected for 24 h. **Significantly different ($p<0.01$) from mice fed NPD; n=5.

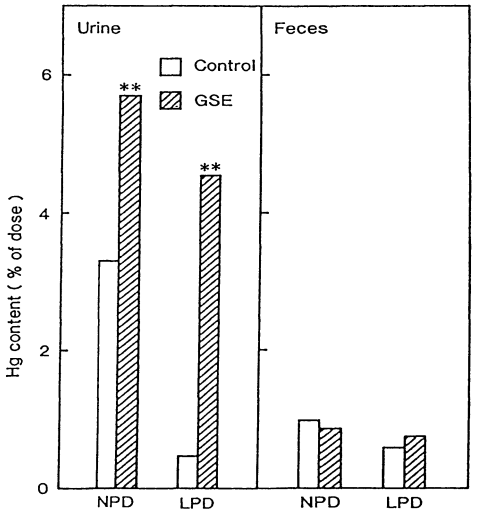

Fig. 4. Effect of GSE on Hg excretion after administration of MeHg in mice fed NPD or LPD. Male mice were fed NPD or LPD diet for 8 days. On day 6, they were orally administered MeHgCl (5 mg/kg). After 24 and 36 h, they were intraperitoneally administered 50 mg/kg of glutathione isopropylester (GSE). Control group was administered saline. Then, urine and feces were collected for 24 h. **Significantly different ($p<0.01$) from control; n=5.

increased significantly in BHA treated mice (Fig. 2). At this time, Hg levels in liver, blood and plasma decreased, while its levels in the brain increased (Table 2).

Effect of LPD on the fate of MeHg

To study the influence of nutritional conditions on the fate of MeHg, mice were fed NPD or LPD. Hepatic GSH levels significantly decreased in mice fed LPD (from 9.29 ± 0.39 to 6.95 ± 1.48 mM and 9.41 ± 0.49 to 6.92 ± 1.40 mM in males and females, respectively). Also, LPD decreased Hg excretion in urine in both male and females (Fig. 3). GSE increased urinary Hg excretion in NPD and LPD group but not in feces. By GSE treatment, decreased Hg excretion in mice fed LPD restored toward that in mice fed NPD.

Discussion

Our previous report [1] suggested that the rate of MeHg elimination closely correlated with the rate of hepato-renal GSH efflux. Consistent with this notion is the present finding that urinary excretion of MeHg markedly increased in BHA treated mice whose hepato-renal GSH efflux and plasma GSH levels were increased significantly. BHA also increased fecal excretion of Hg. GSH efflux occurs across sinusoidal and canalicular membranes [10,11]. BHA increased hepatic turnover and biliary efflux of GSH [12]. Thus, BHA might increase both sinusoidal and canalicular efflux of GSH and increase Hg excretion in both urine and feces.

Since the major fraction of plasma GSH is degraded by renal peritubular γ-glutamyltransferase [13], the increase in plasma GSH levels might also increase plasma cysteine levels. It has been reported that cysteine increases MeHg uptake by the brain [14]. Thus, the accelerated uptake of MeHg by the brain in BHA treated mice might reflect the increase in plasma cysteine levels.

Mice fed LPD showed lower hepatic GSH levels and urinary MeHg excretion than mice fed NPD. Moreover, GSE, a prodrug for GSH, restored urinary Hg levels in mice fed LPD to that in mice fed NPD. Since glutathione ester increases tissue GSH levels [7], these results suggest that the depletion of hepatic GSH is a predominant factor for decreasing urinary Hg excretion in animals fed LPD.

These results suggest that dietary protein status plays an important role in determining the *in vivo* fate and the toxicity of MeHg in relation to GSH metabolism.

References

1. Hirayama K, Yasutake A and Inoue M (1987) Biochem. Pharmacol. 36: 1919–1924.
2. Yasutake A and Hirayama K (1988) Toxicology 51: 47–55.

3. Tateishi N, Higashi T, Naruse A, Nakashima K, Shiozaki H and Sakamoto Y (1977) J. Nutr. 107: 51–60.
4. Boeble KP and Baker DH (1983) Proc. Soc. Exp. Biol. Med. 172: 498–501.
5. Jaeschke H and Wendel A (1985) Toxicology 36: 77–85.
6. Bauman PF, Smith TK and Bray TM (1988) J. Nutr. 118: 1048–1054.
7. Anderson ME, Powrie F, Puri RN and Meister A (1985) Arch. Biochem. Biophys. 239: 538–548.
8. Jacob MB, Yamaguchi S and Goldwater LD and Gilbert H (1960) Am. Ind. Hyg. Ass. J. 21: 475–480.
9. Teitze F (1969) Anal. Biochem. 27: 503–522.
10. Inoue M, Kinne R, Tran T and Arias IM (1983) Eur. J. Biochem. 134: 467–471.
11. Inoue M, Kinne R, Tran T and Arias IM (1984) Eur. J. Biochem. 138: 491–495.
12. Jaeschke H and Wendel A (1988) Toxicology 52: 225–235.
13. Inoue M (1985) In: Kinne RKH (ed.) Renal Biochemistry. Elsevier, Amsterdam, pp. 225–265.
14. Hirayama K (1982) Biochem. Pharmacol. 34: 2030–2032.

Address for correspondence: Kimiko Hirayama, Kumamoto University College of Medical Science, 24–1 Kuhonji 4 Chome, Kumamoto 862, Japan.

Altered capacities for amino acid transport in response to liver injury by CCl_4 and during subsequent regeneration

Rolf Gebhardt and Ludger Schöls

Physiologisch-chemisches Institut der Universität, D-7400 Tübingen, F.R.G.

Abstract

Exposure of rats to CCl_4 resulted in necrosis of the acinar zone 3 associated with the disappearance of glutamine synthetase-positive pericentral hepatocytes. Histologic and immunohistochemical observations indicated the almost complete remodelling of the pericentral zone within 2 weeks. Immediately after intoxication as well as during subsequent regeneration dramatic changes in the extent of the hormonal regulation of the amino acid transport systems A, N, and G^- were noted in cultured hepatocytes characterized by the individual response of each system. The changes occurring during the regenerative period could partially be mimicked by inducing transient hepatocyte proliferation through plating at low cell density and addition of growth factors *in vitro*. It is obvious from these results that the alterations in the induction of hepatic amino acid transport systems observed after CCl_4 intoxication are due to: (a) disturbance and reacquisition of acinar heterogeneity, (b) onset and finish of hepatocellular proliferation.

Introduction

Exposure of rat liver to CCl_4 is well known to cause severe necrosis in zone 3 of the hepatic acinus [1]. After cessation of the treatment regeneration will take place which leads to a normal histology after 1–2 weeks. It has recently become apparent that liver injury by CCl_4 results in a considerable disturbance of ammonia metabolism [2–4] and, related to this, the metabolism of glutamate and glutamine [5,6], because of the exclusive localization of glutamine synthetase (GS) at the pericentral end plate which is completely destroyed [7,8]. This seems to be associated with alterations in amino acid transport capacities, particularly for glutamate, the Na^+-dependent uptake of which seems to be restricted to the GS-positive hepatocyte population [9–11].

In the present study we have investigated the alteration in hepatic amino acid transport caused by exposure to CCl_4 and further influenced by the regenerating process. The observed changes were compared to those found in proliferating hepatocytes *in vitro*. Furthermore, these changes were correlated to liver histology and to the reappearance of GS determined at various times after exposure to CCl_4.

Experimental procedures

Exposure to CCl_4

Male Sprague-Dawley rats (170–250 g) were injected i.p. with CCl_4 (1 ml/kg) with an equal amount of corn oil on three consecutive days as described [7,8]. At various times thereafter, livers were fixed for immunohistochemistry or used for the isolation of hepatocytes by collagenase perfusion [8]. The day of the last injection was considered as the onset of regeneration.

Immunohistochemistry

Liver sections (after fixation and paraffin imbedding) or cultured hepatocytes were stained for glutamine synthetase (GS) by the peroxidase antiperoxidase technique of Sternberger [12] as modified [7,8]. An antiserum against rat liver GS was used (diluted 1:400 with PBS).

Hepatocyte cultures

Hepatocytes were cultured for 48 h (treated rats) or up to 96 h (normal rats) in serum-free (except first 2 h) Williams Medium E supplemented with or without (controls) dexamethasone (10^{-7} M) as described [3,7]. Addition of other hormones for appropriate stimulation [13,14] is indicated for the individual experiments. Cultivation for studies on hepatocyte growth *in vitro* was performed according to Gebhardt *et al.* [15]. In this case the medium was changed only once after 48 h and growth factors were present only before this change.

Amino acid transport

α-aminoisobutyrate (AIB), histidine (HIS) and glutamate (GLU) were used as substrates for systems A, N, and G^-, respectively. The Na^+-dependent uptake was determined as described [13,14]. Statistical evaluation was based on Student's t-test.

Results

Exposure of rats to CCl_4 for 3 days resulted in a strong pericentral necrosis characterized by the almost complete disappearance of GS (Fig. 1) as described previously [7–8]. During regeneration the necrotic tissue is replaced by new hepatocytes. This process could be divided into an early phase of regeneration up to day 5 characterized by a still disturbed morphology including an incomplete encirculation of the terminal hepatic venules (THV) by GS-positive hepatocytes, and into a late phase (days 12 to 21) where the parenchyma seemed intact and the

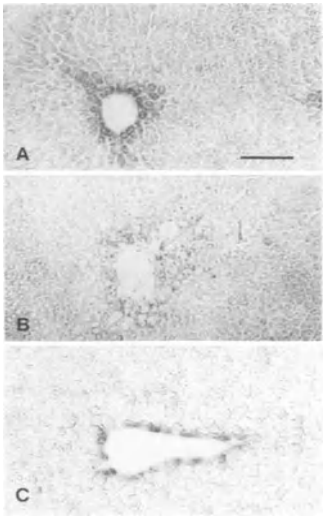

Fig. 1. Distribution of GS in livers exposed to CCl_4. A) Paraffin section of normal rat liver. GS-positive cells are found in 1 to 3 cell layers surrounding the central veins. B) Necrotic zone surrounding the central vein. One day after exposure to CCl_4. C) 5th day of regeneration. GS is present in one cell layer only. Bar: 100 μm.

distribution of GS was normal with the exception that only one cell layer around the THV was enzyme positive. Most likely, the original pattern of distribution of GS was not completely restored [1,6] (Fig. 1). The most active cell proliferation was found to be confined to the early phase of regeneration [17,18].

Determination of the capacities for amino acid uptake during the different phases of injury and regeneration revealed considerable changes particularly in the hormonal induction of the various amino acid transport systems (Table 1). The individual transport systems responded quite differently. System A showed a strong reinforcement of the induction by dexamethasone and glucagon immediately after exposure to CCl_4 but returned to normal during early regeneration. System N dropped during early regeneration and increased during late regeneration, particularly its induction by dexamethasone and insulin. System G^- remained unchanged in controls, but showed a reduced induction by dexamethasone after exposure to CCl_4 as described earlier [7]. However, during early and late regeneration a continuous increase of this induction was observed which exceeded by far the capacity of controls. Similar changes were noted if glucagon was added in addition to dexamethasone, while addition of insulin strongly repressed the induction throughout.

These changes seem to result as a consequence of both the heterogeneous distribution of amino acid transport systems [9,10] and the specific requirements of

Table 1. Hormonal induction of amino acid transport systems A, N and G$^-$ in hepatocytes isolated after exposure to CCl_4 and during regeneration

Transport system	Hormonal conditions	Specific uptake (pmol·min^{-1}·mg^{-1})[a]			
		Control animals	Time after last injection of CCl_4[b]		
			1 day	3–5 days	12–21 days
System A	none	216±151 (6)	194±65 (4)	180±88 (4)	239±132 (6)
	D[c]	240±186 (6)	360±224 (4)	190±34 (4)	307±198 (6)
	D/G	851±597 (6)	1884±981 (4)[d]	903±387 (4)	955±556 (6)[e]
System N	none	95±48 (5)	114±41 (4)	59±32 (4)	145±54 (6)
	D	n.d.	n.d.	168±91 (4)	285 (2)
	D/I	203±39 (5)	302±89 (4)[d]	213±48 (4)	435±132 (6)[f]
System G$^-$	none	13±17 (6)	15±15 (4)	11±8 (4)	16±13 (7)
	D	609±267 (6)	267±117 (4)[d]	489±131 (4)	890±226 (7)[d,g]
	D/I	[218]	[26]	215±173 (4)	79 (2)
	D/G	443±166 (6)	364±188 (4)	741±330 (4)[d,e]	873±525 (6)[e]

[a]Values represent means ± SD. Numbers of determinations in parenthesis. Single values are given in square brackets [b]3–5 days, early regeneration; 12–21 days, late regeneration.[c]hormonal conditions: D, dexamethasone 10^{-7}; G, glucagon 10^{-6} M; I, Insulin 10^{-6} M n.d.: not determined. Statistically different from control value: [d], $p<0.05$; [f], $p<0.01$ Statistically different from 1 day value: [e], $p<0.05$; [g], $p<0.001$.

Table 2. Hormonal regulation of amino acid transport systems A and G$^-$ in hepatocytes cultured under different growth promoting conditions

Transport system	Hormonal conditions	specific uptake (pmoles·min^{-1}·mg^{-1})			
		High density[b]		Low density	
		48 h[c]	96 h	48 h	96 h
System A	control	192 ± 34	321 ± 29	612 ± 54[e]	184 ± 15
	D[d]	121 ± 11	282 ± 21	484 ± 38[e]	109 ± 17
	D/G	297 ± 33	351 ± 37	1682 ± 113[e]	622 ± 84[e]
	G1 → D/G	n.d.	n.d.	649 ± 144[e]	319 ± 41
	G2 → D/G	442 ± 60	514 ± 48	1903 ± 198[e]	841 ± 146[e]
System G$^-$	control	37 ± 21	8 ± 3	13 ± 4[e]	7 ± 2
	D[d]	621 ± 68	45 ± 6	133 ± 17[e]	19 ± 3
	D/G	526 ± 47	81 ± 11	137 ± 13[e]	76 ± 9
	G1 → D/G	12 ± 3	2 ± 3	6 ± 2	117 ± 17[e]
	G2 → D/G	197 ± 18	192 ± 24	52 ± 26[e]	153 ± 10

[a]Values represent means ± SD of 3 to 4 determinations [b]High density: $125 \cdot 10^3/cm^2$; low density: $25 \cdot 10^3/cm^2$. [c]hepatocytes were cultured for 48 h or 96 h with only one medium change after 48 h· [d]hormonal conditions: D, dexamethasone 10^{-7} M; G, glucagon 10^{-6} M. G1: mixture of D, insulin 10^{-6} M, EGF 30 ng/ml. G2: mixture of G1, lactate 40 mM, pyruvate 5 mM; n.d.: not determined. Statistically different from respective value at high density: [e]$p<0.001$.

proliferating hepatocytes [19]. Further modification may result from changes of receptor concentrations at the cell surface [20]. The influence of the acinar distribution is obvious for the immediate changes produced by the CCl_4 intoxication and is most prominent for system G^- which seems to disappear in relation to the GS-positive cell population [7]. The enhanced stimulation of system A at this time cannot be explained on this basis, but seems to result from the rapid response of this system to alterations in the hormonal environment [14,21] and thus reflects the first indication for the adaptation to regenerative growth. This is strongly suggested by comparison with results obtained after *in vitro* induction of hepatocyte growth by low cell density and growth factors (Table 2). Under these conditions (i.e. in proliferating hepatocytes after 48 h) the capacity of AIB uptake is strikingly enhanced, whereas removal of growth factors resulted in a diminution at 96 h. These changes fit well with similar observations made by Le Cam *et al.* [22] after partial hepatectomy. The changes observed for system G^- in the transiently growing hepatocytes reflect a quite different behavior of this system. The growth conditions lead to the repression of the induction both with dexamethasone and with dexamethasone and glucagon, while cessation of growth restored this induction to some extent. These results as well as those shown in Table 1 indicate a potent inhibition by insulin of the dexamethasone dependent induction. Thus, the decrease of system G^- activity and inducibility may be due not only to acinar heterogeneity but also to the onset of growth. The late increase of system G^- on the other hand, may be due to the slow adaptation of this transport activity [13]. It suggests that the influence of insulin (or insulin-like activities) is diminished after cessation of growth. Whether the striking enhancement of the stimulation of system G^- during late regeneration might be due to the influence of inhibitory growth factors like TGF-ß [23] is currently being investigated.

In conclusion, these results demonstrate that necrotic destruction and regeneration of the liver acinus after intoxication with CCl_4 is associated with prominent changes in the capacities and inducibility of some important amino acid transport systems. Although the early changes may be explained by the loss of the GS-positive hepatocyte population and by the onset of proliferation, the late variations do not completely correlate with the remodeling of the parenchyma, since some changes persist beyond the morphologic completion of the regenerating process.

Acknowledgement

We thank Mrs. H. Fitzke and Mr. C. Mayer for their excellent technical assistance. This work was supported by the Deutsche Forschungsgemeinschaft.

References

1. Recknagel RO (1967) Pharmacol. Rev. 19: 145–208.
2. O'Donovan DJ (1980) Int. J. Biochem. 12: 85–87.

3. Gebhardt H and Mecke D (1983) EMBO 2: 587–570.
4. Häussinger D (1983) Eur. J. Biochem. 133: 269–275.
5. Häussinger D and Gerok W (1984) Chem. Biol. Interactions 48: 191–194.
6. Häussinger D and Gerok W (1988) In: Thurman RG, Kauffman FC and Jungermann K (eds.) Regulation of Hepatic Metabolism. Intra- and Intercellular Compartmentation. Plenum Press, New York, pp. 253–291.
7. Gebhardt R and Burger H-J (1987) J. Hepatol. 4: 381–389.
8. Gebhardt R, Burger H-J, Heini H, Schreiber KL and Mecke D (1988) Hepatology 8: 822–830.
9. Gebhardt R (1989) In: Petzinger E, Kinne RK-H and Sies H (eds.) Hepatic Transport in Organic Substances. Springer-Verlag, Berlin, Heidelberg, pp. 177–187.
10. Burger H-J, Gebhardt R, Mayer C and Mecke D (1989) Hepatology 9: 22–28.
11. Taylor PM and Rennie MJ (1987) FEBS Lett. 221: 370–374.
12. Sternberger LA, Hardy PH, Cuculis JJ and Meyer HG (1970) J. Histochem. Cytochem. 18: 315–333.
13. Gebhardt H and Mecke D (1983) FEBS Lett. 161: 275–278.
14. Gebhardt R and Kleemann E (1987) Eur. J. Biochem. 166: 339–344.
15. Gebhardt R, Cruise J, Houck KA, Luetteke NC, Novotny A, Thaler F and Michalopoulos GK (1986) Differentiation 33: 45–55.
16. Schöls L, Gebhardt R and Mecke D (1987) Z. Gastroenterol. 25: 69–70.
17. Leevy CM, Hollister HM, Schid H, MacDonald HA and Davidson CS (1959) Proc. Soc. Exp. Biol. Med. 102: 672–675.
18. Schultze B, Gerhard H, Schump E and Maurer W (1973) Virchows Arch. B. Zell. Path. 14: 329–343.
19. Christensen HN, Rothwell JT, Sears HA and Streicher JA (1948) J. Biol. Chem. 175: 101–105.
20. Mourelle M and Rubalcava B (1981) J. Biol. Chem. 256: 1656–1660.
21. Kilberg A, Barber EF and Handlogten ME (1986) Curr. Top. Cell. Regul. 25: 133–163.
22. LeCam A, Rey J-F, Fehlmann M, Kitabgi P and Freychet P (1979) Am. J. Physiol. 5: E594-E602.
23. Braun L, Mead JE, Panzica M, Mikumo R, Bell GI and Fausto N (1988) Proc. Natl. Acad. Sci. USA 85: 1539–1543.

Address for correspondence: Doz. Dr. R. Gebhardt, Physiologisch-chemisches Institut, Hoppe-Seyler-Str. 4, D-7400 Tübingen, F.R.G.

Effects of some amino acids and peptide growth factors on wool growth and wool follicle function in sheep

Ralph E. Chapman

Division of Animal Production, CSIRO, PO Box 239, Blacktown, NSW 2148, Australia

Abstract

Wool growth and wool follicle function are affected by the amounts of lysine, cyst(e)ine and methionine reaching the intestines of sheep. In pre-ruminant lambs and sheep fed abomasally on diets of low lysine content, a series of deleterious events occurs in the wool follicles, commencing with apoptosis of cells in the follicle bulbs. This is followed by impaired synthesis and improper keratinization of the fibres, distortion of the mid- and distal parts of the follicles, gross enlargement of the distal outer root sheaths and partial degradation of the fibres before they emerge from the skin in a very weakened state. Small supplements of cyst(e)ine or methionine given via the abomasum stimulate wool growth of sheep fed roughage diets, but supplements of methionine depress wool growth and weaken the fibres when sheep are fed a diet of whole wheat. The same sequence of deleterious changes occurs in the follicles, as in lambs on low lysine intakes.

Epidermal growth factor, transforming growth factor α and transforming growth factor ß all induce regression of wool follicles and cessation of fibre growth when either infused subcutaneously or intravenously or injected intradermally.

Introduction

The amount of wool grown by sheep is influenced by many genetic, environmental and physiological factors. For any particular genotype of sheep, wool production can be markedly affected by the environmental factors of dietary intake and composition. These, together with the outflow of microbial protein from the rumen, largely govern the nutrient supply available to the wool follicles. While effective utilization of nutrients is influenced by the ratio of protein to energy in the intestines, the major limitations to wool production are the amount and composition of amino acids available [1–3]. Wool growth can be adversely affected by deficiencies of essential amino acids and by diets based on proteins deficient in these amino acids *eg.* gelatin and zein [4,5].

Other environmental factors such as photoperiodism [6,7] and climatic stress, be it heat or cold [8], as well as various physiological states such as age, sex, pregnancy, lactation [9] and state of health [10] also influence wool growth. These operate, *inter alia*, through changes in the concentrations of circulating hormones [7,11]. Interest is also growing in the roles of peptide growth factors.

This paper reviews, in particular, the effects on wool growth and wool follicle function of lysine and sulphur-containing amino acids, and of epidermal growth factor and transforming growth factors α and ß.

Amino acids

Wool fibres consist of an outer cuticle of one to three layers of overlapping flattened cells surrounding the cortex, which in coarse wool fibres may surround a central medulla of vacuolated cells [12]. The cortex comprises most of the mass of the fibres and consists of keratin-filled cells held together by intercellular material. The cortical cells are composed of intermediate filament proteins (or microfibrils) of *c.* 7.5 nm diameter embedded in a matrix of non-filamentous intermediate filament-associated proteins. The intermediate filaments are partly α-helical assemblies in which there are two families (Types I and II) of polypeptides of low cyst(e)ine content (low-sulphur proteins) [13]. These contain all of the methionine and much of the lysine present in wool and are also rich in glutamic acid [14]. The matrix consists of two heterogeneous families, one of which has high contents of cyst(e)ine, proline and serine (high-sulphur and ultra-high sulphur proteins) [14,15], while the other is rich in tyrosine and glycine (high-tyrosine proteins) [16]. Within the latter there are two major sub-families, Type I with a low content of cyst(e)ine but rich in phenylalanine, and Type II moderately rich in cyst(e)ine but poor in phenylalanine [17], not to be confused with the Type I and Type II polypeptides of the low-sulphur proteins.

Because of the complexity of wool proteins it is not surprising that the supply of amino acids to the follicles can affect follicle function both in terms of wool production and composition. In some instances there can be associated changes in follicle morphology, as will be described later.

Evaluation of proteins or amino acids given as dietary supplements to sheep is complicated by microbial degradation and fermentation in the rumen and by various aspects of rumen function [18]. These ruminal complications have been avoided in many studies by giving the substances as abomasal or parenteral supplements to a basal diet fed per os.

With the exception of the sulphur-containing amino acids, abomasal administration of various single amino acids to sheep fed roughage diets does not stimulate wool growth [19]. In contrast, abomasal infusion of a mixture of 10 essential amino acids (ie. the same 10 amino acids essential for growth in rats) in proportions approximating those in casein stimulates wool growth to an extent similar to the infusion of an equivalent amount of casein [20]. Omission of any one of methionine, lysine, leucine or isoleucine depresses wool growth with the additional effect of reducing the tensile strength of the wool fibres when either methionine or lysine is omitted. Similar loss of tensile strength occurs, along with a slight depression of wool growth and marked reduction of fibre thickness, during abomasal infusion of zein [5]. Zein is devoid of lysine and deficient in tryptophan [21] and the adverse effects of zein can be eliminated by the inclusion of lysine in the zein infusate [22].

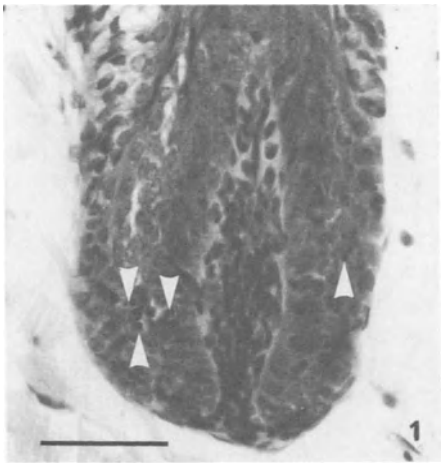

Fig. 1. Longitudinal section of the bulb of a wool follicle with cells containing apoptotic bodies (arrowheads) in the skin of a lamb fed 0.12 g lysine/(kg live weight)$^{0.75}$ daily. Scale bar = 50 μm [23].

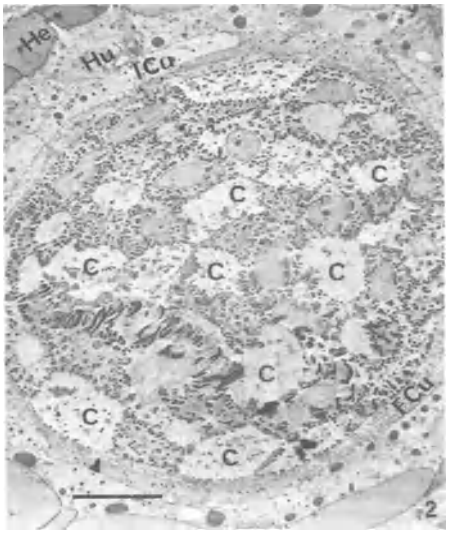

Fig. 2. Transverse section near the middle of the keratogenous zone of a wool follicle in the skin of a lamb fed 0.12 g lysine/(kg live weight)$^{0.75}$ daily. Some cortical cells (C) of the fibre have decreased ribosomal content and depressed formation of macrofibrils. FCu = fibre cuticle, ICu = inner root sheath cuticle, Hu = Huxley's layer, He = Henle's layer. Scale bar = 10μm [23].

Lysine intake markedly influences follicle function of pre-ruminant lambs [23]. A daily lysine intake of *c.* 0.9 g/(kg live weight)$^{0.75}$ in liquid diets fed abomasally is required for normal follicle function. When lesser quantities are fed, apoptosis [24] occurs in follicle bulb cells (Fig. 1). In addition, keratin synthesis is impaired in the keratogenous zone of the fibres, as indicated by decreased ribosomal content and depressed formation of macrofibrils (ie. intermediate filaments and associated proteins) in the cortical cells (Fig. 2). Keratinization of the fibres is also impaired and this leads to kinking of the fibres at the mid-dermal level in some follicles and to severe distortion and partial degradation of the fibres in the distal parts of most follicles (Fig. 3). This is accompanied by gross enlargement of the surrounding follicle outer root sheaths. Presumably the proteolytic process which normally breaks down the inner root sheath cells in the distal part of the follicles also partially degrades the poorly keratinized fibres within the thickened outer root sheaths. Upon emergence from the skin, the distorted fibres are weak, are often fragmented at bends and break easily. Most are irregular in cross-section, are incompletely filled with keratin and appear to lack intercellular cementing material. Some are also devoid of surface scale pattern. Almost all follicles and fibres are affected when daily lysine intake falls below 0.4 g/kg$^{0.75}$.

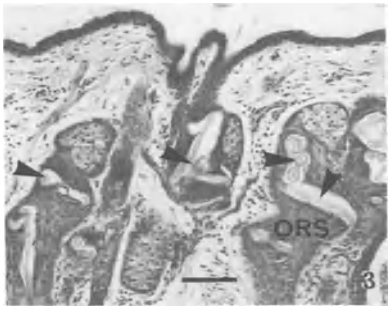

Fig. 3. Longitudinal sections of wool follicles in which the fibres (arrowheads) are distorted and partially degraded within grossly thickened distal outer root sheaths (ORS), in the skin of a lamb fed 0.27 g lysine/(kg live weight)$^{0.75}$ daily. Scale bar = 100μm [23].

There is a time sequence in the development of the above abnormalities when pre-ruminant lambs are changed suddenly from a diet with adequate lysine (1.35 g/kg$^{0.75}$.day) to one containing little lysine (0.12 g/kg$^{0.75}$.day). Apoptotic bodies develop in the majority of follicle bulbs within one day after the change, whereas impaired keratin formation in the fibres is not evident until 2 days and gross distortion in the distal parts of follicles is not seen until 3–4 days. Hence the cells in the keratogenous zone of the fibre at the time of the change in diet appear to be unaffected by the reduced lysine intake. The differences in times for the various effects to occur are similar to the times for cells of the fibre to migrate from the follicle bulb into the keratogenous zone and distal part of the follicle respectively [25]. So the population of cells which are first to exhibit defective keratin synthesis in the keratogenous zone are those which were first to be affected during the previous day by apoptotis in the follicle bulb. This raises the question as to whether those cells that are involved in phagocytosing apoptotic bodies have subsequently impaired ability to synthesize keratin proteins.

When pre-ruminant lambs are returned to a diet with adequate lysine, there is again a similar time sequence in the disappearance of apoptosis in the bulb cells and in the return to apparently normal keratin synthesis in the keratogenous zone of the fibre. However, disappearance of the gross enlargement of outer root sheaths is slower than its development, presumably as a result of the time required for accumulated outer root sheath cells to be exfoliated.

The supply of sulphur-containing amino acids to the follicles can also markedly affect wool growth [26,27]. When given as dietary supplements, these amino acids are readily degraded in the rumen and do little to stimulate wool growth, except when the diet is deficient in sulphur [28]. However, when these amino acids are given as abomasal or intravenous supplements to sheep, the effects are dependent on the nature of the basal diet. Given to sheep on roughage diets, equimolar amounts of *c.* 2 g/day of cyst(e)ine or methionine stimulate wool growth to similar extents [29], although with high-producing sheep methionine may be more stimu-

latory than cystine [30]. The presence of some methionine appears to be obligatory, because methionine cannot be replaced entirely by cyst(e)ine or homocyst(e)ine. However, increasingly larger supplements of methionine become less stimulatory, a feature not observed with cystine supplementation [29].

Abomasal infusions of cystine do not stimulate wool growth when given at either 5 g/day to sheep fed a diet of whole wheat [31] or 2 g/day to sheep consuming oat grain [32]. In contrast, daily intraperitoneal injections of 1.5–4.5 g methionine stimulate the wool growth of sheep fed a diet based on ground corn [33], whereas abomasal infusions of 1.5–6.0 g methionine/day into sheep receiving a diet of whole wheat not only depress wool growth but also cause a marked weakening of the wool [31,34]. This loss of strength in the wool is caused by the same sequence of changes in the wool follicles as occurs in pre-ruminant lambs fed a lysine deficient diet, *viz.* apoptosis in cells in the follicle bulbs, poor fibre formation, impaired keratinization of the fibres and distortion and partial degradation of the fibres within grossly enlarged distal outer root sheaths [34]. This same sequence also occurs in wool follicles in lambs fed diets deficient in zinc [35] or folic acid (J.L. Black, W.F. Colebrook and R.E. Chapman, unpublished data). It appears, therefore, to be a manner in which follicles respond to various nutritional insults which depress wool growth but still allow mitotic activity to proceed in the follicle bulbs.

Peptide growth factors

Most studies of the effects of peptide growth factors on wool growth and wool follicle function relate to the effects of epidermal growth factor (EGF) prepared from submaxillary glands of male mice [36] or by a recombinant DNA technique [37] and administered to sheep by subcutaneous or intravenous infusion [37–44] or by intradermal injection [45,46].

EGF stimulates cell proliferation in the epidermis and sebaceous glands but, paradoxically, inhibits cell division in follicle bulbs and induces follicle regression and cessation of fibre growth. Following subcutaneous or intravenous infusion of EGF for periods up to 28 h, the increases in mitotic activity in the epidermis and sebaceous glands are transient and last for only 2–3 days. However; the resultant hyperplasia in the epidermis takes *c.* 3 weeks to begin to subside, whereas the increase in sebaceous gland size lasts only 1–2 days. In contrast, mitotic activity ceases within 24 h in follicle bulbs, which decrease in size as the bulb cells migrate from around the dermal papillae. Also within 24 h apoptosis starts to occur at the suprabulbar level in cells destined to form the fibre. This EGF-induced apoptosis appears to be secondary to the inhibition of mitotic activity in the follicle bulbs, whereas the apoptosis induced by dietary manipulation is the first effect to occur.

Regression of some follicles continues for *c.* 4 days and becomes maximal with cessation of fibre growth and the formation of irregularly tapered fibre ends, frequently enclosed by hardened inner root sheath cells (Fig. 4). In these follicles, apoptosis occurs in some of the epithelial cells that form the stalk between the fibre

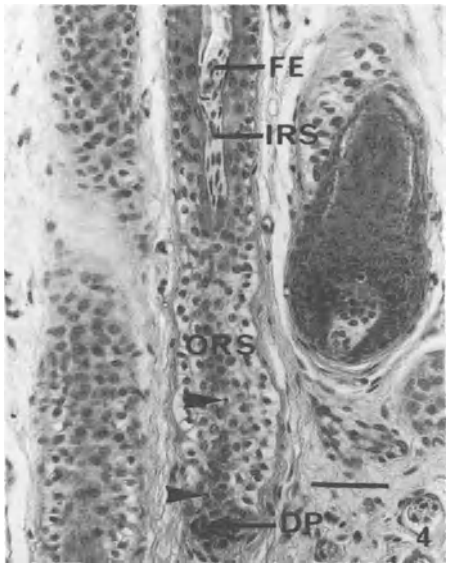

Fig. 4. Longitudinal section of the lower part of a wool follicle which regressed following intradermal administration of EGF. The end of the fibre (FE), which has ceased growing, is surrounded by the last of the inner root sheath cells (IRS). Apoptotic bodies (arrowheads) are present in the stalk of outer root sheath cells (ORS) between the fibre end and the dermal papilla (DP). Scale bar = 50 μm [46].

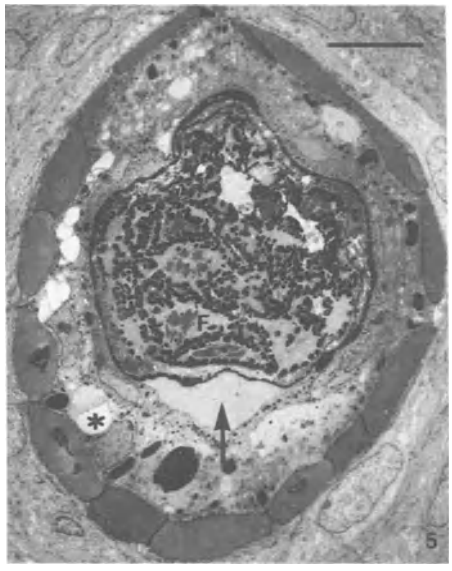

Fig. 5. Transverse section near the middle of the keratogenous zone of a wool follicle towards the end of an intravenous infusion of EGF. Endoplasmic reticulum is dilated (*) in inner root sheath cells and fluid and flocculent material (arrow) have accumulated intercellularly, distorting the wool fibre (F) Scale bar = 10 μm [44].

end and dermal papilla cells. This is similar to the apoptosis that occurs during the normal catagen phase of the cyclic hair growth in mice [47]. Regeneration of the regressed follicles commences in 4–8 days. In the remaining follicles, fibre growth continues but the fibres are markedly reduced in thickness for several days after the infusion of EGF. The proportions of follicles in which fibre growth ceases or continues are dose-dependent. When more than *c.* 250 μg EGF/(kg live weight)$^{0.75}$ are infused subcutaneously or intravenously, about half of the fibres stop growing and the remainder become so thin that they can be readily broken, thus permitting the fleece to be removed from the sheep. This depilatory action of EGF is the basis of a method being developed for harvesting fleeces from sheep as an alternative to conventional mechanical shearing.

EGF also induces mitochondrial swelling as well as dilation and vesiculation of endoplasmic reticulum in cells of Huxley's layer of the inner root sheath in the mid-keratogenous zone of the follicles. These changes develop as early as 1 h after the start of the infusion. Subsequently, by 6 h and until the infusion ceases, cells of

the inner root sheath and fibre cuticles and peripheral cortical cells are also affected and flocculent material accumulates intercellularly (Fig. 5). This results in a segment of fibre irregular in cross-section and with an aberrant cuticle pattern. By 24 h, hardening of the inner root sheath cells is retarded and this permits a length of fibre of increased diameter to form proximal to the segment of irregular cross-section before the fibre either ceases growing or becomes very thin.

Twice daily intradermal injections of 5 μg EGF for 3–4 days produce changes in the epidermis, follicles and fibres similar to those induced by infused depilatory amounts of EGF. However, epidermal thickening persists for a shorter time and follicle regression occurs more slowly after intradermal injection than after infusion.

Similar intradermal injections into sheep of either human or rat transforming growth factor α (TGF-α) (Bachem Inc. Torrance CA, U.S.A.) also induce follicle regression and inhibit wool growth (B.A. Panaretto and R.E. Chapman, unpublished data). This resembles the inhibition of hair growth by daily subcutaneous injections of TGF-α into mice [48]. Compared with the effects of intradermal injections of EGF into sheep, intradermal injections of TGF-α induce less thickening of the epidermis and less enlargement of sebaceous glands. Although TGF-α binds to receptors for EGF [49], these lesser effects may be the result of less effective binding of human or rat TGF-α to receptors in sheep epidermis and sebaceous glands than occurs with EGF of mouse origin.

Twice daily intradermal injections of 300 ng human transforming growth factor ß (TGF-ß) (R&D Systems Inc., Minneapolis MN, U.S.A.) into sheep for 4 days induce intense proliferation of fibroblasts and pronounced thickening of the connective tissue in the lower dermis (B.A. Panaretto and R.E. Chapman, unpublished data). Following cessation of injections, these effects subside within 2–3 days and the dermis regains its normal thickness. These responses resemble those produced by daily subcutaneous injections of human TGF-ß into newborn mice [50]. In addition to the dermal responses, some of the wool follicles exhibit partial extrusion of dermal papilla cells from within the bulbs, compaction of bulb cells and apoptosis in cells in the bulbar and suprabulbar regions during the course of the injections. These effects may be indirect responses mediated through either TGF-ß-induced alterations in extracellular matrix components or pressure generated by the rapid thickening of the underlying dermis. Alternatively, in view of the inhibition by TGF-ß of proliferation of various epithelial cell lines in culture, including keratinocytes [51,52] they may be direct responses to TGF-ß. Once initiated, they are apparently not immediately reversible because within 2–3 days after cessation of the injections some follicles regress and cease producing fibres. The time course for subsequent regeneration of the regressed follicles is yet to be determined.

The above results indicate that wool follicles and skin of adult sheep respond to administration of exogenous peptide growth factors. Other studies at this laboratory are concerned with establishing the existence and concentrations of endogenous growth factors in sheep tissues and their roles in foetal development and maintenance of wool follicle function in adult sheep.

References

1. Kempton TJ (1979) In: Black JL and Reis PJ (eds.) Physiological and Environmental Limitations to Wool Growth. University of New England Publishing Unit, Armidale, pp. 209–222.
2. Reis PJ (1979) In: Black JL and Reis PJ (eds.) Physiological and Environmental Limitations to Wool Growth. University of New England Publishing Unit, Armidale, pp. 223–242.
3. Reis PJ (1989) In: Rogers GE, Reis PJ, Ward KA and Marshall RC (eds.) Chapman and Hall, London, pp. 185–203.
4. Colebrook WF and Reis PJ (1969) Aust. J. Biol. Sci. 22: 1507–1516.
5. Reis PJ and Colebrook WF (1972) Aust. J. Biol. Sci. 25: 1057–1071.
6. Nagorcka BN (1979) In: Black JL and Reis PJ (eds.) Physiological and Environmental Limitations to Wool Growth. University of New England Publishing Unit, Armidale, pp. 127–137.
7. Panaretto BA (1979) In: Black JL and Reis PJ (eds.) Physiological and Environmental Limitations to Wool Growth. University of New England Publishing Unit, Armidale, pp. 327–336.
8. Hopkins PS and Richards MD (1979) In: Black JL and Reis PJ (eds.) Physiological and Environmental Limitations to Wool Growth. University of New England Publishing Unit, Armidale, pp. 321–325.
9. Corbett JL (1979) In: Black JL and Reis PJ (eds.) Physiological and Environmental Limitations to Wool Growth. University of New England Publishing Unit, Armidale, pp. 79–98.
10. Donald AD (1979) In: Black JL and Reis PJ (eds.) Physiological and Environmental Limitations to Wool Growth. University of New England Publishing Unit, Armidale, pp. 99–114.
11. Wallace ALC (1979) In: Black JL and Reis PJ (eds.) Physiological and Environmental Limitations to Wool Growth. University of New England Publishing Unit, Armidale, pp. 257–268.
12. Chapman RE (1979) In: Orfanos CE (ed.) Haar und Haarkrankheiten. Gustav Fischer Verlag, Stuttgart, pp. 167–204.
13. Gillespie JM (1983) In: Goldsmith LA (ed.) Biochemistry and Physiology of the Skin. Oxford University Press, New York, pp. 475–510.
14. Marshall RC and Gillespie JM (1977) Aust. J. Biol. Sci. 30: 389–400.
15. Gillespie JM and Broad A (1972) Aust. J. Biol. Sci. 25: 139–145.
16. Zahn H and Biela M (1968) Eur. J. Biochem. 5: 567–573.
17. Gillespie JM and Frenkel MJ (1976) Proc. Fifth Int. Wool. Text. Res. Conf. Aachen 2: 265–274.
18. Faichney GJ and Black JL (1979) In: Black JL and Reis PJ (eds.) Physiological and Environmental Limitations to Wool Growth. University of New England Publishing Unit, Armidale, pp. 179–192.
19. Reis PJ (1970) Aust. J. Biol. Sci. 23: 441–446.
20. Reis PJ and Tunks DA (1978) J. Agric. Sci. 90: 173–183.
21. Block RJ and Mitchell HH (1946) Nutr. Abstr. Rev. 16: 249–278.
22. Reis PJ and Tunks DA (1976) J. Agric. Sci. 86: 475–482.
23. Chapman RE, Colebrook WF and Black JL (1983) J. Agric. Sci. 101: 139–145.
24. Kerr JFR, Wyllie AH and Currie AR (1972) Br. J. Cancer 26: 239–257.
25. Chapman RE, Downes AM and Wilson PA (1980) Aust. J. Biol. Sci. 33:587–603.
26. Reis PJ and Schinckel PG (1963) Aust. J. Biol. Sci. 16: 218–230.
27. Reis PJ and Schinckel PG (1964) Aust. J. Biol. Sci. 17: 532–547.
28. Downes AM, Langlands JP and Reis PJ (1975) In: McLachlan KD (ed.) Sulphur in Australasian Agriculture. Sydney University Press, Sydney, pp. 117–124.
29. Reis PJ, Tunks DA and Downes AM (1973) Aust. J. Biol. Sci. 26: 249–258.
30. Williams AJ, Robards GE and Saville DG (1972) Aust. J. Biol. Sci. 25: 1269–1276.
31. Reis PJ and Tunks DA (1974) Aust. J. Agric. Res. 25: 919–929.
32. Lindsay JR, Hogan JP and Weston RH (1978) Proc. Nutr. Soc. Aust. Annu. Conf. 3: 76.
33. Wright PL (1971) J. Anim. Sci. 33: 137–141.
34. Chapman RE and Reis PJ (1978) Aust. J. Biol. Sci. 31: 161–172.
35. Masters DG, Chapman RE and Vaughan JD (1985) Aust. J. Biol. Sci. 38: 355–364.
36. Savage CR Jr. and Cohen S (1972) J. Biol. Chem. 247: 7609–7611.

37. Allen G, Winther MD, Henwood CA, Beesley J, Sharry LF, O'Keefe J, Bennett JW, Chapman RE, Hollis DE, Panaretto BA, Van Dooren P, Edols RW, Inglis AS, Wynn PC and Moore GPM (1987) J. Biotechnol. 5: 93–114.
38. Moore GPM, Panaretto BA and Robertson D (1981) Search (Syd.) 12: 128–129.
39. Moore GPM, Panaretto BA and Robertson D (1982) Aust. J. Biol. Sci. 35: 163–172.
40. Moore GPM, Panaretto BA and Carter NB (1985) J. Invest. Dermatol. 84: 172–175.
41. Hollis DE, Chapman RE, Panaretto BA and Moore GPM (1983) Aust. J. Biol. Sci. 36: 419–434.
42. McDonald BJ, Waters MJ, Richards MD, Thorburn GD and Hopkins PS (1983) Res. Vet. Sci. 35: 91–99.
43. Hollis DE and Chapman RE (1987) J. Invest. Dermatol. 88: 455–458.
44. Hollis DE and Chapman RE (1989) Aust. J. Agric. Res. 40: 1047–1063.
45. Hardy MH and Chapman RE (1986) Can. Fed. Biol. Soc. Proc. 29: 117.
46. Chapman RE and Hardy MH (1988) Aust. J. Biol. Sci. 41: 261–268.
47. Weedon D and Strutton G (1981) Acta Dermato-Venereol. 61: 335–339.
48. Tam JP (1985) Science 229:673–675.
49. Roberts AB, Frolik CA, Anzano MA and Sporn MB (1983) Fed. Proc. 42:2621–2626.
50. Roberts AB, Sporn MB, Assoian RK, Smith JM, Roche NS, Wakefield LM, Heine UL, Liotta LA, Falanga V, Kehrl JH and Fauci AS (1986) Proc. Natl. Acad. Sci. USA 83: 4167–4171.
51. Moses HL, Tucker RF, Leof EB, Coffey RJ, Halper J and Shipley GD (1985) Cancer Cells (Cold Spring Harbor) 3: 65–71.
52. Shipley GD, Pittelkow MR, Wille JJ, Scott RE and Moses HL (1986) Cancer Res. 46: 2068–2071.

Address for correspondence: Dr. R.E. Chapman, Division of Animal Production, CSIRO, P.O. Box 239, Blacktown, NSW 2148, Australia.

L-Arginine transport and regulation of endothelium-derived relaxing factor (nitric oxide) in cultured vascular endothelial cells*

C.-J. Sheriff[a], J.D. Pearson[b] and G.E. Mann[a]

[a]Biomedical Sciences Division, King's College London, Campden Hill Road, London W8 7AH, U.K.
[b]Section of Vascular Biology, MRC Clinical Research Centre, Harrow, U.K.

Abstract

Endothelial cells are involved in regulating vascular tone through their release of endothelium-derived relaxing factor (EDRF) and prostacyclin [1,2]. In cultured vascular endothelial cells release of nitric oxide is indistinguishable from EDRF, and recent evidence implicates L-arginine as an important physiological precursor for nitric oxide biosynthesis [3,4]. We have presently investigated the specificity and kinetics of L-arginine transport in perfused microcarrier cultures of bovine aortic endothelial cells using a dual isotope dilution technique, applied previously to cultured human umbilical vein endothelial cells [5]. L-arginine transport was saturable ($K_t = 206\ \mu M$, $V_{max} = 8.26$ nmol/min per 3×10^6 cells) and inhibited specifically by N^G-monomethyl-L-arginine and the cationic amino acids L-ornithine, L-lysine and L-citrulline. Although L-leucine was another effective inhibitor, 2-methylaminolsobutyric acid (System A analogue) was a poor competitor. We are currently investigating whether transport of exogenous L-arginine is rate-limiting for biosynthesis of nitric oxide in normal and diseased vascular endothelium.

Introduction

Endothelium-derived relaxing factor (EDRF), recently identified as nitric oxide [3], plays an essential role in the relaxation of arterial smooth muscle [1,2]. The term EDRF was introduced by Furchgott and Zawadzki [1] to describe the powerful vasodilator substance released from endothelial cells by acetylcholine, bradykinin and ATP. By activating soluble guanylate cyclase in vascular smooth muscle EDRF induces vascular relaxation and inhibits platelet aggregation and adhesion. Increased cGMP levels most likely mediate the sustained endothelium-dependent relaxation induced by acetylcholine and other relaxants [2].

Recent studies in cultured porcine aortic endothelial cells have shown that release of nitric oxide is indistinguishable from EDRF in its stability, biological activity and specificity of action [3,4]. Subsequently, Palmer and Moncada [6] demonstrated that a novel NADPH-dependent enzyme may be involved in the

* Supported by the British Heart Foundation, Medical Research Council (U.K.), SERC/CASE Cooperative Award with Wellcome Research Laboratories (U.K.) and King's College Academic Development Fund. C-J Sheriff is the recipient of a SERC PhD studentship.

generation of nitric oxide from the terminal guanidino nitrogen atom(s) of L-arginine [6]. The importance of L-arginine, and possibly other polypeptides rich in arginine, lysine and ornithine [7,8], in the generation of nitric oxide, prompted us to investigate L-arginine transport in perfused microcarrier cultures of bovine aortic endothelial cells using rapid tracer techniques. A preliminary abstract of this work has been published [9].

Materials and Methods

Culture and perfusion of bovine aortic endothelial cells in microcarrier bead columns

Endothelial cells were isolated from bovine aortae using collagenase and first passage cells were grown to confluence on Blosilon microcarrier beads [10], as described previously for porcine [11] and bovine [9] aortic endothelial cells. Briefly, flasks of confluent primary cells (approx. 10^6 cells) were subcultured into 50 ml of Dulbecco's modified Eagles medium (DMEM) supplemented with 10% newborn and 10% fetal calf serum in a silicone-treated 125 ml Techne stirring flask containing 2 ml of sterile microcarrier beads. Flasks were gassed with 95% air-5% CO_2 and incubated at 37°C during continuous stirring at 40 rpm. Within 5–7 days cells became confluent and each bead contained about 30–50 cells.

Microcarrier beads with confluent aortic endothelial cells were then transferred to the barrel of a 1 ml disposable syringe and, after inserting a modified plunger, were perfused at 37°C from below at 0.35 ml/min [5,9] with a HEPES buffered Krebs-Henseleit medium of the following composition (mmol/l): NaCl, 131; KCl, 5.6; $CaCl_2$, 2.5; $MgCl_2$, 1.0; $NaHCO_3$, 25; NaH_2PO_4,, 1.0; D-glucose, 5.5.

Measurement of endothelial cell amino acid and D-glucose transport

Unidirectional nutrient transport was measured using a rapid dual isotope dilution technique [12], employed previously for studies of amino acid, glucose and catecholamine uptake in cultured human umbilical vein endothelial cells [5]. After 45–60 min equilibration with an amino acid-free solution, endothelial cells were challenged (100 µl) with L-[^{3}H]arginine (or another ^{3}H-amino acid) and D-[^{14}C]mannitol (extracellular reference) and the column effluent was collected sequentially (Fig. 1A). Fractional [^{3}H] uptake was calculated for each of the successive effluent samples: uptake = [1 − (L-[^{3}H]arginine/D-[^{14}C]mannitol)] (Fig. 1B).

The inhibitory effects of different possible 'competitor' amino acids were examined by adding a given unlabelled amino acid (1 mM) to successive 100 µl isotope challenges containing tracer doses of L-[^{3}H]arginine and D-[^{14}C]mannitol. These experiments enabled us to screen the selectivity of L-arginine uptake at the

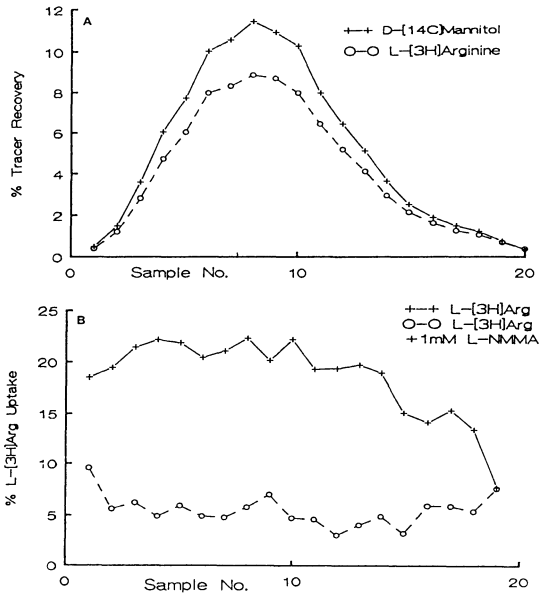

Fig. 1. Unidirectional L-arginine uptake by cultured bovine aortic endothelial cells. A) paired effluent dilution profiles for D-[^{14}C]mannitol (extracellular reference) and L-[^{3}H]arginine were obtained after challenging an endothelial cell column with both tracers. The column effluent was collected sequentially for 2 min and tracer recoveries are normalized with respect to the challenge doses. B) time course of L-[^{3}H]arginine uptake relative to D-[^{14}C]mannitol was calculated from the successive effluent samples shown in Fig. 1A. Figure 1A also shows an uptake profile for L-[^{3}H]arginine (dilution data not shown) obtained following a successive challenge of the same column with 1 mM N^{G}-monomethyl-L-arginine.

luminal surface of confluent endothelial cells. In kinetic experiments unlabelled L-arginine was added to the control perfusate and isotope challenges at concentrations ranging from 25–400 μM. Endothelial cells were equilibrated for 2 min with each concentration before measuring influx in the continued presence of substrate. Unidirectional transport of L-arginine was estimated from the maximal fractional tracer uptake (U_{max}), the perfusion rate (F, ml/min) and perfusate concentration of L-arginine (Ca): influx ($-F \times \ln(1 - U_{max}) \times C_a$. Michaelis-Menten kinetic constants were estimated assuming a single entry site analysis.

Materials

L-[2,3-^{3}H]arginine (41.9 Ci/mmol), L-[2,3-^{3}H]ornithine (50 Ci/mmol), L-[4,5-^{3}H]lysine (97.3 Ci/mmol), 2-[^{14}C]MeAIB (46.4 mCi/mmol), L-[3-^{3}H]serine (37 Ci/mmol), L-[4,5-^{3}H]leucine (143.7 Ci/mmol), L-[4-^{3}H]phenylalanine (26 Ci/mmol), D-[1-^{3}H]glucose, D-[1-^{14}C]mannitol (52 mCi/mmol) and D-[1-^{3}H]manni-

tol (19 Ci/mmol) were obtained from either NEN, Dreieich, F.R.G. or Amersham International plc, U.K. Unlabelled amino acids and other analytical grade reagents were purchased from Sigma. N^G-monomethyl-L-arginine was kindly provided by Dr S. Moncada from the Wellcome Research Laboratories, Beckenham, Kent, U.K.

Results

Amino acid uptake by bovine aortic endothelial cells

Figure 1A shows representative effluent tracer dilution profiles obtained with confluent bovine aortic endothelial cells perfused in a microcarrier bead column. Recovery of L-[^{3}H]arginine was less than that of D-[^{14}C]mannitol (extracellular tracer), indicating endothelial cell uptake of L-[^{3}H]arginine [9]. The time course of L-[^{3}H]arginine uptake reached a maximum within 15 s, and thereafter gradually decreased with time due to [^{3}H] efflux (Fig. 1B). When the same endothelial cells were rechallenged with 1 mM N^Gmonomethyl-L-arginine (an inhibitor of nitric oxide production, 13), uptake of L-[^{3}H]arginine was inhibited significantly (Fig. 1B). This rapid inhibition suggests *cis-inhibition* of inward transport.

Cultured aortic endothelial cells rapidly transport cationic and neutral amino acids (Fig. 2), and at identical packed microcarrier bead volumes tracer uptakes were similar to values measured previously in perfused microcarrier cultures of human umbilical vein endothelial cells [5]. Tracer amino acids have been grouped according to the specific transporters known to mediate their uptake in other mammalian cell types [14]. Unlike our earlier findings in venous endothelium [5], aortic endothelial cells exhibit a small but measurable uptake for the System A

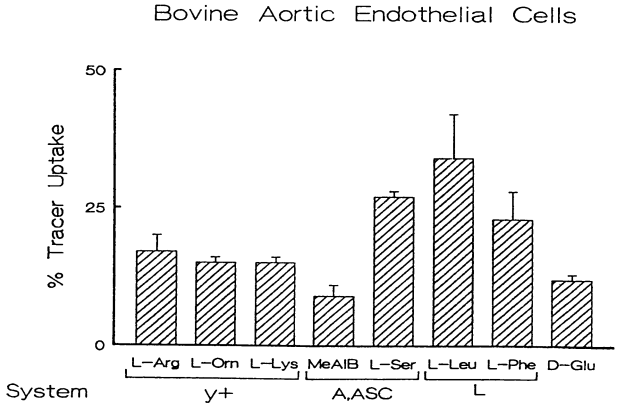

Fig. 2. Uptake of amino acids and glucose by bovine aortic endothelial cells. Unidirectional uptakes relative to D-mannitol were assessed at tracer concentrations during perfusion of endothelial cells with an amino acid-free medium containing 5.5 mM D-glucose. Values denote the mean ± S.E. of measurements in at least 3 different cell cultures.

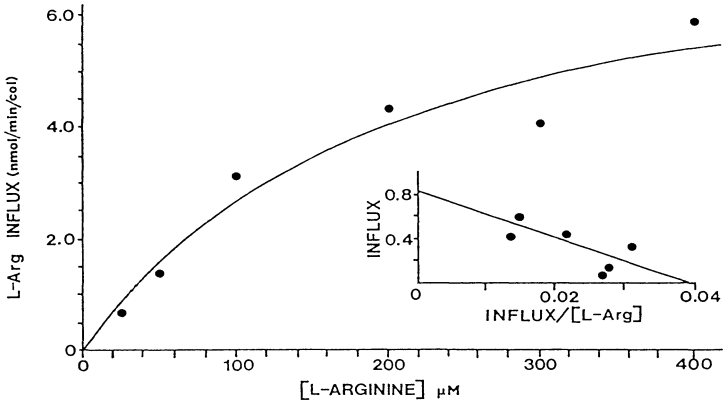

Fig. 3. Saturation of L-arginine transport in bovine aortic endothelial cells. Unidirectional transport of L-arginine was measured during perfusion of endothelial cells at 0.35 ml/min with different concentration of unlabelled L-arginine. The curve is a rectangular hyperbola obtained by a direct fit to the influx values. The inset illustrates an Eadie-Hofstee transformation of the data.

analogue 2-MeAIB. Although uptake of D-[^{3}H]glucose was low during perfusion of cells with 5.5 mM glucose, this uptake reflects a unidirectional transport rate of 0.25 μmol/min per 3×10^6 cells.

Saturation of L-arginine transport

When L-arginine transport was examined at physiological plasma concentrations (25–400 μm), influx was saturable with an apparent $K_t = 206$ μM and $V_{max} = 8.26$ nmol/min per 3×10^6 cells (Fig. 3). Over this range of substrate concentrations transport appeared to be mediated by a single entry site. Further detailed kinetic inhibition studies are necessary to establish whether at higher substrate concentrations entry of L-arginine is mediated by an additional diffusional pathway described recently in bovine aortic monolayers [15]. As tracer efflux is prominent in perfused aortic endothelial cell cultures, measurements of net uptake in microcarrier columns, and particularly static endothelial cell monolayers [15], would not reflect unidirectional transport.

Inhibition of L-arginine transport by cationic and neutral amino acids

In these experiments aortic endothelial cells were challenged with L-[^{3}H]arginine and D-[^{14}C]mannitol in the absence or presence of different unlabelled amino acids (1 mM). As shown in Fig. 4, uptake of L-[^{3}H]arginine was significantly inhibited during perfusion of cells with 1 mM N^G-monomethyl-L-arginine (L-NMMA). Although L-arginine transport was restored to control levels upon washout of N^G-monomethyl-L-arginine, further kinetic experiments are necessary to determine

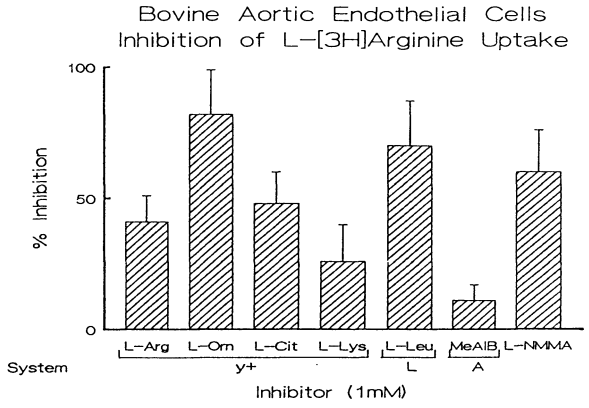

Fig. 4. Specificity of aortic endothelial cell amino acid transport. Endothelial cells were perfused with an amino acid-free medium, and unidirectional L-[^{3}H]arginine uptake was measured in the absence (U_c) or presence (U_i) of a given unlabelled amino acid (1 mM). Percentage inhibition in tracer uptake was calculated from $[(1 - U_i/U_c) \times 100]$, and the values denote the mean ± S.E. of measurements in at least 3 different cell cultures. Inhibitor amino acids are identified using standard three-letter nomenclature and are grouped according to their known effectiveness in inhibiting specific amino acid transporters in other cell types.

whether this analogue is a transportable competitor of L-arginine uptake. The cationic amino acids L-ornithine, L-citrulline and L-lysine, as well as, the neutral substrate L-leucine were also effective inhibitors. Interestingly, uptake was negligibly affected by the non-metabolized System A analogue MeAIB (Fig. 4).

Discussion

The present study has established that cultured bovine aortic endothelial cells perfused in microcarrier bead columns rapidly transport cationic and neutral amino acids. L-arginine transport appears to be carrier-mediated with an apparent, K_t = 206 μM and V_{max} = 8.26 nmol/min × 10^6 cells and is inhibited significantly by cationic and large neutral amino acids and N^Gmonomethyl-L-arginine.

In macrophages formation of oxides of nitrogen (NO_2, NO_3) from the guanidino nitrogen atom(s) of L-arginine appear to be involved in macrophage cytotoxic activity [16,17]. Nitric oxide (NO) reacts rapidly with O_2 to produce NO_2 which then generates NO_2 and NO_3 in neutral aqueous solution. Similar to observations in cultured aortic endothelial cells [13] N^G-monomethyl-L-arginine effectively inhibits formation of NO-containing compounds. However, macrophages and endothelial cells exhibit unexplained differences in their substrate specificity [4,16,17].

The role of other polypeptides rich in arginine, lysine and ornithine merits detailed further study, as it has been suggested that basic peptides containing L-arginine stimulate EDRF release, thereby inducing vascular relaxation [7].

Ignarro *et al.* [8] have reported that basic polyamino acids elicit endothelium- and cGMP-dependent relaxation of pulmonary artery and vein. These authors suggested that basic polyamino acids serve as partial or alternative substrates for the enzyme system(s) that catalyze conversion of L-arginine to nitric oxide in endothelial cells. Clearly, further studies are necessary to resolve the substrate specificity of this enzyme system(s) and whether transport of exogenous L-arginine is rate-limiting for nitric oxide production in normal and diseased vascular endothelium.

Abnormalities in endothelial cell mediated control of underlying vascular smooth muscle may serve as important clinical signs of atherosclerosis, hypertension [18] and coronary artery disease [19]. Our unique experimental approach provides the basis for establishing whether L-arginine is the principal exogenous precursor for nitric oxide biosynthesis in vascular endothelium.

References

1. Furchgott RF and Zawadzki JV (1980) Nature 288: 373–376.
2. Vanhoutte PM (1988) In: Vanhoutte PM (ed.) Relaxing and Contracting Factors, Humana Press Inc., New Jersey.
3. Palmer RJ, Ferrige AG and Moncada S (1987) Nature 327: 524–526.
4. Palmer RJ, Ashton DS and Moncada S (1988) Nature 333: 664–666.
5. Mann GE, Pearson JD, Sheriff C-J and Toothill VJ (1989) J. Physiol. 410: 325–339.
6. Palmer RJ and Moncada S (1989) Biochem. Biophys. Res. Comm. 158: 340–353.
7. Thomas G, Hecker M and Ramwell PW (1989) Biochem. Biophys. Res. Comm. 158: 177–180.
8. Ignarro LJ, Gold ME, Buga GM, Byrns RE, Wood KS, Chaudhuri G and Frank G (1989) Cir. Res. 64: 315–329.
9. Mann GE, Pearson JD and Sheriff C-J (1989) J. Physiol., 415: 81P.
10. Jaffe EA, Nachman RL, Becker CG and Minick CR (1973) J. Clin. Invest. 52: 2745–2756.
11. Needham L, Cusack NJ, Pearson JD and Gordon JL (1987) Eur. J. Pharmacol. 134: 199–209.
12. Yudilevich DL and Mann GE (1982) Fed. Proc. 41: 3045–3053.
13. Palmer RJ, Rees DD, Ashton DG and Moncada S (1988) Biochem. Biophys. Res. Comm. 153: 1251–1256.
14. Christensen HN and Kilberg MS (1987) In: Yudilevich DL and Boyd CAR (eds.) Amino Acid Transport in Animal Cells. Manchester Univ. Press. pp. 1–46.
15. Sneddon JM, Bearpark TM and Vane JR (1989) Br. J. Pharmacol. 97: 514P.
16. Hibbs JB, Taintor RR and Vavrin Z (1987) Science 235: 473–476.
17. Iyengar R, Stuehr DJ and Marletta MA (1987) Proc. Natl. Acad. Sci. USA 84: 6369–6373.
18. Van de Voorde J, Vanheel B and Leusen I (1988) Pflugers Arch. 411: 500–504.
19. Werns SW, Walton JA, Hsia HH, Nabel EG, Sanz ML and Pitt B (1989) Cir. Res. 79: 287–291.

Address for correspondence: Dr G.E. Mann, Physiology, Biomedical Sciences Division, King's College London, Campden Hill Road, London W8 7AH, U.K.

Error rates and mechanism of substrate recognition in aminoacylation of tRNAs by aminoacyl-tRNA synthetases

Wolfgang Freist

Max-Planck-Institut für experimentelle Medizin, Abteilung Chemie, Göttingen, F.R.G.

Abstract

Substrate specificity with regard to naturally occurring amino acids has been investigated with four aminoacyl-tRNA synthetases. Discrimination factors D were calculated from k_{cat} and K_m values observed in aminoacylation of tRNA-C-C-A. Highest specificities were found for tyrosyl-tRNA synthetase from yeast with D values of 30,000–500,000 which show that tyrosine is 30,000–500,000 times more often attached to tRNA than noncognate amino acids at the same amino acid concentration. Arginyl- and isoleucyl-tRNA synthetases exhibit generally medium D values of 10,000–70,000 but with regard to a few amino acids (Cys, Arg, Trp) even lower values of 300–3,000.

Lower specificities are observed in aminoacylation of the modified substrate tRNA-C-C-A(3'NH_2) (D_1 = 20–55,000). From kinetic constants and AMP-formation stoichiometry observed in aminoacylation of this tRNA species as well as in acylating tRNA-C-C-A hydrolytic proofreading factors could be calculated for a pretransfer (π_1) and a posttransfer (π_2) proofreading step. The observed values show that pretransfer proofreading is the main correction step for most amino acids.

Initial discrimination factors caused by differences in Gibbs free energy of binding are calculated from discrimination and proofreading factors. Assuming a two step binding process two factors (I_1 and I_2) were determined which can be related to hydrophobic interaction forces and hydrogen bonding.

Introduction

Protein biosynthesis is achieved by translation of the genetic code into protein structures by a translation apparatus working with extraordinary high precision. Incorrect translation would cause incorporation of 'wrong' amino acids into proteins and as one consequence accumulation of malfunctioning enzymes. Increasing error rates in translation of the genetic code have been discussed as a reason of biological ageing [1,2]. Although today this proposed 'error catastrophy' is no longer accepted as the only reason of biological ageing [3–5] error rates in protein biosynthesis are still a matter of interest with regard to stability of the translation apparatus [6,7].

A crucial step in protein biosynthesis is the esterification of a special tRNA with its cognate amino acid. Aminoacyl-tRNA synthetases, the enzymes which catalyse this step, have to recognize their cognate tRNA in a population of about sixty species and their cognate amino acid among twenty naturally occurring compounds. Attachment of a 'wrong' amino acid to the tRNA would result in erroneous proteins.

Specificity of aminoacyl-tRNA synthetases with regard to amino acids was intensively investigated with isoleucyl-tRNA synthetases from *Escherichia coli* and yeast and with the enzymes specific for tyrosine and arginine prepared from yeast. Experiments with chemically modified tRNAs allowed to draw conclusions on the single steps of the recognition process and special properties of these enzymes which enable them to work with high accuracy.

Materials and Methods

Isoleucyl-tRNA synthetases from *E. coli* MRE 600 and yeast have been isolated as given in [8] and [9], tyrosyl- and arginyl-tRNA synthetases as described in [10] and [11]. The preparations had specific activities of 0.420, 0.493, 8.74 and 2.44 U/mg protein in the aminoacylation reaction. One enzyme unit catalysed the aminoacylation of 1 μmol tRNA in 1 min at 37°C under standard conditions. The absence of other aminoacyl-tRNA synthetases in the preparations was proven as described in [12]. For determination of k_{cat} values the concentrations of isoleucyl- and tyrosyl-tRNA synthetases were determined by the nitrocellulose filter assay as in [13], that of arginyl-tRNA synthetase as in [14].

Pure *E. coli* $tRNA^{Ile}$ was isolated from *E. coli* MRE 600 purchased from Boehringer (Mannheim, F.R.G.) [9], pure yeast $tRNA^{Ile}$, $tRNA^{Tyr}$ and $tRNA^{Arg}$ from commercially available yeast tRNA (Boehringer Mannheim, F.R.G.) as described in [15–17]. The preparations were tested for presence of other tRNAs as in [12]. From these tRNA preparations the modified tRNA species $tRNA^{Ile}$-C-C-A(3'NH_2), $tRNA^{Tyr}$-C-C-A(3'NH_2) and $tRNA^{Arg}$-C-C-A(3'NH_2) were prepared with the aid of nucleotidyltransferase (EC 2.7.7.25) from yeast by reaction of 3'-deoxy-3'-amino-ATP with tRNA-C-C and analysed as indicated in [12].

^{14}C-labelled amino acids were from the same sources and of the same specific activities as given in [12].

[8-^{14}C]Adenosine 5'-triphosphate with a specific activity of 546 Ci/mol was purchased from Amersham Buchler GmbH (Braunschweig, F.R.G.) and diluted with the tenfold amount of unlabelled material.

Aminoacylation of tRNA-C-C-A and tRNA-C-C-A(3'NH_2) with ^{14}C-labelled amino acids

The standard reaction mixture (0.1 ml) contained 0.15 M Tris/ HCl buffer pH 7.65, 0.1 M KCl, 0.015 M $MgSO_4$, 2–5 mM ATP, 1–10 μM tRNA and ^{14}C-labelled amino acids in the range of 20–200 μM. The reaction mixture was preincubated at 37°C, then the enzymes were added to concentrations of 30–150 pM. The velocity of the esterification reaction was measured by the amount of ^{14}C-labelled amino acids incorporated into tRNA as described in [12].

For calculation of K_m and k_{cat} values, data were given from the scintillation counter directly to a Personal Computer (Y-E Data Inc. 8105, Tokyo, Japan);

aminoacylation velocities and Lineweaver-Burk plots were calculated by linear regression programs. For the resulting D and D_1 values medium errors of 20% are estimated.

AMP formation under aminoacylation conditions

The assay mixture contained 0.15 M Tris/HCl buffer pH 7.65, 0.1 M KCl, 0.015 M $MgS0_4$, 0.2 mM [^{14}C]ATP, 0.02 mM ^{14}C-labelled amino acid and 1–10 μM tRNA. All experiments were run as in [12]. The total experimental error in π'or π_1 values is estimated to be in a range of ± 20%. When I_1 and I' values are calculated from D_1 and π_1 or D and π' values mean errors of 30% may occur. These typical errors may cause mean deviations of $\Delta\Delta G_{I1}$ and $\Delta\Delta G_{I2}$ values of ±0.8 kJ (0.2 kcal) due to the logarithmic function by which they are calculated ($\Delta\Delta G = RTlnI$).

Results and Discussion

Discrimination of amino acids in aminoacylation of tRNA-C-C-A: overall discrimination factors D

For discrimination between cognate and noncognate substrates the quotient of reaction velocities is decisive by which the substrates are converted to products. This quotient depends on substrate concentration and a discrimination factor D:

$$v_c/v_n = D\cdot([aa_c]/[aa_n])$$

Factor D can be calculated from kinetic constants [18]:

$$D = (k_{cat}/K_m)_c/(k_{cat}/K_m)_n$$

D values obtained in aminoacylation of naturally occurring specific tRNA-C-C-A with four aminoacyl-tRNA synthetases are listed in Table 1. These factors differ considerably. Comparing isoleucyl-tRNA synthetases from *E. coli* and yeast higher specificity of the bacterial enzyme is observed. In most cases D values of the *E. coli* enzyme are 2–9 times as high as those of the yeast enzyme; in some cases even about 40 times as high. Both enzymes achieve the best discrimination against valine, the amino acid structurally most similar to the cognate substrate. Tyrosyl- and arginyl-tRNA synthetases from yeast show higher discrimination factors than isoleucyl-tRNA synthetase from the same source. D values of the first enzyme are about tenfold higher; D values of the latter enzyme are in a medium range. Both enzymes show the lowest specificity in discrimination of amino acids with structures most similar to the cognate one. A common property which is observed for all the four enzymes is a relatively low specificity in discrimination between the cognate substrate and cysteine and tryptophan. However, even these

Table 1. Overall discrimination factors D calculated from k_{cat} and K_m values observed with isoleucyl-tRNA synthetases from *E. coli* and yeast and tyrosyl- and arginyl-tRNA synthetases from yeast in aminoacylation of tRNA-C-C-A

Amino acid	D values of enzymes specific for			
	Ile (*E. coli*)	Ile (yeast)	Tyr (yeast)	Arg (yeast)
Gly	63,100	16,600	>500,000	30,300
Ala	68,400	1,800	>500,000	29,000
Ser	42,700	12,800	>500,000	15,200
Cys	620	300	39,500	2,200
Pro	49,700	7,200	463,100	52,500
Asp	39,100	700	370,700	32,100
Thr	25,600	20,800	285,600	31,000
Asn	24,100	600	378,600	18,200
Val	71,900	38,000	263,600	21,000
Gln	48,800	9,200	178,500	18,200
Ile	1	1	369,900	24,800
Leu	21,600	12,200	285,600	22,700
Glu	38,300	6,100	136,700	19,500
His	25,600	3,600	142,800	19,500
Met	26,600	16,600	117,400	18,200
Phe	42,100	6,300	29,400	31,000
Lys	21,000	7,800	153,500	8,000
Tyr	28,500	3,100	1	11,400
Arg	2,800	1,800	122,700	1
Trp	3,400	700	28,600	800

low specificities should be sufficient to keep the translation apparatus stable as was shown in experiments on bacterial growth with error promoting drugs [19].

Discrimination of amino acids in aminoacylation of tRNA-C-C-A(3'NH_2): discrimination factors D_1

Chemically modified tRNAs as tRNA-C-C-A(3'NH_2) with an amino group in position 3' of the terminal ribose of the tRNA could be used as valuable tools in elucidation of the recognition process. When the discrimination factors (called D_1) were determined in the aminoacylation reaction with these tRNA species, considerably lower specificities than in acylation of tRNA-C-C-A were observed [12,20,21] (Table 2). Comparing these D_1 values observed with the four enzymes a

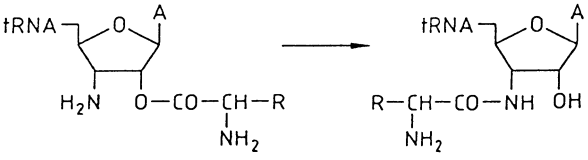

Table 2. Overall discrimination factors D_1 calculated from k_{cat} and K_m values observed with isoleucyl-tRNA synthetases from *E. coli* and yeast and tyrosyl- and arginyl-tRNA synthetases from yeast in aminoacylation of tRNA-C-C-A(3'NH_2)

Amino acid	Ile (*E. coli*)	Ile (yeast)	Tyr (yeast)	Arg (yeast)
Gly	4,348	1,191	54,800	204
Ala	3,750	617	29,100	349
Ser	1,633	641	13,300	572
Cys	26	22	490	17
Pro	2,222	249	4,000	596
Asp	1,944	167	780	336
Thr	800	362	2,400	371
Asn	727	139	2,300	89
Val	100	167	10,000	333
Gln	2,432	427	6,700	304
Ile	1	1	16,900	485
Leu	692	556	6,650	381
Glu	1,600	407	6,650	867
His	899	69	4,900	286
Met	2,069	617	3,700	371
Phe	1,961	556	780	143
Lys	1,613	177	13,900	84
Tyr	2,469	388	1	191
Arg	1,010	128	8,500	1
Trp	210	69	2,000	51

similar picture is obtained as for the D values, only on a lower level. To explain the lower specificities one has to consider the different structures of the tRNAs. During aminoacylation the amino acid is attached to the hydroxy group of the terminal ribose and migrates spontaneously to the amino group in the position 3' yielding an aminoacyl amide instead an aminoacyl ester [12,20,21]. These amides are much more stable against hydrolysis than the esters and a special correction step which is described below cannot be carried out by the enzymes.

Pretransfer proofreading factors π_1 and initial discrimination factors I_1

$$E + aa + ATP \rightarrow E{\cdot}aa\text{-}AMP + PP_i$$

$$E{\cdot}aa\text{-}AMP + tRNA \rightarrow E + aa\text{-}tRNA + AMP$$

According to the two step reaction mechanism which is generally accepted for aminoacylation of tRNAs for each aminoacyl-tRNA generated also one molecule of AMP must be formed. When the stoichiometry of AMP formation was investigated in aminoacylation of tRNA-C-C-A(3'NH_2) it turned out that in misacylation with noncognate amino acids considerably more AMP was generated than one molecule per one acylated tRNA. This observation could be explained by a special

'proofreading' step in which aminoacyl-tRNA synthetases reject misactivated noncognate amino acids by hydrolysis of the aminoacyl-adenylate, the intermediate formed in the first reaction step [22,23,20,12]. This process called 'pretransfer proofreading' is characterized by a pretransfer proofreading factor π_1 which gives the quotient of the number of AMP molecules formed in a misactivation and the number of AMP molecules generated with the cognate substrate. These factors are listed in Table 3, for isoleucyl- and tyrosyl-tRNA synthetases they appear in a range of 10–280, only for arginyl-tRNA synthetase values below 10 are observed.

Because discrimination of amino acids is also dependent on the different Gibbs free energies of binding in the special amino acid binding site discrimination factors D_1 are the product of an initial discrimination factor I_1 which is due to the different binding energies and of proofreading factor π_1: $D_1 = I_1.\pi_1$ [23,12,20]. Thus, factors I_1 can be calculated as $I_1 = D_1/\pi_1$. Their values vary in a range of 1–1,000 (Table 3).

Posttransfer proofreading factors π_2 and initial discrimination factors I_2

When AMP formation rates in aminoacylation of natural tRNA-C-C-A are measured higher numbers of AMP molecules per one acylated tRNA-C-C-A are found [23,12,20]. This phenomenon is due to a second proofreading step occurring after transfer of the amino acid to the tRNA-C-C-A. In aminoacylation of tRNA-C-C-A(3'NH_2) this step was blocked because stable amides were formed. The 'posttransfer proofreading' is achieved by the enzyme hydrolysing the aminoacyl-tRNA esters of the natural tRNA-C-C-A. The overall proofreading factors π' are given by the quotient of AMP formation rates of noncognate and of cognate substrates. Because factor π' is the product of the pretransfer and the posttransfer proofreading factor factors π_2 can be calculated as $\pi_2 = \pi'/\pi_1$ [23,12,20]. The obtained values given in Table 3 are in most cases considerably lower than factors π_1 indicating that pretransfer proofreading is the main correction step for most amino acids.

When overall initial discrimination factors are calculated as $I' = D/\pi'$ values are obtained which are higher than factors I_1. As a rational explanation for this observation higher binding energies caused by a more densely packed binding site are assumed, and in acylation of tRNA-C-C-A(3'NH_2) this pocket may not be complete. In acylation of tRNA-C-C-A binding of amino acids is achieved in a two step process for which two initial binding factors, I_1 and I_2, must be assumed [23,12,20]. These factors multiply to the overall initial discrimination factors I', and I_2 can be calculated as $I_2 = I'/I_1$. They vary between 2 and 300 (Table 3).

The complete process of amino acid recognition is achieved in at least four steps which are shown in Scheme 1. Two 'physical' steps enable the enzyme to distinguish the amino acids by different binding energies (factors I_1 and I_2), in two chemical steps 'wrong' products are hydrolysed (factors π_1 and π_2). However, in some cases posttransfer proofreading is marginal and may be neglected.

Table 3. Proofreading factors π_1 and π_2 calculated from AMP formation stoichiometry and initial discrimination factors I_1 and I_2 calculated from factors D_1, D and π_1 and π_2 obtained for isoleucyl-tRNA synthetases from *E. coli* and yeast and tyrosyl- and arginyl-tRNA synthetases from yeast

Amino acid	Ile (*E. coli*)				Ile (yeast)				Tyr (yeast)				Arg (yeast)			
	π_1	I_1	π_2	I_2	π_1	I_1	π_2	I_2	π_1	I_1	π_2	I_2	π_1	I_1	π_2	I_2
Gly	30	144.9	1.3	13.7	14	84.5	1.1	12.7	55	999.4	—	—	56	3.6	0.5	300.6
Ala	54	69.4	3.0	6.2	28	22.3	0.5	5.8	81	359.4	—	—	4.7	74.3	6.4	13.0
Ser	51	32.0	1.1	24.0	31	20.4	0.9	23.0	56	237.5	—	—	31	18.5	1.5	17.9
Cys	12	2.2	2.9	8.2	7	3.2	1.1	12.3	280	1.8	1.8	44	3.3	5.2	0.8	151.1
Pro	65	34.2	1.3	17.0	62	4.0	0.9	32.6	65	61.5	2.8	41	54	11.0	0.7	130.3
Asp	109	17.8	1.3	15.6	61	2.8	0.5	8.8	12	65.0	47.5	10	71	4.7	0.8	119.8
Thr	100	8.0	3.1	10.2	61	5.9	1.1	55.1	64	37.5	4.2	29	4.2	88.3	10.7	7.8
Asn	59	12.3	2.1	16.1	25	5.6	0.6	6.9	53	43.4	2.8	58	26	3.4	1.1	184.6
Val	22	4.5	61.6	11.8	51	3.3	3.0	76.5	28	357.1	1.3	21	70	4.6	2.3	35.4
Gln	72	33.8	1.0	19.6	40	10.8	0.7	29.7	106	63.2	1.4	19	16	19.0	5.7	10.5
Ile	1	1.0	1.0	1.0	1	1.0	1.0	1.0	236	71.6	1.4	15	35	13.9	1.6	32.4
Leu	121	5.7	8.9	3.5	70	7.9	0.7	31.7	75	88.7	1.2	35	48	7.9	2.6	22.4
Glu	61	26.2	2.2	10.6	56	7.3	0.6	27.0	48	138.5	1.0	22	45	19.3	2.9	7.7
His	68	13.2	1.9	15.3	41	1.7	1.5	33.9	92	53.3	1.1	27	24	11.9	2.7	18.3
Met	161	12.9	2.1	6.2	33	7.5	1.3	51.1	127	29.1	1.3	25	120	3.1	0.8	59.5
Phe	119	16.5	1.4	9.3	85	6.5	0.5	24.1	92	8.5	1.8	20	2.4	59.6	1.7	130.0
Lys	84	19.2	1.4	9.3	46	3.9	1.5	29.6	97	143.3	1.0	11	64	1.7	1.2	62.0
Tyr	41	60.2	1.2	9.5	33	11.7	0.6	14.4	1	1.0	1.0	1	62	3.1	1.5	40.0
Arg	98	10.3	1.2	2.1	76	1.7	0.6	25.1	141	60.3	1.9	7.4	1	1.0	1.0	1.0
Trp	56	3.8	1.4	10.5	66	1.0	1.1	9.6	48	41.7	2.4	6.0	2.6	25.8	7.3	1.6

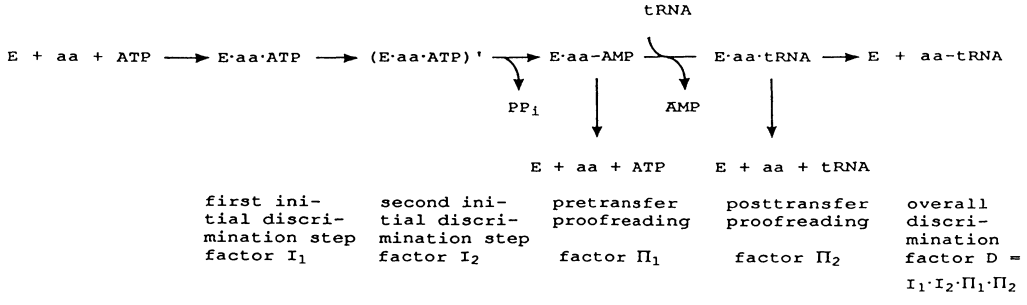

Scheme 1. Four step recognition of amino acids.

Relation of initial discrimination factors I_1 and I_2 to accessible surface areas of amino acids

In binding of amino acids at the specific binding pockets hydrophobic interaction plays an important role. The interaction energy is determined by the accessible surface areas of amino acids which are removed from contact with water, a medium energy gain of 105 J/mol (25 cal/mol) is given per 0.01 nm^2 (1 $Å^2$) for such interaction in literature [24–26]. Initial discrimination factors I_1 and I_2 which are due to different Gibbs free energies of binding of cognate and noncognate

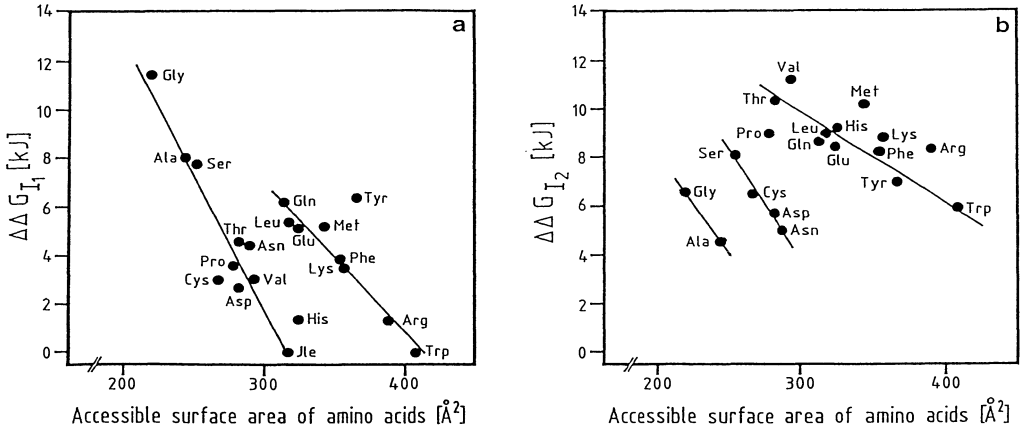

Fig. 1. Plots of $\Delta\Delta G_{I1}$ values (a) and $\Delta\Delta G_{I2}$ values (b) against accessible surface areas of amino acids [32] measured for $tRNA^{Ile}$-C-C-A(3'NH_2) and $tRNA^{Ile}$-C-C-A in aminoacylation with isoleucyl-tRNA synthetase from yeast.

substrates are related to these energy differences by the equation

$$I = e^{\Delta\Delta G / RT}$$

and thus $\Delta\Delta G$ values can be calculated as $\Delta\Delta G = RT\ln I$.

If $\Delta\Delta G_{I_1}$ or $\Delta\Delta G_{I_2}$ values obtained for the different amino acids are plotted against accessible surface areas of the acids linear relationships are observed. In Fig. 1a this is shown for aminoacylation of $tRNA^{Ile}C\text{-}C\text{-}A(3'NH_2)$ by isoleucyl-tRNA synthetase from yeast. Here two groups of amino acids can be distinguished. Generally the first group consists of acids with side chains smaller than the isobutyl moiety of isoleucine; the second group is composed of amino acids with longer side chains. In the first group from the slope of the plot a Gibbs free energy of 11.1 kJ/nm^2 (26.5 cal/Å^2) can be calculated, in the second group a value of 6.1 kJ/nm^2 (14.6 cal/Å^2); these numbers are very well in the range of hydrophobic interaction energies of amino acid side chains in proteins [24–26].

The existence of two groups of amino acids may be explained by a simple model [12]: The enzyme possesses a binding cavity which is suitable for the surface and length of the isoleucine side chain. The length of this cavity may be restricted by a bulky 'stopper' group. If amino acids are longer than isoleucine this 'stopper' has to be pushed aside and the free energy value of this conformational change corresponds to the difference in $\Delta\Delta G_{I1}$ between the two straight lines at the jumping point. If $\Delta\Delta G_{I2}$ values are plotted against accessible surface areas of amino acids similar linear relations are obtained (Fig. 1b), but in this group the values must be assigned to three lines and it must be suspected that two 'stopper' groups are responsible for this distribution.

These observations may be explained by an extended model of the isoleucine binding cavity [27]: After binding of the amino acid at the initial binding site (characterized by $\Delta\Delta G_{I1}$) a conformational change of the enzyme may occur which makes it possible that another part of the protein comes also in contact with the substrate (characterized by $\Delta\Delta G_{I2}$). In this way the binding pocket is completed to a dense package (Fig. 2). Shape and length of the amino acid side chains are checked by one limiting 'stopper' of the binding cavity in the first step and by two stoppers in the second step.

Very similar pictures are obtained for $\Delta\Delta G$ values calculated for tyrosyl-tRNA synthetase [20] and a very similar model of the binding cavity can be made. However, this amino acid is not only bound by hydrophobic interaction but according to X-ray analyses [28,29] also by two hydrogen bonds formed with the hydroxy group of the side chain. In fact tyrosine deviates from the straight lines by energy values due to the hydrogen bonds [20]. Very similar values had been found in site-directed mutagenesis experiments [30,31] and thus confirm the results obtained with $\Delta\Delta G$ plots.

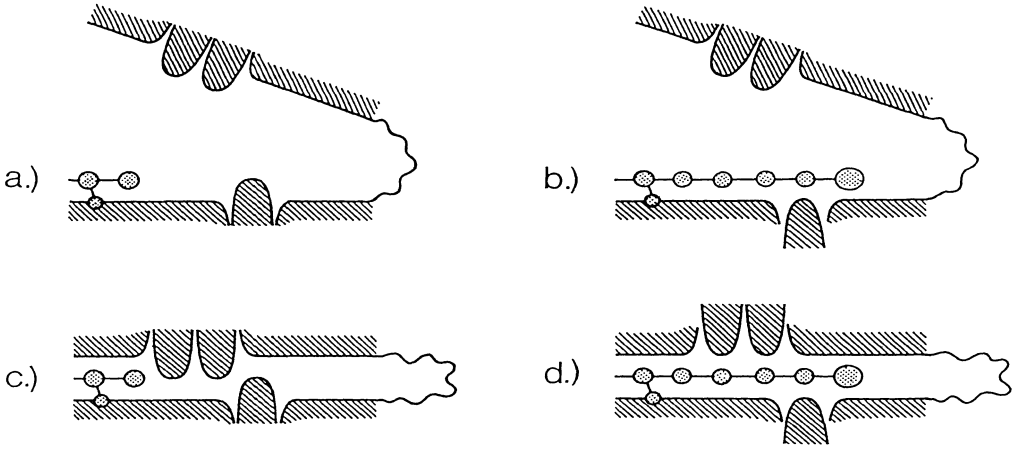

Fig. 2. Schematic view of isoleucine binding site of isoleucyl-tRNA synthetase. a) An alanine attached to the initial binding site responsible for the first initial discrimination step, which sorts amino acids with initial discrimination factor I_1 and represents the binding cavity for side chains of amino acids in aminoacylation of $tRNA^{Ile}$-C-C-A(3'NH_2). b) A lysine attached to the initial binding site, one 'stopper' group is pushed aside. c) An alanine side chain bound to the complete binding site as it is structured after conformational change of the enzyme in aminoacylation of $tRNA^{Ile}$-C-C-A. In this complete 'densely packed' binding pocket, isoleucine and the other amino acids are discriminated by factor $I' = I_1.I_2$. d) A lysine side chain bound in the complete pocket, three stopper groups are pushed aside.

Concluding remarks

Recognition of amino acids is a complicated multistep process. The high specificity of aminoacyl-tRNA synthetases can only be achieved using 'physical' and 'chemical' steps. At present four steps are known, two of each category. Whereas in early stages of investigations of these enzymes their high specificities seemed to be mysterious, this important property can now be referred to simple phenomena like hydrophobic interaction, hydrogen bonds and enzymatic hydrolysis.

References

1. Orgel LE (1963) Proc. Natl. Acad. Sci. USA 49: 517–521.
2. Orgel LE (1970) Proc. Natl. Acad. Sci. USA 67: 1476.
3. Parker J, Flanagan I, Murphy I and Gallant I (1981) Mech. Ageing Dev. 16: 127–139
4. Edelmann P and Gallant J (1977) Proc. Natl. Acad. Sci. USA 74: 3396–3398.
5. Baird MB, Samis HV, Massie HR and Zimmerman JA (1975) Gerontologia 21: 57–63.
6. Hoffmann GW (1974) J. Mol. Biol. 86: 349–362 .

7. Kirkwood TBL and Holliday R (1975) J. Mol. Biol. 97: 257–265.
8. von der Haar F (1973) Eur. J. Biochem. 34: 84-90.
9. Freist W, Sternbach H and Cramer F (1982) Eur. J. Biochem. 128: 315–329.
10. Faulhammer HG and Cramer F (1977) Eur. J. Biochem. 75: 561–570.
11. Freist W, Sternbach H, von der Haar F and Cramer F (1978) Eur. J. Biochem. 84: 499–502.
12. Freist W, Sternbach H and Cramer, F (1987) Eur. J. Biochem. 169: 33–39.
13. Fersht AR and Kaethner MM (1976) Biochemistry 15: 818–823.
14. Lin SX, Shi JP, Cheng XP and Wang YL (1988) Biochemistry 27: 6343–6348.
15. von der Haar F and Cramer F (1978) Biochemistry 17: 3139–3145.
16. Faulhammer HG and Cramer F (1977) Eur. J. Biochem. 75:561–570.
17. Freist W, Sternbach H and Cramer F (1981) Eur. J. Biochem. 119: 477–482
18. Fersht AR (1977) Enzyme Structure and Mechanism WH Freeman, Reading and San Francisco.
19. Gallant JA and Prothero J (1980) J. Theoret. Biol. 83: 561–578.
20. Freist W and Sternbach H (I988) Eur. J. Biochem. 177: 425–433
21. Freist W, Sternbach H and Cramer F (1988) Eur. J. Biochem. 186: 535–541.
22. Hopfield II, Yamane T, Yue V and Coutts SM (1976) Proc. Natl. Acad. Sci. USA 73: 1164–1168.
23. Freist W, Pardowitz I and Cramer F (1985) Biochemistry 24: 7014–7023.
24. Chothia C (1974) Nature. London 248: 338–339.
25. Chothia C (1975) Nature. London 254: 304–308.
26. Chothia C (1976) J. Mol. Biol. 105: 1–14.
27. Freist W, Sternbach H and Cramer F (1988) Eur. J. Biochem. 173: 27–34.
28. Monteilhet C and Blow DM (1978) J. Mol. Biol. 122: 407–417.
29. Blow DM and Brick P (1985) In: Jurnak F and McPherson A (eds.) Biological Macromolecules and Assemblies, Vol 2: Nucleic Acids and Interactive Proteins. Wiley, New York, pp. 443–469.
30. Fersht AR (1987) Biochemistry 26: 8031–8037.
31. Fersht AR (1988) Biochemistry 27: 1577–1580.

Effect of *Escherichia coli* endotoxin on some aspects of amino acid and protein metabolism by the rat small intestine*

D.A. Ameh and J.R. Thompson

Department of Animal Science, University of Alberta, Edmonton, Alberta T6G 2P5, Canada

Abstract

There is a paucity of information concerning the metabolism of the small intestine in the presence of bacterial endotoxins. The effect *Escherichia coli* (055:B5) endotoxin (50 ng/ml) on nitrogen metabolism was studied in isolated rat enterocytes incubated in the presence or absence of glutamine and/or glucose as energy substrates.

Considerable amounts of glutamate and alanine are produced by enterocytes incubated in the presence of 5 mM glutamine or 5 mM glutamine plus 10 mM glucose for 1 h at 37°C. Glutamate production averaged 126.93 ± 11.37 and 121.79 ± 12.66 nmol/h/mg, respectively, while alanine production averaged 25.34 ± 2.37 and 52.77 ± 4.83 nmol/h/mg, respectively. Inclusion of endotoxin in the incubation medium slightly decreased ($p<0.05$) enterocyte net glutamate production but had no effect on net alanine production. The net release of tyrosine and the essential amino acids to the incubation media increased three to fourfold ($p<0.001$) following the addition of 5 mM glutamine to both the control and the endotoxin treatments. This effect was not influenced by the addition of 10 mM glucose. The inclusion of endotoxin in the incubation medium increased ($p<0.001$) the rate of protein breakdown as measured by the release of ^{3}H-phenylalanine from prelabeled protein approximately threefold in the presence or absence of energy substrates or plasma concentrations of amino acids. The relatively high concentration of taurine in the enterocytes was not affected by addition of endotoxin to the incubation medium. In addition, endotoxin treatment did not affect ethanolamine production in the enterocytes.

Introduction

Altered glucose metabolism [1] and plasma amino acid concentrations [2] following sepsis or injection of purified bacterial endotoxin have been reported in experimental animals including the rat and sheep. Continuous infusion or bolus injection of *Escherichia coli* endotoxin is commonly associated with hypoglycemia [3], decreased plasma concentrations of a number of amino acids [2], decreased gastrointestinal tract motility [4] as well as increased plasma concentrations of cortisol and catecholamines and suppressed thyroid hormone concentrations [5,6]. Marked changes in protein metabolism including an increase in overall protein turnover rate have been reported following sepsis or trauma [7,8]. Under normal physiological conditions, a significant amount of glutamine is used by the small intestine for meeting its energy requirements [9,10]. It is therefore not

* This project was supported by the Natural Sciences and Engineering Research Council of Canada.

unlikely that glutamine might play a role in the regulation of the functional and metabolic activities of the small intestine under these conditions.

Very little is known about the metabolism of the small intestine in the presence of bacterial endotoxins. Changes in the metabolic activity and the functional integrity of the small intestine may be a significant part of the mechanism through which changes in the plasma concentrations of several metabolites of dietary nutrients is achieved following endotoxin administration. This study was therefore designed to determine some aspects of the effects of *E. coli* (055: B5) endotoxin on amino acid and protein metabolism by isolated enterocytes from the rat small intestine.

Materials and Methods

Male Sprague-Dawley rats weighing 250–310 g provided feed and water *ad libitum* were used in all experiments unless stated otherwise. Endotoxin (from *E. coli* (055:B5)) and all chemicals used were obtained from Sigma Chemical Co., St. Louis MO. L-[2,6-^{3}H] phenylalanine was obtained from Amersham International, U.K. Endotoxin-free saline was obtained from Travenol Canada Inc., Mississauga Ont.

Isolation of rat enterocytes

The method of Reiser and Christiansen [11] as modified by Watford *et al.* [12] was used for isolating enterocytes from the small intestine. Following a 12 h fast, each rat was killed by a blow on the head and the abdomen was rapidly opened. A 90 cm segment of the small intestine beginning 5 cm below the pylorus was excised and cut into two equal portions. The intestinal contents were flushed out of each portion with ice-cold Krebs-Ringer bicarbonate buffer (KRB) saturated with O_2/CO_2 (19:1). A further 20 ml of gassed KRB were passed through the intestine to remove mucus. One end of each portion was ligated with 3–0 Dexon and the intestine was filled with KRB containing 1.5 mg/ml hyaluronidase and 2.5 mg/ml bovine serum albumin. The other ends were ligated and the portions were incubated in 100 ml of KRB for 15 min at 37°C with constant agitation and gassing with O_2/CO_2 (19:1). The contents were then discarded and the intestines refilled with pre-gassed KRB. Following ligation, the portions were gently patted for 1 min with finger tips on ice-blocks covered with a polythene sheet to release enterocytes into the intestinal lumen. The KRB, containing enterocytes, from both portions was pooled in polythene tubes and centrifuged at 1,000 × g for 3 min. The cells were washed with cold KRB and resuspended in 10 ml KRB for subsequent metabolic studies. The average cell density (dry weight of enterocytes per ml of suspension) was determined by drying three 0.2 ml portions of the suspension to a constant weight in an oven maintained at 105°C.

Measurement of net glutamate and alanine production and tyrosine release by enterocytes

In a preliminary study tyrosine release and the net production of glutamic acid and alanine were measured in enterocytes from each of six animals. Two hundred microlitres of the enterocyte preparation were added to 3.1 ml incubation media containing KRB alone or KRB plus 10 mM glucose, 5 mM glutamine, or 5 mM glutamine plus 10 mM glucose in the presence or absence of *E. coli* endotoxin (50 ng/ml). A concentration range of between 10–100 ng endotoxin per gram body weight has been reported to give fibrile responses in rats [13]. The incubation medium was constantly gassed with O_2/CO_2 (19:1) throughout the incubation period. Enterocytes placed in 4% perchloric acid at time 0 min were used to measure the concentration of free amino acids before incubation. At the end of the 1 h incubation period, the reaction was terminated by addition of 0.2 ml 70% perchloric acid bringing the total volume to 3.5 ml and the medium was spun at 2,500 × g for 10 min. The pellet was homogenised in 1.0 ml 4% perchloric acid. One hundred microliters of the incubation media and 200 µl of the tissue homogenate were analysed for free amino acids by high performance liquid chromatography (HPLC) according to the method of Jones and Gilligan [14].

Measurement of protein degradation

Eight young rats weighing approximately 100 g each were injected intraperitoneally with 0.50 ml physiological saline containing 0.4 mM L-[2,6-^{3}H]phenylalanine (150 µCi/100 g body weight) and were fed rat chow and water *ad libitum* until 12 h prior to killing. The rats were housed in individual metallic cages and all urine and faeces were collected to prevent radioactive contamination.

The enterocytes were isolated as described earlier. The freshly harvested enterocytes were washed with five 10 ml portions of a 0.4 mM solution of non-radioactive phenylalanine in KRB to remove free ^{3}H-phenylalanine. To ascertain the effectiveness of removal of free ^{3}H-phenylalanine, the washes were counted for radioactivity. After five washes the radioactivity in the wash was similar to the background value. The cells were resuspended in 10 ml KRB and used for the metabolic studies.

Sixteen 200 µl portions of the enterocyte suspension from each rat were incubated with one of the following treatments; 3.1 ml KRB (blank) or 3.1 ml KRB containing 5 mM, glutamine, 5 mM glutamine plus 10 mM glucose or 10 mM glucose for 1 h in the presence or absence of 50 ng/ml endotoxin. In addition, two incubation conditions were used, one in which amino acids were absent from the media and the other in which plasma concentrations of amino acids [22] were present. At the end of the incubation period, the reaction was terminated by addition of 0.2 ml of 70% perchloric acid. The enterocytes were spun down at 1,000 × g for 5 min and the supernatant collected. One ml of the supernatant was counted for radioactivity in a liquid scintillation spectrometer to estimate the

amount of ^{3}H-phenylalanine released from protein. The pellet was sonicated for 3 min in 2 ml ice-cold 4% perchloric acid. The radioactivity in ^{3}H-phenylalanine in 1 ml of this solution was counted.

To determine the amount of protein-bound ^{3}H-phenylalanine, 1 ml of the cell suspension was hydrolysed with 6 N HCl at 110 °C for 24 h. The hydrolysate was evaporated to dryness and taken up in 3 ml of water. One ml of the solution was counted for ^{3}H-phenylalanine radioactivity while 0.2 ml was analysed for phenylalanine by HPLC. The rate of protein degradation was calculated by dividing the ^{3}H-phenylalanine radioactivity released into the incubation medium during the 1 h incubation period by the specific radioactivity of protein-bound ^{3}H-phenylalanine. Results were analysed using analysis of variance [16].

Results and Discussion

Glutamine metabolism and amino acid production by the enterocytes

In the preliminary study, the effects of endotoxin and the energy substrates glutamine and glucose on net alanine and glutamate production by rat enterocytes were studied. Substantially greater ($p<0.001$) amounts of glutamate and alanine were produced by enterocytes incubated in the presence of 5 mM glutamine or 5 mM glutamine plus 10 mM glucose than by enterocytes incubated in the presence of 10 mM glucose alone (Table 1). These observations are consistent with the well established fate of glutamine in the small intestine [12,17]. The finding that glutamine is extensively metabolised to glutamate is in agreement with the high glutaminase activity reported in the small intestine [9,18,19]. The inclusion of endotoxin in the incubation media was found to slightly decrease ($p<0.05$) net glutamate production by the enterocytes but had no significant effect on net alanine production. The inclusion of 10 mM glucose in the presence of 5 mM glutamine

Table 1. Effect of endotoxin and glutamine on alanine and glutamate production by rat enterocytes

	Alanine (nmol/h/mg)		Glutamate (nmol/h/mg)	
	Control	Endotoxin	Control	Endotoxin
10 mM glucose	14.23 ± 0.44^{a}	15.52 ± 1.03^{a}	5.44 ± 0.24^{a}	6.28 ± 0.62^{a}
5 mM gln	25.34 ± 2.37^{b}	25.37 ± 2.91^{b}	126.93 ± 11.37^{b}	111.70 ± 9.20^{b}
5 mM gln & 10 mM glucose	52.77 ± 4.83^{c}	50.48 ± 0.93^{c}	121.79 ± 12.66^{b}	106.04 ± 12.56^{b}

Enterocytes isolated from the small intestine of the rat were incubated for 1 h at 37°C in the presence of 10 mM glucose or 5 mM glutamine or 5 mM glutamine plus 10 mM glucose. Means within a column followed by different superscripts are significantly different ($p<0.05$) from control values. The rate of glutamate production was significantly ($p<0.05$) reduced in the presence of endotoxin plus glutamine. n=6.

Table 2. Effect of glutamine and glucose on tyrosine and essential amino acid release by rat enterocytes in the absence or presence of amino acids

Amino acid	Amino acid release (nmol/h/mg tissue)		
	In KRB	5 mM Gln	5 mM Gln & 10 mM glucose
Absence of amino acids			
Threonine	5.26 ± 0.89[a]	11.47 ± 2.24[b]	10.53 ±1.72[b]
Tryptophan	1.08 ± 0.21[a]	1.88 ± 0.25[b]	1.92 ± 0.22[b]
Methionine	1.09 ± 0.33[a]	3.27 ± 0.57[b]	2.82 ± 0.36[b]
Valine	5.82 ± 0.79[a]	10.25 ± 2.18[b]	9.09 ± 1.58[b]
Phenylalanine	2.79 ± 0.37[a]	5.91 ± 0.78[b]	5.43 ± 0.50[b]
Isoleucine	3.82 ± 0.44[a]	6.50 ± 1.21[b]	5.46 ± 0.84[b]
Leucine	6.88 ± 1.28[a]	12.39 ± 2.12[b]	11.02 ± 1.36[b]
Lysine	12.38 ± 2.14[a]	17.78 ± 3.18[b]	15.91 ± 2.18[b]
Tyrosine	3.93 ± 0.41[a]	11.64 ± 0.62[b]	11.49 ± 0.65[b]
Presence of amino acids			
Threonine	21.57 ± 3.61[a]	17.95 ± 4.23[a]	15.63 ± 1.98[a]
Tryptophan	4.70 ± 0.48[a]	3.72 ± 0.43[b]	2.75 ± 0.48[c]
Methionine	4.63 ± 0.52[a]	3.69 ± 0.64[b]	1.76 ± 0.79[c]
Valine	9.46 ± 0.93[a]	7.15 ± 1.31[b]	2.70 ± 1.47[c]
Phenylalanine	4.15 ± 0.64[a]	2.54 ± 1.15[b]	0.92 ± 1.36[c]
Isoleucine	3.99 ± 0.26[a]	3.68 ± 0.58[a]	2.51 ± 0.46[b]
Leucine	10.37 ± 0.77[a]	9.47 ± 1.20[a]	6.87 ± 1.36[b]
Lysine	20.27 ± 4.03[a]	15.25 ± 4.05[a]	14.27 ± 3.50[a]
Tyrosine	3.84 ± 0.40[a]	12.93 ± 1.04[b]	12.89 ± 0.81[b]

Isolated enterocytes from rats were incubated for 1 h at 37°C in KRB or KRB plus 5 mM glutamine or 5 mM glutamine plus 5 mM glucose in the presence or absence of plasma amino acid concentrations. Means within the same row followed by different superscripts are significantly different ($p<0.05$). n=8.

increased net alanine production by approximately 100%, suggesting that the carbon skeleton of alanine arose from glycolysis. Hanson and Parsons [17] proposed that glutamate derived from glutamine leaves the mitochondria to be transaminated in the cytosol with extramitochondrial pyruvate derived from glucose. In addition to the shifts in alanine and glutamate production there were increases in the net production of the other amino acids at the end of the incubation period similar to those reported in Table 2.

In addition to amino acids that are protein constituents, a relatively high concentration of taurine (10.54 ± 1.26 nmol/mg) was found in the enterocytes. Taurine concentrations did not increase during the 1 h incubation period, implying that this amino acid is not produced within the enterocytes. Quirk *et al.* [20] also reported high concentrations of taurine in enterocytes isolated from the chicken jejunum. Glucose and glutamine had no effect on enterocyte taurine concentrations. Enterocytes may serve as a taurine reserve which can be readily mobilised for hepatic biodetoxification of xenobiotics as tauroconjugates and may also be

involved in the recycling of bile acids as tauroconjugates. The addition of *E. coli* endotoxin to the incubation media did not influence enterocyte taurine concentrations during the incubation period (data not shown).

Relatively high concentrations of ethanolamine were also found in the incubation medium after the 1 h incubation period. The total amount of ethanolamine approximately doubled during the incubation period from 4.18 ± 1.13 to 10.15 ± 1.00 nmol/mg. The exact source of ethanolamine is not clear. However, Quirk *et al.* [20] have reported the presence of a serine ethanolamine phosphodiester in chicken enterocytes which may serve as the precursor of ethanolamine in this tissue. The energy substrates, glucose and glutamine, had no effect on enterocyte ethanolamine concentrations during the period of incubation. The addition of *E. coli* endotoxin to the incubation media also did not influence ethanolamine concentration (data not shown).

Tyrosine release and protein turnover

The release of amino acids from a tissue depends upon the relative rates of protein synthesis and degradation as well as the extent of metabolism of the amino acid within the tissue. The release of tyrosine has been used as an index of protein breakdown in tissues such as skeletal muscle where it is thought not to be metabolised [21]. The metabolism of tyrosine in small intestinal enterocytes has not been thoroughly studied. The possibility of using tyrosine as a measure of protein breakdown in rat enterocytes was examined in the preliminary study. Glutamine (5 mM) caused a significant increase in tyrosine release from the enterocytes which was not reversed by glucose (Table 3). This is suggestive of an increased rate of protein breakdown following the addition of glutamine if tyrosine is not metabolised in the enterocytes. However, as can be seen from Table 2, the three fold increase in net tyrosine release cannot be completely explained by an increased rate of proteolysis alone since the relative increase in net release of

Table 3. Effect of *E. coli* endotoxin on tyrosine release by rat enterocytes in the absence of amino acids

	Total tyrosine	
	Control (nmol/mg)	Endotoxin (nmol/mg)
Krebs-Ringer buffer	2.53 ± 0.15[a]	2.86 ± 0.12[a]
5 mM glutamine	14.51 ± 0.81[b]	14.70 ± 0.84[b]
5 mM gln & 10 Mm glucose	14.88 ± 1.07[b]	15.09 ± 0.84[b]
10 mM glucose	2.36 ± 0.06[a]	2.68 ± 0.14[a]

Enterocytes isolated from the small intestine of the rat were incubated for 1 h at 37°C in Krebs-Ringer buffer or in the presence of 5 mM glutamine or 5 mM glutamine plus 10 mM glucose or 10 mM glucose. Means within a column followed by different superscripts are significantly different ($p<0.001$). n=6.

Table 4. Effect of *E. coli* endotoxin and different energy substrates on protein degradation by rat enterocytes in the absence or presence of amino acids

	Protein degradation (nmol Phe/h/mg tissue)	
	Control	Endotoxin
Amino acids absent from incubation media		
Krebs-Ringer buffer	1.72 ± 0.07[a]	5.11 ± 0.38[b]
Plus 5 mM gln	1.75 ± 0.23[a]	6.38 ± 0.88[b]
Plus 5 mM gln & 10 mM glucose	1.70 ± 0.19[a]	4.38 ± 0.41[b]
Plus 10 mM glucose	1.77 ± 0.22[a]	5.03 ± 0.80[b]
Amino acids present in incubation media		
Krebs-Ringer buffer	1.67 ± 0.19[a]	4.75 ± 0.42[b]
Plus 5 mM gln	1.89 ± 0.25[a]	5.14 ± 0.67[b]
Plus 5 mM gln & 10 mM glucose	1.67 ± 0.21[a]	4.90 ± 0.70[b]
Plus 10 mM glucose	1.63 ± 0.18[a]	5.19 ± 0.46[b]

Enterocytes isolated from the small intestine of the rat containing ^{3}H-phenylalanine labeled protein, were incubated for 1 h at 37°C in the presence or absence of plasma concentrations of amino acids plus 5 mM glutamine or 5 mM glutamine plus 10 mM glucose. Protein degradation was determined by measuring the release of ^{3}H-phenylalanine from the enterocytes. Means within the same row followed by different superscripts are significantly different ($p<0.001$). n=8.

essential amino acids such as lysine which is not metabolised in this tissue was considerably smaller. Therefore it remains possible that enterocytes may produce tyrosine. This observation is further supported by the drop in phenylalanine concentration in the presence of glutamine when all amino acids were present at plasma concentrations, suggesting that hydroxylation of phenylalanine to tyrosine has been increased. To obtain a more direct estimation of protein breakdown, rats were injected with ^{3}H-phenylalanine 24 h before sacrifice to prelabel enterocyte proteins. The release of ^{3}H-phenylalanine from the prelabeled proteins was measured as an index of the relative rates of protein breakdown in control and endotoxin treated enterocytes and in enterocytes exposed to glutamine and glucose. The rate of ^{3}H-phenylalanine release provides a good estimate of protein degradation since the amount of phenylalanine in the extracellular free amino acid pool is overwhelmingly larger than the intracellular pool thereby making the chance of re incorporation of released ^{3}H-phenylalanine very slim.

The inclusion of *E. coli* endotoxin in the incubation medium extensively increased ($p<0.001$) the rate of enterocyte protein degradation both in the presence and in the absence of plasma concentrations of amino acids (Table 4). In contrast, the inclusion of endotoxin in the incubation medium was previously shown not to influence tyrosine release (Table 3). Subcutaneous administration of *E. coli* endotoxin to the rat has been reported to cause a 60–100% increase in muscle protein degradation, and a 52% fall in the rate of muscle protein synthesis [22]. The fractional rate of protein synthesis was increased by 35% in the liver in the same

experiment. The effect of endotoxin on the rate of protein synthesis in the small intestine was not measured in their experiment.

The addition of 10 mM glucose, 5 mM glutamine or 5mM glutamine plus 10 mM glucose to the incubation media did not influence the rate of protein degradation (Table 4), but did increase the net release of tyrosine three-fold (Table 2). The measurement of tyrosine release for assessing protein breakdown therefore appears unsuitable in the rat enterocytes. These preliminary findings demonstrate that glutamine influences tyrosine metabolism and that endotoxin has a dramatic effect on protein metabolism in enterocytes. Considerable additional work is required to delineate the effects of glutamine on amino acid metabolism and the effects of bacterial endotoxins on amino acid and protein metabolism in these cells.

Acknowledgements

The authors gratefully acknowledge suggestions from ABR Thomson, technical assistance from G Sedgewick and B Turner, R Niskala for caring for the animals and the Association of Universities and Colleges of Canada who supports DA Ameh in Canada as a Commonwealth Scholar.

References

1. Kelleher DL, Puinno PA, Fong BC and Spitzer JA (1982) Metabolism 31: 252–257.
2. Southorn BG and Thompson JR (1986) Can. J. Vet. Res. 50: 374–379.
3. Lang CH, Bagby GJ and Spitzer JJ (1984) Metabolism 33: 959–963.
4. Lohius JACM, Verheijden JHM, Burvenich C and van Miert ASJPAM (1988) Vet Quarterly 10: 109–125.
5. Messom GV, Kuhn ER and Burvenich C (1986) Arch. Int. Physiol. Biochim. 94: 61–62.
6. Bernabe J, Messom GV, Roets E and Burvenich C (1986) Arch. Int. Physiol. Biochim. 94: 67–68.
7. Garlick PJ , McNurlan MA, Fern EB, Tomkins AM and Waterlow JC (1980) Br. Med. J. 281: 263–265.
8. Tomkins AM, Carlick PJ, Schofield WN and Waterlow JC (1983) Clin. Sci. 65: 313–324.
9. Watford M , Erbelding EJ and Smith EM (1987) Biochem. J. 242: 61–68.
10. King PA, Goldstein L and Newsholme EA (1983) Biochem. J. 216: 523–525.
11. Reiser S and Christiansen PA (1971) Biochim. Biophys. Acta 225: 123–139.
12. Watford M, Lund P and Krebs HA (1979) Biochem. J. 178: 589–596.
13. van Miert ASJPAM and Frens J (1968) Zentbl. Vet. Med. A15: 532–543.
14. Jones BN and Gilligan JP (1983) J. Chromatog. 266: 471–482.
15. Ardawi MSM (1988) Clin. Sci. 74: 165–172.
16. Steel RCD and Torrie JH (1980) Principles and Procedures of Statistics. McCraw-Hill, New York.
17. Hanson PJ and Parsons DS (1980) Biochem. Soc. Trans. 8: 506–509.
18. Nagy LE, and Kretchmer N (1986) Arch. Biochem. Biophys. 248: 80–86.
19. Pinkus LM and Windmueller HG (1977) Arch. Biochem. Biophys. 182: 506–517.
20. Quirk PG, King GF, Campbell ID and Boyd CAR (1989) Am. J. Physiol. 256: G423–G429.
21. Tischler ME, Desautels M and Goldberg AL (1982) J. Biol. Chem. 257: 1613–1621.
22. Jepson MM, Pell JM, Bates PC and Millward DJ (1986) Biochem. J. 235: 329–336.

Development of high-capacity, low-affinity L-arginine transport in a proximal tubular cell line during differentiation

Johann S. Schwegler[a], Edgar Schömig[b], Almut Heuner[a] and Stefan Silbernagl[a]

[a]Dept. of Physiology, University of Würzburg, Röntgenring 9, D-8700 Würzburg, F.R.G.
[b]Dept. of Pharmacology and Toxicology, University of Würzburg, Versbacherstr. 9, D-8700 Würzburg, F.R.G.

Abstract

The kinetics of L-arginine transport were investigated dependent on culture age in an established proximal tubular cell line (OK). Initial uptake rates were determined by radiochemical methods. The cell membrane depolarization that is induced by L-arginine transport (ΔPD_m) was measured with microelectrodes.

Initial L-[^{3}H]arginine uptake follows Michaelis-Menten-kinetics with a Hill-coefficient near unity. Twenty four h after plating at subconfluent density (6.3×10^4 cells/cm^2) K_m is 50 ± 14 µmol/l, and v_{max} 6.6 $\pm$ 0.6 nmol/(mg protein $\times$ min) (n=4). K_m and v_{max} increase linearly with culture age ($r>0.94$ between 1 and 14 days). Seven days after plating, K_m is 4-fold, v_{max} 5.5-fold higher than after 1 day ($p<0.05$). Thus, total L-arginine transport capacity increases, while substrate affinity decreases during differentiation of OK cells. This corresponds with the development of a specific low-affinity transport system for the reabsorption of the bulk of filtered cationic amino acids in the renal proximal tubule.

Electrogenic L-arginine transport was measured by microelectrode techniques in single OK cells of various culture ages. Extracellular application of 3 mmol/l L-arginine results in a cell membrane depolarization of 5.2 ± 0.6 mV, irrespective of the time after plating. In old cultures (7 days after confluent seeding), PD_m repolarizes during sustained extracellular L-arginine superfusion. This repolarization is slower than it is expected for a potential driven electrogenic L-arginine transport. This indicates that up-regulation of the L-arginine uptake capacity is probably an electroneutral process.

Introduction

Like most other organic solutes of low molecular weight, cationic amino acids are nearly completely reabsorbed in the proximal renal tubule [26]. The proximal renal tubule needs capacitive amino acid transport systems because plasma amino acid concentration and GFR rise e.g. after a protein rich meal. The transport system for cationic amino acids is of major pathophysiological interest because in cystinuria there is a reabsorption defect of the common proximal cystin and cationic amino acid carrier [28].

There are quite contradictory results in literature concerning the kinetics and sodium requirement of L-arginine transport, depending on the applied method. Microperfusion experiments *in vivo et situ* revealed relatively low-affinity Na^+-dependent Larginine transport [25,4,18] with K_m's in the millimolar range. In

contrast, brush border membrane vesicle preparations possess high-affinity (K_m about 0.1 mmol/l) Na^+-independent L-arginine uptake [3,6]. In isolated cortical tubules, low-affinity Na^+-independent lysine transport was observed [2]. These discrepancies can be explained by up- and down-regulation of the cationic amino acid carrier(s). Proximal tubule cells are highly specialized for huge transepithelial solute transport. Therefore, such a change in the kinetics of the carrier might be effected by differentiation processes.

This question was investigated in cultured proximal tubule cells. The OK culture was originally established from a kidney preparation of the American opossum [9]. Later on, Malmström *et al.* demonstrated that the OK cell line shares many characteristics with proximal tubule cells [12]. In particular, parathyrin is able to inhibit phosphate uptake [13] and Na^+/H^+-exchange [15]. OK cells – like other non-transformed renal epithelial cell lines (e.g. LLC-PK_1 and MDCK) – grow in a dedifferentiated fibroblast like shape when seeded at a low densitiy. After having reached cell-to-cell contact OK cells stop logarithmic growth, form confluent monolayers with a polygonal cell shape, and polarize. Microvilli now occur on the apical membrane [5] and the enzymatic pattern resembles proximal tubule characteristics [12]. When grown on an impermeable support, transepithelial vectorial solute transport is reflected by the uprising of domes. Thus, the monolayer formation proves to be an adequate model for differentiation of renal tubule cells.

We recently demonstrated electrogenic transport of neutral and dibasic amino acids in confluent monolayers of OK cells. We found that rheogenic L-arginine transport is Na^+-independent and has a high substrate affinity (K_m<0.05 mmol/l) [22]. In this study we combine radiotracer uptake with microelectrode techniques to distinguish between electrogenic and electroneutral transport of L-arginine during the process of cell monolayer formation.

Materials and Methods

Cell culture

Experiments were performed with OK cells of the passages 99 to 107 (obtained at passage 95 from Dr. Gstraunthaler, Innsbruck). The cells were maintained in plastic culture flasks (Falcon, D-6900 Heidelberg, F.R.G.) and grown in Minimal Essential Medium (MEM) containing 10% fetal calf serum (Biochrom, D-1000 Berlin-W.) and 24 mmol/l bicarbonate without antibiotics. The flasks were kept in a humidified atmosphere at 37°C and 5% CO_2. Confluent monolayers were disintegrated by washing them for 1 min with Ca^{2+}- and Mg^{2+}-free Ringer solution (10 ml) containing (in mmol/l): 137 NaCl, 2.7 KCl, 8 Na_2HPO_4, 1.5 KH_2PO_4, 0.7 EDTA (titrated to a pH of 7.3 with 1 mol/l HCl) and 10 min of trypsination (2 ml trypsin 0.25 g/l, Serva, D-6900 Heidelberg, F.R.G.). Cultures were split once a week at a split ratio of 1:3 or 1:4. The medium was changed 3 times a week.

Radiotracer uptake studies

For [^{3}H]-arginine uptake experiments, the OK cells were grown on plastic dishes (60 mm ∅, Falcon). Thirty min before the experiment the culture medium was replaced by 3 ml of buffer A. Subsequently, initial rates of uptake were determined by incubation with [^{3}H]arginine for 20 seconds at 37°C. The incubation was stopped by rinsing the dishes four times with 3.5 ml of ice-cold buffer A. Finally, the cells were solubilized by 0.1% v/v Triton X-100 (in 5 mmol/l Tris·HCl, pH 7.4), and radioactivity was determined by liquid scintillation counting. In all experiments, the concentration of labeled [^{3}H]arginine was kept constant (2.0 nmol/l, 1×10^{-7} Ci/ml). Saturation of uptake was determined by the addition of unlabeled arginine. In a pilot experiment, the amount of [^{3}H]arginine which was incorporated into proteins after an incubation period of 20 seconds was determined. The cells were osmotically lysed by pure H_2O. Subsequently, proteins were precipitated with trichloracetic acid (9% v/v). More than 90% of [^{3}H]arginine remained soluble. By way of contrast, after an incubation period of 30 min less than 20% remained soluble.

Microelectrode measurements

Confluent monolayers of OK cells grown on 3 cm ∅ plastic petri dishes were washed with control solution and fixed on an inverted microscope (IM35, Zeiss, D-7082 Oberkochen, F.R.G.). The monolayer was constantly superfused through a constant-temperature tube system (37°C) at a rate of 4 ml/min. Microelectrodes were fixed to a mechanical micromanipulator (Leitz, D-6330 Wetzlar, F.R.G.). PD_m-signals were amplified by a high-impedance electrometer (Frankenberger, D-8034 Germering, F.R.G.; Biologic, F-38130 Echirolles, France).

Cell membrane potential measurements were carried out by conventional microelectrodes (input resistance about 5×10^7 ohms). Filament-containing borosilicate glass tubes with an outer diameter of 1.5 mm (Hilgenberg, D-3509 Malsfeld, FRG) were drawn by a vertical microelectrode puller (Narishige, Tokyo, Japan). The electrodes were filled with 1 mmol/l KCl. As a reference electrode we used an Ag/AgCl half cell imbedded in 3 mol/l KCl-Agar (25 g/l) that was fitted into a Pasteur pipette.

Calculations

K_m and v_{max} were calculated according to modified Michaelis-Menten-kinetics [23]:

$$V_{max} = \frac{v \cdot [I]^{nH}}{IC_{50}{}^{nH} + [I]^{nH}} \quad (1)$$

where [I] = concentration of unlabeled L-arginine; nH = Hill-coefficient.

Apparent transference numbers for potassium (t'_{K+}) were calculated from the PD_m-changes in response to extracellular K^+ concentration steps from 5.4 (control) to 20 mmol/l according to the equation:

$$t_{K+} = PD_m / S \cdot \log_{10}(C_1/C_2) \tag{2}$$

where PD_m = observed change in PD_m; S = Nernst'ian slope (–61,2 mV for monovalent ions at 37°C); C_1 = control concentration of K^+; C_2 = changed concentration of K^+.

We postulated that the cell membrane repolarization during constant superfusion with L-arginine is due to an intracellular accumulation of this amino acid. Our model further implies that the one-fold positively charged form of arginine is the only one that is transported and that transport stoichiometry is 1 arginine : 1 elementary charge [22]. Then the maximum intracellular concentration of L-arginine $[arg_i]_m$ directly depends on cell membrane potential PD_m and the extracellular L-arginine concentration $[arg_e]$ according to the Nernst equation:

$$[arg_i]_m = [arg_e] \cdot 10^{(PD_m/S)} \tag{3}$$

Assuming that the initial depolarization in response to extracellular L-arginine application (ΔPD_{mi}) reflects initial electrogenic uptake of the substrate, rheogenic uptake current [I] can be quantified per cm^2 cell surface area (A) by the use of the value for specific cell membrane resistance ($R_s = R \cdot A$):

$$\frac{I}{A} = \frac{\Delta PD_{mi}}{R_s} \tag{4}$$

The initial depolarization can be delineated from PD_m-recovery under the assumption that the time course of recovery follows a negative exponential curve. This is justified because $[arg_e]$ remains constant and thus intracellular accumulation follows first order kinetics. Then, electrogenic arginine influx ($d\upsilon/dt$) per cell surface area can be calculated by making use of the Faraday-constant ($F=Q/\upsilon$):

$$\frac{d\upsilon}{dt \cdot A} = \frac{\Delta PD_{mi}}{F \cdot R_s} \tag{5}$$

Electrically, OK cells are not coupled to one another in a confluent monolayer [21]. Thus, electrogenic L-arginine influx can be determined for each individual cell. Under the assumption of a hemispherical shape with a flat bottom, volume (V) and surface area can be calculated from optically measured cell diameter (d):

$$V = 2/3 \cdot (d/2)^3 \cdot \pi \tag{6}$$

$$A = 3 \cdot (d/2)^2 \cdot \pi \tag{7}$$

Cell surface area can therefore be expressed as:

$$A = 9/d \cdot V \tag{8}$$

For ($d\upsilon/dt \cdot V$) is nothing else but the rise of intracellular L-arginine concentration by rheogenic uptake per time, we can express [5] as:

$$\frac{d[arg_i]}{dt} = \frac{9 \cdot \Delta PD_{mi}}{F \cdot R_s \cdot d} \tag{9}$$

Since extracellular arginine concentration does not change, the rate constant (λ) for the intracellular saturation with arginine follows first order saturation kinetics:

$$\lambda = \frac{d[arg_i]}{dt} \cdot \frac{1}{[arg_i]_m} = \frac{9 \cdot \Delta PD_{mi}}{F \cdot R_s \cdot d \cdot [arg_i]_m} \tag{10}$$

and with respect to (3):

$$\lambda = \frac{9 \cdot \Delta PD_{mi}}{F \cdot R_s \cdot d \cdot [arg_i]_e \cdot 10^{(PD_m/S)}} \tag{11}$$

Data are usually given as means ± SEM, significance was tested by Wilcoxon's U-test because amino acid induced depolarization in OK cells does not follow a Gauss-distribution [22]. IC_{50}-values were calculated by a computer assisted non-linear least square method based on the Hill-equation for multisite inbibition [23].

Chemicals and solutions

The control solution for electrical experiments containe (in mmol/l) NaCl 122.5, KCl 5.4, $MgCl_2$ 0.8, $CaCl_2$ 1.2, Na_2HPO_4 0.8, NaH_2PO_4 0.2, N-(2-Hydroxyethyl)-piperazine-N'-2-ethansulfonic acid (HEPES)·NaOH 10, pH 7.4. Solutions with increased K^+-concentrations were prepared by exchanging NaCl by KCl. Solution A for uptake experiments contained (in mmol/l) NaCl 125, KCl 4.8, KH_2PO_4 1.2, $CaCl_2$ 1.2, HEPES·NaOH 25, pH 7.4, L-[+]ascorbic acid 1, D-[+]glucose 5.6, bovine albumin 1 g/l. Radioactive L-arginine (L-[2,3,4,5-^{3}H]arginine monohydrochloride) was purchased from Amersham (Braunschweig, FRG, TRK.698, batch 26), all other chemicals from Merck (Darmstadt, FRG).

Results

Radiochemical uptake studies

We studied the uptake of a tracer amount of L-[^{3}H]arginine (2.0 nmol/l) into OK cells of different age. Radiotracer uptake is linear for the first 30s (r=0.94; n=10), then deviates from linearity, but does not reach saturation until 15 min incubation at 37°C. This allows determination of initial uptake rates at an incubation time of 20 s.

Figure 1 shows that L-[^{3}H]arginine uptake is virtually completely inhibited by high concentrations of unlabeled L-arginine (96.5 ± 0.3% inhibition at 10 mmol/l L-arginine; n=12). This inhibition follows Michaelis-Menten kinetics with a mean Hill coefficient of 0.87 ± 0.06 (n=20). The L-arginine concentration which is necessary for half-maximum inhibition of L-[^{3}H]arginine uptake (IC_{50}) is more than 4 orders of magnitude higher than the applied radioligand concentration. Thus, IC_{50} and K_m are nearly identical.

Twenty-four hour after seeding the cells at a subconfluent density of 6.3 * 10^4 cells/cm^2, L-[^{3}H]arginine uptake shows a high substrate affinity (K_m=50 ± 14 µmol/l; n=4). The maximum uptake rate (v_{max}) – calculated from L-[^{3}H]arginine uptake in the presence of 0.3 mmol/l unlabeled L-arginine – is 6.6 ± 0.6 nmol/(mg protein * min) (n=4). With increasing age of the culture, the inhibition curve shifts to the right, indicating a decreasing substrate affinity of the uptake system. Seven days after plating, K_m is 210 ± 14.3 µmol/l (n=4). Also v_{max} is now higher than in a 1 day old culture (36 ± 2.2 nmol/(mg protein * min); n=4; $p<0.05$). In spite of the fact that monolayer formation has been completed about 5 days after plating, K_m and v_{max} continue to rise linearly up to 2 weeks (r=0.97 and 0.96, resp; n=20; Fig. 2).

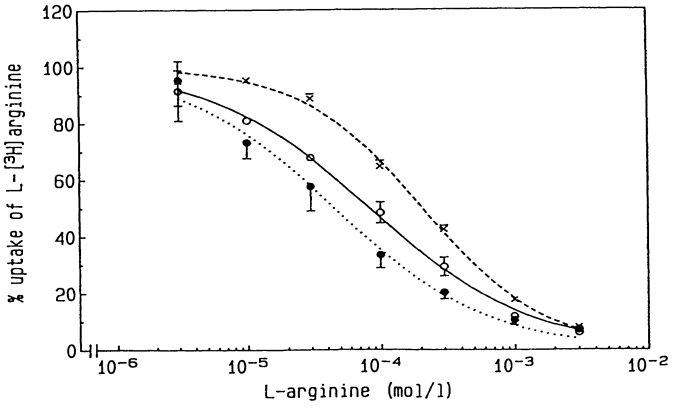

Fig. 1. Inhibition of L-[^{3}H]arginine uptake (2.0 nmol/l) into OK cells by unlabeled L-arginine at different culture age (1 day: filled circles and dotted line, 3 days: open circles and solid line, 7 days: × and dashed line). Each point represents the means ± SEM of n=4 independent experiments. The curves represent the best fit to Michaelis-Menten equation.

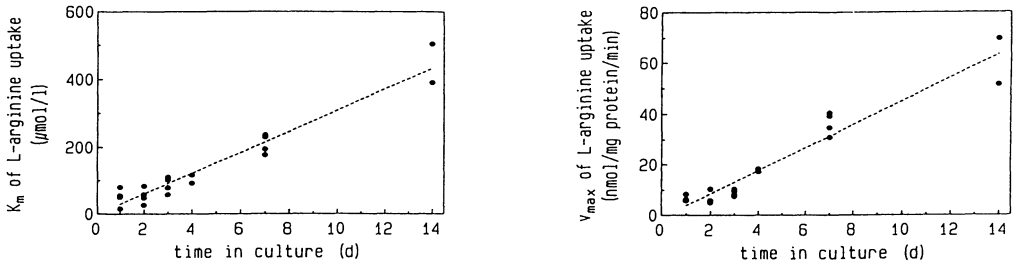

Fig. 2. Alterations of K_m (left) and v_{max} (right) for L[^{3}H]arginine uptake (2.0 nmol/l) at different culture age. The curves represent least squares linear regression (r=0.97 for K_m and 0.96 for v_{max}).

Unfortunately, uptake studies with those old cultures (>7 days) are technically hampered by the loose attachment of the cells to the culture dish, making rapid washing difficult.

The observed decrease in affinity and increase in capacity of transmembrane L-arginine transport might be explained by two distinct carrier populations whose expression is differentially regulated or by one carrier type with shifting kinetics. For this reason we looked for comparable changes in the electrogenic portion of L-arginine transport during monolayer formation.

Microelectrode measurements

We investigated the depolarization of OK cells (ΔPD_m) that is induced by the extracellular application of high L-arginine concentrations (3 mmol/l) at different time periods after plating. We recently demonstrated that this depolarization reflects stereospecific, sodium-independent, electrogenic amino acid uptake with high substrate affinity [22]. The seeding densitiy for these experiments was higher than for radiotracer studies, so that the culture reached confluency about 3 days after plating.

Figure 3 shows that ΔPD_m in response to L-arginine is largely variable from cell to cell, ranging from 0 to 12 mV depolarization (5.2 ± 0.6 mV; n=31). There is, however, no consistent difference between old and young cells as would have been expected considering the observed tenfold v_{max}-increase between 1 and 14 days after plating.

It is most important to note that the voltage drop at a cell membrane that is induced by a carrier mediated current is the result of both the current itself and also the cell membrane conductance (according to Ohm's law). Therefore, we studied the time course of two major electric cell membrane properties, membrane potential (PD_m) and apparent potassium transference number (t'_{K+}).

Figure 4 shows that neither PD_m nor t'_{K+} is significantly influenced by the age of the impaled cells. Also, cell membrane resistance (measured by microelectrode input resistance) remains virtually constant (data not shown). Thus, gross electrical

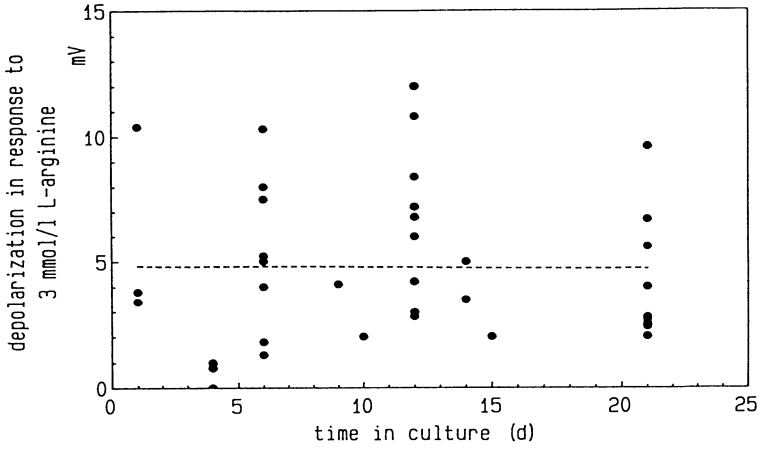

Fig. 3. Depolarization of PD_m in response to extracellular application of 3 mmol/l L-arginine at different culture age. Each dot represents an individual single cell in a subconfluent or confluent monolayer. The curve is the least squares linear regression line (r=–0.01; n=38).

properties of the OK cell membrane can be considered as being rather constant over the investigated time period.

Our data suggest that electrogenic L-arginine transport is not subdued to up- or down-regulation during the process of monolayer formation. This favors the hypothesis that 2 different L-arginine carriers co-exist in OK cell membranes, one

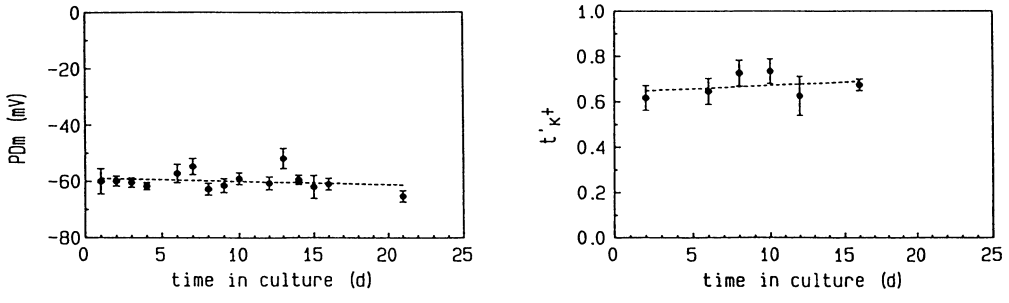

Fig. 4. Cell membrane potential difference (PD_m) (left) and apparent transference number (relative conductance) for K^+ (right) of OK cells at different culture age. Each dot represents the means ± S.E.M. of at least 3 results from different cell impalements. The curves are the least squares linear regression lines.

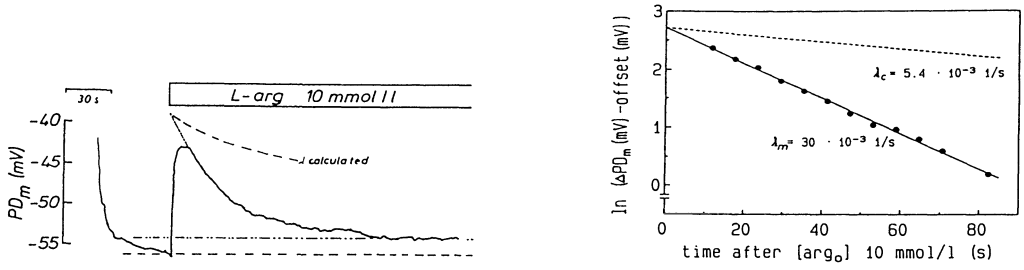

Fig. 5. Kinetics of the slow cell membrane repolarization after sustained extracellular L-arginine application (10 mmol/l) in a cell with 25 μm diameter (7 days after plating, original tracing, left). PD_m does not reach control level (dashed line) but rises to a lower 'steady state' value (dashed-dotted line). The half-logarithmic plot of PDm-recovery (right) clearly shows negative exponential kinetics (solid line), that allow a delination of initial depolarization (t = 0). The time constant λ_m is 6-fold higher than calculated according to [11] (dashed line). 'Offset' is the difference between control PD_m and steady state PD_m in mV.

of them being upregulated by differentiation but being invisible to electrophysiological methods because it is electroneutral.

This hypothesis is further supported by the investigation of a slow cell membrane potential recovery during sustained L-arginine superfusion. Figure 5 shows an original recording of such a recovery phenomenon. The repolarization in the presence of L-arginine follows an exponential time course. We have recently shown that this recovery is also observed in the presence of 3 mmol/l $BaCl_2$ [21] and hence does not reflect changes in the K^+-conductance. Therefore, we postulate that the potential recovery simply reflects the intracellular L-arginine accumulation. The initial depolarization is masked by the onset of the recovery itself and has to delineated from the time course of repolarization (see 'Methods'). The so-calculated time course for solely electrogenic L-arginine uptake, however, is about sixfold slower than the observed repolarization (calculated $\lambda_c = 5.4 \times 10^{-3}$ 1/s, observed $\lambda_m = 30 \times 10^{-3}$ 1/s). Similar results were observed in another 5 cells. Figure 5 also shows that the recovery is not complete – PD_m does not fully reach control level. This suggests that a hypothetical high-capacity electroneutral L-arginine uptake is driven by a smaller electrochemical driving force than PD_m. Then, L-arginine accumulation stops at a lower intracellular arginine concentration than is expected for the electrogenic, potential-driven transport. At that elevated $[arg_i]$, electrogenic uptake still works and produces the remaining ('steady state') cell membrane depolarization.

In addition, we found that the potential repolarization in the presence of L-arginine is more pronounced at high L-arginine concentrations. If there were only the high-affinity rheogenic system present, we should observe the opposite phenomenon because the rate constant λ for PD_m-recovery is inversely proportional to the extracellular L-arginine concentration (see equation (11)).

We look upon these facts as indirect supplementory evidence for the existence of a high-capacity electroneutral L-arginine uptake system that exists in parallel with the rheogenic transport of cationic amino acids.

Discussion

The cell density influences transmembrane amino acid transport in a variety of cultured cells. Most commonly, the uptake systems for neutral amino acids are down-regulated when the cells reach contact to one another. This has first been shown for transformed and untransformed 3T3 cells [1]. There, uptake for system A amino acid but not for lysine is affected by increasing cell density. More recently, Scheinman [20] demonstrated that alanine uptake decreases in the mammalian proximal tubule cell lines LLC-PK_1 and OK during monolayer formation. The substrate affinity (K_m) remains constant and only v_{max} decreases. In confluent monolayers of LLC-PK_1 [16,17] and MDCK cells [11], amino acid transport is predominantly localized at the basolateral membrane. These results indicate a qualitative difference between cultured cell monolayers and the intact tubule, for apical amino acid transport systems play the most important role in transtubular reabsorption *in vivo*.

In the present study we show that in contrast to these findings the uptake activity into OK cells for the cationic amino acid L-arginine rises with culture aging. Not only the v_{max}, but also the K_m is affected by this up-regulation in that substrate affinity decreases, but capacity increases with time after plating. It is interesting to note that these changes are not at all confined to the time before monolayer formation has been completed (about 5 days after plating under our conditions), but continue far beyond that period. The rise in K_m and v_{max} is linear up to 14 days without any sign of beginning 'saturation'. Longer maintenance in culture is possible, but then the cells are so loosely attached to their support that uptake studies are not feasible any longer.

Furthermore, we focused on the question whether the up-regulated L-arginine carrier system is electrogenic or not. We used the cell membrane depolarization in response to superfusion with L-arginine as a measure for transmembrane electrogenic L-arginine flux [8]. Stieger *et al.* [27] report both electrogenic (Na^+-dependent) and electroneutral (Na^+-independent) cationic amino acid transport in rat renal brush border membrane vesicles. Cationic amino acid uptake of LLC-PK_1 and MDCK cells was found to be driven by their cell membrane potential [24]. In OK cells we recently demonstrated the presence of an electrogenic, sodium-independent transport system for L-arginine that has a considerable high substrate affinity. Half-maximal cell membrane depolarization occurs at about 0.02 mmol/l [22]. This transport system has some considerable similarities to system y^+ that is best investigated in liver cells and there contributes to the function of the urea cycle [29].

The present study shows that the maximum activity of this electrogenic L-arginine transport system is not changed by culture age. Despite the large variability of

the electric response to 3 mmol/l extracellular L-arginine there is no tenedency to higher values in old cultures. These data taken alone are not unambiguous because a higher carrier mediated current could be masked by a decreasing cell membrane resistance, both effects together producing the same depolarization as before. However, the cell membrane potential and the relative potassium conductance (t'_{K+}) are not subject to time-dependent alterations. As potassium conductance is responsible for the cell membrane potential of OK cells [21], it is unlikely that there are major changes in cell membrane conductance during monolayer formation.

We could also demonstrate that the velocity of cell membrane repolarization during sustained L-arginine application is too fast to be explained by a simple potential driven intracellular accumulation. Rehwald *et al.* [18,10] report that repolarization during phenylalanine perfusion in frog kidney is partly due to the opening of K^+-conductance. This does not seem to be true in OK cells because 1.) blocking of K^+-channels by barium does not inhibit recovery, 2.) there is no transient intracellular alkalinization in OK cells after L-arginine superfusion [22] like found in frog tubule cells [14] that could account for opening of potassium channels. The kinetic differences between our mathematical model and experimental data might be explained by a carrier stoichiometry that shuttles less positive charges than arginine molecules. Then, however, we have to assume a stoichiometry of about 6 to 1 that is very unusual in biological carrier systems.

More realistic seems the assumption that in confluent OK monolayers the greatest part of arginine transport occurs electroneutrally. We observed that the repolarization is never complete. This suggests that the electrochemical driving force for electroneutral L-arginine uptake is smaller than PD_m. If there was a K^+/arg^+ (1/1) antiporter, the driving force for arginine accumulation would be greater than PD_m because intracellular potassium concentration is about 113 mmol/l (unpublished observations). Thus, it may be speculated if electroneutral arginine uptake occurs via Cl^-/arg^+ symport. Another possible explanation for the fact that PD_m does not reach control level is an intracellular sink for L-arginine by metabolism. Further studies are necessary to clarify this question.

In vivo microperfusion studies of the proximal tubule both by electrophysiological [19] and radiochemical methods [25] have revealed a K_m in the millimolar range (3.1 and 1.6 mmol/l, resp.). But in most studies dealing with brush border membrane vesicles derived from rodent kidney, the cationic amino acid transport was found to be much higher affine [3,6,7]. This discrepancy corresponds to the remarkable fact that the low-affinity L-arginine uptake system presented in this study 'vanishes' after trypsination.

In conclusion, OK cells probably possess at least two distinct transport systems for cationic amino acids: a high-affinity electrogenic system y^+ whose activity remains rather constant during monolayer formation, and an electroneutral low-affinity uptake system for cationic amino acids that contributes to the largest part of net arginine uptake in differentiated monolayers. The simultaneous rise in v_{max} and K_m can , however, also be interpreted as the reverse of a kinetic phenomenon

which according to Segel [23] is called 'uncompetitive inhibition'. We cannot make a clear decision between these alternatives yet.

Acknowledgements

The authors acknowledge the skilful technical assistance of S. Mildenberger and E. Fekete. They are grateful for many stimulating discussions with Drs. W. Steigner, H. Oberleithner and U. Kersting during the course of this study and for the careful language editing by K.P. Thiele.

References

1. Borghetti AF, Piedimonte G, Tramacere M, Severini A, Ghiringhelli P and Giudotti GG (1980) J. Cell. Physiol. 105: 39–49.
2. Bowring AM, Forman JW, Lee J and Segal S (1987) Biochem. Biophys. Acta 901: 23–29.
3. Busse D (1978) Arch. Biochem. Biophys. 191: 551–560.
4. Frömter E (1982) Pflügers Arch. 393: 179–189.
5. Gstraunthaler GJA (1988) Renal Physiol. Biochem. 11: 1–42.
6. Hammermann MR (1982) Biochem. Biophys. Acta 685: 71–77.
7. Hilden SA and Sacktor B (1981) Arch. Biochem. Biophys. 210: 289–297.
8. Hoshi T, Sudo K and Suzuku Y (1976) Biochem. Biophys. Acta 448: 492–504.
9. Koyama H, Goodpasture C, Miller MM, Teplitz RL and Riggs AD (1978) In vitro 14: 239–246.
10. Lang F, Messner G, Rehwald W (1986) Am. J. Physiol. 250: F953–F962.
11. Lever JA, Kennedy BG and Vasan R (1984) Arch. Biochem. Biophys. 234: 330–340.
12. Malmström K, Stange G and Murer H (1987) Biochim. Biophys. Acta 902: 269–277.
13. Malmström K, Stange G and Murer H (1988) Biochem. J. 251: 207–213.
14. Messner G, Koller H and Lang F (1985) Pflügers Arch. 404: 145–149.
15. Pollock AS, Warnock DG and Strewler GJ (1986) Am. J. Physiol. 250: F217–F225.
16. Rabito CA and Karish MV (1982) J. Biol. Chem. 257: 6802–6808.
17. Rabito CA and Karish MV (1983) J. Biol. Chem. 258: 2543–2547.
18. Rehwald W and Lang F (1987) Pflügers Arch. 410: 505–509.
19. Samarzija I and Frömter E (1982) Pflügers Arch. 393, 210–214.
20. Scheinman SJ (1988) J. Cell. Physiol. 135: 122–126.
21. Schwegler JS, Heuner A and Silbernagl S (1989) Electrical Properties of Cultured Renal Tubular cells (OK) Grown in Confluent Monolayers. Pflügers Arch. 415: 183–190.
22. Schwegler JS, Heuner A and Silbernagl S (1989) Electrogenic Transport of Neutral and Dibasic Amino Acids in a Cultured Opossum Kidney Cell Line. Pflügers Arch. 414: 543–550.
23. Segel IH (1975) Enzyme kinetics. John Wiley, New York, London, Sydney, Toronto.
24. Sepulveda FV and Pearson JD (1985) J. Cell. Physiol. 123: 144–150.
25. Silbernagl S and Deetjen P (1972) Pflügers Arch. 336: 79–86.
26. Silbernagl S (1988) Physiol. Rev. 68: 911–1007.
27. Stieger B, Stange G, Biber J and Murer H (1983) Pflügers Arch. 397: 106–113.
28. Wellner D and Meister A (1981) Ann. Rev. Biochem. 50: 911–968.
29. White MF (1985) Biochem. Biophys. Acta 822: 355–374.

Address for correspondence: J.S. Schwegler, Dept. of Physiology, University of Würzburg, Röntgenring 9, D-8700 Würzburg, F.R.G.

Regulation of lysine biosynthesis in the fungus *Penicillium chrysogenum*

C.P. Kubicek, C. Hönlinger, W.M. Jaklitsch, K. Affenzeller, R. Mach, T.-U. Gerngross and Lu Ying

Department of Microbial Biochemistry, Institute of Biochemical Technology and Microbiology, University of Technology, Getreidemarkt 9/1725, A-1060 Wien, Austria

Abstract

Two completely different pathways have evolved in nature for the biosynthesis of the essential amino acid lysine, i.e. the diaminopimelic acid pathway in bacteria, phycomycetes and green plants, and the α-aminoadipate pathway in higher fungi and euglenids. Regulation of the α-aminoadipate pathway has been studied extensively in the unicellular fungi, but little is known on this from multicellular fungi.

Regulation of biosynthesis in *Penicillium chrysogenum* occurs at multiple levels: the general amino acid control circuit is operative at the level of gene expression, whereas no lysine repression is apparent. On the other hand, lysine specifically inhibits homocitrate synthase (the first enzyme, which is localized in the mitochondrium), and α-aminoadipate reductase (the first enzyme located in the cytosol). Results presented in evidence for this will include studies on purified enzymes and isolation of respective mutants. Evidence will also be presented for a compartmentation of the α-aminoadipate pool in *P. chrysogenum*, which enables this fungus to tolerate high intracellular concentrations of this intermediate, which are toxic to yeast.

Introduction

Lysine is biosynthesized via two mutually exclusive pathways: the diaminopimelate pathway and the α-aminoadipate pathway [1]. The latter pathway is used by Euglenids, some Phycomycetes (Chytridiales, Blastocladiales, and Mucorales), yeasts and higher fungi (Ascomycetes and Basidiomycetes). A scheme of the pathway, the metabolites and enzymes involved is given in Fig. 1. Its structure and genetics have mainly been elucidated with *Saccharomyces cerevisiae* and *Neurospora crassa* as model organisms [2]. Except for yeast, little is known on the regulation of the pathway in fungi.

The key intermediate of the pathway, α-aminoadipate, is involved in the biosynthesis of several secondary metabolites, i.e. α- and ß-lactams [3–5]. In the case of the ß-lactam penicillin, production by *Penicillium chrysogenum* has been shown to be stimulated by increased intracellular pool levels of α-aminoadipate [6]. High producing strains of *P. chrysogenum* exhibit a high intracellular concentration of α-aminoadipate [6]. In order to find out how the intracellular concentration of α-aminoadipate is regulated in *P. chrysogenum*, we have carried out a

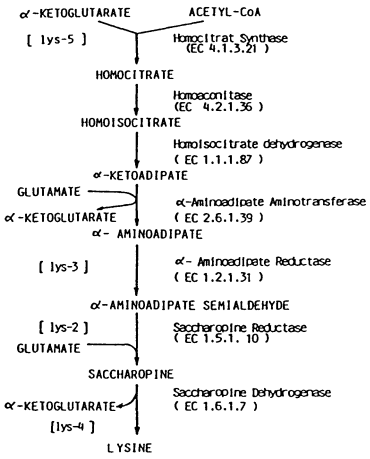

Fig. 1. The lysine biosynthetic pathway in *P. chrysogenum*. EC numbers of enzymes catalyzing individual steps are indicated. Designation lys-x gives numbers of loci identified in *Neurospora crassa*.

thorough investigation on the regulation of lysine biosynthesis in several strains of this fungus, which will be reviewed here. Parts of this report have already been published in detail [7–11].

Regulation of synthesis of lysine biosynthetic enzymes

In yeast, synthesis of lysine biosynthetic enzymes is regulated by (a) lysine repression and (b) the general amino acid control [2]. In *P. chrysogenum*, repression by lysine cannot be demonstrated [7], except for homocitrate synthase, albeit at very high (50 mM) extracellular concentrations [12] which are unlikely to

Table 1. Specific activities of lysine biosynthetic enzymes in *P. chrysogenum* strains Q176, D6/1014/A and P2 upon histidine depletion by 10 mM Amitrol[a]

Amitrol	Q176		D6/1014/A		P2	
	+	−	+	−	+	−
Homocitrate synthase	0.020	0.019	0.025	0.025	0.025	0.025
α-Aminoadipate aminotransferase	0.060	0.065	0.056	0.061	0.046	0.043
α-Aminoadipate reductase	0.023	0.023	0.063	0.170	0.060	0.115
Saccharopine reductase	1.00	1.65	1.05	1.90	1.40	2.20
Saccharopine dehydrogenase	0.210	0.350	0.190	0.420	0.130	0.290

[a]Values in parenthesis indicate standard errors of determination.

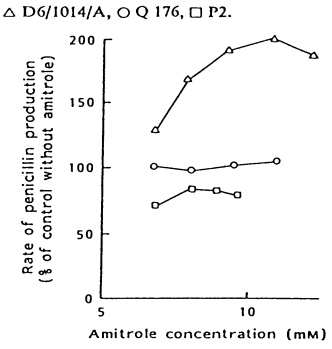

Fig. 2. Effect of amitrole on penicillin biosynthesis in *P. chrysogenum*. Different strains are indicated in the figure. Penicillin production was carried out in a defined medium described recently [6], but omitting cycloheximide and chloramphenicol. Penicillin production rates were calculated from the linear increase in extracellular penicillin during the first 3 h. Δ = D6/1014/A, ○ = Q 176, ❑ = P2.

resemble physiological conditions. The general amino acid control is operating at the enzymes following α-aminoadipate, i.e. α-aminoadipate reductase, saccharopine reductase and saccharopine dehydrogenase (Table 1). A brief description of the genes and proteins involved in the general control, deduced from [13] is shown in Fig. 2. This mode of control is involved in balancing amino acid pools under conditions of starvation for particular amino acids. Interestingly, different strains with different capacity to produce penicillin show a different pattern of control [7]. This different behaviour is also reflected in a differential effect of the general amino acid control on penicillin biosynthesis, mediated via its effect on the α-aminoadipate pool (Fig. 3).

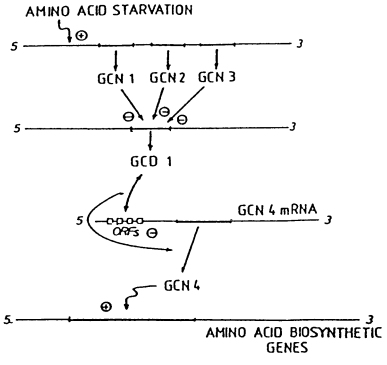

Fig. 3. A model summarizing regulatory interactions among the upstream open reading frames (ORF) of the GCN 4-mRNA and the negative regulator GCD 1 and the positive regulators GCN 1, GCN 2 and GCN 3. ⊕ indicates activation, O indicates inhibition of transcription (in the case of GCN 1, 2 or 3 GCD 1 or amino acid biosynthetic genes) or translation (in the case of GCN 4-mRNA). Please note that the neighbourhood of GCN 1–3 genes is artificially drawn, and does not mean that these genes are clustered in fungi.

Regulation of activities of lysine biosynthetic enzymes

There appear to be two major points of fine control within the lysine biosynthetic pathway: (a) homocitrate synthase and (b) α-aminoadipate reductase.

Homocitrate synthase has also shown to regulatory in yeast [2], but evidence *in vitro* for filamentous fungi has so far not been obtained. We have recently purified this enzyme from *P. chrysogenum* to homogeneity (see paper by WM Jaklitsch and CP Kubicek, this volume) and investigated its kinetics in detail. The enzyme is strongly inhibited by lysine, depending on the pH: hence, at pH 7.8 the Ki is 20 μM, but at pH 7.0, virtually no inhibition can be observed. In view of changes in pH related to the energy state of the cell, this may be a mechanism of controlling lysine biosynthesis depending on the cells needs.

α-aminoadipate reductase has first been shown by us to form a regulatory point in lysine biosynthesis [9], by being susceptible to lysine inhibition (Fig. 4). Using (6-^{14}C)-α-aminoadipate, this inhibition can also be demonstrated *in vivo* [9].

Compartmentation of lysine biosynthesis in *P. chrysogenum*

In yeast, lysine biosynthesis is known to be compartmentalized in the mitochondrium and the cytosol [2]. Cell fractionation of *P. chrysogenum* has been performed, but no clear evidence for or against this situation in *P. chrysogenum* has yet been obtained (WM Jaklitsch, A Pfitzner and CP Kubicek, unpublished results). However, the dipartite control of the pathway, and the low Ki of homocitrate synthase for lysine would favour a compartmentation similar to yeast which is depicted in Fig. 5.

Moreover, we have recently obtained evidence for the existence of two distinct α-aminoadipate pools in *P. chrysogenum*, one of which – located in the cytosol – is used for lysine biosynthesis, whereas the other one is used for ß-lactam synthesis (named 'penicillinosome',[10]). Lysine appears to be compartmentized analogous to yeast, being located to 85% in the vacuole; interestingly, less vacuolar lysine is found under conditions of carbon catabolite repression [10].

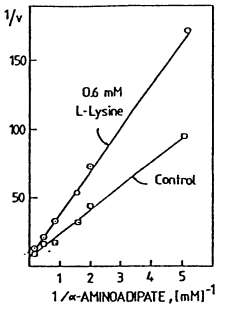

Fig. 4. Lineweaver-Burk plot of affinity of α-aminoadipate reductase for its substrate at 0 (❑—❑) and at 0.6 mM L-lysine (○—○).

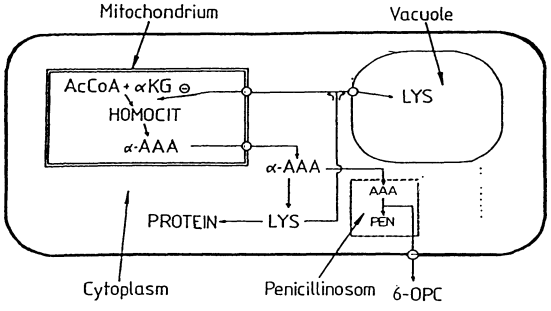

Fig. 5. A hypothetical scheme of compartmentation of lysine biosynthesis and associated pathways in *P. chrysogenum*. Please note that meanwhile (see 'Note added in proof'), a second cytosolic homocitrate synthase has been identified [11].

α-Aminoadipate toxicity

In yeast, α-aminoadipate is toxic at 1 mM, which is probably due to a disturbance of amino acid biosynthesis by elevated concentrations of α-aminoadipate semialdehyde [14]. This phenomenon can be used to select for yeast mutants defective in α-aminoadipate reductase. In *P. chrysogenum*, this phenomenon is only observed at very high concentrations of α-aminoadipate (20 mM) [15]. This is due to the compartmentation of α-aminoadipate, which preferentially traps α-aminoadipate into the penicillinosom [10]. Additionally, *P. chrysogenum* forms and excretes 6-oxopiperidine-2-carboxylic acid, a δ-lactam of α-aminoadipate (Fig. 6) by an as yet unknown mechanism immediately upon addition of exogenous α-aminoadipate [16].

These two mechanisms may relieve *P. chrysogenum* from the accumulation of a potentially toxic metabolite. Using 20 mM of aminoadipate, however, we have been able to isolate α-aminoadipate reducatse defective mutants analogous to yeast [15].

Conclusions

Regulation of lysine biosynthesis in *P. chrysogenum* differs from that in yeast by relying more strongly on fine control mechanisms and compartmentation. Hence,

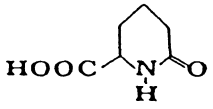

6-oxopiperidine-2-carboxylic acid

Fig. 6. Chemical formula of 6-oxopiperidine-2-carboxylic acid.

the transport of key metabolites, α-aminoadipate and lysine between the compartments actively and passively involved in lysine biosynthesis may deserve more investigation in future, since it may be crucial to the regulation of secondary metabolism from lysine and α-aminoadipate.

Note added in proof

During revision of the manuscript [11] we have obtained evidence that homocitrate synthase in *P. chrysogenum* occurs in at least two isoenzymic forms, one of which solely occurs in the cytoplasm. Hence, a complete cytosolic pathway of lysine biosynthesis and a standard pathway coexist in this organism.

References

1. Vogel HJ (1964) Am. Natur. 98: 435–446.
2. Bhattacharjee JK (1985) CRC Crit. Rev. Microbiol. 12: 131–151.
3. Turner WB and Aldridge DC (1983) Fungal Metabolites II: Academic Press New York.
4. Herbert RB (1989) The Biosynthesis of Secondary Metabolites. Chapman and Hall. 2nd Ed.
5. Demain AL (1983) In: Demain AL and Solomons NA (eds.) Handbook of Experimental Pharmacology. Vol. 67/1. Springer Verlag Berlin, New York, pp. 189–228.
6. Jaklitsch WM, Hampel WA, Röhr M, Kubicek CP and Gamerith G (1986) Can. J. Microbiol. 32: 473–480.
7. Jaklitsch WM, Röhr M and Kubicek CP (1987) Exp. Mycol. 11: 141–149.
8. Hönlinger C, Hampel WA, Röhr M and Kubicek CP (1988) J. Antibiot. 41: 255–257.
9. Affenzeller K, Jaklitsch WM, Hönlinger C and Kubicek CP (1989) FEMS Microbiol. Letts. 58: 293–298.
10. Hönlinger C and Kubicek CP (1989) Biochim. Biophys. Acta 993: 204–211.
11. Jaklitsch WM and Kubicek CP (1989) Biochem J., in press.
12. Luengo JM, Revilla G, Lopez-Nieto MJ, Villanueva JR and Martin JF (1980) J. Bacteriol. 144: 869–875.
13. Hinnebusch AG (1988) Microbiol. Rev. 52: 248–273.
14. Zaret KS and Sherman F (1985) J. Bacteriol. 162: 579–583.
15. Mach R, Affenzeller K and Kubicek CP (1989) 6th International Symposium on Genetics of Industrial Microorganisms, Strasbourg, France, Abstract.
16. Hönlinger C, Gerngross TU, Affenzeller K and Kubicek CP (1989) Fourth European Congress on Industrial Biotechnology. Varese, Italy, Abstract.

The relationships between the availability of L-tryptophan in serum and HPA-axis function in postpartum females

M. Claes, M. Maes, L. Delbeke, C. Schotte, Y. Jacquemyn and S. Scharpe
University Hospital of Antwerp, Belgium

Abstract

L-Tryptophan (L-Trp), the sum of five competing amino-acids (CAA) – i.e. valine, leucine, isoleucine, tyrosine, phenylalanine – cortisol and adrenocorticotrophic hormone (ACTH) were determined both before and after treatment with 1 mg dexamethasone in 24 females 3 days after childbirth. Basal L-Trp concentrations were significantly lower in postpartum females as compared to normative values. There was a significant suppressing effect for dexamethasone on the availability of L-Trp. Up to 75% of all females showed cortisol non-suppression (postdexamethasone cortisol ≥5 μg/dl). The baseline cortisol and ACTH levels were significantly positively related to the availability of L-Trp. We found a positive relationship between basal L-Trp values and the post dexamethasone ACTH values.

Introduction

Five days postpartum, a disordered dexamethasone suppression test (DST) is found in 80% of normal females [1,2]. As with the majority of amino-acids, circulating L-tryptophan (L-Trp) is reduced during pregnancy [3]. Plasma L-Trp increases over the first five days postpartum [4]. Absence of the early postpartum peak in plasma total L-Trp is associated with postpartum blues and the later occurrence of postpartum depression. From the second till the fifth day postpartum, plasma L-Trp tends to rise and plasma cortisol concentrations tend to decrease [5].

A proportion (35–60%) of patients with major depression show disturbances in the hypothalamic-pituitaryadrenal (HPA) axis as evidenced by disorders in the dexamethasone suppression test [6,7]. A significantly decreased total L-Trp and L-Trp/CAA ratio is established in patients suffering from major depression [7]. In one of our previous papers, we reported on significantly negative correlations between postdexamethasone cortisol and both L-Trp and the L-Trp/CAA ratio in depression [7]. Handley *et al.* [4] observed negative correlations between the availability of L-Trp and serum cortisol in postpartum females.

The brain serotonin synthesis largely depends on the availability of L-Trp; the ratio of L-Trp to the CAA in serum (competing amino-acids: valine, leucine, isoleucine, tyrosine, phenylalanine) which compete with L-Trp for passage through the blood-brain-barrier, is as index of the availability of L-Trp to the brain [8].

Several major hypotheses may account for the negative correlation between HPA-axis hyperactivity and decreased availability of L-Trp in the serum. One is

that, through hypersecretion of corticosteroids the peripheral nicotinamide biosynthesis is induced so that L-Trp is withdrawn from the serum [9]. A second hypothesis is that the deficiency of L-Trp in the serum attenuates the negative feedback exerted by glucocorticoids on pituitary corticotrophic cells [7]; this feedback mechanism is possibly stimulated through serotonergic structures [10].

This prospective study was undertaken in order to investigate (1) if the availability of L-Trp, pre- and postdexamethasone cortisol, and ACTH values are disordered in postpartum females, and (2) if the disposal of L-Trp to the brain and HPA-axis function are negatively interrelated in those females.

Patients and Methods

Patients

In the present study, 24 postpartum females participated. All were inpatients admitted to the University Hospital of Antwerp. Inclusion criteria were: (1) an uncomplicated childbirth for mother and child, (2) medication free, (3) breast feeding, and (4) disease free patients. Also 5 healthy controls (i.e. staff members) participated.

Measurements

Self-rating scales were administered three days after childbirth (i.e. Zung depression, Zung anxiety, Beck depression inventory) to evaluate the severity of maternal distress. Three days after childbirth, basal L-Trp, the sum of the 5 CAA, cortisol and ACTH were determined at 8 a.m. after an overnight fasting. The same day at 11 p.m. 1 mg dexamethasone was administered orally. The next day samples for postdexamethasone cortisol, ACTH, L-Trp and CAA measurements were taken at 8 a.m. In the healthy controls, only basal 8 a.m. L-Trp, CAA, cortisol and ACTH were determined.

The average age of the 24 postpartum females (28.0 ± 3.0 years) was not different from the healthy controls (27.8 ± 1.9 years). The mean Zung depression score of the 24 patients was 31.4 (± 6.5); the Zung anxiety score was 30.3 (± 6.0); the Beck depression inventory averaged 4.7 (± 3.2). According to these scores, no postpartum females with depressive or anxiety disorders were included in this study.

Methods

The methods and interassay coefficients of variation for the determination of the amino-acids, cortisol and ACTH are described elsewhere [11].

Table 1. Results of L-TRP, CAA, and L-TRP/CAA, ACTH and cortisol in postpartum females and in healthy controls

Biological markers	Healthy controls	Postpartum females	F statistic	p value
L-TrP (10^{-6} mole/l)	71.2 (± 10.5)	53.3 (± 10.1)	12.8	0.002
CAA (10^{-6} mole/l)	782.0 (± 204)	579.0 (± 75)	15.5	0.001
L-TRP/CAA × 100	9.32 (± 1.4)	9.23 (± 1.4)	0.02	0.9
ACTH (pg/ml)	34.0 (± 6.0)	23.4 (± 23.2)	0.9	0.6
Cortisol (μg/dl)	20.8 (± 6.0)	35.8 (± 4.9)	36.2	$<10^{-5}$

All results of ANOVA.

Statistics

To test group mean differences we used the analysis of variance (ANOVA). Repeated ANOVA's were used to assess treatment effects of dexamethasone administration on the several biological data. Relationships between variables were ascertained by means of Pearson's product moment correlation coefficients. The significance level was set at a 0.05 (two tailed).

Results

Table 1 lists baseline L-Trp, CAA, L-Trp/CAA ratio, ACTH and cortisol in 5 healthy controls and in 24 postpartum females. Basal L-Trp and sum of CAA were significantly lower in postpartum females compared to healthy controls. The ratio L-Trp/CAA was not different between both groups. Baseline cortisol values were significantly higher in postpartum females whereas basal ACTH was not different between both groups.

Table 2 displays the effects of treatment with 1 mg dexamethasone on the several biological parameters. We found significant suppressive effects for dexamethasone treatment on L-Trp, the L-Trp/CAA ratio, ACTH and cortisol. Up to 70% of all postpartum females exhibited a disturbed DST (i.e. postdexamethasone cortisol ≥ 5 μg/dl).

Table 2. Effects of 1 mg dexamethasone on L-TrP, CAA, L-Trp/CAA, ACTH and cortisol in 24 postpartum females

Biological markers	Baseline values	Postdexamethasone values	F statistic	p values
L-Trp (10^{-6} mole/l)	53.3 (± 10.1)	47.6 (± 12.7)	4.6	0.04
CAA (10^{-6} mole/l)	579.0 (± 75)	604.0 (± 99)	0.9	0.6
L-Trp/CAA × 100	9.32 (± 1.43)	7.87 (± 1.46)	18.7	0.0005
ACTH (pg/ml)	23.4 (± 23.2)	18.5 (± 23.6)	3.9	0.05
Cortisol (μg/dl)	35.8 (± 4.9)	13.1 (± 9.9)	77.3	$<10^{-5}$

All results of repeated ANOVA.

Table 3. Intercorrelations between the baseline L-Trp, L-Trp/CAA, and pre and postdexamethasone cortisol, ACTH data in 24 postpartum females

Variables	Predexamethasone cortisol	Predexamethasone ACTH	Postdexamethasone cortisol	Postdexamethasone ACTH
L-Trp	0.47 (p = 0.02)	0.43 (p = 0.03)	0.05 (p = 0.81)	0.36 (p = 0.07)
CAA	0.12 (p = 0.56)	0.20 (p = 0.66)	0.17 (p = 0.57)	0.15 (p = 0.51)
L-TrP/CAA	0.45 (p = 0.02)	0.34 (p = 0.09)	–0.18 (p = 0.61)	0.43 (p = 0.03)

Listed are Pearson's product moment correlation coefficients with exact p-value (between brackets).

Table 3 shows the intercorrelations between basal L-Trp, CAA, L-Trp/CAA values, and the pre- and postdexamethasone cortisol or ACTH data in the 24 postpartum females. The availability of L-Trp was significantly positively correlated with the predexamethasone ACTH and cortisol values, and with the postdexamethasone ACTH values.

Discussion

In the present study, basal L-Trp and the sum of CAA were significantly lower in postpartum females compared to healthy controls. This is in accordance with the findings of Handley *et al.* [4]. The ratio L-Trp/CAA was not different between both groups.

We found that baseline cortisol values were significantly higher in postpartum females compared to healthy controls. These findings corroborate those of Handley *et al.* [5].

In our study, there was a significant suppressive effect for dexamethasone treatment on L-Trp, L-Trp/CAA ratio, ACTH and cortisol. No effect for dexamethasone on the CAA was established. Consequently, the suppressive effects of dexamethasone on the availability of L-Trp are induced by the decrements in L-Trp circulating levels. These findings consolidate earlier reports [9,12].

Up to 70% of all postpartum females showed cortisol non-suppression. This is in agreement with the findings of other authors [1,2]. A hypothesis which could explain the abnormal DST's in postpartum females, is that the disturbance of the HPA-axis, known to be present in pregnancy, persists for a while into the puerperium [1]. As a result, using the DST in the initial postpartum period as a biological marker of postpartum depression, can not be validated.

In this paper we reported that the availability of L-Trp is significantly positively correlated with the basal ACTH and cortisol values, and with the postdexamethasone ACTH values. These findings are in sharp contrast with the results of earlier publications reporting on a negative correlation between postdexamethasone cortisol and the availability of L-Trp in depression or a negative correlation between L-Trp and serum cortisol in postpartum females [4,7].

Conclusions

The biological alterations detected in postpartum females, did not only show similarities (lower basal L-Trp, higher baseline cortisol values, cortisol non-suppression), but also dissimilarities (normal ratio L-Trp/CAA, positive correlation between HPA-axis hyperactivity and L-Trp availability) with the biological characteristics of major depression [7].

References

1. Greenwood J and Parkes G (1984) Austr. N. Z. J. Psychiatry 18: 282–285.
2. Singl B, Gilhotra M, Smith R, Brinsmead B, Lewin F and Hall C (1986) J. Affect. Disord. 11: 173–177.
3. Cox BD and Calane DP (1978) Horm. Met. Res. 10: 428–433.
4. Handley SL, Dunn TL, Waldron JM and Baker JM (1980) Br. J. Psychiatry 136: 493–508.
5. Handley SL, Dunn TL, Baker JM et al. (1977) Br. Med. J. 2: 18–22.
6. Feinberg M and Carroll BJ (1984) Arch. Gen. Psychiatry 41: 1080–1085.
7. Maes M, De Ruyter M, Hobin P and Suy E (1987) Psychiatr. Res. 21: 323–335.
8. Fernstrom JD and Faller V (1978) J. Neurochem. 30: 1531.
9. Morgan CJ and Badawy AA-B (1988) Biol. Psychiatry 25: 360–362.
10. Nuller JL and Ostroumova JL (1980) Acta Psychiatr. Scand. 61: 169–177.
11. Maes M, Vandewoude M, Maes L, Schotte C and Cosyns P (1989) J. Affect. Disord. 16: 197–221.
12. Maes M, Minner B and Suy E (1989) Acta Psychiatr. Scand., in press.

Address for correspondence: Dr. M. Maes, Department of Psychiatry, University Hospital, UZA, Wilrijkstraat 10, 2520 Edegem, Belgium.

Biosynthetic mechanism and physiological role of heterocyclic ß-substituted alanines in higher plants

Fumio Ikegami[a], Fernand Lambein[b], Leslie Fowden[c] and Isamu Murakoshi[a]

[a]Faculty of Pharmaceutical Sciences, Chiba University, Yayoi-cho 1–33, Chiba 260, Japan
[b]Faculty of Medicine, State University of Ghent, K.L. Ledeganckstraat 35, B-9000 Ghent, Belgium
[c]Rothamsted Experimental Station, Harpenden, U.K.

Abstract

Purification of cysteine synthase from the seedlings of *Leucaena leucocephala* reveals the presence of two forms of this enzyme, separated by chromatography on DEAE-Sephadex A-50. Both isoenzymes have the same *Mr* of 64,000 consisting of two identical subunits each. The subunits contain one molecule of pyridoxal 5'-phosphate. Cysteine synthases from *L. leucocephala* catalyzed the formation of some heterocyclic ß-substituted alanines such as ß-(pyrazol-1-yl)-L-alanine from O-acetyl-L-serine as an additional catalytic activity, but only isoenzyme B catalyzed the formation of L-mimosine in the same manner as the formation of L-quisqualic acid in *Quisqualis indica* var. *villosa*. The properties of the cysteine synthase isoenzymes purified in this study suggest that all cysteine synthases in higher plants can be multifunctional enzymes that are involved in the biosynthesis of ß-substituted alanines, and that these enzymes may have different substrate specificities. The physiological role of these enzymes in higher plants is also described.

Introduction

Plants produce a number of non-protein amino acids that may be regarded as heterocyclic ß-substituted alanines such as L-quisqualic acid, L-mimosine, ß-(pyrazol-1-yl)-L-alanine and L-willardiine (Scheme 1). In such plants, *Quisqualis indica* (Combretaceae) and *Leucaena leucocephala* (Leguminosae) are utilized as traditional medicines. They contain the neuroexcitatory amino acid L-quisqualic acid [1] and the thyrotoxic amino acid L-mimosine [2], respectively.

It has been demonstrated by Murakoshi *et al.* [3–9] that these naturally occurring heterocyclic ß-substituted alanines are enzymatically synthesized by condensation of the appropriate N-heterocyclic compounds with O-acetyl-L-serine (OAS) as an activated form of L-serine.

The biosynthesis of non-protein amino acids in plants may be due to the action of enzymes normally involved in the biosynthesis of protein amino acids that, during the course of evolution, have acquired a different specificity. In the case of the heterocyclic ß-substituted alanines, it was first suggested that these natural compounds may arise by a non-specific action of tryptophan synthase [10–12].

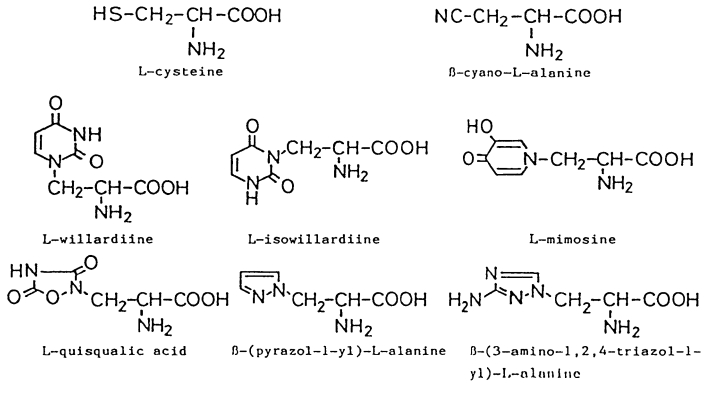

Scheme 1. Some ß-substituted alanines in higher plants.

When OAS was recognized as the donor for the alanyl moiety [3–9], the enzymatic formation of heterocyclic ß-substituted alanines was compared to the biosynthetic mechanism of S-substituted L-cysteines formed by the cysteine synthase (O-acetyl-serine sulfhydrylase) [13–16] as shown in Scheme 2.

The group of enzymes producing heterocyclic ß-substituted alanines generally establishes an N-C bond between the ß-carbon of alanine and a ring-nitrogen. Occasionally a C-C bond is formed in a natural product [6] or an O-C bond is formed with a synthetic precursor *in vitro* [8].

In the course of our ongoing study on the ß-substituted alanine synthases in higher plants forming heterocyclic ß-substituted alanines and also to obtain a better understanding of the relationship between protein amino acid metabolism and the metabolism of this group of non-protein amino acids, we have attempted the purification of the enzymes catalyzing the formation of heterocyclic ß-substituted alanines and of the cysteine synthase from some higher plants [17–23], and we

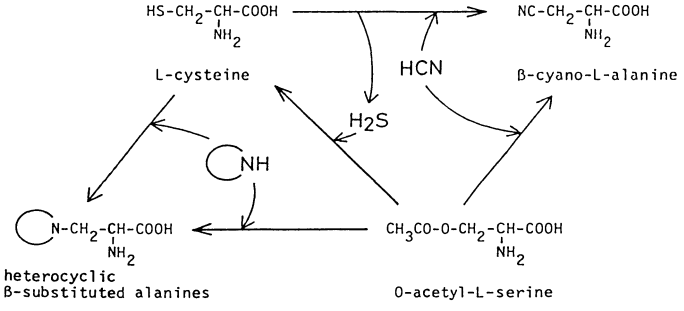

Scheme 2. Biosynthetic pathways for heterocyclic ß-substituted alanines, L-cysteine and ß-cyano-L-alanine in higher plants.

presented evidence that some cysteine synthases from plants, as an additional catalytic activity, can also catalyze the formation of some ß-substituted alanines, including ß-cyano-L-alanine, without jeopardizing the synthesis of L-cysteine as a primary metabolite.

In this paper we describe the existence of isoenzymes of cysteine synthases catalyzing the formation of heterocyclic ß-substituted alanines such as L-quisqualic acid and L-mimosine, and also describe the physiological role of these enzymes in higher plants.

Experimental procedures

Materials

L. leucocephala de Wit seeds were collected at Ogasawara Islands (Japan), sown in moistened vermiculite and grown in the dark for 7–8 days at 26–28°C. Seedlings were harvested, washed and the cotyledons removed; they were then cooled for 1 h at 0–4°C before enzyme extraction. Sephadex G-25 and G-100, DEAE-Sephadex A-50 and AH-Sepharose 4B were purchased from Pharmacia LKB Biotechnology, Inc. SDS-PAG Plate 4/20 was obtained from Daiichi Pure Chemicals. All other chemicals used were of the highest commercial grade available.

Activity assays

The enzyme preparations obtained were dissolved in 50 mM potassium phosphate buffer (pH 8.0). Substrate concentrations were 4–6 mM for sulphide or 12.5 mM for 3,4-dihydroxypyridine and 12.5 mM for OAS. Incubation was at 30°C for 10 min; the total reaction volume was 0.5 ml, utilizing up to 0.2 ml of enzyme (corresponding to 2–400 µg of protein). Reactions were terminated by the addition of 0.1 ml of 7.5% trichloroacetic acid and the formation of L-cysteine was spectrophotometrically measured at 560 nm using an acidic ninhydrin reagent [24]. The formation of L-mimosine was determined by using 2% ammonium dihydrogen phosphate buffer (pH 2.4) on HPLC (Wakosil 5C18 column, Hitachi 655) [25]. The unit of enzyme activity used in this paper is equivalent to 1 µ mol of L-cysteine or L-mimosine produced per min. Protein was determined by a dye-binding method [26].

Purification of cysteine synthase isoenzymes from L. leucocephala

All operations were carried out at 0–4°C. Cysteine synthases were prepared from 420 g of fresh etiolated seedlings (cotyledons removed) by the same procedure up to ammonium sulfate fractionation as previously described [17–23]. The 30–70% saturated $(NH_4)_2SO_4$ fraction was collected and dissolved in 30 mM potassium phosphate buffer (pH 8.0) containing 10 mM mercaptoethanol (buffer A). The

resulting solutions were then applied to the DEAE-Sephadex A-50 column (2 × 10 cm) pre-equilibrated with buffer A. The column was washed extensively with buffer A and the enzymes eluted with a linear gradient of potassium phosphate (30–350 mM) in the same buffer. Cysteine synthase activities were eluted at 110–150 mM and 150–210 mM potassium phosphate buffer, respectively, and were concentrated by Immersible membrane filter CX-10 (Millipore). The first and second active fractions were individually applied to a column (2 × 95 cm) of Sephadex G-100 pre-equilibrated with buffer A. The eluates were collected in 2 ml fractions, and two series of active fractions were pooled and concentrated by Immersible membrane filter CX-10. The resulting solutions were individually subjected to preparative polyacrylamide gel electrophoresis (PAGE) on 7.5% gels at pH 8.3 (Tris-glycine buffer). Cysteine synthase fractions obtained from gel slices were finally applied to a column (1.0 × 3.5 cm) of AH-Sepharose 4B pre-equilibrated in buffer A and then eluted with a linear gradient of potassium phosphate (30–200 mM) in buffer A. The highly purified enzyme fractions (isoenzyme A: 75–85 mM, isoenzyme B: 80–100 mM) were concentrated by Immersible membrane filter CX-10 and these enzyme preparations in 50 mM potassium phosphate buffer (pH 8.0) were used as isoenzymes A and B in all further experiments.

Spectrophotometric measurements of cysteine synthase isoenzymes

The absorption spectra of purified enzymes were measured at 200–600 nm by using an automatic spectrophotometer (Hitachi 557). The protein concentrations were 0.4 and 0.25 mg per ml of 50 mM potassium phosphate buffer (pH 8.0) for isoenzyme A and B respectively. The identification of bound pyridoxal 5'-phosphate (PLP) in the purified enzymes was determined by measuring the *A* at 410 nm in comparison with that of standard PLP [27].

Molecular weight determination

Native molecular weight of the purified enzymes was determined by gel filtration chromatography using Sephadex G-100 (1.5 × 115 cm) according to the method of Andrews [28]. The column was equilibrated with buffer A, which contained 0.1 M NaCl. The enzyme was detected by assaying fractions for activity at 0.04 ml min^{-1}. The following standard marker proteins (Pharmacia) were used: chymotrypsinogen A (*Mr* = 25,000), ovalbumin (*Mr* = 43,000) and bovine serum albumin (*Mr* = 67,000). The column void volume was determined in a separate run by using Blue Dextran 2,000.

SDS-Polyacrylamide gel electrophoresis

The purified enzymes were subjected to dodecylsulfate electrophoresis on 4–20% gradient gels at pH 8.3 (Tris-glycine buffer) following the method of King and

Laemmli [29] and the running time was 1 h at 60 mA/gel. Gels were stained with Coomassie Brilliant Blue R-250, followed by destaining in HOAc-MeOH-H_2O (1:5:5) The enzyme concentrations were 0.5–2 μg/well and protein standards were α-lactalbumin (Mr = 14,400), trypsin inhibitor (Mr = 20,100), carbonic anhydrase (Mr = 30,000), ovalbumin (Mr = 43,000) and bovine serum albumin (Mr = 67,000) and bromophenol blue was marker.

Kinetics and other properties

The pH optima, curves relating enzyme activities to OAS and sulphide concentrations, etc. were determined under standard assay conditions by using 100 μl samples of purified enzymes.

Identification of heteterocyclic ß-substituted alanines and S-substituted L-Cysteines as reaction products

The normal reaction mixtures contained 12.5 mM of OAS, 70 mM of thiol compounds or N-heterocyclic compounds and 200 μl of enzyme preparation (corresponding to 4 μg of protein), in a final volume of 0.5 ml of 50 mM potassium phosphate buffer (pH 8.0). Incubation was at 30°C for 10–30 min and the reactions were terminated by the addition of 30 μl of 1 N potassium hydroxide. The resulting solution acidified with 15 μl of 6 N HCl was examined for the formation of heterocyclic ß-substituted alanines and S-substituted L-cysteines by using an automatic amino acid analyzer (Hitachi 835–10) under standard operating conditions (2.6 × 25 cm column, 33–68°C, Li-citrate buffer system pH 3.0–7.0, flow rate 0.275 ml min^{-1})[30].

Results

Enzyme purification

Initially the extraction and purification of cysteine synthase from 420 g fresh weight of 7–8 day-old seedlings (cotyledons removed) of *L. leucocephala* followed our previous methods [17–23]. The enzyme was prepared simultaneously with the L-mimosine synthase activity by a procedure including heat treatment, ammonium sulfate fractionation, gel filtration on Sephadex G-100, ion-exchange chromatography on DEAE-Sephadex A-50, preparative PAGE and hydrophobic chromatography on AH-Sepharose 4B. Two peaks exhibiting cysteine synthase activity were separated completely after the DEAE-Sephadex A-50 column was eluted with a concentration gradient of potassium phosphate buffer. Cysteine synthase A was eluted at 110–150 mM and cysteine synthase B at 150–210 mM, respectively, and the enzyme activity for L-mimosine synthase was completely overlapped with the peak of cysteine synthase B (Fig. 1). The complete procedure

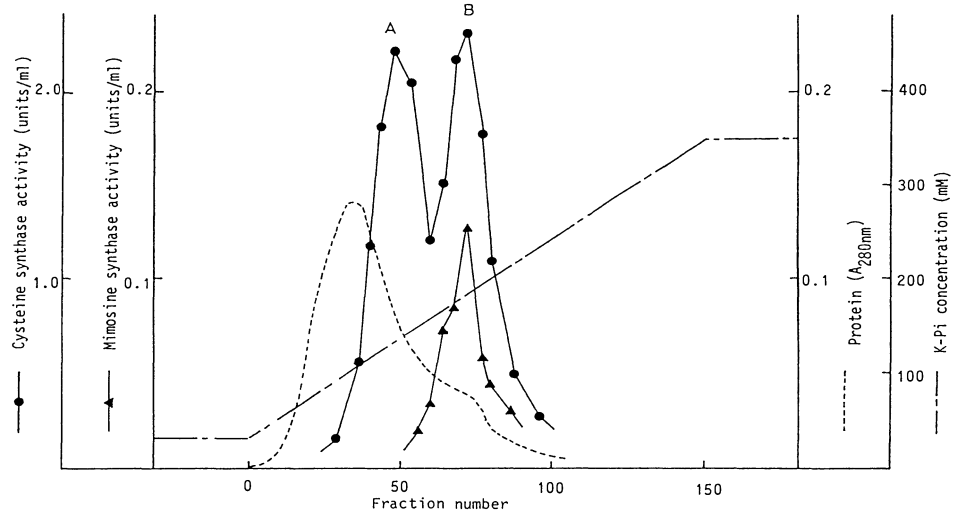

Fig. 1. Elution patterns of cysteine synthases and mimosine synthase activities after the DEAE-Sephadex A-50 column chromatography. Cysteine synthase activity (•—•), mimosine synthase activity (▲—▲) and protein (A_{280},- - -) were monitored as shown in the Experimental Procedures.

afforded apparent purifications of *ca* 500-fold for isoenzymes A and B; with the specific activity of 82.5 U/mg protein for A, 95.7 U/mg protein for B, and yields of 3.2 and 2.3%. respectively, as compared to the total cysteine synthase activity of the crude extract.

Properties of isoenzymes

The *Mrs* of the purified enzymes were estimated by analytical gel filtration using Sephadex G-100. Cysteine synthase activity of isoenzymes A and B was found invariably as a single peak, corresponding to *Mr*s of 64,000. The purified isoenzymes were subjected to SDS-PAGE on 4–20% gradient gels to determine their subunit structures. This suggests that both native enzymes are composed of two identical subunits similar to the cysteine synthases from other plant sources (Table 1).

The purified enzymes had absorbance peaks 280 and 410 nm, typical for a PLP-enzyme. Direct spectrophotometric measurements indicated that both cysteine synthase isoenzymes in *L. leucocephala* had one molecule of PLP bound to each subunit also similar to the cysteine synthases from other sources [19–23, 31–33].

The enzymes exhibited a single pH optimum at pH 8, although there was a rapid acetyl shift from O to N atoms in OAS above *ca* pH 8.

The isoenzymes of cysteine synthase from *L. leucocephala* display somewhat different relative activities, but their responses to OAS are essentially the same.

Table 1. Some properties of cysteine synthases in higher plants

Enzyme source	Enzyme	Molecular weight		Pyridoxal 5'-phosphate (mol/enzyme)	K_m value (mM)	
		Native enzyme	Subunit		O-acetyl-L-serine	H_2S
Leucaena leucocephala	Cysteine synthase					
	Isoenzyme A	64,000	32,000	2	16.7	–[a]
	Isoenzyme B	64,000	32,000	2	6.7	–
Quisqualis indica	Cysteine synthase					
var. *villosa* [20]	Isoenzyme A	58,000	29,000	n.d.[b]	1.9	0.059
	Isoenzyme B	58,000	29,000	n.d.	7.1	n.d.
Pisum sativum [21]	Cysteine synthase					
	Isoenzyme A	52,000	26,000	2	2.1	0.036
	Isoenzyme B	52,000	26,000	2	2.3	0.038
Citrullus vulgaris [22]	Cysteine synthase					
	Isoenzyme A	58,000	29,000	2	2.6	0.036
	Isoenzyme B	58,000	29,000	2	1.5	0.033
Spinacia oleracea [19]	Cysteine synthase	60,000	30,000	2	2.9	0.022
Brassica juncea [23]	Cysteine synthase	52,000	26,000	2	2.5	0.043
Brassica chinensis	Cysteine synthase	62,000	31,000	2	6.1	n.d.
var. *Komatsuna* [31]						
Raphanus sativus [32]	Cysteine synthase	66,000	33,000	n.d.	2.2	n.d.
Phaseolus vulgaris [33]	Cysteine synthase					
	Isoenzyme A }	65,000~	n.d.	n.d.	3.8	0.28
	Isoenzyme B }	70,000	n.d.	n.d.	2.3	0.33

[a] Hill numbers are 2.3 for each enzyme.
[b] Not determined.

Isoenzymes A and B have K_m values of 16.7 and 6.7 mM for OAS, respectively, but they show no indication of inhibition by OAS at concentrations up to 20 mM. The K_m value for OAS of isoenzyme B has almost the same value as that determined for L-mimosine synthase from the same plant [18] and is also very close to the value determined for isoenzyme B of cysteine synthase from *Q. indica* var. *villosa* [20]. The response of isoenzymes A and B to sulphide concentrations below 0.2 mM was also examined, and the kinetic parameters obtained indicate Hill numbers of approximately 2.3 for each of the isoenzymes. The K_m values for sulphide of other cysteine synthases were obtained before [19–23].

The addition of PLP had an inhibitory effect on the activities of both enzymes, the decrease being about 5% at a concentration of 0.1 mM, and was further inhibitory at higher concentration, 1 mM causing 30% and 15% inhibition of isoenzymes A and B respectively. Similar inhibitory effects of PLP have been reported for cysteine synthases [19–23]. Both isoenzymes were sensitive to PLP-enzyme inhibitors: sodium borohydride at a concentration of 10 mM caused about 95% inhibition, while 10 mM hydroxylamine had a less inhibitory effect, the decrease being 35% and 50% for isoenzymes A and B respectively.

Substrate specificity

Under standard assay conditions, the cysteine synthase isoenzymes from *L. leucocephala* seedlings clearly appear to be specific for OAS as a donor of the alanyl moiety, an observation in line with previous findings [19–23]. In isoenzyme B, the activity was 72.4% and 8% in the presence of ß-chloro-L-alanine and O-sulfo-L-serine, respectively, in comparison with the activity with OAS at 12.5 mM under identical conditions. No detectable activity was found with O-phospho-L-serine or with L-serine.

Isoenzymes A and B also showed a distinct substrate specificity when a variety of thiol compounds or N-heterocyclic compounds were used as an acceptor for the alanyl moiety (Table 2). The relative activities of the purified enzymes with different substrates were compared with that of L-cysteine formed by each enzyme. Isoenzyme A could not synthesize L-quisqualic acid, L-willardiine or L-isowillardiine when suitable substrate were provided, while this enzyme synthesized S-substituted L-cysteines. However, isoenzyme A could synthesize ß-(pyrazol-1-yl)-L-alanine, ß- (3-amino-1,2,4-triazol-1-yl)- L-alanine, L-mimosine and ß- cyano-L-alanine at low rates. Isoenzyme B, on the other hand, synthesized L-mimosine, ß-(pyrazol-1-yl)-L-alanine and ß- (3-amino-1,2,4-triazol-1-yl)-L-alanine, although this enzyme also could not synthesize L-quisqualic acid, L-willardiine, L-isowillardiine or ß-cyano-L-alanine. The different heterocyclic substrates were tested under the same conditions described previously [19-23]. Thus, both isoenzyme A and B show different substrate specificities as compared with cysteine synthases from other sources [19–23, 31–33].

Table 2. Relative synthetic rates of S-substituted L-cysteines and ß-substituted alanines by cysteine synthases in higher plants

Amino acid synthesized	*Leucaena leucocephala* Cysteine synthase		*Quisqualis indica* var. *villosa* Cysteine synthase		*Pisum sativum* Cysteine synthase		*Citrullus vulgaris* Cysteine synthase		*Spinacia oleracea* Cysteine synthase
	Iso-enzyme A	Iso-enzyme B	Iso-enzyme A	Iso-enzyme B	Iso-enzyme A	Iso-enzyme B	Iso-enzyme A	Iso-enzyme B	
L-Cysteine	100[a]	100	100	100	100	100	100	100	100
S-Methyl-L cysteine	29.6	12.7	7.7	n.d.[b]	4.0	1.75	21.5	71.9	31.7
S-Allyl-L-cysteine	21.6	73.2	4.0	n.d.	2.6	7.08	0.46	5.76	17.6
S-Carboxymethyl-L-cysteine	0.35	0.97	0	n.d.	2.31	1.62	3.46	2.81	2.5
L-Quisqualic acid	0	0	0	0.33	0	0	0	0	0
L-Mimosine	0.03	15.7	n.d.	n.d.	0	0	0	0	0
L-Willardiine	0	0	0	0	0	0	0	0	0
L-Isowillardiine	0	0	0	0	0	0	0	0	0
ß-(Pyrazol-1-yl)-L-alanine	0.23	0.19	1.2	0.44	1.33	0.54	1.88	1.99	3.8
ß-(3-Amino-1,2,4-triazol-1-yl)-L-alanine	0.74	0.33	0.59	0.48	0.74	0.65	0.98	1.31	0.97
ß-Cyano-L-alanine	0.13	0	1.58	0	22.1	0	35.1	0	0

[a]The relative rates of synthesis (%) were compared with that of L-cysteine formed by each enzyme, respectively.
[b]Not determined.

Discussion

Several different types of cysteine synthase have been isolated from various higher plants [19–23, 31–33], and the existence of isoenzymes of cysteine synthases catalysing the formation of heterocyclic ß-substituted alanines has been reported previously [20–22]. In the present study, we have purified two cysteine synthases from *L. leucocephala* seedlings to apparent homogeneity and a comparison has been made of their properties and substrate specificities with those of the previously purified enzymes [19–23] from the viewpoint of the biosynthesis of heterocyclic ß-substituted alanines in higher plants.

The two enzymes purified in this study have very similar physicochemical properties: they have the same *Mrs* of 64,000 and consist of two identical subunits, they have the same pH optimum of 8 and they contain one molecule of PLP per subunit. The physicochemical properties of the enzymes we have purified from *L. leucocephala* seedlings are almost the same as those of cysteine synthases from other plant sources (Table 1): the *Mrs* for plant cysteine synthases have been reported to be in the range 52,000–70,000, they can be dissociated into two identical subunits of *Mrs* approximately half of that of the intact enzyme, they contain 2 mol of PLP, they have almost the same pH optimum of 8.0 and the K_m values for OAS are also within the range of 1.5–7.1 mM [19–23, 31–33].

Among the substrates studied thus far (Table 2), cysteine synthases from *L. leucocephala* could catalyse the formation of S-substituted L-cysteines and also heterocyclic ß-substituted alanines such as ß-(pyrazol-1-yl)-L-alanine and ß-(3-amino-1,2,4-triazol-1-yl)-L-alanine in low yields, but could not catalyse the formation of L-quisqualic acid, L-willardine or L-isowillardine. These observations are in line with our previous findings [19–23]. On the biosynthesis of L-willardiine and L-isowillardiine, they are synthesized by the uracilylalanine synthases in pea seedlings [21]. Morerover, the cysteine synthase isoenzyme B from *L. leucocephala* could catalyze the formation of L-mimosine in relatively high yield. When the physicochemical properties of this enzyme are compared with those of L-mimosine synthase purified before [18], they are almost the same. Therefore, we consider that the isoenzyme B of cysteine synthase from *L. leucocephala* seedlings also functions as a L-mimosine synthase in the same manner as the formation of L-quisqualic acid in *Q. indica* var. *villosa* [20] and ß-(pyrazol-1-yl)-L-alanine in *Citrullus vulgaris* [22] are also catalysed by a cysteine synthase isoenzyme. The purified isoenzyme A, on the other hand, catalyzed the formation of ß-cyano-L-alanine from OAS and CN^-as an additional activity, this activity is different from the biosynthesis of ß-cyano-L-alanine from L-cysteine and CN^- as catalyzed by the ß-cyanoalanine synthases from microorganisms and some higher plants [34–36].

All our findings concerning plant cysteine synthases suggest that this group of enzymes can play a role in the detoxification of endogenous- or eventually exogenous-toxic molecules such as cyanide, hydrogen sulphide or pyrazole in higher plants without jeopardizing the synthesis of L-cysteine as a primary metabolite, thereby forming secondary metabolites like the ß-substituted alanines,

which may have an ecological role as allelochemicals. A similar metabolic detoxification by alanyl-substitution of unnatural heterocyclic chemicals has been described before in plants [37,38].

This is in agreement with earlier statements by Fowden [39] and Bell [40], proposing that some non-protein amino acids may have arisen by a modification of common pathways for the biosynthesis of the protein amino acids. This modification can thus be effected by a change in substrate specificity of the enzymes involved.

When the known amino acid compositions of cysteine synthases purified before [21–23] are compared by a mathematical method [41], it is suggested that cysteine synthases from higher plants seem to be closely related to each other. This makes it likely that a phylogenetic relationship exists among those enzymes.

References

1. Takemoto T, Takagi N, Nakajima T and Koike K (1975) Yakugaku Zasshi 95: 176–179.
2. Hegarty MP, Schinckel PG and Court RD (1964) Aust. J. Agric. Res. 15: 153–167.
3. Murakoshi I, Kuramoto H, Haginiwa J and Fowden L (1972) Phytochemistry 11: 177–182.
4. Murakoshi I, Kato F, Haginiwa J and Takemoto T (1974) Chem. Pharm. Bull. 22: 473–475.
5. Murakoshi I, Kato F and Haginiwa J (1974) Chem. Pharm. Bull. 22: 480–481.
6. Murakoshi I, Ikegami F, Kato F, Haginiwa J, Lambein F, Van Rompuy L and Van Parijs R (1975) Phytochemistry 14: 1515–1517.
7. Murakoshi I, Ikegami F, Ookawa N, Ariki T, Haginiwa J, Kuo Y -H and Lambein F (1978) Phytochemistry 17: 1571–1576.
8. Murakoshi I, Ikegami F, Harada K and Haginiwa J (1978) Chem. Pharm. Bull. 26: 1942–1945.
9. Murakoshi I, Koide C, Ikegami F and Nasu K (1983) Chem. Pharm. Bull. 31: 1777–1779.
10. Dunnill PM and Fowden L (1963) J. Exp. Botany 14: 237–248.
11. Hadwiger LA, Floss HG, Stoker JR and Conn EE (1965) Phytochemistry 4: 825–830.
12. Tiwari HP, Penrose WR and Spenser ID (1967) Phytochemistry 6: 1245–1248.
13. Giovanelli J and Mudd SH (1968) Biochem Biophys. Res. Commun. 31: 275–280.
14. Thompson JF and Moore DP (1968) Biochem. Biophys. Res. Commun. 31: 281–286.
15. Smith IK and Thompson JF (1971) Biochim. Biophys. Acta 227: 288–295.
16. Ng BH and Anderson JW (1978) Phytochemistry 17: 2069–2074.
17. Murakoshi I, Ikegami F, Hinuma Y and Hanma Y (1984) Phytochemistry 23: 973–977.
18. Murakoshi I, Ikegami F, Hinuma Y and Hanma Y (1984) Phytochemistry 23: 1905–1908.
19. Murakoshi I, Ikegami F and Kaneko M (1985) Phytochemistry 24, 1907–1911.
20. Murakoshi I, Kaneko M, Koide C and Ikegami F (1986) Phytochemistry 25: 2759–2763.
21. Ikegami F, Kaneko M, Lambein F, Kuo Y-H and Murakoshi I (1987) Phytochemistry 26: 2699–2704.
22. Ikegami F, Kaneko M, Kamiyama H and Murakoshi I (1988) Phytochemistry 27: 697–701.
23. Ikegami F, Kaneko M, Kobori M and Murakoshi I (1988) Phytochemistry 27: 3379–3383.
24. Gaitonde MK (1967) Biochem. J 104: 627–633.
25. Lowry JB, Tangendjaja B and Cook NW (1985) J. Sci. Food Agric. 36: 799–807.
26. Bradford MM (1976) Anal. Biochem. 72: 248–254.
27. Kumagai H, Yamada H, Matsui H, Ohkishi H and Ogata K (1970) J. Biol. Chem. 245: 1773–1777.
28. Andrews P (1965) Biochem. J. 96: 595–606.
29. King J and Laemmli UK (1971) J. Mol. Biol. 62: 465–477.
30. Murakoshi I, Ikegami F, Hama T and Nishino K (1984) Shoyakugaku Zasshi 38: 355–358.

31. Masada M, Fukushima K and Tamura G (1975) J. Biochem. 77: 1107–1115.
32. Tamura G, Iwasawa T, Masada M and Fukushima K (1976) Agric. Biol. Chem. 40: 637–638.
33. Bertagnolli BL and Wedding RT (1977) Plant Physiol. 60: 115–121.
34. Ikegami F, Takayama K, Tajima C and Murakoshi I (1988) Phytochemistry 27: 2011–2016.
35. Manning K (1986) Planta 168: 61–66.
36. Ikegami F, Takayama K and Murakoshi I (1988) Phytochemistry 27: 3385–3389.
37. Massini P (1963) Acta Bot. Neerl. 12: 64–72.
38. Murakoshi I, Ikegami F, Nishimura T and Tomita K (1985) Phytochemistry 24: 1693–1695.
39. Fowden L, Lea PJ and Bell EA (1979) Adv. Enzymol. 50: 117–175.
40. Bell EA (1976) FEBS Letters 64: 29–35.
41. Chernoff H (1973) J. Am. Stat. Assoc. 68: 361–368.

Address for correspondence: Fumio Ikegami, PhD, Faculty of Pharmaceutical Sciences, Chiba University, Yayoi-cho 1–33, Chiba 260, Japan.

Tryptophan side chain oxidase: Types I and II from *Pseudomonas*

Akira Kanda, Hidefumi Yoshii, Eiko Nakamaru, Masaki Shiraishi and Katsuji Takai

The Department of Biochemistry and Nutrition, School of Health Sciences, Faculty of Medicine, The University of Tokyo, Tokyo 113, Japan

Abstract

Tryptophan side chain oxidase (TSO), a new type of hemoprotein, is an O_2-linked dehydrogenase that acts on tryptophan residues in peptides and proteins, free tryptophan, and also various 3-substituted indoles, to give corresponding products oxidized at the alanine side chain (Nakamaru *et al.*, this proceedings).

Two types of TSO(TSO I/II), distinguishable in *Mr*, subunit structure, and antigenicity, have been purified from a strain of *Pseudomonas*. TSO II (150-kDa), a simpler type, consisted of two functional units; the dehydrogenase (DH, 80-kDa) and the oxidase (OX, 48-kDa), both isolated as free forms. DH had a substrate binding site (most likely, charge-transfer type), a free radical (g=2.005, spherical) stable under aerobic conditions and at room temperature, and a high potential heme b ($E^{\circ\prime}$= 0.42 V), nonautooxidizable per se. The radical appeared to be another one-electron carrier coupled with heme, the equilibrium being shifted far to the latter. OX combined reversibly with DH ($K_d = 10^{-9}$ M) accepted electrons from reduced DH, and catalyzed 4-electron reduction of O_2, most likely, via an autooxidizable cyanide/nitrite-sensitive heme-like chromophore. The structure and function of TSO I (280-kDa) may be essentially similar to those of TSO II.

TSO thus provided new and crucial issues of biological electron transfer initiated by interaction with tryptophan residues in peptides and proteins, followed by mobilization and abstraction of electrons and, via intra/intermolecular electron transfer, ending up with 4-electron reduction of molecular oxygen.

Introduction

In 1977, a new type of hemoprotein that catalyzes the oxidation of tryptophan to give a hitherto undescribed product, 3-indoleglyoxal, was isolated and crystallized from *Pseudomonas* [1]. At comparable rates, it acted also on tryptophan residues (Trp) in peptides and various 3-substituted indoles. These reactions required O_2 and were cyanide (CN)-sensitive, but a CN-insensitive reaction proceeded under anaerobic conditions in the presence of an electron acceptor such as 2,6-dichlorophenolindophenol (DCPIP) or ferricyanide, indicating that the enzyme was not an oxygenase or hydroxylase, but an O_2-linked dehydrogenase (oxidase). Dehydrogenation at the alanine side chain was eventually established when a product of N-acetyl-L-tryptophanamide (Ac-Trp-NH_2), a model substrate for tryptophan residue in peptides, was identified as Ac-α,ß-dehydro-Trp-NH_2(Ac-Δ-Trp-NH_2). At this stage, the enzyme was termed tryptophan side chain oxidase (TSO). Subse-

quently another type of TSO (TSO II) was isolated and purified from the same strain, which was essentially similar to in reactions but distinct from the original TSO (TSO I) in *Mr*, subunit structure, and antigenicity. Analyses of TSO II showed that it was a multienzyme system consisting of the dehydrogenase component (DH), a b-type cytochrome catalyzing ferricyanide reductase (partial) reaction of TSO II, and the oxidase component (OX) which constituted the O_2-linked TSO activity with DH [2–5, and references therein].

In this paper, we describe first the outline of structure and function of TSO I, TSO II, and the subunits (DH and OX) of TSO II, and then, the results of ongoing analyses of DH on substrate binding, the free radical, b-type heme, and their interrelationships. Accounts for TSO-catalyzed reactions are presented in tandem in this proceedings (Nakamaru *et al.*).

Materials and Methods

TSO I, TSO II, and DH and OX for TSO II, were isolated and purified from *Pseudomonas* essentially as described [5] with modifications to afford a rapid and larger scale (g-order) purification [6]. Holo (O_2-linked) enzyme activity of TSO I/II was assayed either by O_2 consumption or the formation of Ac-Δ-Trp-NH_2 ($\varepsilon_{mM,\ 333nm}$=19.8 cm^{-1}) from Ac-Trp-NH_2, spectrophotometrically [5]. Partial DH activity was assayed by monitoring the reduction of ferricyanide or DCPIP [5], and, for OX activity, CN-sensitive O_2 consumption or ferricyanide formation with ferrocyanide as electron donor, was monitored [6], or else, the sample was preincubated with the fixed amounts of the isolated DH and the reconstituted O_2-linked activity was measured [5]. Assays were performed at 25°C in 0.5 M potassium phosphate (pH 6.0). EPR spectra were recorded on a JEOL model FE-3XG (Tokyo) at room temperature.

Results and Discussion

Properties of TSO I, TSO II, and isolated subunits (DH and OX) of TSO II (Table 1)

Two types of holoenzymes were molecular entities mutually distinguishable in *Mr* of the native forms and subunits, pI, and antigenicity (non cross reactive). TSO I preferred free tryptophan as substrate, whereas TSO II was far more active on Ac-Trp-NH_2, a model substrate for internal tryptophan residues in peptides, but inactive on tryptamine and N-terminal Trp [2,5,7,8].

However, the mode of reactions catalyzed by TSO I and II was identical, both consisted of non-covalently-linked multiple subunits, and contained heme b and Fe at a ratio of 1:2. The absorption spectra of the native and dithionite-reduced (Fig. 1A and *inset*) TSO I and II, and their pyridine hemochromes, indicated that both contained low-spin b-type cytochromes. Upheaval of the absorption at 430–700

Table 1. Physicochemical and catalytic properties of TSO I, TSO II, and dehydrogenase (DH) and oxidase (OX) of TSO II [3,5,9,10]

	TSO I	TSO II	DH	OX
Mr (kDa); native	280	150	64	58
subunits	83[a]	80	80	
	45,40	48		48
Heme b(mol/mol enzyme)	2	1	1	0[b]
Fe (mol/mol enzyme)	4	2	1	1
Substrate specificity (%)[c]				
L-tryptophan	100	100	100	
Ac-Trp-NH_2	47	458	172	
tryptamine	27	3	0	

[a]A value for TSO I purified by a new method [10]. Additional entities (60- and 30-kDa) were often detected. [b]Heme-like chromophore was detected. [c]Expressed as % of activity as compared with that for L-tryptophan.

nm, not accounted for heme b (Fig. 1A, 1B), and Fe in excess over heme (Table 1), were ascribed to one of TSO II subunits as described below.

Two functional subunits (DH) (80-kDa) and OX (48-kDa) of TSO II (150-kDa), were successfully isolated and purified from cell extracts by following ferricyanide reductase activity which was TSO-substrate dependent but not linked to O_2, and a component which reconstituted the TSO II holoactivity with the isolated DH, respectively [2,3,5,9]. They combined with high specificity ($K_d=10^{-9}$ *M*) to form an active molecular complex indistinguishable from TSO II. DH, isolated as a reduced form, was a large-sized (80 kDa) low spin b-type cytochrome (Fig. 1B) with substrate site, nonautooxidizable heme b, and a free radical [9] (see below). The turnover number and substrate specificity of ferricyanide reductase were virtually identical for DH and TSO II. No prosthetic group and metal other than heme and its Fe, have been detected. The isolated OX (48-kDa) contained 1 mol of Fe, most likely combined with a heme-like red/ox chromophore with $\varepsilon_{mM,440nm}$, for reduced OX of $\approx$ 60 cm^{-1} (Fig. 1C). Its isolation and identification are now

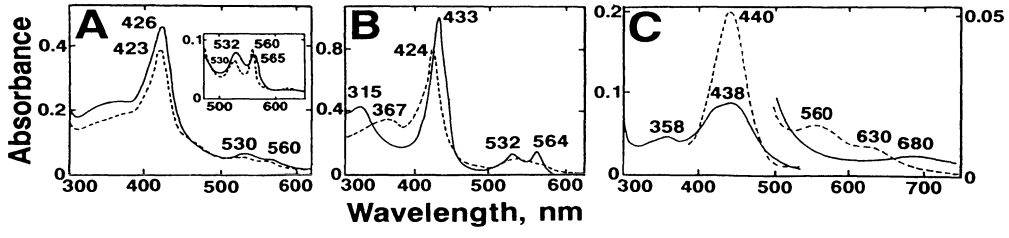

Fig. 1. Absorption spectra of TSO I, TSO II, and DH and OX components of TSO II at pH 6.0 (3,5). A, 0.5 mg/ml native TSO I(- - -) and II(——) and those reduced with dithionite (inset); B, 0.8 mg/ml native (——) and ferricyanide-oxidized (- - -) DH; and C, 0.16 mg/ml native (——) and dithionite-reduced (- - -) OX.

underway. Catalytic amounts of OX readily converted otherwise non-autooxidizable reduced DH to an oxidized form, indicating that OX mediated electron transfer between the reduced DH and O_2. Reduced spectrum of OX returned to the active one by autooxidation or else collapsed by nitric oxide [3,5]. OX showed CN/NO_2^--sensitive ferrocyanide oxidase (partial) activity, its pH optimum, K_m for O_2, and inhibitors were essentially similar to those of O_2-linked TSO II activity [11]. Upon O_2-linked reactions of TSO II and OX, no H_2O_2 was formed, indicating that OX involved in 4-electron reduction of O_2, and peroxidase and catalase activities were undetected in these systems.

TSO II was, thus, established to be a multienzyme system consisting of two functional subunits which were, most likely, coupled as depicted below. Although functional subunits are as yet unavailable, this 'respiratory chain' may run,

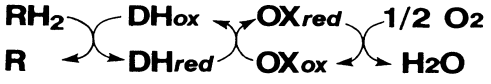

possibly in duplicate, also in TSO I; TSO I showed a partial dehydrogenase activity linked to DCPIP rather than ferricyanide, and CN-sensitive ferrocyanide oxidase activities [11]. Detailed accounts for the first half of TSO system are described below.

Characterization of dehydrogenase component (DH) of TSO II

Although DH was, spectrophotometrically, a mere low-spin b-type cytochrome (Fig. 1B), its *Mr* (80-kDa) was larger than those of electron transfer cytochromes with one heme molecule (Table 1). In this single polypeptide chain, the substrate site, free radical, and heme b may interplay to constitute ferricyanide reductase activity, most likely, initiated by the binding of tryptophan residues followed by abstraction of electrons, intramolecular electron transfer, and finally intermolecular electron transfer to ferricyanide or to OX in holoenzyme. To unravel these issues we began with kinetic studies on the overall reaction of DH.

Almost absolute dependence of the activity on ionic strength, as interpreted by facilitation of electron transfer between samely (negatively) charged DH (pI=4.3) and ferricyanide molecules, was a first premise of the reaction [12]. A ping-pong type steady state kinetics showed that substrate (Ac-Trp-NH_2) dehydrogenation and the reduction of ferricyanide were mutually independent steps [5,12]. For substrate site analysis, a series of *p*-substituted anilines were found to be competitive inhibitors. The plots of K_i vs their pK_B representing the electron densities of aniline nitrogen, gave a concave curve with a minimum for *p*-Br(Cl)-anilines (K_i=5 μM); substituents with either a lower or higher electron density than those of Br(Cl)-substituents showed weaker binding, and *p*-aminophenol, among the highest in the series, even served as slow substrate. These results suggested that the inhibitor and, possibly, the substrate sharing the aniline moiety in its indole ring also bound with the substrate site by a charge-transfer type interaction [4,5,12].

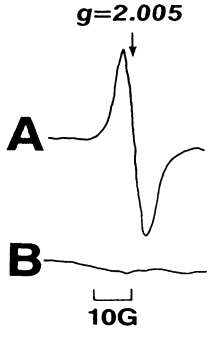

Fig. 2. EPR spectra of dehydrogenase (DH) of TSO II at 22°C and pH 6 (14). 52 μM native (reduced) (A) and ferricyanide-oxidized (B) DH.

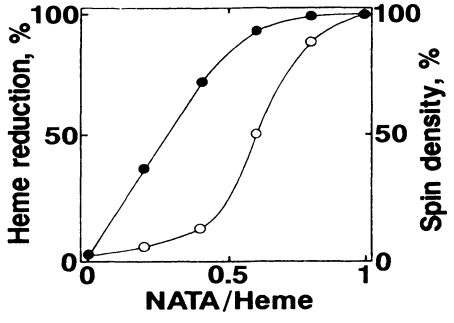

Fig. 3. Titration of oxidized DH with Ac-Trp-NH_2 (NATA) at pH 6 (μ=0.5) and 22°C (14). To 0.7 ml of oxidized DH (15.7 μM heme), 2 μl aliquots of NATA were sequentially added and, each after 10–30 min, A_{433nm} was monitored whereas an aliquot (5 μl) was subjected to recording EPR spectra. Heme reduction (●) was expressed as % increase in A_{433nm} and spin density (○) as % of peak area at g=2.005 as compared with that of fully reduced DH.

The inhibitor induced a marked quenching of the intrinsic fluorescence of tryptophan, but no change in visible spectra of heme suggesting that the substrate site and the tryptophan which probed the binding, may be located apart from the heme (otherwise the potent quencher) [13].

The free radical (g=2,005, spherical) of the native DH was stable under aerobic conditions and at room temperature. The signal showed no hyperfine structure resolved under liquid nitrogen except a modest increase in peak heights. It was totally quenched on oxidation with ferricyanide (Fig. 2), and reappeared by the addition of not only substrate but also dithionite, indicating that substrate and porphyrin radicals may be unlikely [14]. Pyrroloquinoline quinone (PQQ) semiquinone once suspected for the radical [15] suffered from the sparse content (10^{-3} mol/mol enzyme) and the effect of dithionite which may quench PQQ semiquinone. Upon titration of the oxidized DH with 2-electron substrate (Fig. 3), the heme reduction was almost complete with first 1-electron equivalent, followed by the radical formation with another 1-electron equivalent, indicating that the radical served as an additional 1-electron carrier to heme, hence, DH, a 2-electron carrier system. The radical and heme may be electronically coupled, and in an equilibrium shifted far to the latter. The coupling might be of a long-distance nature, since, at any stage of the titration, the peak-to-peak width and the shape of signals were maintained and absorption spectra of heme showed no more than features of reduced and oxidized forms. *p*-Cl-Aniline induced the quenching of the radical

concurrent with that of tryptophan fluorescence (as above), both with a time course up to 30 min [14]. Irrespective of conformational or electronic coupling, substrate binding, thus, appeared to be linked with the radical rather than heme. We, at present, would favor that the radical may derive from an intrinsic structure of the DH protein.

For the heme b in DH (Fig. 1B), an E°' (pH 6.0, μ=0.5) of 0.42 V, an exceptionally high value for b-type cytochromes, was obtained electrochemically and also with ferricyanide-ferrocyanide couple [2–4,5,12]. To assess whether its high potential is critical for catalysis, the turnover numbers of DH with various electron acceptors were correlated with their E°' ranging from 0–0.6 V. The plots of the turnover number vs E°' gave a convex curve with a maximum (3,000–5,000 sec^{-1}) between 0.42 and 0.6 V [12]. For these results, we are in favor of the matching of E°' values of the donor (herein, we assumed heme b of E°'= 0.42 V) and the acceptor to give a maximum rate of electron transfer, rather than a simple estimation of a lower E°' of heme in catalytic cycle, taking into account a huge reorganization energy [16]. Based on these and foregoing results, we would suggest, that the heme b in the depth of DH may most likely serve as a deeply positive electronic trough to support the overall reaction including electron abstraction from tryptophan residues, possibly, its electron transfer to the radical and then to heme, in the red/ox equilibrium manner, and then the feeding electrons outside DH as a rate-limiting step prescribed by a red/ox matching between heme and acceptors. If it is valid, the rate of each preceding step must be as high as or even exceed 5,000 sec^{-1} (a maximum turnover rate in the overall reaction with matched acceptors) in the steady state reaction.

The present studies on TSO systems and DH, thus, provided new and unique issues of a biological electron transfer spanning from protein [8] to molecular oxygen. The outline of our working model is illustrated in Fig. 4.

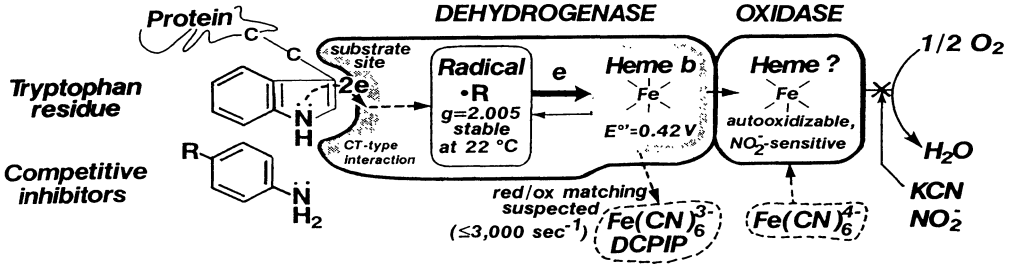

Fig. 4. Working model for electron transfer in TSO system.

References

1. Takai K, Ushiro H, Noda Y, Narumiya S, Tokuyama T and Hayaishi O (1977) J. Biol. Chem. 252: 2648–2656.
2. Takai K (1980) Dev. Biochem. 16: 103–115.
3. Takai K, Müller R, Zavala F, Inoue S, Narumiya S, Ito S and Hayaishi O (1982) In: Nozaki M, Yamamoto S, Ishimura Y, Coon MJ, Ernster L and Estabrook RW (eds.) Oxygenases and Oxygen Metabolism. Academic Press, New York, pp. 159–172.
4. Takai K, Inoue S, Zavala F, Müller R, Hamasaki T and Sasai Y In: Schlossberger HG, Kochen W, Linzen B and Steinhart H (eds.) Progress in Tryptophan and Serotonin Research. Walter de Gruyter, Berlin, pp. 765–768.
5. Takai K, and Hayaishi O (1987) Methods Enzymol. 142: 195–217.
6. Kanda A and Takai K, unpublished results.
7. Ito S, Takai K, Tokuyama T and Hayaishi O (1981) J. Biol. Chem. 256: 7834–7843.
8. Takai K, Sasai Y, Morimoto H, Yamazaki H, Yoshii H and Inoue S (1984) J. Biol. Chem. 259: 4452–4457.
9. Ushiro H, Takai K, Narumiya S, Ito S and Hayaishi O (1979) J. Biol. Chem. 254: 11794–11797.
10. Kanda A and Takai K, unpublished results.
11. Kanda A and Takai K, unpublished results.
12. Yoshii H, Kanda A, Nakamaru E and Takai K, in preparation.
13. Kanda A, Nakamaru E and Takai K, in preparation.
14. Kanda A, Nakamaru E, Yoshii H and Takai K, in preparation.
15. Van der Graaff W, Duine JA, Frank Jzn J and Jongejan JA (1984) In: Schlossberger HG, Kochen W, Linzen B and Steinhart H (eds.) Progress in Tryptophan and Serotonin Research. Walter de Gruyter, Berlin, pp. 762–764.
16. Tollin G, Terrance EM and Cusanovich MA (1986) Biochim. Biophys. Acta 853: 29–41.

Enzymatic derivatizations of tryptophan residues in peptides and proteins, free tryptophan, and its metabolites with tryptophan side chain oxidase types I and II from *Pseudomonas*

Eiko Nakamaru, Takaaki Kawashima, Yoshiki Kamiyama, Hidefumi Yoshii, Akira Kanda and Katsuji Takai

The Department of Biochemistry and Nutrition, School of Health Sciences, Faculty of Medicine, The University of Tokyo, Tokyo 113, Japan

Abstract

Enzymatic derivatizations of tryptophan residues in peptides and proteins, free tryptophan, and its metabolites, have been achieved with a new type of O_2-linked dehydrogenase with broad substrate specificity, termed tryptophan side chain oxidase (TSO) types I and II (TSO I/II) from *Pseudomonas* (Kanda *et al.*, this proceedings).

The mode of TSO-reaction was diverse depending on the substrate used. Free tryptophan gave 3-indoleglyoxal concomitant with the release of NH_3 and CO_2. For tryptophan residues (Trp), their positions in peptides were crucial; (i), N-terminal Trp underwent dehydrogenation followed by hydration to give diastereomeric ß-hydroxy-Trp (ß-OH-Trp), which was further dehydrogenated to ß-keto-Trp; (ii), C-terminal Trp was converted to α,ß-dehydrotryptamine residue and CO_2; (iii), the dehydrogenation of the internal Trp gave simultaneously α,ß-dehydro-Trp (Δ-Trp) and ß-OH-Trp, via pH-dependent nonenzymatic isomerization and hydration of a common indolyloxazoline-type primary intermediate, respectively, as assessed with a model substrate, Ac-Trp-NH_2. Other nucleophiles also reacted with the intermediate to give a variety of ß-substituted-Trp. ß-OH-Trp alike in (i), was converted to ß-keto form, or else, at extreme pH's nonenzymatically dehydrated to Δ-Trp. The diversity of TSO-reactions was, thus, ascribed to the nature of intermediates and nonenzymatic reactions. TSO II was almost inert for N-terminal Trp, whereas TSO I, larger in M_r, was mostly inactive on internal Trp of polypeptides with conformations.

On these bases, we obtained various active peptides and proteins containing Δ-Trp and/or ß-substituted-Trp, and also free ß-substituted tryptophan by peptidase treatment of oligopeptides with TSO-modified Trp. Serotonin, melatonin, and so forth were converted to DL-hydroxy and keto derivatives at the side chain carbon atoms adjacent to the indole C-3 carbon.

Implications of the present results are discussed together with our concept in the search for new amino acid residue metabolisms.

Introduction

Derivatizations of amino acid residues, free amino acids, and their metabolites, have been achieved almost exclusively by organic chemistry. Notwithstanding the wealth of their *in vivo* derivatives such as antibiotics, alkaloids, and so forth[1], enzymatic derivatization *in vitro* as yet suffers from the lack of appropriate enzymes. In this context, the isolation and identification of tryptophan side chain oxidase (TSO) types I and II (TSO I/II) from *Pseudomonas*, opened a new vista for

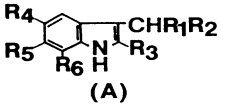

(A)

enzymatic approaches to this end. TSO, an O_2-linked dehydrogenase with broad substrate specificity, acted, roughly at comparable rates, on tryptophan residues (Trp), free tryptophan, and its metabolites conforming to the structure (A) [2–6]. The core enzymatic processes in TSO-reactions were shown to be (i) the abstraction of indole electrons from (A) followed by intersubunit electron transfer to reduce O_2 to give H_2O (Kanda *et al.*, this proceedings), and (ii) the regeneration of the intact from oxidized indole nucleus, coupled with the shifts of oxidative changes to ß-, or α,ß-carbon atoms of the alanine side chain or corresponding positions [2,3,5–8]. The nature of the substrate and conditions prescribed the integrity of these steps and ensuing reactions, providing the bases for versatile derivatizations with TSO's [2,3,5–9].

In this paper, we describe (i) TSO-reactions for various substrates with special reference to nonenzymatic reactions, (ii) derivatizations of Trp in active peptides and proteins, and (iii) those of tryptophan metabolites, and (iv) a strategy to prepare free tryptophan derivatives with TSO's. Implications and prospects of these approaches, and a possible occurrence of enzyme systems similar to TSO but distinct in substrate specificity, are discussed.

Materials and Methods

Free tryptophan substituted at amino and carboxyl groups and oligopeptides containing Trp were from Sigma; active peptides from Protein Research Foundation (Osaka). TSO I and II were purified from *Pseudomonas* essentially as described [5]. Analytical HPLC were performed on ODS (5 μm) columns (4.6 × 250 mm (for (A) and (C)) and 150 mm (for (B) and (D)), Inertsil and Wakosil, respectively) under conditions as follows: (A), 30% methanol at 40°C and 1 ml/min; (B), 30% methanol at 25°C and 1 ml/min; (C), 25% methanol at 22°C and 0.5 ml/min, for (A), (B), and (C), 50 mM ammonium acetate (pH 5.0) was used as buffer; and (D), 20% tetrahydrofuran (THF) in 2 mM Tris/HCl (pH 8.0) at 25°C and 2 ml/min.

Results and Discussion

Free tryptophan

TSO I and II acted on free L-tryptophan (I) to give diverse by-products concomitant with the stoichiometric release of NH_3 and CO_2. The reactive main product,

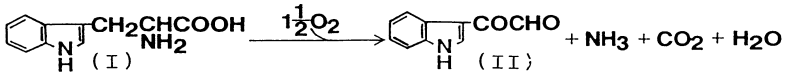

3-indoleglyoxal (II), was efficiently trapped with *o*-phenylenediamine to form a stable adduct identified as 3-indolylquinoxaline [10]. A hitherto undescribed reaction to give (II) may consist of multistep dehydrogenations intervened by hydration. D-Tryptophan also served as substrate but at a slower rate.

N-Terminal Trp

N-Terminal Trp (III) in Trp-Leu and a model compound, Trp-NH_2, underwent two consecutive dehydrogenations; the first dehydrogenation followed by hydration

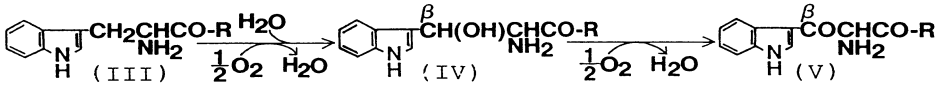

gave diastereomeric ß-hydroxy-Trp(ß-OH-Trp) (IV) (Fig. 1–1) which underwent further dehydrogenation to ß-keto-Trp (V) [2,7], in either step, *threo* form being favored [11]. TSO I, but not II, was active on N-terminal Trp [2,5,7]. On these bases, [*erythro* ß-OH-Trp-1] delta-sleep inducing peptide (DSIP) and also its *threo* conterpart were prepared (Fig. 1–2) [12]. DSIP derivatives lost an activity to modulate sleep/waking patterns of rats [12]. Leucine aminopeptidase treatment of diastereomeric ß-OH-Trp-Leu gave free ß-hydroxy-tryptophan, not available with (I), again *threo* form being favoured (Fig. 1–1) [5,7,11].

C-Terminal Trp

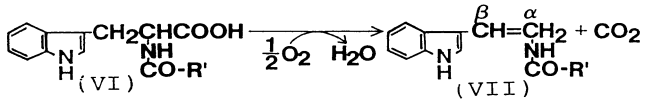

C-Terminal Trp (VI) was dehydrogenated to give α,ß-dehydrotryptamine residue (VII) concomitant with decarboxylation as assessed with Leu-Trp and a model compound Ac-Trp [2,5,7], no hydrated product being detected.

Internal Trp

Upon dehydrogenation of the internal Trp (VIII), accumulated an indolyloxazoline-type primary product (IX), as identified with a model substrate, Ac-Trp-NH_2 (Fig. 1–4, 1–5a) [3,5,8,9].

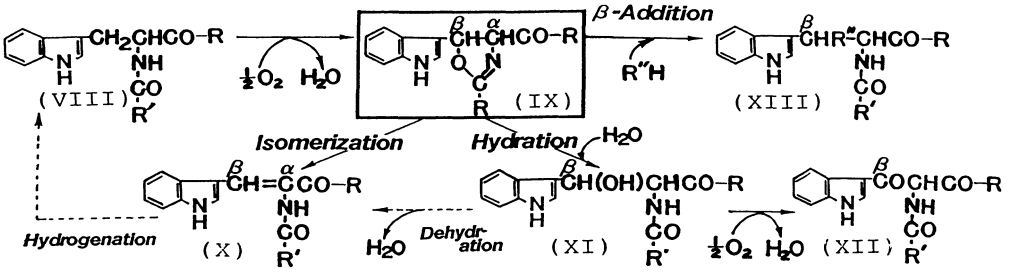

Most likely, the indole nucleus, once deprived of its electrons by TSO, was regenerated concurrent with an intramolecular shift of the electrophiles to the side chain ß-carbon atom followed by the cyclization due to the attack by the peptide amide carbonyl oxygen [3,5,8,9]. The oxazoline ring of (IX), rather stable in hydrophobic environment (Fig. 1–5a) ((IX) from Ac-Trp-NH_2 was stable overnight in CH_2Cl_2), was reactive in aqueous media to give nonenzymatically α,ß-dehydro-Trp (Δ-Trp) (X) (Fig. 1–4, 1–5b) and ß-OH-Trp (XI) (Fig. 1–4, 1–5c), by isomerization and ß-hydration, respectively [3,5,8]. Distinct from (IV), the *threo* to *erythro* ratio of (XI) was close to unity. These dichotomous reactions were pH-dependent (pH=5.8) [2,3,5,8]; higher pH's favored the decay of (IX) to (X), most likely preceded by α-deprotonation, whereas the protonation of imido nitrogen of (IX) may lead to regeneration of amide, facilitating ß-hydration [3,8] at lower pH's. Higher ionic strength accelerated the formation of (X) [5]. ß-OH-Trp (XI) underwent further dehydrogenation, alike (IV) at the N-terminus, to give ß-keto-Trp (XII), or else, unlike (IV), was non-enzymatically dehydrated, but only at extreme pH's, to Δ-Trp. In addition to ß-hydration, nucleophiles such as methanol, cysteine, pyrrole, and so forth, avidly reacted with (IX) to give a variety of ß-substituted-Trp (XIII) [2,3,5,8]; the thiol group of reduced glutathione (GSH) readily reacted with (IX) (Fig. 1–5d) [13]. In view of dichotomous reactions for internal Trp, unilateral reaction and the lack of ß-addition of nucleophiles for N- and C-terminal Trp, may be ascribed to the nature of as yet unassessed intermediates distinct from (IX). TSO-reactions for internal Trp, thus, provided the bases for versatile derivatizations of active peptides and proteins, and also isotope labeling with labeled nucleophiles [2,3,5]. Catalytic hydrogenation of Δ-Trp (X) gave ^3H-labeled peptides with NaB^3H_4 and also inverted the chirality of Trp in peptides. By manipulating these features above, yeast α-factor, LHRH, somatostatin, $ACTH^{1-24}$, and glucagon, have been derivatized [2,3,5,7]. [Δ-Trp-3]LHRH lost biological activity [2,5]. The release of free ß-substituted tryptophans from Leu-ß-substituted-Trp-Leu is underway with peptidases; they failed to act on peptide bonds neighbouring Δ-Trp [2,3,5].

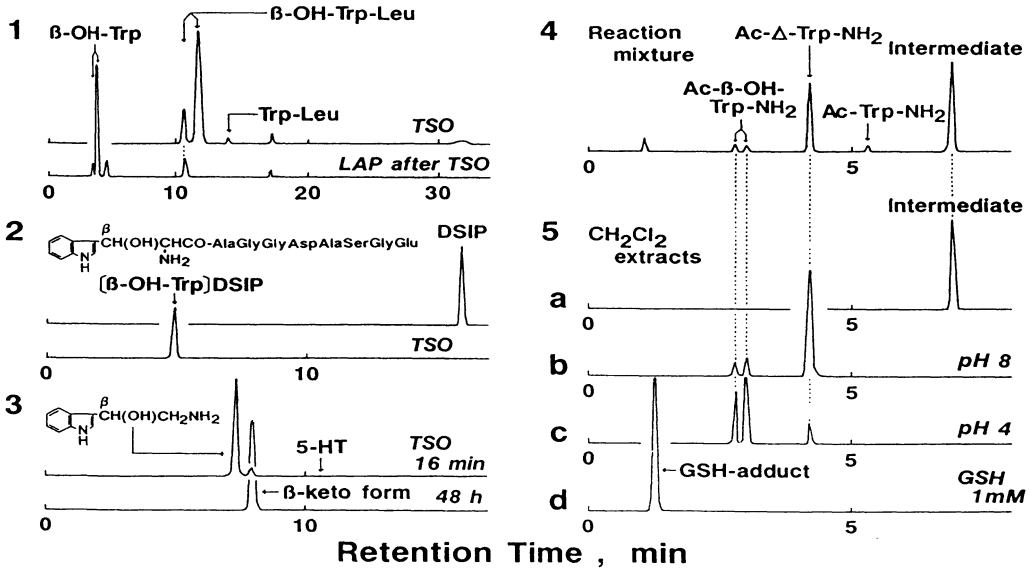

Fig. 1. HPLC analyses of TSO-reaction products: (1), Trp-Leu (1mM/0.1 ml H_2O) incubated for 26 min at 25°C with TSO I (*upper*), and ß-modified-Trp-leu formed as above incubated with leucine aminopeptidase (2 units) in 10 mM Tris/HCl (pH 8.0) containing 1 mM $MgCl_2$; (2), DSIP (1 mM/0.1 ml H_2O) incubated for 30 min with (*lower*) or without (*upper*) TSO I; (3), 5-HT (1 mM/0.1 ml H_2O) incubated with TSO I; (4), Ac-Trp-NH_2 (2.5 mM/0.5 ml) incubated with TSO I in 2 mM Tris/HCl (pH 8.0) at 25°C for 4 min; (5), CH_2Cl_2-extracts (2 × volumes) of (4) (5a), CH_2Cl_2-extracts incubated at 25°C for 20 min, with 2 volumes each of 50 mM Tris/HCl (pH 8.0) (5b), 50 mM sodium acetate (pH 4.0) (5c), and 1 mM GSH at pH 8.0 (5d). Amounts of TSO I used were 0.05 unit. Aliquots of reaction mixtures were analyzed under HPLC conditions (A), (B), (C), and (D) for (1), (2), (3) and (4)/(5), respectively. The elution was monitored by A_{280nm} (arbitrary units).

Tryptophan metabolites

Tryptophan metabolites with biological significance such as serotonin (5-HT), melatonin, 3-indoleacetate, and 5-hydroxyindoleacetate, were derivatized, preferentially with TSO I, to give racemic hydroxy and keto derivatives (Fig. 1–3) [5,14] at the positions corresponding to the ß-carbon of Trp. We are also attempting the release of free α,ß-dehydrotryptamine from (VIII).

Trp in proteins

TSO II, but not I, acted on Trp in human globins to give [Δ-Trp-14]α- and [Δ-Trp-15, Trp-37]ß-globins, inducing structural changes in both the residue and peptide main chain, and also a new chromophore [3,5,6,9]. Entgegen/zusammen

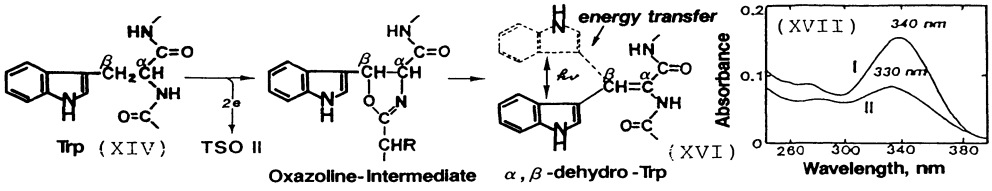

configurations (XVI) of Δ-Trp were distinguishable by UV spectra (XVII). They rapidly photoequilibrated and returned, in the dark, to an initial ratio at a slower rate [5,9]. The modified ß-, but not α-globin, emitted a strong blue fluorescence (430 nm) upon irradiation of Δ-Trp at 340 nm due to the resonance energy transfer (XVI) from Trp-37 to Δ-Trp-15 [5,9]. Thus, the inversion of an electron donor (XIV), to an oxidized form retaining indole nucleus (XVI), provided unique structural and electronic perturbations and also relaxation studies of proteins. An indolyloxazoline structure (XV), obligatory in Δ-Trp formation as established with a model substrate, appeared highly likely also in proteins. If it is valid, the peptide amide carbonyl oxygen must be reactive with electrophiles generated *in situ* in proteins, and the 5-membered ring imposes sizable structural changes of the peptide main chain, mobilizes protons and/or reacts with cysteine or H_2O.

Coda

Enzymatic derivatizations of Trp in peptides and proteins, free tryptophan, and its metabolites, herein achieved with TSO's, promise their applications to biochemistry and pharmacology. However, the enzymatic approaches would be far more prospective, if enzymes similar to TSO but distinct in specificity, may be available, although none of them has been described previously.

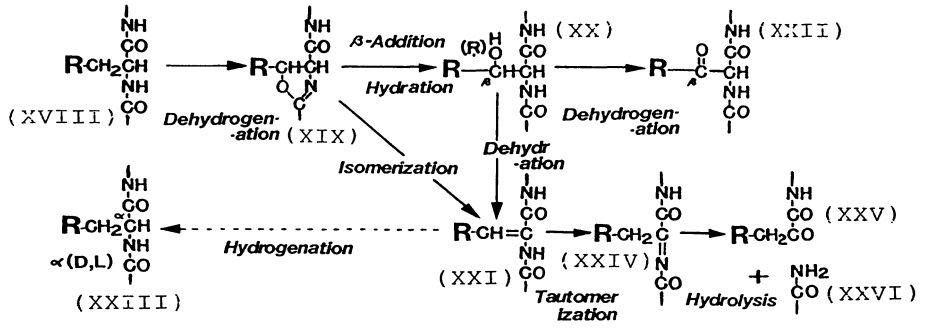

Scheme 1. Working hypothesis for new amino acid residue metabolisms.

In this context, we herein postulate our concept as a working hypothesis (Scheme 1) in the search for new amino acid residue metabolisms and related new enzymes. Besides Δ-Trp, each more than ten α, ß-dehydro (XXI) and diastereomeric ß-hydroxy amino acid residues (XX), and some ß-keto residues (XXII), have been identified in peptides synthesized *in vivo* [15–18], implying that amino acid residue dehydrogenase systems other than TSO may exist in nature [2,3,5,9]. For the formation of Δ-amino acid residues (XXI), intraproteinous α,ß-elimination (dehydration) of (XX) can be applied only to serine, cysteine, and threonine, and hydroxylase (monooxygenases), rigorously stereospecific in general, may not account for the coexistence of *erythro* and *threo* ß-hydroxy-Pro in a peptide, Telomycin [16]. At present, dehydrogenation/hydration systems herein postulated may be more likely. Besides catalytic hydrogenation of Δ-Trp to give D-enantiomer, enzymatic hydrogenation to (XXIII) may also be considered, since no racemase so far known acts on peptides. Scheme 1 incorporates the tautomerization of Δ-amino acid residues (XXI) leading to the cleavage of peptides, *via* enamine structure (XXIV), to give N-terminal α-keto acid residue (XXV) and C-terminal amide (XXVI), as exemplified by microbial histidine decarboxylase [19] and mammalian α-amidase [20], respectively. The assignment of the latter to hydroxylase appeared to be tentative, and no internal Δ-Trp herein formed, underwent nonenzymatic cleavage *via* (XXIV), as yet leaving possibilities for newer mechanisms and enzymes.

References

1. Biosynthesis (1972–76) Vol. 1–5 (Geissman TA (Vol. 1–3) and Bu'Lock JD (Vol. 4–5) senior reporters) The Chemical Society Burlington House, London.
2. Takai K (1980) Dev. Biochem. 16: 103–115.
3. Takai K, Inoue S, Zavala F, Müller R, Hamasaki T and Sasai Y (1983) In: Schlossberger HG, Kochen W, Linzen B and Steinhalt H (eds.) Progress in Tryptophan and Serotonin Research. de Gruyter, Berlin, pp. 765–768.
4. Takai K, Müller R, Zavala F, Inoue S, Narumiya S, Ito S and Hayaishi O (1982) In: Nozaki M, Yamamono S, Ishimura Y, Coon MJ, Ernster L and Estabrook RW (eds.) Oxygenase and Oxygen Metabolism. Academic Press, New York, pp. 159–172.
5. Takai K and Hayaishi O (1987) Methods Enzymol. 142: 195–217.
6. Takai K, Yoshii H, Yasui Y and Sasai Y (1986) In: Bender DA, Joseph MH, Kochen W and Steinhart H (eds.) Progress in Tryptophan and Serotonin Research. de Gruyter, Berlin, pp. 59–60.
7. Ito S, Takai K, Tokuyama T and Hayaishi O (1981) J. Biol. Chem. 256: 7834–7843.
8. Zavala F, Takai K and Hayaishi O (1983) J. Biol. Chem. 258: 344–351.
9. Takai K, Sasai Y, Morimoto H, Yamazaki H, Yoshii H and Inoue S (1984) J. Biol. Chem. 259: 4452–4457.
10. Takai K, Ushiro M, Noda Y, Narumiya S, Tokuyama T and Hayaishi O (1977) J. Biol. Chem. 252: 2648–2656.
11. Nakamaru E, Kawashima T and Takai K, unpublished results.
12. Nakamaru E, Kawashima T, Kamiyama Y and Takai K, unpublished results.
13. Nakamaru E, Kawashima T and Takai K, unpublished results.
14. Nakamaru E, Kawashima T and Takai K, unpublished results
15. Gross E (1970) In: Sober HA (ed.) Handbook of Biochemistry. CRC Press, Cleveland, B–50.

16. Sheehan JS, Mania D, Nakamura S, Stock JA and Maeda K (1968) J. Chem. Soc. 90: 462–470.
17. Uy R and Wold F (1977) Science 198: 890–896.
18. Wold F (1981) Ann. Rev. Biochem. 50: 783–814.
19. Recsei PA and Snell EE (1984) Ann. Rev. Biochem. 53: 357–387.
20. Bradbury AF, Finnie MDA and Smyth DG (1982) Nature 298: 686–688.

Section V
Nutrition

Effect of amino acid, ketoacid supplementation to a low-protein diet on diabetic nephropathy with chronic renal failure

F. Ciardella, E. Morelli, A. Cupisti, M. Meola, F. Niosi, A. Guidi, A. Pasquinucci and G. Barsotti

Clinica Medica 1, Nephrology Unit, University of Pisa, Italy

Abstract

Type 1 diabetics with 'overt' diabetic nephropathy (DN) have a rapid decline of GFR, reaching the uremic status within a few months or years. In the present study we have submitted to a vegetarian a low-protein diet, supplemented with amino acids and their analogues (Supplemented diet, SD) fourteen patients with DN and chronic renal failure (CRF). All the patients were followed up during a 15.8 month (9–25) period of unrestricted protein diet (UPD), and successively during 22.3 months (6–42) of SD. The monthly decrease of creatinine clearance on UPD was -1.42 ± 0.38 ml/min, while on SD it dropped to -0.29 ± 0.24 ml/min ($p<0.001$). Urinary protein loss decreased (6.02 ± 1.74 to 3.28 ± 1.12 g/day; $p<0.01$), independently from any change either in creatinine clearance or in serum albumin concentration. The daily insulin requirement was reduced despite the very high carbohydrate intake. PTH and GH fell, while T3 increased significantly. Serum cortisol decreased from 187.9 ± 42.5 to 139.8 ± 25.6 ng/ml ($p<0.005$).

These results demonstrate that SD protects the residual renal function, lowers urinary protein loss and corrects some hormonal abnormalities strictly related to insulin action and glucose metabolism. The reduction of the daily insulin requirement may be regarded as a consequence of these endocrine effects of SD.

Introduction

The peculiar feature of the 'overt' nephropathy in Type 1 diabetics is the rapid onset of chronic renal failure after the appearance of a dipstick detectable proteinuria [1]. The decline of glomerular filtration rate (GFR) shows various slopes in different patients, ranging from a minimum of 0.6 to a maximum of 2.4 ml/min/month [2].

In the past years the nutritional management of diabetic patients has been based mainly on the reduction of carbohydrate intake in order to achieve a good glycemic control. In 1979 the American Diabetes Association recommended that carbohydrate intake should be increased to cover more than 60% of total energy intake, with a reduction of fat and a normal-high protein intake [3]. Recent studies have shown that a reduction of dietary protein intake early in the course of experimental diabetic nephropathy retards the progression of renal damage [4]. Zeller *et al.* in a preliminary report have demonstrated that a similar beneficial effect can be achieved in human diabetic nephropathy [5].

More recently, we studied the effects of a very low protein, low-phosphate vegetarian diet, supplemented with a mixture of amino acids and their analogues, in eight patients with 'overt' diabetic nephropathy and chronic renal failure. As previously observed in other chronic nephropaties [6,7] the use of very low protein diets supplemented with amino-acids and analogues exerts a lowering effect on the rate of decline of the residual renal function [8].

In addition, a low protein diet, supplemented with amino acids and their analogues (supplemented diet, SD) can reverse some endocrine derangements typical of chronic renal failure, as the secondary hyperparathyroidism [9] and the 'low-T3 syndrome' [10]. A similar dietary regimen seems to reduce hypercortisolism in uremic patients [11]. It is well known that all the above mentioned endocrine derangements interfere with carbohydrate metabolism and insulin action.

The main purpose of the present investigation was to evaluate the effects of a prolonged period of SD (6–42 months) in Type 1 diabetics with chronic renal failure on the residual renal function, urinary protein loss, daily insulin requirement and serum levels of the most important hormones which interfere with insulin action.

Patients and Methods

Fourteen Type 1 diabetics with advanced renal insufficiency due to diabetic nephropathy were recruited. The data concerning age, sex, duration of diabetes, diabetes complications other than nephropathy, and creatinine clearance at the beginning of SD are reported in Table 1.

Table 1.

Name	Sex	Age (yrs)	Duration of diabetes (yrs)	CRrcl at the beginning of SD (ml/min)	Complications other than diabetic nephropathy
1. Dembe.	M	33	18	35.1	Neurop. + Retinopathy
2. Verac.	F	54	21	20.6	Neuropathy
3. Carto.	M	61	26	44.4	Neurop. + Arteriopathy
4. Rovai.	M	60	28	21.8	Arteriopathy
5. Delbr.	F	23	14	39.1	Retinopathy
6. Cozza.	M	49	24	44.3	Neurop. + Retinopathy
7. Marfi.	M	58	21	14.1	Neurop. + Retinop. + Arteriop.
8. Mobil.	F	38	26	4.9	Neurop. + Retinopathy
9. Ferra.	M	59	28	14.6	Neurop. + Retinopathy
10. Molen.	F	34	19	15.5	Retinopathy
11. Cei	M	52	24	7.9	Neurop. + Retinopathy
12. Dei	F	33	19	9.1	Neurop. + Retinopathy
13. Campa.	M	55	24	16.2	Neurop. + Retinop. + Arteriop.
14. Depao.	F	54	26	7.4	Neurop. + Retinopathy
Mean		47.3	22.6	21.1	
± S.D.		12.1	4.5	13.9	

All the studied patients before the SD followed an unrestricted protein diet (UPD). The daily energy supply of UPD was about 30–35 kCal/kg b.w. (60% from carbohydrates, 22% from lipids and 18% from animal and vegetable proteins) and the protein supply was 1.1–1.5 g/kg. During the 15.8 month study period on UPD (9–25 months) we repeatedly measured the creatinine clearance (CRcl), in order to assess the rate of decline of residual renal function during a reasonable time period, and by calculating the slope of CRcl plotted against time. During the last fortnight period before SD, while the patients were on UPD, they did not receive any drug which might interfere with the studied hormonal functions.

Subsequently, all the patients shifted to the SD and were followed during this dietary therapy for a mean period of 22.3 months (6–42 months). The SD is a pure

Table 2. The composition of the low nitrogen, low phosphorus diet, supplemented with essential amino acids and ketoacids (SD)

Kcal (kg/day)	30–35
% from carbohydrates	70
% from lipids	26
% from protein	4
Protein content (g/kg/day)	0.3
Nitrogen supply from proteins (mg/kg/day)	48
Nitrogen supply from supplements (mg/kg/day)	9.6
Protein quality	vegetarian
Inorganic phosphorus (mg/kg/day)	6
Cholesterol content	low
Na^+ content (mEq/kg/day)	0.15
K^+ content (mEq/kg/day)	1.0

Essential amino acid, ketoacid supplementation[a]

Essential amino acids			*Ketoanalogues of EAAs*		
L-lysine	mg	1890	Keto-valine[b]	mg	1584
L-threonine	mg	954	Keto-leucine[b]	mg	1818
L-tryptophan	mg	414	Keto-isoleucine[b]	mg	1206
L-tyrosine	mg	540	Keto-phenylalanine[b]	mg	1224
DL-hydroxy-methionine	mg	1062			
Non-essential amino acids					
L-hystidine	mg	684			

[a]The daily intake of EAAs-KAs mixture for 70 kg B.W.
[b]As calcium salts.

vegetarian, normal-high energy, low-protein and low phosphorus diet, supplemented with a mixture of amino acids and their analogues in tablets (one tablet for one Kg of b.w.) according to Zimmermann's formula [12]. More details concerning SD are reported in Table 2.

Immediately before and during the SD period we repeatedly measured in each patient the following parameters:

- creatinine clearance (24 h urine collection) (CRcl)
- daily urinary protein loss (uPr)
- serum total protein (sTP) and serum albumin (sA)
- body weight (BW)
- daily insulin requirement (IR)
- fasting glucose levels (sG)
- mean arterial pressure (diastolic blood pressure plus one third of pulse pressure) (MAP)
- circulating PTH (M-M fragment)
- T3
- Growth Hormone (GH)
- Cortisol (Cort)

The plasma samples for these determinations were collected at 8.00 a.m., after an overnight fast, at the end of the 24 h urine collection. The arterial blood pressure was repeatedly controlled in a supine position.

Serum and urine creatinine and sG were determined by the standard auto-analytical methods of our clinical laboratory.

Urinary daily protein excretion was measured by the Red-Ponceau colorimetric method, and serum total proteins by the biuret method. Serum albumin was calculated by electrophoretic fractional analysis of serum proteins. Hormonal determination were performed by using the commercial RIA kits. Normal values were: PTH (M–M) = 0.29–0.85 ng/ml; T3 = 80–200 ng/dl; GH = 0–6 ng/ml; Cort (in samples withdrawn at 8.00 a.m.) = 70–220 ng/ml.

The statistical evaluation of the data was performed by the Student's 't' test for paired data. Statistical significance was considered when p was below 0.05.

Results

The slope of CRcl plotted against time during the control period on UPD and during the study period on SD is shown in Fig. 1. The initial and final values of each period are indicated, to make the figure as clear as possible. It can be easily appreciated the significantly different slopes of CRcl in the same patient during UPD and SD. The star-marked cases passed from SD to the maintenance hemodialysis as a consequence of the development of hyperpotassemia (one case), for a further reduction of the residual renal function (two cases) or following a spontaneous decision to stop the SD in the last one. As it can be seen in Fig. 1 we obtained the best results in patients who started the SD early, when their residual renal function was less damaged.

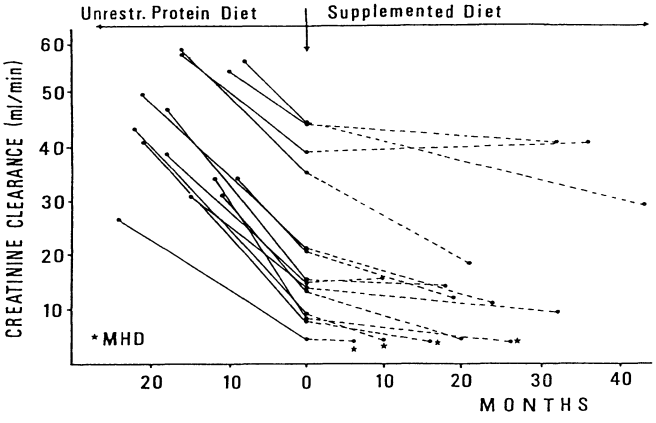

Fig. 1. The CRcl of each studied patient plotted against time, during the pre-treatment follow-up period on UPD (continuous lines) and during the SD treatment (dotted lines). *patients who changed from SD to the MHD.

The rate of decline of CRcl, calculated as the ratio between the differences of initial and final values of CRcl and the time of each study period, was significantly higher in UPD (1.42 ± 0.38 ml/min/month) than in SD patients (0.29 ± 0.24 ml/min/month) ($p<0.001$, Fig. 2).

The daily urinary protein loss decreased from a mean value of 6.02 ± 1.74 g/day on UPD, to 3.28 ± 1.12 g/day on SD ($p<0.01$, Fig. 3). This lowering effect of SD on

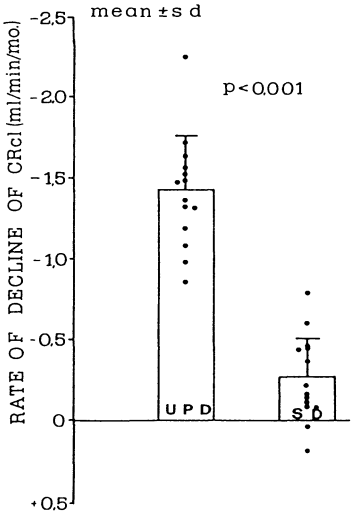

Fig. 2. The rate of decline of the CRcl on UPD and SD.

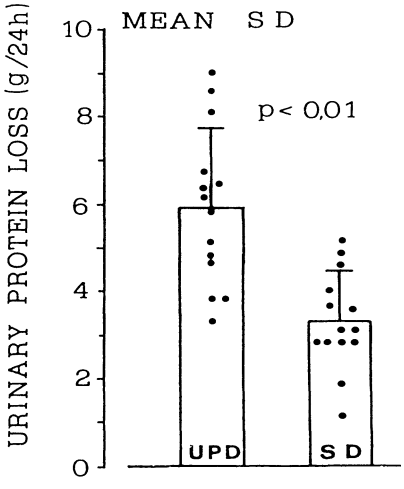

Fig. 3. The urinary protein loss of each patient during UPD and SD period.

Table 3.

	M.A.P. (mmHg)		Body weight (kg)		Fasting glucose levels (mg/dl)		Insulin requirement (U/day)	
	UPD	SD	UPD	SD	UPD	SD	UPD	SD
1. Demb.	123.3	120.0	74.2	70.6	126.3	130.2	60	50
2. Vera.	113.3	116.6	65.2	67.1	121.4	98.1	55	50
3. Cart.	120.0	121.6	74.2	73.5	145.2	112.6	50	45
4. Rova.	113.3	116.3	68.3	69.4	118.4	121.6	60	35
5. Delb.	123.3	116.6	50.2	49.1	136.4	128.2	44	40
6. Cozz.	115.0	115.0	76.5	75.1	126.7	113.6	50	42
7. Marf.	123.3	125.0	89.6	91.8	145.5	138.6	75	55
8. Mobi.	128.3	115.0	50.2	54.6	125.3	134.8	66	44
9. Ferr.	126.6	126.6	89.1	87.6	116.4	123.8	55	35
10. Mole.	110.0	115.0	62.2	58.9	138.0	125.6	38	32
11. Cei	131.6	110.0	64.8	62.6	114.4	132.6	64	38
12. Dei	123.3	125.0	58.2	59.4	144.2	119.5	55	34
13. Camp.	113.3	123.3	74.1	71.3	119.2	123.4	50	36
14. Depa.	118.3	121.6	68.9	70.1	116.4	122.0	42	38
Mean ±	120.2	119.1	69.0	68.6	128.1	123.2	54.6	41.0
S.D.	6.5	4.9	11.9	11.6	11.5	10.3	10.0	6.9
p	n.s.		n.s.		n.s.		<0.001	

uPr was present in all studied patients, reaching the non-nephrotic grade in some cases (Fig. 3).

sTP slightly, but not significantly, increased during SD from 6.54 ± 0.36 g/dl to 6.63 ± 0.34 g/dl.

sA significantly increased on SD from 3.32 ± 0.42 g/dl to 3.68 ± 0.36 g/dl ($p<0.05$), probably as a consequence of the reduced uPr.

Fasting glucose levels and mean arterial pressure did not change during SD, as it appears in Table 3. Body weight decreased slightly, but not significantly on SD, probably as a consequence of the reduced water retention in some patients who had edema at the beginning of SD treatment. The daily insulin requirement was significantly reduced when patients shifted from UPD to the SD, from 54.4 ± 9.9 to 41.5 ± 7.5 U/day ($p<0.01$, Table 3) in spite of the very high carbohydrate supply of SD.

PTH fell in almost all the cases, reaching the normal values in seven out of the fourteen studied patients, from a mean value of 2.53 ± 1.46 ng/ml on UPD to 1.26 ± 0.74 ng/ml on SD ($p<0.0002$). T3 values were low-normal on UPD (84.0 ± 24.0 ng/dl) and increased, reaching the normality on SD (120.7 ± 24.1 ng/dl; $p<0.0002$) (Table 4). Two patients only did not reached the normality. CORT was high-normal on UPD (187.9 ± 42.5 ng/ml) and decreased in almost all the patients on SD (139.8 ± 25.6 ng/dl) ($p<0.005$) (Table 4). GH significantly decreased on SD (from 2.7 ± 0.9 to 1.2 ± 0.9 ng/ml) ($p<0.0001$) (Table 4).

Table 4. Variation of PTH, T3, cort and GH plasma levels following the change from UPD to SD in 14 type 1 diabetics with CRF (mean ± S.D.)

	UPD	SD	p
PTH (M-M) (ng/ml)	2.53 ± 1.46	1.26 ± 0.74	<0.0002
T3 (ng/dl)	84.0 ± 24.0	120.7 ± 24.1	<0.0002
CORT (ng/ml)	187.9 ± 42.5	139.8 ± 25.6	<0.005
GH (ng/ml)	2.7 ± 0.9	1.2 ± 0.9	<0.0001

Discussion

The present investigation confirms preliminary observations on the positive effects on residual renal function and urinary protein loss exerted by low-protein diets with or without essential amino acid and analogues supplementation [5,8,13] in Type 1 diabetics with overt nephropathy and chronic renal failure.

We did not randomize our patients into a study group and a control one for two reasons: first, for the small size of the sample and second, the studied patients were considered as controls of themselves during the pre-treatment follow-up period on UPD. On the other hand, the follow-up on the two dietary regimens was long enough and of comparable length to permit a valid evaluation of the rate of decline of renal function. A similar methodological approach has been previously used to evaluate the effect of the strict glycemic control on the progression of renal insufficiency in diabetics [14].

The protective effect on the residual renal function exerted by SD in diabetic patients seems to be maintained for several months or years. In fact, in our groups of patients, only four out of the fourteen studied subjects shifted from SD into the MHD program. As it appears in Fig. 1, these patients had a very low residual renal function when they started the SD, and in this conditions even a minimal further reduction of the number of residual nephrons might cause oliguria or hyperkalemia. Only in one patient we did not obtain benefit from SD (Fig. 1). The advanced age (60 years), the duration of diabetes (28 years) and the prevalence of vascular involvement, probably account for the poor effect of SD in this patient. It is known, in fact, that the ischemic renal involvement in chronic renal diseases (including diabetic nephropathy) is an important cause of progressive decrease of renal function [15,16].

SD reduces uPr in all the studied patients, and this effect is maintained during the whole period of nutritional therapy. This effect is not apparently related to a decrease of GFR, because the CRcl was unchanged in almost all the cases on SD. The possibility that the fall of uPr was a consequence of a spontaneous remission of the renal disease, or secondary to a reduction or sTP and sAlb might be excluded, because spontaneous remissions are exceptional in the course of overt diabetic nephropathy (if they exist at all), and in our series sTP and sAlb increased during

SD. In experimental animal model of chronic renal damage low-protein diets and SD reduce uPr [4,17,18]. This effect may be related to the changes in the quality and the quantity of the ingested proteins, as it happens in the experimental animal model of proteinuria [19,20], while a corrective effect exerted by the SD on the abnormal glomerular hemodynamic, that is peculiar of diabetic nephropathy [21], cannot be excluded. The correction of glomerular hyperfiltration and the reduction of uPr [22] probably contribute to the preservation of the residual renal function during SD treatment.

An adequate control of arterial hypertension is undoubtedly of critical importance for the progression of diabetic nephropathy [23]. In our patients the hypertension was adequately corrected in almost all the patients by an appropriate treatment (diuretics, calcium channel blockers, vasodilators, clonidine). We did not use the ACE inhibitors in order to avoid any interfering effect on renal function and proteinuria [24]. Finally, the mean blood pressure was similar on UPD and on SD follow-up periods, so that we can reasonably exclude that the better protection of the residual renal function observed on SD was due to a better control of blood pressure.

The daily insulin requirement was significantly reduced during SD, in spite of the increased carbohydrate dietary supply. This effect of a low protein diet in patients with diabetic nephropathy has been previously described [13]. In addition, we observed a fall of PTH, GH and CORT levels, and an increase of circulating T3. Such changes of hormonal pattern cannot be related to an improvement of the renal function, which results unchanged during the SD. It is known that these hormones exert an important action on glucose metabolism and insulin action. PTH counteracts the peripheral action of insulin at the level of the tissue receptors [25] and exerts an opposite metabolic effect inside cells [25]. GH and Cort are well known anti-insular hormones, while the increase of T3 strongly favours an improvement of glucose tolerance, since this hormone directly induces an enhancement of glucagon catabolism [26].

In conclusion, the SD in patients with renal insufficiency due to overt diabetic nephropathy exerts several favourable effects: reduces urinary protein loss, preserves the residual renal function for months or years, even when it is already markedly reduced, corrects some hormonal derangements and reduces the daily insulin requirement. In our patients we never observed negative effects on the nutritional status. In our opinion, the overt diabetic nephropathy seems to represent the most responsive, among the chronic renal diseases, to the SD therapy.

Acknowledgements

The authors are very grateful to the Farma Biagini S.p.A., Castelvecchio Pascoli, Lucca (Italy) and to the Italian National Health Service, USL 12 Area Pisana, for the supply of amino acids and analogues in tablets (Alfa-Kappa).

References

1. Krolewski AS, Warram JH, Christlieb AR, Busick EJ and Kahn CR (1985) The Changing Natural History of Nephropathy in Type 1 Diabetes. Am. J. Med. 78: 785–794.
2. Viberti GC, Bilous RW, Mackintosh D and Keen H (1983) Monitoring Glomerular Function in Diabetic Nephropathy. Am. J. Med. 74: 256–264.
3. American Diabetes Association (1979) Special Report: Principles of Nutrition and Dietary Recommendations for Individuals with Diabetes Mellitus. Diabetes 28: 1027–1042.
4. Wen SF, Huang TP and Moorthy AY (1985) Effect of a Low Protein Diet on Experimental Diabetic Nephropathy in the Rat. J. Lab. Clin. Med. 106: 589–594.
5. Zeller KR, Jacobson H and Raskin P (1987) The Effect of Dietary Protein Modification on Renal Function in Diabetic Nephropathy: Preliminary Report of an Ongoing Study. Kidney Int. 31: 225 (Abstr.).
6. Mitch WE, Walser M, Steinman TI, Hill S, Zeger S and Tungsana K (1984) The effect of a Keto-Amino Acid Supplement to a Restricted Diet on the Progression of Chronic Renal Failure. N. Engl. J. Med. 311: 623–629.
7. Walser M, LaFrance ND, Ward L and VanDuyn MA (1987) Progression of Chronic Renal Failure in Patients Given Ketoacids Following Amino Acids. Kidney Int. 32: 123–128.
8. Barsotti G, Ciardella F, Morelli E, Cupisti A, Mantovanelli A and Giovannetti S (1988) Nutritional Treatment of Renal Failure In Type 1 Diabetic Nephropathy. Clin. Nephrol. 29: 280–287.
9. Barsotti G, Morelli E, Guiducci A, Ciardella F, Giannoni A, Lupetti S and Giovannetti S (1982) Reversal of Hyperparathyroidism in Severe Uremics Following Very Low Protein and Low Phosphorus Diet. Nephron 30: 310–313.
10. Ciardella F, Morelli E, Caprioli R et al. (1986). Restoration of Thyroid Secretion in Uremic Patients Following a Low Protein, Low Phosphorus Diet Supplemented with Essential Aminoacids and Ketoanalogues. Contr. Nephrol. 53: 51–57.
11. Walser M and Ward L (1988) Progression of Chronic Renal Failure is Related to Glucorticoid Production. Kidney Int. 34: 859–866.
12. Zimmermann EW, Meisinger E, Weinel B and Strauch M (1979) Essential Aminoacids/Ketoanalogue Supplementation: An Alternative to Unrestricted Protein Intake in Uremia. Clin. Nephrol. 11: 71–78.
13. Attmann PO, Bucht H, Larsson O and Uddebom G (1983). Protein-reduced Diet in Diabetic Renal Failure. Clin. Nephrol. 19: 217–224.
14. Viberti GC, Bilous RW, Mackintosch D and Bending JJ (1983). Longterm Correction of Hyperglycemia and Progression of Renal Failure in Insulin-Dependent Diabetes. Br. Med. J. 286: 598–603.
15. Sterpetti AV, Schultz RD, Feldhaus RJ and Peetz DJ jr. (1986) Aortic and Renal Atherosclerotic Disease. Surg. Gynecol. Obstet. 163: 54–59.
16. Jacobson HR (1988) Ischemic Renal Disease: An Overlooked Clinical Entity? (Nephrologic Forum) Kidney Int. 34: 729–743.
17. Barsotti G, Cupisti A, Dani L et al. (1986) Protection of Renal Function in Subtotally Nephrectomyzed Rats by Dietary Therapy. Contr. Nephrol. Karger, Basel, pp. 21–30.
18. Remuzzi G, Zoja C and Remuzzi A et al. (1985) Low-Protein Diet Prevents Glomerular Damage in Adriamycin-Treated Rats. Kidney Int. 28: 21–27.
19. Neugarten J, Feiner HD, Schacht RG and Balwin DS (1983) Amelioration of Experimental Glomerulonephritis by Dietary Protein Restriction. Kidney Int. 24: 595–601.
20. Williams AJ, Baker F and Walls J (1987) The Effect of Varying Quantity and Quality of Dietary Protein Intake in Experimental Renal Disease in Rats. Nephron 46: 83–91.
21. Hostetter TH, Troy JL and Brenner BM (1981) Glomerular Hemodynamics in Experimental Diabetes Mellitus. Kidney Int. 19: 410–416.
22. Brenner MB, Meyer TW and Hostetter TH (1982) Dietary Protein Intake and the Progressive Nature of Kidney Disease: The Role of Hemodinamically Mediated Glomerular Injury in the Pathogenesis of Progressive Sclerosis in Aging, Renal Ablation and Intrinsic Renal Disease. N. Engl. J. Med. 307: 652–659.

23. Mogensen CE (1982) Long-Term Antihypertensive Treatment Inhibiting Progression of Diabetic Nephropathy. Br. Med. J. 285: 685–692.
24. Taguma Y, Kitamoto Y, Futaki G et al. (1985) Effect of Captopril on Eavy Proteinuria in Azotemic Diabetics. N. Engl. J. Med. 313: 1617–1623.
25. Massry SG (1985) Current Status of the Role of Parathyroid Hormone in Uremic Toxicity. Contr. Nephrol. 49: 1–11.
26. Burman K, Smallridge RC, Jones L et al. (1980) Glucagon Kinetics in Fasting: Physiological Elevations in Serum 3,5,3-triiodiothyronine Increase the Metabolic Clearance Rate of Glucagon. J. Clin. Endocrinol. Metab. 51: 1158–1165.

Address for correspondence: Prof. Giuliano Barsotti MD, Clinica Medica 1, University of Pisa, Via Roma 67, 56100 Pisa, Italy.

A novel use of amino acid ratios as an indicator of nutritional status

V.G. Oberholzer and A. Briddon
Queen Elizabeth Hospital for Children, London, U.K.

Abstract

Changes in plasma amino acid levels with varying protein intake in normal children [1–3] and in children with malnutrition, [4–6] have been well documented. These changes have led to the use of ratios between amino acids, or groups of amino acids, as possible indicators of the degree of malnutrition [2,5].

In analysing the data in the literature, together with our own data, we have combined and extended the use of such ratios to give a wider picture of nutritional status with respect to both protein and calorie intake that may increase the value of amino acid levels as a means of diagnosis, and in the monitoring of treatment, in the malnourished patient.

Data and Method

Various ratios have been tried in attempts to use amino acid levels as a measure of protein depletion. The ratio of some essential to non-essential amino acids was not found to correlate well with various grades of kwashiorkor, [5] possibly due to difficulties in measuring glutamine and glutamic acid [2]. Better discrimination was obtained using the glycine-valine ratio as an indicator of moderate protein calorie malnutrition [7].

Glycine and branched chain amino acids consistently reflect protein intake. Low protein or protein free diets lead to a lowering of branched chains accompanied by a rise in glycine [6].The ratio of glycine to the sum of branched chain amino acids (BCAA), has therefore been used as a sensitive indicator of changes in protein intake. This ratio, calculated from data in the literature, plotted against protein intake clearly shows a correlation, (Fig. 1). The ratio of alanine to leucine has also ben used but this ratio could be more helpful in the differential diagnosis between marasmus and kwashiorkor [8], as variations in carbohydrate intake are reflected more directly by the alanine level. Using data of Holt [9], the gly-BCAA ratio gives excellent correlation with the degree of severity of kwashiorkor, ($r = 0.987$), but the alanine-BCAA ratio less so, ($r = 0.573$), again suggesting that the glycine-BCAA ratio is a more specific indicator of protein intake.

It is possible that these two ratios together will provide an improved indicator of both protein and calorie components of the intake. In an attempt to combine these two aspects of nutrition we have plotted the glycine-BCAA quotient against that of alanine-BCAA.

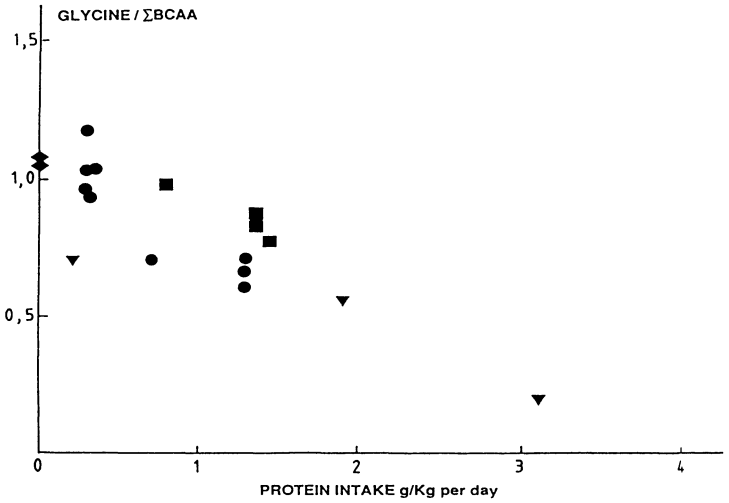

Fig. 1. Change in the ratio of glycine to sum of branched chain amino acids with protein intake. ● Adults, 1–5 weeks on diet. Swendseid, J. Nutr. (1966). ▼ 7–13 years old, 1–2 days, on diet, Homgren, Nutr. Metab. (1974). ◆ 17–22 years old, 7–16 days on diet, Young, Br. J. Nutr. (1968). ■ 8–9 years old, 6 days on diet, Moore, Amer. J. Clin. Nutr. (1966).

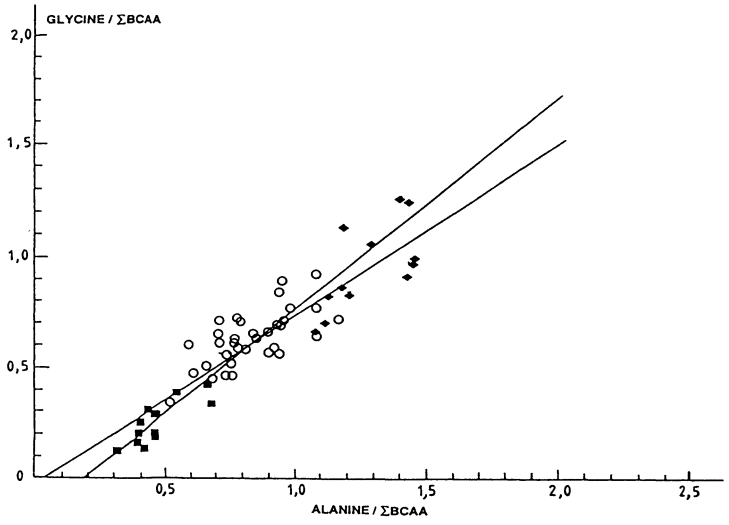

Fig. 2. Correlation between ratio of plasma glycine to sum of branched chain amino acids (BCAA) and of alanine to BCAA. Control values for infants, children and adults taken from the literature: 22 authors, 60 results. Fasting levels following low, normal or high protein intake with adequate calories, and levels following acute loads of protein or glucose. r = 0.903, n = 60. ■ High protein intake, over 6 g/kg per day or 2 h after protein load. ◆ Low protein intake 1.1–1.5 g/kg per day or 2 h after CHO load. ○ Normal protein intake.

Using data from the literature, Fig. 2 shows the correlation obtained between the two ratios for different levels of protein and calorie intake. By applying bivariate regression analysis to this data we have arrived at 95% confidence limits to define the area of low, normal and high protein intake in control subjects. These limits are shown in Figs. 3, 4 and 5.

Figure 3 shows the response of these ratios to experimental dietary changes; reducing protein and increasing CHO intake to maintain calories.

Figure 4 shows data on patients suffering from varying degrees of malnutrition plotted on the 'ratiogram'.

Results and Discussion

Alanine, glycine and branched chain amino acids show the most consistent changes with protein intake. Reliable estimates of these can be made since they are all stable and well separated and accurately measured by ion-exchange chromatography. The glycine-BCAA ratio correlates well with protein intake (Fig. 1), as does the alanine-BCAA ratio provided that calorie intake is maintained. The significance of these quotients was examined by calculation from published data including values from the authors laboratory. Although there was good correlation between each quotient and protein intake there are indications that the alanine-BCAA ratio responds more specifically to changes in CHO intake [8].

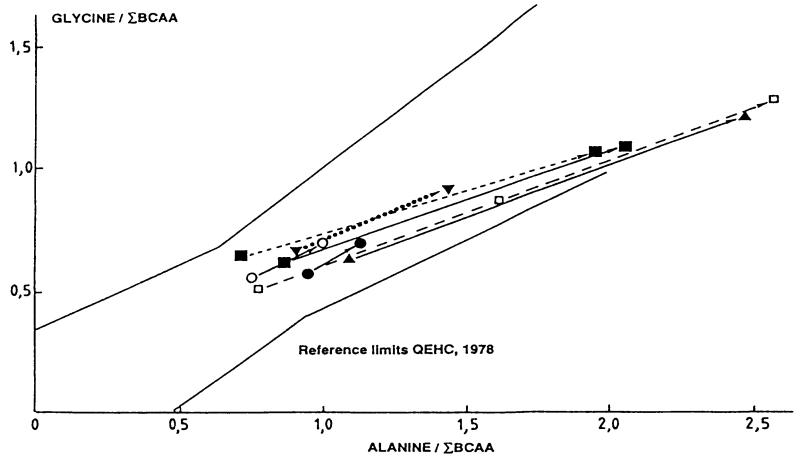

Fig. 3. Effect of reduced protein diets with carbohydrate on amino acid ratios. ● Glucose infusion, fasting and 1 h Crofford, Proc. Soc. Exptl. Biol. Med. (1964). ❑ Nil protein 3 days then CHO feeds (adults) Maher, Amer. J. Clin. Nutr. (1984). ○ Low protein intake for 2 days, 7–13 years old. Holmgren, Nutr. Metab. (1974). ▲ Low protein intake 1–18, adults. Weller, Amer. J. Clin. Nutr. (1969). ▼ CHO load, 0 and 2 h, adults. Vaughan, Amer. J. Clin. Nutr. (1977). ■ Nil protein 7–10 and 16 days, adults. Young, Br. J. Nutr. (1968).

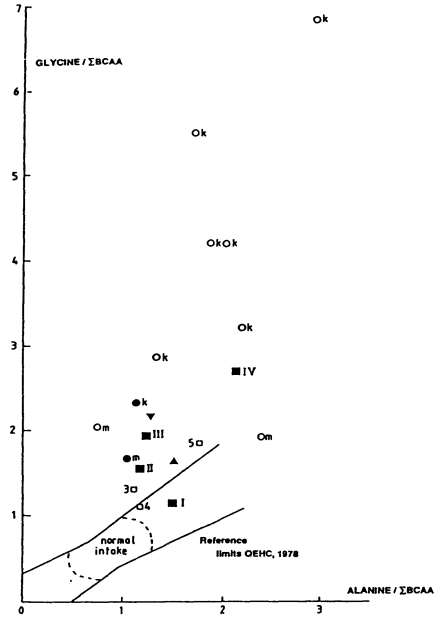

Fig. 4 Effects of malnutrition on amino acid ratios. ● k kwashiorkor, ● m marasmus. Saunders, Lancet (1967).▲ Kwashiorkor. Grimble, Br. J. Nutr. (1971). ■ Kwashiorkor. Holt, Lancet (1963). I–IV degrees of severity. ○ K Kwashiorkor. ○ m Marasmus. Arroyave, Amer. J. Clin. Nutr. (1962). ▼ Kwashiorkor. Padilla, Amer. J. Clin. Nutr. (1961). ❑ 3,4 and 5 degrees of protein deficiencey. Ghisolti, Ped. Res. (1978).

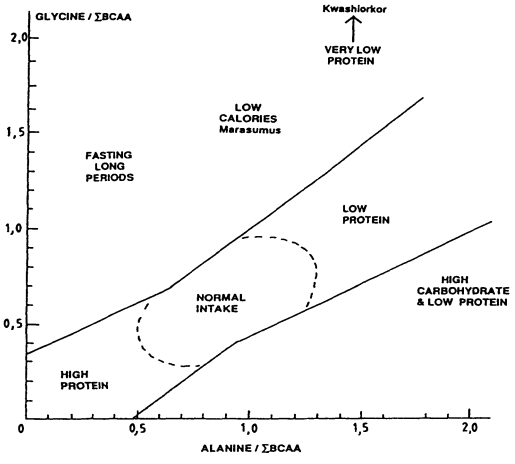

Fig. 5. Interpretation of glycine/BCAA and alanine/BCAA ratiogram based on published data, 92 results from 31 authors, and reference values from 98 children and adults, (Queen Elizabeth Hospital for Children, 1978).

In an attempt to combine both aspects of protein and of calorie intake the glycine-BCAA quotient was plotted against the alanine-BCAA ratio. A remarkable correlation, ($r = 0.903$, $n = 60$) was obtained for control infants, children and adults under varying conditions of protein and calorie intake, with good discrimination between the different intakes as illustrated in Fig. 2; however, in control subjects given adequate calories almost completely in the form of carbohydrate, the ratiogram showed a movement from the normal area as defined in Fig. 2 toward the low protein area and beyond, with a trend toward the lower 95% confidence limit (Fig. 3).

Further data taken from patients under stress of starvation, low protein calorie intake, marasmus and kwashiorkor showed a progressive deviation from the 95% confidence limits with severity of the condition (Fig. 4).

From experimental and clinical data from the literature, plus data from our own laboratory, we have tentatively assigned areas of nutritional significance to the

ratiogram. Data from Felig [10] has illustrated the effect of prolonged starvation (Fig. 5).

The question has arisen as to whether amino acids used in this way reliably reflect degree of protein-calorie depletion rather than recent intake [11]. However, the amino acid pattern of chronically malnourished infants before rehabilitation, and expressed in this way, appears to be a good indicator of nutritional status, (Fig. 4), and may prove a useful aid in monitoring the effectiveness of treatment.

It is possible that areas of the ratiogram close to our 95% confidence limits may be indicative of short term changes or recent dietary intake in healthy people, whereas the more divergent areas may truly reflect chronic clinical situations.

In severe cases of malnutrition the validity of results following dietary treatment would be improved by allowing sufficient time to elapse, ensuring that amino acid levels reflect homeostasis. Clarification of this point and definition of the areas suggested in Fig. 5 requires many more standardised results and clinical study. Our experience so far is that the 'ratiogram' adds greatly to the interpretation of amino acid results by representing their levels in terms of protein-calorie intake.

References

1. Snyderman SE, Holt LE, Norton PM, Roitman E and Phansalker SV (1986) The Plasma Aminogram I. Influence of the Level of Protein Intake and a Comparison of Whole Protein and Amino Acid Diets. Pediat. Res. 2: 131–144.
2. Holmgren G (1974) Effect of Low, Normal and High Dietary Protein Intake on Urinary Amino Acid Excretion and Plasma Aminogram in Children. Nutr. Metab. 16: 223–237.
3. Valman HB, Brown RJK, Palmer T, Oberholzer VG and Levin B (1971) Protein Intake and Plasma Amino Acids of Infants of Low Birth Weight. Br. Med. J. 4: 789–791.
4. Arroyave G, Wilson D, De Funes C and Behar M (1962) The Free Amino Acids in Blood Plasma of Children with Kwashiorkor and Marasmus. Am. J. Nutr. 11: 517–524.
5. Whitehead RG and Dean RFA (1964) Serum Amino Acids in Kwashiorkor. Am. J. Nutr. 14: 313–319.
6. Lindblad BS, Rahimtoola RJ, Rehman HV, Ahmad SS, Fancy K, Singha L and Hussain SS (1978) Plasma Free Amino Acid Levels During Initial Rehabilitation of Protein-Energy Malnutrition with Protracted Diarrhoea Using a Free Amino Acid-Glucose Diet. Acta. Paediatr. Scand. 67: 335–343.
7. Arroyave G (1970) Comparative Sensitivity of Specific Amino Acid Ratios vs 'Essential to Non-Essential' Amino Acid Ratio. Am. J. Clin. Nutr. 23: 703–706.
8. Lindblad BS (1971) In: Jonxis JHP, Visser HRA and Troelstra JA (eds.) The Plasma Aminogram in Small for Date Newborn Infants. Metabolic Processes in the Foetus and Newborn Infant. HE Stenfert Kroese, N.V., The Williams and Wilkins Co., Baltimore, pp. 111–126.
9. Holt LE, Snyderman SE, Norton PM, Roitman E and Finch J (1963) The Plasma Aminogram in Kwashiorkor. Lancet ii: 1343–1348.
10. Felig P, Owen OE, Wahren J and Cahill GF (1969) Amino Acid Metabolism During Prolonged Starvation. J. Clin. Invest. 48: 584–594.
11. Saunders SJ, Truswell AS and Hansen JDL (1967) Plasma Free Amino Acid Pattern in Protein-Calorie Malnutrition. Lancet ii: 795–797.

Address for correspondence: A. Briddon, National Hospital for Nervous Diseases, Queen Square, London WC1N 3BG, U.K.

Lysine and methionine in dairy cows' nutrition

Edna Nachtomi and Israel Bruckental

Department of Nutrition and Physiology of Cattle, Agricultural Research Organization, Volcani Center, P.O.B. 6, Bet Dagan 50–250, Israel

Abstract

Abomasal infusion of lysine alone or lysine with methionine was investigated in lactating dairy cows to assess whether these amino acids were limiting to milk production. Two Israeli-Holstein cows cannulated in the duodenum were utilized in a double reversal experiment for a 72-day period. Cows were fed total mixed rations containing 25% silage and 75% concentrate on a dry matter (DM) basis, with 15% crude protein of which were corn source. Cows were infused continuously over a 12-day period with 2 l/d water, a solution of 30 g/d lysine, or a solution of 30 g lysine plus 8 g/d methionine. Infusion of lysine to cows resulted in a daily increase of 7.4% in DM intake, 9.1% in milk yield, 13.3% in milk protein yield, and a 3.55% decrease in milk fat yield compared to control. Cows infused with lysine and methionine had increases of 11.8% in milk yield, 6% in milk fat, and 12.5% in milk protein production. Addition of methionine to the lysine infusion resulted in a 6% increase in milk fat, but no increase in milk protein.

Introduction

Because of intensive fermentation of protein by rumen microbes, the ruminant is dependent on microbial protein for most of its amino acids supply. Lactating cows may encounter a specific amino acid deficiency in rations that formerly were considered adequate in protein. Efforts have been focused primarily on methionine and also on lysine, because these amino acids have been identified as possibly limiting milk yield and milk protein production under several dietary conditions [1–3].

Corn protein has a relatively low percentage of lysine. An adequate diet based on a high percentage of corn fed to lactating cows, could result in limiting lysine for protein synthesis in high-yielding dairy cows.

An attempt was made to increase the milk yield and milk protein production of cows fed a ration based on a corn feed diet (grain and silage), by lysine and methionine infusion to duodenum.

Experimental procedures

Animals and treatments. Four Israeli Holstein lactating cows were included in the study: two cows cannulated in the duodenum were used for infusion of amino

Table 1. Ingredient composition of total mixed ration. Protein from a corn source constitutes 30% of total protein

Ingredient	% of DM
Soybean	13.2
Corn grain	28.8
Cotton seeds	15.0
Barley grain	15.0
Cereal hay	10.0
Corn silage	15.0
Bentonite salts	1.6
Dicalcium phosphate	3.3
Mineral and vitamins	0.2
Crude protein	15.0

acids, and two cows not cannulated were used for observations on the effects of environmental changes.

Cows were fed *ad libitum* a ration containing 75% concentrate. Rations were formulated to contain 15% crude protein (CP). The composition of the total mixed rations is detailed in Table 1.

Four weeks postpartum the cows were allocated individually to metabolic cages and two cows were infused as follows: 2 l/d water (control), water solution of lysine (30 g/d) or a solution of lysine and methionine (30 g + 8 g/d). Each treatment period lasted 12 days. The treatment's sequence was repeated.

Feed consumption was recorded daily for all cows. Feed composition was analysed according to the AOAC. Cows were milked three times a day, and milk yield recorded. Samples of milk were taken on the last 2 days of each treatment period for analysis.

Data Analysis. Statistical treatment was done according to analysis of covariance, and differences between control and treatments were analysed by student's t-test.

Results and Discussion

Lysine infusion to duodenum increased significantly ($P<0.05$) the DM intake (7.4%), and the milk yield was augmented by 2.8 l/d (9.1%) over the control (Table 2). Infusion of lysine decreased significantly ($P<0.05$) the milk fat percentage (11.4%), and milk protein percentage was elevated slightly (3.8%). The improvement of milk production and milk protein percentage consequently resulted in a remarkable elevation 107 g/d (13.3%) in milk protein production, but milk fat yield was reduced by 29 g/d (–3.3%).

Lysine and methionine infusion depressed slightly the DM intake. Feed intake of ruminants could be depressed by increasing levels of methionine supplementation. Milk yield was increased by 3.6 l/d, and accounted for 2.7% more than that

Table 2. Average DM intake, milk production and composition of cows as affected by lysine or lysine plus methionine infusion. (Lysine was infused at 30 g/d in 21 water and methionine was added at 8 g/d)

Parameter	Infusion			S.E. of mean
	Water	Lysine	Lysine + methionine	
DM intake (kg/d)	14.8	15.9 (7.4)[a]	14.5 (–2.0)	0.23
Milk yield (kg/d)	30.6	33.4 (9.1)	34.2 (11.8)	0.98
4% FCM (kg/d)	24.3	20.2 (7.8)	27.4 (12.7)	0.7
Milk fat (%)	2.90	2.57 (–11.4)[b]	2.75 (–5.2)	0
Milk protein (%)	2.63	2.73 (3.8)	2.65 (0.8)	0
Fat yield (g/d)	887	858 (–3.3)	940 (6.0)	30
Protein yield (g/d)	805	912 (13.3)[b]	906 (12.5)[b]	29

[a]In parentheses percentage difference relative to water infused cows.
[b]Significant difference from control at $p<0.05$.

obtained with lysine alone; the milk fat percentage were still depressed relative to control, but this depression was less (by 6.2%) than that observed with lysine infusion. Milk fat production increased by 53 g/d (6.0%), and could be the result of methionine supplementation only. The protein yield, elevated to 101 g/d, was nearly the same as that obtained with lysine alone (107 g/d). From these results it may be concluded that methionine supplementation does not affect milk protein production.

The performance of cows not infused during parallel periods of experimental infusion or amino acids, tended to decrease according to normal lactation curve postpartum (Table 3). Accordingly, it is concluded that the data presented in Table 2 can be considered as the true results of the effect of amino acid infusion to cows. Methionine seems to be not limiting when infused postruminally with an adequate quantity of lysine. Methionine is one of the essential amino acids which is

Table 3. Average DM intake, milk production and composition of non-infused cows as compared with infused cows, during parallel periods

Parameter	Infusion periods			S.E. of mean
	Water	Lysine	Lysine + methionine	
DM intake (kg/d)	17.8	17.8	15.8 (–11.2)	0.23
Milk yield (kg/d)	29.6	29.3 (–1.0)	30.8 (4.0)	0.86
4% FCM (kg/d)	29.0	27.3 (–5.8)	25.9 (–10.6)	0.6
Milk fat (%)	3.8	3.45 (–9.2)[a]	3.3 (–13.1)[a]	0.15
Milk protein (%)	2.82	2.86	2.7 (–4.2)	0.36
Fat yield (g/d)	1125	1001 (–10)[a]	1016 (–9.6)[a]	36
Protein yield (g/d)	835	838 (0.39)	832 (–0.37)	21

[a]Significant difference from control period at $p<0.05$.

degraded relatively slightly by rumen microorganisms [1], and lysine has lower transport capacity than methionine in cattle intestinal mucosa [4]. Lysine seems to be a more limiting amino acid for milk protein production.

In lactating dairy cows, duodenum infusion of lysine alone resulted in a positive response to milk crude protein secretion; lysine and methionine doubled this response [3]. Feeding rumen-protected methionine increased milk and milk protein content of cows [5], or increased the milk fat percent of cows [6,7]. Feeding rumen protected methionine plus lysine increased the production of milk protein [8].

It is not clear whether the possible requirement for each of the amino acids, lysine and methionine separately or together was actual reason for raising milk protein or fat production.

In conclusion, our results showed that an infusion of lysine (30 g/d) to the duodenum of lactating cows fed a diet containing 15% protein, (composed of 30% protein from a corn source), had increased milk yield and the amount of protein produced, but the supplementation of methionine (8 g/d) in addition to lysine increased the daily milk fat yield.

Acknowledgements

We would like to thank Mrs. Holstein Pia and Mrs. Hana Lehrer for their skillful technical assistance.

References

1. Chalupa W (1976) J. Anim. Sci. 43: 828–834.
2. Clark JH, Spires HR and Davis CL (1978) Fed. Proc. 37: 1233–1238.
3. Schwab CG, Satter LD and Clark AB (1976) J. Dairy Sci. 59: 1254–1270.
4. Guerino F and Baumrucker CR (1987) J. Anim. Sci. 65: 619–629.
5. Illg. DJ, Sommerfeldt JL and Schungoethe DJ (1987) J. Dairy Sci. 70: 620–629.
6. Huber JT, Emery RS, Bergen WG, Liesman JS, Kung L Jr. and King KJ (1984) J. Dairy Sci. 67: 2525–2531.
7. Lundquist RJ, Otterly DE and Linn JG (1985) J. Dairy Sci. 68: 3350–3354.
8. Rogers JA, Krishnamoorthy V and Sniffen CJ (1987) J. Dairy Sci. 70: 789–798.

Address for correspondence: Dr. Edna Nachtomi Dept. Nutri. Phys. of Cattle Agric. Res. Organisation Volcani Center, P.O.B. 6, Bet Dagan 50–250, Israel.

Dietary tyrosine supplementation corrects tyrosine and dopamine deficits in diabetic rat retina

Candace J. Gibson

Department of Pathology, University of Western Ontario, London, Ontario N6A 5C1, Canada

Abstract

The dietary amino acid tyrosine is the precusor of the brain and retinal catecholamine transmitter dopamine (DA). Alterations in tissue level of this precursor may influence the rate at which the catechol is synthesized and released, particularly when the rate-limiting enzyme, tyrosine hydroxylase (TH), is activated. Physiologically, TH is activated in the retinal amacrine DA cell during exposure to light. In diabetic rats we have found that retinal tyrosine level is severely reduced and tyrosine supplementation of the diet can correct this deficiency and hence retinal DA. Retinal tyrosine level in streptozotocin-diabetic male rats was reduced to 0.24 ± 0.05 μg/mg protein from control levels of 0.71 ± 0.02 μg/mg protein. Addition of 4% tyrosine to the 24% casein basal diet increased tyrosine level threefold in both control (to 2.38 ± 0.30 μg/mg protein) and diabetic retina (to 0.62 ± 0.08 μg/mg protein). Retinal DA was also reduced in diabetic rats (controls, 2.23 ± 0.19 ng/mg protein; diabetic, 1.71 ± 0.12 ng/mg protein) and this deficit was reversed by the addition of dietary tyrosine (2.12 ± 0.05 ng/mg protein).

Introduction

The dietary aromatic amino acid, tyrosine is the precursor of the brain and retinal transmitter, dopamine (DA). The first step in DA synthesis involves the hydroxylation of tyrosine, catalyzed by the rate-limiting enzyme, tyrosine hydroxylase (TH). Under normal conditions TH is almost fully saturated with its amino acid substrate (about 75–80%) [1] and increases in precursor level have little influence on DA synthesis. However under conditions in which the synthetic enzyme is activated (i.e. during increased neuronal firing [2]; certain receptor [3] or impulse blocking drugs [4]) tyrosine administration and elevation of tissue tyrosine level results in increased synthesis and release of dopamine.

Retinal TH is normally regulated by exposure to light. Tyrosine hydroxylase activity [5,6] and indices of DA synthesis, such as DOPA accumulation [7]; DA metabolites, DOPAC and HVA [8] are elevated when eyes are exposed to light or during the light portion of the diurnal cycle. Tyrosine administration, by its intraperitoneal injection [9,10] or supplementation in the diet [11] raises retinal tyrosine level and DA turnover in light-exposed rats.

Alterations in tissue tyrosine level, due to diet, disease or disordered metabolism, may ultimately affect transmitter synthesis. Brain and retinal tyrosine levels

are determined not only by blood tyrosine concentration but also by the blood levels of several neutral amino acids which compete with it for uptake into tissue. In diabetic rats, central nervous system (CNS) and retinal levels of tyrosine are reduced due to large increases in three neutral amino acid competitors (leucine, isoleucine and valine) [12,13]. We have investigated the ability of dietary tyrosine supplementation to restore deficient tyrosine levels and retinal DA turnover in diabetic rats.

Materials and Methods

Male, Sprague-Dawley rats (initial weight 180–200 gm, Charles River, St. Constant, Que.) were housed 2–3 per cage under standard lighting conditions (fluorescent lights on from 7 AM to 7 PM) and acclimatized to the animal quarters for 3–5 days before switching to the synthetic casein diets (control diet = 24% casein; 240 g casein, 365 g dextrin, 183 g sucrose, 22 g Vitamin Mix (No. 904654); 40 g Rogers-Harper salt mix, 150 ml corn oil per kg of diet). All diet ingredients were purchased from ICN Biochemicals, Montreal, Que., Canada.

Diabetes was produced by intraperitoneal injection of the pancreatic toxin, streptozotocin (65 mg/kg/ml of 10 mM citrate buffer, pH 4.5; 2 × 24 h) and confirmed by the presence of hyperphagia; polydipsia and weight loss and elevation of serum glucose (>275 mg %). Control rats received vehicle injections. One week after streptozotocin injection half of the control and diabetic rats were placed on a 24% casein diet supplemented with 4% tyrosine (40 gm/kg diet with an equal reduction in dextrin). Two weeks later rats were sacrificed by decapitation between 9–11 a.m. or 9–11 p.m. (under red light). Retina were removed and frozen at −80°C until assay of DA and its metabolites by HPLC [11,13] and tyrosine by fluorometry [14]. Blood was collected from the neck wound and serum analyzed for glucose and tyrosine.

To measure *in vivo* tyrosine hydroxylase activity, rats were injected with the dopa decarboxylase inhibitor, NSD 1015 (100 mg/kg/ml, i.p.) 30 min prior to decapitation. Retina were analyzed for DOPA and tyrosine [11].

Twenty-four hour food intake was similar in control (24% casein) and tyrosine-supplemented rats (31 ± 2 and 34 ± 5 g/day) and was increased in diabetic rats (55 ± 2 and 62 ± 4 g/day). Data were analyzed by 2-way ANOVA (BMDP Statistics Program) and are presented as means ± standard error of the mean (x ± SEM).

Results

Dietary tyrosine supplementation doubled to tripled serum tyrosine levels in controls, from 27.6 ± 1.9 μg/ml to 68.0 ± 3.8 μg/ml (light) and from 29.8 ± 0.9 μg/ml to 74.8 ± 9.0 μg/ml (dark-during time of maximum food consumption). Serum tyrosine was decreased slightly in diabetic rats but was also doubled with

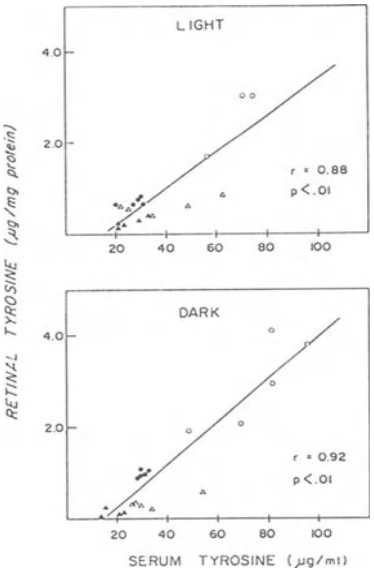

Fig. 1. Correlation of Retinal Tyrosine with Serum Tyrosine Level. Diabetic and control rats were fed 24% casein or 24% casein supplemented with 4% tyrosine ad libitum for two weeks before sacrifice. Closed triangles-diabetic, 24% casein; open triangles-diabetic, 24% casein plus 4% tyrosine; closed circles-control, 24% casein; open circles-control, 24% casein plus 4% tyrosine. Upper graph from rats killed during light phase of cycle (9–11 a.m.); lower graph from rats killed during dark phase of cycle (9–11 p.m.). Serum and retinal tyrosine were measured fluorometrically. (N = 5/group)

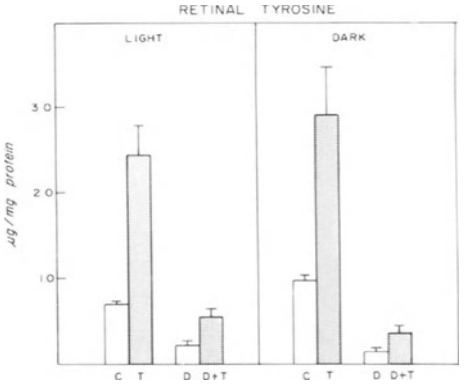

Fig. 2. Effect of Tyrosine Supplementation on Retinal Tyrosine in Control and Diabetic Rats. Control and diabetic rats were fed 24% casein (C or D) or 24% casein plus 4% tyrosine (T or D+T) *ad libitum* for two weeks. Rats (groups of 5) were sacrificed between 9–11 a.m. (light) or between 9–11 p.m. (dark) and retina analyzed for tyrosine and DA (Fig. 3). Data were analyzed by 2-way ANOVA. There was a significant difference ($p<0.00001$) with condition (control vs diabetes, $F(1.16) = 62.01$) and with diet (basal vs 4% tyrosine, $F(1,16) = 52.22$). in light-exposed retina and in dark-exposed retina (control vs diabetes, $F(1,15) = 53.87$, p 0.00001 and basal vs 4% tyrosine, $F(1,15) = 20.62$, $p = 0.0004$).

tyrosine supplementation, from 25.7 ± 2.6 µg/ml to 38.3 ± 8.5 µg/ml (light) and from 17.3 ± 1.8 µg/ml to 34.1 ± 5.8 µg/ml (dark).

Retinal tyrosine level showed a similar pattern, two to three-fold increases following tyrosine supplementation in both light and dark phases of the cycle (Fig. 1 and 2). Serum tyrosine was significantly correlated to retinal tyrosine level ($r = 0.88$, light and $r = 0.92$, dark $p<0.01$) throughout the daily cycle. Retinal tyrosine was severely reduced in diabetic rats to about one-third of normal values in light exposed retina (0.24 ± 0.05/mg protein) and was restored to normal values (0.62 ± 0.08 µg/mg protein) with tyrosine supplementation. In the dark, retinal tyrosine was even more severely reduced to about 15% of normal levels (0.15 ± 0.04 µg/mg

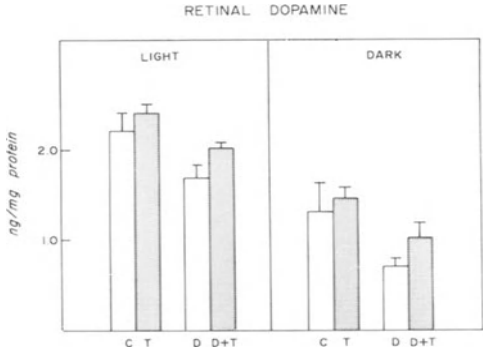

Fig. 3. Effect of Tyrosine Supplementation on Retinal Dopamine in Control and Diabetic Rats. Same legend as Fig. 2. Data were analyzed by 2-way ANOVA. There was a significant difference with condition (control vs diabetic, $(F(1,16) = 11.4, p = 0.0038)$ and with diet (basal vs 4% tyrosine, $F(1,16) = 6.0, p = 0.026$) in light-exposed rats. Under dark conditions, there was a significant difference between control and diabetic rats ($F(1,16) = 11.2, p = 0.004$) but no significant difference with diet ($F(1.16) = 3.19, p = 0.09$).

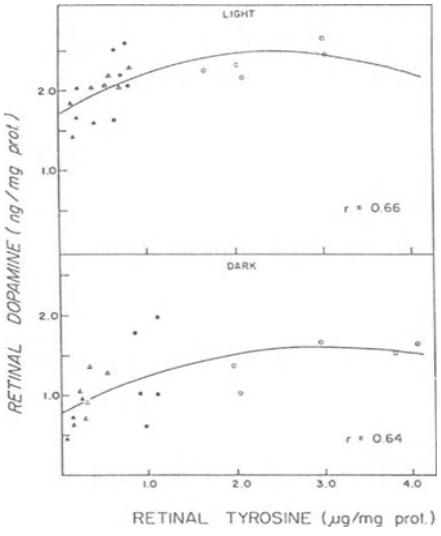

Fig. 4. Correlation of Retinal Dopamine with Retinal Tyrosine Level. Legend as per Fig. 1. Data were best fit to a quadratic equation ($y = -0.123x^2 + 0.62x + 1.71$, light; $y = -0.08x^2 + 0.53x + 0.79$, dark).

protein). Even though tyrosine supplementation significantly doubled retinal tyrosine (0.33 ± 0.07 µg/mg protein) this was below control levels (Fig. 2).

In these experiments, retinal DA was decreased in diabetic rats at both time points, e.g. from 2.23 ± 0.19 to 1.71 ± 0.12 µg/mg protein at 10 a.m. (Fig. 3) and supplementation with tyrosine significantly increased retinal DA (to 2.12 ± 0.05 µg/mg protein). In dark retina, tyrosine supplementation had little effect on DA in control rats but resulted in a 30% increase in diabetic rat retina. DOPAC and HVA followed a similar pattern (data not shown).

There was a significant linear correlation between retinal tyrosine level and retinal DA ($r = 0.62$, light and $r = 0.52$, dark $p<.05$). A better fit was obtained to a quadratic function (Fig. 4). Values of tyrosine and dopamine at the maxima of the quadratic equation were 3.15 µg tyrosine/mg protein, 1.62 ng DA/mg protein in dark-retina (TH in basal state) and 2.52 µg tyrosine/mg protein, 2.49 ng DA/mg

Table 1. The effect of dietary tyrosine supplementation on retinal tyrosine and DOPA

	Basal	4% Tyrosine	Basal	4% Tyrosine
	Tyrosine (μg/mg protein)		DOPA (ng/mg protein)	
Control	1.58 ± 0.13	5.73 ± 0.38[a]	1.99 ± 0.21	2.78 ± 0.22[b]
Diabetic	1.16 ± 0.20[c]	2.13 ± 0.35[c,a]	1.70 ± 0.39	2.41 ± 0.49[b]

Rats were injected with streptozotocin (2 × 65 mg/kg, i.p.) or vehicle (10 mM citrate buffer, pH 4.5) and one week later half of each group (N=5) were placed on the 4% tyrosine supplemented diets. Two weeks later rats were injected with NSD – 1015 (100 mg/kg, i.p.) 30 min prior to sacrifice and removal of retina for tyrosine and DOPA analysis. Data were analyzed by 2-way ANOVA (x ± S.E.M.).
[a] $p<0.00001$, $F(1,14) = 81.91$ significantly differs from basal diet.
[b] $p<0.04$, $F(1,14) = 5.13$ significantly differs from basal diet.
[c] $p<0.00001$, $F(1.14) = 50.55$ diabetic significantly differs from control rats.

protein in light-exposed retina (TH in activated state). The increased peak level of DA in light reflects the increased V_{max} of the synthetic enzyme with light.

An *in vivo* measure of TH activity DOPA accumulation after decarboxylase inhibition indicated that the increase in DA with dietary tyrosine supplementation was due to an increase in DOPA synthesis (Table 1). There was no effect of diabetes or tyrosine on DOPA synthesis during the dark phase of the cycle.

Discussion

In CNS tissues, increasing tyrosine level has little effect on DA synthesis under normal conditions, but can result in increased turnover when the synthetic enzyme is activated [2–4,15]. Physiologically, activation of TH occurs in the retina with exposure to light; thus there is a diurnal rhythm in TH activity, DA synthesis and release [6–8]. After a single injection of tyrosine during the light cycle retinal DA turnover is increased; but there is no change during the dark phase of the cycle [9].

Retinal tyrosine level is determined not only by its serum tyrosine level but also by the level of neutral amino acids which share a common carrier for uptake across endothelial cells of the blood-retinal barrier [13,16]. Insulin promotes the uptake of the branched chain amino acids (leucine, isoleucine and valine) into muscle where they are metabolized. In diabetes, in the absence of insulin, serum levels of these branched chain amino acids are increased 2–3 fold and retinal levels of tyrosine fall [12,13]. In diabetic rats retinal tyrosine is proportional to the serum tyrosine ratio, which is reduced from one-half to one-third of normal values. Retinal tyrosine level was also reduced in these experiments (Fig. 1 and 2) and led to a reduction in retinal DA synthesis as evidenced by a decrease in DA level itself and in the rate of accumulation of DOPA following inhibition of the decarboxylase enzyme. Supplementation of the diet with tyrosine significantly raised serum and

retinal tyrosine in both control and diabetic rats. In animals in the light (when TH is activated) tyrosine supplementation resulted in an increase in DA synthesis (DOPA and DA concentration). Diabetic animals in the dark (TH in basal state) with a 40% reduction in their retinal tyrosine level, and control animals were unresponsive to increased retinal tyrosine. However, if the reduction in tyrosine was severe enough (as in the first experiment where tyrosine was reduced by 85%) in diabetic rats, DA synthesis was also affected and in this case tyrosine supplementation doubled retinal tyrosine and resulted in an increased level of DA.

The relationship between tyrosine and DA in both light and dark conditions fit a quadratic function with maxima at 2.52 μg tyrosine, 2.49 ng DA and 3.15 μg tyrosine, 1.62 ng DA, respectively. Using the maximal DA concentration as a rough *in vivo* index of V_{max} of the enzyme one can see a 50% increase in light-exposed retina. A rough approximation of affinity for tyrosine substrate gives 1.26 μg/mg protein (light) and 1.57 μg/mg protein (dark). In these experiments retinal tyrosine level varied between 0.71–1.58 μg/mg protein which is close to this estimated K_m. In diabetic rats this value fell to 0.24 μg/mg protein which is well below the K_m and hence, resulted in a reduced rate of DA synthesis. In dark-exposed rats, even though the enzyme is in its basal state, severe reductions in retinal tyrosine (due to the influx of large amounts of competing neutrals and reduction in serum tyrosine ratio with night-time feeding) may compromise retinal DA synthesis.

Dietary supplementation with 4% tyrosine effectively doubled to triple retinal tyrosine level and these changes in precusor level were sufficient to result in an increase in retinal DA synthesis. The response to tyrosine is slightly blunted in diabetic rats, due to the persistence of high levels of competing branched chain amino acids (not measured in these studies) and an increase in tyrosine aminotransferase activity in diabetic rat liver [13]. This level of tyrosine supplementation was sufficient to produce a doubling of tissue levels in diabetic rats and positive effects on retinal DA synthesis. Thus, tyrosine supplementation is an effective means of restoring reduced tyrosine levels and neurotransmitter deficits.

References

1. Carlsson A and Lindquist M (1978) Naunyn Schmiedebergs Arch. Pharmacol. 303: 157–164.
2. Melamed E, Hefti F and Wurtman RJ (1980) Proc. Natl. Acad. Sci. 77: 4305–4309.
3. Scally UC, Ulus IH, Wurtman RJ (1977) J. Neural. Transm. 41: 1–6.
4. Sved AF and Fernstrom JD (1981) Life Sci. 29: 743–748.
5. Iuvone PM, Galli CL and Neff NH (1978) Mol. Pharmacol. 14: 1212–1219.
6. Iuvone PM, Galli CL, Garrison-Gund CK and Neff NH (1978) Science 202: 901–902.
7. Wirz-Justice A, DaPrada M and Remé C (1984) Neurosci. Lett. 45: 21–25.
8. Cohen J, Hadjiconstantinou M and Neff NH (1983) Brain Res. 260: 125–127.
9. Gibson CJ, Watkins CJ and Wurtman RJ (1983) J. Neural Trans. 56: 153–160.
10. Fernstrom MH, Volk EA, Fernstrom JD and Iuvone PM (1986) Life Sci. 39: 2049–2057.
11. Gibson CJ (1988) J. Neurochem. 50: 1769–1774.
12. Brosnan JT, Man KC, Hall DE and Colbourne SA (1983) Am. J. Physiol. 244: E151–E158.

13. Gibson CJ (1988) Brain Res. 454: 60–66.
14. Waalkes TP and Udenfriend S (1957) J. Lab. Clin. Med. 50: 733–736.
15. Milner JD and Wurtman RJ (1986) Biochem. Pharmacol. 35: 875–881.
16. Fernstrom MH, Volk EA and Fernstrom JD (1986) Am. J. Physiol. 251: E393–E399.

Address for correspondence: Candace J. Gibson, Ph.D., Department of Pathology, University of Western Ontario, London, Ontario, N6A 5C1, Canada.

Renal immaturity causes taurine depletion in very low birth weight infants fed with prolonged total parenteral nutrition*

Israel Zelikovic[a], Russell W. Chesney[b], Aaron L. Friedman[c] and Charles E. Ahlfors[d]

[a]*Division of Pediatric Nephrology, Department of Pediatrics, University of Tennessee, Memphis TN, U.S.A.*

[b]*Department of Pediatrics, University of Tennessee, Memphis TN, U.S.A.*

[c]*Division of Pediatric Nephrology, Department of Pediatrics, University of Wisconsin, Madison WI, U.S.A.*

[d]*Division of Neonatology, Department of Pediatrics, University of California, Davis, Sacramento CA, U.S.A.*

Introduction

Taurine is a ß amino acid, whose functions include neuromodulation, cell membrane stabilization, antioxidation, detoxification, bile acid conjugation and osmoregulation [1], and is regarded as essential for normal brain and retinal development [2]. Taurine depletion in early life causes degeneration of retinal photoreceptors, CNS abnormalities and growth depression in young animals [1] and atypical electroretinograms in children [3] and auditory brainstem evoked responses in preterm infants [4].

Taurine, while abundant in human milk and in supplemented infant formulas, is not found in many total parenteral nutrition (TPN) solutions. Reduced taurine values in plasma and blood cells have been demonstrated in adults [5] and children [6] receiving long-term parenteral nutrition, but not after a short-term administration (10–12 days) in preterm infants [7]. Taurine status, in very low birth weight (VLBW) infants receiving taurine-devoid TPN solution for extended periods of time, is uncertain.

Immature animals and newborn infants show hypertaurinuria as a part of their neonatal 'physiologic' aminoaciduria [8]. Our lab has recently demonstrated that the renal tubular brush border membrane isolated from suckling 7-day-old rats does not show the adaptive response to various taurine diets 'up' and 'down' regulation of Na^+-taurine cotransport across the membrane which prevails in older rats (Fig. 1) [9]. While term [10] and preterm infants [11,12] fed a low taurine formula show reduced urinary taurine, the capacity of the immature tubule of the VLBW infants to adapt to low taurine intake by enhancing tubular taurine reabsorption is unknown. The purpose of this study is to measure plasma and urinary taurine content in VLBW infants receiving taurine-free TPN solution as compared to VLBW infants receiving human milk or taurine-supplemented formula. Further,

* This study is supported in part by National Institutes of Health Grants P30AM35747 and DK-37223.

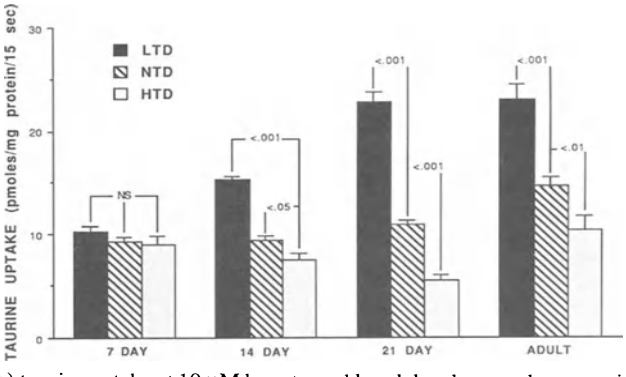

Fig. 1. Initial (15 sec) taurine uptake at 10 μM by rat renal brush border membrane vesicles as influenced by age and diet. LTD-low taurine diet, NTD-normal taurine diet, HTD-high taurine diet (Modified from Chesney RW, et al, Pediatr Res 20:893, 1986). Note the failure of 7-day-old rat membranes to adapt to diet.

the capacity of the immature renal tubular epithelium to adjust to a taurine deficiency state was examined.

Methods

Twenty-two premature, appropriate for gestational age infants were enrolled in a prospective controlled study. The infants were assigned into one of two categories: 1) (E1 & E2) Infants receiving human milk or taurine supplemented (30–40 μmol/dl) infant formula (Pregestimil, Similac Special Care or Enfamil) from day 3–4 of life. Feedings contained 20 or 24 kcal/30 ml at 120–170 ml/kg/day; 2) (P1 & P2) infants receiving TPN from day 3–4 of life because of medical or surgical complications. A standard TPN solution (Travasol, Travenol Company, Deerfield, IL) was provided via peripheral or central vein catheter at 120–160 ml/kg/day of infusate containing 1.5–2.5 g/kg/day amino acids, 7–20 g/kg/day dextrose, electrolytes, trace elements and vitamins. Four hundred mg methionine per 10 g amino acid mixture was present, but the solution was devoid of cysteine or taurine. One to three g/kg/day lipids were provided as 10% or 20% solution (Intralipid, Rabivitrum, Alameda, CA). Total nonprotein energy intake was 90–120 kcal/kg/day. These infants were not fed before or during the period of TPN administration. The infant's condition permitting, feeding was started using taurine-containing formula. TPN was discontinued when the enteral feeding provided at least 50% of the caloric intake.

All infants were followed from the third week of life for a time period ranging from 4–16 weeks. Once weekly, a heparinized blood specimen was obtained. Blood was collected by allowing it to drop spontaneously through a 21-gauge needle inserted into a hand vein in order to avoid lysis of blood cells which contain

high concentrations of taurine [5]. The blood specimen was immediately centrifuged and the plasma stored at −70°C. Two-hour urine collections were obtained using adhesive bags or by extracting urine from the infant's diaper or from cotton wool balls placed inside the diaper [13] and stored.

Ten healthy, full-term, appropriate for gestational age infants served as controls. In these infants plasma taurine was obtained by venous puncture at least 3 h after morning feeding and a 3-h urine collection was performed using adhesive bags.

Taurine concentrations in plasma and urine were determined using reversed phase high pressure liquid chromatography after derivatization of taurine with phenylisothiocyanate [14]. Creatinine levels were determined by a photometric method. Fractional excretion of taurine (FET) was calculated according to the formula: U taurine/P taurine × P creatinine/U creatinine × 100 where U and P represent concentrations in urine and plasma, respectively.

Data points in line graphs represent mean ± S.E.M. of values determined during 2 week periods. Data comparison was made with Student's *t*-test for grouped independent data and analysis of variance.

Results

All 15 infants in groups P1 and E1, which were gestational-age and birth weight-matched groups, were ill and had multisystem disease (Table 1). The infants in group P1 required TPN because of necrotizing enterocolitis (2 infants) or persistent feeding intolerance (abdominal distention, vomiting, etc). Indications for TPN in group P2 infants were gastroschisis and short bowel syndrome. All infants in group E2 had hyaline membrane disease and other prematurity-related manifestations.

Table 1. Study population

	TPN		Enteral		Control
	P1	P2	E1	E2	C
n	7	2	8	5	10
Gestational age (wk)					
Mean	26.3	34	27.3	30.4	39.2
Range	24–28	34	26–28	28–32	37–42
Birth Weight (g)					
Mean	814	2687	898	1374	3367
Range	510–990	2635–2740	750–1000	1070–1640	2800–4090
Duration of TPN (days)					
Mean	40	38.5	——	——	——
Range	32–49	33–44			

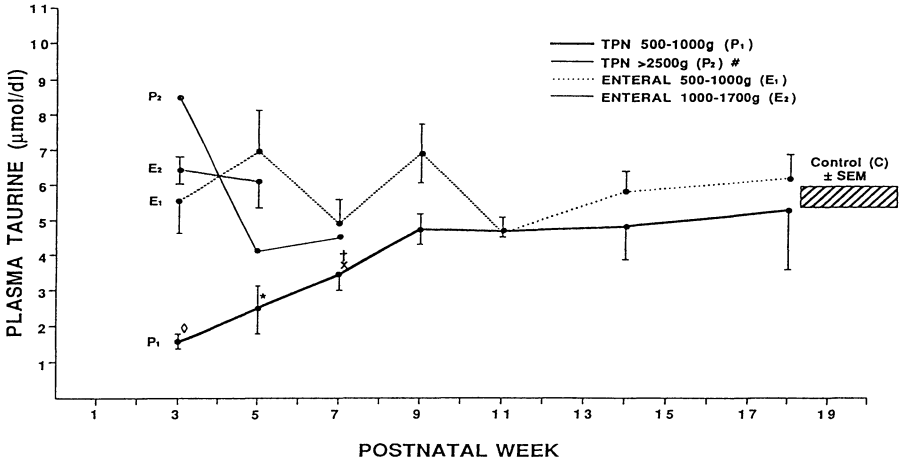

Fig. 2. Plasma taurine concentrations. Each data point represents mean ± S.E.M. of values determined during a 2-week period for each group of infants. ◊ $p<0.001$ vs E1 and C. * $p<0.005$ vs E1 and C. † $p<0.05$ vs E1. × $p<0.005$ vs C. # Data from two infants.

Significantly lower mean plasma taurine values were found between the third and seventh postnatal week in infants with birth weight 500–1000 g who received TPN (P1) as compared to values in the birth weight-matched enterally-fed group of infants (E1) and to control infants (C) (Fig. 2). Over the same time period, infants in group E1, the two larger TPN-requiring-infants (P2) and the infants with birth weight 1000–1700 g who received oral feeding (E2) had plasma taurine concentrations similar to controls. After initiation of feeding in P1 infants (at a mean age of 40 ± 7 days), plasma taurine concentration increased to normal. Mean plasma taurine values at age 1 month in all groups are shown in Fig. 3. Plasma taurine concentrations in P1 were significantly lower than in all other groups. These data

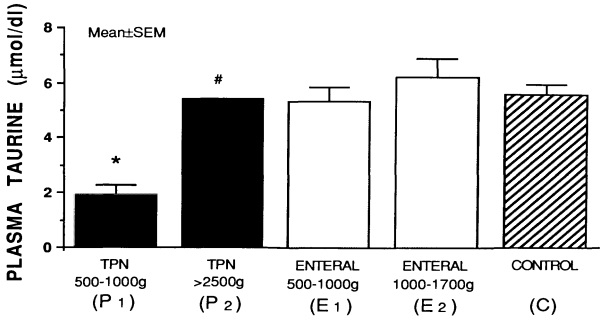

Fig. 3. Plasma taurine concentrations at postnatal age 1 month. Data represent mean ± S.E.M. for each group of infants. * $p<0.001$ vs all other groups. # Data from two infants.

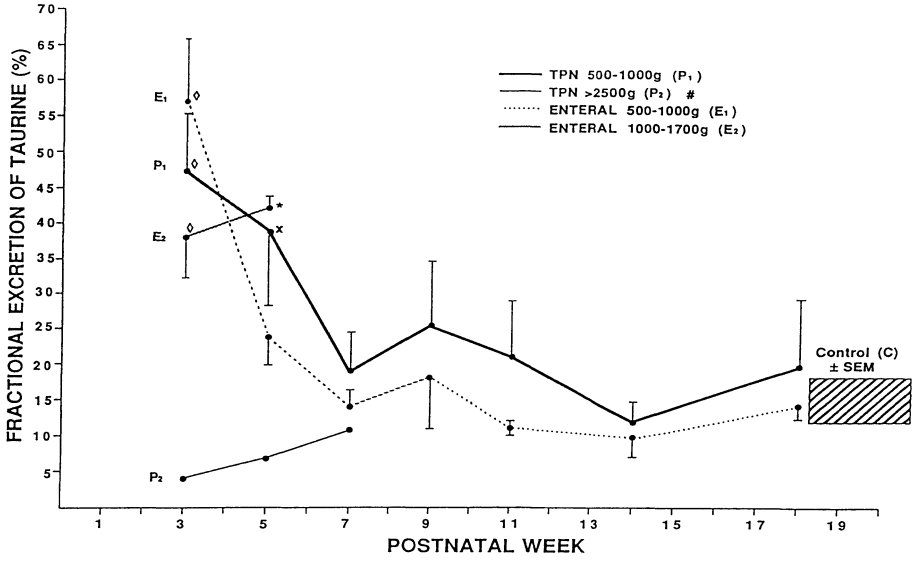

Fig. 4. Urinary fractional excretion of taurine. Each data point represents mean ± S.E.M. of values determined during a 2-week period for each group of infants. * $p<0.001$ vs C. ◊ $p<0.005$ vs C. × $p<0.05$ vs C. # Data from two infants.

indicate severe plasma taurine depletion during early life in sick VLBW infants receiving taurine-devoid TPN solution.

Elevated mean values of FET were found between the third and fifth postnatal week in the small infants in P1, E1 and E2 when compared to controls (C) (Fig. 4). By contrast, low values of FET were found in the two large infants in P2. After the fifth postnatal week, FET was in the control range in all groups. Figure 5 illustrates markedly elevated mean FET values at one month of age in all groups of small infants when compared to controls and to infants with birth weight >2500 g. These

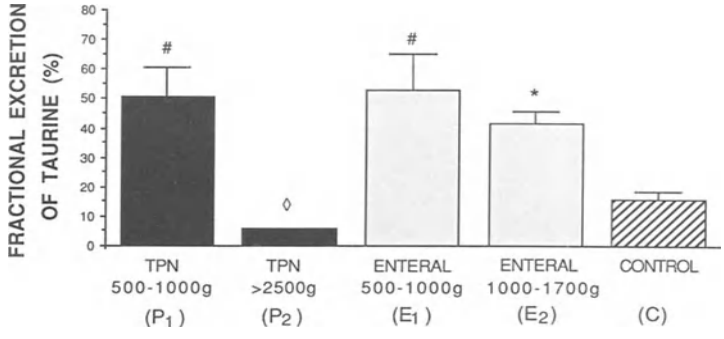

Fig. 5. Urinary fractional excretion of taurine at postnatal age 1 month. Data represent mean ± S.E.M. for each group of infants. # $p<0.005$ vs C. * $p<0.001$ vs C. ◊ Data from two infants.

data demonstrate marked hypertaurinuria in sick VLBW infants during the first weeks of life and indicate that the immature tubule of VLBW infants lacks the capacity to adaptively increase taurine reabsorption even in the face of markedly reduced plasma taurine concentrations.

Discussion

The low plasma and urine taurine concentrations in infants fed a low taurine, casein-based formula [10,11] has led to the supplementation of essentially all infant formulas manufactured in the United States with taurine in concentrations similar to those found in human milk [1]. Many TPN solutions, which can be administered to sick premature infants for prolonged time intervals, contain no taurine. This study demonstrates extremely low plasma taurine values in VLBW infants receiving a taurine-free TPN solution during the first weeks of life (Fig. 2,3). Since most of the taurine in the body is intracellular [1] and since plasma taurine concentrations reflect intracellular taurine stores [5,6], these data suggest that depleted body taurine pools may prevail in these immature infants early in life. This finding is in contrast to normal plasma taurine concentrations during the same time period in birth weight-matched (E1) and larger infants (E2) receiving taurine supplements in their solutions, as well as in two large infants (P2) receiving taurine-free TPN solution (Fig. 2,3).

Low plasma taurine levels were found in children receiving long-term taurine-free parenteral nutrition for gastrointestinal disorders [3]. In nearly all these children parenteral nutrition was administered for more than 1 year. In the very premature infants reported in our study, however, a 3–4 week administration of taurine-devoid TPN solution already resulted in a severe taurine deficiency, probably indicating limited body taurine pools.

During fetal life, taurine is transported from mother to fetus via the placenta and subsequently concentrates in the brain and retina [15,16]. The total body content of taurine increases markedly up to term in all mammals including humans [17]. Thus, markedly decreased body taurine pools exist in prematurely born infants who have been unable to assimilate sufficient reserves of taurine. The activity of cystathionase and cysteine sulfinic acid decarboxylase (CSAD), the rate limiting enzymes in the biosynthesis of taurine from methionine and cysteine, is low in the developing human liver and brain [1]. These low enzyme concentrations mean that the immature infant is totally dependent on external taurine supply after birth. Indeed, taurine deficiency developed in the premature infants reported in Gaull's study [11] and in our study despite adequate supply of methionine and cysteine in the taurine-free formula [11] and of methionine in the taurine-devoid TPN solution, respectively. Taurine containing enteral solutions, however, prevented the development of taurine deficiency, even in the very low birth weight premature infants (Fig. 2,3).

Increased taurine accumulation into isolated renal brush border membrane

vesicles (BBMV) prepared from rats fed a low taurine diet was found as compared to uptake in BBMV from rats on a normal taurine diet [9] (Fig. 1). Diminished uptake is found in vesicles from high taurine diet fed animals. This renal adaptive response to diet, observed in weanling and mature rats (Fig. 1), maintains body pool size and, as a result, the constancy of brain content of taurine [19]. The renal brush border membrane isolated from the suckling 7-day-old rats does not exhibit the adaptive response to diet found in older rats [9] (Fig. 1). This diet-induced adaptive response occurs only as the animal becomes more mature.

The high rate of urinary taurine excretion during early life in VLBW infants (Fig. 4,5) is consistent with the well known neonatal 'physiologic' aminoaciduria in all mammals including humans [8] and reflects the immaturity of the renal tubular transport system. Of importance is the marked hypertaurinuria observed between the third and fifth postnatal week in VLBW infants receiving TPN (P1) (Fig. 4,5), despite extremely low plasma taurine values (Fig. 2,3). This observation indicates the failure of the immature tubular epithelium to adjust to a taurine deficiency state and may represent the human counterpart of the above-mentioned *in vitro* finding in the rat. While taurine supplementation to enterally fed premature infants (E1, E2) maintained normal plasma taurine values (Fig. 2,3), despite excessive urinary excretion of this amino acid (Fig. 4,5), the inability of the very immature kidney to reabsorb taurine resulted in severely depleted body taurine pools in unsupplemented TPN-requiring immature infants.

It is plausible that the two large infants receiving taurine-free TPN solution (P2) did not develop taurine deficiency (Fig. 2,3) partly because their more mature nephron successfully responded to the stimulus of taurine deficiency by decreasing urinary excretion and by avid conservation of taurine (Fig. 4,5). This finding is similar to previous studies demonstrating low urinary taurine concentrations in term [10] and preterm infants with birth weight >1700 g [11] receiving taurine-free formulas.

The role of the immature nephron in taurine depletion observed in P1 infants and the importance of the renal tubule in taurine conservation are further indicated by the demonstration that a gradual decrease in FET (third to seventh postnatal week) (Fig. 4) coincided with the gradual increase in plasma taurine concentrations in this group (Fig. 2) despite ongoing administration of taurine-free TPN solution.

Both values, mean FET and mean plasma taurine concentration, in groups P1 and E1 reached control values at 7th to 8th postnatal week, which in our study population corresponds to an age of 34–35 weeks post conception. This is known to be the time when nephrogenesis has been completed and various tubular functions reach the degree of maturity observed in full-term infants [20].

The mechanisms governing the developmental change in mammalian tubular taurine transport are not clear. Recent studies using rats, however, have provided evidence that changes in the phospholipid content-related fluidity of the brush border membrane [21] or differences in the dissipation rate of the Na^+ gradient necessary for taurine transfer across this membrane [22] may account for the observed maturational differences in tubular taurine transport.

Taurine is the amino acid present in the greatest concentration in the newborn brain of all mammals [23]. Recent studies have shown abnormal ontogeny of neurons in developing cerebellum and visual cortex region of kittens born to taurine-depleted mothers and suckling their taurine-poor milk [24,25]. Furthermore, degeneration of photoreceptor cells have been documented in cats who have a very low capacity to synthesize taurine after being fed taurine-free casein diet [26] and in infant Rhesus monkeys fed taurine-devoid synthetic human infant formula [27]. Children receiving long-term taurine-free TPN solution demonstrated abnormal retinograms which are reversible by taurine supplementation [3]. To date, abnormal auditory brainstem-evoked responses is the only documented clinical manifestation of taurine deficiency in preterm infants [4]. The accumulating evidence for the major role of taurine in CNS function and development strongly suggests that taurine deficiency may adversely affect the rapidly growing, vulnerable brain and retina in VLBW infants.

To summarize, the lack of taurine in TPN solutions administered to VLBW infants combined with diminshed capacity to synthesize taurine and the inability of the immature nephron to adapt to low taurine intake by increasing tubular taurine reabsorption may result in severely depleted body-taurine pools during the first weeks of life. This could potentially have a deleterious effect on the rapidly growing brain and retina of premature infants. These findings strongly suggest the need for taurine supplementation of TPN solutions administered to VLBW infants. A parenteral protein formulation designed to maintain normal plasma concentrations of all amino acids, including taurine, in low birth weight infants requiring parenteral nutrition has been recently developed [28]. Future studies, however, investigating the effect of taurine supplementation of TPN solutions on taurine status and particularly on neurological and ophthalmological outcome of premature infants are warranted.

References

1. Zelikovic I and Chesney RW (In press) In: Friedman M (ed.) Taurine in Biology and Nutrition. Absorption and Utilization of Amino Acids, Vol. 1. Boca Raton: CRC Press, in press.
2. Sturman JA (1986) Nutritional Taurine and Central Nervous System Development. Ann. N.Y. Acad. Sci. 477: 196–213.
3. Geggel HS, Ament ME, Heckenlivery JR, Martin DA and Kopple JD (1985) Nutritional Requirement for Taurine in Patients Receiving Long-term Parenteral Nutrition. N. Engl. J. Med. 312: 142–146.
4. Tyson JE, Lasky R, Flood D, Mize C, Picone T and Paule CL (1989) Randomized Trial of Taurine Supplementation for Infants ≤ 1300 g Birth Weight: Effect on Auditory Brain-Stem Evoked Responses. Pediatrics 83: 406–415.
5. Vinton NE, Laidlaw SA, Ament ME and Kopple JD (1986) Taurine Concentrations in Plasma and Blood Cells of Patients Undergoing Long-term Parenteral Nutrition. Am. J. Clin. Nutr. 44: 398–404.
6. Vinton NE, Laidlaw SA, Ament ME and Kopple JD (1987) Taurine Concentrations in Plasma, Blood Cells and Urine of Children Undergoing Long-term Total Parenteral Nutrition. Pediatr. Res. 21: 399–403.

7. Helms RA, Christensen ML, Mauer EC and Storm MC (1987) Comparison of a Pediatric vs Standard Amino Acid Formulation in Pretern Neonates Requiring Parenteral Nutrition. J. Pediatr. 110: 466–470.
8. Segal S (1981) In: Spitzer A (ed.) Regulatory Aspects of Transport During Development. The Kidney during Development: Morphology and Function. Masson Publishing, New York, pp. 363–375.
9. Chesney RW, Gusowski N, Zelikovic I and Padilla M (1986) Developmental Aspects of Renal ß-amino Acid Transport. V. Brush Border Membrane Transport in Nursing Animals-Effect of Age and Diet. Pediatr. Res. 20: 890–894.
10. Järvenpää AL, Rassin DK, Räihä NCR and Gaull GE (1982) Milk Protein Quantity and Quality in the Term Infant. II. Effect on Acidic and Neutral Amino Acids. Pediatrics 70: 221–230.
11. Rassin DK, Gaull GE, Järvenpää AL and Räihä NCR (1983) Feeding the Low Birth Weight Infant: II Effects of Taurine and Cholesterol Supplementation on Amino Acids and Cholesterol. Pediatrics 71: 179–186.
12. Okamoto E, Rassin DK, Zucker CL, Salen GS and Heird WC (1984) Role of Taurine in Feeding the Low Birth Weight Infant. J. Pediatr. 104: 936–940.
13. Roberts SB and Lucas A (1985) Measurement of Urinary Constituents and Output Using Disposable Napkins. Arch. Dis. Child. 60: 1021–1024.
14. Lippincott S, Friedman AL, Siegal FL, Pityer RM and Chesney RW (1988) HPLC Analysis of the Phenylisothiocyanage (PITC) Derivatives of Taurine from Physiologic Samples. J. Am. Coll. Nutr. 47: 491–498.
15. Sturman JA, Rassin OK and Gaull GE (1977) Taurine In Developing Rat Brain. Maternal-Fetal Transfer of (^{35}S)-Taurine and its Role in the Neonate. J. Neurochem. 28: 31–39.
16. Palou A, Arola L and Alemany M (1977) Plasma Amino Acid Concentrations in Pregnant Rats and in 21 Day Fetuses. Biochem. J. 166: 49–55.
17. Ghisolfi J (1987) Taurine and the Premature. Biol. Neonate 52 Suppl. 1: 78–86.
18. Zelikovic I, Stejskal-Lorenz E, Lohstroh P, Budreau A and Chesney RW (1989) Anion Dependence of Taurine Transport by Rat Renal Brush Border Membrane Vesicles. Am. J. Physiol. 256: F646–F655.
19. Chesney RW, Gusowski N and Dabbagh S (1985) Renal Cortex Taurine Content Regulates Renal Adaptive Response to Altered Dietary Intake of Sulfur Amino Acids. J. Clin. Invest. 76: 2213–2221.
20. Arant BS (1987) Postnatal Development of Renal Function During the First Year of Life. Pediatr. Nephrol. 1: 308–313.
21. Chesney RW, Gusowski N and Zelikovic I (1987) Developmental Aspects of Renal ß-Amino Acid Transport. IV The Role of Membrane Fluidity and Phospholipid Composition in the Renal Adaptive Response in Nursing Animals. Pediatr. Res. 22: 163–167.
22. Zelikovic I, Stejskal-Lorenz E, Lohstroh P and Chesney RW (1988) Na^+/H^+ Exchange is Increased in Renal Brush Border Membrane Vesicles (BBMV) from Neonatal Rat. Kidney Int. 33: 430.
23. Sturman JA and Hayes KC (1980) In: Draper HH (ed.) The Biology of Taurine in Nutrition and Development. Advances in Nutritional Research, Vol. 3. New York, Plenum Press, pp. 231–299.
24. Sturman JA, Mortez RC, French JH and Wisniewski HM (1985) Taurine Deficiency in the Developing Cat: Persistence of the Cerebellar External Granule Cell Layer. J. Neurosci. Res. 13: 405–416.
25. Palackel T, Sturman JA, Mortez RC and Wisniewski HM (1985) Feline Maternal Taurine Deficiency: Abnormal Ontogeny of Visual Cortex. Trans. Am. Soc. Neurochem. 16: 186–190.
26. Hayes KC, Carey RE and Schmidt SY (1975) Retinal Degeneration Associated with Taurine Deficiency in the Cat. Science 88: 949–951.
27. Sturman JA, Wen GY, Wisniewski HM and Neuringer MD (1984) Retinal Degeneration in Primates Raised on a Synthetic Human Infant Formula. Int. J. Dev. Neurosci. 2: 121–129.
28. Heird WC, May W, Helms RA, Storm MC, Kashyap S and Dell RB (1988) Pediatric Parenteral Amino Acid Mixture in Low Birth Weight Infants. Pediatrics 81: 41–50.

Address for corespondence: Russell W. Chesney M.D., Le Bonheur Children's Medical Center, 848 Adams Avenue, Room 306, Memphis TN 38103, U.S.A.

Prophylactic use of amino acids in the treatment of inborn errors of the urea cycle

Steven M. Donn

Department of Pediatrics and Communicable Diseases, Section of Newborn Services University of Michigan Medical Center, Ann Arbor MI, U.S.A.

Abstract

Urea cycle enzymopathies result in the inability to adequately excrete waste nitrogen, leading to the accumulation of ammonia in the plasma. This may result in significant neurologic dysfunction and death if untreated. Arginine cannot be synthesized in the absence of an intact urea cycle and thus becomes an essential amino acid. Provision of supplemental arginine allows for an abbreviated urea cycle in which both molecules of nitrogen (normally excreted as urea) are excreted as argininosuccinic acid.

Since the long-term neurologic sequelae of neonatal hyperammonemia are related to the severity and duration of plasma ammonia concentration, prompt recognition and treatment is necessary. Presented herein are three cases of urea cycle defects in which hyperammonemia was successfully treated by exogenous arginine therapy.

Introduction

Disorders of the urea cycle may occur as inborn errors of metabolism. These enzymopathies result in the inability to dispose of waste nitrogen by the only known metabolic pathway of urea synthesis, leading to a toxic accumulation of ammonia in the plasma [1].

Normally, the urea cycle consists of five major steps. The first two are mitochondrial and involve the enzymes carbamyl phosphate synthetase I (CPS-I) and ornithine transcarbamylase (OTC); the last three are extra-mitochondrial (cytosolic) and involve argininosuccinic acid synthetase (AS), argininosuccinic acid lyase (AL), and arginase (ARG). The estimated incidence of urea cycle defects is 1/30,000 births [2]. Most are autosomal recessive disorders; OTC deficiency is X-linked, AL and AS deficiency have several clinical forms [1].

The major source of endogenous ammonia is the metabolism of protein and amino acids, and there is a significant exogenous source from intestinal flora which decompose urea and other nitrogenous compounds. In the absence of an intact urea cycle, plasma ammonia may rapidly accumulate, leading to dysfunction and death. Clinical manifestations include severe vomiting, tachypnea, lethargy, stupor, or coma. Seizures are frequently observed, and rapid deterioration may occur with subsequent respiratory distress, renal failure (with additional accumulation of ammonia), and cardiovascular collapse [1]. Neurologic injury may stem from

defective myelination, or direct injury to neurons or Alzheimer type 2 glia [3]. Impaired intellectual function and brain injury have been directly correlated to the duration of hyperammonemic coma [4]. Thus, early detection and prompt therapy are necessary to minimize sequelae and maximize outcome.

In the absence of an intact urea cycle, arginine cannot be sythesized *de novo* and becomes an essential amino acid. Administration of exogenous arginine to newborns with urea cycle enzymopathies enables an abbreviated urea cycle to occur. This commences with ornithine and terminates with the excretion of large quantities of argininosuccinic acid, containing the two molecules of nitrogen ordinarily synthesized to urea. Arginine also allows for protein synthesis [5–7].

The following case reports serve to emphasize the role of exogenous arginine administration in controlling (or preventing) neonatal hyperammonemia in three patients with urea cycle enzymopathies.

Case 1[8]

This patient, a 1780 g male, was born at 32 weeks gestation by Cesarean section because of maternal pre-eclampsia. The previous child of this couple was severly affected by argininosuccinic aciduria (AL deficiency) complicated by severe neonatal hyperammonemic coma and subsequent global central nervous system injury. Argininosuccinic aciduria was diagnosed in the 23rd week of the second pregnancy by amniocentesis. The diagnosis was confirmed in the neonatal period. Plasma ammonia was 33 mM at birth and rose to a maximum of 115 mM at 32h of age, when arginine-HCl (4 mmol/kg/d) was begun as a continous infusion. After 48 h of therapy plasma ammonia ranged from 29–65 mM, even with as much dietary protein as 3.0 g/kg/d. He was discharged on dietary supplementation of arginine and ornithine acetate (2 mmol/kg/d of each). His early growth and develpment were reported to be normal; unfortunately he was lost to follow-up when the family suddenly moved to California at six months.

Case 2

This patient, a 3.32 kg term female, was the first-born of a 32 year-old mother. At two days of age poor feeding, vomiting, and lethargy prompted transfer to a regional neonatal center where a diagnosis of hyperammonemia was made. She was immediately transferred to the University of Michigan Medical Center where AS deficiency (citrullinemia) was detected. Hemodialysis was used to lower plasma ammonia, but had to be terminated because of dysequilibrium syndrome. She was given arginine (4 mmol/kg/d) and sodium benzoate (250 mg/kg/d) which stabilized plasma ammonia concentrations within the normal range, even with protein intake at 2.0 g/kg/d. She was discharged at 22 days of age on oral arginine and ornithine acetate. At 5 years of age her height and head circumference are growing appropriately, though below the fifth percentile. She displays speech and language delays and behavioral problems, but is motorically appropriate.

Case 3

This 3.72 kg male infant was delivered by elective repeat Cesarean section at 37 weeks to a 37 year-old mother whose most recent pregnancy had resulted in a neonatal death secondary to AS deficiency. Antenatal diagnosis of citrullinemia was made during this pregnancy by amniocentesis, and was confirmed after birth. The infant was immediately started on intravenous arginine-HCl (4 mmol/kg/d) and gradual introduction of dietary protein, to a maximum of 2.0 g/kg/d. Plasma ammonia remained normal. He was discharged at 14 days on arginine and ornithine acetate and sodium benzoate. Phenylacetate was subsequently added. At 5 years of age he displays normal growth and development.

Discussion

Each patient treated with exogenous arginine displayed a prompt response to therapy with a fall (or no rise) in plasma ammonia concentration and amelioration of clinical symptomatology (if present).

Analysis of the effect of arginine treatment on urea cycle intermediates was performed on Case 1 and his sibling. After 24 h of arginine therapy, plasma ASA concentrations were approximately 1900 mM for each (normal is non-detectable). Homeostasis appears to depend on provision of adequate arginine for effective removal of ammonia but also upon intact renal mechanisms for ASA excretion.

Thus far, the only discernible complication of therapy has been a persistent mild metabolic acidosis (during intravenous infusion only), presumed to result from the hydrochloride salt. This responds to sodium bicarbonate therapy and resolves when oral therapy commences.

Though the numbers of patients treated with arginine therapy remain small, preliminary follow-up has been encouraging. Obviously, where prenatal diagnosis is known, avoidance of neonatal hyperammonemia is feasible and potentially normal outcomes become possible. In cases of unexpected and early-diagnosed disorders, prompt institution of arginine may effect more sustained relief of severe hyperammonemia than invasive methods directed solely at removing ammonia, such as exchange transfusion, peritoneal dialysis, and hemodialysis [9]. Arginine can also serve as a useful therapeutic adjunct to additional means of alternative waste nitrogen systhesis therapies such as sodium benzoate and phenylacetate, transforming a once-uniformly lethal disorder to one with a favorable outcome.

References

1. Donn SM and Banagale RC (1984) Pediatr. Rev., 5: 203–208.
2. Koch R (1981) Pediatrics 68: 271–272.
3. Volpe JJ (1981) Neurology of the Newborn. Philadelphia, W.B. Saunders Co. pp. 367.

4. Msall M, Batshaw ML, Suss R et al. (1984) N. Engl. J. Med. 310: 1500–1505.
5. Brusilow SW and Batshaw ML (1979) Lancet I: 134–136.
6. Batshaw ML and Brusilow SW (1980) J. Pediatr. 97: 893–900.
7. Batshaw ML, Brusilow SW, Waber L et al. (1982) N. Engl. J. Med. 306: 1387–1392.
8. Donn SM and Thoene JG (1985) J. Inher. Metab. Dis. 8: 18–20.
9. Donn SM, Swartz RD and Thoene JG (1979) J. Pediatr. 95: 67–70.

Address for correspondence: L3023 Womens' Hospital/0254 1500 E. Medical Center Drive, Ann Arbor MI 48109-0254, U.S.A.

Effect of methionine supplementation of low protein diets in the rat: A review

J. Leclerc

Station de Recherches sur la qualité des Aliments de l'Homme, INRA, 21034 Dijon Cedex, France

Abstract

The beneficial effect of methionine supplementation to low sulphur amino acid diets has been demonstrated in the human newborn suffering from protein malnutrition.

In the animal, many studies have been made, mainly in the rat, to test the effect of methionine to low protein diets. Generally, methionine supplementation improves weight gain during *growth*, but also leads to a marked increase in the liver lipid content. Lipidosis might be due to a secondary threonine deficiency. As a matter of fact, addition of threonine to the diet suppresses the lipidosis observed during methionine supplementation. However the effect of threonine deficiency on liver lipid content depends on the type of dietary carbohydrate: with glucose or starch, no increase in liver lipid; with fructose or sucrose, marked fatty infiltration.

During *pregnancy*, methionine supplementation of low protein diets stimulates feed intake the days prior to parturition, increases the body weight of the neonate and reduces the liver lipid content of the dam.

During *lactation*, methionine supplementation of low protein diets, strongly reduces the loss weight of the dam, increases milk yield and stimulated the growth of the young. As in the growing rat, the dam exhibits a liver lipidosis, which is also influenced by the type of dietary carbohydrate. However, in this case it is not caused by a secondary threonine deficiency: a large addition of inositol, but not choline, to the diet was found to reduce considerably liver lipidosis.

Introduction

Diets used in animal feeding and containing plant or little animal proteins have generally a low sulphur amino acid content. Thus, the requirement for these amino acids, particularly methionine [1] is not met.

It has been shown in man (newborn and adult) that moderate additions of methionine to low protein diets led to a better nitrogen retention, whereas an excess may be detrimental in the rat [2].

Many experiments have been performed in the animal, mainly in the rat, to study the consequences of methionine supplementation of low protein diets.

The aim of the present paper was to review the influence of methionine supplementation during growth, pregnancy and lactation.

Effects of methionine supplementation

Growth

Effects on feed intake and weight gain

Excess. An excessive addition (5%) of methionine to a low protein diet (10% casein) strongly reduces feed efficiency, whereas the same amount of other amino acids has little or no effect [3]. In normal protein diets, this level of methionine is even toxic [3,4]. This toxicity is due to an abnormal metabolic transformation leading to the production of toxic substances such as methyl-mercaptan [5] or to an excessive excretion of urea, creatinine and ammonia [6]. The excessive level of ammonia in blood might explain the appetite loss [7].

Moderate addition. It has been reported by several workers that methionine supplementation of low protein diet lead to enhancement of diet intake and weight of growing rat [8,9,10]. This may result from an increase in the plasma insulin level which stimulates the feed intake during methionine supplementation [10].

In this case, the more rapid growth is not only due to an increased feed intake at a similar level of intake, rats supplemented with methionine have a higher body weight [11]. Since the nitrogen balance is higher with moderate methionine supplementation [6], the latter plays an anabolizing role, which may be due to a larger thyroid activity [12]. By contrast, an excessive methionine supplementation leads to a lower nitrogen balance [6] and thyroid activity [13]. Adrenaline, which is also involved in protein metabolism might play a role: in adrenalectomized rats, methionine supplementation has no effect on weight gain [12].

In adequate protein diets, moderate methionine supplementation has no effect on feed efficiency [14].

Accordingly it is recommended to supplement low protein diets with moderate amounts (<1%) of methionine in order to stimulate growth [14].

Effects on the liver lipid content

Lipotropic factor. Rats fed choline deficient diets, a factor necessary to the control of liver lipid deposition, exhibit an increase in the liver lipid content [15,16]. In this case, supplementation with methionine, biologic donor of methyl groups contributing to the synthesis of choline, strongly reduces the liver lipid contents [15,16]. For that reason, methionine is generally considered as a lipotropic factor.

Antilipotropic factor. Choline is included in most experimental diets. It has been observed that methionine supplementation of low protein diets contributed to increasing the liver lipid content [11,17,18]. In this case, methionine plays an antilipotrophic role. This liver lipidosis is accompanied by a decrease in the liver [19,20] and plasma [20,21] threonine content. In fact, methionine supplementation

stimulates the activity of the serine-threonine dehydrase, which leads to a threonine deficiency [20,22]. The threonine deficiency increases the liver lipid content [23]. Thus, a complementary threonine supplementation reduces and even suppresses this liver lipidosis [17,18,24].

However, this lipidosis due to an increase in triglycerides [25] would be only transitory. A maximum level is observed within two weeks, but it is much lower during the following weeks [18,26].

According to authors the lipidosis caused by methionine supplementation or threonine deficiency might be due to:
- a decreased oxidation of fatty acids [26];
- an increased lipid synthesis [27–29];
- a decreased transport of lipids from liver into blood [30,31].

Thus, lipidosis caused by methionine supplementation of low protein diets is due to very complex phenomena. Moreover, it should be noticed that this lipidosis is not observed when the diet:
- only contains saturated fatty acids as source of lipids [24],
- is ingested by rats kept at low temperature [32],
- only contains glucose or starch as source of carbohydrates [33],
- is supplemented, not with methionine but with oligo-L-methionine (a mixture of hexamer and heptamer) [34].

In conclusion , during growth it is recommended to supplement low protein diets not only with methionine but also with threonine.

Pregnancy

Excess

As during growth, an excess of dietary methionine is detrimental during pregnancy: it is the most toxic amino acid [35]. Generally, female rats do not proceed to term and the weight of newborns is lower [36–39]. A weight decrease of newborn is not due to a reduced feed intake [39]. Methionine has probably an effect on hormonal production, since oestrone or progesterone additions lead to the maintenance of pregnancy to term [37].

Moderate addition

A moderate addition of methionine to low protein diets has a favourable effect on pregnancy and weight of newborn [40–44]. The higher weight of the latter is probably due to a lower decrease in feed intake in late pregnancy [44].

The slight liver lipidosis observed during malnutrition in the rat in late pregnancy is almost suppressed by methionine supplementation [45].

As during growth, a moderate methionine supplementation of low protein diets is recommended.

Lactation

Effects on reproductive performance

With a diet based on plant proteins (16%), a 0.5% methionine supplementation has a favourable effect on the feed intake of the dam and the weight of the young [46], whereas a 1% supplementation is slightly toxic [46].

With diets based on animal proteins (8–12% casein) methionine supplementation has also a positive effect on the growth of offspring [47–49], whereas with adequate protein diets this supplementation has no effect [49]

In case of low protein diets supplemented with methionine milk production is increased [48,49]. This may be explained by an increase in the free ribosomes of the mammary gland and thus in the stimulation of protein synthesis [50]. Therefore, methionine has an anabolic action since for the same level of feed intake in the dam, the weight of offspring with methionine is higher at weaning when the maternal diet is supplemented with methionine [51].

Effects on liver lipid content

As during growth, methionine supplementation of low protein diets increases the triglyceride content of the liver [52–54], mainly if glucose is substituted by fructose or saccharose [52]. Because of a negative correlation between the plasma threonine content and the neutral lipid content of the liver [53], lipidosis might be attributed to a threonine deficiency. This is not the case however, since a threonine supplementation does not suppress this lipidosis [53]. It is probably due to the lack of secretion of liver lipoproteins and to the transport of the latter towards blood.

It has been demonstrated that inositol is involved in the lipoprotein secretion by the liver which depends on an adequate supply of this element [55]. Thus, an increased addition of inositol to a low protein ie supplemented with methionine highly reduces the lipidosis observed [56].

During lactation, methionine supplementation of a low protein diet (better growth of offspring) should be accompanied by an inositol supply to suppress the liver lipidosis observed in the dam.

Conclusion

During growth, pregnancy and lactation, methionine supplementation is recommended to stimulate growth when the diet used has a low protein content. However, this supplementation should be accompanied by threonine supply during growth and by inositol supply during lactation in order to reduce or suppress the lipidosis observed otherwise.

References

1. National Research Council (1978) in Requirement of Laboratory Animals. National of Academy of Sciences, Washington D.C., pp. 7–37.
2. Anonymous (1974) Bulletin du PAG 4 (2): 27–30.
3. Muramatsu K, Odagiri H, Morishita S and Takeuski H (1971) J. Nutr. 101: 1117–1125.
4. Daniel RG and Waisman HA (1968) Growth 32: 255–265.
5. Benevenga NJ (1974) J. Agric. Food Chem. 22: 2–9.
6. Allison JB (1956) In some aspects of Amino-acid supplementation. Rutgers University, pp. 69.
7. Reifsnyder DH and Svacha AJ (1979) Fed. Proc. 38: 288.
8. Kimura T, Susuki K, Iskikawa M, Yoshida A (1976) Agric. Biol. Chem. 40: 535–542.
9. Peretianu J and Abraham J (1964) Arch. Sci. Physiol. 18: 253–264.
10. Noda K (1971) J. Nutr. 101: 1391–1397.
11. Noda K (1971) J. Japan Soc. Food Nutr. 24: 89–91.
12. Aschkenasy (1954) In: Journées médicales Nestlé, Colloque sur les Acides Aminés. Lausanne, Karger, Bâle, pp. 16–19.
13. Parker HE and Rogers KS (1972) Experentia 28: 208–210.
14. Sarwar G and Beare-Rogers JL (1984), Nutr. Res. 4: 347–351.
15. Aoyama Y, Yasui H and Ashida K (1971) J. Nutr. 101: 739–745.
16. Harper AE, Benton DA, Winje ME and Elvehjem CA (1954) J. Biol. Chem. 209: 171–177.
17. Aoyama Y and Ashida, K (1978) Nutr. Rep. Int. 17: 463–473.
18. Harper AE, Benton DA, Winje ME and Elvehjem CA (1954) J. Biol. Chem. 209: 159–163.
19. Kimura T, Ebihara K and Yoshida A (1975) Agric. Biol. Chem. 39: 651–656.
20. Girard-Globa A, Robin P and Forestier M (1972) J. Nutr. 102: 209–217.
21. Mc Laughan JM (1979) Nutr. Rep. Int. 19: 27–35.
22. Sanchez A and Swendseid M (1969) J. Nutr. 99: 145–151.
23. Aoyama Y and Ashida K (1972) J. Nutr. 102: 1025–1032.
24. Morris L, Arata D and Cederquist DC (1965) J. Nutr. 85: 362–366.
25. Noda K and Okita T (1980) J. Nutr. 110: 505–512.
26. Arata D, Carrol C and Cederquist DC (1964) J. Nutr. 82: 150–156.
27. Wilfred G and Varma TNS (1969) Bioch. Bioph. Acta 187: 442–443.
28. Yoshida A and Harper AE (1960) J. Biol. Chem. 235: 2586–2589.
29. Maeda H, Ikeda I and Sugano M (1975) Nutr. Rep. Int. 12: 61–66.
30. Aoyama Y, Nakanishi M and Ashida K (1973) J. Nutr. 103: 54–60.
31. Katayama Y and Saimei M (1979) J. Nutr. Sci. Vitaminol. 25: 525–542.
32. Yoshida A and Ashida K (1962) Nature 194: 484–485.
33. Harper AE, Monson WJ, Arata DA, Benton DA and Elvehjem CA (1953) J. Nutr. 51: 523–537.
34. Kasai T, Sonoyama K and Kiriyama S (1987) J. Agr. Chem. Soc. Japan, 61: 1425–1434.
35. Matsueda S and Niiyma Y (1982) J. Nutr. Sci. Vitaminol. 28: 557–573.
36. Aly Z, (1976) Dtsch. Tierarztlich Wschr. 83: 239–242.
37. Chandrashekar V and Leathem JH (1977) Fertil and Steril 28: 590–593.
38. Knipfel JE and Elliot JI (1976) Nutr. Rep. Int. 13: 143–148.
39. Viau AT and Leathem JH (1973) J. Reprod. Fertil 33: 109–111.
40. Kinzey WG (1970) Proc. Soc. Exp. Biol. Med. 133: 449–451.
41. Benedetti PC, Tagliamonte B, Semprini ME and Mariani A (1973) Nutr. Rep. Int. 8: 9–20.
42. Stapleton P and Hill DC (1980) Nutr. Rep. Int. 21: 231–242.
43. Tagliamonte B, Benedetti PC, Semprini ME and Mariani A (1973) Nutr. Rep. Int. 8: 301–311.
44. Leclerc J (1985) Int. J. Vit. Nutr. Res. 55: 103–106.
45. Leclerc J and Miller ML (1985) Int. J. Vit. Nutr. Res. 55: 217–222.
46. Tagliamonte B, Benedetti PC, Semprini M and Gentili V (1976) Nutr. Rep. Int. 14: 633–639.
47. Nakamoto T, Alam SQ, Karubé S and Shoji H (1981) Nutr. Rep. Int. 24: 355–360.
48. Leclerc J (1984) Nutr. Rep. Int. 29: 769–774.
49. Leclerc J (1980) Ann. Nutr. Aliment 34: 641–656.

50. Grillmaier H and Bassler RA (1963) Ztschr. ges. exp. Med. 137: 299–320.
51. Haag JR and Wright LD (1940) J. Nutr. 19: 563–568.
52. Leclerc J, Miller ML and Septier C (1985) Nutr. Rep. Int. 32: 1003–1008.
53. Leclerc J, Hamel O and Grynberg A (1988) Nutr. Rep. Int. 38: 635–642.
54. Leclerc J, Miller ML, Chanussot B, Poisson JP and Belleville J (1989) Reprod. Nutr. Dev. 29: 269–276.
55. Yagi Y and Kotaki A (1969) Ann. N.Y. Acad. Sci. 165: 710–725.
56. Leclerc J and Miller ML (1989) Int. J. Vit. Nutr. Res. 59: 180–183.

Address for correspondence: Leclerc J, Station de Recherches sur la qualité des Aliments de l'Homme, INRA, 21034 Dijon Cedex, France.

Potential of γ-L-glutamyl-L-glutamine as an L-glutamine-containing dipeptide for parenteral nutrition

Tadayasu Furukawa and Takahiro Hara

Kyowa Hakko Kogyo Co.,Ltd. Tokyo Research Laboratories, Machida-shi, Tokyo 194, Japan

Abstract

L-Glutamine (Gln) not stable in aqueous solutions can be used for parenteral nutrition in the dipeptide form. In this study, we compared γ-L-glutamyl-L-glutamine (Glu-Gln) with L-alanyl-L-glutamine (Ala-Gln), one of the most widely tested Gln-containing dipeptide, in regard to the heat stability and *in vivo* utilization in mice.

Contrary to Gln, Glu-Gln (10 mM, pH 6.5) was found far resistant to the heat treatment above 80°C, but less stable than Ala-Gln; activation energy to induce the thermal change was calculated as 104 kJ/mole for Gln, 160 kJ/mole for Glu-Gln, and 192 kJ/mole for Ala-Gln, respectively, using the Arrhenius' equation. A tail vein of 6-week-old C3H/He male mouse was injected with a solution of Glu-Gln or Ala-Gln (250 μmole/kg b.w.). During 20 min, blood sample was drawn for the determination of the respective dipeptide concentration. There was a moderate disappearance of injected Glu-Gln giving 2.97 min as half life. Meanwhile, Ala-Gln disappeared very rapidly from the systemic circulation. No hydrolysis of Glu-Gln was observed after the incubation with plasma while the plasma hydrolytic capacity was considerably high for Ala-Gln. Kidney might be a tissue to uptake and utilize Glu-Gln because the injection of this dipeptide gave significantly higher level of renal Gln than that of Ala-Gln.

These results suggest that Glu-Gln might be a new type of Gln-containing dipeptide for parenteral nutrition characterized by receiving no plasma hydrolysis and by presumably having a certain target tissues to be utilized.

Introduction

It has been demonstrated that a marked decrease in the body free L-glutamine (Gln) pool represents one of the most typical features of the metabolic response to the postinjury conditions [1]. Thus, Gln might be an indispensable component of parenteral solutions designed for patients suffering from catabolism. However, the instability of Gln excludes this amino acid from parenteral solution. Recently, the use of Gln-containing synthetic dipeptide such as L-alanyl-L-glutamine (Ala-Gln) or glycyl-L-glutamine (Gly-Gln) stable during heat sterilization has been proposed as the amino acid source for intravenous nutrition [2,3]. For these synthetic dipeptides, plasma hydrolysis is a mechanism of disappearance from circulation [3]. It seems, therefore, interesting to develop Gln-containing dipeptides with minimum hydrolysis in plasma and with a specificity in the tissue uptake and utilization.

In the present study, we have examined the potential of naturally occurring γ-L-glutamyl-L-glutamine (Glu-Gln) for the use of parenteral nutrition comparing it with Ala-Gln in regard to the heat stability and *in vivo* utilization in mice.

Experimental procedures

Reagents

Gln was obtained from Kyowa Hakko Kogyo (Tokyo, Japan). Both Ala-Gln and Glu-Gln were from Kokusan Chemical Works (Tokyo, Japan). All other chemicals were reagent grade and used without further purification.

Heat processing conditions

The sample solutions (10 mM, pH 6.5) in the ampoules were heated for 20 min at 80–132°C using a water bath or an autoclave.

In vitro plasma hydrolysis

Blood from 6-week-old C3H/He male mouse was collected and the plasma was separated by centrifugation. Each 50 μl of the plasma sample was incubated with 5 μl of dipeptide solution (34.4 mM in saline) at 37°C for 2, 5, 10 and 20 min, respectively. The reaction was stopped by adding 5 μl of 30% sulfosalicylic acid (SSA). The resulting protein free supernatant was analyzed for the determination of residual dipeptides [4].

In vivo *utilization*

A tail vein of 6-week-old C3H/He male mouse was injected with 0.2 ml of a saline solution of Glu-Gln or Ala-Gln (250 μmole/kg b.w.). During 20 min, blood sample was obtained and then added with an equal volume of 6% SSA to deproteinize. After the centrifugation at 12,000 × g for 5 min, the supernatant was separated and stored at −80°C until determined for the concentrations of the dipeptide and the constituent amino acids. With respect to tissue study, at 20 min after the injection, liver and kidney were removed and frozen immediately in liquid nitrogen. Each sample was weighed and homogenized in 3% SSA using a glass homogenizer. After the centrifugation, the resulting supernatant was stored at −80°C until analyzed.

Analysis

Concentrations of dipeptides and amino acids were determined by ion-exchange or reversed-phase HPLC detected based on fluorometry with o-phthalaldehyde [5,6].

Statistics

Data are presented as mean ± S.E.M. There were five mice in each experimental group. Student's t-test was used for statistical evaluation.

Results

In the heat processing, Gln started disappearing above 90°C and was almost completely eliminated from the system at 132°C (Fig. 1). The heat-induced disappearance of Glu-Gln was observed above 120°C. Ala-Gln remained unchangeable at 132°C for 20 min, but started disappearing by the prolongation of heating time at this temperature. As a result, activation energy to induce the thermal change was calculated as 104 kJ/mole for Gln, 160 kJ/mole for Glu-Gln, and 192 kJ/mole for Ala-Gln, respectively, using Arrhenius' equation.

In order to estimate hydrolysis of dipeptide prior to tissue uptake, Glu-Gln or Ala-Gln was incubated with the mouse plasma at 37°C. The plasma exhibited measurable hydrolysis activity against Ala-Gln whereas no hydrolysis was observed with Glu-Gln. As a result, the incubation of Ala-Gln for 2, 5, 10 and 20 min gave 13%, 38%, 76% and 89% disappearance of this dipeptide, respectively, to the initial concentration.

Figure 2 summarizes the time course of the blood concentration of dipeptide and glutamine after the injection of Glu-Gln or Ala-Gln to mice. Glu-Gln disappeared moderately from the systemic circulation and gave 2.97 min as half life [7]. In contrast, the administration of Ala-Gln resulted in an extremely rapid disappearance from blood, liberating free Gln. In fact, no Ala-Gln was detectable even at 1 min after the injection of this dipeptide.

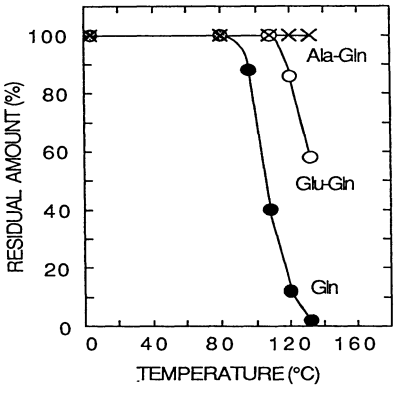

Fig. 1. Heat stability of Gln, Glu-Gln and Ala-Gln. The sample solutions (10 mM, pH 6.5) in the ampoules were heated at 80–132°C for 20 min. Residual amounts were determined by reversed-phase HPLC fluorometrically as described under 'Experimental Procedure'.

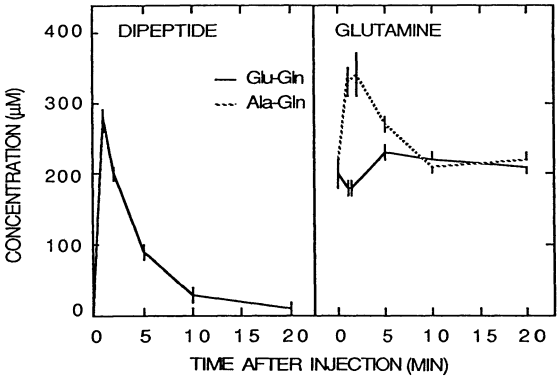

Fig. 2. Blood dipeptide and Gln concentration in mice after the injection of Glu-Gln and Ala-Gln. A tail vein of 6-week-old C3H/He mouse was injected with 0.2 ml of a saline solution of each dipeptide (250 μmole/kg b.w.). Blood sample from each mouse was analyzed as described under 'Experimental Procedure'. Each value represents mean ± S.E.M. (n=5).

Table 1. Intracellular concentration of Gln, glutamate and alanine in kidney removed at 20 min after the injection of Glu-Gln or Ala-Gin (250 μmole/kg b.w.)

Dipeptide injected	Glutamine	Glutamate	Alanine
		μmole/g wet wt.	
Control (saline)	1.07 ± 0.08[a]	4.42 ± 0.32[a]	2.61 ± 0.39[a]
Glu-Gln	1.57 ± 0.12[b]	6.60 ± 0.47[b]	2.31 ± 0.64[a]
Ala-Gln	1.14 ± 0.09[a]	4.87 ± 0.33[a]	2.46 ± 0.43[a]

Kidney sample was homogenized in 3% SSA and the resulting protein-free supernatant were analyzed as described under 'Experimental Procedure'. Each value represents mean ± S.E.M. (n = 5) and those in a column bearing the common superscripts do not differ ([a,b] $P<0.025$).

To investigate tissue utilization of dipeptides, intracellular concentration of Glu-Gln, Ala-Gln and corresponding amino acids in the liver and kidney at 20 min after the injection of these dipeptides were determined. None of these dipeptides was, however, detected in these tissues. As shown in Table 1, there was about 1.5-fold increase ($p<0.025$) of both renal Gln and L-glutamate levels by the injection of Glu-Gln compared to control while no such increases were observed in Ala-Gln. On the other hand, there was no substantial change of hepatic Gln level after the injection of each dipeptide.

Discussion

Currently available amino acid solutions lack Gln because of its instability in free form. To solve this problem, the use of Gln in the dipeptide form has been proposed and both Ala-Gln and Gly-Gln are the leading candidates for the practical use in parenteral nutrition [3,8].

Glu-Gln is a naturally occurring dipeptide and is characterized by including γ-peptide linkage in its molecular structure [9]. It is generally recognized that the carboxyamide group of free Gln is hydrolyzed through a concerted action by the neighboring α-amino group, whereas the latter with its lone electron pair can not participate in this reaction when engaged in peptide linkage [10]. However, Glu-Gln with free, reactive carboxy group in the N-terminus might be somewhat unstable comparing with other Gln-containing dipeptides having α-peptide linkage with neutral amino acid. As expected, Glu-Gln was observed to be resistant to the heat treatment compared with Gln, but less stable than Ala-Gln (Fig. 1).

The possible mechanism for disappearance of injected dipeptide from blood could be both uptake by tissues and hydrolysis by enzyme circulating in plasma. The incubation of Ala-Gln with plasma was confirmed to cause substantial hydrolysis of this dipeptide in agreement with the finding by Adibi *et al.* as reported that dipeptides with L-alanine in the N-terminus receive relatively rapid hydrolysis in plasma [11]. In contrast to Ala-Gln, Glu-Gln was actually free from

plasma hydrolysis. However, after the injection Glu-Gln disappeared moderately, although not so rapidly as Ala-Gln, from blood as shown in Fig. 2. In this study, in order to eliminate further hydrolysis of dipeptides during the plasma preparation, blood was deproteinized immediately after the collection at each timing by adding the SSA solution, followed by HPLC analysis. The explanation for the disappearance from the circulation may be different for each dipeptide because of different behavior to plasma hydrolysis as described above. According to Adibi, minimizing dipeptide hydrolysis in plasma allows a greater fraction of infused dipeptides to reach tissues in intact form and kidney plays a major role in the uptake of circulating dipeptides [3]. In addition, Griffith *et al.* reported that one of the mechanism that mediates amino acid translocation across cell membranes involves the action of γ-glutamyltransferase on intracellular glutathione and extracellular amino acids to form γ-glutamyl amino acids and that kidney has a relatively specific transport system for γ-glutamyl amino acids [12]. It is, therefore, likely that kidney plays a major role in removal of Glu-Gln from the systemic circulation. As a result, the injection of Glu-Gln gave significantly higher level of renal Gln than that of Ala-Gln (Table 1). In the case of Ala-Gln, plasma hydrolysis may contribute to its disappearance from blood considerably.

These results obtained here suggest that Glu-Gln might be a new type of Gln-containing dipeptide for parenteral nutrition characterized by receiving no plasma hydrolysis and by having a certain target tissues, probably including kidney, to be utilized. Further studies where the effects of Glu-Gln administration on catabolic conditions are actually examined would yield more direct evidence for the availability of this dipeptide.

Acknowledgements

The authors are thankful to Dr. H. Minagawa for carrying out animal experiments and to Mr. K. Yamamoto for his valuable comments on the manuscript.

References

1. Askanazi J, Carpentier YA, Michelsen CB, Elwyn DH, Fürst P, Kantrowitz LR, Gump FE and Kinney JM (1980) Ann. Surg. 192: 78–85.
2. Stehle P, Albers S, Amberger I, Pfaender P and Fürst P (1985) Clin. Nutr. Spec. Suppl. 4: 116–123.
3. Adibi SA (1987) Metabolism 36: 1001–1011.
4. Stehle P, Bohlmann F and Fürst P (1988) Clin. Nutr. 7 (Suppl.): 40.
5. Molnar I and Horvath C (1977) J. Chromatogr. 142: 623–640.
6. Spackman DH, Stein WH and Moore S (1958) Anal. Chem. 30: 1190–1206.
7. Adibi SA and Krzysik BA (1977) Clin. Sci. Mol. Med. 52: 205–213.
8. Stehle P, Zander J, Mertes N, Albers S, Puchstein CH, Lavin P and Fürst P (1989) Lancet 8632: 231–233.
9. Meister A (1984) Fed. Proc. 43: 3031–3042.
10. Dimarchi RD, Tam JP, Kent SBH and Merrifield RB (1982) Int. J. Peptide Protein Res. 19: 88–93.
11. Adibi SA, Paleos GA and Morse EL (1986) Metabolism 35: 830–836.
12. Griffith OW, Bridges RJ and Meister A (1979) Proc. Natl. Acad. Sci. USA 76: 6319–6322.

A low-protein diet supplemented with amino acids and their analogues lowers circulating ß-endorphins in chronic uremic patients

G. Barsotti, F. Ciardella, E. Morelli, A. Cupisti, A. Guidi, E. Buoncristiani and S. Giovannetti

Clinica Medica 1, Nephrology Unit, University of Pisa, Italy

Abstract

In twelve male chronic uremics we studied the effect of a pure vegetarian, low-protein diet supplemented with amino acids and analogues on serum ß-endorphin, parathyroid hormone, growth hormone, thyroid hormones, TSH and total cortisol.

ß-endorphin decreased significantly, as well as growth hormone, cortisol and parathyroid hormone. T3 improved, reaching the normal values in some cases.

It is supposed that the correction of the ß-endorphin excess may account, in part, for the improvement of some endocrine and metabolic effects exerted by this diet. The possible pathophysiological mechanisms which could explain the anti-endorphinic action of this treatment in uremic patients are discussed, as well as the possible beneficial endocrine and metabolic effects exerted by the fall of circulating ß-endorphin.

Introduction

Endogenous opioids are implicated in the pathogenesis of some endocrine and metabolic derangements of chronic renal failure (CRF). High serum levels of these polypeptides are known to stimulate the secretion of parathyroid hormone (PTH) [1], growth hormone (GH) [2,3], pituitary TSH [2], gonadotropins (LH, FSH) [4,5], prolactin (PRL) [2] and to cause glucose intolerance [6].

Recently circulating ß-endorphin (B-EP), the most active of the endogenous opioids, has been found to be elevated in CRF [7]. Some years ago a low-protein diet, supplemented with amino acids and analogues (supplemented diet, SD) was introduced in the conservative management of severe CRF [8]. SD slows the decline of the residual renal function [8,9], corrects or improves secondary hyperparathyroidism [10,11], improves TSH and T3 serum levels [12] and restores gonadal testosterone (T) secretion in males [13]. Oral glucose tolerance test also improves following SD therapy.

Since these hormonal and metabolic changes may be even induced through the correction of uremic hyperendorphinism, the present study has been mainly performed to investigate if the SD exerts any effect on the circulating B-EP levels.

Materials and Methods

Twelve male CRF patients (aged 18–42 years) were studied. No drugs were allowed in the five days before the test, while the patients were following a conventional, low-protein (0.6 g/kg/day) diet (CLPD). Blood samples for B-EP determination were withdrawn from the patients on supine position, after an overnight fast. The first blood sample was taken at 8 am, the others (eight milliliters each) were collected at 15 min intervals for one h, through an indwelling catheter in a peripheral arm vein, maintained open by a slow saline infusion. The procedure of repeated sampling for B-EP determination was used to minimize the error due to the spontaneous fluctuations that are known to occur in serum concentration of this hormone. The reported data are the mean of these values.

Blood samples for B-EP determination were put into plastic tube, containing Aprotinin (4000 U) and Sodium EDTA (400 μl), immediately after withdrawal, and centrifuged at 0°C for 10 min. After centrifugation the samples were frozen and stored at −20°C until assay. A single 10 ml blood sample for the determination of GH, T3, T4, TSH, PTH and total cortisol (C) was taken in the same day, as well as a blood sample for serum creatinine determination (sCr). All these samples were immediately centrifuged and frozen at −20°C.

All the hormonal determinations were performed by radioimmunological assay (RIA) techniques. For each hormonal determination the RIA was performed when all the samples had been collected, in order to avoid the inter-assay error. The following commercially available RIA kits were used: B-EP: Nichols Inst., CA, U.S.A.; GH: Pharmacia AB, Sweden; T3 and T4: Clinical Assays, MA, U.S.A.; TSH: Bik, UK; PTH (middle molecule): Immuno Nuclear Corp., MN, U.S.A.; C: Clinical assays, MA, U.S.A. Normal values for B-EP: 32.2 ± 12.5 pg/ml; GH: 0–6 ng/ml; T3: 80–200 ng/dl; T4: 4.5–12.5 μg/dl; TSH: <5 μU/ml; PTH (M-M): <0.8 ng/ml; C: 70–220 ng/ml.

Serum creatinine (sCr) and urinary creatinine (uCr) for creatinine clearance (CRcl) determination were measured by standard Auto-Analyzer procedure.

Subsequently, the patients shifted to the SD, and all these parameters were monthly repeated during the 14 month study period. The SD supplies daily 0.3 g/kg/ of protein from vegetable foods, 350 mg of inorganic phosphorus, 20 mEq of sodium and 72–96 mEq of potassium. The energy supply is 35 kcal/kg/day. A supplementation with amino acids and analogues was performed as previously described [8]. Calcium carbonate (3–6 g/day) was also supplemented.

All the results are reported as mean ± standard deviation. The statistical analysis was performed by using Student's t-test for paired data and Pearson's correlation test. Statistical significance: when $p<0.05$.

Results

All the studied patients had a severe CRF. The mean CRcl was 7.2 ± 2.4 ml/min at the beginning of the SD, and it was virtually unmodified at the end of the study: 6.9

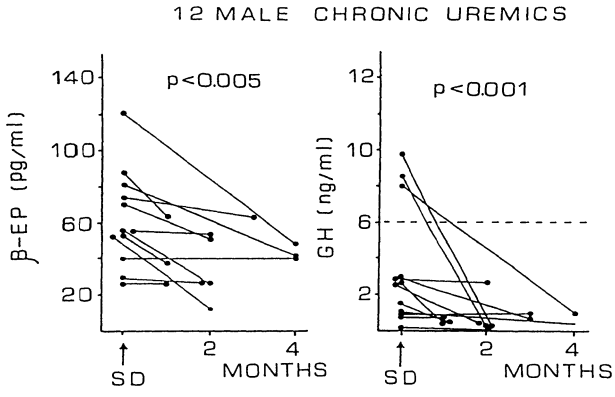

Fig. 1. The behaviour of circulating B-EP and of GH in 12 male chronic uremics who shifted from a conventional low-protein diet to the SD. Dotted lines indicate the upper limit of normal range.

± 2.7 ml/min (p: n.s.). Circulating B-EP was higher than normal before SD (61.7 ± 25 pg/ml) and decreased on SD (41.2 ± 15.5 pg/ml) ($p<0.005$) reaching the normal range in eight out of twelve cases (Fig. 1, left panel). Serum GH was normal, as a mean, before SD (3.5 ± 3.2 ng/ml), having values higher than the normal range in three subjects (Fig. 1, right panel). It fell significantly after SD, reaching in all cases low-normal values (0.8 ± 0.8 ng/ml. $p<0.001$) (Fig. 1, right panel). The per cent decrease of B-EP and GH was quite similar in the single cases, confirming the existence in these patients of a close relationship between the secretion of B-EP and GH, as previously described in normals [2].

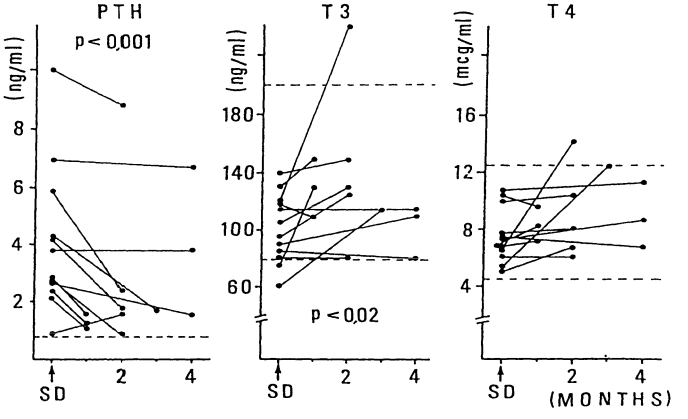

Fig. 2. Changes of circulating PTH (M-M), total T3 and total T4 in 12 male chronic uremics following the change from conventional low-protein diet to the SD. The dotted lines indicate the upper normal limit for PTH and the normal range for thyroid hormones.

PTH was increased before SD, and significantly decreased ($p<0.001$) after SD period (Fig. 2, left panel). T3 levels were low-normal before SD (101.1 ± 22.6 ng/ml) and increased on SD, reaching the normal values (127.8 ± 51 ng/dl) ($p<0.02$) (Fig. 2, central panel). Serum T4 (from 7.5 ± 1.8 to 9.1 ± 2.3 μg/ml (Fig. 2, right panel) and TSH (from 2.6 ± 2.3 to 1.8 ± 2.2 μU/ml) were normal and did not change significantly following the SD treatment. C was high-normal at the beginning of the study (170.7 ± 43 ng/ml) and decreased on SD, reaching the mean value of 115.1 ± 30.9 ng/ml.

Discussion

The stability of the renal function during the SD period, that confirms data already reported, is of great importance to exclude that the fall of B-EP may be due to an improvement of renal function, and makes reasonable to regard such reduction as an effect of dietary treatment itself.

The fall in circulating B-EP may be of crucial value, as high levels of this hormone may contribute, together with other less active endogenous opioids, to cause the endocrine derangements of CRF. The mechanisms through which the SD exerts this lowering effect on B-EP remains to be understood. Some hypothesis may be put forward, however. The supplementation of some amino acids, which are low in uremic serum, may affect the concentration of several neuromediators in the central nervous system (CNS). Tryptophan may cause an increase of melatonin in the pineal gland centers, so reducing the pituitary GH secretion [15], and may also cause an increase of serotonin in the diencephalic centers [16]. Tyrosine may increase dopamine release in the hypothalamus and both serotonin and dopamine are important anti-endorphinic neuromediators [16]. They participate to the regulation of hypothalamic-pituitary axis [17] and, peripherally, to the function of endocrine pancreas [2] and parathyroid glands [18]. The fall of B-EP observed during the SD treatment, might then be considered as a part of a general resetting of most CNS neuromediators, with an increase of anti-endorphinic molecules.

Another possible explanation might be related with the reduction of waste metabolites (uremic toxins) in body fluids caused by the SD: serum urea, sCR, serum inorganic phosphorus, serum uric acid [19], serum methylguanidine [19] and serum oxalic acid [20] decrease during SD. Metabolic acidosis is also corrected [19]. This more physiological condition reached on SD may hinder the hyperproduction of B-EP.

Every chronic 'stress condition', like uremic intoxication, induces a persistent increase of corticotropin-releasing-factor and, subsequently, via pro-opiomelanocortin (POMC) [2], an overproduction of ACTH and B-EP [2]. It is then reasonable to think that SD can reduce B-EP by correcting the CRF 'stress like' condition.

The consequences of the reversal of uremic hyperendorphinism, which has never been obtained with the replacement of renal function [21,22] may explain, at

least in part, the beneficial endocrine and metabolic effect of the SD. The important fall of circulating GH, in parallel with that of B-EP, may be explained by the decrease of the stimulatory effect of B-EP on the GH production [2,3]. The decrease of PTH may be due in part to the fall of the endorphinic stimulation [1,6], as well as to the correction of the calcium and phosphorus serum levels. The lowering effect of the amino acid-analogue mixture on PTH levels in dialyzed patients on a free mixed diet [23] suggest, indeed, that the SD influences PTH levels also by mechanisms other than the correction of the calcium-phosphate abnormalities. Normal values for PTH were not always reached in our experience, probably because the follow up period on SD was not long enough [10].

The increase of T3 during SD, previously observed in other experiences [12], may be attributed to the decrease of PTH levels [24] and to the good nutritional state. Also this endocrine change may be regarded in part as a consequence of the fall of circulating B-EP.

An excess of B-EP may cause insulin deficiency, impairing its secretion mechanism [2]. This might contribute to explain our previous observation, of an improvement of glucose tolerance in uremics during SD [14]. GH and PTH have a significant anti-insular action and the decrease of the serum levels of these hormones, as well as the increase of T3 (which favours carbohydrate tolerance) [25] may contribute to improve glucose metabolism.

Finally, another possible explanation to understand the important lowering effect of amino acids and their analogues on circulating B-EP, can be found in the recent finding of a real neuromediator role for some amino acids (unpublished observations).

Acknowledgements

We are gratefully indebted to the our Local Health Service Unit (USL 12, Area Pisana. Pisa, Italy) for the generous supply to our chronic uremics of essential amino acids and analogue tablets, as well as to the Farma Biagini S.p.A., Castelvecchio Pascoli, Lucca, Italy that produces this dietary supplement.

References

1. Grzeszczak W, Kokot F and Dulawa J (1986) Einfluss von Naloxone auf die Parathormone und Kalcitonin Secretion bei Kranken mit akuter und chronischer Niereninsuffizienz. Z. Klin. Med. 41: 435–437.
2. Rosemblatt M (1987) The Endogenous Opiate Peptides. In: Harrison's Principles of Internal Medicine. McGraw-Hill Book Comp, N.Y., 378–382.
3. Pfeiffer A, Braun S, Mann K, Meyer HD and Bronte W (1986) Anterior Pituitary Hormone Responses to a K-opiod agonist in man. J. Clin. Endocrinol Metab. 62: 181–185.
4. Blankstein J, Reyes Fi, Winter JSD and Faiman C (1981) Endorphins and the regulation of the human menstrual cycle. Clin. Endocrinol. 14: 287–294.

5. Bruni JF, Van Vugt D, Marshall S and Meites J (1981) Effects of Naloxone, Morphine and Methionine-Enkefalin on Serum PRL, LH, FSH, TSH and GH. Life Sci. 21: 461–466.
6. Grzeszczak W, Kokot F and Dulawa J (1987) Effect of Naloxone Administration on Endocrine Abnormalities in Chronic Renal Failure. Am. J. Nephrol. 7: 93–100.
7. Nakao K, Nakai J, Oky S, Matsubata S, Konishi H et al. (1980) Immunoreactive ß-endorphin in human cerebrospinal fluid. J. Clin. Endocrinol Metab. 50: 230–233.
8. Barsotti G, Guiducci A, Ciardella F and Giovannetti S (1982) Effect on Renal Function of a Low-Nitrogen Diet Supplemented with Essential Aminoacids and Ketoanalogues and of Hemodialysis and Free Protein Supply in Patients with Chronic Renal Failure. Nephron. 27: 113–177.
9. Walser M, La France ND, Ward L and Van Duin MA (1987) Progression of Chronic Renal Failure in Patients given Ketoacids Following Aminoacids. Kidney Int. 32: 123–128.
10. Barsotti G, Morelli E, Guiducci A, Ciardella F et al. (1982) Reversal of Hyperparathyroidism in Severe Uremics Following very Low Protein and Low Phosphorus Diet. Nephron. 30: 310–313.
11. Froehling PT, Kokot F, Schmicker R, Kaschube I, Lindenau K and Vetter K (1983) Influence of Ketoacids on Serum Parathyroid Hormone Levels in Patients with Chronic Renal Failure. Clin. Nephrol. pp. 212–215.
12. Ciardella F, Morelli E, Caprioli R et al. (1986) Restoration of Thyroid Secretion in Uremic Patients Following a Low Protein, Low Phosphorus Diet Supplemented with Essential Aminoacids and Ketoanalogues. Contr. Nephrol. 53: 51–57.
13. Barsotti G, Ciardella F, Morelli E et al. (1985) Restoration of Blood Levels of Testosterone in Male Uremics Following a Low-Protein Diet Supplemented with Essential Amino Acids and Keto-analogues. Contr. Nephrol. 49: 63–69.
14. Aparicio M, Bouchet JL and Gin H et al. (1987) Effect of a Low Protein Diet Supplemented with Essential Amino Acids and Ketoanalogues (SD) on Triglyceridemia and Carbohydrate Metabolism in Uremia. Xth International Congress of Nephrology, London Abstract Book, pp. 496.
15. Reichlin S (1985) Neuroendocrinology. In: 'Williams Textbook of Endocrinology' pp. 492–567.
16. Maher JT (1984) In: Adibi SA, Fekl W, Langenbeck U and Schauder P (eds.) Plasma Branched Chain Aminoacids as Regulators of Brain Neurotransmitters. Branched Chain Amino and Keto Acids in Health and Disease. Karger, Basel, pp. 242-249.
17. Grzeszczac W, Kokot F and Dulawa J (1984) Influence of Naloxone on Prolactin Secretion in Patients with Acute and Chronic Renal Failure. Clin. Nephrol. 21: 47–49.
18. Auerbach JD, Marx SJ and Spiegel AM (1985) In: Wilson JD, Foster DW, (eds.) Parathyroid Hormone, Calcitonin and the Calciferols. Williams Textbook of Endocrinology, Saunders, Philadelphia, pp. 1137–1217.
19. Giovannetti S (1985) Dietary Treatment of Chronic Renal Failure: Why Is It Not Used More Frequently? Nephron. 40: 1–12.
20. Barsotti G, Cristofano C, Morelli E et al. (1984) Serum Oxalic Acid in Uremia: Effect of a Low-Protein Diet Supplemented with Essential Aminoacids and Ketoanalogues. Nephron. 38: 54–56.
21. Zoccali C, Ciccarelli M, Mallamaci F and Maggiore Q (1986) Enkephalins in Plasma of Patients with Chronic Renal Failure. XXIIIrd E.D.T.A.-E.R.A. Congress. Budapest Abs. Book, p. 54.
22. Aronin N and Krieger DT (1983) Plasma Immunoreactive Betaendorphin is Elevated in Uremia. Clin. Endocrinol. 18: 459–464.
23. Lindenau K, Kokot F and Froehling P (1986) Suppression of Parathyroid Hormone by Therapy with a Mixture of Ketoanalogues/Aminoacids in Hemodialysis Patients. Nephron. 43: 84–86.
24. Kaptein EM, Fenstein EI and Massry SG (1982) Thyroid Hormone Metabolism in Renal Disease. Contr. Nephrol. 33: 112–135.
25. Burman kd, Smallridge RC, Jones L et al. (1980) Glucagon Kinetics in Fasting: Physiological Elevations in Serum 3, 5,3'-Triiodiothyronine Increases the Metabolic Clearance Rate of Glucagon. J. Clin. Endocr. Metab. 51: 1158–1162.

Address for correspondence: Dr. Fulvio Ciardella MD, Clinica Medica 1, University of Pisa, Via Roma 57, 56100 PISA, Italy.

Amino acids as energy sources in genetically fat and lean chickens

P.A. Geraert, M.L. Grisoni, S. Guillaumin, C. Law and M. Larbier
Station de Recherches Avicoles, INRA 37380 Nouzilly, France

Abstract

In the first experiment, *in vivo* incorporation into body lipids, oxidation to CO_2 and hepatic gluconeogenesis from glucogenic amino acids were studied in genetically lean (LL) or fat (FL) chickens. L-U-^{14}C alanine and glutamic acid were injected intraperitoneally. In fed birds, lipogenesis from labelled alanine or glutamic acid was greater in fat than in lean chickens: 13.71 and 6.95% respectively of the activity injected as alanine were recovered in body lipids 4 h after administration. No significant difference was found in fasted birds. No divergence in amino acid oxidation was reported between FL and LL birds whatever the nutritional status.

In the second experiment, ^{14}C incorporation into abdominal fat lipids and total oxidation from uniformly labelled alanine were investigated in FL and LL chickens fed experimental diets differing in protein concentrations (190 and 250 g/kg) or lysine contents (9 and 13 g/kg). No difference in oxidation between fat and lean lines was reported. However FL chickens exhibited significantly higher lipogenesis from alanine than LL birds. This difference between lines was not affected by the dietary composition.

Introduction

To understand the physiological mechanisms involved in the excessive fat deposition of fast-growing chickens, a problem that is causing increasing concern, two experimental lines have been divergently selected: a fat (FL) and a lean (LL) ones [1]. Unlike in genetically obese rodents [2]. Previous studies [3,4] have shown that the differences in fat content could not be explained by divergence in energy metabolism: intake or expenditure. However, for the same protein intake, FL chickens retained less protein than LL birds whatever the dietary protein concentration (from 130–250 g/kg) [4,5]. This lower protein retention efficiency is accompanied by a higher uric acid excretion which revealed greater amino acid degradation. Furthermore, the FL exhibited lower total plasma free amino acid levels than the LL irrespective of the nutritional status: fasted or fed [3]. This difference was mainly due to glucogenic amino acids; the levels of which were 10–15% lower in the FL.

The first study was therefore performed to investigate the degradative fate of carbon chain of two glucogenic amino acids: alanine and glutamic acid through lipogenesis, oxidation or gluconeogenesis in FL and LL chickens. The second experiment was conducted in order to determine how the partition between these

different pathways was affected in each line by either the dietary protein concentration (190 or 250 g/kg) or the essential amino acid supply (lysine, 9 or 13 g/kg).

Materials and Methods

Experiment 1

Male chickens of the FL and LL lines were housed in floor pens from hatching to 4 weeks of age. They were fed *ad libitum* a complete diet containing 210 g protein and 3100 kcal metabolisable energy per kg (Table 1).

For lipogenesis study, 36 chickens of each line were then transferred in individual battery cages and divided into four groups. At 35 days of age, all chickens, fasted for 20 hours or fed *ad libitum* with the same diet than during the starting period, received intraperitoneally about 2.5 μCi per kg bodyweight of L-U-^{14}C alanine (300 mCi/mmol, Amersham France) or L-U-^{14}C glutamic acid (150 mCi/mmol, Amersham France). All chickens were slaughtered by intracardiac injection of sodic pentobarbital 4 h after ^{14}C-amino acid administration. Carcasses including feathers were minced twice and freeze-dried. The lipids extracted in a Soxhlet apparatus were transferred with diethyl ether in counting vials. After evaporation, the vials were weighed and a toluene-PPO-POPOP mixture was added. The radioactivity was measured in a liquid scintillation counter Tricarb 460 (Packard Instr.). The results were expressed in specific activity (DPM/g lipid) and in total activity as a percentage of injected activity.

For oxidation studies, 5-week-old male chickens were individually placed in an open-circuit calorimeter. After 30 min for the acclimatization period, the bird was intraperitoneally injected with 10 or 5 μCi per kg bodyweight of L-U-^{14}C alanine or glutamic acid, respectively for fasted or fed birds. The total CO_2 production was determined using an infrared CO_2 analyser (UNOR 5, Schlumberger) and the $^{14}CO_2$ was measured during the 4 h following injection using the original device described by Geraert and Simonnet [6]. A proportion of the air extracted from the respiratory chamber was diverted through a modified scintillation vial placed

Table 1. Nutrient contents of experimental diets

Diet	Starter	Low protein		High protein	
Lysine content		low	high	low	high
Calculated values (g/kg)					
Metabolizable energy (kcal/g)	3100	3205	3207	3203	3206
Protein	210	190	190	250	250
Lysine	1.2	9.0	13.0	9.1	13.0
Sulphur amino acid	8.6	8.2	8.2	9.9	9.9
Tryptophane		1.8	1.8	2.1	2.1
Threonine		7.0	7.0	9.1	9.1

between the two photomultipliers of a FLO ONE liquid scintillation counter (Radiomatic Instr., France). The measurement of radioactivity was done during bubbling of the gas through the liquid scintillation mixture. The counting efficiency was about 90%.

Lastly for gluconeogenesis measurement, 40 fed chickens were used. The liver was rapidly removed after slaughtering. After a quick mincing in cold conditions, two 1 g-samples were taken and treated according to Bloom *et al.* [7]. The radioactivity of the glucose molecules from the glycogen was determined.

Experiment 2

One hundred and fourty-four male chickens from the FL and LL were used. Husbandry conditions were as in Exp. 1. At 4 weeks of age, the birds transferred in individual battery cages were allocated according to a factorial design as follows: 2 lines (FL & LL) × 2 dietary protein concentrations (190 & 250 g/kg) × 2 lysine levels (9 or 13 g/kg) × 18 replicates. They were fed *ad libitum* for eight days on the experimental diets (Table 1).

Oxidation and lipogenesis investigations from L-U-^{14}C alanine were done on 40 birds: 2 lines × 4 diets × 5 replicates. Degradation in $^{14}CO_2$ was measured as described above. However specific activity was also determined on $Ba^{14}CO_3$ precipitates using barium hydroxide trapping according to Simonnet and Bocquet [16]. Ninety minutes after intravenous injection of about 5 μCi/kg bodyweight of L-U-^{14}C alanine, birds were sacrificed by intracardiac administration of sodic pentobarbital. Total abdominal fat, a part of the subcutaneous fat and of the breast muscle were quickly removed and frozen until further analyses. Lipids from the adipose tissues were determined gravimetrically after extraction in chloroform-methanol (2:1 v/v) [8]. Preparation of samples for radioactivity determinations was done as previously.

Results and Discussion

Irrespective of the amino acid used (alanine, glutamic acid), in fasted birds, the specific activity of total body lipids was twice higher in the LL than in the FL (1993 v 963 DPM/g lipid with alanine) while the total body lipid content was half higher in the fat birds (Table 2). This would reveal similar lipogenic activity from glucogenic amino acids in both genotypes. Conversely, in fed chickens, specific activity of body lipids is equal in both lines suggesting an increased lipogenesis from alanine or glutamic acid in fatter birds. These results confirmed *in vivo* measurements done with tritiated water [17] indicating higher hepatic lipogenesis in fed FL birds but no differences when fasted. Expressed in % of injected activity, the incorporation into body lipids was then twice higher in fat chickens (13.71 v 6.95 % with alanine) as reported in obese Zucker rats [9] and in genetically fat chickens injected with ^{14}C-leucine [10]. However these data did not distinguish the different adipose tissues.

Table 2. ^{14}C incorporation from L-U-^{14}C alanine and glutamic acid into body lipids in 5-week-old fat line (FL) and lean line (LL) chickens (4 h after intraperitoneal injection of 2.5 μCi/kg body weight)

Line	LL		FL		Statistical analysis[a]		
Nutritional status	Fasted	Fed	Fasted	Fed	RSD	line	nutr. stat.
Alanine							
n[b]	9	8	8	8			
Body weight (BW,g)	709	823	724	840	51	NS	***
Lipids (g/100 g BW)	7.1	7.8	11.4	11.4	1.2	***	NS
Specific activity (DPM/g lipid)	1993	5899	963	6654	450	NS	***
^{14}C labelled lipids (% injected activity)	1.56	6.95	1.41	13.71	0.90	**	***
Glutamic acid							
n	9	9	8	9			
Body weight (BW, g)	699	824	715	837	57	NS	***
Lipids (g/100 g BW)	7.2	7.7	11.2	12.3	1.9	***	NS
Specific activity (DPM/g lipid)	1066	3000	616	2922	395	NS	***
^{14}C labelled lipids (% injected activity)	0.88	3.45	0.84	5.40	0.70	**	***

[a] RSD: residual standard deviation; * $P<0.05$, ** $P<0.01$, *** $P<0.001$. NS, not significant. No interactions were significant.
[b] n: number of replicates.

On the other hand, measurements of $^{14}CO_2$ expired in both genotypes at 5 weeks of age after ^{14}C-amino acid administration (Table 3) did not indicate any divergence whatever the amino acid injected or the nutritional status. These data did not agree with reports from Saunderson and Whitehead [11] on VLDL-selected lines of chickens or from Dunn and Hartsook [9] on Zucker rats which indicated higher $^{14}CO_2$ production in the fat lines. Nevertheless in both cases, fat animals were significantly hyperphagic and when adjusting food intakes by means of pair-feeding or age, the differences in oxidation disappeared [9,11].

Unlike in Zucker rats [13], fat and lean chickens did not show any significant difference in hepatic glycogen content (9–10 mg/g liver). In the case of alanine, incorporation of ^{14}C in hepatic glycogen seemed to be enhanced in the LL compared to the FL when expressed in DPM/g liver (+40%) or in DPM/mg glycogen (+67%) while no difference appeared with glutamic acid. So, FL chickens did not exhibit an increased gluconeogenesis from amino acids as observed in obese rodents [18], but rather a decrease as reported by Bloxham and York [14] in Fa/Fa rats.

Finally, alanine and glutamic acid exhibited different metabolic pathways in chickens. While glutamic acid was relatively more oxidized into CO_2, alanine was more potent for lipogenesis and hepatic gluconeogenesis.

Table 3. $^{14}CO_2$ excretion in 5-week-old FL and LL chickens, fasted for 24 h or fed *ad libitum*, 4 h after intraperitoneal administration of L-U-^{14}C alanine or glutamic acid (5 or 10 μC/kg body weight for fed and fasted birds respectively)

Line	LL		FL		Statistical analysis[a]		
Nutritional status	Fasted	Fed	Fasted	Fed	RSD	line	nutr. stat.
Alanine							
n[b]	6	7	6	7			
Body weight (g)	814	830	803	871	21	NS	**
Total activity (% injected activity)	3.07	14.64	3.44	13.24	0.68	NS	***
Time of maximum oxidation (min)	30	35	30	35			
Glutamic acid							
n	5	8	6	9			
Body weight (g)	822	802	831	774	17	NS	NS
Total activity (% injected activity)	5.10	19.51	5.39	19.34	0.67	NS	**
Time of maximum oxidation (min)	60	45	60	45			

[a] [b] see Table 2.

The results on body composition (Table 5) confirm that the selection has led to the production of two divergent lines: the abdominal fat ratio was 0.74 in the LL and 2.14 g/100 g body weight for the FL. Moreover, the abdominal fat of the FL exhibited higher lipid content. Hermier *et al.* [15] found similar results and concluded that the difference in abdominal fat pad weight was the consequence of a divergence in cell number as well as a difference in cell size. As observed for ^{14}C incorporation into total body lipids in the 1st experiment, there was no significant

Table 4. ^{14}C incorporation from L-U-^{14}C alanine and glutamic acid into hepatic glycogen in 5-week-old fat line (FL) and lean line (LL) chickens (4 h after intraperitoneal injection)

Amino acid (AA)	Alanine		Glutamic acid		Statistical analysis[a]		
Line	LL	FL	LL	FL	RSD	line	AA
Body weight (g)	755	860	760	891	24	***	NS
Liver weight (LW, g)	22.2	26.3	22.9	26.7	1.0	***	NS
Glycogen (mg/g LW)	8.59	9.39	10.60	10.93	1.02	NS	NS
^{14}C glycogen (DPM/g LW)	278	196	103	93	19	NS	***
Specific activity (DPM/mg glycogen)	35	21	11	9	5	*	***

[a] see Table 2.
n = 10 birds per treatment.

Table 5. Effects of dietary protein concentration (190 and 250 g/kg) and lysine content (9 and 13 g/kg) on utilization of L-U-^{14}C alanine for lipogenesis or oxidation in 5-week-old genetically fat and lean chickens (1 h 30 min after intravenous injection of 5 μCi/kg body weight)

Dietary protein (g/kg)		190		250		Statistical analysis[a]		
Lysine(g/kg)		9	13	9	13	RSD	line	diet
Abdominal fat (AF, g)	LL	6.16	6.66	6.39	4.94	1.42	***	NS
	FL	17.85	17.58	13.57	18.13			
Abdominal fat	LL	0.73	0.87	0.77	0.60	0.22	***	NS
(g/100 g bodyweight)	FL	2.30	2.24	1.74	2.28			
Lipid content	LL	80.95	80.41	83.71	77.21	2.24	***	NS
(g/100 g AF)	FL	86.70	88.86	85.34	87.12			
Specific activity	LL	1638	3495	2362	2487	915	NS	NS
(DPM/g lipid AF)	FL	1906	6523	5319	2651			
Total activity	LL	7658	16291	11283	10997	10180	***	NS
(DPM/AF)	FL	29689	89483	54174	39893			
$^{14}CO_2$	LL	53208	58143	60002	53166	181	NS	**
(DPM/mmol CO_2)	FL	53505	56779	63272	51967			

[a]see Table 2.
n = 5 birds per treatment.

divergence in specific activity of abdominal fat (DPM/g lipides) also suggesting higher lipogenic activity from alanine in fat birds. Furthermore when expressed on a total abdominal fat weight basis, incorporation of ^{14}C from alanine was significantly enhanced in FL birds compared to lean chickens.

Measurements of alanine oxidation indicated no overall difference between genotypes but a significant increase in specific activity (DPM/mmol CO_2) when increasing the dietary protein concentration (from 190–250 g/kg) for low lysine

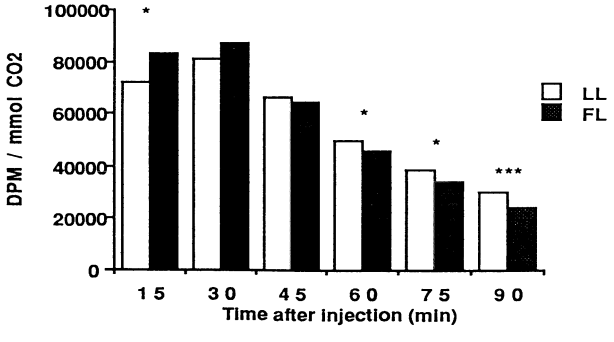

Statistical significance : * P<0.05, *** P<0.001

Fig. 1. Specific activity of $^{14}CO_2$ exhaled by FL and LL chicken during 90 min following intravenous injection of 5 μCi/kg body weight of L-U-^{14}C alanine (5 birds per treatment).

content. This tendency was not statistically confirmed for lipid synthesis due to a greater variability. Furthermore, for high protein level (250 g/kg), an increase in lysine level (from 0.9–1.3%) resulted in a decrease in alanine oxidation (Table 5) which could be explained by a higher rate of protein synthesis. Figure 1 showed the $^{14}CO_2$ production over 90 min in both lines after intravenous administration of uniformly labelled alanine. The specific activity of $^{14}CO_2$ appeared higher in FL chickens than in LL ones during the first 30 min after injection and on the contrary, LL birds exhibited greater specific activity when measured between 60 and 90 min after labelled alanine administration. This would suggest either an enhanced uptake of amino acid in the FL hepatocyte or a dilution phenomenon: the FL having lower plasma free alanine level than the LL [3]. Both hypotheses might be involved.

Finally, the two experimental lines showed similar changes in amino acid degradation with increasing dietary protein concentration or with increasing of essential amino acid content. This would led to the conclusion that no significant divergence in total or essential amino acid requirement existed between FL and LL birds as suggested in previous studies [5].

The divergence of fattening between FL and LL chickens could then only be explained by the fact that some dietary amino acids are diverted from protein synthesis towards lipogenesis while no difference appeared in amino acid oxidation or gluconeogenesis.

References

1. Leclercq B, Blum JC and Boyer JP (1980) Br. Poult. Sci. 21: 107–113.
2. Bray GA and York DA (1979) Physiol. Rev. 59: 719–809.
3. Geraert PA, Leclercq B and Larbier M (1987) Rep. Nutr. Develop. 27: 1041–1051.
4. Geraert PA, MacLeod MG, Larbier M and Leclercq B (1988) J. Nutr. 118: 1232–1239.
5. Geraert PA, MacLeod MG Larbier M and Leclercq B (1990) Poult. Sci. in press.
6. Geraert PA and Simonnet F (1986) Int. J. Rad. Appl. Instr. 37A: 450–454.
7. Bloom WL, Lewis GT, Schumpert MZ and Shen TM (1950) J. Biol. Chem. 188: 631–636.
8. Folch J, Lees M and Stanley GHS (1957) J. Biol. Chem. 226: 497–509.
9. Dunn MA and Hartsook EW (1980) J. Nutr. 110: 1865–1879.
10. Mamier B, Geraert PA and Larbier M (1986) Comp. Biochem. Physiol. 83A: 735–737.
11. Saunderson CL and Whitehead CC (1987) Comp. Biochem. Physiol. 86B: 419–422.
12. Whitehead CC and Saunderson CL (1988) Comp. Biochem. Physiol. 89B: 107–129.
13. Koubi H and Freminet A (1985) Comp. Biochem. Physiol. 81B: 103–110.
14. Bloxham DP and York DA (1977) Biochem. Soc. Trans. 4: 989–993.
15. Hermier D, Quignard-Boulangé A, Dugail I, Guy G, Salichon MR, Brigant L, Ardouin B and Leclercq B (1989) J. Nutr., in press.
16. Simonnet F, Bocquet C (1980) Rapport CEA-R-5060, Dec 80.
17. Saadoun A, Leclercq B (1986) Comp. Biochem. Physiol. 83B: 607–611.
18. Triscari J, Stern JS, Johnson PR, Sullivan AC (1979) Metabolism 28: 183–189.

Address for correspondence: Station de Recherches Avicoles, I.N.R.A. 37380 Nouzilly, France.

Amino acid requirements of guinea pigs using chemically defined diets*

John T. Typpo[a], Donna J. Curtis[a], Linette S. Ayers[a], Sara C. Mokros[a], Jane E. Link[a] and Gary F. Krause[b]

[a]*Department of Human Nutrition and Foods, University of Missouri, Columbia, MO 65211, U.S.A.*
[b]*Department of Agronomy, University of Missouri, Columbia, MO 65211, U.S.A.*

Abstract

At the University of Missouri in Columbia we have been studying the nutritional requirements of the guinea pig using chemically defined diets. The purpose of this longterm study has been to enhance the value of this species as an animal model for human research. This presentation includes the results of over twenty experiments, 22 days in duration and involving over 1500 guinea pigs from 3–6 weeks of age.

In 1982 we published the results of our first studies on indispensable amino acid nitrogen and total nitrogen requirements. The amino acid content and composition of these diets was patterned after casein and soy protein based diets reported in the literature. Four levels of total dietary nitrogen (2.5, 2.9, 3.6 and 4.3%) and three levels of indispensable amino acid nitrogen (1.7, 2.0 and 2.4%) were tested. The level selected was 3.6% total dietary nitrogen and 1.7% total indispensable amino acid nitrogen. The remainder of our research on specific amino acid requirements has been conducted using 3.6% of total dietary nitrogen. When individual indispensable amino levels have been altered they have been replaced by a corresponding change in the dispensable amino acid nitrogen component. The total dietary level of indispensable amino acid nitrogen has been reduced from 1.7% to 0.98% while maintaining the total dietary nitrogen level constant at 3.6%. During the process of this research the growth rate of the animals has increased by over 20%, attesting to a better balance of nutrients. Our most recent research suggests that total dietary nitrogen can be reduced by 20% to about 2.9%.

The nutritive requirements of the guinea pig are not well documented. The research reported here is focused on designing a chemically defined diet for guinea pigs 2–6 weeks of age which will make this animal a more useful model for human research. These studies deal with the assessment of the indispensable amino acid (IAA) and the total nitrogen (TN) requirements of the growing guinea pig [1–3]. The requirements for Arg, Lys, Met and Trp have been previously estimated using diets supplemented with crystalline amino acids and based on either casein or soybean protein [4–7].

Methods

A number of years ago when this research was first conceived, we calculated the approximate protein, IAA, TN and mineral content of diets which had supported good growth in young guinea pigs. We then chose a level of each IAA which was slightly higher than the lowest value we had found among the diets. These levels were then used to formulate the first IAA mixture made up entirely of crystalline L-amino acids (Table 1). The length of study used throughout this research was 21

* Contribution from the Missouri Agricultural Experiment Station, Journal Series Number 10,856.

Table 1. Indispensable amino acid mixture[a]

Amino acid[b]	g/100 g mixture
Arg	17.30
Cys	2.90
His	5.80
Ile	10.20
Leu	11.60
Lys·HCl	13.66
Met	4.40
Phe	9.45
Thr	7.30
Trp	2.15
Tyr	5.80
Val	9.45

[a]This mixture was originally designed after the amino acid composition of a number of successful natural protein diets. The selected level for each amino acid was based on the diet containing the lowest level of that amino acid plus a small safety factor. Cys and Tyr were included with the indispensable amino acids because of their ability to spare Met and Phe respectively.
[b]All amino acids are present in the L form.

day for growth data and 22 day for autopsy information. Nitrogen balance data were collected over a 4 day period, usually from day 17 through day 20. Guinea pigs were purchased from commercial suppliers and shipped to our animal research facility at the University of Missouri. Upon arrival they were placed in stainless steel wire mesh cages in a temperature and humidity controlled environment. The animals were weighed daily and had free access to feed and water. Animals were allowed a 4 to 7 day pretrial acclimation period prior to the 22 day trial. At the end of the pretrial period, those which had exhibited no symptoms of poor health and had gained consistently were admitted to the study. At autopsy the animals were rendered unconscious with ether (earlier studies) or CO_2 (later studies). Blood for hemoglobin and hematocrit determinations was collected by direct heart puncture and liver and carcass weights were recorded.

The dispensable amino acid (DAA) mixture used throughout these studies is shown in Table 2. The composition of this mixture was based upon a relatively broad range of dispensable amino acids. Previous work with the rat suggested that some DAA were perhaps semi-essential, so in formulating our DAA mixture we included Glu, Asn, Pro along with Ala, Asp, Gly and Ser [8–10]. The ratio of indispensable to dispensable amino acids was also of concern. Others studying this question with rats and chicks, respectively, found that approximately 30–40% of total dietary nitrogen was most satisfactory [11,12]. The acidity of the diet was of some concern, so we replaced some of the Glu with Glu-Na as shown in Table 2. The DAA mixture has remained unchanged throughout these studies. When an IAA is being investigated the diet is kept isonitrogenous by either raising or lowering the amount of the DAA mixture.

Table 2. Dispensable amino acid mixture[a]

Amino acid[b]	g/100 g mixture
Ala	7.05
Asn·H_2O	5.81
Asp	5.81
Glu	34.82
Glu-Na	23.20
Gly	11.69
Pro	5.81
Ser	5.81

[a]This mixture was used in all diets reported here. Only the amount of mixture varied from diet to diet. This mixture has remained essentially unchanged throughout all of our studies.
[b]All amino acids except Gly are present in the L form.

A special mineral mixture (Table 3) was developed for use with the crystalline amino acid based diet. It is a modification of the mixture developed for semi-purified diets [15]. Final modifications of this mixture were made in 1988 and the amount used in the diet was reduced to 6.3%.

Table 3. Mineral mixture[a]

Ingredient	g/100 g mixture
$CaHPO_4$	38.80
$CaCO_3$	6.60
NaCl	6.40
KCl	8.60
$MgSO_4$	5.10
$FeC_8H_5O_7 \cdot nH_2O$	0.71
$MnSO_4 \cdot H_2O$	0.41
$KC_2H_3O_2$	27.70
MgO	5.50
$ZnCO_3$	0.143
KIO_3	0.0045[b]
$CuSO_4$	0.0201[b]
$KCr(SO_4)_2 \cdot 12H_2O$	0.0128
$Na_2MoO_4 \cdot 2H_2O$	0.00067
$NiCl_2 \cdot 6H_2O$	0.00026
Na_2SeO_3	0.00026
NaF	0.0085[c]
$SnCl_2$	0.0045[c]
$Na_2SiO_3 \cdot 5H_2O$	2.910[c]
$VOSO_4 \cdot 2H_2O$	0.0006[c]

[a]This mineral mixture has been adapted for use with chemically defined diets where all nitrogen is supplied by crystalline amino acids. This mixture is fed at 7.5% of the diet.
[b]Changed to levels indicated in 1980. [c]Added to mixture in 1988.

Table 4. Fat soluble vitamin mixture

Ingredient	g/100 g mixture
Vitamin D3	0.0002
D,L-alpha tocopherol acetate	0.20
Menadione	0.01
Vitamin A palmitate in oil[a]	0.26
Corn oil	99.5298

This mixture is used in all diets at the rate of 2 g/100 g diet.
[a]1,000,000 USP units/g oil.

Table 5. Water soluble vitamin mixture

Ingredient	g/100 g mixture
Thiamine HCl	0.08
Riboflavin	0.08
Pyridoxine HCl	0.08
D-calcium pantothenate	0.20
Nicotinic acid	1.00
Folic acid	0.05
Biotin	0.0025
Cobalamin[a]	0.25
Glucose·H_2O	98.2575

This mixture is used in all diets at the rate of 2 g/100 g diet.
[a]0.1% trituration in mannitol.

Table 6. Composition of chemically defined basal diet

Ingredient	g/100 g diet
Indispensable amino acid mixture[a]	10.7
Dispensable amino acid mixture[b]	16.1
Mineral mixture[c]	7.5
Corn oil	3.0
Sucrose	
Granulated	5.4
Powdered	21.5
Glucose·H_2O	16.2
Non-nutritive fiber[d]	15.0
Fat soluble vitamin mixture[e]	2.0
Water soluble vitamin mixture[f]	2.0
Ascorbic acid	0.2
Choline chloride	0.2
Inositol	0.2

[a]See Table 1.
[b]See Table 2.
[c]See Table 3.
[d]Cellophane spangles or solka floc.
[e]See Table 4.
[f]See Table 5.

The vitamin mixtures used throughout these studies remained unchanged in composition and amount. These mixtures were stored in amber glass bottles and refrigerated at +4°C (Tables 4 and 5).

Table 6 shows the composition of the diet selected to be used in the study of the amino acid requirements of young growing guinea pigs. As the IAA were studied individually, diets were maintained isonitrogenous and isoenergetic by increasing or decreasing the DAA mixture and sugar corresponding to changes in IAA.

Results and Discussion

The first study was directed to the determination of the most suitable level of TN for young guinea pigs. The ratio of IAAN to TN was maintained at about 0.67:1 as TN was fed at 4.3, 3.6, 2.9 and 2.5% of the diet. The lowest level of IAA mixture used provided all IAA at levels slightly above the lowest levels found in adequate natural protein diets. The lowest level of TN which supported growth not significantly different from the casein control was 3.6% (Table 7a).

The 3.6% level of TN was then fed in two diets combined with IAAN levels of 1.7 and 2.0%. As indicated in Table 7b, the growth response to the casein control diet and both chemically defined diets was equal.

Thus the diet selected for completing the studies on the amino acid requirements was diet 3A, which contains 3.6% TN and 1.7% IAAN and with a ratio of 0.47:1 of IAAN to TN. Lysine was the first amino acid studied using the diet developed for this purpose. Table 8 shows the results of the three parameters used in assessing the Lys requirement.

Total gain, CWT, and N-bal clearly indicate that the 0.5% level of dietary Lys is limiting and the 0.6% level appears marginal. At levels of 0.7% Lys and above, the

Table 7a. Effect of varying dietary levels of total nitrogen on growth of young guinea pigs

	Diets and nitrogen sources				
	Casein Control	Crystalline amino acids			
		1A	2B	3C	4D
IAAN (%)	2.4	1.7	2.0	2.4	2.9
TN (%)	4.4	2.5	2.9	3.6	4.3
IAAH/TN	0.55	0.68	0.70	0.67	0.67
Casein (%)	30.3	——	——	——	——
Gain	140 ± 7^{a}	94 ± 10^{b}	96 ± 10^{b}	108 ± 17^{ab}	128 ± 16^{ab}

The ratio of indispensable amino acid nitrogen (IAAN) to total dietary nitrogen (TN) was kept constant at about 0.67:1. The lowest level of IAAN used (1.7%) was the sum of the lowest levels of the individual amino acids as determined in Table 1. The nitrogen component of the diets is presented as well as gain during the 21 day study. Gains (in g) are presented as means ± S.E.

[ab]Means with same superscript are not significantly different ($p>0.05$).

Table 7b. Effect of varying dietary levels of indispensable amino acid nitrogen on growth of young guinea pigs

	Diets and nitrogen sources		
	Casein Control	Crystalline amino acids	
		3A	3B
IAAN (%)	2.4	1.7	2.0
DAAH (%)	2.0	1.9	1.6
TN (%)	4.4	3.6	3.6
Gain	121 ± 8[a]	122 ± 8[a]	121 ± 7[a]

Indispensable amino acid nitrogen (IAAN) was varied while total nitrogen (TN) was kept constant at 3.6% of the diet. The nitrogen component of the diet is presented as well as gain during the 21 day study. Gains (in g) are presented as means ± S.E.

[a] Means with same letter superscript are not significantly different ($p>0.05$).

requirement appears to have been met. Performance at levels of over 0.7% Lys seems to generally plateau with no indication of toxic effects. In the study of Ile (Table 9) the changes in the IAA mixture reflected the amino acids which had been previously studied. The DAA mixture was increased to keep the level of dietary nitrogen constant between studies.

Eight levels of Ile were fed (0.2–0.8% and 1.2% of the diet). The 0.2 and 0.3% levels supported suboptimal performance in all parameters studied, but the 0.4% level approached the level of performance of the higher levels of Ile fed. Only the total gain in weight was slightly, though significantly, lower than the highest gain recorded (0.7% level). The 0.5% level of Ile was selected as the lowest level supporting performance not significantly different from the higher levels fed. The daily gain of these animals approached 7 g/day.

The current status of this research is shown in Tables 10 and 11. The amount of the IAA mixture used in the current diet (3.6% TN) is only 59% of the amount used in the original diet (3A) as shown in Table 10. The level of the DAA mixture used

Table 8. Effect of graded levels of Lys on growth related parameters

	Dietary Lys (%)					
	0.5	0.6	0.7	0.8	0.9	1.1
G	75 ± 5[a]	105 ± 5[b]	118 ± 5[bc]	123 ± 5[c]	114 ± 5[bc]	119 ± 5[c]
CWT	187 ± 5[a]	212 ± 5[b]	224 ± 4[c]	229 ± 4[c]	217 ± 5[bc]	222 ± 5[bc]
N-bal	0.80 ± 0.04[a]	1.04 ± 0.04[b]	1.20 ± 0.04[bc]	1.20 ± 0.04[c]	1.04 ± 0.04[b]	1.04 ± 0.04[b]

All diets are isonitrogenous and isoenergetic. Based on the data, 0.7% Lys was chosen as the minimum requirement. Gain (G), carcass weight (CWT), and nitrogen balance (N-bal) are presented as means (in g) ± S.E.

[a–c] Means with same letter superscript in same row are not significantly different ($p>0.05$).

Table 9. Effect of graded levels of dietary Ile on growth parameters

	Dietary Ile							
	0.2	0.3	0.4	0.5	0.6	0.7	0.8	1.2
G	23 ± 8^{a}	75 ± 8^{b}	125 ± 10^{c}	146 ± 8^{cd}	142 ± 10^{cd}	153 ± 8^{d}	133 ± 10^{cd}	131 ± 10^{cd}
CWT	154 ± 8^{a}	195 ± 8^{b}	248 ± 9^{c}	254 ± 8^{c}	252 ± 9^{c}	267 ± 9^{c}	245 ± 9^{c}	245 ± 9^{c}
N-bal	0.05 ± 0.10^{a}	0.49 ± 0.10^{b}	0.92 ± 0.11^{c}	0.92 ± 0.10^{c}	0.99 ± 0.11^{c}	0.76 ± 0.11^{bc}	0.93 ± 0.11^{c}	0.78 ± 0.11^{bc}

To keep diets isonitrogenous and isoenergetic, each g change in Ile was matched by a change of 0.913 g of the DAA mixture. Any changes in total weight of diet are adjusted by increasing or decreasing the sugar component. Based on the data presented here, 0.5% Ile was chosen as the minimum requirement. Gain (G), carcass weight (CWT), and nitrogen balance (N-bal) are presented as means (in g) ± S.E.

[a–d] Means with same letter superscript in same row are not significantly different ($p>0.05$).

Table 10. Indispensable amino acid mixture. A comparison of the original and final composition

Amino acid[a]	Old g/100 g mixture	New g/100 g mixture
Arg	17.30	15.81
Cys	2.90	3.16
His	5.80	4.74
Ile	10.20	7.91
Leu	11.60	14.23
Lys·HCl	13.66	13.83
Met	4.40	4.74
Phe	9.45	7.11
Thr	7.30	7.91
Trp	2.15	2.37
Tyr	5.80	7.11
Val	9.45	11.07

The old indispensable amino acid mixture (IAA) was used at the rate of 10.7 g/100 g diet, while the new IAA mixture was used at 6.3 g/100 g diet.
[a]All amino acids are present in the L form.

in the original diet was 16.1 g/100 g and currently is 22.4 g/100 g of diet when all IAA are included at their required levels.

Recent work in our laboratory with the TN requirements of young guinea pigs suggests that performance is not affected by lowering the DAAN to 1.89 g/100 g diet or lowering TN to 2.86%. Weight gains of about 7 g/day are usually seen with this reduced TN level[1]. We started out with an IAAN to TN ratio of 0.67:1 and now it is 0.34:1. It appears now that we have developed a chemically defined diet which will permit the inclusion or exclusion of any given nutrient at any desired level. If

Table 11. Dispensable amino acid mixture

Amino acid[a]	g/100 g mixture
Ala	7.05
Asn·H_2O	5.81
Asp	5.81
Glu	34.82
Glu-Na	23.20
Gly	11.69
Pro	5.81
Ser	5.81

This mixture was used in all diets reported here. Only the amount of mixture varied from diet to diet. This mixture has remained essentially unchanged throughout all of our studies. The amount of this mixture used in initial and final studies is 16.1 and 16.0 g/100 g diet respectively.
[a]All amino acids except Gly are present in the L form.

[1] D. Bavarati and J.T. Typpo, unpublished results.

this proves to be so, then the guinea pig will become more valuable as a model for human research.

References

1. Jeffery DM and Typpo JT (1982) J. Nutr. 112: 1118–1125.
2. Typpo JT, Anderson HL, Wause GF and Yu DT (1985) J. Nutr. 115: 579–587.
3. Ayers LS, Typpo JT and Krause GF (1987) J. Nutr. 117: 1098–1101.
4. Reid ME and Mickelsen O (1963) J. Nutr. 80: 25–32.
5. Heinicke HR, Harper AE and Elvehjem CA (1955) J. Nutr. 57: 483–496.
6. Reid ME (1966) J. Nutr. 88: 397–402.
7. Reid ME and Von Sallmann L (1960) J. Nutr. 70: 329–336.
8. Hepburn FN, Calhoun WK and Bradley WB (1960) J. Nutr. 72: 163–176.
9. Breuer LH, Pond WG, Warner RG and Loosli JK (1964) J. Nutr. 82: 499–506.
10. Adkins JS, Wertz JM and Hove EL (1966) Proc. Soc. Exp. Biol. Med. 122: 519–523.
11. Frost DV and Sandy HR (1951) J. Biol. Chem. 189: 249–260.
12. Kumta VS and Harper AE (1960) J. Nutr. 71: 310–316.
13. Stucki WP and Harper AE (1961) J. Nutr. 74: 377–383.
14. Stucki WP and Harper AE (1962) J. Nutr. 78: 278–286.
15. Liu KC, Typpo JT, Lu JY and Briggs GM (1967) J. Nutr. 93: 480–484.

Address for correspondence: John T. Typpo, Ph.D., Room 16, Gwynn Hall, Department of Human Nutrition and Foods, University of Missouri, Columbia, MO 65211, U.S.A.

Bioavailability of homocyst(e)ine in rats and humans

D. de Weck-Gaudard and P.A. Finot

Nestlé Research Centre, Nestec Ltd., Vers-chez-les-Blanc, CH-1000 Lausanne 26, Switzerland

Abstract

It has been reported that the growth of certain lines of cultured malignant cells is methionine-dependent: replacement of methionine in the culture medium with homocystine does not allow growth to occur. A dietetic approach may therefore be proposed to treat *in vivo* methionine-dependent tumours, under the condition that the bioavailability of homocystine to healthy cells is good.

In weanling rats, the replacement of dietary methionine by equivalent amounts of homocystine, or homocysteine thiolactone. in the L or DL forms to a limiting level in the diet, resulted in a decrease of the growth rate by 58%. The addition of further levels of folic acid, vitamin B12 and choline, which are involved in the methylation of homocysteine into methionine did not improve growth.

In 200 g rats, when homocystine was provided instead of methionine, growth rate was markedly reduced, although protein deposition was maintained at 76% of that obtained with the methionine containing diets, and liver glutathione reduced by 39%. Normal growth can be obtained with additional levels of homocystine.

In human volunteers, a diet providing homocystine but no methionine for 24 h, improved the nitrogen balance as compared to a methionine free diet.

Introduction

Methionine is an essential amino acid for normal growth and development of mammals, the primary source of which is protein. Methionine and its metabolic derivatives are essential components in several indispensable biological reactions. Protein synthesis requires both methionine and cysteine. S-adenosyl-methionine is the obligatory methyl donor in almost all transmethylation reactions and, following decarboxylation, is the donor of propylamine groups in the synthesis of polyamines-spermine and spermidine. By means of the transsulfuration sequence, methionine can be the precursor of cysteine and its important derivatives such as glutathione, for example, which plays a very important role in the catabolism of drugs [1] and the removal of free radicals generated by chemotherapy [2].

In vivo methionine can be derived by methylation of homocysteine using either the methyl donors methyltetrahydrofolate and B12 (after methylation) or choline. *In vitro* the growth of a number of cultured malignant cells is methionine dependent: replacement of methionine in the culture medium with homocystine does not allow growth to occur. Different explanations have been proposed: i) these malignant cells do not have the capacity to methylate homocysteine to methionine [3–6]; ii) they are not able to synthetize S-adenosyl-methionine [7–9] and thus

provide the necessary methyl donors to the cell; iii) polyamines are possibly increased in the maligant cell as a result of its high division rate.

A dietary approach may therefore be possible to treat *in vivo* methionine-dependant tumours in which the replacement of dietary methionine by homocystine effects specifically malignant cells rather than healthy ones.

In growth tests we have determined the bioavailability of L- and DL-homocystine, DL-homocysteine thiolactone and D-methionine relative to L-methionine in young rats and the bioavailability of L-homocystine in 200 g rats. The possibility to improve the homocysteine methylation by increasing the dietary concentrations of cofactors involved in homocysteine methylation (vitamin B12, choline and folic acid) or by high dietary levels of homocystine was studied. To assess more precisely if adult rat utilised homocysteine, food conversion efficiency (FCE) was calculated for the different diets as well as the protein and lipid deposition during the test.

The influence of dietary replacement of methionine by homocystine on hepatic glutathione level was studied in the presence or absence of dietary serine and glycine, both of which are also required for glutathione synthesis.

Finally, the bioavailability of L-homocystine in humans was examined by comparing the nitrogen balance obtained with a methionine-free diet with that of one containing homocystine.

Experimental procedures

Animals and diets

Male Sprague-Dawley rats (Interfauna, Tuttlingen, RFA) weighing 60 g (young rats) or 200 g were used. During a four day adaptation period all rats were fed a low-methionine diet after which they were matched for weight and allocated to one of the dietary groups. All rats were fed ad libitum. The rats and the food were weighed three times per week. At the end of the test, the gut contents of the adult rats were removed prior to carcass analysis. The carcasses were lyophylised and lipids were extracted in a methanol/chloroform solution (1:2). After digestion in hydrochloric acid (25%). the nitrogen content was measured by the Kjeldahl method.

The basal diet contained the free amino acid mixture (Fluka, AG, Buchs, CH) described by Rogers and Harper [10] with the exceptions that it was methionine free and that the concentrations of serine and glutamic acid were modified to 6.0% and to 17.4% respectively. The diet also contained 10 mg/kg folic acid, 2 g/kg choline bitartrate and 50µg/kg vitamin B12. The diets contained 20% crude protein.

Experiment 1

L-methionine, DL-methionine, L-homocystine, DL-homocystine and DL-homocysteine thiolactone were tested for 15 days each at the levels 0.10% and 0.16% calculated in methionine equivalents days. Each group was composed of 6 young rats fed the same diet throuthout the experiment.

Experiment 2

Four groups of 10 young rats were fed L-methionine or Lhomocystine at the level of 0.16% incorporated in diets containing the same concentration of vitamin B12, folic acid and choline as the basal diet or three-fold greater concentrations for 30 days.

Experiment 3

Two groups of 10 young rats were fed diets containing 0.16% L-homocystine for 21 days. The level of vitamin B12 was 50 μg/kg in both diets but in addition the diet of the experimental group contained 150 μg/kg methylcobalamin.

Experiment 4

L-methionine and L-homocystine were tested at the levels 0.10% and 0.16% in adult rats (6 per group) for 21 days. One group was sacrified at the beginning of the experimental period and was used as reference for body composition.

Experiment 5

Ten groups of 6 adult rats were fed diets containing 10 μg/kg vitamin B12, 2 mg/kg folic acid and 2 g/kg choline bitartrate for 20 days. L-Methionine was tested at the following levels: 0.16%. 0.28%, 0.40% and 0.56%; DL-homocystine at the levels of 0.16%, 0.36%, 0.56%, 0.76% and 0.96%. The last group was fed a diet containing 0.56% L-homocystine. A reference group was sacrificed at the beginning of the experimental period.

Experiment 6

An amino acid mixture without serine, glycine and cystine was prepared. For 28 days, four groups of adult rats were fed 0.40% L-methionine or DL-homocystine with or without serine and glycine. The absence of serine and glycine was compensated for by supplementary adjunction of arginine, alanine, proline, aspartic acid and asparagine to keep all diets isonitrogenous. At the end of the growth test, a piece of liver was taken by the freeze-clamp method and stored in liquid nitrogen for glutathione analysis. Free glutathione (oxidised and reduced) was analysed by a method adapted from Griffith [11].

Human study

This was approved by the ethical comittee of the Nestle Research Centre. Two experimental periods of 24 h were each preceeded by two days of adaptation and were separated by 6 days. During the adaptation period the food ingestion and physical activity of the six volunteers was controlled. During the experimental period, the diet consisted of a mixture of amino acids (food grade quality, Welding Pharma AG, Zurich,CH) simulating the egg protein, which was served as a drink, and differents foods prepared without proteins. The urine was collected throughout the experimental period, beginning at 8 am and ending at 8 am one day later. The quantity of all the differents nutrients were adapted to the body weight of each volunteer and given in 7 equilibrated meals every two hours during the day.time period. The mixture provided the equivalent of 1 g/kg protein, and the complete diet 125 kJ/kg body weight. Blood was taken at the beginning and end of the experimental period and plasma was stored at −80°C. Urinary nitrogen was determined by the Kjeldahl method. Plasma urea was analysed on an automatic analyser Cobas-Fara (Hoffman-la Roche and Co, AG Roche-Diagnostica, Basle, CH) by an enzymatic method involving urease and glutamate dehydrogenase.

Results and Discussion

Bioavailability of homocyst(e)ine for young rats

The daily weight gain and the growth rate relative to methionine are presented in Table 1. The results were treated by multivariate analysis of variance. The racemic form of either amino acids did not influence the growth of the rat. The replacement of methionine by one of its metabolic precursors, homocystine or homocysteine, modified significantly the growth of the rat ($p<0.001$) but both did so to the same extent. The solubility of homocysteine thiolactone makes it an interesting molecule for parenteral nutrition. The replacement of methionine in experimental diets resulted in a decrease in weight gain of 52% (9% sem) when the sulfur amino acid was present at 0.10% in the diet, and 63% (3%) when present at 0.16%. The relative efficiency of the diets are also given in Table 1. The efficiency of the diet was decreased by 46% (12%) when methionine was replaced by a precursor at 0.10% and by 30% (5%) at the level of 0.16%. These results demonstrate that some growth can be supported by homocyst(e)ine and indicate that homocysteine is converted to methionine which is then incorporated into protein. The relative food conversion efficiency is higher than the relative growth rate (weight gain/day). It demonstrates that the decrease in growth is partially due to a decrease in food conversion efficiency. However, a spontaneous reduction in food intake also occured. In the second experiment, the growth rate obtained was 4.41 (0.26 sem) g/d with L-methionine and 4.40 (0.29) g/day with dietary supplements of vitamin B12, folic acid and choline. When homocystine replaced methionine in the diet, the

Table 1. Growth of young rats fed different methionine precursors for 15 days. Absolute and relative growth rate and relative food conversion efficiency. Means of 6 rats ± S.E.M.

Dietary sulfur amino acid	Level in the diet[a] %	Weight gain per day g/day	Relative growth rate[b]	Relative FCE[b,c] %
L-methionine	0.10	1.19 ± 0.06	100.0	100
	0.16	4.16 ± 0.39	100.0	100
L-homocystine	0.10	0.68 ± 0.09	57.5 ± 0.4	66.8 ± 0.5
	0.16	1.58 ± 0.08	37.9 ± 0.9	73.9 ± 0.2
DL-homocystine	0.10	0.49 ± 0.07	41.5 ± 0.3	43.3 ± 0.6
	0.16	1.65 ± 0.13	39.7 ± 0.9	72.7 ± 0.2
DL-homocystine thiolactone	0.10	0.52 ± 0.04	43.7 ± 0.3	53.0 ± 0.3
	0.16	1.39 ± 0.06	33.5 ± 0.9	64.3 ± 0.2
DL-methionine	0.10	1.22 ± 0.09	102.9 ± 0.8	97.7 ± 0.4
	0.16	3.57 ± 0.31	85.7 ± 1.3	99.5 ± 0.2

[a]The level in the diets is given in methionine equivalent. [b]The relative growth rate and FCE are given in % of the growth and of the FCE obtained with the same level of L-methionine. [c]FCE: food conversion efficiency.

growth rates obtained without and with supplements of cofactors were, respectively. 2.02 (0.17) g/day and 2.12 (0.15) g/day which are equivalent to 45.8% (0.4) and 48.2% (0.5) of the growth obtained with methionine. In the third experiment, the growth rates obtained with diets containing 0.16% L-homocystine in the absence or in the presence of a supplement of methylcobalamine were 2.18 (0.13) g/day and 2.44 (0.15) g/day respectively (NS). These results demonstrate that it is not possible to improve growth by the addition to the diet of high levels of cofactors implicated in the methylation of homocysteine into methionine. The dietary pool of homocysteine can not be totally incorporated into proteins, this intermediate product is partially metabolized by other biochemical pathways.

Bioavailability of homocystine for the adult rat

Since homocystine and homocysteine thiolactone gave the same growth rate in young rats, only homocystine was tested in this case. The absolute and the relative growth rates are presented in Table 2. They demonstrate that some growth is also possible in older animals. The maintenance requirement of 200 g rats is higher than that of 60 g rats, which would explain the low growth rate obtained with 0.10% homocystine. The food conversion efficiency of homocystine relative to methionine is also presented in Table 2. With young rats, the relative food conversion efficiency was higher than the relative growth rate (weight gain/day). This suggests that in addition to the decrease in food efficiency, a reduction in food intake again occured, when homocystine was used to replace dietary methionine.

The protein and fat content of the carcasses of the rats killed at the end of the study was compared with that of the animals killed at the start of the study. This allowed fat and protein gains to be calculated. These results are presented in Table 3 as a function of food intake. They demonstrate that dietary homocystine was preferentially used for protein rather than lipid deposition. The high incorporation of homocystine into protein may be a beneficial factor for its use in clinical nutrition. Cancer patients often suffer from increased muscle protein catabolism, the incorporation in their diet of homocystine would be profitable. All the results presented thus far concern limiting levels of sulfur amino acids in the diet.

In experiment 5, we studied the possibility of compensating for the lack of complete utilisation of homocystine by increasing the amount of this amino acid in the diet. Thus, we compared the growth of 200 g rats fed high levels of methionine with that of rats fed higher levels of homocystine. Because of the appreciable amount of homocystine used in this experiment, and, therefore the cost, DL-homocystine was used rather than its L-isomer. The group receiving 0.56% L-homocystine was included to verify that L- and DL-homocystine are equally bioavailable to the adult rat as they are to the young rat. The growth presented in Fig. 1 was not different (by analysis of variance), for the different groups fed methionine, with the exception of the group fed only 0.16% L-methionine. For the rats fed homocystine (see Fig. 2) the growth curves of the rats fed 0.36%, 0.56%, 0.76% and 0.96% were not significantly different. Thus 0.36% homocystine was

Table 2. Growth of adult rats fed 21 days methionine or homocystine. Absolute and relative growth rate and relative food conversion efficiency. Means of 6 rats ± S.E.M.

Dietary sulfur amino acid	Level in the diet %	Weight gain per day g/day	Relative growth rate %	Relative FCE %
L-methionine	0.10	2.06 ± 0.24	100	100
L-methionine	0.16	5.81 ± 0.46	100	100
L-homocystine	0.10	0.52 ± 0.26	25.2 ± 1.5	34.7 ± 0.4
L-homocystine	0.16	2.38 ± 0.19	41.0 ± 0.6	61.8 ± 0.3

The presentation of data and the abbreviations are the same as that described in the legend of Table 1.

Table 3. Protein and lipid gain during the growth test (expressed as a proportion of food intake). Homocystine utilisation relative to methionine

Dietary sulfur amino acid	Level in the diet %	Protein weight gain / Food intake	Lipid weight gain / Food intake
L-methionine	0.10	0.020 ± 0.003	0.039 ± 0.006
L-methionine	0.16	0.046 ± 0.001	0.055 ± 0.008
L-homocystine	0.10	0.015 ± 0.002	0.010 ± 0.005
L-homocystine	0.16	0.030 ± 0.005	0.317 ± 0.006
Relative utilization of homocystine[a]	0.10	75.8 ± 2.9	25.5 ± 2.7
	0.16	64.6 ± 0.6	56.2 ± 2.4

[a]The relative utilization of homocystine is given in % of the utilization obtained with the same level of methionine.

enough to obtain maximal growth. The groups fed 0.56% of L- and DL-homocystine also had similar growth rates. As for the young rat the racemic form did not influence bioavailability in the adult and allows the groups fed methionine and homocystine to be compared. To determine if an excess of homocystine can replace methionine, we compared the growth rates of each group fed methionine with groups fed a higher level of homocystine. Among these comparisons, only two groups showed a significant difference in growth: the group fed 0.40% L-methionine compared to the group fed 0.56% L-homocystine. However this difference was due in part to a tendancy to a decreased food intake and not only to a

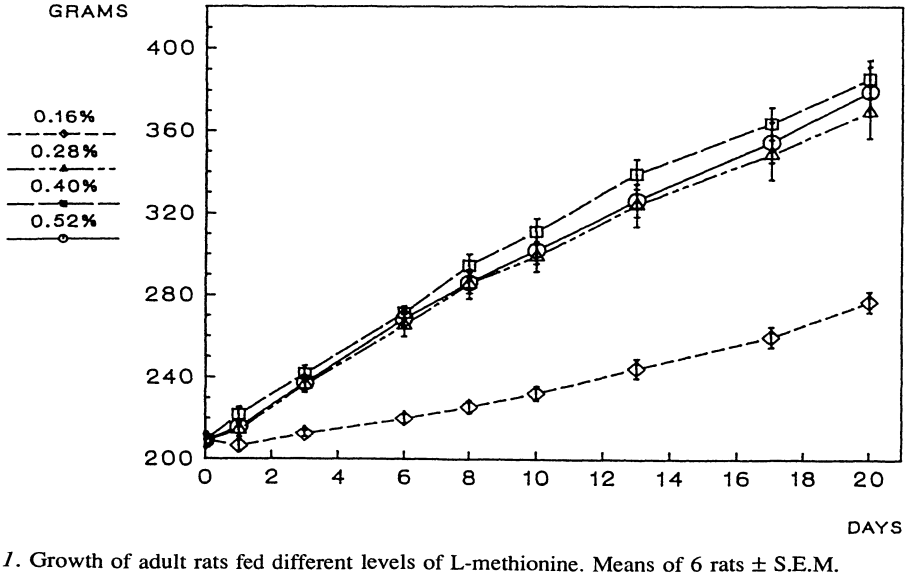

Fig. 1. Growth of adult rats fed different levels of L-methionine. Means of 6 rats ± S.E.M.

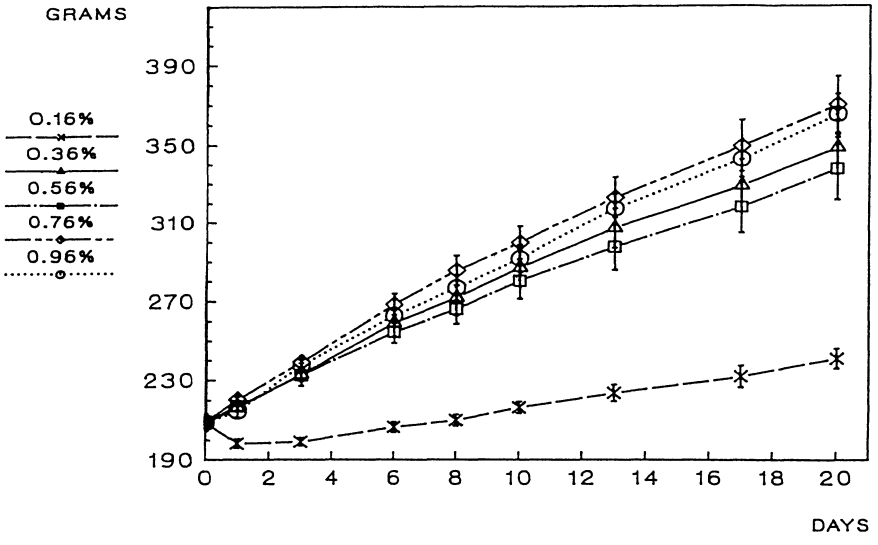

Fig. 2. Growth of adult rats fed different levels of DL-homocystine, expressed as in methionine equivalent. Means of 6 rats ± SEM.

difference in the efficiency of the diet. Thus, maximal growth can be obtained by dietary homocystine in replacement of methionine. The deposition of protein and lipid during the study periods are presented in Table 4 for methionine containing diets and Table 5 for homocystine*. The comparisons made between groups fed methionine and groups fed a higher level of homocystine, indicated some significant differences, but these again are related in part to the tendancy of the rats fed 0.40% methionine to eat more and to be heavier than the rats fed 0.56% homocystine. If one consider all the overall situation, it can be seen that homocystine, at a high level, can totally replace dietary methionine without altering body composition.

Table 4. Total protein and lipid weight gains during the growth test (20 d) of rats fed different levels of L-methionine. Means of 6 rats ± S.E.M.

Dietary level %	0.16	0.28	0.40	0.52
Total weight gain[a] g	69.1 ± 5.8	159.4 ± 12.7	174.5 ± 8.8	166.0 ± 11.3
Protein weight gain g	12.2 ± 0.9	31.9 ± 2.2	32.1 ± 1.4	32.2 ± 1.8
Lipid weight gain g	12.4 ± 2.9	30.5 ± 4.6	35.7 ± 3.9	24.9 ± 3.4

[a]The weight gain presented here is the carcass weight gain.

* At the level of 0.16%, the relative utilization of homocystine for protein deposition was 86.1% (0.4).

Table 5. Total protein and lipid weight gains during the growth test (20 d) of rats fed different levels of DL-homocystine. Mean of 6 rats ± S.E.M.

Dietary level %	0.16	0.36	0.56	0.76	0.96
Total weight gain g	31.4 ± 2.6	137.1 ± 12.4	130.1 ± 15.4	143.6 ± 17.5	137.8 ± 22.1
Protein weight gain g	7.7 ± 0.3	25.8 ± 2.5	24.8 ± 2.7	25.3 ± 4.1	26.7 ± 4.1
Lipid weight gain g	4.1 ± 1.2	26.2 ± 2.1	18.5 ± 4.1	27.1 ± 2.5	22.6 ± 2.3

See footnote *a* of Table 4.

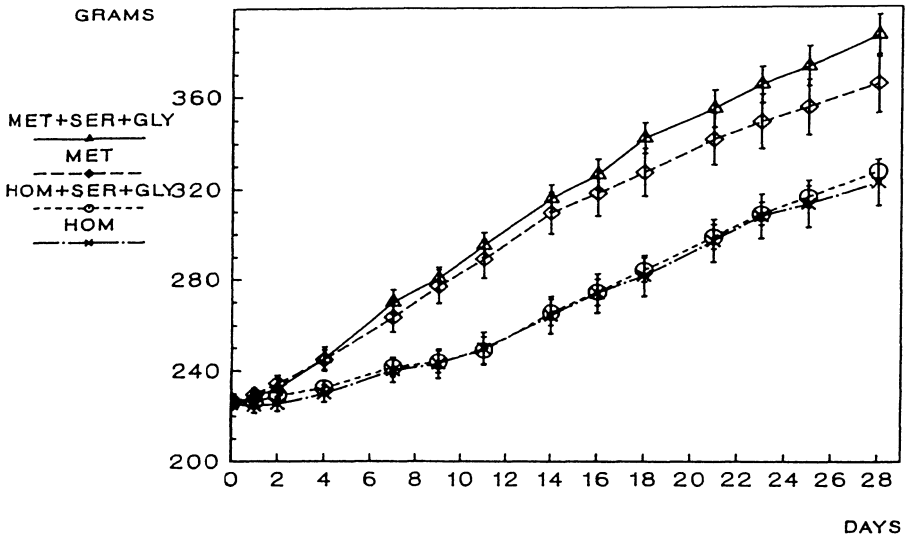

Fig. 3. Growth of rats fed diets without cysteine, containing 0.40% methionine or homocystine, in the presence or absence of serine and glycine. Means of 10 rats ± SEM.

In the last rat experiment, the basal diet did not contain cysteine, serine or glycine. The rate of growth presented in Fig. 3 was not significantly decreased by the absence of serine and glycine. These amino acids are not essential, even when their requirements are increased by the absence of dietary cystine. Hepatic glutathione levels are presented in Table 6. Analysis of variance showed that the absence of dietary serine and glycine had no significant influence on the size of the glutathione pool. The substitution of dietary methionine with homocystine led to a decrease of hepatic glutathione levels, with or without dietary serine and glycine. A possible explanation for this is cellular compartmentation of homocysteine. There is evidence to suggest that homocysteine in the cell is contained in at least two pools one arising from demethylatilon of methionine and the other from conversion

Table 6. Hepatic concentration of glutathione (μmol/g) in rats fed 28 days 0.40 % of methionine or the equivalent in homocystine in the presence or absence of dietary serine and glycine. All diets were exempted of cysteine. Means of 10 rats ± S.E.M.

Dietary sulfur amino acid	with serine and glycine	without serine nor glycine
Methionine	4.30 ± 0.42	3.50 ± 0.21
Homocystine	2.49 ± 0.23	2.27 ± 0.11

Table 7. Nitrogen balance in humans. During the first experimental day, the diet contained no sulfur amino acids; during the second experimental day, it contained homocystine

Volunteer	Nitrogen balance	
	1st exper. day g	2nd exper. day g
1	−1.240	−0.901
2	−3.773	−2.112
3	−1.202	+1.671
4	−2.914	−0.556
5	−1.195	−0.461
6	−2.288	−2.495
Mean ± S.E.M.	− 2.102 ± 0.442	− 0.809 ± 0.602

of homocystine. Thus precursor availability for glutathione synthesis may not be the same in each case. The importance of glutathione in drug and free radical catabolism indicates that this aspect should be studied further in relation to clinical nutrition.

Homocystine bioavailability in humans

The nitrogen balances of all the subjects, as calculated by the method given in reference 12, are presented in Table 7. The results obtained in the absence of dietary sulfur amino acid or with the diet containing homocystine were compared by a paired t-test. The presence of homocystine in the amino acids mixture improved the nitrogen balance significantly. This result demonstrates that homocystine is, at least partially, converted to methionine, which is important to establish before any clinical studies are performed.

References

1. Dethmers JK and Meister A (1981) Proc. Nat. Acad. Sci. USA 78: 7492–7496.
2. Meister A (1984) Nutr. Rev. 42: 397–410.
3. Halpern BC, Clark BR, Hardy DN, Halpern RM and Smith RA (1974) Proc. Nat. Acad. Sci. USA 71: 1133–1136.
4. Halpern BC, Ezzell R, Hardy DN, Clark BC, Ashe H, Halpern RM and Smith RA (1975) In Vitro 11: 14–19.
5. Halpern RM, Halpern BC, Clark BR, Ashe H, Hardy DN, Jenkinson PY, Chou SC and Smith RA (1975) Proc. Nat. Acad. Sci. USA 72: 4018–4022.
6. Ashe H, Clark BR, Chu F, Hardy DN, Halpern BC, Halpern RM and Smith RA (1974) Biochem. Biophys. Res. Comm. 57: 417–425.

7. Tisdale MJ (1980) Br. J. Cancer 42: 121–128.
8. Hoffmann RM and Erbe RW (1976) Proc. Nat. Acad. Sci. USA 73: 1523–1527.
9. Coalson DW, Mecham JO, Stern PH and Hoffmann RM (1982) Proc. Nat. Acad. Sci. USA 79: 4248–4251.
10. Rogers QR and Harper AE (1965) J. Nutr. 87: 267–273.
11. Griffith OW (1985) In: Bergmeyer HU (ed.) Methods of Enzymatic Analysis. Academic Press, New York, Vol. 8, pp. 521–529.
12. Fern EB, Garlick PJ, McNurlan MA and Waterlow JC (1981) Clin. Sci. 61(1): 217–228.

Feeding behavior, growth and tissue amino acids of rats fed diets containing norleucine or homoarginine

Jean K. Tews
Department of Biochemistry, University of Wisconsin-Madison, Madison, WI 53706, U.S.A.

Introduction

Amino acid analogs may interfere with normal metabolism in a variety of ways [1]. Also, analogs such as 2-(methylamino)isobutyrate and 2-aminobicyclo[2,2,1] heptane-2-carboxylate are widely used as specific models for the A and L systems for transport of small and large neutral amino acids (SNAA and LNAA), respectively [2]. Of particular interest is the ability of certain analogs to compete for transport of natural amino acids into various tissues, especially at the blood-brain barrier (BBB) [3–5].

Amino acid transport into brain

We have used the carotid injection technique, in which blood amino acid composition has little effect on uptake [6], to show that transport of LNAA such as valine or histidine was inhibited in the presence of LNAA analogs including norvaline and norleucine; basic amino acids (BAA) were not inhibitory [3]. Similarly, transport of lysine was not affected by LNAA or their analogs, while the BAA analog homoarginine almost completely suppressed lysine passage across the BBB [3].

Transport of valine or lysine from blood into brain in rats, as measured by a constant infusion procedure in which the amino acid composition of the blood affects influx of a given substrate, was also depressed when selected analogs were included in amino acid diets [4]. When rats consumed a diet containing extra valine, its influx into brain was almost fivefold above that observed in rats fed a valine-limiting, control diet. Dietary norleucine caused high plasma levels of norleucine and a 50% depression of valine influx; the concomitant presence of valine partially overcame this effect. Addition of homoarginine to a lysine-limiting diet caused high plasma homoarginine, tended to reduce lysine entry into brain, and completely prevented the 5-fold increase in lysine influx seen when additional dietary lysine was included in the control diet. These effects were specific as equimolar dietary serine (a SNAA) or ornithine (a BAA) had no effect on influx of valine (a LNAA); also, neither tyrosine (a LNAA) nor serine altered influx of lysine. These transport effects are associated with altered feeding behavior and growth of rats and with selective and often striking effects on tissue amino acid profiles.

Feeding behavior and growth

Norleucine, added to a diet containing leucine at 65% and other indispensable amino acids (IAA) at 75% of their requirements for growth of the rat, reduced food intake and weight gain (Table 1A). Extra leucine increased food intake and weight gain of rats fed the norleucine diet, but complete reversal of the norleucine effects was not obtained. Norleucine also depressed food intake and growth when the remaining IAA were 125% of requirements; additional leucine then completely prevented the adverse effects of norleucine (Table 1B). Homoarginine reduced food intake and growth of rats fed a lysine-limiting diet (Table 1C). Supplemental lysine increased weight gain. primarily by raising the efficiency of food utilization rather than by a distinct increase in food intake [7]. Except for additional leucine or lysine, other individual amino acids already present in relative excess should not

Table 1. Food intakes and growth of rats fed an amino acid diet limiting in leucine or lysine without or with added amino acid analogs

Leucine-limiting diet A		
	Food intake (g)	Weight gain (g)
Control	148.4 ± 2.1[a]	39.2 ± 1.1[a]
0.64% Leucine	156.9 ± 5.0[a]	43.2 ± 1.5[a]
1.12% Norleucine	103.2 ± 2.2[b]	15.8 ± 1.6[b]
Norleucine + Leucine	123.2 ± 4.2[c]	28.3 ± 1.5[c]
Leucine-limiting diet B		
	Food intake (g)	Weight gain (g)
Control	123.9 ± 7.8[a]	33.0 ± 3.1[a]
0.64% Leucine	128 ± 4.6[a]	40.5 ± 1.9[b]
1.12% Norleucine	79.6 ± 4.0[b]	7.7 ± 1.4[c]
Norleucine + Leucine	132.1 ± 2.8[a]	46.0 ± 1.7[b]
Lysine-limiting diet C		
	Food intake (g)	Weight gain (g)
Control	128.4 ± 9.0[a]	22.1 ± 1.4[a]
0.88% Lysine·HCl	126.1 ± 5.3[a]	32.9 ± 2.4[b]
1.92% Homoarginine·HCl	89.9 ± 4.0[b]	6.1 ± 1.0[c]
Homoarginine + Lysine	103.4 ± 4.8[b]	16.9 ± 1.4[d]

Control Diet Contained: A) 8% L-amino acids with leucine at 65% and other IAA at 75% of requirements; B) 8% L-amino acids with leucine at 65% and other IAA at 125% of requirements; C) 8% L-amino acids with lysine at 50% and other IAA at 125% of requirements. Additional leucine or lysine raised their levels to 150% of requirements. Within each section different letters indicate significant differences among groups (1-way ANOVA; $P<0.05$); 10-day cumulative values.

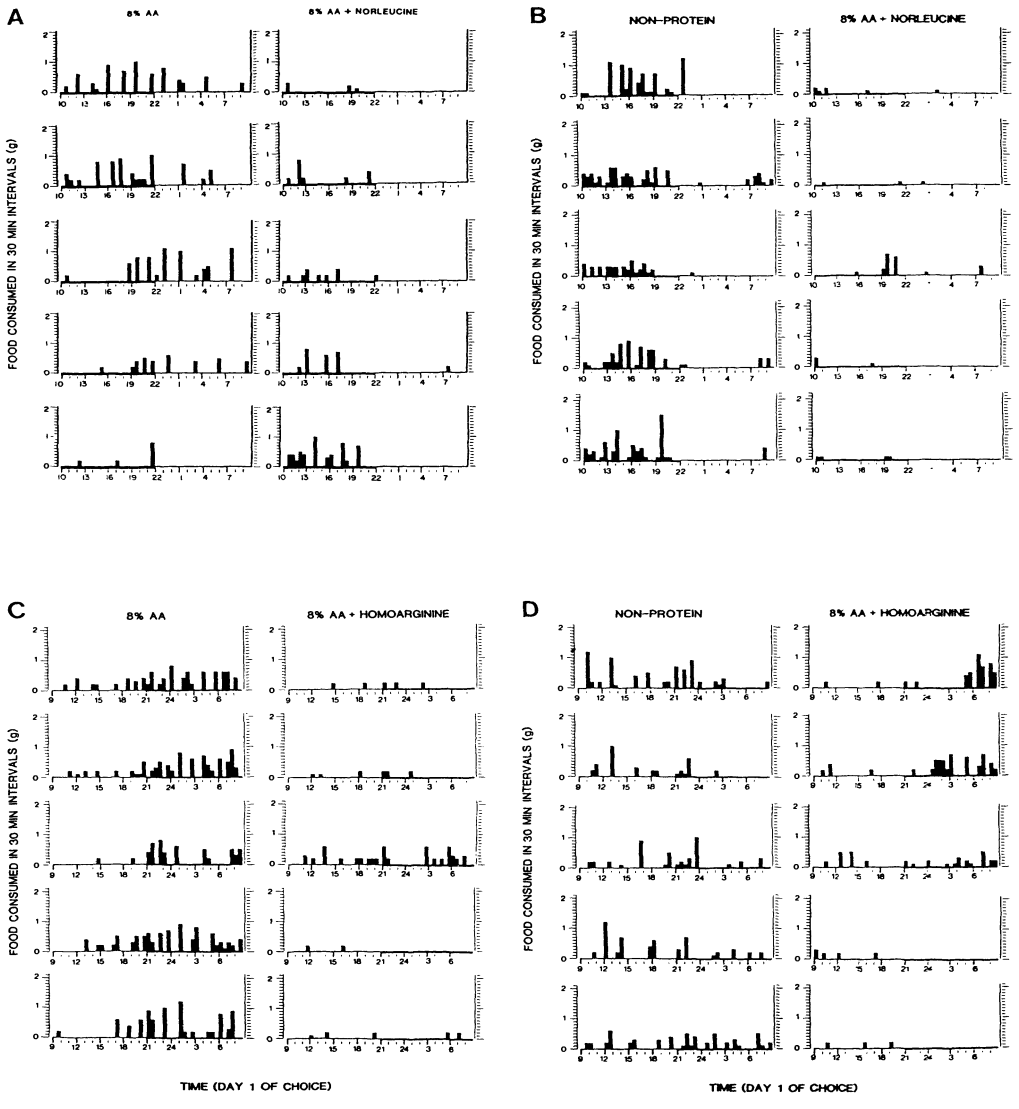

Fig. 1. Feeding patterns on day 1 of rats offered choices between diets shown across top of each section. Diets contained 8% amino acids with leucine at 65% (Fig. 1A, 1B), or lysine at 50% (Fig. 1C, 1D), and other IAA at 125% of requirements; non-protein diet was amino acid-free. Heavy lines on abscissas show 12 h dark period. Results are for separate groups of 5 rats each, with choices by each rat shown individually in the horizontal rows (see ref. 8 for method).

have beneficial effects; additional valine and isoleucine did not reverse the effects of dietary norleucine, and arginine was ineffective vs. homoarginine.

Rats tend to choose diets which will maintain a 'normal' plasma amino acid pattern. Rats generally selected only small amounts of a leucine-limiting diet containing norleucine during the first 12 h of exposure (Fig. 1A). They almost invariably preferred the control diet, especially after the first day, thereby avoiding a high plasma level of norleucine which in turn could interfere with transport of already limiting amounts of leucine into various tissues. These rats later selected a diet containing norleucine + leucine rather than one containing norleucine; however, the same norleucine + leucine diet was often avoided when the succeeding choice was between this diet and one containing extra leucine alone. Rats first offered a choice between the norleucine diet and one containing no amino acids, almost exclusively ate this non-protein diet for a 6-day period (Fig. 1B). However, when other rats had first selected between a non-protein diet and the non-aversive norleucine + leucine diet they clearly preferred the latter diet. They then subsequently chose the norleucine diet (without added leucine) rather than the non-protein diet; 3 rats maintained this preference for 6 days, despite a presumably high plasma content of norleucine, while 2 rats had switched to the non-protein diet. Sequence of diet presentation can thus be important in determining diet choice.

Rats selected a lysine-limiting control diet rather than this diet containing homoarginine (Fig. 1C; [8]); except for one rat, these animals tended to avoid the homoarginine diet on day 1 even more strongly than rats did the norleucine diet in Fig. 1A. Other rats generally selected more of the non-protein than of the homoarginine diet on the first day (Fig. 1D), but later preferred the homoarginine diet (8-fold difference by day 6). After an initial period during which diet taste may have temporarily affected choice, the lysine-limiting homoarginine diet seemed to be less aversive than the leucine-limiting norleucine diet. Rats choosing between leucine-limiting and lysine-limiting control diets selected almost 10-fold as much of the latter diet on day 1 (not shown), consistent with their relative insensitivity to a lysine deficiency [9].

Tissue amino acid profiles: Leucine/norleucine effects

Tissue concentrations of leucine, isoleucine and valine (BCAA) depended on the relative amounts of leucine and the other IAA in the diet (Figs. 2,3). When rats consumed a control diet containing leucine at 65% and other IAA at 75% of the requirements, tissue leucine concentrations tended to be two- to three-fold above those of rats fed a control diet containing leucine at 65% and other IAA at 125% of requirements. Average concentrations of methionine, phenylalanine and histidine (MPH) and BAA were consistently higher in rats fed the larger amounts of IAA. When dietary leucine was fed at 150% of requirement, absolute concentrations of leucine were higher in tissues of rats fed IAA at 75% than at 125% of requirements. Additional dietary leucine induced a marked decline in tissue valine and iso-

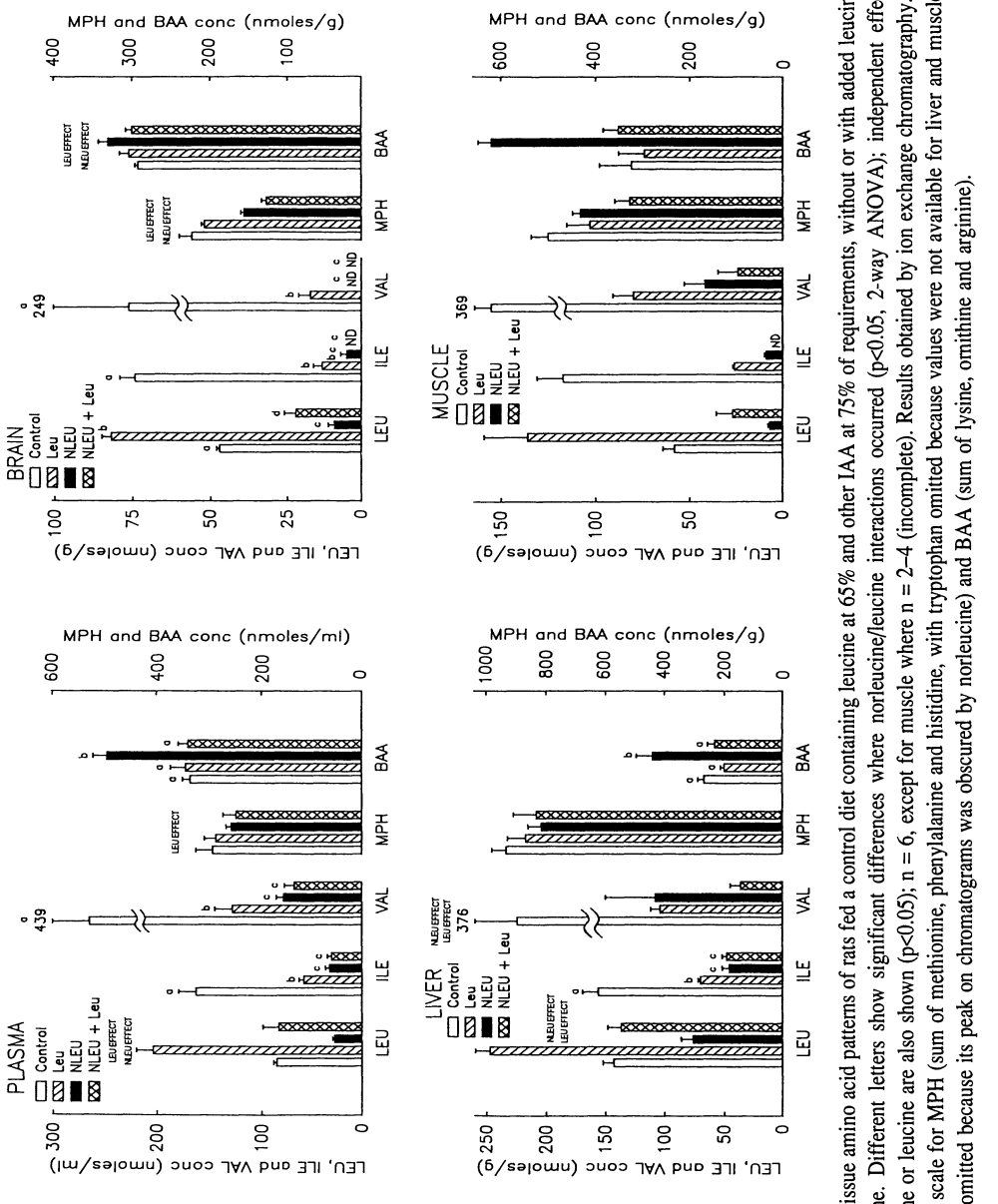

Fig. 2. Tissue amino acid patterns of rats fed a control diet containing leucine at 65% and other IAA at 75% of requirements, without or with added leucine and norleucine. Different letters show significant differences where norleucine/leucine interactions occurred ($p<0.05$, 2-way ANOVA); independent effects of norleucine or leucine are also shown ($p<0.05$); n = 6, except for muscle where n = 2–4 (incomplete). Results obtained by ion exchange chromatography. Note different scale for MPH (sum of methionine, phenylalanine and histidine, with tryptophan omitted because values were not available for liver and muscle, and tyrosine omitted because its peak on chromatograms was obscured by norleucine) and BAA (sum of lysine, ornithine and arginine).

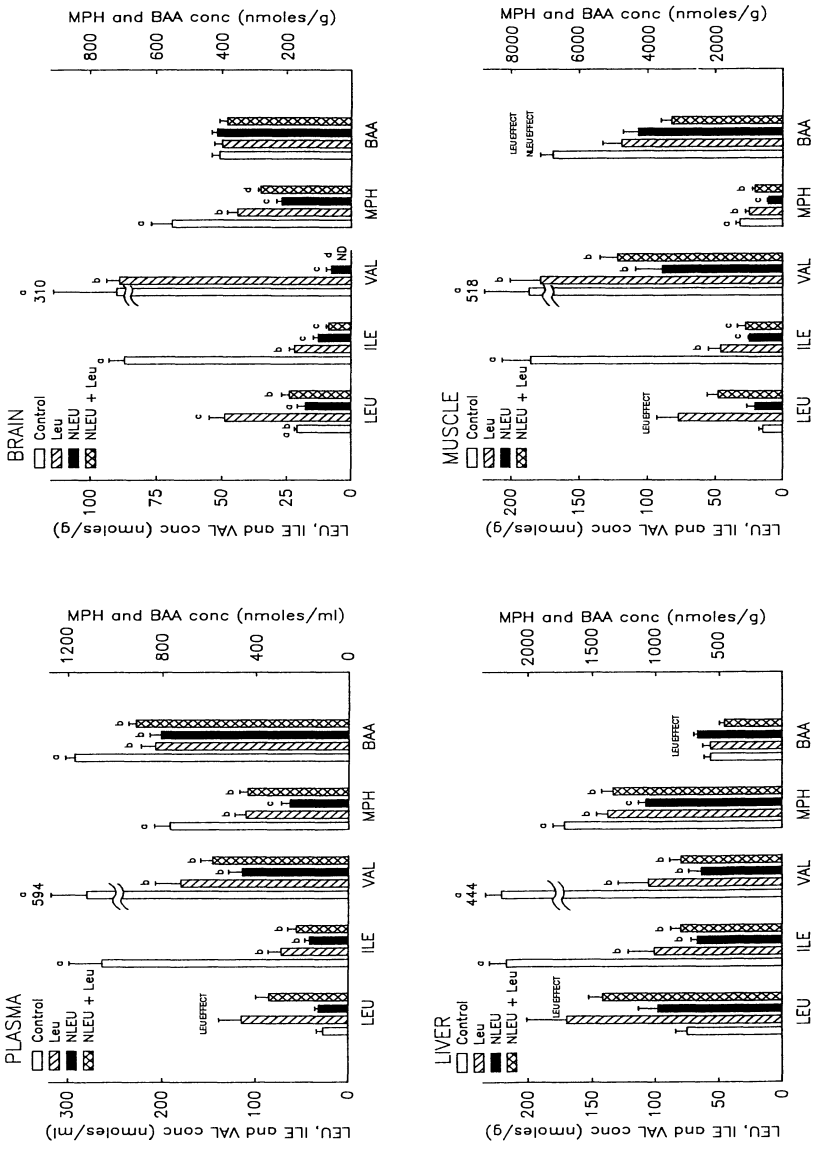

Fig. 3. Tissue amino acid patterns of rats fed a control diet containing leucine at 65% and other IAA at 125% of requirements, without or with added leucine and norleucine. n = 6; other details as in Fig. 2.

leucine, especially in brain in which valine concentration was about 7% (Fig. 2) or 28% (Fig. 3) and that of isoleucine was 18% (Fig. 2) or 25% (Fig. 3) of control values; levels were also low in plasma, liver and muscle. Concentrations of MPH were not always clearly altered by additional dietary leucine.

Norleucine also markedly reduced tissue BCAA when the leucine-limiting diet contained other IAA at 75% of requirement (Fig. 2). Valine was consistently undetectable in brain (<5 nmoles/g) and isoleucine concentration was only 6% of the control value. When norleucine and extra leucine were fed together, the increase in tissue leucine induced by extra leucine alone was completely prevented in plasma and liver; leucine concentration of brain was far below that of the control group not fed extra leucine, and isoleucine and valine were undetectable. MPH levels were only moderately affected by norleucine, while concentrations of BAA were not reduced.

If norleucine was included in the diet with other IAA at 125% of requirements, tissue leucine concentrations did not fall below initially low levels (Fig. 3), although norleucine completely prevented the rise in brain leucine induced by extra dietary leucine alone. Valine and isoleucine concentrations were again greatly reduced in tissues of rats fed norleucine, and were even lower in brain but not in other tissues when extra leucine was also included in the norleucine diet. In tissues of rats fed norleucine alone, MPH concentrations were consistently reduced and BAA levels were unaffected in brain and liver (Fig. 3). SNAA showed little change in the studies of Figs. 2 and 3.

Lysine/homoarginine effects

Plasma lysine concentration of rats fed a lysine-limiting control diet (Fig. 4) was only half that of the rats fed the leucine-limiting control diet containing IAA, including lysine, at 75% of requirements. Raising dietary lysine to 150% of requirement caused large increases in tissue lysine concentrations [7]. Plasma, brain and liver ornithine and brain arginine concentrations were low. Dietary homoarginine raised plasma, liver and muscle lysine content, possibly because of slow hydrolysis via arginase to form lysine and urea [10], but reduced lysine concentrations when dietary lysine was high; under these conditions tissue concentrations of ornithine or arginine were not below those observed in rats fed homoarginine alone.

Comment

We have employed amino acid analogs in attempts to clarify previously observed associations between dietary amino acid modifications and feeding behavior, growth and brain amino acid concentrations. In general, food intake is depressed and food choices are altered if rats are fed a low protein (or amino acid) diet containing disproportionate amounts of amino acids or of various analogs [7,8,11,12]. High plasma levels of the amino acid(s) added to create the dispropor-

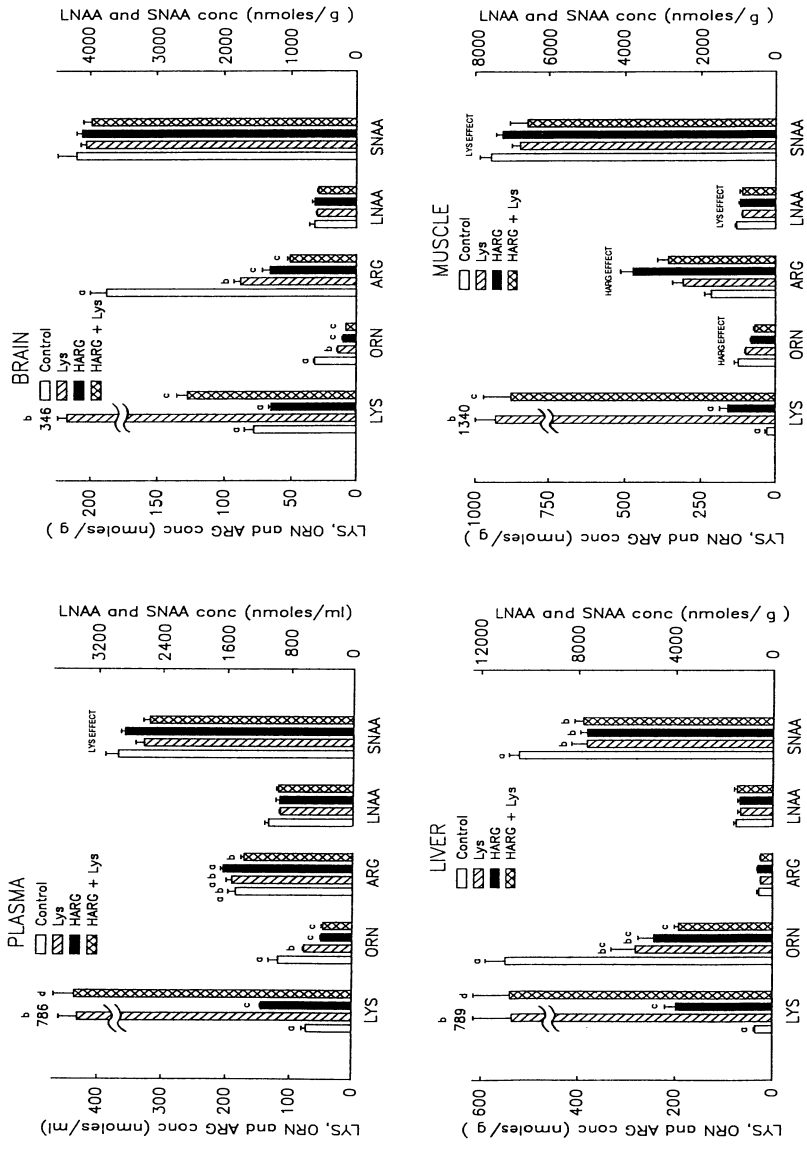

Fig. 4. Tissue amino acid patterns of rats fed a control diet containing lysine at 50% and other IAA at 125% of requirements, without or with added lysine and homoarginine. Note different scale for LNAA (sum of BCAA and MPH) and SNAA (sum of threonine, serine and alanine); n = 6; other details as in Fig. 2.

tion, and depressed levels in plasma [11,13] and especially in brain [13,14] of that amino acid most limiting in the diet usually occur. These effects on brain presumably are related to the high sensitivity of amino acid transport across the BBB to competition from amino acids in the blood [15]. Changes in dietary protein content [16,17] or dietary additions of amino acid analogs [4] selectively affect influx of individual amino acids from blood into brain. Distribution ratios (brain/plasma concentrations) are depressed for the amino acid limiting in the diet (or those closely related metabolically), but are little affected for amino acids of other transport classes. Ratios calculated from Fig. 2 or 3 were markedly lower for each of the BCAA when leucine and norleucine were added to the diet, while ratios for other amino acids were far less affected (MPH) or remained essentially constant (BAA and SNAA); only ratios for the BAA were decreased in the presence of dietary lysine and homoarginine (Fig. 4).

An obvious explanation of the effects of feeding diets containing disproportionate amounts of amino acids is that the selectively depressed concentration in brain of a specific amino acid leads to altered feeding behavior. There generally appears to be a close relationship between these factors, but there may be situations in which rats do not invariably avoid a diet associated with depleted brain levels of an amino acid. Although some rats of Figs. 2 and 3 had non-detectable levels of valine in the brain, they readily consumed the diet causing this condition and grew well; however, it may be important in this situation that the valine content of the diet was well above the requirement for growth of rats. Obviously, rats must regulate their selection and intake of food by some neural mechanism(s). Possibilities include effects of altered blood and hence brain amino acid profiles on synthesis of a brain peptide(s) or protein(s) or of a pertinent neurotransmitter(s).

Amino acid analogs may provide specific models for investigating aspects of amino acid disproportions, while avoiding some of the complications resulting from nutritional and metabolic interactions among the natural amino acids.

References

1. Arfin SM and JS Gantt (1983) Trends Biochem. Sci. 8: 163–164.
2. Christensen HN (1975) Biological Transport. Benjamin, Reading MA.
3. Tews JK and Harper AE (1983) Am. J. Physiol. 245: R556–R563.
4. Tews JK, Greenwood J, Pratt OE and Harper AE (1988) J. Nutr. 118: 756–763.
5. Tovar A, Tews JK, Torres N and Harper AE (1988) J. Neurochem. 51: 1285–1293.
6. Oldendorf WH (1971) Am. J. Physiol. 221: 1629–1639.
7. Tews JK and Harper AE (1986) J. Nutr. 116: 1910–1921.
8. Tews JK, Repa JJ, Lichy R and Harper AE (1987) Nutr. Rep. Int. 36: 989–1002.
9. Bender AE (1961) In: Meeting Protein Needs of Infants and Children (publication 843), pp. 407–424. National Academy of Sciences, Washington D.C.
10. Ryan WL, Barak AJ and Johnson RJ (1968) Arch. Biochem. Biophys. 123: 294–297.
11. Harper AE, Benevenga NJ and Wohlhueter RM (1970) Physiol. Rev. 50: 428–558.
12. Tews JK and Harper AE (1986) J. Nutr. 116: 1464–1472.

13. Peng Y, Tews JK and Harper AE (1972) Am. J. Physiol. 222: 314–321.
14. Tews JK, Kim YWL and Harper AE (1980) J. Nutr. 110: 394–408.
15. Pardridge WM (1983) Physiol. Rev. 63: 1481–1535.
16. Tews JK, Greenwood J, Pratt OE and Harper AE (1987) Am. J. Physiol. 252: R78–R84.
17. Tews JK, Greenwood J, Pratt OE and Harper AE (1987) J. Neurochem. 48: 1879–1886.

Toxicity of D-proline

D. Kampel, R. Kupferschmidt and G. Lubec

Department of Paediatrics and Psychiatry, University of Vienna, Waehringer Guertel 18, A-1090 Vienna, Austria

Abstract

Sprague-Dawley rats, white, female, 150–180g were fed for a period of one month with D-proline (n = 7), L-proline (n = 7), L-lysine (n = 6) in a mean dosage of 50 mg/kg body weight/ day orally in tap water; 10 healthy rats served as controls. The animals were sacrificed after one month by guillotinization.

On autopsy of all the groups no remarkable microscopical changes could be found. In the group fed with D-proline histology of the liver showed severe pathological changes as fibrosis and necrosis of liver cells, histological changes of renal structures revealed severe tubular lesions as the major pathological finding. In the group of L-proline fed animals and healthy controls no histological changes of liver and kidney could be observed.

In the panel fed with L-lysine severe tubular changes were found on histology, no pathological findings of liver sections were detected.

Serum parameters for GOT, GPT, alkaline phosphatase, gamma GT, LDH, HBDH and creatinine were elevated significantly in the groups fed with D-proline and L-lysine as compared to healthy animals and L-proline fed rats.

D-proline was determined in serum, liver, kidney homogenates and rat urine as well as in collagen type IV extracted from the kidney: it could not be detected by chirospecific HPLC using Cyclobond I columns (beta-cyclodextrine).

The highly toxic effect cannot be due to D-proline, which was not found in tissue homogenates and serum. Intestinal bacteria, known to contain high levels and activity of D-amino acid oxidases, proline racemase and D-proline reductase must have been converting or degrading D-proline. We cannot answer the question which mediator has been responsible for renal and hepatotoxicity as D-proline itself could not be found in the corresponding organs.

The toxic effect could be dedicated to an intermediate originating from the conversions of D to L-proline or a toxin formed secondarily or released by an intermediate.

Introduction

Isomers of amino acids are normal constituents of food and the biological environment. It cannot be predicted from the conformation whether an amino acid is toxic in its D or L form. D and L forms differ in its nutritional value, bio-availability, resorption and utilisation [1].

In the specific situation of proline, there are many biological activities reported in literature: Sugahara reported that D-proline is equal to L-proline in promoting growth [2]. Adult and coworkers published the effect of isomers on depolarization of rat spinal motoneurons: D-proline was shown to depolarize spinal roots four

times less than its L-isomers [3]. Pico and coworkers reported that L-proline induced amnesia in chicken in contrast to D-proline [4]. Nadler observed paralleling these results that D-proline destroyed less hippocampal neurons than L-proline [5]. Cherkin described the effect of D-proline on antispreading depression in the chick: L-proline had a shorter latency of pecking and a higher pecking rate than its D-isomer [6]. Another difference in central nervous system activity was found by Cherkin and coworkers: D-proline, injected intraventricularly into chicken produced convulsions and lethality whereas the L-form was non-convulsant [7].

It was the aim of the study to evaluate the toxicity of D-proline to the rat; furthermore it should be investigated whether D-proline can be incorporated into collagen instead of its L-form.

Materials and Methods

Animals

Sprague-Dawley rats, white, female, 150–180 g (Forschungsinstitut fuer Versuchstierzucht, Himberg, Austria) were used in the experiments.

They were given an oral administration of L-proline, D-proline, L-lysine (50 mg/kg body weight/day) into tap water; 10 animals served as controls. They had free access to rat cake and the healthy controls to tap water. They were kept at 23 °C under a day/night rhythm. Animals were sacrificed by guillotinization at the end of the month and the body weight was taken. Autopsy of the animals was performed, biopsies were taken from liver and kidney and used for histology.

Histology

Liver and kidney biopsies were fixed by 10% buffered formaldehyde and stained by hematoxylin-eosin after a standard procedure.

Electron microscopy

Kidney cortices were fixed in buffered glutaraldehyde, Epoxy embedded, cut and stained by osmiumtetroxide after a routine method. Glomerular basement membrane thickness was measured according to a previous publication [8].

Serum parameters

GOT, GPT, gamma GT, alkaline phosphatase, LDH, HBDH, creatinine and serum total protein were determined in serum on a Greiner electronic autoanalyzer according to a standard procedure.

Liver and kidney were homogenized in a Sorvall homogenizer on an ice bath and stored in liquid nitrogen until use.

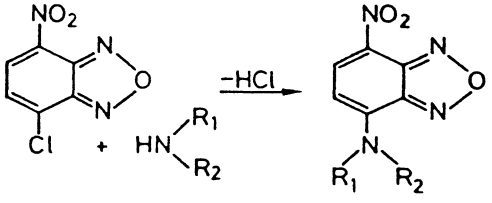

Fig. 1. Derivative formation with Nbd-Cl.

Determination of D-proline and L-proline

A highly sensitive HPLC method was established and the principle is given as follows:

Standards of D- and L-proline (SIGMA P 4266, P 0380) and samples were derivatized by o-phthalaldehyde (PIERCE No.26025): 50 µl of the amino acid standard (or sample) were mixed with 50 µl 0.1 M borate buffer pH 10.4 and 50 µl o-phthalaldehyde (10 mg/ml ethanol) and incubated in the dark for 10 min at 23 degrees C. After this incubation period NBD-Cl (7-chloro-4-nitrobenz-2-oxa-1, 3-diazole] 50 µl (10 mg/ml ethanol) was added and subject to further incubation at the same conditions for 10 min (Fig. 1). After this procedure 50 µl of 70% per-chloric acid (MERCK, 517, Suprapur) were added in order to destroy the OPD derivatives, NBD-Cl-derivatives are stable under these conditions. The resulting precipitate (containing precipitated OPD-derivatives) was spun down in a centrifuge 3000 × g for 5 min. The supernatant was added to the mobile phase (1:10) and 5 µl were injected.

Fluorescence was measured at 535 nm emission and at 465 nm of excitation wavelength. The separation was carried out at room temperature (23 °C) with a mobile phase consisting of 10% (Vol.) methanol (Rathburn, HPLC grade) and 90% TEA (1%) acetate buffer ph 6.0.

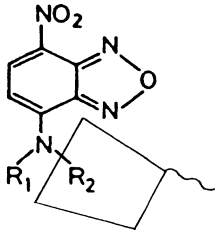

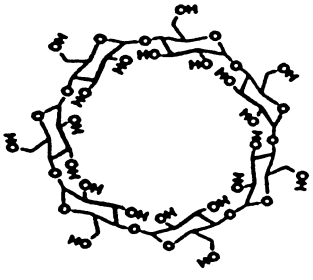

Beta-Cyclodextrin

Fig. 2.

The column used was a Cyclobond I (250 + 100) × 4.6 mm (ASTEC) Inc., Whippany, N.J., USA. The flow applied was 0.4 ml/min.

The mechanism of the enantiomeric separation on the bonded beta-cyclodextrinphase can be explained by the formation of an inclusion complex of the amino acid derivatives within the beta-cyclodextrin cavity. Hydrogen bonding of the samples' polar residues to the beta-cyclodextrin hydroxyl functions can take place. This interaction with the chiral carbons of the beta-cyclodextrin might explain the selectivity of this stationary phase (Fig. 2).

50 µl of the homogenates (50 µl of deproteinized serum, 50 µl collagen hydrolyzate and 50 µl of ion exchanged rat urine) which were adjusted to a protein concentration of 100 mg/ml were derivatized and subject to separation.

Isolation of collagen type IV from rat kidneys

The isolation procedure was performed according to the principle of Dixit [9]. 1 mg of each collagen sample isolated from the kidney was used for acid hydrolysis (6 N HCl, 16 h at 105 °C). The samples were evaporated to dryness and redissolved in distilled water. 50 µl were used for HPLC as given above.

For comparison of groups Tukey's studentized range (HSD) test was applied [10].

Results

There were no significant differences in body weight at the end of the study ($p = 0.09$).

On autopsy no macroscopical changes could be observed.

Histological changes

a) On liver sections animal organs treated with L-proline, L-lysine and healthy controls did not show any pathological changes. Animals treated by D-proline showed periportal fibrosis and necrosis of liver cells.
b) On kidney sections animal organs treated with L-proline and healthy animals showed normal histoarchitectonics and structure and no pathological changes. In the L-lysine as well as in the D-proline treated group severe proximal tubular dystrophy and necrosis was observed. Glomerular mesangial crescents were observed in those panels.

Electron microsopical studies

The extracellular matrix of the kidney was without pathological findings. The glomerular basementmembrane thickness measured after the principle given in a previous publication was not different between the groups.

Serum parameters

The results of serum parameters for GOT, GPT, alkaline phosphatase, gamma GT, LDH, HBDH, creatinine and serum total protein are given in Table 1.

HPLC determinations

Baseline separation was obtained for the proline isomers. As given in Fig. 3 two clearly discriminated peaks were observed after a retention time of 53 min for D-proline and 56 min for L-proline at an isocratic run.

D-proline could not be detected in serum , the homogenates of liver and kidney, the collagen hydrolyzate and rat urine.

D-proline, however, could be found in homogenates spiked with D-proline.

Discussion

As given in the results D-proline turned out to be a highly toxic amino acid isomer to the rat.

Previous studies on the toxicity of D-proline revealed the neurotoxic effect only as described above. Studies on toxic effects of D-proline on other organ systems were not reported. As revealed by histomorphological examinations D-proline (DP) in our study showed severe renal tubular lesions. These morphological changes were comparable to tubulotoxic effects of L-lysine, found in our study confirming previous observations given by Racusen and coworkers [11]. L-proline in the same dosage failed to produce renal toxicity. Serum creatinine as an indicator of renal damage was significantly increased in the D-proline and L-lysine groups. The

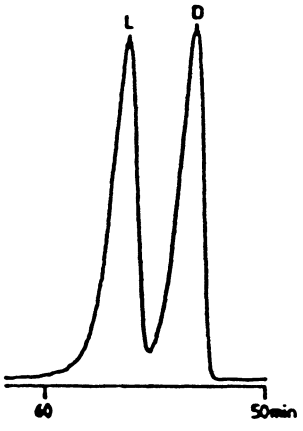

Fig. 3. Separation of D- and L-proline on CB I column.

Table 1a. Means and standard deviation of serum parameters

	GOT	GPT	Alkaline phosphatase	Gamma GT	LDH	HBDH	Serum protein	Creatinine
Controls	30 ± 15	35 ± 22	89 ± 22	62 ± 20	180 ± 51	68 ± 33	6.8 ± 0.3	0.9 ± 0.3
DP	493 ± 227	224 ± 107	222 ± 87	268 ± 91	447 ± 225	205 ± 55	6.3 ± 0.5	2.0 ± 0.6
LP	28 ± 10	29 ± 12	79 ± 13	66 ± 22	184 ± 30	56 ± 22	6.5 ± 0.6	0.9 ± 0.3
LL	95 ± 30	102 ± 59	191 ± 94	56 ± 21	172 ± 34	49 ± 27	6.8 ± 0.3	1.5 ± 0.2

Table 1b. Results of Tukey's studentized range HSD test on serum parameters (s = $p<0.05$)

	GOT	GPT	Alkaline phosphatase	GammaGT	LDH	HBDH	Serum protein	Creatinine
C vs DP	s	s	s	s	s	s	ns	s
C vs LP	ns	ns	ns	ns	ns	ns	ns	s
C vs LL	ns	ns	s	ns	ns	ns	ns	s
DP vs LP	s	s	s	s	s	s	ns	s
DP vs N	s	s	s	s	s	s	ns	s
DP vs LL	s	s	ns	s	s	s	ns	ns
LP vs DP	s	s	s	s	s	s	ns	s
LP vs N	ns	ns	ns	ns	ns	ns	ns	ns
LP vs LL	ns	ns	s	ns	ns	ns	ns	ns
LL vs DP	s	s	ns	s	s	s	ns	ns
LL vs LP	ns	ns	s	ns	ns	ns	ns	ns
LL vs C	ns	ns	s	ns	ns	ns	ns	s

mechanism for the renal damage is suggested and described by Racusen as tubular obstruction [11]. It is in addition highly probable that another mechanism could lie in the block of tubular reabsorption which was found for lysine by Mogensen and coworkers [12]. Lysine and D-proline are sharing the basic and nucleophilic properties. Electron microscopy of renal extracellular matrix did not reveal structural abnormalities.

The nephrotoxic effect of another D-amino acid was reported by Kaltenbach and coworkers: renal tubular necrosis was found in rats (not in hamsters, dogs, guinea pigs, rabbits, mice) after the administration of D-serine [13]. The authors described however the nonnephrotoxic effect of D-threonine, D-homoserine, D-alanine, D-cysteine etc. Thus concluding that the D-conformation alone is not responsible for toxicity.

Histology of liver sections revealed normal morphology in controls, L-lysine and L-proline treated animals. On liver sections of D-proline periportal fibrosis and hepatocellular necrosis were detected. These morphological changes were accompanied by serum parameters of liver damage: GOT, GPT, alkaline phosphatase, HBDH and gammaGT were significantly elevated in D-proline fed animals and in L-lysine fed rats, which, however, did not reveal morphological alterations. Hepatotoxicity was described for a series of D-amino acids to name but D-ethionine in mice [14].

The reason for LDH and HBDH elevation in rat plasma of D-proline treated rats could be interpreted as induction of hemolysis in those animals. Hemolysis was found after the administration of D-OH-methionine in the chick system [15].

HPLC results are clearly indicating that D-proline itself could not be detected in serum, liver and kidney homogenates, was not incorporated into the glomerular basement membrane collagen and not excreted into urine. This observation rises the question wether D-proline is present transiently in those specimen with subsequent degradation or a toxic intermediate is formed by the conversion of D-proline to L-proline. These effects on D-proline are under physiological circumstances obtained by the activity of intestinal bacteria. High activities and concentrations of D-amino acid oxidases (E.C. 1.4.3.3.) are acting in the mammalian intestine. D-proline incubated with D-amino acid oxidase can lead to two possible reaction products: a) the oxidation derivative of D-proline, 1, 2-dehydroproline, or, after ring cleavage, to the alpha-oxo-acid [16]. An intermediate resulting from these conversions, not detected in our system, could be responsible for the toxic effects.

Proline racemase (E.C.5.1.1.4.) purified from Clostridium sticklandii leads to conversion only by dissociation and re-formation of the alpha-carbon-hydrogen bond [17]. Intermediates of this enzymatic reaction could have been detected in our system.

Delta-aminovaleric acid derived after ring cleavage catalyzed by D-proline-reductase (E.C.1.4.1.6.), first described by T.C. Stadtmann in 1957 [18], could be another possible toxic intermediate.

The possibility that a mediator of tissue injury was released by D-proline is theoretically existing as well.

There was no influence of D-proline, L-proline, L-lysine on body weight and growth ruling out severe nutritional influences.

We are concluding that feeding of rats with D-proline leads to severe renal and hepatic damage though the substance itself could not be found neither in the damaged organs, nor in serum and urine. An unknown intermediate or release of mediators for tissue injury are incriminated as the interpretation that D-proline itself is present transiently is highly inprobable.

References

1. Sunde ML, (1972) Poultry Science 51: 44–55.
2. Sugahara M, Morimoto T, Kobayashi T and Ariyosi S (1967) Agr. Biol. Chem. 31: 77–84.
3. Ault B, Wang Ch.M and Yawn BC (1987) Br. J. Pharmac. 92: 319–326.
4. Pico RM, Keller E, Cherkin A and Davis JL (1983) Development Brain Research 9: 227–230.
5. Nadler JV, Wang A and Hakim A (1988) Brain Research 456: 168–172.
6. Cherkin A and Van Harreveld A (1978) Brain Research 156: 265–273.
7. Cherkin A, Davis JL and Garman MW (1978) Pharmacology Biochemistry & Behaviour 8: 623–625.
8. Lubec G, Kitz K and Adamiker D (1979) Renal Physiol. 2: 79–82.
9. Dixit SN (1979) FEBS Lett. 106: 379–387.
10. SAS User's Guide (1982) Alice Allen Ray (ed.), Cary NC, USA.
11. Racusen LC, Finn WF, Whelton A and Solez K (1985) Kidney International 27: 617–522.
12. Mogensen CD and Solling K (1977) Scand. J. Clin. Lab. Invest. 37: 477–486.
13. Kaltenbach JP, Ganote CE and Carone FA (1979) Exp. Mol. Pathol. 30: 209–214.
14. Friedman MA, Berry DE and Elzay RP (1977) Cancer Lett. 3: 71–76.
15. Baker DH and Boebel KP (1980) J. Nutr. 110: 959–964.
16. Dixon M and Kleppe K (1965) Biochim. Biophys. Acta 96: 357–367.
17. Cardinale GJ and Abeles RH (1968) Biochemistry 7(11): 3970–3978.
18. Stadtman TC and Elliott P (1957) JBC 228: 983–997.

D-Amino acids as ubiquitous constituents in fermented foods

Hans Brückner and Michael Hausch

Institute of Food Technology, University of Hohenheim, D-7000 Stuttgart 70, F.R.G.

Abstract

Fermented foods such as Trappist cheese, Parmesan cheese, curdled milk, fermented juices of cabbage and carrots, beer, red wine, vinegar, cacao, tea, soy sauce and Miso have been investigated quantitatively for their total contents of free amino acids (AA) and D-AA. For analyses, the foodstuffs were deproteinized by addition of picric acid, defatted with a mixture of light petroleum/diethyl ether, and decolorized if necessary by treatment with polyamide-6; the free amino acids were then absorbed on Dowex WX 8 cation exchanger and desorbed by aqueous ammonia. For the determination of the total amount of AA automated amino acid analysis by ion-exchange chromatography the Stein and Moor procedure was used.

Determination of the ratio of D- and L-AA was performed as their N(O)-pentafluoropropionyl AA 1-(and 2-) propyl esters by employing gas chromatography with fused silica capillary columns coated with the chiral stationary phases 'Chirasil-L-Val' or 'XE-60-L-Val-(S-)-α-phenylethylamide'. From these analyses the absolute amount of D-AA was calculated. It is shown that all fermented foods contain D-AA, from as much as totally 404 mg D-AA in 100 g Parmesan cheese, to as little as 0.28 mg D-AA in 100 ml of a German beer. From the results it is concluded that D-AA are common in fermented foods and originate from microorganisms which are added as either starter cultures in food processing or which are involved in traditional fermentation processes. The ubiquitous presence of free D-AA in fermented foods has to be taken into account when the nutritional, sensorial and physiological aspects of fermented foods are discussed.

Introduction

It has been shown and investigated in detail that treatment of proteinaceous food or food proteins under certain technologically relevant or experimental conditions causes the epimerization (usually refered to as racemization) of protein (peptide)-bonded L-amino acids (L-AA) [1–3]. The formation of D-amino acids (D-AA) has consequences with regard to nutritional, including possible toxicological, physiological and food technological aspects [4]. In the majority of instances, relatively drastic treatment of food proteins is necessary in order to obtain significant effects, and these conditions are frequently far beyond those of accepted manufacturing practice. We have recently shown, however, that even a relatively mild treatment, such as heating gelatin in water, causes the formation of surprisingly high amounts of D-Asp in this food protein and that free D-amino acids are present in fermented dairy products such as yogurt and kefir [5,6]. As shown in this paper, extension of our analytical methodologies for sample work-up and enantioseparation of AA to a great variety of foods in which fermentation processes are involved revealed that D-AA are ubiquitous constituents in fermented foodstuffs.

Materials and Methods

Instruments

Gas-liquid chromatography (GC) was carried out by using the following instruments and chiral capillary columns: A. Model HRGC 5160 gas chromatograph (Carlo Erba, Milan, Italy) and a Chirasil-L-Val column (25 m × 0.25 mm. i.d., Macherey Nagel, Düren, F.R.G.); B. same instrument but with a Chirasil-L-Val column having a different elution profile as compared to A. (C.G.C. Analytic, Mössingen, F.R.G.); C. Model Mega 4100 gas chromatograph (Carlo Erba) and a XE-60-L-Val-S-α-phenylethylamide column (50 m × 0.22 mm i.d. (Chrompack, Middelburg, The Netherlands). The instruments were equipped with a flame ionization detector (FID), a Model 410 LT programmer, an EL 440 electrometer, and a Chromatopac C-R3A integrator-printerplotter (Shimadzu, Kyoto, Japan). Temperature injector and detector, 250°C; split injection, split ratio approx. 1:30; temperature program: column A, 5 min at 80°C, then at 4°C/min to 128°C, 4 min at 128°C, then at 4°C/min to 155°C, then at 5°C/min to 195°C, then 10 min at 195°C; column B, 5 min at 70°C, then at 3.5°C/min to 195°C, then 10 min at 195°C; column C, 3 min at 95°C, then at 4.5°C to 190°C, then 20 min at 190°C. Carrier gas, hydrogen; pressure, A., B., 450 kPa, C., 1100 kPa. For automated amino acid analysis by ion-exchange chromatography (IEC) a Biotronik LC 6001 amino acid analyzer (Braun Diesel, Melsungen, F.R.G.) was used with lithium citrate buffers, postcolumn derivatization of amino acids with ninhydrin and an elution program for the separation physiological amino acids.

Origin of food samples

The food samples investigated (Parmesan cheese, curdled milk, lactic acid fermented cabbage and carrots, beer, red wine, vinegar, cacao powder, tea, and fermented soy products) were commercial products and are specified in detail in Table 1. Trappist cheese was manufactured at the Dairy of the University of Hohenheim from cow milk and by use of a freeze-dried starter culture containing *Streptococcus cremoris, Str. lactis, Str. diacetylactis, Leuconostoc cremoris* (Laboratorium Wiesby, Niebüll, F.R.G.) and a commercial culture of read smear (Drewes, Seesen, F.R.G.).

Preparation of food samples

(a) Fifteen grammes of curdled milk were suspended in 45 ml of methanol/water (8:2), stirred for 10 min at ambient temperature, centrifuged at 1630 × g, and the supernatant was concentrated *in vacuo* to a volume of approx. 10 ml. For the further treatment, method (aa) was applied: 10 ml of a saturated aqueous solution of picric acid were added, the mixture was centrifuged at 1630 × g, the supernatant was diluted with water to a volume of approx. 60 ml, and extracted three times with

20 ml portions of light petroleum (b.p. 40–60°C)/diethyl ether (1:1). The aqueous phase was evaporated *in vacuo* to a volume of approx. 10 ml and passed through a column packed with Dowex 50 WX 8 cation exchanger (particle size, 200–400 mesh, Serva, Heidelberg, F.R.G.). After washing the ion exchanger with dist. water, the amino acids were eluted with approx. 30 ml of 2 N aqu. ammonia, the eluate was evaporated to dryness, and aliquots were subjected to derivatization for gas chromatography and amino acid analysis by means of the Biotronik amino acid analyzer. For the investigation of Trappist cheese, Parmesan cheese, Miso, cacao powder, and tea leaves, 5 g each of the ground materials were suspended in 70 ml of water, stirred for 30 min at 50°C and, after addition of 30 ml methanol, stirred for another 15 min at 50°C, and then centrifuged at 1630 × g. The supernatants were treated as described under (aa). To 10 ml each of beer, vinegar, and lactic acid fermented cabbage and carrots juice, 10 ml of a saturated solution of picric acid were added and the mixture was treated as described under (aa). To 10 ml each of Italian balsamic vinegar and French red wine, 10 ml of a saturated solution of picric acid were added and the mixture was centrifuged and extracted with light petroleum/diethyl ether as described under (aa). After evaporation to volumes of approx. 10 ml, the pH was adjusted to approx. 2 by addition of 0.1 M HCl, the solution decolorized by use of a column packed with polyamide-6 powder (Serva, Heidelberg, F.R.G.), and the eluate subjected to Dowex 50 WX 8 as described above. To 2 ml of soy sauce, 2 ml of saturated picric acid were added, the resulting mixture was filtered by means of a cellulose filter; the filtrate was defatted with organic solvents, treated with polyamide-6, and subjected to Dowex WX8 as described above for balsamic vinegar and red wine.

Amino acid analyses by GC IEC

For GC, to approx. 3 mg samples of amino acid mixtures in 1 ml 'reacti vials' (Wheaton, Millville, NJ, U.S.A.) 200 µl of 1-propanol/acetyl chloride (8:2), or 200 µl of 2-propanol/acetyl chloride (8:2), and approx. 1.5 mg of the antioxidant 2.6-di-*tert*-butyl-*p*-cresol (BHT, Fluka) were added. The vials were then tightly closed with teflon-lined screw caps and the mixtures were heated at 100°C for 1 h. Solvents were removed in a stream of nitrogen, 200 µl of dichloromethane (DCM) and 50 µl of pentafluoropropionic anhydride (Pierce, Rockford, IL., U.S.A.) added and the mixture was heated at 100°C for 20 min. Solvents were removed in a stream of nitrogen and the residues dissolved in 50 to 100 µl of DCM. Aliquots of approx. 0.6 µl were subjected to GC in the split mode. For IEC, food samples were treated separately as described for GC, with the exception that α-aminoguanidino-propionic acid (Pierce) was added to the samples at the beginning to serve as internal standard. The residue obtained after treatment with Dowex WX8 as described above was dissolved in 5 ml of pH 2.2 lithium citrate buffer and aliquots of 50 µl were subjected to IEC.

Results and Discussion

The total amounts of AA as determined by IEC and the kinds and amounts of D-AA as determined by GC and found in the various types of food are compiled in Table 1 and selected gas chromatograms are shown in Figs. 1a–f. It can be seen that Parmesan cheese has about seven times as much free AA as Trappist cheese. This is attributed to the much longer ripening time of the former (usually 1–2 years) as compared to the latter (5 weeks). Consequently, the amount of D-AA is about ten times higher in Parmesan cheese than in Trappist cheese. L-allo-Ile which is found in Trappist cheese (Fig. 1a) is not found in Parmesan cheese. This AA, however, is also found in curdled milk that has, as a result of the short treatment with starter cultures, a very low content of D-AA. D-allo-Ile is found in lactic fermented juices of cabbage and carrots (Table 1 and Fig. 1b). In addition to a number of D-AA, interestingly γ-aminobutyric acid (GABA) is found in lactic fermented cabbage juice (cf. Fig. 1b). This AA is also found in beer, vinegar and cacao. Red wine, as compared to beer, contains a relatively smaller amount of D-AA and L-pipecolic acid (L-Pip) can be seen in the chromatogram of the latter. The absolute amount of D-AA in two types of vinegar is about the same as that of red wine. In vinegar made from red wine, in contrast to red wine itself, D-Pro and about equal amounts of D- and allo-Ile are found (Table 1). Tea contains about five times as much free amino acids as cacao. The relative amount of D-AA of the latter, however, is about twice that of tea. Furthermore, the kinds of D-AA found in cacao show a greater diversity as compared to those of tea (Fig. 1e). The total amount of free amino acids in the fermented soy products Miso and soy sauce are roughly equal. However, the amount of DAA in soy sauce is about four times that in Miso and D-allo-Ile is found only in soy sauce. No D-Ala was found in Miso, in contrast to all other fermented foods investigated (cf. Table 1). From Table 1 it can be seen that the absolute, combined amount of D-AA ranges from 404 mg/100 g (Parmesan cheese) and 187 mg/100 g (soy sauce) to 0.28 mg/100 ml ('Altbier').

From these results, the question arises as to the origin of D-AA in fermented foods and possible nutritional and food technological aspects. It is assumed that free D-AA in fermented foods originate as a result of the action of microorganisms i.e. bacteria, yeasts, and fungi. This is supported by the fact that D-Ala, D-Asp, and D-Glu, in particular, which occur in all fermented foods, are among the constituents of the peptide moieties of the peptidoglycans that form the bacterial cell walls [7]. The determination of oligopeptides containing D-AA is therefore routinely used for the chemotaxonomical assignment of bacteria species and strains [7]. Moreover, the D-enantiomers of almost all protein AA have been found to be constituents of various microbial peptides, in particular peptide antibiotics [8]. It is also likely that bacterial amino acid racemazes and epimerases are involved in the formation of D-AA in fermented foods [9]. From nutritional points of view, D-AA do not contribute to the nutritional value of foods and their amount should thus be subtracted from the total amount of AA in

Table 1. Free D-amino acids[a] and L-allo-Ile in fermented foods

Amino acid	Dairy products					
	Trappist cheese[e,f]		Parmesan cheese[g]		Curdled milk[h]	
	rel. amount (%)	abs. amount[d] (mg/100 g)	rel. amount (%)	abs. amount (mg/100 g)	rel. amount (%)	abs. amount (mg/100g)
D-Asx[b]	12.0	1.08	13.8	49.0	14.1	0.25
D-Glx[b]	15.7	22.9	5.4	69.2	4.0	0.58
D-Ala	16.4	7.08	42.5	173	38.6	0.46
D-Leu	0.4	0.57	10.2	88.4	18.4	0.15
D-Val	–	–	4.6	23.5	6.8	0.04
D-allo-Ile[c]	–	–	–	–	17.1	0.02
L-allo-Ile[c]	19.9	10.3	–	–	–	–
D-Lys	1.6	2.10	–	–	3.1	0.13
D-Ser	–	–	0.2	0.99	–	–
free amino acids (total)	939 mg/100 g		7302 mg/100 g		36.8 mg/100 g	
free D-amino acids	44.0 mg/100 g		404 mg/100 g		1.63 mg/100 g	

Amino acid	Fermented vegetables			
	Cabbage juice[e,i]		Carrot juice[j]	
	rel. amount (%)	abs. amount (mg/100 ml)	rel. amount (%)	abs. amount (mg/100 ml)
D-Asx[b]	3.3	1.24	0.9	0.97
D-Glx[b]	10.1	6.02	5.0	1.69
D-Ala	8.8	7.38	13.5	6.42
D-Leu	5.2	0.99	13.8	0.56
D-Val	1.0	0.30	8.2	0.72
D-allo-Ile[c]	7.0	1.51	19.0	0.93
L-allo-Ile[c]	–	–	4.0	0.19
D-Lys	5.9	0.68	–	–
D-Ser	1.5	0.43	–	–
D-Phe	–	–	4.9	0.18
D-Met	–	–	17.7	0.11
free amino acids (total)	502 mg/100 ml		311 mg/100 ml	
free D-amino acids	18.6 mg/100ml		11.8 mg/100 ml	

Table 1. (continued)

Amino acid	Alcoholic beverages			
	Beer[e,k]		Red wine[l]	
	rel. amount (%)	abs. amount (mg/100 ml)	rel. amount (%)	abs. amount (mg/100 ml)
D-Asx[b]	32.5	0.11	3.8	0.44
D-Glx[b]	14.4	0.06	2.2	0.34
D-Ala	12.6	0.11	3.2	0.77
free amino acids (total)	40.7 mg/100 ml		215 mg/100 ml	
free D-amino acids	0.28 mg/100 ml		1.55 mg/100 ml	

Amino acid	Vinegars			
	Aceto balsamico[e,m]		Vinegar[n]	
	rel. amount (%)	abs. amount (mg/100 ml)	rel. amount (%)	abs. amount (mg/100 ml)
D-Asx[b]	4.1	0.41	12.2	0.09
D-Glx[b]	2.3	0.22	10.5	0.18
D-Ala	4.5	0.50	20.3	0.48
D-Leu	1.9	0.09	5.5	0.11
D-Val	1.2	0.06	2.4	0.04
D-allo-Ile[c]	–	–	8.4	0.10
D-allo-Ile[c]	–	–	9.8	0.12
D-Pro	–	–	2.4	0.38
D-Phe	2.1	0.09	–	–
free amino acids (total)	189 mg/100 ml		33.3 mg/100 ml	
free D-amino acids	1.37 mg/100 ml		1.50 mg/100 ml	

Table 1. (continued)

Amino acid	Stimulants			
	Cacao powder[e,o]		Tea[p]	
	rel. amount (%)	abs. amount (mg/100 g)	rel. amount (%)	abs. amount (mg/100 g)
D-Asx[b]	9.3	1.45	1.1	2.19
D-Glx[b]	4.0	0.34	0.6	0.93
D-Ala	14.5	2.28	1.4	0.56
D-Leu	3.8	0.73	–	–
D-Val	1.2	0.17	–	–
D-allo-Ile[c]	3.1	0.33	–	–
D-Pro	2.3	0.63	–	–
D-Phe	4.0	0.63	–	–
D-Tyr	4.2	0.55	–	–
D-Ser	5.3	0.33	–	–
free amino acids (total)	172 mg/100 g		827 mg/100 g	
free D-amino acids	7.44 mg/100 g		3.68 mg/100 g	

Amino acid	Asian type of fermented foods			
	Soy sauce[e,q]		Miso[r]	
	rel. amount (%)	abs. amount (mg/100 g)	rel. amount (%)	abs. amount (mg/100 g)
D-Asx[b]	11.7	47.8	7.8	24.1
D-Glx[b]	5.0	51.2	3.1	13.8
D-Ala	4.8	22.5	–	–
D-Leu	12.6	22.7	–	–
D-allo-Ile[c]	7.4	7.14	–	–
D-Pro	4.0	19.6	2.0	14.1
D-Phe	5.1	11.0	–	–
D-Tyr	6.8	5.87	–	–
free amino acids (total)	4589 mg/100 g		3739 mg/100 g	
free D-amino acids	188 mg/100 g		52.0 mg/100 g	

Footnotes to Table 1

[a] $\%\ \text{D–AA} = \dfrac{\text{D} \times 100}{\text{D} + \text{L}}$

[b] Asx = Asp + Asn, calculated as Asp.
Glx = Glu + Gln, calculated as Glu.

[c] $\%\ \text{D–allo–Ile} = \dfrac{\text{D–allo–Ile} \times 100}{\text{D–allo–Ile} + \text{L–allo–Ile} + \text{D–Ile} + \text{L–Ile}}$

$\%\ \text{L–allo–Ile} = \dfrac{\text{L–allo–Ile} \times 100}{\text{D–allo–Ile} + \text{L–allo–Ile} + \text{D–Ile} + \text{L–Ile}}$

(D–Ile not found)

[d] Determined by IEC, precision ± 3%.
[e] For gas chromatograms see Fig. 1.
[f] See Materials and Methods.
[g] "Parmigiano reggiano" from an Italian market (Cannobio, Italy).
[h] "Sauermilch" from a German local dairy factory.
[i] Lactic fermented "Sauerkrautsaft" (German product).
[j] Lactic fermented "Karottenmost" (German product).
[k] "Altbier", specially brewed German beer.
[l] "Morgon", 1978, appellation controlée (France).
[m] Balsamic vinegar, stored in different types of wooden barrels (Modena, Italy).
[n] Vinegar made of red wine (Varvello, Italy).
[o] Dark, medium fat content.
[p] Tea leaves (Ceylon–Assam blend).
[q] Based on soy/wheat (Singapore).
[r] Fermented soy paste (Chinese product).

foods for nutritional calculations. From a sensorial point of view, the occurrence of D-AA in foods may be of interest since most D-AA have a sweet taste in contrast to many L-AA, which taste bitter [10]. Although toxicological [11] and immunosuppressive [12] effects of D-AA in experimental animals have been reported, the question as to whether any noxious effects of free D-AA in foods have to be taken into account still remains unanswered [13–18]. They certainly depend on the amounts and composition of the D-AA consumed as well as on the food matrix that contains D-AA. Furthermore, possible synergistic effects with other food constituents have to be considered. Factors such as nutritional and cultural preferences and behaviour, age, sex, race, and state of health may be of significance for the sensitivity of individuals towards foodstuffs containing D-AA.

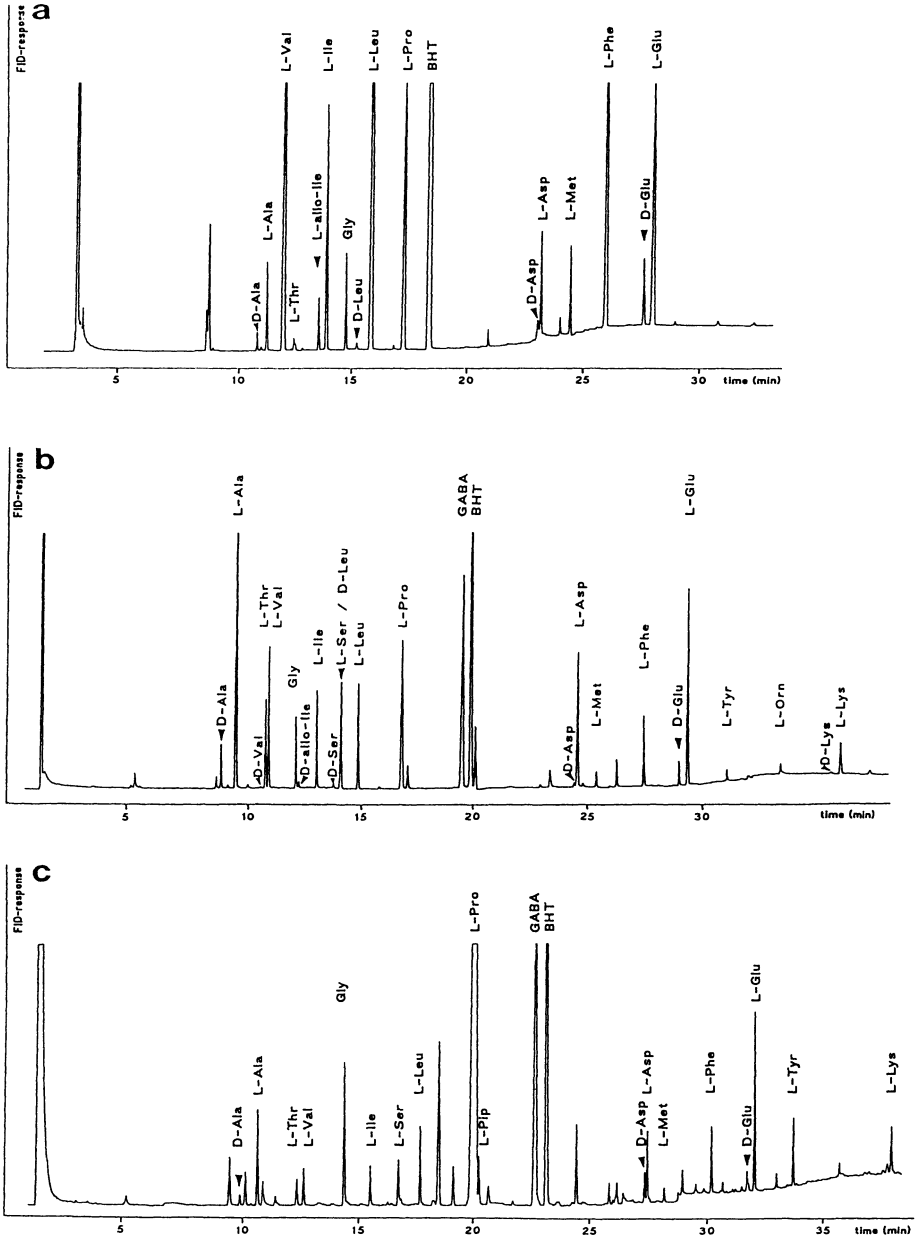

Fig 1. Gas chromatograms of N(O)-pentafluoropropionyl amino acid 1-propyl esters of free amino acids isolated from fermented foods. (a) Trappist cheese, (b) lactic fermented cabbage juice, (c) beer, (d) bal-

(continued)

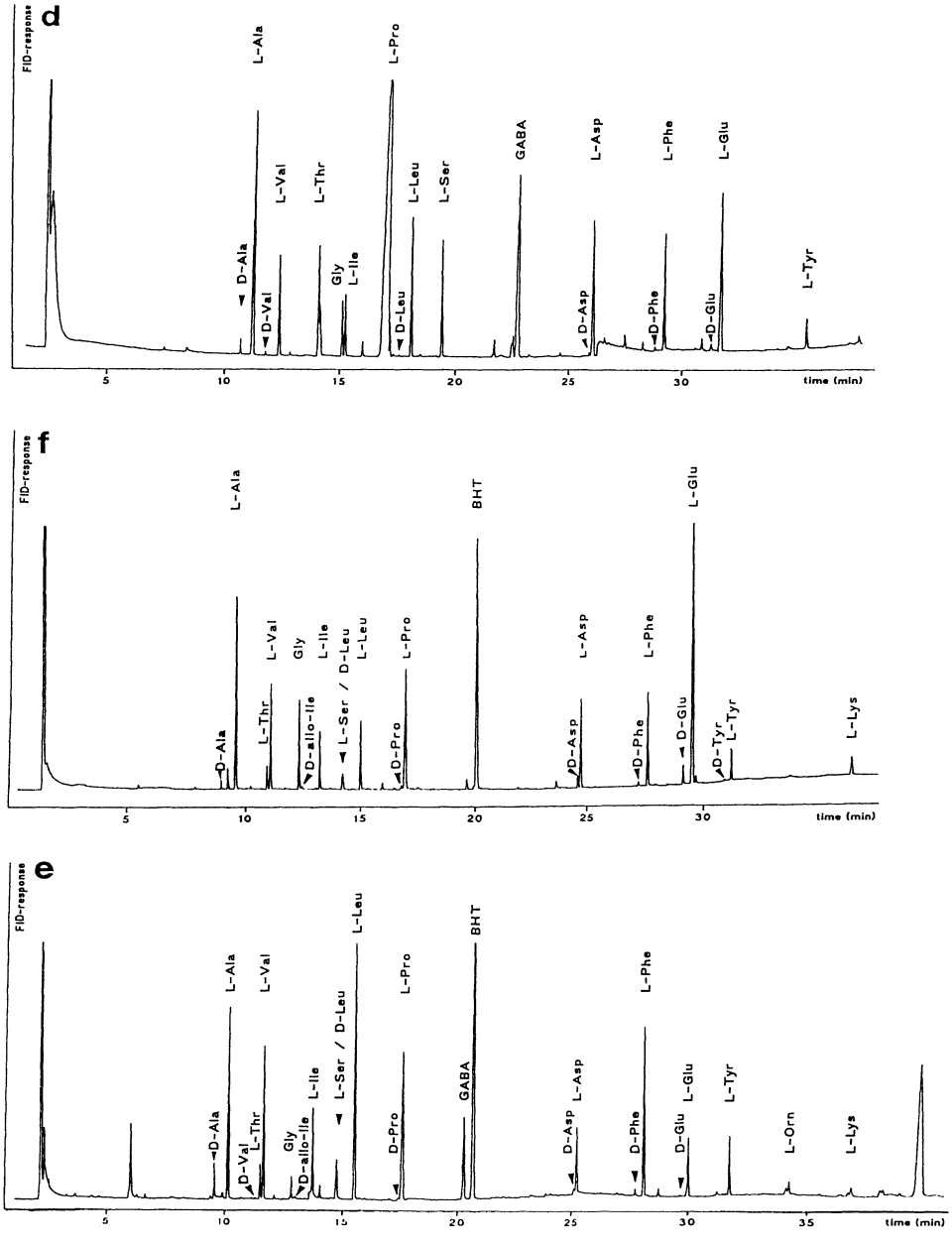

samic vinegar, (e) cacao, and (f) soy sauce. For origin of foods see Table 1. Chiral stationary phases and chromatographic conditions: (a) XE-60-S-Val-S-phenylethylamide, C; (b), (c), (e), (f), Chirasil-L-Val, A; (d) Chirasil-L-Val, B; (for specification of A, B, and C, see Materials and Methods).

References

1. Whitaker JR and Feeney RE (1983) CRC Crit. Rev. Food Sci. Nutr. 19: 173–212.
2. Masters PM and Friedman M (1979) J. Agric. Food Chem. 27: 507–511.
3. Friedman M and Liardon R (1985) J. Agric. Food Chem. 33: 666–672.
4. Tovar LR and Schwass DE (1983) Am. Chem. Soc. Symp. Ser. 234: 169–185.
5. Brückner H, Wittner R, Hausch M and Godel H (1989) Fresenius Z. Anal. Chem. 333: 775–776.
6. Brückner H and Hausch M (1990) In: Franck H, Holmsted B and Testa B (eds.) Chirality and Biological Activity. Liss, New York, pp. 129–136.
7. Schleifer KH and Kandler O (1972) Bacteriol. Rev. 36: 407–477.
8. Davies JS (1977) In: Weinstein B, (ed.) Chemistry and Biochemistry of Amino Acids, Peptides, and Proteins. Decker, New York, Basel, Vol. 4: pp. 1–27.
9. Johnston MM and Diven WF (1969) J. Biol. Chem. 244: 5414–5420.
10. Wieser H, Jugel H and Belitz HD (1977) Z. Lebensm. Unters.-Forsch. 164: 277–282.
11. Ganote CE and Carone FA (1974) Am. J. Path. 77: 269–276.
12. Inoue Y, Zama Y and Suzuki M (1981) Jpn. J. Exp. Med. 51: 363–366.
13. Brückner H and Hausch M (1989) J. High Resol. Chromatogr. 12: 680–684.
14. Brückner H and Hausch M (1989) Chromatographia 28: 487–492.
15. Lubec G, Wolf Chr and Bartosch B (1989) The Lancet, Dec. 9, 1392–1393.
16. Segal W (1990) The Lancet, Febr. 24, 470.
17. Brückner H and Hausch M (1990) Milchwissenschaft 45(6) and 45(7), in press.
18. Kampel D, Kupferschmidt R and Lubec G (1990) In: Lubec G and Rosenthal GA (eds.) Amino Acids: Chemistry, Biology and Medicine. ESCOM, Leiden, pp. 1164–1171.

Address for correspondence: H. Brückner, M. Hausch, Institute of Food Technology, University of Hohenheim, D-7000 Stuttgart 70, F.R.G.

Author index

Subject index